frontiers | Research Topics

Advances in neuroprotective agents for cerebral ischemia treatment

Edited by
Yongjun Sun, Li-Nan Zhang, Toshiko Yamazawa, Zibin Gao and Long Wang

Published in
Frontiers in Pharmacology
Frontiers in Neuroscience

ISSN 1664-8714
ISBN 978-2-83252-115-1
DOI 10.3389/978-2-83252-115-1

About Frontiers

Frontiers is more than just an open access publisher of scholarly articles: it is a pioneering approach to the world of academia, radically improving the way scholarly research is managed. The grand vision of Frontiers is a world where all people have an equal opportunity to seek, share and generate knowledge. Frontiers provides immediate and permanent online open access to all its publications, but this alone is not enough to realize our grand goals.

Frontiers journal series

The Frontiers journal series is a multi-tier and interdisciplinary set of open-access, online journals, promising a paradigm shift from the current review, selection and dissemination processes in academic publishing. All Frontiers journals are driven by researchers for researchers; therefore, they constitute a service to the scholarly community. At the same time, the *Frontiers journal series* operates on a revolutionary invention, the tiered publishing system, initially addressing specific communities of scholars, and gradually climbing up to broader public understanding, thus serving the interests of the lay society, too.

Dedication to quality

Each Frontiers article is a landmark of the highest quality, thanks to genuinely collaborative interactions between authors and review editors, who include some of the world's best academicians. Research must be certified by peers before entering a stream of knowledge that may eventually reach the public - and shape society; therefore, Frontiers only applies the most rigorous and unbiased reviews. Frontiers revolutionizes research publishing by freely delivering the most outstanding research, evaluated with no bias from both the academic and social point of view. By applying the most advanced information technologies, Frontiers is catapulting scholarly publishing into a new generation.

What are Frontiers Research Topics?

Frontiers Research Topics are very popular trademarks of the *Frontiers journals series*: they are collections of at least ten articles, all centered on a particular subject. With their unique mix of varied contributions from Original Research to Review Articles, Frontiers Research Topics unify the most influential researchers, the latest key findings and historical advances in a hot research area.

Find out more on how to host your own Frontiers Research Topic or contribute to one as an author by contacting the Frontiers editorial office: frontiersin.org/about/contact

Advances in neuroprotective agents for cerebral ischemia treatment

Topic editors

Yongjun Sun — Hebei University of Science and Technology, China
Li-Nan Zhang — Hebei Medical University, China
Toshiko Yamazawa — Jikei University School of Medicine, Japan
Zibin Gao — Hebei University of Science and Technology, China
Long Wang — California State University, Long Beach, United States

Citation

Sun, Y., Zhang, L.-N., Yamazawa, T., Gao, Z., Wang, L., eds. (2023). *Advances in neuroprotective agents for cerebral ischemia treatment*.
Lausanne: Frontiers Media SA. doi: 10.3389/978-2-83252-115-1

Table of contents

06 Inhibiting YAP in Endothelial Cells From Entering the Nucleus Attenuates Blood-Brain Barrier Damage During Ischemia-Reperfusion Injury
Shuaishuai Gong, Huifen Ma, Fan Zheng, Juan Huang, Yuanyuan Zhang, Boyang Yu, Fang Li and Junping Kou

19 Ginkgolide With Intravenous Alteplase Thrombolysis in Acute Ischemic Stroke Improving Neurological Function: A Multicenter, Cluster-Randomized Trial (GIANT)
Xuting Zhang, Wansi Zhong, Xiaodong Ma, Xiaoling Zhang, Hongfang Chen, Zhimin Wang, Min Lou and GIANT Investigators

28 Resveratrol has an Overall Neuroprotective Role in Ischemic Stroke: A Meta-Analysis in Rodents
Jianyang Liu, Jialin He, Yan Huang and Zhiping Hu

41 Metabolomic Profiling of Brain Protective Effect of Edaravone on Cerebral Ischemia-Reperfusion Injury in Mice
Hui-fen Ma, Fan Zheng, Lin-jie Su, Da-wei Zhang, Yi-ning Liu, Fang Li, Yuan-yuan Zhang, Shuai-shuai Gong and Jun-ping Kou

55 Inhibiting Sphingosine 1-Phosphate Receptor Subtype 3 Attenuates Brain Damage During Ischemia-Reperfusion Injury by Regulating nNOS/NO and Oxidative Stress
Xuehui Fan, Hongping Chen, Chen Xu, Yingju Wang, Pengqi Yin, Meng Li, Zhanbin Tang, Fangchao Jiang, Wan Wei, Jihe Song, Guozhong Li and Di Zhong

67 Treatment of Cerebral Ischemia Through NMDA Receptors: Metabotropic Signaling and Future Directions
Yuanyuan Li, Xiaokun Cheng, Xinying Liu, Le Wang, Jing Ha, Zibin Gao, Xiaoliang He, Zhuo Wu, Aibing Chen, Linda L. Jewell and Yongjun Sun

74 Bibliometric Analysis of Ferroptosis in Stroke From 2013 to 2021
Yuhua Chen, Tianlin Long, Quanhua Xu and Chi Zhang

86 A Meta-Analysis of Using Protamine for Reducing the Risk of Hemorrhage During Carotid Recanalization: Direct Comparisons of Post-operative Complications
Yongli Pan, Zhiqiang Zhao, Tao Yang, Qingzheng Jiao, Wei Wei, Jianyong Ji and Wenqiang Xin

98 Economic Evaluation of Ticagrelor Plus Aspirin Versus Aspirin Alone for Acute Ischemic Stroke and Transient Ischemic Attack
Jigang Chen, Linjin Ji, Xin Tong, Mingyang Han, Songfeng Zhao, Yongkai Qin, Zilong He, Zhiqun Jiang and Aihua Liu

107 A Network-Based Approach to Investigate the Neuroprotective Effects and Mechanisms of Action of Huangqi-Chuanxiong and Sanleng-Ezhu Herb Pairs in the Treatment of Cerebral Ischemic Stroke
Lin Zhao, Li Dong Ding, Zi Hao Xia, Peng Sheng, Meng Meng Shen, Zhong Ming Cai and Bing Chun Yan

120 Acute Administration of Metformin Protects Against Neuronal Apoptosis Induced by Cerebral Ischemia-Reperfusion Injury *via* Regulation of the AMPK/CREB/BDNF Pathway
Ke Liu, Lulu Li, Zhijun Liu, Gang Li, Yanqing Wu, Xingjun Jiang, Mengdie Wang, Yanmin Chang, Tingting Jiang, Jianheng Luo, Jiahui Zhu, Hongge Li and Yong Wang

136 Corrigendum: Acute Administration of Metformin Protects Against Neuronal Apoptosis Induced by Cerebral Ischemia-Reperfusion Injury *via* Regulation of the AMPK/CREB/BDNF Pathway
Ke Liu, Lulu Li, Zhijun Liu, Gang Li, Yanqing Wu, Xingjun Jiang, Mengdie Wang, Yanmin Chang, Tingting Jiang, Jianheng Luo, Jiahui Zhu, Hongge Li and Yong Wang

137 Preclinical Evidence of Paeoniflorin Effectiveness for the Management of Cerebral Ischemia/Reperfusion Injury: A Systematic Review and Meta-Analysis
Anzhu Wang, Wei Zhao, Kaituo Yan, Pingping Huang, Hongwei Zhang and Xiaochang Ma

155 The Emerging Role of Extracellular Vesicle Derived From Neurons/Neurogliocytes in Central Nervous System Diseases: Novel Insights Into Ischemic Stroke
Fan Li, Xiaokui Kang, Wenqiang Xin and Xin Li

168 Magnetic Resonance Imaging Investigation of Neuroplasticity After Ischemic Stroke in Tetramethylpyrazine-Treated Rats
Xue-Feng Feng, Jian-Feng Lei, Man-Zhong Li, Yu Zhan, Le Yang, Yun Lu, Ming-Cong Li, Yu-Ming Zhuang, Lei Wang and Hui Zhao

183 Diprotin A TFA Exerts Neurovascular Protection in Ischemic Cerebral Stroke
Ming-Yue Zhou, Ya-Jie Zhang, Hong-Mei Ding, Wei-Feng Wu, Wei-Wei Cai, Yan-Qiang Wang and De-Qin Geng

194 Neuroprotective Effects of Quercetin on Ischemic Stroke: A Literature Review
Leilei Zhang, Jingying Ma, Fan Yang, Sishi Li, Wangran Ma, Xiang Chang and Lin Yang

208 Effect of Celastrol on LncRNAs and mRNAs Profiles of Cerebral Ischemia-Reperfusion Injury in Transient Middle Cerebral Artery Occlusion Mice Model
Jiandong Liu, Xiangna Guo, Lu Yang, Tao Tao, Jun Cao, Zexuan Hong, Fanning Zeng, Yitian Lu, Chunshui Lin and Zaisheng Qin

223 miRNA Involvement in Cerebral Ischemia-Reperfusion Injury
Maria-Adriana Neag, Andrei-Otto Mitre, Codrin-Constantin Burlacu, Andreea-Ioana Inceu, Carina Mihu, Carmen-Stanca Melincovici, Marius Bichescu and Anca-Dana Buzoianu

247 *Panax notoginseng* Saponins Stimulates Neurogenesis and Neurological Restoration After Microsphere-Induced Cerebral Embolism in Rats Partially *Via* mTOR Signaling
Jiale Gao, Jianxun Liu, Mingjiang Yao, Wei Zhang, Bin Yang and Guangrui Wang

261 Elevated plasma syndecan-1 as glycocalyx injury marker predicts unfavorable outcomes after rt-PA intravenous thrombolysis in acute ischemic stroke
Fangfang Zhao, Rongliang Wang, Yuyou Huang, Lingzhi Li, Liyuan Zhong, Yue Hu, Ziping Han, Junfen Fan, Ping Liu, Yangmin Zheng and Yumin Luo

271 A synthetic BBB-permeable tripeptide GCF confers neuroprotection by increasing glycine in the ischemic brain
Juan Chen, Yang Zhuang, Ya Zhang, Huabao Liao, Rui Liu, Jing Cheng, Zhifeng Zhang, Jiangdong Sun, Jingchen Gao, Xiyuran Wang, Shujun Chen, Liang Zhang, Fengyuan Che and Qi Wan

285 Antioxidant and neuroprotective actions of resveratrol in cerebrovascular diseases
Qing Wang, Qi Yu and Min Wu

303 DL-3-n-butylphthalide (NBP) alleviates poststroke cognitive impairment (PSCI) by suppressing neuroinflammation and oxidative stress
Hui Zhang, Laifa Wang, Yongping Yang, Chuanhai Cai, Xueqin Wang, Ling Deng, Binsheng He, Wenhu Zhou and Yanhui Cui

frontiers in Pharmacology

ORIGINAL RESEARCH
published: 26 November 2021
doi: 10.3389/fphar.2021.777680

Inhibiting YAP in Endothelial Cells From Entering the Nucleus Attenuates Blood-Brain Barrier Damage During Ischemia-Reperfusion Injury

Shuaishuai Gong†, Huifen Ma†, Fan Zheng, Juan Huang, Yuanyuan Zhang, Boyang Yu, Fang Li and Junping Kou**

State Key Laboratory of Natural Medicines, Jiangsu Key Laboratory of TCM Evaluation and Translational Research, Department of Pharmacology of Chinese Material Medical, School of Traditional Pharmacy, China Pharmaceutical University, Nanjing, China

Blood-brain barrier (BBB) damage is a critical event in ischemic stroke, contributing to aggravated brain damage. Endothelial cell form a major component of the BBB, but its regulation in stroke has yet to be clarified. We investigated the function of Yes-associated protein 1 (YAP) in the endothelium on BBB breakdown during cerebral ischemia/reperfusion (I/R) injury. The effects of YAP on BBB dysfunction were explored in middle cerebral artery occlusion/reperfusion (MCAO/R)-injury model mice and using brain microvascular endothelial cells (BMEC) exposed to oxygen-glucose deprivation/reoxygenation (OGD/R) injury. The degree of brain injury was estimated using staining (2,3,5-Triphenyltetrazolium chloride, hematoxylin and eosin) and the detection of cerebral blood flow. BBB breakdown was investigated by examining the leakage of Evans Blue dye and evaluating the expression of tight junction (TJ)-associated proteins and matrix metallopeptidase (MMP) 2 and 9. YAP expression was up-regulated in the nucleus of BMEC after cerebral I/R injury. Verteporfin (YAP inhibitor) down-regulated YAP expression in the nucleus and improved BBB hyperpermeability and TJ integrity disruption stimulated by cerebral I/R. YAP-targeted small interfering RNA (siRNA) exerted the same effects in BMEC cells exposed to OGD/R injury. Our findings provide new insights into the contributions made by YAP to the maintenance of BBB integrity and highlight the potential for YAP to serve as a therapeutic target to modulate BBB integrity following ischemic stroke and related cerebrovascular diseases.

Keywords: YAP, verteporfin, endothelial cells, blood-brain barrier, ischemic stroke

OPEN ACCESS

Edited by:
Li-Nan Zhang,
Hebei Medical University, China

Reviewed by:
Bun Tsoi,
The University of Hong Kong, Hong Kong SAR, China
Shu Shu,
Nanjing Drum Tower Hospital, China

****Correspondence:***
Fang Li
lifangcpu@163.com
Junping Kou
junpingkou@cpu.edu.cn

†These authors have contributed equally to this work

Specialty section:
This article was submitted to Neuropharmacology, a section of the journal Frontiers in Pharmacology

Received: *15 September 2021*
Accepted: *08 November 2021*
Published: *26 November 2021*

Citation:
Gong S, Ma H, Zheng F, Huang J, Zhang Y, Yu B, Li F and Kou J (2021) Inhibiting YAP in Endothelial Cells From Entering the Nucleus Attenuates Blood-Brain Barrier Damage During Ischemia-Reperfusion Injury. Front. Pharmacol. 12:777680. doi: 10.3389/fphar.2021.777680

1 INTRODUCTION

Ischemic stroke is often accompanied by vascular dysfunction due to damage to the blood-brain barrier (BBB) (Feigin et al., 2018; Ozen et al., 2018). The BBB is a specialized barrier comprised of endothelial cells (ECs), tight junctions (TJs), pericytes, astrocytic end-feet processes, and the basement membrane. These components are crucial for the establishment of a highly regulated microenvironment, which ensures appropriate neuronal function (Moskowitz et al., 2010; Lallukka et al., 2018; Sweeney et al., 2019). Therefore, protection against BBB destruction represents an effective strategy for the clinical prevention and treatment of ischemic stroke.

ECs represent the most important component of the BBB, lining the entire microvasculature, and forming TJs to limit paracellular transport, ECs also display considerably a limited rate of transcellular transport for hydrophilic molecules, which contributes to the maintenance of barrier function (Armulik et al., 2010; Guclu et al., 2014). The appropriate regulation and maintenance of the barrier integrity of the ECs that line within blood vessels represent an essential feature of the BBB. The prevention of early cytoskeletal changes in microvascular ECs can attenuate BBB breakdown and secondary tissue injury, resulting in the amelioration of long-term neurological deficits (Fernandez-Klett et al., 2013; Hall et al., 2014). However, the molecular mechanisms that underlie the regulation of EC function and the associated BBB alterations that occur under pathological conditions remain incompletely understood.

The Hippo/Yes-associated protein 1 (YAP) kinase cascade has been reported to serve as a critical regulator of organ size, tissue regeneration, and tumor suppression (Halder and Johnson, 2011; Lin et al., 2017). The Hippo pathway negatively regulates the activity of transcriptional co-activators, including YAP and transcriptional co-activator with PDZ-binding motif (TAZ) (Varelas, 2014). In the nucleus, YAP transcribes genes that control cell proliferation, apoptosis, and cell fate (Szymaniak et al., 2015). YAP localization becomes dramatically altered upon tissue damage, and in some tissues, nuclear YAP abundance is associated with increased regeneration (Choi and Kwon, 2015). YAP has been shown to be involved in BBB dysfunction during ischemic stroke (Ouyang et al., 2020; Gong et al., 2019), although the function of YAP in the maintenance of the cerebral endothelial barrier (CEB) remains unclear. We postulated that YAP might be essential for EC protection and the maintenance of CEB integrity following ischemic stroke.

In the present study, we investigated the effects of YAP on the CEB in mouse and cell models of ischemic-reperfusion injury, with the aim of determining whether YAP represents a potential therapeutic target for regulating BBB integrity after ischemic stroke and related cerebrovascular diseases.

2 MATERIALS AND METHODS

2.1 Ethical Approval of the Study Protocol

The welfare of all animals was ensured, and all experimental procedures were performed in accordance with the Guide for the Care and Use of Laboratory Animals established by the National Institutes of Health. The Animal Ethics Committee of China Pharmaceutical University (Nanjing, China) approved all protocols [No. SYXK(Su)2018-0008].

2.2 Animals

Male C57BL/6J mice were purchased from the Animal Center of Yangzhou University (Yangzhou, China). Adequate food and water were provided. Animals were housed in cage in an environment maintained at a constant temperature (22–24°C) with a normal circadian rhythm.

2.3 Cell Culture

bEnd.3 cells were purchased from Bioleaf Biotech (Shanghai, P.R. China) and cultured in Dulbecco's modified Eagle's medium (DMEM; Gibco, Billings, MT, United States) supplemented with 15% fetal bovine serum (FBS; Gibco), 100 U/mL penicillin and 100 U/mL streptomycin (Ameresco, Framingham, MA, United States) at 37°C in a humidified atmosphere of 5% CO_2 and 95% air. Cells were plated onto cell culture dishes and grown to 80–90% confluence before experimentations.

2.4 Middle Cerebral Artery Occlusion/ Reperfusion Model

Mice were anesthetized in an induction chamber using 3–4% isoflurane in 30% O_2/70% N_2. Anesthetization was confirmed after approximately 2 min when respiration slowed to one breathe per second. Animals were removed from the induction chamber and placed in an anesthesia mask, which maintained an isoflurane concentration of 1–1.5%. Middle cerebral artery occlusion/reperfusion (MCAO/R) was induced using a method based on intraluminal filaments with slight modification as described previously (Gong et al., 2019). Briefly, the right middle cerebral artery of mouse was occluded by inserting a blunt-tip 4-0 nylon monofilament for 1 h followed with reperfusion for 24 h.

2.5 Oxygen and Glucose Deprivation/ Reperfusion Model

bEnd.3 cells were placed in a 37°C anaerobic chamber (0.2% O_2, 5% CO_2, 95% N_2) and cultured in glucose-free medium for 6 h. After the oxygen-glucose deprivation, the cells were placed in glucose-containing DMEM with 15% FBS and incubated under normoxic conditions for hours in order to imitate I/R-like conditions Cao et al. (2016).

2.6 Transendothelial Electrical Resistance Assay

The protective effects of verteporfin (VP, CAS No. 129497-78-5) were examined *in vitro*. Cells were divided into four groups (n = 3): Control, OGD/R, VP (1 μM, **Supplementary Figure S1**) treatment after 6 h OGD, and edaravone (Edara, 1 μM, CAS No. 89-25-8). Edara is a commonly used drug for the clinical treatment of ischemic stroke and is often used as a positive drug in basic research (Bao et al., 2018). bEnd.3 cells were cultured on top of gelatin-coated transwell inserts in 24-well plates for 7 days. The Transendothelial electrical resistance (TEER) of the EC monolayer was monitored daily using a Millicell-ERS voltohmmeter (Millipore, United States). The results obtained from the experimental groups were measured after subtracting the value of a blank, cell-free filter.

2.7 TTC Staining

The protective effects of VP were examined in mice that were randomly divided into four groups (n = 6 per group): sham,

MCAO/R, VP (10 mg/kg, i. p.) after 1 h MCAO, and Edara (5 mg/kg, i. p.). After 24 h of reperfusion, the mice brains were quickly removed and frozen at −70°C. The frozen brain was coronally cut into five slices, then incubated individually using a 24-well culture plate with 1% triphenyl tetrazolium chloride (TTC) solution at 37°C for 15 min. The infarct area was measured by computerized planimetry after photographing with a digital camera. The infarct volume is calculated by summing infarct areas on each slice and multiplying by slice thickness. The personnel conducting the TTC staining was blinded to the study group assignment in order to avoid subjective factors affecting the experimental results Tsubokawa et al. (2017).

2.8 Determination of Cerebral Edema and Neurological Deficits

The mice were sacrificed after MCAO/R induction. The brains were taken out and the wet weight of tissue was accurately measured. After dried in an oven at 100°C for 48 h, the lung tissues were weighed again, recording as dry weight. The content of water in brain were calculated to determine the degree of brain edema. The neurological deficits of the experimental animals were graded on an 18-point scale, as previously described Wu et al. (2019). The evaluation indicators include body symmetry, gait, climbing, circling behavior, forelimb symmetry, compulsory circling and whisker response. The index scores are added together as the final score. The higher the score, the more severe the neurological deficit.

2.9 Hematoxylin and Eosin Staining

Animal brains were removed 24 h after reperfusion, mice were euthanized, the brains excised rapidly, and dipped in 4% paraformaldehyde. Examination was completed in the Pathology Department of the Jiangsu Center for Safety Evaluation of Drugs (Jiangsu, P.R. China) and the brain slices were observed by a digital scanner (NanoZoomer 2.0 RS, Hamamatsu, Japan).

2.10 Cerebral Blood Flow Measurement

After anesthesia with 3% pentobarbital sodium, an incision of about 1–2 cm was made in the abdominal cavity of mice. Cerebral blood flow (CBF) in the mesentery was measured using a laser Doppler flowmeter Laser. Images were acquired at ischemia onset and during reperfusion (n = 6 per group).

2.11 Evans Blue Analysis

Evans Blue (EB) extravasation was used to determine BBB integrity as described previously Wu et al. (2019). At 22 h after reperfusion, 2% EB dye (3 ml/kg, Sigma, United States) was injected *via* the tail vein. The mice were euthanized at 2 h after injection of EB and then perfused with saline. The brains were rapidly taken out and imaged. Then the right hemisphere of brain tissue was weighed, homogenized in formamide (0.1 g/ml) and centrifuged at 5,000 g for 30 min after incubated at 60°C for 18 h. The supernatants were collected to determine the quantity of EB, the absorbance at 620 nm was measured spectrophotometrically using an Infinite M200 Pro plate reader (Tecan, NC, United States). EB leakage into the brain tissue was assessed with a standard curve and expressed as micrograms per Gram of wet brain tissue.

2.12 *In vitro* Permeability Assay

Cells were incubated in the Millicell™ cell culture inserts in a humidified atmosphere of 5% CO_2 and 95% air for 7 days. After exposure to OGD/R conditions and drugs, the medium was removed. 200 μL of EB solution (0.67 mg evans blue powder dissolved in 4% BSA solution) were added into the Millicell cell culture inserts and 600 μL of 4% BSA solution were added into the external chamber. The cells were continuously incubated for another 1 h and then the external solution was collected and the absorbance at 620 nm was measured spectrophotometrically using an Infinite M200 Pro plate reader (Tecan, NC, United States). The EB leakage of each group was calculated according to the standard curve and expressed as a percentage of the values of control group.

2.13 siRNA Transfection and Plasmid

2.13.1 YAP-siRNA Treatment

YAP-siRNA (sense: 5′-GACAUCUUCUGGUCAGAGA-3′, and anti-sense: 3′-AGUACCGGAGGUAACAGAG-5′) were constructed by Genomeditech Co., Ltd, (Shanghai, China). Cells were divided randomly into four groups: Control, Control + siRNA, OGD/R, OGD/R + siRNA. bEnd.3 cells were treated with YAP-siRNA or control solvent for 6 h in DEME medium and proliferated for another 24 h. OGD/R was treated subsequently in DMEM medium. After testing the expression of YAP by western blot, the cells with adequate interference efficiency were used in the evaluation of the downstream signaling pathways.

2.14 Cell Viability

Culture medium containing 5 mg/ml 3-(4,5-Dimethylthiazol-2-yl)-2,5-diphenyltetrazolium bromide (MTT) solution replaced the complete medium Four hours after incubation at 37°C, the reaction solution was removed, and 150 μL DMSO was added to each well. A microplate reader (Epoch, Bio Tek, Winooski, VT, United States) was used to record the absorbance with dual waves at 570 and 650 nm after 10 min of shaking.

2.15 Western Blot Analysis

The cells or brain tissue samples (n = 6, for each group) were decapitated and rapidly collected. The prepared cells or tissues (brain tissues from the ischemic penumbra) were homogenized in 1:10 (w/v) ice-cold protein extraction buffer in glass homogenizers. To detect the levels of YAP and phospho- (p)-YAP in the nucleus, a Nuclear Extraction Kit (Solarbio, Cat: SN0020) was used to isolate and purify nuclear and cytoplasmic fractions. To examine the levels of zonula occludens-1 (ZO-1), occludin, matrix metalloproteinase (MMP)-2 and MMP-9, soluble proteins were extracted from cell lysates by centrifugation at 12,000 × g for 10 min at 4°C and collecting the supernatant. The membranes were blocked with phosphate-buffered saline containing Tween20 (PBST) containing 5% skim

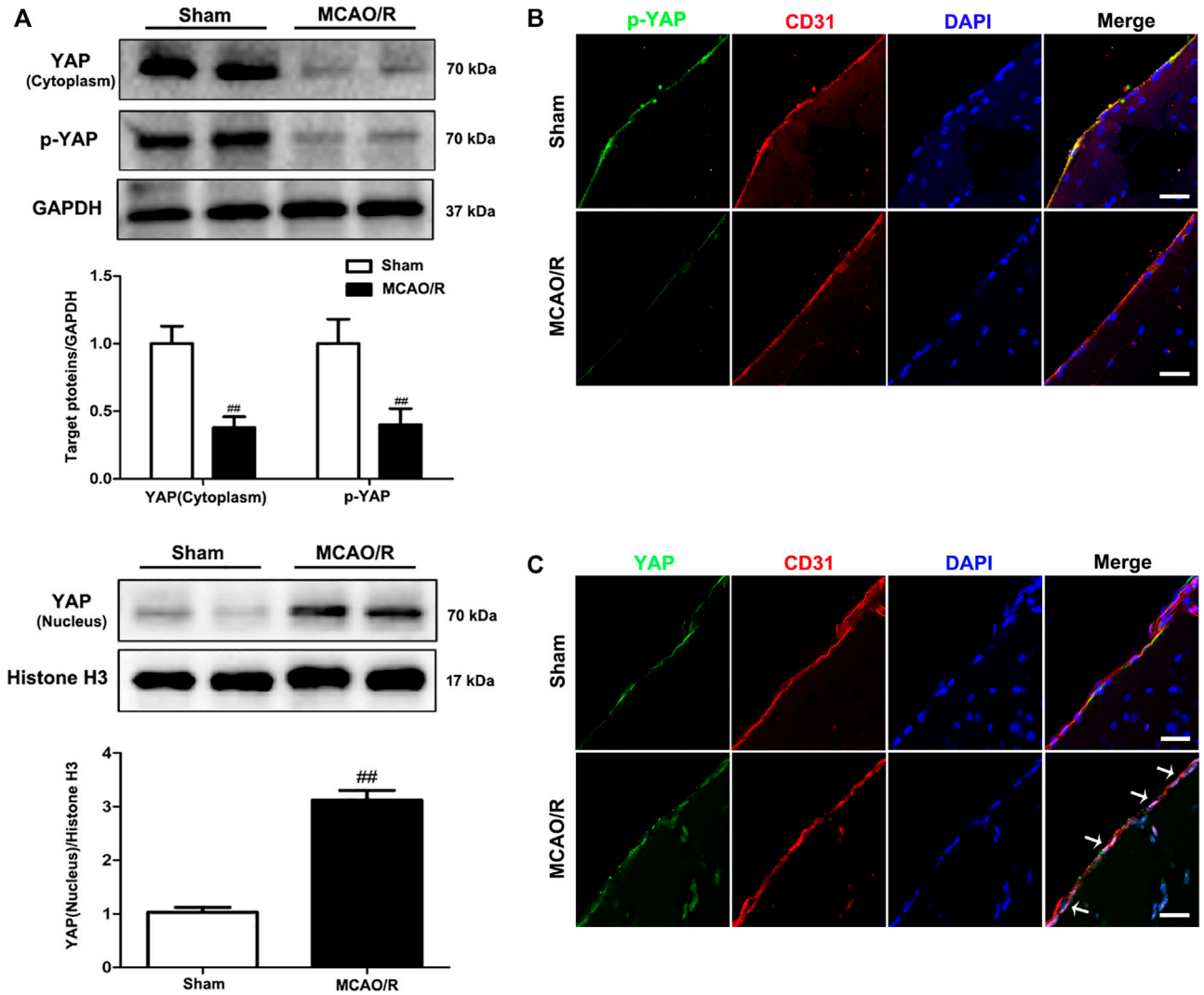

FIGURE 1 | Expression of YAP/p-YAP in the brain endothelial cells following MCAO/R-induced injury. Mice were subjected to 1 h of ischemia and 24 h of reperfusion. **(A)** MCAO/R-induced changes in YAP/p-YAP protein expression levels in the cytoplasm and nucleus were detected by western blotting analysis. **(B)** and **(C)** MCAO/R-induced changes in YAP/p-YAP protein expression levels were detected by immunofluorescence analysis using a combination of anti-YAP (green), anti-p-YAP (green), CD31 (red) and DAPI (blue) staining in mice. The white arrow represents the number of YAP protein into the nucleus. Scale bar = 50 μm. Data are expressed as the mean ± SD, $n = 3$. $^{\#\#}p < 0.01$ *vs*. Sham group.

milk for 2 h at room temperature and then incubated with primary rabbit monoclonal antibody overnight at 4°C (YAP, p-YAP, 1:500; Proteintech Group, United States ZO-1, occludin 1:500; Abcam, United Kingdom MMP-2, MMP-9, 1: 800; CST, United States). The membranes were then washed and incubated with secondary antibody (anti-rabbit IgG, 1:3,000; Proteintech Group, United States) for 1.5 h at room temperature. The anti-actin antibody (1:1,000; Proteintech Group, United States) served as a loading control. The protein bands were visualized with enhanced chemiluminescence reagents (ECL), and the signal densitometry was quantified using a western blotting detection system (Quantity One, Bio-Rad Laboratories, United States) by an observer blinded to the groups of animals or cells being examined.

2.16 *In vivo* and *In vitro* Immunofluorescence

Specimens were sectioned at thickness 10 μm to adhesive slides and bEnd.3 cells were cultured on laser confocal dishes. Specimens were treated with blocking buffer (5% bovine serum albumin, 0.2%Triton-100) for 1 h at 4 °C and then incubated overnight at 4°C with primary antibody against YAP, p-YAP, and ZO-1 (ZO-1, 1:200;

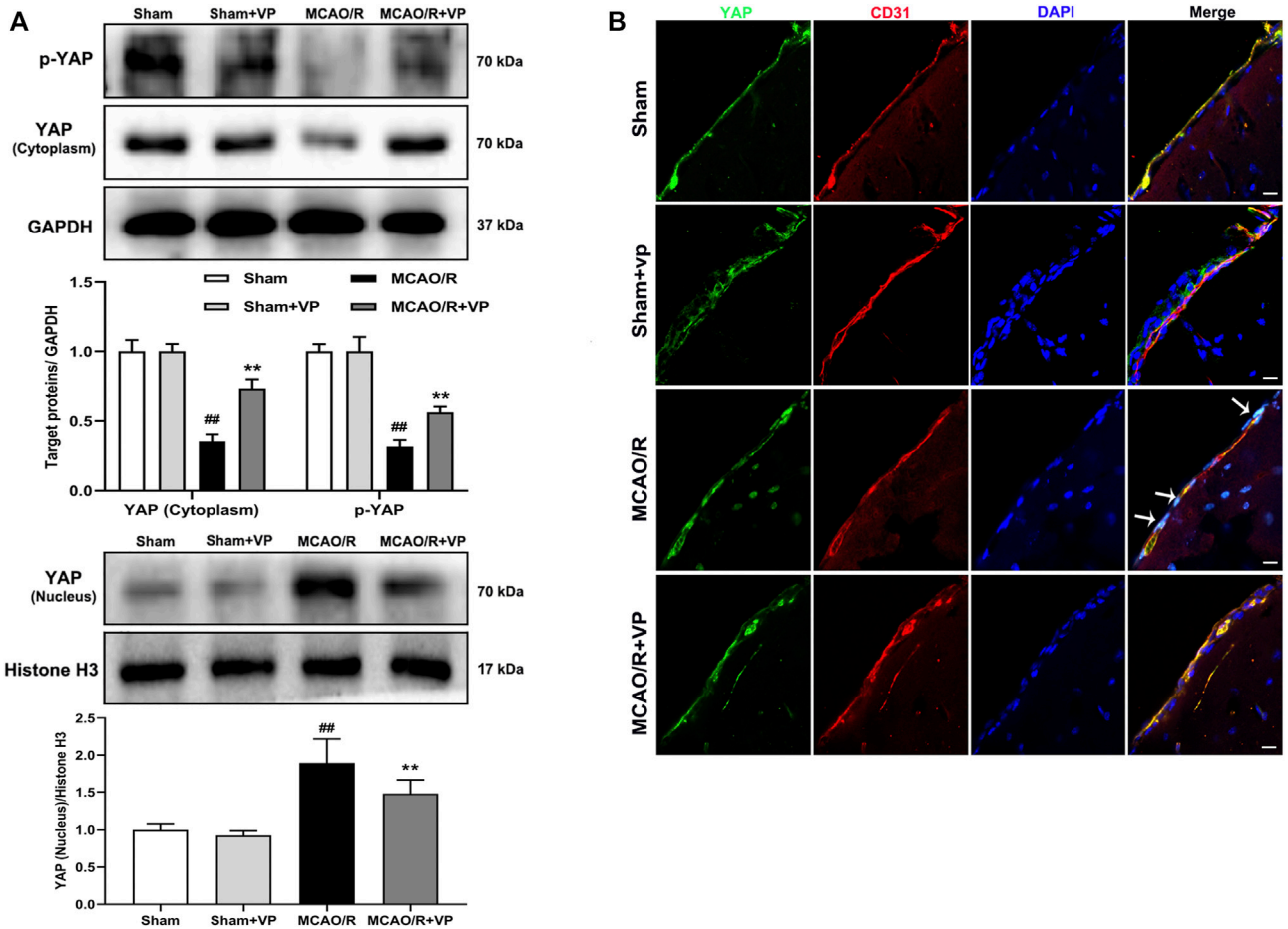

FIGURE 2 | Effects of VP treatment on YAP/p-YAP expression levels following MCAO/R injury in mice. Mice were subjected to 1 h of ischemia and 24 h of reperfusion. **(A)** Representative western blots and quantitative analyses of the expression levels of p-YAP, YAP (cytoplasm), and YAP (nucleus) *in vivo*. **(B)** Representative microscopic images of YAP (green), based on immunofluorescence analyses. DAPI-stained nuclei are depicted in blue. The white arrow represents the number of YAP protein into the nucleus. Data are expressed as the mean ± SD, $n = 6$. $^{\#\#}p < 0.01$ *vs*. Sham group, $^{**}p < 0.01$ *vs*. MCAO/R group. Scale bar = 50 μm.

Proteintech Group, United States; YAP, 1:300; p-YAP, 1:100; Abcam, United Kingdom), followed by incubation with an Alexa Fluor 488-conjugated donkey anti-rabbit IgG (HþL) antibody (Invitrogen, Carlsbad, CA, United States) and 4′,6-Diamidino-2-phenylindole (Beyotime Biotechnology). Fluorescent images were observed with a confocal laser scanning microscope (LSM700; Zeiss, Jena, Germany) and processed using ZEN imaging software. Regarding the IF brain slice, the location of the studied brain area was showed as an illustration figure in **Supplementary Figure S1**.

2.17 Statistical Analysis

Data are expressed as the mean ± SEM. Statistical analyses were carried out using the Student's t-test (two-tailed) for comparison between two groups and one-way analysis of variance (ANOVA) followed by Dunnett's test if the data involved three or more groups. Tests were considered significant at $p < 0.05$. Analyses were carried out using Prism v5.01 (GraphPad, San Diego, CA, United States).

3 RESULTS

YAP is highly expressed in the nuclei of brain endothelial cells from mice subjected to MCAO/R injury *in vivo*.

To determine the specific role played by YAP in ischemic stroke, YAP expression levels were evaluated in the brain after MCAO/R injury using western blotting and IF analyses. After 1 h of cerebral ischemia and 24 h of reperfusion, the expression levels of YAP and p-YAP were reduced in the cytoplasm, and the expression level of YAP was significantly increased in the nucleus (**Figure 1** and **Supplementary Figures S3–5**).

Verteporfin (a small molecule inhibitor of YAP) inhibits the expression of YAP in the nucleus under MCAO/R injury conditions.

The western blot analysis results showed that VP (10 mg/kg), when i. p. injected 1 h after MCAO, significantly increased the expression levels of p-YAP and YAP in the cytoplasm and decreased YAP expression levels in the nucleus (**Figure 2A**). In addition, the IF results also showed that the fluorescence intensity of p-YAP significantly increased (**Supplementary**

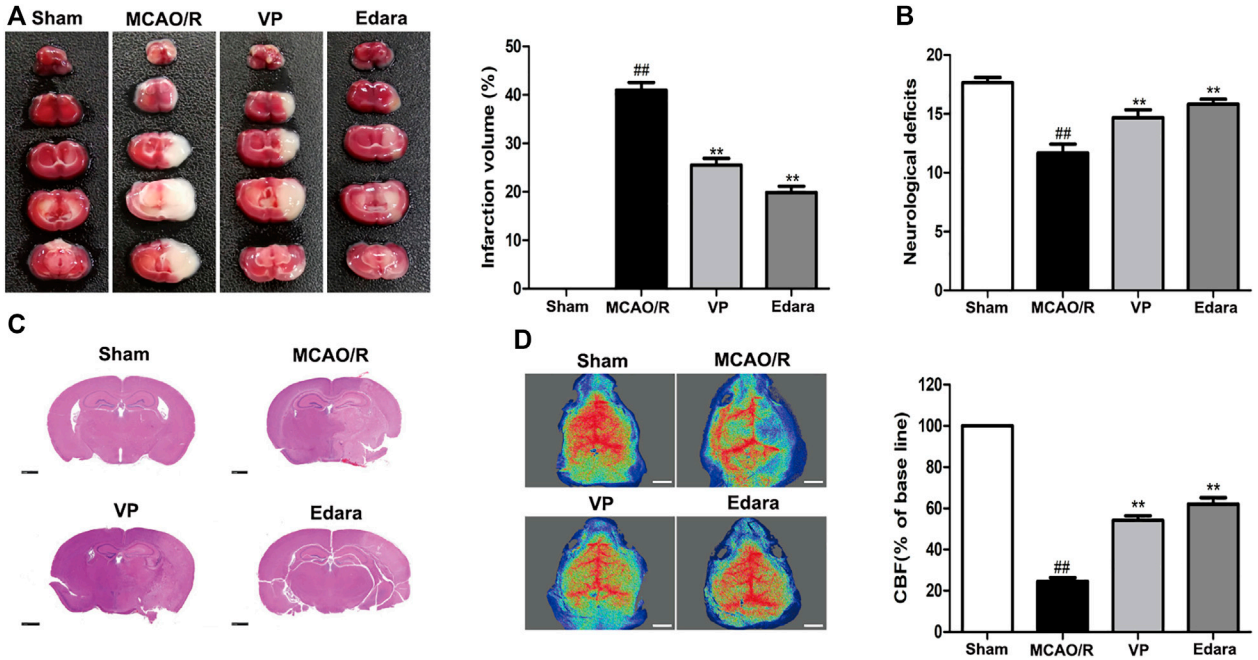

FIGURE 3 | Effects of VP treatment on brain damage caused by MCAO/R injury in mice. Mice were subjected to 1 h of ischemia and 24 h of reperfusion. Mice were treated with VP (10 mg/kg) after 1 h of ischemia. **(A)** Mouse brains were evaluated for infarct volumes using TTC staining, which was quantified using imaging software, after I/R injury. **(B)** Quantitation of the neurological deficits measured in different groups. **(C)** H and E-stained images of mouse brain sections from different groups, examined under a light microscope. **(D)** CBF quantification in ischemic brain regions. Data are expressed as the mean ± SD, $n = 6$. $^{\#\#}p < 0.01$ *vs*. Sham group, $^{**}p < 0.01$ *vs*. MCAO/R group. Scale bar = 50 μm.

Fig. 7), and the intensity of YAP in nucleus significantly decreased after the administration of VP compared with the intensities observed in the untreated MCAO/R group (**Figure 2B** and **Supplementary Figure S6**).

3.1 Inhibition of YAP Attenuates MCAO/R-Induced Brain Damage

VP (10 mg/kg) significantly reduced cerebral infarct volume, cerebral edema, and neurological deficits after MCAO/R injury (**Figures 3A,B**, **Supplementary Figures S8 and 9**). The damaged area of the brain was reduced significantly in MCAO/R model mice after the administration of VP compared with the untreated MCAO/R mice (**Figure 3C**). CBF improved in the ischemic hemisphere of MCAO/R mice after the administration of VP compared with untreated MCAO/R mice (**Figure 3D**). The efficacy of VP was similar to that observed for Edara, which was used as a positive control, which indicated that VP treatment induced improvements following ischemic brain injury in mice.

3.2 The Inhibition of YAP Results in the Maintenance of BBB Integrity Following MCAO/R Injury

Compared with the untreated MCAO/R group, the administration of VP significantly reduced EB leakage, increased the expression levels of ZO-1 and occludin, and decreased the expression levels of matrix metallopeptidase (MMP)-2 and MMP-9 in brain tissues (**Figure 4**). The efficacy of VP was similar to Edara, which indicated that VP could improve BBB integrity following MCAO/R injury.

3.3 YAP is Highly Expressed in the Nucleus of Cells Exposed to OGD/R Injury *In vitro*

To evaluate changes in YAP expression in an *in vitro* model of cerebral I/R injury, YAP/p-YAP expression levels were examined in the brain-derived EC line bEnd.3 following the induction of an OGD/R model. YAP/p-YAP expression levels in the cytoplasm reduced gradually after 6 h of OGD and 6 h of reoxygenation, whereas YAP expression increased gradually in the nucleus (**Figure 5A**). IF analysis also showed changes in YAP/p-YAP expression occurred after 6 h of OGD followed by 6 h of reoxygenation (**Figure 5B**), which was consistent with the results of *in vivo* studies.

3.4 VP Inhibits the Expression of YAP in the Nucleus Under OGD/R Injury Conditions

Whether VP can inhibit the expression of YAP in the nucleus under OGD/R injury conditions remains to be elucidated. The expression levels of the Hippo pathway target kinase YAP and p-YAP in the Hippo pathway were measured by western blotting and IF analyses *in vitro* after the administration of VP. The results showed that VP (1 μM) significantly increased the expression levels of p-YAP and YAP in the cytoplasm and decreased YAP

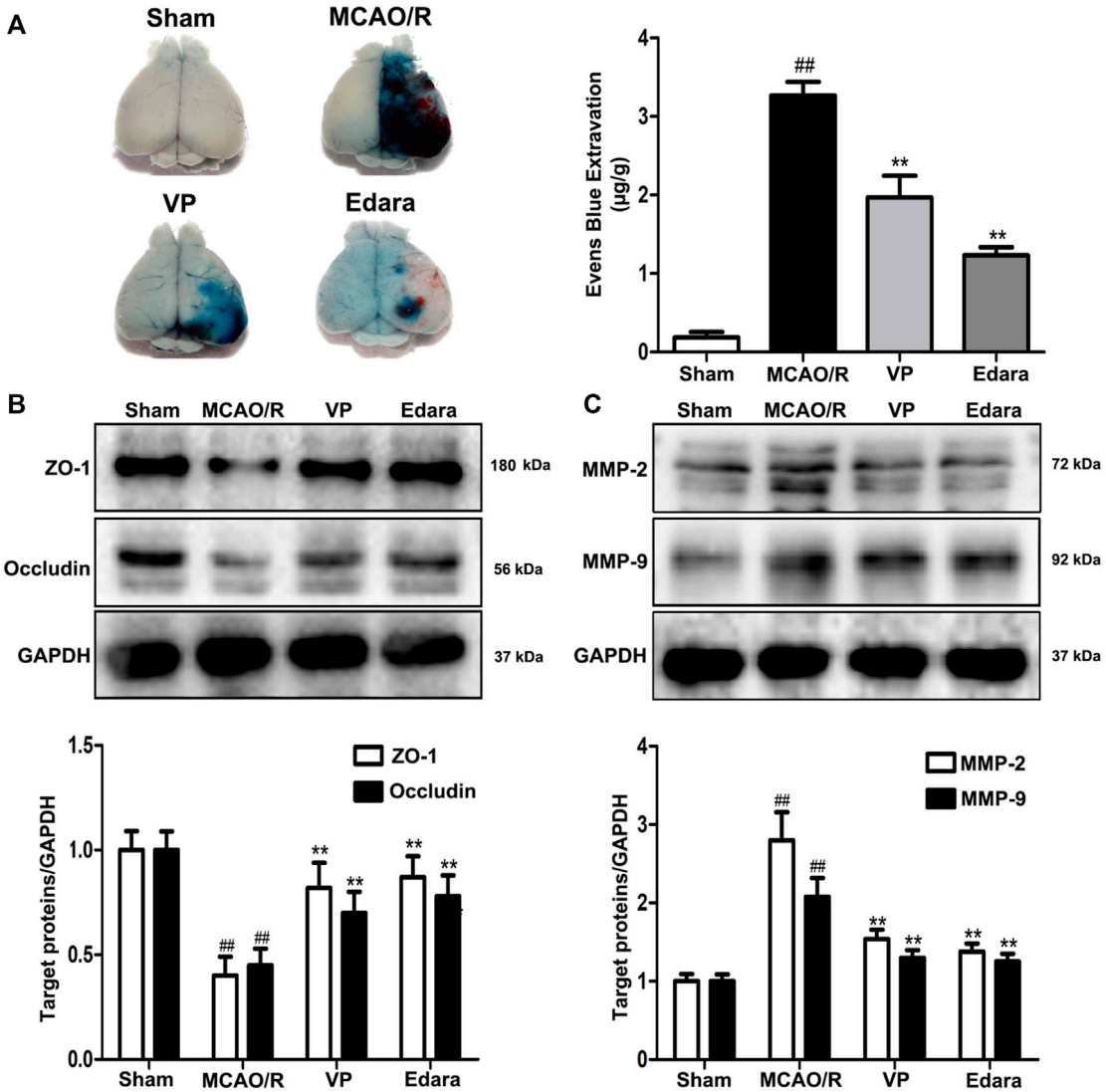

FIGURE 4 | Effects of VP treatment on BBB damage caused by MCAO/R injury in mice. Mice were subjected to 1 h of ischemia and 24 h of reperfusion. Mice were treated with VP (10 mg/kg) after 1 h of ischemia. **(A)** Representative gross appearance of EB-stained brains from a mouse subjected to 1 h of ischemia followed by 24 h of reperfusion. **(B)** Representative western blots and quantitative analyses of ZO-1 and occludin expression levels after the administration of VP in mice. **(C)** Representative western blots and quantitative analyses of MMP-2/9 expression levels after the administration of VP in mice. Data are expressed as the mean ± SD, $n = 6$. $^{\#\#}p < 0.01$ *vs*. Sham group, $^{**}p < 0.01$ *vs*. MCAO/R group.

expression levels in the nucleus (**Figures 6A–C**). Further analysis showed that under OGD/R conditions, the ratio of translocated YAP protein into the nucleus was approximately 85%, and after VP administration, the ratio of translocated YAP into the nucleus was approximately 30% (**Supplementary Figure S10**).

3.5 Inhibition of YAP Ameliorates the Loss of Endothelial Barrier Integrity Induced by OGD/R Injury

To further investigate the protective effects of VP *in vitro*, bEnd.3 cells exposed to OGD/R injury were utilized. Compared with the control group, the cell viability of the OGD/R group decreased, based on the results of an MTT assay (**Figure 7A**, **Supplementary Figure S11**). Treatment with VP (1 μM) and Edara (1 μM) significantly increased cell survival following OGD/R injury. TEER was lower after OGD/R injury compared with the control group and increased significantly following treatment with VP and Edara (**Figure 7B**). EB leakage increased in the OGD/R group compared with that in the control group, and VP significantly inhibited OGD/R-induced EB leakage to an equivalent level as observed for Edara (**Figure 7C**). Compared with the OGD/R group, the protein expression levels of ZO-1 and occludin were increased, and MMP−2 and −9 expression levels were decreased significantly after VP administration (**Figures 7D,E**).

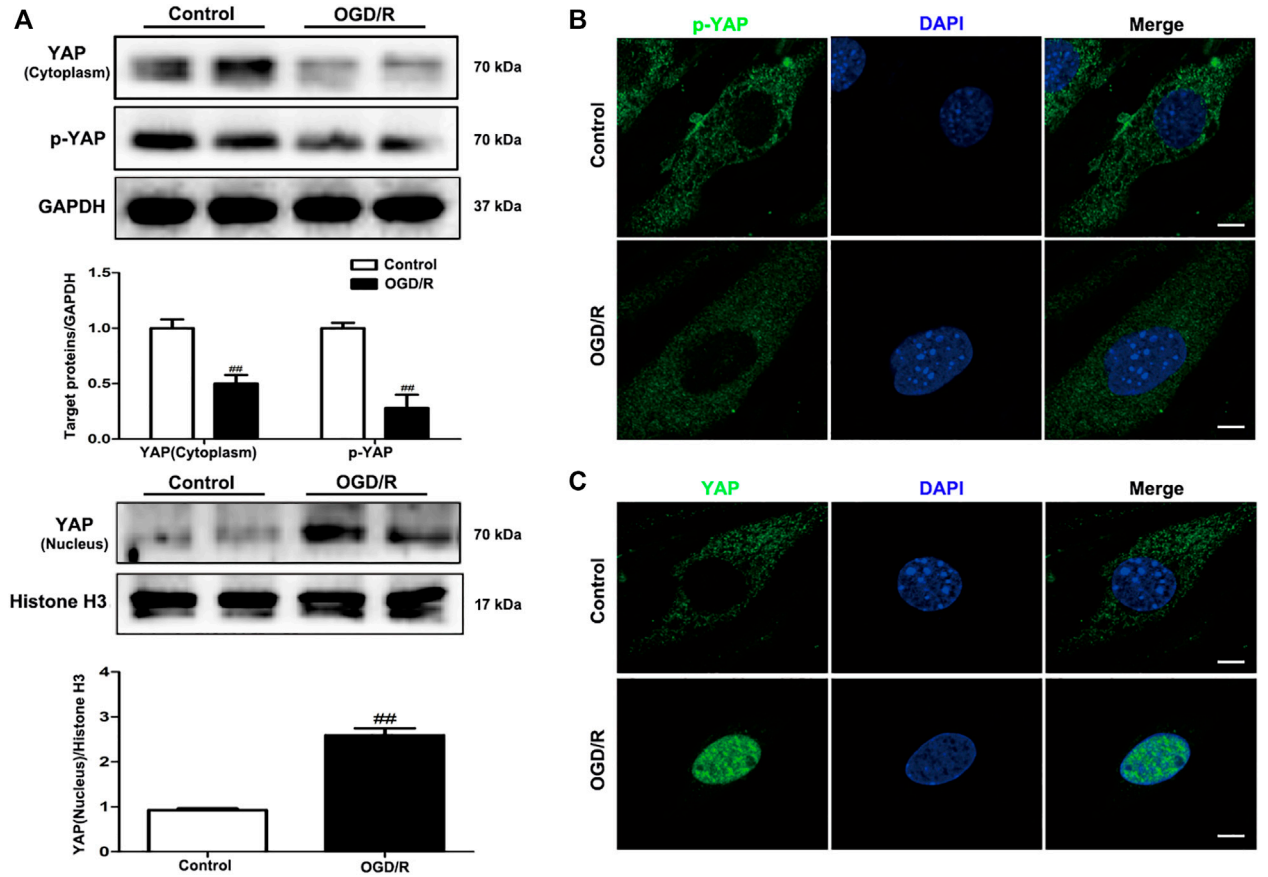

FIGURE 5 | Expression levels of YAP/p-YAP in brain endothelial cells following OGD/R-induced injury. bEnd.3 cells were exposed to 6 h of OGD and 6 h of reoxygenation. **(A)** OGD/R-induced changes in YAP/p-YAP protein expression levels in the cytoplasm and nucleus, as detected by western blotting analysis. **(B)** and **(C)** OGD/R-induced changes in YAP/p-YAP protein expression levels were detected by immunofluorescence using a combination of anti-YAP (green), anti-p-YAP (green), and DAPI (blue) staining in bEnd.3 cells. Scale bar = 50 μm. Data are expressed as the mean ± SD, $n = 3$. $^{\#\#}p < 0.01$ *vs*. Control group.

3.6 YAP-siRNA Attenuates OGD/R Injury-Induced Endothelial Barrier Disruption

To further evaluate the effects of YAP on TJs between ECs, we knocked down YAP expression in bEnd.3 cells using YAP-siRNA *in vitro* (**Supplementary Figures S11 and 12**). Compared with the control group, the TEER of cells subjected to OGD/R. Treatment with YAP-siRNA induced a significant increase in TEER (**Figure 8A**). EB leakage increased in the OGD/R group compared with the control group. YAP-siRNA significantly inhibited OGD/R-induced EB leakage to an equivalent level (**Figure 8B**). Compared with the OGD/R group, the protein expressions levels of ZO-1 and occludin increased significantly after the administration of YAP-siRNA (**Figure 8C**). The IF results also showed that the fluorescence intensity of ZO-1 increased significantly after the administration of YAP-siRNA compared with that in the OGD/R group (**Figure 8D**).

4 DISCUSSION

Here, we identified a previously unrecognized role for YAP in the maintenance of endothelial TJ stability. The increased expression of YAP in the nucleus was observed in both cellular and animal models of cerebral I/R injury. The specific role played by YAP was investigated through the use of a YAP inhibitor and the use of YAP siRNA. The results showed YAP inhibition improved cerebral I/R injury-induced BBB dysfunction. We identified YAP as a regulator of BBB integrity during pathological injury. Thus, the inhibition of YAP expression during cerebral I/R injury may represent a novel strategy for the promotion of ischemic stroke recovery.

The Hippo/YAP signaling pathway plays an essential role in central nervous system development Bao et al. (2017). YAP participates in a range of cellular functions, including migration, adhesion, phagocytosis, and signal transduction Guichet et al. (2018). YAP regulates adherens junction dynamics and EC distribution during vascular development

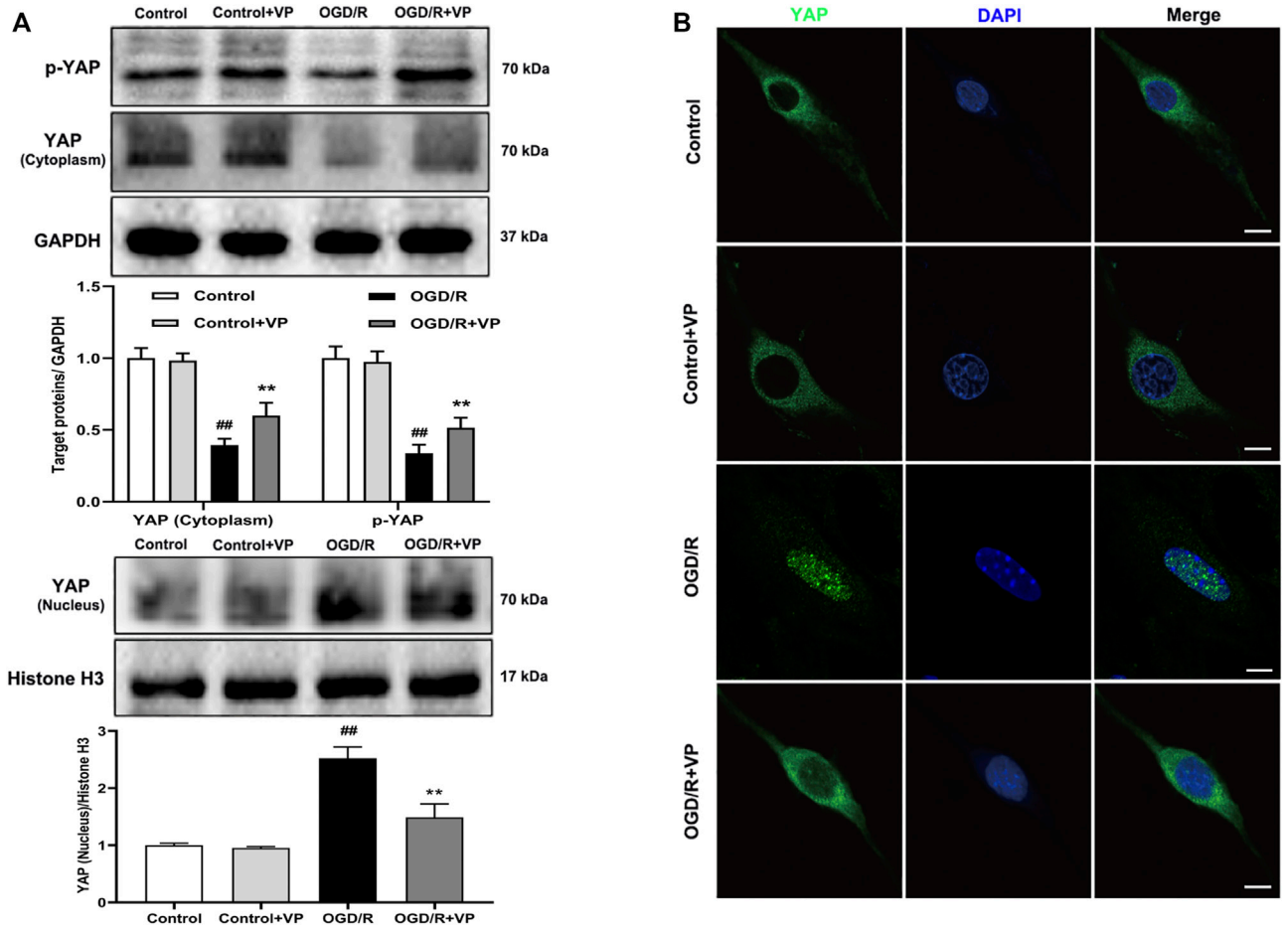

FIGURE 6 | Effects of VP treatment on YAP/p-YAP expression levels following OGD/R injury in brain endothelial cells. bEnd.3 cells were treated with VP (1 μM) and subsequently exposed to 6 h of OGD and 6 h of reoxygenation. **(A)** Representative western blots and quantitative analyses showing the expression levels of p-YAP, YAP (cytoplasm), and YAP (nucleus) *in vitro*. **(B)** Representative microscopic images of YAP (green) based on immunofluorescence analyses. DAPI-stained nuclei are depicted in blue. Data are expressed as the mean ± SD, $n = 6$. $^{\#\#}p < 0.01$ *vs*. Control group, $^{**}p < 0.01$ *vs*. OGD/R group. Scale bar = 50 μm.

(Dieterich et al., 2000; Nagasawa-Masuda and Terai, 2017). The Hippo/YAP signaling pathway has been reported to be involved in the destruction of the BBB in an *in vivo* model (Gong et al., 2019; Jin et al., 2020). However, no studies have investigated the function of YAP in the maintenance of CEB integrity in mice and brain EC models of ischemic stroke. In this study, we found that YAP was highly expressed in the nucleus following cerebral I/R injury model induction (**Figures 1–5**), which indicated that the Hippo/YAP signaling pathway was linked to CEB injury after ischemic stroke. We postulate that YAP acts as a key target protein, which participates in the pathological process and biologic function of ischemic stroke; however, few studies have investigated the involvement of YAP in CEB regulation in ischemic stroke.

To further explore the role played by YAP during brain injury induced by cerebral I/R, we used a YAP inhibitor, verteporfin (VP), which is a benzoporphyrin derivative that is clinically used in photodynamic therapy for neovascular macular degeneration (Brodowska et al., 2014). Recently, studies have shown that VP inhibits YAP activation by disrupting YAP-TEA domain transcription factor (TEAD) interactions, which prevented YAP-induced oncogenic growth (Liu-Chittenden et al., 2012). However, whether and how VP regulates YAP expression during the development of ischemic stroke remains unknown. In this study, VP treatment was found to significantly increase the expression levels of p-YAP and YAP in the cytoplasm and decreased YAP expression levels in the nucleus under cerebral I/R model conditions (**Figures 2–6**). Furthermore, VP treatment was able to reduce the cerebral infarct volume and brain water contents and improve neurological deficits and CBF in cerebral I/R model mice. Cerebral infarct volume, neurological deficits, brain edema, and CBF are often used to evaluate the degree of brain injury (Lochhead et al., 2017). H and E staining is an important method used to evaluate the degree of pathological changes in tissue sections (Campbell et al., 2017). Our results suggested that VP ameliorated MCAO/R-induced brain damage *in vivo* (**Figure 3**, **Supplemental Figure S8**).

The evolution of BBB breakdown after cerebral I/R occurs along the following path: I/R rapidly induces cytoskeletal alterations in BMECs, due to the activation of a variety of

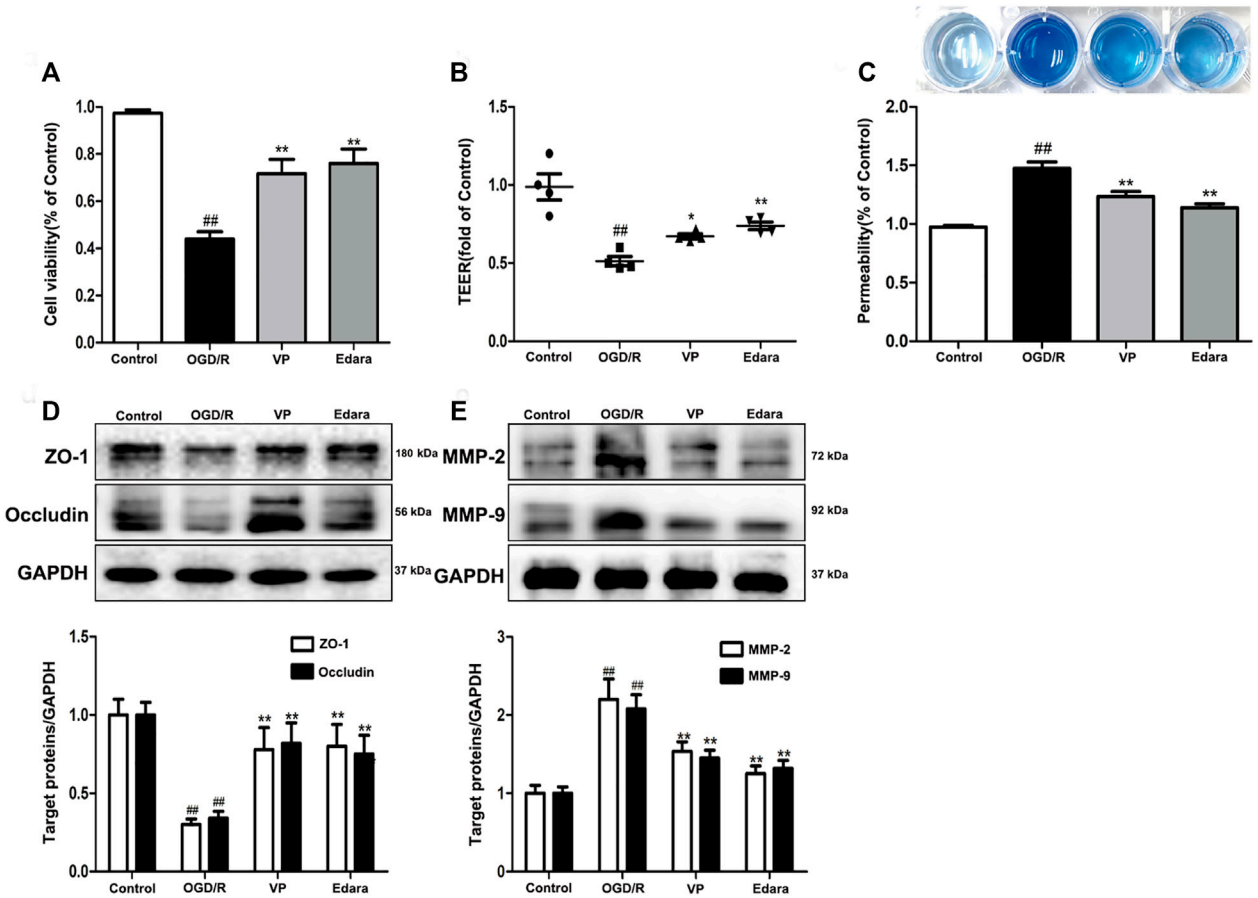

FIGURE 7 | Effects of VP treatment on endothelial barrier injuries induced by OGD/R. bEnd.3 cells were treated with VP (1 μM) and subsequently exposed to 6 h of OGD and 6 h of reoxygenation. **(A)** The protective effect of VP in endothelial cells was detected by MTT assays. **(B)** and **(C)** The protective effect of VP on the endothelial cell barrier was detected using TEER and EB assays. **(D)** Representative western blots and quantitative analyses showing ZO-1 and occludin expression levels. **(E)** Representative western blots and quantitative analyses of MMP-2 and MMP-9 expression levels. Data are expressed as the mean ± SD, $n = 3$. $^{\#\#}p < 0.01$ *vs*. Control group, $^{**}p < 0.01$ *vs*. OGD/R group.

protease and signaling pathways. Cytoskeletal alterations cause EC contraction and the disassembly of TJs through junctional-accessory proteins (for example, ZO-1, occludin). The disassembly and redistribution of TJs result in subtle BBB hyperpermeability, inducing the extravasation of fluid and small macromolecules from the blood to the central nervous system. The weakened barrier becomes more vulnerable to the MMP-2/9-mediated degradation of TJs, further damaging the BBB and permitting the eventual leakage of large macromolecules Shi et al. (2016). *In vivo*, EB staining is often used to evaluate the degree of BBB damage (Nishiyama et al., 2008). VP treatment in MCAO/R model mice was able to significantly decrease EB leakage and MMP2/9 expression levels and increase the expression levels of ZO-1 and occludin compared with untreated MCAO/R model mice (**Figure 4**). *In vitro*, VP remarkably alleviated OGD/R-induced endothelial-barrier injury, mitigated bEnd.3 cell leakage, and inhibited the degradation of TJ proteins (**Figure 7**) in OGD/R exposed cells compared with the untreated control, indicating the protective effects of VP against I/R-induced CEB damage. Meanwhile, bEnd.3 cells transfected with YAP-siRNA were used to evaluate the effects of YAP on endothelial barrier integrity *in vitro*. YAP expression decreased in following siRNA interference in bEnd3 cells exposed to OGD/R (**Figure 8**). These results indicated that YAP-siRNA was able to maintain the integrity of the endothelial barrier by promoting the preservation of TJ, which further indicated that YAP is a vital target molecule for the maintenance of BBB integrity.

Cerebral ECs are key components involved in the maintenance of BBB integrity. The loss of BBB integrity is a pathophysiological hallmark of brain diseases, including Alzheimer's disease, epilepsy, and cranial trauma (Straight et al., 2003; Schmidt et al., 2014; Sharma and Goyal, 2016). Studies have reported that Hippo (MST)-YAP signaling is involved in brain vessel in various diseases, including cerebral I/R injury and subarachnoid hemorrhage, suggesting the potential for the modulation of this signaling pathway to influence the prognosis of many types of neurological disorders (Gong et al., 2019; Zhao et al., 2016; Qu et al., 2018). Future studies remain necessary to elucidate the specific roles played by this pathway in the development of these

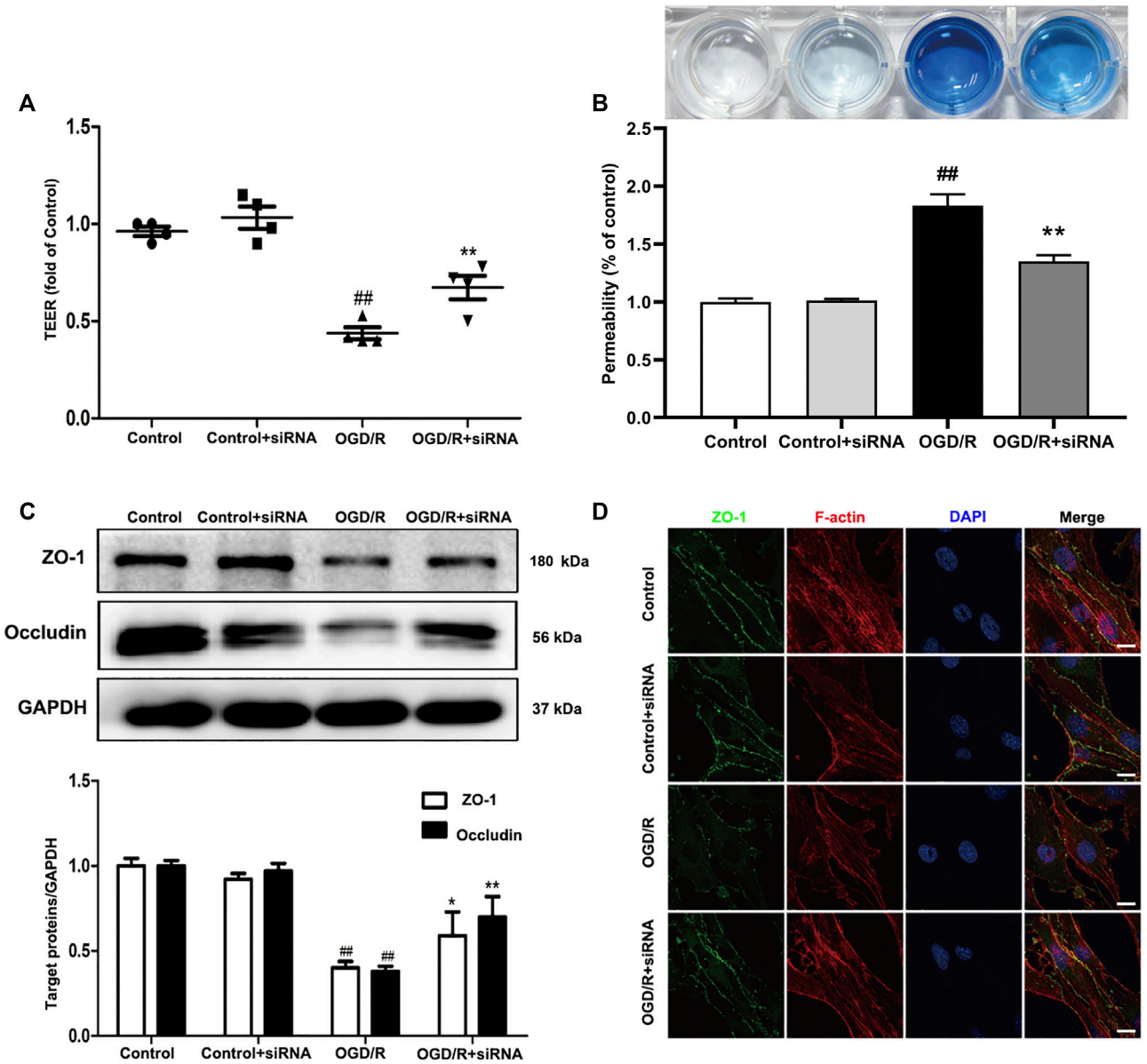

FIGURE 8 | Effects of YAP-siRNA on endothelial barrier injury induced by OGD/R. bEnd.3 cells were treated with YAP-siRNA and subsequently exposed to 6 h of OGD and 6 h of reoxygenation. **(A)** and **(B)** A barrier-protective effect for YAP-siRNA was detected using TEER and EB assays. **(C)** Representative western blots and quantitative analyses for ZO-1 and occludin expression levels. **(D)** Representative microscope images (based on immunofluorescence analyses) of ZO-1 (green), F-actin (red), and DAPI-stained nuclei (blue). Scale bar = 20 μm. Data are expressed as the mean ± SD, $n = 3$. $^{\#\#}p < 0.01$ *vs*. Control group, $^{*}p < 0.05$, $^{**}p < 0.01$ *vs*. OGD/R group.

various neurological disorders. As an essential component of this signaling pathway, YAP has been shown to be involved in several diseases, including the discord caused by viruses or bacteria (Lee et al., 2013). Our results suggested that YAP might act as a key mediator in I/R-induced CEB injury. Our findings provide broad insights into brain injury characterized by BBB hyperpermeability and indicate new therapeutic strategies for severe diseases associated with dysfunctional TJ signaling.

In summary, the inhibition of YAP expression in the nucleus beneficially antagonizes the high endothelial permeability induced by cerebral I/R injury, both *in vivo* and *in vitro*. As a regulatory molecule, YAP contributes to the maintenance of CEB integrity (**Figure 9**). Taken together, our findings extend the current understanding of the regulatory mechanisms associated with TJ function and present potential novel targets for the development of efficacious drugs that may prevent and treat damage associated with ischemic stroke and other related diseases.

In conclusion, we clarified a key role for YAP in BBB maintenance during stroke. YAP could represent a potential target in ECs for pharmacotherapeutic interventions designed

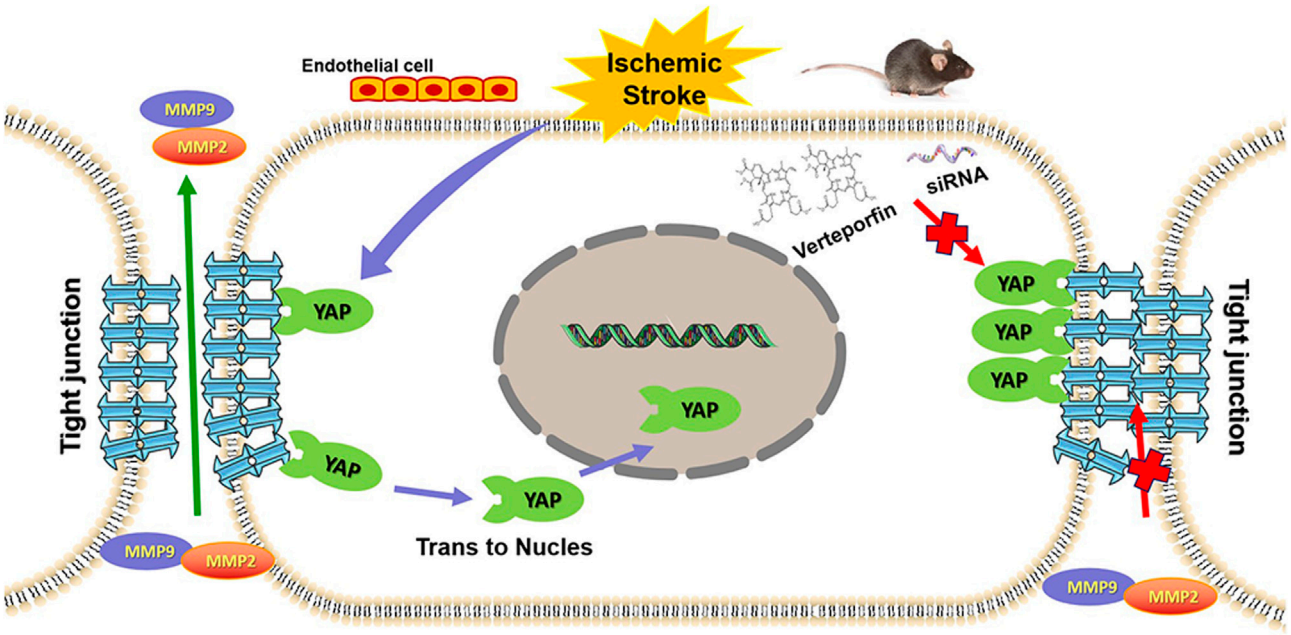

FIGURE 9 | Graphic abstract depicting the role played by YAP to protect against BBB disruption in cerebral ischemia-reperfusion injury.

to protect the BBB. Our data revealed new opportunities for the prevention of brain damage aggravation following ischemic stroke.

DATA AVAILABILITY STATEMENT

The original contributions presented in the study are included in the article/**Supplementary Material**, further inquiries can be directed to the corresponding authors.

ETHICS STATEMENT

The animal study was reviewed and approved by The Animal Ethics Committee of China Pharmaceutical University.

AUTHOR CONTRIBUTIONS

SG and JK conceived this project and designed the experiments. SG performed most experiments and interpreted the data. JH and FZ performed some of the *in vitro* experiments. YZ and HM performed some of the *in vivo* experiments. JK and BY conceived this project. SG and HM wrote the manuscript. JK and FL revised the manuscript.

FUNDING

This research was supported by the National Natural Science Foundation of China (No. 82074058, No. 82104438, No. 82104437), Project funded by China Postdoctoral Science Foundation (No. 2021M693518, No. 2021M693519), Natural Science Foundation of Jiangsu Province (No. SBK2021043206, No. SBK20210431), the National Science Foundation for the third batch of special funding for postdoctoral fellows (No. 2021TQ0367), and supported by "Double First-Class" University Project (CPU2018GF07).

ACKNOWLEDGMENTS

The authors thank the staff of the Key Laboratory of Natural Products, Jiangsu Key Laboratory of TCM Evaluation and Translational Research, China Pharmaceutical University for their valuable support.

SUPPLEMENTARY MATERIAL

The Supplementary Material for this article can be found online at: https://www.frontiersin.org/articles/10.3389/fphar.2021.777680/full#supplementary-material

REFERENCES

Armulik, A., Genové, G., Mäe, M., Nisancioglu, M. H., Wallgard, E., Niaudet, C., et al. (2010). Pericytes Regulate the Blood-Brain Barrier. *Nature* 468, 557–561. doi:10.1038/nature09522

Bao, X. M., He, Q., Wang, Y., Huang, Z. H., and Yuan, Z. Q. (2017). The Roles and Mechanisms of the Hippo/YAP Signaling Pathway in the Nervous System. *Hereditas* 39, 630–641.

Brodowska, K., Al-Moujahed, A., Marmalidou, A., Meyer Zu Horste, M., Cichy, J., Miller, J. W., et al. (2014). The Clinically Used Photosensitizer Verteporfin (VP) Inhibits YAP-TEAD and Human Retinoblastoma Cell Growth *In Vitro* without Light Activation. *Exp. Eye Res.* 124, 67–73. doi:10.1016/j.exer.2014.04.011

Cao, G. S., Chen, H. L., Zhang, Y. Y., Li, F., Liu, C. H., Xiang, X., et al. (2016). YiQiFuMai Powder Injection Ameliorates the Oxygen-Glucose Deprivation-Induced Brain Microvascular Endothelial Barrier Dysfunction Associated with the NF-κB and ROCK1/MLC Signaling Pathways. *J. Ethnopharmacol.* 183, 18–28.

Campbell, H. K., Maiers, J. L., and Demali, K. A. (2017). Interplay between Tight Junctions & Adherens Junctions. *Exp. Cel Res* 358, 39–44. doi:10.1016/j.yexcr.2017.03.061

Choi, H. J., and Kwon, Y. G. (2015). Roles of YAP in Mediating Endothelial Cell Junctional Stability and Vascular Remodeling. *BMB Rep.* 48, 429–430. doi:10.5483/bmbrep.2015.48.8.146

Dieterich, P., Odenthal-Schnittler, M., Mrowietz, C., Krämer, M., Sasse, L., Oberleithner, H., et al. (2000). Quantitative Morphodynamics of Endothelial Cells within Confluent Cultures in Response to Fluid Shear Stress. *Biophys. J.* 79, 1285–1297. doi:10.1016/S0006-3495(00)76382-X

Feigin, V. L., Feigin, V. L., Nguyen, G., Cercy, K., Johnson, C. O., Alam, T., et al. (2018). Global, Regional, and Country-specific Lifetime Risks of Stroke, 1990 and 2016. *N. Engl. J. Med.* 379, 2429–2437. doi:10.1056/NEJMoa1804492

Fernández-Klett, F., Potas, J. R., Hilpert, D., Blazej, K., Radke, J., Huck, J., et al. (2013). Early Loss of Pericytes and Perivascular Stromal Cell-Induced Scar Formation after Stroke. *J. Cereb. Blood Flow Metab.* 33, 428–439. doi:10.1038/jcbfm.2012.187

Gong, P., Zhang, Z., Zou, C., Tian, Q., Chen, X., Hong, M., et al. (2019). Hippo/YAP Signaling Pathway Mitigates Blood-Brain Barrier Disruption after Cerebral Ischemia/reperfusion Injury. *Behav. Brain Res.* 356, 8–17. doi:10.1016/j.bbr.2018.08.003

Guclu, M., Demirogullari, B., Barun, S., Ozen, I. O., Karakus, S. C., Poyraz, A., et al. (2014). The Effects of Melatonin on Intestinal Adaptation in a Rat Model of Short Bowel Syndrome. *Eur. J. Pediatr. Surg.* 24, 150–157. doi:10.1055/s-0033-1343081

Guichet, P. O., Masliantsev, K., Tachon, G., Petropoulos, C., Godet, J., Larrieu, D., et al. (2018). Fatal Correlation Between YAP1 Expression and Glioma Aggressiveness: Clinical and Molecular Evidence. *J. Pathol.* 246, 205–216.

Halder, G., and Johnson, R. L. (2011). Hippo Signaling: Growth Control and beyond. *Development* 138, 9–22. doi:10.1242/dev.045500

Hall, C. N., Reynell, C., Gesslein, B., Hamilton, N. B., Mishra, A., Sutherland, B. A., et al. (2014). Capillary Pericytes Regulate Cerebral Blood Flow in Health and Disease. *Nature* 508, 55–60. doi:10.1038/nature13165

Jin, J., Zhao, X., Fu, H., and Gao, Y. (2020). The Effects of YAP and its Related Mechanisms in central Nervous System Diseases. *Front. Neurosci.* 14, 595. doi:10.3389/fnins.2020.00595

Lallukka, T., Ervasti, J., Lundström, E., Mittendorfer-Rutz, E., Friberg, E., Virtanen, M., et al. (2018). Trends in Diagnosis-specific Work Disability before and after Stroke: A Longitudinal Population-Based Study in Sweden. *J. Am. Heart Assoc.* 7, e006991. doi:10.1161/JAHA.117.006991

Lee, J. E., Jeon, I. S., Han, N. E., Song, H. J., Kim, E. G., Choi, J. W., et al. (2013). Ubiquilin 1 Interacts with Orai1 to Regulate Calcium Mobilization. *Mol. Cell* 35, 41–46. doi:10.1007/s10059-013-2268-7

Lin, K. C., Moroishi, T., Meng, Z., Jeong, H. S., Plouffe, S. W., Sekido, Y., et al. (2017). Regulation of Hippo Pathway Transcription Factor TEAD by P38 MAPK-Induced Cytoplasmic Translocation. *Nat. Cel Biol* 19, 996–1002. doi:10.1038/ncb3581

Liu-Chittenden, Y., Huang, B., Shim, J. S., Chen, Q., Lee, S. J., Anders, R. A., et al. (2012). Genetic and Pharmacological Disruption of the TEAD-YAP Complex Suppresses the Oncogenic Activity of YAP. *Genes Dev.* 26, 1300–1305. doi:10.1101/gad.192856.112

Lochhead, J. J., Ronaldson, P. T., and Davis, T. P. (2017). Hypoxic Stress and Inflammatory Pain Disrupt Blood-Brain Barrier Tight Junctions: Implications for Drug Delivery to the central Nervous System. *Aaps J.* 19, 910–920. doi:10.1208/s12248-017-0076-6

Moskowitz, M. A., Lo, E. H., and Iadecola, C. (2010). The Science of Stroke: Mechanisms in Search of Treatments. *Neuron* 67, 181–198. doi:10.1016/j.neuron.2010.07.002

Nagasawa-Masuda, A., and Terai, K. (2017). Yap/Taz Transcriptional Activity Is Essential for Vascular Regression via Ctgf Expression and Actin Polymerization. *PLoS One* 12, e0174633. doi:10.1371/journal.pone.0174633

Nishiyama, Y., Akaishi, J., Katsumata, T., Katsura, K., and Katayama, Y. (2008). Cerebral Infarction in a Patient with Macrothrombocytopenia with Leukocyte Inclusions (MTCP, May-Hegglin Anomaly/Sebastian Syndrome). *J. Nippon Med. Sch.* 75, 228–232. doi:10.1272/jnms.75.228

Ouyang, T., Meng, W., Li, M., Hong, T., and Zhang, N. (2020). Recent Advances of the Hippo/YAP Signaling Pathway in Brain Development and Glioma. *Cell. Mol. Neurobiol.* 40, 495–510.

Özen, I., Roth, M., Barbariga, M., Gaceb, A., Deierborg, T., Genové, G., et al. (2018). Loss of Regulator of G-Protein Signaling 5 Leads to Neurovascular protection in Stroke. *Stroke* 49, 2182–2190. doi:10.1161/STROKEAHA.118.020124

Qu, J., Zhao, H. L., Li, Q., Pan, P. Y., Ma, K., Liu, X., et al. (2018). MST1 Suppression Reduces Early Brain Injury by Inhibiting the NF-κB/MMP-9 Pathway After Subarachnoid Hemorrhage in Mice. *Behav. Neurol.* 2018, 6470957.

Schmidt, S., Liu, G., Liu, G., Yang, W., Honisch, S., Pantelakos, S., et al. (2014). Enhanced Orai1 and STIM1 Expression as Well as Store Operated Ca2+ Entry in Therapy Resistant Ovary Carcinoma Cells. *Oncotarget* 5, 4799–4810. doi:10.18632/oncotarget.2035

Sharma, A., and Goyal, R. (2016). Experimental Brain Ischemic Preconditioning: A Concept to Putative Targets. *CNS Neurol. Disord. Drug Targets* 15, 489–495. doi:10.2174/1871527314666150821112228

Shi, Y. J., Zhang, L. L., Pu, H. J., Mao, L. L., Hu, X. M., Jiang, X. Y., et al. (2016). Rapid Endothelial Cytoskeletal Reorganization Enables Early Blood-Brain Barrier Disruption and Long-Term Ischaemic Reperfusion Brain Injury. *Nat. Commun.* 7, 10523.

Straight, A. F., Cheung, A., Limouze, J., Chen, I., Westwood, N. J., Sellers, J. R., et al. (2003). Dissecting Temporal and Spatial Control of Cytokinesis with a Myosin II Inhibitor. *Science* 299, 1743–1747. doi:10.1126/science.1081412

Sweeney, M. D., Zhao, Z., Montagne, A., Nelson, A. R., and Zlokovic, B. V. (2019). Blood-Brain Barrier: From Physiology to Disease and Back. *Physiol. Rev.* 99, 21–78. doi:10.1152/physrev.00050.2017

Szymaniak, A. D., Mahoney, J. E., Cardoso, W. V., and Varelas, X. (2015). Crumbs3-mediated Polarity Directs Airway Epithelial Cell Fate through the Hippo Pathway Effector Yap. *Dev. Cel* 34, 283–296. doi:10.1016/j.devcel.2015.06.020

Tsubokawa, T., Jadhav, V., Solaroglu, I., Shiokawa, Y., Konishi, Y., Zhang, J. H., et al. (2007). Lecithinized Superoxide Dismutase Improves Outcomes and Attenuates Focal Cerebral Ischemic Injury via Antiapoptotic Mechanisms in Rats. *Stroke* 38, 1057–1062.

Varelas, X. (2014). The Hippo Pathway Effectors TAZ and YAP in Development, Homeostasis and Disease. *Development* 141, 1614–1626. doi:10.1242/dev.102376

Wu, K. W., Lv, L. L., Lei, Y., Qian, C., and Sun, F. Y. (2019). Endothelial Cells Promote Excitatory Synaptogenesis and Improve Ischemia-Induced Motor Deficits in Neonatal Mice. *Neurobiol. Dis.* 121, 230–239.

Zhao, S. Q., Yin, J., Zhou, L. J., Yan, F., He, Q., Huang, L., et al. (2016). Hippo/MST1 Signaling Mediates Microglial Activation Following Acute Cerebral Ischemia-Reperfusion Injury. *Brain Behav. Immun.* 55, 236–248.

Conflict of Interest: The authors declare that the research was conducted in the absence of any commercial or financial relationships that could be construed as a potential conflict of interest.

Publisher's Note: All claims expressed in this article are solely those of the authors and do not necessarily represent those of their affiliated organizations, or those of the publisher, the editors and the reviewers. Any product that may be evaluated in this article, or claim that may be made by its manufacturer, is not guaranteed or endorsed by the publisher.

frontiers in Pharmacology

ORIGINAL RESEARCH
published: 03 December 2021
doi: 10.3389/fphar.2021.792136

Ginkgolide With Intravenous Alteplase Thrombolysis in Acute Ischemic Stroke Improving Neurological Function: A Multicenter, Cluster-Randomized Trial (GIANT)

Xuting Zhang[1†], Wansi Zhong[1†], Xiaodong Ma[2], Xiaoling Zhang[3], Hongfang Chen[4], Zhimin Wang[5], Min Lou[1] and GIANT Investigators*

[1]Department of Neurology, The Second Affiliated Hospital of Zhejiang University, School of Medicine, Hangzhou, China, [2]Department of Neurology, Haiyan People's Hospital, Jiaxing, China, [3]Department of Neurology, The Second Affiliated Hospital of Jiaxing University, Jiaxing, China, [4]Department of Neurology, Affiliated Jinhua Hospital, Zhejiang University School of Medicine, Jinhua, China, [5]Department of Neurology, The First People's Hospital of Taizhou, Taizhou, China

OPEN ACCESS

Edited by:
Yongjun Sun,
Hebei University of Science and Technology, China

Reviewed by:
Wenbo Zhao,
Capital Medical University, China
Jie Chen,
Army Medical University, China
Miao Chen,
University of Shanghai for Science and Technology, China

***Correspondence:**
Min Lou
lm99@zju.edu.cn

[†]These authors have contributed equally to this work

Specialty section:
This article was submitted to Neuropharmacology, a section of the journal Frontiers in Pharmacology

Received: 09 October 2021
Accepted: 04 November 2021
Published: 03 December 2021

Citation:
Zhang X, Zhong W, Ma X, Zhang X, Chen H, Wang Z, Lou M and GIANT Investigators (2021) Ginkgolide With Intravenous Alteplase Thrombolysis in Acute Ischemic Stroke Improving Neurological Function: A Multicenter, Cluster-Randomized Trial (GIANT). Front. Pharmacol. 12:792136. doi: 10.3389/fphar.2021.792136

Background and Purpose: We aimed to investigate the effect of Ginkgolide® treatment on neurological function in patients receiving intravenous (IV) recombinant tissue plasminogen activator (rt-PA).

Methods: This cluster randomized controlled trial included acute ischemic stroke patients in 24 centers randomized to intervention of intravenous Ginkgolide® or control group within the first 24 h after IV rt-PA therapy (IVT). Clinical outcome at 90 days was assessed with modified Rankin Scale (mRS) score and dichotomized into good outcome (0–2) and poor outcome (3–6). Hemorrhagic transformation represented the conversion of a bland infarction into an area of hemorrhage by computed tomography. Symptomatic intracerebral hemorrhage (sICH) was defined as cerebral hemorrhagic transformation in combination with clinical deterioration of National Institutes of Health Stroke Scale (NIHSS) score ≥4 points at 7-day or if the hemorrhage was likely to be the cause of the clinical deterioration. We performed logistic regression analysis and propensity score matching analysis to investigate the impact of Ginkgolide® treatment with IV rt-PA on good outcome, hemorrhagic transformation and sICH, respectively.

Results: A total of 1113 patients were finally included and 513 (46.1%) were in the intervention group. Patients in the Ginkgolide® group were more likely to have good outcomes (78.6 vs. 66.7%, $p < 0.01$) and lower rate of sICH (0 vs. 2.72%, $p < 0.01$), compared with patients in the control group. The intra-cluster correlation coefficient (ICC) for good outcome at 90 days was 0.033. Binary logistic regression analysis revealed that

Abbreviations: AIS, acute ischemic stroke; BBB, blood brain barrier permeability; CI, confidence intervals; DNA, deoxyribonucleic acid; ENI, early neurological improvement; ER, endoplasmic reticulum; HI, hemorrhagic infarction; ICC, intra-cluster correlation coefficient; IVT, intravenous thrombolysis; IQR, interquartile range; MCAO, middle cerebral artery occlusion; mRS, modified Rankin scale; NIHSS, National Institute of Health Stroke Scale; ONT, onset to reperfusion therapy; OR, odds ratios; PH, parenchymal hemorrhage; PPS, per-protocol set; PAF, platelet-activating factor; rt-PA, recombinant tissue plasminogen activator; SOD, superoxide dismutase; sICH, symptomatic intracranial hemorrhage.

treatment with Ginkgolide® was independently associated with 90-day mRS in patients with IV rt-PA therapy (OR 1.498; 95% CI 1.006–2.029, $p = 0.009$). After propensity score matching, conditional logistic regression showed intervention with Ginkgolide® was significantly associated with 90-day good outcome (OR 1.513; 95% CI 1.073–2.132, $p = 0.018$). No significant difference in hemorrhage transformation was seen between the 2 matched cohorts (OR 0.885; 95% CI 0.450–1.741, $p = 0.724$).

Conclusion: Using Ginkgolide® within 24-hour after IV rt-PA is effective and safe and might be recommended in combination with rtPA therapy in acute ischemic stroke.

Clinical Trial Registration: http://www.clinicaltrials.gov, identifier NCT03772847.

Keywords: Ginkgolide®, stroke, intravenous alteplase, prognosis, improve

INTRODUCTION

Intravenous recombinant tissue plasminogen activator (rt-PA) administered within 4.5 h of onset (or later if a favorable perfusion imaging profile is present) could improve neurological outcome in patients with acute ischemic stroke (AIS). Treatments for AIS continue to evolve after the superior value of endovascular thrombectomy was confirmed over systemic thrombolysis. Unfortunately, up to 50% of such patients with successful recanalization still have an unfavorable outcome (Hussein et al., 2018), and numerous neuroprotective drugs have failed to show benefit in the treatment of AIS (Zhao et al., 2020). New methods to enhance the general efficacy of intravenous thrombolysis (IVT) are imperative in patients with AIS (Knecht et al., 2018).

The core problem in acute stroke is the loss of neuronal cells which makes recovery difficult or even not possible in the late states. Several key players in neuronal cell death within the penumbra have been identified, including excitotoxicity, oxidative stress, and inflammation. Oxidative stress directly leads to DNA damage that occurs within minutes after cerebral ischemic strokes (Li et al., 2018). Reperfusion therapy accompanying re-entry of oxygen and glucose into the ischemic brain fuels an excess production of reactive oxygen species (ROS) that overwhelms endogenous antioxidant reserves and leads to reperfusion injury. Researchers observed that cerebral ROS generation peaked 1 day after transient middle cerebral artery occlusion (MCAO) in mice, coinciding with an increase in Nrf2, a transcription factor that regulates antioxidant enzymes (Takagi et al., 2014; Yumiko et al., 2017).

Ginkgo biloba leaves extracts can protect against neuronal death caused by ischemia in animal stroke models (Feng et al., 2019). These pharmacological effects are attributed to two major groups of chemical constituents, namely, flavonoids and terpene lactones. Terpene lactones includes ginkgolides A, B, and C, and bilobalide, which are the main components of Ginkgolides®. In MCAO rats, ginkgolides B treatment could significantly increase the expressions of anti-oxidative stress-related proteins, including superoxide dismutase (SOD). Diterpene ginkgolides (ginkgolide A, ginkgolide B and ginkgolide C) were reported to activate Akt signaling and lead to the nuclear location of Nrf2, which has protective effects against oxidative stress (Liu et al., 2019). Furthermore, in Sprague daw rats with MCAO, pretreatment with bilobalide improved neurological function and increased SOD activity while decreasing infarct volume and brain edema (Jiang et al., 2014).

The immune-mediated inflammatory response that follows AIS is a therapeutic target under current investigation. Previous studies have shown that ginkgolides can reduce inflammation, ameliorate the metabolic disturbances caused by rt-PA. A derivate of ginkgolide B named XQ-1H, suppressed neutrophils infiltration and inflammatory mediators, including matrix metalloproterinase-9 in the ischemic region of the brain (Fang et al., 2015). Down-regulated matrix metalloproterinase-9 expression could reduce extracellular matrix degradation and protect blood brain barrier permeability (BBB) via tight junction in brain endothelial cells (Wei et al., 2013). Finally, pre-administration of XQ-1H reduced cerebral infarct size and diminished brain edema after stroke in rats.

Ginkgolide was found to be specific and selective antagonist of platelet activating factor (PAF) (Koch, 2005), which was involved in thrombosis for strong platelet aggregation. Thus, Ginkgolide may enhance the general efficacy of IVT through its antioxidation, anti-inflammatory and antithrombotic mechanisms. But so far, there is no large-scale clinical trial to confirm the general efficacy of Ginkgolide® in AIS with IVT therapy. Moreover, whether Ginkgolide can increase the risk of hemorrhagic transformation after intravenous thrombolysis in AIS patients is unclear. Thus, we aimed to determine the clinical efficacy and safety of Ginkgolide® combined with IV rt-PA in AIS.

METHODS

Study Design and Participants

GIANT was an open label, prospective, multicenter cluster-randomized clinical trial involving 24 hospitals in China (NCT03772847). We enrolled patients who 1) were 18 years or older; 2) were AIS patients who met the criteria of IVT (William et al., 2019); 3) or his/her family member signed an informed consent. We excluded patients who 1) were diagnosed as cerebral arteritis; 2) with baseline alanine aminotransferase or aspartate aminotransferase ≥3 times the upper limit of normal, or baseline serum creatinine ≥1.5 times the upper limit of

normal; 3) were allergic to ginkgo drugs, alcohol or glycerol; 4) participated in other clinical trials. The criteria for intravenous thrombolysis was as follows: 1) Inclusion criteria:Clinical diagnosis of ischemic stroke causing measurable neurologic deficit; Onset of symptoms <4.5 h before beginning treatment; Age ≥18 years; 2) Exclusion criteria: Ischemic stroke or severe head trauma in the previous 3 months; Previous intracranial hemorrhage; Intra-axial intracranial neoplasm; Gastrointestinal malignancy; Gastrointestinal/ Urinary hemorrhage in the previous 21 days; Major surgery in the preceding 14 days; Had an arterial puncture of a noncompressible blood vessel in the previous 7 days; Intracranial or intraspinal surgery within the prior 3 months; Symptoms suggestive of subarachnoid hemorrhage; Persistent blood pressure elevation (systolic ≥185 mmHg or diastolic ≥110 mmHg); Glucose levels <50 or >400 mg/dl; Active internal bleeding; Presentation consistent with infective endocarditis; Stroke known or suspected to be associated with aortic arch dissection; Acute bleeding diathesis; Platelet count <100,000/mm^3; Current anticoagulant use with an INR >1.7 or PT > 15 s or aPTT >40 s; Therapeutic doses of low molecular weight heparin received within 24 h; Current use of a direct thrombin inhibitor or direct factor Xa inhibitor with evidence of anticoagulant effect by laboratory tests such as aPTT, INR, ECT, TT, or appropriate factor Xa activity assays; Evidence of hemorrhage; Extensive regions of obvious hypodensity consistent with irreversible injury.

The human ethics committee of the Second Affiliated Hospital of Zhejiang University (SAHZU), School of Medicine, approved the trial protocol. The clinical trial was conducted according to the principle expressed in the Declaration of Helsinki. Written consent was obtained from patients or their relatives.

Randomization

The randomization was conducted by using a computer generating randomization sequence where twenty-four hospitals were assigned to the Ginkgolide intervention or control group randomly. Data on all thrombolytic patients in both groups were consecutively recorded in a secure, purpose-built web-based data entry system.

Interventions

Patients in hospitals which were allocated to the treatment arm received rt-PA (0.9 mg/kg) and an intravenous infusion of Ginkgolide® (10 ml dissolved in a vehicle containing 250 ml normal saline, once a day, continuous intravenous injection for at least 7 days). The recommended course of treatment is 14 days, so our study requires the intervention group to take medication for at least 7 days. Ginkgolide® was infused intravenously within 24 h after the initiation of alteplase, and the researcher should record the time from thrombolysis to Ginkgolide® use. Patients in hospital which were allocated to the control arm received rt-PA and 250 ml normal saline combined standard-of-care therapy following current clinical guidelines. Patients were followed at 7 and 90 days.

Ginkgolide® was obtained from Chengdu Baiyu Pharmaceutical Company Limited (each 2 ml per vial, containing terpene lactone 10 mg, batch: No.13110002). Intravenous rt-PA treatment was initiated at a standard dose and regimen (0.9 mg/kg, initial bolus of 10% of the final dose and the remaining dose as an intravenous infusion lasting 60 min) following current clinical guidelines. When a patient met all the inclusion/exclusion criteria and signed the informed consent, Ginkgolide® infusion was initiated within 24 h after starting the infusion of rt-PA treatment.

Outcome Measures

The primary outcome was the proportion of patients with modified Rankin scale (mRS) ≤2 at 90 days. A structured modified Rankin Score at 90 days of AIS patients was followed up with telephone questionnaires by external clinical evaluators who were blinded to the patients' clinical data. The telephone questionnaire had been validated and was used in previous trial (Collaboration, 2019). The process of telephone assessment was recorded and could be reviewed at any time. Secondary outcomes included National Institute of Health Stroke Scale (NIHSS) scores at 24 h; early neurological improvement (ENI), which was defined as (baseline NIHSS—NIHSS at 7 days)/baseline NIHSS*100%≥18% at 7 days. NIHSS scores were performed by staffs who were not aware of treatment allocation. The mRS scale at 90 days was also followed up with telephone questionnaires by external clinical evaluators who were blinded to the patients' clinical data. The safety outcomes included any intracranial hemorrhage transformation and symptomatic intracranial hemorrhage on the 7-day follow-up. CT scan was performed within 24 h and on 7 ± 1th day after thrombolysis for assessment of hemorrhage, and additional images might be performed in the case of clinical worsening or at the discretion of the treating physicians. Hemorrhagic transformation was classified into hemorrhagic infarction (HI) and parenchymal hemorrhage (PH). An intracerebral hemorrhage was defined as symptomatic intracranial hemorrhage (sICH) if the patient had clinical deterioration causing an increase of NIHSS ≥4 points and if the hemorrhage was likely to be the cause of the clinical deterioration (Hacke et al., 1998).

Sample Size

A pre-randomization survey at participating clusters was conducted. According to previous study, the neurological prognosis was increased 21.1% after the treatment of Ginkgolide. Therefore, a total of 894 patients at 14 hospitals (considering a median of 80 AIS patients treated with rt-PA per hospital) would be required to detect a 21% improvement in AIS patients treated with Ginkgolide combined rt-PA (Yuan and Guo, 2017), with 90% power, 5% significance level, and an intra-cluster correlation coefficient (ICC) of 0.05. Taking into account an estimated 20% rate of non-assessable patients, each arm was required to enroll 560 patients. The sample size calculation formula is as follows (Nijders and Bosker, 1999):

$$N = \left(Z_{1-\alpha/2} + Z_{1-\beta}\right)^2 * [p1(1-p1) + p0(1-p0)] \\ [1 + (nj-1)\rho I]/(p1-p0)^2$$

Z 1-α/2 and Z1-β: Z statistic of type I errors and type II errors; p1: Hypothetical rate of primary outcome in the intervention

group; p0: Hypothetical rate of primary outcome in the control group; nj: the median number of AIS patients treated with rt-PA per hospital; ρI: intra-cluster correlation coefficient.

Statistical Analysis

We retrieved demographic and clinical data, the vascular risk factors, time interval from stroke onset to reperfusion therapy (ONT), baseline NIHSS, 24-hour NIHSS and 7-day NIHSS. Clinical outcome at 90 days was assessed with mRS score and dichotomized into good outcome (0–2) and poor outcome (3–6).

Full analysis set analyses were conducted. Per-protocol set (PPS) analyses were conducted: for these analyses we only included completers who received therapy at least 7 days and didn't experience PH transformation within 24 h after thrombolysis. Our data analyses focused on the predefined primary and secondary outcomes of the trial in our pre-registration (NCT03772847). Fisher's exact test was used to compare the dichotomous variables between groups, while independent samples two-tailed *t*-test or Mann-Whitney U test was used for the continuous variables, depending on the normality of the distribution. Intra-cluster correlation coefficients (ICC) were calculated using the correlation-based estimation methods for categorical outcomes. To statistically analyze whether there were differences in primary/secondary outcome and safety outcomes between two groups, binary logistic regression analysis was conducted.

Since several baseline factors showed significant differences, we further created a cohort at a 1:1 ratio using propensity score-matching techniques. The use of propensity score analyses balanced the distribution of covariates between treatment and control groups and therefore minimized the influence of potential bias. The resulting propensity score for the treatment of Ginkgolide® included the following 6 variables: age, sex, baseline NIHSS, history of smoking, hypertension, atrial fibrillation. An additional conditional logistic regression was done for primary outcome and safety outcomes by adjusting baseline NIHSS. Odds ratios (OR), 95% confidence intervals (CI), and p values were calculated. All tests were two-sided, and statistical significance was set at a probability value of <0.05. All statistical analyses were performed with SPSS 20.0, SAS 9.4 and R 4.0.1 package.

RESULTS

Hospital and Patients' Characteristics

Twenty-four hospitals were involved in the trial, but 4 hospitals in control group withdrew at the beginning of the study period. 1189 patients fulfilled the inclusion/exclusion criterion. We excluded 29 patients in the control group and 5 patients in the intervention group because of PH transformation within 24-hour after IV alteplase. We excluded 42 patients in the intervention group because they did not receive treatment for at least 7 days. Finally, 1113 patients were enrolled in the PPS analysis. Of these, 513 were in the intervention group and 600 were in the control group. Study design and timeframe including number of enrolled cases are provided in **Figure 1**.

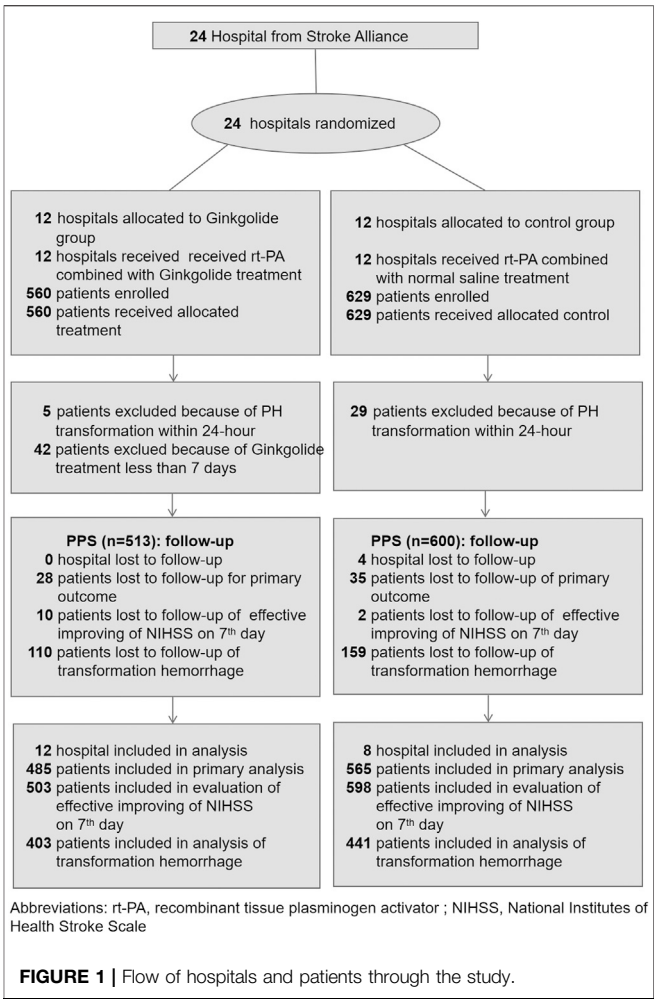

FIGURE 1 | Flow of hospitals and patients through the study.

The median age was 69 years (mean 69 ± 12 years, range 60–78 years), 452 (40.6%) patients were women. The median baseline NIHSS score was 5 (IQR 3–10). The median onset to IVT was 153 min (IQR 108–203 min). The median time from thrombolysis to Ginkgolide use was 115 min (IQR 15–961 min). A total of 758/1050 (72.2%) patients experienced good outcome. Good outcome was achieved in 78.6% patients in the Ginkgolide group and 66.7% in the control group. Follow-up scans after treatment revealed hemorrhage transformation in 66/844 (7.8%) patients, and sICH was observed in 12/844 (1.4%) patients. Baseline characteristics are shown in **Table 1**. Results of full analysis set analysis are shown in **Supplementary Tables S1, S2**.

Unmatched Analysis

As **Table 1** shows, patients in the Ginkgolide® group had higher rates of smoking (37.2 vs. 30.3%, $p = 0.015$) and hypertension (68.4 vs. 60.8%, $p < 0.01$) than patients in the control group. However, the intervention group had lower baseline NIHSS (5 (2–9) vs. 5 (3–12), $p < 0.001$) and lower rates of atrial fibrillation (16.2 vs. 21.0%, $p = 0.04$). There were no significant differences in other variables. Patients in the Ginkgolide® group were more likely to have good outcomes (78.6 vs. 66.7%, $p < 0.01$) and lower

TABLE 1 | Univariate comparison of characteristics stratified by intervention in unmatched and propensity-matched patients.

	Unmatched		*p* Value	Propensity-matched[a]		*p* Value
	Ginkgolide *n* = 513	Control *n* = 600		Ginkgolide *n* = 404	Control *n* = 404	
Age (year)	67 ± 12	69 ± 13	0.074	68 ± 12	68 ± 12	0.528
Female, n (%)	208 (40.5%)	244 (40.7%)	0.967	252 (62.4%)	240 (59.4%)	0.428
Smoking, n (%)	191 (37.2%)	182 (30.3%)	0.015	153 (37.9%)	143 (35.4%)	0.511
Hypertension, n (%)	351 (68.4%)	365 (60.8%)	0.008	264 (25.3%)	262 (64.9%)	0.941
Diabetes mellitus, n (%)	88 (17.1%)	86 (14.3%)	0.196	65 (16.1%)	65 (16.1%)	1.000
Atrial fibrillation, n (%)	83 (16.2%)	126 (21.0%)	0.040	66 (16.3%)	67 (16.6%)	1.000
Baseline NIHSS	5 (2–9)	5 (3–12)	<0.001	5 (3–9)	4 (2–9)	0.292
24-hour NIHSS	3 (1–6)	4 (1–9)	<0.001	2 (1–5)	3 (1–6)	0.485
Onset-to-needle time (min)	150 (100–205)	156 (112–203)	0.121	148 (98–203)	158 (115–204)	0.280

[a]*This cohot was created at a 1:1 ratio using propensity score-matching techniques for primary outcome of "good outcome at 90 days".*

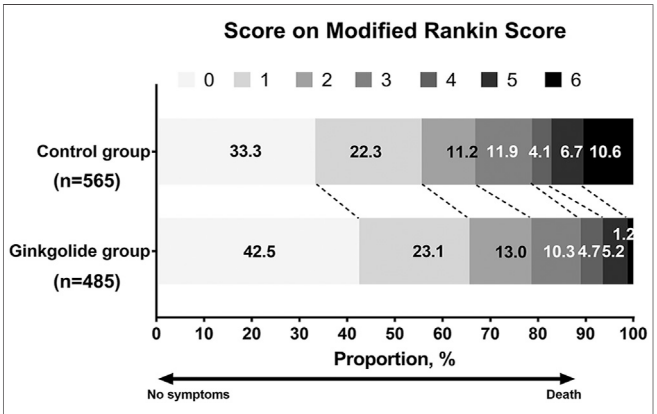

FIGURE 2 | Distribution of Modified Rankin Scores at 90 days Among Eligible Patients with Ginkgolide intervention vs. Control Group.

rate of sICH (0 vs. 2.72%, $p < 0.01$), compared with patients in the control group. **Figure 2** shows the distribution of mRS values at 90 days. Patients in the Ginkgolide® group were more likely to have early neurological improvement (intervention vs control: 74.0 vs 67.7%, $p = 0.02$). As **Table 2** shows, binary logistic regression analysis revealed that the usage of Ginkgolide® was independently associated with good outcome (OR 1.498; 95% CI 1.006–2.029, $p = 0.009$) and early neurological improvement (OR 1.395; 95% CI 1.068–1.814, $p = 0.014$). The usage of Ginkgolide® was also not associated with hemorrhage transformation (OR 0.708; 95% CI 0.412–1.218, $p = 0.212$).

Propensity-Matched Analysis

Propensity score analysis, balanced for age, gender, baseline NIHSS, history of smoking, hypertension, diabetes mellitus and atrial fibrillation, identified 404 matched patient pairs for outcome of "good outcome at 90 days." As **Table 1** shows, all baseline variables were comparable between two groups. Considering the powerful effect of baseline NIHSS on primary outcome, conditional logistic regression was done for outcomes by adjusting baseline NIHSS. Intervention with Ginkgolide® significantly associated with 90-day good outcome (OR 1.513; 95% CI 1.073–2.132, $p = 0.018$) and early neurological improvement (OR 1.574; 95% CI 1.164–2.128, $p = 0.003$) (**Table 3**). No significant difference in safety outcome of hemorrhage transformation was seen between the 2 matched cohorts (**Table 3**).

DISCUSSION

This cluster-randomized trial showed that Ginkgolide® was effective in improving neurological deficit after rtPA therapy in AIS patients. Additionally, the safety data analysis demonstrated that Ginkgolide® did not increase the incidence of hemorrhage transformation events.

Although mechanical thrombectomy has recently been established as the standard of care for selected patients with large vessel occlusions, less than 10% of all stroke patients are currently eligible for mechanical thrombectomy based on current guidelines. In this regard, intravenous thrombolysis with alteplase remains a viable treatment for the majority of AIS patients in many centers. A number of experimental studies showed the neuroprotective efficacy of Ginkgolide, which can inhibit the platelet aggregation and increase vascular recanalization in AIS patients (Feng et al., 2019; Dong et al., 2021). Ginkgolide played a role as an inhabitation of PAF receptor, which was induced by ischemic stroke (Joseph et al., 1989). The reduction in PAF and its pathway were reportedly helpful to reduce the volume of infarction in acute phase (Oberpichler et al., 1990). A recently clinical trial also confirmed that Ginkgolide helped in decreasing accumulation of PAF after ischemic stroke, which might be one of the mechanisms in reducing stroke recurrence (Dong et al., 2021). Both Ginkgo biloba extract and its constituent ginkgolide were proved effectively attenuating the rtPA-induced disturbances in neurotransmitter, amino acid, energy, lipid, and nucleotide metabolisms (Pietri et al., 1997; Huang et al., 2012; Li et al., 2013; Chen et al., 2018; Feng et al., 2019; Liu et al., 2019). Chen et al. showed that rtPA upregulated the production of glutamic acid, aspartic acid, N-acetyl-l-aspartic acid, and glutamine. Although both diterpene ginkgolide and ginkgo biloba extract ameliorated the upregulation of aspartic acid and glutamine, diterpene ginkgolide also ameliorated the upregulation of glutamic acid and N-acetyl-l-aspartic acid (Chen et al., 2018). Thus,

TABLE 2 | Neurological Outcome and Complication Among Ginkgolide intervention vs. Control Group after binary logistic regression.

Variables	ICC	Ginkgolide group, no. of events/Total patients (%)	Control group, no. of events/Total patients (%)	Odds ratio (95% CI)[a]	*p* Value
Primary outcome					
Good outcome at 90 days, No. (%)	0.033	381/485 (78.6)	377/565 (66.7)	1.498 (1.106–2.029)	0.009
Secondary outcome					
Early neurological improvement, No. (%)	0.002	372/503 (74.0%)	405/598 (67.7%)	1.392 (1.068–1.814)	0.014
Safety outcome					
sICH, No. (%)	0.031	0/403 (0%)	12/441 (2.72%)	-	-
Hemorrhage transformation, No. (%)	0.041	24/403 (6.0%)	42/441 (9.5%)	0.708 (0.412–1.218)	0.212

[a]*Adjusted for age, hypertension, atrial fibrillation, smoking and baseline NIHSS.*

TABLE 3 | Neurological Outcome and Complication Among matched cohorts between two groups after conditional logistic regression.

Variables[a]	Ginkgolide group, no. of events/Total patients (%)	Control group, no. of events/Total patients (%)	Odds ratio (95% CI)[b]	*p* Value
Primary outcome				
Good outcome at 90 days, No. (%)	311/404 (77.0)	285/404 (70.5)	1.513 (1.073,2.132)	0.018
Secondary outcome				
Early neurological improvement, No. (%) (%)	321/423 (75.9)	282/423 (66.7)	1.574 (1.164,2.128)	0.003
Safety outcome				
sICH, No. (%)	0/318 (0)	5/318 (1.6)	—	—
Hemorrhage transformation, No.(%)	18/318 (5.7)	20/318 (6.3)	0.885 (0.450,1.741)	0.724

[a]*We created different cohorts according to the specific outcome at a 1:1 ratio using propensity score-matching techniques.*
[b]*Adjusted for baseline NIHSS.*

diterpene ginkgolide may exert its neuroprotective effects by reducing the excess production of glutamate and aspartate excitotoxicity, while ginkgo biloba extract may partially ameliorate the excitotoxicity induced by rtPA. But so far, there have been few clinical trials of Ginkgolide. GIANT attained more encouraging results than previous trials because only patients that received thrombolytic therapy were allowed in this study. To the best of our knowledge, this was the largest study to address the management of Ginkgolide® within the first 24 h after IVT.

In our study, 66.7% of rt-PA-treated patients in the control group had good outcome after 3 months, which was in accordance to results in the Thrombolysis Implementation and Monitor of Acute Ischemic Stroke in China (Zhou et al., 2020). In our study, the degree of improvement of the neurological impairment was more pronounced in the Ginkgolide® combined with IVT, compared with the control group, indicating that early use of Ginkgolide® within 24 h after IVT might improve the neurological function of AIS patients. This result was consistent with those of previous studies that showed ginkgolide B and bilobalide might provide neuroprotective effects against rt-PA-induced toxicity.

The antioxidant effects of Ginkgolide® could have contributed to the clinical benefits reported in the trial. Researchers found ginkgolide B reduced reactive oxygen species and restored cerebral blood flow in hyperglycemic rats (Huang et al., 2012). Of note, ginkgolide B treatment could significantly increase the expressions of anti-oxidative stress-related proteins, such as Nrf2. Ginkgolide B was also believed to interfere with the production of free radicals after ischemia (Pietri et al., 1997). These characteristics may support the Ginkgolide® as an antioxidant in AIS patients within the first 24 h after IVT. Furthermore, ginkgolide B could also protect brain from endoplasmic reticulum (ER) stress, which was also an essential signaling event in the progression of brain ischemic/reperfusion injury. In a cell model, preincubation with ginkgolide B could attenuate bupivacaine-induced ER stress and cell apoptosis (Li et al., 2013). Another important component of Ginkgolide®, bilobalide, can also reduce ER stress by increasing the expression of catalase and glutathione (Lu et al., 2016). Hence, the early use of Ginkgolide® after IVT may prevent further oxidative stress injury and ER stress and thereby improve the functional outcome.

The N-methyl-D-aspartate receptor also played a pivotal role in the process of glutamate-induced excitotoxicity in stroke (Wu and Tymianski, 2018). Intravenous rt-PA can potentiate excitotoxic lesions and lead to neuronal death induced by NMDA (Nicole et al., 2001). Administration of Ginkgo biloba extract effectively inhibited NMDA-receptor and ameliorated

metabolic disturbances induced by rt-PA (Chen et al., 2018). Moreover, bilobalide enhanced cell viabilities, inhibited apoptosis, and attenuated mitochondrial membrane potential depolarization (Shi et al., 2010; Shi et al., 2011). By triggering various pathways, Ginkgolide® seemed to interrupt the development of pathological processes that lead to ischemic/reperfusion injury after rtPA therapy.

During recent years, several cases of hemorrhage including subdural hematoma (Rowin and Lewis, 1996), subarachnoid hemorrhage (Vale, 1998), intracerebral hemorrhage (Matthews, 1998), have been reported to occur in coincidence with the use of Ginkgo products and those observations have generally been explained by the platelet-activating factor (PAF)-antagonistic action of ginkgolides. However, in this study, ultra-early administration of Ginkgolide® after IVT did not involve a higher risk of hemorrhage transformation or sICH. Indeed, results from different studies consistently indicated that Ginkgo does not significantly affect hemostasis nor the safety of co-administered aspirin, warfarin and other antiplatelet drugs (Bone, 2008). E Koch confirmed that induction of aggregation of human platelets by PAF requires higher concentration, which were generally more than 100 times higher as the peak plasma values measured after oral intake ginkgo biloba extract at recommended doses (Koch, 2005). Therefore, the likelihood of hemorrhage transformation due to PAF is very low, and those case reports might be coincidences. *In vitro* multicellular network model, pretreatment with Ginkgo biloba extract or ginkgolide B enhanced the *trans*-endothelial electrical resistance of capillary endothelial monolayers, reduced the endothelial permeability coefficients for sodium fluorescein, and increased the expression levels of tight junction proteins, namely, ZO-1 and occludin, in endothelial cells (Yang et al., 2017). Results demonstrated the preventive effects of Ginkgo biloba extract on neuronal cell death and enhancement of the function of brain capillary endothelial monolayers after oxygen–glucose deprivation/reoxygenation injury *in vitro*. Ginkgolides® are mainly composed of ginkgo diterpene lactones (ginkgolide A, B, and C) and bilobalide. Ginkgo diterpene lactone mainly plays a role in inhibiting platelet aggregation caused by PAF and inhibiting the production of inflammatory molecules during ischemia-reperfusion, while bilobalide mainly functions to maintain the integrity of vascular endothelial cells and promote vascular endothelial proliferation. Our result also showed the use of Ginkgolide® was not associated with hemorrhage transformation after adjusting baseline NIHSS, indicating that ginkgolides could not increase hemorrhage transformation in AIS patients receiving IV rt-PA, indicating that it is safe and effective to use Ginkgolides® within 24 h after intravenous thrombolysis. It may be due to the anti-platelet aggregation and anti-inflammation of ginkgolides, while bilobalide protects blood brain barrier permeability, which may further diminish the risk of hemorrhage transformation.

Limitations include biased baseline characters such as baseline NIHSS, hypertension and atrial fibrillation, although after adjusting for baseline NIHSS and these comorbidities, intervention with Ginkgolide® was still significantly associated with 90-day mRS. Secondly, the underlying mechanism of Ginkgolide improving neurological deficits was not revealed in our study, which need further imaging or lab markers. Thirdly, we analyzed patients mostly in the Yangtze River Delta, which may introduce geographic bias.

CONCLUSION

In summary, the present study suggests that Ginkgolide® use in patients within the first 24 h after IVT was safe and could have a favorable impact on functional outcome. Ginkgolide® therapy might be the treatment of choice for patients at the first 24 h after IVT. Confirmation of these findings in a larger randomized trial is needed.

GIANT INVESTIGATORS

Gu Qun, Department of Neurology, The First People's Hospital of Huzhou, Huzhou, China; Wang Yaxian, Department of Neurology, Huzhou Central Hospital, Huzhou, China; Chen Chaochan, Department of Neurology, The First People's Hospital of Yonkang, Jinhua, China; Sui Yi, Department of Neurology, The First People's Hospital of Shenyang, Shenyang, China; Lan Likang, Department of Neurology, Lishui City People's Hospital, Lishui, China; Zhong Jianbin, Department of Neurology, Guangzhou Zengcheng District People's Hospital, Guangzhou, China; Xu Dongjuan, Department of Neurology, Donyang People's Hospital, Jinhua, China; Hu Haifang, Department of Neurology, The First People's Hospital of Hangzhou Xiaoshan District, Hangzhou, China; Huang Huadong, Department of Neurology, Sahzu.Changxing Campus, Huzhou, China; Cai Xueli, Department of Neurology, Lishui Central Hospital, Lishui, China; Hou Shuangxing, Department of Neurology, ShangHai Pudong Hospital, Shanghai, China; Zhang Ningyuan, Department of Neurology, The First People's Hospital of Tongxiang, Jiaxin, China; Bi Yong, Department of Neurology, ShangHai Fourth People's Hospital, Shanghai, China; Zhang Dechou, Department of Neurology, Affiliated TCM hospital of Southwest Medical University, Sichuan, China; Zhong Lianjiang, Department of Neurology, The Second People's Hospital of Tongxiang, Jiaxin, China;

DATA AVAILABILITY STATEMENT

The raw data supporting the conclusion of this article will be made available by the authors, without undue reservation.

ETHICS STATEMENT

The studies involving human participants were reviewed and approved by the Human Ethics Committee of the Second Affiliated Hospital of Zhejiang University, School of Medicine. The patients/participants provided their written informed consent to participate in this study.

AUTHOR CONTRIBUTIONS

ML led the conception and design of the trial and reviewing the manuscript. XZ wrote the manuscript and involved in design of the trial. WZ was closely involved in data collection, data curation and wrote original draft preparation. XM, XZ, HC, and ZW were involved in the design of the study, participated in data interpretation, and revised the manuscript critically for important intellectual content. QG, YW, CC, YS, LL, JZ, DX, HH, HH, XC, SH, NZ, YB, and DZ participated in data collection. All authors read and approved the final manuscript.

FUNDING

This study was supported by the National Natural Science Foundation of China (81971101), the National Key Research and Development Program of China (2016YFC1301503), and the Science Technology Department of Zhejiang Province (2018C04011). All interventions and placebo were sponsored by Chendu Hundred Pharmaceutical Co. Ltd. Otherwise, the funder and the sponsor had no role in the design and interpretation of data; in the writing of the manuscript; and in the decision to submit this manuscript for publication.

ACKNOWLEDGMENTS

We thank all participating hospitals, their physicians, and nurses.

SUPPLEMENTARY MATERIAL

The Supplementary Material for this article can be found online at: https://www.frontiersin.org/articles/10.3389/fphar.2021.792136/full#supplementary-material

REFERENCES

Bone, K. M. (2008). Potential Interaction of Ginkgo Biloba Leaf With Antiplatelet or Anticoagulant Drugs: what Is the Evidence? *Mol. Nutr. Food Res.* 52, 764–771. doi:10.1002/mnfr.200700098

Chen, Z., Bai, S., Hu, Q., Shen, P., Wang, T., Liang, Z., et al. (2018). Ginkgo Biloba Extract and its Diterpene Ginkgolide Constituents Ameliorate the Metabolic Disturbances Caused by Recombinant Tissue Plasminogen Activator in Rat Prefrontal Cortex. *Neuropsychiatr. Dis. Treat.* 14, 1755–1772. doi:10.2147/NDT.S167448

Collaboration, F. T. (2019). Effects of Fluoxetine on Functional Outcomes After Acute Stroke (Focus): a Pragmatic, Double-Blind, Randomised, Controlled Trial. *Lancet.* 393, 265–274. doi:10.1016/S0140-6736(18)32823-X

Dong, Y., Zhang, J., Wang, Y., Zhao, L., Li, R., Wei, C., et al.GISAA committee (2021). Effect of Ginkgolide in Ischemic Stroke Patients With Large Artery Atherosclerosis: Results From a Randomized Trial. *CNS Neurosci. Ther.* 00, 1–9. doi:10.1111/cns.13742

Fang, W., Sha, L., Kodithuwakku, N. D., Wei, J., Zhang, R., Han, D., et al. (2015). Attenuated Blood-Brain Barrier Dysfunction by XQ-1H Following Ischemic Stroke in Hyperlipidemic Rats. *Mol. Neurobiol.* 52, 162–175. doi:10.1007/s12035-014-8851-1

Feng, Z., Sun, Q., Chen, W., Bai, Y., Hu, D., and Xie, X. (2019). The Neuroprotective Mechanisms of Ginkgolides and Bilobalide in Cerebral Ischemic Injury: a Literature Review. *Mol. Med.* 25 (1), 57. doi:10.1186/s10020-019-0125-y

Hacke, W., Kaste, M., Fieschi, C., von Kummer, R., Davalos, A., Meier, D., et al. (1998). Randomised Double-Blind Placebo-Controlled Trial of Thrombolytic Therapy With Intravenous Alteplase in Acute Ischaemic Stroke (ECASS II). Second European-Australasian Acute Stroke Study Investigators. *Lancet.* 352 (9136), 1245–1251. doi:10.1016/s0140-6736(98)08020-9

Huang, M., Qian, Y., Guan, T., Huang, L., Tang, X., and Li, Y. (2012). Different Neuroprotective Responses of Ginkgolide B and Bilobalide, the Two Ginkgo Components, in Ischemic Rats With Hyperglycemia. *Eur. J. Pharmacol.* 677, 71–76. doi:10.1016/j.ejphar.2011.12.011

Hussein, H. M., Saleem, M. A., and Qureshi, A. I. (2018). Rates and Predictors of Futile Recanalization in Patients Undergoing Endovascular Treatment in a Multicenter Clinical Trial. *Neuroradiology.* 60 (5), 557–563. doi:10.1007/s00234-018-2016-2

Jiang, M., Li, J., Peng, Q., Liu, Y., Liu, W., Luo, C., et al. (2014). Neuroprotective Effects of Bilobalide on Cerebral Ischemia and Reperfusion Injury Are Associated With Inhibition of Pro-inflammatory Mediator Production and Down-Regulation of JNK1/2 and P38 MAPK Activation. *J. Neuroinflammation.* 11, 167. doi:10.1186/s12974-014-0167-6

Joseph, R., Welch, K. M., and D'Andrea, G. (1989). Effect of Therapy on Platelet Activating Factor-Induced Aggregation in Acute Stroke. *Stroke.* 20 (5), 609–611. doi:10.1161/01.str.20.5.609

Knecht, T., Borlongan, C., and Dela Peña, I. (2018). Combination Therapy for Ischemic Stroke: Novel Approaches to Lengthen Therapeutic Window of Tissue Plasminogen Activator. *Brain Circ.* 4 (3), 99–108. doi:10.4103/bc.bc_21_18

Koch, E. (2005). Inhibition of Platelet Activating Factor (PAF)-Induced Aggregation of Human Thrombocytes by Ginkgolides: Considerations on Possible Bleeding Complications After Oral Intake of Ginkgo Biloba Extracts. *Phytomedicine.* 12 (1-2), 10–16. doi:10.1016/j.phymed.2004.02.002

Li, L., Zhang, Q. G., Lai, L. Y., Wen, X. J., Zheng, T., Cheung, C. W., et al. (2013). Neuroprotective Effect of Ginkgolide B on Bupivacaine-Induced Apoptosis in SH-Sy5y Cells. *Oxid Med. Cell Longev.* 2013, 159864. doi:10.1155/2013/159864

Li, P., Stetler, R. A., Leak, R. K., Shi, Y., Li, Y., Yu, W., et al. (2018). Oxidative Stress and DNA Damage After Cerebral Ischemia: Potential Therapeutic Targets to Repair the Genome and Improve Stroke Recovery. *Neuropharmacology.* 134, 208–217. doi:10.1016/j.neuropharm.2017.11.011

Liu, Q., Jin, Z., Xu, Z., Yang, H., Li, L., Li, G., et al. (2019). Antioxidant Effects of Ginkgolides and Bilobalide Against Cerebral Ischemia Injury by Activating the Akt/Nrf2 Pathway *In Vitro* and *In Vivo*. *Cell Stress Chaperones.* 24 (2), 441–452. doi:10.1007/s12192-019-00977-1

Lu, L., Wang, S., Fu, L., Liu, D., Zhu, Y., and Xu, A. (2016). Bilobalide Protection of Normal Human Melanocytes from Hydrogen Peroxide-Induced Oxidative Damage via Promotion of Antioxidase Expression and Inhibition of Endoplasmic Reticulum Stress. *Clin. Exp. Dermatol.* 41, 64–73. doi:10.1111/ced.12664

Matthews, M. K., JR. (1998). Association of Ginkgo Biloba With Intracerebral Hemorrhage. *Neurology.* 50, 1933–1934. doi:10.1212/wnl.50.6.1933

Nicole, O., Docagne, F., Ali, C., Margaill, I., Carmeliet, P., MacKenzie, E. T., et al. (2001). The Proteolytic Activity of Tissue-Plasminogen Activator Enhances NMDA Receptor-Mediated Signaling. *Nat. Med.* 7 (1), 59–64. doi:10.1038/83358

Nijders, S. T. A. B., and Bosker, R. J. (1999). *Multilevel Analysis*. 1st ed. New Delhi: SAGE.

Oberpichler, H., Sauer, D., Rossberg, C., Mennel, H. D., and Krieglstein, J. (1990). PAF Antagonist Ginkgolide B Reduces Postischemic Neuronal Damage in Rat Brain Hippocampus. *J. Cereb. Blood Flow Metab.* 10 (1), 133–135. doi:10.1038/jcbfm.1990.17

Pietri, S., Maurelli, E., Drieu, K., and Culcasi, M. (1997). Cardioprotective and Anti-Oxidant Effects of the Terpenoid Constituents of Ginkgo Biloba Extract (EGb 761). *J. Mol. Cell Cardiol.* 29 (2), 733–742. doi:10.1006/jmcc.1996.0316

Rowin, J., and Lewis, S. L. (1996). Spontaneous Bilateral Subdural Hematomas Associated With Chronic Ginkgo Biloba Ingestion. *Neurology.* 46 (6), 1775–1776. doi:10.1212/wnl.46.6.1775

Shi, C., Wu, F., Yew, D. T., Xu, J., and Zhu, Y. (2010). Bilobalide Prevents Apoptosis through Activation of the PI3K/Akt Pathway in SH-Sy5y Cells. *Apoptosis.* 15, 715–727. doi:10.1007/s10495-010-0492-x

Shi, C., Zou, J., Li, G., Ge, Z., Yao, Z., and Xu, J. (2011). Bilobalide Protects Mitochondrial Function in Ovariectomized Rats by Up-Regulation of mRNA and Protein Expression of Cytochrome C Oxidase Subunit I. *J. Mol. Neurosci.* 45, 69–75. doi:10.1007/s12031-010-9388-z

Takagi, T., Kitashoji, A., Iwawaki, T., Tsuruma, K., Shimazawa, M., Yoshimura, S., et al. (2014). Temporal Activation of Nrf2 in the Penumbra and Nrf2 Activator-Mediated Neuroprotection in Ischemia-Reperfusion Injury. *Free Radic. Biol. Med.* 72, 124–133. doi:10.1016/j.freeradbiomed.2014.04.009

Vale, S. (1998). Subarachnoid Haemorrhage Associated With Ginkgo Biloba. *Lancet.* 352, 36. doi:10.1016/S0140-6736(05)79516-7

Wei, J., Fang, W., Sha, L., Han, D., Zhang, R., Hao, X., et al. (2013). XQ-1H Suppresses Neutrophils Infiltration and Oxidative Stress Induced by Cerebral Ischemia Injury Both *In Vivo* and *In Vitro*. *Neurochem. Res.* 38, 2542–2549. doi:10.1007/s11064-013-1176-z

William, J., Rabinstein Alejandro, A., Ackerson, T., Adeoye Opeolu, M., Bambakidis Nicholas, C., Becker, K., et al. (2019). Guidelines for the Early Management of Patients With Acute Ischemic Stroke: 2019 Update to the 2018 Guidelines for the Early Management of Acute Ischemic Stroke: A Guideline for Healthcare Professionals From the American Heart Association/American Stroke Association. *Stroke.* 50 (12), e344–e418. doi:10.1016/j.phymed.2004.02.002

Wu, Q. J., and Tymianski, M. (2018). Targeting NMDA Receptors in Stroke: New Hope in Neuroprotection. *Mol. Brain.* 11, 15. doi:10.1186/s13041-018-0357-8

Yang, X., Zheng, T., Hong, H., Cai, N., Zhou, X., Sun, C., et al. (2017). Neuroprotective Effects of Ginkgo Biloba Extract and Ginkgolide B Against Oxygen-Glucose Deprivation/Reoxygenation and Glucose Injury in a New *In Vitro* Multicellular Network Model. *Front. Med.* 12, 307–318. doi:10.1007/s11684-017-0547-2

Yuan, L. F., and Guo, H. L. (2017). Effect and Mechanism of Ginkgolide Injection Combined with Edaravone on Acute Cerebral Infarction. *Chin. J. Prim. Med. Pharm.* 24 (18), 2820–2823.

Yumiko, N., Toru, Y., Qian, L., Kota, S., Yasuyuki, O., Ryuta, M., et al. (2017). Time-dependent Change of *In Vivo* Optical Imaging of Oxidative Stress in a Mouse Stroke Model. *J. Neurosci. Res.* 95, 2030–2039.

Zhao, W., Wu, C., Dornbos, D., 3rd, Li, S., Song, H., Wang, Y., et al. (2020). Multiphase Adjuvant Neuroprotection: A Novel Paradigm for Improving Acute Ischemic Stroke Outcomes. *Brain Circ.* 6 (1), 11–18. doi:10.4103/bc.bc_58_19

Zhou, H. Y., Chen, W. Q., Pan, Y. S., Suo, Y., Meng, X., Li, H., et al. (2020). Effect of Sex Differences on Prognosis of Intravenous Thrombolysis: Data From the Thrombolysis Implementation and Monitor of Acute Ischemic Stroke in China (TIMS-China). *Stroke Vasc. Neurol.* 6 (1), 1015, 2020 svn-2020-000351. doi:10.1136/svn-2020-000351

Conflict of Interest: The authors declare that the research was conducted in the absence of any commercial or financial relationships that could be construed as a potential conflict of interest.

Publisher's Note: All claims expressed in this article are solely those of the authors and do not necessarily represent those of their affiliated organizations, or those of the publisher, the editors and the reviewers. Any product that may be evaluated in this article, or claim that may be made by its manufacturer, is not guaranteed or endorsed by the publisher.

frontiers in Pharmacology

SYSTEMATIC REVIEW
published: 20 December 2021
doi: 10.3389/fphar.2021.795409

Resveratrol has an Overall Neuroprotective Role in Ischemic Stroke: A Meta-Analysis in Rodents

Jianyang Liu[1], *Jialin He*[1], *Yan Huang*[2] *and Zhiping Hu*[1]*

[1]Department of Neurology, The Second Xiangya Hospital, Central South University, Changsha, China, [2]National Health Commission Key Laboratory of Birth Defects Research, Prevention, and Treatment, Hunan Provincial Maternal and Child Health Care Hospital, Changsha, China

Background: Resveratrol, a natural polyphenolic phytoalexin, is broadly presented in dietary sources. Previous research has suggested its potential neuroprotective effects on ischemic stroke animal models. However, these results have been disputable. Here, we conducted a meta-analysis to comprehensively evaluate the effect of resveratrol treatment in ischemic stroke rodent models.

Objective: To comprehensively evaluate the effect of resveratrol treatment in ischemic stroke rodent models.

Methods: A literature search of the databases Pubmed, Embase, and Web of science identified 564 studies that were subjected to pre-defined inclusion criteria. 54 studies were included and analyzed using a random-effects model to calculate the standardized mean difference (SMD) with corresponding confidence interval (CI).

Results: As compared with controls, resveratrol significantly decreased infarct volume (SMD −4.34; 95% CI −4.98 to −3.69; $p < 0.001$) and the neurobehavioral score (SMD −2.26; 95% CI −2.86 to −1.67; $p < 0.001$) in rodents with ischemic stroke. Quality assessment was performed using a 10-item checklist. Studies quality scores ranged from 3 to 8, with a mean value of 5.94. In the stratified analysis, a significant decrease of infarct volume and the neurobehavioral score was achieved in resveratrol sub-groups with a dosage of 20–50 mg/kg. In the meta-regression analysis, the impact of the delivery route on an outcome is the possible source of high heterogeneity.

Conclusion: Generally, resveratrol treatment presented neuroprotective effects in ischemic stroke models. Furthermore, this study can direct future preclinical and clinical trials, with important implications for human health.

Keywords: resveratrol, ischemic stroke, meta-analysis, neuroprotection, therapy

OPEN ACCESS

Edited by:
Toshiko Yamazawa, Jikei University School of Medicine, Japan

Reviewed by:
Fabiola Paciello, Catholic University of the Sacred Heart, Italy
Yoshinori Mikami, Toho University, Japan

***Correspondence:**
Zhiping Hu
zhipinghu@csu.edu.cn

Specialty section:
This article was submitted to Neuropharmacology, a section of the journal Frontiers in Pharmacology

Received: *15 October 2021*
Accepted: *03 December 2021*
Published: *20 December 2021*

Citation:
Liu J, He J, Huang Y and Hu Z (2021) Resveratrol has an Overall Neuroprotective Role in Ischemic Stroke: A Meta-Analysis in Rodents. Front. Pharmacol. 12:795409. doi: 10.3389/fphar.2021.795409

INTRODUCTION

Ischemic stroke is one of the major causes of morbidity and long-term disability in the worldwide population. At present, intravenous thrombolysis and endovascular thrombectomy are effective therapy within a limited time window (Fisher and Saver, 2015). Owing to the poor regenerative ability of the adult brain, stroke-induced neuronal injury is permanent and results in a long-term

neurological deficiency. Therefore, various effective therapy to reduce post-ischemic neuronal cell or tissue loss remain in further research.

Resveratrol (3,5,4′-trihydroxystilbene) (PubChem CID: 445154) is a natural estrogen-like phytosterol that mainly is found in grapes, blueberries, peanuts, red wine, Semen Cassiae, and other dietary constituents (Walle, 2011). This compound exists in two isoforms *cis*- and *trans*-resveratrol, the isomer *trans* being more active than the *cis*-form (Amri et al., 2012). In preclinical studies, resveratrol has neuroprotective properties in both ischemic stroke, intracerebral hemorrhage (Bonsack et al., 2017; Zhao et al., 2019; Abd Aziz et al., 2020), subarachnoid hemorrhage (Zhao et al., 2017; Li and Han, 2018), and neurodegenerative disease (Griñán-Ferré et al., 2021). Resveratrol was reported to promote neurogenesis (Li et al., 2020) and reduce neurotoxicity by altering glial activity and signaling. In a randomized controlled trial, co-administration of resveratrol significantly improved the outcome of patients receiving delayed recombinant tissue plasminogen activator treatment (Chen et al., 2016). Subsequent preclinical studies have indicated that resveratrol treatment could reduce ischemic brain damage, yet there are some disputes over results. Some studies suggested that the low dosage of resveratrol was unable to induce a significant reduction (Pang et al., 2015; Faggi et al., 2018), and resveratrol administration without nanoparticles did not confer any neurological function recovery (Lu et al., 2020). Moreover, the administration dose, frequency, timing of treatment, and route in each study are so divergent that the overall therapeutic effect is difficult to evaluate. Treatment in some studies was a single dose of 100 mg/kg (He et al., 2017), while in other studies was a single dose of 20 mg/Kg (Teertam et al., 2020). To date, there is no meta-analysis available investigating the potential effects of resveratrol therapy in pre-clinical models of ischemic stroke. Addressing all these problems, we systematically assessed the bias of included studies and then summarized the optimal pattern of resveratrol therapy. This meta-analysis may provide significant clues and information for future clinical research.

MATERIALS AND METHODS

Preferred Reporting Items for Systematic Reviews and Meta-Analysis (PRISMA) was used to conduct this study (Moher et al., 2009). This meta-analysis was not registered in the International prospective register of systematic reviews (PROSPERO). However, the PROSPERO was carefully examined to make sure there is no registered meta-analysis that is investigating a similar topic.

Search Strategy

Studies of resveratrol-based therapy for rodent models of cerebral ischemia were identified from PubMed, EMBASE, and Web of Science, from their inception to July 15, 2021, and using the following search strategy: (stroke OR cerebrovascular OR cerebral infarct OR cerebral ischemia/reperfusion OR middle cerebral artery OR middle cerebral artery occlusion) AND (resveratrol). The publication language was limited to English.

Inclusion and Exclusion Criteria

The inclusion criteria were set up based on the PICOS-scheme (population, intervention, control, outcome, and study design). Published studies were included if they met the following criteria: 1) ischemic stroke animal model (rodent models); 2) testing the effects of purified resveratrol in at least one experimental group (no additional chemicals or drugs were used); 3) setting a control group with placebo; 4) providing adequate data on the functional outcome (neurobehavioral score measured on any scale/rotarod test) or the structural outcome (infarct volume) determined by a recognized method (such as TTC staining/Magnetic Resonance Imaging); 5) study: experimental studies presented in original research articles and 6) published in English.

The exclusion criteria were as follows: 1) animals treated with resveratrol analogues; 2) studies that only tested the effects of resveratrol combined with other chemicals or drugs (such as nanoparticles); 3) not reporting the number of animals in groups; 4) repeated publications or duplicate report, and abstracts without full text.

Data Collection

The following information was abstracted by two investigators independently and discrepancies were resolved by consensus and then checked by a third investigator. 1) authors, year published, study country, 2) characteristics of the animals used, including species of animals, animal model, animal gender, anesthetic type, and animal number per group, 3) treatment information, including dosage, administration route, and timing, follow-up (the longest observation time of outcomes after occlusion), 4) the outcomes data: functional outcome (neurobehavioral score measured on any scale/rotarod test), structural outcome (infarction volume determined by TTC staining/Magnetic Resonance Imaging/cresyl violet staining/silver staining).

If a study comprised multi-experimental groups distinguished by dosage, frequency, delivery route, and timing that were compared with the control group, these experimental groups would be considered as independent comparisons. If the outcomes were evaluated at different follow-up times, only the longest follow-up time was collected. The GetData Graph Digitizer software was applied when only graphs were available.

Quality Assessment

To evaluate the quality of the eligible studies, we used the Collaborative Approach to Meta-Analysis and Review of Animal Data from Experimental Studies (CAMARADES) checklists (Macleod et al., 2004). A sum of the quality scores was recorded for each study, with a total score of 10 points. Two researchers independently scored the included studies. Discrepancies were resolved by consensus and then adjudicated by a third investigator.

Statistical Analysis

During data abstraction, we found that infarction volume determined by TTC staining (n = 46) and functional outcome determined by neurobehavioral score (n = 24) were available in large numbers of original studies. Thus, we decided to choose these as co-primary outcomes in this meta-analysis. Other

secondary outcomes were rotarod test, and infarction volume determined by Magnetic Resonance Imaging/cresyl violet staining/silver staining. The combined effect size was calculated as standardized mean difference (SMD) with corresponding confidence interval (CI) between BMSCs treated group and control group. The random-effects model and Hedges calculation (Durlak, 2009) were used for the pooled SMD, and all analysis was performed with Stata 14.0 software. A p value <0.05 was considered statistically significant. The inconsistency index (I^2) was used to analyze heterogeneity (Higgins et al., 2003).

Four clinical characteristics were used to group the effect size of outcome: resveratrol dosage (<10, ≥10, ≤20, >20, and <50, 50–200 mg/Kg), frequency of treatment (single treatment; irregularly treatment; daily treatment), the timing of administration (pre-stroke onset; post-stroke onset), administration route (intraperitoneally; intravenously; oral gavage; intracarotid arterial). Subgroup analysis and meta-regression analysis (Higgins and Thompson, 2002) were conducted to explore the impact of the above clinical characteristics on outcomes and the possible sources of heterogeneity.

A leave-one-out sensitivity analysis was conducted by iteratively removing each study one by one to estimate the influence of each study.

Publication bias was evaluated by Egger's tests, Trim and Fill analysis, and funnel plot (Egger et al., 1997; Vahidy et al., 2016). Plotting the SMD against the SE can cause distortion of funnel plots, especially when the included studies have small sample sizes. Thus, we plotted the SMD against $1/\sqrt{n}$, a sample size-based precision estimate (Zwetsloot et al., 2017). Each funnel plot displays all studies in one plot with SMD as the x-value and $1/\sqrt{n}$ as the y-value.

RESULTS

Study Selection

Electronic searching identified 295 articles in PubMed, 101 articles in EMBASE, and 503 articles in Web of Science. After removing duplicates, 564 articles were screened by abstract and/or title, resulting in 424 irrelevant records excluded. We retrieved the full text of the remaining 140 records for further assessment. Among them, 86 records were excluded due to review, abstracts without full text, not having purified resveratrol, no *in vivo* experiment, not reporting the number of animals in groups, and or no adequate outcomes (infarction volume or functional outcome determined by neurobehavioral score measured on any scale/rotarod test). Therefore, 54 studies (Huang et al., 2001; Sinha et al., 2002; Inoue, 2003; Gao et al., 2006; Tsai et al., 2007; Dong et al., 2008; Yousuf et al., 2009; Li et al., 2010; Sakata et al., 2010; Shin et al., 2010; Ren et al., 2011; Li et al., 2012; Shin et al., 2012; Hurtado et al., 2013; Lanzillotta et al., 2013; Lin et al., 2013; Orsu et al., 2013; Yan et al., 2013; Saleh et al., 2014; Wang et al., 2014; Fang et al., 2015; Hermann et al., 2015; Ishrat et al., 2015; Koronowski et al., 2015; Li et al., 2015; Narayanan et al., 2015; Pandey et al., 2015; Pang et al., 2015; Abdel-Aleem et al., 2016; Jeong et al., 2016; Li et al., 2016; Lopez et al., 2016; Su et al., 2016; Wan et al., 2016; Yang et al., 2016; Al Dera, 2017; He et al., 2017; Koronowski et al., 2017; Yu et al., 2017; Faggi et al., 2018; Hou et al., 2018; Liu et al., 2018; Dou et al., 2019; Grewal et al., 2019; Park et al., 2019; Yan et al., 2019; Alquisiras-Burgos et al., 2020; Lu et al., 2020; Mota et al., 2020; Pineda-Ramírez et al., 2020; Teertam et al., 2020; Yao et al., 2020; McDonald et al., 2021; Yu et al., 2021) met our criteria and were used for meta-analysis (**Figure 1**).

Study Characteristics

The baseline characteristics of all studies are shown in **Supplementary Tables S1, S2**. All studies were carried out in rodents (rats and mice). The most common model of ischemic stroke was the t-MCAO induced with nylon monofilament, although other methods were also used, such as the photothrombosis, electrocoagulation, and embolic MCAO. The most common delivery route used for resveratrol was the intraperitoneal route. Others used were the intravenous, intracarotid arterial, and oral gavage routes. The dosage of resveratrol with intraperitoneal route ranged from 2.5 mg/kg to 100 mg/kg. Resveratrol was administrated either immediately after ischemic insult or over a period before ischemia onset. The follow-up time in most studies is 24 h. Infarction outcome was assessed by TTC staining in 46 studies, cresyl violet staining in four studies, silver-staining in one study, and MRI in one study. Behavioral outcomes were evaluated by behavioral scale (0 represents no neurological deficit) in 24 studies, rotarod test in four studies, limb function (beam walking test, limb-use asymmetry test, grip test, and gait assessment) in 5 studies, corner test in 2 studies, and Morris water maze test in one study. Considering that TTC staining and neurobehavioral score are the most common evaluations used in rodent studies of ischemic stroke, we took them as co-primary outcomes in this meta-analysis.

Quality Assessment

The quality assessment of included studies is summarized in **Table 1**. The quality scores varied from 3 to 8, with a mean value of 5.94. All included studies were peer-reviewed publications. Most studies reported compliance with animal welfare regulations. However, only one study was performed on aged animals (20-month-old aged mice) (Jeong et al., 2016), no study reported a sample size calculation. Control of temperature was stated in 40 studies. 38 studies reported random allocation to treatment or control, 31 studies reported blinding assessment of outcome, 23 studies stated blinded induction of model, and 32 studies declared no potential conflict of interests. The details of the quality assessment are presented in **Supplementary Table S3**.

Meta-Analysis

Our primary aim was to evaluate whether resveratrol had neuroprotective effects on ischemic stroke. The primary outcome was composed of two aspects: infarction volume determined by TTC staining, and behavioral outcomes determined by neurobehavioral score. Meta-analysis of 46 studies with 68 comparisons showed significant effects of

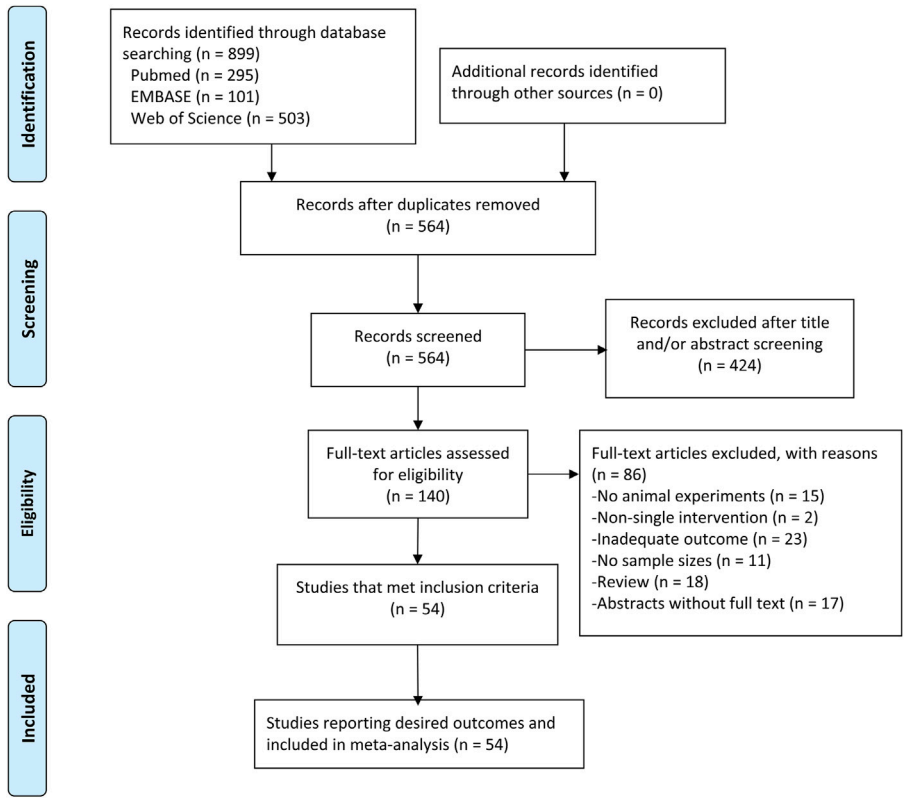

FIGURE 1 | PRISMA flow diagram for review and selection process of studies included in meta-analysis of resveratrol in rodent models of ischemic stroke.

TABLE 1 | Percentage of included studies satisfying each criterion of CAMARADES checklists.

Quality score criterion	Percentage of qualified studies (%)
Publication in a peer-reviewed journal	100
Control of temperature	74.07
Randomized treatment allocation	70.37
Allocation concealment	42.59
Use of aged animal models	1.85
Blind assessment of outcome	57.41
Avoidance neuroprotective anesthetics	94.44
Sample size calculation	0
Compliance with animal welfare regulations	92.59
Statement of conflict of interest	59.25

resveratrol for reducing infarct volume compared with control groups (SMD −4.34; 95% CI −4.98 to −3.69; $p < 0.001$; $I^2 = 85.6\%$; **Figure 2A**).

Meta-analysis of 24 studies with 34 comparisons reported the neurobehavioral score. The pooled analysis showed that resveratrol can significantly improve the neurological function compared with the control groups (SMD −2.26; 95% CI −2.86 to −1.67; $p < 0.001$; $I^2 = 82.0\%$; **Figure 2B**).

We also conducted pooled analysis for the secondary outcomes: infarction outcome assessed by cresyl violet-staining/silver-staining/MRI ($n = 10$), and behavioral outcomes evaluated by rotarod test ($n = 5$). The result was similar: The composite weighted mean (95% CI) effect size for rotarod tests was 2.59 (0.74, 4.44) ($p < 0.001$, $I^2 = 91.9\%$), and −1.63 (−2.68, −0.58) ($p < 0.0011$, $I^2 = 87.0\%$) for infarction outcome assessed by cresyl violet-staining/silver-staining/MRI. (**Supplementary Figures S1A,B**).

Stratified Analysis

To identify heterogeneity potentially influencing the analysis, articles were divided into several groups based on dosage, frequency of treatment, the timing of administration, and administration route. **Table 2** summarizes the data of primary outcomes in diverse subgroup analysis. Due to the insufficient number of comparisons, stratified analysis for rotarod test and infarction outcome assessed by cresyl violet-staining/silver-staining/MRI were not conducted.

For TTC staining, no significant between-subgroup heterogeneity was found in administration timing ($p = 0.32$). Significant differences between-subgroup were found in the dosage ($p = 0.044$), and frequency of administration ($p < 0.001$), and administration route ($p < 0.001$). Among them, there was a clear difference in therapeutic effect by the dosage of resveratrol. Compared with −3.93 (95% CI, −4.92 to −2.94) for doses between 10 and 20 mg/kg and −3.76 (95% CI, −4.88 to −2.64) for doses less than 10 mg/kg, the effects size for doses between 20 and 50 mg/kg is −6.02 (95% CI, −7.92 to −4.13) (**Table 2**).

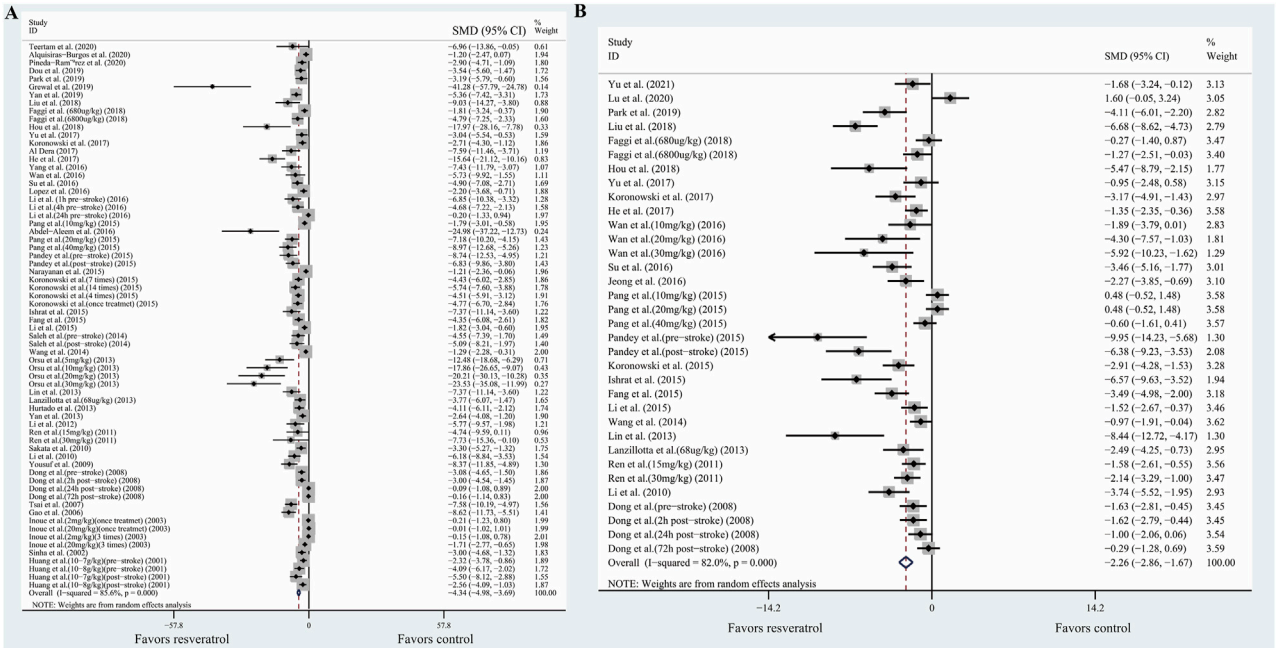

FIGURE 2 | Forest plot shows mean effect size and 95% CI for **(A)** TTC staining, **(B)** neurobehavioral score between resveratrol therapy group and control group. Weights have been calculated using random effects model. Degree of heterogeneity in the pooled estimates is represented at I^2 statistic. Abbreviations: SMD, standardized mean difference; CI: confidence interval.

For the neurobehavioral score, no significant between-subgroup heterogeneity was found in administration timing (p = 0.731) and frequency of administration (p = 0.09). Significant differences between-subgroup were found in the dosage (p = 0.002), and administration route (p = 0.001). Similarly, there was a significant difference in treatment effect by dosage of resveratrol. Compared with −1.22 (95% CI, −2.32 to −0.12) for doses between 10 and 20 mg/kg and −2.15 (95% CI, −3.63 to −0.67) for doses less than 10 mg/kg, the effects size for doses between 20 and 50 mg/kg is −3.10 (95% CI, −4.20 to −1.99) (**Table 2**). Thus, we speculated that resveratrol treatment with 20–50 mg/kg achieves the greatest effects.

However, in the included studies, resveratrol dosage was confounded with other variables. For instance, out of the 18 comparisons involving lower doses (<10 mg/kg), 15 of them administered the resveratrol with a single treatment instead of daily treatment. This makes it difficult to identify whether the difference in treatment effect was related to the dosage or the frequency of administration. To elucidate the effect of dose independently from administration frequency, we assessed the dosage effect for comparisons only involving single treatment. In the comparisons involving a single treatment, the estimated effect of the 20–50 mg/kg dose in this subset was similar to the full analysis (**Figures 3A,B**). This implied that the smaller effect estimated in the lower dose (<10 mg/kg) are indeed associated with the lower dose instead of administration frequency.

Except for the administration frequency, the routes of administration may be correlated to the different effects in dosage. In the 16 comparisons involving 20–50 mg/kg dose, 15 of them administered the resveratrol with the intraperitoneal route. To elucidate the effect of dosage independently from administration routes, we assessed the dosage effect for comparisons only involving the intraperitoneal route. For TTC staining, significant differences between-subgroup were found (p < 0.001). Compared with −4.219 (95% CI, −5.282 to −3.156) for dosage between 10 and 20 mg/kg and −4.23 (95% CI, −6.26 to −2.211) for dosage less than 10 mg/kg, the effects size for dosage between 20 and 50 mg/kg is −5.754 (95% CI, −7.666 to −3.843). This implied that the smaller effect estimated in the lower dose (<20 mg/kg) is indeed associated with the lower dose instead of administration routes. Similar results were also found in the outcomes of the neurobehavioral scores. However, in the comparisons only involving the intraperitoneal route, the dosage between 50 and 200 mg/kg achieved the greatest effects size (SMD, −8.35; 95% CI, −11.63 to −5.07), which is different from the full analysis. We speculated that the difference may owe to the administration routes. In the full analysis, some studies using dosage between 50 and 200 mg/kg delivered the resveratrol orally. The bioavailability of the oral route is less than the intraperitoneal route. Thus, the larger effects estimated in the higher dose (>50 mg/kg) may associate with the administration routes.

Meta-Regression Analysis

For infarct volume, we discovered that administration timing (p = 0.448), frequency (p = 0.787), and dosage (p = 0.288) had no significant relation with heterogeneity, only delivery route presented significantly related with the reduction of infarction volume (p = 0.033). Similarly, for neurobehavioral score, delivery

TABLE 2 | Subgroup analysis of primary outcomes (TTC staining and neurobehavioral score) in animal models of ischemic stroke associated with resveratrol therapy.

Variable	TTC staining						Neurobehavioral score					
	No. of reports	Pooled estimates (95% CI)	Q statistic	*p* Value for heterogeneity	I^2 value (%)	Between group *p* value	No. of reports	Pooled estimates (95% CI)	Q statistic	*p* Value for heterogeneity	I^2 value (%)	Between group *p* value
Dosage						0.044						0.002
<10	18	−3.76 (−4.88, −2.64)	107.68	<0.001	84.2%		5	−2.15 (−3.63, −0.67)	17.33	<0.001	76.9%	
≥10 and ≤20	23	−3.93 (−4.92, −2.94)	129.49	<0.001	83.0%		9	−1.22 (−2.32, −0.12)	46.26	<0.001	82.7%	
>20 and <50	16	−6.02 (−7.92, −4.13)	118.37	<0.001	87.3%		12	−3.10 (−4.20, −1.99)	55.82	<0.001	80.3%	
50–200	11	−4.72 (−6.55, −2.90)	100.84	<0.001	90.1%		8	−2.48 (−3.73, −1.23)	48.73	<0.001	85.6%	
Frequency						0.001						0.09
Once	34	−4.32 (−5.27, −3.37)	230.36	<0.001	85.7%		11	−2.59 (−3.80, −1.37)	63.47	<0.001	84.2%	
Daily	29	−4.31 (−5.30, −3.32)	199.26	<0.001	85.9%		21	−2.01 (−2.71, −1.31)	105.36	<0.001	81.0%	
Unregularly	5	−4.79 (−6.77, −2.81)	21.73	<0.001	81.6%		2	−3.83 (−8.77,1.09)	9.2	<0.001	89.1%	
Administration timing						0.32						0.731
Pre	42	−4.02 (−4.78, −3.27)	266.72	<0.001	84.6%		21	−2.43 (−3.23, −1.64)	115.54	<0.001	82.7%	
Post	26	−5.03 (−6.26, −3.79)	196.77	<0.001	87.3%		13	−2.03 (−2.97, −1.11)	67.2	<0.001	82.1%	
Administration route						<0.001						0.001
Intraperitoneal	43	−5.14 (−6.01, −4.27)	232.99	<0.001	82.0%		24	−2.89 (−3.59, −2.20)	99.91	<0.001	77.0%	
Intravenous	10	−4.07 (−5.38, −2.75)	36.87	<0.001	75.6%		1	NA	NA	NA	NA	
Oral	15	−2.52 (−3.57, −1.47)	111.83	<0.001	87.5%		8	−0.71 (−1.37, −0.06)	20.04	0.001	65.1%	
Intraarterial	NA	NA	NA	NA	NA		1	NA	NA	NA	NA	

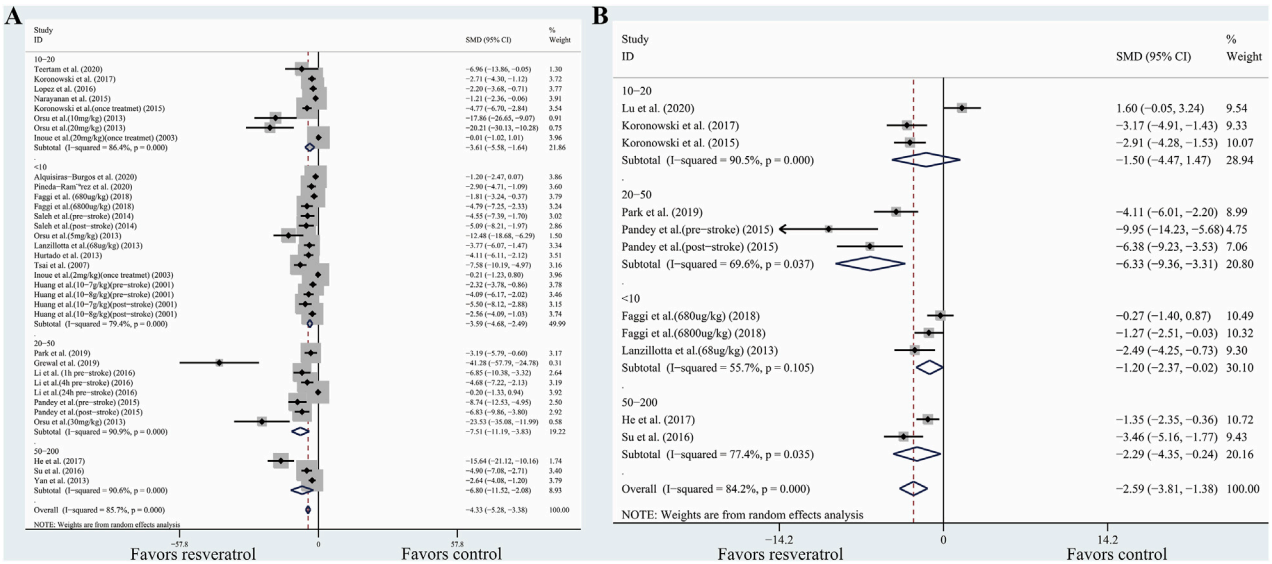

FIGURE 3 | (A) Effect of resveratrol dose on TTC staining (only including comparisons with single treatment). **(B)** Effect of resveratrol dose on neurobehavioral score (only including comparisons with single treatment). Abbreviations: SMD, standardized mean difference; CI: confidence interval.

TABLE 3 | Meta-regression analysis.

Covariates	TTC staining			Neurobehavioral score		
	Coefficient	95% CI	*p* Value	Coefficient	95% CI	*p* Value
Dosage	−0.493915	−1.414301; 0.427471	0.288	−0.470948	−1.186008; 0.244111	0.188
Frequency	−0.213211	−1.78268; 1.356259	0.787	−0.258621	−1.755727; 1.238486	0.726
Timing	−0.781463	−2.828497; 1.265571	0.448	0.038947	−1.619807; 1.697703	0.962
Route	1.215059	0.099148; 2.33097	0.033	1.227027	0.470639; 1.983415	0.002

route ($p = 0.002$) was a significant source of heterogeneity, while administration timing ($p = 0.962$), frequency ($p = 0.726$), and dosage ($p = 0.188$) had little effect on heterogeneity (**Table 3**). Thus, the impact of the delivery route on the outcome is the possible source of high heterogeneity.

Sensitivity Analysis and Publication Bias

To assess the robustness of the estimated pooled analysis for infarction volume and neurobehavioral score, we used a leave-one-out sensitivity analysis by systematically removing each study and recalculating the pooled effect size of the remaining studies. For TTC staining and neurobehavioral score, the pooled effect was stable, which indicates that the results were not driven by any single study.

The publication bias was evaluated by funnel plots and Egger's regression test. It has been demonstrated that the use of SMD to assess publication bias can lead to distortion of results due to over-estimation (Zwetsloot et al., 2017). For this reason, the funnel plot is a graphical representation of trial size plotted against the reported effect size. Inspection of the funnel plots revealed slight asymmetry for TTC staining and neurobehavioral score (**Figures 4A,B**). In addition, we performed Egger's test, which indicated that no significant publication bias for TTC staining ($p = 0.480$) and neurobehavioral score ($p = 0.691$).

DISCUSSION

To our knowledge, this is the first preclinical meta-analysis to investigate the neuroprotective effect of resveratrol treatment in animals subjected to ischemic stroke.

Summary of Evidence

The following is a summary of these results: 1) Resveratrol has neuroprotective effects in alleviating infarct volume and ameliorating neurobehavioral defects in rodent models of ischemic stroke. 2) The dose of resveratrol was correlated with effect size in TTC staining and neurobehavioral score. 20–50 mg/kg resveratrol therapy showed the greatest efficacy. 3) Compared with the administration of resveratrol intravenous and oral, intraperitoneal treatment presented more effective to reduce infarction volume. However, in clinical application, the intravenous and oral route is more common. The subgroup analysis in our meta-analysis suggested that intravenous treatment achieved greater

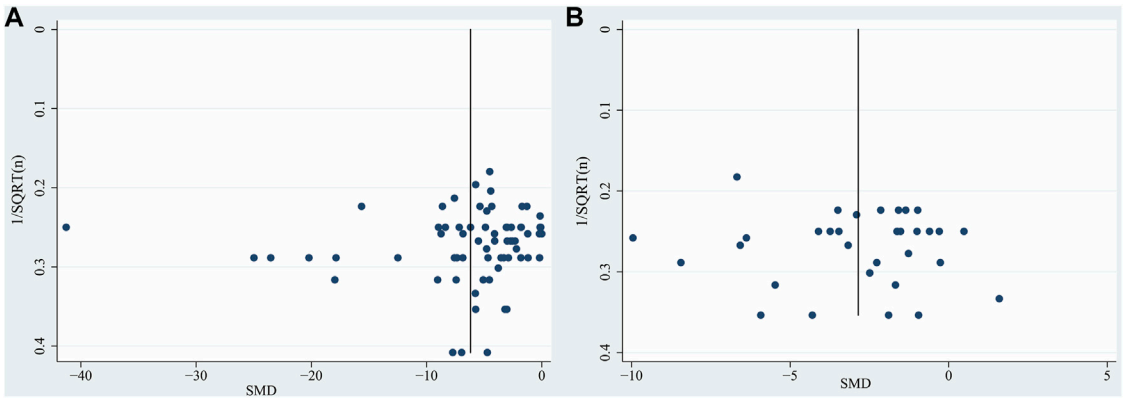

FIGURE 4 | Funnel plot for **(A)** TTC staining, **(B)** neurobehavioral score. Each funnel plot displays all studies in one plot with SMD as the x-value and $1/\sqrt{n}$ as the y-value. Abbreviations: SMD, standardized mean difference.

efficacy than oral treatment, possibly due to the increased bioavailability with intravenous treatment. 4) There were no significant differences between the estimated pooled effect size for a single treatment and daily treatment. 5) The administration timing of resveratrol in our included studies ranges from 30-days before ischemia onset to 3-days after ischemia onset. The neuroprotection between the pre-stroke treatment sub-group and post-stroke treatment sub-group was not significant, which suggested that resveratrol has a relatively long therapeutic time window.

Pharmacokinetics and Pharmacodynamics Properties of Resveratrol

The pharmacokinetics and pharmacodynamics properties of resveratrol have been studied in several studies. Due to resveratrol's low water solubility (<50 μg/ml) and high permeability, it is classified as the second class of the biopharmaceutical classification system (Singh and Pai, 2015). The principal absorption site is at the intestine through passive diffusion or forming complexes with membrane transporters (Sergides et al., 2016). Resveratrol can be absorbed through the bloodstream to the liver, where it is metabolized to form glucuronide, and sulphate derivatives or free. The free form can be bound in a non-covalent manner to proteins, such as albumin and lipoproteins (Burkon and Somoza, 2008). These complexes can be dissociated at cellular membranes that have receptors for albumin and lipoproteins, leaving the resveratrol free and allowing it to enter cells. The peak plasma concentration in humans was reached at 90 min with a single oral dose treatment of 25 mg. The half-life time of plasma concentration is around 9.2 h (Walle et al., 2004). Owing to its lipophilic characteristics, resveratrol has high absorption (at least 70% after oral consumption), and a high volume of distribution supporting its potential to accumulate in tissues such as the brain. Although resveratrol has a high absorption rate (Walle et al., 2004), the rapid metabolism of resveratrol leads to approximately 1% bioavailability of the parent compound (Walle, 2011). Except for the low solubility and high metabolism, an additional specific problem for the delivery of appropriate therapeutic resveratrol concentrations in the brain tissues is the presence of the blood-brain barrier. Peripheral administration of resveratrol could increase the antioxidant enzyme activities in the brain of healthy rats, which suggested that resveratrol is able to traverse the blood-brain barrier, and have biological activity in the brain (Mokni et al., 2007). A previous study suggested that only 2% of plasmatic resveratrol can cross the blood-brain barrier (Asensi et al., 2002). Despite its low bioavailability, resveratrol presents significant efficacy in the brain tissues, and which may ascribe to the metabolites (Walle et al., 2004). The metabolites of resveratrol, such as resveratrol-3-*O*-glucuronide, resveratrol-*O*-glucuronide, resveratrol-3-*O*-sulfate, and resveratrol-4′-*O*-sulfate, possess anti-inflammatory and antioxidant properties (Luca et al., 2020). A previous study reviewed the neuroprotection provided by resveratrol in brain tissues of animals, such as preserving mitochondrial function, inhibiting the lipid peroxidation, and inducing phosphorylation of several mitogen activated protein kinases (Shetty, 2011). Despite the ability of resveratrol to cross the blood-brain barrier, recent research aims to explore the methods improving the permeability and stability of resveratrol in the central nervous system. Nanotechnology has been proposed for the incorporation of resveratrol-loaded nanocarriers designed to deliver resveratrol to brain tissues (Fonseca-Santos and Chorilli, 2020). The nanocarriers containing resveratrol reduced infarct volume and improved neurobehavioral outcomes after ischemic stroke in rats (Ashafaq et al., 2021).

As dietary polyphenolic phytoalexin, resveratrol appeared to be well tolerated, and non-toxic. In an experimental study, resveratrol did not cause any adverse effects in rats at 28 daily doses of 50, 150, or 500 mg/kg (Williams et al., 2009). In a clinical trial conducted in healthy volunteers, resveratrol was demonstrated to be safe with 29 daily doses of 0.5, 1.0, 2.5, and 5.0 g, except the 2.5 and 5.0 g doses caused gastrointestinal

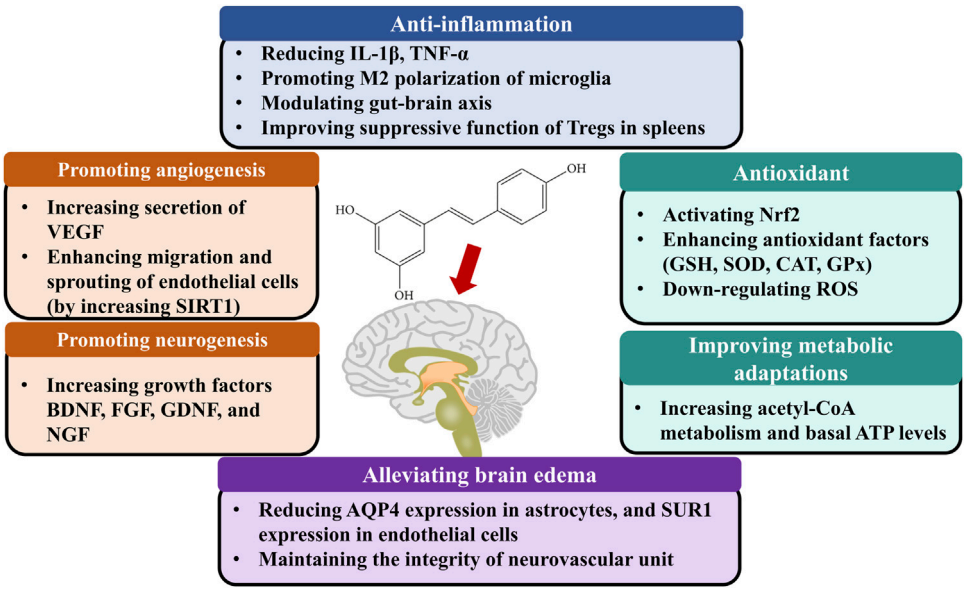

FIGURE 5 | The possible mechanisms of resveratrol therapy for ischemic stroke. Abbreviations: BDNF, Brain-derived neurotrophic factor; CAT, Catalase; EGF, Epidermal growth factor; FGF, Fibroblast growth factor; NGF, Nerve growth factor; Nrf2, Transcription factor nuclear factor (erythroid-derived 2)-like 2; GDNF, Glial cell line-derived neurotrophic factor; Glial cell-derived neurotrophic factor; GPx, glutathione peroxidase; GSH, Glutathione; Interleukin 1β, IL-1β; SOD, Superoxide dismutase; SIRT1, Silent mating type information regulation 2 homolog 1; TNF-α, Tumor necrosis factor-alpha; VEGF, Vascular endothelial growth factor.

symptoms, including nausea, flatulence, abdominal discomfort, and diarrhea (Brown et al., 2010).

Possible Mechanism of Resveratrol-Mediated Neuroprotection

The studies included in our meta-analysis indicated the main mechanisms of neuroprotection include the following biological activities (**Figure 5**): 1) Promoting angiogenesis. In an *in vitro* study, resveratrol-induced endothelial nitric oxide synthase phosphorylation led to prompt generation of nitric oxide in endothelial cells. The elevated nitric oxide increased the secretion of VEGF and matrix metalloproteinases (MMPs) (Simão et al., 2012). *In vivo* model, resveratrol administration elevated matrix metalloproteinase-2 and vascular endothelial growth factor levels (Dong et al., 2008). Moreover, resveratrol is an activator of silent information regulator 2 homologue 1, which enhances angiogenesis through migration, and sprouting of endothelial cells (Koronowski et al., 2017). 2) Promoting neurogenesis. Resveratrol treatment significantly increased the expression rates of neuronal markers with bromodeoxyuridine in the ischemic lesion site (Hermann et al., 2015). 3) Inhibiting neuroinflammation. Resveratrol reduced interleukin-1β, tumor necrosis factor-α protein levels, and immunoglobulin G extravasation in the brain tissues (Jeong et al., 2016). Meanwhile, Resveratrol promoted the M2 polarization of microglia after cerebral ischemia (Ma et al., 2020). In addition, resveratrol modulated inflammation by targeting the gut-brain axis, such as regulating Th17/Tregs and Th1/Th2 polarity shift in the small intestinal lamina propria (Dou et al., 2019). Resveratrol pretreatment also improved the suppressive function of Tregs in the spleens, which increased levels of anti-inflammatory factors, and decreased levels of pro-inflammatory factors in the plasma and ischemic hemisphere (Yang et al., 2016). 4) Antioxidant. Oxidative stress plays a pivotal role in neurological dysfunction. Resveratrol delayed the increases in oxygen species in brain tissue after ischemia, decreased xanthine oxidase activity and expression levels of inducible nitric oxide synthase, and increased levels of antioxidant enzymes such as superoxide dismutase, glutathione peroxidase, and chloramphenicol acetyltransferase (Su et al., 2016; Al Dera, 2017; Alquisiras-Burgos et al., 2020). 5) Improving metabolic adaptations. Brain tissues may lack metabolic plasticity due to their tight regulation of energy metabolism (Khoury et al., 2016). Compared with the control group, the cortex with resveratrol preconditioning presented increasing acetyl-CoA metabolism, basal ATP levels, and long-term ischemic tolerance (Khoury et al., 2019). 6) Alleviating brain edema. Astrocytic swelling mediated by AQP4 plays a significant role in cytotoxic edema. Sulfonylurea receptor 1 (SUR1) interacted with AQP4 to form a heteromultimeric complex favoring ion/water osmotic coupling and cell swelling. Following brain injury, SUR1 is up-regulated in the cells from the neurovascular unit. Resveratrol was demonstrated to reduce AQP4 expression (Li et al., 2015; Alquisiras-Burgos et al., 2020) in astrocytes, and SUR1 expression in endothelial cells (Alquisiras-Burgos et al., 2020) after ischemic stroke. Except for the endothelial cell and astrocyte, the interconnections between cells also contribute to brain edema. The neurovascular unit is a physiological and functional unit encompassing human brain microvascular endothelial cells, pericytes, smooth muscle cells, astrocytes, microglia, and neurons. The integrity of the neurovascular unit may determine the evolution of blood-brain barrier damage, neuronal death, and neuroinflammation. MMP-9 has been shown to degrade components of the basal lamina matrix. Some studies

found that resveratrol could inhibit MMP-2 and MMP-9 activity in human cerebral microvascular endothelial cells (Cavdar et al., 2012; Pandey et al., 2015; Wei et al., 2015), which maintain the integrity of the neurovascular unit and decrease BBB permeability. However, how resveratrol regulates cell-cell signaling in the neurovascular unit remains further studied.

Limitations

There are several limitations in terms of drawing definitive conclusions. 1) our study only included published data in English, which may lead to a certain degree of selective bias. 2) we limited outcomes measures in infarct volume and neurobehavioral score. Thus, we may disregard results seen in other outcomes. 3) the follow-up time in most included studies is 24 h, few studies evaluated the outcomes on 28 days post-stroke. Thus, it remains further research whether resveratrol plays an effective long-term treatment therapy for ischemic stroke.

Clinical Application

Some previous treatments that have shown great efficacy in animal studies have failed to apply in humans, possibly owing to the side effects, and narrow therapeutic time windows (Mergenthaler and Meisel, 2012). The present preclinical meta-analysis suggested that resveratrol has a relatively long therapeutic time window in the animal model. The administration timing of resveratrol in our included studies ranges from 30-days before ischemia onset to 3-days after ischemia onset. However, there is still significant work to be done for clinical application. First, age is one of the non-modifiable risk factors of ischemic stroke (Campbell and Khatri, 2020). Nevertheless, the included studies are based almost exclusively on healthy adult animals. It is doubtful whether resveratrol can achieve the same effect in the elderly animal models. In addition, no studies in the present meta-analysis evaluated the potential side effects of resveratrol injection on ischemic stroke. Resveratrol, when administered at a high dose (1,000 mg/kg/day), may cause renal and hepatic toxicity (Crowell et al., 2004; Rocha et al., 2009). We are incapable of evaluating the safety of resveratrol treatment from the meta-analysis. However, a previous clinical study suggested that resveratrol 2000 mg twice daily was well tolerated by healthy subjects (la Porte et al., 2010). Thus, the translation of resveratrol for the therapy of ischemic stroke is promising.

CONCLUSION

Based on the data of this meta-analysis, resveratrol treatment presents neuroprotection compared with control groups, by assessing the treatment outcomes including infarct volume, and neurobehavioral score. Furthermore, we suggested that the dosage ranging from 20 to 50 mg/kg showed the greatest efficacy. The results of this meta-analysis may provide certain references and a baseline for further preclinical and clinical studies with important implications for human health.

DATA AVAILABILITY STATEMENT

The original contributions presented in the study are included in the article/**Supplementary Material**, further inquiries can be directed to the corresponding author.

AUTHOR CONTRIBUTIONS

JL: Conceptualization, Methodology, Software. JL and ZH: Data curation, Writing—Original draft preparation. JL and JH: Visualization, Investigation. JH and YH: Supervision, Software, Validation. ZH: Writing—Reviewing and Editing.

FUNDING

This work was supported by Grants from the National Natural Science Foundation of China (No. 81974213).

SUPPLEMENTARY MATERIAL

The Supplementary Material for this article can be found online at: https://www.frontiersin.org/articles/10.3389/fphar.2021.795409/full#supplementary-material

Supplementary Figure 1 | Forest plot shows mean effect size and 95 % CI for **(A)** infarction outcome assessed by cresyl violet-staining/silver-staining/MRI, **(B)** rotarod tests between resveratrol therapy group and control group. Weights have been calculated using random effects model. Degree of heterogeneity in the pooled estimates is represented at I2 statistic. Abbreviations: SMD, standardized mean difference; CI: confidence interval.

REFERENCES

Abd Aziz, N. A. W., Iezhitsa, I., Agarwal, R., Abdul Kadir, R. F., Abd Latiff, A., and Ismail, N. M. (2020). Neuroprotection by Trans-resveratrol against Collagenase-Induced Neurological and Neurobehavioural Deficits in Rats Involves Adenosine A1 Receptors. *Neurol. Res.* 42 (3), 189–208. doi:10.1080/01616412.2020.1716470

Abdel-Aleem, G. A., Khaleel, E. F., Mostafa, D. G., and Elberier, L. K. (2016). Neuroprotective Effect of Resveratrol against Brain Ischemia Reperfusion Injury in Rats Entails Reduction of DJ-1 Protein Expression and Activation of PI3K/Akt/GSK3b Survival Pathway. *Arch. Physiol. Biochem.* 122 (4), 200–213. doi:10.1080/13813455.2016.1182190

Al Dera, H. (2017). Neuroprotective Effect of Resveratrol against Late Cerebral Ischemia Reperfusion Induced Oxidative Stress Damage Involves Upregulation of Osteopontin and Inhibition of Interleukin-1beta. *J. Physiol. Pharmacol.* 68 (1), 47–56.

Alquisiras-Burgos, I., Ortiz-Plata, A., Franco-Pérez, J., Millán, A., and Aguilera, P. (2020). Resveratrol Reduces Cerebral Edema through Inhibition of De Novo SUR1 Expression Induced after Focal Ischemia. *Exp. Neurol.* 330, 113353. doi:10.1016/j.expneurol.2020.113353

Amri, A., Chaumeil, J. C., Sfar, S., and Charrueau, C. (2012). Administration of Resveratrol: What Formulation Solutions to Bioavailability Limitations? *J. Control. Release* 158 (2), 182–193. doi:10.1016/j.jconrel.2011.09.083

Asensi, M., Medina, I., Ortega, A., Carretero, J., Baño, M. C., Obrador, E., et al. (2002). Inhibition of Cancer Growth by Resveratrol Is Related to its Low

Bioavailability. *Free Radic. Biol. Med.* 33 (3), 387–398. doi:10.1016/s0891-5849(02)00911-5

Ashafaq, M., Intakhab Alam, M., Khan, A., Islam, F., Khuwaja, G., Hussain, S., et al. (2021). Nanoparticles of Resveratrol Attenuates Oxidative Stress and Inflammation after Ischemic Stroke in Rats. *Int. Immunopharmacol* 94, 107494. doi:10.1016/j.intimp.2021.107494

Bonsack, F., Alleyne, C. H., Jr., and Sukumari-Ramesh, S. (2017). Resveratrol Attenuates Neurodegeneration and Improves Neurological Outcomes after Intracerebral Hemorrhage in Mice. *Front Cell Neurosci* 11, 228. doi:10.3389/fncel.2017.00228

Brown, V. A., Patel, K. R., Viskaduraki, M., Crowell, J. A., Perloff, M., Booth, T. D., et al. (2010). Repeat Dose Study of the Cancer Chemopreventive Agent Resveratrol in Healthy Volunteers: Safety, Pharmacokinetics, and Effect on the Insulin-like Growth Factor axis. *Cancer Res.* 70 (22), 9003–9011. doi:10.1158/0008-5472.can-10-2364

Burkon, A., and Somoza, V. (2008). Quantification of Free and Protein-Bound Trans-resveratrol Metabolites and Identification of Trans-resveratrol-c/o-conjugated Diglucuronides - Two Novel Resveratrol Metabolites in Human Plasma. *Mol. Nutr. Food Res.* 52 (5), 549–557. doi:10.1002/mnfr.200700290

Campbell, B. C. V., and Khatri, P. (2020). Stroke. *Lancet* 396 (10244), 129–142. doi:10.1016/s0140-6736(20)31179-x

Cavdar, Z., Egrilmez, M. Y., Altun, Z. S., Arslan, N., Yener, N., Sayin, O., et al. (2012). Resveratrol Reduces Matrix Metalloproteinase-2 Activity Induced by Oxygen-Glucose Deprivation and Reoxygenation in Human Cerebral Microvascular Endothelial Cells. *Int. J. Vitam Nutr. Res.* 82 (4), 267–274. doi:10.1024/0300-9831/a000119

Chen, J., Bai, Q., Zhao, Z., Sui, H., and Xie, X. (2016). Resveratrol Improves Delayed R-tPA Treatment Outcome by Reducing MMPs. *Acta Neurol. Scand.* 134 (1), 54–60. doi:10.1111/ane.12511

Crowell, J. A., Korytko, P. J., Morrissey, R. L., Booth, T. D., and Levine, B. S. (2004). Resveratrol-associated Renal Toxicity. *Toxicol. Sci.* 82 (2), 614–619. doi:10.1093/toxsci/kfh263

Dong, W., Li, N., Gao, D., Zhen, H., Zhang, X., and Li, F. (2008). Resveratrol Attenuates Ischemic Brain Damage in the Delayed Phase after Stroke and Induces Messenger RNA and Protein Express for Angiogenic Factors. *J. Vasc. Surg.* 48 (3), 709–714. doi:10.1016/j.jvs.2008.04.007

Dou, Z., Rong, X., Zhao, E., Zhang, L., and Lv, Y. (2019). Neuroprotection of Resveratrol against Focal Cerebral Ischemia/Reperfusion Injury in Mice through a Mechanism Targeting Gut-Brain Axis. *Cell Mol Neurobiol* 39 (6), 883–898. doi:10.1007/s10571-019-00687-3

Durlak, J. A. (2009). How to Select, Calculate, and Interpret Effect Sizes. *J. Pediatr. Psychol.* 34 (9), 917–928. doi:10.1093/jpepsy/jsp004

Egger, M., Davey Smith, G., Schneider, M., and Minder, C. (1997). Bias in Meta-Analysis Detected by a Simple, Graphical Test. *BMJ* 315 (7109), 629–634. doi:10.1136/bmj.315.7109.629

Faggi, L., Pignataro, G., Parrella, E., Porrini, V., Vinciguerra, A., Cepparulo, P., et al. (2018). Synergistic Association of Valproate and Resveratrol Reduces Brain Injury in Ischemic Stroke. *Int. J. Mol. Sci.* 19 (1), 172. doi:10.3390/ijms19010172

Fang, L., Gao, H., Zhang, W., Zhang, W., and Wang, Y. (2015). Resveratrol Alleviates Nerve Injury after Cerebral Ischemia and Reperfusion in Mice by Inhibiting Inflammation and Apoptosis. *Int. J. Clin. Exp. Med.* 8 (3), 3219–3226.

Fisher, M., and Saver, J. L. (2015). Future Directions of Acute Ischaemic Stroke Therapy. *Lancet Neurol.* 14 (7), 758–767. doi:10.1016/s1474-4422(15)00054-x

Fonseca-Santos, B., and Chorilli, M. (2020). The Uses of Resveratrol for Neurological Diseases Treatment and Insights for Nanotechnology Based-Drug Delivery Systems. *Int. J. Pharm.* 589, 119832. doi:10.1016/j.ijpharm.2020.119832

Gao, D., Zhang, X., Jiang, X., Peng, Y., Huang, W., Cheng, G., et al. (2006). Resveratrol Reduces the Elevated Level of MMP-9 Induced by Cerebral Ischemia-Reperfusion in Mice. *Life Sci.* 78 (22), 2564–2570. doi:10.1016/j.lfs.2005.10.030

Grewal, A. K., Singh, N., and Singh, T. G. (2019). Effects of Resveratrol Postconditioning on Cerebral Ischemia in Mice: Role of the Sirtuin-1 Pathway. *Can. J. Physiol. Pharmacol.* 97 (11), 1094–1101. doi:10.1139/cjpp-2019-0188

Griñán-Ferré, C., Bellver-Sanchis, A., Izquierdo, V., Corpas, R., Roig-Soriano, J., Chillón, M., et al. (2021). The Pleiotropic Neuroprotective Effects of Resveratrol in Cognitive Decline and Alzheimer's Disease Pathology: From Antioxidant to Epigenetic Therapy. *Ageing Res. Rev.* 67, 101271. doi:10.1016/j.arr.2021.101271

He, Q., Li, Z., Wang, Y., Hou, Y., Li, L., and Zhao, J. (2017). Resveratrol Alleviates Cerebral Ischemia/reperfusion Injury in Rats by Inhibiting NLRP3 Inflammasome Activation through Sirt1-dependent Autophagy Induction. *Int. Immunopharmacol* 50, 208–215. doi:10.1016/j.intimp.2017.06.029

Hermann, D. M., Zechariah, A., Kaltwasser, B., Bosche, B., Caglayan, A. B., Kilic, E., et al. (2015). Sustained Neurological Recovery Induced by Resveratrol Is Associated with Angioneurogenesis rather Than Neuroprotection after Focal Cerebral Ischemia. *Neurobiol. Dis.* 83, 16–25. doi:10.1016/j.nbd.2015.08.018

Higgins, J. P., Thompson, S. G., Deeks, J. J., and Altman, D. G. (2003). Measuring Inconsistency in Meta-Analyses. *BMJ* 327 (7414), 557–560. doi:10.1136/bmj.327.7414.557

Higgins, J. P., and Thompson, S. G. (2002). Quantifying Heterogeneity in a Meta-Analysis. *Stat. Med.* 21 (11), 1539–1558. doi:10.1002/sim.1186

Hou, Y., Wang, K., Wan, W., Cheng, Y., Pu, X., and Ye, X. (2018). Resveratrol Provides Neuroprotection by Regulating the JAK2/STAT3/PI3K/AKT/mTOR Pathway after Stroke in Rats. *Genes Dis.* 5 (3), 245–255. doi:10.1016/j.gendis.2018.06.001

Huang, S. S., Tsai, M. C., Chih, C. L., Hung, L. M., and Tsai, S. K. (2001). Resveratrol Reduction of Infarct Size in Long-Evans Rats Subjected to Focal Cerebral Ischemia. *Life Sci.* 69 (9), 1057–1065. doi:10.1016/s0024-3205(01)01195-x

Hurtado, O., Hernández-Jiménez, M., Zarruk, J. G., Cuartero, M. I., Ballesteros, I., Camarero, G., et al. (2013). Citicoline (CDP-Choline) Increases Sirtuin1 Expression Concomitant to Neuroprotection in Experimental Stroke. *J. Neurochem.* 126 (6), 819–826. doi:10.1111/jnc.12269

Inoue, H., Jiang, F. X., Katayama, T., Osada, S., Umesono, K., and Namura, S. (2003). Brain protection by Resveratrol and Fenofibrate against Stroke Requires Peroxisome Proliferator-Activated Receptor α in Mice. *Neurosci. Lett.* 352, 203–206. doi:10.1016/j.neulet.2003.09.001

Ishrat, T., Mohamed, I. N., Pillai, B., Soliman, S., Fouda, A. Y., Ergul, A., et al. (2015). Erratum to: Thioredoxin-Interacting Protein: a Novel Target for Neuroprotection in Experimental Thromboembolic Stroke in Mice. *Mol. Neurobiol.* 51 (2), 779–780. doi:10.1007/s12035-014-9025-x

Jeong, S. I., Shin, J. A., Cho, S., Kim, H. W., Lee, J. Y., Kang, J. L., et al. (2016). Resveratrol Attenuates Peripheral and Brain Inflammation and Reduces Ischemic Brain Injury in Aged Female Mice. *Neurobiol. Aging* 44, 74–84. doi:10.1016/j.neurobiolaging.2016.04.007

Khoury, N., Koronowski, K. B., and Perez-Pinzon, M. A. (2016). Long-term Window of Ischemic Tolerance: An Evolutionarily Conserved Form of Metabolic Plasticity Regulated by Epigenetic Modifications? *J. Neurol. Neuromedicine* 1 (2), 6–12. doi:10.29245/2572.942x/2016/2.1021

Khoury, N., Xu, J., Stegelmann, S. D., Jackson, C. W., Koronowski, K. B., Dave, K. R., et al. (2019). Resveratrol Preconditioning Induces Genomic and Metabolic Adaptations within the Long-Term Window of Cerebral Ischemic Tolerance Leading to Bioenergetic Efficiency. *Mol. Neurobiol.* 56 (6), 4549–4565. doi:10.1007/s12035-018-1380-6

Koronowski, K. B., Dave, K. R., Saul, I., Camarena, V., Thompson, J. W., Neumann, J. T., et al. (2015). Resveratrol Preconditioning Induces a Novel Extended Window of Ischemic Tolerance in the Mouse Brain. *Stroke* 46 (8), 2293–2298. doi:10.1161/strokeaha.115.009876

Koronowski, K. B., Khoury, N., Saul, I., Loris, Z. B., Cohan, C. H., Stradecki-Cohan, H. M., et al. (2017). Neuronal SIRT1 (Silent Information Regulator 2 Homologue 1) Regulates Glycolysis and Mediates Resveratrol-Induced Ischemic Tolerance. *Stroke* 48 (11), 3117–3125. doi:10.1161/strokeaha.117.018562

la Porte, C., Voduc, N., Zhang, G., Seguin, I., Tardiff, D., Singhal, N., et al. (2010). Steady-State Pharmacokinetics and Tolerability of Trans-resveratrol 2000 Mg Twice Daily with Food, Quercetin and Alcohol (Ethanol) in Healthy Human Subjects. *Clin. Pharmacokinet.* 49 (7), 449–454. doi:10.2165/11531820-000000000-00000

Lanzillotta, A., Pignataro, G., Branca, C., Cuomo, O., Sarnico, I., Benarese, M., et al. (2013). Targeted Acetylation of NF-kappaB/RelA and Histones by Epigenetic Drugs Reduces post-ischemic Brain Injury in Mice with an Extended Therapeutic Window. *Neurobiol. Dis.* 49, 177–189. doi:10.1016/j.nbd.2012.08.018

Li, C., Yan, Z., Yang, J., Chen, H., Li, H., Jiang, Y., et al. (2010). Neuroprotective Effects of Resveratrol on Ischemic Injury Mediated by Modulating the Release of Neurotransmitter and Neuromodulator in Rats. *Neurochem. Int.* 56 (3), 495–500. doi:10.1016/j.neuint.2009.12.009

Li, W., Tan, C., Liu, Y., Liu, X., Wang, X., Gui, Y., et al. (2015). Resveratrol Ameliorates Oxidative Stress and Inhibits Aquaporin 4 Expression Following Rat Cerebral Ischemia-Reperfusion Injury. *Mol. Med. Rep.* 12 (5), 7756–7762. doi:10.3892/mmr.2015.4366

Li, W., Ye, A., Ao, L., Zhou, L., Yan, Y., Hu, Y., et al. (2020). Protective Mechanism and Treatment of Neurogenesis in Cerebral Ischemia. *Neurochem. Res.* 45 (10), 2258–2277. doi:10.1007/s11064-020-03092-1

Li, Z., Fang, F., Wang, Y., and Wang, L. (2016). Resveratrol Protects CA1 Neurons against Focal Cerebral Ischemic Reperfusion-Induced Damage via the ERK-CREB Signaling Pathway in Rats. *Pharmacol. Biochem. Behav.* 146-147, 21–27. doi:10.1016/j.pbb.2016.04.007

Li, Z., and Han, X. (2018). Resveratrol Alleviates Early Brain Injury Following Subarachnoid Hemorrhage: Possible Involvement of the AMPK/SIRT1/autophagy Signaling Pathway. *Biol. Chem.* 399 (11), 1339–1350. doi:10.1515/hsz-2018-0269

Li, Z., Pang, L., Fang, F., Zhang, G., Zhang, J., Xie, M., et al. (2012). Resveratrol Attenuates Brain Damage in a Rat Model of Focal Cerebral Ischemia via Up-Regulation of Hippocampal Bcl-2. *Brain Res.* 1450, 116–124. doi:10.1016/j.brainres.2012.02.019

Lin, Y., Chen, F., Zhang, J., Wang, T., Wei, X., Wu, J., et al. (2013). Neuroprotective Effect of Resveratrol on Ischemia/reperfusion Injury in Rats through TRPC6/CREB Pathways. *J. Mol. Neurosci.* 50 (3), 504–513. doi:10.1007/s12031-013-9977-8

Liu, Y., Yang, H., Jia, G., Li, L., Chen, H., Bi, J., et al. (2018). The Synergistic Neuroprotective Effects of Combined Rosuvastatin and Resveratrol Pretreatment against Cerebral Ischemia/Reperfusion Injury. *J. Stroke Cerebrovasc. Dis.* 27 (6), 1697–1704. doi:10.1016/j.jstrokecerebrovasdis.2018.01.033

Lopez, M. S., Dempsey, R. J., and Vemuganti, R. (2016). Resveratrol Preconditioning Induces Cerebral Ischemic Tolerance but Has Minimal Effect on Cerebral microRNA Profiles. *J. Cereb. Blood Flow Metab.* 36 (9), 1644–1650. doi:10.1177/0271678x16656202

Lu, X., Dong, J., Zheng, D., Li, X., Ding, D., and Xu, H. (2020). Reperfusion Combined with Intraarterial Administration of Resveratrol-Loaded Nanoparticles Improved Cerebral Ischemia-Reperfusion Injury in Rats. *Nanomedicine* 28, 102208. doi:10.1016/j.nano.2020.102208

Luca, S. V., Macovei, I., Bujor, A., Miron, A., Skalicka-Woźniak, K., Aprotosoaie, A. C., et al. (2020). Bioactivity of Dietary Polyphenols: The Role of Metabolites. *Crit. Rev. Food Sci. Nutr.* 60 (4), 626–659. doi:10.1080/10408398.2018.1546669

Ma, S., Fan, L., Li, J., Zhang, B., and Yan, Z. (2020). Resveratrol Promoted the M2 Polarization of Microglia and Reduced Neuroinflammation after Cerebral Ischemia by Inhibiting miR-155. *Int. J. Neurosci.* 130 (8), 817–825. doi:10.1080/00207454.2019.1707817

Macleod, M. R., O'Collins, T., Howells, D. W., and Donnan, G. A. (2004). Pooling of Animal Experimental Data Reveals Influence of Study Design and Publication Bias. *Stroke* 35 (5), 1203–1208. doi:10.1161/01.str.0000125719.25853.20

McDonald, M. W., Jeffers, M. S., Issa, L., Carter, A., Ripley, A., Kuhl, L. M., et al. (2021). An Exercise Mimetic Approach to Reduce Poststroke Deconditioning and Enhance Stroke Recovery. *Neurorehabil. Neural Repair* 35 (6), 471–485. doi:10.1177/15459683211005019

Mergenthaler, P., and Meisel, A. (2012). Do stroke Models Model Stroke? *Dis. Model. Mech.* 5 (6), 718–725. doi:10.1242/dmm.010033

Moher, D., Liberati, A., Tetzlaff, J., Altman, D. G., and Group, P. (2009). Preferred Reporting Items for Systematic Reviews and Meta-Analyses: the PRISMA Statement. *BMJ* 339 (10), b2535–1012. doi:10.1016/j.jclinepi.2009.06.00510.1136/bmj.b2535

Mokni, M., Elkahoui, S., Limam, F., Amri, M., and Aouani, E. (2007). Effect of Resveratrol on Antioxidant Enzyme Activities in the Brain of Healthy Rat. *Neurochem. Res.* 32 (6), 981–987. doi:10.1007/s11064-006-9255-z

Mota, M., Porrini, V., Parrella, E., Benarese, M., Bellucci, A., Rhein, S., et al. (2020). Neuroprotective Epi-Drugs Quench the Inflammatory Response and Microglial/macrophage Activation in a Mouse Model of Permanent Brain Ischemia. *J. Neuroinflammation* 17 (1), 361. doi:10.1186/s12974-020-02028-4

Narayanan, S. V., Dave, K. R., Saul, I., and Perez-Pinzon, M. A. (2015). Resveratrol Preconditioning Protects against Cerebral Ischemic Injury via Nuclear Erythroid 2-Related Factor 2. *Stroke* 46 (6), 1626–1632. doi:10.1161/strokeaha.115.008921

Orsu, P., Murthy, B. V., and Akula, A. (2013). Cerebroprotective Potential of Resveratrol through Anti-oxidant and Anti-inflammatory Mechanisms in Rats. *J. Neural Transm. (Vienna)* 120 (8), 1217–1223. doi:10.1007/s00702-013-0982-4

Pandey, A. K., Bhattacharya, P., Shukla, S. C., Paul, S., and Patnaik, R. (2015). Resveratrol Inhibits Matrix Metalloproteinases to Attenuate Neuronal Damage in Cerebral Ischemia: a Molecular Docking Study Exploring Possible Neuroprotection. *Neural Regen. Res.* 10 (4), 568–575. doi:10.4103/1673-5374.155429

Pang, C., Cao, L., Wu, F., Wang, L., Wang, G., Yu, Y., et al. (2015). The Effect of Trans-resveratrol on post-stroke Depression via Regulation of Hypothalamus-Pituitary-Adrenal axis. *Neuropharmacology* 97, 447–456. doi:10.1016/j.neuropharm.2015.04.017

Park, D. J., Kang, J. B., Shah, F. A., and Koh, P. O. (2019). Resveratrol Modulates the Akt/GSK-3β Signaling Pathway in a Middle Cerebral Artery Occlusion Animal Model. *Lab. Anim. Res.* 35, 18. doi:10.1186/s42826-019-0019-8

Pineda-Ramírez, N., Alquisiras-Burgos, I., Ortiz-Plata, A., Ruiz-Tachiquín, M.-E., Espinoza-Rojo, M., and Aguilera, P. (2020). Resveratrol Activates Neuronal Autophagy through AMPK in the Ischemic Brain. *Mol. Neurobiol.* 57 (2), 1055–1069. doi:10.1007/s12035-019-01803-6

Ren, J., Fan, C., Chen, N., Huang, J., and Yang, Q. (2011). Resveratrol Pretreatment Attenuates Cerebral Ischemic Injury by Upregulating Expression of Transcription Factor Nrf2 and HO-1 in Rats. *Neurochem. Res.* 36 (12), 2352–2362. doi:10.1007/s11064-011-0561-8

Rocha, K. K., Souza, G. A., Ebaid, G. X., Seiva, F. R., Cataneo, A. C., and Novelli, E. L. (2009). Resveratrol Toxicity: Effects on Risk Factors for Atherosclerosis and Hepatic Oxidative Stress in Standard and High-Fat Diets. *Food Chem. Toxicol.* 47 (6), 1362–1367. doi:10.1016/j.fct.2009.03.010

Sakata, Y., Zhuang, H., Kwansa, H., Koehler, R. C., and Doré, S. (2010). Resveratrol Protects against Experimental Stroke: Putative Neuroprotective Role of Heme Oxygenase 1. *Exp. Neurol.* 224 (1), 325–329. doi:10.1016/j.expneurol.2010.03.032

Saleh, M. C., Connell, B. J., Rajagopal, D., Khan, B. V., Abd-El-Aziz, A. S., Kucukkaya, I., et al. (2014). Co-administration of Resveratrol and Lipoic Acid, or Their Synthetic Combination, Enhances Neuroprotection in a Rat Model of Ischemia/reperfusion. *PLoS One* 9 (1), e87865. doi:10.1371/journal.pone.0087865

Sergides, C., Chirilă, M., Silvestro, L., Pitta, D., and Pittas, A. (2016). Bioavailability and Safety Study of Resveratrol 500 Mg Tablets in Healthy Male and Female Volunteers. *Exp. Ther. Med.* 11 (1), 164–170. doi:10.3892/etm.2015.2895

Shetty, A. K. (2011). Promise of Resveratrol for Easing Status Epilepticus and Epilepsy. *Pharmacol. Ther.* 131 (3), 269–286. doi:10.1016/j.pharmthera.2011.04.008

Shin, J. A., Lee, H., Lim, Y. K., Koh, Y., Choi, J. H., and Park, E. M. (2010). Therapeutic Effects of Resveratrol during Acute Periods Following Experimental Ischemic Stroke. *J. Neuroimmunol* 227 (1-2), 93–100. doi:10.1016/j.jneuroim.2010.06.017

Shin, J. A., Lee, K. E., Kim, H. S., and Park, E. M. (2012). Acute Resveratrol Treatment Modulates Multiple Signaling Pathways in the Ischemic Brain. *Neurochem. Res.* 37 (12), 2686–2696. doi:10.1007/s11064-012-0858-2

Simão, F., Pagnussat, A. S., Seo, J. H., Navaratna, D., Leung, W., Lok, J., et al. (2012). Pro-angiogenic Effects of Resveratrol in Brain Endothelial Cells: Nitric Oxide-Mediated Regulation of Vascular Endothelial Growth Factor and Metalloproteinases. *J. Cereb. Blood Flow Metab.* 32 (5), 884–895. doi:10.1038/jcbfm.2012.2

Singh, G., and Pai, R. S. (2015). Trans-resveratrol Self-Nano-Emulsifying Drug Delivery System (SNEDDS) with Enhanced Bioavailability Potential: Optimization, Pharmacokinetics and *In Situ* Single Pass Intestinal Perfusion (SPIP) Studies. *Drug Deliv.* 22 (4), 522–530. doi:10.3109/10717544.2014.885616

Sinha, K., Chaudhary, G., and Gupta, Y. K. (2002). Protective Effect of Resveratrol against Oxidative Stress in Middle Cerebral Artery Occlusion Model of Stroke in Rats. *Life Sci.* 71 (6), 655–665. doi:10.1016/s0024-3205(02)01691-0

Su, Q., Pu, H., and Hu, C. (2016). Neuroprotection by Combination of Resveratrol and Enriched Environment against Ischemic Brain Injury in Rats. *Neurol. Res.* 38 (1), 60–68. doi:10.1080/01616412.2015.1133027

Teertam, S. K., Jha, S., and Prakash Babu, P. (2020). Up-regulation of Sirt1/miR-149-5p Signaling May Play a Role in Resveratrol Induced protection against Ischemia via P53 in Rat Brain. *J. Clin. Neurosci.* 72, 402–411. doi:10.1016/j.jocn.2019.11.043

Tsai, S. K., Hung, L. M., Fu, Y. T., Cheng, H., Nien, M. W., Liu, H. Y., et al. (2007). Resveratrol Neuroprotective Effects during Focal Cerebral Ischemia Injury via Nitric Oxide Mechanism in Rats. *J. Vasc. Surg.* 46 (2), 346–353. doi:10.1016/j.jvs.2007.04.044

Vahidy, F. S., Rahbar, M. H., Zhu, H., Rowan, P. J., Bambhroliya, A. B., and Savitz, S. I. (2016). Systematic Review and Meta-Analysis of Bone Marrow-Derived Mononuclear Cells in Animal Models of Ischemic Stroke. *Stroke* 47 (6), 1632–1639. doi:10.1161/strokeaha.116.012701

Walle, T. (2011). Bioavailability of Resveratrol. *Ann. N. Y Acad. Sci.* 1215, 9–15. doi:10.1111/j.1749-6632.2010.05842.x

Walle, T., Hsieh, F., DeLegge, M. H., Oatis, J. E., Jr., and Walle, U. K. (2004). High Absorption but Very Low Bioavailability of Oral Resveratrol in Humans. *Drug Metab. Dispos* 32 (12), 1377–1382. doi:10.1124/dmd.104.000885

Wan, D., Zhou, Y., Wang, K., Hou, Y., Hou, R., and Ye, X. (2016). Resveratrol Provides Neuroprotection by Inhibiting Phosphodiesterases and Regulating the cAMP/AMPK/SIRT1 Pathway after Stroke in Rats. *Brain Res. Bull.* 121, 255–262. doi:10.1016/j.brainresbull.2016.02.011

Wang, R., Liu, Y. Y., Liu, X. Y., Jia, S. W., Zhao, J., Cui, D., et al. (2014). Resveratrol Protects Neurons and the Myocardium by Reducing Oxidative Stress and Ameliorating Mitochondria Damage in a Cerebral Ischemia Rat Model. *Cell Physiol Biochem* 34 (3), 854–864. doi:10.1159/000366304

Wei, H., Wang, S., Zhen, L., Yang, Q., Wu, Z., Lei, X., et al. (2015). Resveratrol Attenuates the Blood-Brain Barrier Dysfunction by Regulation of the MMP-9/TIMP-1 Balance after Cerebral Ischemia Reperfusion in Rats. *J. Mol. Neurosci.* 55 (4), 872–879. doi:10.1007/s12031-014-0441-1

Williams, L. D., Burdock, G. A., Edwards, J. A., Beck, M., and Bausch, J. (2009). Safety Studies Conducted on High-Purity Trans-resveratrol in Experimental Animals. *Food Chem. Toxicol.* 47 (9), 2170–2182. doi:10.1016/j.fct.2009.06.002

Yan, W., Fang, Z., Yang, Q., Dong, H., Lu, Y., Lei, C., et al. (2013). SirT1 Mediates Hyperbaric Oxygen Preconditioning-Induced Ischemic Tolerance in Rat Brain. *J. Cereb. Blood Flow Metab.* 33 (3), 396–406. doi:10.1038/jcbfm.2012.179

Yan, Y., Tong, F., and Chen, J. (2019). Endogenous BMP-4/ROS/COX-2 Mediated IPC and Resveratrol Alleviated Brain Damage. *Curr. Pharm. Des.* 25 (9), 1030–1039. doi:10.2174/1381612825666190506120611

Yang, H., Zhang, A., Zhang, Y., Ma, S., and Wang, C. (2016). Resveratrol Pretreatment Protected against Cerebral Ischemia/Reperfusion Injury in Rats via Expansion of T Regulatory Cells. *J. Stroke Cerebrovasc. Dis.* 25 (8), 1914–1921. doi:10.1016/j.jstrokecerebrovasdis.2016.04.014

Yao, Y., Zhou, R., Bai, R., Wang, J., Tu, M., Shi, J., et al. (2020). Resveratrol Promotes the Survival and Neuronal Differentiation of Hypoxia-Conditioned Neuronal Progenitor Cells in Rats with Cerebral Ischemia. *Front. Med.* 15, 472–485. doi:10.1007/s11684-021-0832-y

Yousuf, S., Atif, F., Ahmad, M., Hoda, N., Ishrat, T., Khan, B., et al. (2009). Resveratrol Exerts its Neuroprotective Effect by Modulating Mitochondrial Dysfunctions and Associated Cell Death during Cerebral Ischemia. *Brain Res.* 1250, 242–253. doi:10.1016/j.brainres.2008.10.068

Yu, P., Wang, L., Tang, F., Guo, S., Liao, H., Fan, C., et al. (2021). Resveratrol-mediated Neurorestoration after Cerebral Ischemic Injury - Sonic Hedgehog Signaling Pathway. *Life Sci.* 280, 119715. doi:10.1016/j.lfs.2021.119715

Yu, P., Wang, L., Tang, F., Zeng, L., Zhou, L., Song, X., et al. (2017). Resveratrol Pretreatment Decreases Ischemic Injury and Improves Neurological Function via Sonic Hedgehog Signaling after Stroke in Rats. *Mol. Neurobiol.* 54 (1), 212–226. doi:10.1007/s12035-015-9639-7

Zhao, Q., Che, X., Zhang, H., Tan, G., Liu, L., Jiang, D., et al. (2017). Thioredoxin-Interacting Protein Mediates Apoptosis in Early Brain Injury after Subarachnoid Haemorrhage. *Int. J. Mol. Sci.* 18 (4), 854. doi:10.3390/ijms18040854

Zhao, R., Zhao, K., Su, H., Zhang, P., and Zhao, N. (2019). Resveratrol Ameliorates Brain Injury via the TGF-β-Mediated ERK Signaling Pathway in a Rat Model of Cerebral Hemorrhage. *Exp. Ther. Med.* 18 (5), 3397–3404. doi:10.3892/etm.2019.7939

Zwetsloot, P. P., Van Der Naald, M., Sena, E. S., Howells, D. W., IntHout, J., De Groot, J. A., et al. (2017). Standardized Mean Differences Cause Funnel Plot Distortion in Publication Bias Assessments. *Elife* 6, e24260. doi:10.7554/eLife.24260

Conflict of Interest: The authors declare that the research was conducted in the absence of any commercial or financial relationships that could be construed as a potential conflict of interest.

Publisher's Note: All claims expressed in this article are solely those of the authors and do not necessarily represent those of their affiliated organizations, or those of the publisher, the editors and the reviewers. Any product that may be evaluated in this article, or claim that may be made by its manufacturer, is not guaranteed or endorsed by the publisher.

frontiers in Pharmacology

ORIGINAL RESEARCH
published: 14 February 2022
doi: 10.3389/fphar.2022.814942

Metabolomic Profiling of Brain Protective Effect of Edaravone on Cerebral Ischemia-Reperfusion Injury in Mice

Hui-fen Ma†, Fan Zheng†, Lin-jie Su, Da-wei Zhang, Yi-ning Liu, Fang Li, Yuan-yuan Zhang, Shuai-shuai Gong and Jun-ping Kou**

State Key Laboratory of Natural Medicines, Jiangsu Key Laboratory of TCM Evaluation and Translational Research, Department of Pharmacology of Chinese Materia Medica, School of Traditional Pharmacy, China Pharmaceutical University, Nanjing, China

OPEN ACCESS

Edited by:
Li-Nan Zhang,
Hebei Medical University, China

Reviewed by:
Achuthan Raghavamenon,
Amala Cancer Research Centre, India
Guoxiang Xie,
University of Hawaii Cancer Center, United States

***Correspondence:**
Shuai-shuai Gong
1520210030@cpu.edu.cn
Jun-ping Kou
junpingkou@cpu.edu.cn

†These authors have contributed equally to this work

Specialty section:
This article was submitted to Neuropharmacology, a section of the journal Frontiers in Pharmacology

Received: *14 November 2021*
Accepted: *14 January 2022*
Published: *14 February 2022*

Citation:
Ma H-f, Zheng F, Su L-j, Zhang D-w, Liu Y-n, Li F, Zhang Y-y, Gong S-s and Kou J-p (2022) Metabolomic Profiling of Brain Protective Effect of Edaravone on Cerebral Ischemia-Reperfusion Injury in Mice. Front. Pharmacol. 13:814942. doi: 10.3389/fphar.2022.814942

Edaravone (EDA) injection has been extensively applied in clinics for treating stroke. Nevertheless, the metabolite signatures and underlying mechanisms associated with EDA remain unclear, which deserve further elucidation for improving the accurate usage of EDA. Ischemia stroke was simulated by intraluminal occlusion of the right middle cerebral artery for 1 h, followed by reperfusion for 24 h in mice. Brain infarct size, neurological deficits, and lactate dehydrogenase (LDH) levels were improved by EDA. Significantly differential metabolites were screened with untargeted metabolomics by cross-comparisons with pre- and posttreatment of EDA under cerebral ischemia/reperfusion (I/R) injury. The possibly involved pathways, such as valine, leucine, and isoleucine biosynthesis, and phenylalanine, taurine, and hypotaurine metabolisms, were enriched with differential metabolites and relevant regulatory enzymes, respectively. The network of differential metabolites was constructed for the integral exhibition of metabolic characteristics. Targeted analysis of taurine, an important metabolic marker, was performed for further validation. The level of taurine decreased in the MCAO/R group and increased in the EDA group. The inhibition of EDA on cerebral endothelial cell apoptosis was confirmed by TdT-mediated dUTP nick-end labeling (TUNEL) stain. Cysteine sulfinic acid decarboxylase (CSAD), the rate-limiting enzyme of taurine generation, significantly increased along with inhibiting endothelial cell apoptosis after treatment of EDA. Thus, CSAD, as the possible new therapeutic target of EDA, was selected and validated by Western blot and immunofluorescence. Together, this study provided the metabolite signatures and identified CSAD as an unrecognized therapeutic intervention for EDA in the treatment of ischemic stroke *via* inhibiting brain endothelial cell apoptosis.

Keywords: metabolomic, edaravone, ischemia stroke, taurine, endothelial cells

Abbreviations: CSAD, cysteine sulfinic acid decarboxylase; EDA, edaravone; LDH, lactate dehydrogenase; MCAO/R, middle cerebral artery occlusion/reperfusion; TUNEL, TdT-mediated dUTP nick-end labeling; H&E, hematoxylin and eosin; EC, endothelial cell; I/R, ischemia/reperfusion.

INTRODUCTION

Stroke, one of the neurovascular diseases, is the leading cause of disability and death globally, resulting from an increasing burden of vascular risk factors. Ischemic stroke is the most common type, accounting for 70% of all strokes (Benjamin et al., 2019; Montaner et al., 2020). Although the precise mechanism underlying ischemic injury has not been fully elucidated, vascular pathology has been reported the most common cause. As a part of the vascular pathologies, endothelial cell (EC) death could affect the surrounding cellular environment, which made it a potential target mechanism for the treatment and prevention of stroke, and ECs line the entire microvasculature and are also important for maintaining normal brain function. Therefore, it is necessary to choose the appropriate drugs for ischemic stroke.

Edaravone injection (EDA), as a commonly neurovascular protective agent, has been widely used in patients with acute ischemic stroke owing to its scavenging effect on oxygen-free radical and neurovascular protective effects (Kikuchi et al., 2013). It has been proven that EDA attenuates the Ca^{2+}-induced swelling of mitochondria and inhibits neuron apoptosis by decreasing the expression of Fas-associated death domain protein, death-associated protein, and caspase-8 immunoreactivity in the middle cerebral artery occlusion (MCAO) model (Zhang et al., 2005). EDA could suppress the response to endoplasmic reticulum stress and subsequent apoptotic signaling in hypoxic/ischemic injury and exhibit neuroprotective effects *via* its antioxidant actions, such as suppression of lipid peroxidation and oxidant-induced DNA damage (Amemiya et al., 2005; Yung et al., 2007). In addition, EDA also could inhibit vascular endothelial growth factor (VEGF) expression, aquaporin-4 expression, nuclear factor-κB (NF-κB), inducible nitric oxide synthase (iNOS), cytokines, cyclooxygenase-2, reactive oxygen species (ROS) generation, and ROS-induced inflammatory reactions in stroke mice and patients (Kikuchi et al., 2013). However, few of the literature comprehensively elucidate action characteristics of EDA; thus, further studies are still needed.

Metabolites are small molecules (typically <1.5 kDa), including lipids, amino acids, carbohydrates, and nucleotides, that could reflect the downstream function of the gene, protein expression, and environmental changes, such as drug intake; as a result, metabolome could provide information about related mechanisms (Shah et al., 2012). What is more, disease-specific metabolites can be biomarkers for the diagnosis of diseases and provide reference for the precise use of drugs in the clinic. The functional characteristics of Huang-Lian-Jie-Du decoction and gross saponins of *Tribulus terrestris* fruit were elucidated for ischemic stroke with metabolomics (Fu et al., 2019; Wang et al., 2019). By contrast, the value of metabolites of EDA for stroke has not been systematically studied. Therefore, the metabolomics was selected to investigate the potential mechanism of EDA.

Herein, we intended to discover the therapeutic mechanism of EDA for stroke as comprehensively as possible according to the metabolite variation characteristics. In this study, untargeted metabolic profiling was applied to examine the serum and urine metabolic signature of EDA for improving stroke. The metabolic network was constructed with differential metabolites. Finally, we performed targeted metabolic profiling and verified the potential therapeutic targets.

MATERIALS AND METHODS

Chemicals and Reagents

The standard compounds of taurine and caffeic acid were obtained from Shanghai Yuanye Bio-technology Co., Ltd. (Shanghai, China). Deionized water used in the experiment was supplied by a Milli-Q Academic ultrapure water system (Milford, Millipore, United States). Acetonitrile and methanol were obtained from Merck (Chromatographic, Germany); formic acid was obtained from Tedia (Chromatographic, United States). Edaravone injection was obtained from China National Medicines Guorui pharmaceutical Co., Ltd. (Anhui, China; lot number: 2005018). The lactate dehydrogenase (LDH) assay kit was purchased from Nanjing Jiancheng Bioengineering Institute (Nanjing, China), and cysteine sulfinic acid decarboxylase (CSAD) was obtained from Abcam (Cambridge, England).

Animals and Middle Cerebral Artery Occlusion/Reperfusion (MCAO/R) Model

Adult male specified-pathogen-free (SPF) C57BL/6J mice weighing 18–22 g were obtained from the Experimental Animal Research Centre of Yangzhou University (Yangzhou, China; certificate no SCXK 2017–0007). All experimental protocols were performed according to the National Institutes of Health (NIH) guidelines and the research was approved by the Institutional Animal Care and Use Committee of the Animal Ethics Committee of the School of Chinese Materia Medica, China Pharmaceutical University. All mice were housed with a 12:12 h light–dark cycle at 23 ± 1°C. Prior to experiments, mice were split randomly into three groups: sham, MCAO/R, and MCAOR + EDA. Stroke was induced by the MCAO/R model in mice as reported previously (Cao et al., 2016). In addition, the right middle cerebral artery was occluded with a blunt-tip 6-0 nylon monofilament for 1 h. Then the animals were reperfused by the careful withdrawal of the filament. Sham-operated control mice underwent the same surgical procedures except for the occlusion by nylon monofilament. EDA was administrated intraperitoneally to mice with 3 mg/kg (refer to the clinical dose) after 1 h of ischemia, the remaining model mice were given an equal volume of normal saline. Neurological function was evaluated at 24 h after reperfusion. Neurological deficit was graded on a score of 0–4 as previously reported (Cao et al., 2016) with slight modifications, as follows: 0, no observable deficit; 1, forelimb flexion and preference to walk in one direction; 2, unable to walk straight or to turn in both directions, circling to the affected side when held by the tail on the bench; 3, circling on the spot and walking circling; and 4, no spontaneous locomotor activity or barrel rolling, upon stimulation circling.

Hematoxylin and Eosin (H&E) Staining

H&E staining was used for histomorphological analysis. In short, brain slices were put into hematoxylin and eosin solution, redehydrated in gradient ethanol solution again, treated with dimethylbenzene, and covered with coverslips. The pathological images were scanned with a digital pathological section scanner (Hamamatsu, Japan) and analyzed with NDPView2 software.

TTC Staining

After ischemia/reperfusion (I/R), mice were euthanized and perfused by normal saline. Then, the whole brains were taken out, frozen at −20° followed by cutting into 1 mm thick slices rapidly. These brain slices were incubated in 1% TTC for 10 min at 37°C. The infarcted areas were analyzed with ImageJ software (NIH, Bethesda, MD).

Transmission Electron Microscopy

After I/R, mice were euthanized and perfused by normal saline followed by perfusion with the fixative (2% glutaraldehyde and 2% lanthanum nitrate in 0.1M sodium cacodylate pH 7.4–7.5) at room temperature, as previously described (Wang Q. et al., 2007). 1 mm^3 sample obtained from the region encompassing ischemic infarction of removed brains was kept in the same fixative overnight at 4°C. The samples were postfixed in 1% osmium tetroxide for 1 h followed by embedding in Epon 812. After polymerization, three blocks were randomly selected from each brain sample. An Ultratome (Nova, LKB, Bromma, Sweden) was used for cutting ultrathin sections. Then, ultrath insections were mounted on mesh grids (6–8 sections/grid) and stained with uranyl acetate and lead citrate. Finally, the prepared samples were examined under a transmission electron microscope (JEOL Ltd., Tokyo, Japan).

Untargeted Metabolomics Analysis

Sample Pretreatment

Serum and urine of mice were collected after 24 h reperfusion. After standing for about 60 min, the blood was centrifuged with 3,500 r/min for 10 min at 15°C. The obtained serum samples were sub-packed and stored at −80°C until the analysis. Urine samples were collected at 4°C and kept at −80 °C until the analysis. 200 μl of serum and urine were used for untargeted metabolomics analysis and 600 μl of methanol was added into samples for precipitating protein. Samples were subsequently centrifuged (13,000 rpm, 15 min) at 4°C followed by swirling 60 s. The supernatant was transferred to a tube and dried under a gentle stream of nitrogen at room temperature. Then, the residue was dissolved with 200 μl methanol and centrifuged (13,000 rpm, 15 min) at 4°C for further analysis.

HPLC-Q-TOF/MS Analysis

The detection of metabolites in urine and serum samples was performed on an Agilent Technologies 6540 Accurate-Mass Q-TOF LC/MS (United States) with electrospray ionization (ESI) source and the data were collected by a mass hunter workstation. The eluant A and B were deionized water (0.1% formic acid) and acetonitrile (0.1% formic acid), respectively. Serum analyses were achieved on a SynergiTM Fusion-RP C18 column (50 × 2 mm i.d., 2.5 μm) with a gradient elution program: 0–5 min, 5–5% B; 5–10 min, 5–30% B; 10–15 min, 30–60% B; 15–20 min, 60–70% B; 20–22 min, 70–80% B; 22–25 min, 80–95% B; 25–30 min, 95–95% B. Urine analyses were achieved on a TSK-GEL Amide-80 column (150 × 2.0 mm i.d., 5 μm) with a gradient elution program: 0–7 min, 90–90% B; 7–9 min, 90–75% B; 9–11 min, 75–75% B; 11–13 min, 75–50% B; 13–20 min, 50–50% B. Both of the flow rates were set at 0.2 ml/min with the injection volume of 10 μl. The Q-TOF/MS operating parameters were set as follows: fragment voltage, 120 V; nebulizer gas, 35 psig; capillary voltage, 4000 V; drying gas flow rate, 9 L/min; temperature, 325°C; detection range, m/z 50–1,500 in full scan mass spectra. The MS data acquisition was carried out in positive and negative ionization modes.

Validation of System Stability

The repeatability and robustness of the experiment were validated with the pooled quality control sample (QC) (Peron et al., 2020). The QC sample was prepared to mix equal volumes (30 μl) of each test sample, and treated with the same method as the test samples. QC samples were randomly injected throughout the sequence list.

Data Analysis of Metabolomics Strategies

Before multivariate analysis, the data format (.mzdata) files obtained by MassHunter Workstation Software (version B.06.00, Agilent Technologies) were processed by XCMS software performing on the R+ package (R Foundation for Statistical Computing, Vienna, Austria), and the data pretreatment procedures include non-linear retention time alignment, peak discrimination, filtering, alignment, and matching. All detected peaks were tabulated with tR-m/z pairs and outputted for statistical analyses. In order to screen the significant compounds that were responsible for the difference between model and model + EDA, metabolomic strategies were subsequently used to dispose the data. Principal component analysis (PCA), orthogonal partial least square discriminant analysis (OPLS-DA), volcano Plot, and heatmap developed by Metaboanalyst (https://www.metaboanalyst.ca/) were adopted to do the preliminary screening. PCA is a multivariate technique which can select the typical variables from a data table by several linear transformations, and OPLS-DA is a supervised machine learning model. The online database including HMDB (http://www.hmdb.ca/), METLIN (http://metlin.scripps.edu/), and MassBank (http://www.massbank.jp/) was performed to identify the potential metabolites by matching with the message of ion fragments.

Targeted Analysis for Taurine by HPLC-QQQ-MS/MS

Targeted analysis was performed on a triple quadrupole tandem high-performance liquid chromatography-mass spectrometry (HPLC-QQQ-MS/MS) system (Agilent, 6465) with caffeic acid as the internal standard. Chromatographic separation was performed on a TSK-GEL Amide-80 column (150 × 2.0 mm i.d., 5 μm) with a gradient elution program: 0–1 min, 75–75% B;

1–2 min, 75–60% B; 2–3 min, 60–60% B; 3–5 min, 60–50% B. The mobile phase system consists of deionized water containing 0.1% formic acid (A) and acetonitrile containing 0.1% formic acid (B) at a flow rate of 0.2 ml/min. Multiple reaction monitoring transitions in the negative mode were performed at m/z124→79.9 for the target analyte taurine and m/z 179→135 for the internal standard compound. MS parameters for the LC-MS/MS system, including the fragment and voltage collision energy of taurine and internal standard were 110, 21, and 90 V, 17 V, respectively.

Western Blot Analysis

The RIPA buffer supplemented with protease inhibitor cocktail was adopted for lysing ischemic penumbra of the brain tissues, and obtained samples were used for Western blotting as described previously (Zhai et al., 2017). Protein concentration of tissues was determined by Bicinchoninic Acid (BCA) Protein Assay Kit (Biyuntian Biotech. Co., Ltd., China) after centrifuging (12,000 rpm, 10 min, 4°C). The supernatant was diluted by loading buffer to 1 μg/μl followed by heating at 100°C for 5 min. Equal protein amounts of different groups were electrophoresed on SDS-PAGE gels and transferred to a polyvinylidene fluoride (PVDF) membrane. Then, the obtained PVDF membrane was blocked with 5% BSA solution for 2 h and incubated with specific primary antibodies overnight at 4°C followed by suitable secondary antibodies at room temperature for 2 h. Protein signals were detected with the ECL plus system and imaged by the gel imaging system (BioRad, Hercules, CA, United States). The protein levels were calculated by protein signals to correlative GAPDH or β-actin.

Immunofluorescence Staining

After perfusion with PBS and 4% paraformaldehyde, brain tissues were picked up and put into 4% paraformaldehyde. After 24 h, brain tissues were dehydrated with 40% sucrose for 5 days, embedded in OTC, and frozen at −80°C. Brain tissues were sectioned into slices of 10 μm thickness with a cryotome (Leica, Mannheim, Germany). Brain sections were fixed in 4% paraformaldehyde, permeabilized with 0.3% Triton X-100 in PBS, blocked with 5% bovine serum albumin, and incubated with specific primary antibodies overnight at 4°C. The next day, tissue sections were incubated with appropriate fluorescence-conjugated secondary antibodies at room temperature, and the cell nucleus was stained with DAPI. The immunofluorescence TUNEL assay was performed according to the instructions of the manufacturer. Fluorescent images were observed by confocal laser scanning microscopy (CLSM, LSM700, Zeiss, Germany).

Statistical Analysis

Student's t-test and one-way analysis of variance (ANOVA) followed by Dunnett's *post hoc* test operating on the GraphPad Prism 8.0 (Graph Pad Software, La Jolla, CA, United States) were used for analyzing two group comparisons and multiple comparisons, respectively. Differences were considered significant at $p < .05$.

RESULTS

EDA Effectively Ameliorated Brain Ischemia Reperfusion Injury in Mice

The results of TTC staining demonstrated the marked infarct area of the brain appeared after cerebral I/R and could be reduced by EDA (**Figures 1A,B**). H&E staining of brain sections showed that cerebral I/R induced cell loss and numerous vacuolated spaces, whereas EDA ameliorated such histopathological damage, as shown in **Figure 1C**. Additionally, the neurobehavioral deficits could be improved by EDA administration compared with the model group (**Figure 1D**). The electron microscope was applied for observing the morphology of endothelium, the key elements of the blood–brain barrier. Obviously, the endothelial cells were destroyed after cerebral I/R and improved by EDA (**Figure 1E**). The morphology of cerebral microvascular endothelial cells in MCAO/R mice changed. Additionally, the cell membrane integrity was also destroyed in MCAO/R mice. These injuries of microvascular endothelial cells could be improved by EDA. Besides, the level of LDH in serum increased in MCAO/R mice and could be significantly inhibited by EDA (**Figure 1F**). Taken together, EDA effectively alleviated the brain injury and inflammation in MCAO/R mice.

Multivariate Statistical Analysis of Metabolites in Urine and Serum Samples

Analytical stability was validated by contrasting the difference in retention time of the QC samples. The overlapped total ion chromatograms of QC samples showed that retention time deviation was acceptable (**Supplementary Figures 1A–D**). Three ions were randomly chosen from QC samples including serum-positive, serum-negative, urine-positive, and urine-negative to evaluate the system reproducibility in the metabolomic raw data acquisition throughout the whole experiment. The relative standard deviations (RSD) of the retention times and corresponding peak areas of the 3 selected ions in the QC samples were 0.59–2.54 and 1.14%–3.78%, as shown in **Table 1**. The results proved that the repeatability and stability of the HPLC-Q-TOF/MS system were reliable.

PCA was applied to perform unsupervised data analysis on Sham, MCAO/R, and EDA groups, and these groups could be easily distinguished from each other (**Figures 2A–D**). The phenomenon of the EDA group closing to the sham group compared with the MCAO/R group showed the improvement of EDA on brain injury. To screen the influential compounds that caused the difference between EDA and the model group, OPLS-DA was applied to classify the different samples and select the differential compounds from obtained data. **Figures 2E–H** suggested that the metabolic profiles in the EDA group were significantly different from those in the MCAO/R group in both urine and serum samples, and the ions of variable importance parameters (VIP > 1) were obtained. S-plot was applied to show those changed ions which significantly contributed to the classification between EDA and MCAO/R group (**Figures 2I–L**). Depending on VIP > 1 and p-value ($p < .05$) acquired

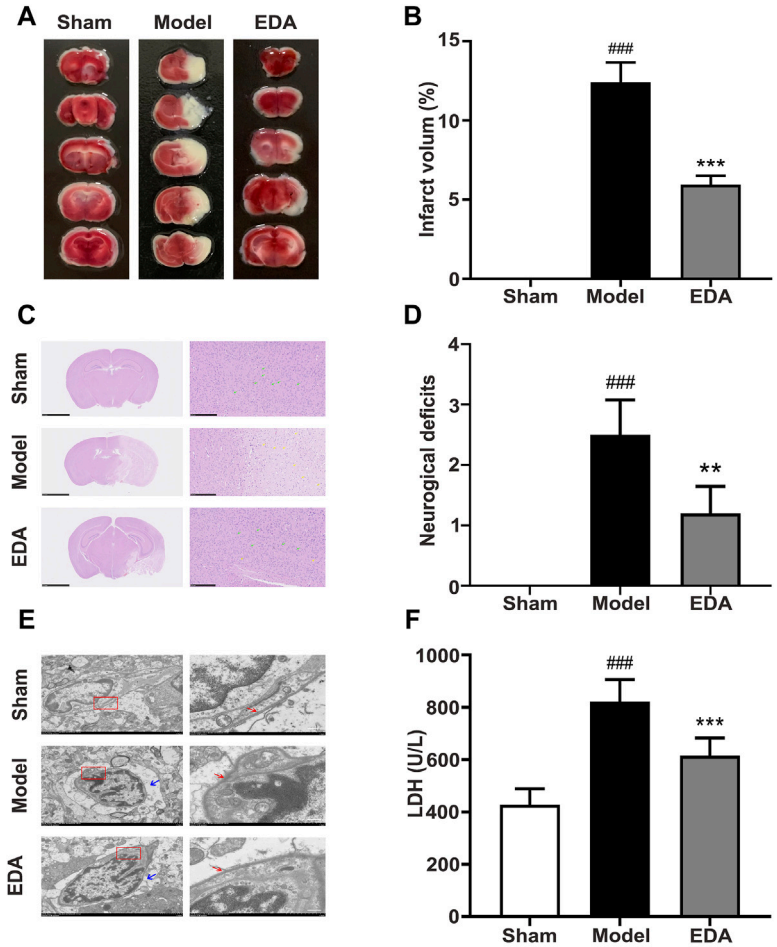

FIGURE 1 | EDA protects against cerebral I/R injury and endothelial injury. Mice were subjected to 1 h of ischemia, followed by 24 h of reperfusion. EDA (3 mg/kg) was administered intraperitoneally after ischemia. **(A)** Representative TTC-stained brain sections. **(B)** Quantitative analysis of infarct volume. **(C)** Stained H&E sections of mice brains. Shrunken cells with pyknotic nuclei are indicated with yellow arrows, while intact cells are indicated with green arrows. **(D)** Neurological deficit scores in different groups. **(E)** The structure and morphology of cerebral microvascular endothelial cells in different groups were examined by electron microscopy. Red arrow: brain microvascular endothelial cell membrane. Blue arrow: the degree of edema around brain microvascular endothelial cells. **(F)** LDH activity. All data are presented as the means ± SEM, $n = 6$. Scale bar = 50 μm. $^{\#}p < .05$, $^{\#\#}p < .01$, $^{\#\#\#}p < .001$, *vs*. Sham group, $^{*}p < .05$, $^{**}p < .01$, $^{***}p < .001$, *vs*. MCAO/R group.

TABLE 1 | Relative standard deviation (RSD%) of retention time and peak area in QC samples.

Sample	Model	m/z	Retention time (RSD%)	Peak area (RSD%)
Serum	Positive	203.0541	1.34	2.01
		274.2751	0.95	1.93
		675.6783	1.12	3.56
	Negative	215.0316	1.27	3.78
		809.2477	2.08	2.69
		279.2312	2.54	2.17
Urine	Positive	174.1122	1.83	2.98
		114.0654	0.81	1.74
		263.1456	1.96	3.14
	Negative	172.9869	1.53	1.14
		208.0667	0.59	1.22
		195.0460	1.21	1.65

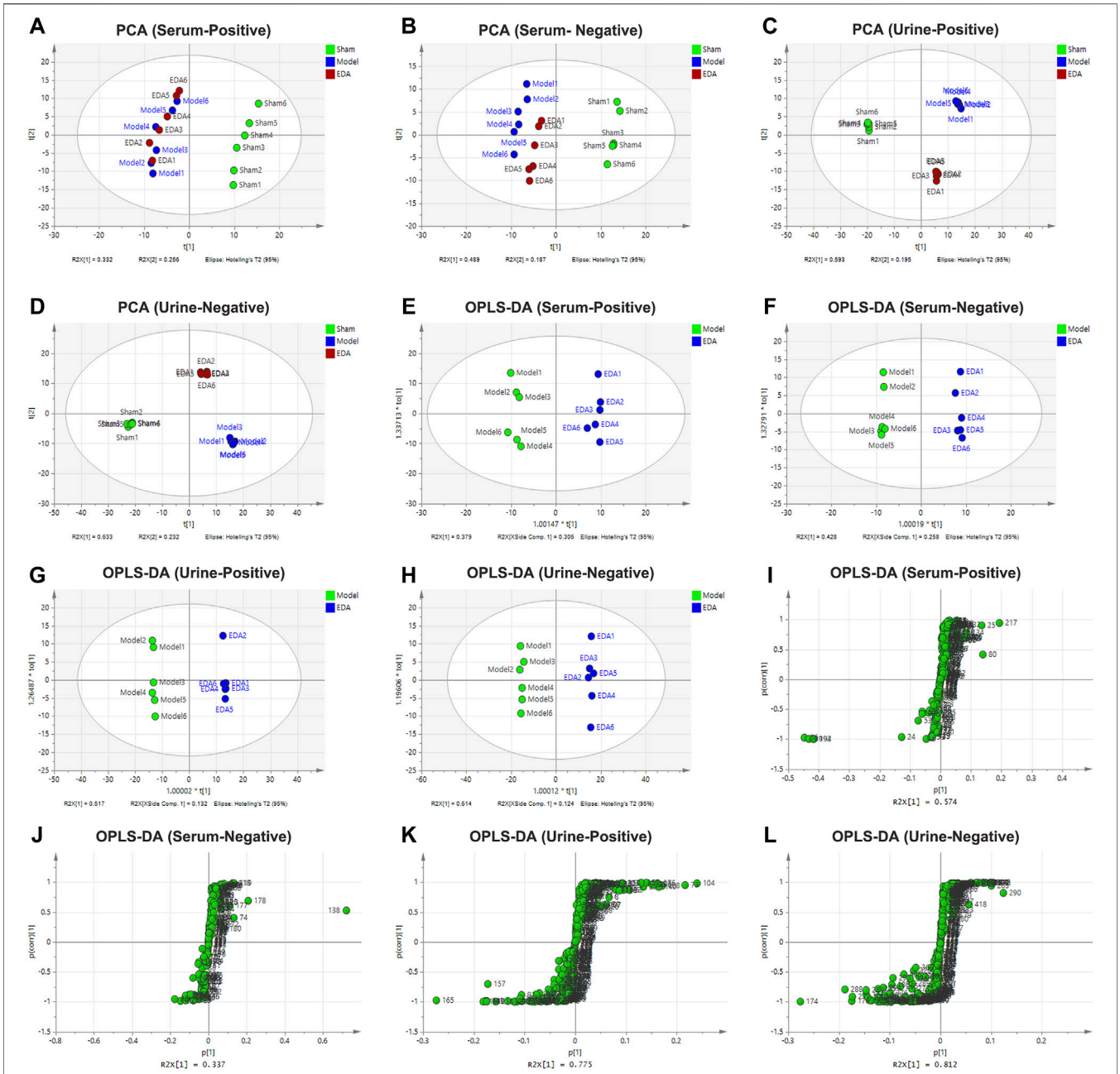

FIGURE 2 | PCA, OPLS-DA score plot, and S-plot of sham, model, and EDA group based on HPLC-Q-TOF/MS system for serum and urine analysis. **(A–D)** PCA score plot of model and EDA group. **(E–H)** OPLS-DA score plot of model and EDA group. **(I–L)** S-plot of model and EDA group.

through two-tailed Student's t-test and showed in volcano plot (**Figures 3A–D**), the variables can be selected for further screening. According to the above screening procedures, the ions were screened and the metabolites were identified, which were considered as potential biomarkers listed in **Supplementary Table S1**. Comparing EDA and MCAO/R groups, 51 and 56 differential metabolites were identified in serum and urine, respectively. The hierarchical clustering heatmap exhibited the change of metabolites more intuitively (**Figures 3E,F**). The heatmaps showed that EDA and MCAO/R could be grouped into two parts according to the identified metabolites. The above data exposed that numerous metabolites changed by EDA. Among these metabolites, taurine with 30.795 of fold change showed the greatest change.

Enrichment Analysis of Metabolic Pathway and Regulatory Enzymes Changed by EDA

In order to comprehensively observe the changes in metabolic pathways, Metaboanalyst 4.0 (https://www.metaboanalyst.ca/)

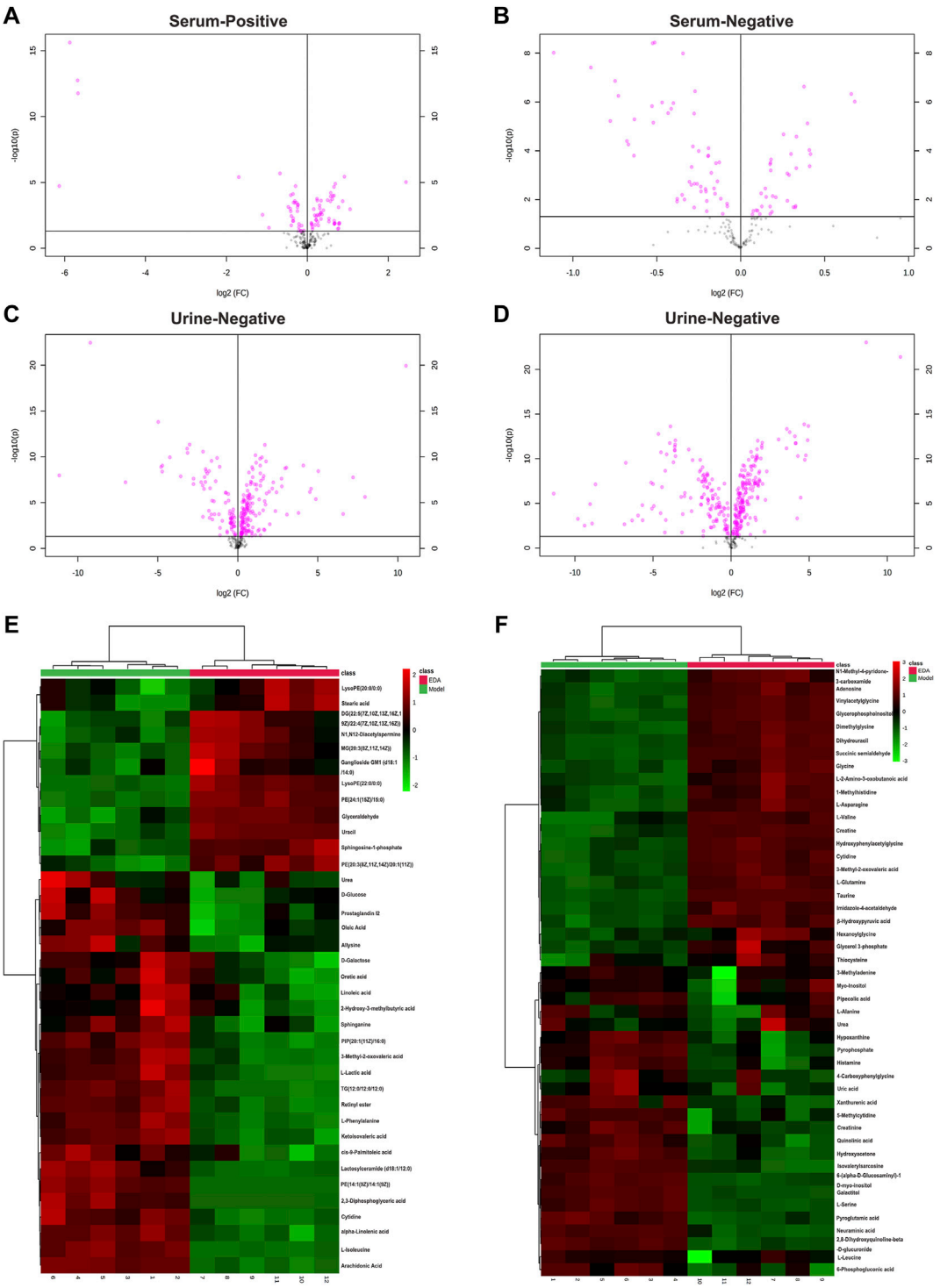

FIGURE 3 | Volcano plot and heatmap of the differential endogenous metabolites between the model and EDA group in serum and urine. **(A–D)** Volcano plot of model and EDA group. **(E)** Heatmap of the differential endogenous metabolites between the model and EDA group in serum. **(F)** Heatmap of the differential endogenous metabolites between the model and EDA group in urine. Red represented the metabolites in high abundance; green represented the metabolites in low abundance.

was applied for pathway and biological function enrichment by introducing all significant metabolites of serum and urine. The perturbed pathways including valine, leucine, and isoleucine biosynthesis, and phenylalanine, taurine, and hypotaurine metabolism were screened out (**Figures 4A,B**). And the correlations between biological functions are also shown in

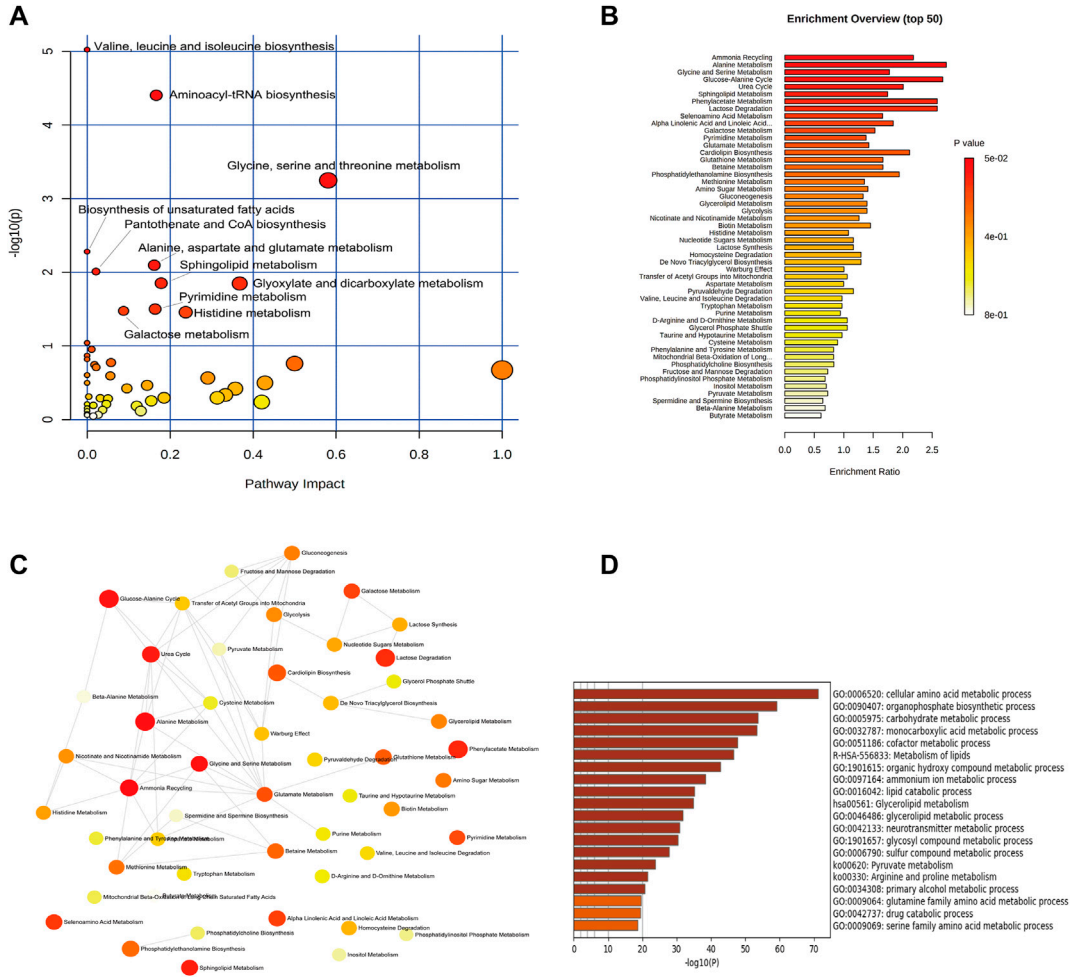

FIGURE 4 | Enrichment analysis of metabolic pathway and related regulatory enzymes. **(A)** Bubble plots of altered metabolic pathways. **(B)** Overview of biological function related to the differential endogenous metabolites. **(C)** Network map of pathways. **(D)** Regulatory enzyme GO enrichment analysis results.

Figure 4C. The results suggested that EDA could improve many pathways under MCAO/R. Moreover, the interaction network of related regulatory enzymes built up with STRING (https://string-db.org/) is exhibited in **Supplementary Figure S2A**. And the GO enrichment analysis of related regulatory enzymes performed by Metascape (https://www.metascape.org/) showed that cellular amino acid metabolic process, monocarboxylic acid metabolic process, metabolism of lipids, and so on were regulated by EDA (**Figure 4D**), and the relations of them are exhibited in **Supplementary Figure S2B**. According to the results described previously, a schematic diagram of the changed metabolic pathways in serum and urine is exhibited in **Figure 5**.

Semiquantitative Analysis of Taurine and Validation of CSAD Expression in Pre- and Posttreatment by EDA

Identification of taurine was characterized by MS profile and confirmed with a standard compound, as shown in **Supplementary Figure S3**. Analyses of all samples showed that taurine decreased in MCAO/R mice compared with sham groups and could be improved by EDA (**Figure 6A**). To explore the possible reasons for the change of taurine, the level of CSAD, which is the predominant enzyme that regulates taurine biosynthesis in the brain, was determined. The expression of CSAD in the brain decreased in MCAO/R mice and dramatically increased in mice with the treatment of EDA (**Figure 6B**). The results of immunofluorescent staining proved the same tendency of CSAD expression in brain ECs (**Figures 6C,D**). These results demonstrate that the level of taurine was increased by EDA through promoting the expression of CSAD.

EDA Alleviates MCAO/R Induced Brain EC Apoptosis *In Vivo*

As shown in **Figures 7A,B**, TUNEL assays of brain sections counterstained with CD31 to mark endothelium proved that TUNEL-positive brain ECs increased significantly in the MCAO/R mice, while the number of TUNEL-positive brain ECs was decreased after treatment with EDA. The levels of

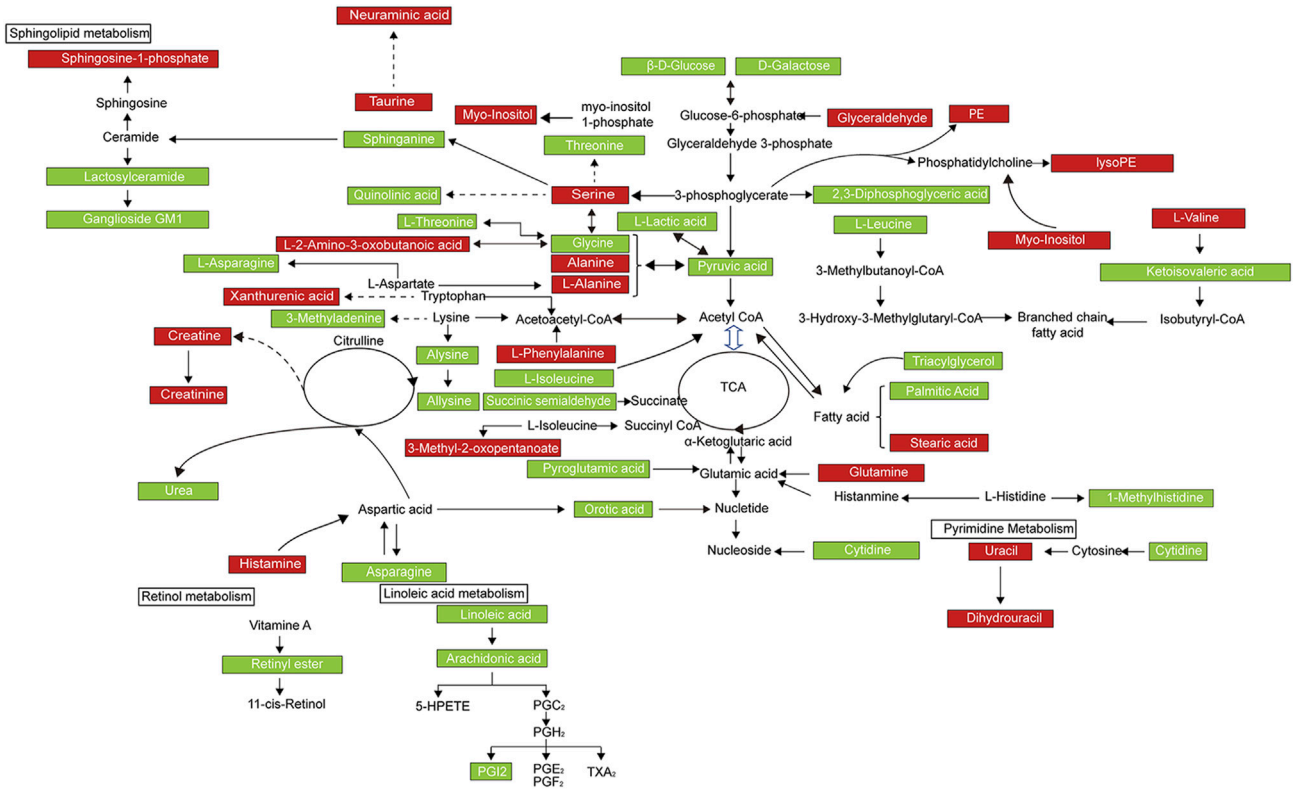

FIGURE 5 | Metabolic network of the significantly changed endogenous metabolites in both serum and urine. Compared with the model group, elevated metabolites in the EDA group were represented by red, and the reduced metabolites were represented by green.

apoptosis proteins were measured with Western blot. The results showed that EDA significantly inhibited the expression of Bax and cleaved caspase-3, and upregulated the expression of Bcl-2 compared with the MCAO/R group (**Figures 7C,D**). These results suggested that EDA had a protective effect on MCAO/R-induced brain EC apoptosis.

DISCUSSION

In this study, through analysis of high-through metabolomics data and multistep validations, we attempted to find the untapped therapeutic targets of EDA, a first-line drug for the clinical treatment of stroke, toward elucidating the therapeutic mechanisms. Initially, we verified that EDA could significantly decrease cerebral infarction, inflammatory infiltration, neurological deficits, endothelium injury, and apoptosis in MCAO/R mice (**Figure 1**). The above investigations showed that EDA could effectively alleviate the cerebral ischemia-reperfusion injury in MCAO/R mice, thereby providing reliable samples for subsequent metabolomic analysis.

The results of metabolomic analyses presented the metabolic signature of EDA improvement of cerebral I/R injury, offering insights into the therapeutic mechanisms (**Figure 5**). The metabolites influenced by EDA were mainly lipids, fatty acids in serum, and were mainly amino acids in urine. Notably, oleic acid, linoleic acid, triacylglycerol (TG), palmitic acid, prostaglandin I2, urea, and leucine were reduced by EDA, while sphingosine-1-phosphate, taurine, valine, glutamine, and creatine were improved by EDA, especially taurine (**Supplementary Table S1**). The increased level of oleic acid leads to mitochondrial-derived reactive oxygen species production, resulting in endothelial dysfunction and blood–brain barrier disruption (Han et al., 2013; Gremmels et al., 2015). Linoleic acid associated with cardiovascular and cerebrovascular diseases significantly activates pro-inflammatory signaling in ECs, such as PI3K/Akt and ERK1/2, thus causing vessel inflammation, endothelial dysfunction, and death (Hennig et al., 2006; Bin et al., 2013; Satoh, 2013; Marchix et al., 2015). Adults with high triacylglycerol have increased risks of incident coronary heart disease and stroke, while lowering triglyceride levels of serum improves endothelial function, leading to a decrease in cardiovascular diseases (Hirano et al., 2008; Kajikawa et al., 2016; Lee et al., 2017). Similarly, the elevated palmitic acid level is related to the development of inflammation and endothelial dysfunction (Yang et al., 2019). Palmitic acid also induces energy metabolism disorders and apoptosis *via* activation of the apoptotic mitochondrial pathway (Adrian et al., 2017; Wen et al., 2017). Additionally, excess prostaglandin I2, urea, and leucine could similarly result in vascular endothelial injury and even lead to the disruption of barrier (Dorovini-Zis et al., 1987; De Bock et al., 2013; Lau and Vaziri, 2017; d'Apolito et al., 2018; Zhenyukh et al., 2018). Vessel inflammation, endothelial dysfunction, and death were the main factors causing

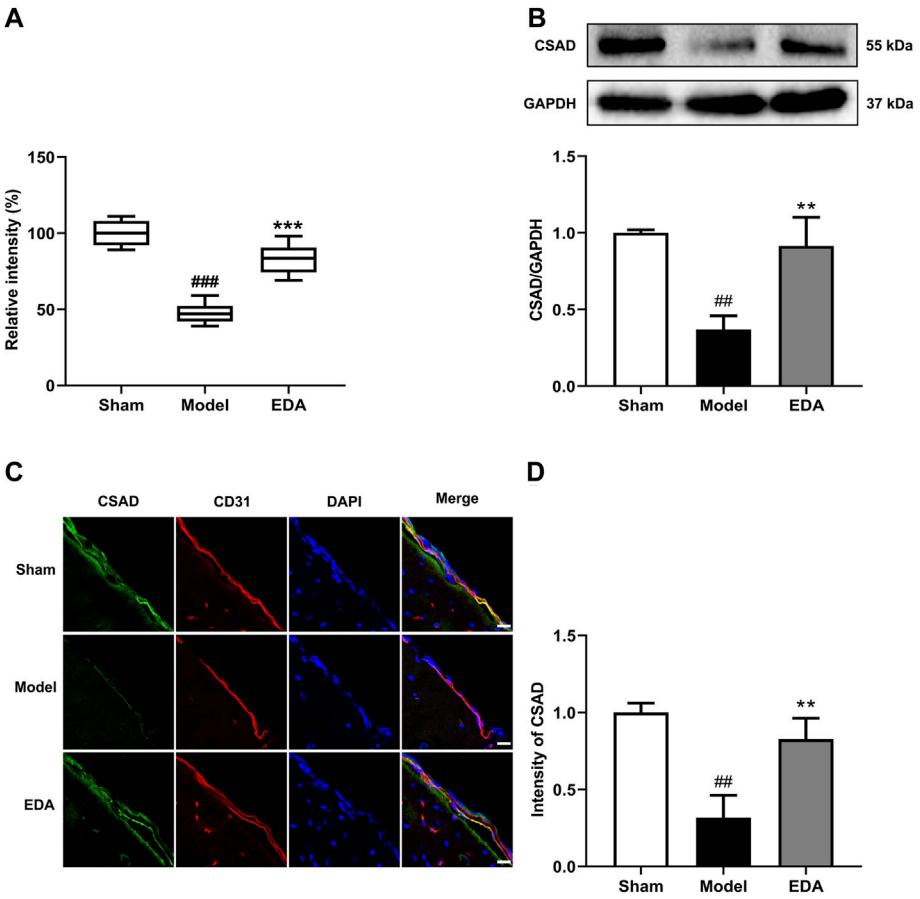

FIGURE 6 | Effect of EDA on taurine and CSAD in MCAO/R mice. **(A)** Level of taurine in the different groups. **(B)** Representative Western blots and quantitative analyses of CSAD expression. **(C)** Immunofluorescence staining for CSAD (green) and CD31 (red) were performed on frozen brain sections, and the nuclei were counterstained with DAPI (blue) (scale bar = 20 μm). **(D)** Quantitative analyses of CSAD expression in endothelial cells. All data are presented as the means ± SEM, $n = 6$. $^{\#}p < .05$, $^{\#\#}p < .01$, $^{\#\#\#}p < .001$, *vs.* Sham group, $^{*}p < .05$, $^{**}p < .01$, $^{***}p < .001$, *vs.* MCAO/R group.

cardiovascular and cerebrovascular diseases including stroke. Thus, reducing levels of differential metabolites damaging ECs is the potential mechanism of EDA for improving I/R injury. Sphingosine-1-phosphate, a bioactive intermediate of the sphingolipid metabolism, serves important physiological functions, such as proliferation, differentiation, survival, and migration, and is a key regulator of lymphocyte trafficking, endothelial barrier function, and vascular tone (Książek et al., 2015). Taurine, a semi-essential sulfur-containing amino acid, is present in several organs including the brain and has extensive physiological activities such as anti-inflammation and anti-oxidative stress, as well as regulation of energy metabolism, gene expression, osmosis, and quality control of protein. Thus, taurine protects against injuries of ECs and has potential ameliorating effects against cardiovascular diseases and neurological disorder events such as neurodegenerative diseases, stroke, and diabetic neuropathy (Ulrich-Merzenich et al., 2007; Murakami, 2014; Jakaria et al., 2019). Additionally, taurine has been reported to have a protective effect on the brain in stroke by down-regulating PARP and NF-κB, and activating GABAA and glycine receptors, as well as attenuating cell death (Wang GH. et al., 2007; Sun et al., 2012). Valine, one of the eight essential amino acids and sugar-producing amino acids for the human body, could promote the normal growth of the body, regulate protein and energy metabolism, and neurological functions (Shimomura and Kitaura, 2018). Glutamine metabolism is important for ECs in health and disease conditions, especially in cardiovascular diseases. Glutamine not only possesses potent antioxidant and anti-inflammatory effects in the circulation but also drives key processes in vascular cells, including proliferation, migration, apoptosis, senescence, and extracellular matrix deposition by serving as a substrate for the synthesis of DNA, ATP, proteins, and lipids (Rohlenova et al., 2018; Durante, 2019). Creatine exhibits ergogenic effects under a number of conditions including neurodegenerative diseases by maintaining cellular ATP stores. Moreover, creatine could improve ischemic stroke and other cerebrovascular diseases due to antioxidant activity, neurotransmitter-like behavior, and prevention of the opening of the mitochondrial permeability pore (Balestrino et al., 2016). The metabolites described above could replicate some of the previous research findings of the treatment of stroke. In this study, the level of oleic acid and palmitic acid decreased after treating with EDA, which appears to be in line with the treatment of gross saponins of *Tribulus*

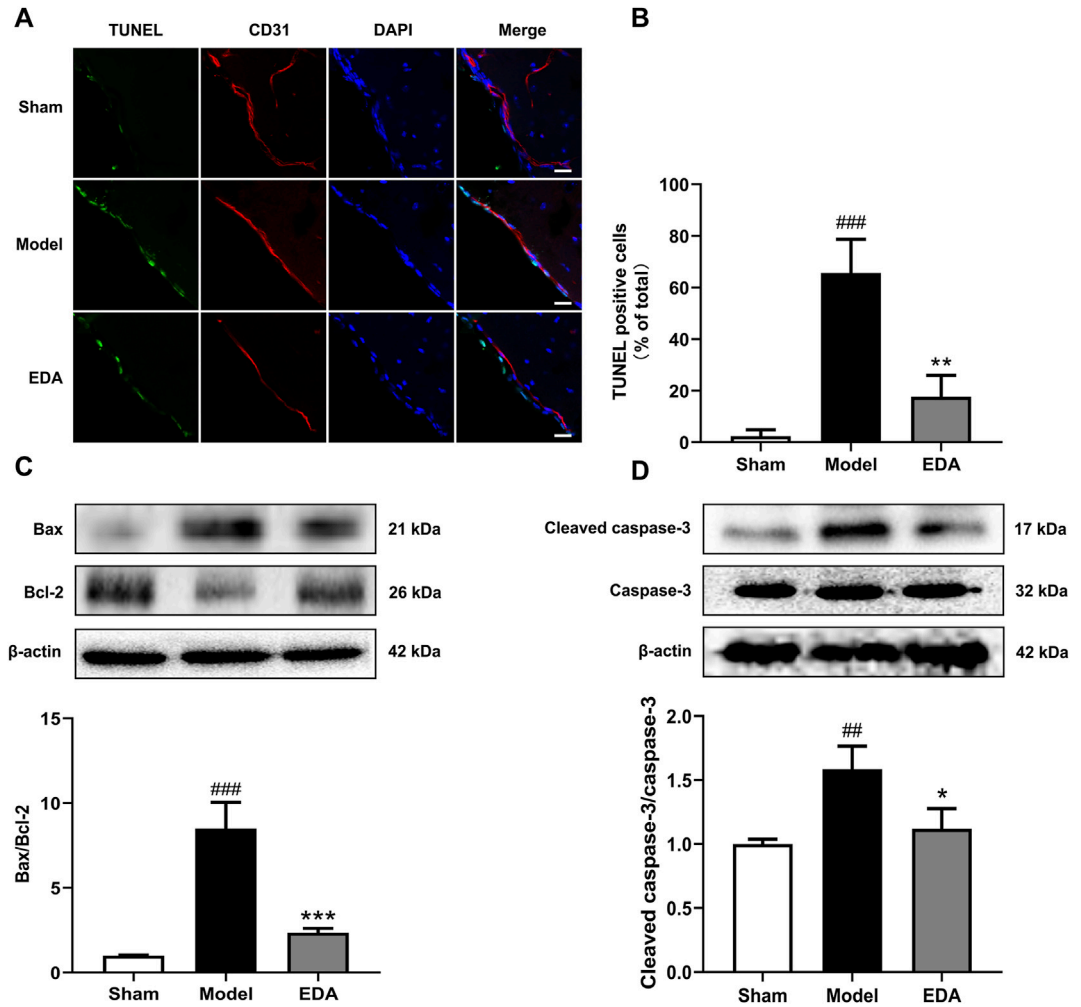

FIGURE 7 | EDA mitigates cerebral endothelial apoptosis stimulated by MCAO/R in mice. **(A)** Brain-frozen sections were stained with TUNEL (green) and CD31 was used as a marker for endothelial cells; the nuclei were stained with DAPI (blue) (scale bar = 20 μm). **(B)** Quantitative analyses of apoptotic cells in endothelial cells. **(C)** Western blot analysis for the expression of Bax and Bcl-2 in brain tissues. **(D)** Western blot analysis for the expression of cleaved caspase-3 in brain tissues. All data are presented as the means ± SEM, $n = 6$. $^{\#}p < .05$, $^{\#\#}p < .01$, $^{\#\#\#}p < .001$, *vs.* Sham group, $^{*}p < .05$, $^{**}p < .01$, $^{***}p < .001$, *vs.* MCAO/R group.

terrestris fruit (Wang et al., 2019). Similarly, the decrease of phenylalanine was in accordance with the previous report (Fu et al., 2019). Therefore, the possible mechanisms of EDA improvement of stroke were anti-inflammation and anti-oxidative stress, as well as a decrease of endothelial dysfunction and blood–brain barrier disruption by regulating the metabolites described above.

Subsequently, the pathways mediated by EDA were enriched with the differential metabolites. The results highlighted amino acid metabolisms, fatty acid metabolisms, and lipid metabolisms, such as valine, leucine, and isoleucine biosynthesis, biosynthesis of unsaturated fatty acids, sphingolipid metabolism as well as taurine and hypotaurine metabolism pathways (**Figures 4A–C**). As described above, valine, leucine, and isoleucine metabolism and most fatty acid metabolisms were directly associated with endothelial dysfunction through increasing reactive oxygen species generation and inflammation, and the change of these pathways, as well as taurine and hypotaurine metabolism, were the important pathological factors in stroke (Hennig et al., 2006; Gremmels et al., 2015; Zhenyukh et al., 2018). Consequently, EDA mainly improves endothelial dysfunction and blood–brain barrier function by interfering with these metabolic pathways, which might be the metabolism mechanism of EDA alleviating cerebral impairment induced by ischemia-reperfusion.

ECs are the key part of the blood–brain barrier which maintains the normal function of the central nervous system and metabolism activity of brain tissue. The death of ECs occurs at the primary stage of stroke which plays a vital role in the early impairment of neurological functions and may interfere with later recovery (Zille et al., 2019). Thus, EC is the potential target mechanism for the treatment of stroke. Interestingly, taurine, one of the mainly increased metabolites by EDA, possesses the effect of endothelium protection. EDA might inhibit the death of ECs by increasing the level of taurine. Hence, taurine was selected for

the follow-up validation to explore the potential targets of EDA. Our research demonstrated that EDA could effectively elevate the level of taurine. In order to further confirm the mechanism of EDA increase of taurine, the key regulatory enzymes of taurine were verified. CSAD is the key synthetase of taurine and expresses in the brain, while its biofunction in MCAO/R has not been clarified yet (Park et al., 2014). We found that EDA could significantly increase the expression of CSAD, which indicated that EDA might elevate the level of taurine in MCAO/R mice by increasing CSAD. Therefore, CSAD is a potential target of EDA therapy for stroke.

Apoptosis is a common way of cell death, and the apoptosis of ECs is an important pathological process in stroke (Yang et al., 2018). Bax, Bcl-2, and cleaved caspase-3 are the characteristic proteins of apoptosis. We found that EDA could effectively inhibit Bax, Bcl-2, and cleaved caspase-3 by increasing taurine (**Figure 7**). Thus, EDA inhibited apoptosis of ECs and ameliorated cerebral microvascular endothelial dysfunction, thereby alleviating brain injury induced by I/R. Meanwhile, the EC apoptosis was inhibited along with the expression of CSAD increasing. In summary, taurine and CSAD have a critical role in inhibiting ECs apoptosis, which might be an important metabolism mechanism of EDA treatment stroke.

Our current study still has several limitations. EDA treats stroke with many complex mechanisms. Numerous differential metabolites and pathways were found to be associated with therapeutic stroke of EDA. Thus, more differential metabolites need to be further investigated.

CONCLUSION

In the present study, a functional metabolomics strategy was used to characterize metabolite signatures and their underlying mechanisms associated with the therapeutic stroke of EDA. We not only constructed the differential metabolic network map providing clues for investigating mechanisms but also identified the biological function of taurine in the process of EDA improving stroke. It is interesting to note that taurine and its regulatory enzyme CSAD seem to play a key role in inhibiting EC apoptosis induced by I/R. Therefore, this study elucidated that EDA improves stroke *via* the influence of metabolites and provided a potential therapeutic target for stroke.

DATA AVAILABILITY STATEMENT

The original contributions presented in the study are included in the article/**Supplementary Material**, further inquiries can be directed to the corresponding authors.

ETHICS STATEMENT

The animal study was reviewed and approved by the Institutional Animal Care and Use Committee of the Animal Ethics Committee of the School of Chinese Materia Medica, China Pharmaceutical University.

AUTHOR CONTRIBUTIONS

H-fM, S-sG and J-pK conceived this project and designed the experiments. H-fM, FZ and L-jS performed most experiments and interpreted the data. D-wZ and Y-nL collected samples. FZ and Y-yZ aided in the data analysis. H-fM wrote the manuscript. J-pK, S-sG and FL revised the manuscript. All authors read and approved the final article.

FUNDING

This research was supported by the National Natural Science Foundation of China (Nos. 82074058, 82104438, and 82104437), Project funded by the China Postdoctoral Science Foundation (Nos. 2021M693518 and 2021M693519), the Natural Science Foundation of Jiangsu Province (Nos. SBK20210432 and SBK20210431), and the National Science Foundation for the third batch of special funding for postdoctoral fellows (No. 2021TQ0367), and supported by "Double First-Class" University project (CPU2018GF07). This research project was supported by the grant from China Pharmaceutical University.

SUPPLEMENTARY MATERIAL

The Supplementary Material for this article can be found online at: https://www.frontiersin.org/articles/10.3389/fphar.2022.814942/full#supplementary-material

REFERENCES

Adrian, L., Lenski, M., Tödter, K., Heeren, J., Böhm, M., and Laufs, U. (2017). AMPK Prevents Palmitic Acid-Induced Apoptosis and Lipid Accumulation in Cardiomyocytes. *Lipids* 52, 737–750. doi:10.1007/s11745-017-4285-7

Amemiya, S., Kamiya, T., Nito, C., Inaba, T., Kato, K., Ueda, M., et al. (2005). Anti-apoptotic and Neuroprotective Effects of Edaravone Following Transient Focal Ischemia in Rats. *Eur. J. Pharmacol.* 516, 125–130. doi:10.1016/j.ejphar.2005.04.036

Balestrino, M., Sarocchi, M., Adriano, E., and Spallarossa, P. (2016). Potential of Creatine or Phosphocreatine Supplementation in Cerebrovascular Disease and in Ischemic Heart Disease. *Amino Acids* 48, 1955–1967. doi:10.1007/s00726-016-2173-8

Benjamin, E. J., Muntner, P., Alonso, A., Bittencourt, M. S., Callaway, C. W., Carson, A. P., et al. (2019). Heart Disease and Stroke Statistics-2019 Update: a Report from the American Heart Association. *Circulation* 139, e56–e528. doi:10.1161/CIR.0000000000000659

Bin, Q., Rao, H., Hu, J. N., Liu, R., Fan, Y. W., Li, J., et al. (2013). The Caspase Pathway of Linoelaidic Acid (9t, 12t-C18:2)-Induced Apoptosis in Human Umbilical Vein Endothelial Cells. *Lipids* 48, 115–126. doi:10.1007/s11745-012-3728-4

Cao, G., Jiang, N., Hu, Y., Zhang, Y., Wang, G., Yin, M., et al. (2016). Ruscogenin Attenuates Cerebral Ischemia-Induced Blood-Brain Barrier Dysfunction by Suppressing TXNIP/NLRP3 Inflammasome Activation

and the MAPK Pathway. *Int. J. Mol. Sci.* 17, 1418. doi:10.3390/ijms17091418

d'Apolito, M., Colia, A. L., Manca, E., Pettoello-Mantovani, M., Sacco, M., Maffione, A. B., et al. (2018). Urea Memory: Transient Cell Exposure to Urea Causes Persistent Mitochondrial Ros Production and Endothelial Dysfunction. *Toxins (Basel)* 10, 410. doi:10.3390/toxins10100410

De Bock, M., Wang, N., Decrock, E., Bol, M., Gadicherla, A. K., Culot, M., et al. (2013). Endothelial Calcium Dynamics, Connexin Channels and Blood-Brain Barrier Function. *Prog. Neurobiol.* 108, 1–20. doi:10.1016/j.pneurobio.2013.06.001

Dorovini-Zis, K., Bowman, P. D., Betz, A. L., and Goldstein, G. W. (1987). Hyperosmotic Urea Reversibly Opens the Tight Junctions between Brain Capillary Endothelial Cells in Cell Culture. *J. Neuropathol. Exp. Neurol.* 46, 130–140. doi:10.1097/00005072-198703000-00002

Durante, W. (2019). The Emerging Role of L-Glutamine in Cardiovascular Health and Disease. *Nutrients* 11, 2092. doi:10.3390/nu11092092

Fu, X., Wang, J., Liao, S., Lv, Y., Xu, D., Yang, M., et al. (2019). 1H NMR-Based Metabolomics Reveals Refined-Huang-Lian-Jie-Du-Decoction (BBG) as a Potential Ischemic Stroke Treatment Drug with Efficacy and a Favorable Therapeutic Window. *Front. Pharmacol.* 10, 337. doi:10.3389/fphar.2019.00337

Gremmels, H., Bevers, L. M., Fledderus, J. O., Braam, B., van Zonneveld, A. J., Verhaar, M. C., et al. (2015). Oleic Acid Increases Mitochondrial Reactive Oxygen Species Production and Decreases Endothelial Nitric Oxide Synthase Activity in Cultured Endothelial Cells. *Eur. J. Pharmacol.* 751, 67–72. doi:10.1016/j.ejphar.2015.01.005

Han, H. S., Jang, J. H., Park, J. S., Kim, H. J., and Kim, J. K. (2013). Transient Blood Brain Barrier Disruption Induced by Oleic Acid Is Mediated by Nitric Oxide. *Curr. Neurovasc. Res.* 10, 287–296. doi:10.2174/15672026113109990024

Hennig, B., Lei, W., Arzuaga, X., Ghosh, D. D., Saraswathi, V., and Toborek, M. (2006). Linoleic Acid Induces Proinflammatory Events in Vascular Endothelial Cells via Activation of PI3K/Akt and ERK1/2 Signaling. *J. Nutr. Biochem.* 17, 766–772. doi:10.1016/j.jnutbio.2006.01.005

Hirano, K., Ikeda, Y., Zaima, N., Sakata, Y., and Matsumiya, G. (2008). Triglyceride deposit Cardiomyovasculopathy. *N. Engl. J. Med.* 359, 2396–2398. doi:10.1056/NEJMc0805305

Jakaria, M., Azam, S., Haque, M. E., Jo, S. H., Uddin, M. S., Kim, I. S., et al. (2019). Taurine and its Analogs in Neurological Disorders: Focus on Therapeutic Potential and Molecular Mechanisms. *Redox Biol.* 24, 101223. doi:10.1016/j.redox.2019.101223

Kajikawa, M., Maruhashi, T., Matsumoto, T., Iwamoto, Y., Iwamoto, A., Oda, N., et al. (2016). Relationship between Serum Triglyceride Levels and Endothelial Function in a Large Community-Based Study. *Atherosclerosis* 249, 70–75. doi:10.1016/j.atherosclerosis.2016.03.035

Kikuchi, K., Tancharoen, S., Takeshige, N., Yoshitomi, M., Morioka, M., Murai, Y., et al. (2013). The Efficacy of Edaravone (Radicut), a Free Radical Scavenger, for Cardiovascular Disease. *Int. J. Mol. Sci.* 14, 13909–13930. doi:10.3390/ijms140713909

Książek, M., Chacińska, M., Chabowski, A., and Baranowski, M. (2015). Sources, Metabolism, and Regulation of Circulating Sphingosine-1-Phosphate. *J. Lipid Res.* 56, 1271–1281. doi:10.1194/jlr.R059543

Lau, W. L., and Vaziri, N. D. (2017). Urea, a True Uremic Toxin: the empire Strikes Back. *Clin. Sci. (Lond)* 131, 3–12. doi:10.1042/CS20160203

Lee, J. S., Chang, P. Y., Zhang, Y., Kizer, J. R., Best, L. G., and Howard, B. V. (2017). Triglyceride and HDL-C Dyslipidemia and Risks of Coronary Heart Disease and Ischemic Stroke by Glycemic Dysregulation Status: the strong Heart Study. *Diabetes Care* 40, 529–537. doi:10.2337/dc16-1958

Marchix, J., Choque, B., Kouba, M., Fautrel, A., Catheline, D., and Legrand, P. (2015). Excessive Dietary Linoleic Acid Induces Proinflammatory Markers in Rats. *J. Nutr. Biochem.* 26, 1434–1441. doi:10.1016/j.jnutbio.2015.07.010

Montaner, J., Ramiro, L., Simats, A., Tiedt, S., Makris, K., Jickling, G. C., et al. (2020). Multilevel Omics for the Discovery of Biomarkers and Therapeutic Targets for Stroke. *Nat. Rev. Neurol.* 16, 247–264. doi:10.1038/s41582-020-0350-6

Murakami, S. (2014). Taurine and Atherosclerosis. *Amino acids* 46, 73–80. doi:10.1007/s00726-012-1432-6

Park, E., Park, S. Y., Dobkin, C., and Schuller-Levis, G. (2014). Development of a Novel Cysteine Sulfinic Acid Decarboxylase Knockout Mouse: Dietary Taurine Reduces Neonatal Mortality. *J. Amino Acids* 2014, 346809. doi:10.1155/2014/346809

Peron, G., Sut, S., Dal Ben, S., Voinovich, D., and Dall'Acqua, S. (2020). Untargeted UPLC-MS Metabolomics Reveals Multiple Changes of Urine Composition in Healthy Adult Volunteers after Consumption of Curcuma Longa L. Extract. *Food Res. Int.* 127, 108730. doi:10.1016/j.foodres.2019.108730

Rohlenova, K., Veys, K., Miranda-Santos, I., De Bock, K., and Carmeliet, P. (2018). Endothelial Cell Metabolism in Health and Disease. *Trends Cel Biol* 28, 224–236. doi:10.1016/j.tcb.2017.10.010

Satoh, K. (2013). Linoleic Acid. A Novel Mechanism of Endothelial Cell Dysfunction. *Circ. J.* 77, 2702–2703. doi:10.1253/circj.cj-13-1155

Shah, S. H., Kraus, W. E., and Newgard, C. B. (2012). Metabolomic Profiling for the Identification of Novel Biomarkers and Mechanisms Related to Common Cardiovascular Diseases: Form and Function. *Circulation* 126, 1110–1120. doi:10.1161/CIRCULATIONAHA.111.060368

Shimomura, Y., and Kitaura, Y. (2018). Physiological and Pathological Roles of Branched-Chain Amino Acids in the Regulation of Protein and Energy Metabolism and Neurological Functions. *Pharmacol. Res.* 133, 215–217. doi:10.1016/j.phrs.2018.05.014

Sun, M., Zhao, Y., Gu, Y., and Xu, C. (2012). Anti-inflammatory Mechanism of Taurine against Ischemic Stroke Is Related to Down-Regulation of PARP and NF-Kb. *Amino Acids* 42, 1735–1747. doi:10.1007/s00726-011-0885-3

Ulrich-Merzenich, G., Zeitler, H., Vetter, H., and Bhonde, R. R. (2007). Protective Effects of Taurine on Endothelial Cells Impaired by High Glucose and Oxidized Low Density Lipoproteins. *Eur. J. Nutr.* 46, 431–438. doi:10.1007/s00394-007-0682-7

Wang, G. H., Jiang, Z. L., Fan, X. J., Zhang, L., Li, X., and Ke, K. F. (2007a). Neuroprotective Effect of Taurine against Focal Cerebral Ischemia in Rats Possibly Mediated by Activation of Both GABAA and glycine Receptors. *Neuropharmacology* 52, 1199–1209. doi:10.1016/j.neuropharm.2006.10.022

Wang, Q., Luo, W., Zheng, W., Liu, Y., Xu, H., Zheng, G., et al. (2007b). Iron Supplement Prevents lead-induced Disruption of the Blood-Brain Barrier during Rat Development. *Toxicol. Appl. Pharmacol.* 219, 33–41. doi:10.1016/j.taap.2006.11.035

Wang, Y., Zhao, H., Liu, Y., Guo, W., Bao, Y., Zhang, M., et al. (2019). GC-MS-based Metabolomics to Reveal the Protective Effect of Gross Saponins of Tribulus Terrestris Fruit against Ischemic Stroke in Rat. *Molecules* 24, 793. doi:10.3390/molecules24040793

Wen, S. Y., Velmurugan, B. K., Day, C. H., Shen, C. Y., Chun, L. C., Tsai, Y. C., et al. (2017). High Density Lipoprotein (HDL) Reverses Palmitic Acid Induced Energy Metabolism Imbalance by Switching CD36 and GLUT4 Signaling Pathways in Cardiomyocyte. *J. Cel Physiol.* 232, 3020–3029. doi:10.1002/jcp.26007

Yang, H., Xi, X., Zhao, B., Su, Z., and Wang, Z. (2018). KLF4 Protects Brain Microvascular Endothelial Cells from Ischemic Stroke Induced Apoptosis by Transcriptionally Activating MALAT1. *Biochem. Biophys. Res. Commun.* 495, 2376–2382. doi:10.1016/j.bbrc.2017.11.205

Yang, Q., Han, L., Li, J., Xu, H., Liu, X., Wang, X., et al. (2019). Activation of Nrf2 by Phloretin Attenuates Palmitic Acid-Induced Endothelial Cell Oxidative Stress via AMPK-dependent Signaling. *J. Agric. Food Chem.* 67, 120–131. doi:10.1021/acs.jafc.8b05025

Yung, H. W., Korolchuk, S., Tolkovsky, A. M., Charnock-Jones, D. S., and Burton, G. J. (2007). Endoplasmic Reticulum Stress Exacerbates Ischemia-Reperfusion-Induced Apoptosis through Attenuation of Akt Protein Synthesis in Human Choriocarcinoma Cells. *Faseb. J.* 21, 872–884. doi:10.1096/fj.06-6054com

Zhai, K. F., Zheng, J. R., Tang, Y. M., Li, F., Lv, Y. N., Zhang, Y. Y., et al. (2017). The Saponin D39 Blocks Dissociation of Non-muscular Myosin Heavy Chain IIA from TNF Receptor 2, Suppressing Tissue Factor Expression and Venous Thrombosis. *Br. J. Pharmacol.* 174, 2818–2831. doi:10.1111/bph.13885

Zhang, N., Komine-Kobayashi, M., Tanaka, R., Liu, M., Mizuno, Y., and Urabe, T. (2005). Edaravone Reduces Early Accumulation of Oxidative Products and Sequential Inflammatory Responses after Transient Focal

Ischemia in Mice Brain. *Stroke* 36, 2220–2225. doi:10.1161/01.STR.0000182241.07096.06

Zhenyukh, O., González-Amor, M., Rodrigues-Diez, R. R., Esteban, V., Ruiz-Ortega, M., Salaices, M., et al. (2018). Branched-chain Amino Acids Promote Endothelial Dysfunction through Increased Reactive Oxygen Species Generation and Inflammation. *J. Cel Mol. Med.* 22, 4948–4962. doi:10.1111/jcmm.13759

Zille, M., Ikhsan, M., Jiang, Y., Lampe, J., Wenzel, J., and Schwaninger, M. (2019). The Impact of Endothelial Cell Death in the Brain and its Role after Stroke: A Systematic Review. *Cell Stress* 3, 330–347. doi:10.15698/cst2019.11.203

Conflict of Interest: The authors declare that the research was conducted in the absence of any commercial or financial relationships that could be construed as a potential conflict of interest.

Publisher's Note: All claims expressed in this article are solely those of the authors and do not necessarily represent those of their affiliated organizations, or those of the publisher, the editors, and the reviewers. Any product that may be evaluated in this article, or claim that may be made by its manufacturer, is not guaranteed or endorsed by the publisher.

frontiers in Neuroscience

ORIGINAL RESEARCH
published: 15 February 2022
doi: 10.3389/fnins.2022.838621

Inhibiting Sphingosine 1-Phosphate Receptor Subtype 3 Attenuates Brain Damage During Ischemia-Reperfusion Injury by Regulating nNOS/NO and Oxidative Stress

Xuehui Fan, Hongping Chen, Chen Xu, Yingju Wang, Pengqi Yin, Meng Li, Zhanbin Tang, Fangchao Jiang, Wan Wei, Jihe Song, Guozhong Li and Di Zhong**

Department of Neurology, The First Affiliated Hospital of Harbin Medical University, Harbin, China

OPEN ACCESS

Edited by:
Yongjun Sun,
Hebei University of Science and Technology, China

Reviewed by:
Rehab Rifaai,
Minia University, Egypt
Bhakta Prasad Gaire,
University of Maryland, Baltimore, United States

***Correspondence:**
Guozhong Li
lgzhyd1962@163.com
Di Zhong
dityan@163.com

Specialty section:
This article was submitted to Neuropharmacology, a section of the journal Frontiers in Neuroscience

Received: *18 December 2021*
Accepted: *17 January 2022*
Published: *15 February 2022*

Citation:
Fan X, Chen H, Xu C, Wang Y, Yin P, Li M, Tang Z, Jiang F, Wei W, Song J, Li G and Zhong D (2022) Inhibiting Sphingosine 1-Phosphate Receptor Subtype 3 Attenuates Brain Damage During Ischemia-Reperfusion Injury by Regulating nNOS/NO and Oxidative Stress. Front. Neurosci. 16:838621. doi: 10.3389/fnins.2022.838621

Background: Ischemic stroke (IS) is a common disease endangering human life and health. Cerebral ischemia triggers a series of complex harmful events, including excitotoxicity, inflammation and cell death, as well as increased nitric oxide production through the activation of nitric oxide synthase (NOS). Oxidative stress plays a major role in cerebral ischemia and reperfusion. Sphingosine 1-phosphate receptor subtype 3 (S1PR3), a member of S1P's G protein-coupled receptors S1PR1-S1PR5, is involved in a variety of biological effects in the body, and its role in regulating oxidative stress during cerebral ischemia and reperfusion is still unclear.

Methods: Transient middle cerebral artery occlusion (tMCAO) mice were selected as the brain ischemia–reperfusion (I/R) injury model. Male C57/BL6 mice were treated with or without a selective S1PR3 inhibition after tMCAO, and changes in infarct volume, Nissl staining, hematoxylin-eosin (H&E) staining and NOS protein, nitric oxide (NO), superoxide dismutase (SOD), and malondialdehyde (MDA) content after tMCAO were observed.

Results: In the cerebral ischemia–reperfusion model, inhibition of S1PR3 improved the infarct volume and neuronal damage in mice after tMCAO. Similarly, inhibition of S1PR3 can reduce the expression of NO synthase subtype neuronal NOS (nNOS) and reduce the production of NO after cerebral ischemia. After cerebral ischemia and reperfusion, the oxidative stress response was enhanced, and after the administration of the S1PR3 inhibitor, the SOD content increased and the MDA content decreased, indicating that S1PR3 plays an important role in regulating oxidative stress response.

Conclusion: Inhibiting S1PR3 attenuates brain damage during I/R injury by regulating nNOS/NO and oxidative stress, which provides a potential new therapeutic target and mechanism for the clinical treatment of IS.

Keywords: S1PR3, cerebral ischemia-reperfusion injury, nitric oxide, oxidative stress, CAY-10444

INTRODUCTION

Cerebrovascular disease is the main disease that endangers human health. Ischemic stroke (IS) is the most common type of stroke, accounting for 60–70% of all strokes (Wang et al., 2020). When brain tissue is ischemic for a long period of time, the restoration of blood flow will further damage brain tissue, which is cerebral ischemia–reperfusion (I/R) injury (Taoufik and Probert, 2008). Oxidative stress is a pathophysiological phenomenon in which cells in the body are affected by the outside world, which causes excessive production of reactive oxygen species (ROS), and leads to impairment between oxidation and antioxidant systems, making the system prone to oxidation and cell damage. In cerebral I/R injury, oxidative stress can damage nerve cells through direct damage to reactive oxygen species and activation of other signaling pathways (Frantseva et al., 2001). Nitric oxide (NO) has dual neuroprotective and neurotoxic functions in cerebral ischemic injury (Beray-Berthat et al., 2003), which depends on factors such as the time period after ischemic brain injury, the nitric oxide synthase (NOS) subtype of NO, and the source of cells. Immediately after cerebral ischemia, the NO released by endothelial nitric oxide synthase (eNOS) plays a protective role by promoting vasodilation and inhibiting the aggregation and adhesion of microvessels. However, after the occurrence of cerebral ischemia, NO produced by the excessive activation of neuronal NOS (nNOS) and by later inducible nitric oxide synthase (iNOS) contributes to brain damage (Moro et al., 2004).

Sphingosine 1-phosphate (S1P) is produced by the phosphorylation of sphingosine by sphingosine kinase. S1P is synthesized in the cell and then acts as a bioactive molecule in the extracellular or intracellular pathways. To date, there are five subtypes of S1P receptors: S1P receptor subtype 1 (S1PR1), S1PR2, S1PR3, S1PR4, and S1PR5, among which S1PR1, S1PR2, and S1PR3 are commonly expressed in tissues, S1PR4 is mainly expressed in lymphoid tissues, and S1PR5 is limited to expression in the brain and spleen (Chun et al., 2010). FTY720, a new class of immunomodulator, has an excitatory effect on all four receptor subtypes except S1PR2 (Albert et al., 2005). The study found that S1P and CYM5442 are full agonists for S1PR3 (Wang et al., 2018). FTY720-P is a partial agonist for S1PR3 and requires a certain level of receptor reserve to initiate the response (Stepanovska and Huwiler, 2020). FTY720-P may also inhibit S1P-induced leukocyte rolling and P-selectin mobilization by interfering with S1PR3 (Nussbaum et al., 2015). In addition, TY-52156 and CAY-10444 have been widely used as specific S1PR3 receptor antagonists (Murakami et al., 2010; Li et al., 2015; Shirakawa et al., 2017; Patil et al., 2019). To study the pathophysiological mechanism mediated by S1PR3, these agonists and antagonists have been widely used in experimental studies.

The pathogenicity of S1PR1 in cerebral ischemia is related to neuroinflammation. Inhibition of S1PR1 activity with AUY954 not only alleviated the pro-inflammatory response but also enhanced the anti-inflammatory response after cerebral ischemia. In addition, the regulatory role of S1PR1 in proinflammatory response after cerebral ischemia may be related to the activation of microglia. Such as increasing the number of microglia and cell proliferation, promoting microglia to amoeboid cells transformation (Gaire et al., 2018a, 2019). Another independent study also suggested that S1PR2 was involved in neuroinflammatory after tMCAO, and S1PR2 may mainly participate in the pro-inflammatory response of activated microglia during cerebral ischemia (Sapkota et al., 2019). However, it is not clear whether S1PR4 or S1PR5 are involved in the pathogenesis of cerebral ischemia. In the mouse brain I/R model, S1PR3 is beneficial to the activation of microglia and polarization of M1-type macrophages (Gaire et al., 2018b). It is still unclear whether S1PR3 is involved in mediating NO production and oxidative stress in I/R. We used the S1PR3 antagonist CAY-10444 to study the role of S1PR3 in cerebral ischemia and reperfusion to provide new methods for the treatment of stroke.

MATERIALS AND METHODS

Animal Studies

For this experiment, C57BL/6 male mice were selected. The mice were SPF grade and weighed approximately 20–25 g. All experimental mice were purchased from Liaoning Changsheng Biotechnology Co., Ltd. All experimental animals were managed and used strictly in accordance with the experimental animal management guidelines of the First Affiliated Hospital of Harbin Medical University, as recommended by the US National Institutes of Health. During the experiment, the mice were housed in an environment with a humidity of 50–60% and a temperature of 23–25°C, the natural circadian rhythm was simulated with a 12/12 h alternating light mode, and the mice were able to eat and drink water freely. Mice are randomly assigned to each group, 4 mice per group.

Construction of the Transient Middle Cerebral Artery Occlusion Model

Cerebral ischemia was established by generating the tMCAO model using a modified intraluminal technique (Liu et al., 2010). The mice were anesthetized with 3% pentobarbital sodium, their heads were skinned and disinfected, and the anal temperature probe was inserted to keep the body temperature at 37 ± 0.5°C. The skin of the neck was cut open to isolate and expose the common carotid artery, internal carotid artery and external carotid artery. An incision was made on the right common carotid artery, where a 0.21 mm thread was inserted into the internal carotid artery through the common carotid artery until the middle cerebral artery was reached. The depth reached approximately 9 ± 1 mm at the bifurcation of the internal and external carotid arteries. If there was any resistance, the thread was stopped. One hour after ischemia, the thread plug was removed, the skin was sutured, and the mouse was placed on a heating pad. After waking up, the mice were placed in a constant temperature incubator for 24 h. The animals in the sham group were subjected to the same operation process except that the middle cerebral artery (MCA) was not occluded. An inspector unknowingly scored mice for neurological deficits. The deficits were scored as follows: 0, no deficits; 1, forelimb weakness and torso turning to the ipsilateral side when

held by tail; 2, unable to extend the opposite forepaw completely; 3, turning to the paralyzed side; 4, dumping to the opposite side; and 5, unable to walk spontaneously, loss of consciousness. It is considered that the tMCAO model is successful when score is 1–4 points. Mice after tMCAO were excluded from this study: (1) one that died before euthanasia; (2) one with a subarachnoid hemorrhage or intraparenchymal hemorrhage; (3) one with a 0 score or 5 score at the time point of euthanasia. When the mice were operated, the neck skin opening is narrowed to reduce the wound surface and unnecessary exposure. The operation is gentle, reducing the physical strain on the tissue. From the beginning of anesthesia to awake, the mice are placed on the 37°C constant temperature heating plate to make the mice in a more comfortable environment, promoting their recovery. Each batch of 20 mice were randomly assigned to 4 cages, and the average success rate of the model was over 90%.CAY-10444 was purchased from Cayman Company and was injected intraperitoneally into mice at 0.5 mg/kg during reperfusion (Gaire et al., 2018b). CAY-10444 was dissolved in dimethylsulfoxide (DMSO, less than 2%). Mice in the V + tMCAO group were intraperitoneally injected with vehicle (DMSO, less than 2%) after ischemia and reperfusion. Mice were randomly divided into the following groups: (1) sham group; (2) 24 h-tMCAO group; (3) CAY-10444 + tMCAO group; and (4) V + tMCAO group.

2,3,5-Triphenyltetrazolium Chloride (TTC) Staining

After the mouse was sacrificed, the brain was extracted and cut into seven pieces from the rostral tip (1 mm thick) of the frontal lobe. The tissue was incubated with 2% 2,3,5-triphenyltetrazolium chloride solution (2% TTC, Solarbio) at 37°C in the dark for 30 min and then fixed with 4% paraformaldehyde. Finally, brain slices were imaged with a camera, and the infarct volume was evaluated by ImageJ software. Measure the infarct area and total area of each slice. The infarct volume of each layer is the product of the infarct area and the thickness of the layer. The sum of the infarct volume of each layer is the total infarct volume.

Nissl Staining, and Hematoxylin-Eosin Staining

The specimens were fixed in 4% buffered formaldehyde, paraffin-embedded and 4 μm thick histological sections were stained with H&E. In Nissl staining, the sections were put into toluidine blue, the staining tank was placed in a constant temperature box at 50–60°C for 25–50 min, 70% ethanol was added for washing, and finally 95% ethanol was used for rapid differentiation. Absolute ethanol dehydrates quickly. The tissue sections were examined and imaged with an optical microscope (Nikon, Y-TV55, JAPAN).

Immunofluorescent Staining

At the time of 24 h after tMCAO on set, the mice brain tissues were taken and their hearts were perfused. Firstly, pre-cooled saline was used for perfusion and flushing until all blood was released, and then 4% paraformaldehyde was perfused until the mice became stiff. Secondly, the tissues were obtained by dissection at 4°C, fixed in 4% paraformaldehyde for more than 24 h, putting the tissues fixed in paraformaldehyde in a 30% sucrose solution for dehydration for 24–48 h, then it was embedded with OCT and placed in a −80°C refrigerator. The frozen brain tissues were sliced using a cryostat with a thickness of 7 μm, and the slices were directly subjected to immunofluorescence staining. We cover the tissue with 0.5% Triton X-100, permeate it at room temperature for 20 min, and then incubate it with 10% goat serum at room temperature for 1 h (Fulgenzi et al., 2020). The samples were incubated at 4°C overnight with primary antibodies specifically raised against the following proteins: NeuN (Abcam, ab104224, 1:1,000), Iba1 (Abcam, ab178846, 1:500), GFAP (Wanlei, WL0836, 1:100), nNOS (GeneTex, GTX133403, 1:50). Subsequently, the samples were incubated with the appropriate fluorophore-conjugated secondary antibodies (BOSTER, BA1089, 1:100) for 1 h at room temperature in the dark. DAPI (Abcam, ab104139) was used to stain cell nuclei. Images were captured using a fluorescence microscope (Nikon, Y-TV55, JAPAN).

Fluoro Jade C Staining

Fluoro Jade C (FJC), a polyanionic fluorescein derivative that binds sensitively and selectively to degenerating neurons, was used to examine dynamic time-course changes in dying neurons in the brains of the animal models described above (Schmued et al., 2005). Sections were first treated as for IF staining, and then FJC staining was performed. We immersed the slides in 80% ethanol solution containing 1% NaOH for 5 min. They were rinsed in 70% ethanol for 2 min, then incubated them in 0.06% potassium permanganate solution for 10 min. After rinsing with distilled water for 2 min, the treated slides were stained in 0.0001% concentration of FJ-C (United States, Biosensis) solution for 10 min, adding Solution D (DAPI) to the above FJC solution. Finally, Slides were mounted with DPX, sections were examined under a fluorescence microscope and images were captured for demonstration.

Western Blot Analysis

Brain tissue from the right hemisphere was obtained, and proteins were extracted on the first day after I/R. The protein concentration of the samples was determined by the BCA protein detection Kit. In addition, 30 μg of protein from each group were loaded onto an 7.5 or 10% SDS–PAGE gel. After electrophoresis, the brain proteins were transferred to polyvinylidene fluoride (PVDF) membranes, blocked with 5% skim milk at room temperature for 1 h, and then incubated with the primary antibody overnight in a 4°C refrigerator. After an incubation with goat anti-mouse and anti-rabbit (Abmart, M21003, 1:2,000) secondary antibodies for 45 min at room temperature, membranes were washed with TBST, and then incubated with enhanced chemiluminescence (ECL) reagent (biosharp, BL520A, China)

for detection. Primary antibodies included: anti-iNOS (1:1,000, 22226-1-AP, Proteintech, United States), anti-nNOS (1:1,000, ab76067, Abcam, United States, United States), and anti-eNOS (1:1,000, ab199956, Abcam, United States). β-Tubulin (1:1,000, 10094-1-AP, Proteintech, United States) was used for internal comparison. ImageJ software was used to quantitatively analyze the gray values of all protein bands.

Nitric Oxide Detection

NO detection kit was purchased from Nanjing Jiancheng Institute of Bioengineering. Since NO metabolism will eventually lead to the production of nitrite, the NO content is measured by quantifying the levels of nitrate and nitrite in the sample. To this end, cadmium is used to convert nitrate to nitrite, then the Griess reaction is performed, and the NO content in each sample is measured using a microplate reader at 570 nm.

Superoxide Dismutase and Malondialdehyde Detection

A commercial kit (Wanleibio, Shenyang, China) was used to measure MDA and SOD levels in the right brain tissue of mice. All measurements were performed in accordance with the manufacturer's instructions. MDA and SOD were determined by the absorbance at 532 and 570 nm, respectively.

Statistical Analysis

Use GraphPad Prism 8.0 statistical software for statistical analysis, and the experimental data are expressed as mean ± SEM. Differences between groups were analyzed using one-way ANOVA followed by the Tukey *post hoc* test. $P < 0.05$ was regarded as statistically significant.

RESULTS

Inhibition of Sphingosine 1-Phosphate Receptor Subtype 3 Can Improve Infarct Volume and Neuron Damage in Mice After Transient Middle Cerebral Artery Occlusion

In our previous studies, we found that the expression of S1PR3 was highest 24 h after tMCAO and then decreased, so we chose to extract the brain 24 h after tMCAO. To confirm that inhibition of S1PR3 can reduce cerebral I/R injury, we performed TTC staining. Compared with the 24 h tMCAO group, the cerebral infarction volume of mice was reduced following CAY-10444 administration ($P < 0.05$) (**Figures 1A,B**). The brain tissue morphology of mice was examined after tMCAO. H&E staining showed that the tissue surrounding the infarct was damaged after tMCAO, the peripheral neuron was characterized by nuclear pyknosis, the staining was darker, the penumbra area was swollen, neuropil vacuolation, glial cell hyperplasia. In the pyramidal cell layer and granular layer of the cerebral cortex, H&E staining showed that CAY + 24 h-tMCAO mice had pyknosis and deep staining of nuclei around the infarct, the number of unclear structures decreased, the neuropil vacuolation of the infarct focus are alleviated, and the number of glial cells around the infarct was also reduced (**Figure 2A**). Nissl staining of mice after tMCAO showed the disappearance of Nissl bodies in neurons. Compared with the 24 h tMCAO group, there were more Nissl bodies in neurons in the CAY + 24 h tMCAO group (**Figure 2B**). Fluoro-Jade C staining was performed on mice brain tissues. The results showed that the number of Fluoro-Jade C-positive cells in the 24 h-tMCAO group and the V + 24 h-tMCAO group increased significantly ($P < 0.001$ and $P < 0.001$, respectively),

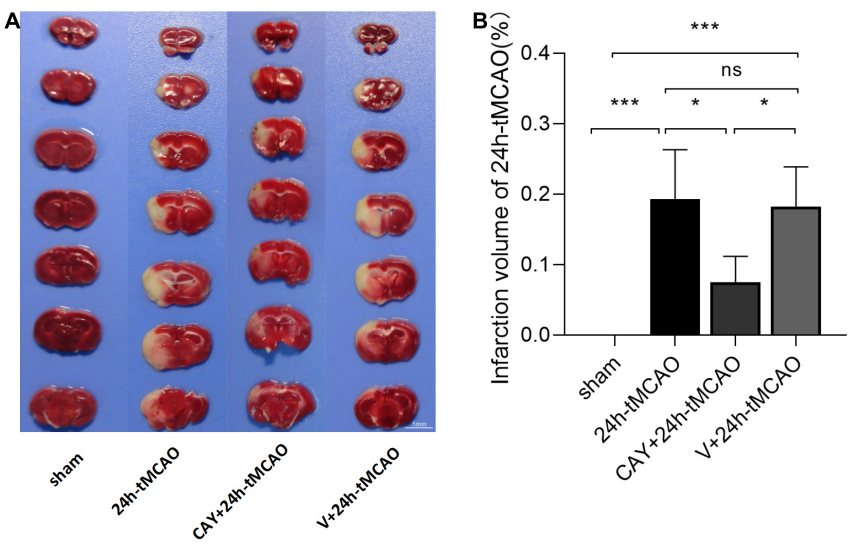

FIGURE 1 | Infarction volume of mice subjected to tMCAO after administration of an S1PR3-specific antagonist. **(A,B)** Representative images and statistical results of TTC staining of brain tissues in different groups ($n = 4$). Scale bar = 5 mm. Data are presented as the mean ± SEM. *P*-values were determined by ANOVA followed by the Tukey *post hoc* test, $^{*}P < 0.05$; $^{***}P < 0.001$; and ns, not significant.

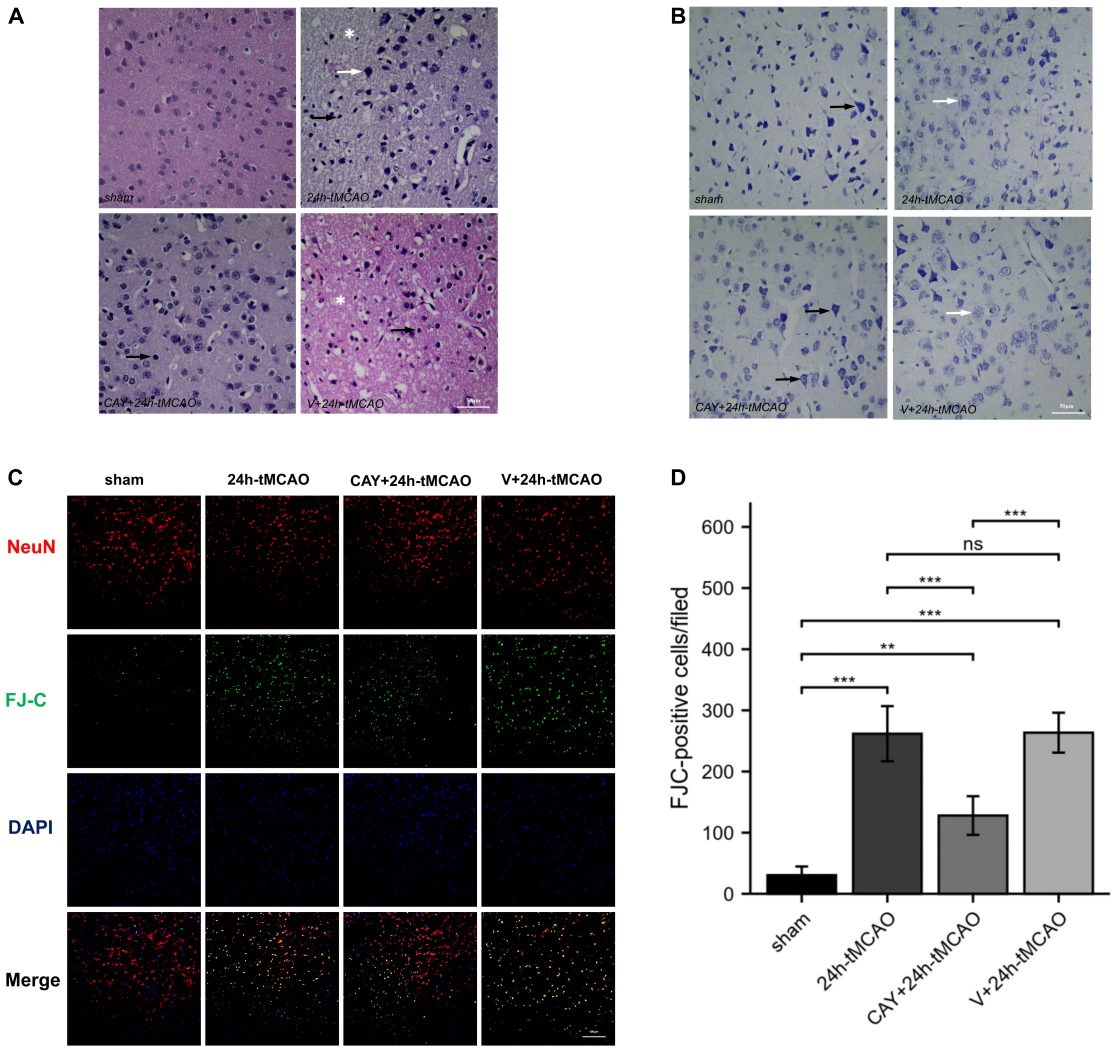

FIGURE 2 | H&E, Nissl and FJC staining in brain tissue of mice subjected to tMCAO after administration of an S1PR3-specific antagonist. **(A)** H&E staining in brain tissue of mice subjected to tMCAO after administration of an S1PR3-specific antagonist. Vacuolated neuropil in brain tissue (*). The black arrow points to the glial cells and the white arrow points to the nucleus of neurons that were reduced and trachychromatic (→), $n = 4$. Scale bar = 50 μm. **(B)** Nissl staining in brain tissue of mice subjected to tMCAO after administration of an S1PR3-specific antagonist. The black arrow points to neurons with Nissl bodies. The white arrow points to neurons with absent Nissl bodies, $n = 4$. Scale bar = 50 μm. **(C,D)** DAPI (blue)/FJC (green)/NeuN (red) Representative immunofluorescence images and statistical results of mouse brain tissue slices after tMCAO ($n = 4$). Data are presented as the mean ± SEM. *P*-values were determined by ANOVA followed by the Tukey *post hoc* test, $^{**}P < 0.01$; $^{***}P < 0.001$; and ns, not significant. Scale bar = 100 μm.

while the number of Fluoro-Jade C-positive cells of the mice treated with CAY-10444 significantly decreased ($P < 0.001$ and $P < 0.001$, respectively) (**Figures 2C,D**). Subsequently, we stained brain tissues for Iba1 and GFAP, we found that the number of Iba1-positive cells around the infarct area increased significantly after tMCAO ($p < 0.001$), showing amoeboid-like changes. After administrating of CAY-10444, the number of Iba1-positive cells decreased ($p < 0.001$) (**Figures 3A,B**), the number of amoeboid microglia also significantly reduced. Compared with the Sham group, the number of GFAP-positive cells increased significantly after tMCAO in mice ($p < 0.001$), while the number of GFAP-positive cells showed a decreasing trend after CAY-10444 was administered ($p < 0.01$) (**Figures 3C,D**).

Inhibition of Sphingosine 1-Phosphate Receptor Subtype 3 Can Inhibit the Expression of Neuronal NOS After Ischemia–Reperfusion

To confirm the effect of S1PR3 on the expression of nNOS, iNOS and eNOS proteins after cerebral I/R, we used Western blotting to detect the expression of related proteins 24 h after I/R. As shown in **Figure 4**, the expression of nNOS protein in the tMCAO group increased ($p < 0.001$), and after CAY-10444 was administered, the expression decreased ($p < 0.01$) (**Figure 4C**). After tMCAO, the expression of iNOS and eNOS both increased ($p < 0.01$ and $p < 0.001$, respectively) (**Figures 4B,D**). After CAY-10444

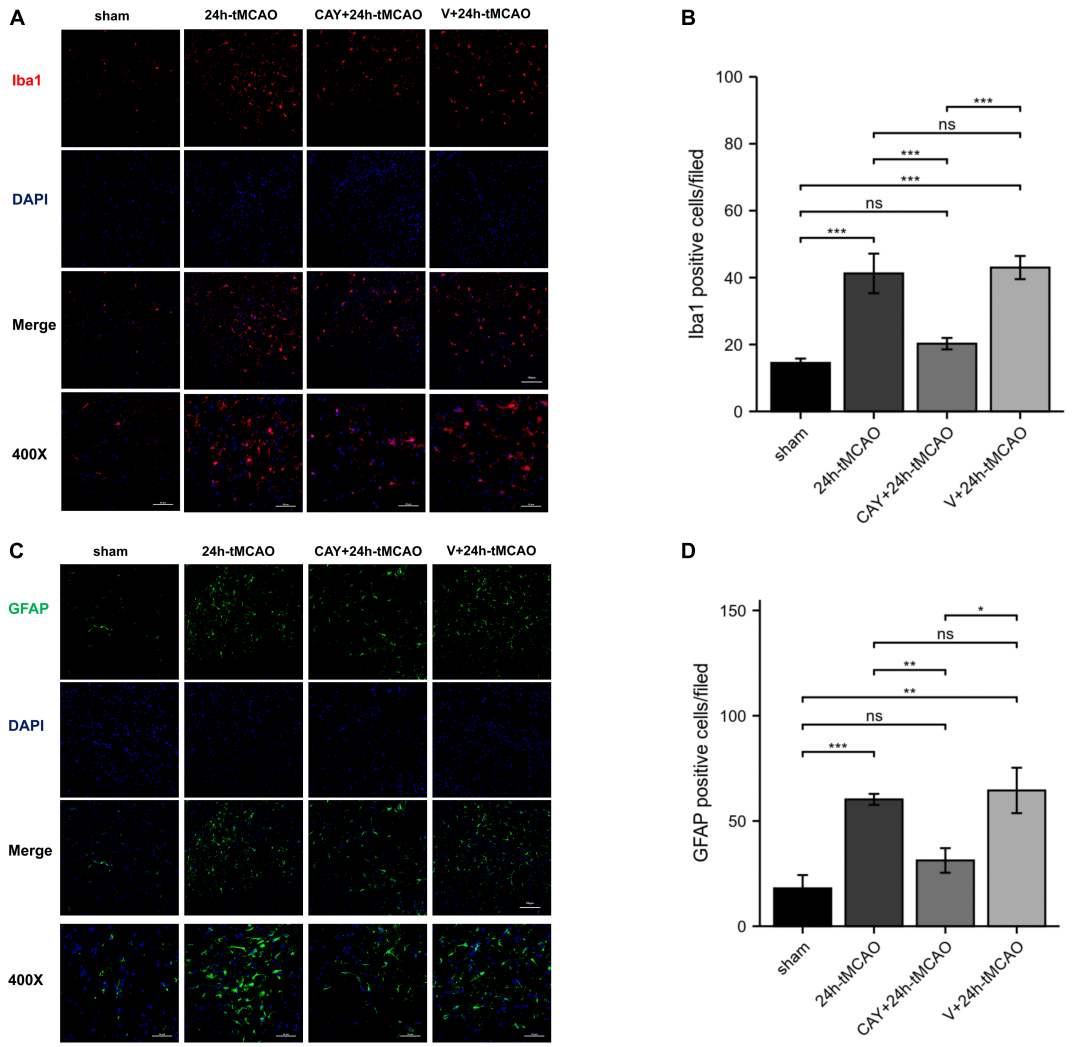

FIGURE 3 | Inhibition of S1PR3 attenuates microglia and astrocyte activation after tMCAO. **(A,B)** DAPI (blue)/Iba1 (red) Representative immunofluorescence images and statistical results of mouse brain tissue slices after tMCAO ($n = 4$). **(C,D)** DAPI (blue)/GFAP (green) Representative immunofluorescence images and statistical results of mouse brain tissue slices after tMCAO ($n = 4$). Data are presented as the mean ± SEM. *P*-values were determined by ANOVA followed by the Tukey *post hoc* test, $^{*}P < 0.05$; $^{**}P < 0.01$; $^{***}P < 0.001$; and ns, not significant. Scale bar = 100 μm. 400×, Scale bar = 50 μm.

administration, the expression of iNOS and eNOS did not change significantly ($P > 0.05$) (**Figures 4B,D**). Subsequently, we performed immunofluorescence staining on mouse brain slices (**Figure 5A**). The results showed that 24 h after tMCAO, there was more fluorescent staining of nNOS in the peri-ischemic regions ($p < 0.01$). After CAY-10444 administration, nNOS fluorescence staining was reduced ($p < 0.05$) (**Figure 5B**). This shows that after tMCAO, inhibition of S1PR3 reduces the expression of nNOS.

Inhibition of Sphingosine 1-Phosphate Receptor Subtype 3 Can Inhibit the Formation of Nitric Oxide After Ischemia–Reperfusion

To determine whether S1PR3 mediates the production of NO and causes brain damage, we measured the content of nitric oxide in brain tissue. NO content determination in brain tissue showed that after 24 h of I/R, the NO level in the tMCAO group was significantly higher than that in the sham group ($p < 0.001$). Compared with 24 h-tMCAO and V + 24 h-tMCAO, the NO level of the CAY-10444 + 24 h-tMCAO group was significantly lower ($p < 0.01$) (**Figure 5C**). This suggests that in I/R injury, S1PR3 regulates the production of NO by regulating nNOS.

Sphingosine 1-Phosphate Receptor Subtype 3 Participates in the Regulation of Superoxide Dismutase and Malondialdehyde After Ischemia–Reperfusion

To study whether S1PR3 is involved in the oxidative stress response in the brain tissue of tMCAO model mice, we examined

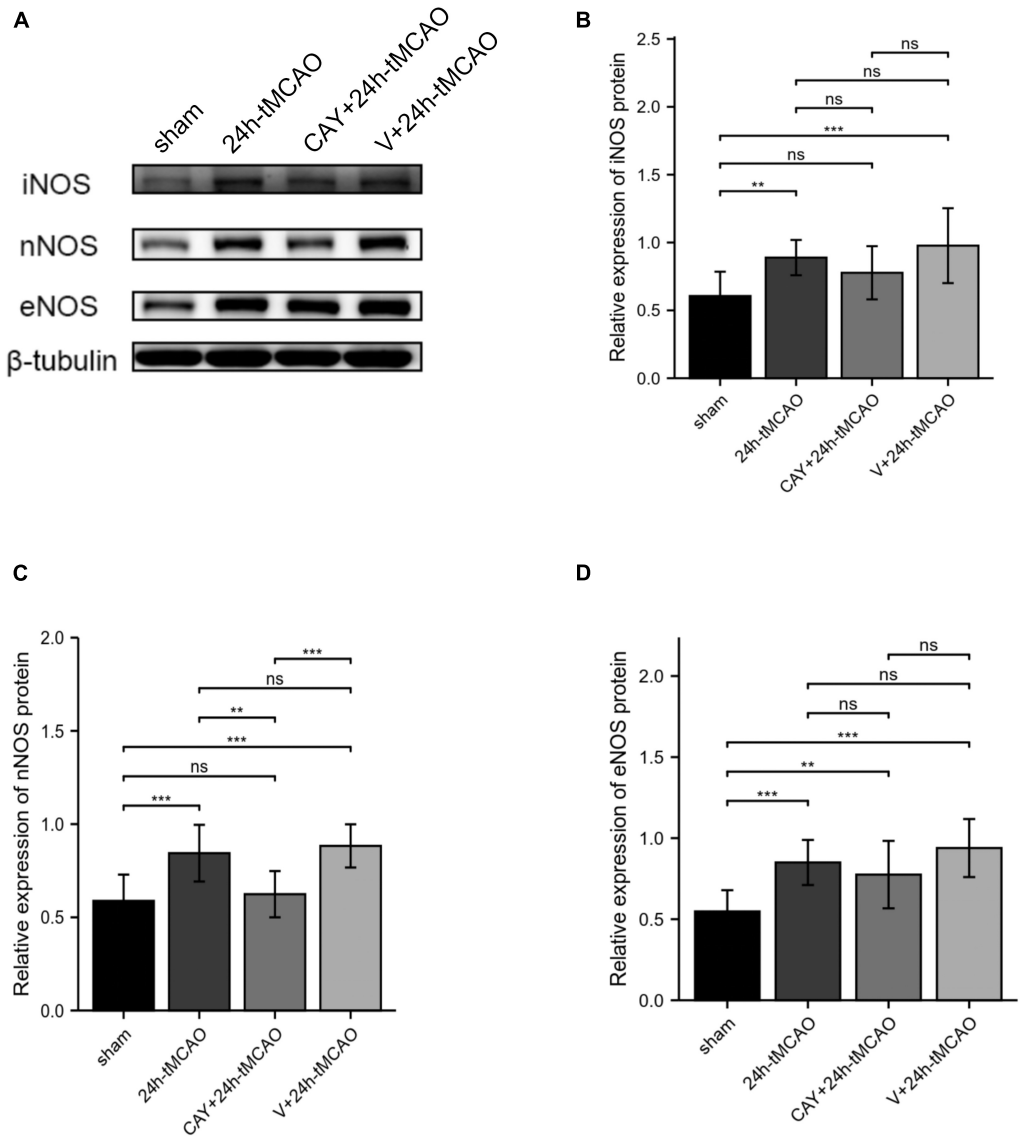

FIGURE 4 | Inhibition of S1PR3 inhibited the expression of nNOS after I/R. **(A)** Western blot of the sham group, 24 h tMCAO group, CAY10444 + 24 h tMCAO group, V + 24 h tMCAO group, and iNOS, nNOS and eNOS expression. **(B–D)** The expression levels of iNOS, nNOS and eNOS proteins ($n = 4$). Data are presented as the mean ± SEM. *P*-values were determined by ANOVA followed by the Tukey *post hoc* test, $^{**}P < 0.01$; $^{***}P < 0.001$; and ns, not significant.

the changes in SOD vitality and MDA content in brain tissue after brain I/R. Compared with the sham group, the SOD vitality in the brain tissue of mice in the 24 h-tMCAO group was significantly reduced ($p < 0.001$). Compared with that of the 24 h tMCAO group, the SOD vitality of the CAY + 24 h tMCAO group was significantly higher ($p < 0.01$) (**Figure 6A**). MDA content determination results showed that compared with the sham group, the MDA content in the brain tissue of the 24 h-tMCAO group increased significantly up ($p < 0.001$) and compared with the 24 h-tMCAO group, the MDA content of the CAY + 24 h-tMCAO group was significantly decreased ($p < 0.01$) (**Figure 6B**). These results show that S1PR3 is involved in the regulation of oxidative stress after I/R.

DISCUSSION

Studies have found that S1PR3 plays a role in cell inflammation, cell proliferation, cell migration, tumor invasion, I/R, tissue fibrosis, and vascular activity (Fan et al., 2021). In an *in vivo* mouse model of myocardial I/R, it was observed that high-density lipoprotein and its component S1P protect the heart from I/R damage through an independent signaling pathway mediated by S1PR3 (Levkau et al., 2004). S1PR3(–/–) mice are protected from kidney I/R damage through mechanisms involving bone marrow-derived dendritic cells (BMDCs) and their immunomodulatory functions (Bajwa et al., 2012). Bajwa et al. (2016) found that adoptively transferred S1PR3(–/–)

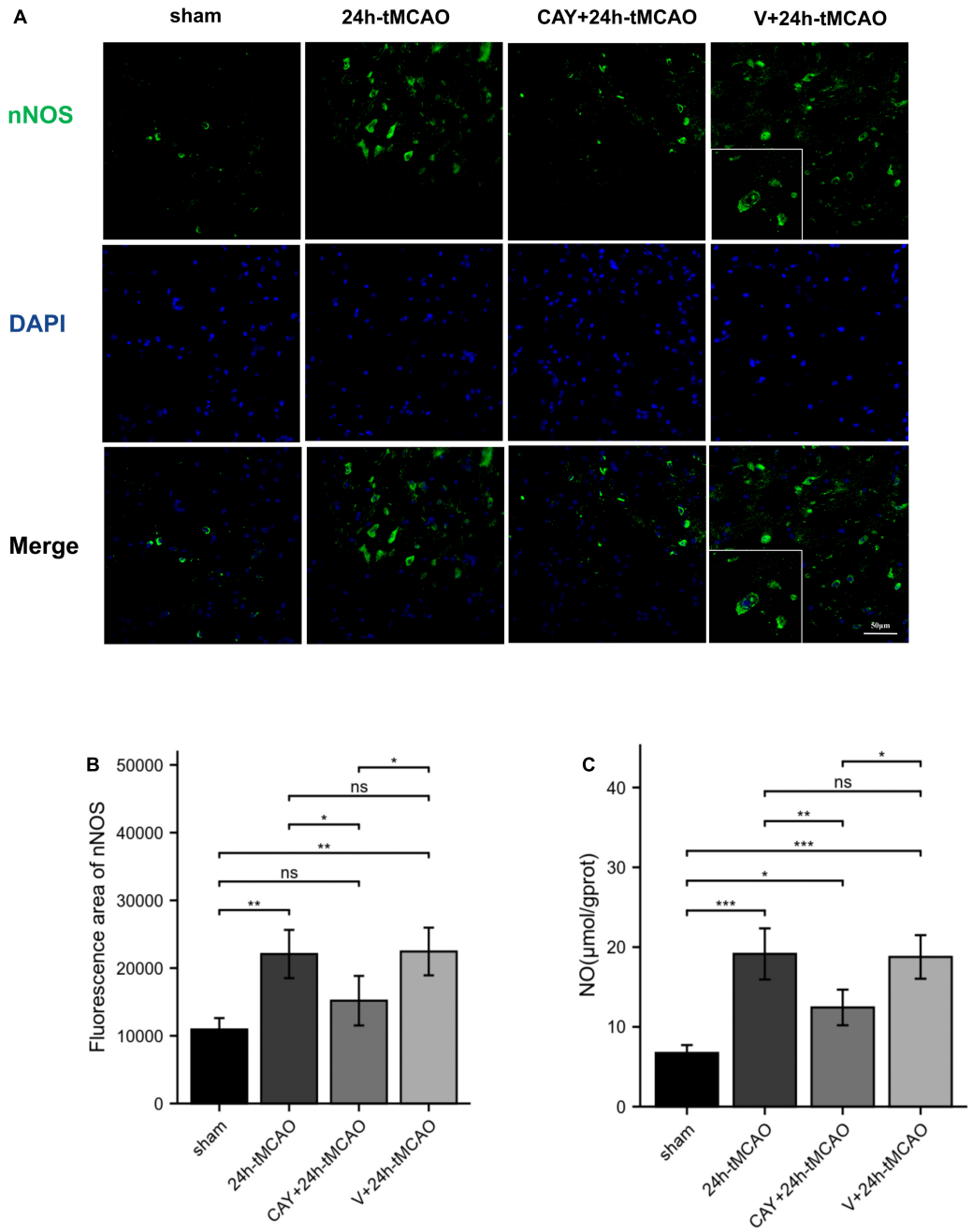

FIGURE 5 | nNOS fluorescence image and NO content expression. **(A,B)** DAPI (blue)/nNOS (green) Representative immunofluorescence images and statistical results of mouse brain tissue slices after tMCAO. **(C)** NO production was measured ($n = 4$). Data are presented as the mean ± SEM. *P*-values were determined by ANOVA followed by the Tukey *post hoc* test, $^{*}P < 0.05$; $^{**}P < 0.01$; $^{***}P < 0.001$; and ns, not significant.

BMDCs prevent kidney I/R damage through interaction in the spleen and expansion of splenic CD4 + Foxp3 + T regulatory cells (Tregs). In contrast to the protective effect on heart I/R, S1PR3 shows the opposite effect on kidney I/R, which is speculated to be due to the existence of cells and tissues at different developmental stages of disease. S1PR1 and S1PR2 has previously been found to be involved in the activation of microglia during cerebral ischemia reperfusion (Gaire et al., 2018a, 2019; Sapkota et al., 2019). A recent study showed that S1PR3 contributes to the activation of microglia and the polarization of M1 macrophages in a mouse brain I/R model (Gaire et al., 2018b). In our study, we found that inhibition of S1PR3 reduced I/R injury, which was confirmed by the reduction of infarct volume. The results of H&E, Nissl and FJC staining confirmed the point that S1PR3 mediates brain damage during cerebral ischemia and reperfusion.

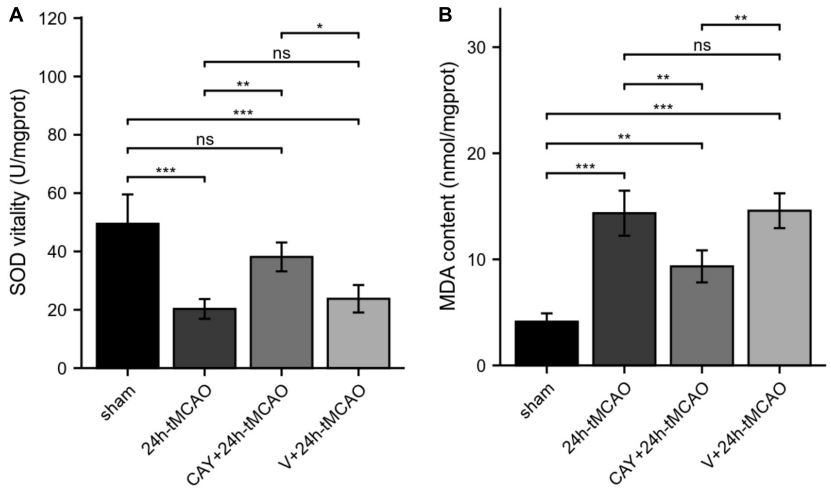

FIGURE 6 | SOD vitality and MDA content in mice subjected to tMCAO. **(A)** SOD vitality was measured ($n = 4$). **(B)** MDA content was measured ($n = 4$). Data are presented as the mean ± SEM. *P*-values were determined by ANOVA followed by the Tukey *post hoc* test, $^{*}P < 0.05$; $^{**}P < 0.01$; $^{***}P < 0.001$; and ns, not significant.

nNOS mediates early neurological damage, and overexpression of nNOS plays a key role in the early stages of ischemia and excitotoxic injury (Von Arnim et al., 2001). iNOS subsequently increased, and both changes have adverse effects on cerebral ischemia. The production of nitric oxide (NO) is one branch of the ornithine cycle, which is catalyzed by L-arginine and oxygen NOS. NO can react with superoxide to form peroxynitrite (ONOO), which is an effective and destructive oxidant (Zhang et al., 2018). During ischemia, the NO produced by nNOS and iNOS may be neurotoxic, partly because the formation of peroxynitrite free radicals causes direct damage to mitochondrial enzymes and DNA (Zhao et al., 2000; Sims and Anderson, 2002). In addition, the increase in NO produced by nNOS or iNOS can promote ischemic damage through free radical damage, tissue inflammation and microcirculation failure (Iadecola, 1997). In a cerebral ischemia model, nNOS knockout mice showed smaller infarct sizes and fewer neurological defects after middle cerebral artery occlusion (Nakamura et al., 2015). Compared with wild-type mice, mice lacking the iNOS gene showed fewer neurological deficits and infarct volumes after MCAO (Yang et al., 2019). In our experiment, the expression of nNOS and iNOS was higher than that of the sham group after cerebral ischemia, which is consistent with previous studies. After inhibiting S1PR3, we found reduced nNOS expression, and significantly reduced NO content. Heo and Im (2019) found that inhibiting S1PR3 can reduce the expression of LPS-induced inflammatory genes, such as iNOS and cyclooxygenase-2 (COX-2). However, our research found that inhibition of S1PR3 did not reduce the expression of iNOS, indicating that S1PR3 reduces the expression of NO by reducing nNOS.

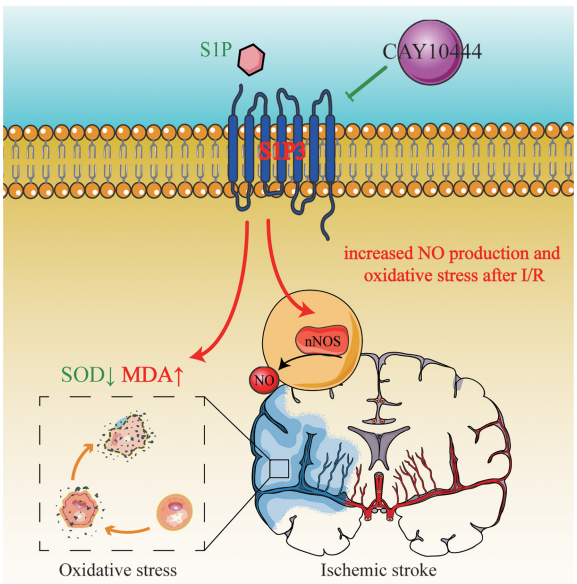

FIGURE 7 | S1PR3 mediates nNOS/NO and oxidative stress during cerebral ischemia and reperfusion.

Studies have shown that eNOS protein expression in cerebral blood vessels after focal cerebral ischemia protects against cerebral ischemia by protecting cerebral blood flow (Muid et al., 2016). Lv et al. (2020) found that sphingosine kinase 1 (Sphk1)/S1P signaling may mediate angiogenesis after cerebral ischemia by regulating eNOS activity and NO production. We found that the expression of eNOS increased after cerebral ischemia and reperfusion, but inhibition of S1PR3 did not affect the expression of eNOS, suggesting that S1PR3 does not play a relevant role in regulating eNOS activity in the tMCAO model.

We previously mentioned that S1PR3 is involved in regulating the production of NO and that NO is involved in excitotoxicity. During cerebral ischemia, NO can mediate glutamate neurotoxicity in cortical and hippocampal neurons.

After cerebral ischemic attack, oxidative stress plays a major role in neuroinflammatory diseases. Mitochondria play a key role in energy metabolism in the body. When energy metabolism is dysregulated, mitochondria produce a large amount of ROS and cause tissue oxidative stress damage (Hussain et al., 2018). Under normal physiological conditions, SOD (superoxide dismutase), GPX (glutathione peroxidase), catalase and other antioxidant enzymes can protect brain tissue from ROS poisoning through catalysis and maintain sexual balance (Ouyang et al., 2015; Zhang et al., 2016). During cerebral ischemia and reperfusion, the production of ROS is significantly increased, and SOD can be consumed by catalase reactions. As a result, the body's oxidation and anti-oxidation balance is broken, making the body more susceptible to oxidation and causing cells to undergo oxidative damage (Wang et al., 2019). MDA (malondialdehyde) is an indicator for the severity of oxidative stress within the tissue, and the level of MDA can indirectly measure the degree of tissue damage. High blood lipid levels and high oxygen consumption are the causes of brain oxidative stress damage (Ozkul et al., 2007). In our study, after cerebral ischemia, the activity of SOD decreased, and the content of MDA increased. After the S1PR3 inhibitor CAY-10444 was administered to tMCAO mice, the MDA content in the brain tissues decreased significantly, and the SOD vitality increased, indicating that S1PR3 is involved in the regulation of cerebral ischemia and oxidative stress. Previous studies have found that S1P induces NADPH oxidase activity and intracellular ROS generation in a time-dependent manner (Lin et al., 2016). Therefore, more research is needed to confirm whether S1P is an oxidative stress process regulated by S1PR3 during cerebral ischemia and reperfusion.

CAY10444 has been widely used as a specific antagonist of S1PR3, but other modes of action have been found. Previous studies have found that CAY10444 (10 μM) inhibits $[Ca^{2+}]i$ increases via purinergic P2 receptor or α1A-adrenoceptor stimulation and α1A-adrenoceptor-mediated contraction, while not affecting the S1PR3-mediated decrease of forskolin-induced cAMP accumulation (Jongsma et al., 2006). The proliferation of ovarian cancer cells was not affected by S1PR3 inhibitor CAY10444 (1 μM) (Illuzzi et al., 2010). S1PR3 specific inhibitor CAY10444 (10 μM) showed no effect on the protection of platelet-activating factor induced mesenteric venular microvascular permeability by S1P (Zhang et al., 2010). The concentrations of CAY-10444 used in these studies may be too low, mostly 1 or 10 μm, to significantly block the S1PR3 receptor. In previous studies, the use of CAY10444 reduced the polarization of microglia and proved the effectiveness of the inhibitor for this model 30305119 (Gaire et al., 2018b). Therefore, we chose this concentration for the experiment. However, it is necessary to use gene knockout in future research.

CONCLUSION

In summary, our results provide a new evidence that S1PR3 participates in the regulation of oxidative stress after cerebral ischemia and reperfusion and regulates brain damage after cerebral ischemia through regulation of nNOS/NO. **Figure 7** shows that S1PR3 mediates nNOS/NO and oxidative stress during cerebral ischemia-reperfusion. The results of this study provide new potential therapeutic targets and mechanisms for the treatment of cerebral ischemia and reperfusion injury. These results may provide pharmacological evidence for the potential application of CAY-10444 in the treatment of cerebral ischemic injury and as an effective treatment for IS.

DATA AVAILABILITY STATEMENT

The original contributions presented in the study are included in the article/supplementary material, further inquiries can be directed to the corresponding author/s.

ETHICS STATEMENT

The animal study was reviewed and approved by the Laboratory Animals Ethics Committee of the First Affiliated Hospital of Harbin Medical University.

AUTHOR CONTRIBUTIONS

XF performed experiments and wrote the manuscript. HC conceived the idea of the study. CX, YW, PY, and ML designed the experiments. ZT, FJ, WW, and JS analyzed the data. GL and DZ revised the final manuscript. All authors contributed to the article and approved the submitted version.

FUNDING

This work was supported by the National Natural Science Foundation of China (Grant No. 81873746) and Heilongjiang Province Key R&D Program (Grant No. GA21C005).

REFERENCES

Albert, R., Hinterding, K., Brinkmann, V., Guerini, D., Müller-Hartwieg, C., Knecht, H., et al. (2005). Novel immunomodulator FTY720 is phosphorylated in rats and humans to form a single stereoisomer. *J. Med. Chem.* 48, 5373–5377. doi: 10.1021/jm050242f

Bajwa, A., Huang, L., Kurmaeva, E., Gigliotti, J. C., Ye, H., Miller, J., et al. (2016). Sphingosine 1-phosphate receptor 3-Deficient dendritic cells modulate splenic responses to ischemia-reperfusion injury. *J. Am. Soc. Nephrol. :JASN* 27, 1076–1090. doi: 10.1681/ASN.2015010095

Bajwa, A., Huang, L., Ye, H., Dondeti, K., Song, S., Rosin, D. L., et al. (2012). Dendritic cell sphingosine 1-phosphate receptor-3 regulates Th1-Th2 polarity in kidney ischemia-reperfusion injury. *J. immunol.* 189, 2584–2596. doi: 10.4049/jimmunol.1200999

Beray-Berthat, V., Palmier, B., Plotkine, M., and Margaill, I. (2003). Neutrophils do not contribute to infarction, oxidative stress, and NO synthase activity in

severe brain ischemia. *Exp. Neurol.* 182, 446–454. doi: 10.1016/s0014-4886(03)00106-7

Chun, J., Hla, T., Lynch, K. R., Spiegel, S., and Moolenaar, W. H. (2010). International union of basic and clinical pharmacology. LXXVIII. lysophospholipid receptor nomenclature. *Pharmacol. Rev.* 62, 579–587. doi: 10.1124/pr.110.003111

Fan, X., Liu, L., Shi, Y., Guo, F., He, X., Zhao, X., et al. (2021). Recent advances of the function of sphingosine 1-phosphate (S1P) receptor S1P3. *J. Cell Physiol.* 236, 1564–1578. doi: 10.1002/jcp.29958

Frantseva, M. V., Carlen, P. L., and Perez Velazquez, J. L. (2001). Dynamics of intracellular calcium and free radical production during ischemia in pyramidal neurons. *Free Radic. Biol. Med.* 31, 1216–1227. doi: 10.1016/s0891-5849(01)00705-5

Fulgenzi, G., Hong, Z., Tomassoni-Ardori, F., Barella, L. F., Becker, J., Barrick, C., et al. (2020). Novel metabolic role for BDNF in pancreatic β-cell insulin secretion. *Nat. Commun.* 11:1950. doi: 10.1038/s41467-020-15833-5

Gaire, B. P., Bae, Y. J., and Choi, J. W. (2019). S1P(1) regulates M1/M2 polarization toward brain injury after transient focal cerebral ischemia. *Biomol. Ther. (Seoul)* 27, 522–529. doi: 10.4062/biomolther.2019.005

Gaire, B. P., Lee, C. H., Sapkota, A., Lee, S. Y., Chun, J., Cho, H. J., et al. (2018a). Identification of sphingosine 1-Phosphate receptor subtype 1 (S1P(1)) as a pathogenic factor in transient focal cerebral ischemia. *Mol. Neurobiol.* 55, 2320–2332. doi: 10.1007/s12035-017-0468-8

Gaire, B. P., Song, M. R., and Choi, J. W. (2018b). Sphingosine 1-phosphate receptor subtype 3 (S1P(3)) contributes to brain injury after transient focal cerebral ischemia via modulating microglial activation and their M1 polarization. *J. Neuroinflamm.* 15:284. doi: 10.1186/s12974-018-1323-1

Heo, J. Y., and Im, D. S. (2019). Pro-Inflammatory Role of S1P(3) in macrophages. *Biomol. Ther. (Seoul)* 27, 373–380. doi: 10.4062/biomolther.2018.215

Hussain, G., Rasul, A., Anwar, H., Aziz, N., Razzaq, A., Wei, W., et al. (2018). Role of plant derived alkaloids and their mechanism in neurodegenerative disorders. *Int. J. Biol. Sci.* 14, 341–357. doi: 10.7150/ijbs.23247

Iadecola, C. (1997). Bright and dark sides of nitric oxide in ischemic brain injury. *Trends Neurosci.* 20, 132–139. doi: 10.1016/s0166-2236(96)10074-6

Illuzzi, G., Bernacchioni, C., Aureli, M., Prioni, S., Frera, G., Donati, C., et al. (2010). Sphingosine kinase mediates resistance to the synthetic retinoid N-(4-hydroxyphenyl)retinamide in human ovarian cancer cells. *J. Biol. Chem.* 285, 18594–18602. doi: 10.1074/jbc.M109.072801

Jongsma, M., Hendriks-Balk, M. C., Michel, M. C., Peters, S. L., and Alewijnse, A. E. (2006). BML-241 fails to display selective antagonism at the sphingosine-1-phosphate receptor. S1P(3). *Br. J. Pharmacol.* 149, 277–282. doi: 10.1038/sj.bjp.0706872

Levkau, B., Hermann, S., Theilmeier, G., Van Der Giet, M., Chun, J., Schober, O., et al. (2004). High-density lipoprotein stimulates myocardial perfusion in vivo. *Circulation* 110, 3355–3359. doi: 10.1161/01.CIR.0000147827.43912.AE

Li, C., Li, J.-N., Kays, J., Guerrero, M., and Nicol, G. D. (2015). Sphingosine 1-phosphate enhances the excitability of rat sensory neurons through activation of sphingosine 1-phosphate receptors 1 and/or 3. *J. Neuroinflamm.* 12:70. doi: 10.1186/s12974-015-0286-8

Lin, C. C., Yang, C. C., Cho, R. L., Wang, C. Y., Hsiao, L. D., and Yang, C. M. (2016). Sphingosine 1-Phosphate-Induced ICAM-1 expression via NADPH Oxidase/ROS-Dependent NF-κB cascade on human pulmonary alveolar epithelial cells. *Front. Pharmacol.* 7:80. doi: 10.3389/fphar.2016.00080

Liu, D. Z., Tian, Y., Ander, B. P., Xu, H., Stamova, B. S., Zhan, X., et al. (2010). Brain and blood microRNA expression profiling of ischemic stroke, intracerebral hemorrhage, and kainate seizures. *J. Cereb. Blood Flow Metab.* 30, 92–101. doi: 10.1038/jcbfm.2009.186

Lv, M. H., Li, S., Jiang, Y. J., and Zhang, W. (2020). The Sphkl/SlP pathway regulates angiogenesis via NOS/NO synthesis following cerebral ischemia-reperfusion. *CNS Neurosci. Ther.* 26, 538–548. doi: 10.1111/cns.13275

Moro, M. A., Cárdenas, A., Hurtado, O., Leza, J. C., and Lizasoain, I. (2004). Role of nitric oxide after brain ischaemia. *Cell Calcium* 36, 265–275. doi: 10.1016/j.ceca.2004.02.011

Muid, S., Froemming, G. R., Rahman, T., Ali, A. M., and Nawawi, H. M. (2016). Delta- and gamma-tocotrienol isomers are potent in inhibiting inflammation and endothelial activation in stimulated human endothelial cells. *Food Nutr. Res.* 60:31526. doi: 10.3402/fnr.v60.31526

Murakami, A., Takasugi, H., Ohnuma, S., Koide, Y., Sakurai, A., Takeda, S., et al. (2010). Sphingosine 1-phosphate (S1P) regulates vascular contraction via S1P3 receptor: investigation based on a new S1P3 receptor antagonist. *Mol. Pharmacol.* 77, 704–713. doi: 10.1124/mol.109.061481

Nakamura, T., Prikhodko, O. A., Pirie, E., Nagar, S., Akhtar, M. W., Oh, C. K., et al. (2015). Aberrant protein S-nitrosylation contributes to the pathophysiology of neurodegenerative diseases. *Neurobiol. Dis.* 84, 99–108. doi: 10.1016/j.nbd.2015.03.017

Nussbaum, C., Bannenberg, S., Keul, P., Gräler, M. H., Gonçalves-De-Albuquerque, C. F., Korhonen, H., et al. (2015). Sphingosine-1-phosphate receptor 3 promotes leukocyte rolling by mobilizing endothelial P-selectin. *Nat. Commun.* 6:6416. doi: 10.1038/ncomms7416

Ouyang, Y. B., Stary, C. M., White, R. E., and Giffard, R. G. (2015). The use of microRNAs to modulate redox and immune response to stroke. *Antioxid Redox Signal.* 22, 187–202. doi: 10.1089/ars.2013.5757

Ozkul, A., Akyol, A., Yenisey, C., Arpaci, E., Kiylioglu, N., and Tataroglu, C. (2007). Oxidative stress in acute ischemic stroke. *J. Clin. Neurosci.* 14, 1062–1066.

Patil, M. J., Meeker, S., Bautista, D., Dong, X., and Undem, B. J. (2019). Sphingosine-1-phosphate activates mouse vagal airway afferent C-fibres via S1PR3 receptors. *J. Physiol.* 597, 2007–2019. doi: 10.1113/JP277521

Sapkota, A., Gaire, B. P., Kang, M. G., and Choi, J. W. (2019). S1P(2) contributes to microglial activation and M1 polarization following cerebral ischemia through ERK1/2 and JNK. *Sci. Rep.* 9:12106. doi: 10.1038/s41598-019-48609-z

Schmued, L. C., Stowers, C. C., Scallet, A. C., and Xu, L. (2005). Fluoro-Jade C results in ultra high resolution and contrast labeling of degenerating neurons. *Brain Res.* 1035, 24–31.

Shirakawa, H., Katsumoto, R., Iida, S., Miyake, T., Higuchi, T., Nagashima, T., et al. (2017). Sphingosine-1-phosphate induces Ca(2+) signaling and CXCL1 release via TRPC6 channel in astrocytes. *Glia* 65, 1005–1016. doi: 10.1002/glia.23141

Sims, N. R., and Anderson, M. F. (2002). Mitochondrial contributions to tissue damage in stroke. *Neurochem. Int.* 40, 511–526. doi: 10.1016/s0197-0186(01)00122-x

Stepanovska, B., and Huwiler, A. (2020). Targeting the S1P receptor signaling pathways as a promising approach for treatment of autoimmune and inflammatory diseases. *Pharmacol. Res.* 154:104170. doi: 10.1016/j.phrs.2019.02.009

Taoufik, E., and Probert, L. (2008). Ischemic neuronal damage. *Curr. Pharm. Des.* 14, 3565–3573. doi: 10.2174/138161208786848748

Von Arnim, C. A., Timmler, M., Ludolph, A. C., and Riepe, M. W. (2001). Chemical preconditioning in mice is not mediated by upregulation of nitric oxide synthase isoforms. *Neurosci. Lett.* 299, 130–134. doi: 10.1016/s0304-3940(00)01762-6

Wang, H., Huang, H., and Ding, S. F. (2018). Sphingosine-1-phosphate promotes the proliferation and attenuates apoptosis of Endothelial progenitor cells via S1PR1/S1PR3/PI3K/Akt pathway. *Cell Biol. Int.* 42, 1492–1502. doi: 10.1002/cbin.10991

Wang, J., Huang, L., Cheng, C., Li, G., Xie, J., Shen, M., et al. (2019). Design, synthesis and biological evaluation of chalcone analogues with novel dual antioxidant mechanisms as potential anti-ischemic stroke agents. *Acta Pharm. Sin. B* 9, 335–350. doi: 10.1016/j.apsb.2019.01.003

Wang, M., Chen, W., Geng, Y., Xu, C., Tao, X., and Zhang, Y. (2020). Long Non-Coding RNA MEG3 promotes apoptosis of vascular cells and is associated with poor prognosis in ischemic stroke. *J. Atheroscler. Thromb.* 27, 718–726. doi: 10.5551/jat.50674

Yang, C., Hawkins, K. E., Doré, S., and Candelario-Jalil, E. (2019). Neuroinflammatory mechanisms of blood-brain barrier damage in ischemic stroke. *Am. J. Physiol. Cell Physiol.* 316, C135–C153. doi: 10.1152/ajpcell.00136.2018

Zhang, G., Xu, S., Qian, Y., and He, P. (2010). Sphingosine-1-phosphate prevents permeability increases via activation of endothelial sphingosine-1-phosphate receptor 1 in rat venules. *Am. J. Physiol. Heart Circ. Physiol.* 299, H1494–H1504. doi: 10.1152/ajpheart.00462.2010

Zhang, L., Wu, J., Duan, X., Tian, X., Shen, H., Sun, Q., et al. (2016). NADPH oxidase: a potential target for treatment of stroke. *Oxid. Med. Cell. Longev.* 2016:5026984. doi: 10.1155/2016/5026984

Zhang, Y., Zhang, W. X., Zhang, Y. J., Liu, Y. D., Liu, Z. J., Wu, Q. C., et al. (2018). Melatonin for the treatment of spinal cord injury. *Neural Regen. Res.* 13, 1685–1692.

Zhao, X., Haensel, C., Araki, E., Ross, M. E., and Iadecola, C. (2000). Gene-dosing effect and persistence of reduction in ischemic brain injury in mice lacking inducible nitric oxide synthase. *Brain Res.* 872, 215–218.

Conflict of Interest: The authors declare that the research was conducted in the absence of any commercial or financial relationships that could be construed as a potential conflict of interest.

Publisher's Note: All claims expressed in this article are solely those of the authors and do not necessarily represent those of their affiliated organizations, or those of the publisher, the editors and the reviewers. Any product that may be evaluated in this article, or claim that may be made by its manufacturer, is not guaranteed or endorsed by the publisher.

frontiers in Pharmacology

MINI REVIEW
published: 21 February 2022
doi: 10.3389/fphar.2022.831181

Treatment of Cerebral Ischemia Through NMDA Receptors: Metabotropic Signaling and Future Directions

Yuanyuan Li[1†], Xiaokun Cheng[2,3,4,5†], Xinying Liu[2], Le Wang[4,6], Jing Ha[1,7,8], Zibin Gao[1,7,8], Xiaoliang He[9], Zhuo Wu[10], Aibing Chen[11]*, Linda L. Jewell[12] and Yongjun Sun[1,7,8]**

[1]Department of Pharmacy, Hebei University of Science and Technology, Shijiazhuang, China, [2]Institute for the Development of Energy for African Sustainability, University of South Africa, Pretoria, South Africa, [3]Department of Chemical Engineering, University of South Africa, Florida, South Africa, [4]Department of Pharmaceutical Engineering, Hebei Chemical & Pharmaceutical College, Shijiazhuang, China, [5]New Drug Research & Development Co., Ltd., North China Pharmaceutical Group Corporation, Shijiazhuang, China, [6]Hebei Technological Innovation Center of Chiral Medicine, Shijiazhuang, China, [7]Hebei Research Center of Pharmaceutical and Chemical Engineering, Hebei University of Science and Technology, Shijiazhuang, China, [8]State Key Laboratory Breeding Base—Hebei Province Key Laboratory of Molecular Chemistry for Drug, Shijiazhuang, China, [9]College of Food Science and Biology, Hebei University of Science and Technology, Shijiazhuang, China, [10]Department of Pharmacy, Huashan Hospital, Fudan University, Shanghai, China, [11]College of Chemical and Pharmaceutical Engineering, Hebei University of Science and Technology, Shanghai, China, [12]Department of Chemical Engineering, University of South Africa, Pretoria, South Africa

OPEN ACCESS

Edited by:
Antonio Rodriguez Moreno, Universidad Pablo de Olavide, Spain

Reviewed by:
Valeria Bruno, Sapienza University of Rome, Italy
Yuniesky Andrade Talavera, Universidad Pablo de Olavide, Spain

***Correspondence:**
Zhuo Wu
zwu14@fudan.edu.cn
Aibing Chen
chen_ab@163.com
Yongjun Sun
yj_sun1@aliyun.com

[†]These authors have contributed equally to this work

Specialty section:
This article was submitted to Neuropharmacology, a section of the journal Frontiers in Pharmacology

Received: *08 December 2021*
Accepted: *28 January 2022*
Published: *21 February 2022*

Citation:
Li Y, Cheng X, Liu X, Wang L, Ha J, Gao Z, He X, Wu Z, Chen A, Jewell LL and Sun Y (2022) Treatment of Cerebral Ischemia Through NMDA Receptors: Metabotropic Signaling and Future Directions. Front. Pharmacol. 13:831181. doi: 10.3389/fphar.2022.831181

Excessive activation of N-methyl-D-aspartic acid (NMDA) receptors after cerebral ischemia is a key cause of ischemic injury. For a long time, it was generally accepted that calcium influx is a necessary condition for ischemic injury mediated by NMDA receptors. However, recent studies have shown that NMDA receptor signaling, independent of ion flow, plays an important role in the regulation of ischemic brain injury. The purpose of this review is to better understand the roles of metabotropic NMDA receptor signaling in cerebral ischemia and to discuss the research and development directions of NMDA receptor antagonists against cerebral ischemia. This mini review provides a discussion on how metabotropic transduction is mediated by the NMDA receptor, related signaling molecules, and roles of metabotropic NMDA receptor signaling in cerebral ischemia. In view of the important roles of metabotropic signaling in cerebral ischemia, NMDA receptor antagonists, such as GluN2B-selective antagonists, which can effectively block both pro-death metabotropic and pro-death ionotropic signaling, may have better application prospects.

Keywords: NMDA receptor, ion-flow independent, metabotropic signaling, cerebral ischemia, NMDA receptor antagonists

INTRODUCTION

Glutamate receptors mediate glutamate's excitatory role in physiological processes such as memory, learning, and synaptic plasticity (Hansen et al., 2021); thus, they also play a part in several common neurological diseases, such as depression (Xia et al., 2021), Alzheimer's disease (Srivastava et al., 2020) and epilepsy (Alcoreza et al., 2021). Glutamate receptors are both ionotropic and metabotropic. The ionotropic N-methyl-D-aspartate (NMDA) glutamate receptor is a tetrameric complex containing two obligatory GluN1 subunits and two additional subunits, either GluN2

(GluN2A-D) or GluN3 (GluN3A-B) (Sun et al., 2019). The diversity of NMDA receptor subtypes endows the receptor family with a variety of physiological and pathological functions (Paoletti et al., 2013; Perez-Otano et al., 2016).

The traditional view on signal transduction through ionotropic glutamate receptors (NMDA receptors, α-amino-3-hydroxy-5-methyl-4-isoxazolepropionic acid (AMPA) receptors, and kainate (KA) receptors) is that glutamate binding opens ion channels, which allow Na^+, K^+, or Ca^{2+} to enter or exit the cell and subsequently transmit ion-dependent excitatory signaling (Rajani et al., 2020). However, the discovery of the metabotropic action of KA receptors in 1998 revealed another mode of signal transduction (Rodriguez-Moreno and Lerma, 1998). The metabotropic activities of both KA receptors and AMPA receptors have been found to modulate neurotransmitter release (Falcon-Moya and Rodriguez-Moreno, 2021). With the deepening of research into this subject, there is increasing evidence that NMDA receptors can also mediate both ionotropic and metabotropic signaling (Dore et al., 2016; Dore et al., 2017; Montes De Oca Balderas, 2018). Metabotropic NMDA receptor signaling, which is independent of ion flow, is involved in long-term depression (LTD) (Nabavi et al., 2013), synaptic depression induced by β-amyloid (Aβ) (Kessels et al., 2013; Tamburri et al., 2013; Birnbaum et al., 2015), dendritic spine shrinkage (Stein et al., 2015; Stein et al., 2020) and long-term potentiation (LTP)-induced spine growth (Stein et al., 2021). Recent studies have found that ion-independent metabotropic NMDA receptor signaling plays an important role in the regulation of cerebral ischemic injury (Weilinger et al., 2016; Chen et al., 2017). Metabotropic NMDA receptor signaling has not been found in some other important processes, such as spike timing-dependent plasticity (Rodriguez-Moreno and Paulsen, 2008; Banerjee et al., 2014; Andrade-Talavera et al., 2016) and presynaptic glutamate release modulation (Abrahamsson et al., 2017; Prius-Mengual et al., 2019). This mini review provides a discussion on how metabotropic transduction is mediated by the NMDA receptor, known related signaling molecules, and their interplay in cerebral ischemia.

NMDA RECEPTOR METABOTROPIC OPERATION

The prevailing view on NMDA receptors states that agonist glutamate and co-agonist glycine (or D-serine) jointly activate the receptor, initiating excitatory signaling. Unlike this classical mode, transduction of metabotropic NMDA receptor signaling only requires ligand binding to either one of the two agonist-binding sites, the one for glutamate, GluN2, or the one for glycine, GluN1 (Rajani et al., 2020). By measuring Förster resonance energy transfer (FRET) between fluorescently tagged GluN1 subunits of NMDA receptors, Malinow et al. demonstrated that NMDA exposure induced conformational changes in the cytoplasmic domain of NMDA receptors, provoking synaptic inhibition (Aow et al., 2015; Dore et al., 2015). This phenomenon can be blocked by the glutamate-binding site antagonist amino-phosphonovalerate (APV), but not by the glycine-binding site antagonist 7-chlorokynurenate (7CK) (Aow et al., 2015; Dore et al., 2015). Low-frequency stimulation (LFS) in acute hippocampal slices was shown to induce ion-independent and NMDA receptor-dependent LTD, which could be blocked by the glutamate-binding site antagonist D-amino-phosphonovalerate (D-APV), but not 7CK (Nabavi et al., 2013). In calcium-free extracellular solutions with calcium chelator EGTA or BAPTA, glycine exposure increased the level of Akt phosphorylation in cultured mouse cortical neurons, which was inhibited by the glycine-binding site antagonist, L-689560, and the addition of NMDA receptor ion-channel blocker, MK-801 or GluN2B-selective antagonist, Ro 25-6981 could not prevent this effect (Hu et al., 2016).

Similar to non-channel transmembrane receptors, agonist-induced conformational change in the cytoplasmic domain of NMDA receptors is a key requirement for metabotropic signaling transduction. Using the FRET technique, Dore et al. showed that in the presence of 7CK or MK-801, FRET between different GluN1 subunits on individual NMDA receptors could be reduced after NMDA was administered, which indicated that the binding of NMDA to NMDA receptors causes conformational changes in the cytoplasmic domain in the absence of ion flow (Dore et al., 2015). Intracellular infusion of a GluN1 C-terminus antibody that can bind and immobilize two nearby cytoplasmic domains of the GluN1 subunit prevented FRET changes induced by NMDA exposure (Dore et al., 2015).

The relative position change and resulting interaction between different molecules coupled to the C-terminus of NMDA receptors induced by conformational changes are the underlying molecular mechanisms of metabotropic NMDA signaling transduction. Studies have shown that both protein phosphatase 1 (PP1) and calcium/calmodulin-dependent protein kinase II (CaMKII) bind to the intracellular C-terminus of NMDA receptors (Aow et al., 2015; Sun et al., 2018). Without ligands binding to NMDA receptors, the distance between PP1 and CaMKII is too large for any interaction to occur. However, when NMDA binds to NMDA receptors, the relative positions of PP1 and CaMKII change, and the distance between them is reduced. In this situation, the catalytic site of PP1 can contact CaMKII, and dephosphorylate it at Thr286 (Aow et al., 2015). Thereafter, CaMKII is repositioned on the NMDA receptor and subsequently activates downstream signaling molecules, thereby inducing synaptic inhibition in an ion-independent manner (Aow et al., 2015).

Although it is independent of ion transmembrane flow, metabotropic NMDA receptor signaling may require the involvement of intracellular calcium and its effectors. Studies have indicated that the metabotropic actions of KA receptors are involved in modulating glutamate release in a biphasic manner (Falcon-Moya and Rodriguez-Moreno, 2021). KA receptor-mediated facilitation of glutamate release is dependent on Ca^{2+}, calmodulin, and

TABLE 1 | Downstream signaling molecules of metabotropic NMDA receptor signaling.

Pathophysiological processes	Related subunits	Downstream signaling molecule	References
Spine shrinkage	Not reported	nNOS, NOSIAP, p38, MK2, cofilin CaMKII	Nabavi et al. (2013); Stein et al. (2020)
Synaptic depression	GluN2	p38	Stein et al. (2020)
LTD	GluN2	p38	Nabavi et al. (2013); Birnbaum et al. (2015)
	Not reported	PP1, CaMKII	Coultrap et al. (2014); Aow et al. (2015)
LTP	Not reported	CaMKII	Coultrap et al. (2014)
Enhance the function of the AMPA receptor	GluN2A	ERK1/2	Li et al. (2016)
Excitotoxic injury	GluN1, GluN2A	Akt	Hu et al. (2016)
	GluN1	Src, Panx1	Weilinger et al. (2012); Weilinger et al. (2016)
	GluN2B	PI3K, NOX2	Minnella et al. (2018)

protein kinase A (PKA) (Andrade-Talavera et al., 2012; Andrade-Talavera et al., 2013; Falcon-Moya et al., 2018; Falcon-Moya and Rodriguez-Moreno, 2021). KA receptor-mediated depression of glutamate release is dependent on Ca^{2+}, calmodulin, protein kinase A (PKA), and G-protein (Falcon-Moya et al., 2018; Falcon-Moya and Rodriguez-Moreno, 2021). Whether these signaling molecules are involved in metabotropic NMDA receptor-mediated actions should be studied in the future.

SIGNALING MOLECULES MEDIATING METABOTROPIC NMDA RECEPTOR SIGNALING

Metabotropic NMDA receptor actions involve signaling molecules, such as kinases, second messengers, and other molecules that have been found to be related to synaptic plasticity and cerebral ischemia (**Table 1**).

Signaling Molecules Related to Synaptic Plasticity

Neuronal nitric oxide synthase (nNOS)/nitric oxide synthase one adaptor protein (NOS1AP)/p38/MAPK-activated protein kinase 2 (MK2)/cofilin is a key metabotropic NMDA receptor signaling pathway for gating the structural plasticity of dendritic spines. nNOS is a member of the NMDA receptor complex that anchors to the scaffold protein postsynaptic density-95 (PSD-95) (Sun et al., 2015). NOS1AP is a carboxy-terminal ligand of nNOS (Zhu et al., 2020). L-TAT-GESV, an uncoupling agent of the nNOS/NOS1AP complex (Li et al., 2013), interferes with dendritic spine shrinkage driven by metabotropic NMDA receptor signaling (Stein et al., 2020). The NOS inhibitor l-NNA was shown to abolish high-frequency uncaging (HFU)-induced NMDA receptor-dependent spine shrinkage mediated by non-ionotropic signaling (Stein et al., 2020). p38, MK2, and cofilin are specific downstream signaling molecules of NOS1AP (Stein et al., 2020). Interestingly, during strong Ca^{2+} influx following LTP induction, this signaling pathway promotes spine growth (Stein et al., 2021). It is still unclear how metabotropic NMDA receptor signaling affects nNOS. Although nNOS is a member of the NMDA receptor complex, it may play a physiological role in an NMDA receptor-independent manner. For example, nNOS-derived NO is involved in the recently discovered developmental switch from an NMDA receptor-dependent form of spike timing-dependent LTD to NMDA receptor-independent LTP (Falcon-Moya et al., 2020).

PP1 and CaMKII are two important downstream signaling molecules of metabotropic NMDA receptor signaling involved in the process of synaptic depression. PP1 becomes an indirect coupling molecule of the GluN1 subunit by binding to yotiao (Westphal et al., 1999). CaMKII is a direct binding partner of GluN2 subunits. Both residues 1120–1482 or residues 839–1120 in GluN2B and the 1389–1464 sequence in the C-terminus of GluN2A are sufficient for the binding of CaMKII (Sun et al., 2018). NMDA binding was shown to produce a transient change in the relative position between PP1 and CaMKII, allow PP1 to act on CaMKII and dephosphorylate CaMKII at Thr286 (Aow et al., 2015). This change induced a reorientation of CaMKII within the C-terminus of NMDA receptors and caused CaMKII to potentially catalyze substrates necessary for LTD (Aow et al., 2015).

p38 is also involved in synaptic depression mediated by metabotropic NMDA receptor signaling. NMDA exposure increased p38 phosphorylation in cultured neurons, which could be blocked by D-APV but not by MK-801 (Nabavi et al., 2013). Synaptic depression can be induced by Aβ exposure, and the p38 inhibitor SB239063 abolishes this phenomenon (Birnbaum et al., 2015). Because p38 is not a member of the NMDA receptor complex, further studies are needed to identify the related upstream signaling molecules.

Extracellular signal-regulated kinase 1/2 (ERK1/2) participates in the transduction of metabotropic NMDA receptor signaling. Co-incubation of hippocampal slices with metabotropic glutamate receptor type 5 (mGluR5) agonist CHPG (15 μM) and NMDA (5 μM) induced a robust increase in the phosphorylation level of ERK1/2, which could be inhibited by AP5, but not by MK-801 (Krania et al., 2018). This phenomenon could also be prevented by the Src inhibitor PP1, which indicated the involvement of Src in this process (Krania et al., 2018). Glycine increased ERK1/2 phosphorylation in a dose-dependent manner, in hippocampal neurons exposed to a Ca^{2+}-free extracellular solution with EGTA, MK-801, and

strychnine (Li et al., 2016). This effect of glycine appeared in HEK293 cells transfected with cDNAs of GluN1 and GluN2A, but not in cells transfected with cDNAs of GluN1 and GluN2B (Li et al., 2016).

Signaling Molecules Related to Cerebral Ischemia

The NMDA receptor, Src, and pannexin 1 (Panx1) comprise a metabotropic signaling complex that is involved in the process of cerebral ischemia (Li et al., 2021). Src indirectly associates with NMDA receptors by interacting with NADH dehydrogenase subunit 2 (ND2) via amino acids 40–80 (Gingrich et al., 2004; Liu et al., 2008; Sun et al., 2016). Src is anchored to NMDA receptors through the interaction between the PDZ3 domain of PSD-95 and the SH2 domain of Src (Kalia and Salter, 2003; Sun et al., 2016). Panx1 interacts with Src via the amino acid sequence 305–318 at the C terminus (Weilinger et al., 2012). The relative amount of Src associated with the NMDA receptor complex increased following NMDA and glycine exposure, and the phosphorylation level at Tyr416 also increased (Weilinger et al., 2016). Src can open Panx1 channels by phosphorylating Panx1 at Tyr308, which can be prevented by the SFK inhibitor PP2 (Weilinger et al., 2012; Weilinger et al., 2016). NMDA receptor competitive antagonists APV plus CGP-78608, but not MK-801, can prevent NMDA-induced Panx1 currents (Weilinger et al., 2016).

Akt is another downstream metabotropic signaling molecule involved in cerebral ischemia. In a modified calcium-free extracellular solution with EGTA or BAPTA, treating mouse cortical neurons with glycine significantly enhanced the activity of Akt, which could be blocked by L-689560, but not by MK-801 or the glycine receptor antagonist, strychnine (Hu et al., 2016). After inhibiting ion flow by NMDA receptors, glycine exposure increased Akt phosphorylation level in GluN1/GluN2A transfected HEK293 cells, but not in GluN1/GluN2B-transfected cells (Hu et al., 2016). This indicates that glycine can enhance Akt phosphorylation through the metabotropic signaling of NMDA receptors containing GluN2A. Similarly, glycine could also reduce the infarct volume in the brain of ischemic stroke rats pre-injected with MK-801 and strychnine; this effect was sensitive to L-689560 and Akt inhibitor IV (Chen et al., 2017).

In addition to participating in the regulation of synaptic plasticity, p38 is involved in neuronal damage induced by cerebral ischemia. p38 activation induced by glutamate exposure or NO donors contributes to excitotoxic neuronal cell death (Cao et al., 2005). The nNOS-PBD (PSD95-binding domain) construct containing the nNOS PDZ domain and the adjacent β finger, which binds PSD95 in a manner similar to nNOS, reduced p38 activation and decreased glutamate-induced pyknosis in neurons (Cao et al., 2005). The NMDA receptor-PSD-95-nNOS-NOS1AP-MAP kinase 3 (MKK3) is the upstream signaling pathway of p38 (Cao et al., 2005; Li et al., 2013; Sun et al., 2015).

In contrast to previous signaling pathways, NADPH oxidase-2 (NOX2) activation requires both ionotropic and metabotropic NMDA receptor signaling. In mouse cortical neuron cultures, NMDA-induced superoxide production was blocked by the application of 7CK, L-689560, or MK-801, and after additional addition of ionomycin to provide a Ca^{2+} influx, superoxide production was restored (Minnella et al., 2018). However, AP5 prevented NMDA-induced NOX2 activation, and this effect could not be reversed by co-incubation with ionomycin (Minnella et al., 2018). NOX2 does not form a complex with the NMDA receptor. The upstream signaling molecule phosphatidylinositol 3-kinase (PI3K) binds to GluN2B via its p85 regulatory subunit (Wang and Swanson, 2020). After NMDA stimulation, the activation of PI3K induces the formation of phosphatidylinositol (3,4,5) trisphosphate (PIP3) and PIP3 activates protein kinase C (PKC) and phosphorylates the $p47^{phox}$ organizing subunit of NOX2 (Brennan-Minnella et al., 2015; Wang and Swanson, 2020).

ROLES OF METABOTROPIC NMDA RECEPTOR SIGNALING IN CEREBRAL ISCHEMIA

Metabotropic NMDA receptor signaling regulates the damage induced by cerebral ischemia in a bidirectional manner (**Figure 1**). In general, metabotropic signaling mediated by GluN2B-containing NMDA receptors plays an important role in promoting neuronal death, whereas GluN2A-containing NMDA receptors play a neuroprotective role.

Pro-Death Effect

The metabotropic NMDA receptor-Src-Panx1 signaling pathway exerts a pro-death effect in cerebral ischemia. Over-activation of NMDA receptors activates Src, induces phosphorylation of Panx1 at the Tyr308 site, opens the Panx1 half-channel, and ion-independently causes neuronal death (Weilinger et al., 2012; Weilinger et al., 2016). A combination of the competitive glutamate site antagonist APV and glycine site antagonist CGP-78608 blocked the opening of the Panx1 half channel and prevented excitotoxic damage in hippocampal CA1 pyramidal neurons (Weilinger et al., 2016). Polypeptide Src48, which interferes with GluN1-Src interaction, or Tat-Panx308, which interferes with Panx1 phosphorylation, showed a neuroprotective effect *in vitro* (Weilinger et al., 2016). In an *in vivo* model of stroke, Tat-Panx308 reduced infarction volume by approximately 9.7% (Weilinger et al., 2016).

The NMDA receptor-PI3K-PKC-NOX2 is a pro-death metabotropic NMDA receptor signaling pathway. NOX2 is the primary source of neuronal superoxide production in response to NMDA receptor activation (Brennan-Minnella et al., 2015; Minnella et al., 2018). Superoxide production largely contributes to neuronal death during excitotoxicity following cerebral ischemia (Brennan-Minnella et al., 2015).

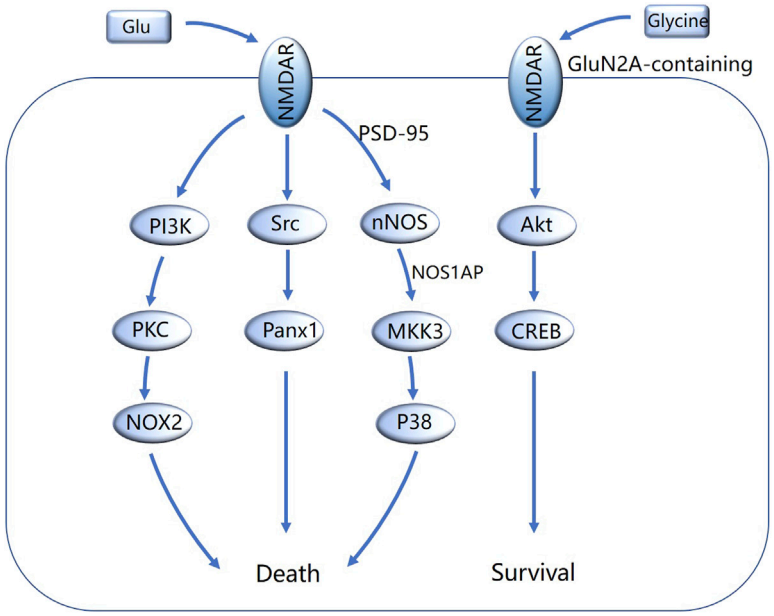

FIGURE 1 | Overview of metabotropic NMDA receptor (NMDAR) signaling pathways involved in cerebral ischemia. Excessive glutamate binds to the GluN2 subunit of NMDA receptors and initiates several pro-death signaling pathways, such as PI3K-PKC-NOX2, Src-PanX1 and nNOS-MKK3-p38. Glycine binds to the GluN1 subunit of GluN2A-containing NMDA receptors, activates Akt-CREB signaling pathway and promotes the survival of neurons.

The signaling pathway that links NMDA receptors to NOX2 activation as well as superoxide production is triggered by NMDA binding, but not glycine binding, which can be blocked by the glutamate-binding site antagonist AP5 (Minnella et al., 2018; Wang and Swanson, 2020). Neurons deficient in GluN2B or expressing chimeric GluN2B/GluN2A C-terminus subunits did not exhibit NMDA-induced superoxide production, indicating that GluN2B-containing NMDA receptors are preferentially involved in NMDA-induced superoxide production (Minnella et al., 2018).

p38 may also be a downstream pro-death metabotropic signaling molecule of NMDA receptors during cerebral ischemia. p38 is strongly involved in excitotoxicity, and the cell-permeable peptide, TAT-GESV effectively inhibits excitotoxic p38 activation, which protects against excitotoxic neuronal damage and reduces ischemic injury in neonatal hypoxia-ischemia rats (Li et al., 2013). NMDA exposure in cultured neurons activates p38 in an ion-independent manner (Nabavi et al., 2013).

Pro-Survival Effect

The metabotropic NMDA receptor signaling mediated by GluN2A may play a neuroprotective role in cerebral ischemia. Glycine administration reduced infarct volume in middle cerebral artery occlusion (MCAO) animals pretreated with MK-801 and strychnine; this effect was sensitive to glycine site antagonists and can also be blocked by Akt inhibitors (Chen et al., 2017). After inhibiting ion flow by NMDA receptors, glycine exposure increased Akt phosphorylation level in GluN1/GluN2A transfected HEK293 cells, but not in GluN1/GluN2B-transfected cells (Hu et al., 2016). This indicates that glycine can enhance Akt phosphorylation through the metabotropic signaling mediated by NMDA receptors containing GluN2A.

FUTURE DIRECTIONS OF NMDA RECEPTOR ANTAGONISTS

The roles of NMDA receptors in cerebral ischemia are complex. NMDA receptors mediate both pro-death and pro-survival ionotropic signaling. Similarly, the metabotropic signaling of NMDA receptors can either be beneficial or harmful to neuronal survival. This makes the design of effective treatment strategies based on NMDARs difficult. The complexity of NMDA receptor signaling may be one of the important underlying reasons for the failure of NMDA receptor antagonists in the treatment of cerebral ischemia. Researchers should study how to effectively block all pro-death ionotropic and pro-death metabotropic signaling. Among all NMDA receptor antagonists, ion-channel blockers and glycine-binding site antagonists cannot block pro-death metabotropic signaling. Although glutamate-binding site antagonists can inhibit both ionotropic and metabotropic signaling, they have no selectivity for GluN2A and GluN2B. In theory, GluN2B-selective antagonists may have unique advantages for blocking the pro-death effect of both ionotropic and metabotropic signaling without influencing the pro-survival effect of GluN2A. However, existing

GluN2B-selective antagonists are negative allosteric regulators and have the disadvantages of off-target effects and activity dependence (Kew et al., 1996; Fischer et al., 1997; Dey et al., 2016). GluN2B-selective glutamate-binding site antagonists may be a promising research and development direction for NMDAR antagonists.

AUTHOR CONTRIBUTIONS

YL and XC drafted the work; LW and JH performed the literature search and data analysis; ZG and XH revised the work; XL, ZW, AC, LJ, and YS put forward the idea and revised the work.

FUNDING

This work was supported by the Natural Science Foundation of China (NSFC 82071333, 81771265), the Biological Medicine Joint Fund of Natural Science Foundation of Hebei Province (H2020208016, H2020208024, H2021208010, H2021208011), and open fund of Hebei technological innovation center of chiral medicine (ZXJJ20210205).

REFERENCES

Abrahamsson, T., Chou, C. Y. C., Li, S. Y., Mancino, A., Costa, R. P., Brock, J. A., et al. (2017). Differential Regulation of Evoked and Spontaneous Release by Presynaptic NMDA Receptors. *Neuron* 96, 839–e5. doi:10.1016/j.neuron.2017.09.030

Alcoreza, O. B., Patel, D. C., Tewari, B. P., and Sontheimer, H. (2021). Dysregulation of Ambient Glutamate and Glutamate Receptors in Epilepsy: An Astrocytic Perspective. *Front. Neurol.* 12, 652159. doi:10.3389/fneur.2021.652159

Aow, J., Dore, K., and Malinow, R. (2015). Conformational Signaling Required for Synaptic Plasticity by the NMDA Receptor Complex. *Proc. Natl. Acad. Sci. U S A.* 112, 14711–14716. doi:10.1073/pnas.1520029112

Banerjee, A., González-Rueda, A., Sampaio-Baptista, C., Paulsen, O., and Rodríguez-Moreno, A. (2014). Distinct Mechanisms of Spike Timing-dependent LTD at Vertical and Horizontal Inputs onto L2/3 Pyramidal Neurons in Mouse Barrel Cortex. *Physiol. Rep.* 2, e00271. doi:10.1002/phy2.271

Birnbaum, J. H., Bali, J., Rajendran, L., Nitsch, R. M., and Tackenberg, C. (2015). Calcium Flux-independent NMDA Receptor Activity Is Required for Aβ Oligomer-Induced Synaptic Loss. *Cell Death Dis* 6, e1791. doi:10.1038/cddis.2015.160

Brennan-Minnella, A. M., Won, S. J., and Swanson, R. A. (2015). NADPH Oxidase-2: Linking Glucose, Acidosis, and Excitotoxicity in Stroke. *Antioxid. Redox Signal.* 22, 161–174. doi:10.1089/ars.2013.5767

Cao, J., Viholainen, J. I., Dart, C., Warwick, H. K., Leyland, M. L., and Courtney, M. J. (2005). The PSD95-nNOS Interface: a Target for Inhibition of Excitotoxic P38 Stress-Activated Protein Kinase Activation and Cell Death. *J. Cel Biol* 168, 117–126. doi:10.1083/jcb.200407024

Chen, J., Hu, R., Liao, H., Zhang, Y., Lei, R., Zhang, Z., et al. (2017). A Non-ionotropic Activity of NMDA Receptors Contributes to Glycine-Induced Neuroprotection in Cerebral Ischemia-Reperfusion Injury. *Sci. Rep.* 7, 3575. doi:10.1038/s41598-017-03909-0

Coultrap, S. J., Freund, R. K., O'leary, H., Sanderson, J. L., Roche, K. W., Dell'acqua, M. L., et al. (2014). Autonomous CaMKII Mediates Both LTP and LTD Using a Mechanism for Differential Substrate Site Selection. *Cell Rep* 6, 431–437. doi:10.1016/j.celrep.2014.01.005

Dey, S., Schepmann, D., and Wünsch, B. (2016). Role of the Phenolic OH Moiety of GluN2B-Selective NMDA Antagonists with 3-benzazepine Scaffold. *Bioorg. Med. Chem. Lett.* 26, 889–893. doi:10.1016/j.bmcl.2015.12.067

Dore, K., Aow, J., and Malinow, R. (2015). Agonist Binding to the NMDA Receptor Drives Movement of its Cytoplasmic Domain without Ion Flow. *Proc. Natl. Acad. Sci. U S A.* 112, 14705–14710. doi:10.1073/pnas.1520023112

Dore, K., Aow, J., and Malinow, R. (2016). The Emergence of NMDA Receptor Metabotropic Function: Insights from Imaging. *Front. Synaptic Neurosci.* 8, 20. doi:10.3389/fnsyn.2016.00020

Dore, K., Stein, I. S., Brock, J. A., Castillo, P. E., Zito, K., and Sjöström, P. J. (2017). Unconventional NMDA Receptor Signaling. *J. Neurosci.* 37, 10800–10807. doi:10.1523/JNEUROSCI.1825-17.2017

Duque-Feria, Y., Negrete-Diaz, P., Negrete-Díaz, J. V., Flores, T. S., Rodriguez-Moreno, G., and Rodríguez-Moreno, A. (2012). Presynaptic Kainate Receptor-Mediated Facilitation of Glutamate Release Involves Ca2+ -calmodulin at Mossy fiber-CA3 Synapses. *J. Neurochem.* 122, 891–899. doi:10.1111/j.1471-4159.2012.07844.x

Duque-Feria, Y., Paulsen, P., Rodriguez-Moreno, O., and Rodríguez-Moreno, A. (2016). Presynaptic Spike Timing-dependent Long-Term Depression in the Mouse Hippocampus. *Cereb. Cortex* 26, 3637–3654. doi:10.1093/cercor/bhw172

Duque-Feria, Y., Sihra, P., Rodriguez-Moreno, T. S., and Rodríguez-Moreno, A. (2013). Pre-synaptic Kainate Receptor-Mediated Facilitation of Glutamate Release Involves PKA and Ca(2+) -calmodulin at Thalamocortical Synapses. *J. Neurochem.* 126, 565–578. doi:10.1111/jnc.12310

Falcón-Moya, R., Losada-Ruiz, P., Sihra, T. S., and Rodríguez-Moreno, A. (2018). Cerebellar Kainate Receptor-Mediated Facilitation of Glutamate Release Requires Ca2+-Calmodulin and PKA. *Front. Mol. Neurosci.* 11, 195. doi:10.3389/fnmol.2018.00195

Falcón-Moya, R., Pérez-Rodríguez, M., Prius-Mengual, J., Arroyo-Garcia, Y., Arroyo-García, L. E., Pérez-Artés, R., et al. (2020). Astrocyte-mediated Switch in Spike Timing-dependent Plasticity during Hippocampal Development. *Nat. Commun.* 11, 4388. doi:10.1038/s41467-020-18024-4

Falcón-Moya, R., and Rodríguez-Moreno, A. (2021). Metabotropic Actions of Kainate Receptors Modulating Glutamate Release. *Neuropharmacology* 197, 108696. doi:10.1016/j.neuropharm.2021.108696

Fischer, G., Mutel, V., Trube, G., Malherbe, P., Kew, J. N., Mohacsi, E., et al. (1997). Ro 25-6981, a Highly Potent and Selective Blocker of N-Methyl-D-Aspartate Receptors Containing the NR2B Subunit. Characterization *In Vitro*. *J. Pharmacol. Exp. Ther.* 283, 1285–1292.

Gingrich, J. R., Pelkey, K. A., Fam, S. R., Huang, Y., Petralia, R. S., Wenthold, R. J., et al. (2004). Unique Domain Anchoring of Src to Synaptic NMDA Receptors via the Mitochondrial Protein NADH Dehydrogenase Subunit 2. *Proc. Natl. Acad. Sci. U S A.* 101, 6237–6242. doi:10.1073/pnas.0401413101

Hansen, K. B., Wollmuth, L. P., Bowie, D., Furukawa, H., Menniti, F. S., Sobolevsky, A. I., et al. (2021). Structure, Function, and Pharmacology of Glutamate Receptor Ion Channels. *Pharmacol. Rev.* 73, 298–487. doi:10.1124/pharmrev.120.000131

Hu, R., Chen, J., Lujan, B., Lei, R., Zhang, M., Wang, Z., et al. (2016). Glycine Triggers a Non-ionotropic Activity of GluN2A-Containing NMDA Receptors to Confer Neuroprotection. *Sci. Rep.* 6, 34459. doi:10.1038/srep34459

Kalia, L. V., and Salter, M. W. (2003). Interactions between Src Family Protein Tyrosine Kinases and PSD-95. *Neuropharmacology* 45, 720–728. doi:10.1016/s0028-3908(03)00313-7

Kessels, H. W., Nabavi, S., and Malinow, R. (2013). Metabotropic NMDA Receptor Function Is Required for β-amyloid-induced Synaptic Depression. *Proc. Natl. Acad. Sci. U S A.* 110, 4033–4038. doi:10.1073/pnas.1219605110

Kew, J. N., Trube, G., and Kemp, J. A. (1996). A Novel Mechanism of Activity-dependent NMDA Receptor Antagonism Describes the Effect of Ifenprodil in Rat Cultured Cortical Neurones. *J. Physiol.* 497 (Pt 3), 761–772. doi:10.1113/jphysiol.1996.sp021807

Krania, P., Dimou, E., Bantouna, M., Kouvaros, S., Tsiamaki, E., Papatheodoropoulos, C., et al. (2018). Adenosine A2A Receptors Are Required for Glutamate mGluR5- and Dopamine D1 Receptor-Evoked ERK1/2 Phosphorylation in Rat hippocampus: Involvement of NMDA Receptor. *J. Neurochem.* 145, 217–231. doi:10.1111/jnc.14268

Li, L. J., Hu, R., Lujan, B., Chen, J., Zhang, J. J., Nakano, Y., et al. (2016). Glycine Potentiates AMPA Receptor Function through Metabotropic Activation of GluN2A-Containing NMDA Receptors. *Front. Mol. Neurosci.* 9, 102. doi:10.3389/fnmol.2016.00102

Li, L. L., Ginet, V., Liu, X., Vergun, O., Tuittila, M., Mathieu, M., et al. (2013). The nNOS-p38MAPK Pathway Is Mediated by NOS1AP during Neuronal Death. *J. Neurosci.* 33, 8185–8201. doi:10.1523/JNEUROSCI.4578-12.2013

Li, Y. L., Liu, F., Zhang, Y. Y., Lin, J., Huang, C. L., Fu, M., et al. (2021). NMDAR1-Src-Pannexin1 Signal Pathway in the Trigeminal Ganglion Contributed to Orofacial Ectopic Pain Following Inferior Alveolar Nerve Transection. *Neuroscience* 466, 77–86. doi:10.1016/j.neuroscience.2021.04.032

Liu, X. J., Gingrich, J. R., Vargas-Caballero, M., Dong, Y. N., Sengar, A., Beggs, S., et al. (2008). Treatment of Inflammatory and Neuropathic Pain by Uncoupling Src from the NMDA Receptor Complex. *Nat. Med.* 14, 1325–1332. doi:10.1038/nm.1883

Minnella, A. M., Zhao, J. X., Jiang, X., Jakobsen, E., Lu, F., Wu, L., et al. (2018). Excitotoxic Superoxide Production and Neuronal Death Require Both Ionotropic and Non-ionotropic NMDA Receptor Signaling. *Sci. Rep.* 8, 17522. doi:10.1038/s41598-018-35725-5

Montes De Oca Balderas, P. (2018). Flux-Independent NMDAR Signaling: Molecular Mediators, Cellular Functions, and Complexities. *Int. J. Mol. Sci.* 19, 3800. doi:10.3390/ijms19123800

Nabavi, S., Kessels, H. W., Alfonso, S., Aow, J., Fox, R., and Malinow, R. (2013). Metabotropic NMDA Receptor Function Is Required for NMDA Receptor-dependent Long-Term Depression. *Proc. Natl. Acad. Sci. U S A.* 110, 4027–4032. doi:10.1073/pnas.1219454110

Paoletti, P., Bellone, C., and Zhou, Q. (2013). NMDA Receptor Subunit Diversity: Impact on Receptor Properties, Synaptic Plasticity and Disease. *Nat. Rev. Neurosci.* 14, 383–400. doi:10.1038/nrn3504

Pérez-Otaño, I., Larsen, R. S., and Wesseling, J. F. (2016). Emerging Roles of GluN3-Containing NMDA Receptors in the CNS. *Nat. Rev. Neurosci.* 17, 623–635. doi:10.1038/nrn.2016.92

Prius-Mengual, J., Pérez-Rodríguez, M., Rodriguez-Moreno, Y., and Rodríguez-Moreno, A. (2019). NMDA Receptors Containing GluN2B/2C/2D Subunits Mediate an Increase in Glutamate Release at Hippocampal CA3-CA1 Synapses. *Mol. Neurobiol.* 56, 1694–1706. doi:10.1007/s12035-018-1187-5

Rajani, V., Sengar, A. S., and Salter, M. W. (2020). Tripartite Signalling by NMDA Receptors. *Mol. Brain* 13, 23. doi:10.1186/s13041-020-0563-z

Rodríguez-Moreno, A., and Lerma, J. (1998). Kainate Receptor Modulation of GABA Release Involves a Metabotropic Function. *Neuron* 20, 1211–1218. doi:10.1016/s0896-6273(00)80501-2

Rodríguez-Moreno, A., and Paulsen, O. (2008). Spike Timing-dependent Long-Term Depression Requires Presynaptic NMDA Receptors. *Nat. Neurosci.* 11, 744–745. doi:10.1038/nn.2125

Srivastava, A., Das, B., Yao, A. Y., and Yan, R. (2020). Metabotropic Glutamate Receptors in Alzheimer's Disease Synaptic Dysfunction: Therapeutic Opportunities and Hope for the Future. *J. Alzheimers Dis.* 78, 1345–1361. doi:10.3233/JAD-201146

Stein, I. S., Gray, J. A., and Zito, K. (2015). Non-Ionotropic NMDA Receptor Signaling Drives Activity-Induced Dendritic Spine Shrinkage. *J. Neurosci.* 35, 12303–12308. doi:10.1523/JNEUROSCI.4289-14.2015

Stein, I. S., Park, D. K., Claiborne, N., and Zito, K. (2021). Non-ionotropic NMDA Receptor Signaling gates Bidirectional Structural Plasticity of Dendritic Spines. *Cel Rep* 34, 108664. doi:10.1016/j.celrep.2020.108664

Stein, I. S., Park, D. K., Flores, J. C., Jahncke, J. N., and Zito, K. (2020). Molecular Mechanisms of Non-ionotropic NMDA Receptor Signaling in Dendritic Spine Shrinkage. *J. Neurosci.* 40, 3741–3750. doi:10.1523/JNEUROSCI.0046-20.2020

Sun, Y., Chen, Y., Zhan, L., Zhang, L., Hu, J., and Gao, Z. (2016). The Role of Non-receptor Protein Tyrosine Kinases in the Excitotoxicity Induced by the Overactivation of NMDA Receptors. *Rev. Neurosci.* 27, 283–289. doi:10.1515/revneuro-2015-0037

Sun, Y., Feng, X., Ding, Y., Li, M., Yao, J., Wang, L., et al. (2019). Phased Treatment Strategies for Cerebral Ischemia Based on Glutamate Receptors. *Front Cel Neurosci* 13, 168. doi:10.3389/fncel.2019.00168

Sun, Y., Xu, Y., Cheng, X., Chen, X., Xie, Y., Zhang, L., et al. (2018). The Differences between GluN2A and GluN2B Signaling in the Brain. *J. Neurosci. Res.* 96, 1430–1443. doi:10.1002/jnr.24251

Sun, Y., Zhang, L., Chen, Y., Zhan, L., and Gao, Z. (2015). Therapeutic Targets for Cerebral Ischemia Based on the Signaling Pathways of the GluN2B C Terminus. *Stroke* 46, 2347–2353. doi:10.1161/STROKEAHA.115.009314

Tamburri, A., Dudilot, A., Licea, S., Bourgeois, C., and Boehm, J. (2013). NMDA-receptor Activation but Not Ion Flux Is Required for Amyloid-Beta Induced Synaptic Depression. *PLoS One* 8, e65350. doi:10.1371/journal.pone.0065350

Wang, J., and Swanson, R. A. (2020). Superoxide and Non-ionotropic Signaling in Neuronal Excitotoxicity. *Front. Neurosci.* 4, 861. doi:10.3389/fnins.2020.00861

Weilinger, N. L., Lohman, A. W., Rakai, B. D., Ma, E. M., Bialecki, J., Maslieieva, V., et al. (2016). Metabotropic NMDA Receptor Signaling Couples Src Family Kinases to Pannexin-1 during Excitotoxicity. *Nat. Neurosci.* 19, 432–442. doi:10.1038/nn.4236

Weilinger, N. L., Tang, P. L., and Thompson, R. J. (2012). Anoxia-induced NMDA Receptor Activation Opens Pannexin Channels via Src Family Kinases. *J. Neurosci.* 32, 12579–12588. doi:10.1523/JNEUROSCI.1267-12.2012

Westphal, R. S., Tavalin, S. J., Lin, J. W., Alto, N. M., Fraser, I. D., Langeberg, L. K., et al. (1999). Regulation of NMDA Receptors by an Associated Phosphatase-Kinase Signaling Complex. *Science* 285, 93–96. doi:10.1126/science.285.5424.93

Xia, C. Y., He, J., Du, L. D., Yan, Y., Lian, W. W., Xu, J. K., et al. (2021). Targeting the Dysfunction of Glutamate Receptors for the Development of Novel Antidepressants. *Pharmacol. Ther.* 226, 107875. doi:10.1016/j.pharmthera.2021.107875

Zhu, L. J., Shi, H. J., Chang, L., Zhang, C. C., Si, M., Li, N., et al. (2020). nNOS-CAPON Blockers Produce Anxiolytic Effects by Promoting Synaptogenesis in Chronic Stress-Induced Animal Models of Anxiety. *Br. J. Pharmacol.* 177, 3674–3690. doi:10.1111/bph.15084

Conflict of Interest: Author XC was employed by New Drug Research & Development Co., Ltd. LW was employed by the company Hebei Technological Innovation Center of Chiral Medicine.

The remaining authors declare that the research was conducted in the absence of any commercial or financial relationships that could be construed as a potential conflict of interest.

frontiers in Pharmacology

REVIEW
published: 21 February 2022
doi: 10.3389/fphar.2021.817364

Bibliometric Analysis of Ferroptosis in Stroke From 2013 to 2021

Yuhua Chen[1,2,3†], *Tianlin Long*[2†], *Quanhua Xu*[2] *and Chi Zhang*[3,4*]

[1]Department of Central Laboratory, Xi'an Peihua University, Xi'an, China, [2]Department of Neurosurgery, Bijie Traditional Chinese Medicine Hospital, Bijie, China, [3]Department of Neurosurgery, Xiangya Hospital, Central South University, Changsha, China, [4]The Institute of Skull Base Surgery and Neurooncology at Hunan Province, Changsha, China

Background: Stroke is a major cause of long-term disability and death, but the clinical therapeutic strategy for stroke is limited and more research must be conducted to explore the possible avenues for stroke treatment and recovery. Since ferroptosis is defined, its role in the body has become the focus of attention and discussion, including in stroke.

Methods: In this work, we aim to systematically discuss the "ferroptosis in stroke" research by bibliometric analysis. Documents were retrieved from the Web of Science Core Collection database on October 30, 2021. Statistical analysis and visualization analysis were conducted by the VOSviewer 1.6.15.

Results: Ninety-nine documents were identified for bibliometric analysis. Research on "ferroptosis in stroke" has been rapidly developing and has remained the focus of many scholars and organizations in the last few years, but the Chinese groups in this field still lacked collaboration with others. Documents and citation analysis suggested that Rajiv R. Ratan and Brent R. Stockwell are active researchers, and the research by Qingzhang Tuo, Ishraq Alim, and Qian Li are more important drivers in the development of the field. Keywords associated with lipid peroxidation, ferroptosis, iron, oxidative stress, and cell death had high frequency, but apoptosis, necroptosis, pyroptosis, and autophagy had scant research, and there may be more research ideas in the future by scholars.

Conclusion: Further exploration of the mechanisms of crosstalk between ferroptosis and other programmed cell death may improve clinical applications and therapeutic effects against stroke. Scholars will also continue to pay attention to and be interested in the hot topic "ferroptosis in stroke", to produce more exciting results and provide new insights into the bottleneck of stroke treatment.

Keywords: bibliometric analysis, Web of Science, stroke, ferroptosis, programmed cell death

OPEN ACCESS

Edited by:
Toshiko Yamazawa, Jikei University School of Medicine, Japan

Reviewed by:
Hartmut Kuhn, Charité University Medicine Berlin, Germany
Charareh Pourzand, University of Bath, United Kingdom

***Correspondence:**
Chi Zhang
chizhang25@163.com

†These authors have contributed equally to this work and share first authorship

Specialty section:
This article was submitted to Neuropharmacology, a section of the journal Frontiers in Pharmacology

Received: *18 November 2021*
Accepted: *29 December 2021*
Published: *21 February 2022*

Citation:
Chen Y, Long T, Xu Q and Zhang C (2022) Bibliometric Analysis of Ferroptosis in Stroke From 2013 to 2021. Front. Pharmacol. 12:817364. doi: 10.3389/fphar.2021.817364

BACKGROUND

With about 3.0 million new cases occurring every year, stroke is a primary reason of disability and death in China and the United States (Wu et al., 2019; Barthels and Das, 2020). The burden is expected to increase further due to population aging, continued high prevalence of risk factors such as hypertension, and poor management. Although overall access to health services has improved, access to specialist stroke cure and care is patchy across regions and particularly uneven in backward areas (Wu et al., 2019; Zhang et al., 2020). Research has shown that people with hypertension, obesity, and diabetes have a higher incidence of stroke (Barthels and Das, 2020). The vast majority of

TABLE 1 | The top 10 funding sources.

Ranking	Funding Source	Frequency
1	National Natural Science Foundation of China	43
2	National Institutes of Health	22
3	United States Department of Health Human Services	22
4	NIH National Institute of Neurological Disorders Stroke	12
5	American Heart Association	6
6	Burke Foundation	6
7	Dr Miriam And Sheldon G Adelson Medical Research Foundation	6
8	European Commission	6
9	NIH National Institute on Aging	6
10	NIH National Cancer Institute	5

strokes fall into two categories, hemorrhagic stroke (HS) induced by ruptured brain blood vessels and ischemic stroke (IS) caused by blocked brain arteries, both of which lead to local hypoxia and brain tissue damage (Campbell et al., 2019; Barthels and Das, 2020). Currently, tissue plasminogen activator (tPA), a powerful thrombolysis for the dissolution of acute thromboembolism, is the only ischemic stroke drug approved by the Food and Drug Administration (Kuo et al., 2020). But the tPA has a strict time window for treatment. Stroke patients must receive tPA within 3 h of the onset of stroke symptoms, but no longer than 4.5 h, and if the treatment window is exceeded, it may lead to hemorrhagic transformation, which can cause additional damage to the brain (Hughes et al., 2021). Routine prophylactic drug interventions, such as anticoagulants and blood pressure-lowering and cholesterol-lowering drugs, are necessary for people who have experienced stroke because they are at increased risk for a second stroke occurring immediately after the first stroke (Barthels and Das, 2020). Dismayingly, there is still no effective treatment for HS (Yin et al., 2021). Overall, the clinical therapeutic strategy for stroke is limited, and more research must be conducted to explore possible avenues for stroke treatment and recovery.

Ferroptosis is a programmed cell death (PCD) characterized by iron-dependent lipid peroxidation, including impaired intracellular cysteine uptake, glutathione depletion, membrane damage, and damage-related molecule release (Galluzzi et al., 2018; Tang and Kroemer, 2020; Hassannia et al., 2021; Wu et al., 2021). The term "ferroptosis" was coined by Scott J Dixon in 2012 and used to describe a type of cell death caused by erastin and also suppressed by lipophilic antioxidants or iron chelators such as ferrostatin-1 (Dixon et al., 2012). Recent studies have shown that the cell phenotype and molecular events of ferroptosis are different from apoptosis, autophagy, necroptosis, pyroptosis, and other PCDs (Galluzzi et al., 2018; Zhou et al., 2020). PCD is crucial to the occurrence and development of multiple diseases, including dysgenopathy, immune system diseases, central nervous system (CNS) disease, and cancer (Gibellini and Moro, 2021; Kist and Vucic, 2021; Moujalled et al., 2021). Moreover, common molecular events involved in ferroptosis are logically linked to the occurrence and development of many diseases, such as oxidative stress and abnormal iron, glutamate, and lipid metabolism (Stockwell et al., 2020; Plascencia-Villa and Perry, 2021; Yu et al., 2021). Ferroptosis involves nerve disorders (David et al., 2021), such as Alzheimer's disease (AD) (Plascencia-Villa and Perry, 2021), Parkinson's disease (PD) (Mahoney-Sánchez et al., 2021, spinal cord injury (SCI) (Ge et al., 2021), traumatic brain injury (TBI) (Rui et al., 2020), stroke (Alim et al., 2019; Zhou et al., 2020), and depression (Cao et al., 2021). The novel findings provide potential strategies for the clinical treatment and prognosis of stroke, such as targeting ferroptosis. However, to the best of our knowledge, the objective and overall reports on the publishing trend, powerful research, institutions and their collaborations, and the hotspots of "ferroptosis in stroke" are lacking.

In this work, we aim to systematically discuss the "ferroptosis in stroke" research from 2013 to 2021 by bibliometric analysis. The bibliometric analysis combines mathematical and statistical methods with data visualization (Chen G. et al., 2021), to present the annual publications, countries/regions, institutions, journals, authors, and co-citation; to evaluate global patterns of collaboration between authors, institutions, and countries; and to determine the study trend and hotspot in "ferroptosis in stroke".

DATA AND METHOD

Data Collection

The keywords of ferroptosis and stroke were indexed in the Web of Science Core Collection (WOSCC). Articles from 2013 to 2021 (deadline October 30, 2021) were retrieved, and search themes were as follows: "TS=(ferroptosis) OR TS=(ferroptotic)", AND "TS=(stroke) OR TS=(cerebrovascular accident) OR TS=(cerebrovascular apoplexy)", AND Language: English, AND Reference Type: Article OR Review". A total of 99 references were chosen and then used to perform a bibliometric analysis.

Data Analysis

Firstly, through the analysis and retrieval results in WOSCC, the general information of the literature is preliminarily analyzed, including the year of publication, country, organization, journal, and author. Then, the VOSviewer 1.6.15 software was used to conduct bibliometric and visual analysis, including main author, keyword, scientific research partnership, cited analysis, and co-cited analysis. The standard tournament ranking method was used for ranking order, and Linlog/modularization was applied in the VOSviewer software.

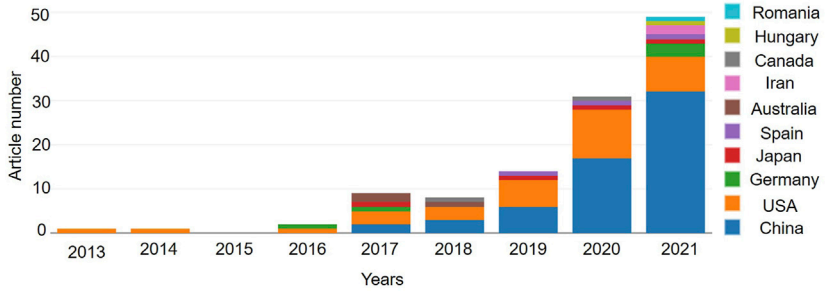

FIGURE 1 | The annual publication indexed in the WOSCC from 2013 to 2021 by online bibliometric analysis. And the article number of the top 10 countries/regions with "ferroptosis in stroke" were presented.

RESULTS

Publication Outputs

There were 99 items on "ferroptosis in stroke" in the WOSCC from 2013 to 2021 (October 30, 2021), including 51 articles (51.52%) and 48 reviews (48.48%). The annual publication is exhibited in **Figure 1**. There was one publication in 2013, which subsequently increased year by year, and it was 28 in 2020 and 42 on October 30, 2021 (**Figure 1**). The number of publication was small, but it rose steadily rise. A total of 185 sources of funding supported the research on "ferroptosis in stroke". The top three major sources of funding were the National Natural Science Foundation of China (frequency, 43), National Institutes Of Health (frequency, 22), and United States Department of Health Human Services (frequency, 22) **Table 1**.

Countries and Organization

There were 15 countries and 193 organizations in the 99 documents of "ferroptosis in stroke", which had been published in the past 8 years. China (63), the United States (38), and Germany (5) were the top three countries/regions, and early research began in the United States and China, which have published documents mainly since 2017 (**Figure 1**). The United States had the most citation with 2,834, but the citation of publication in China was 2,262. Cooperation on this subject has been concentrated between China and the United States, with weak cooperation between other countries (**Figure 2**). As shown in **Table2**, the top 10 institutions in terms of publications were from China (50%) and the United States (50%). The top three institutions in terms of publications were Columbia University (United States, six documents), Weill Cornell Medicine (United States, six documents), and Zhejiang University (China, six documents), but the top three institutions ranked by citations were Columbia University (1,819), Yale University (1,731), and Memorial Sloan Kettering Cancer Center (1,596) (**Table 2**). Cooperation between institutions is presented in **Figure 3**. The top organizations showed extensive relationships with others (**Figure 3**), but some gray circles indicated that the institutions were isolated. The data suggest that the top institutions with "ferroptosis in stroke" research lack cooperation with each other; in particular, the Chinese institutions should improve cooperation with their counterparts.

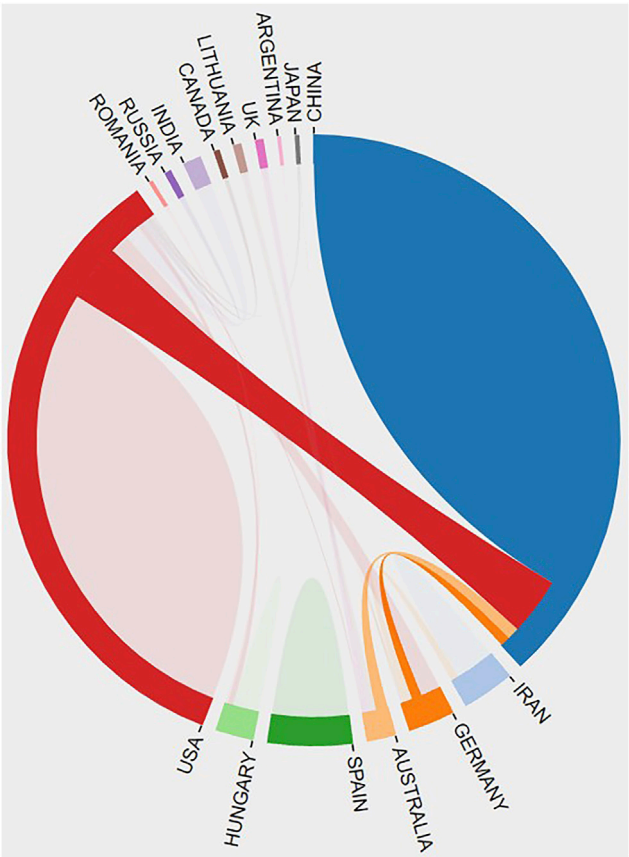

FIGURE 2 | The cooperative relationship between countries was generated by the online bibliometric analysis.

Journals

There were 72 journals with documents on "ferroptosis in stroke". In **Table 4**, the top 10 journals were shown to have published about 34.34% of documents (34/99). *Frontiers in Cellular*

TABLE 2 | Top 10 most productive organizations.

Rank	Organizations	Country	Documents	Citations
1	Columbia University	United States	6	1819
2	Weill Cornell Medicine	United States	6	459
3	Zhejiang University	China	6	27
4	Sichuan University	China	5	245
5	Memorial Sloan Kettering Cancer Center	United States	4	1596
6	Johns Hopkins University	United States	4	443
7	Central South University	China	4	24
8	Jilin University	China	4	24
9	Yale University	United States	3	1731
10	Harbin Medical University	China	3	200

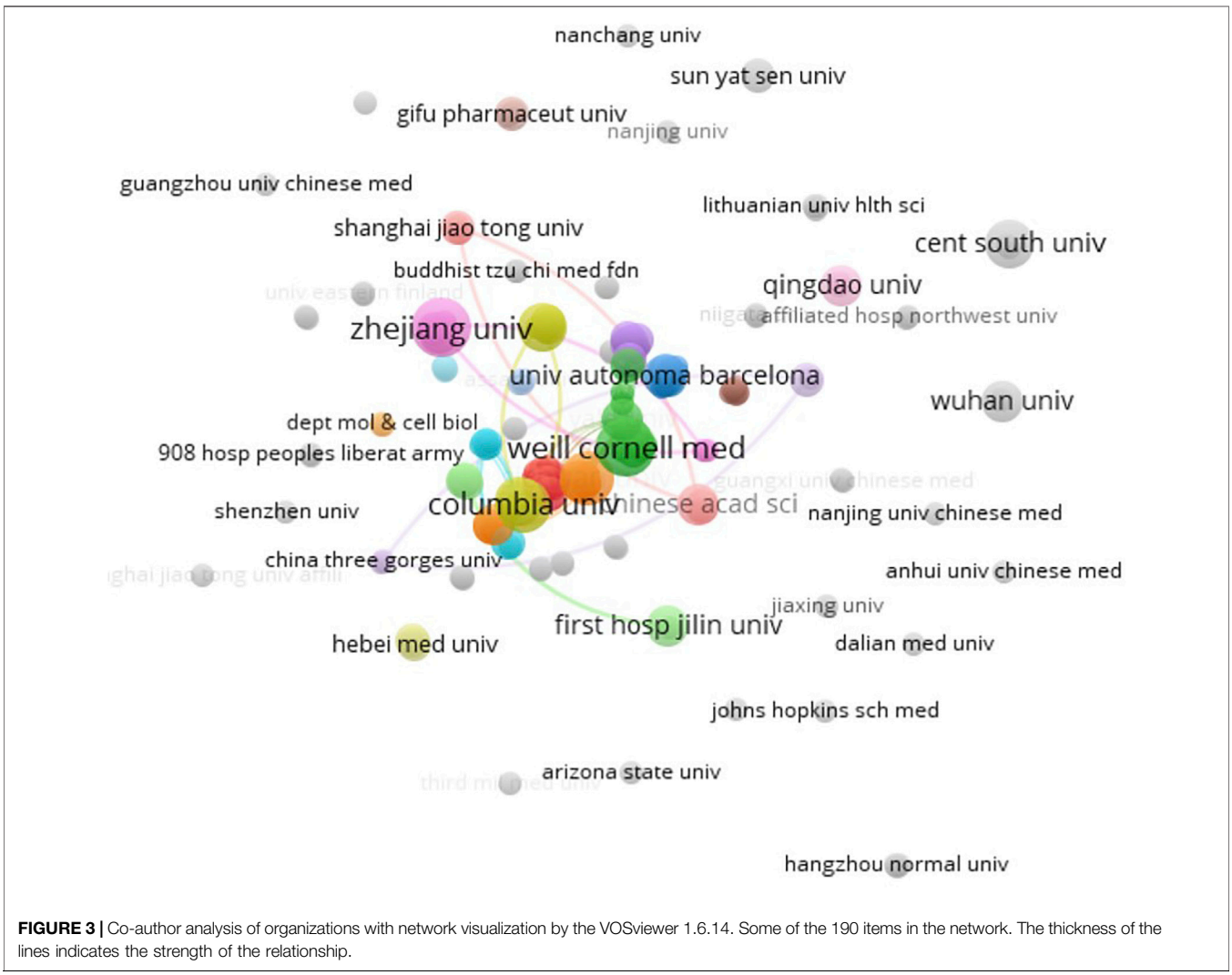

FIGURE 3 | Co-author analysis of organizations with network visualization by the VOSviewer 1.6.14. Some of the 190 items in the network. The thickness of the lines indicates the strength of the relationship.

Neuroscience was the most active journal, followed by *Frontiers in Neuroscience*, *Frontiers in Cell and Developmental Biology*, *Frontiers in Pharmacology*, *Life Sciences*, *Frontiers in Neurology*, *Cell*, *Cellular and Molecular Life Sciences*, *Pharmacology and Pharmacy*, and *Cell Chemical Biology*. All of the journals had a higher level of JCR partition (70% Q1 and 30% Q2), and *Cell Chemical Biology* had a minimum IF of 4.003 (Q2) (**Table 3**). Encouragingly, one article and one review were published in the *Cell* journal (Q1, 41.584). The publication of these articles in the corresponding high-level journals is enough to indicate that "ferroptosis in stroke" is exciting and interesting.

TABLE 3 | Top 10 journals with the largest number of publications.

Rank	Journals	Documents	2020 Impact Factor	2020 JCR Partition
1	*Frontiers in Cellular Neuroscience*	8	5.505	Q1
2	*Frontiers in Neuroscience*	4	4.677	Q2
3	*Frontiers in Cell and Developmental Biology*	3	6.684	Q1/Q2
4	*Frontiers in Pharmacology*	3	5.811	Q1
5	*Life Sciences*	3	5.037	Q1/Q2
6	*Frontiers in Neurology*	3	4.003	Q2
7	*Cell*	2	41.584	Q1
8	*Cellular and Molecular Life Sciences*	2	9.261	Q1
9	*Pharmacology and Pharmacy*	2	7.658	Q1
10	*Cell Chemical Biology*	2	8.116	Q2

TABLE 4 | Top 10 active authors with most documents.

Rank	Authors	Organizations	Documents	Citations
1	Rajiv R Ratan	Weill Cornell Medicine	7	531
2	Jian Wang	Johns Hopkins University	5	477
3	Saravanan S Karuppagounder	Weill Cornell Medicine	5	492
4	Brent R Stockwell	Columbia University	4	441
5	Zhen-Ni Guo	Jilin University	4	24
6	Xuejun Jiang	Memorial Sloan Kettering Cancer Center	4	218
7	Peng Lei	Sichuan University	4	243
8	Qing-Zhang Tuo	Sichuan University	4	243
9	Xiu-Li Yan	Jilin University	4	24
10	Yi Yang	Jilin University	4	24

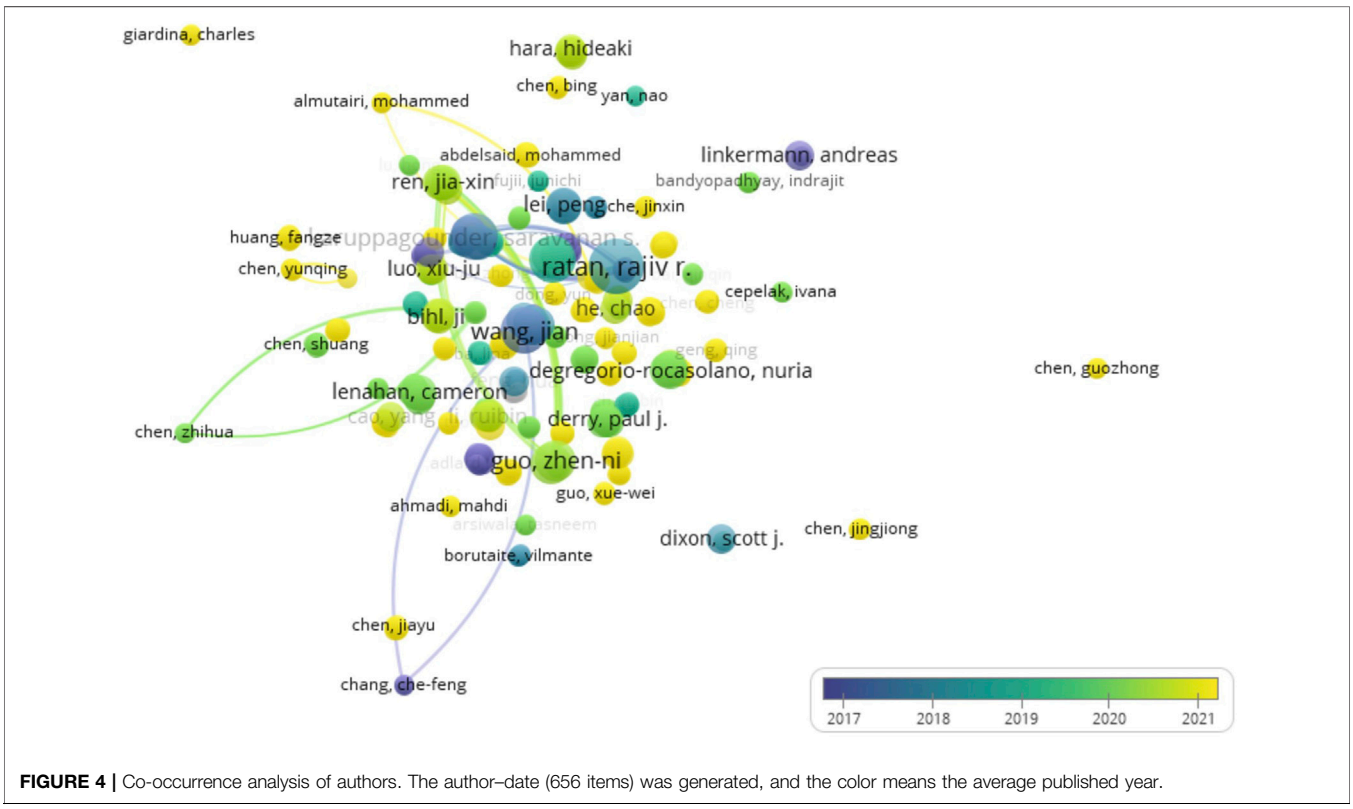

FIGURE 4 | Co-occurrence analysis of authors. The author–date (656 items) was generated, and the color means the average published year.

TABLE 5 | Top 10 co-citation of cited references on "ferroptosis in stroke".

Rank	Title	Type	First author	Source	Publication year	Total citations
1	Ferroptosis: an iron-dependent form of nonapoptotic cell death	Review	SJ Dixon	Cell	2012	82
2	Regulation of ferroptotic cancer cell death by GPX4	Article	WS Yang	Cell	2014	51
3	Ferroptosis: a regulated cell death nexus linking metabolism, redox biology, and disease	Review	BR Stockwell	Cell	2017	50
4	Inactivation of the ferroptosis regulator Gpx4 triggers acute renal failure in mice	Article	JPF Angeli	Nat Cell Biol	2014	44
5	Tau-mediated iron export prevents ferroptotic damage after ischemic stroke	Article	QZ Tuo	Mol Psychiatr	2017	42
6	Selenium drives a transcriptional adaptive program to block ferroptosis and treat stroke	Article	I Alim	Cell	2019	42
7	Inhibition of neuronal ferroptosis protects hemorrhagic brain	Article	Q Li	JCI Insight	2017	39
8	Ferroptosis: process and function	Review	Y Xie	Cell Death Differ	2016	39
9	Glutaminolysis and transferrin regulate ferroptosis	Article	MH Gao	Mol Cell	2015	39
10	ACSL4 dictates ferroptosis sensitivity by shaping cellular lipid composition	Article	S Doll	Nat Chem Biol	2017	37

Authors

A total of 656 authors drafted the 99 documents in "ferroptosis in stroke". Rajiv R. Ratan (Weill Cornell Medicine) contributed seven documents and ranked first (531 citations), followed by Saravanan S. Karuppagounder (Weill Cornell Medicine), Jian Wang (Johns Hopkins University), Brent R. Stockwell (Columbia University), and Zhenni Guo (Jilin University). Seventy percent of authors were from China (**Table 4**). In a co-authorship map, yellow indicated that many scholars have only recently begun to work on this topic (**Figure 4**). Some researchers were also scattered independently with other active scholars, and Rajiv R. Ratan, Jian Wang, and Brent R. Stockwell were the center, but they had not been able to reach all groups (**Figure 4**). The data suggest that the active authors on "ferroptosis in stroke" still lack collaboration with other scholars.

Citations

The top 10 highly cited references and the citation analysis of documents on "ferroptosis in stroke" are shown in **Tables 5**, **6**. "Ferroptosis: an iron-dependent form of nonapoptotic cell death" was the most cited reference in "ferroptosis in stroke" (**Table 5**), as Dixon et al. (2012) firstly came up with the concept of ferroptosis. Two reviews of Brent R. Stockwell were included in the highly cited references: "Ferroptosis: a regulated cell death nexus linking metabolism, redox biology, and disease" with 1,378 citations and "Emerging mechanisms and disease relevance of ferroptosis" with 84 citations (**Table 6**). Four of the documents appeared on both lists: "Ferroptosis: a regulated cell death nexus linking metabolism, redox biology, and disease" (review), "Tau-mediated iron export prevents ferroptotic damage after ischemic stroke" (article), "Selenium drives a transcriptional adaptive program to block ferroptosis and treat stroke" (article), and "Inhibition of neuronal ferroptosis protects hemorrhagic brain" (article), which were respectively completed by the team of Brent R. Stockwell, Qingzhang Tuo, Ishraq Alim, and Qian Li. The data suggest that Brent R. Stockwell is very interested in the research on "ferroptosis in stroke", but the research of Qingzhang Tuo, Ishraq Alim, and Qian Li are more important drivers in the development of the field, and articles of "ferroptosis in stroke" with a high number of citations have been widely accepted and have inspired recent researches, and recent studies should improve scale and breakthrough.

Figure 5 showed the keyword subnetwork and its clustering graph, and the circle size represented the number of occurrences of keywords. The top six keywords in terms of occurrence were "ferroptosis", "oxidative stress", "iron", "cell death", "lipid peroxidation", and "intracerebral hemorrhage" (**Figure 5**). In the overlay visualization (**Figure 6**), the keywords apoptosis, necroptosis, pyroptosis, autophagy, NLRP3 inflammasome activation, and Chinese herbal medicine were are also related to ferroptosis but had few research.

DISCUSSION

In the last few years, research on "ferroptosis in stroke" has been rapidly developing and remained the focus of scholars and organizations. Some countries, organizations, and scholars collaborated on research on "ferroptosis in stroke", but the Chinese groups in this field still lacked collaboration with others. The documents and citation analysis suggested that Rajiv R. Ratan and Brent R. Stockwell were active researchers, and the research of Qingzhang Tuo, Ishraq Alim, and Qian Li are more important drivers in the development of the field. Keywords associated with lipid peroxidation, ferroptosis, iron, oxidative stress, and cell death were highly frequent, but apoptosis, necroptosis, pyroptosis, and autophagy were used in few research, so there may be more research ideas in the future by scholars. "Ferroptosis in stroke" is an emerging research topic that will continue to produce more exciting results and provide new insights into the bottleneck of stroke treatment.

***Ferroptosis, a newly defined class of PCD in 2012 (Dixon et al., 2012), quickly became the focus of attention and discussion because of its important function in the body, and publication on this topic has increased year by year. In 2013, Louandre et al. demonstrated that sorafenib induces ferroptosis in hepatocellular carcinoma (HCC) cells, and triggering ferroptosis may improve the antitumor effect of sorafenib in HCC (Louandre et al., 2013);

TABLE 6 | Top 10 citation analysis of documents on "ferroptosis in stroke".

Rank	Title	Type	First author	Source	Publication year	Total citations
1	Ferroptosis: a regulated cell death nexus linking metabolism, redox biology, and disease	Review	BR Stockwell	Cell	2017	1378
2	Neuronal cell death	Review	M Fricker	Physiol Rev	2018	275
3	Inhibition of neuronal ferroptosis protects hemorrhagic brain		Q Li	JCI Insight	2017	223
4	Neuronal death after hemorrhagic stroke *in vitro* and *in vivo* shares features of ferroptosis and necroptosis	Article	M Zille	Stroke	2017	192
5	Tau-mediated iron export prevents ferroptotic damage after ischemic stroke	Article	QZ Tuo	Mol Psychiatr	2017	183
6	Selenium drives a transcriptional adaptive program to block ferroptosis and treat stroke	Article	I Alim	Cell	2019	161
7	Ischemia-induced ACSL4 activation contributes to ferroptosis-mediated tissue injury in intestinal ischemia/reperfusion	Article	Y Li	Cell Death Differ	2019	132
8	Ferroptosis and its role in diverse brain diseases	Review	A Weiland	Mol Neurobiol	2019	94
9	Ferroptosis: mechanisms, biology and role in disease	Review	XJ Jiang	Nat Rev Mol Cell Biol	2021	93
10	Emerging mechanisms and disease relevance of ferroptosis	Review	BR Stockwell	Trends Cell Biol	2020	84

Henke et al. (2013) found that dysregulated ORAI1-mediated Ca^{2+} influx contributes to ferroptosis in HT22 cells; based on their previous research, Speer et al. (2013) suggested that iron chelators inhibit ferroptosis in primary neurons by targeting the HIF prolyl hydroxylases. Since then, research on "ferroptosis" and "ferroptosis in stroke" has been gradually reported.

Studies have confirmed that ferroptosis involves the failure of GPX4 activity and the metabolic processes of iron, amino acids, and lipid peroxide, which results in the accumulation of intracellular reactive oxygen species (ROS) and ferroptotic death (Stockwell et al., 2017; Wan et al., 2019; Cheng et al., 2021). Ferroptosis is mediated by nuclear factor E2-related factor 2 (NRF2) and Hippo pathways by regulating GPX4 activity (Liu et al., 2021). There are still polymolecules involved in ferroptosis, such as acyl-CoA synthetase long-chain family member 4 deferoxamine (ACSL4), ferritin, divalent metal transporter 1 (DMT1), glutathione (GSH), imidazole ketone erastin, lysophosphatidylcholine acyltransferase 3 (LPCAT3), nicotinamide adenine dinucleotide phosphate (NADPH), oxidized glutathione (GSSG), solute carrier family three member 2 (SLC3A2), transferrin, and transferrin receptor 1 (TFR1) (Liu et al., 2021; Zhang et al., 2021). With the deepening of research, the regulatory network of ferroptosis in stroke is gradually revealed (Bai et al., 2020; DeGregorio-Rocasolano, et al., 2019; Zille et al., 2017). Ferritin reduces robust ROS production and GSH consumption; its decrease is necessary for cerebral ischemia-induced hippocampal neuronal ferroptosis through p53 and SLC7A11 in middle cerebral artery occlusion (MCAO) rats (Chen W. et al., 2021), and mice lacking mitochondrial ferritin show graver brain injury and neurological deficits, accompanied by typical ferroptotic event after cerebral ischemia/reperfusion (I/R) (Wang et al., 2021). ACSL4 enhances ischemic stroke by increasing ferroptosis-induced brain damage and neuroinflammation while inhibiting ACSL4, which promotes the recovery of neurological function following stroke (Li et al., 2019; Chen J. et al., 2021; Cui et al., 2021). Tuo et al. (2017) demonstrated that tau suppression reduces MCAO-induced ferroptosis and influences ischemic stroke outcome. Nuclear receptor coactivator 4 (NCOA4) facilitates ferritinophagy-mediated ferroptosis, and NCOA4 deletion protects neurons from ferritinophagy-mediated ferroptosis after ischemic stroke (Li C. et al., 2021). Guo et al. (2021) hypothesized that PIEZO1 involves cerebral I/R injury *via* ferroptosis regulation. In addition, noncoding RNAs are also involved in ferroptosis-mediated stroke. The lncRNA-MEG3/p53 signaling pathway mediates ferroptosis of rat brain microvascular endothelial cells *via* regulation of the GPX4 transcription and expression (Chen C. et al., 2021). The level of lncRNA-PVT1 is upregulated and the miR-214 level is downregulated in the plasma of acute ischemic stroke patients, and PVT1 involves ferroptosis *via* miR-214-mediated TFR1 and TP53 levels in brain I/R (Lu et al., 2020). By the bioinformatic analysis, three ferroptosis-related biomarkers are found as potential diagnostic biomarkers for ischemic stroke, namely, PTGS2, MAP1LC3B, and TLR4, which are upregulated in ischemic stroke and provide more evidence about the important role of ferroptosis (Chen G. et al., 2021). Therefore, extensive evidence suggests that ferroptosis is one of the key pathological mechanisms of nerve injury and neurological dysfunction after stroke, which is a potentially promising therapeutic target (Jin Y. et al., 2021; Li Y. et al., 2021).

Previous studies show that ferroptosis is reversed by iron chelators (deferoxamine and ceruloplasmin), lipophilic antioxidants (ferrostatin-1, trolox, liproxstatin-1, and *N*-acetylcysteine (NAC)), and selenoprotein activator (selenium) (**Figure 7**) (Liu et al., 2021; Zhang et al., 2021). Then, significant progress has been made in preclinical studies targeting ferroptosis in the treatment of stroke. Intracerebral hemorrhage-induced neurological defects, dysmnesia, and brain atrophy were decreased by the ferroptosis inhibitor ferrostatin-1 (Chen et al., 2019). NAC, a clinically approved redox regulatory compound containing mercaptan, prevents hemin-induced ferroptosis by inhibiting toxic lipid generated by arachidonic acid-dependent ALOX5 activity (Karuppagounder et al., 2018). Deferoxamine treatment prevents post-stroke cognitive impairment in diabetes while increasing AQP4 polarity and blood–brain barrier permeability (Abdul et al., 2021). Pyridoxal isonicotinoyl hydrazine protects mice against hemorrhage stroke, by reducing

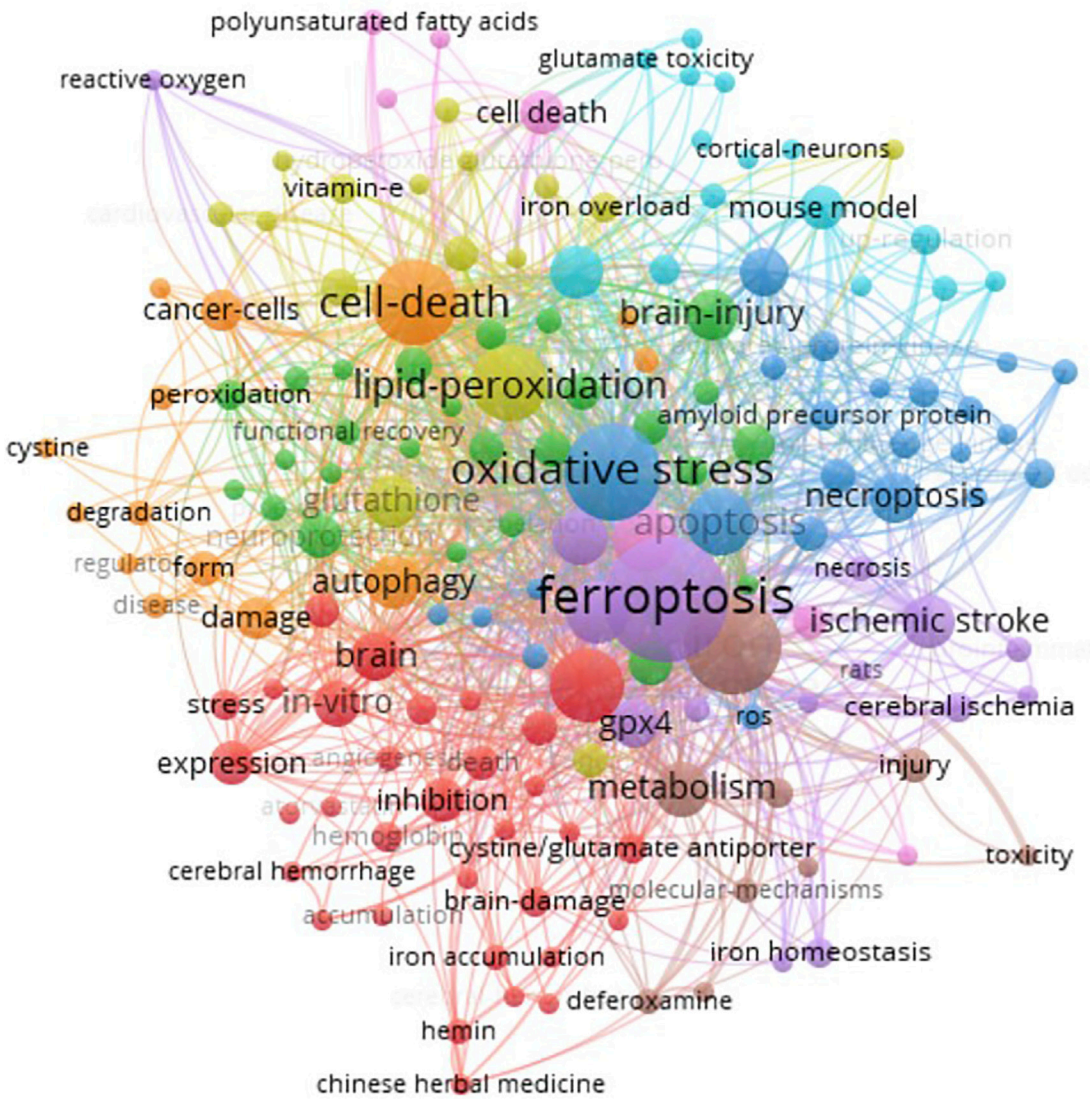

FIGURE 5 | Co-occurrence analysis of author keywords. Two minimum number of occurrences of a keyword, and 158 meet the threshold of the 554 keywords. The network visualization of the keywords (158 items) was conducted.

ferroptosis, including ROS production, iron accumulation, and lipid peroxidation in perihematoma (Zhang et al., 2021). Pharmacological selenium inhibits GPX4-dependent ferroptotic death, and selenome protects neurons and improves behavior following hemorrhagic stroke through regulating TFAP2c and Sp1 (Alim et al., 2019). And pretreatment with selenium compounds, such as methylselenocysteine or selenocystamine, also protects I/R neuronal ferroptosis *in vivo* (Tuo et al., 2021). Some natural products and traditional Chinese medicine-related content have also been confirmed to improve the prognosis of stroke by regulating ferroptosis. The baicalin, carthamin yellow, dauricine, (−)-epicatechin, kaempferol, and paeonol ameliorate neuronal ferroptosis *in vitro* or *in vivo* stroke models via regulating ACSL4, GPX4, TFR1, Fe^{2+}, and NRF2 pathways (Chang et al., 2014; Duan et al., 2021; Guo et al., 2021; Jin Z. L. et al., 2021; Peng et al., 2021; Yuan et al., 2021), which show great potential in the treatment of stroke. Treating MCAO rats with Naotaifang (a traditional Chinese herbal medicine compound) extract involves inhibition of acute cerebral ischemia-induced neuronal ferroptosis and neurobehavioral disorder through TFR1/DMT1 and SCL7A11/GPX4 pathways (Lan et al., 2020). Electroacupuncture inhibits ferroptosis to protect against MCAO via regulating iron and oxidative stress-related protein (Li G. et al., 2021). Furthermore, the new inhibitors of ferroptosis are also being explored. Yang et al. conducted promethazine derivatives and screened a promising lead compound, 2-(1-(4-(4-methylpiperazin-1-yl)phenyl)ethyl)-10*H*-phenothiazine, as a new type of ferroptosis inhibitor, which displays favorable pharmacokinetic properties, good ability to permeate the blood–brain barrier, and excellent therapeutic effect in the

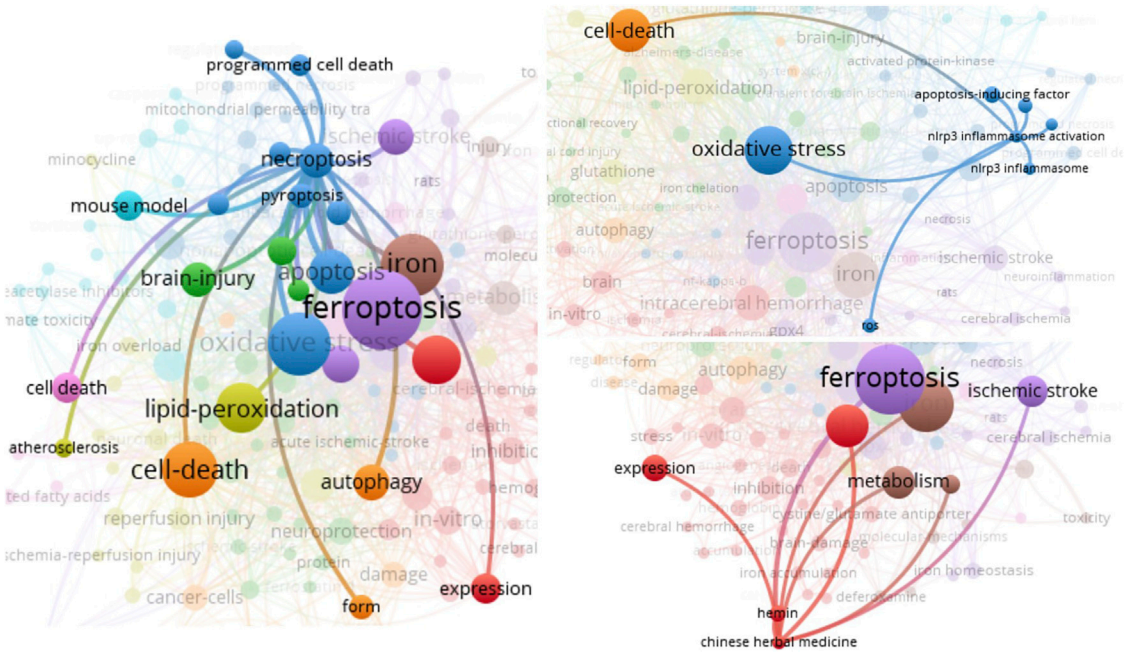

FIGURE 6 | The crosstalk of author keywords necroptosis, NLRP3 inflammasome activation, and Chinese herbal medicine was presented.

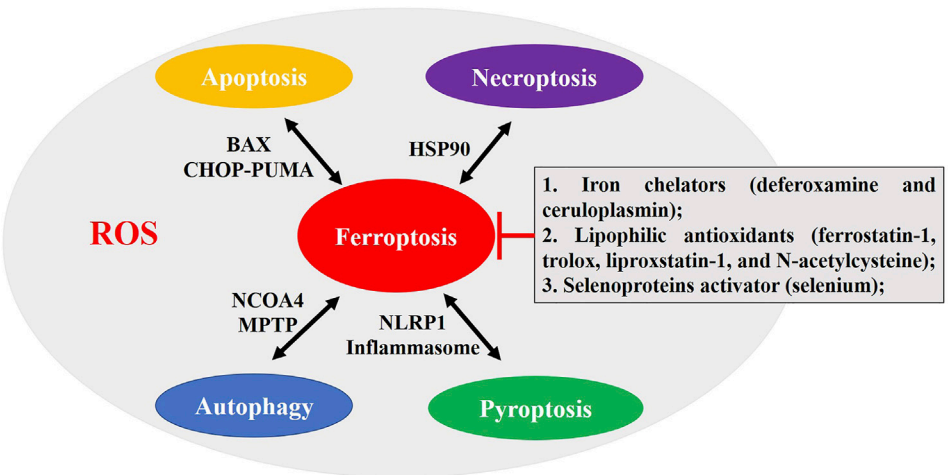

FIGURE 7 | The crosstalk between ferroptosis and autophagy, apoptosis, necroptosis, and pyroptosis. The iron chelators (deferoxamine and ceruloplasmin), lipophilic antioxidants (ferrostatin-1, trolox, liproxstatin-1, and *N*-acetylcysteine), and selenoprotein activator (selenium) can reverse ferroptosis. Mitochondrial function and ROS production may be key to the crosstalk. Some molecules participate in the crosstalk between them, including ROS; BAX; HSP90; mitochondrial permeability transition pore (MPTP); NCOA4; NACHT, LRR, and PYD domains-containing protein 1 (NLRP1) inflammasome; C/EBP-homologous protein (CHOP); and p53 upregulated modulator of apoptosis (PUMA).

ischemic stroke model (Yang et al., 2021). Keuters et al. (2021) demonstrated that the benzo[b]thiazine derivative efficiently suppresses GSH or GPX4 inhibition-induced ferroptosis in neuronal cell lines and decreases infarction volume, edema, and pro-inflammatory levels after stroke. Thus, ferroptosis inhibitors and targeting them are potential treatment options for stroke, but more direct clinical evidence remains to be explored.

The keyword analysis revealed that multiple PCDs were involved in the progression of stroke pathology, and apoptosis, necroptosis, pyroptosis, and autophagy were related to ferroptosis. Some reports show that apoptosis, autophagy, pyroptosis, and ferroptosis are present together in stroke-induced neuronal damage (Guo et al., 2021; Li et al., 2018). The crosstalk between ferroptosis and other PCDs is fascinating (**Figure 7**). Lee et al. (2018, 2020) showed ferroptotic and

apoptotic agent interactions via the B-cell lymphoma-2 associated X (BAX)-dependent mitochondrial pathway and ER stress-mediated PERK-eIF2α-ATF4-CHOP-PUMA pathway. Studies have found that ferritinophagy-mediated ROS production contributes to ferroptosis and apoptosis (Li L. et al., 2021). Ferroptosis, an autophagic cell death process, leads to autophagy activation and consequent ferritin and NCOA4 degradation (Gao et al., 2016), and NCOA4-regulated ferritinophagy maintains ferroptosis via mediating cellular iron homeostasis, which is also present in stroke (Li C. et al., 2021). Mitochondrial permeability transition pore opening is a common event of ferroptosis and necroptosis, which stimulates formation of autophagosome, mitophagy, and ROS production, causing necroptosis/ferroptosis (Basit et al., 2017). Heat shock protein 90 (HSP90) is defined as a common regulatory nodal between ferroptosis and necroptosis (Wu et al., 2019). Friedmann Angeli et al. demonstrated that necrostatin-1 (RIP1 inhibitor) inhibits ferroptosis through a necroptosis/RIP1-independent manner, but ferroptosis inhibitors cannot inhibit necroptosis (Friedmann Angeli et al., 2014) and the specific link between ferroptosis and necroptosis remains to be clarified after stroke (Zille et al., 2017; Zhou et al., 2021). Carthamin yellow attenuates cerebral I/R injury via suppressing NF-κB/NLRP3-mediated pyroptosis and ACSL4-mediated ferroptosis in rats (Guo et al., 2021b). The regulatory relationship between ferroptosis and pyroptosis has been proved. Meihe et al. found that silenced or upregulated NLRP1 inflammasome positively affects ferroptosis in the oxidative stress model, and NLRP1, NLRP3, IL-1β, and caspase-1 levels are positively correlated with ferroptosis following ferroptosis inhibition or ferroptosis activation (Meihe et al., 2021). However, whether ferroptosis facilitates apoptosis, autophagy, necroptosis, pyroptosis, or other PCDs or their mutual regulation following stroke requires the further studies.

LIMITATIONS

This is the first bibliometric analysis of "ferroptosis in stroke", but some limitations are presented. Firstly, the retrieval time is October 30, 2021, but the database continues to be updated. Secondly, the search terms "TS=(Ferroptosis) OR TS=(Ferroptotic)", AND "TS=(stroke) OR TS=(cerebrovascular accident) OR TS=(cerebrovascular apoplexy)", AND Language: English, AND Reference Type: Article OR Review" are used to define the topic of this studies in the WOSCC database; some productions may not be contained. Thirdly, there are still some articles that are not included in the WOSCC database, so they are left out. However, WOSCC is the dominant database for bibliometric analysis, and we believe this work could represent the overall situation and general trend for "ferroptosis in stroke".

CONCLUSION

Our study discussed the research status of "ferroptosis in stroke" by bibliometric analysis, which is an increasingly hot research topic, with more and more scholars, institutions, and countries pouring in and publishing a lot of high-quality productions. Most of them are Chinese scholars, but most of them are isolated and lack communication and cooperation. Researchers need to strengthen the sharing of results on this topic and promote the exploration of relevant hotspots. The mechanisms of apoptosis, necroptosis, pyroptosis, and autophagy engage crosstalk with ferroptosis in the pathological processes of stroke, and the different types of PCD is as a single, but in which the individual pathway is highly interconnected and concertedly compensated for others (Bedoui et al., 2020). The ferroptosis inhibitors and targeting them are potential treatment options for stroke, but more direct clinical evidence remains to be explored. Further exploring the mechanisms of crosstalk between ferroptosis and other PCDs improves clinical applications and therapeutic effects against stroke, and a combination of ferroptosis with other harmful pathway suppression may provide valid therapies for stroke and brain disorder. The scholars will also continue to pay attention to and be interested in the hot topic of "ferroptosis in stroke".

AUTHOR CONTRIBUTIONS

Conceptualization: YC, TL, and CZ. Data collection and analysis: QX and TL. Writing—original draft: YC. Writing—review and editing: CZ.

FUNDING

This study was supported by the National Natural Science Foundation of China (82072229 and 81901270), Guizhou Traditional Chinese Medicine Administration (201815797), and Guizhou Provincial Health and Family Planning Commission (2019XMSB00022878).

REFERENCES

Abdul, Y., Li, W., Ward, R., Abdelsaid, M., Hafez, S., Dong, G., et al. (2021). Deferoxamine Treatment Prevents Post-Stroke Vasoregression and Neurovascular Unit Remodeling Leading to Improved Functional Outcomes in Type 2 Male Diabetic Rats: Role of Endothelial Ferroptosis. *Transl Stroke Res.* 12 (4), 615–630. doi:10.1007/s12975-020-00844-7

Alim, I., Caulfield, J. T., Chen, Y., Swarup, V., Geschwind, D. H., Ivanova, E., et al. (2019). Selenium Drives a Transcriptional Adaptive Program to Block Ferroptosis and Treat Stroke. *Cell* 177 (5), 1262–e25. doi:10.1016/j.cell.2019.03.032

Bai, Q., Liu, J., and Wang, G. (2020). Ferroptosis, a Regulated Neuronal Cell Death Type after Intracerebral Hemorrhage. *Front Cel Neurosci* 14, 591874. doi:10.3389/fncel.2020.591874

Barthels, D., and Das, H. (2020). Current Advances in Ischemic Stroke Research and Therapies. *Biochim. Biophys. Acta Mol. Basis Dis.* 1866 (4), 165260. doi:10.1016/j.bbadis.2018.09.012

Basit, F., van Oppen, L. M., Schöckel, L., Bossenbroek, H. M., van Emst-de Vries, S. E., Hermeling, J. C., et al. (2017). Mitochondrial Complex I Inhibition

Triggers a Mitophagy-dependent ROS Increase Leading to Necroptosis and Ferroptosis in Melanoma Cells. *Cell Death Dis* 8 (3), e2716. doi:10.1038/cddis.2017.133

Bedoui, S., Herold, M. J., and Strasser, A. (2020). Emerging Connectivity of Programmed Cell Death Pathways and its Physiological Implications. *Nat. Rev. Mol. Cel Biol* 21 (11), 678–695. doi:10.1038/s41580-020-0270-8

Campbell, B. C. V., De Silva, D. A., Macleod, M. R., Coutts, S. B., Schwamm, L. H., Davis, S. M., et al. (2019). Ischaemic Stroke. *Nat. Rev. Dis. Primers* 5 (1), 70. doi:10.1038/s41572-019-0118-8

Cao, H., Zuo, C., Huang, Y., Zhu, L., Zhao, J., Yang, Y., et al. (2021). Hippocampal Proteomic Analysis Reveals Activation of Necroptosis and Ferroptosis in a Mouse Model of Chronic Unpredictable Mild Stress-Induced Depression. *Behav. Brain Res.* 407, 113261. doi:10.1016/j.bbr.2021.113261

Chang, C. F., Cho, S., and Wang, J. (2014). (-)-Epicatechin Protects Hemorrhagic Brain via Synergistic Nrf2 Pathways. *Ann. Clin. Transl Neurol.* 1 (4), 258–271. doi:10.1002/acn3.54

Chen, B., Chen, Z., Liu, M., Gao, X., Cheng, Y., Wei, Y., et al. (2019). Inhibition of Neuronal Ferroptosis in the Acute Phase of Intracerebral Hemorrhage Shows Long-Term Cerebroprotective Effects. *Brain Res. Bull.* 153, 122–132. doi:10.1016/j.brainresbull.2019.08.013

Chen, C., Huang, Y., Xia, P., Zhang, F., Li, L., Wang, E., et al. (2021). Long Noncoding RNA Meg3 Mediates Ferroptosis Induced by Oxygen and Glucose Deprivation Combined with Hyperglycemia in Rat Brain Microvascular Endothelial Cells, through Modulating the p53/GPX4 axis. *Eur. J. Histochem.* 65 (3), 3224. doi:10.4081/ejh.2021.3224

Chen, G., Li, L., and Tao, H. (2021). Bioinformatics Identification of Ferroptosis-Related Biomarkers and Therapeutic Compounds in Ischemic Stroke. *Front. Neurol.* 12, 745240. doi:10.3389/fneur.2021.745240

Chen, J., Yang, L., Geng, L., He, J., Chen, L., Sun, Q., et al. (2021). Inhibition of Acyl-CoA Synthetase Long-Chain Family Member 4 Facilitates Neurological Recovery after Stroke by Regulation Ferroptosis. *Front. Cel Neurosci* 15, 632354. doi:10.3389/fncel.2021.632354

Chen, W., Jiang, L., Hu, Y., Tang, N., Liang, N., Li, X. F., et al. (2021). Ferritin Reduction Is Essential for Cerebral Ischemia-Induced Hippocampal Neuronal Death through p53/SLC7A11-Mediated Ferroptosis. *Brain Res.* 1752, 147216. doi:10.1016/j.brainres.2020.147216

Cheng, Y., Song, Y., Chen, H., Li, Q., Gao, Y., Lu, G., et al. (2021). Ferroptosis Mediated by Lipid Reactive Oxygen Species: A Possible Causal Link of Neuroinflammation to Neurological Disorders. *Oxid Med. Cel Longev* 2021, 20215005136. doi:10.1155/2021/5005136

Cui, Y., Zhang, Y., Zhao, X., Shao, L., Liu, G., Sun, C., et al. (2021). ACSL4 Exacerbates Ischemic Stroke by Promoting Ferroptosis-Induced Brain Injury and Neuroinflammation. *Brain Behav. Immun.* 93, 312–321. doi:10.1016/j.bbi.2021.01.003

David, S., Jhelum, P., Ryan, F., Jeong, S. Y., and Kroner, A. (2021). Dysregulation of Iron Homeostasis in the CNS and the Role of Ferroptosis in Neurodegenerative Disorders. *Antioxid. Redox Signaling.* doi:10.1089/ars.2021.0218

DeGregorio-Rocasolano, N., Martí-Sistac, O., and Gasull, T. (2019). Deciphering the Iron Side of Stroke: Neurodegeneration at the Crossroads between Iron Dyshomeostasis, Excitotoxicity, and Ferroptosis. *Front. Neurosci.* 13, 85. doi:10.3389/fnins.2019.00085

Dixon, S. J., Lemberg, K. M., Lamprecht, M. R., Skouta, R., Zaitsev, E. M., Gleason, C. E., et al. (2012). Ferroptosis: an Iron-dependent Form of Nonapoptotic Cell Death. *Cell* 149 (5), 1060–1072. doi:10.1016/j.cell.2012.03.042

Duan, L., Zhang, Y., Yang, Y., Su, S., Zhou, L., Lo, P. C., et al. (2021). Baicalin Inhibits Ferroptosis in Intracerebral Hemorrhage. *Front. Pharmacol.* 12, 62937. doi:10.3389/fphar.2021.629379

Friedmann Angeli, J. P., Schneider, M., Proneth, B., Tyurina, Y. Y., Tyurin, V. A., Hammond, V. J., et al. (2014). Inactivation of the Ferroptosis Regulator Gpx4 Triggers Acute Renal Failure in Mice. *Nat. Cel Biol* 16 (12), 1180–1191. doi:10.1038/ncb3064

Galluzzi, L., Vitale, I., Aaronson, S. A., Abrams, J. M., Adam, D., Agostinis, P., et al. (2018). Molecular Mechanisms of Cell Death: Recommendations of the Nomenclature Committee on Cell Death 2018. *Cell Death Differ* 25 (3), 486–541. doi:10.1038/s41418-017-0012-4

Gao, M., Monian, P., Pan, Q., Zhang, W., Xiang, J., and Jiang, X. (2016). Ferroptosis Is an Autophagic Cell Death Process. *Cell Res* 26 (9), 1021–1032. doi:10.1038/cr.2016.95

Ge, H., Xue, X., Xian, J., Yuan, L., Wang, L., Zou, Y., et al. (2021). Ferrostatin-1 Alleviates White Matter Injury via Decreasing Ferroptosis Following Spinal Cord Injury. *Mol. Neurobiol.* doi:10.1007/s12035-021-02571-y

Gibellini, L., and Moro, L. (2021). Programmed Cell Death in Health and Disease. *Cells* 10 (7), 1765. doi:10.3390/cells10071765

Guo, H., Zhu, L., Tang, P., Chen, D., Li, Y., Li, J., et al. (2021b). Carthamin Yellow Improves Cerebral Ischemia-reperfusion I-njury by A-ttenuating I-nflammation and F-erroptosis in R-ats. *Int. J. Mol. Med.* 47 (4), 52. doi:10.3892/ijmm.2021.4885

Guo, X. W., Lu, Y., Zhang, H., Huang, J. Q., and Li, Y. W. (2021). PIEZO1 Might Be Involved in Cerebral Ischemia-Reperfusion Injury through Ferroptosis Regulation: a Hypothesis. *Med. Hypotheses* 146, 110327. doi:10.1016/j.mehy.2020.110327

Hassannia, B., Van Coillie, S., and Vanden Berghe, T. (2021). Ferroptosis: Biological Rust of Lipid Membranes. *Antioxid. Redox Signal.* 35 (6), 487–509. doi:10.1089/ars.2020.8175

Henke, N., Albrecht, P., Bouchachia, I., Ryazantseva, M., Knoll, K., Lewerenz, J., et al. (2013). The Plasma Membrane Channel ORAI1 Mediates Detrimental Calcium Influx Caused by Endogenous Oxidative Stress. *Cel Death Dis* 4 (1), e470. doi:10.1038/cddis.2012.216

Hughes, R. E., Tadi, P., and Bollu, P. C. (2021). "TPA Therapy," in *StatPearls*. Treasure Island, Florida: StatPearls Publishing.

Jin, Y., Zhuang, Y., Liu, M., Che, J., and Dong, X. (2021). Inhibiting Ferroptosis: A Novel Approach for Stroke Therapeutics. *Drug Discov. Today* 26 (4), 916–930. doi:10.1016/j.drudis.2020.12.020

Jin, Z. L., Gao, W. Y., Liao, S. J., Yu, T., Shi, Q., Yu, S. Z., et al. (2021). Paeonol Inhibits the Progression of Intracerebral Haemorrhage by Mediating the HOTAIR/UPF1/ACSL4 axis. *ASN Neuro* 13, 17590914211010647. doi:10.1177/17590914211010647

Karuppagounder, S. S., Alin, L., Chen, Y., Brand, D., Bourassa, M. W., Dietrich, K., et al. (2018). N-acetylcysteine Targets 5 Lipoxygenase-Derived, Toxic Lipids and Can Synergize with Prostaglandin E2 to Inhibit Ferroptosis and Improve Outcomes Following Hemorrhagic Stroke in Mice. *Ann. Neurol.* 84 (6), 854–872. doi:10.1002/ana.25356

Keuters, M. H., Keksa-Goldsteine, V., Dhungana, H., Huuskonen, M. T., Pomeshchik, Y., Savchenko, E., et al. (2021). An Arylthiazyne Derivative Is a Potent Inhibitor of Lipid Peroxidation and Ferroptosis Providing Neuroprotection *In Vitro* and *In Vivo*. *Sci. Rep.* 11 (1), 3518. doi:10.1038/s41598-021-81741-3

Kist, M., and Vucic, D. (2021). Cell Death Pathways: Intricate Connections and Disease Implications. *EMBO J.* 40 (5), e106700. doi:10.15252/embj.2020106700

Kuo, P. C., Weng, W. T., Scofield, B. A., Furnas, D., Paraiso, H. C., Intriago, A. J., et al. (2020). Interferon-β Alleviates Delayed tPA-Induced Adverse Effects via Modulation of MMP3/9 Production in Ischemic Stroke. *Blood Adv.* 4 (18), 4366–4381. doi:10.1182/bloodadvances.2020001443

Lan, B., Ge, J. W., Cheng, S. W., Zheng, X. L., Liao, J., He, C., et al. (2020). Extract of Naotaifang, a Compound Chinese Herbal Medicine, Protects Neuron Ferroptosis Induced by Acute Cerebral Ischemia in Rats. *J. Integr. Med.* 18 (4), 344–350. doi:10.1016/j.joim.2020.01.008

Lee, Y. S., Kalimuthu, K., Park, Y. S., Luo, X., Choudry, M. H. A., Bartlett, D. L., et al. (2020). BAX-dependent Mitochondrial Pathway Mediates the Crosstalk between Ferroptosis and Apoptosis. *Apoptosis* 25 (9-10), 625–631. doi:10.1007/s10495-020-01627-z

Lee, Y. S., Lee, D. H., Choudry, H. A., Bartlett, D. L., and Lee, Y. J. (2018). Ferroptosis-Induced Endoplasmic Reticulum Stress: Cross-Talk between Ferroptosis and Apoptosis. *Mol. Cancer Res.* 16 (7), 1073–1076. doi:10.1158/1541-7786.MCR-18-0055

Li, C., Sun, G., Chen, B., Xu, L., Ye, Y., He, J., et al. (2021). Nuclear Receptor Coactivator 4-mediated Ferritinophagy Contributes to Cerebral Ischemia-Induced Ferroptosis in Ischemic Stroke. *Pharmacol. Res.* 174, 105933. doi:10.1016/j.phrs.2021.105933

Li, G., Li, X., Dong, J., and Han, Y. (2021). Electroacupuncture Ameliorates Cerebral Ischemic Injury by Inhibiting Ferroptosis. *Front. Neurol.* 12, 619043. doi:10.3389/fneur.2021.619043

Li, L., Li, H., Li, Y., Feng, J., Guan, D., Zhang, Y., et al. (2021). Ferritinophagy-Mediated ROS Production Contributed to Proliferation Inhibition, Apoptosis, and Ferroptosis Induction in Action of Mechanism of 2-Pyridylhydrazone

Dithiocarbamate Acetate. *Oxid Med. Cel Longev* 2021, 5594059. doi:10.1155/2021/5594059

Li, Q., Weiland, A., Chen, X., Lan, X., Han, X., Durham, F., et al. (2018). Ultrastructural Characteristics of Neuronal Death and White Matter Injury in Mouse Brain Tissues after Intracerebral Hemorrhage: Coexistence of Ferroptosis, Autophagy, and Necrosis. *Front. Neurol.* 9, 581. doi:10.3389/fneur.2018.00581

Li, Y., Feng, D., Wang, Z., Zhao, Y., Sun, R., Tian, D., et al. (2019). Ischemia-induced ACSL4 Activation Contributes to Ferroptosis-Mediated Tissue Injury in Intestinal Ischemia/reperfusion. *Cel Death Differ* 26 (11), 2284–2299. doi:10.1038/s41418-019-0299-4

Li, Y., Liu, Y., Wu, P., Tian, Y., Liu, B., Wang, J., et al. (2021). Inhibition of Ferroptosis Alleviates Early Brain Injury after Subarachnoid Hemorrhage *In Vitro* and *In Vivo* via Reduction of Lipid Peroxidation. *Cell Mol Neurobiol* 41 (2), 263–278. doi:10.1007/s10571-020-00850-1

Liu, Y., Fang, Y., Zhang, Z., Luo, Y., Zhang, A., Lenahan, C., et al. (2021). Ferroptosis: An Emerging Therapeutic Target in Stroke. *J. Neurochem.* 160, 64–73. doi:10.1111/jnc.15351

Louandre, C., Ezzoukhry, Z., Godin, C., Barbare, J. C., Mazière, J. C., Chauffert, B., et al. (2013). Iron-dependent Cell Death of Hepatocellular Carcinoma Cells Exposed to Sorafenib. *Int. J. Cancer* 133 (7), 1732–1742. doi:10.1002/ijc.28159

Lu, J., Xu, F., and Lu, H. (2020). LncRNA PVT1 Regulates Ferroptosis through miR-214-Mediated TFR1 and P53. *Life Sci.* 260, 118305. doi:10.1016/j.lfs.2020.118305

Mahoney-Sánchez, L., Bouchaoui, H., Ayton, S., Devos, D., Duce, J. A., and Devedjian, J. C. (2021). Ferroptosis and its Potential Role in the Physiopathology of Parkinson's Disease. *Prog. Neurobiol.* 196, 101890. doi:10.1016/j.pneurobio.2020.101890

Meihe, L., Shan, G., Minchao, K., Xiaoling, W., Peng, A., Xili, W., et al. (2021). The Ferroptosis-NLRP1 Inflammasome: The Vicious Cycle of an Adverse Pregnancy. *Front Cel Dev Biol* 9, 707959. doi:10.3389/fcell.2021.707959

Moujalled, D., Strasser, A., and Liddell, J. R. (2021). Molecular Mechanisms of Cell Death in Neurological Diseases. *Cel Death Differ* 28 (7), 2029–2044. doi:10.1038/s41418-021-00814-y

Peng, C., Fu, X., Wang, K., Chen, L., Luo, B., Huang, N., et al. (2022). Dauricine Alleviated Secondary Brain Injury after Intracerebral Hemorrhage by Upregulating GPX4 Expression and Inhibiting Ferroptosis of Nerve Cells. *Eur. J. Pharmacol.* 914, 174461. doi:10.1016/j.ejphar.2021.174461

Plascencia-Villa, G., and Perry, G. (2021). Preventive and Therapeutic Strategies in Alzheimer's Disease: Focus on Oxidative Stress, Redox Metals, and Ferroptosis. *Antioxid. Redox Signal.* 34 (8), 591–610. doi:10.1089/ars.2020.8134

Rui, T., Li, Q., Song, S., Gao, Y., and Luo, C. (2020). Ferroptosis-relevant Mechanisms and Biomarkers for Therapeutic Interventions in Traumatic Brain Injury. *Histol. Histopathol* 35 (10), 1105–1113. doi:10.14670/HH-18-229

Speer, R. E., Karuppagounder, S. S., Basso, M., Sleiman, S. F., Kumar, A., Brand, D., et al. (2013). Hypoxia-inducible Factor Prolyl Hydroxylases as Targets for Neuroprotection by "antioxidant" Metal Chelators: From Ferroptosis to Stroke. *Free Radic. Biol. Med.* 62, 26–36. doi:10.1016/j.freeradbiomed.2013.01.026

Stockwell, B. R., Friedmann Angeli, J. P., Bayir, H., Bush, A. I., Conrad, M., Dixon, S. J., et al. (2017). Ferroptosis: A Regulated Cell Death Nexus Linking Metabolism, Redox Biology, and Disease. *Cell* 171 (2), 273–285. doi:10.1016/j.cell.2017.09.021

Stockwell, B. R., Jiang, X., and Gu, W. (2020). Emerging Mechanisms and Disease Relevance of Ferroptosis. *Trends Cel Biol* 30 (6), 478–490. doi:10.1016/j.tcb.2020.02.009

Tang, D., and Kroemer, G. (2020). Ferroptosis. *Curr. Biol.* 30 (21), R1292–R1297. doi:10.1016/j.cub.2020.09.068

Tuo, Q.-Z., Masaldan, S., Southon, A., Mawal, C., Ayton, S., Bush, A. I., et al. (2021). Characterization of Selenium Compounds for Anti-ferroptotic Activity in Neuronal Cells and after Cerebral Ischemia-Reperfusion Injury. *Neurotherapeutics*. doi:10.1007/s13311-021-01111-9

Tuo, Q. Z., Lei, P., Jackman, K. A., Li, X. L., Xiong, H., Li, X. L., et al. (2017). Tau-mediated Iron export Prevents Ferroptotic Damage after Ischemic Stroke. *Mol. Psychiatry* 22 (11), 1520–1530. doi:10.1038/mp.2017.171

Wan, J., Ren, H., and Wang, J. (2019). Iron Toxicity, Lipid Peroxidation and Ferroptosis after Intracerebral Haemorrhage. *Stroke Vasc. Neurol.* 4 (2), 93–95. doi:10.1136/svn-2018-000205

Wang, P., Cui, Y., Ren, Q., Yan, B., Zhao, Y., Yu, P., et al. (2021). Mitochondrial Ferritin Attenuates Cerebral Ischaemia/reperfusion Injury by Inhibiting Ferroptosis. *Cel Death Dis* 12 (5), 447. doi:10.1038/s41419-021-03725-5

Wu, H., Wang, Y., Tong, L., Yan, H., and Sun, Z. (2021). Global Research Trends of Ferroptosis: A Rapidly Evolving Field with Enormous Potential. *Front. Cel Dev Biol* 9, 646311. doi:10.3389/fcell.2021.646311

Wu, S., Wu, B., Liu, M., Chen, Z., Wang, W., Anderson, C. S., et al. (2019). Stroke in China: Advances and Challenges in Epidemiology, Prevention, and Management. *Lancet Neurol.* 18 (4), 394–405. doi:10.1016/S1474-4422(18)30500-3

Wu, Z., Geng, Y., Lu, X., Shi, Y., Wu, G., Zhang, M., et al. (2019). Chaperone-mediated Autophagy Is Involved in the Execution of Ferroptosis. *Proc. Natl. Acad. Sci. U S A.* 116 (8), 2996–3005. doi:10.1073/pnas.1819728116

Yang, W., Liu, X., Song, C., Ji, S., Yang, J., Liu, Y., et al. (2021). Structure-activity Relationship Studies of Phenothiazine Derivatives as a New Class of Ferroptosis Inhibitors Together with the Therapeutic Effect in an Ischemic Stroke Model. *Eur. J. Med. Chem.* 209, 112842. doi:10.1016/j.ejmech.2020.112842

Yin, J., Wan, J., Zhu, J., Zhou, G., Pan, Y., and Zhou, H. (2021). Global Trends and Prospects about Inflammasomes in Stroke: a Bibliometric Analysis. *Chin. Med.* 16 (1), 53. doi:10.1186/s13020-021-00464-9

Yu, Y., Yan, Y., Niu, F., Wang, Y., Chen, X., Su, G., et al. (2021). Ferroptosis: a Cell Death Connecting Oxidative Stress, Inflammation and Cardiovascular Diseases. *Cell Death Discov* 7 (1), 193. doi:10.1038/s41420-021-00579-w

Yuan, Y., Zhai, Y., Chen, J., Xu, X., and Wang, H. (2021). Kaempferol Ameliorates Oxygen-Glucose Deprivation/Reoxygenation-Induced Neuronal Ferroptosis by Activating Nrf2/SLC7A11/GPX4 Axis. *Biomolecules* 11 (7), 923. doi:10.3390/biom11070923

Zhang, H., Wen, M., Chen, J., Yao, C., Lin, X., Lin, Z., et al. (2021). Pyridoxal Isonicotinoyl Hydrazone Improves Neurological Recovery by Attenuating Ferroptosis and Inflammation in Cerebral Hemorrhagic Mice. *Biomed. Res. Int.*, 20219916328. doi:10.1155/2021/9916328

Zhang, T., Zhao, J., Li, X., Bai, Y., Wang, B., Qu, Y., et al. (2020). Chinese Stroke Association Guidelines for Clinical Management of Cerebrovascular Disorders: Executive Summary and 2019 Update of Clinical Management of Stroke Rehabilitation. *Stroke Vasc. Neurol.* 5 (3), 250–259. doi:10.1136/svn-2019-000321

Zhang, Y., Lu, X., Tai, B., Li, W., and Li, T. (2021). Ferroptosis and its Multifaceted Roles in Cerebral Stroke. *Front. Cel Neurosci* 15, 615372. doi:10.3389/fncel.2021.615372

Zhou, S. Y., Cui, G. Z., Yan, X. L., Wang, X., Qu, Y., Guo, Z. N., et al. (2020). Mechanism of Ferroptosis and its Relationships with Other Types of Programmed Cell Death: Insights for Potential Interventions after Intracerebral Hemorrhage. *Front. Neurosci.* 14, 589042. doi:10.3389/fnins.2020.589042

Zhou, Y., Liao, J., Mei, Z., Liu, X., and Ge, J. (2021). Insight into Crosstalk between Ferroptosis and Necroptosis: Novel Therapeutics in Ischemic Stroke. *Oxid Med. Cel Longev*, 20219991001. doi:10.1155/2021/9991001

Zille, M., Karuppagounder, S. S., Chen, Y., Gough, P. J., Bertin, J., Finger, J., et al. (2017). Neuronal Death after Hemorrhagic Stroke *In Vitro* and *In Vivo* Shares Features of Ferroptosis and Necroptosis. *Stroke* 48 (4), 1033–1043. doi:10.1161/STROKEAHA.116.015609

Conflict of Interest: The authors declare that the research was conducted in the absence of any commercial or financial relationships that could be construed as a potential conflict of interest.

Publisher's Note: All claims expressed in this article are solely those of the authors and do not necessarily represent those of their affiliated organizations, or those of the publisher, the editors and the reviewers. Any product that may be evaluated in this article, or claim that may be made by its manufacturer, is not guaranteed or endorsed by the publisher.

frontiers in Pharmacology

SYSTEMATIC REVIEW
published: 25 February 2022
doi: 10.3389/fphar.2022.796329

A Meta-Analysis of Using Protamine for Reducing the Risk of Hemorrhage During Carotid Recanalization: Direct Comparisons of Post-operative Complications

Yongli Pan[1†], Zhiqiang Zhao[2†], Tao Yang[2†], Qingzheng Jiao[3], Wei Wei[4], Jianyong Ji[5†] and Wenqiang Xin[6*]*

[1]Department of Neurology, Weifang Medical University, Weifang, China, [2]Department of Neurosurgery, Heji Hospital Affiliated Changzhi Medical College, Changzhi, China, [3]Second Department of Internal Medicine, Gucheng Country Hospital, Shijiazhuang, China, [4]Department of Neurology, Mianyang Central Hospital, Mianyang, China, [5]Department of Neurosurgery, Liaocheng People's Hospital, Liaocheng, China, [6]Department of Neurosurgery, Tianjin Medical University General Hospital, Tianjin, China

OPEN ACCESS

Edited by:
Yongjun Sun,
Hebei University of Science and Technology, China

Reviewed by:
Zhouqing Chen,
Soochow University, China
Amit Kumar,
Rajendra Institute of Medical Sciences, India

***Correspondence:**
Jianyong Ji
jijianyong2005@163.com
Wenqiang Xin
xinwenqiangdr@126.com

[†]These authors have contributed equally to this work and share first authorship

Specialty section:
This article was submitted to Neuropharmacology, a section of the journal Frontiers in Pharmacology

Received: 16 October 2021
Accepted: 24 January 2022
Published: 25 February 2022

Citation:
Pan Y, Zhao Z, Yang T, Jiao Q, Wei W, Ji J and Xin W (2022) A Meta-Analysis of Using Protamine for Reducing the Risk of Hemorrhage During Carotid Recanalization: Direct Comparisons of Post-operative Complications. Front. Pharmacol. 13:796329. doi: 10.3389/fphar.2022.796329

Background: Protamine can decrease the risk of hemorrhage during carotid recanalization. However, it may cause severe side effects. There is no consensus on the safety and efficacy of protamine during surgery. Thus, we conduct a comprehensive review and meta-analysis to compare the differences between the protamine and the no-protamine group.

Method: We systematically obtained literature from Medline, Google Scholar, Cochrane Library, and PubMed electronic databases. All four databases were scanned from 1937 when protamine was first adopted as a heparin antagonist until February 2021. The reference lists of identified studies were manually checked to determine other eligible studies that qualify. The articles were included in this meta-analysis as long as they met the criteria of PICOS; conference or commentary articles, letters, case report or series, and animal observation were excluded from this study. The Newcastle-Ottawa Quality Assessment Scale and Cochrane Collaboration's tool are used to assess the risk of bias of each included observational study and RCT, respectively. Stata version 12.0 statistical software (StataCorp LP, College Station, Texas) was adopted as statistical software. When $I^2 < 50\%$, we consider that the data have no obvious heterogeneity, and we conduct a meta-analysis using the fixed-effect model. Otherwise, the random-effect model was performed.

Result: A total of 11 studies, consisting of 94,618 participants, are included in this study. Our analysis found that the rate of wound hematoma had a significant difference among protamine and no-protamine patients (OR = 0.268, 95% CI = 0.093 to 0.774, $p = 0.015$). Furthermore, the incidence of hematoma requiring re-operation (0.7%) was significantly

Abbreviations: CEA, Carotid endarterectomy; CAS, Carotid artery stenting; MI, Myocardial Infarction; RDs, Risk differences; ORs, Odds ratios; FDA, Food and Drug Administration; CIs, Confidence Intervals; RCTs, Randomized Controlled Trials; TIA, Transient Ischemic Attacks.

lower than that of patients without protamine (1.8%). However, there was no significant difference in the incidence of stroke, wound hematoma with hypertension, transient ischemic attacks (TIA), myocardial infarction (MI), and death.

Conclusion: Among included participants undergoing recanalization, the use of protamine is effective in reducing hematoma without increasing the risk of having other complications. Besides, more evidence-based performance is needed to supplement this opinion due to inherent limitations.

Keywords: protamine, carotid recanalization, meta-analysis, carotid stenosis, hemorrhage - cerebral

INTRODUCTION

Ischemic stroke accounts for the mortality of approximately more than ten million lives per year all over the world (Yip et al., 2016), and it is an important public health concern. Considerable research evidence demonstrates that the prevalence of carotid stenosis is about 7% (Dharmakidari et al., 2017), which is becoming an important public health issue (Abbott et al., 2015). Carotid endarterectomy (CEA), performed to prevent embolus, is considered a conventional treatment (Howell, 2007). Carotid artery stenting (CAS), a minimally invasive procedure (Spiliopoulos et al., 2019), has emerged as an effective treatment modality for carotid artery stenosis (Setacci et al., 2018). Although these two surgical interventions have improved the prognosis of ischemic stroke, they may carry hemorrhage as a severe complication (Spence et al., 2016). Heparin is a robust anticoagulant used routinely during both CEA and CAS surgeries to avoid thromboembolic complications (Lynch and Kavanagh, 2016; Sokolowska et al., 2016). After such surgeries, some surgeons advocate the adoption of protamine to achieve a systemic anticoagulant effect to decrease the risk of hemorrhage (Liang et al., 2021). Protamine is known to be arginine-rich, making it a positively charged protein (Bakchoul et al., 2016), and is an approved drug by the Food and Drug Administration (FDA). Despite its neutralization action, protamine may cause severe side effects such as systemic hypotension, anaphylactic reaction, pulmonary hypertension, and tissue damage of the lungs, kidneys, and red blood cells (Sokolowska et al., 2016). Hence, the use of protamine can have a significant difference in short-term and long-term morbidity and mortality (Al-Kassou et al., 2020). As one study reviewed 10,059 CEAs performed in 9,260 patients from 2003 to 2012, protamine use remained stable from 2003 through 2007 at 43%. Then, there was a significant increase in protamine use to 52% from the beginning in January 2008 (Patel et al., 2013). Theoretically, protamine can bind with the glucosaminoglycan of heparin to form a stable complex, which, in turn, suppresses the activity of antithrombin, herein counteracting the anticoagulant effect of heparin and achieving the effect of hemostasis. Some surgeons advocate the routine use of protamine to minimize bleeding complications, whereas some others avoid heparin reversal to minimize the risk of stroke through thrombus formation on the endarterectomy surface of the artery (Cho et al., 2012). Therefore, the purpose of this study is to evaluate the safety and efficacy of protamine to reduce the risk of hemorrhage during carotid recanalization.

MATERIALS AND METHODS

Literature Search Strategy

We systematically obtained literature from Medline, Google Scholar, Cochrane Library, and PubMed electronic databases. We utilized controlled vocabulary to build the search terms such as the National Library of Medicine in this study. All four databases were scanned from 1937 when protamine was first adopted as a heparin antagonist until February 2021 for the keywords of protamine, carotid endarterectomy, and carotid artery stenosis in combination with Boolean logic (Jaques, 1973). The specific search strategy is shown in **Table 1**. After the original search, the relevant studies and their references were searched manually by two authors. Beyond that, all references to previous reviews and related clinical trials were manually checked to identify potential publications that were not included in our electronic search results.

Inclusion and Exclusion Criteria

Studies are considered eligible if they fulfilled the predefined inclusion criteria: (1) population: participant with carotid stenosis; (2) intervention: all patients strictly undergoing carotid recanalization; (3) comparison intervention: use of protamine to no-protamine group; (4) outcome measures: one or more of the following outcomes were reported: complications of wound hematoma, hematoma requiring re-operation, wound hematoma with hypertension, transient ischemic attacks (TIA), myocardial infarction (MI), stroke, and death; and (5) official published prospective and retrospective studies in English.

The exclusion criteria are listed as follows: (1) conference or commentary articles and letters, (2) atypical patients and outcome data, (3) case report and case series, and (4) animal observation.

Data Extraction and Outcome Measures

Data were extracted by using a form prepared in advance and from the eligible researchers. Each relevant study was independently captured by two authors for the following essential details: the first author of the study, publication year, type of study, quality assessment, endpoints, and study

TABLE 1 | The specific search strategy.

Carotid stenosis OR carotid artery stenosis OR carotid disease OR carotid artery disease
AND
CAS OR carotid artery stenting OR carotid angioplasty OR carotid stenting OR CEA OR carotid endarterectomy OR endarterectomy OR carotid surgery OR carotid revascularization
AND
Protamine

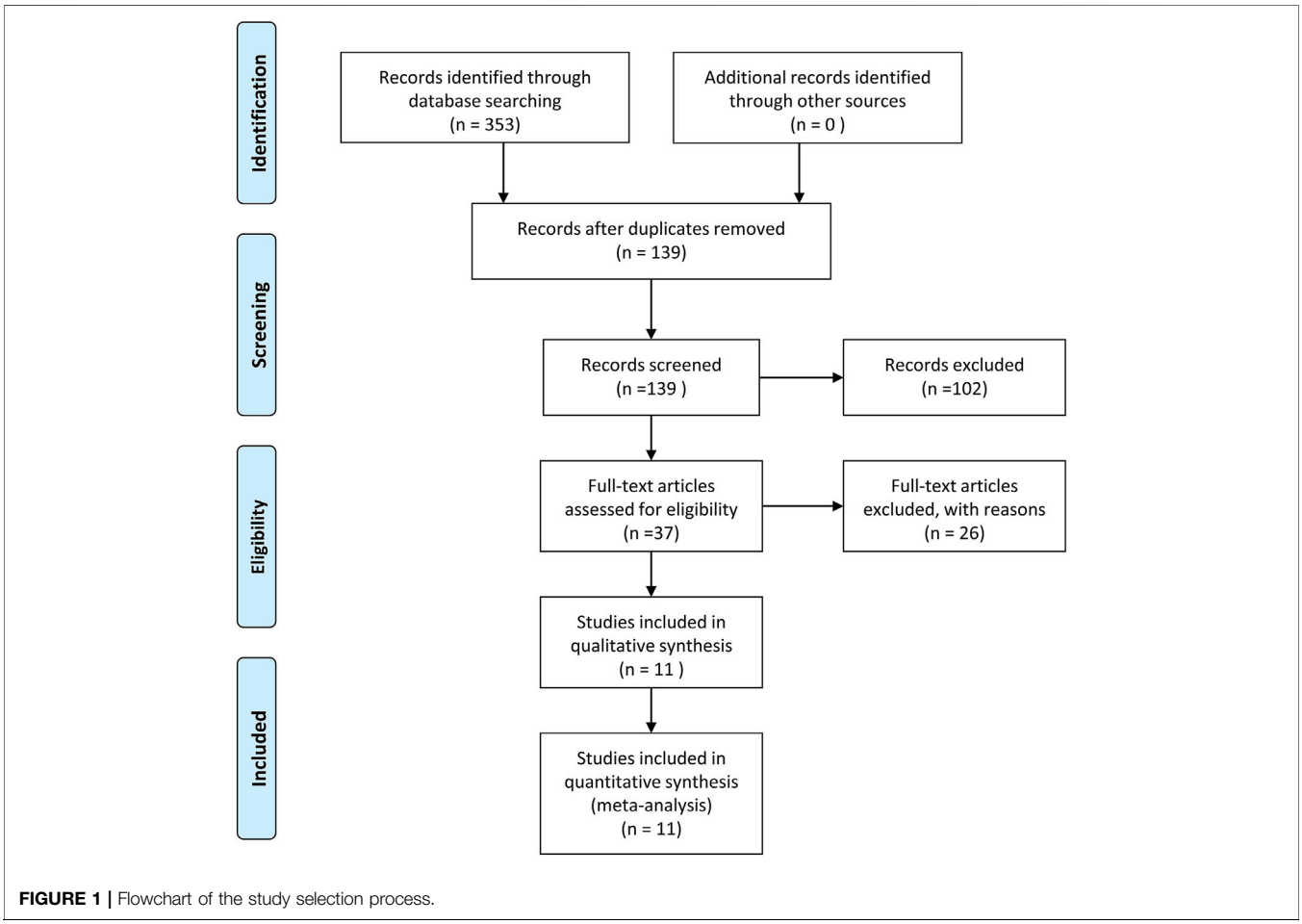

FIGURE 1 | Flowchart of the study selection process.

characteristics including the number of populations in total, mean age, and gender ratio, among others. All disagreements were discussed until a final decision is reached. The primary study endpoint measurements are relevant to hemorrhagic damage including wound hematoma, hematoma requiring re-operation, and hematoma with hypertension, and secondary endpoints were the composite of ischemic injuries including stroke, TIA, and MI. Herein, in primary endpoints, all hematoma was defined as wound hematoma. In secondary endpoints, stroke was defined as 1 or more of the following: (1) an increase in the National Institute of Health stroke scale (NIHSS) score of >4 points from pre-stroke score; (2) an increase in the MRS score of >2 points from the pre-stroke score; or (3) stroke leading to a modified Rankin scale (MRS) score of 5 or more.

Statistical Analysis

Stata version 12.0 statistical software (StataCorp LP, College Station, Texas) was adopted as statistical software. The risk differences (RDs) or odds ratios (ORs) with the corresponding 95% confidence intervals (95% CIs) were used as measures of the treatment effect of protamine. We accessed the heterogeneity with the Higgins *I*-square (I^2), which indicated the percentage of the observed between-study viability. I^2 over 25% and less than 75% was considered as moderately heterogeneous or significant heterogeneity. If I^2 was under 50%, the endpoint item was

TABLE 2 | Characteristics of publication year, country, study type, cases, general anesthesia, and mean age in each group for included studies.

Study	Years	Country	Study design	General anesthesia	Sample size		Mean age (Years)	
					Protamine	No protamine	Protamine	No protamine
Protamine use in carotid endarterectomy (CEA)								
Treiman et al.	1990	United States	Non-RCT	100%	328	369	71	71
Mauney et al.	1995	United States	Non-RCT	98.3%	193	155	65.9	68.8
Fearn et al.	1997	United Kingdom	RCT	100%	31	33	66	61.9
Levison, et al.	1999	United States	Non-RCT	NA	365	42	70.6	69
Dellagrammaticas et al.	2008	United Kingdom	RCT	50%	594	1,513	70	70.4
Stone et al.	2010	United States	Non-RCT	50%	2,087	2,500	69.2	70
Mazzalai et al.	2014	Italy	Non-RCT	100%	201	1,294	75.7	75.1
Stone et al.	2020	United States	Non-RCT I	100%	53,349	23,966	70.0 ± 9.1	69.1 ± 9.2
Protamine use in carotid artery stenting (CAS)								
Mcdonald et al.	2013	United States	Non-RCT	NA	555	555	NA	NA
Liang et al.	2020	United States	Non-RCT	NA	944	944	72.7 ± 9.7	73.2 ± 9.4
Liang et al.	2021	United States	Non-RCT	NA	2,300	2,300	70.6 ± 9.5	70.4 ± 9.7

Note: NA: not available; RCT, randomized controlled trials.

considered to be homogeneous, and we ran a meta-analysis by using a fixed-effect model according to the Cochrane Handbook for Systematic Reviews of Interventions. Otherwise, the random-effect model was performed.

Quality of Evidence Assessment

We used the guidance from the Grading of Recommendations Assessment, Development and Evaluation (GRADE) working group to assess the quality of evidence for the primary outcome (Li et al., 2019). The GRADE summary of findings table was produced using the GradePRO software.

RESULTS

Search Result

The screening process is displayed in **Figure 1**, which is based on the inclusion and exclusion criteria. The search initially yielded a total of 353 articles. After the exclusion of duplicated or irrelevant articles, 139 eligible studies were enrolled in this study. Later, after evaluating the full text of the remaining articles, 37 articles met our inclusion criteria. Finally, 11 studies were involved in our quantitative synthesis.

Characteristics of Included Studies

Detailed characteristics of the 11 observational articles, including 94,618 participants (median sample size, 1,495; range, 64 to 77,315) with an average age of 76 years (range, 59.1 to 82.6), are listed in **Table 2**. The majority of studies were performed in the United States (Liang et al., 2021; Treiman et al., 1990; Stone et al., 2010; Stone et al., 2020; McDonald et al., 2013; Liang et al., 2020). Two were in the United Kingdom (Fearn et al., 1997; Dellagrammaticas et al., 2008), and another one was from Italy (Mazzalai et al., 2014). There were 9 Non-RCTs (Randomized Controlled Trials) (Liang et al., 2021; Treiman et al., 1990; Stone et al., 2010; Stone et al., 2020; McDonald et al., 2013; Liang et al., 2020; Mazzalai et al., 2014; Mauney et al., 1995) (n = 92,447) and 2 RCTs (Fearn et al., 1997; Dellagrammaticas et al., 2008) involving 2,171 patients randomized to either protamine of heparin or not restrictedly undergoing CEA. In the protamine group, out of the 60,947 patients, 57,148 were allocated to CEA, and 3,799 were from CAS, with an average age from 65.9 to 79.1 years old. In the no protamine group, 57.8% of enrolled participants were from CEA. Nearly all surgeries considered age, whereas only McDonald et al. (2013) ignored this.

Quality Assessment

Methodological quality and risk of bias in the included observational studies are assessed by two reviewers independently by using the Newcastle-Ottawa Quality Assessment Scale (Mitchell-Jones et al., 2017), which consists of three main categories: selection, comparability, and outcome, with questions in each area corresponding to the study quality (Newhall et al., 2016). The evaluation scores for all non-RCT are listed in **Table 3** with the highest quality of 9 points. Studies that scored lower than 5 points equate to low quality, and a score of 6–7 points is regarded as moderate quality. Additionally, the Cochrane Collaboration's tool is used for assessing the risk of bias of each included RCT. The results of the quality assessment of RCT are provided in **Table 4**.

The Outcome of the Meta-Analysis

There were nearly ten thousand participants, 92% of whom have been undergoing CEA and 8% had been treated with CAS. The detailed results and GRADE assessment of outcomes are shown in **Table 5**.

Wound Hematoma

We include four independent pieces of research of CEA with 4,706 patients (1,488 of protamine and 3,218 of no-protamine). Among these studies, the incidence of wound hematoma in the protamine group is 3.8% (57 of 1,488), which is smaller than the no-protamine group (9.5%, 305 of 3,218). This comparison fully indicates that the group of protamine is associated with a significantly lower incidence of wound hematoma than participants treated with non-protamine (OR = 0.268, 95% CI = 0.093 to 0.774, p = 0.015, **Figure 2**). Similarly, in the subgroup of CEA, the results are the same. However, a significant heterogeneity was observed (I^2 = 77.2%, p = 0.004). A

TABLE 3 | The quality assessment in randomized controlled trials.

Author, year	Design	Newcastle-Ottawa scale (NOS)			
		Selection	Comparability	Exposure	Total score
Treiman et al. 1990	Non-RCT	3	1	3	7
Mauney et al. 1995	Non-RCT	3	2	3	8
Levison, et al. 1999	Non-RCT	3	2	2	7
Stone et al. 2010	Non-RCT	3	2	2	7
Mazzalai et al. 2014	Non-RCT	4	1	3	8
Stone et al. 2020	Non-RCT	4	2	2	8
Mcdonald et al. 2013	Non-RCT	3	2	3	8
Liang et al. 2020	Non-RCT	3	1	3	7
Liang et al. 2021	Non-RCT	4	2	2	8

Note: NOS , Newcastle-Ottawa scale.

TABLE 4 | Cochrane Collaboration's tool for quality assessment in randomized controlled trials.

Trials	Sequence generation	Allocation concealment	Blinding of outcome assessors	Incomplete outcome data	Selective outcome reporting	Others
Fearn et al. 1997	Low	Unclear	Low	Low	Low	Low
Dellagrammaticas et al. 2008	Low	Low	Low	Low	Low	Unclear

TABLE 5 | The post-operative outcomes of this meta-analysis. The bold values refer to p-value < 0.05.

Outcomes	Study numbers	Event rates		Overall effect			Heterogeneity		EQ
		Protamine	No protamine	Effect estimates	95% CIs	p-Value	I^2 (%)	p-Value	(GRADE)
The use of protamine in carotid recanalization									
Wound hematoma (WH)	4	57/1,488 (3.83%)	305/3,218 (9.48%)	OR (0.268)	0.093–0.774	**0.015**	77.2	0.004	Low
WH requiring re-operation	8	409/ 60,013 (0.68%)	591/ 32,714 (1.81%)	OR (0.475)	0.282–0.798	**0.005**	77.3	0.000	Low
WH with hypertension	3	170/1,471 (11.56%)	347/2,607 (13.31%)	OR (0.704)	0.358–1.388	0.311	76.0	0.015	Low
Transient Ischemic Attacks	5	50/4,193 (1.19%)	91/5,248 (1.73%)	OR (0.793)	0.546–1.151	0.222	44.4	0.126	Low
Myocardial Infarction	7	430/ 60,030 (0.72%)	245/ 33,072 (0.74%)	OR (0.935)	0.797–1.096	0.408	0.0	0.446	High
Post-operative Stroke	10	735/ 60,916 (1.21%)	426/ 33,638 (1.27%)	OR (1.071)	0.944–1.214	0.286	30.1	0.168	Low
Post-operative Death	7	138/ 56,638 (0.24%)	82/30,526 (0.36%)	RD (0.000)	–0.001–0.001	0.877	0.0	0.719	Low
The use of protamine in CEA									
Wound hematoma (WH)	4	57/1,488 (3.83%)	305/3,218 (9.48%)	OR (0.268)	0.093–0.774	**0.015**	77.2	0.004	Low
WH requiring re-operation	6	379/ 56,769 (0.67%)	546/ 29,470 (1.85%)	OR (0.429)	0.265–0.694	**0.001**	61.0	0.025	Low
WH with hypertension	2	22/527 (4.17%)	209/1,663 (12.57%)	OR (0.333)	0.057–1.959	0.224	67.6	0.079	Low
Transient Ischemic Attacks	2	3/394 (0.76%)	41/1,449 (2.83%)	OR (0.255)	0.068–0.947	**0.041**	0.0	0.366	High
Myocardial Infarction	4	399/ 56,231 (0.71%)	222/ 29,273 (0.76%)	OR (0.902)	0.764–1.065	0.224	0.0	0.661	High
Post-operative Stroke	7	641/ 57,117 (1.12%)	354/ 29,839 (1.19%)	OR (1.029)	0.897–1.180	0.687	37	0.146	Low
Post-operative Death	4	106/ 52,839 (0.20%)	54/26,727 (0.20%)	RD (0.000)	–0.001–0.001	0.878	0.0	0.967	High

Note. CIs, confidence intervals; RD, risk difference; OR, odds ratio; EQ , evidence quality.

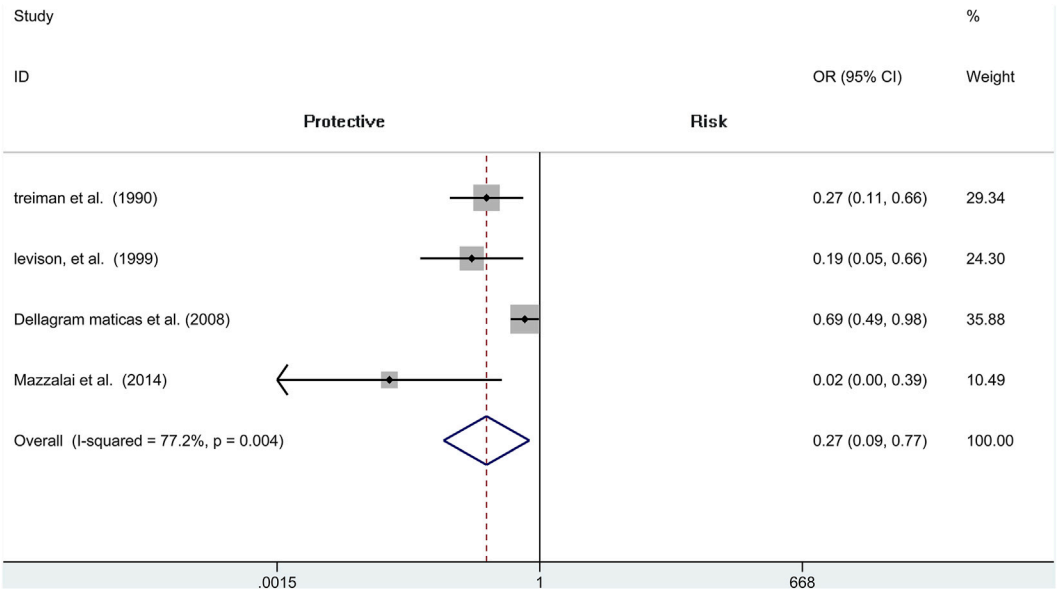

FIGURE 2 | Forest plot for meta-analysis of the incidence of wound hematoma.

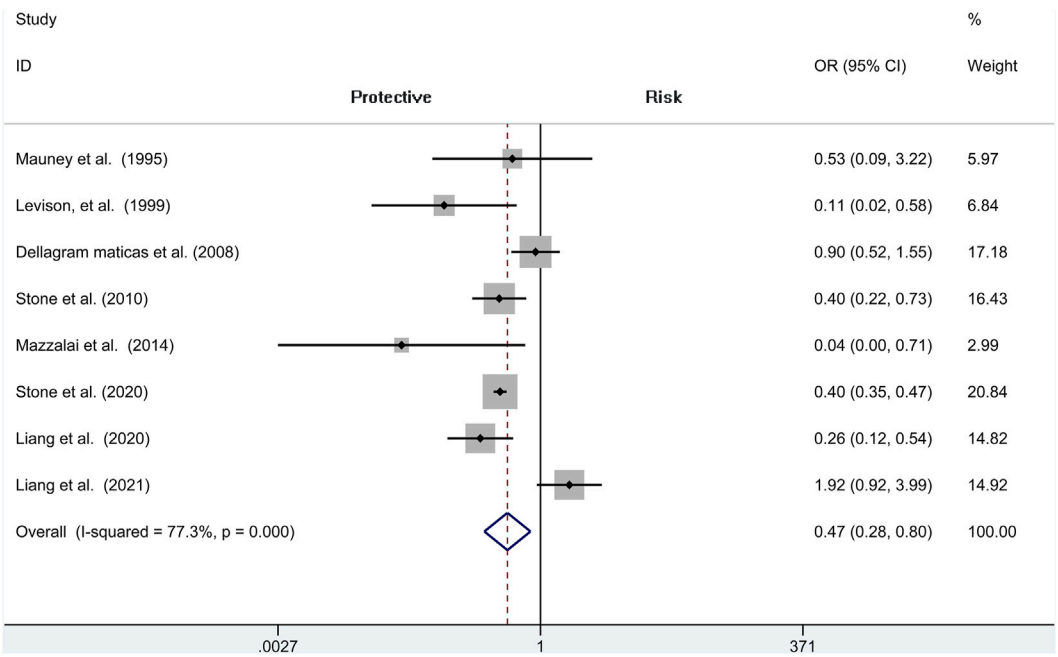

FIGURE 3 | Forest plot for meta-analysis of the incidence of hematoma requiring re-operation.

sensitivity analysis was performed to reveal that the heterogeneity was decreased by deleting the study conducted by Dellagrammaticas et al. (I^2 = 51.6%, p = 0.127).

Hematoma Requiring Re-operation

Analysis of risk of hematoma requiring re-operation between the protamine and no-protamine groups is provided in eight studies. The proportion estimated in protamine and no-protamine groups is 0.7% (409 of 60,013) versus 1.8% (591 of 32,714). However, a significant heterogeneity was observed, and a random effects model was used (I^2 = 77.3%, p < 0.001). A specific OR of 0.475 (95% CI = 0.282 to 0.798, p = 0.005; **Figure 3**) is obtained, suggesting that the incidence of hematoma requiring re-operation is significantly lower than

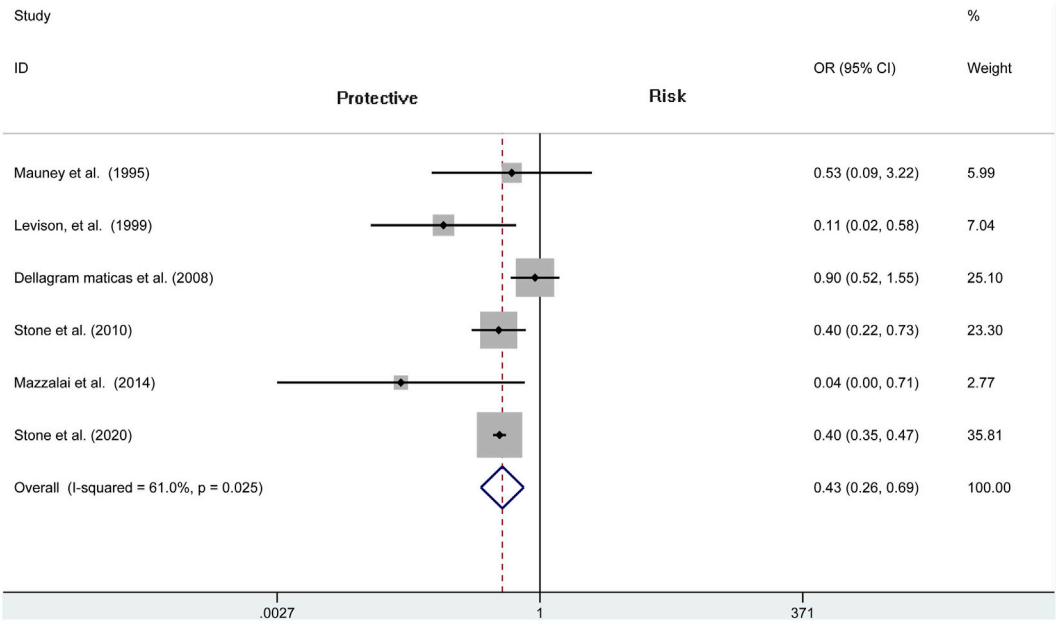

FIGURE 4 | Forest plot for meta-analysis of the incidence of hematoma requiring re-operation in the subgroup of CEA.

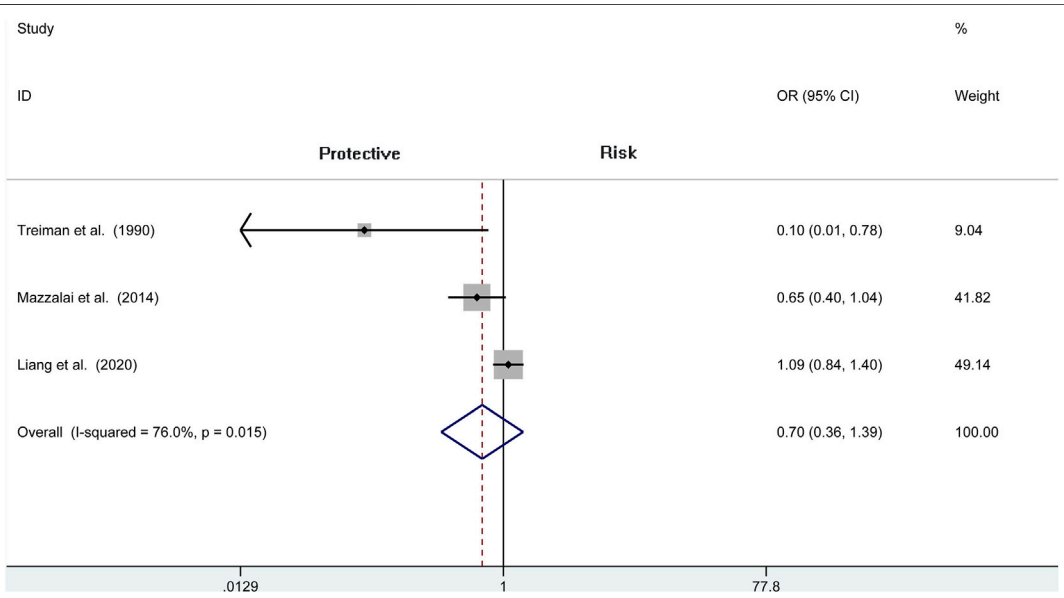

FIGURE 5 | Forest plot for meta-analysis of the incidence of wound hematoma with hypertension.

patients without protamine. Given a significant heterogeneity, we conducted a subgroup analysis, and the results showed that the heterogeneity was decreased (I^2 = 61%, p = 0.025) and that there is also a significant difference in the subgroup of CEA between the two groups (OR = 0.429, 95% CI = 0.265 to 0.694, p = 0.001; **Figure 4**). In addition, we perform a sensitivity analysis and found that the heterogeneity was significantly decreased by deleting the study conducted by Dellagrammaticas et al. (I^2 = 17.7%, p = 0.302).

Wound Hematoma With Hypertension

Three articles (N = 4,078) report the wound hematoma with hypertension. This analysis does not find a significant difference between the two groups (OR = 0.704, 95% CI = 0.358 to 1.388, p = 0.311; **Figure 5**), whereas a high heterogeneity is presented in these studies (I^2 = 76%, p = 0.015). Therefore, we also analyze the subgroup of CEA and reveal that there is no difference among the protamine and no-protamine groups (OR = 0.333, 95% CI = 0.057 to 1.959, p = 0.224; **Figure 6**). However, a high heterogeneity in

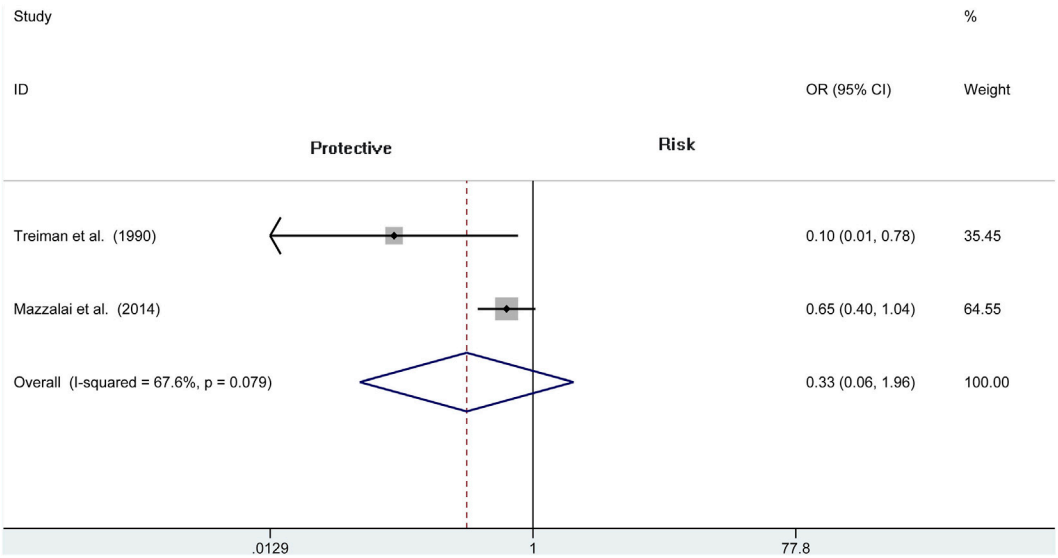

FIGURE 6 | Forest plot for meta-analysis of the incidence of wound hematoma with hypertension in the subgroup of CEA.

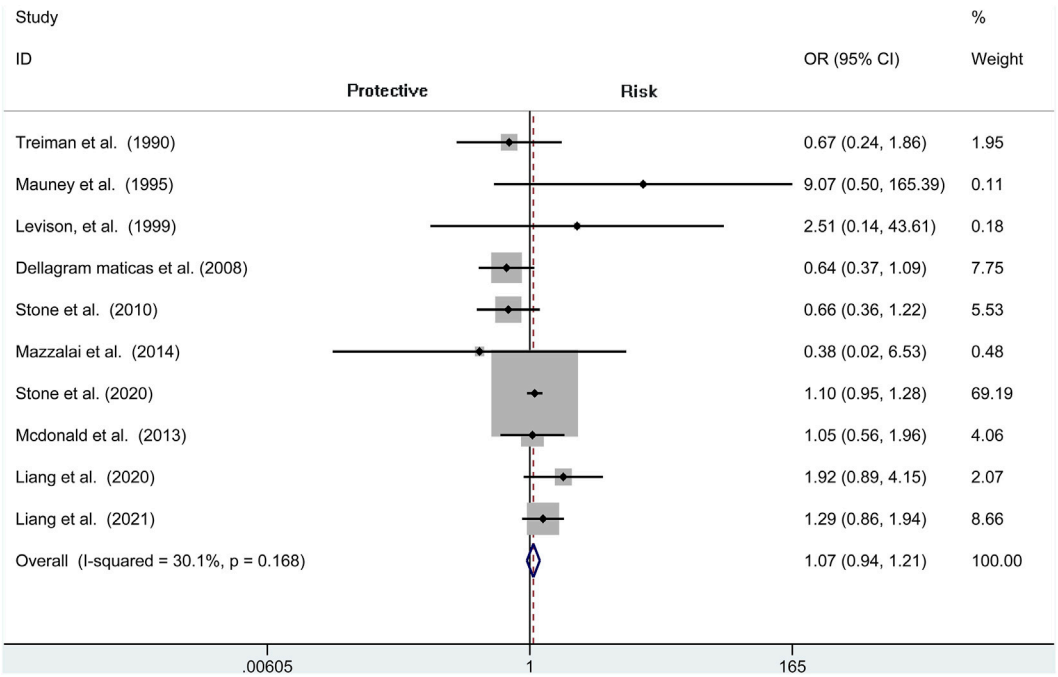

FIGURE 7 | Forest plot for meta-analysis of the incidence of stroke.

these studies was also observed ($I^2 = 67.6\%$, $p = 0.079$). Moreover, we performed a sensitivity analysis, but no significant difference was revealed in the changes of heterogeneity.

Stroke

A total of seven independent studies compare protamine with no protamine in participants undergoing CEA, while three studies include participants with carotid stenting. There is no significant heterogeneity among these studies ($I^2 = 30.1\%$, $p = 0.168$). We think that patients treated with protamine did not have a lower rate of stroke than those treated with no protamine (OR = 1.071, 95% CI = 0.944–1.214, $p = 0.286$, **Figure 7**). In the subgroup of CEA, there is also no significant difference between the two groups (OR = 1.029, 95% CI = 0.897 to 1.180, $p = 0.687$; **Figure 8**).

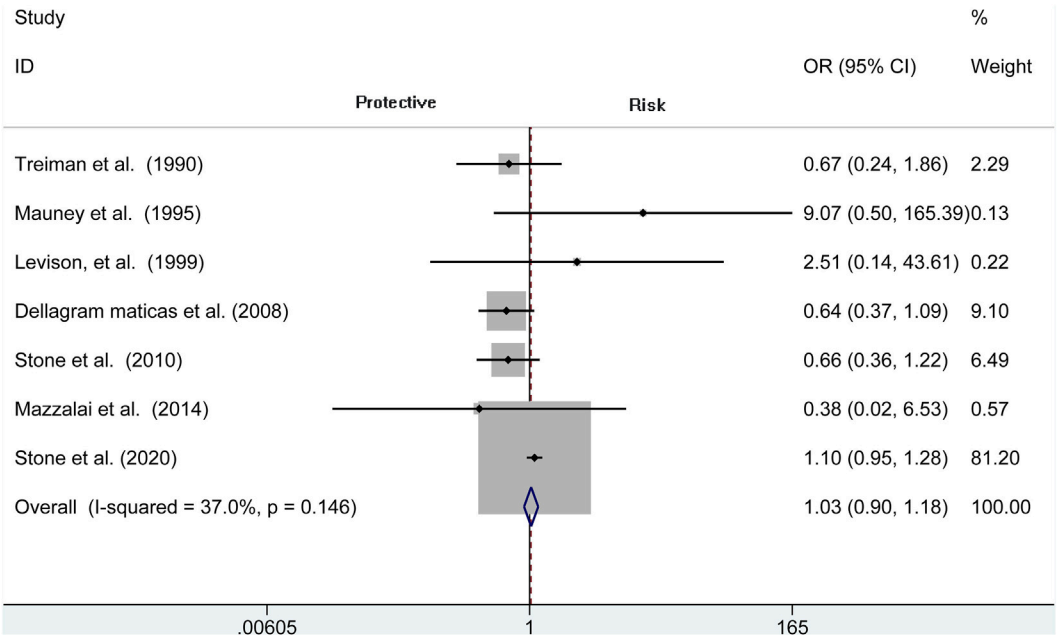

FIGURE 8 | Forest plot for meta-analysis of the incidence of stroke in the subgroup of CEA.

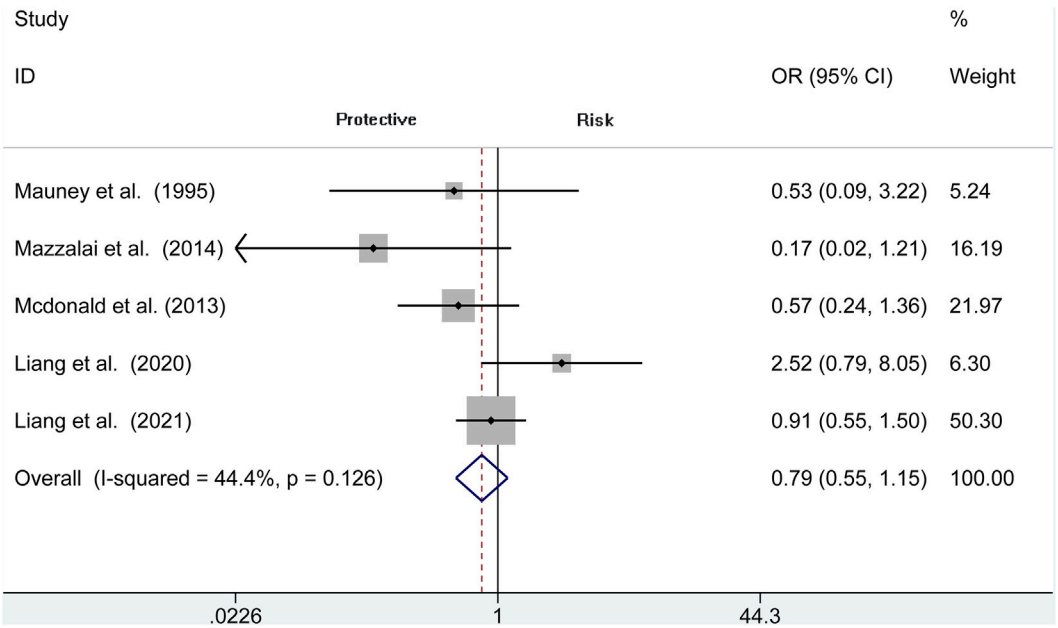

FIGURE 9 | Forest plot for meta-analysis of the incidence of transient ischemic attacks.

Transient Ischemic Attacks

The risk of TIA is reported in 5 observational studies (N = 9,441). Perioperative TIA occurred in the protamine (50 of 4,193, 1.2%) and no-protamine group (91 of 5,248, 1.7%). No evidence of significant heterogeneity is revealed in these studies (I^2 = 44.4%, p = 0.126). The overall analysis does not prove an apparent difference in TIA rates between protamine and no-protamine groups (OR = 0.793, 95% CI = 0.546 to 1.151, p = 0.222; **Figure 9**). However, a difference is presented in the subgroup of CEA among these two groups (OR = 0.255, 95% CI = 0.068 to 0.947, p = 0.041; **Supplementary Figure S1**).

Myocardial Infarction (MI)

The MI is reported in seven studies. In these publications, 60,030 and 33,072 patients are enrolled in the protamine and no-protamine groups, respectively. The results reveal that there is no significant difference in occurrence of MI (OR = 0.935, 95% CI = 0.797 to 1.096, p = 0.408, **Supplementary Figure S2**) and between-study heterogeneity is low (I^2 = 0.0%, p = 0.446). Similarly, we find that there is also no difference among protamine and no-protamine patients in the subgroup of CEA (OR = 0.902, 95% CI = 0.764 to 1.065, p = 0.224, **Supplementary Figure S3**).

Death

Seven publications report post-operative death enrolling 87,164 patients. No significant difference in mortality between the protamine and no-protamine group is seen (RD = 0.000, 95% CI = −0.001 to 0.001, p = 0.877, **Supplementary Figure S4**). The same result is found in the subgroup of CEA as well (RD = 0.000, 95% CI = −0.001 to 0.001, p = 0.878, **Supplementary Figure S5**).

DISCUSSION

Carotid artery stenosis is a major cause of stroke, which is the most common risk for long-term disability. Surgical treatment (carotid recanalization) is considered significantly meaningful for artery stenosis. Even though it reduces the risk of stroke, it carries a risk of hematoma (Rerkasem et al., 2020). Protamine, which was primarily isolated from salmon fish sperm, is a small, arginine-rich, positively charged protein with similarities to histones in that it has a role in stabilizing DNA in the sperm head (Bakchoul et al., 2016; Boer et al., 2018). It is adopted in a variety of vascular and cardiac procedures to reserve systemic heparin anticoagulation (Phair et al., 2020), especially for carotid recanalization (Lamanna et al., 2019). However, this inevitably leads to bleeding and then further cause major or minor strokes, myocardial infarction, or death (Yuan et al., 2018). Herein, we wonder whether protamine did affect the efficiency and safety of carotid recanalization and try to illustrate its safety and effectiveness in this surgery. Our results demonstrate that protamine can reduce the risk of bleeding without increasing the risk of having other complications.

Reoperation or reintervention is needed if bleeding happened during carotid recanalization, which is associated with the chance of perioperative stroke, MI, or even death. Miklosz et al. (2019) measured the platelet numbers, collagen-induced aggregation, etc. in blood extracted from mice and rats and then furthermore found that protamine has a short-term antiplatelet activity. In 2016, Kakisis et al. (2016) did a meta-analysis showing that the incidence of wound hematoma in the no-protamine group was 6%, whereas only 1.7% happened in the protamine group. They finally indicated that protamine significantly reduced the risk of wound hematoma by 64% without increasing the risk of post-operative stroke. Similarly, our analysis found that the incidence of wound hematoma in the protamine group is 3.8% (57 of 1,488), which is lower than that in the no-protamine group (9.5%, 305 of 3,218). Furthermore, a specific OR of 0.475 (95% CI = 0.282–0.798, p = 0.005) was obtained, suggesting that the rates of hematoma requiring re-operation was lower than that in patients without protamine. However, we thought the high rates of wound hematoma may be related to a higher risk of hypertension, but there is no difference presented in the two groups (OR = 0.704, 95% CI = 0.358–1.388, p = 0.311). We cannot distinguish whether this result is directly related to protamine use. As far as we know, protamine is a multi-cation strong alkaline polypeptide, which can combine with the glucosaminoglycan of heparin to form a stable complex and inhibit the activity of antithrombin, thus counteracting the anticoagulant effect of heparin and playing the effect of hemostasis. Protamine-induced circulatory changes have been demonstrated by Jastrzebski et al. (Cho et al., 2012), who explicated the role of it by endogenously liberating vasoactive substances.

Cerebral recanalization therapy, either intravenous thrombolysis or mechanical thrombectomy, improves the outcomes of patients with artery stenosis (Zhang et al., 2019), which exerts an increased impact on ischemic diseases. However, some complications involving ischemic injuries such as stroke, TIA, and MI sometimes inevitably followed. We included these three complications in our observations. One study had 365 patients who were subjected to 407 recanalization; 365 (89.6%) received protamine and 42 (10.4%) patients did not; 2.5% (10/407) happened post-operatively in the protamine group. This meta-analysis did not find an association between protamine and stroke (Levison et al., 1999). Likely, in our research, even though the stroke rates were slightly lower than without protamine, our results did not obtain statistical significance (OR = 1.071, 95% CI = 0.944 to 1.214, p = 0.286), the same result as TIA. Even though protamine did not affect the incidence of stroke and TIA by multivariate analysis, the risk of MI has also been studied extensively. In light of the 0.7% rate of MI in our study with protamine showing no significant difference (OR = 0.935, 95% CI = 0.797 to 1.096, p = 0.408). Furthermore, we should note that the protamine did not change the rate of death among these two groups (RD = 0.000, 95% CI = −0.001 to 0.001, p = 0.877). Meanwhile, other studies related to this topic did not find an association between protamine and stroke, TIA, MI, and death. We suspect that there may be a certain stimulation factor of protamine that causes a reduction in bleeding.

Our research has several limitations. The dosage of protamine was not standardized, which may confound the outcomes. Besides the primary inclusion and exclusion criteria, the characteristics of the participants were a little different from each other, potentially causing bias. The number of recent and high-quality studies was too small. Additionally, some heterogeneity was found among included trials due to the different study protocols, patient characteristics, and definitions of clinical endpoints. Moreover, the current study is not registered and there may be a slight deviation, but we strictly followed the procedures of systematic evaluation. Finally, the exact sequence of disease for the included patients cannot be known exactly and protamine might have been administered after a complication occurred rather than before, which might have affected our results.

CONCLUSION

This study has crucial implications. The current meta-analysis demonstrates that surgeons should consider routinely using protamine during carotid recanalization especially for CEA, due to the lower incidence of wound hematoma and hematoma requiring re-operation with its use. These findings, however, have inherent limitations, such as obvious heterogeneity and data from retrospective reviews; therefore, they cannot be regarded robust enough to provide a firm recommendation in clinical practice. With regard to the carotid artery stenting, there were fewer studies examining the effect of protamine; herein, further research is necessary to illustrate whether consistent results exist across all types of carotid revascularization.

BRIEF STATEMENT

Protamine, which was primarily isolated from salmon fish sperm, is a small, arginine-rich, positively charged protein with similarities to histones in that it has a role in stabilizing DNA in the sperm head. Despite it being adopted in a variety of vascular and cardiac procedures to reserve systemic heparin anticoagulation, especially for carotid recanalization, this inevitably leads to bleeding and then further causes major or minor strokes, myocardial infarction, or death. Herein, a comprehensive review and meta-analysis are necessary to illustrate the efficiency of protamine for carotid recanalization. This study demonstrated that protamine was effective in reducing hematoma without increasing the risk of having other complications.

DATA AVAILABILITY STATEMENT

The original contributions presented in the study are included in the article/**Supplementary Material**, further inquiries can be directed to the corresponding authors.

AUTHOR CONTRIBUTIONS

YP and WX designed and conceptualized the article. QJ and WW prepared the figures and tables. All authors significantly contributed to writing the paper and provided important intellectual content.

SUPPLEMENTARY MATERIAL

The Supplementary Material for this article can be found online at: https://www.frontiersin.org/articles/10.3389/fphar.2022.796329/full#supplementary-material

REFERENCES

Abbott, A. L., Paraskevas, K. I., Kakkos, S. K., Golledge, J., Eckstein, H. H., Diaz-Sandoval, L. J., et al. (2015). Systematic Review of Guidelines for the Management of Asymptomatic and Symptomatic Carotid Stenosis. *Stroke* 46 (11), 3288–3301. doi:10.1161/STROKEAHA.115.003390

Al-Kassou, B., Kandt, J., Lohde, L., Shamekhi, J., Sedaghat, A., Tabata, N., et al. (2020). Safety and Efficacy of Protamine Administration for Prevention of Bleeding Complications in Patients Undergoing TAVR. *JACC Cardiovasc. Interv.* 13 (12), 1471–1480. doi:10.1016/j.jcin.2020.03.041

Bakchoul, T., Jouni, R., and Warkentin, T. E. (2016). Protamine (Heparin)-induced Thrombocytopenia: a Review of the Serological and Clinical Features Associated with Anti-protamine/heparin Antibodies. *J. Thromb. Haemost.* 14 (9), 1685–1695. doi:10.1111/jth.13405

Boer, C., Meesters, M. I., Veerhoek, D., and Vonk, A. B. A. (2018). Anticoagulant and Side-Effects of Protamine in Cardiac Surgery: a Narrative Review. *Br. J. Anaesth.* 120 (5), 914–927. doi:10.1016/j.bja.2018.01.023

Cho, Y. D., Lee, J. Y., Seo, J. H., Kang, H. S., Kim, J. E., Kwon, O. K., et al. (2012). Early Recurrent Hemorrhage after Coil Embolization in Ruptured Intracranial Aneurysms. *Neuroradiology* 54 (7), 719–726. doi:10.1007/s00234-011-0950-3

Dellagrammaticas, D., Lewis, S. C., and Gough, M. J. (2008). Is Heparin Reversal with Protamine after Carotid Endarterectomy Dangerous? *Eur. J. Vasc. Endovasc Surg.* 36 (1), 41–44. doi:10.1016/j.ejvs.2008.01.021

Dharmakidari, S., Bhattacharya, P., and Chaturvedi, S. (2017). Carotid Artery Stenosis: Medical Therapy, Surgery, and Stenting. *Curr. Neurol. Neurosci. Rep.* 17 (10), 77. doi:10.1007/s11910-017-0786-2

Fearn, S. J., Parry, A. D., Picton, A. J., Mortimer, A. J., and McCollum, C. N. (1997). Should Heparin Be Reversed after Carotid Endarterectomy? A Randomised Prospective Trial. *Eur. J. Vasc. Endovasc Surg.* 13 (4), 394–397. doi:10.1016/s1078-5884(97)80082-2

Howell, S. J. (2007). Carotid Endarterectomy. *Br. J. Anaesth.* 99 (1), 119–131. doi:10.1093/bja/aem137

Jaques, L. B. (1973). Protamine--antagonist to Heparin. *Can. Med. Assoc. J.* 108 (10), 1291–1297.

Kakisis, J. D., Antonopoulos, C. N., Moulakakis, K. G., Schneider, F., Geroulakos, G., and Ricco, J. B. (2016). Protamine Reduces Bleeding Complications without Increasing the Risk of Stroke after Carotid Endarterectomy: A Meta-Analysis. *Eur. J. Vasc. Endovasc Surg.* 52 (3), 296–307. doi:10.1016/j.ejvs.2016.05.033

Lamanna, A., Maingard, J., Barras, C. D., Kok, H. K., Handelman, G., Chandra, R. V., et al. (2019). Carotid Artery Stenting: Current State of Evidence and Future Directions. *Acta Neurol. Scand.* 139 (4), 318–333. doi:10.1111/ane.13062

Levison, J. A., Faust, G. R., Halpern, V. J., Theodoris, A., Nathan, I., Kline, R. G., et al. (1999). Relationship of Protamine Dosing with Postoperative Complications of Carotid Endarterectomy. *Ann. Vasc. Surg.* 13 (1), 67–72. doi:10.1007/s100169900222

Li, Q., Gao, Y., Xin, W., Zhou, Z., Rong, H., Qin, Y., et al. (2019). Meta-Analysis of Prognosis of Different Treatments for Symptomatic Moyamoya Disease. *World Neurosurg.* 127, 354–361. doi:10.1016/j.wneu.2019.04.062

Liang, P., Motaganahalli, R., Swerdlow, N. J., Dansey, K., Varkevisser, R. R. B., Li, C., et al. (2021). Protamine Use in Transfemoral Carotid Artery Stenting Is Not Associated with an Increased Risk of Thromboembolic Events. *J. Vasc. Surg.* 73 (1), 142–e4. doi:10.1016/j.jvs.2020.04.526

Liang, P., Motaganahalli, R. L., Malas, M. B., Wang, G. J., Eldrup-Jorgensen, J., Cronenwett, J. L., et al. (2020). Protamine Use in Transcarotid Artery Revascularization Is Associated with Lower Risk of Bleeding Complications without Higher Risk of Thromboembolic Events. *J. Vasc. Surg.* 72 (6), 2079–2087. doi:10.1016/j.jvs.2020.02.019

Lynch, N. P., and Kavanagh, E. G. (2016). Does Routine Reversal of Heparin with Protamine Sulphate in Patients Undergoing Carotid Endarterectomy Reduce Bleeding Complications without Leading to Increased Thromboembolic Complications? *Eur. J. Vasc. Endovasc Surg.* 51 (1), 150. doi:10.1016/j.ejvs.2015.09.001

Mauney, M. C., Buchanan, S. A., Lawrence, W. A., Bishop, A., Sinclair, K., Daniel, T. M., et al. (1995). Stroke Rate Is Markedly Reduced after Carotid Endarterectomy by Avoidance of Protamine. *J. Vasc. Surg.* 22 (3), 264–270. ; discussion 269-70. doi:10.1016/s0741-5214(95)70140-0

Mazzalai, F., Piatto, G., Toniato, A., Lorenzetti, R., Baracchini, C., and Ballotta, E. (2014). Using Protamine Can Significantly Reduce the Incidence of Bleeding Complications after Carotid Endarterectomy without Increasing the Risk of

Ischemic Cerebral Events. *World J. Surg.* 38 (5), 1227–1232. doi:10.1007/s00268-013-2347-4

McDonald, J. S., Kallmes, D. F., Lanzino, G., and Cloft, H. J. (2013). Protamine Does Not Increase Risk of Stroke in Patients with Elective Carotid Stenting. *Stroke* 44 (7), 2028–2030. doi:10.1161/STROKEAHA.113.001188

Miklosz, J., Kalaska, B., Kaminski, K., Rusak, M., Szczubialka, K., Nowakowska, M., et al. (2019). The Inhibitory Effect of Protamine on Platelets Is Attenuated by Heparin without Inducing Thrombocytopenia in Rodents. *Mar. Drugs* 17 (9). doi:10.3390/md17090539

Mitchell-Jones, N., Gallos, I., Farren, J., Tobias, A., Bottomley, C., and Bourne, T. (2017). Psychological Morbidity Associated with Hyperemesis Gravidarum: a Systematic Review and Meta-Analysis. *BJOG* 124 (1), 20–30. doi:10.1111/1471-0528.14180

Newhall, K. A., Saunders, E. C., Larson, R. J., Stone, D. H., and Goodney, P. P. (2016). Use of Protamine for Anticoagulation during Carotid Endarterectomy: A Meta-Analysis. *JAMA Surg.* 151 (3), 247–255. doi:10.1001/jamasurg.2015.3592

Patel, R. B., Beaulieu, P., Homa, K., Goodney, P. P., Stanley, A. C., Cronenwett, J. L., et al. (2013). Shared Quality Data Are Associated with Increased Protamine Use and Reduced Bleeding Complications after Carotid Endarterectomy in the Vascular Study Group of New England. *J. Vasc. Surg.* 58 (6), 1518–e1. doi:10.1016/j.jvs.2013.06.064

Phair, J., Futchko, J., Trestman, E. B., Carnevale, M., Friedmann, P., Shukla, H., et al. (2020). Protamine Sulfate Use during Tibial Bypass Does Not Appear to Increase Thrombotic Events or Affect Short-Term Graft Patency. *Vascular* 28 (6), 708–714. doi:10.1177/1708538120924149

Rerkasem, A., Orrapin, S., Howard, D. P., and Rerkasem, K. (2020). Carotid Endarterectomy for Symptomatic Carotid Stenosis. *Cochrane Database Syst. Rev.* 9, CD001081. doi:10.1002/14651858.CD001081.pub4

Setacci, C., Sterpetti, A., and de Donato, G. (2018). Introduction: Carotid Endarterectomy versus Carotid Stenting-A Never-Ending story. *Semin. Vasc. Surg.* 31 (1), 1–3. doi:10.1053/j.semvascsurg.2018.03.001

Sokolowska, E., Kalaska, B., Miklosz, J., and Mogielnicki, A. (2016). The Toxicology of Heparin Reversal with Protamine: Past, Present and Future. *Expert Opin. Drug Metab. Toxicol.* 12 (8), 897–909. doi:10.1080/17425255.2016.1194395

Spence, J. D., Song, H., and Cheng, G. (2016). Appropriate Management of Asymptomatic Carotid Stenosis. *Stroke Vasc. Neurol.* 1 (2), 64–71. doi:10.1136/svn-2016-000016

Spiliopoulos, S., Vasiniotis Kamarinos, N., Reppas, L., Palialexis, K., and Brountzos, E. (2019). Carotid Artery Stenting: an Update. *Curr. Opin. Cardiol.* 34 (6), 616–620. doi:10.1097/HCO.0000000000000679

Stone, D. H., Giles, K. A., Kubilis, P., Suckow, B. D., Goodney, P. P., Huber, T. S., et al. (2020). Protamine Reduces Serious Bleeding Complications Associated with Carotid Endarterectomy in Asymptomatic Patients without Increasing the Risk of Stroke, Myocardial Infarction, or Death in a Large National AnalysisStroke, Myocardial Infarction, or Death in a Large National Analysis. *Eur. J. Vasc. Endovasc Surg.* 60 (6), 800–807. doi:10.1016/j.ejvs.2020.08.047

Stone, D. H., Nolan, B. W., Schanzer, A., Goodney, P. P., Cambria, R. A., Likosky, D. S., et al. (2010). Protamine Reduces Bleeding Complications Associated with Carotid Endarterectomy without Increasing the Risk of Stroke. *J. Vasc. Surg.* 51 (3), 559–e1. 564 e1. doi:10.1016/j.jvs.2009.10.078

Treiman, R. L., Cossman, D. V., Foran, R. F., Levin, P. M., Cohen, J. L., and Wagner, W. H. (1990). The Influence of Neutralizing Heparin after Carotid Endarterectomy on Postoperative Stroke and Wound Hematoma. *J. Vasc. Surg.* 12 (4), 440–446. doi:10.1016/0741-5214(90)90046-d

Yip, H. K., Sung, P. H., Wu, C. J., and Yu, C. M. (2016). Carotid Stenting and Endarterectomy. *Int. J. Cardiol.* 214, 166–174. doi:10.1016/j.ijcard.2016.03.172

Yuan, G., Zhou, S., Wu, W., Zhang, Y., Lei, J., and Huang, B. (2018). Carotid Artery Stenting versus Carotid Endarterectomy for Treatment of Asymptomatic Carotid Artery Stenosis. *Int. Heart J.* 59 (3), 550–558. doi:10.1536/ihj.17-312

Zhang, Z., Pu, Y., Mi, D., and Liu, L. (2019). Cerebral Hemodynamic Evaluation after Cerebral Recanalization Therapy for Acute Ischemic Stroke. *Front. Neurol.* 10, 719. doi:10.3389/fneur.2019.00719

Conflict of Interest: The authors declare that the research was conducted in the absence of any commercial or financial relationships that could be construed as a potential conflict of interest.

Publisher's Note: All claims expressed in this article are solely those of the authors and do not necessarily represent those of their affiliated organizations, or those of the publisher, the editors, and the reviewers. Any product that may be evaluated in this article, or claim that may be made by its manufacturer, is not guaranteed or endorsed by the publisher.

frontiers in Pharmacology

ORIGINAL RESEARCH
published: 18 March 2022
doi: 10.3389/fphar.2022.790048

Economic Evaluation of Ticagrelor Plus Aspirin Versus Aspirin Alone for Acute Ischemic Stroke and Transient Ischemic Attack

Jigang Chen[1,2†], Linjin Ji[3†], Xin Tong[1,2], Mingyang Han[4], Songfeng Zhao[4], Yongkai Qin[4], Zilong He[4], Zhiqun Jiang[3] and Aihua Liu[1,2,5*]*

[1]Department of Interventional Neuroradiology, Beijing Tiantan Hospital, Capital Medical University, Beijing, China, [2]Beijing Neurosurgical Institute, Capital Medical University, Beijing, China, [3]Department of Neurosurgery, The First Affiliated Hospital of Nanchang University, Nanchang, China, [4]Department of Neurosurgery, The Third Xiangya Hospital, Central South University, Changsha, China, [5]China National Clinical Research Centre for Neurological Diseases, Beijing, China

OPEN ACCESS

Edited by:
Yongjun Sun,
Hebei University of Science and Technology, China

Reviewed by:
Mohammadreza Amirsadri,
Isfahan University of Medical Sciences, Iran
Weiting Liao,
Sichuan University, China

***Correspondence:**
Aihua Liu
liuaihuadoctor@163.com
Zhiqun Jiang
jzq315@gmail.com

[†]*These authors have contributed equally to this work*

Specialty section:
This article was submitted to Neuropharmacology, a section of the journal Frontiers in Pharmacology

Received: *06 October 2021*
Accepted: *31 January 2022*
Published: *18 March 2022*

Citation:
Chen J, Ji L, Tong X, Han M, Zhao S, Qin Y, He Z, Jiang Z and Liu A (2022) Economic Evaluation of Ticagrelor Plus Aspirin Versus Aspirin Alone for Acute Ischemic Stroke and Transient Ischemic Attack. Front. Pharmacol. 13:790048. doi: 10.3389/fphar.2022.790048

Background: Although ticagrelor plus aspirin is more effective than aspirin alone in preventing the 30-day risk of a composite of stroke or death in patients with an acute mild-to-moderate ischemic stroke (IS) or transient ischemic attack (TIA), the cost-effectiveness of this combination therapy remains unknown. This study aims to determine the cost-effectiveness of ticagrelor plus aspirin compared with aspirin alone.

Methods: A combination of decision tree and Markov model was built to estimate the expected costs and quality-adjusted life-years (QALYs) associated with ticagrelor plus aspirin and aspirin alone in the treatment of patients with an acute mild-to-moderate IS or TIA. Model inputs were extracted from published sources. One-way sensitivity, probabilistic sensitivity, and subgroup analyses were performed to test the robustness of the findings.

Results: Compared with aspirin alone, ticagrelor plus aspirin gained an additional lifetime QALY of 0.018 at an additional cost of the Chinese Yuan Renminbi (¥) of 269, yielding an incremental cost-effectiveness ratio of ¥15,006 (US$2,207)/QALY. Probabilistic sensitivity analysis showed that ticagrelor plus aspirin had a probability of 99.99% being highly cost-effective versus aspirin alone at the current willingness-to-pay threshold of ¥72,447 (US$10,500)/QALY in China. These findings remain robust under one-way sensitivity and subgroup analyses.

Conclusions: The results indicated that early treatment with a 30-days ticagrelor plus aspirin for an acute mild-to-moderate IS or TIA is highly cost-effective in a Chinese setting.

Keywords: ticagrelor, aspirin, stroke, transient ischemic attack, cost-effectiveness analysis

INTRODUCTION

The risk of another ischemic stroke (IS) occurring after an acute mild-to-moderate IS or transient ischemic attack (TIA) is very high, and nearly 5%–10% of patients would have a stroke in the first few months (Johnston et al., 2000; Giles and Rothwell, 2007). Aspirin has been used for secondary stroke prevention among these patients with only modest benefits (Chen, 1997; International Stroke Trial

Collaborative Group, 1997). Two trials show that adding clopidogrel to aspirin is superior to aspirin alone in reducing the risk of stroke and other major ischemic events (Wang et al., 2013; Johnston et al., 2018). Yet, the efficacy of clopidogrel varies among individuals with different metabolic activations due to the reduced function of cytochrome *CYP2C19*, and a considerable number of strokes still occur even with clopidogrel or dual antiplatelet therapy (Pan et al., 2017).

Ticagrelor is a platelet aggregation inhibitor that reversibly binds and inhibits the $P2Y_{12}$ receptor. It has the advantage of being unaffected by *CYP2C19* polymorphisms. The Acute Stroke or Transient Ischemic Attack Treated with Ticagrelor and ASA (acetylsalicylic acid) for Prevention of Stroke and Death (THALES) trial showed that early treatment with ticagrelor plus aspirin for the first 30 days was superior to aspirin alone in reducing the 30-day risk of a composite of stroke or death [5.5% vs. 6.5%; hazard ratio (HR), 0.83; 95% confidence interval (CI), 0.71–0.96] (Johnston et al., 2020). Adding ticagrelor to aspirin also reduced the total burden of disability (odds ratio, 0.77; 95% CI, 0.65–0.91) owing to IS recurrence (Amarenco et al., 2021). However, the incidence of severe bleeding was significantly higher in the ticagrelor–aspirin group (0.5% vs. 0.1%; HR, 3.99; 95% CI, 1.74–9.14) (Johnston et al., 2020).

Although the combination of ticagrelor and aspirin could reduce the risk of a composite of stroke or death, it is associated with higher adverse events and higher costs when compared with aspirin alone. Therefore, medical decision analysis is needed to evaluate the advantage or disadvantage of ticagrelor plus aspirin over aspirin alone. Currently, the best method of doing this is cost-effectiveness analysis, which aims to assess the overall costs of different drugs and treatment procedures as well as the overall effectiveness related to different outcomes. In this study, we aim to determine the cost-effectiveness of adding ticagrelor to aspirin in patients with an acute mild-to-moderate IS or TIA.

METHODS

Model Overview

This study was conducted according to the Consolidated Health Economic Evaluation Reporting Standards (CHEERS) reporting guidelines (Husereau et al., 2013). A combination of decision tree and Markov model was developed using TreeAge Pro 2020 software (Tree Age Software, Inc., One Bank Street, Williamstown, MA, United States of America) to estimate the long-term costs and outcomes of two antiplatelet therapies: 1) ticagrelor plus aspirin therapy: a loading dose of 180 mg ticagrelor (given as two 90-mg tablets) followed by a maintenance dose of 90 mg ticagrelor twice daily on day 2 to day 30 plus a loading dose of 300 mg aspirin on day 1 followed by a maintenance dose of 75–100 mg aspirin daily on day 2 to day 30; 2) aspirin-alone therapy: a loading dose of 300 mg aspirin on day 1 followed by a maintenance dose of 75–100 mg aspirin daily on day 2 to day 30. The target population was analogous to that of the THALES trial (Johnston et al., 2020). Patients were 65 years old on average. They had either an acute mild-to-moderate IS or TIA and were not undergoing intravenous or endovascular thrombolysis. Patients in the two treatment arms entered the Markov model at the health state of modified Rankin scale (mRS) score of 0 and transited to other health states including mRS 1, 2, 3, 4, 5, and 6 (death) in the next cycle. The occurrence of adverse events such as IS, intracranial hemorrhage (ICH), and major extracranial hemorrhage (ECH), as defined according to the Global Utilization of Streptokinase and Tissue Plasminogen Activator for Occluded Coronary Arteries trial (Gusto Investigators, 1993), was incorporated into the model with additional costs and disutility. The cycle length was 1 month, and the time horizon was 30 years. The schematic structure of the model is provided in **Figure 1**.

Input Parameters

Input parameters of this model were obtained from the THALES trial (Johnston et al., 2020; Amarenco et al., 2021) and the most recently published literature if possible (**Table 1**). In the aspirin-alone group, the probability of a primary outcome (the composite of stroke or death) in the first 30 days was 0.066. In the ticagrelor-plus-aspirin group, the probability of primary outcome was estimated based on the HR (0.83) between these two groups. The proportion of death, IS, and ICH among patients with primary outcome and the probability of major ECH were extracted according to their respective event data reported by the THALES trial (Johnston et al., 2020).

All the patients were assumed to enter the model in the state of mRS 0, and they would be distributed to different states from mRS 0 to mRS 6 at the end of the first month after receiving ticagrelor plus aspirin or aspirin alone. The proportion of patients in different health states at the end of the first month was obtained from the THALES trial and has been provided in **Table 1** (Amarenco et al., 2021).

After the initial month, the proportion of patients distributed to different health states was decided by the recurrent rate of stroke and the age-specific non-stroke death rates. The recurrent rate of stroke after the first 30 days was estimated from the China National Stroke Registry (CNSR) (Xu et al., 2007), and we assumed that the risk of stroke recurrence would increase by 1.03-fold per life-year (Pennlert et al., 2014). The death rate after recurrent stroke was reported to be 0.1933 (Xu et al., 2007), and patients who remained alive were assumed to be reallocated equally among health states of equal and greater disability (Pan et al., 2014; Peultier et al., 2020).

We obtained the age-specific non-stroke death rates from the most recent published census of China and adjusted the rates according to the causes of death in 2018 reported in the China Health Statistics Yearbook 2019 (National Bureau of Statistics of China, 2021a; National Health Commission of the People's Republic of China, 2019). Dependent patients (mRS 3, 4, or 5) were reported to have increased mortality compared with independent patients (mRS 0, 1, or 2) (Slot et al., 2009), and we obtained mRS state-specific hazard ratios from previous reports (Samsa et al., 1999; Peultier et al., 2020). Patients who

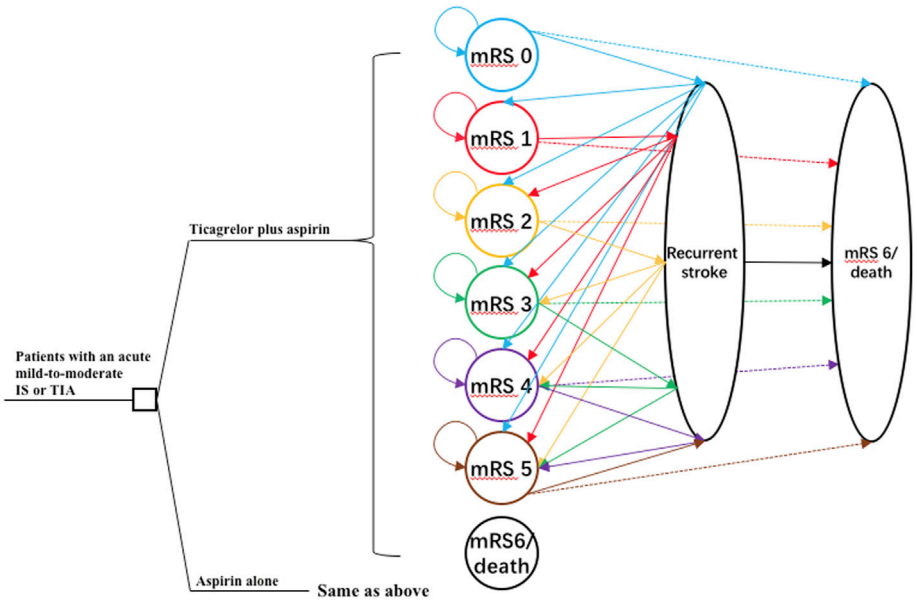

FIGURE 1 | The schematic structure of the model. A patient with an acute mild-to-moderate IS or TIA entered the model at 65 years old receiving either ticagrelor plus aspirin or aspirin alone for the first 30 days. Patients would distribute among different health statuses determined by mRS scores at 30 days and transit to a state of equal or greater disability after recurrent stroke or die after 30 days. IS, ischemic stroke; mRS, modified Rankin Scale; TIA, transient ischemic attack.

were alive and did not experience a recurrent stroke would remain in the same health state at the end of one cycle.

Costs

This study was conducted from the perspective of Chinese healthcare payers, and only direct medical costs were included. The additional cost of ticagrelor was estimated according to the median retail price of ticagrelor from the widely used Chinese Drug Price database (Tuling, www.315jiage.cn). This database provides information about reference prices in different regions of China for the same drug. We validated the price of ticagrelor from this database with other famous Chinese online pharmacies as well as our institutional clinical database, and the prices were very close. One-time hospitalization costs for major events and posthospitalization costs were obtained from the most recent published studies conducted in China. To account for the uncertainty, a wide range of ±25% was used for all costs. Costs were converted to 2020 Chinese Yuan Renminbi (¥) according to the consumer price index (National Bureau of Statistics of China, 2020).

Utility

Health-related quality of life value (utility scores) was assigned to all health states. Quality-adjusted life-years (QALYs) were calculated by multiplying the length period the patient spent in a particular state by the corresponding utility score. Utility scores for mRS 0, mRS 1, mRS 2, mRS 3, mRS 4, and mRS 5 were defined as 0.85 (0.8–1), 0.8 (0.8–0.95), 0.7 (0.68–0.9), 0.51 (0.45–0.65), 0.30 (0.1–0.4), and 0.15 (0–0.32), respectively (Gage et al., 1998; Earnshaw et al., 2009; Nelson et al., 2016; Peultier et al., 2020). Patients with recurrent stroke or major ECH were assumed to have a disutility of 0.66 and 0.2, respectively (Pan et al., 2014). All costs and utilities were discounted by 3% per year (Weinstein et al., 1996).

Statistical Analysis

The primary measure in this study was the incremental cost-effectiveness ratio (ICER), which was defined as the incremental cost per additional QALY gained. One strategy was considered cost-effective when compared to another if the ICER was below the willingness-to-pay (WTP) threshold. As recommended by the World Health Organization, the WTP threshold was chosen as 1 × gross domestic product (GDP) per capita if one strategy was to be highly cost-effective. This WTP threshold corresponded to ¥72,447 (US dollars $10,500)/QALY in China in the year 2020 (National Bureau of Statistics of China, 2021b).

The base-case analysis was conducted using the mean value of all parameters. To identify key parameters related to the robustness of the results, one-way sensitivity analyses were performed by varying one parameter while keeping others fixed. To perform a probabilistic sensitivity analysis, all parameters were assigned with a distribution accordingly. These parameters varied simultaneously in the probabilistic sensitivity analysis with Monte Carlo simulation (10,000 iterations) to evaluate the impact of uncertainty. Moreover, subgroup analyses were performed in the prespecified subgroups as defined in the THALES trial by varying the HRs of primary outcomes between two antiplatelet therapy groups. The mean and range for these HRs were obtained from the subgroups reported in this trial (Johnston et al., 2020).

TABLE 1 | List of input parameters.

Parameters	Base case value	Range	Distribution	Source
30-day outcome of aspirin alone				
Probability of primary outcome	0.066	0.060–0.073	Beta, SD: 0.003	Johnston et al. (2020)
Proportion of death	0.075	0.052–0.106	Beta, SD: 0.014	Johnston et al. (2020)
Proportion of IS	0.953	0.926–0.970	Beta, SD: 0.011	Johnston et al. (2020)
Proportion of ICH	0.017	0.008–0.036	Beta, SD: 0.007	Johnston et al. (2020)
Probability of major ECH	0.001	0.000–0.003	Beta, SD: 0.001	Johnston et al. (2020)
Proportion of mRS 0	0.365	—	—	Amarenco et al. (2021)
Proportion of mRS 1	0.395	—	—	Amarenco et al. (2021)
Proportion of mRS 2	0.140	—	—	Amarenco et al. (2021)
Proportion of mRS 3	0.056	—	—	Amarenco et al. (2021)
Proportion of mRS 4	0.034	—	—	Amarenco et al. (2021)
Proportion of mRS 5	0.004	—	—	Amarenco et al. (2021)
30-day outcome of ticagrelor added to aspirin				
HR of primary outcome	0.830	0.710–0.960	Beta: SD: 0.060	Johnston et al. (2020)
Proportion of death	0.119	0.087–0.160	Beta, SD: 0.018	Johnston et al. (2020)
Proportion of IS	0.911	0.874–0.938	Beta, SD: 0.016	Johnston et al. (2020)
Proportion of ICH	0.066	0.043–0.100	Beta, SD: 0.014	Johnston et al. (2020)
Probability of major ECH	0.005	0.004–0.007	Beta, SD: 0.001	Johnston et al. (2020)
Proportion of mRS 0	0.372	—	—	Amarenco et al. (2021)
Proportion of mRS 1	0.390	—	—	Amarenco et al. (2021)
Proportion of mRS 2	0.139	—	—	Amarenco et al. (2021)
Proportion of mRS 3	0.057	—	—	Amarenco et al. (2021)
Proportion of mRS 4	0.031	—	—	Amarenco et al. (2021)
Proportion of mRS 5	0.004	—	—	Amarenco et al. (2021)
Probabilities				
Recurrent rate of stroke per life-year	0.122	0.116–0.128	Beta, SD: 0.003	Xu et al. (2007)
Proportion of ICH	0.075	0.075–0.146	Beta, SD: 0.018	Johnston et al. (2020)
RR of stroke recurrence per life-year	1.030	1.020–1.040	Lognormal, SD: 0.005	Pennlert et al. (2014)
Death after recurrent stroke	0.193	0.174–0.213	Beta, SD: 0.010	Xu et al. (2007)
Mortality hazard ratios				
mRS 0	1.000	—	Lognormal, SD: 0.050	Samsa et al. (1999)
mRS 1	1.000	—	Lognormal, SD: 0.050	Samsa et al. (1999)
mRS 2	1.110	—	Lognormal, SD: 0.083	Samsa et al. (1999)
mRS 3	1.270	—	Lognormal, SD: 0.127	Samsa et al. (1999)
mRS 4	1.710	—	Lognormal, SD: 0.171	Samsa et al. (1999)
mRS 5	2.370	—	Lognormal, SD: 0.237	Samsa et al. (1999)
Cost (2020 Chinese Yuan Renminbi, ¥)				
Additional cost of ticagrelor	394	174–593	Gamma, SD: 105	Tuling
Hospitalization cost for IS, independent	10,958	13,698–8,219	Gamma, SD: 1370	Wang et al. (2018), Pan et al. (2020)
Hospitalization cost for IS, dependent	13,605	10,204–17,006	Gamma, SD: 1701	Wang et al. (2018), Pan et al. (2020)
Hospitalization cost for IS, death	11,970	8,978–14,963	Gamma, SD: 1496	Wang et al. (2018), Pan et al. (2020)
Hospitalization cost for ICH, independent	13,174	9,881–16,468	Gamma, SD: 1647	Pan et al. (2014)
Hospitalization cost for ICH, dependent or death	17,490	13,118–21,863	Gamma, SD: 2186	Pan et al. (2014)
Hospitalization cost for major ECH	8,535	6,401–10,669	Gamma, SD: 1067	Pan et al. (2014)
Annual posthospitalization cost for independent	8,310	6,233–10,388	Gamma, SD: 1039	Pan et al. (2018)
Annual posthospitalization cost for dependent	12,771	9,578–15,964	Gamma, SD: 1596	Pan et al. (2018)
Utility				
mRS 0	0.850	0.800–1.000	Beta, SD: 0.050	Gage et al. (1998), Earnshaw et al. (2009), Nelson et al. (2016), Peultier et al. (2020)
mRS 1	0.800	0.800–0.950	Beta, SD: 0.038	Gage et al. (1998), Earnshaw et al. (2009), Nelson et al. (2016), Peultier et al. (2020)
mRS 2	0.700	0.680–0.900	Beta, SD: 0.055	Gage et al. (1998), Earnshaw et al. (2009), Nelson et al. (2016), Peultier et al. (2020)
mRS 3	0.510	0.450–0.650	Beta, SD: 0.050	Gage et al. (1998), Earnshaw et al. (2009), Nelson et al. (2016), Peultier et al. (2020)
mRS 4	0.300	0.100–0.400	Beta, SD: 0.075	Gage et al. (1998), Earnshaw et al. (2009), Nelson et al. (2016), Peultier et al. (2020)
mRS 5	0.150	0.000–0.320	Beta, SD: 0.080	Gage et al. (1998), Earnshaw et al. (2009), Nelson et al. (2016), Peultier et al. (2020)
mRS 6 or death	0.000			
Disutility of recurrent stroke	0.660	0.640–0.680	Beta, SD: 0.010	Ganesalingam et al. (2015)
Disutility of major ECH	0.200	0.160–0.230	Beta, SD: 0.018	Pan et al. (2014)

ECH, extracranial hemorrhage; HR, hazard ratio; ICH, intracranial hemorrhage; IS, ischemic stroke; mRS, modified Rankin scale; RR, relative risk; SD, standard deviation

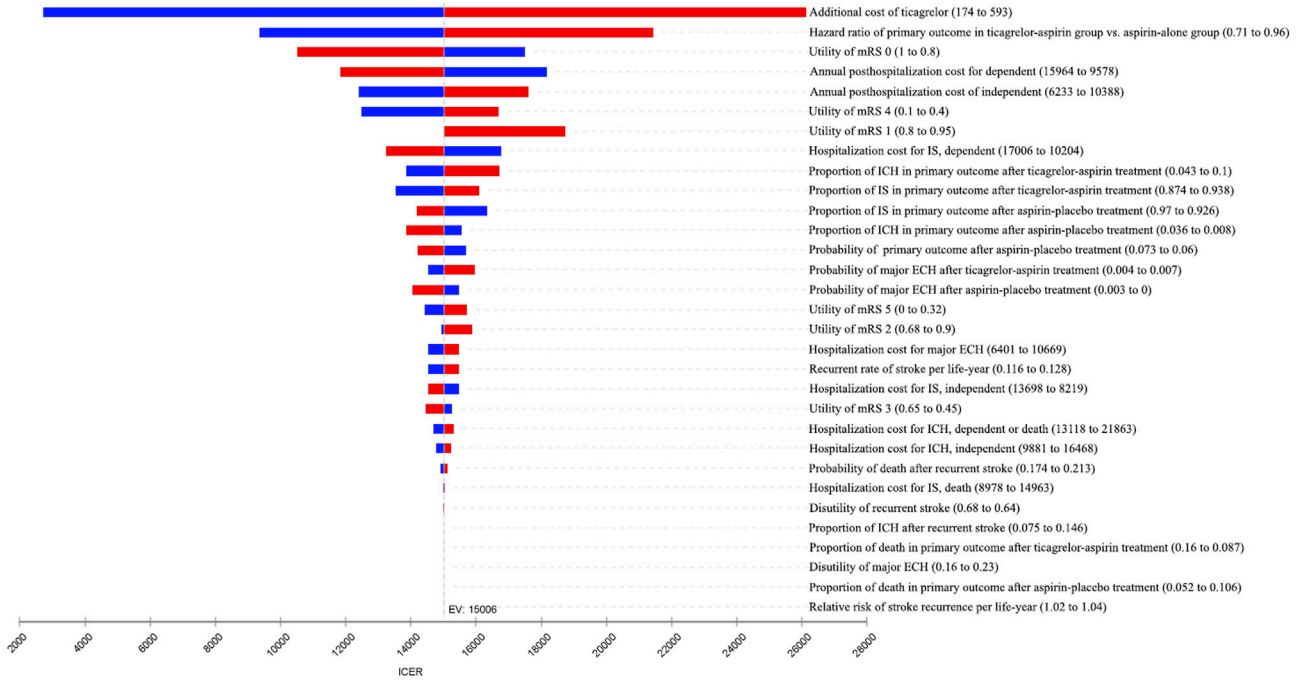

FIGURE 2 | Tornado diagram of one-way sensitivity analyses. The plot shows how varying one input parameter to its limits at a time affects the incremental cost-effectiveness ratio (ICER). ECH, extracranial hemorrhage; EV, expected value; ICH, intracranial hemorrhage; IS, ischemic stroke; mRS, modified Rankin Scale.

RESULTS

Base-Case Analysis

In the base-case scenario, patients treated with aspirin alone lived an average of 6.764 QALYs, incurring a cost of ¥147,122. Those treated with ticagrelor plus aspirin lived an average of 6.782 QALYs (that is, an additional 0.018 QALY), with a lifetime cost of ¥147,391 or an additional cost of ¥269. The ICER for ticagrelor-plus-aspirin therapy relative to aspirin-alone therapy was ¥15,006 ($2,207)/QALY. Under the current threshold of ¥72,447/QALY, ticagrelor-plus-aspirin therapy was highly cost-effective in the base-case scenario.

Sensitivity Analyses

One-way sensitivity analyses were conducted to account for the impact of the uncertainty of different parameters on the ICER, and the results were presented in the tornado diagram (**Figure 2**). Overall, the results were most sensitive to the additional cost of ticagrelor as well as HR of primary outcome between two antiplatelet therapy groups. When the additional cost of ticagrelor ranged between ¥174 and ¥593, the corresponding ICER was between ¥2,712/QALY and ¥26,127/QALY. When the HR ranged between 0.71 and 0.96, the corresponding ICER was between ¥9,354/QALY and ¥21,440/QALY. All the ICERs, including those obtained by other varying parameters, were below the WTP threshold, indicating that the study results were robust.

The result of probabilistic sensitivity analysis is shown in **Figure 3**. Among the 10,000 simulation runs, ticagrelor-plus-aspirin therapy was superior in 99.99% of the simulations at a WTP threshold of ¥72,447/QALY.

Subgroup Analyses

By varying the HRs for primary outcome between two antiplatelet therapy groups in the THALES trial subpopulations, subgroup analyses were conducted among the following subgroups including age, sex, race, weight, body mass index, geographic region, diagnosis of index event, time from index event to randomization, time from index event to loading dose, diabetes mellitus, hypertension, previous ischemic stroke or TIA, previous aspirin therapy, previous statin therapy, and smoking status. All the ICERs were below the WTP threshold, indicating that ticagrelor plus aspirin was cost-effective compared with aspirin alone in these subgroups (**Figure 4**).

DISCUSSION

For patients with an acute mild-to-moderate IS or TIA, adding ticagrelor to aspirin for 1 month increased life expectancy by 0.018 QALY over a lifetime, near 1 week of perfect health, at excellent value. This dual antiplatelet therapy gained an additional cost of ¥269, resulting in an ICER of ¥15,006/QALY. The robustness of our overall conclusion that ticagrelor-plus-aspirin therapy was cost-effective compared to aspirin-alone therapy was supported by the sensitivity and subgroup analyses. In the one-way sensitivity analyses, all the ICERs were below the WTP threshold when the input variables

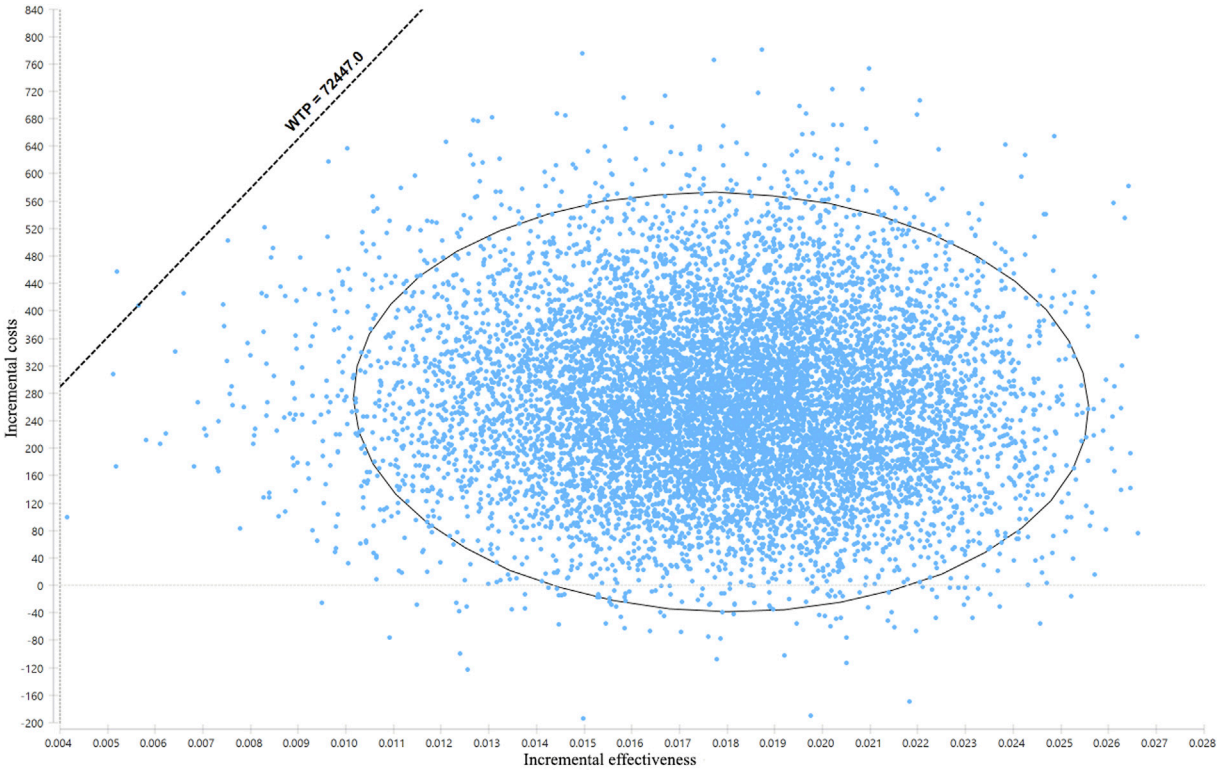

FIGURE 3 | Results of the probabilistic sensitivity analysis. The dots that lie to the right of the willingness-to-pay (WTP) line mean the cases where ticagrelor plus aspirin is cost-effective when compared with aspirin alone.

varied in their plausible ranges one by one. In the probabilistic sensitivity analysis, ticagrelor-plus-aspirin therapy was superior in 99.99% of simulations. Moreover, with the variations of HRs for the primary outcome, this dual antiplatelet therapy was favored in all the THALES trial subpopulations.

Our results were comparable to other similar studies. For example, the lifetime additional gain of QALY by ticagrelor-plus-aspirin therapy is 0.018 in the current study, while the lifetime QALY gain is 0.17 for clopidogrel when compared with aspirin for secondary prevention among stroke patients (Schleinitz et al., 2004) and 0.037 for clopidogrel plus aspirin when compared with aspirin alone (Pan et al., 2014). The gain of QALY associated with ticagrelor plus aspirin in our study is relatively smaller than other treatments. This is mainly because the 30-day incidence of disability did not differ significantly between the two groups in the THALES trial. Moreover, the incidence of adverse events such as major ECH was significantly higher when ticagrelor was added to aspirin, thus leading to a higher disutility of patients treated with this therapy. Notwithstanding, the comparable results between the current and other studies demonstrated the validity of our model.

To our knowledge, this study provides the first economic data on ticagrelor added to aspirin for the prevention of recurrent stroke. The advantage of this study is that we have utilized data from the THALES trial, which is a large-scale randomized trial that compares ticagrelor plus aspirin with aspirin alone directly. We conducted this study from the perspective of Chinese healthcare payers. There are over two million new cases of stroke in China every year, and it is related to the highest disability-adjusted life-years lost of any disease (Wu et al., 2019). Moreover, the stroke burden is expected to increase as a result of population aging and inadequate management. China has the largest population around the world, and there are fast-increasing demands for limited healthcare budgets. This drives policymakers to move towards a data-driven and evidence-supporting healthcare system with China's national health strategy. Our cost-effectiveness study has the merits of providing an evidence-based reference regarding the secondary prevention practices for recurrent stroke.

A large body of studies has been published to assess the cost-effectiveness of acute stroke treatment and prevention in the last 2 decades. For acute ischemic stroke, intravenous alteplase is the recommended treatment, and investigators have evaluated its cost-effectiveness within different time windows after the stroke onset from the perspective of different countries including the United States, United Kingdom, China, and so on (Joo et al., 2017). These studies showed that intravenous alteplase was a dominant strategy compared with traditional treatment. Likewise, economic evaluation of mechanical thrombectomy, a recommended treatment for acute IS with a large vessel occlusion, has been increasingly conducted in recent years. According to a recent review, 25 studies from 12 different countries were

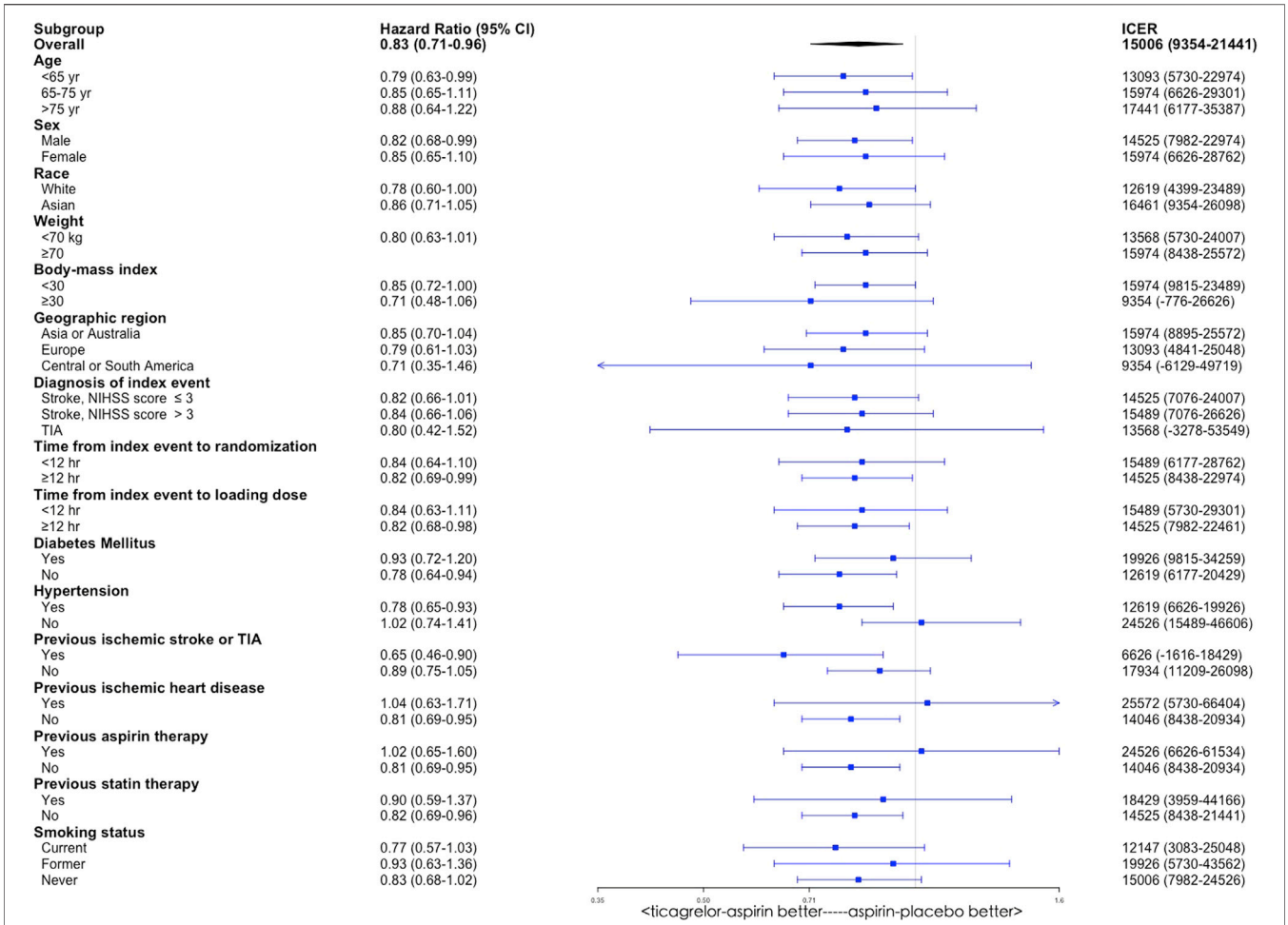

FIGURE 4 | Subgroup analyses of incremental cost-effectiveness ratio (ICER) by varying the hazard ratio of primary outcome between the ticagrelor-plus-aspirin group and the aspirin-alone group. CI, confidence interval.

published, and all these studies but one suggested that mechanical thrombectomy for stroke treatment was cost-effective (Waqas et al., 2021). The cost-effective evaluations regarding the long-term secondary prevention of IS with different drugs were published. These studies showed that clopidogrel, statin, warfarin, and dabigatran are regarded as the most cost-effective treatment for secondary stroke prevention. However, there is a lack of long-term outcome and resource use data, which adds great uncertainty to the cost-effectiveness (Pan et al., 2012).

Some limitations of our study should be noted. First, different treatment methods for IS were not incorporated into our model, while the mRS distribution of IS patients was significantly associated with treatment methods. However, we used the 30-day mRS scores as the post-treatment outcomes in our model as they were expected to be highly correlated with the post-treatment 90-day mRS scores (Rost et al., 2016). Moreover, the cost of IS treatment in the aspirin-alone group would be higher than the aspirin-plus-ticagrelor group, making aspirin alone less favorable. Second, our results were based on the efficacy findings of the THALES trial that was performed internationally, and the participants were mainly from Europe. It is unknown whether the combination therapy would show similar effects if the participants were restricted to Chinese patients. What is more, the utility scores were not Chinese population-specific. However, we have considered the difference in the sensitivity analyses, and the conclusion remains unchanged. Third, the one-time hospitalization costs and annual posthospitalization costs were different only between patients in independent and dependent status. Costs associated with different mRS scores were not obtained because no literature was available for these costs in China. Fourth, we assumed that patients who remained alive would be reallocated equally among health states of equal and greater disability. Dependent and independent patients were assumed to have the same probability of recurrent stroke. These assumptions might not reflect a real-world situation. However, they are not unprecedented in other cost-effectiveness studies (Pan et al., 2014; Peultier et al., 2020). Fifth, only direct costs were included in this analysis. If indirect and intangible costs such as loss of productivity were taken into consideration, it might produce a different result. Last, our model was built from the Chinese perspective and only reflected cost and event rates in

China. Results might not accurately reflect the cost-effectiveness of ticagrelor added to aspirin in other countries.

CONCLUSION

Early treatment with a 30-day ticagrelor plus aspirin for an acute mild-to-moderate IS or TIA is highly cost-effective in a Chinese setting. However, more studies are needed to evaluate the benefit and risks of this therapy.

DATA AVAILABILITY STATEMENT

The original contributions presented in the study are included in the article/supplementary material; further inquiries can be directed to the corresponding authors.

AUTHOR CONTRIBUTIONS

JC and LJ were responsible for the study design. ZJ and AL built the model and conducted the statistical analysis. JC and LJ prepared the manuscript. XT, MH, SZ, YQ, and ZH collected the data. All the authors reviewed the model structure, data source, formula, and results. All authors contributed to the article and approved the submitted version.

FUNDING

This work was supported by Beijing Health Science and Technology Achievements and Appropriate Technology Promotion Project (NO. BHTPP202011).

REFERENCES

Amarenco, P., Denison, H., Evans, S. R., Himmelmann, A., James, S., Knutsson, M., et al. (2021). Ticagrelor Added to Aspirin in Acute Ischemic Stroke or Transient Ischemic Attack in Prevention of Disabling Stroke: a Randomized Clinical Trial. *JAMA Neurol.* 78 (2), 177–185. doi:10.1001/jamaneurol.2020.4396

Chen, Z.-M. (1997). CAST: Randomised Placebo-Controlled Trial of Early Aspirin Use in 20,000 Patients with Acute Ischaemic Stroke. CAST (Chinese Acute Stroke Trial) Collaborative Group. *Lancet* 349 (9066), 1641–1649. doi:10.1016/s0140-6736(97)04010-5

Earnshaw, S. R., Jackson, D., Farkouh, R., and Schwamm, L. (2009). Cost-effectiveness of Patient Selection Using Penumbral-Based MRI for Intravenous Thrombolysis. *Stroke* 40 (5), 1710–1720. doi:10.1161/STROKEAHA.108.540138

Gage, B. F., Cardinalli, A. B., and Owens, D. K. (1998). Cost-effectiveness of Preference-Based Antithrombotic Therapy for Patients with Nonvalvular Atrial Fibrillation. *Stroke* 29 (6), 1083–1091. doi:10.1161/01.str.29.6.1083

Ganesalingam, J., Pizzo, E., Morris, S., Sunderland, T., Ames, D., and Lobotesis, K. (2015). Cost-utility Analysis of Mechanical Thrombectomy Using Stent Retrievers in Acute Ischemic Stroke. *Stroke* 46 (9), 2591–2598. doi:10.1161/STROKEAHA.115.009396

Giles, M. F., and Rothwell, P. M. (2007). Risk of Stroke Early after Transient Ischaemic Attack: a Systematic Review and Meta-Analysis. *Lancet Neurol.* 6 (12), 1063–1072. doi:10.1016/S1474-4422(07)70274-0

Gusto Investigators (1993). An International Randomized Trial Comparing Four Thrombolytic Strategies for Acute Myocardial Infarction. *N. Engl. J. Med.* 329 (10), 673–682. doi:10.1056/NEJM199309023291001

Husereau, D., Drummond, M., Petrou, S., Carswell, C., Moher, D., Greenberg, D., et al. (2013). Consolidated Health Economic Evaluation Reporting Standards (CHEERS) Statement. *BMC Med.* 11, 80f1049. doi:10.1186/1741-7015-11-80

International Stroke Trial Collaborative Group (1997). The International Stroke Trial (IST): a Randomised Trial of Aspirin, Subcutaneous Heparin, Both, or Neither Among 19435 Patients with Acute Ischaemic Stroke. International Stroke Trial Collaborative Group. *Lancet* 349 (9065), 1569–1581.

Johnston, S. C., Gress, D. R., Browner, W. S., and Sidney, S. (2000). Short-term Prognosis after Emergency Department Diagnosis of TIA. *JAMA* 284 (22), 2901–2906. doi:10.1001/jama.284.22.2901

Johnston, S. C., Easton, J. D., Farrant, M., Barsan, W., Conwit, R. A., Elm, J. J., et al. (2018). Clopidogrel and Aspirin in Acute Ischemic Stroke and High-Risk TIA. *N. Engl. J. Med.* 379 (3), 215–225. doi:10.1056/nejmoa1800410

Johnston, S. C., Amarenco, P., Denison, H., Evans, S. R., Himmelmann, A., James, S., et al. (2020). Ticagrelor and Aspirin or Aspirin Alone in Acute Ischemic Stroke or TIA. *N. Engl. J. Med.* 383 (3), 207–217. doi:10.1056/NEJMoa1916870

Joo, H., Wang, G., and George, M. G. (2017). A Literature Review of Cost-Effectiveness of Intravenous Recombinant Tissue Plasminogen Activator for Treating Acute Ischemic Stroke. *Stroke Vasc. Neurol.* 2 (2), 73–83. doi:10.1136/svn-2016-000063

National Bureau of Statistics of China (2020). Health Care and Personal Articles of Consumer Price Indices. Available at: http://data.stats.gov.cn/english/easyquery.htm?cn=C01 (Accessed July 10, 2021).

National Bureau of Statistics of China (2021). The 2010 Population Census of the People's Republic of China. (in Chinese). Available at: http://www.stats.gov.cn/tjsj/pcsj/rkpc/6rp/indexch.html (Accessed July 25, 2021).

National Bureau of Statistics of China (2021). Available at: http://www.stats.gov.cn/english/PressRelease/202102/t20210228_1814177.html (Accessed July 6, 2021).

National Health Commission of the People's Republic of China (2019). *China Health Statistics Yearbook 2019*. Beijing: Peking Union Medical College Press. (in Chinese).

Nelson, R. E., Okon, N., Lesko, A. C., Majersik, J. J., Bhatt, A., and Baraban, E. (2016). The Cost-Effectiveness of Telestroke in the Pacific Northwest Region of the USA. *J. Telemed. Telecare* 22 (7), 413–421. doi:10.1177/1357633X15613920

Pan, F., Hernandez, L., and Ward, A. (2012). Cost-effectiveness of Stroke Treatments and Secondary Preventions. *Expert Opin. Pharmacother.* 13 (12), 1751–1760. doi:10.1517/14656566.2012.699522

Pan, Y., Wang, A., Liu, G., Zhao, X., Meng, X., Zhao, K., et al. (2014). Cost-effectiveness of Clopidogrel-Aspirin versus Aspirin Alone for Acute Transient Ischemic Attack and Minor Stroke. *J. Am. Heart Assoc.* 3 (3), e000912. doi:10.1161/JAHA.114.000912

Pan, Y., Chen, W., Xu, Y., Yi, X., Han, Y., Yang, Q., et al. (2017). Genetic Polymorphisms and Clopidogrel Efficacy for Acute Ischemic Stroke or Transient Ischemic Attack: a Systematic Review and Meta-Analysis. *Circulation* 135 (1), 21–33. doi:10.1161/CIRCULATIONAHA.116.024913

Pan, Y., Cai, X., Huo, X., Zhao, X., Liu, L., Wang, Y., et al. (2018). Cost-effectiveness of Mechanical Thrombectomy within 6 hours of Acute Ischaemic Stroke in China. *BMJ Open* 8 (2), e018951. doi:10.1136/bmjopen-2017-018951

Pan, Y., Zhang, L., Li, Z., Meng, X., Wang, Y., Li, H., et al. (2020). Cost-Effectiveness of a Multifaceted Quality Improvement Intervention for Acute Ischemic Stroke in China. *Stroke* 51 (4), 1265–1271. doi:10.1161/STROKEAHA.119.027980

Pennlert, J., Eriksson, M., Carlberg, B., and Wiklund, P. G. (2014). Long-term Risk and Predictors of Recurrent Stroke beyond the Acute Phase. *Stroke* 45 (6), 1839–1841. doi:10.1161/STROKEAHA.114.005060

Peultier, A. C., Pandya, A., Sharma, R., Severens, J. L., and Redekop, W. K. (2020). Cost-effectiveness of Mechanical Thrombectomy More Than 6 hours after Symptom Onset Among Patients with Acute Ischemic Stroke. *JAMA Netw. Open* 3 (8), e2012476. doi:10.1001/jamanetworkopen.2020.12476

Rost, N. S., Bottle, A., Lee, J. M., Randall, M., Middleton, S., Shaw, L., et al. (2016). Stroke Severity Is a Crucial Predictor of Outcome: an International Prospective Validation Study. *J. Am. Heart Assoc.* 5 (1), e002433. doi:10.1161/JAHA.115.002433

Samsa, G. P., Reutter, R. A., Parmigiani, G., Ancukiewicz, M., Abrahamse, P., Lipscomb, J., et al. (1999). Performing Cost-Effectiveness Analysis by Integrating Randomized Trial Data with a Comprehensive Decision Model: Application to Treatment of Acute Ischemic Stroke. *J. Clin. Epidemiol.* 52 (3), 259–271. doi:10.1016/s0895-4356(98)00151-6

Schleinitz, M. D., Weiss, J. P., and Owens, D. K. (2004). Clopidogrel versus Aspirin for Secondary Prophylaxis of Vascular Events: a Cost-Effectiveness Analysis. *Am. J. Med.* 116 (12), 797–806. doi:10.1016/j.amjmed.2004.01.014

Slot, K. B., Berge, E., Sandercock, P., Lewis, S. C., Dorman, P., and Dennis, M. (2009). Causes of Death by Level of Dependency at 6 Months after Ischemic Stroke in 3 Large Cohorts. *Stroke* 40 (5), 1585–1589. doi:10.1161/STROKEAHA.108.531533

Wang, Y., Wang, Y., Zhao, X., Liu, L., Wang, D., Wang, C., et al. (2013). Clopidogrel with Aspirin in Acute Minor Stroke or Transient Ischemic Attack. *N. Engl. J. Med.* 369, 11–19. doi:10.1056/NEJMoa1215340

Wang, Y., Li, Z., Zhao, X., Wang, C., Wang, X., Wang, D., et al. (2018). Effect of a Multifaceted Quality Improvement Intervention on Hospital Personnel Adherence to Performance Measures in Patients with Acute Ischemic Stroke in China: a Randomized Clinical Trial. *JAMA* 320 (3), 245–254. doi:10.1001/jama.2018.8802

Waqas, M., Gong, A. D., Levy, B. R., Dossani, R. H., Vakharia, K., Cappuzzo, J. M., et al. (2021). Is Endovascular Therapy for Stroke Cost-Effective Globally? A Systematic Review of the Literature. *J. Stroke Cerebrovasc. Dis.* 30 (4), 105557. doi:10.1016/j.jstrokecerebrovasdis.2020.105557

Weinstein, M. C., Siegel, J. E., Gold, M. R., Kamlet, M. S., and Russell, L. B. (1996). Recommendations of the Panel on Cost-Effectiveness in Health and Medicine. *JAMA* 276 (15), 1253–1258. doi:10.1001/jama.276.15.1253

Wu, S., Wu, B., Liu, M., Chen, Z., Wang, W., Anderson, C. S., et al. (2019). Stroke in China: Advances and Challenges in Epidemiology, Prevention, and Management. *Lancet Neurol.* 18 (4), 394–405. doi:10.1016/S1474-4422(18)30500-3

Xu, G., Liu, X., Wu, W., Zhang, R., and Yin, Q. (2007). Recurrence after Ischemic Stroke in Chinese Patients: Impact of Uncontrolled Modifiable Risk Factors. *Cerebrovasc. Dis.* 23 (2-3), 117–120. doi:10.1159/000097047

Conflict of Interest: The authors declare that the research was conducted in the absence of any commercial or financial relationships that could be construed as a potential conflict of interest.

Publisher's Note: All claims expressed in this article are solely those of the authors and do not necessarily represent those of their affiliated organizations, or those of the publisher, the editors, and the reviewers. Any product that may be evaluated in this article, or claim that may be made by its manufacturer, is not guaranteed or endorsed by the publisher.

frontiers in Pharmacology

ORIGINAL RESEARCH
published: 23 March 2022
doi: 10.3389/fphar.2022.844186

A Network-Based Approach to Investigate the Neuroprotective Effects and Mechanisms of Action of Huangqi-Chuanxiong and Sanleng-Ezhu Herb Pairs in the Treatment of Cerebral Ischemic Stroke

Lin Zhao[1,2†], *Li Dong Ding*[3†], *Zi Hao Xia*[1,2], *Peng Sheng*[1,2], *Meng Meng Shen*[1,2], *Zhong Ming Cai*[4] *and Bing Chun Yan*[1,2*]

[1]Medical College, Institute of Translational Medicine, Yangzhou University, Yangzhou, China, [2]Jiangsu Key Laboratory of Integrated Traditional Chinese and Western Medicine for Prevention and Treatment of Senile Diseases, Yangzhou University, Yangzhou, China, [3]Department of Neurology, Taizhou Second People's Hospital, Taizhou, China, [4]Department of Neurology, Yangzhou Hospital of Chinese Medicine, Yangzhou, China

OPEN ACCESS

Edited by:
Li-Nan Zhang,
Hebei Medical University, China

Reviewed by:
Yucong Peng,
Zhejiang University, China
Feng Zhang,
Third Hospital of Hebei Medical University, China

***Correspondence:**
Bing Chun Yan
bcyan@yzu.edu.cn

[†]These authors have contributed equally to this work

Specialty section:
This article was submitted to Neuropharmacology, a section of the journal Frontiers in Pharmacology

Received: 27 December 2021
Accepted: 18 February 2022
Published: 23 March 2022

Citation:
Zhao L, Ding LD, Xia ZH, Sheng P, Shen MM, Cai ZM and Yan BC (2022) A Network-Based Approach to Investigate the Neuroprotective Effects and Mechanisms of Action of Huangqi-Chuanxiong and Sanleng-Ezhu Herb Pairs in the Treatment of Cerebral Ischemic Stroke. Front. Pharmacol. 13:844186. doi: 10.3389/fphar.2022.844186

Objective: We aimed to investigate the effect and mechanisms of action of two drug pairs [Huangqi-Chuanxiong and Sanleng-Ezhu Herb (HCSE)] on the treatment of ischemic stroke.

Materials and methods: We mined the current literature related to ischemic stroke and formulated a new formulation of Chinese herbs. Then, we identified the main candidate target genes of the new formulation by network pharmacology. Next, we performed enrichment analysis of the target genes to identify the potential mechanism of action of the new formulation in the treatment of ischemic stroke. Next, we experimentally validated the mechanism of action of the new formulation against ischemic stroke. Infarct volume and neurological deficits were evaluated by 2,3,5-triphenyltetrazolium (TTC) staining and Longa's score, respectively. The predicted pathways of signal-related proteins were detected by western blotting.

Results: We mined the current literature and identified a new formulation of Chinese herbs for the treatment of ischemic stroke. The formulation included Huangqi, Chuanxiong, Sanleng and Ezhu. Next, we used network pharmacological analysis to identify 23 active compounds and 327 target genes for the new formulation. The key target genes were *MAPK3*, *MAPK1*, *HSP90AA1*, *STAT3*, *PIK3R1*, *PIK3CA* and *AKT1*. Kyoto Encyclopedia of Genes and Genomes (KEGG) enrichment analysis revealed significant enrichment of the PI3K/AKT and MAPK/ERK signaling pathways. By performing experiments, we found that the new formulation reduced the infarct volume of middle cerebral artery occlusion (MCAO) induced mice and activated the PI3K/AKT and MAPK/ERK signaling pathways. These

findings confirmed that the new formulation has a significant protective effect against ischemic stroke injury by activating the PI3K/AKT and MAPK/ERK signaling pathways.

Conclusion: We identified a new treatment formulation for ischemic stroke by data mining and network pharmacological target prediction. The beneficial effects of the new formulation act by regulating multiple target genes and pathways. The mechanism of action of the new formulation may be related to the AKT and ERK signaling pathways. Our findings provide a theoretical basis for the effects of the new formulation on ischemic stroke injury.

Keywords: huangqi-chuanxiong, sanleng-ezhu herb, ischemic stroke, clinical data mining, network pharmacology

INTRODUCTION

Stroke has become the second leading cause of global death and is the leading cause of death and disability among adults in China. Ischemic stroke accounts for 69.6–77.8% of stroke cases and is associated with mortality and recurrence rates of 7 and 16%, respectively (Wang et al., 2017; Yiping Chen et al., 2020). Ischemic stroke causes irreversible damage to the brain tissue by influencing the distribution of affected blood vessels, thus leading to a variety of neurological symptoms and signs. Ischemic stroke adversely affects the health of patients and places significant socioeconomic burden on their families (Mukundan and Seidenwurm, 2018).

According to the theory of traditional Chinese medicine (TCM) (Liu et al., 2007), the main syndromes and causes of ischemic stroke are Qi deficiency and blood stasis syndrome (Li et al., 2014; Zhai et al., 2020). Therefore, the main principle of treatment for ischemic stroke is the invigoration of Qi and the promotion of blood circulation (Yu Wang et al., 2020). Based on this principle, practitioners of ancient Chinese medicine have suggested many treatments for stroke (Xu et al., 2019). The most commonly used and most effective treatment is Buyang Huanwu Decoction, invented by Wang Qingren, a famous doctor in the Qing Dynasty. Several studies have shown that the modified Buyang Huanwu Decoction has significant positive effects on the neurological deficits of patients with ischemic stroke (Xi Chen et al., 2020). When using Buyang Huanwu Decoction, the effect of invigoration of Qi and the promotion of blood circulation is mainly induced by two specific drugs: Huangqi and Chuanxiong. Some drugs mainly treated blood stasis, such as Taoren (Xi et al., 2013). However, research on the molecular effects associated with the invigoration of Qi and the promotion of blood circulation is scarce. Therefore, in the present study, we investigated the molecular mechanisms underlying the traditional methods used to prevent and treat ischemic stroke.

Data mining and network pharmacology can systematically evaluate the interactions between diseases and drugs and identify the specific mechanisms of action of drugs on their gene targets. Many previous studies have used data mining and network pharmacology to investigate the treatment of diseases by TCM (Li and Zhang, 2013; Sun et al., 2020). These strategies can provide new ideas for research and allow for the more accurate application of TCM.

In the present study, data mining and network pharmacology were used to evaluate the related mechanisms and effects of Huangqi-Chuanxiong and Sanleng-Ezhu Herb pairs (HCSE) on the treatment of patients suffering from ischemic stroke with Qi deficiency and blood stasis syndrome. Our findings provide scientific evidence to support the application of the new formulation for the treatment of ischemic stroke.

MATERIALS AND METHODS

Data Mining

Literature Review

First, we searched the China National Knowledge Infrastructure, Wanfang Data, and PubMed using the keywords “stroke” and “ischemic stroke with Qi deficiency and blood stasis syndrome” to identify articles published the 1st September 2011 and the 1st September 2021. Then, we used the keywords “circulating blood and removing stasis” and “broking blood stasis” to search the clinical literature on the use of TCM to treat ischemic stroke with Qi deficit and blood stasis syndrome (Liu et al., 2012).

Data Screening

The prescriptions included in the retrieved literature were analyzed, and matrix distribution was performed.

Association Analysis

The drugs were analyzed using the *a priori* module included in SPSS Modeler software (version 18.0; IBM Corp., Armonk, NY, USA). The minimum number of conditional supports, indicating the number of drug combinations in the prescriptions, was set to 10. The minimum rule confidence, indicating the probabilities of occurrence for the first and second terms of the rule, was set to 80%. Drug pairs were then identified based on the association rules, and the new formulations were combined using TCM theory analysis.

Network Pharmacology

Prediction of Target Genes for the Drug Ingredients

The active compounds of the drugs were screened based on an oral bioavailability (OB) ≥ 30%, a drug-likeness (DL) ≥ 0.18, and a blood-brain barrier (BBB) ≥ −0.3 using the TCMSP database (https://tcmsp-e.com/) (Ru et al., 2014). Target proteins of the

TABLE 1 | Drug associations.

Serial number	Drug pair	Support (%)	Confidence (%)
1	Chuanxiong/Huangqi	90.79	86.96
2	Huangqi/Chuanxiong	84.21	93.75
3	Chishao/Honghua	67.11	82.35
4	Dilong/Honghua	67.11	86.27
5	Danggui/Honghua	67.11	88.23

TABLE 2 | Drug associations.

Serial number	Drug pair	Support (%)	Confidence (%)
1	Ezhu/Sanleng	53.62	86.49
2	Sanleng/Ezhu	52.17	88.89
3	Honghua/Danggui	50.72	85.71
4	Chuanxiong/Danggui	50.72	80.00
5	Chuanxiong/Taoren	42.01	86.21

active ingredients were identified using SwissTargetPrediction (Swiss Institute of Bioinformatics, Basel, Switzerland; http://www.swisstargetprediction.ch/) (Daina et al., 2019).

Disease Target Identification

The keyword "ischemic stroke" was used to search disease targets in the GeneCards database (https://www.genecards.org/) (Safran et al., 2021). According to the principles of TCM, the main symptoms of ischemic stroke with Qi deficiency and blood stasis syndrome are a pale white complexion, a shortness of breath, palpitations, spontaneous sweating, loose stools, limb swelling, angular salivation, a purple tongue, a thin and whitish tongue coating, and a deep and faint pulse. We used these keywords as search terms in the GeneCards database. These symptoms were then selected as the targets for Qi deficiency and blood stasis syndrome. Overlapping targets were considered as potential targets of ischemic stroke with Qi deficiency and blood stasis syndrome.

Predicting Overlapping Drug and Disease Targets

Drug and disease targets were imported into Jvenn software (http://jvenn.toulouse.inra.fr/app/example.html) (Bardou et al., 2014) to construct a Venn diagram; overlapping targets were then considered to be potential therapeutic targets for the new treatment for ischemic stroke.

Construction of a Protein-Protein Interaction Network

A PPI network was constructed for the potential therapeutic target proteins of the new treatment formulation using the STRING database (https://string-db.org). The results were then visualized using Cytoscape software (version 3.8.2; https://cytoscape.org/). The degree of freedom was indicated by node size and color. The topological properties of the target genes were analyzed using the CytoNCA tool (Cytoscape software plugin) (Tang et al., 2015; Bei Yin et al., 2020). The PPI network was used to screen key targets of the new treatment based on a degree centrality (DC) > two-fold of the median and betweenness centrality (BC), closeness centrality (CC), and an eigenvector centrality (EC) > one-fold of the median. Higher quantitative values were correlated with a greater importance of the node.

Gene Ontology Enrichment and Kyoto Encyclopedia of Genes and Genomes Pathway Analyses

Metascape (https://metascape.org/) was used to perform GO and KEGG pathway enrichment analyses of 327 candidate target genes, according to the molecular function (MF), biological process (BP), and cellular component (CCT) categories (Zhou et al., 2019). p values were used to evaluate the proteins each GO annotation, thus reflecting the significance of the biological function. In addition, the FDR error control method (FDR <0.05) was used to test and correct the p value. The threshold value of $p < 0.05$ was finally used to screen the biological processes with significant differences. GO and KEGG enrichment analyses were visualized by the Bioinformatics platform (http://www.bioinformatics.com.cn/).

Experimental Verification

Experimental Animals

Healthy male Institute of Cancer Research mice (ICR; body weight: 32–35 g) were provided by the Comparative Medicine Center of Yangzhou University (Yangzhou, China) and used after 1 week of acclimation. The mice were housed in a controlled condition with a 12-h light/dark cycle at 23°C and 60% humidity with free access to food and water. All experimental investigation procedures for animals were permitted by the Yangzhou University Institutional Animal Care and Use Committee (Grant No. YIACUC-14-0015).

Middle Cerebral Artery Occlusion

The middle cerebral artery occlusion (MCAO) model was created using the following procedure. The mice were continuously anesthetized by the inhalation of a mixture of 30% oxygen, 70% nitrogen and 3–4% isoflurane (RWD Life Science, Guangdong Province, China). The mice were then fixed in the supine position. Next, we sterilized and dissected the skin of the middle of the neck. The left common carotid artery (CCA), the internal carotid artery (ICA), and the external carotid artery (ECA), were then separated with a blunt instrument. The ECA was ligated, the CCA and ICA were clamped with a bulldog clip, and a "V" incision was made in the ECA with ophthalmic scissors. A 0.23 mm monofilament nylon suture (Beijing Biotechnology Co., Ltd.) was then inserted through the "V" incision into the ICA until slight resistance was achieved. After 45 min of arterial occlusion, the monofilament nylon suture was removed, and the blood was reperfused for 24 h. In the Sham group, only the CCA, ICA and ECA were separated; no monofilament nylon suture was inserted. The body temperature of the mice was maintained at 37.0–37.5°C during surgery.

Experimental Groups and Drug Treatments

The mice were randomly divided into four groups as follows (n = 21 in each group): 1) a control group and 2) a pre-HCSE (13.65 g/kg) group. Each of these two groups was then further divided into a Sham group and a MCAO group. All animals were

TABLE 3 | Active compounds contained in the new formulation.

Serial number	Herb	Active component	Mol ID	OB	DL	BBB
1	Huangqi	Betulinic acid	MOL000211	55.38	0.78	0.22
2	Huangqi	Kumatakenin	MOL000239	50.83	0.29	−0.22
3	Huangqi	Hederagenin	MOL000296	36.91	0.75	0.96
4	Huangqi	Beta-sitosterol	MOL000033	36.23	0.78	1.09
5	Huangqi	3,9,10-Trimethoxypterocarpan	MOL000371	53.74	0.48	0.63
6	Huangqi	7-O-Methylisomucronulatol	MOL000378	74.69	0.3	0.84
7	Huangqi	Astrapterocarpan	MOL000380	64.26	0.42	0.55
8	Huangqi	Bifendate	MOL000387	31.1	0.67	−0.06
9	Huangqi	Formononetin	MOL000392	69.67	0.21	0.02
10	Huangqi	Isoflavanone	MOL000398	109.99	0.3	0.17
11	Huangqi	Isomucronulatol 7-O-glucoside	MOL000438	67.67	0.26	0.34
12	Huangqi	3,4-(4-methoxy-6-hydroxy-1,2-phenyleneoxy)-5-hydroxy-7-methoxy-2H-1-benzopyran	MOL000442	39.05	0.48	−0.04
13	Chuanxiong	Ethyl linoleate	MOL001494	42	0.19	1.14
14	Chuanxiong	Myricanone	MOL002135	40.6	0.51	−0.08
15	Chuanxiong	Perlolyrine	MOL002140	65.95	0.27	0.15
16	Chuanxiong	Senkyunone	MOL002151	47.66	0.24	0.5
17	Chuanxiong	Wallichilide	MOL002157	42.31	0.71	0.73
18	Chuanxiong	3-Epi-beta-sitosterol	MOL000359	36.91	0.75	0.87
19	Sanleng	trans-11-eicosenoic acid	MOL001297	30.7	0.2	0.89
20	Sanleng	Hederagenin	MOL000296	36.91	0.75	0.96
21	Sanleng	beta-Sitosterol	MOL000358	36.91	0.75	0.99
22	Sanleng	Formononetin	MOL000392	69.67	0.21	0.02
23	Sanleng	Stigmasterol	MOL000449	43.83	0.76	1
24	Ezhu	Hederagenin	MOL000296	36.91	0.75	0.96
25	Ezhu	Wenjine	MOL000906	47.93	0.27	0.3
26	Ezhu	Bisdemethoxycurcumin	MOL000940	77.38	0.26	−0.08

FIGURE 1 | Venn diagram of the overlapping drug and disease target genes. The red circle represents the targets for ischemic stroke with Qi deficiency and blood stasis syndrome. The blue circle represents the targets for the new formulation. The 327 overlapping genes are potential therapeutic targets for the new formulation against ischemic stroke with Qi deficiency and blood stasis syndrome.

killed at 24 h after cerebral ischemia reperfusion. The method used to prepare HCSE involved mixing 225 g of Huangqi (100 g), Chuanxiong (50 g), Sanleng (45 g), and Ezhu (30 g) with eight times the volume of distilled water, followed by boiling for 2 h. Then, the filtrate was collected, and the filtrate was extracted again with three times the volume of distilled water. The filtrate was mixed twice and concentrated to 225 ml by a rotary evaporator. Therefore, the final crude drug concentration was 1 g/ml. All herbs were purchased from the Yangzhou Hospital of Chinese Medicine, Jiangsu Province, China. According to the dose used for ischemic stroke patients in the clinic (90 ml per day), we determined the dose for our experimental animals by extrapolation from the human dose in accordance with a previous study (Reagan-Shaw et al., 2008). Finally, a dose of 13.65 g/kg was obtained for administration. We chose 6.83 g/kg, 13.65 g/kg, and 27.3 g/kg as the HCSE doses in our preliminary study. We found that the neuroprotective effects (as determined by TTC staining) of the 13.65 g/kg and 27.3 g/kg doses were better than those with the 6.83 g/kg dose. Therefore, we selected a dose of 13.65 g/kg for use in the present study.

HCSE was administered intra-gastrically the same day, 24 h, and 48 h before ischemic surgery, and was administered twice a day. The Sham group and the ischemia group received the same amount of 0.9% saline intra-gastrically for the same durations. Following the last administration, the mice underwent ischemia/reperfusion or Sham operation.

Neurological Deficit Assessment

The degree of neurological deficit was assessed 24 h after reperfusion using the Longa score, as follows: 1) no neurological deficit: 0 points; 2) inability to fully extend the front paw on the paralyzed side: 1 point; 3) circling to the paralyzed side during walking: 2 points; 4) leaning towards the paralyzed side when walking: 3 points; and 5) inability to walk spontaneously, with loss of consciousness: 4 points. A score of more than 1 indicates that the MCAO model had been successfully established.

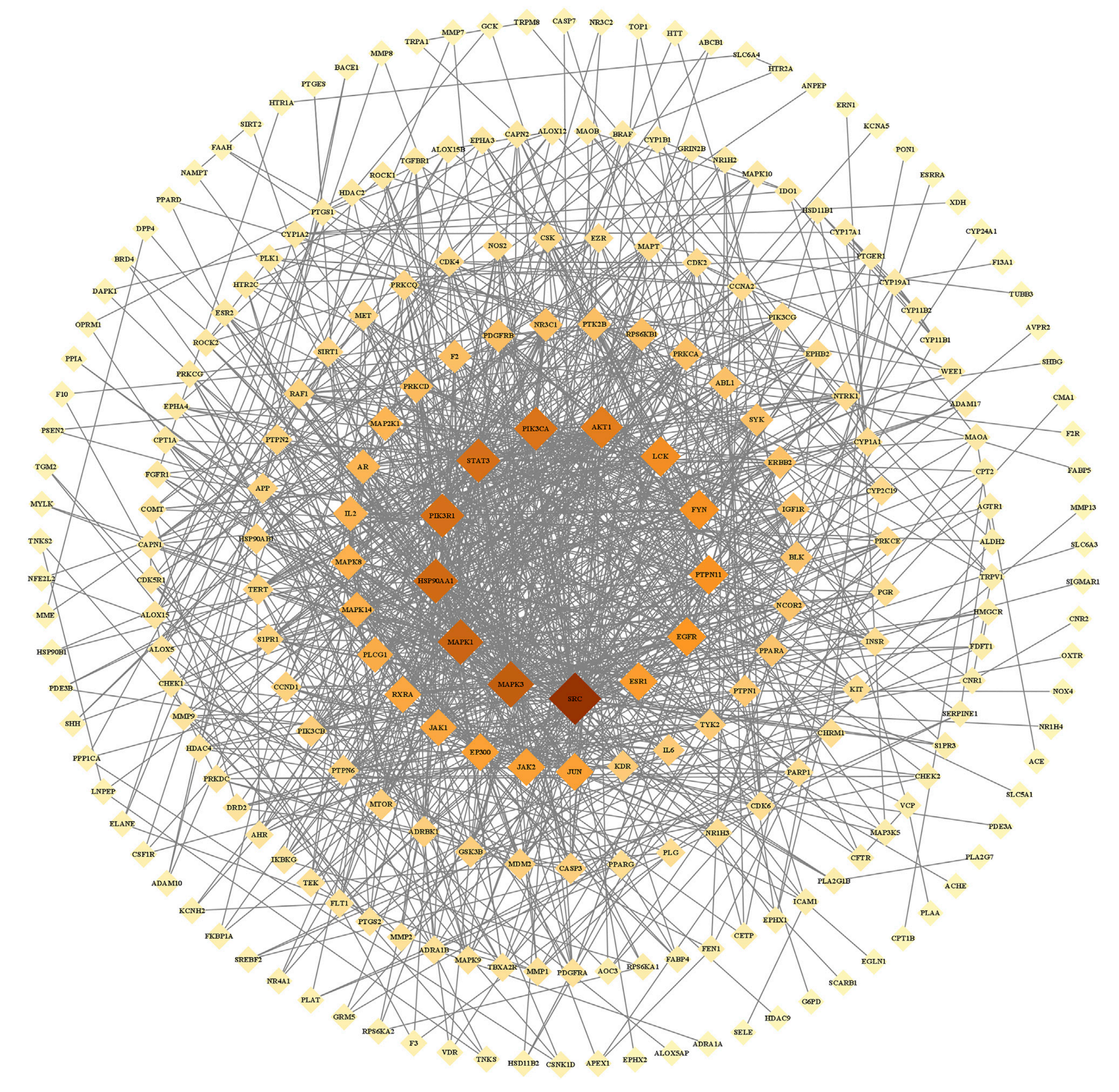

FIGURE 2 | Protein-protein interaction network of the core proteins targeted by the new formulation for the treatment of ischemic stroke with Qi deficiency and blood stasis syndrome. The network included 244 nodes and 1,081 edges. Diamonds repr6+ the target proteins, with darker colors indicating increasing importance.

TTC Staining and the Quantification of Infarct Volume

Next, we performed TTC staining experiments with reference to relevant published literature (Liu et al., 2020; Zhang et al., 2021). After 24 h of ischemia/reperfusion, mice were anesthetized by isoflurane inhalation and killed by cervical dislocation. Brain tissue was then removed and cut into 2 mm thick coronal sections. The sections were then stained using 2% 2,3,5-triphenyltetrazolium chloride (Sigma-Aldrich, St. Louis, MO) in the dark at 37.0°C for 30 min. After staining, the brain sections were fixed in 4% paraformaldehyde buffer. The live portion of the brain section was red, and the infarcted portion was pale white. The infarct volume and whole volume of each brain slice were measured using Image Pro Plus 6.0 software (Media Cybernetics, Bethesda, MD, USA). The infarct volume of each section was multiplied by the layer thickness (2 mm) to calculate the total infarct volume. The ratio of total infarct volume/whole brain volume × 100% was used as the total infarct ratio.

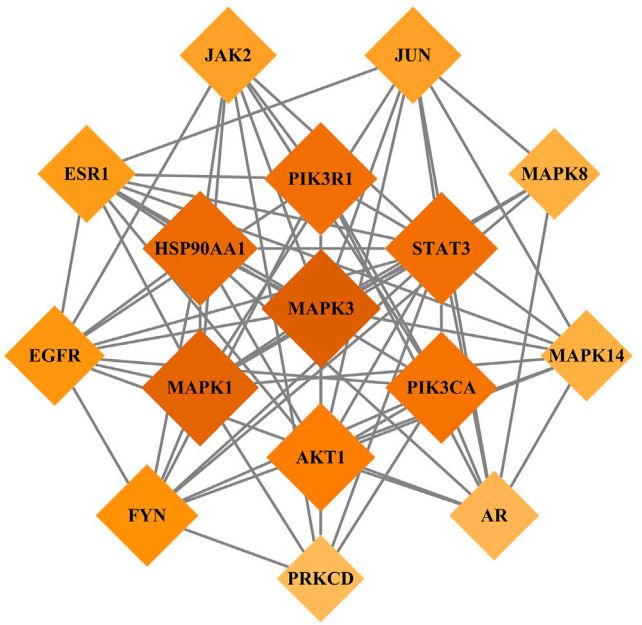

FIGURE 3 | Key target genes of the new treatment formulation for ischemic stroke with Qi deficiency and blood stasis syndrome. Diamonds represent target genes, with darker colors indicating increasing importance.

Western Blot Analysis

Western blotting was carried out as described in our previous article (Liu et al., 2021). First, hippocampal and cortical tissues were lysed with a Whole Protein Extraction Kit (Solarbio, Beijing, China). The protein concentration of each sample was then measured using a BCA protein assay kit (Vazyme, Nanjing, China). Equal amounts of protein (30 μg) were then separated by 10% sodium dodecyl sulfate polyacrylamide gel electrophoresis (SDS-PAGE) and transferred to nitrocellulose membranes (Millipore, Bedford, USA). The membranes were cultured in 5% BSA in TBS containing 0.1% Tween 20 for 90 min to prevent non-specific protein binding sites from binding to antibodies. The membranes were cut according to molecular weight and then incubated overnight at 4°C with rabbit anti-AKT (1:1,000, Cell Signaling Technology), rabbit anti-p-AKT (1:2000, Cell Signaling Technology), rabbit anti-ERK 1/2 (1:1,000, Cell Signaling Technology), rabbit anti-p-ERK 1/2 (1:1,000, Cell Signaling Technology). Subsequently, the membrane was incubated with a corresponding secondary antibody at room temperature for 2 h. The protein membranes were then to Super Signal West Pico chemiluminescence substrates (CWBIO, Beijing, China) and observed by Fluor Chem M (Protein Simple, USA). Western blot results were analyzed by Image Pro Plus 6.0.

Data Analysis

Data are expressed as a mean ± standard deviation ($\bar{X} \pm SD$) and analyzed by GraphPad Prism 8.0. SPSS software (version 21.0; IBM, Armonk, NY, USA). The student's two-tailed *t*-test was used for comparisons between two groups and one-way analysis of variance followed by Dunnett's test was used for the comparison of three or more groups. $p < 0.05$ was considered statistically significant.

RESULTS

Data Mining

Literature Analysis

We identified 177 articles related to TCM treatment of ischemic stroke with Qi deficiency and blood stasis syndrome, including 76 prescriptions based on 119 TCM drugs. In total, 77 articles were related to breaking blood and removing blood stasis for the treatment of ischemic stroke with Qi deficiency and blood stasis syndrome; these articles included 52 prescriptions based on 94 TCM drugs.

Types of TCM Drugs

The 10 most common TCM drugs used for the treatment of ischemic stroke with Qi deficiency and blood stasis syndrome were Huangqi ($n = 69$), Chuanxiong ($n = 64$), Honghua ($n = 51$), Danggui ($n = 50$), Dilong ($n = 50$), Chishao ($n = 46$), Taoren ($n = 40$), Danshen ($n = 27$), Shuizhi ($n = 20$), Jixueteng ($n = 19$), and Sanqi ($n = 14$). The 10 most common TCM drugs used for breaking blood and removing stasis were Chuanxiong ($n = 46$), Honghua ($n = 39$), Sanleng ($n = 37$), Ezhu ($n = 37$), Danshen ($n = 35$), Danggui ($n = 35$), Chishao ($n = 29$), Taoren ($n = 29$), Huangqi ($n = 26$), and Dilong ($n = 19$).

Association Analyses

The five most commonly used drug combinations for TCM treatment of ischemic stroke with Qi deficiency and blood stasis syndrome were Chuanxiong/Huangqi, Huangqi/Chuanxiong, Chishao/Honghua, Dilong/Honghua, and Danggui/Honghua (**Table 1**). The five most commonly used drug combinations for breaking blood and removing blood stasis for the treatment of ischemic stroke with Qi deficiency and blood stasis syndrome were Ezhu/Sanleng, Sanleng/Ezhu, Honghua/Danggui, Chuanxiong/Danggui, and Chuanxiong/Taoren (**Table 2**). Based on these results, we decided to combine Huangqi, Chuanxiong, Sanleng, and Ezhu to form a new formulation (HCSE).

Network Pharmacology

Chemical Component Analysis

After excluding components with undiscovered targets, 26 candidate components of Huangqi, Chuanxiong, Sanleng, and Ezhu were identified in the TCMSP database based on specific thresholds (OB ≥ 30%, DL ≥ 0.18, and BBB ≥ −0.3). In total, 12, 5, 5, and 3 compounds were identified from Huangqi, Chuanxiong, Sanleng and Ezhu, respectively (**Table 3**). Of these, Huangqi, Sanleng and Ezhu all contain Hederagenin as a key ingredient; Huangqi and Sanleng both contain Formononetin as a key ingredient.

Integration of Disease and Drug Target Genes

The GeneCards database was used to integrate 3,854 genes related to ischemic stroke and 5,103 genes related to the syndrome of Qi deficiency and blood stasis syndrome; these analyses identified a total of 2,696 genes. Then, the target genes of the drug

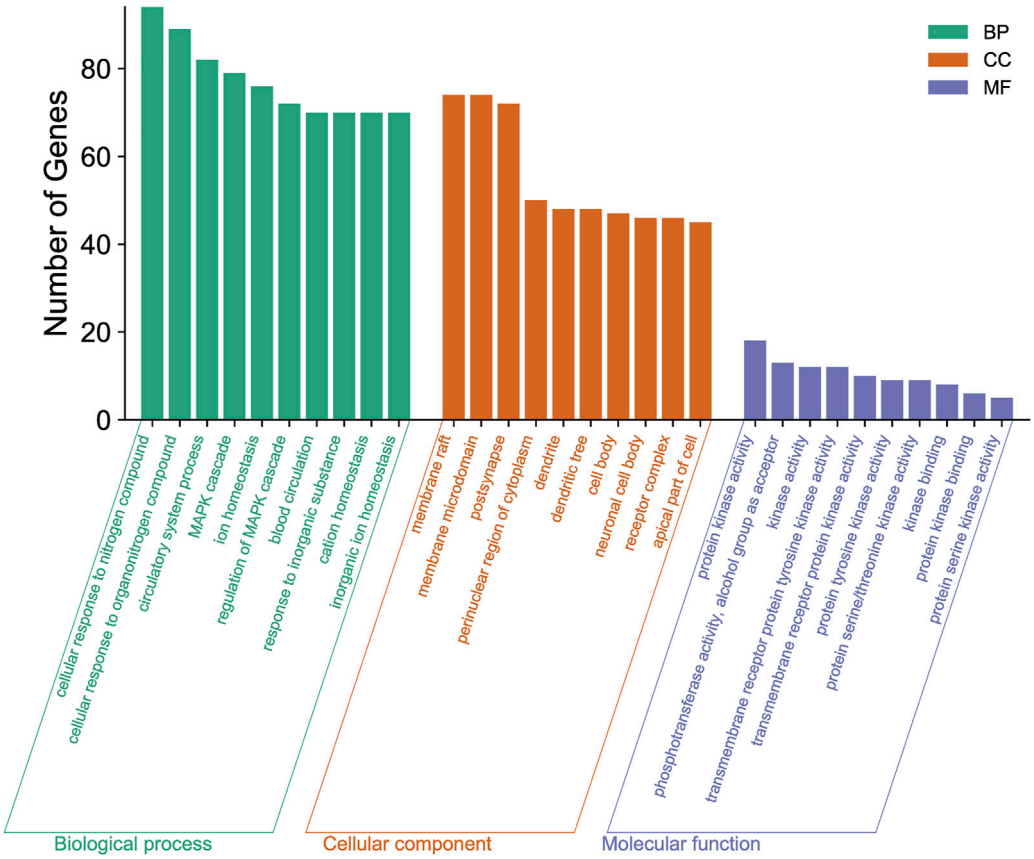

FIGURE 4 | Gene Ontology (GO) enrichment analysis of the new treatment formulation for ischemic stroke with Qi deficiency and blood stasis syndrome. The top 10 biological processes, cellular components, and molecular functions are shown as a bar chart. The *x*-axis represents the GO terms and the *y*-axis represents the number of annotated genes.

components and disease were compared in a Venn diagram using Jvenn software. The Venn diagram showed that 327 genes were potential targets of the new formulation for the treatment of ischemic stroke with Qi deficiency and blood stasis syndrome (**Figure 1**).

PPI Network

We imported the 327 potential therapeutic target genes into the STRING database. Then, we imported target genes with a confidence >0.9 into Cytoscape 3.8.2 software to construct a PPI network. In the PPI network, the nodes represent the target genes, and the node size and color represent the degrees of freedom. As shown in **Figure 2**, the network consisted of 244 nodes and 1,081 edges. The central properties of the nodes were estimated by topological analysis. Sixteen key gene targets of the new formulation for the treatment of ischemic stroke with Qi deficiency and blood stasis syndrome were screened using the following criteria: DC > 11, BC > 728.62274, CC > 0.37587029, and EC > 0.09713785. In **Figure 3**, the size of the nodes is proportional to the DC. Notably, MAPK3, MAPK1, HSP90AA1, STAT3, PIK3R1, PIK3CA, and AKT1 were the main target proteins involved in the pathogenesis of ischemic stroke with Qi deficiency and blood stasis syndrome. Among these targets, MAPK3 (degree = 50) was shown to be the most important protein in the PPI network.

GO Enrichment Analysis

To explore the functional distribution of the gene targets for the formulation, we imported the 327 predicted target genes into the Metascape database for GO enrichment analysis. These genes were found to be associated with multiple BP, CCT, and MF categories ($p < 0.01$; **Figure 4**). The main BP terms were involved in cellular response to nitrogen compound, cellular response to organonitrogen compound, circulatory system processes, the MAPK cascade, and ion homeostasis. The CCT terms included membrane rafts, membrane microdomains, post-synapse, the perinuclear region of the cytoplasm, and dendrites. The MF terms included protein kinase activity, phosphotransferase activity, alcohol group as acceptor kinase activity, transmembrane receptor protein tyrosine kinase activity, and transmembrane receptor protein kinase activity.

KEGG Pathway Annotation

The 327 potential target genes were imported into the Metascape database for KEGG pathway enrichment analysis. Analysis showed that these targets were enriched in 191

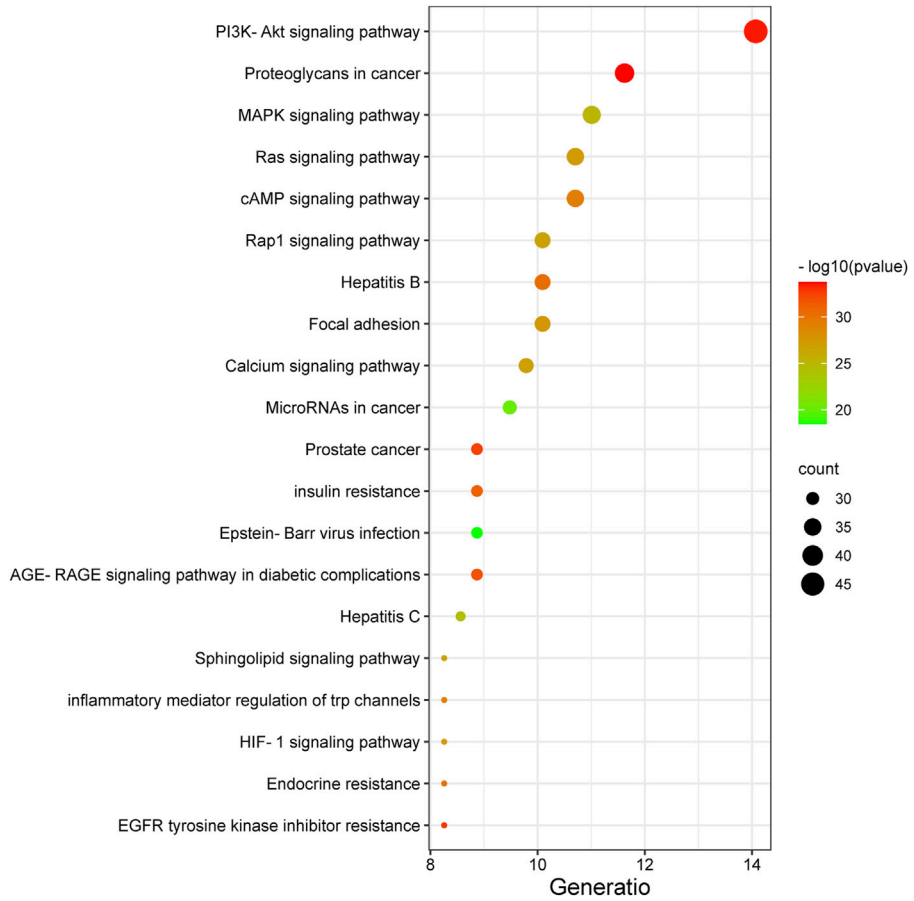

FIGURE 5 | The top 20 pathways identified by KEGG analysis of the new treatment formulation for ischemic stroke with Qi deficiency and blood stasis syndrome. The *y*-axis represents the name of each pathway, and the size of the dots corresponds to the number of genes annotated in the pathway. The *x*-axis represents the ratio corresponding to the significance of the differential protein enrichment, with higher ratios indicating higher reliability.

pathways ($p < 0.01$). The top 20 pathways were analyzed using a bioinformatics database (**Figure 5**). Among these, the PI3K/AKT and MAPK signaling pathways were highly associated with the target genes, thus suggesting that the active ingredients of the new formulation exert beneficial effects on Qi and blood stasis by regulating the PI3K/AKT and MAPK signaling pathways.

Experimental Verifications

The Neuroprotective Effects of HCSE on Ischemic Stroke

The volume of cerebral infarcts was determined by TTC staining. As shown in **Figures 6A,B**, no cerebral infarction was seen in the Sham and Sham + HCSE groups. However, the infarct volume in the MCAO group accounted for approximately 44% of the whole brain ($p < 0.05$). Compared with the MCAO group, the infarct volume in the MCAO + HCSE group was significantly smaller (approximately 23% of the brain volume; $p < 0.05$). In addition, the neurological function of the mice was assessed by applying the Longa (0–4) scale. As shown in **Figure 6C**, no neurological impairment was observed in the Sham and Sham + HCSE groups, although mice in the MCAO group had the highest score (approximately 3.64 points) ($p < 0.05$). Mice in the MCAO + HCSE group had significantly lower neurological function scores (approximately 2.35 points) compared to the MCAO group ($p < 0.05$).

The Effect of HCSE on the Levels of AKT/P-AKT/ERK 1/2/p-ERK 1/2 Signaling-Related Proteins in the Hippocampus and Cortex With Ischemic Stroke in Mice

To investigate the possible mechanisms of HCSE against ischemic stroke, we investigated the expression levels of AKT/p-AKT/ERK 1/2/p-ERK 1/2 signaling related proteins by Western blotting. In hippocampal tissue, as shown in **Figure 7**, there was no significant difference in the p-AKT/AKT and p-ERK 1/2/ERK 1/2 protein ratios in the Sham + HCSE group when compared with the Sham group ($p < 0.05$). The p-AKT/AKT protein ratio in the MCAO group was lower than that in the Sham group ($p < 0.05$), while the p-ERK 1/2/ERK 1/2 protein ratio was higher than that in the Sham group ($p < 0.05$). However, the p-AKT/AKT protein ratio in the MCAO + HCSE group was significantly

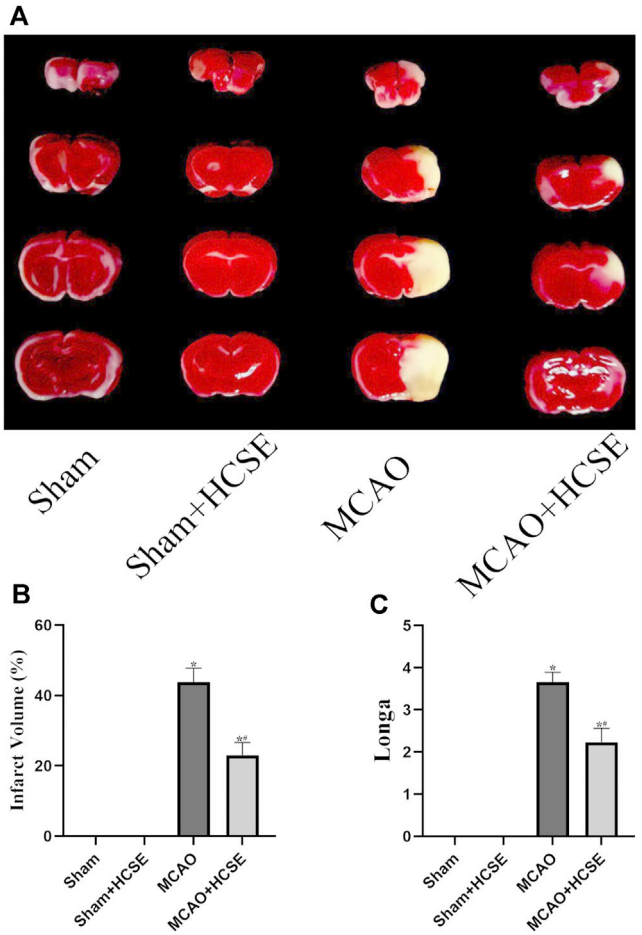

FIGURE 6 | The neuroprotective effects of HCSE. **(A)** TTC staining in the Sham, Sham + HCSE, MCAO and MCAO + HCSE groups. **(B)** The infarct volume was expressed as the ratio of (infarct volume/the whole brain volume) × 100%. **(C)** Longa score. (n = 7 per group; *p < 0.05, significantly different from the corresponding Sham group, #p < 0.05, significantly different from the MCAO group).

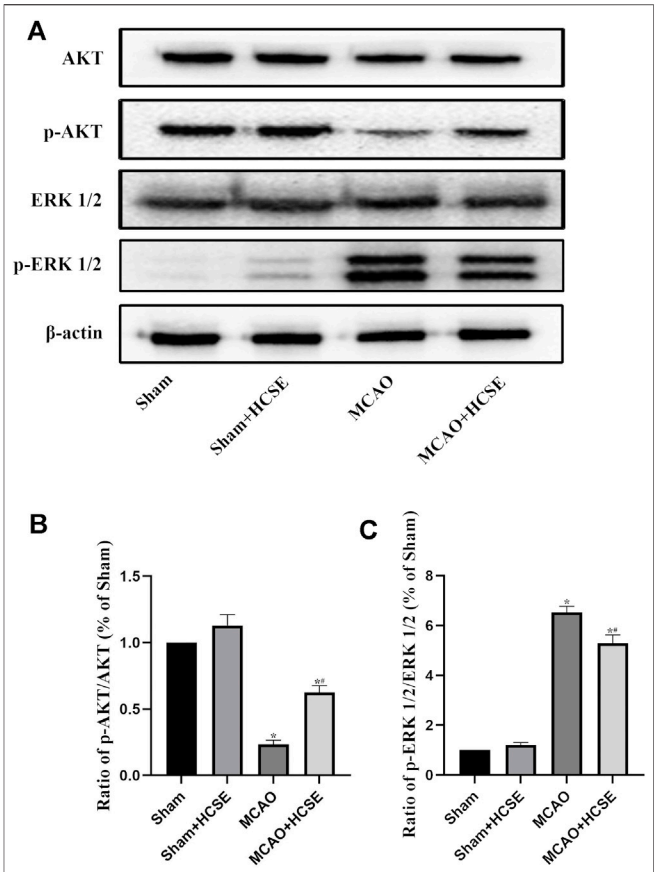

FIGURE 7 | Changes in the levels of proteins related to the AKT/p-AKT/ERK1/2/p-ERK 1/2 signaling pathway in the hippocampus. **(A)** Western blotting of related proteins. **(B)** The ratio of p-AKT/AKT. **(C)** The ratio of p-ERK 1/2/p-ERK 1/2. (n = 7 per group; *p < 0.05, significantly different from the corresponding Sham group, #p < 0.05, significantly different from the MCAO group).

higher than that in the MCAO group (p < 0.05), and the p-ERK 1/2/ERK 1/2 protein ratio was significantly lower than that in the MCAO group (p < 0.05). Western blot analyses of cortical tissues revealed the same trend as the hippocampal tissue. As shown in **Figure 8**, the p-AKT/AKT protein ratio in the MCAO + HCSE group was significantly higher than that in the MCAO group (p < 0.05). In addition, the p-ERK 1/2/ERK 1/2 protein ratio was significantly lower than that in the MCAO group (p < 0.05).

DISCUSSION

Although the treatment of stroke is rapidly evolving, research on the use of TCM to treat ischemic stroke is scarce. In the present study, we identified a new treatment formulation for ischemic stroke by the application of data mining and identified the mechanism of action of this treatment formulation using network pharmacology. The new formulation consists of Huangqi, Chuanxiong, SanLeng, and Ezhu. We concluded that the main active ingredients of the new formulation include trans-11-eicosenoic acid, ethyl linoleate, 7-O-methylisomucronulatol, myricanone, bisdemethoxycurcumin, wallichilide, astrapterocarpan, and kumatakenin. The active ingredients target a series of genes, including *MAPK3*, *MAPK1*, *HSP90AA*1, *STAT3*, *PIK3R1*, *PIK3CA* and *AKT1*, and can potentially regulate the PI3K/AKT, MAPK/ERK, Ras, cAMP and Rap1 signaling pathways to exert a neuroprotective role in patients with ischemic stroke, Qi deficiency and blood stasis syndrome. The cerebral protective effects of each of the drugs that constitutes HCSE have been extensively reported in previous studies; Huangqi promotes the proliferation of neural stem cells, Chuanxiong inhibits inflammation, Sanleng prevents the aggregation of platelets, and Ezhu inhibits autophagy (Huang et al., 2018; Fei Yin et al., 2020; Min Wang et al., 2020; Jia et al., 2021; Wang et al., 2021). In the present study, we found that HCSE effectively reduced cerebral infarcts and the neuronal dysfunction caused by ischemic stroke with Qi deficiency and blood stasis syndrome. KEGG pathway annotation suggested that

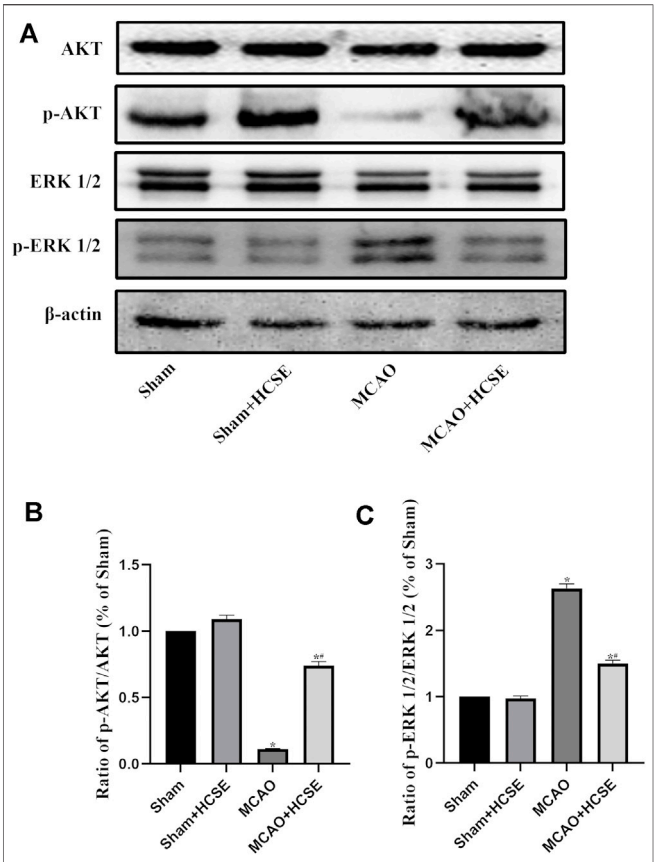

FIGURE 8 | Changes in the levels of proteins related to the AKT/p-AKT/ERK1/2/p-ERK1/2 signaling pathway in the cortex. **(A)** Western blotting of related proteins. **(B)** The ratio of p-AKT/AKT. **(C)** The ratio of p-ERK1/2/p-ERK 1/2. (n = 7 per group; *p < 0.05, significantly different from the corresponding Sham group, #p < 0.05, significantly different from the MCAO group).

the active ingredients of the new formulation exert beneficial effects by regulating the PI3K/AKT and MAPK signaling pathways. By analyzing the KEGG enrichment of these targets in ischemic stroke with Qi deficiency and blood stasis syndrome, we found that the PI3K/AKT and MAPK signaling pathway were the main pathways involved. Thus, by regulating the PI3K/AKT and MAPK signaling pathways, it may be possible to improve Qi and blood in patients with ischemic stroke.

The PI3K and MAPK signaling pathways are abnormally regulated in cerebral ischemia; by modulating these pathways, it is possible to alleviate the neuronal injury caused by ischemia (Tu et al., 2015). Research has also shown that HSP90 inhibitors protect against ischemia-induced neural progenitor cell death via the PI3K/AKT and MAPK/ERK pathways (Kwon et al., 2008; Wang et al., 2011; Bradley et al., 2014). On the one hand, the PI3K/AKT signaling pathway is known to play key roles in regulating cell proliferation, differentiation, apoptosis, and migration (Samakova et al., 2019) and is critical for neuronal growth and survival following cerebral ischemia (Zhao et al., 2016). Previous studies have reported that modulation of the PI3K/AKT/mTOR pathway upregulates the bcl-2 protein and increases ischemic tolerance in the semi-dark zone, thereby reducing apoptosis, increasing VEGF expression, and promoting cerebral angiogenesis (Hou et al., 2018; Liang et al., 2018). On the other hand, the extracellular signal-regulated kinases MAPK1/ERK2 and MAPK3/ERK1 are members of the MAP kinase family and are involved in cell proliferation, differentiation, transcriptional regulation, and apoptosis. A series of cascade reactions are known to be involved in ischemic stroke (Sun and Nan, 2016). Numerous previous studies have shown that the MAPK/ERK signaling pathway disrupts the blood-brain barrier, affects neurocyte apoptosis, and enhances the expression of neuronal inflammatory factors after ischemic stroke (Irving et al., 2000; Cao et al., 2016; Wang et al., 2019). The downregulation of MAPK1 has been shown to reduce the levels of TNF-α, IL-6, and reactive oxygen species, thereby reducing neuroinflammation, oxidative stress, and neuronal damage (Zhang et al., 2020). In a previous study, Mostajeran found that inhibition of the ERK signaling pathway by U0126 reduced neuronal death and significantly upregulated the expression of Tie-2, thereby promoting post-stroke vascular stabilization and angiogenesis (Mostajeran et al., 2017).

The cascade response of the PI3K and MAPK signaling pathways is regulated by complex feedback and crosstalk mechanisms. Zhou et al. reported negative crosstalk between the MAPK and PI3K/AKT signaling pathways, with AKT inhibiting the MAPK signaling pathway by phosphorylating and inhibiting the Raf1 node during cerebral ischemia (Zhou et al., 2015). This is consistent with the results of the present study, in which phosphorylated AKT levels were significantly lower, and phosphorylated ERK 1/2 levels were significantly higher, in mice suffering from ischemic stroke. Levels of phosphorylated AKT were increased while levels of phosphorylated ERK 1/2 were decreased in mice with ischemic stroke when treated with HCSE. We suggest that HCSE protects against post-ischemic injury not only by reducing ERK activity, but also by increasing crosstalk between AKT and ERK. The reduction in ERK activity exerts cerebral protective effects.

In summary, we used data mining and network pharmacological target prediction to identify a new treatment formulation (HCSE) for patients suffering from ischemic stroke with Qi deficiency and blood stasis syndrome. HCSE significantly reduced infarct volume and improved neurological function. We found that multiple target genes and pathways participated in the action of HCSE against cerebral ischemia stroke. The mechanisms underlying the neuroprotective effects of HCSE were closely related to activation of the PI3K/AKT and MAPK/ERK signaling pathways. Our results provided evidence for the positive effects of HCSE on ischemic stroke with Qi deficiency and blood stasis syndrome. However, further research now needs to verify the mechanisms underlying the action of HSCE on the improvement of cerebral ischemic injury *via* the regulation of the PI3K/AKT and MAPK/ERK pathways; it is possible that other neuroprotective mechanisms are involved. In addition, it is important to investigate the internal mechanisms that link Qi deficiency, blood stasis syndrome and cerebral ischemic injury, as this could provide a more enhanced theoretical basis for the prevention and treatment of stroke with TCM.

DATA AVAILABILITY STATEMENT

The raw data supporting the conclusion of this article will be made available by the authors, without undue reservation.

ETHICS STATEMENT

The animal study was reviewed and approved by And all experimental investigation procedures were authorized by the Yangzhou University Institutional Animal Care and Use Committee (YIACUC-14–0015).

AUTHOR CONTRIBUTIONS

LZ performed the experiments, LZ and LDD drafted the manuscript. ZHX, PS, MMS, LDD, and ZC analyzed the data; BCY designed the experiments. All authors have discussed the results, reviewed the manuscript and approved the final version for publication.

FUNDING

This work was partially supported by the National Natural Science Foundation of China (81401005).

REFERENCES

Bardou, P., Mariette, J., Escudié, F., Djemiel, C., and Klopp, C. (2014). Jvenn: an Interactive Venn Diagram Viewer. *BMC Bioinformatics* 15, 293. doi:10.1186/1471-2105-15-293

Bradley, E., Zhao, X., Wang, R., Brann, D., Bieberich, E., and Wang, G. (2014). Low Dose Hsp90 Inhibitor 17AAG Protects Neural Progenitor Cells from Ischemia Induced Death. *J. Cel. Commun Signal* 8 (4), 353–362. doi:10.1007/s12079-014-0247-5

Cao, G., Jiang, N., Hu, Y., Zhang, Y., Wang, G., Yin, M., et al. (2016). Ruscogenin Attenuates Cerebral Ischemia-Induced Blood-Brain Barrier Dysfunction by Suppressing TXNIP/NLRP3 Inflammasome Activation and the MAPK Pathway. *Int. J. Mol. Sci.* 17 (9), 1418. doi:10.3390/ijms17091418

Daina, A., Michielin, O., and Zoete, V. (2019). SwissTargetPrediction: Updated Data and New Features for Efficient Prediction of Protein Targets of Small Molecules. *Nucleic Acids Res.* 47 (W1), W357–W364. doi:10.1093/nar/gkz382

Fei Yin, F., Zhou, H., Fang, Y., Li, C., He, Y., Yu, L., et al. (2020). Astragaloside IV Alleviates Ischemia Reperfusion-Induced Apoptosis by Inhibiting the Activation of Key Factors in Death Receptor Pathway and Mitochondrial Pathway. *J. Ethnopharmacol.* 248, 112319. doi:10.1016/j.jep.2019.112319

Hou, Y., Wang, K., Wan, W., Cheng, Y., Pu, X., and Ye, X. (2018). Resveratrol Provides Neuroprotection by Regulating the JAK2/STAT3/PI3K/AKT/mTOR Pathway after Stroke in Rats. *Genes Dis.* 5 (3), 245–255. doi:10.1016/j.gendis.2018.06.001

Huang, L., Chen, C., Zhang, X., Li, X., Chen, Z., Yang, C., et al. (2018). Neuroprotective Effect of Curcumin against Cerebral Ischemia-Reperfusion via Mediating Autophagy and Inflammation. *J. Mol. Neurosci.* 64 (1), 129–139. doi:10.1007/s12031-017-1006-x

Irving, E. A., Barone, F. C., Reith, A. D., Hadingham, S. J., and Parsons, A. A. (2000). Differential Activation of MAPK/ERK and P38/SAPK in Neurones and Glia Following Focal Cerebral Ischaemia in the Rat. *Brain Res. Mol. Brain Res.* 77 (1), 65–75. doi:10.1016/s0169-328x(00)00043-7

Jia, J., Li, X., Ren, X., Liu, X., Wang, Y., Dong, Y., et al. (2021). Sparganii Rhizoma: A Review of Traditional Clinical Application, Processing, Phytochemistry, Pharmacology, and Toxicity. *J. Ethnopharmacol.* 268, 113571. doi:10.1016/j.jep.2020.113571

Kwon, H. M., Kim, Y., Yang, S. I., Kim, Y. J., Lee, S. H., and Yoon, B. W. (2008). Geldanamycin Protects Rat Brain through Overexpression of HSP70 and Reducing Brain Edema after Cerebral Focal Ischemia. *Neurol. Res.* 30 (7), 740–745. doi:10.1179/174313208X289615

Li, S., and Zhang, B. (2013). Traditional Chinese Medicine Network Pharmacology: Theory, Methodology and Application. *Chin. J. Nat. Med.* 11 (2), 110–120. doi:10.1016/S1875-5364(13)60037-0

Li, S. M., Xu, H., and Chen, K. J. (2014). The Diagnostic Criteria of Blood-Stasis Syndrome: Considerations for Standardization of Pattern Identification. *Chin. J. Integr. Med.* 20 (7), 483–489. doi:10.1007/s11655-014-1803-9

Liang, Z., Chi, Y. J., Lin, G. Q., Luo, S. H., Jiang, Q. Y., and Chen, Y. K. (2018). MiRNA-26a Promotes Angiogenesis in a Rat Model of Cerebral Infarction via PI3K/AKT and MAPK/ERK Pathway. *Eur. Rev. Med. Pharmacol. Sci.* 22 (11), 3485–3492. doi:10.26355/eurrev_201806_15175

Liu, S. Z., Bao, Z. X., and Zhang, R. L. (2007). Theory Discuss of the Pathogenesis Theory of Deficiency of Qi and Blood Stasis in Lschemic Stroke. *Chin. Arch. Tradit. Chin.* 25, 97–98. doi:10.13193/j.archtcm.2007.01.99.liuszh.040

Liu, Y., Yin, H. J., Shi, D. Z., and Chen, K. J. (2012). Chinese Herb and Formulas for Promoting Blood Circulation and Removing Blood Stasis and Antiplatelet Therapies. *Evid. Based Complement. Alternat Med.* 2012, 184503. doi:10.1155/2012/184503

Liu, D., Bai, X., Ma, W., Xin, D., Chu, X., Yuan, H., et al. (2020). Purmorphamine Attenuates Neuro-Inflammation and Synaptic Impairments after Hypoxic-Ischemic Injury in Neonatal Mice via Shh Signaling. *Front. Pharmacol.* 11, 204. doi:10.3389/fphar.2020.00204

Liu, J., Wang, F., Sheng, P., Xia, Z., Jiang, Y., and Yan, B. C. (2021). A Network-Based Method for Mechanistic Investigation and Neuroprotective Effect on Treatment of Tanshinone I against Ischemic Stroke in Mouse. *J. Ethnopharmacol.* 272, 113923. doi:10.1016/j.jep.2021.113923

Wang, M., Yao, M., Liu, J., Takagi, N., Yang, B., Zhang, M., et al. (2020). Ligusticum Chuanxiong Exerts Neuroprotection by Promoting Adult Neurogenesis and Inhibiting Inflammation in the hippocampus of ME Cerebral Ischemia Rats. *J. Ethnopharmacol.* 249, 112385. doi:10.1016/j.jep.2019.112385

Mostajeran, M., Edvinsson, L., Warfvinge, K., Singh, R., and Ansar, S. (2017). Inhibition of Mitogen-Activated Protein Kinase 1/2 in the Acute Phase of Stroke Improves Long-Term Neurological Outcome and Promotes Recovery Processes in Rats. *Acta Physiol. (Oxf)* 219 (4), 814–824. doi:10.1111/apha.12632

Mukundan, G., and Seidenwurm, D. J. (2018). Economic and Societal Aspects of Stroke Management. *Neuroimaging Clin. N. Am.* 28 (4), 683–689. doi:10.1016/j.nic.2018.06.009

Reagan-Shaw, S., Nihal, M., and Ahmad, N. (2008). Dose Translation from Animal to Human Studies Revisited. *FASEB J.* 22 (3), 659–661. doi:10.1096/fj.07-9574LSF

Ru, J., Li, P., Wang, J., Zhou, W., Li, B., Huang, C., et al. (2014). TCMSP: a Database of Systems Pharmacology for Drug Discovery from Herbal Medicines. *J. Cheminform* 6, 13. doi:10.1186/1758-2946-6-13

Safran, M., Rosen, N., Twik, M., BarShir, R., Stein, T. I., Dahary, D., et al. (2021). "The GeneCards Suite," in *Practical Guide to Life Science Databases*. Editors I. Abugessaisa and T. Kasukawa. (Singapore: Springer), 27–56. doi:10.1007/978-981-16-5812-9_2

Samakova, A., Gazova, A., Sabova, N., Valaskova, S., Jurikova, M., and Kyselovic, J. (2019). The PI3k/Akt Pathway Is Associated with Angiogenesis, Oxidative Stress and Survival of Mesenchymal Stem Cells in Pathophysiologic Condition in Ischemia. *Physiol. Res.*68, S131–S138. doi:10.33549/physiolres.934345

Sun, J., and Nan, G. (2016). The Mitogen-Activated Protein Kinase (MAPK) Signaling Pathway as a Discovery Target in Stroke. *J. Mol. Neurosci.* 59 (1), 90–98. doi:10.1007/s12031-016-0717-8

Sun, J. H., Sun, F., Yan, B., Li, J. Y., and Xin, L. (2020). Data Mining and Systematic Pharmacology to Reveal the Mechanisms of Traditional Chinese Medicine in Mycoplasma Pneumoniae Pneumonia Treatment. *Biomed. Pharmacother.* 125, 109900. doi:10.1016/j.biopha.2020.109900

Tang, Y., Li, M., Wang, J., Pan, Y., and Wu, F. X. (2015). CytoNCA: a Cytoscape Plugin for Centrality Analysis and Evaluation of Protein Interaction Networks. *Biosystems* 127, 67–72. doi:10.1016/j.biosystems.2014.11.005

Tu, X. K., Yang, W. Z., Chen, J. P., Chen, Y., Chen, Q., Chen, P. P., et al. (2015). Repetitive Ischemic Preconditioning Attenuates Inflammatory Reaction and Brain Damage after

Focal Cerebral Ischemia in Rats: Involvement of PI3K/Akt and ERK1/2 Signaling Pathway. *J. Mol. Neurosci.* 55 (4), 912–922. doi:10.1007/s12031-014-0446-9

Wang, G., Krishnamurthy, K., and Tangpisuthipongsa, D. (2011). Protection of Murine Neural Progenitor Cells by the Hsp90 Inhibitor 17-Allylamino-17-Demethoxygeldanamycin in the Low Nanomolar Concentration Range. *J. Neurochem.* 117 (4), 703–711. doi:10.1111/j.1471-4159.2011.07239.x

Wang, W., Jiang, B., Sun, H., Ru, X., Sun, D., Wang, L., et al. (2017). Prevalence, Incidence, and Mortality of Stroke in China: Results from a Nationwide Population-Based Survey of 480 687 Adults. *Circulation* 135 (8), 759–771. doi:10.1161/CIRCULATIONAHA.116.025250

Wang, Q. C., Lu, L., and Zhou, H. J. (2019). Relationship between the MAPK/ERK Pathway and Neurocyte Apoptosis after Cerebral Infarction in Rats. *Eur. Rev. Med. Pharmacol. Sci.* 23 (12), 5374–5381. doi:10.26355/eurrev_201906_18206

Wang, Y., Liu, X., Hu, T., Li, X., Chen, Y., Xiao, G., et al. (2021). Astragalus Saponins Improves Stroke by Promoting the Proliferation of Neural Stem Cells through Phosphorylation of Akt. *J. Ethnopharmacol* 277, 114224. doi:10.1016/j.jep.2021.114224

Chen, X., Chen, H., He, Y., Fu, S., Liu, H., Wang, Q., et al. (2020). Proteomics-Guided Study on Buyang Huanwu Decoction for its Neuroprotective and Neurogenic Mechanisms for Transient Ischemic Stroke: Involvements of EGFR/PI3K/Akt/Bad/14-3-3 and Jak2/Stat3/Cyclin D1 Signaling Cascades. *Mol. Neurobiol.* 57 (10), 4305–4321. doi:10.1007/s12035-020-02016-y

Xi, S., Qian, L., Tong, H., Yue, L., Zhao, H., Wang, D., et al. (2013). Toxicity and Clinical Reasonable Application of Taoren (Semen Persicae) Based on Ancient and Modern Literature Research. *J. Tradit Chin. Med.* 33 (2), 272–279. doi:10.1016/s0254-6272(13)60139-9

Xu, H. Y., Zhang, Y. Q., Liu, Z. M., Chen, T., Lv, C. Y., Tang, S. H., et al. (2019). ETCM: an Encyclopaedia of Traditional Chinese Medicine. *Nucleic Acids Res.* 47 (D1), D976–D982. doi:10.1093/nar/gky987

Chen, Y., Wright, N., Guo, Y., Turnbull, I., Kartsonaki, C., Yang, L., et al. (2020). Mortality and Recurrent Vascular Events after First Incident Stroke: a 9-year Community-Based Study of 0·5 Million Chinese Adults. *Lancet Glob. Health* 8 (4), e580–e590. doi:10.1016/S2214-109X(20)30069-3

Wang, Y., Zhang, L., Pan, Y. J., Fu, W., Huang, S. W., Xu, B., et al. (2020). Investigation of Invigorating Qi and Activating Blood Circulation Prescriptions in Treating Qi Deficiency and Blood Stasis Syndrome of Ischemic Stroke Patients: Study Protocol for a Randomized Controlled Trial. *Front. Pharmacol.* 11, 892. doi:10.3389/fphar.2020.00892

Yin, B., Bi, Y. M., Fan, G. J., and Xia, Y. Q. (2020). Molecular Mechanism of the Effect of Huanglian Jiedu Decoction on Type 2 Diabetes Mellitus Based on Network Pharmacology and Molecular Docking. *J. Diabetes Res.* 2020, 5273914. doi:10.1155/2020/5273914

Zhai, X., Wang, X., Wang, L., Xiu, L., Wang, W., and Pang, X. (2020). Treating Different Diseases with the Same Method-A Traditional Chinese Medicine Concept Analyzed for its Biological Basis. *Front. Pharmacol.* 11, 946. doi:10.3389/fphar.2020.00946

Zhang, L., Wang, J., Liu, Q., Xiao, Z., and Dai, Q. (2020). Knockdown of Long Non-coding RNA AL049437 Mitigates MPP+ -induced Neuronal Injury in SH-Sy5y Cells via the microRNA-205-5p/MAPK1 axis. *Neurotoxicology* 78, 29–35. doi:10.1016/j.neuro.2020.02.004

Zhang, J., Rui, Y., Gao, M., Wang, L., and Yan, B. C. (2021). Expression of Long Non-coding RNA RGD1566344 in the Brain Cortex of Male Mice after Focal Cerebral Ischemia-Reperfusion and the Neuroprotective Effect of a Non-coding RNA RGD1566344 Inhibitor. *Cell Mol Neurobiol* 41 (4), 705–716. doi:10.1007/s10571-020-00877-4

Zhao, E. Y., Efendizade, A., Cai, L., and Ding, Y. (2016). The Role of Akt (Protein Kinase B) and Protein Kinase C in Ischemia-Reperfusion Injury. *Neurol. Res.* 38 (4), 301–308. doi:10.1080/01616412.2015.1133024

Zhou, J., Du, T., Li, B., Rong, Y., Verkhratsky, A., and Peng, L. (2015). Crosstalk between MAPK/ERK and PI3K/AKT Signal Pathways during Brain Ischemia/Reperfusion. *ASN Neuro* 7 (5), 1759091415602463. doi:10.1177/1759091415602463

Zhou, Y., Zhou, B., Pache, L., Chang, M., Khodabakhshi, A. H., Tanaseichuk, O., et al. (2019). Metascape Provides a Biologist-Oriented Resource for the Analysis of Systems-Level Datasets. *Nat. Commun.* 10 (1), 1523. doi:10.1038/s41467-019-09234-6

Conflict of Interest: The authors declare that the research was conducted in the absence of any commercial or financial relationships that could be construed as a potential conflict of interest.

Publisher's Note: All claims expressed in this article are solely those of the authors and do not necessarily represent those of their affiliated organizations, or those of the publisher, the editors and the reviewers. Any product that may be evaluated in this article, or claim that may be made by its manufacturer, is not guaranteed or endorsed by the publisher.

GLOSSARY

AKT Protein Kinase B

BBB Blood-Brain Barrier

BC Betweenness Centrality

BCA Bicinchonininc Acid

bcl-2 B-Cell Lymphoma-2

BP Biological Process

BSA Bovine Serum Albumin

cAMP Cyclic Adenosine Monophosphate

CC Cellular ComponentCloseness Centrality

CC Cellular ComponentCloseness Centrality

CCA Common Carotid artery

DC Degree Centrality

DL Drug-Likeness

EC Eigenvector Centrality

ECA External Carotid artery

ERK Extracellular Regulated Protein Kinases 1 and 2

FDR False Discovery Rate

GO Gene Ontology

HCSE Huangqi-Chuanxiong and Sanleng-Ezhu

HSP90 Heat Shock Protein 90

HSP90AA1 Heat Shock Protein 90 Alpha Family Class A Member 1

ICA Internal Carotid artery

ICR Institute of Cancer Research

IL6 Interleukin 6

KEGG Kyoto Encyclopedia of Genes and Genomes

MAPK Mitogen-Activated Protein Kinases

MAPK1 Mitogen-Activated Protein Kinase 1

MAPK3 Mitogen-Activated Protein Kinase 3

MCAO Middle Cerebral artery Occlusion

MF Molecular Functions

mTOR Mechanistic Target of Rapamycin Kinase

OB Oral Bioavailability

p-AKT Phospho-Protein kinase B

p-ERK1/2 Phospho-Extracellular Regulated Protein Kinases 1 and 2

PI3K Phosphoinositide 3-kinase

PIK3CA Phosphatidylinositol-4,5-Bisphosphate 3-Kinase Catalytic Subunit Alpha

PIK3R1 Phosphoinositide-3-Kinase Regulatory Subunit 1

PPI Protein-Protein Interaction

Raf1 Raf-1 Proto-Oncogene, Serine/Threonine Kinase

Ras Rat Sarcoma

SDS-PAGE Sodium Dodecyl Sulfate Polyacrylamide Gel Electrophoresis

STAT3 Signal Transducer and Activator of Transcription 3

TBS Tris Buffered Saline

TCM Traditional Chinese Medicine

Tie-2 Tyrosine-Protein Kinase

TNF-α Tumor Necrosis Factor-α

TTC 2, 3, 5-Triphenyl Tetrazolium Chloride

VEGF Vascular Endothelial Growth Factor

frontiers | Frontiers in Pharmacology

ORIGINAL RESEARCH
published: 01 April 2022
doi: 10.3389/fphar.2022.832611

Acute Administration of Metformin Protects Against Neuronal Apoptosis Induced by Cerebral Ischemia-Reperfusion Injury *via* Regulation of the AMPK/CREB/BDNF Pathway

Ke Liu[1†], Lulu Li[2†], Zhijun Liu[1†], Gang Li[1], Yanqing Wu[1], Xingjun Jiang[1], Mengdie Wang[1], Yanmin Chang[1], Tingting Jiang[1], Jianheng Luo[1], Jiahui Zhu[1], Hongge Li[1] and Yong Wang[1]**

[1]Department of Neurology, Union Hospital, Tongji Medical College, Huazhong University of Science and Technology, Wuhan, China, [2]Department of Neurology, People's Hospital of Zhengzhou, People's Hospital of Henan University of Chinese Medicine, Zhengzhou, China

Metformin is a first-line anti-diabetic agent with a powerful hypoglycemic effect. Several studies have reported that metformin can improve the prognosis of stroke patients and that this effect is independent of its hypoglycemic effect; however, the specific mechanism remains unclear. In this research, we explored the effect and specific mechanism of metformin in cerebral ischemia-reperfusion (I/R) injury by constructing a transient middle cerebral artery occlusion model *in vivo* and a glucose and oxygen deprivation/reoxygenation (OGD/R) model *in vitro*. The results of the *in vivo* experiments showed that acute treatment with low-dose metformin (10 mg/kg) ameliorated cerebral edema, reduced the cerebral infarction volume, improved the neurological deficit score, and ameliorated neuronal apoptosis in the ischemic penumbra. Moreover, metformin up-regulated the brain-derived neurotrophic factor (BDNF) expression and increased phosphorylation levels of AMP-activated protein kinase (AMPK) and cAMP-response element binding protein (CREB) in the ischemia penumbra. Nevertheless, the above-mentioned effects of metformin were reversed by Compound C. The results of the *in vitro* experiments showed that low metformin concentrations (20 μM) could reduce apoptosis of human umbilical vein endothelial cells (HUVECs) under OGD/R conditions and promote cell proliferation. Moreover, metformin could further promote BDNF expression and release in HUVECs under OGD/R conditions *via* the AMPK/CREB pathway. The Transwell chamber assay showed that HUVECs treated with metformin could reduce apoptosis of SH-SY5Y cells under OGD/R conditions and this effect could be partially reversed by transfection of BDNF siRNA in HUVECs. In summary, our results suggest that metformin upregulates the level of BDNF in the cerebral ischemic penumbra *via* the AMPK/CREB pathway, thereby playing a protective effect in cerebral I/R injury.

Keywords: cerebral ischemia-reperfusion injury, metformin, AMP-activated protein kinase, neuronal apoptosis, brain-derived neurotrophic factor

OPEN ACCESS

Edited by:
Yongjun Sun,
Hebei University of Science and Technology, China

Reviewed by:
Yuxiang Fei,
China Pharmaceutical University, China
Junke Song,
Chinese Academy of Medical Sciences and Peking Union Medical College, China

****Correspondence:***
Hongge Li
hgeli0609@163.com
Yong Wang
370687495@qq.com

[†]These authors have contributed equally to this work

Specialty section:
This article was submitted to Neuropharmacology, a section of the journal Frontiers in Pharmacology

Received: *10 December 2021*
Accepted: *28 February 2022*
Published: *01 April 2022*

Citation:
Liu K, Li L, Liu Z, Li G, Wu Y, Jiang X, Wang M, Chang Y, Jiang T, Luo J, Zhu J, Li H and Wang Y (2022) Acute Administration of Metformin Protects Against Neuronal Apoptosis Induced by Cerebral Ischemia-Reperfusion Injury via Regulation of the AMPK/CREB/BDNF Pathway. Front. Pharmacol. 13:832611. doi: 10.3389/fphar.2022.832611

INTRODUCTION

Acute ischemic stroke is the most prevailing type of cerebrovascular disease. Due to its high morbidity, mortality, and disability, it has received widespread attention and imposes a substantial burden on national health and the social economy. Intravenous recombinant tissue plasminogen activator thrombolysis (National Institute of Neurological Disorders and Stroke rt-PA Stroke Study Group, 1995) and mechanical arterial thrombectomy (Goyal et al., 2015; Campbell et al., 2015; Berkhemer et al., 2015) are currently the most efficient treatments for opening occluded blood vessels and restoring cerebral blood perfusion. However, rapid reperfusion after cerebral ischemia can cause secondary damage, named cerebral ischemia-reperfusion (I/R) injury, which is even more serious than simple cerebral ischemic injury. Cerebral I/R injury often results in the death of a large number of neurons, leading to widespread cerebral infarction and severe cognitive dysfunction (Lin et al., 2016). Therefore, there is an urgent need to identify the pathogenesis of cerebral I/R injury and find effective therapies.

The neurovascular unit is a concept that emphasizes the interaction between the cerebrovascular system and brain tissue cells, which contains neurons, vascular endothelial cells (ECs), glial cells, and the basement membrane (Iadecola, 2017). As one of the central components of the neurovascular unit, ECs can not only provide blood flow and nutrients for the brain but also play a neuroprotective role by secreting neurotrophic factors. This effect of ECs is known as nerve-vascular coupling (Guo et al., 2008; Alhusban et al., 2013; Fouda et al., 2017). Neurotrophic factors play a crucial role in the nervous system *via* regulating the survival and differentiation of neurons (Mizui et al., 2016). Brain-derived neurotrophic factor (BDNF), as a member of neurotrophic factors, has powerful neurogenesis, neuroprotection, and angiogenesis effects (Caporali and Emanueli, 2009; Greenberg et al., 2009) and is also relevant to learning and memory (Tyler et al., 2002; Bekinschtein et al., 2014). Some studies have found that BDNF is involved in the nerve-vascular coupling between ECs and nerve cells (Guo et al., 2008). Furthermore, several studies have shown that BDNF can be upregulated and has an important neuroprotective effect after experimental stroke (Guo et al., 2008; Alhusban et al., 2013; Fouda et al., 2017).

Metformin, a first-line biguanide drug, is widely used in patients with type 2 diabetes because of its hypoglycemic effect. Several clinical studies have revealed that metformin can also improve the prognosis of stroke patients (Mima et al., 2016) and decrease the risk of long-term cardiovascular events (UK Prospective Diabetes Study (UKPDS) Group, 1998; Nathan, 1998; Selvin and Hirsch, 2008). Furthermore, the activation of AMP-activated protein kinase (AMPK) plays a dominant role in the protective effect of metformin (Alexander et al., 2013). Related studies have shown that AMPK is a vital endogenous defense factor that plays a protective effect in ischemic stroke *via* alleviating neuroinflammation, reducing oxidative stress, improving mitochondrial dysfunction, and inhibiting cell apoptosis (Jiang et al., 2018). Metformin has also been confirmed in many studies to promote phosphorylation of AMPK protein, thereby exerting neuroprotective effects by activating downstream molecules that reduce the adverse influences of cerebral I/R injury (Ashabi et al., 2014; Venna et al., 2014; Ashabi et al., 2015).

The specific mechanism by which metformin alleviates cerebral I/R injury remains ambiguous. Nevertheless, various *in vivo* and *ex vivo* experimental models have shown that metformin can promote BDNF expression (Patil et al., 2014; Han et al., 2018; Keshavarzi et al., 2019). Subsequently, we hypothesized that metformin can upregulate BDNF expression to exert a neuroprotective effect, thus alleviating cerebral I/R injury in an experimental model of ischemic stroke. Our study aimed to further understand the mechanism by which metformin improves cerebral I/R injury and to provide new evidence and support for metformin as a therapy that can be synchronized with vascular recanalization as a treatment for acute cerebral infarction.

MATERIALS AND METHODS

Animals

Male specific pathogen-free Sprague-Dawley rats (age, 6–8 weeks; weight, 280–300 g) were purchased from Sipeifu Biotechnology Co., Ltd. (Beijing, China). During the experiments, two rats per cage were housed in a specific pathogen-free environment (temperature 21–24°C, humidity 55%–65% and a 12-h light/dark cycle) with free access to food and water. All experiments were performed in accordance with the Experimental Animal Management Committee of Tongji Medical College of Huazhong University of Science and Technology (IACUC Number: 2499).

Construction of a tMCAO Model and Drug Administration *in vivo*

After anesthesia with 2% sodium pentobarbital (40 mg/kg, i.p.), a transient middle cerebral artery occlusion (tMCAO) rodent model was constructed based on previous studies (Yuan et al., 2016). In brief, a neck incision was made, the common carotid artery was exposed, and the internal carotid and external carotid arteries were then carefully separated. Next, the blood flow in the right middle cerebral artery was blocked with a 4-0 monofilament nylon suture (Cinontech, Beijing, China) coated with poly-L-lysine. Thereafter, the sutures were pulled out after 60 min of ischemia. At the beginning of the reperfusion period, rats in each group were administered metformin (10 mg/kg, i.p.; Sigma-Aldrich, United States) and Compound C (CC, 20 mg/kg, i.p.; an AMPK inhibitor, APExBIO, United States), according to the experimental design (the specific experimental groups are shown in **Figure 1**). The concentration and mode of administration of metformin and Compound C were based on previous research by Jiang et al. (2014). The sham operation group underwent the same surgical procedure except for the insertion of the suture and received an equal volume of the vehicle at the beginning of the reperfusion period. All rats were euthanized 24 h after the reperfusion period, then the brain tissues of the ischemic core, the ischemic penumbra, and the contralateral cerebral

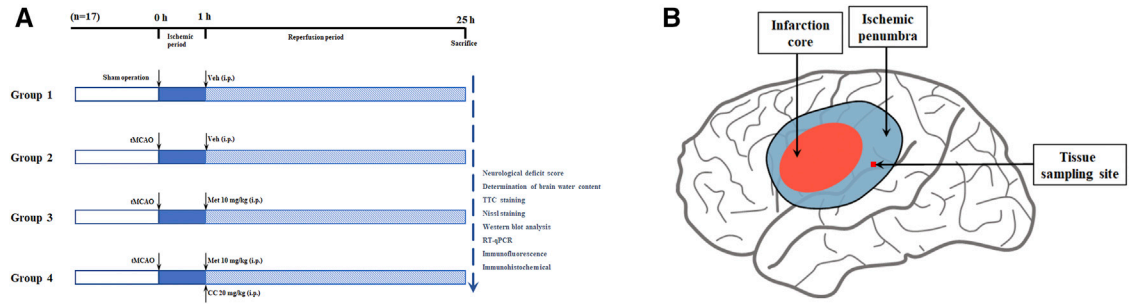

FIGURE 1 | Schematic diagram of animal experiment groupings and ischemic penumbra. **(A)** The schematic diagram of animal experiment groupings (n = 17 in each group). Abbreviations: tMCAO, transient middle cerebral artery occlusion; Veh, vehicle; Met, metformin; CC, Compound C. **(B)** The schematic diagram of ischemic penumbra.

hemisphere were collected and stored at -80°C for later use. The body temperature of rats was maintained at 37.1 ± 0.5°C from after anesthesia to before euthanasia with a heating pad.

Neurological Deficit Score

After successful modeling, all rats were evaluated for neurological deficits using the Zea-Longa five-point scoring system (Longa et al., 1989) before they were euthanized: 0 points, normal; 1 point, weakness of the left forelimb and incomplete extension; 2 points, turning to the left side when walking; 3 points, cannot bear weight on the left side; and 4 points, no spontaneous activity, and disturbed consciousness.

TTC Staining

After the rats were euthanized, the volume of cerebral infarction was measured using the 2,3,5-triphenyltetrazolium chloride (TTC) staining method. Briefly, the brain was removed and rapidly frozen in a refrigerator at -20°C for 20 min and cut into 6–7 slices of 2-mm thickness. Next, the slices were stained with 2% TTC solution for 20 min. The volume of cerebral infarction was measured *via* an Image-Pro Plus analysis system.

Determination of Brain Water Content

We used our previous experiments (Wang et al., 2018) to determine the water content of the brain tissue and evaluate brain edema in the rats in each group. After the brains were taken out and the cerebellum and brain stem were removed, wet weights (WW) were obtained. Next, the dry weights (DW) were obtained after the brain was dried in an oven at 100°C for 24 h. The brain water content was calculated *via* the following formula: brain water content (%) = (WW-DW)/WW×100%.

Immunohistochemical Analysis

After successful modeling, several rats were selected for anesthesia, followed by perfusion with normal saline and 4% paraformaldehyde. The brain was then taken out, embedded in paraffin, and cut coronally into 5-μm thick brain slices. Next, paraffin sections of the brain tissues in each group were deparaffinized by xylene and then rehydrated with gradient alcohol (100%, 95%, 80%, and 75%). The tissue sections were sequentially subjected to antigen retrieval (citric acid antigen retrieval buffer, high temperature, and pressure conditions), blocking endogenous peroxidase (3% H_2O_2 solution, protected from light for 25 min), and serum sealing (5% BSA solution, 40 min). The brain slices were then incubated with the prepared BDNF primary antibody (1:500; Abcam, United States) at 4°C for 18–24 h. After washing, brain slices were incubated with the secondary antibody of the corresponding species for 2 h. After washing again, the brain slices were developed by 3,3′-diaminobenzidine and counterstained with hematoxylin. Finally, after dehydration with gradient alcohol and transparent xylene, the brain slices were mounted with neutral gum for microscopic examination. Images were obtained using an Olympus photomicroscope (Nikon, Tokyo, Japan).

Nissl Staining

Paraffin sections were deparaffinized and rehydrated as previously described. Next, the brain slices were stained with Nissl solution, washed with distilled water, dried, and mounted with neutral gum. Finally, the slices were observed and images were acquired using the Olympus photomicroscope.

Cell Culture

Human umbilical vein endothelial cells (HUVECs) and SH-SY5Y cells were purchased from the China Center for Type Culture Collection (Hubei, China). Both types of cells were cultured in Dulbecco's modified Eagle's medium (DMEM; Gibco, Waltham, MA, United States) containing 10% fetal bovine serum and 1% penicillin-streptomycin solution (Solarbio, Beijing, China) and incubated in a humidified incubator filled with 5% CO_2 and 95% O_2 at 37°C.

Transfection With Small Interfering RNAs

BDNF small interfering RNA (siRNA) and negative control siRNA were obtained from Genomeditech (Shanghai, China). The BDNF siRNA sequence was as follows: 5′-GAAUUGGCUGGCGAUUCA UAA-3′ and 3′-CUUAACCGACCGCUAAGUAUU-5' (the blocking effect of BDNF siRNA is shown in **Supplementary Figure S3**). The HUVECs were cultured in the upper chamber. After the cells grew normally and the confluence reached 30–50%, transfection was performed according to the manufacturer's

protocols (RiboBio, Guangzhou, China) with a final concentration of 50 nM siRNA. The cells were used for the subsequent Transwell chamber assay 48 h after the transfection.

Construction of an OGD/R Model and Drug Administration *in vitro*

For oxygen-glucose deprivation (OGD), the cells were discarded from the original medium and rinsed twice with phosphate-buffered saline, glucose-free DMEM was added and then cultured in a humidified anaerobic incubator (containing 1% O_2, 5% CO_2, and 94% N_2) at 37°C to simulate the ischemic environment *in vitro*. In this study, HUVECs and SH-SY5Y cells were maintained under OGD conditions for 2, 4, 6, or 8 h and 0.5, 1, 2, or 4 h, respectively. The culture medium was then replaced with complete DMEM and the cells were placed in a normal incubator (containing 95% O_2 and 5% CO_2) at 37°C for reoxygenation for 12 h to mimic reperfusion *in vitro*. At the beginning of the reoxygenation phase, metformin (0, 5, 10, 20, 50, and 100 μM), AICAR (an AMPK agonist, 500 μM; MedChemExpress, China), Compound C (10 μM), and KG-501 (a CREB inhibitor, 25 μM; Sigma-Aldrich, United States) were added to the culture medium to treat HUVECs, and BDNF (0, 10, 20, 50, and 100 ng/ml; R&D Systems, United States) was added to treat SH-SY5Y cells in different groups. All cells were collected for later experiments at the end of the reoxygenation period.

Cell Counting Kit-8 Assay

Approximately 5,000 cells/well were seeded in a 96-well plate. After the cell processing of each well was completed, the original medium was discarded, and 100 μL of new DMEM and 10 μL of Cell Counting Kit-8 (CCK-8) solution (Dojindo Technologies, Japan) were added and incubated for 2 h. Finally, the absorbance of each well was measured at 450 nm by a microplate reader for subsequent analysis.

Western Blot Analysis

The brain tissue samples in the ischemic penumbra, and the processed HUVECs were homogenized in RIPA lysis buffer and then centrifuged to obtain tissue and cell proteins. The protein concentration was measured using the BCA protein assay kit (Beyotime, China), and 20 μg of protein was separated for electrophoresis. Proteins were then transferred to a 0.45-μm PVDF membrane (Merck, Germany). After blocking with 5% non-fat milk for 1 h at 18–20°C, the membranes were incubated with the corresponding primary antibodies at 4°C for 18–24 h. After washing three times, the membranes were incubated with secondary antibodies of the corresponding species for 1 h. Finally, the protein bands were visualized by chemiluminescence and analyzed using ImageJ software. The primary antibodies used in this study were as follows: AMPK (1:1000; CST, United States), p-AMPK (1:1000; Abcam, United States), CREB (1:1000; CST), p-CREB (1:1000; Abcam), BDNF (1:1000; Abcam), and GAPDH (1:3000; Proteintech, China).

Enzyme-Linked Immunosorbent Assay

Plasma samples were obtained by centrifuging the blood samples at 1,200 g for 10 min. To detect the BDNF concentration in the plasma of rats and culture supernatant of HUVECs, a BDNF enzyme-linked immunosorbent assay (ELISA) kit (Multi Sciences, China) was used according to the manufacturer's protocols.

Real-Time Quantitative PCR

TRIzol and reverse transcription kits (Takara, Japan) were used for RNA extraction and reverse transcription according to the manufacturer's instructions. ChamQ SYBR qPCR Master Mix (Vazyme, China), cDNA, and primers were mixed in the polymerase chain reaction (PCR) plate, after which the transcription level of BDNF was analyzed using the StepOnePlus real-time PCR System. The primers used in this experiment were as follows: actin (human, 5′-3′, forward/reverse), AGAGCTACGAGC TGCCTGAC and AGCACTGTGTTGGCGTACAG; BDNF (human, 5′-3′, forward/reverse) TGTTGGATGAGGACCAGA AAGTT and GCCTCCTCTTCTCTTTCTGCTGG; actin (rat, 5′-3′, forward/reverse) TTGTCACCAACTGGGACGATATGG and GGGTGTTGAAGGTCTCAAACATG; BDNF (rat, 5′-3′, forward/reverse) CAGGGGCATAGACAAAAG and CTTCCC CTTTTAATGGTC.

Immunofluorescence

Immunofluorescence was used to measure BDNF expression in ECs in the penumbra of cerebral ischemia. Paraffin sections of brain tissues were deparaffinized and rehydrated, and antigen retrieval and serum blocking were performed as described above. The cells were then incubated at 4°C with the CD31 (1:50; R&D Systems, United States) and BDNF (1:500; Abcam, United States) primary antibodies for 18–24 h. After washing, the samples were incubated with a fluorescent secondary antibody of the corresponding species for 1 h at 18–20°C. Finally, after DAPI staining, the slices were mounted with anti-fluorescence quenching mounting tablets and examined under a microscope.

Immunofluorescence staining was also performed to detect BDNF expression in HUVECs. The cells were seeded on slides and processed accordingly. After fixation, permeabilization and serum blocking, the cell slides were incubated at 4°C with the BDNF primary antibodies (1:500; Abcam, United States) for 18–24 h. After washing, the cell slides were incubated with a fluorescent secondary antibody of the corresponding species for 1 h at 18–20°C. Finally, after DAPI staining, the cell slices were mounted with anti-fluorescence quenching mounting tablets and examined under a microscope.

Analysis of Apoptosis

Apoptosis of neurons in the ischemic penumbra area *in vivo* and apoptosis of HUVECs and SH-SY5Y cells under OGD/R conditions *in vitro* was detected using a one-step TdT-mediated dUTP nick-end labeling (TUNEL) apoptosis assay kit (Beyotime, China) according to the manufacturer's instructions. Related steps are referred to in the immunofluorescence section. The primary antibody used was as follows: NeuN (1:100; Proteintech, China).

Apoptosis of HUVECs and SH-SY5Y cells under OGD/R conditions was also detected using the Annexin V-FITC/PI apoptosis kit (Multi Sciences, China). After the staining, the

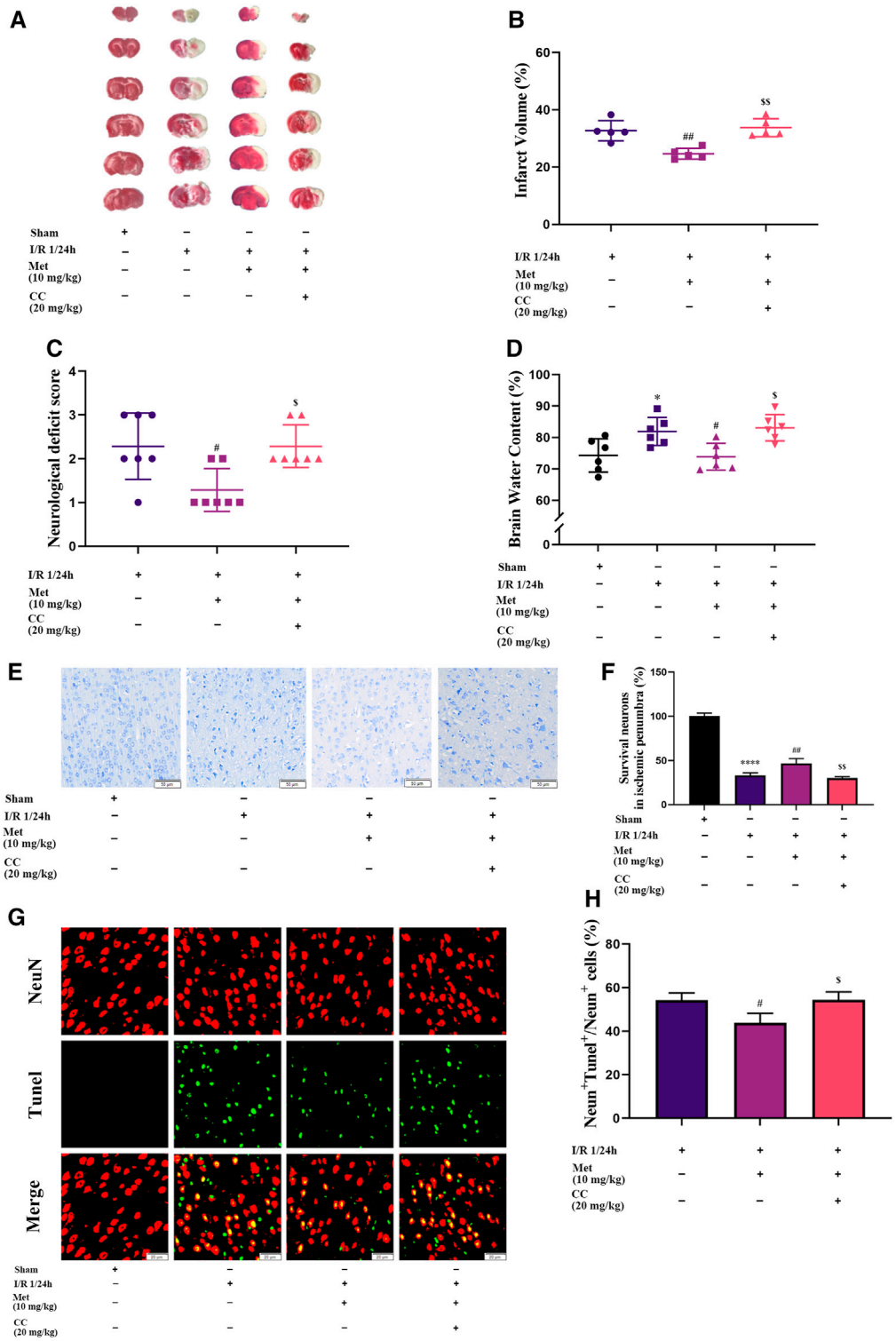

FIGURE 2 | Metformin alleviates cerebral edema, reduces cerebral infarct volume, improves the neurological deficit score, and ameliorates neuronal apoptosis in the ischemic penumbra. However, Compound C significantly reduces the above-mentioned effects of metformin. **(A,B)** Cerebral infarct volume was assessed by TTC staining ($n = 5$). **(C)** The neurological deficit score was assessed by the Zea-Longa five-point scoring system ($n = 7$). **(D)** Brain edema was evaluated by measuring the brain water content ($n = 6$). **(E–H)** Survival and apoptosis of neurons around the ischemic penumbra were evaluated by Nissl staining ($n = 3$, bar = 50 μm) and TUNEL staining ($n = 3$, bar = 20 μm), respectively. ($^{*}p < 0.05$, $^{****}p < 0.0001$ vs. sham; $^{\#}p < 0.05$, $^{\#\#}p < 0.01$ vs. I/R 1/24 h; $^{\$}p < 0.05$, $^{\$\$}p < 0.01$, vs. I/R 1/24 h + Met).

cells were immediately detected using a flow cytometer (BD Biosciences, United States). The results were analyzed by FlowJo software.

The Transwell chamber assay was used to explore the effect of metformin-treated HUVECs on apoptosis of SH-SY5Y cells under OGD/R conditions. Briefly, HUVECs were seeded in the upper chamber and exposed to OGD conditions for 5 h after transfection with siRNA. SH-SY5Y cells were then seeded in the lower chamber and co-cultured with HUVECs under OGD conditions for 1 h (from hour 5 to hour 6). Subsequently, HUVECs located in the upper chamber were treated accordingly at the beginning of the reoxygenation period (schematic representations of each treatment group are shown in **Figure 8A**and schematic diagram for transwell chamber assay is shown in **Supplementary Figure S2**). After a 12-h reoxygenation period, the cells in the lower chamber were collected and apoptosis rate was detected by flow cytometry and TUNEL staining.

Statistical Analysis

All data were analyzed using GraphPad Prism 8 software and expressed as the mean ± SD. Comparisons between two groups were performed by the independent-samples *t*-test. Pairwise comparisons between multiple groups were performed by ordinary one-way analysis of variance and Tukey's multiple comparisons test. Neurological deficit scores were compared between groups using the Mann-Whitney *U* test. $p < 0.05$ was considered statistically significant.

RESULTS

Metformin Alleviated Cerebral Edema, Reduced the Volume of Cerebral Infarction, Improved the Neurological Deficit Score, and Ameliorated Neuronal Apoptosis in the Ischemic Penumbra *in vivo*

To explore the function of metformin on cerebral I/R injury *in vivo*, brain edema, the volume of cerebral infarction, and the neurological deficit score were subjected to statistical analysis after the reperfusion period. As shown in **Figure 2C**, treatment with metformin dramatically improved the neurological deficit score after cerebral I/R injury *in vivo*. In addition, after the administration of metformin, cerebral edema improved remarkably (**Figure 2D**). TTC staining revealed that the volume of cerebral infarction was also dramatically reduced by treatment with metformin (**Figures 2A,B**). Nissl staining implied that the number of normal neurons in the ischemic penumbra was significantly higher in the metformin group than in the operation group (**Figures 2E,F**). Moreover, TUNEL staining showed that apoptosis of neurons in the metformin group was markedly reduced (**Figures 2G,H**). However, it is intriguing that treatment with Compound C at the same time as treatment with metformin reversed the aforementioned positive effects. This finding suggests that the protective role of metformin in cerebral I/R injury is at least partially mediated by activation of AMPK.

Metformin Improved Cerebral I/R Injury *via* Regulating BDNF Expression *in vivo*

We speculated that metformin plays an active role in cerebral I/R injury *via* regulating BDNF expression. To verify our hypothesis, we used quantitative PCR and western blotting to measure the mRNA and protein levels of BDNF in the cortex of the cerebral ischemic penumbra, and ELISA was used to assess the BDNF concentration in the plasma of the rats in each group. Western blotting revealed that administration of metformin further increased BDNF expression (**Figures 3A,B**), and ELISA showed that metformin treatment also upregulated BDNF concentrations in the plasma (**Figure 3E**). The results of quantitative PCR showed that metformin also increased the level of BDNF transcription (**Figure 3D**), indicating that metformin regulated BDNF expression at the transcription level. Furthermore, consistent with the above results, brain slice immunohistochemistry indicated that administration of metformin significantly upregulated BDNF expression in the penumbra of cerebral ischemia (**Figure 3C**). Interestingly, immunofluorescence staining of brain slices revealed that metformin can act on ECs to promote BDNF expression in ECs. However, treatment with Compound C inhibited the metformin-mediated upregulation of BDNF expression (**Figure 3F**). Therefore, metformin plays a protective role in cerebral I/R injury at least in part *via* regulating BDNF expression in ECs at the transcriptional level, with AMPK activation as part of the process.

AMPK and CREB Were Involved in Regulating BDNF Expression in Cerebral I/R Injury

To further explore whether AMPK was involved in regulating BDNF expression, we detected the AMPK and p-AMPK expression levels in the brain tissue around the ischemic penumbra by western blotting. The results showed that metformin significantly increased the phosphorylation of AMPK, and this effect was inhibited by Compound C (**Figures 4A,B**). Furthermore, previous studies have found that transcriptional induction of BDNF was closely related to the CREB protein family (Tao et al., 1998) and have suggested that metformin could induce BDNF expression at the transcriptional level. Consequently, we speculated that CREB might participate in the regulation of BDNF expression in cerebral I/R injury, and tested this possibility by western blotting to detect CREB and p-CREB protein levels in the ischemic penumbra. We found that metformin could increase the phosphorylation level of CREB, and this phenomenon could also be reversed by Compound C (**Figures 4A,C**). Therefore, it could be concluded that metformin regulated BDNF expression in cerebral I/R injury at least in part by regulating the phosphorylation of AMPK and CREB.

Metformin Upregulated BDNF Expression and Release, Promoted Proliferation of HUVECs, and Inhibited Cell Apoptosis Under OGD/R Conditions *in vitro*

Based on the results of our *in vivo* experiments, we used HUVECs to construct an OGD/R model *in vitro* to simulate cerebral I/R injury

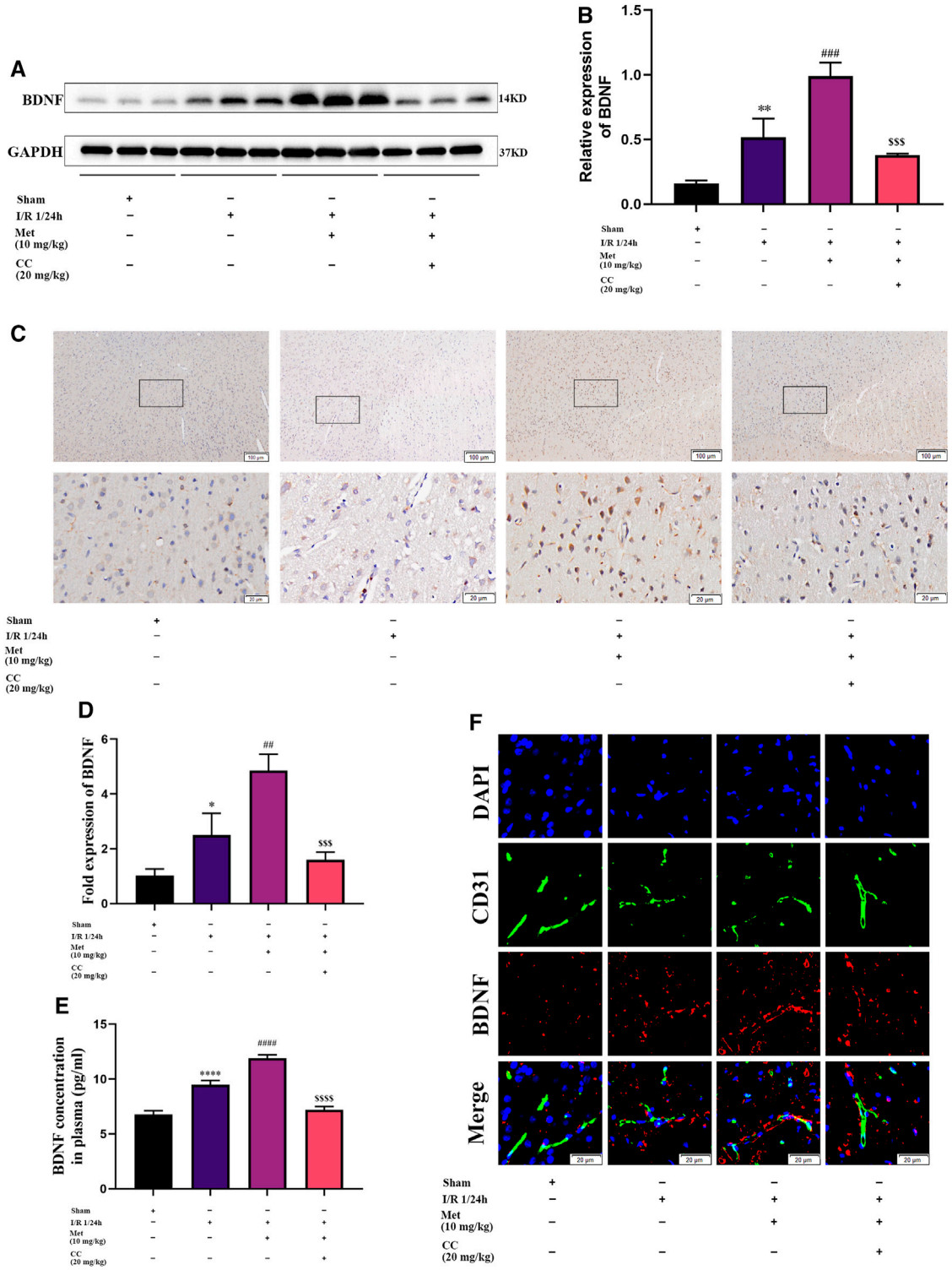

FIGURE 3 | Metformin improves cerebral ischemia/reperfusion (I/R) injury by regulating the expression of BDNF. **(A–C)** BDNF protein expression in the ischemic penumbra area was evaluated by western blotting and immunohistochemistry ($n = 3$, bar = 100 μm/20 μm). **(D)** The BDNF transcription level in the ischemic penumbra area was assessed by RT-qPCR ($n = 3$). **(E)** The BDNF concentration in the plasma assessed by ELISA ($n = 3$). **(F)** BDNF expression in endothelial cells in the ischemic penumbra was evaluated by immunofluorescence staining ($n = 3$, bar = 20 μm). ($^{*}p < 0.05$, $^{**}p < 0.01$, $^{****}p < 0.0001$ vs. sham; $^{\#\#}p < 0.01$, $^{\#\#\#}p < 0.001$, $^{\#\#\#\#}p < 0.0001$ vs. I/R 1/24 h; $^{\$\$\$}p < 0.001$, $^{\$\$\$\$}p < 0.0001$ vs. I/R 1/24 h + Met).

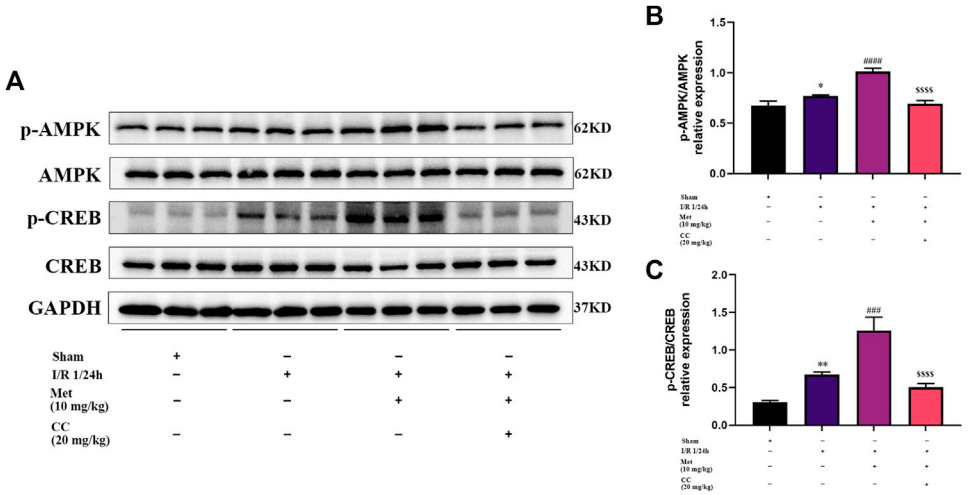

FIGURE 4 | AMPK and CREB are involved in the regulation of BDNF expression by metformin in cerebral ischemia-reperfusion (I/R) injury. **(A–C)** The phosphorylation levels of AMPK and CREB proteins was detected by western blotting ($n = 3$). (*$p < 0.05$, **$p < 0.01$ vs. sham; $^{###}p < 0.001$, $^{####}p < 0.0001$ vs. I/R 1/24 h; $^{\$\$\$\$}p < 0.0001$ vs. I/R 1/24 h + Met).

and further explore the effect of metformin in cerebral I/R injury. As shown in **Figures 5A,B**, HUVECs could upregulate the expression of BDNF under conditions of OGD/R 2, 4, 6, and 8 h/12 h and could significantly upregulate the expression of BDNF under conditions of OGD/R 4, 6, and 8 h/12 h. Selecting OGD/R 6 h/12 h conditions for follow-up studies, we found that metformin could further promote the expression and release of BDNF in HUVECs at a concentration of 20 μM. As the treatment concentration increased, the effect of metformin continued to weaken (**Figures 5C–E**). Furthermore, as shown in **Figures 5F–J**, metformin at a concentration of 20 μM promoted the proliferation of HUVECs and reduced cell apoptosis under OGD/R conditions.

Metformin Promoted HUVECs to Express BDNF Under OGD/R Conditions *via* the AMPK/CREB Pathway *in vitro*

We then explored whether AMPK and CREB were involved in the regulation of BDNF expression in HUVECs by metformin under OGD/R conditions. We treated HUVECs with metformin, AICAR (an AMPK activator), Compound C, and KG-501 (a CREB inhibitor) at the beginning of the reoxygenation period. Western blotting revealed that metformin and AICAR significantly increased the expression of BDNF and phosphorylation levels of AMPK and CREB at the same time, while Compound C inhibited the positive effect of metformin and AICAR (**Figures 6A–D**). Immunofluorescence staining of the cell slides also revealed that metformin and AICAR could further upregulate BDNF expression in HUVECs, while Compound C reversed the effect of metformin and AICAR (**Figures 6F,G**). Moreover, quantitative PCR results showed that metformin and AICAR promoted BDNF expression at the transcription level, and Compound C exerted an inhibitory effect also at the transcription level (**Figure 6E**). We also found that KG-501 could inhibit the increase in BDNF expression and CREB phosphorylation caused by metformin but had no effect on the AMPK phosphorylation level increased by metformin (**Figures 6H–K**). This suggests that AMPK is located upstream of CERB. Therefore, we concluded that metformin regulated phosphorylation of CREB and further regulated BDNF expression by affecting the phosphorylation level of AMPK in HUVECs under OGD/R conditions. In brief, metformin promotes BDNF expression in HUVECs under OGD/R conditions through the AMPK/CREB pathway.

BDNF Promoted the Proliferation of SH-SY5Y Cells and Inhibited Cell Apoptosis Under OGD/R Conditions *in vitro*

To explore the protective mechanism of BDNF on neurons under OGD/R conditions, we constructed an *in vitro* OGD/R model using SH-SY5Y cells and treatment with BDNF at the beginning of the reoxygenation period. After the intervention, the proliferation of SH-SY5Y cells was detected using the CCK-8 assay. The results revealed that the conditions of OGD/R 0.5, 1, 2, and 4 h/12 h dramatically reduced the proliferation of SH-SY5Y cells, and OGD/R 1 h/12 h treatment was selected for follow-up studies (**Figure 7B**). After treatment with various concentrations of BDNF, the CCK-8 assay revealed that the proliferation of SH-SY5Y cells was dramatically increased under OGD/R conditions when the BDNF concentration was 20 or 50 ng/ml (**Figure 7C**). Apoptosis of SH-SY5Y cells was detected using TUNEL staining and flow cytometry. The flow cytometry results revealed that BDNF concentrations of 20 and 50 ng/ml significantly reduced OGD/R-induced apoptosis in SH-SY5Y cells (**Figures 7D,E**). Furthermore, TUNEL staining revealed that when the concentration of BDNF was 20 ng/ml, apoptosis of SH-SY5Y cells under OGD/R 1 h/12 h conditions was significantly reduced (**Figures 7F,G**). Therefore, BDNF could promote the proliferation of SH-SY5Y cells and reduce apoptosis under OGD/R conditions.

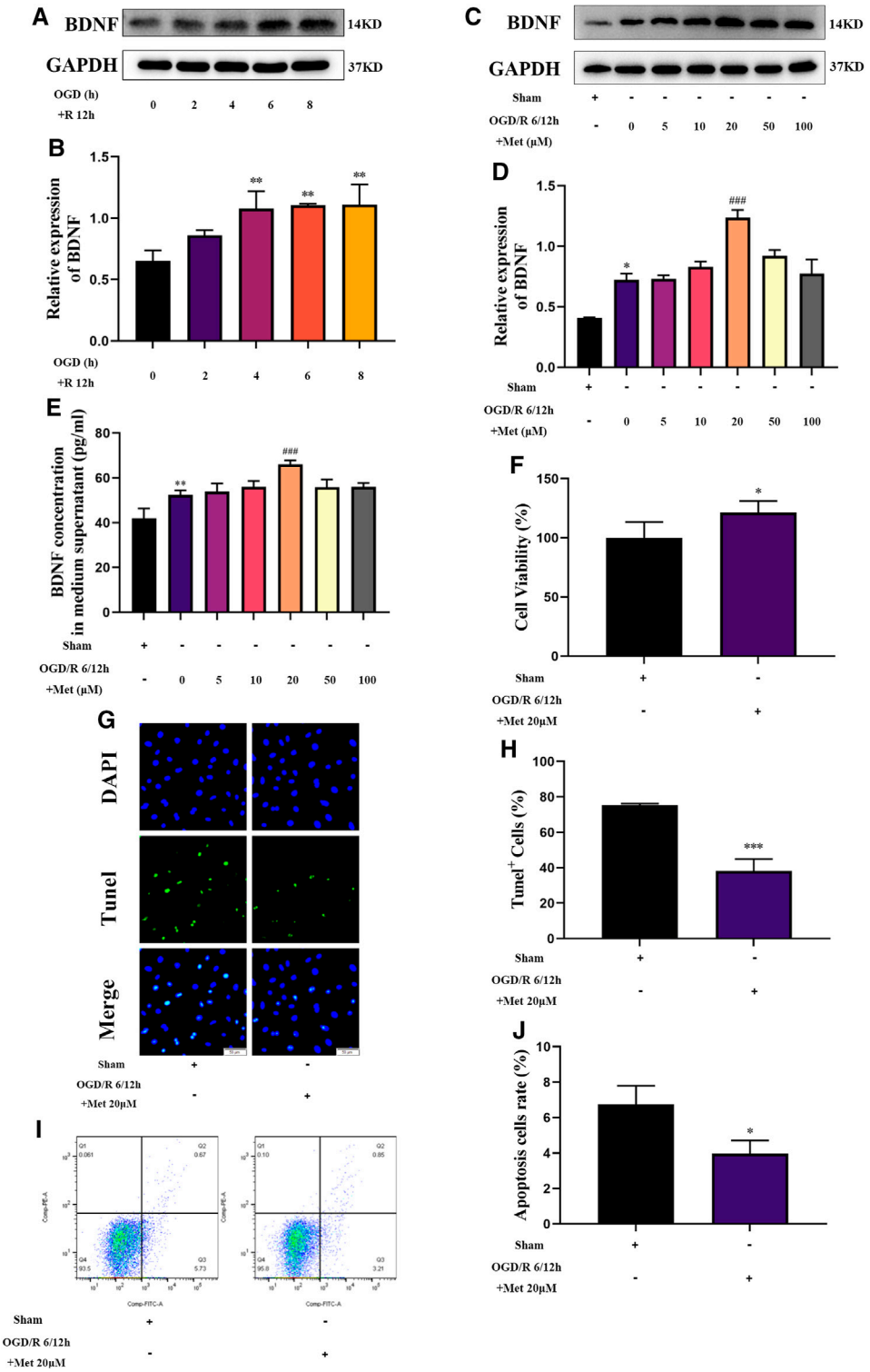

FIGURE 5 | Metformin upregulates BDNF expression and release, promotes HUVECs proliferation, and inhibits cell apoptosis under OGD/R conditions. **(A–D)** The BDNF expression level of metformin-treated HUVECs was detected by western blotting ($n = 3$). **(E)** The BDNF concentration in the culture supernatant of metformin-treated HUVECs was detected by ELISA ($n = 3$). **(F)** Proliferation of HUVECs was detected by CCK-8 assay ($n = 5$). **(G–J)** Apoptosis of HUVECs was detected by TUNEL staining ($n = 3$, bar = 50 μm) and flow cytometry ($n = 3$). ($^{*}p < 0.05$, $^{**}p < 0.01$ vs. sham; $^{\#}p < 0.05$, $^{\#\#\#}p < 0.001$ vs. OGD/R 6/12 h).

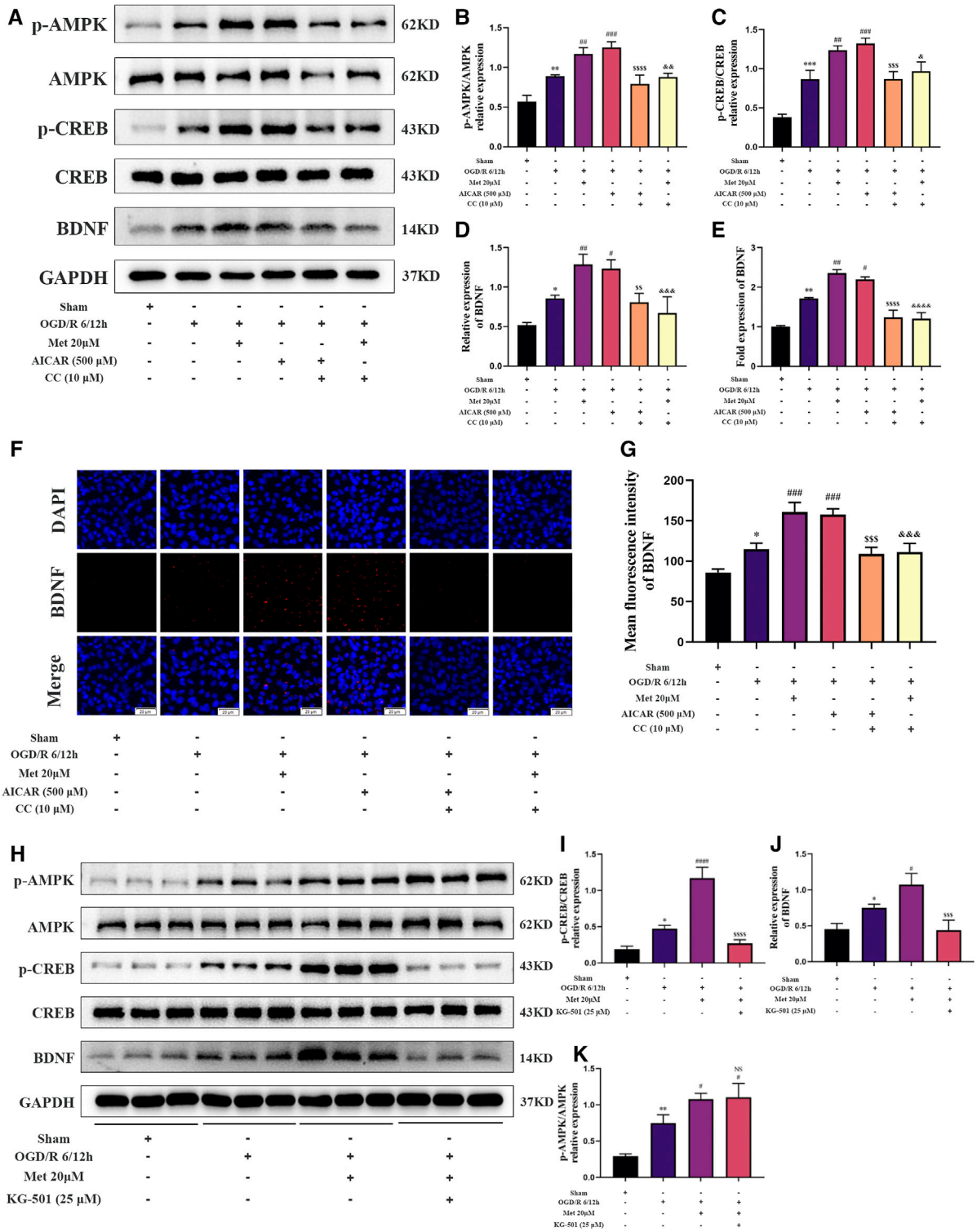

FIGURE 6 | Metformin promotes the expression of BDNF in HUVECs under OGD/R conditions through the AMPK/CREB pathway. **(A–D)** The BDNF expression level and AMPK and CREB phosphorylation levels in HUVECs treated with metformin, AICAR, and Compound C under OGD/R conditions detected were by western blotting ($n = 3$). **(E)** The BDNF transcription level under the above conditions was detected by RT-qPCR (n = 4). **(F,G)** Immunofluorescence staining and quantification of BDNF under the above conditions ($n = 3$, bar = 20 μM). **(H–K)** BDNF expression level and AMPK and CREB phosphorylation levels in HUVECs treated with metformin and KG-501 under OGD/R conditions were detected by western blotting ($n = 3$). ($^{*}p < 0.05$, $^{**}p < 0.01$, $^{***}p < 0.001$ vs. sham; $^{\#}p < 0.05$, $^{\#\#}p < 0.01$, $^{\#\#\#}p < 0.001$, $^{\#\#\#\#}p < 0.0001$ vs. OGD/R 6/12 h; NS, not significant, $^{\$\$}p < 0.01$, $^{\$\$\$}p < 0.001$, $^{\$\$\$\$}p < 0.0001$ vs. OGD/R 6/12 h + AICAR; $^{\&}p < 0.05$, $^{\&\&}p < 0.01$, $^{\&\&\&}p < 0.001$, $^{\&\&\&\&}p < 0.0001$ vs. OGD/R 6/12 h + Met 20 μM).

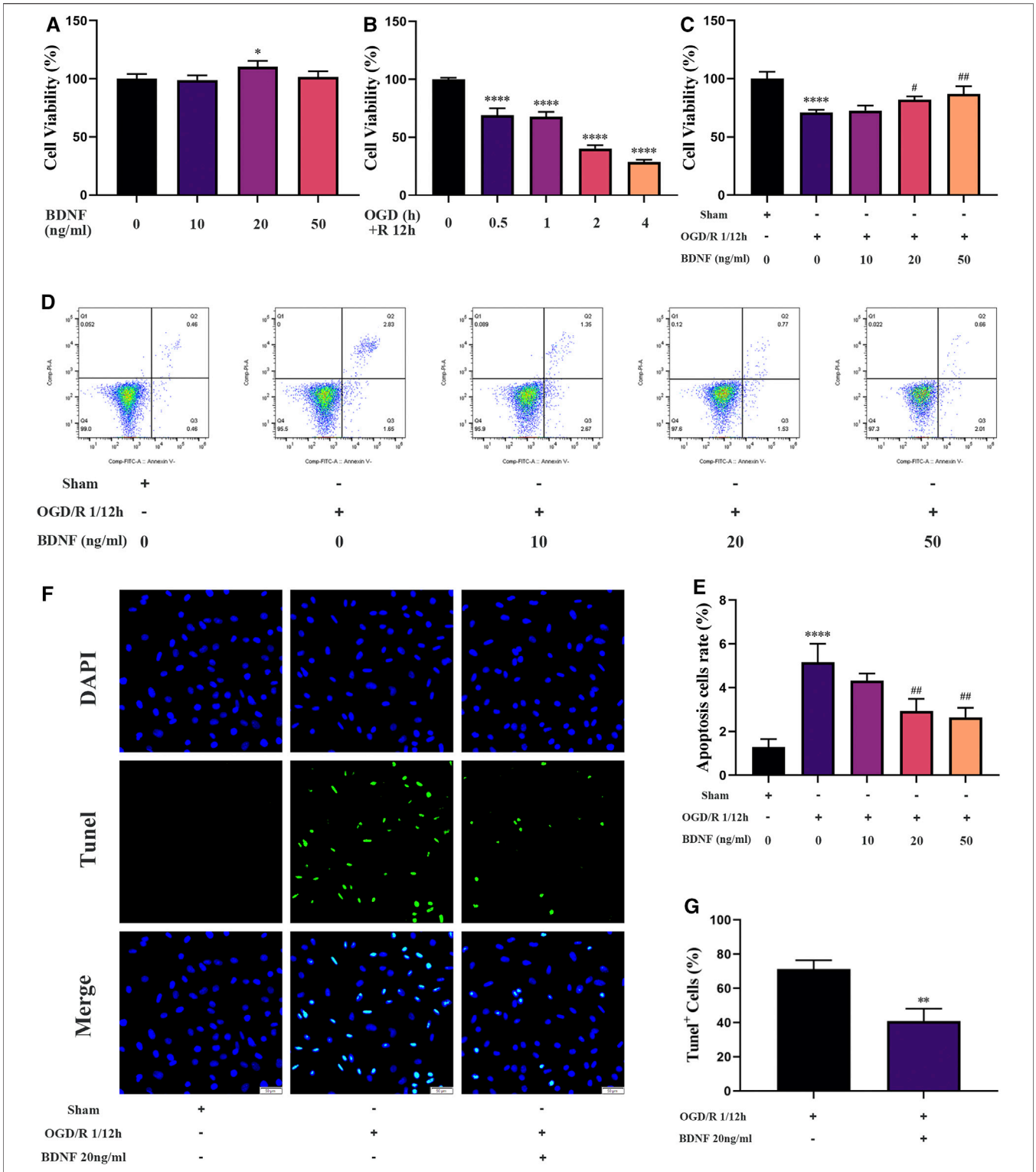

FIGURE 7 | BDNF promotes the proliferation of SH-SY5Y cells and inhibits cell apoptosis under OGD/R conditions. **(A–C)** The effect of BDNF on the proliferation of SH-SY5Y cells was detected by CCK-8 assay under OGD/R conditions (n = 4). **(D–G)** The effect of BDNF on apoptosis of SH-SY5Y cells was detected by TUNEL staining (n = 3, bar = 50 μm) and flow cytometry (n = 3). (*p < 0.05, **p < 0.01, ****p < 0.0001 vs. sham; $^{\#}p$ < 0.05, $^{\#\#}p$ < 0.01 vs. OGD/R 1/12 h).

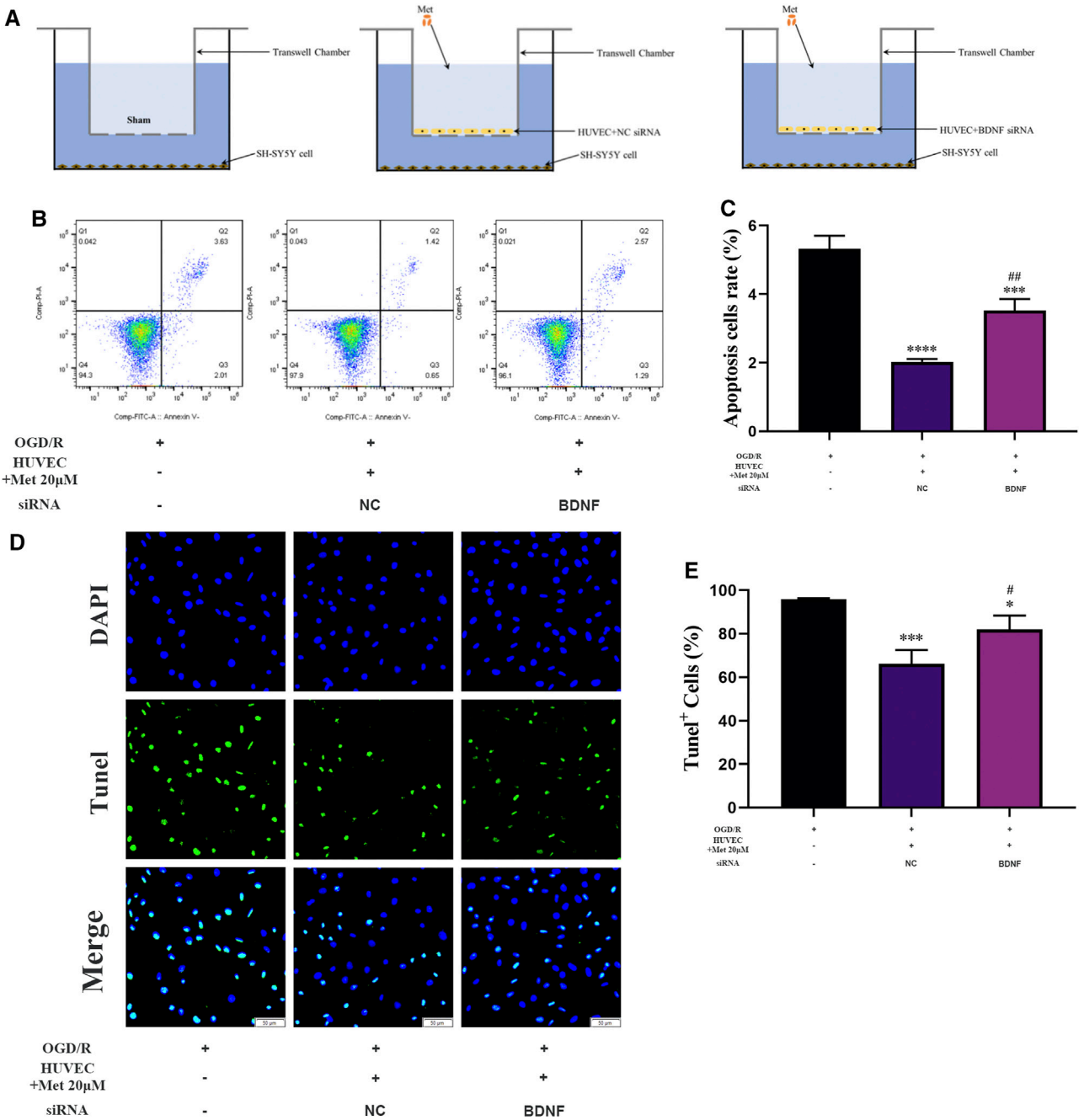

FIGURE 8 | HUVECs treated with metformin reduce apoptosis of SH-SY5Y cells under OGD/R conditions. **(A)** Schematic diagram of grouping in the Transwell chamber assay. **(B–E)** Apoptosis of SH-SY5Y cells was detected by TUNEL staining (n = 3, bar = 50 μm) and flow cytometry (n = 3). (*p < 0.05, ***p < 0.001, ****p < 0.0001 vs. OGD/R; $^{\#}p$ < 0.05, $^{\#\#}p$ < 0.01 vs. OGD/R + HUVEC + Met 20 μM + NC siRNA; NC, negative control).

HUVECs Treated With Metformin Alleviated Apoptosis of SH-SY5Y Cells Under OGD/R Conditions *in vitro*

We examined the function of metformin-treated HUVECs on apoptosis of SH-SY5Y cells using a Transwell chamber assay under OGD/R conditions. Flow cytometry revealed that apoptosis of SH-SY5Y cells could be alleviated in the metformin-treated HUVEC group (Figures 8B,C). Consistent with the above results, TUNEL staining showed that metformin-treated HUVECs could reduce the number of SH-SY5Y cells positive for TUNEL staining more effectively than in the control group (**Figures 8D,E**). However, the improved apoptosis level of SH-SY5Y cells *via* metformin-treated HUVECs was partially reversed by transfecting BDNF siRNA in HUVECs. Therefore, metformin may decrease the

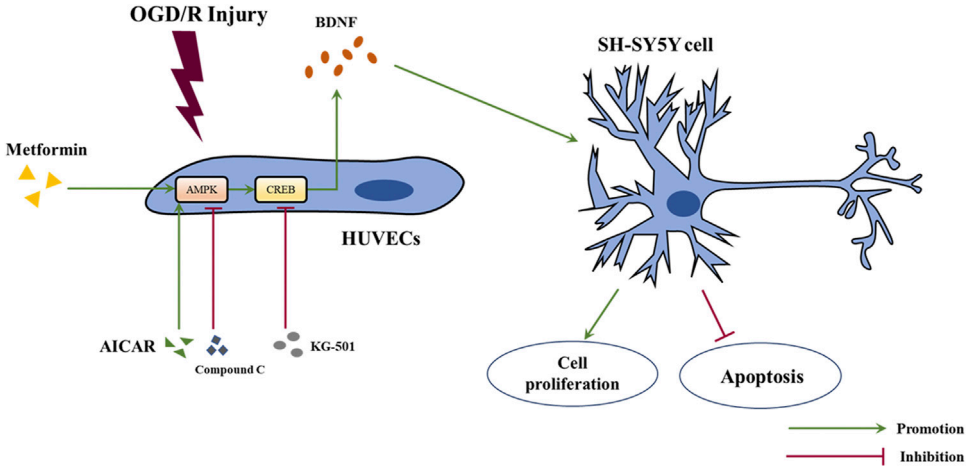

FIGURE 9 | Schematic diagram of the mechanism of metformin in this study. Abbreviations: OGD/R, oxygen-glucose deprivation/reoxygenation; HUVECs, human umbilical vein endothelial cells; BDNF, brain-derived neurotrophic factor.

apoptosis of SH-SY5Y cells partially by upregulating BDNF expression in HUVECs under OGD/R conditions.

DISCUSSION

In this study, we revealed that acute treatment with low-dose metformin upregulated the expression of BDNF in ECs in the ischemic penumbra area in an AMPK-dependent manner, thereby improving cerebral edema, cerebral infarct volume, the neurological deficit score, and neuronal apoptosis caused by cerebral I/R injury *in vivo*. Metformin also promoted BDNF expression in HUVECs *via* the AMPK/CREB pathway, thereby promoting the proliferation of SH-SY5Y cells and reducing cell apoptosis under OGD/R conditions *in vitro*. The mechanism of metformin observed in this research is summarized in **Figure 9**.

AMPK is the main energy homeostasis regulator in the body and can be activated by phosphorylation when the AMP/ATP ratio increases (Hardie et al., 2012). Many studies have suggested that AMPK is an important mediator in the pathogenesis of stroke (Manwani and Mccullough, 2013). Similarly, we found that AMPK could be activated by phosphorylation both in cerebral I/R injury *in vivo* and under OGD/R conditions *in vitro* and that treatment with metformin can further promote phosphorylation of AMPK. Moreover, we found that the active influence of metformin in cerebral I/R injury and promotion of BDNF expression in HUVECs under OGD/R conditions depend on the activation of AMPK, because the above-mentioned effects of metformin are all inhibited by Compound C.

As a transcription factor, CREB is widely expressed in various organs and participates in the proliferation, differentiation, and survival of various cell types (Kitagawa, 2007). Related studies have reported that CREB could be activated by phosphorylation in the ischemic penumbra area in a model of focal cerebral ischemia (Tanaka et al., 1999). Moreover, many studies have suggested that the activation of CREB phosphorylation can have a neuroprotective effect in models of cerebral ischemia (Miyata et al., 2001; Lee et al., 2004), which is consistent with our results. Furthermore, our *in vitro* data showed that the activation of CREB depends on the activation of AMPK phosphorylation; that is, AMPK is located upstream of CREB. Because AMPK agonists and inhibitors can upregulate and downregulate the phosphorylation level of CREB, but CERB inhibitors cannot affect the phosphorylation level of AMPK (**Figure 6**).

BDNF, as a neurotrophic factor, is widely distributed throughout the brain, especially in the hippocampus and cortex, and has a wide range of neuroprotective and neurotrophic functions (Eyileten et al., 2021). More and more studies have revealed that BDNF can upregulate and exert neuroprotective effects in cerebral ischemia (Ferrer et al., 2001; Zhang and Pardridge, 2001). A study by Dmitrieva et al. found that in acute ischemic stroke, the body's endogenous self-protection mechanism can be stimulated to increase the expression of endogenous BDNF, thereby promoting repair of damaged neurons; however, this compensation cannot completely offset the neuronal damage caused by ischemia (Dmitrieva et al., 2010). Similarly, our study found an increased expression of BDNF in both the cortex of the ischemic penumbra in cerebral I/R injury *in vivo* and in HUVECs under OGD/R conditions *in vitro* and that metformin could further promote the expression of BDNF. Increased BDNF expression in the cortex of the ischemic penumbra was accompanied by the improvement in cerebral I/R injury *in vivo*, which suggests that metformin reduces cerebral I/R injury by promoting BDNF expression.

As a first-line hypoglycemic agent, metformin not only has a good hypoglycemic effect (Sanchez-Rangel and Inzucchi, 2017) but can also reduce the risk of cardiovascular (Ghotbi et al., 2013) and cerebrovascular (UK Prospective Diabetes Study (UKPDS) Group, 1998) events and improve the prognosis of stroke patients (Mima et al., 2016). Previous studies have suggested that metformin could play

a positive role in neurodegenerative conditions, such as Parkinson's disease (Fitzgerald et al., 2017; Mor et al., 2020) and Alzheimer's disease (Luchsinger et al., 2016; Farr et al., 2019; Xu et al., 2021). In the present study, we found that acute treatment with low-dose metformin (10 mg/kg) reduced cerebral I/R injury in a rat model of tMCAO. Interestingly, acute treatment with a low concentration of metformin (20 μM) promoted BDNF expression in HUVECs under OGD/R conditions *in vitro*, while BDNF expression continued to decrease as the concentration of metformin increased. This implies that acute treatment with metformin can only exert a protective effect at low concentrations.

Moreover, metformin not only reduces cerebral I/R injury in a global cerebral ischemia model (Ashabi et al., 2014; Ashabi et al., 2015; Ge et al., 2017) but also has a neuroprotective effect in a model of focal cerebral ischemia (Li et al., 2010; Venna et al., 2014). The above findings were also observed under long-term chronic metformin treatment. A study by Li et al. revealed that acute treatment with metformin aggravated brain damage in the focal ischemia model, which seems to be inconsistent with our experimental results (Li et al., 2010). There are several possible explanations for these conflicting findings. First, the dose of metformin used in our experiment was 10 mg/kg, which is much smaller than the 100 mg/kg dose used in the study by Li et al. Treatment with the various concentrations of metformin resulted in differences in the degree of AMPK activation. Moderate AMPK activation can counteract cerebral ischemic damage by strengthening catabolic pathways and reducing ATP consumption (Manwani and Mccullough, 2013; Jiang et al., 2018). A study by Jiang et al. found that pretreatment with acute low-dose metformin can moderately activate AMPK and has a neuroprotective effect in a model of focal cerebral ischemia (Jiang et al., 2014). Moreover, high-dose metformin has been shown to markedly enhance AMPK activation and lactic acid accumulation, promote ATP consumption, and ultimately aggravate neuronal death (Jiang et al., 2018). Second, metformin was administered at the beginning of the reperfusion period in our study, while it was administered as preconditioning before ischemia in the study by Li et al. Our treatment was a therapeutic intervention, whereas theirs was a preventive intervention, and different intervention times sometimes have different results.

Interestingly, BDNF siRNA transfection in HUVECs was able to partially reverse the metformin-dependent increase in SH-SY5Y cells apoptosis under OGD/R conditions based on the results of the Transwell chamber assay. This result indicates that metformin can reduce the apoptosis level of SH-SY5Y cells by promoting the BDNF expression of HUVECs but also through other currently unclear mechanisms. In addition, according to the ELISA results of the metformin-treated HUVECs culture supernatant, BDNF concentration was approximately 66 pg/ml, while our *in vitro* experiments showed that BDNF could reduce apoptosis levels of SH-SY5Y cells at 20 ng/ml under OGD/R conditions. These results also indicate that metformin not only promoted the BDNF expression of HUVECs, but also enhanced the protective effect of BDNF through an uncertain mechanism. This will be further explored in our future studies.

This research also has many shortcomings. First, we only focused on the effects of metformin in the acute phase and did not investigate the effects and mechanisms of chronic low-dose metformin. We will address these issues in future experiments. Second, we only explored whether BDNF promoted the proliferation of SH-SY5Y cells and reduced apoptosis under OGD/R conditions but not the specific mechanism of BDNF functions, which will be also one of our later research focuses. Finally, the intraperitoneal injection method used in in vivo experiments can greatly reduce the first-pass effect of the drug, but it is also more invasive. Therefore, the protective effects of oral metformin against ischemic stroke should be investigated.

In conclusion, this study shows that acute treatment with low-dose metformin can upregulate BDNF expression in the ischemic penumbra *via* the AMPK/CREB pathway, thereby reducing cerebral I/R injury. The ability of exogenous BDNF to enter the brain tissue is extremely limited because of the blood-brain barrier; this study may lead to a new and effective way of activating endogenous BDNF. Furthermore, our findings provide new evidence and support for metformin as a treatment that can be synchronized with the revascularization of acute cerebral infarction.

DATA AVAILABILITY STATEMENT

The original contributions presented in the study are included in the article/**Supplementary Material**, further inquiries can be directed to the corresponding authors.

ETHICS STATEMENT

The animal study was reviewed and approved by the Experimental Animal Management Committee of Tongji Medical College of Huazhong University of Science and Technology (No. 2499).

AUTHOR CONTRIBUTIONS

KL, GL, ZL, HL, LL, and YoW conceived and designed the study. KL, GL, ZL, LL, YoW, XJ, MW, YC, TJ, JL, JZ, HL, and YaW performed the experiments. KL and ZL analyzed the data. KL and GL wrote the manuscript. HL and YoW revised the manuscript. All authors read and approved the final version of the manuscript.

FUNDING

This work was supported by grants from the National Natural Science Foundation of China (No. 81801181).

ACKNOWLEDGMENTS

We would like to thank Editage for the English language editing.

SUPPLEMENTARY MATERIAL

The Supplementary Material for this article can be found online at: https://www.frontiersin.org/articles/10.3389/fphar.2022.832611/full#supplementary-material

REFERENCES

Alexander, S. P., Benson, H. E., Faccenda, E., Pawson, A. J., Sharman, J. L., Spedding, M., et al. (2013). The Concise Guide to PHARMACOLOGY 2013/14: Enzymes. *Br. J. Pharmacol.* 170 (8), 1797–1867. doi:10.1111/bph.12451

Alhusban, A., Kozak, A., Ergul, A., and Fagan, S. C. (2013). AT1 Receptor Antagonism Is Proangiogenic in the Brain: BDNF a Novel Mediator. *J. Pharmacol. Exp. Ther.* 344 (2), 348–359. doi:10.1124/jpet.112.197483

Ashabi, G., Khodagholi, F., Khalaj, L., Goudarzvand, M., and Nasiri, M. (2014). Activation of AMP-Activated Protein Kinase by Metformin Protects against Global Cerebral Ischemia in Male Rats: Interference of AMPK/PGC-1α Pathway. *Metab. Brain Dis.* 29 (1), 47–58. doi:10.1007/s11011-013-9475-2

Ashabi, G., Khalaj, L., Khodagholi, F., Goudarzvand, M., and Sarkaki, A. (2015). Pre-treatment with Metformin Activates Nrf2 Antioxidant Pathways and Inhibits Inflammatory Responses through Induction of AMPK after Transient Global Cerebral Ischemia. *Metab. Brain Dis.* 30 (3), 747–754. doi:10.1007/s11011-014-9632-2

Bekinschtein, P., Cammarota, M., and Medina, J. H. (2014). BDNF and Memory Processing. *Neuropharmacology* 76, 677–683. doi:10.1016/j.neuropharm.2013.04.024

Berkhemer, O. A., Fransen, P. S. S., Beumer, D., van den Berg, L. A., Lingsma, H. F., Yoo, A. J., et al. (2015). A Randomized Trial of Intraarterial Treatment for Acute Ischemic Stroke. *N. Engl. J. Med.* 372, 11–20. doi:10.1056/NEJMoa1411587

Campbell, B. C., Mitchell, P. J., Kleinig, T. J., Dewey, H. M., Churilov, L., Yassi, N., et al. (2015). Endovascular Therapy for Ischemic Stroke with Perfusion-Imaging Selection. *N. Engl. J. Med.* 372 (11), 1009–1018. doi:10.1056/NEJMoa1414792

Caporali, A., and Emanueli, C. (2009). Cardiovascular Actions of Neurotrophins. *Physiol. Rev.* 89 (1), 279–308. doi:10.1152/physrev.00007.2008

Dmitrieva, V. G., Povarova, O. V., Skvortsova, V. I., Limborska, S. A., Myasoedov, N. F., and Dergunova, L. V. (2010). Semax and Pro-gly-pro Activate the Transcription of Neurotrophins and Their Receptor Genes after Cerebral Ischemia. *Cell. Mol. Neurobiol.* 30 (1), 71–79. doi:10.1007/s10571-009-9432-0

Eyileten, C., Sharif, L., Wicik, Z., Jakubik, D., Jarosz-Popek, J., Soplinska, A., et al. (2021). The Relation of the Brain-Derived Neurotrophic Factor with MicroRNAs in Neurodegenerative Diseases and Ischemic Stroke. *Mol. Neurobiol.* 58 (1), 329–347. doi:10.1007/s12035-020-02101-2

Farr, S. A., Roesler, E., Niehoff, M. L., Roby, D. A., Mckee, A., and Morley, J. E. (2019). Metformin Improves Learning and Memory in the SAMP8 Mouse Model of Alzheimer's Disease. *J. Alzheimers Dis.* 68 (4), 1699–1710. doi:10.3233/JAD-181240

Ferrer, I., Krupinski, J., Goutan, E., Martí, E., Ambrosio, S., and Arenas, E. (2001). Brain-derived Neurotrophic Factor Reduces Cortical Cell Death by Ischemia after Middle Cerebral Artery Occlusion in the Rat. *Acta Neuropathol.* 101 (3), 229–238. doi:10.1007/s004010000268

Fitzgerald, J. C., Zimprich, A., Carvajal Berrio, D. A., Schindler, K. M., Maurer, B., Schulte, C., et al. (2017). Metformin Reverses TRAP1 Mutation-Associated Alterations in Mitochondrial Function in Parkinson's Disease. *Brain* 140 (9), 2444–2459. doi:10.1093/brain/awx202

Fouda, A. Y., Alhusban, A., Ishrat, T., Pillai, B., Eldahshan, W., Waller, J. L., et al. (2017). Brain-Derived Neurotrophic Factor Knockdown Blocks the Angiogenic and Protective Effects of Angiotensin Modulation after Experimental Stroke. *Mol. Neurobiol.* 54 (1), 661–670. doi:10.1007/s12035-015-9675-3

Ge, X. H., Zhu, G. J., Geng, D. Q., Zhang, H. Z., He, J. M., Guo, A. Z., et al. (2017). Metformin Protects the Brain against Ischemia/reperfusion Injury through PI3K/Akt1/JNK3 Signaling Pathways in Rats. *Physiol. Behav.* 170, 115–123. doi:10.1016/j.physbeh.2016.12.021

Ghotbi, A. A., Køber, L., Finer, N., James, W. P., Sharma, A. M., Caterson, I., et al. (2013). Association of Hypoglycemic Treatment Regimens with Cardiovascular Outcomes in Overweight and Obese Subjects with Type 2 Diabetes: a Substudy of the SCOUT Trial. *Diabetes Care* 36 (11), 3746–3753. doi:10.2337/dc13-0027

Goyal, M., Demchuk, A. M., Menon, B. K., Eesa, M., Rempel, J. L., Thornton, J., et al. (2015). Randomized Assessment of Rapid Endovascular Treatment of Ischemic Stroke. *N. Engl. J. Med.* 372 (11), 1019–1030. doi:10.1056/NEJMoa1414905

Greenberg, M. E., Xu, B., Lu, B., and Hempstead, B. L. (2009). New Insights in the Biology of BDNF Synthesis and Release: Implications in CNS Function. *J. Neurosci.* 29 (41), 12764–12767. doi:10.1523/JNEUROSCI.3566-09.2009

Guo, S., Kim, W. J., Lok, J., Lee, S. R., Besancon, E., Luo, B. H., et al. (2008). Neuroprotection via Matrix-Trophic Coupling between Cerebral Endothelial Cells and Neurons. *Proc. Natl. Acad. Sci. U S A.* 105 (21), 7582–7587. doi:10.1073/pnas.0801105105

Han, X., Wang, B., Sun, Y., Huang, J., Wang, X., Ma, W., et al. (2018). Metformin Modulates High Glucose-Incubated Human Umbilical Vein Endothelial Cells Proliferation and Apoptosis through AMPK/CREB/BDNF Pathway. *Front. Pharmacol.* 9, 1266. doi:10.3389/fphar.2018.01266

Hardie, D. G., Ross, F. A., and Hawley, S. A. (2012). AMPK: A Nutrient and Energy Sensor that Maintains Energy Homeostasis. *Nat. Rev. Mol. Cel Biol.* 13 (4), 251–262. doi:10.1038/nrm3311

Iadecola, C. (2017). The Neurovascular Unit Coming of Age: A Journey through Neurovascular Coupling in Health and Disease. *Neuron* 96 (1), 17–42. doi:10.1016/j.neuron.2017.07.030

Jiang, T., Yu, J. T., Zhu, X. C., Wang, H. F., Tan, M. S., Cao, L., et al. (2014). Acute Metformin Preconditioning Confers Neuroprotection against Focal Cerebral Ischaemia by Pre-activation of AMPK-dependent Autophagy. *Br. J. Pharmacol.* 171 (13), 3146–3157. doi:10.1111/bph.12655

Jiang, S., Li, T., Ji, T., Yi, W., Yang, Z., Wang, S., et al. (2018). AMPK: Potential Therapeutic Target for Ischemic Stroke. *Theranostics* 8 (16), 4535–4551. doi:10.7150/thno.25674

Keshavarzi, S., Kermanshahi, S., Karami, L., Motaghinejad, M., Motevalian, M., and Sadr, S. (2019). Protective Role of Metformin against Methamphetamine Induced Anxiety, Depression, Cognition Impairment and Neurodegeneration in Rat: The Role of CREB/BDNF and Akt/GSK3 Signaling Pathways. *Neurotoxicology* 72, 74–84. doi:10.1016/j.neuro.2019.02.004

Kitagawa, K. (2007). CREB and cAMP Response Element-Mediated Gene Expression in the Ischemic Brain. *FEBS J.* 274 (13), 3210–3217. doi:10.1111/j.1742-4658.2007.05890.x

Lee, J. H., Kim, K. Y., Lee, Y. K., Park, S. Y., Kim, C. D., Lee, W. S., et al. (2004). Cilostazol Prevents Focal Cerebral Ischemic Injury by Enhancing Casein Kinase 2 Phosphorylation and Suppression of Phosphatase and Tensin Homolog Deleted from Chromosome 10 Phosphorylation in Rats. *J. Pharmacol. Exp. Ther.* 308 (3), 896–903. doi:10.1124/jpet.103.061853

Li, J., Benashski, S. E., Venna, V. R., and Mccullough, L. D. (2010). Effects of Metformin in Experimental Stroke. *Stroke* 41 (11), 2645–2652. doi:10.1161/STROKEAHA.110.589697

Lin, L., Wang, X., and Yu, Z. (2016). Ischemia-reperfusion Injury in the Brain: Mechanisms and Potential Therapeutic Strategies. *Biochem. Pharmacol. (Los Angel)* 5 (4), 213. doi:10.4172/2167-0501.1000213

Longa, E. Z., Weinstein, P. R., Carlson, S., and Cummins, R. (1989). Reversible Middle Cerebral Artery Occlusion without Craniectomy in Rats. *Stroke* 20 (1), 84–91. doi:10.1161/01.str.20.1.84

Luchsinger, J. A., Perez, T., Chang, H., Mehta, P., Steffener, J., Pradabhan, G., et al. (2016). Metformin in Amnestic Mild Cognitive Impairment: Results of a Pilot Randomized Placebo Controlled Clinical Trial. *J. Alzheimers Dis.* 51 (2), 501–514. doi:10.3233/JAD-150493

Manwani, B., and Mccullough, L. D. (2013). Function of the Master Energy Regulator Adenosine Monophosphate-Activated Protein Kinase in Stroke. *J. Neurosci. Res.* 91 (8), 1018–1029. doi:10.1002/jnr.23207

Mima, Y., Kuwashiro, T., Yasaka, M., Tsurusaki, Y., Nakamura, A., Wakugawa, Y., et al. (2016). Impact of Metformin on the Severity and Outcomes of Acute Ischemic Stroke in Patients with Type 2 Diabetes Mellitus. *J. Stroke Cerebrovasc. Dis.* 25 (2), 436–446. doi:10.1016/j.jstrokecerebrovasdis.2015.10.016

Miyata, K., Omori, N., Uchino, H., Yamaguchi, T., Isshiki, A., and Shibasaki, F. (2001). Involvement of the Brain-Derived Neurotrophic factor/TrkB Pathway in Neuroprotecive Effect of Cyclosporin A in Forebrain Ischemia. *Neuroscience* 105 (3), 571–578. doi:10.1016/s0306-4522(01)00225-1

Mizui, T., Ishikawa, Y., Kumanogoh, H., and Kojima, M. (2016). Neurobiological Actions by Three Distinct Subtypes of Brain-Derived Neurotrophic Factor: Multi-Ligand Model of Growth Factor Signaling. *Pharmacol. Res.* 105, 93–98. doi:10.1016/j.phrs.2015.12.019

Mor, D. E., Sohrabi, S., Kaletsky, R., Keyes, W., Tartici, A., Kalia, V., et al. (2020). Metformin Rescues Parkinson's Disease Phenotypes Caused by Hyperactive

Mitochondria. *Proc. Natl. Acad. Sci. U S A.* 117 (42), 26438–26447. doi:10.1073/pnas.2009838117

Nathan, D. M. (1998). Some Answers, More Controversy, from UKPDS. *Lancet* 352, 832–833. doi:10.1016/s0140-6736(98)22937-0

National Institute of Neurological Disorders and Stroke rt-PA Stroke Study Group (1995). Tissue Plasminogen Activator for Acute Ischemic Stroke. *N. Engl. J. Med.* 333, 1581–1587. doi:10.1056/NEJM199512143332401

Patil, S. P., Jain, P. D., Ghumatkar, P. J., Tambe, R., and Sathaye, S. (2014). Neuroprotective Effect of Metformin in MPTP-Induced Parkinson's Disease in Mice. *Neuroscience* 277, 747–754. doi:10.1016/j.neuroscience.2014.07.046

Sanchez-Rangel, E., and Inzucchi, S. E. (2017). Metformin: Clinical Use in Type 2 Diabetes. *Diabetologia* 60 (9), 1586–1593. doi:10.1007/s00125-017-4336-x

Selvin, E., and Hirsch, A. T. (2008). Contemporary Risk Factor Control and Walking Dysfunction in Individuals with Peripheral Arterial Disease: NHANES 1999-2004. *Atherosclerosis* 201 (2), 425–433. doi:10.1016/j.atherosclerosis.2008.02.002

Tanaka, K., Nagata, E., Suzuki, S., Dembo, T., Nogawa, S., and Fukuuchi, Y. (1999). Immunohistochemical Analysis of Cyclic AMP Response Element Binding Protein Phosphorylation in Focal Cerebral Ischemia in Rats. *Brain Res.* 818 (2), 520–526. doi:10.1016/s0006-8993(98)01263-3

Tao, X., Finkbeiner, S., Arnold, D. B., Shaywitz, A. J., and Greenberg, M. E. (1998). Ca2+ Influx Regulates BDNF Transcription by a CREB Family Transcription Factor-dependent Mechanism. *Neuron* 20 (4), 709–726. doi:10.1016/s0896-6273(00)81010-7

Tyler, W. J., Alonso, M., Bramham, C. R., and Pozzo-Miller, L. D. (2002). From Acquisition to Consolidation: on the Role of Brain-Derived Neurotrophic Factor Signaling in Hippocampal-dependent Learning. *Learn. Mem.* 9 (5), 224–237. doi:10.1101/lm.51202

UK Prospective Diabetes Study (UKPDS) Group (1998). Effect of Intensive Blood-Glucose Control with Metformin on Complications in Overweight Patients with Type 2 Diabetes (UKPDS 34). *Lancet* 352, 854–865.

Venna, V. R., Li, J., Hammond, M. D., Mancini, N. S., and Mccullough, L. D. (2014). Chronic Metformin Treatment Improves post-stroke Angiogenesis and Recovery after Experimental Stroke. *Eur. J. Neurosci.* 39 (12), 2129–2138. doi:10.1111/ejn.12556

Wang, Y., Wang, M. D., Xia, Y. P., Gao, Y., Zhu, Y. Y., Chen, S. C., et al. (2018). MicroRNA-130a Regulates Cerebral Ischemia-Induced Blood-Brain Barrier Permeability by Targeting Homeobox A5. *FASEB J.* 32 (2), 935–944. doi:10.1096/fj.201700139RRR

Xu, X., Sun, Y., Cen, X., Shan, B., Zhao, Q., Xie, T., et al. (2021). Metformin Activates Chaperone-Mediated Autophagy and Improves Disease Pathologies in an Alzheimer Disease Mouse Model. *Protein Cell* 12 (10), 769–787. doi:10.1007/s13238-021-00858-3

Yuan, L., Liu, J., Dong, R., Zhu, J., Tao, C., Zheng, R., et al. (2016). 14,15-epoxyeicosatrienoic Acid Promotes Production of Brain Derived Neurotrophic Factor from Astrocytes and Exerts Neuroprotective Effects during Ischaemic Injury. *Neuropathol. Appl. Neurobiol.* 42 (7), 607–620. doi:10.1111/nan.12291

Zhang, Y., and Pardridge, W. M. (2001). Neuroprotection in Transient Focal Brain Ischemia after Delayed Intravenous Administration of Brain-Derived Neurotrophic Factor Conjugated to a Blood-Brain Barrier Drug Targeting System. *Stroke* 32 (6), 1378–1384. doi:10.1161/01.str.32.6.1378

Conflict of Interest: The authors declare that the research was conducted in the absence of any commercial or financial relationships that could be construed as a potential conflict of interest.

frontiers | Frontiers in Pharmacology

CORRECTION
published: 02 June 2022
doi: 10.3389/fphar.2022.929835

Corrigendum: Acute Administration of Metformin Protects Against Neuronal Apoptosis Induced by Cerebral Ischemia-Reperfusion Injury *via* Regulation of the AMPK/CREB/BDNF Pathway

Ke Liu[1†], Lulu Li[2†], Zhijun Liu[1†], Gang Li[1], Yanqing Wu[1], Xingjun Jiang[1], Mengdie Wang[1], Yanmin Chang[1], Tingting Jiang[1], Jianheng Luo[1], Jiahui Zhu[1], Hongge Li[1] and Yong Wang[1]**

[1]Department of Neurology, Union Hospital, Tongji Medical College, Huazhong University of Science and Technology, Wuhan, China, [2]Department of Neurology, People's Hospital of Zhengzhou, People's Hospital of Henan University of Chinese Medicine, Zhengzhou, China

Keywords: cerebral ischemia-reperfusion injury, metformin, AMP-activated protein kinase, neuronal apoptosis, brain-derived neurotrophic factor

OPEN ACCESS

Approved by:
Frontiers Editorial Office, Frontiers Media SA, Switzerland

****Correspondence:***
Hongge Li
hgeli0609@163.com
Yong Wang
370687495@qq.com

†These authors have contributed equally to this work

Specialty section:
This article was submitted to Neuropharmacology, a section of the journal Frontiers in Pharmacology

Received: *27 April 2022*
Accepted: *29 April 2022*
Published: *02 June 2022*

Citation:
Liu K, Li L, Liu Z, Li G, Wu Y, Jiang X, Wang M, Chang Y, Jiang T, Luo J, Zhu J, Li H and Wang Y (2022) Corrigendum: Acute Administration of Metformin Protects Against Neuronal Apoptosis Induced by Cerebral Ischemia-Reperfusion Injury via Regulation of the AMPK/CREB/BDNF Pathway. Front. Pharmacol. 13:929835. doi: 10.3389/fphar.2022.929835

A Corrigendum on

Acute Administration of Metformin Protects Against Neuronal Apoptosis Induced by Cerebral Ischemia-Reperfusion Injury via Regulation of the AMPK/CREB/BDNF Pathway
by Liu K, Li L, Liu Z, Li G, Wu Y, Jiang X, Wang M, Chang Y, Jiang T, Luo J, Zhu J, Li H and Wang Y (2022). Front. Pharmacol. 13:832611. doi: 10.3389/fphar.2022.832611

In the published article, there was an error in **Affiliation 1**. Instead of "Department of Neurology, Tongji Medical College, Union Hospital, Huazhong University of Science and Technology, Wuhan, China," it should be "Department of Neurology, Union Hospital, Tongji Medical College, Huazhong University of Science and Technology, Wuhan, China."

The authors apologize for this error and state that this does not change the scientific conclusions of the article in any way. The original article has been updated.

frontiers | Frontiers in Pharmacology

SYSTEMATIC REVIEW
published: 08 April 2022
doi: 10.3389/fphar.2022.827770

Preclinical Evidence of Paeoniflorin Effectiveness for the Management of Cerebral Ischemia/Reperfusion Injury: A Systematic Review and Meta-Analysis

Anzhu Wang[1,2], *Wei Zhao*[3], *Kaituo Yan*[3], *Pingping Huang*[1,2], *Hongwei Zhang*[1,2] *and Xiaochang Ma*[1,4]*

[1]Xiyuan Hospital, China Academy of Chinese Medical Sciences, Beijing, China, [2]Graduate School, China Academy of Chinese Medical Sciences, Beijing, China, [3]Yidu Central Hospital of Weifang, Weifang, China, [4]National Clinical Research Center for Chinese Medicine Cardiology, Beijing, China

Background: Vessel recanalization is the main treatment for ischemic stroke; however, not all patients benefit from it. This lack of treatment benefit is related to the accompanying ischemia-reperfusion (I/R) injury. Therefore, neuroprotective therapy for I/R Injury needs to be further studied. *Paeonia lactiflora Pall.* is a commonly used for ischemic stroke management in traditional Chinese medicine; its main active ingredient is paeoniflorin (PF). We aimed to determine the PF's effects and the underlying mechanisms in instances of cerebral I/R injury.

Methods: We searched seven databases from their inception to July 2021.SYRCLE's risk of bias tool was used to assess methodological quality. Review Manager 5.3 and STATA 12.0 software were used for meta-analysis.

Results: Thirteen studies, including 282 animals overall, were selected. The meta-analyses showed compared to control treatment, PF significantly reduced neurological severity scores, cerebral infarction size, and brain water content (p = 0.000). In the PF treatment groups, the apoptosis cells and levels of inflammatory factors (IL-1β) decreased compared to those in the control groups (p = 0.000).

Conclusion: Our results suggest that PF is a promising therapeutic for cerebral I/R injury management. However, to evaluate the effects and safety of PF in a more accurate manner, additional preclinical studies are necessary.

Keywords: preclinical evidence, potential mechanisms, paeoniflorin, cerebral ischemia-reperfusion injury, animal studies

OPEN ACCESS

Edited by:
Li-Nan Zhang,
Hebei Medical University, China

Reviewed by:
Yong Zhao,
Chongqing Medical University, China
Ted Carl Kejlberg Andelius,
Aarhus University, Denmark
Xiaoli Liu,
Zhejiang Hospital, China

***Correspondence:**
Xiaochang Ma
maxiaochang@x263.net

Specialty section:
This article was submitted to Neuropharmacology, a section of the journal Frontiers in Pharmacology

Received: *02 December 2021*
Accepted: *24 March 2022*
Published: *08 April 2022*

Citation:
Wang A, Zhao W, Yan K, Huang P, Zhang H and Ma X (2022) Preclinical Evidence of Paeoniflorin Effectiveness for the Management of Cerebral Ischemia/Reperfusion Injury: A Systematic Review and Meta-Analysis. Front. Pharmacol. 13:827770. doi: 10.3389/fphar.2022.827770

INTRODUCTION

Stroke is the second leading cause of death worldwide, and 84.4% of stroke cases are related to ischemia (Collaborators, 2019). Although mechanical thrombectomy and intravenous thrombolysis have been widely recommended and used in the treatment of acute ischemic stroke patients, the treatments are not effective in all patients (Powers et al., 2018; Liu et al., 2020). Besides some known

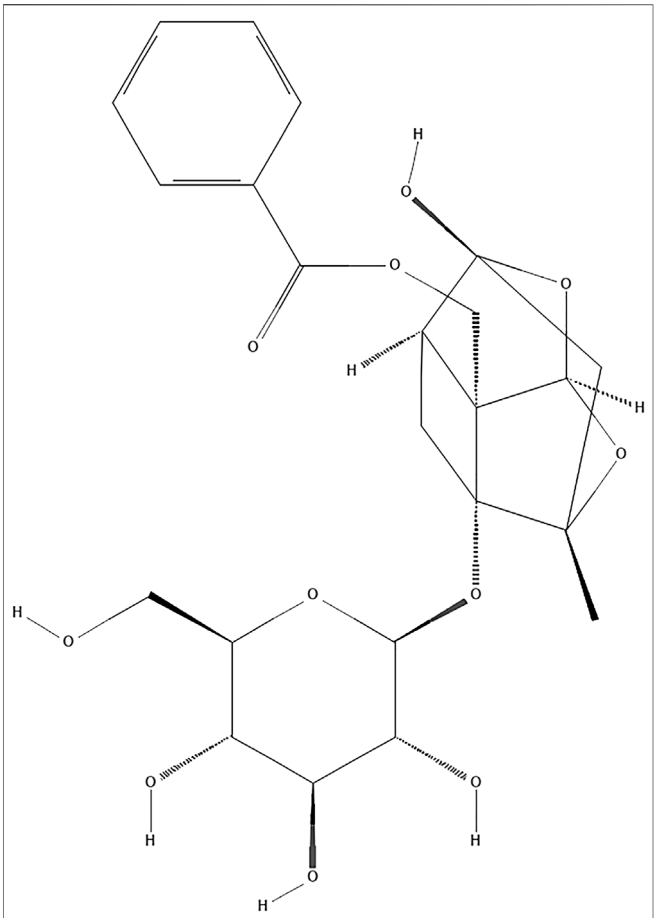

FIGURE 1 | Chemical structure of paeoniflorin.

complications, subsequent ischemia/reperfusion (I/R) injury may be the most important factor resulting in a poor prognosis (Kalogeris et al., 2016). Cerebral I/R injury is characterized by a biochemical cascade of ischemic reactions that result in brain tissue deterioration, limiting the beneficial effects of vascular recanalization (Hu et al., 2015). I/R injury is involved in some complicated pathophysiological mechanisms, such as the release of excitatory neurotransmitters, the acceleration of Ca^{2+} influx into cells, free radical damage, neuronal apoptosis, neuroinflammation, and fat decomposition (Siesjo, 1992; Wang and Lo, 2003; Wu et al., 2018). Therefore, currently used neuroprotective therapies aimed at I/R injury management need further research.

Animal models of ischemic stroke are crucial for determining the pathophysiology of ischemic stroke and creating novel stroke therapies. *In vivo* stroke models are now predominantly mice and rats, which is understandable given the lower costs of procurement and maintenance, as well as the ease of monitoring and tissue processing (Sommer, 2017). The intraluminal suture middle cerebral artery occlusion (MCAO) model, which does not need craniectomy, is the most commonly used experimental model for ischemic stroke in rats (Alrafiah, 2021).

Paeoniflorin (PF, C23H28O11; **Figure 1**) is a natural compound derived from *Paeonia lactiflora Pall.* (Family Ranunculaceae, molecular mass: 480.5) (Sterne et al., 2019). Traditional Chinese medicine (TCM) theory believes that *Paeonia lactiflora Pall.* has the function of clearing heat and cooling blood, promoting blood circulation and removing blood stasis. As an important component of traditional TCM compounds such as Buyanghuanwu Decoction and Huangqi Guizhi Wuwu Decoction, *Paeonia lactiflora Pall.* is widely used in stroke treatment in China (Chen et al., 2019; He et al., 2021). The neuroprotective benefits of PF have received a lot of attention in recent years. At present, the effects and mechanisms of PF on the central nervous system mainly come from *in vitro* experiments on nerve cells (such as primary cortical and hippocampal neurons, PC12 cells, and microglia cells) and *in vivo* investigations (Hu et al., 2018; Cong et al., 2019; Cheng et al., 2021). Studies have confirmed that PF can cross the blood-brain barrier, and its mechanism may be related to the mode of cell death, inflammation, oxidative stress and epigenetics (Jiao et al., 2021). Furthermore, PF has demonstrated its potential therapeutic utility in preventing I/R damage in a variety of tissues (Xie et al., 2018; Wen et al., 2019).Because of the complexity of clinical medicine, many differences between preclinical and clinical studies have prevented the further application of PF. A systematic review can not only offer reliable evidence but also facilitate the choice of an appropriate medicine for clinical experiments (van Luijk et al., 2013). However, no thorough examination of the effectiveness of PF pooled in preclinical investigations has been done to date. For this reason, we conducted a full systematic review and meta-analysis to evaluate PF's effects in small-animal research on brain I/R Injury.

MATERIALS AND METHODS

This is a systematic review and meta-analysis based on Preferred Reporting Items for Systematic Reviews and Meta-Analyses (PRISMA).

Search Strategy

We systematically searched the following seven databases: China National Knowledge Infrastructure, Wanfang Database, VIP Database, PubMed, Cochrane Library, Web of Science, and EMBASE from their inception to July 2021. The search terms used were as follows: ("Paeoniflorin" OR "Peoniflorin") AND ("Brain Ischemia" OR "Ischemic Encephalopathy" OR "Cerebral Ischemia") AND ("Reperfusion Injury" OR "Reperfusion Damage" OR "Ischemia-Reperfusion Injury"). In addition, all review articles, meeting abstracts, and their references were examined thoroughly without language limitations. The search target was research on animals.

Inclusion and Exclusion Criteria

The inclusion criteria were as follows: (1) establishment of I/R experimental models through MCAO; (2) PF as the only consistent therapeutic medication and the use of placebo or no

treatment in animals in the control group; and (3) animal research. The exclusion criteria were as follows: (1) establishment of I/R experimental models through other means; (2) PF not being the only intervention; (3) treatment of animals by using PF analogs; (4) literature with repetitive content; and (5) *in vitro* studies.

Data Extraction

Two reviewers (Anzhu Wang and Pingping Huang) independently selected literature per the abovementioned criteria and resolved differences by discussion with assistance from a third reviewer (Xiaochang Ma). The following information was extracted from each study and is summarized in a table: (1) study features (names of the first authors and publication data); (2) animal characteristics including species, sex, weight, and age; (3) key elements of the MCAO model—the types of anesthetics used and duration of ischemia; (4) information about interventions—administration route, dose, and treatment time; and (5) mean and standard deviation values of the results. When findings were recorded at different time points, only those corresponding to the latest time point were considered. When different doses of a medicine were administered, the reviewers only record the highest dose. If data was reported in the form of a figure, the reviewers used a digital ruler, specifically the Adobe ruler, to determine the numerical values. If there were several publications with similar data, we only chose the earliest one or the one with the most samples.

Quality Assessment

The included studies were assessed for bias by using the SYRCLE's risk of bias tool by two independent reviewers (Anzhu Wang and Pingping Huang) (Hooijmans et al., 2014): which are: selection bias (sequence generation, baseline characteristics, and allocation concealment), performance bias (random housing and blinding of investigators), detection bias (random outcome assessment and blinding of the assessor to outcomes), withdrawal bias (availability of incomplete outcome data), selective reporting bias (selective outcome reporting), and other bias (other sources of bias). When one required standard was reached, one point was assigned. After evaluating 10 standards, each piece of literature was assigned a comprehensive quality score. Two reviewers, Anzhu Wang and Pingping Huang, resolved differences through discussion and with assistance from Xiaochang Ma, the third reviewer.

Statistical Analysis

Reviewers adopted Review Manager 5.3 and STATA 12.0 for data analysis. Outcomes were presented as standardized mean differences with a 95% confidence interval. $p < 0.05$ indicated statistically significant. There was statistical heterogeneity between the Q test and I^2 results for the literature assessed. $p < 0.1$ and $I^2 > 50\%$ were regarded to indicate significant heterogeneity; outcomes were assessed using a random-effects model. $p > 0.1$ and $I^2 \leq 50\%$ were regarded as indicating no heterogeneity; the outcomes were evaluated using a fixed-effects model. Potential publication bias was examined and evaluated by applying Egger's test. Sensitivity and subgroup analyses for a single study were performed using Metaninf.

RESULTS

Study Selection

We identified 452 studies in the database search, and 219 studies remained after eliminating repeated studies. After reading titles and abstracts, 44 studies are considered. Overall, 175 pieces of literature were eliminated for the following reasons: (1) PF was not the intervention drug, no animal experiment, or no MCAO model; and (2) the articles were reviews or case reports. Finally, 13 were considered after reading the full text and 31 were eliminated. The reasons for exclusion were: (1) non-continuous administration; (2) redundant publications; (3) no ischemia-reperfusion injury; and (4) non-availability of data. The process of literature selection is shown in **Figure 2**.

Study Characteristics

A total of 13 studies (Xiao, 2005; Wang, 2008; Tang et al., 2010; He, 2014; Mao et al., 2014; Rao, 2014; Zhang et al., 2015; Liu, 2016; Chu et al., 2017; Ko et al., 2018; Liao, 2018; Yu et al., 2018; Tang et al., 2021), including five English studies (Tang et al., 2010; Zhang et al., 2015; Chu et al., 2017; Ko et al., 2018; Tang et al., 2021) and eight Chinese studies (Xiao, 2005; Wang, 2008; He, 2014; Mao et al., 2014; Rao, 2014; Liu, 2016; Liao, 2018; Yu et al., 2018),were considered. The studies were published from 2005 to 2021. Five of these were master's or doctoral theses (Xiao, 2005; Wang, 2008; He, 2014; Rao, 2014; Liao, 2018). All of them were concerned with 282 male Sprague–Dawley rats, whose weight varied from 180 to 350 g. In one study, pentobarbital sodium was used to anesthetize animals (Yu et al., 2018), while isoflurane was used in another (Ko et al., 2018). Chloral hydrate was used in the remaining 11 (Xiao, 2005; Wang, 2008; Tang et al., 2010; He, 2014; Mao et al., 2014; Rao, 2014; Zhang et al., 2015; Liu, 2016; Chu et al., 2017; Liao, 2018; Tang et al., 2021). Moreover, in five studies, PF was used before treatment (Xiao, 2005; Wang, 2008; He, 2014; Mao et al., 2014; Liu, 2016), and in seven, it was used after treatment (Rao, 2014; Zhang et al., 2015; Chu et al., 2017; Ko et al., 2018; Liao, 2018; Yu et al., 2018; Tang et al., 2021). In one study, it was used both before and after treatment (Tang et al., 2010). Furthermore, in nine out of 13 studies, intraperitoneal administration was adopted (Xiao, 2005; Wang, 2008; He, 2014; Zhang et al., 2015; Liu, 2016; Chu et al., 2017; Ko et al., 2018; Yu et al., 2018; Tang et al., 2021), while in three, intravenous tail injection was performed (Tang et al., 2010; Liao, 2018; Yu et al., 2018). In the final study, intragastric administration was adopted (Mao et al., 2014). Neurological severity scores (NSS) were reported in all studies. Three studies (Xiao, 2005; Tang et al., 2010; Mao et al., 2014) referred to the scoring method of Bederson et al. (1986), while three others (Chu et al., 2017; Ko et al., 2018; Tang et al., 2021) referred to the scoring method of Chen et al. (2001). In seven studies (Wang, 2008; He, 2014; Rao, 2014; Zhang et al., 2015; Liu, 2016; Liao, 2018; Yu et al., 2018), the scoring method of Longa et al. (1989) was used. Cerebral infarction size (CIS) was reported in nine studies (Xiao, 2005; Wang, 2008; Tang et al., 2010; He, 2014; Rao, 2014; Zhang et al., 2015; Liu, 2016; Liao, 2018; Yu et al., 2018). One out of the nine studies did not mention the exact

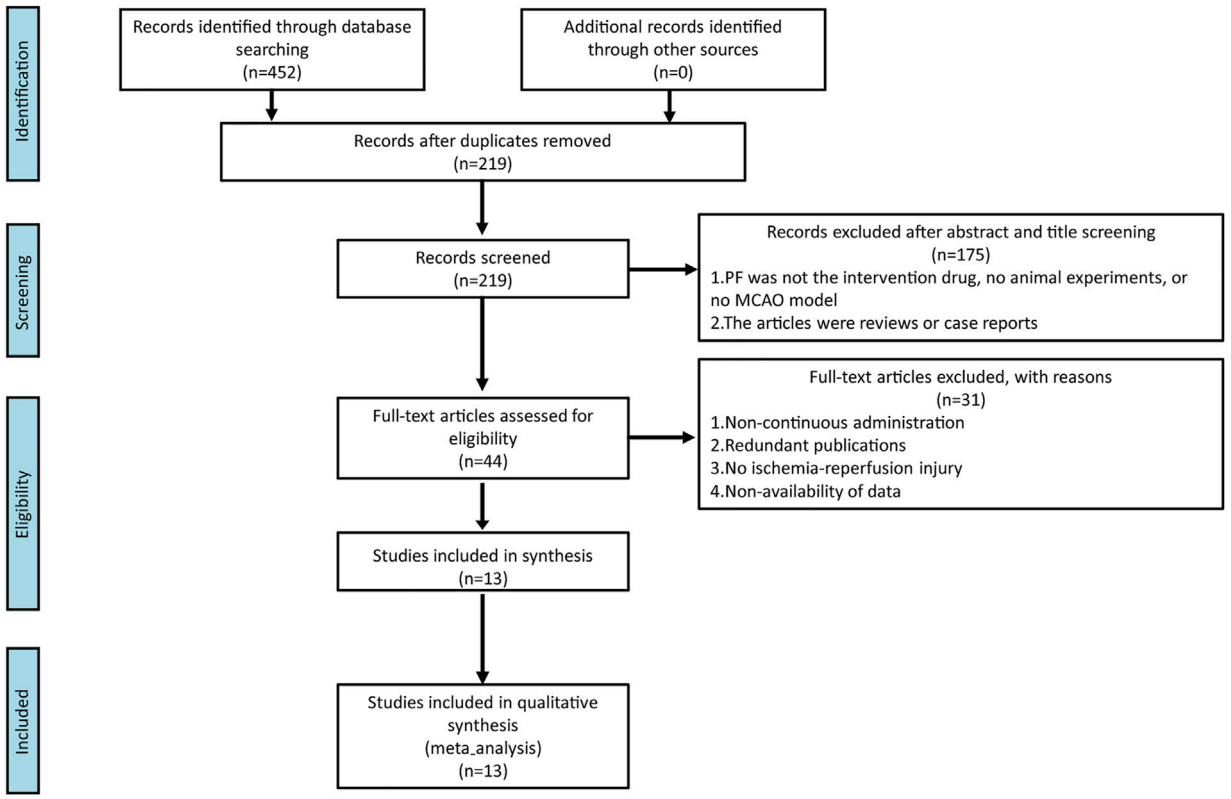

FIGURE 2 | Flow diagram of the study-search process.

method (Liu, 2016). In three of the nine studies, infarct area/contralateral brain area was used for CIS determination (Xiao, 2005; He, 2014; Rao, 2014). In the remaining five studies, CIS determination was based on infarction area/total brain area (Wang, 2008; Tang et al., 2010; Zhang et al., 2015; Liao, 2018; Yu et al., 2018). In five studies, the expression of the associated protein was determined by western blot (WB) (Xiao, 2005; Wang, 2008; He, 2014; Chu et al., 2017; Tang et al., 2021), while in two, reverse transcription-polymerase chain reaction (RT-PCR) was used (Xiao, 2005; He, 2014). In seven studies, the TUNEL assay was performed (Wang, 2008; Tang et al., 2010; Mao et al., 2014; Zhang et al., 2015; Liu, 2016; Ko et al., 2018; Tang et al., 2021). In eight studies, immunohistochemistry (IHC) was performed (Wang, 2008; Tang et al., 2010; Mao et al., 2014; Zhang et al., 2015; Liu, 2016; Ko et al., 2018; Liao, 2018; Yu et al., 2018), while in two, an immunofluorescence (IF) assay was conducted (Ko et al., 2018; Tang et al., 2021). Three studies reported brain water content (BWC) (He, 2014; Rao, 2014; Chu et al., 2017). In two studies, correlated factors were determined using an enzyme linked immunosorbent assay (ELISA) (Liao, 2018; Tang et al., 2021). Two studies focused on morphological changes (Rao, 2014; Yu et al., 2018). One study reported results for peripheral blood cells (Tang et al., 2010). One study reported superoxide dismutase (SOD) levels (He, 2014), and another reported brain specific gravity and blood-brain barrier (BBB) permeability (Chu et al., 2017). One study reported the Rotarod test (Ko et al., 2018), and another reported the foot fault test (Tang et al., 2021). The general features of the included studies are listed in **Table 1**.

Methodological Quality of the Included Studies

The quality scores of studies ranged from 3 to 6. Two studies did not report random grouping (Tang et al., 2010; Tang et al., 2021). Only three studies out of 11 reported the exact randomization method (He, 2014; Liao, 2018; Yu et al., 2018), despite the fact that 11 studies reported randomization (Xiao, 2005; Wang, 2008; He, 2014; Mao et al., 2014; Rao, 2014; Zhang et al., 2015; Liu, 2016; Chu et al., 2017; Ko et al., 2018; Liao, 2018; Yu et al., 2018). In five studies (Tang et al., 2010; Rao, 2014; Chu et al., 2017; Ko et al., 2018; Tang et al., 2021), the modeling method was assessed using doppler analysis, and in six studies (Wang, 2008; He, 2014; Mao et al., 2014; Liu, 2016; Liao, 2018; Yu et al., 2018), NSS was used to guarantee the unification of experimental baseline standards. In the remaining studies, the modeling method was not assessed. Four studies (Tang et al., 2010; Chu et al., 2017; Ko et al., 2018; Tang et al., 2021) reported the feeding environment of the animals. However, none of the studies reported allocation concealment, blinding of investigators, or random outcome assessments. In four studies (Tang et al., 2010; Zhang et al., 2015; Chu et al., 2017; Ko et al., 2018), assessors were blinded to outcomes. The data reported in three studies were incomplete (He, 2014; Liao, 2018; Yu et al.,

TABLE 1 | Basic characteristics of the included studies.

Author	Type	Species	Anesthetic	Ischemia duration	Time of PF administration	Control group	Experimental group (daily dosage, approach, duration)	Outcome measures	Proposed mechanism
Xiao, (2005)	Doctoral thesis	Rat/M/SD 220–250 g	Chloral hydrate	90 min	48 h before MCAO	NS	40 mg/kg,ip, 24 h	1.CIS,2. NSS,3.RT-PCR(COX-2↓), 4.WB(COX-2↓)	Activation of adenosine A1 receptors and downregulation of COX-2
Wang, (2008)	Master's thesis	Rat/M/SD 250 ± 30 g	Chloral hydrate	90 min	30 min before MCAO	NS	60 mg/kg,ip, 24 h	1.CIS,2. NSS,3.TUNEL,4.IHC(FAS↓, TNF-α↓), 5.WB(P-P38↓, iNOS↓)	Anti-apoptosis, downregulation of p-p38, iNOS, FAS, and TNF-α
Tang et al. (2010)	Journal	Rat/M/SD 300–350 g	Chloral hydrate	90 min	10 min before MCAO/ 30 min after MCAO	PBS	20 mg/kg,iv, 24 h	1.NSS, 2. CIS, 3.IHC(ED1↓, IL-1β↓, TNF-α↓, ICAM-1↓, MPO↓),4.TUNEL	Anti-inflammation and anti-apoptosis
He, (2014)	Master's thesis	Rat/M/SD 250–300 g	Chloral hydrate	90 min	48 h before MCAO	NS	20 mg/kg,ip, 72 h	1.CIS,2. NSS,3.BWC,4.SOD↑,5.RT-PCR(Nrf2↑),6.WB(Nrf2↑)	Anti-oxidative stress, activation of SOD, and upregulation of the Nrf2 pathway
Mao et al. (2014)	Journal	Rat/M/SD 250 ± 10 g	Chloral hydrate	90 min	3d before MCAO	PBS	200 mg/kg,ig, 24 h	1.NSS.2.TUNEL.3.IHC(CHOP↓)	Anti-apoptosis, downregulation of CHOP
Rao, (2014)	Master's thesis	Rat/M/SD 260–300 g	Chloral hydrate	90 min	30 min after MCAO	NS	40 mg/kg (20 mg/kg,bid), ip, 24 h	1.NSS,2.CIS,3.BWC.4.Morphological changes	Downregulation of arachidonic acid expression via cyclooxygense pathways, activation of CBR2
Zhang et al. (2015)	Journal	Rat/M/SD 280 ± 20 g	Chloral hydrate	2 h	2 h after MCAO	NS	10 mg/kg (5 mg/kg,bid),ip,7d	1.NSS,2.CIS,3.IHC(NeuN↑, GFAP↑, MAP-2↓),4.TUNEL	Deactivation of astrocytes and anti-apoptosis
Liu, (2016)	Journal	Rat/M/SD 250–300 g	Chloral hydrate	24 h	30 min before MCAO	NS	60 mg/kg,ip, 24 h	1.NSS,2.CIS,3.TUNEL,4.IHC (Bcl-2↑, Bax↓)	Anti-apoptosis by downregulation Bax and activation Bcl-2
Chu et al. (2017)	Journal	Rat/M/SD 280–300 g	Chloral hydrate	90 min	1 h after I/R	NM	10 mg/kg (5 mg/kg), bid,ip,7d	1.NSS,2.BWC,3.Brain specific gravity, 4.BBB permeability,5.WB(Cx43↓,AQP4↓,p-JNK↑,p-ERK↔,p-p38↔), 6.IF(AQP4↓)	Downregulation Cx43 and AQP4 via JNK pathway activation
Liao, (2018)	Master's thesis	Rat/M/SD 200 ± 20 g	Chloral hydrate	1 h	8 h after I/R	NS	5 mg/kg,iv,7d	1.NSS,2.CIS,3.ELISA(IL-1β↓, TNF-α↓), 4.IHC(NF-kB/P65↓)	Downregulation NF-kB pathway, anti-inflammation
Yu et al. (2018)	Journal	Rat/M/SD 180–220 g	Pentobarbital sodium	1 h	6 h after I/R	NS	5 mg/kg,iv,7d	1.NSS,2.CIS,3.Morphological changes, 4.IHC(p-Akt↑)	Activation PI3K/Akt signaling pathway
Ko et al. (2018)	Journal	Rat/M/SD 250–350 g	Isoflurane	15 min	24 h after MCAO	NM	20 mg/kg,ip,6d	1.NSS, 2.Rotarod test, 3.IHC(nAChRs α4β2↓, Ki67↑), 4.IF(CD68↑, nAChR α7↑), 5.TUNEL	Anti-apoptosis and promotion of neurogenesis
Tang et al. (2021)	Journal	Rat/M/SD 200–250 g	Chloral hydrate	2 h	2 h after MCAO	Vehicle (PBS + DMSO)	10 mg/kg,ip,14d	1.NSS,2.foot-fault test,3.WB(Iba-1↓, JNK↔,p-JNK↓,nuclear P65↓),4.ELISA(TNF-α↓, IL-1β↓ and IL-6↓),5.IF(Iba-1↓, vWF↑,DCX↑,P65↓),6.TUNEL	Anti-inflammation and promotion of neurogenesis

AKT, Protein kinase B; AQP4, Aquaporin4; BAX, BCL-2, associated X; BBB, Blood-brain barrier; BCL-2, B-cell lymphoma-2; Bid, Bis in di; BWC, brain water content; CBR2, Cannabinoid 2 receptors; CHOP, C/EBP, homologous protein; CIS, cerebral infarction size; COX-2, Cyclooxygenase 2; Cx43, Connexin43; d, Day; DCX, doublecortin; ED1, Mouse anti rat CD68; ELISA, Enzyme linked immunosorbent assay; ERK, Extracellular signal-regulated kinase; FAS, fas cell surface death receptor; GFAP, glial fibrillary acidic protein; h, Hour; i.g, Irrigation; i.p., intraperitoneal; i.v., intravenous; Iba-1, Ionized calcium-binding adapter molecule 1; ICAM-1, Intercellular adhesion molecule-1; IF, immunofluorescence; IHC, immunohistochemistry; IL-1β, Interleukin-1β; IL-6, Interleukin-6; iNOS, inducible nitric oxide synthase; JNK, c-Jun N-terminal kinase; Ki67, Mitotic cell marker; MAP-2, Microtubule-associated protein 2; MCAO, middle cerebral artery occlusion; min, Minute; MPO, myeloperoxidase; nAChRsα4β2, α4β2 nicotinic acetylcholine receptors; nAChRα7, α7 nicotinic acetylcholine receptor; NeuN, Neuron-specific nuclear; NF-κB/P65, Nuclear transcription factor-kappa B; NM, not mentioned; Nrf2, Nuclear factor erythroid 2-related factor 2; NS, normal saline; NSS, neurological severity score; p-AKT, Phosphorylated AKT; PBS, Phosphate-buffered saline; p-ERK, Phosphorylated ERK; PI3K, Phosphoinositide 3-kinases; p-JNK, Phosphorylated JNK; p-P38, Phosphorylated P38; RT-PCR, Reverse transcription-polymerase chain reaction; SD, Sprague-Dawley; SOD, Superoxide dismutase; TNF-α, Tumor necrosis factor-α; vWF, von willebrand factor; WB, Western blot. ↑, upregulated; ↓, downregulated; ↔, No difference.

TABLE 2 | The research quality of the included studies.

Study	①	②	③	④	⑤	⑥	⑦	⑧	⑨	⑩	Scores
Xiao, (2005)	0	0	0	0	0	0	0	1	1	1	3
Wang, (2008)	0	1	0	0	0	0	0	1	1	1	4
Tang et al. (2010)	0	1	0	1	0	0	1	1	1	1	6
He, (2014)	1	1	0	0	0	0	0	0	1	1	4
Mao et al. (2014)	0	1	0	0	0	0	0	1	1	0	3
Rao, (2014)	0	1	0	0	0	0	0	1	1	1	4
Zhang et al. (2015)	0	0	0	0	0	0	1	1	0	1	3
Liu, (2016)	0	1	0	0	0	0	0	1	0	1	3
Chu et al. (2017)	0	1	0	1	0	0	1	1	1	1	6
Liao, (2018)	1	1	0	0	0	0	0	0	1	1	4
Yu et al. (2018)	1	1	0	0	0	0	0	0	1	1	4
Ko et al. (2018)	0	1	0	1	0	0	1	1	1	1	6
Tang et al. (2021)	0	1	0	1	0	0	0	1	1	1	5

①Sequence generation; ②Baseline characteristics; ③Allocation concealment; ④Random housing; ⑤Blinding of investigators; ⑥Random outcome assessment; ⑦Blinding of assessors to the outcomes; ⑧Incomplete outcome data; ⑨Selective outcome reporting; ⑩Other sources of bias.

2018). Results were inconsistent with the research methods in two studies (Zhang et al., 2015; Liu, 2016). One study reported the supply of new animals (Mao et al., 2014). The general features of the included studies are shown in **Table 2** and **Figure 3**.

NSS

According to $p < 0.1$ and $I^2 > 50\%$,an analysis of NSS data in 13 studies (Xiao, 2005; Wang, 2008; Tang et al., 2010; He, 2014; Mao et al., 2014; Rao, 2014; Zhang et al., 2015; Liu, 2016; Chu et al., 2017; Ko et al., 2018; Liao, 2018; Yu et al., 2018; Tang et al., 2021) showed significant heterogeneity among the results of the studies ($p = 0.000$, $I^2 = 74.6\%$). A random-effects model was used for the analyses, and in comparison with the control group, PF was shown to reduce the NSS (SMD = −2.04, 95% CI = [−2.64, −1.43], $p = 0.000$). After sensitivity analysis of the included studies, PF was still shown to reduce the NSS in comparison with the control group (**Figure 4**). Subgroup analysis indicated that the improvement in the NSS summarized estimated value did not depend on the PF intervention time, duration, daily dosage, and ischemia time (**Table 3**). Meta-regression did not demonstrate a prominent influence of the covariates (intervention time, duration, daily dosage, ischemia time, sample size, route of administration and anesthetic) on the effects of PF (**Table 4**).

CIS

Nine studies (Xiao, 2005; Wang, 2008; Tang et al., 2010; He, 2014; Rao, 2014; Zhang et al., 2015; Liu, 2016; Liao, 2018; Yu et al., 2018) presented CIS data. According to $p < 0.1$ and $I^2 > 50\%$, and the results showed significant heterogeneity ($p = 0.000$, $I^2 = 88.1\%$). In comparison with the control group, PF was shown to reduce the CIS in the random-effects model (SMD = −4.78, 95% CI = [−6.51, −3.05], $p = 0.000$). After sensitivity analysis of the included studies, PF was still shown to reduce the CIS in comparison with the control group (**Figure 5**).

BWC

Three studies (He, 2014; Rao, 2014; Chu et al., 2017) presented data for BWC, and the results showed no heterogeneity according to $p > 0.1$ and $I^2 \leq 50\%$ ($p = 0.383$, $I^2 = 0.0\%$). In comparison with the control group, PF was shown to alleviate BWC in analyses with the fixed-effects model (SMD = −3.03, 95% CI = [−4.35, −1.71], $p = 0.000$; **Figure 6**).

Other Outcomes

Seven studies (Wang, 2008; Tang et al., 2010; Mao et al., 2014; Zhang et al., 2015; Liu, 2016; Ko et al., 2018; Tang et al., 2021) presented the results of TUNEL staining. Among these, one study (Zhang et al., 2015) was ruled out because the data were not available, and another study (Tang et al., 2021) was ruled out because of substantial heterogeneity in the data. A fixed-effects model was used with the last five studies (Wang, 2008; Tang et al., 2010; Mao et al., 2014; Liu, 2016; Ko et al., 2018) because of no heterogeneity among them according to $p > 0.1$ and $I^2 \leq 50\%$ ($p = 0.103$, $I^2 = 48.1\%$). In comparison with the control group, PF was shown to inhibit apoptosis (SMD = −2.62, 95% CI = [−3.32, −1.93], $p = 0.000$; **Figure 7A**).

Two studies presented the results of ELISA (Liao, 2018; Tang et al., 2021), of which one reported the findings for interleukin-1β (IL-1β), tumor necrosis factor-α(TNF-α), and interleukin-6(IL-6) (Tang et al., 2021), while the other one reported data for IL-1β and TNF-α (Liao, 2018). According to $p > 0.1$ and $I^2 \leq 50\%$, the IL-1β results showed no heterogeneity ($p = 0.360$, $I^2 = 0.0\%$). In comparison with the control group using the fixed-effects model, PF was shown to decrease the level of IL-1β (SMD = −8.45, 95% CI = [−11.22, −5.69], $p = 0.000$; **Figure 7B**), and the TNF-α results showed significant heterogeneity ($p = 0.002$, $I^2 = 89.9\%$) according to $p < 0.1$ and $I^2 > 50\%$. In analyses with a random-effects model, in comparison with the control group, PF was shown to decrease the level of TNF-α, but the difference was not statistically significant (SMD = −10.57, 95% CI = [−21.54, 0.39], $p = 0.059$; **Figure 7C**).

Two studies reported morphological changes (Rao, 2014; Yu et al., 2018). In comparison with the control group, most nerve cells in the hippocampus of cornu ammonis 1(CA1) in the PF group were characterized by structural integrity, light morphological changes, and less karyopyknosis. In other analyses, one study reported that PF could improve the

FIGURE 3 | Evaluation of the literature quality results obtained through SYRCLE's risk of bias based on the Cochrane tool. **(A)** Risk of bias summary. **(B)** Risk of bias graph.

activity of SOD in the MCAO model (He, 2014); one study reported that PF could increase brain-specific gravity and reduce BBB permeability in the MCAO model (Chu et al., 2017); one study (Ko et al., 2018) reported the findings for the Rotarod test and one study (Tang et al., 2021) reported the findings for the foot-fault test, and the results of both tests showed that PF could improve neurological symptoms. The results of WB (Xiao, 2005; Wang, 2008; He, 2014; Chu et al., 2017; Tang et al., 2021), RT-PCR (Xiao, 2005; He, 2014), IHC (Wang, 2008; Tang et al., 2010; Mao et al., 2014; Zhang et al., 2015; Liu, 2016; Ko et al., 2018; Liao, 2018; Yu et al., 2018), and IF (Ko et al., 2018; Tang et al., 2021) are shown in **Table 1**. Complete data can be found in the **Supplementary Table S1** and the PRISMA 2020 Checklist is in the **Supplementary Table S2**.

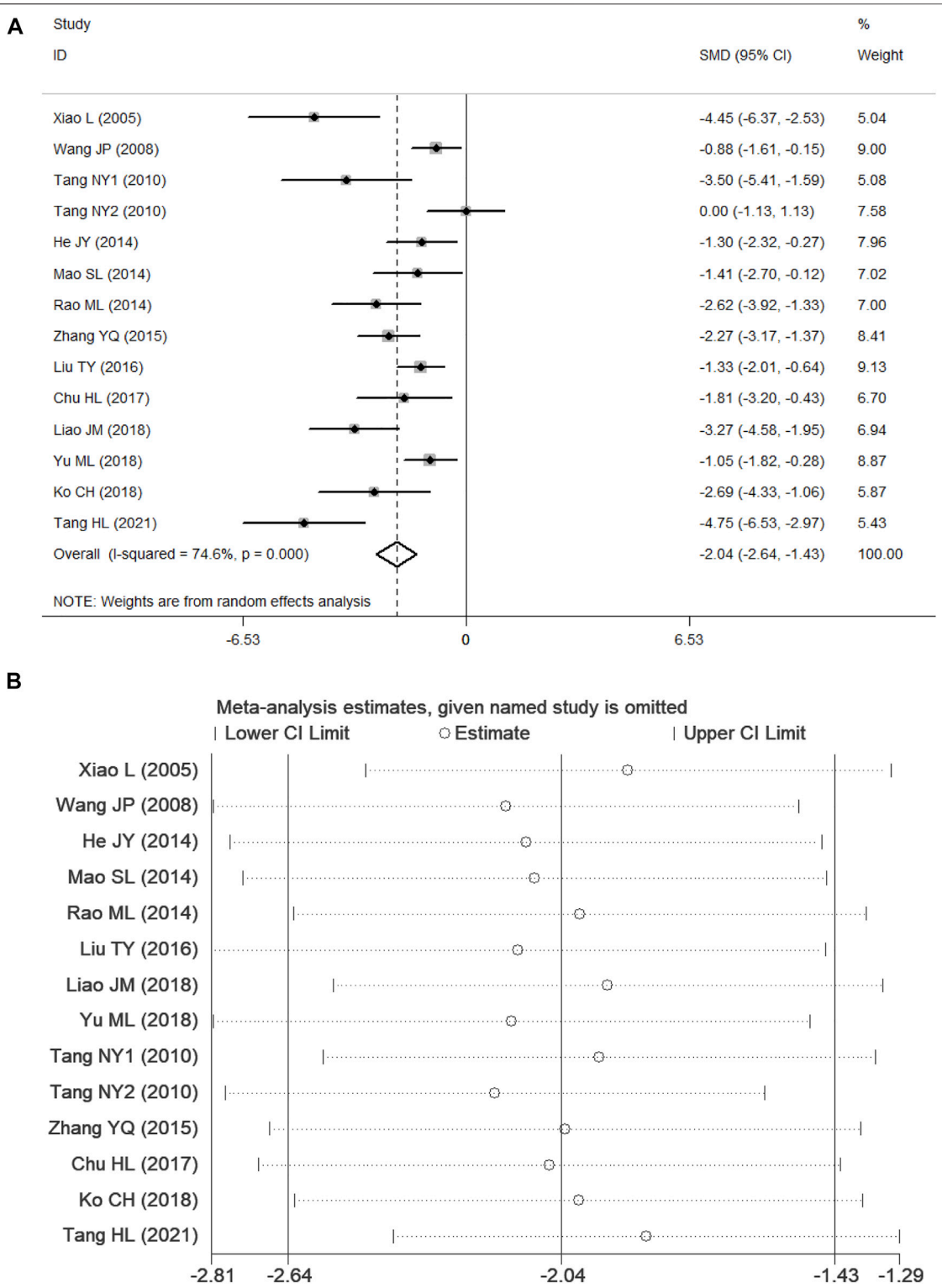

FIGURE 4 | Forest plots of PF for NSS. **(A)** Effects of PF on decreasing the NSS in comparison with the control group; **(B)** sensitivity analysis of PF for NSS.

Publication Bias

For the NSS subset, Egger's linear regression test was performed, and it indicated the possibility of publication bias (P > ItI = 0.004 for Egger's test). The adjusted random-effects pooled HR of −2.036 (95% CI, −2.638 to −1.435), obtained using the trim-and-fill method, was unchanged because no trimming was performed (**Figure 8**).

TABLE 3 | Study characteristics accounting for heterogeneity in the NSS subgroup analysis.

Analysis	References	Fixed-effects model, HR (95% CI)	*p*	Random-effects model HR (95% CI)	*p*	I^2 (%)	ph
NSS	Chu et al. (2017), He, (2014), Ko et al. (2018), Liao, (2018), Liu, (2016), Mao et al. (2014), Rao, (2014), Tang et al. (2021), Tang et al. (2010), Wang, (2008), Xiao, (2005), Yu et al. (2018), Zhang et al. (2015)	−1.657(−1.943, −1.370)	0.000	−2.036 (−2.638, −1.435)	0.000	74.6	0.000
Subgroup 1							
pre-treatment	He, (2014), Liu, (2016), Mao et al. (2014), Tang et al. (2010), Wang, (2008), Xiao, (2005)	−1.430(−1.835–1.025)	0.000	−1.806 (−2.620, −0.992)	0.000	69.5	0.006
post-treatment	Chu et al. (2017), Ko et al. (2018), Liao, (2018), Rao, (2014), Tang et al. (2021), Tang et al. (2010), Yu et al. (2018), Zhang et al. (2015)	−1.883 (−2.288, −1.479)	0.000	−2.198 (−3.107, −1.289)	0.000	78.3	0.000
Subgroup 2							
Duration = 24 h	Liu, (2016), Mao et al. (2014), Rao, (2014), Tang et al. (2010), Wang, (2008), Xiao, (2005)	−1.387 (−1.778, −0.995)	0.000	−1.791 (−2.677, −0.906)	0.000	76.6	0.002
Duration >24 h	Chu et al. (2017), He, (2014), Ko et al. (2018), Liao, (2018), Tang et al. (2021), Yu et al. (2018), Zhang et al. (2015)	−1.967(−2.387, −1.547)	0.000	−2.291 (−3.131, −1.452)	0.001	72.1	0.001
Subgroup 3							
Daily dosage ≤10 mg/kg	Liao, (2018), Tang et al. (2021), Yu et al. (2018)	−1.994 (−2.614, −1.373)	0.000	−2.912 (−5.104, −0.721)	0.000	89.3	0.000
Daily dosage ≤20 mg/kg	Chu et al. (2017), He, (2014), Ko et al. (2018), Tang et al. (2010), Zhang et al. (2015)	−1.681 (−2.173, −1.189)	0.000	-1.802 (-2.712,-0.892)	0.000	68.1	0.008
Daily dosage >20 mg/kg	Liu, (2016), Mao et al. (2014), Rao, (2014), Wang, (2008), Xiao, (2005)	−1.478(−1.906, −1.051)	0.000	−1.873 (−2.790, −0.957)	0.000	73.4	0.005
Subgroup 4							
Ischemia time ≤90 min	Chu et al. (2017), He, (2014), Ko et al. (2018), Liao, (2018), Mao et al. (2014), Rao, (2014), Tang et al. (2010), Wang, (2008), Xiao, (2005), Yu et al. (2018)	−1.536 (−1.878,-1.193)	0.000	−1.905 (−2.595, −1.216)	0.000	72.5	0.000
Ischemia time >90 min	Liu, (2016), Tang et al. (2021), Zhang et al. (2015)	−1.938(-2.461, −1.416)	0.000	−2.562 (−4.076, −1.048)	0.001	84.8	0.001

TABLE 4 | Meta-regression analysis of potential sources of heterogeneity.

Heterogeneity factor	Coefficient	SE	t	p-value	95% CI
Intervention time	1.255402	2.6493	0.47	0.660	−6.100234, 8.611038
Duration	2.497039	4.00392	0.62	0.567	−8.619626, 13.6137
Daily dosage	2.375791	3.072568	0.77	0.483	−6.155026, 10.90661
Ischemia time	−0.0238451	2.307099	−0.01	0.992	−6.429379, 6.381689
Sample size	1.095033	1.722891	0.64	0.560	−3.688479, 5.878546
Route of administration	0.6597497	1.856658	0.36	0.740	−4.495158, 5.814658
Anesthetic	0.5705356	2.355482	0.24	0.821	−5.96933, 7.110401

DISCUSSION

The main targets in the treatment of acute stroke are recovery of cerebral blood flow, and mechanical thrombectomy and intravenous thrombolysis are the main therapeutic strategies at present. However, the narrow time windows and contraindications are major obstacles to the universal application of these therapeutic approaches. On the other hand, vascular recanalization and I/R are often interrelated (Smith et al., 2019). The supply of oxygen and glucose is reduced after the onset of cerebral ischemia, and the recovered oxygen-rich blood from the ischemic damaged brain tissue would offer the necessary substrate for the generation of reactive oxygen species (ROS) if recanalization occurs after the key time window (Eltzschig and Eckle, 2011). ROS can not only lead to direct cell injuries and apoptosis but can also trigger the activation of adaptive immunity and brain innate immunity. This process can induce the formation of various destructive immunological mediators and effectors, eventually creating a vicious circle (Mizuma and Yenari, 2017). The mechanisms underlying ischemic stroke have been explored in depth over many years, although clinical studies did not often yield good outcomes. Thus, there is a constant need for the identification of novel neuroprotective agents (Chamorro, 2018). The neuroprotective effect of PF may be relevant to some molecular mechanisms, such as the mode of cell death, inflammation, oxidative stress and epigenetics.

Cell death triggered by I/R injury not only consists of cell necrosis but also includes programmed cell deaths such as apoptosis (Liao et al., 2020), autophagia (Shen et al., 2021), and pyroptosis (Gou et al., 2021). These procedures are monitored by multiple signaling mechanisms by interfering with a relevant signal pathway to save damaged cells (Datta

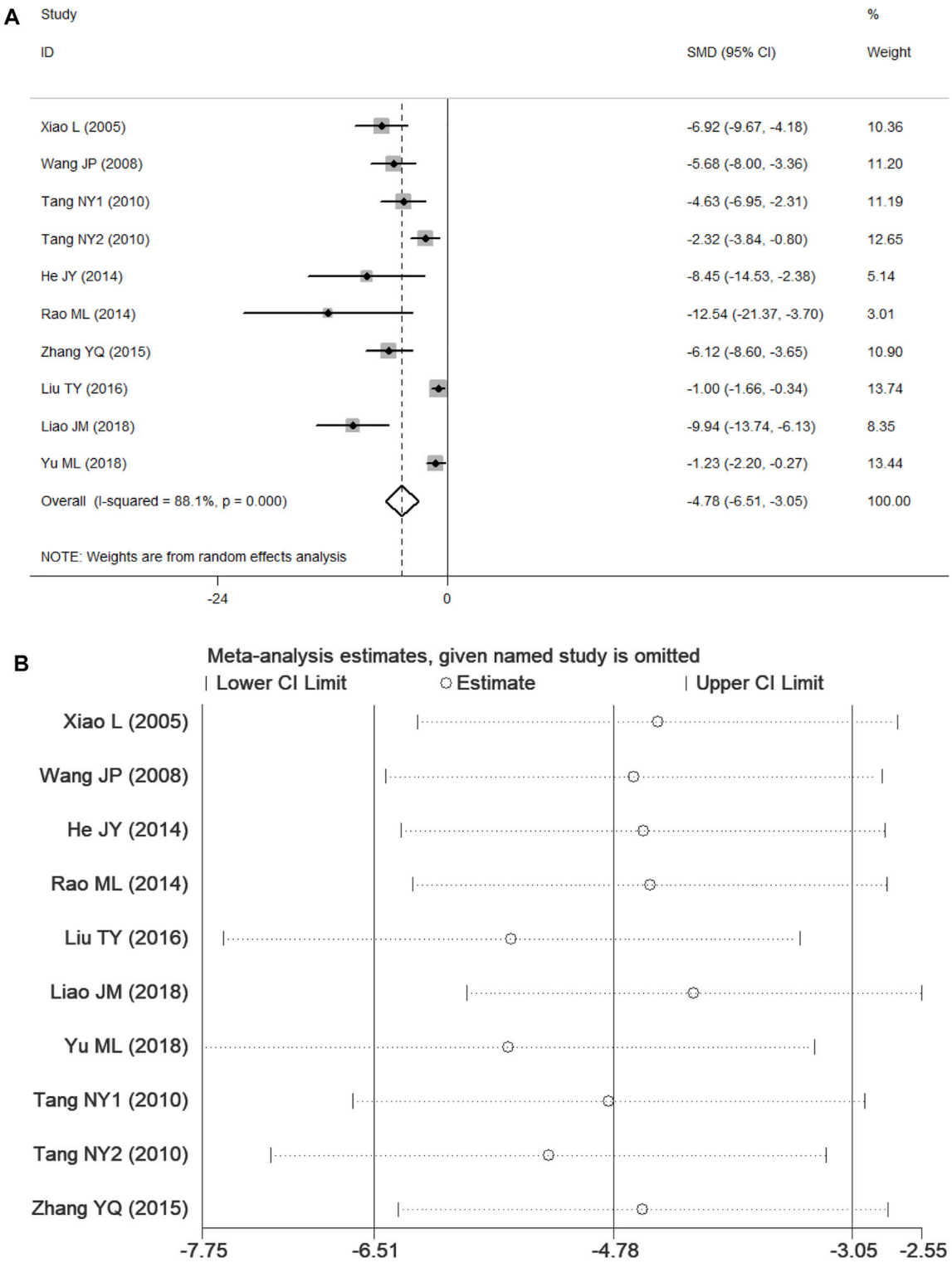

FIGURE 5 | Forest plots of PF for CIS. **(A)** Effects of PF on decreasing the CIS in comparison with the control group; **(B)** sensitivity analysis of PF for CIS.

et al., 2020). Apoptotic pathways consist of the intrinsic apoptotic pathway mediated by mitochondria and the extrinsic apoptotic pathway mediated by death receptors, among which caspase and the B-cell lymphoma 2 (BCL-2) protein family are major molecules (Arya and White, 2015). Studies have shown that PF can maintain the integrity of the

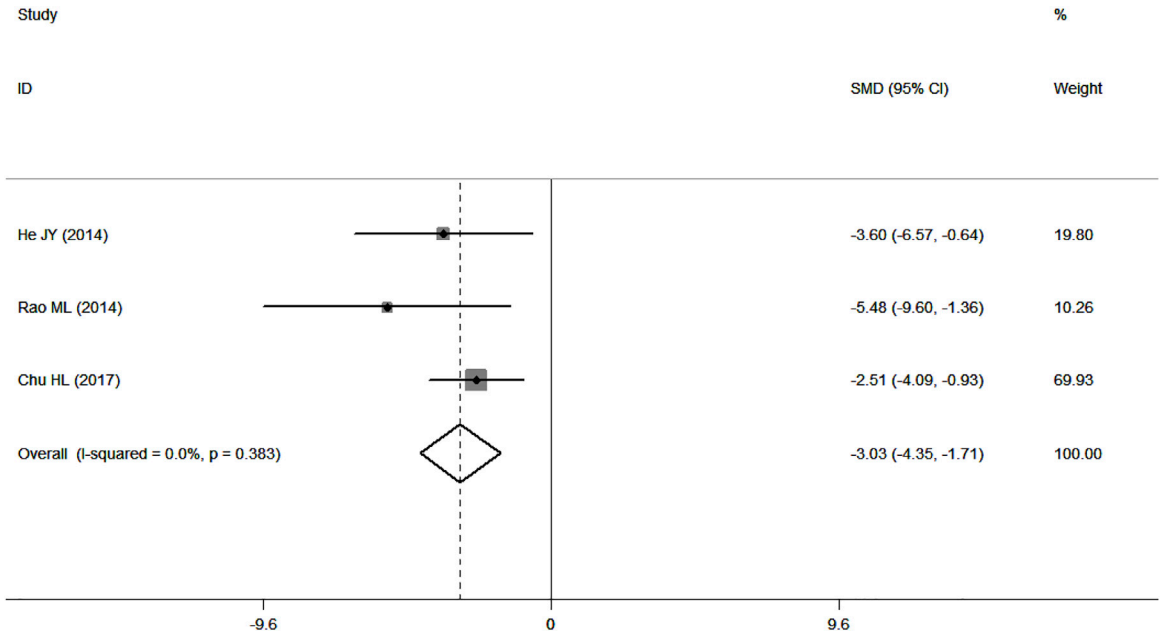

FIGURE 6 | Forest plots of PF for BWC.

mitochondrial membrane, reduce the level of BCL-2 associated X (BAX), BCL-2 associated agonist of cell death (BAD), downstream caspase-3 and caspase-9, and increase the levels of BCL-2 and B cell lymphoma-extra large (BCL-XL), thereby showing anti-apoptotic effects (Chen et al., 2017; Cong et al., 2019; Liu et al., 2021; Zhang and Yang, 2021). In autophagia, which is under the control of autophagia-related genes, lysosomes are used to degrade unnecessary or damaged organelles and proteins to maintain cellular homeostasis. The activation conditions of I/R injuries (such as energy deprivation, oxidative stress and endoplasmic reticulum stress) could result in autophagia (Wu et al., 2018). Appropriate autophagia could offer nerve protection and facilitate improvements in clinical results by significantly decreasing the levels of neurons, glial, and endothelial cells (Ajoolabady et al., 2021). PF has been shown to promote autophagy by regulating the lipidation of microtubule associated protein 1 light chain 3 (LC3-II) (Cao et al., 2010). Pyroptosis is a kind of programmed death of inflammatory cells, which could cause lysis and oligomerization of gasdermin protein family members, including gasdermin D (GSDMD), cell perforation, or even worse, cell death. The process is triggered by the activation of inflammasome-mediated caspases, including caspase-1 (Tuo et al., 2021). In comparison with apoptosis, pyroptosis occurs more rapidly and is associated with a greater release of proinflammatory factors (Tsuchiya, 2021). PF has been shown to alleviate astrocyte pyroptosis caused by hypoxia through the Caspase 1/GSDMD signal pathway (She et al., 2019).

Cerebral I/R injury triggers inflammation without microorganism participation, although the inflammation shows features common with those caused by invading pathogens. This immunologic response involves the collection and activation of pattern recognition receptors, including Toll-Like receptors (TLRs), immune cells of the innate and adaptive immune systems, and the activation of complement systems to pass signal events. Because these responses may have adverse consequences, targeted immune activation has become an emerging treatment modality for I/R injuries (Carbone et al., 2019; Stoll and Nieswandt, 2019). Some studies have shown that PF may have anti-inflammatory effects through the signal pathway of TLR4- Myeloid differentiation factor 88 (MyD88)/Nuclear transcription factor-kappa B(NF-κB) (Zhang et al., 2017; Yang et al., 2021) and Janus kinase 2 (JAK2)/Signal transducer and activator of transcription 3(STAT3) (Zhang and Yang, 2021).

Oxidative stress, which is generated as a result of elevated levels of ROS and reactive nitrogen species and reduced levels of antioxidants, can cause damage to cell components, including proteins, lipids, and DNA (Zhao et al., 2016). Malondialdehyde (MDA), as the end product of lipid oxidation, can induce crosslinking polymerization of proteins, nucleic acids, and other macromolecules. In addition, due to MDA's cytotoxicity, the stronger its activity becomes, the stronger the lipid peroxidization, which can trigger oxidative stress damage (Menon et al., 2020). SOD, an important active ingredient in organisms, can eliminate harmful substances and maintain good metabolic conditions. The lower the levels of SOD, the weaker the cells' ability to prevent oxidative damage (Cherubini et al., 2000). Glutathione (GSH), a tripeptide consisting of γ-amido bonds and sulfydryl, can perform integrated detoxification and antioxidation functions. GSH measurements are also a common index to evaluate antioxidation ability (Higashi et al., 2021). Unsaturated double bonds in cytomembrane phospholipids are easily attacked by oxygen radicals, resulting

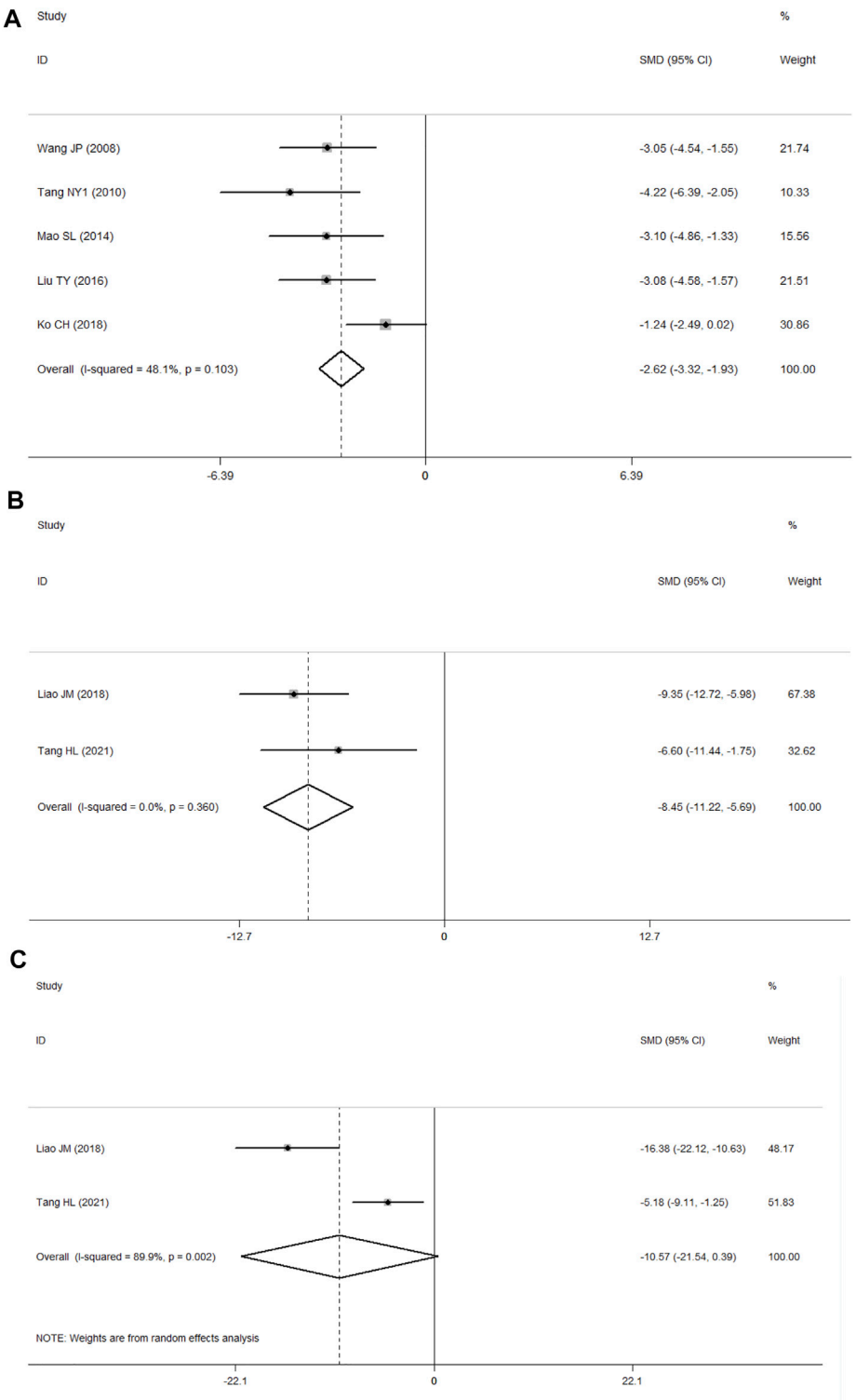

FIGURE 7 | (A) Forest plots of PF for TUNEL staining; **(B)** forest plots of PF for IL-1β; **(C)** forest plots of PF for TNF-α.

in the invagination of phosphatidylserine on cytomembranes, incompleteness of cytomembranes, and release of lactate dehydrogenase (LDH) (Bhowmick and Drew, 2017). Studies have shown that PF can improve these targets and alleviate the brain damage (Liu and Wang, 2013; Wang et al., 2020; Wu et al., 2020; Zhang and Yang, 2021).

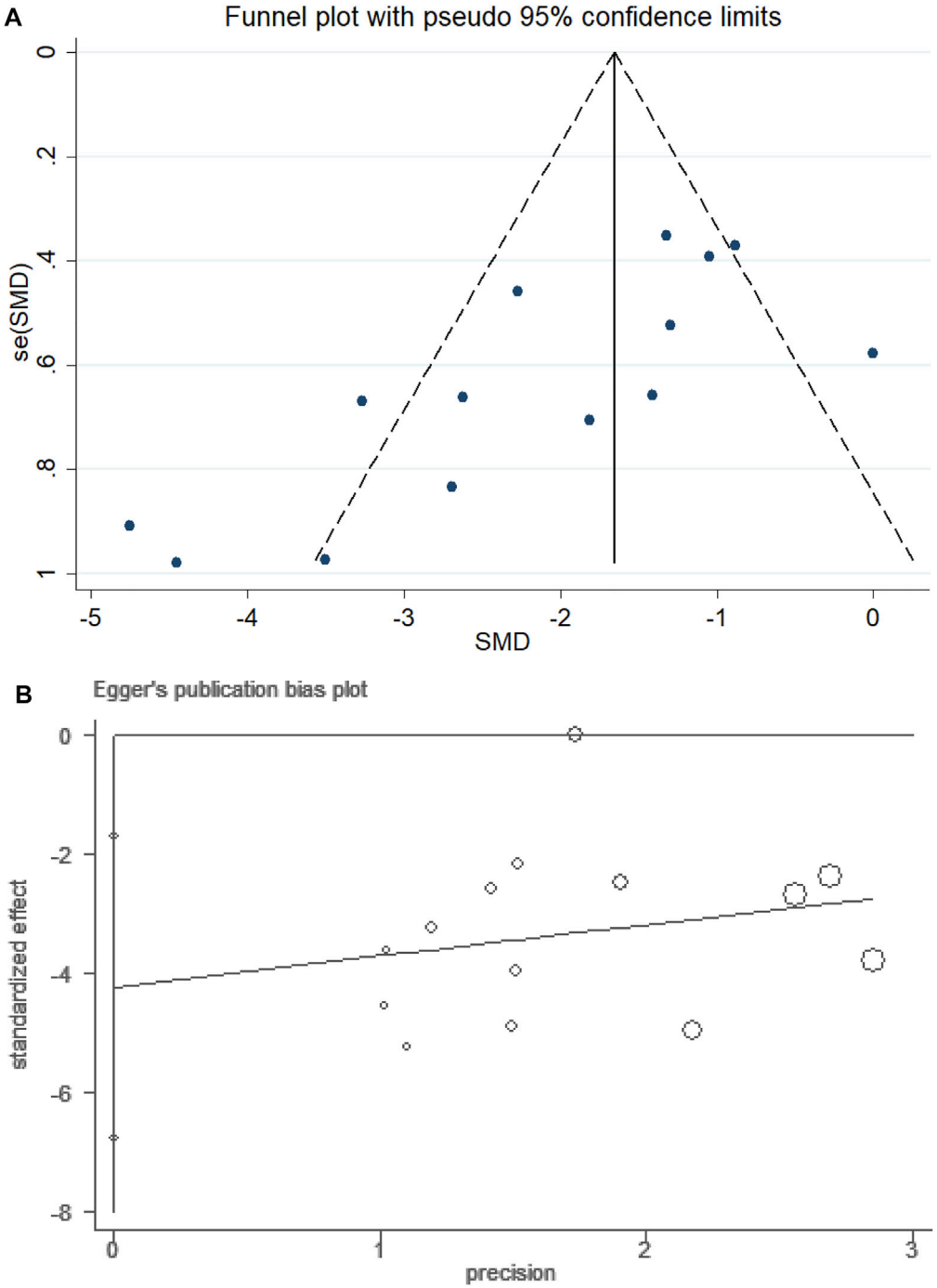

FIGURE 8 | Funnel plot of PF for NSS. **(A)** Assessment of publication bias in a funnel plot. **(B)** Bias assessment plot by Egger's test.

Epigenetics, the transitive variation of phenotypic characters, is unrelated to DNA changes, but may be influenced by external and environmental factors. These factors can turn on and off genes and thus affect the ways in which cells read genes. There are three primary epigenetic mechanisms: DNA methylation, histone modification, and non-coding RNA (Patsouras and Vlachoyiannopoulos, 2019). (1) Members of the histone deacetylase (HDAC) family compete with histone acetyltransferase (HAT) for the right to control lysine residue acetylation that forms histone, thereby ensuring post-translational acetylation of chromatin and many other non-histones (He et al., 2013). Many studies have reported the neuroprotective roles of HDAC inhibitors in ischemic stroke (Patnala et al., 2017; Brookes et al., 2018), and PF has been shown to reduce ischemic brain injuries

triggered by caspase 3-induced HDAC4 nuclear accumulation during stroke (Liu et al., 2021). (2) The common non-coding RNA consists of lncRNAs and miRNAs, and miRNAs have especially attracted considerable attention in cerebral I/R injuries studies in recent years (Ghafouri-Fard et al., 2020). miRNAs can not only influence gene expression by inhibiting mRNA translation or inducing degradation of mRNA, but also act as damage-associated molecular patterns and cofactors activating inflammatory cascades and thrombosis (Hu et al., 2015; Forouzanfar et al., 2019; Mahjoubin-Tehran et al., 2021). Studies show that PF could alleviate brain damage by manipulating miR-210 (Jiang et al., 2021) and miR-135a (Zhai et al., 2019).

This is the first preclinical meta-analysis to investigate the efficacy of PF for cerebral I/R Injury. The findings confirmed that, in comparison with the control group, PF showed improvements in the NSS, CIS, and BWC by modulating a wide range of biological mechanisms such as neuroinflammation, oxidative stress, and apoptosis. The results of subgroup analysis showed that the longer the ischemia duration, the more severe the injury and the better the treatment effect of PF. The effect of PF administered post-MCAO was better than that administered pre-MCAO, but this phenomenon could be explained by the long observation period. Daily dosage ≤10 mg/kg or >20 mg/kg for PF were better than daily dosages ≤20 mg/kg, indicating a "U-Shaped Dose-Response Curve" between PF dosage and therapeutic effect. There are barriers to turning experimental findings into clinically viable therapies, particularly in the research of cerebrovascular disorders. It is important to confirm PF's efficacy in larger animal models, to evaluate the therapeutic benefit of combination application with other neuroprotective treatments, and to clarify its potential side effects and safety in order to advance PF into clinical trials as soon as feasible.

LIMITATIONS

First, the studies evaluated in this meta-analysis had problems related to nonstandard methodologies and incomplete reports, which may have influenced the effectiveness of our conclusions. None of the included studies mentioned power calculation. The lack of a formal sample size calculation leads to uncertainty about the validity of statistical analysis. Particularly for allocation concealment, blinding methods to address performance bias and random outcome evaluation were not mentioned in any studies. A few studies have also been reported on "random housing." This could be an issue as cage size, material, placement, bedding, and the number of animals placed in the cage may affect thermoregulation and stress level. Lack of information on these elements could potentially contribute to bias. Second, ischemic stroke shows high complexity and heterogeneity. Stroke experiment models can only cover specific features of multiple diseases (Sommer, 2017). Clinical conditions are more complex; for example, many factors may affect prognosis, including hypertension, diabetes, and atrial fibrillation (Boehme et al., 2017). The design differences between experimental studies and clinical studies can result in a gradual decrease in effectiveness from early clinical trials to phase III trials (Schmidt-Pogoda et al., 2020). Thus, to connect preclinical and clinical studies, the quality of animal research methods requires improvement through more systematic methods for the analysis of experimental data and greater collaboration between clinical and animal researchers. Third, the funnel plot shows high asymmetry, indicating a publication bias in this study. The results of the Egger test further validated this finding. However, the findings using the trim-and-fill method were unchanged because no trimming was performed. However, similar to other meta-analyses, these conclusions are influenced by the fact that preclinical studies are usually published if the analyses with experimental animals yield positive results. The resultant lack of studies showing lack of effectiveness or negative findings can result in overestimation of the overall curative effects.

CONCLUSION

This preclinical meta-analysis suggests that PF could alleviate cerebral I/R injuries and potentially serve as a neuroprotective agent. Despite the lack of clinical trial data and potential publication biases, these conclusion are worth consideration.

DATA AVAILABILITY STATEMENT

The original contributions presented in the study are included in the article/**Supplementary Material**, further inquiries can be directed to the corresponding author.

AUTHOR CONTRIBUTIONS

AW: Conceptualization, methodology, validation, formal analysis, investigation, data curation, writing—original draft, visualization. WZ: Conceptualization, methodology, writing—review and editing. KY: Conceptualization, methodology, writing—review and editing. PH: Investigation, formal analysis, data Curation. HZ: Validation, investigation. XM: Conceptualization, writing–review and editing, supervision, project administration.

FUNDING

This work was supported by the National Key Research and Development Program of China (No.: 2018YFC1707410-02).

ACKNOWLEDGMENTS

We would like to acknowledge Hong Liu of Qingzhou Station Primary School, Weifang, China for writing assistance.

SUPPLEMENTARY MATERIAL

The Supplementary Material for this article can be found online at: https://www.frontiersin.org/articles/10.3389/fphar.2022.827770/full#supplementary-material

REFERENCES

Ajoolabady, A., Wang, S., Kroemer, G., Penninger, J. M., Uversky, V. N., Pratico, D., et al. (2021). Targeting Autophagy in Ischemic Stroke: From Molecular Mechanisms to Clinical Therapeutics. *Pharmacol. Ther.* 225, 107848. doi:10.1016/j.pharmthera.2021.107848

Alrafiah, A. R. (2021). Secondary Cerebellar Cortex Injury in Albino Male Rats after MCAO: A Histological and Biochemical Study. *Biomedicines* 9 (9). doi:10.3390/biomedicines9091267

Arya, R., and White, K. (2015). Cell Death in Development: Signaling Pathways and Core Mechanisms. *Semin. Cell Dev Biol* 39, 12–19. doi:10.1016/j.semcdb.2015.02.001

Bederson, J. B., Pitts, L. H., Tsuji, M., Nishimura, M. C., Davis, R. L., and Bartkowski, H. (1986). Rat Middle Cerebral Artery Occlusion: Evaluation of the Model and Development of a Neurologic Examination. *Stroke* 17 (3), 472–476. doi:10.1161/01.str.17.3.472

Bhowmick, S., and Drew, K. L. (2017). Arctic Ground Squirrel Resist Peroxynitrite-Mediated Cell Death in Response to Oxygen Glucose Deprivation. *Free Radic. Biol. Med.* 113, 203–211. doi:10.1016/j.freeradbiomed.2017.09.024

Boehme, A. K., Esenwa, C., and Elkind, M. S. (2017). Stroke Risk Factors, Genetics, and Prevention. *Circ. Res.* 120 (3), 472–495. doi:10.1161/CIRCRESAHA.116.308398

Brookes, R. L., Crichton, S., Wolfe, C. D. A., Yi, Q., Li, L., Hankey, G. J., et al. (2018). Sodium Valproate, a Histone Deacetylase Inhibitor, Is Associated with Reduced Stroke Risk after Previous Ischemic Stroke or Transient Ischemic Attack. *Stroke* 49 (1), 54–61. doi:10.1161/STROKEAHA.117.016674

Cao, B. Y., Yang, Y. P., Luo, W. F., Mao, C. J., Han, R., Sun, X., et al. (2010). Paeoniflorin, a Potent Natural Compound, Protects PC12 Cells from MPP+ and Acidic Damage via Autophagic Pathway. *J. Ethnopharmacol* 131 (1), 122–129. doi:10.1016/j.jep.2010.06.009

Carbone, F., Bonaventura, A., and Montecucco, F. (2019). Neutrophil-Related Oxidants Drive Heart and Brain Remodeling after Ischemia/Reperfusion Injury. *Front. Physiol.* 10, 1587. doi:10.3389/fphys.2019.01587

Chamorro, Á. (2018). Neuroprotectants in the Era of Reperfusion Therapy. *J. Stroke* 20 (2), 197–207. doi:10.5853/jos.2017.02901

Chen, A., Wang, H., Zhang, Y., Wang, X., Yu, L., Xu, W., et al. (2017). Paeoniflorin Exerts Neuroprotective Effects against Glutamate-induced PC12 C-ellular C-ytotoxicity by I-nhibiting A-poptosis. *Int. J. Mol. Med.* 40 (3), 825–833. doi:10.3892/ijmm.2017.3076

Chen, J., Li, Y., Wang, L., Zhang, Z., Lu, D., Lu, M., et al. (2001). Therapeutic Benefit of Intravenous Administration of Bone Marrow Stromal Cells after Cerebral Ischemia in Rats. *Stroke* 32 (4), 1005–1011. doi:10.1161/01.str.32.4.1005

Chen, Z. Z., Gong, X., Guo, Q., Zhao, H., and Wang, L. (2019). Bu Yang Huan Wu Decoction Prevents Reperfusion Injury Following Ischemic Stroke in Rats via Inhibition of HIF-1 α, VEGF and Promotion β-ENaC Expression. *J. Ethnopharmacol* 228, 70–81. doi:10.1016/j.jep.2018.09.017

Cheng, J., Chen, M., Wan, H. Q., Chen, X. Q., Li, C. F., Zhu, J. X., et al. (2021). Paeoniflorin Exerts Antidepressant-like Effects through Enhancing Neuronal FGF-2 by Microglial Inactivation. *J. Ethnopharmacol* 274, 114046. doi:10.1016/j.jep.2021.114046

Cherubini, A., Polidori, M. C., Bregnocchi, M., Pezzuto, S., Cecchetti, R., Ingegni, T., et al. (2000). Antioxidant Profile and Early Outcome in Stroke Patients. *Stroke* 31 (10), 2295–2300. doi:10.1161/01.str.31.10.2295

Chu, H., Huang, C., Gao, Z., Dong, J., Tang, Y., and Dong, Q. (2017). Reduction of Ischemic Brain Edema by Combined Use of Paeoniflorin and Astragaloside IV via Down-Regulating Connexin 43. *Phytother Res.* 31 (9), 1410–1418. doi:10.1002/ptr.5868

Collaborators, G. B. D. S. (2019). Global, Regional, and National burden of Stroke, 1990-2016: a Systematic Analysis for the Global Burden of Disease Study 2016. *Lancet Neurol.* 18 (5), 439–458. doi:10.1016/S1474-4422(19)30034-1

Cong, C., Kluwe, L., Li, S., Liu, X., Liu, Y., Liu, H., et al. (2019). Paeoniflorin Inhibits Tributyltin Chloride-Induced Apoptosis in Hypothalamic Neurons via Inhibition of MKK4-JNK Signaling Pathway. *J. Ethnopharmacol* 237, 1–8. doi:10.1016/j.jep.2019.03.030

Datta, A., Sarmah, D., Mounica, L., Kaur, H., Kesharwani, R., Verma, G., et al. (2020). Cell Death Pathways in Ischemic Stroke and Targeted Pharmacotherapy. *Transl Stroke Res.* 11 (6), 1185–1202. doi:10.1007/s12975-020-00806-z

Eltzschig, H. K., and Eckle, T. (2011). Ischemia and Reperfusion-Ffrom Mechanism to Translation. *Nat. Med.* 17 (11), 1391–1401. doi:10.1038/nm.2507

Forouzanfar, F., Shojapour, M., Asgharzade, S., and Amini, E. (2019). Causes and Consequences of MicroRNA Dysregulation Following Cerebral Ischemia-Reperfusion Injury. *CNS Neurol. Disord. Drug Targets* 18 (3), 212–221. doi:10.2174/1871527318666190204104629

Ghafouri-Fard, S., Shoorei, H., and Taheri, M. (2020). Non-coding RNAs Participate in the Ischemia-Reperfusion Injury. *Biomed. Pharmacother.* 129, 110419. doi:10.1016/j.biopha.2020.110419

Gou, X., Xu, D., Li, F., Hou, K., Fang, W., and Li, Y. (2021). Pyroptosis in Stroke-New Insights into Disease Mechanisms and Therapeutic Strategies. *J. Physiol. Biochem.* 77, 511–529. doi:10.1007/s13105-021-00817-w

He, J. Y. (2014). *Effect of Paeoniflorin on Superoxide Dismu Tase and Nuclear Factor E2-Related Factor2Expression in Brain Tissues of Rats with Middle Cerebral Artery Occlusion and its Neuroprotection*. ChongQing: ChongQing Medical University. Master's thesis.

He, M., Zhang, B., Wei, X., Wang, Z., Fan, B., Du, P., et al. (2013). HDAC4/5-HMGB1 Signalling Mediated by NADPH Oxidase Activity Contributes to Cerebral Ischaemia/reperfusion Injury. *J. Cell Mol Med* 17 (4), 531–542. doi:10.1111/jcmm.12040

He, Y., Zheng, H., Zhong, L., Zhong, N., Wen, G., Wang, L., et al. (2021). Identification of Active Ingredients of Huangqi Guizhi Wuwu Decoction for Promoting Nerve Function Recovery after Ischemic Stroke Using HT22 Live-Cell-Based Affinity Chromatography Combined with HPLC-MS/MS. *Dddt* 15, 5165–5178. doi:10.2147/DDDT.S333418

Higashi, Y., Aratake, T., Shimizu, T., Shimizu, S., and Saito, M. (2021). Protective Role of Glutathione in the Hippocampus after Brain Ischemia. *Ijms* 22 (15), 7765. doi:10.3390/ijms22157765

Hooijmans, C. R., Rovers, M. M., de Vries, R. B., Leenaars, M., Ritskes-Hoitinga, M., and Langendam, M. W. (2014). SYRCLE's Risk of Bias Tool for Animal Studies. *BMC Med. Res. Methodol.* 14, 43. doi:10.1186/1471-2288-14-43

Hu, B., Xu, G., Zhang, X., Xu, L., Zhou, H., Ma, Z., et al. (2018). Paeoniflorin Attenuates Inflammatory Pain by Inhibiting Microglial Activation and Akt-NF-Kb Signaling in the Central Nervous System. *Cell Physiol Biochem* 47 (2), 842–850. doi:10.1159/000490076

Hu, Y., Deng, H., Xu, S., and Zhang, J. (2015). MicroRNAs Regulate Mitochondrial Function in Cerebral Ischemia-Reperfusion Injury. *Int. J. Mol. Sci.* 16 (10), 24895–24917. doi:10.3390/ijms161024895

Jiang, Z., Chen, J., Chen, J., Lei, Z., Chen, H., Wu, J., et al. (2021). Anti-inflammatory Effects of Paeoniflorin Caused by Regulation of the hif1a/miR-210/caspase1/GSDMD Signaling Pathway in Astrocytes: a Novel Strategy for Hypoxia-Induced Brain Injury in Rats. *Immunopharmacol Immunotoxicol* 43 (4), 410–418. doi:10.1080/08923973.2021.1924194

Jiao, F., Varghese, K., Wang, S., Liu, Y., Yu, H., Booz, G. W., et al. (2021). Recent Insights into the Protective Mechanisms of Paeoniflorin in Neurological, Cardiovascular, and Renal Diseases. *J. Cardiovasc. Pharmacol.* 77 (6), 728–734. doi:10.1097/FJC.0000000000001021

Kalogeris, T., Baines, C. P., Krenz, M., and Korthuis, R. J. (2016). Ischemia/Reperfusion. *Compr. Physiol.* 7 (1), 113–170. doi:10.1002/cphy.c160006

Ko, C. H., Huang, C. P., Lin, Y. W., and Hsieh, C. L. (2018). Paeoniflorin Has Anti-inflammation and Neurogenesis Functions through Nicotinic Acetylcholine Receptors in Cerebral Ischemia-Reperfusion Injury Rats. *Iran J. Basic Med. Sci.* 21 (11), 1174–1178. doi:10.22038/ijbms.2018.30371.7322

Liao, J. M. (2018). *Synergistic Protective Effect of Hydroxysafflower Yellow A and Paeonifolrin on NF-Kb Pathway in Cerebral Ischemia Reperfusion Injury Rats*. GuangZhou: Southern Medical University. Master's thesis.

Liao, S., Apaijai, N., Chattipakorn, N., and Chattipakorn, S. C. (2020). The Possible Roles of Necroptosis during Cerebral Ischemia and Ischemia/Reperfusion Injury. *Arch. Biochem. Biophys.* 695, 108629. doi:10.1016/j.abb.2020.108629

Liu, L., Chen, W., Zhou, H., Duan, W., Li, S., Huo, X., et al. (2020). Chinese Stroke Association Guidelines for Clinical Management of Cerebrovascular Disorders: Executive Summary and 2019 Update of Clinical Management of Ischaemic

Cerebrovascular Diseases. *Stroke Vasc. Neurol.* 5 (2), 159–176. doi:10.1136/svn-2020-000378

Liu, L., and Wang, S. Y. (2013). Protective Effects of Paeoniflorin against aBETA25-35-Induced Oxidative Stress in PC12 Cells. *Zhongguo Zhong Yao Za Zhi* 38 (9), 1318–1322.

Liu, T. Y. (2016). The Effects of Peoniflorin on Cellular Apoptosis of the Rats with Cerebral Ischchemia Reperfusion Injury and its Mechanism. *West. J. Traditional Chin. Med.* 29 (5), 8–11.

Liu, Y.-f., Zhang, L., Wu, Q., and Feng, L.-y. (2021). Paeoniflorin Ameliorates Ischemic Injury in Rat Brain via Inhibiting Cytochrome c/caspase3/HDAC4 Pathway. *Acta Pharmacol. Sin* 43, 273–284. doi:10.1038/s41401-021-00671-y

Longa, E. Z., Weinstein, P. R., Carlson, S., and Cummins, R. (1989). Reversible Middle Cerebral Artery Occlusion without Craniectomy in Rats. *Stroke* 20 (1), 84–91. doi:10.1161/01.str.20.1.84

Mahjoubin-Tehran, M., Rezaei, S., Jesmani, A., Birang, N., Morshedi, K., Khanbabaei, H., et al. (2021). New Epigenetic Players in Stroke Pathogenesis: From Non-coding RNAs to Exosomal Non-coding RNAs. *Biomed. Pharmacother.* 140, 111753. doi:10.1016/j.biopha.2021.111753

Mao, S. L., Ma, Y. H., Zhang, H. D., Qi, J., and Li, F. (2014). Effect of Paeoniflor in Pretreatment to Brain Cells Apoptosis and the Expression of CHOP on Cerebral Ischemia Reperfusion Injury in Rat. *Shandong Med. J.* (32), 14–16.

Menon, B., Ramalingam, K., and Kumar, R. (2020). Evaluating the Role of Oxidative Stress in Acute Ischemic Stroke. *J. Neurosci. Rural Pract.* 11 (1), 156–159. doi:10.1055/s-0039-3402675

Mizuma, A., and Yenari, M. A. (2017). Anti-Inflammatory Targets for the Treatment of Reperfusion Injury in Stroke. *Front. Neurol.* 8, 467. doi:10.3389/fneur.2017.00467

Patnala, R., Arumugam, T. V., Gupta, N., and Dheen, S. T. (2017). HDAC Inhibitor Sodium Butyrate-Mediated Epigenetic Regulation Enhances Neuroprotective Function of Microglia during Ischemic Stroke. *Mol. Neurobiol.* 54 (8), 6391–6411. doi:10.1007/s12035-016-0149-z

Patsouras, M. D., and Vlachoyiannopoulos, P. G. (2019). Evidence of Epigenetic Alterations in Thrombosis and Coagulation: A Systematic Review. *J. Autoimmun.* 104, 102347. doi:10.1016/j.jaut.2019.102347

Powers, W. J., Rabinstein, A. A., Ackerson, T., Adeoye, O. M., Bambakidis, N. C., Becker, K., et al. (2018). 2018 Guidelines for the Early Management of Patients with Acute Ischemic Stroke: A Guideline for Healthcare Professionals from the American Heart Association/American Stroke Association. *Stroke* 49 (3), e46–e110. doi:10.1161/STR.0000000000000158

Rao, M. L. (2014). *Neuroprotective Effects of Paeoniflorin against Middle Cerebral Artery Occlusion Injury in Rats and its Mechanism*. ChongQing: ChongQing Medical University. Master's thesis.

Schmidt-Pogoda, A., Bonberg, N., Koecke, M. H. M., Strecker, J. K., Wellmann, J., Bruckmann, N. M., et al. (2020). Why Most Acute Stroke Studies Are Positive in Animals but Not in Patients: A Systematic Comparison of Preclinical, Early Phase, and Phase 3 Clinical Trials of Neuroprotective Agents. *Ann. Neurol.* 87 (1), 40–51. doi:10.1002/ana.25643

She, Y., Shao, L., Zhang, Y., Hao, Y., Cai, Y., Cheng, Z., et al. (2019). Neuroprotective Effect of Glycosides in Buyang Huanwu Decoction on Pyroptosis Following Cerebral Ischemia-Reperfusion Injury in Rats. *J. Ethnopharmacol* 242, 112051. doi:10.1016/j.jep.2019.112051

Shen, L., Gan, Q., Yang, Y., Reis, C., Zhang, Z., Xu, S., et al. (2021). Mitophagy in Cerebral Ischemia and Ischemia/Reperfusion Injury. *Front. Aging Neurosci.* 13, 687246. doi:10.3389/fnagi.2021.687246

Siesjö, B. K. (1992). Pathophysiology and Treatment of Focal Cerebral Ischemia. Part I: Pathophysiology. *J. Neurosurg.* 77 (2), 169–184. doi:10.3171/jns.1992.77.2.0169

Smith, M., Reddy, U., Robba, C., Sharma, D., and Citerio, G. (2019). Acute Ischaemic Stroke: Challenges for the Intensivist. *Intensive Care Med.* 45 (9), 1177–1189. doi:10.1007/s00134-019-05705-y

Sommer, C. J. (2017). Ischemic Stroke: Experimental Models and Reality. *Acta Neuropathol.* 133 (2), 245–261. doi:10.1007/s00401-017-1667-0

Sterne, J. A. C., Savović, J., Page, M. J., Elbers, R. G., Blencowe, N. S., Boutron, I., et al. (2019). RoB 2: a Revised Tool for Assessing Risk of Bias in Randomised Trials. *BMJ* 366, l4898. doi:10.1136/bmj.l4898

Stoll, G., and Nieswandt, B. (2019). Thrombo-inflammation in Acute Ischaemic Stroke - Implications for Treatment. *Nat. Rev. Neurol.* 15 (8), 473–481. doi:10.1038/s41582-019-0221-1

Tang, H., Wu, L., Chen, X., Li, H., Huang, B., Huang, Z., et al. (2021). Paeoniflorin Improves Functional Recovery through Repressing Neuroinflammation and Facilitating Neurogenesis in Rat Stroke Model. *PeerJ* 9, e10921. doi:10.7717/peerj.10921

Tang, N. Y., Liu, C. H., Hsieh, C. T., and Hsieh, C. L. (2010). The Anti-inflammatory Effect of Paeoniflorin on Cerebral Infarction Induced by Ischemia-Reperfusion Injury in Sprague-Dawley Rats. *Am. J. Chin. Med.* 38 (1), 51–64. doi:10.1142/S0192415X10007786

Tsuchiya, K. (2021). Switching from Apoptosis to Pyroptosis: Gasdermin-Elicited Inflammation and Antitumor Immunity. *Ijms* 22 (1), 426. doi:10.3390/ijms22010426

Tuo, Q. Z., Zhang, S. T., and Lei, P. (2021). Mechanisms of Neuronal Cell Death in Ischemic Stroke and Their Therapeutic Implications. *Med. Res. Rev.* 42, 259–305. doi:10.1002/med.21817

van Luijk, J., Leenaars, M., Hooijmans, C., Wever, K., de Vries, R., and Ritskes-Hoitinga, M. (2013). Towards Evidence-Based Translational Research: the Pros and Cons of Conducting Systematic Reviews of Animal Studies. *ALTEX* 30 (2), 256–257. doi:10.14573/altex.2013.2.256

Wang, J. P. (2008). *The Effects of Paeoniflorin on Neuronal Apoptosis' Gene and p38MAPK of Focal Cerebral Ischemia/reperfusion Injury in Rats*. BengBu: BengBu Medical College. Master's thesis.

Wang, T., Xu, L., Gao, L., Zhao, L., Liu, X. H., Chang, Y. Y., et al. (2020). Paeoniflorin Attenuates Early Brain Injury through Reducing Oxidative Stress and Neuronal Apoptosis after Subarachnoid Hemorrhage in Rats. *Metab. Brain Dis.* 35 (6), 959–970. doi:10.1007/s11011-020-00571-w

Wang, X., and Lo, E. H. (2003). Triggers and Mediators of Hemorrhagic Transformation in Cerebral Ischemia. *Mol. Neurobiol.* 28 (3), 229–244. doi:10.1385/MN:28:3:229

Wen, J., Xu, B., Sun, Y., Lian, M., Li, Y., Lin, Y., et al. (2019). Paeoniflorin Protects against Intestinal Ischemia/reperfusion by Activating LKB1/AMPK and Promoting Autophagy. *Pharmacol. Res.* 146, 104308. doi:10.1016/j.phrs.2019.104308

Wu, M. Y., Yiang, G. T., Liao, W. T., Tsai, A. P., Cheng, Y. L., Cheng, P. W., et al. (2018). Current Mechanistic Concepts in Ischemia and Reperfusion Injury. *Cell Physiol Biochem* 46 (4), 1650–1667. doi:10.1159/000489241

Wu, W., Qiu, C., Feng, X., Tao, X., Zhu, Q., Chen, Z., et al. (2020). Protective Effect of Paeoniflorin on Acute Cerebral Infarction in Rats. *Curr. Pharm. Biotechnol.* 21 (8), 702–709. doi:10.2174/1389201021666191224151634

Xiao, L. (2005). *Protective and Therapeutic Effects of Paeoniflorin on Cerebral Ischemic Pharmacological Preconditioning in Rats*. Shanghai: Shanghai Institutes for Biological Sciences. Doctoral thesis.

Xie, T., Li, K., Gong, X., Jiang, R., Huang, W., Chen, X., et al. (2018). Paeoniflorin Protects against Liver Ischemia/reperfusion Injury in Mice via Inhibiting HMGB1-TLR4 Signaling Pathway. *Phytother Res.* 32 (11), 2247–2255. doi:10.1002/ptr.6161

Yang, F., Li, Y., Sheng, X., and Liu, Y. (2021). Paeoniflorin Treatment Regulates TLR4/NF-Kb Signaling, Reduces Cerebral Oxidative Stress and Improves white Matter Integrity in Neonatal Hypoxic Brain Injury. *Korean J. Physiol. Pharmacol.* 25 (2), 97–109. doi:10.4196/kjpp.2021.25.2.97

Yu, M. L., Qin, S. S., Liao, J. M., Xu, Y. L., Deng, L. X., Zhu, Y., et al. (2018). Effect of HSYA and Paeoniflorin Combination on Expression of P-AKT in Rats with Cerebral Ischemia-Reperfusion Injury. *Traditional Chin. Drug Res. Clin. Pharmacol.* 29 (01), 13–18.

Zhai, A., Zhang, Z., and Kong, X. (2019). Paeoniflorin Alleviates H2O2-Induced Oxidative Injury through Down-Regulation of MicroRNA-135a in HT-22 Cells. *Neurochem. Res.* 44 (12), 2821–2831. doi:10.1007/s11064-019-02904-3

Zhang, X., Fei, X., Tao, W., Li, J., Shen, H., Wang, X., et al. (2017). Neuroprotective Effect of Modified Xijiao Dihuang Decoction against Oxygen-Glucose Deprivation and Reoxygenation-Induced Injury in PC12 Cells: Involvement of TLR4-MyD88/NF-Kb Signaling Pathway. *Evid. Based Complement. Alternat Med.* 2017, 3848595. doi:10.1155/2017/3848595

Zhang, Y., Li, H., Huang, M., Huang, M., Chu, K., Xu, W., et al. (2015). Paeoniflorin, a Monoterpene Glycoside, Protects the Brain from Cerebral

Ischemic Injury via Inhibition of Apoptosis. *Am. J. Chin. Med.* 43 (3), 543–557. doi:10.1142/s0192415x15500342

Zhang, Z., and Yang, W. (2021). Paeoniflorin Protects PC12 Cells from Oxygen-Glucose Deprivation/reoxygenation-Induced Injury via Activating JAK2/STAT3 Signaling. *Exp. Ther. Med.* 21 (6), 572. doi:10.3892/etm.2021.10004

Zhao, H., Han, Z., Ji, X., and Luo, Y. (2016). Epigenetic Regulation of Oxidative Stress in Ischemic Stroke. *Aging Dis.* 7 (3), 295–306. doi:10.14336/AD.2015.1009

Conflict of Interest: The authors declare that the research was conducted in the absence of any commercial or financial relationships that could be construed as a potential conflict of interest.

Publisher's Note: All claims expressed in this article are solely those of the authors and do not necessarily represent those of their affiliated organizations, or those of the publisher, the editors and the reviewers. Any product that may be evaluated in this article, or claim that may be made by its manufacturer, is not guaranteed or endorsed by the publisher.

GLOSSARY

AKT Protein kinase B
AQP4 Aquaporin4
BAD BCL-2 associated agonist of cell death
BAX BCL-2 associated X
BBB Blood-brain barrier
BCL-2 B-cell lymphoma-2
BCL-XL B cell lymphoma-extra large
Bid Bis in die
BWC Brain water content
CA1 Cornu ammonis 1
CBR2 Cannabinoid 2 receptors
CHOP C/EBP homologous protein
CIS Cerebral infarction size
COX-2 Cyclooxygenase 2
Cx43 Connexin43
d Day
DCX Doublecortin
ED1 Mouse anti rat CD68
ELISA Enzyme linked immunosorbent assay
ERK Extracellular signal-regulated kinase
FAS Fas cell surface death receptor
GFAP Glial fibrillary acidic protein
GSDMD Gasdermin D
GSH Glutathione
h Hour
HAT Histone acetyltransferase
HDAC Histone deacetylase
i.g Irrigation
i.p. Intraperitoneal
i.v. Intravenous
I/R Ischemia/reperfusion
Iba-1 Ionized calcium-binding adapter molecule 1
ICAM-1 Intercellular adhesion molecule-1
IF Immunofluorescence
IHC Immunohistochemistry
IL-1β Interleukin-1β
IL-6 Interleukin-6
iNOS Inducible Nitric Oxide Synthase
JAK2 Janus kinase 2
JNK c-Jun N-terminal kinase
Ki67 Mitotic cell marker
LC3-II Lipidation of microtubule associated protein 1 light chain 3
LDH Lactate dehydrogenase
MAP-2 Microtubule-associated protein 2
MCAO Middle cerebral artery occlusion
MDA Malondialdehyde
min minute
MPO Myeloperoxidase
MyD88 Myeloid differentiation factor 88
nAChRsα4β2 α4β2 nicotinic acetylcholine receptors
nAChRα7 α7 nicotinic acetylcholine receptor
NeuN Neuron-specific nuclear
NF-κB/P65 Nuclear transcription factor-kappa B
NM Not mentioned
Nrf2 Nuclear factor erythroid 2-related factor 2
NS Normal saline
NSS Neurological severity score
p-AKT Phosphorylated AKT
PBS Phosphate-buffered saline
p-ERK Phosphorylated ERK
PF Paeoniflorin
PI3K Phosphoinositide 3-kinases
p-JNK Phosphorylated JNK
p-P38 Phosphorylated P38
PRISMA Preferred Reporting Items for Systematic Reviews and Meta-Analyses
ROS Reactive oxygen species
RT-PCR Reverse transcription-polymerase chain reaction
SD Sprague-Dawley
SOD Superoxide dismutase
STAT3 Signal transducer and activator of transcription 3
TCM Traditional Chinese medicine
TLRs Toll-Like receptors
TNF-α Tumor necrosis factor-α
vWF Von Willebrand Factor
WB Western blot

frontiers | Frontiers in Pharmacology

REVIEW
published: 26 April 2022
doi: 10.3389/fphar.2022.890698

The Emerging Role of Extracellular Vesicle Derived From Neurons/Neurogliocytes in Central Nervous System Diseases: Novel Insights Into Ischemic Stroke

Fan Li[1], *Xiaokui Kang*[2], *Wenqiang Xin*[3] *and Xin Li*[2]*

[1]Department of Neurosurgery, Heji Hospital Affiliated Changzhi Medical College, Shanxi, China, [2]Department of Neurosurgery, Liaocheng People's Hospital, Liaocheng, China, [3]Department of Neurosurgery, Tianjin Medical University General Hospital, Tianjin, China

Neurons and neurogliocytes (oligodendrocytes, astrocytes, and microglia) are essential for maintaining homeostasis of the microenvironment in the central nervous system (CNS). These cells have been shown to support cell-cell communication *via* multiple mechanisms, most recently by the release of extracellular vesicles (EVs). Since EVs carry a variety of cargoes of nucleic acids, lipids, and proteins and mediate intercellular communication, they have been the hotspot of diagnosis and treatment. The mechanisms underlying CNS disorders include angiogenesis, autophagy, apoptosis, cell death, and inflammation, and cell-EVs have been revealed to be involved in these pathological processes. Ischemic stroke is one of the most common causes of death and disability worldwide. It results in serious neurological and physical dysfunction and even leads to heavy economic and social burdens. Although a large number of researchers have reported that EVs derived from these cells play a vital role in regulating multiple pathological mechanisms in ischemic stroke, the specific interactional relationships and mechanisms between specific cell-EVs and stroke treatment have not been clearly described. This review aims to summarize the therapeutic effects and mechanisms of action of specific cell-EVs on ischemia. Additionally, this study emphasizes that these EVs are involved in stroke treatment by inhibiting and activating various signaling pathways such as ncRNAs, TGF-β1, and NF-κB.

Keywords: extracellular vesicles, oligodendrocytes, astrocytes, microglia, ischemic stroke, non-coding RNAs

OPEN ACCESS

Edited by:
Yongjun Sun,
Hebei University of Science and Technology, China

Reviewed by:
Alejandro Villarreal,
University of Freiburg, Germany
Yong Luo,
Chongqing Medical University, China
Huaqiu Zhang,
Huazhong University of Science and Technology, China

***Correspondence:**
Xin Li
lixinliaocheng@163.com

Specialty section:
This article was submitted to Neuropharmacology, a section of the journal Frontiers in Pharmacology

Received: *06 March 2022*
Accepted: *07 April 2022*
Published: *26 April 2022*

Citation:
Li F, Kang X, Xin W and Li X (2022) The Emerging Role of Extracellular Vesicle Derived From Neurons/Neurogliocytes in Central Nervous System Diseases: Novel Insights Into Ischemic Stroke. Front. Pharmacol. 13:890698. doi: 10.3389/fphar.2022.890698

1 INTRODUCTION

The neurovascular unit (NVU), which plays a vital role in neurological disorders, is a multifunctional and morphological entity composed of many cells and materials, including neurons, neurogliocytes, cells of brain vessels (pericytes, endothelial cells, smooth muscle cells), and the extracellular matrix (Potjewyd et al., 2018; Forró et al., 2021). Neurons and neurogliocytes, including oligodendrocytes, astrocytes, and microglia, are key players in maintaining the homeostasis of the microenvironment in the central nervous system (CNS). Under ischemic stroke conditions, hypoxia induces cell death and apoptosis and directly contributes to the release of pro- or anti-inflammatory cytokines and autophagy-related proteins from glia and neurons, leading to neuroprotection or neurotoxicity

(Pan et al., 2021; Xin et al., 2021; Hou et al., 2022). Extracellular vesicles (EVs), present in multiple bodily fluids, are cell-derived nanoscale particles enclosed by a protein-rich lipid bilayer (Rodríguez and Vader, 2022). Based on their size, EVs can be classified into three types as follows (Saltarella et al., 2021): 1) apoptotic bodies (1,000–5,000 nm) are derived from apoptotic or necrotic cells that break up into multiple vesicles (Théry et al., 2009; Saltarella et al., 2021); 2) microvesicles (200–1,000 nm) are pinched off from the cell membrane directly (Théry et al., 2009; Saltarella et al., 2021); and 3) exosomes, the smallest EVs (30–150 nm), are produced *via* an active, energy-dependent, and organized process (Théry et al., 2009; Brinton et al., 2015; Saltarella et al., 2021). Although all classes of EVs and their heterogeneous subsets differ in their biogenesis, diameter, and cargo, owing to their natural composition, EVs have been suggested to exhibit a common feature of good biocompatibility and to transfer homing properties to specific cell types (Möller and Lobb, 2020; Roefs et al., 2020). Therefore, EVs are said to play an important role in intercellular communication as a new paracrine mediator (Möller and Lobb, 2020; Nagelkerke et al., 2021). All the aforementioned types of cells have been found to naturally secrete EVs under normal, physiological, and pathological conditions, owing to the dynamics of the cell membrane (Zhang et al., 2021a; Forró et al., 2021). A great deal of evidence has demonstrated that EVs derived from these cells exert biological functions by modulating specific aspects, such as participation in inflammatory reactions, cell migration, proliferation, apoptosis, and autophagy (Gao et al., 2020; Zhang et al., 2021a; Tallon et al., 2021). However, data on the precise mechanisms underlying such a therapeutic approach are limited. In this review, we summarize the effect of neuron/neurogliocyte-EVs in preclinical studies on treating neurological disorders by regulating different signaling pathways of cellular processes, such as cell apoptosis, inflammation, angiogenesis, and autophagy, and summarize the mutual mechanisms of the interaction between neuron/glial cell-EVs and ischemic stroke conditions.

2 THE CHARACTERISTICS AND BIOGENESIS OF EXTRACELLULARVESICLES

Despite the identification of well-recognized classes of cell-to-cell communication approaches, EVs have been a hot topic in the past several decades as an essential method for transferring cargo to short or long distances between cells (van Niel et al., 2018). Nevertheless, only a few people are aware of the discovery of EVs that can be traced back to the 19th century using a different nomenclature (Kaddour et al., 2021). In the 1840s, Gulliver's first studied milky particles in the blood serum, which he called "the molecular base of the chyle," with very small globules of active Brownian movement and a size ranging from −0.5 to 1 micron; this may have been the first encounter with EVs in the report (Gage and Fish, 1924). All eukaryotes can secrete EVs and exhibit a snapshot of the secreting cells, encapsulating active and specific biomolecules from the donor cell (Marzan and Stewart, 2021). Once EVs are produced in the extracellular space, these nanosized particles can be uptake by recipient cells, and in turn act as messengers and perform biological functions *via* the delivery of plenty of functional biomolecules including proteins, nucleic acids, lipids, and metabolites, into recipient cells, both near and far from the secreting cell (Palviainen et al., 2019; Marzan et al., 2021). Currently, there are three main subsets of EVs: exosomes, microvesicles, and apoptotic bodies. Exosomes are small EVs with a diameter of 30–150 nm and density of 1.13–1.19 g/ml (Yang et al., 2020). Exosome production is mainly classified into three stages: endocytosis, multivesicular body formation, and release. First, the plasma membranes start endocytosis, which is followed by the fusion of multiple intraluminal vesicles to produce endosomes. Second, the loading of bioactive molecules such as non-coding RNAs (ncRNAs), lipids, and proteins facilitates the formation of multivesicular bodies (van Niel et al., 2018). Finally, multivesicular bodies and plasma membranes are fused to achieve exosome release. Microvesicles with a diameter of 200–1,000 nm are slightly larger EVs generated by budding directly from the cell plasma membrane (Thietart and Rautou, 2020). This process involves lipid rearrangements concerning the asymmetry of the plasma membrane accelerated by membrane translocases, scramblases, and calpain. Conversely, apoptotic bodies, the largest among all types of EVs, are 1,000–5,000 nm in diameter, are secreted by dying cells, and are even more abundant than exosomes or microvesicles under specific conditions (Doyle and Wang, 2019; Battistelli and Falcieri, 2020). Many efforts have been made to identify the emerging role of exosomes and microvesicles in intercellular communication. However, there is little evidence on the value of apoptotic bodies in nanomedicine.

3 EXTRACELLULAR VESICLES-DERIVED FROM NEURONS/NEUROGLIOCYTES REGULATE CELL DEATH AND APOPTOSIS IN CENTRAL NERVOUS SYSTEM DISEASES

Cell death is the consequence of multiple cellular processes that occur during neurological diseases, including mitochondrial dysfunction, protein aggregation, free radical generation, excitotoxicity, and inflammation (Salucci et al., 2021). Numerous studies have revealed that EVs derived from these cells are involved in cell death in neurological disorders. A previous study assessed the overall effects of exosomes derived from normoxic and hypoxic neurons on the survival and neuritogenesis of rat cortical neurons (Chiang et al., 2021). As presented by Chiang et al. (2021), hypoxic concentrated conditioned media, but not normoxic concentrated conditioned media, significantly reduced neuronal viability. They further pelleted exosomes from both normoxic and hypoxic concentrated conditioned media, and then examined the effects after administration of PBS and 25, 100, or 200 μg/ml exosomes in cultured cortical neurons using the CCK-8 assay.

TABLE 1 | Preclinical studies assessing the effect of EVs-derived from neurons/neurogliocytes on regulating cell death and apoptosis in CNS diseases.

Author, year	Country	Species	Model	Route	Cell source	Mechanism	Disease	Effect	References
Datta Chaudhuri et al. (2020)	United States	Rats	NA	co-incubation	AS	NA	NA	Inhibit	Datta Chaudhuri et al. (2020)
Song et al. (2019a)	China	Mice, Cells	MCAO	IV, co-incubation	BV2	miR-124	NA	Inhibit	Song et al. (2019a)
Xu et al. (2019)	China	Cells	OGD	co-incubation	Astrocytes	miR-92b-3p	Stroke	Inhibit	Xu et al. (2019)
Bu et al. (2020)	China	Rats, Cells	MCAO, OGD	IV, co-incubation	AS	miR-361/AMPK/mTOR/CTSB	Stroke	Inhibit	Bu et al. (2020)
Huang et al. (2020)	China	Cells	OGD	co-incubation	N2A	NA	Stroke	Promote	Huang et al. (2020)
Casella et al. (2020)	United States	Mice, Cells	MS	IV	OI	IL-10	MS	Inhibit	Casella et al. (2020)
Chen et al. (2021)	China	Rats, Cells	NA	co-incubation	AS	GDNF	NA	Promote	Chen et al. (2021)
Chiang et al. (2021)	Tianwan	Rats, Cells	OGD	co-incubation	neuron	microRNAs	Stroke	Promote	Chiang et al. (2021)
Chun et al. (2021)	United States	Cells	NA	co-incubation	AS	NA	NA	Inhibit	Chun et al. (2021)
Qi et al. (2021)	China	Rats, Cells	VD	IV	HNSCs	MIAT/miR-34b-5p/CALB1	VD	Inhibit	Qi et al. (2021)
Zhang et al. (2021a)	Germany	Mice, Cells	MCAO, OGD	IV	microglia	TGF-β/Smad2/3	Stroke	Inhibit	Zhang et al. (2021a)

NA, not available; AS, astrocytes; MCAO, middle cerebral artery occlusion; OGD, oxygen-glucose-deprivation; ECs, endothelial cells; OI, oligodendrocyte; MS, multiple sclerosis; GDNF, glial cell line-derived neurotrophic factor; VD, vascular dementia; HNSCs, hippocampal neural stem cells; AD, Alzheimer's disease; Ref, Reference.

They noted a linear trend in the decrease in viability with increasing hypoxic exosome dose, revealing that hypoxic exosomes impair neuronal survival in a dose-dependent manner. However, low concentrations (25 and 100 μg/ml) of normoxic exosomes did not affect neuronal viability. To further evaluate the effect on axonal outgrowth, dissociated cortical neurons were treated with exosomes and subjected to immunostaining with an anti-Tau antibody. The results showed that exosomes derived from hypoxic neurons, but not EVs obtained from normoxic neurons, impaired both dendritic and axonal outgrowths of cultured cortical neurons (Chiang et al., 2021). Among the various programmed cell death pathways (Datta et al., 2020), apoptosis accounts for a large proportion of cell death through brain injury (Radak et al., 2017), which efficiently removes damaged cells from DNA damage or during development (Fan et al., 2020). Apoptosis plays an essential role in the homeostasis of normal tissues, and scientists have identified that EVs play essential roles in regulating cell apoptosis. Huang et al. (2020) indicated that not only hypoxic neuron-concentrated conditioned media but also EVs derived from hypoxic neurons exacerbate hypoxia-induced injury on transplanted mesenchymal stem cell viability, apoptosis, and oxidative stress *in vitro*. In addition to neuronal EVs, the effects of EVs derived from glial cells on cell death and apoptosis regulation have been studied more extensively. Bu et al. (2020) performed a series of *in vitro* experiments and demonstrated that astrocyte-derived exosomes promoted hypoxia-inhibited PC12 cell activity and suppressed cell apoptosis. Likewise, Chun et al. (2021) reported that astrocyte-derived EVs enhanced the survival and electrophysiological function of human cortical neurons. Notably, neuronal apoptosis was significantly increased upon treatment with conditioned medium from necroptotic astrocytes *via* EVs delivery (Chen et al., 2021). Furthermore, Casella et al. (2020) uncovered oligodendrocyte-derived EVs as an antigen-specific therapy for experimental autoimmune encephalomyelitis. This process was safe and restored immune tolerance by inducing apoptosis of autoreactive $CD4^+$ T cells. Concerning the EVs derived from microglia, EV derived from both hypoxic and normoxic microglia can repress neuronal apoptosis and promote neuronal viability in hypoxic cortical neurons (Li et al., 2021a; Zhang et al., 2021a). To date, many studies have assessed the effect of EVs derived from neurons/glial cells in the regulation of apoptosis in CNS diseases (Song et al., 2019a; Xu et al., 2019; Bu et al., 2020; Casella et al., 2020; Datta Chaudhuri et al., 2020; Gao et al., 2020; Nogueras-Ortiz et al., 2020; Zhang et al., 2021a; Chen et al., 2021; Chun et al., 2021; Qi et al., 2021). The characteristics of these studies are summarized in **Table 1.**

4 EXTRACELLULAR VESICLE-DERIVED FROM NEURONS/NEUROGLIOCYTES REGULATE AUTOPHAGY IN CENTRAL NERVOUS SYSTEM DISEASES

Autophagy is an evolutionarily conserved cellular mechanism (Wang et al., 2018), which is a program caused by the regulation of the internal conditions of cells (Sun et al., 2018), such as starvation, hypoxic nutrient deficiencies, and infection (Mo et al., 2020), leading to the degradation of toxic proteins, damaged organelles, and invading pathogens *via* the lysosomal pathway (Liu et al., 2020). On the one hand, autophagy can maintain cellular nerve homeostasis, since it is associated with degraded misfolded or nonfunctional proteins and damaged organelle, suggesting that it plays an essential housekeeping role in the

TABLE 2 | Preclinical studies assessing the effect of EVs-derived from neurons/neurogliocytes on regulating autophagy in CNS diseases.

Author, year	Country	Species	Model	Route	Cell source	Mechanism	Disease	Effect	References
Pei et al. (2019)	China	Mice, Cells	MCAO, OGD	IV, co- incubation	AS	NA	stroke	Inhibit	Pei et al. (2019)
Pei et al. (2019)	China	Cells	OGD	co-incubation	AS	miR-190b	stroke	Inhibit	Pei et al. (2020)
Zang et al. (2020)	China	Mice, Cells	MCAO, OGD	SI, co-incubation	BV2	PDE1-B	stroke	NA	Zang et al. (2020)
Liu et al. (2021a)	China	Mice, Cells	MCAO, OGD	IV, co-incubation	microglia	miRNA-135a-5p/TXNIP/NLRP3	stroke	Inhibit	Liu et al. (2021a)
Guo et al. (2020)	China	Cells	NA	co-incubation	microglia	a-synuclein transmission	PD	NA	Guo et al. (2020)
Li et al. (2019)	China	Mice, Cells	TBI	co-culture, IV	BV2	miR-21	TBI	Inhibit	Li et al. (2019)

NA, not available; AS, astrocytes; MCAO, middle cerebral artery occlusion; OGD, oxygen-glucose-deprivation; SI, stereotaxic injection; IV, intravenous injection; α-syn, alpha-synuclein; TBI, traumatic brain injury; PD, Parkinson's disease; Ref, reference.

CNS (Peker and Gozuacik, 2020). On the other hand, autophagy is also associated with the promotion of cell death. It is possible that excessive upregulation of autophagy and long-term autophagy eventually result in self-digestion or have harmful effects (Bar-Yosef et al., 2019). Abundant evidence indicates that autophagy and exosomes are inseparable. Autophagy plays a vital role in the synthesis and degradation of extracellular vesicles (EVs). It has been reported that autophagosomes not only have a strong ability to fuse with lysosomes, but also fuse with multivesicular bodies to form amphiphiles. The amphiphiles eventually fuse with lysosomes and dissolve the inner material of the intraluminal vesicles, resulting in a significant reduction in the release of exosomes. Taken together, these results suggest that autophagosome formation plays a key role in EVs secretion and transport (Xu et al., 2018). In addition, much direct evidence has verified that autophagy could be a therapeutic target in neurological treatment by using neuron/neurogliocyte-EVs. For example, in traumatic brain injury, Li et al. (2019) illustrated that neuronal EVs enriched with miR-21-5p can suppress neuronal autophagy induced by scratch injury, directly targeting the Rab11a 3′UTR region to reduce its translation, thus attenuating trauma-induced, autophagy-mediated nerve injury *in vitro*. Likewise, Liu et al. (2021a) found that M2 type microglia derived EVs could transfer miR-135a-5p into neurons to suppress the expression of thioredoxin-interacting protein, which in turn suppresses the activation of the nod-like receptor protein 3 inflammasome, thereby inhibiting neuronal autophagy induced by ischemia. To date, a vast number of studies have assessed the interaction between neuron/glial cell-EVs and autophagy in CNS diseases (Li et al., 2019; Pei et al., 2019; Guo et al., 2020; Pei et al., 2020; Zang et al., 2020; Liu et al., 2021a). The characteristics of these studies are summarized in **Table 2.**

5 EXTRACELLULAR VESICLE-DERIVED FROM NEURONS/NEUROGLIOCYTES REGULATE ANGIOGENESIS IN CENTRAL NERVOUS SYSTEM DISEASES

Angiogenesis is the appearance of new microvessels that branch off from pre-existing vessels (Ruan et al., 2015). Hypoxic or insulted tissues can produce vascular endothelial growth factors, and angiogenesis begins along the concentration gradient of vascular endothelial growth factor in neonates (Carmeliet and Tessier-Lavigne, 2005). Angiogenesis plays a vital role in brain injury recovery following an injury because it promotes blood flow and metabolic nutrients to reach the injured regions to promote neural tissue repair by facilitating neurogenesis and synaptic initiation (Hatakeyama et al., 2020; Ma et al., 2021). To investigate whether microglial EVs regulate angiogenesis *in vitro*, Zhang et al. (2021a) showed that EVs derived from hypoxia-preconditioned microglia labeled with DiI were taken up by bEnd.3 endothelial cells. Further experiments concerning the therapeutic impact of these EVs against hypoxic injury of bEnd.3 cells were performed to evaluate cell viability and cytotoxicity *via* the MTT and LDH release assays, respectively. The results demonstrated that decreased cell viability and increased cytotoxicity after hypoxia were suppressed by these EVs (Zhang et al., 2021a). Moreover, these EVs can significantly promote bEnd.3 migration during hypoxia according to the scratch migration assay. Meanwhile, EVs derived from preconditioned microglia reversed this effect of impaired tube formation in bEnd.3 cells caused by hypoxia. Following the aforementioned *in vitro* findings, Zhang et al. (2021a) further indicated that EV administration induces angiogenesis and diminishes cell injury in the ischemic mouse hemispheres. Taken together, the evidence suggests that EVs derived from hypoxic microglia promote cell viability, migration, and angiogenesis in hypoxic injury. As such, the ability of EVs derived from neurons and other glial cells to regulate angiogenesis is unclear, and additional and reliable data are urgently needed.

6 EXTRACELLULAR VESICLE-DERIVED FROM NEURONS/NEUROGLIOCYTES REGULATE NEUROINFLAMMATION IN CENTRAL NERVOUS SYSTEM DISEASES

Neuroinflammation is integral to the neurological pathophysiological process and results in damage to tissue homeostasis (DiSabato et al., 2016; Alawieh et al., 2018), involving acidosis, excitotoxicity, promotion of cytoplasmic Ca^{2+} concentrations, loss of glucose and oxygen, destruction of the blood-brain barrier, and damage to mitochondria (Xu et al.,

TABLE 3 | Preclinical studies assessing the effect of EVs-derived from neurons/neurogliocytes on regulating neuroinflammation in CNS diseases.

Author, year	Country	Species	Model	Route	Cell source	Mechanism	Disease	Effect	References
Casella et al. (2018)	Italy	Mice, Cells	EAE	intrathecal injection-incubation	BV2	IL-4	MS	Inhibit	Casella et al. (2018)
Huang et al. (2018)	China	Mice, Cells	TBI, neuronal scratch-injury	IV, co-incubation	BV2	miR-124-3p	TBI	Inhibit	Huang et al. (2018)
Rojas et al. (2018)	United States	Mice, Cells	brain inflammation	IV	AS	DPTIP	NA	Inhibit	Rojas et al. (2018)
Chen et al. (2019)	China	Human	NA	NA	AS	IL-6	ALS	Inhibit	Chen et al. (2019)
Casella et al. (2020)	United States	Mice	EAE	IV	OI	IL-10	MS	Inhibit	Casella et al. (2020)
Datta Chaudhuri et al. (2020)	United States	Cells	NA	co-incubation	AS	ATP, IL-1β	NA	Inhibit	Datta Chaudhuri et al. (2020)
Li et al. (2020)	United States	Cells	NA	co-incubation	AS	CK1	AD	Inhibit	Li et al. (2020)
Zhang et al. (2020)	China	Mice, Cells	TBI	IV	BV2	miR-711	AD	Inhibit	Zhang et al. (2020)
Tallon et al. (2021)	United States	Mice, Cells	striatal IL1-β injection	IV	neurons, OI, microglia	nSMase2	NA	NA	Tallon et al. (2021)
Long et al. (2020)	China	Mice, Cells	LPS and TBI	IV, co-incubation	AS	miR-873a-5p	TBI	Inhibit	Long et al. (2020)

NA, not available; EAE, experimental autoimmune encephalomyelitis; MS, multiple sclerosis; TBI, traumatic brain injury; AS, astrocytes; DPTIP, 2,6-Dimethoxy-4-(5-Phenyl- 4-Thiophen-2-yl-1H-Imidazol-2-yl)-Phenol; ALS, amyotrophic lateral sclerosis; EAE, experimental autoimmune encephalomyelitis; OI, oligodendrocyte; AD, Alzheimer's disease; nSMase2, neutral sphingomyelinase 2; Ref, reference.

2021; Chen et al., 2020a; Forrester et al., 2018). However, the inflammatory response is a double-edged sword after injury because it not only intensifies secondary injury to the brain, but also promotes the recovery of neurological function, thereby demonstrating that neuroinflammation is related to the pathogenesis and prognosis of CNS disorders (Zhang et al., 2021a). Several studies have revealed that various neuron/glial cell-EVs are involved in the regulation of inflammation and microglial activation in neurological diseases. Microglia serve as "brain-resident macrophages" that comprise approximately 10% of all the cells in the CNS (Fakhoury, 2018), the activation of microglia represents the first step of an inflammatory response, followed by the activation of other immune cells like neutrophils, T cells, natural killer cells, etc. (Xin et al., 2021; Iadecola and Anrather, 2011; Jin et al., 2010). Thus, the effects of microglial EVs on inflammation regulation have also been studied extensively. Casella et al. (2018) engineered a murine microglia cell line, BV-2 cell, to produce EVs enriched with the endogenous "eat me" signal Lactadherin on the surface to target phagocytes while overexpressing the anti-inflammatory cytokine IL-4. A single injection of these EVs into the cisterna magna upregulated anti-inflammatory markers, such as chitinase 3-like 3 and arginase-1, and significantly suppressed tissue damage in a mouse model of multiple sclerosis and experimental autoimmune encephalomyelitis. Likewise, overexpression of miR-124-3p in EVs derived from microglia following traumatic brain injury can reduce neuronal inflammation and contribute to neurite outgrowth by transferring these EVs into neurons (Huang et al., 2018). Similarly, BV2 cell-secreted EVs enriched with miR-711 could target and suppress Itpkb, thereby suppressing M1 microglial polarization and promoting M2 microglial polarization (Zhang et al., 2020). Besides that, the EVs derived from other glial cells, such as astrocyte and oligodendrocyte, also are involved in the regulation of inflammation (Casella et al., 2020; Li et al., 2020). The additional details are provided in **Table 3.** EVs derived from glial cells might, therefore, contribute to suppressing inflammation and microglial activation (Casella et al., 2018; Huang et al., 2018; Zhang et al., 2020), information regarding the modulation of neuronal EVs in inflammation is scarce. An overview of how EVs derived from neurons/glial cells affect neurological recovery is shown in **Figure 1.**

7 THE ROLE OF EXTRACELLULAR VESICLES-DERIVED FROM NEURONS/ NEUROGLIOCYTES IN ISCHEMIC STROKE

A comprehensive literature search of electronic databases, including PubMed, Cochrane Library, EMBASE, Web of Science, and China National Knowledge Infrastructure, was conducted from the inception of these databases until 28 February 2022. We retrieved studies assessing the effect of EV-derived from neurons/glial cells on ischemic stroke adopting the following keywords in accordance with Boolean logic: ("ischemic stroke" OR "middle cerebral artery occlusion" OR "MCAO" OR "ischemia") and ("exosome" OR "EVs" OR "Extracellular vesicles" OR "microvesicles") AND ("microglia" OR "neuron" OR "astrocyte" OR "oligodendrocyte"). In addition, all references from the included articles were manually checked to identify potential qualifying studies that were missed in the electronic search results. The process was repeated until no further studies would be obtained. A total of 29 studies were identified in this section (Frühbeis et al., 2013; Fröhlich et al., 2014; Guitart et al., 2016; Xin et al., 2017; Xu et al., 2017; Hira et al., 2018; Yang et al., 2018; Song et al., 2019a; Song et al., 2019b; Pei et al., 2019; Tian

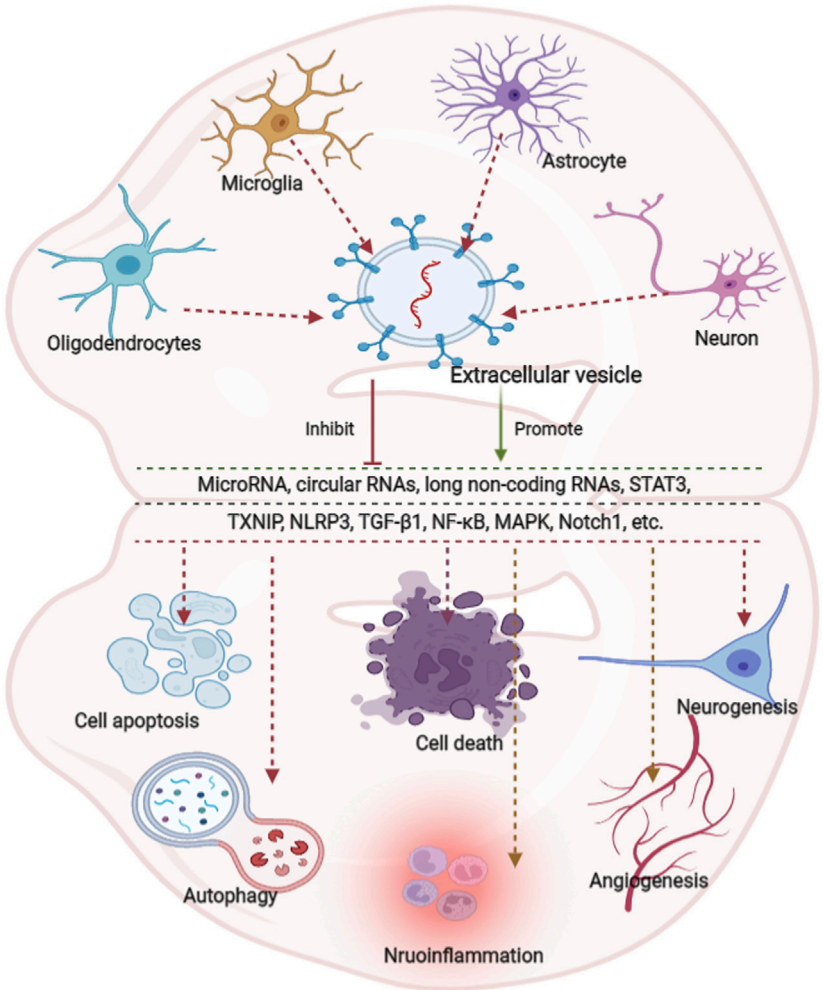

FIGURE 1 | Overview of the effects of extracellular vesicle-derived from neurons/neurogliocytes on neurological recovery in central nervous system diseases. Predominantly extracellular derived from neurons/glial cells predominantly modulate autophagy, cell death, apoptosis, regeneration, and inflammation through various pathways. Glial cells are composed of astrocytes, microglia and oligodendrocytes. MicroRNAs (miRNAs) play key roles in various pathways.

et al., 2019; Xu et al., 2019; Chen et al., 2020b; Bu et al., 2020; Frühbeis et al., 2020; Huang et al., 2020; Pei et al., 2020; Wu et al., 2020; Xie et al., 2020; Zang et al., 2020; Liu et al., 2021a; Yang et al., 2021a; Zhang et al., 2021a; Li et al., 2021b; Liu et al., 2021b; Zhang et al., 2021b; Chiang et al., 2021; Du et al., 2021; Raffaele et al., 2021), conducted from 2016 to 2021. The most extensively adopted species and associated stroke models are mice and middle cerebral artery occlusion, respectively. Among these 29 publications, 10 focused on microglia-EVs (Yang et al., 2018; Song et al., 2019a; Tian et al., 2019; Xie et al., 2020; Zang et al., 2020; Liu et al., 2021a; Zhang et al., 2021a; Li et al., 2021b; Zhang et al., 2021b; Raffaele et al., 2021), 11 focused on astrocyte-EVs (Guitart et al., 2016; Xin et al., 2017; Hira et al., 2018; Pei et al., 2019; Xu et al., 2019; Chen et al., 2020b; Bu et al., 2020; Pei et al., 2020; Wu et al., 2020; Liu et al., 2021b; Du et al., 2021), 3 focused on oligodendrocytes (Frühbeis et al., 2013; Fröhlich et al., 2014; Frühbeis et al., 2020) and 5 focused on neuron-EVs (Xu et al., 2017; Song et al., 2019b; Huang et al., 2020; Yang et al., 2021a; Chiang et al., 2021), demonstrating that it is sufficient to suggest that EVs derived from neurons/glial cells play an important role in regulating the progress and prognosis of ischemic stroke.

7.1 The Extracellular Vesicles Derived From Neurons

Accumulating evidence has demonstrated that neurons have the potential to release EVs from their somatodendritic compartments (Fauré et al., 2006; Lachenal et al., 2011) to regulate local synaptic plasticity, trans-synaptic communication, and post-stroke recovery. As mentioned, microglia are professional phagocytes that are, in part, beneficial due to their ability to reduce neuroinflammation *via* phagocytosis of dead neurons and neuronal debris (Sierra et al., 2013). Previous studies have revealed that neurons could inhibit microglial activation and promote M2-type microglial polarization, which in turn modulates neuronal survival during ischemic stroke (Norris et al., 2018; Pluvinage et al., 2019). As such, Yang et al.

(2021a) indicated that these EV-derived miR-98 act as an intercellular signal mediating neuronal and microglial communication by suppressing platelet-activating factor receptor-mediated microglial phagocytosis during the recovery of neurological function induced by an ischemic stroke. Likewise, Song et al. (2019b) conducted an ischemic brain injury study that resulted in MCAO. They found that EVs derived from hypoxic neurons inhibited the expression of chemokine (C-X-C motif) ligand 1 (CXCL1) and inflammatory factors in astrocytes, suggesting that EVs derived from cortical neurons exert protective effects against neuroinflammation in astrocytes *via* downregulation of CXCL1. Additionally, Xu et al. (2017) demonstrated that these EVs could promote brain vascular integrity by modulating the levels of vascular endothelial cadherin binding to eukaryotic elongation factor 2 kinase. Herein, miR-132 serves as an intercellular signal that mediates the neural regulation of brain vascular integrity. Interestingly, as previously mentioned, EVs derived from hypoxic neurons, but not EVs obtained from normoxic neurons, impaired both dendritic, and axonal outgrowths of cultured cortical neurons (Chiang et al., 2021). Taken together, EVs derived from neurons have been shown to be collectively effective in the recovery of ischemic stroke patients; however, information regarding this aspect is scarce. Therefore, more evidence-based information is needed.

7.2 The Extracellular Vesicles Derived From Oligodendrocytes

Oligodendrocytes are neural tube-derived cells that have the ability to form myelin, a compact lamellar wrapping revealed on properly large fiber axons, thereby accelerating nerve conduction (Cohen, 2005). EVs derived from oligodendrocytes also mediate neuroprotection and promote neuronal homeostasis. Frühbeis et al. (2013) indicated that, triggered by neuronal signals, oligodendrocytes can release EVs derived from the multi-vesicular body which appears prevalent at periaxonal sites in myelinated nerves. In turn, neurons can internalize EVs derived from oligodendrocytes by endocytosis and recover EV cargo, thereby importing bioactive molecules. The supply of cultured neurons with EVs derived from oligodendrocytes increased neuronal viability under conditions of cell stress. Electrophysiological analysis using *in vitro* multi-electrode arrays also demonstrated an improved firing rate of neurons exposed to EVs derived from oligodendrocytes, and further western blot analysis showed increased activation of pro-survival signaling pathways (Fröhlich et al., 2014). These EVs can directly deliver antioxidant enzymes, such as catalase and superoxide dismutase 1. Additionally, Frühbeis et al. (2020) pointed out that oligodendrocyte-to-neuron EVs transfer promotes long-term neuronal maintenance by improving the metabolic state and promoting axonal transport in nutrient-deprived neurons, suggesting a novel mechanistic link between myelin diseases and secondary loss of axonal integrity. Oligodendrocyte-EVs might therefore contribute to supporting neurons; information regarding this aspect, however, is scarce.

7.3 The Extracellular Vesicles Derived From Microglia

Microglia are highly dynamic cells with the potential to transform their morphology from ramified to amoeboid and alter their phenotypes in response to ischemic insult (Xin et al., 2021). These opposing roles of microglia under ischemic conditions correlate with a distinct phenotype, as suggested by the proinflammatory M1 and anti-inflammatory M2 types (Xin et al., 2021). M1 phenotype microglia participate in exacerbating brain damage by secreting interleukin (IL)-6, IL-1β, nitric oxide, and tumor necrosis factor-α (Tang and Le, 2016; Cheng et al., 2019). M2 microglia remove necrotic tissue and stimulate tissue repair by releasing IL-4, IL-10, and transforming growth factor-β, thereby maintaining homeostasis (Ma et al., 2018; Zhang et al., 2018). Microglia have been shown to support cell-cell communication in the treatment of stroke *via* multiple mechanisms, most recently through the release of EVs. Correspondingly, a variety of pathological conditions also regulate microglial secretion, thereby affecting the main components of EVs. For example, inflammation induced by LPS can alter EV production in microglial cells and alter the cytokine levels and protein composition carried by EVs (Yang et al., 2018). Likewise, Zang et al. (2020) illustrated that the increase in autophagic flux using vinpocetine is related to the alteration of microglial EVs contents and properties to protect the survival and neurite structure of neurons against ischemic stroke. Taken together, microglia under different conditions may alter the cargo of microglial EVs, and thus have different functions. For example, M2 microglial EVs can reduce glial scar formation by repressing the expression of astrocyte proliferation gene signal transducer and activator of transcription 3 and glial fibrillary acidic protein. Similarly, M2 microglial EVs can also reduce neuronal autophagy and apoptosis, which further inhibits ischemic brain injury (Song et al., 2019a; Liu et al., 2021a). EVs secreted by microglial cell lines also play a significant role in the treatment of stroke. Tian et al. (2019) showed that IL-4-polarized microglial cells can ameliorate the injury induced by ischemic stroke by improving angiogenesis through the secretion of exosomes. Zhang et al. (2021b) reported that EVs derived from BV2 in the M2 phenotype were taken up by neurons and suppressed neuronal apoptosis in response to ischemic injury, which further reduced the infarct volume and behavioral deficits in MCAO mice. In addition, ischemic preconditioning can change the composition of EVs secreted by microglia, which plays a crucial role in the treatment of stroke. Xie et al. (2020) indicated that EVs derived from ischemia-preconditioned microglia regulate the TGF-β/Smad2/3 pathway to promote angiogenesis in a tube formation assay and neurological recovery in stroke mice. However, Zhang et al. (2021a) reported that microglial EVs inhibited brain microvascular endothelial cell proliferation and angiogenesis by impairing brain microvascular endothelial cell viability and integrity, as well as the loss of vascular formation. The EVs isolation process was conducted by ultracentrifugation, whereas Zhang et al. (2021a) adopted the method of PEG combined with ultracentrifugation. Different extraction methods of EVs may have different therapeutic effects on stroke owing to the alteration

TABLE 4 | Preclinical studies assessing the interaction between EVs-derived from microglia and ischemic stroke.

Author, year	Cell status	Main effects	Main mechanisms
Yang et al. (2018)	Normoxic	Inflammation alters cytokine levels and protein composition in microglial-EVs	IL-6, neuroinflammation
Song et al. (2019a)	M2 type	Attenuate ischemic brain injury and promote neuronal survival	miR-124
Tian et al. (2019)	IL-4-polarized BV2	Ameliorate the ischemia damage by promoting angiogenesis	miR-26a
Xie et al. (2020)	hypoxic	Aggravate ischemia induced brain microvascular endothelial cells damage and permeability	miR-424-5p/FGF2/STAT3
Zhang et al. (2021a)	hypoxia	Regulate inflammatory response, promote angiogenesis and repress apoptosis *in vivo* and vitro	TGF-β/Smad2/3
Li et al. (2021a)	M2 type	Glial scar formation *via* inhibiting astrocyte proliferation and migration	miR-124/STAT3
Liu et al. (2021a)	M2 type	Inhibit TXNIP and NLRP3, thereby reducing neuronal autophagy and ischemic brain injury	miR-135a-5p/TXNIP/NLRP3
Raffaele et al. (2021)	Normoxic	Improve post-stroke recovery by preventing immune cell senescence and favoring oligodendrogenesis	TNF
Zang et al. (2020)	Hypoxia	PDE1-B regulates autophagic flux and EVs biogenesis, in turn regulates neuronal survival under	PDE1-B
Zhang et al. (2021b)	M2 type BV2	Attenuate neuronal apoptosis and promote the recovery of neurological function	miR-137/Notch1

EVs, extracellular vesicles; TGF, transforming growth factor; N-SMase-2, neutral sphingomyelinase-2; STAT3, signal transducer and activator of transcription 3; TXNIP, thioredoxin-interacting protein; NLRP3, nod-like receptor protein 3; TNF, tumor necrosis factor; PDE, phosphodiesterase enzyme.

of the components of EVs. A series of studies have assessed the interaction between EVs derived from diverse microglia and stroke conditions. The main effects and primary mechanisms of these studies are summarized in **Table 4**, demonstrating that microglial EVs may offer a promising strategy for the treatment of ischemic stroke.

7.4 The Extracellular Vesicles Derived From Astrocyte

Astrocytes are the most numerous glial cell types in the mammalian CNS that regulate brain function, synaptic function, neuronal viability, integrity of the blood-brain barrier, and neural plasticity *via* interaction with neurons, and play essential roles in the progression of ischemia (Tahir et al., 2022). As such, astrocyte-derived EVs have been shown to improve neuronal survival, inhibit microglial inflammation, and promote post-stroke functional recovery. In terms of neuronal survival, these EVs can not only directly promote neuronal viability but also indirectly inhibit neuronal autophagy, inflammation, and apoptosis under hypoxic conditions. For instance, Pei et al. (2020) used the mouse hippocampal neuronal cell line HT-22 under oxygen and glucose deprivation (OGD) conditions to mimic ischemic injury. Confocal laser microscopy revealed that EVs isolated from primary astrocytes were taken up by the HT-22 cells. Further experiments demonstrated that these EVs promoted HT-22 cell vitality and apoptosis, as determined by the CCK-8 assay and TUNEL staining, respectively, and regulated the expression of inflammation-related factors (TNF-α, IL-6, and IL-1β) analyzed by ELISA, levels of apoptosis-related proteins (cleaved caspase-3, Bax, and Bcl-2), and autophagy-related proteins (Beclin-1, LC3-I/II, Atg7, and P62) by western blot. Similarly, Pei et al. (2019) and Chen et al. (2020b) revealed that astrocyte-derived EVs could suppress autophagy and ameliorate neuronal damage, and further findings showed the effect of EVs on the inhibition of OGD-induced neurons apoptosis *via* regulating autophagy (Pei et al., 2019). In addition to EVs derived from normoxic astrocytes, Xu et al. (2019) indicated that EVs released from ischemic preconditioned astrocytes ameliorated OGD-induced cell death and apoptosis. Concerning the regulation of inflammation and functional recovery, Liu et al. (2021b) established an OGD N9 microglial model and an MCAO rat model. These findings revealed that astrocyte-derived EVs inhibited OGD-induced injury and inflammation by regulating NLPR3, oxidative stress, and inflammatory factors (IL-1β and IL-18) in N9 microglia; reduced brain infarction; and improved MCAO rat neural functions. Additionally, a series of specialized *in vitro* experiments have confirmed that these EVs can alleviate nerve damage and promote functional recovery after stroke. Bu et al. (2020) showed that these EVs improved neurocognitive function by evaluating the neurological deficit score and reduced the cerebral infarct size by TTC staining and cerebral edema. The main effects and primary mechanisms of astrocytes-EVs on the treatment of ischemic stroke are summarized in **Table 5.**

7.5 The Mechanism of Extracellular Vesicles Derived From Neurons/Glial Cells in the Effect on Regulating Stroke

7.5.1 Non-Coding RNAs, Especially microRNAs, are the Key Players

Unlike messenger RNAs (mRNAs), which do not encode proteins, ncRNAs are ubiquitous throughout the human genome (Yang et al., 2021b). ncRNAs play an essential regulatory role in various biological processes such as cell proliferation, epigenetic modification, and cell apoptosis (Yang et al., 2021b). The top three most commonly described ncRNA molecules are miRNAs, long ncRNAs (lncRNAs), and circular RNAs (circRNAs) (Smith et al., 2021). miRNAs are a group of non-coding RNA molecules with a length of 19–25 nucleotides that participate in the regulation of gene expression after transcription by targeting the 3untranslated region of the target mRNA sequence and inhibiting mRNA levels (Navabi et al., 2022). lncRNAs are a class of single-stranded RNA molecules with more than 200 nucleotides that are important in molecular networks (Guo et al., 2022). CircRNAs are a class of non-coding RNAs with

TABLE 5 | Preclinical studies assessing the interaction between EVs-derived from astrocyte and ischemic stroke.

Author, year	Cell status	Main effects	Main mechanisms
Guitart et al. (2016)	Hypoxic	PrP-carrying EVs under ischemic stress protects against oxidative stress, hypoxia, ischemia, and hypoglycemia	PrP
Hira et al. (2018)	Sema3A	Increase prostaglandin D2 synthase and GSK-3β+, thus contribute to axonal outgrowth and functional recovery	GTPase 1/R-Ras/Akt/GSK-3β
Pei et al. (2019)	Normoxic	Suppress autophagy response, enhance neurons viability and ameliorate ischemic damage *in vivo* and vitro	LC3, P62
Xu et al. (2019)	Hypoxic	Protect neurons against OGD injury and elevate the cell viability	miR-92b-3p
Chen et al. (2020a)	Hypoxic	Suppress neuronal apoptosis and ameliorate neuronal damage *via* regulating autophagy *in vivo* and vitro	miR-7670-3p/SIRT1
Du et al. (2021)	Normoxic	Decrease BNIP2 expression, reduce oxidative stress, and inflammation in HIBD rats	miR-17-5p
Wu et al. (2020)	Normoxic	Downregulate the NF-κB/MAPK axis, thereby promote proliferation and inhibit apoptosis	miR-34c/NF-κB/MAPK/TLR7
Bu et al. (2020)	Normoxic	Increase cell activity and suppress cell apoptosis *in vitro* and alleviate nerve damage in rats	miR-36/AMPK/mTOR
Pei et al. (2020)	Normoxic	Attenuate neuronal apoptosis by suppressing autophagy	miR-190b/Atg7
Liu et al. (2021b)	Hypoxic	Inhibit inflammation *in vitro*, reduce brain infarction, and improve neural functions *in vivo*	miR-29a/NF-κB/NLRP3

EVs, extracellular vesicles; PrP, prion protein; Sema3A, semaphorin 3A; HIBD, hypoxic-ischemic brain damage; TLR7, Toll-like receptor 7; MAPK, mitogen-activated protein kinase; SIRT1, sirtuin 1; CTSB, cathepsin B.

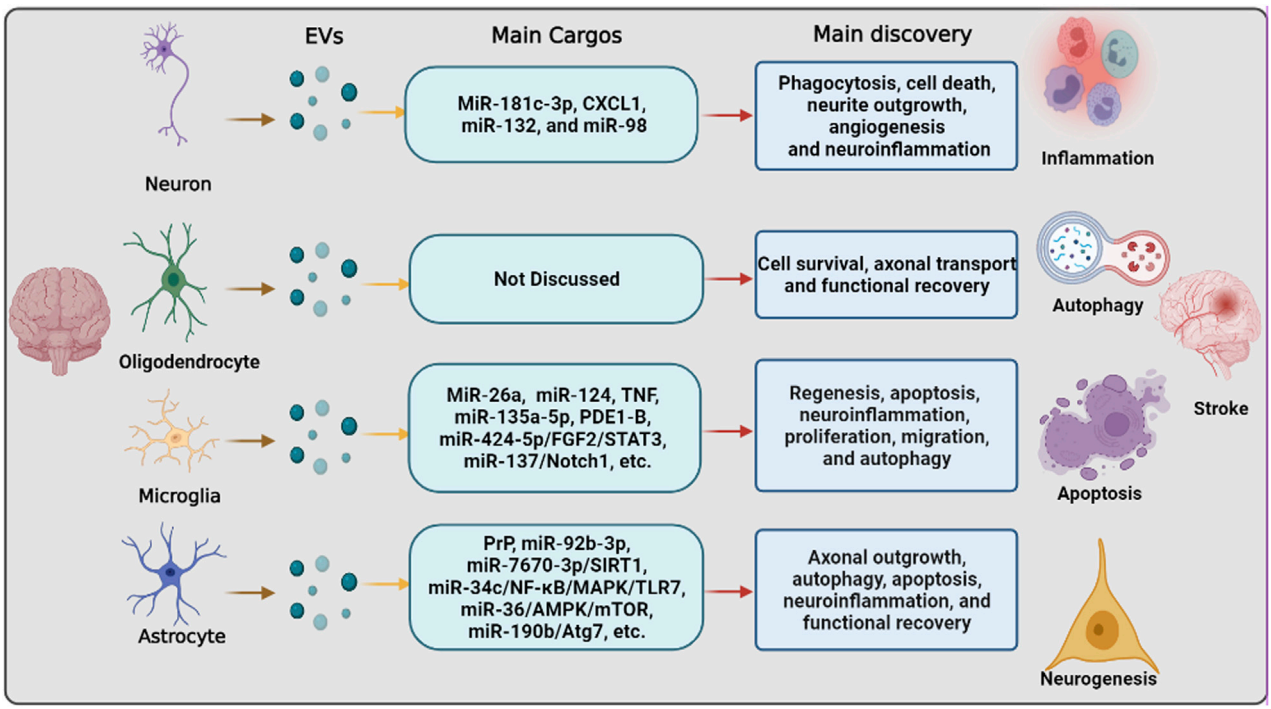

FIGURE 2 | The pathways that are involved in extracellular vesicle derived from neurons/neurogliocytes to regulate stroke recovery. Neurons and various glial cells, including astrocytes, microglia, and oligodendrocytes, can regulate recipient cells by transferring extracellular vesicles to regulate various biological processes, including inflammation, autophagy, apoptosis, and neurogenesis, thereby regulating ischemic stroke progression and recovery.

high stability and significant clinical relevance (Long et al., 2022). Intriguingly, as essential components, ncRNAs are selectively enriched in EVs, and ncRNAs loaded into EVs exert biological functions that modulate specific aspects of the onset and progression of ischemic stroke. Emerging evidence has demonstrated that a similar observation was also made for EV-derived ncRNAs derived from the aforementioned neurons/glial cells in ischemic stroke. For instance, Chen et al. (2020b) suggested that circSHOC2 expression was significantly upregulated in EVs released from ischemic-preconditioned astrocytes. Overexpression of circSHOC2 in neurons yielded the same protective effects as those from ischemic-preconditioned astrocyte-EVs *in vitro*, and similar results were also observed in MCAO mice by sponging miR-7670-3p, which regulates SIRT1 expression (Chen et al., 2020b). In addition to circRNAs, miRNAs are the most commonly reported miRNAs, as indicated in a series of

publications. As mentioned above, M2 microglial EVs reduce glial scar formation and neuronal autophagy, mechanistically, M2 microglial EVs take effect *via* miR-124/STAT3 pathway and microRNA-135a-5p/TXNIP/NLRP3 axis, respectively. Meanwhile, neuronal EV-shuttled miRNA-181c-3p inhibited inflammation by downregulating CXCL1 in astrocytes in a rat model of ischemic brain injury (Song et al., 2019b).

7.5.2 The Role of a Variety of Messenger RNAs Upon Extracellular Vesicle-Regulation in Stroke

mRNAs have been previously shown to have great potential for therapeutic applications in the treatment of ischemic stroke. Delivery systems for mRNAs, including lipid- and polymer-based carriers, have been developed to improve mRNA bioavailability. Among these systems, EVs are the most common carriers. For example, under OGD conditions, EVs derived from OGD-preconditioned primary microglia stimulated both angiogenesis and tube formation in bEnd.3 endothelial cells and repressed neuronal injury. Mechanistically, OGD induces upregulation of TGF-β1 in OGD-preconditioned microglia and EVs derived from non-hypoxic microglia or from different reoxygenation periods (24, 48, and 72 h) (Zhang et al., 2021a). Zhang et al. (2021a) used TGF-β1 siRNA to transfect microglia and obtained the corresponding EVs. Enriched TGF-β1 in EVs secreted from OGD-preconditioned microglia, but not microglia transfected with TGF-β1 siRNA, turned out to be a vital compound for the therapeutic potential of microglial EVs, affecting the Smad 2/3 pathway in both endothelial cells and neurons (Zhang et al., 2021a). This is in addition to the direct interaction between EVs and mRNA. Thus, neurons/glial cell-EVs can not only directly interact with mRNA but also indirectly affect mRNA by acting on miRNAs. Nuclear factor-kB (NF-κB) is present in almost all cell types and primarily serves as a transcription factor implicated in various biological processes (Barnabei et al., 2021). It has been shown to promote multiple pro-inflammatory mediators, and suppression of NF-κB signaling correlates with beneficial effects in ischemic stroke by EV-miRNAs. Liu et al. (2021b) reported that miR-29a in astrocyte-derived EVs inhibits brain ischemia-reperfusion injury by downregulating the NF-κB/NLRP3 axis. Wu et al. (2020) indicated that astrocytes-EVs transported miR-34c downregulates the NF-κB/MAPK axis and relieves neurological damage in ischemic stroke. Additionally, a great number of other mRNAs were revealed as the downstream of EV-miRNAs, such as Notch1 (Zhang et al., 2021b), AMPK/mTOR, (Bu et al., 2020), FGF2/STAT3 (Xie et al., 2020), etc. (Liu et al., 2021a). Besides that, there are, of course, many other pathways that are involved in EVs derived from neurons/glial cells to regulate stroke recovery as shown in **Figure 2.**

8 CONCLUSION

EVs, ranging in size from 30 to 5,000 nm, secreted by different cell types, are surrounded by cell-segregated membrane complexes with a lipid bilayer and play an important role in the pathological and physiological environments of target cells by transferring a variety of cargo of nucleic acids, lipids, and proteins. Neurons and neurogliocytes, including oligodendrocytes, astrocytes, and microglia, play essential roles in maintaining homeostasis of the microenvironment in the CNS. These cells have been shown to support cell-cell communication *via* multiple mechanisms, most recently by the release of EVs, which further regulate various mechanisms underlying CNS disorders, including angiogenesis, autophagy, apoptosis, cell death, and inflammation. Ischemic stroke following cerebral artery occlusion is a major cause of chronic disability worldwide. Neuron/neurogliocyte-EVs are involved in the treatment of ischemic stroke under preclinical conditions. Among the mechanisms of these EVs in the treatment of stroke, ncRNAs play a key role, and they can also modulate directly or indirectly various mRNAs signaling pathways such as TGF-β1and NF-κB.

AUTHOR CONTRIBUTIONS

All authors made a significant contribution to the work prepared, they participated in drafting, revising, critically reviewing, and approving the final manuscript for publication.

REFERENCES

Alawieh, A., Langley, E. F., and Tomlinson, S. (2018). Targeted Complement Inhibition Salvages Stressed Neurons and Inhibits Neuroinflammation after Stroke in Mice. *Sci. Transl Med.* 10 (441). PubMed PMID: 29769288. doi:10.1126/scitranslmed.aao6459

Bar-Yosef, T., Damri, O., and Agam, G. (2019). Dual Role of Autophagy in Diseases of the Central Nervous System. *Front Cel Neurosci* 13, 196. PubMed PMID: 31191249. doi:10.3389/fncel.2019.00196

Barnabei, L., Laplantine, E., Mbongo, W., Rieux-Laucat, F., and Weil, R. (2021). NF-κB: At the Borders of Autoimmunity and Inflammation. *Front. Immunol.* 12, 716469. PubMed PMID: 34434197. doi:10.3389/fimmu.2021.716469

Battistelli, M., and Falcieri, E. (2020). Apoptotic Bodies: Particular Extracellular Vesicles Involved in Intercellular Communication. *Biology (Basel)* 9 (1). PubMed PMID: 31968627. doi:10.3390/biology9010021

Brinton, L. T., Sloane, H. S., Kester, M., and Kelly, K. A. (2015). Formation and Role of Exosomes in Cancer. *Cell Mol Life Sci* 72 (4), 659–671. PubMed PMID: 25336151. doi:10.1007/s00018-014-1764-3

Bu, X., Li, D., Wang, F., Sun, Q., and Zhang, Z. (2020). Protective Role of Astrocyte-Derived Exosomal microRNA-361 in Cerebral Ischemic-Reperfusion Injury by Regulating the AMPK/mTOR Signaling Pathway and Targeting CTSB. *Ndt* 16, 1863–1877. PubMed PMID: 32801720. doi:10.2147/ndt.S260748

Carmeliet, P., and Tessier-Lavigne, M. (2005). Common Mechanisms of Nerve and Blood Vessel Wiring. *Nature* 436 (7048), 193–200. PubMed PMID: 16015319. doi:10.1038/nature03875

Casella, G., Colombo, F., Finardi, A., Descamps, H., Ill-Raga, G., Spinelli, A., et al. (2018). Extracellular Vesicles Containing IL-4 Modulate Neuroinflammation in a Mouse Model of Multiple Sclerosis. *Mol. Ther.* 26 (9), 2107–2118. PubMed PMID: 30017878. doi:10.1016/j.ymthe.2018.06.024

Casella, G., Rasouli, J., Boehm, A., Zhang, W., Xiao, D., Ishikawa, L. L. W., et al. (2020). Oligodendrocyte-derived Extracellular Vesicles as Antigen-specific Therapy for Autoimmune Neuroinflammation in Mice. *Sci. Transl Med.* 12 (568). PubMed PMID: 33148622. doi:10.1126/scitranslmed.aba0599

Chen, W., Guo, C., Feng, H., and Chen, Y. (2020). Mitochondria: Novel Mechanisms and Therapeutic Targets for Secondary Brain Injury after Intracerebral Hemorrhage. *Front. Aging Neurosci.* 12, 615451. PubMed PMID: 33584246. doi:10.3389/fnagi.2020.615451

Chen, W., Wang, H., Zhu, Z., Feng, J., and Chen, L. (2020). Exosome-Shuttled circSHOC2 from IPASs Regulates Neuronal Autophagy and Ameliorates Ischemic Brain Injury *via* the miR-7670-3p/SIRT1 Axis. *Mol. Ther. Nucleic Acids* 22, 657–672. PubMed PMID: 33230464. doi:10.1016/j.omtn.2020.09.027

Chen, Y., Xia, K., Chen, L., and Fan, D. (2019). Increased Interleukin-6 Levels in the Astrocyte-Derived Exosomes of Sporadic Amyotrophic Lateral Sclerosis Patients. *Front. Neurosci.* 13, 574. PubMed PMID: 31231184. doi:10.3389/fnins.2019.00574

Chen, Z., Tang, H. B., Kang, J. J., Chen, Z. Y., Li, Y. L., Fan, Q. Y., et al. (2021). Necroptotic Astrocytes Induced Neuronal Apoptosis Partially through EVs-Derived Pro-BDNF. *Brain Res. Bull.* 177, 73–80. PubMed PMID: 34555432. doi:10.1016/j.brainresbull.2021.09.014

Cheng, Q., Shen, Y., Cheng, Z., Shao, Q., Wang, C., Sun, H., et al. (2019). Achyranthes Bidentata Polypeptide K Suppresses Neuroinflammation in BV2 Microglia through Nrf2-dependent Mechanism. *Ann. Transl Med.* 7 (20), 575. PubMed PMID: 31807556. doi:10.21037/atm.2019.09.07

Chiang, C. S., Fu, S. J., Hsu, C. L., Jeng, C. J., Tang, C. Y., Huang, Y. S., et al. (2021). Neuronal Exosomes Secreted under Oxygen-Glucose Deprivation/Reperfusion Presenting Differentially Expressed miRNAs and Affecting Neuronal Survival and Neurite Outgrowth. *Neuromolecular Med.* 23 (3), 404–415. PubMed PMID: 33389598. doi:10.1007/s12017-020-08641-z

Chun, C., Smith, A. S. T., Kim, H., Kamenz, D. S., Lee, J. H., Lee, J. B., et al. (2021). Astrocyte-derived Extracellular Vesicles Enhance the Survival and Electrophysiological Function of Human Cortical Neurons *In Vitro*. *Biomaterials* 271, 120700. PubMed PMID: 33631652. doi:10.1016/j.biomaterials.2021.120700

Cohen, R. I. (2005). Exploring Oligodendrocyte Guidance: 'to Boldly Go where No Cell Has Gone before'. *Cel Mol Life Sci* 62 (5), 505–510. PubMed PMID: 15747057. doi:10.1007/s00018-004-4485-1

Datta, A., Sarmah, D., Mounica, L., Kaur, H., Kesharwani, R., Verma, G., et al. (2020). Cell Death Pathways in Ischemic Stroke and Targeted Pharmacotherapy. *Transl Stroke Res.* 11 (6), 1185–1202. PubMed PMID: 32219729. doi:10.1007/s12975-020-00806-z

Datta Chaudhuri, A., Dasgheyb, R. M., DeVine, L. R., Bi, H., Cole, R. N., and Haughey, N. J. (2020). Stimulus-dependent Modifications in Astrocyte-Derived Extracellular Vesicle Cargo Regulate Neuronal Excitability. *Glia* 68 (1), 128–144. PubMed PMID: 31469478. doi:10.1002/glia.23708

DiSabato, D. J., Quan, N., and Godbout, J. P. (2016). Neuroinflammation: the Devil Is in the Details. *J. Neurochem.* 139 Suppl 2 (Suppl. 2), 136–153. PubMed PMID: 26990767. doi:10.1111/jnc.13607

Doyle, L. M., and Wang, M. Z. (2019). Overview of Extracellular Vesicles, Their Origin, Composition, Purpose, and Methods for Exosome Isolation and Analysis. *Cells* 8 (7). PubMed PMID: 31311206. doi:10.3390/cells8070727

Du, L., Jiang, Y., and Sun, Y. (2021). Astrocyte-derived Exosomes Carry microRNA-17-5p to Protect Neonatal Rats from Hypoxic-Ischemic Brain Damage *via* Inhibiting BNIP-2 Expression. *Neurotoxicology* 83, 28–39. PubMed PMID: 33309839. doi:10.1016/j.neuro.2020.12.006

Fakhoury, M. (2018). Microglia and Astrocytes in Alzheimer's Disease: Implications for Therapy. *Curr. Neuropharmacol* 16 (5), 508–518. PubMed PMID: 28730967. doi:10.2174/1570159x15666170720095240

Fan, J., Saft, M., Sadanandan, N., Gonzales-Portillo, B., Park, Y. J., Sanberg, P. R., et al. (2020). LncRNAs Stand as Potent Biomarkers and Therapeutic Targets for Stroke. *Front. Aging Neurosci.* 12, 594571. PubMed PMID: 33192490. doi:10.3389/fnagi.2020.594571

Fauré, J., Lachenal, G., Court, M., Hirrlinger, J., Chatellard-Causse, C., Blot, B., et al. (2006). Exosomes Are Released by Cultured Cortical Neurones. *Mol. Cel Neurosci* 31 (4), 642–648. PubMed PMID: 16446100. doi:10.1016/j.mcn.2005.12.003

Forrester, S. J., Kikuchi, D. S., Hernandes, M. S., Xu, Q., and Griendling, K. K. (2018). Reactive Oxygen Species in Metabolic and Inflammatory Signaling. *Circ. Res.* 122 (6), 877–902. PubMed PMID: 29700084. doi:10.1161/CIRCRESAHA.117.311401

Forró, T., Bajkó, Z., Bălașa, A., and Bălașa, R. (2021). Dysfunction of the Neurovascular Unit in Ischemic Stroke: Highlights on microRNAs and Exosomes as Potential Biomarkers and Therapy. *Ijms* 22 (11), 5621. PubMed PMID: 34070696. doi:10.3390/ijms22115621

Fröhlich, D., Kuo, W. P., Frühbeis, C., Sun, J.-J., Zehendner, C. M., Luhmann, H. J., et al. (2014). Multifaceted Effects of Oligodendroglial Exosomes on Neurons: Impact on Neuronal Firing Rate, Signal Transduction and Gene Regulation. *Phil. Trans. R. Soc. B* 369 (1652), 20130510. PubMed PMID: 25135971. doi:10.1098/rstb.2013.0510

Frühbeis, C., Fröhlich, D., Kuo, W. P., Amphornrat, J., Thilemann, S., Saab, A. S., et al. (2013). Neurotransmitter-triggered Transfer of Exosomes Mediates Oligodendrocyte-Neuron Communication. *Plos Biol.* 11 (7), e1001604. PubMed PMID: 23874151. doi:10.1371/journal.pbio.1001604

Frühbeis, C., Kuo-Elsner, W. P., Müller, C., Barth, K., Peris, L., Tenzer, S., et al. (2020). Oligodendrocytes Support Axonal Transport and Maintenance *via* Exosome Secretion. *Plos Biol.* 18 (12), e3000621. PubMed PMID: 33351792. doi:10.1371/journal.pbio.3000621

Gage, S. H., and Fish, P. A. (1924). Fat Digestion, Absorption, and Assimilation in Man and Animals as Determined by the Dark-Field Microscope, and a Fat-Soluble Dye. *Am. J. Anat.* 34 (1), 1–85. doi:10.1002/aja.1000340102

Gao, B., Zhou, S., Sun, C., Cheng, D., Zhang, Y., Li, X., et al. (2020). Brain Endothelial Cell-Derived Exosomes Induce Neuroplasticity in Rats with Ischemia/Reperfusion Injury. *ACS Chem. Neurosci.* 11 (15), 2201–2213. PubMed PMID: 32574032. doi:10.1021/acschemneuro.0c00089

Guitart, K., Loers, G., Buck, F., Bork, U., Schachner, M., and Kleene, R. (2016). Improvement of Neuronal Cell Survival by Astrocyte-Derived Exosomes under Hypoxic and Ischemic Conditions Depends on Prion Protein. *Glia* 64 (6), 896–910. PubMed PMID: 26992135. doi:10.1002/glia.22963

Guo, M., Wang, J., Zhao, Y., Feng, Y., Han, S., Dong, Q., et al. (2020). Microglial Exosomes Facilitate α-synuclein Transmission in Parkinson's Disease. *Brain* 143 (5), 1476–1497. PubMed PMID: 32355963. doi:10.1093/brain/awaa090

Guo, Y., Xie, Y., and Luo, Y. (2022). The Role of Long Non-coding RNAs in the Tumor Immune Microenvironment. *Front. Immunol.* 13, 851004. Epub 2022/03/01PubMed PMID: 35222443; PubMed Central PMCID: PMCPMC8863945. doi:10.3389/fimmu.2022.851004

Hatakeyama, M., Ninomiya, I., and Kanazawa, M. (2020). Angiogenesis and Neuronal Remodeling after Ischemic Stroke. *Neural Regen. Res.* 15 (1), 16–19. PubMed PMID: 31535636. doi:10.4103/1673-5374.264442

Hira, K., Ueno, Y., Tanaka, R., Miyamoto, N., Yamashiro, K., Inaba, T., et al. (2018). Astrocyte-Derived Exosomes Treated with a Semaphorin 3A Inhibitor Enhance Stroke Recovery *via* Prostaglandin D2 Synthase. *Stroke* 49 (10), 2483–2494. PubMed PMID: 30355116. doi:10.1161/strokeaha.118.021272

Hou, W., Hao, Y., Sun, L., Zhao, Y., Zheng, X., and Song, L. (2022). The Dual Roles of Autophagy and the GPCRs-Mediating Autophagy Signaling Pathway after Cerebral Ischemic Stroke. *Mol. Brain* 15 (1), 14. PubMed PMID: 35109896. doi:10.1186/s13041-022-00899-7

Huang, S., Ge, X., Yu, J., Han, Z., Yin, Z., Li, Y., et al. (2018). Increased miR-124-3p in Microglial Exosomes Following Traumatic Brain Injury Inhibits Neuronal Inflammation and Contributes to Neurite Outgrowth *via* Their Transfer into Neurons. *FASEB J.* 32 (1), 512–528. PubMed PMID: 28935818. doi:10.1096/fj.201700673R

Huang, Y., Liu, Z., Tan, F., Hu, Z., and Lu, M. (2020). Effects of the Insulted Neuronal Cells-Derived Extracellular Vesicles on the Survival of Umbilical Cord-Derived Mesenchymal Stem Cells Following Cerebral Ischemia/Reperfusion Injury. *Oxid Med. Cel Longev* 2020, 9768713. PubMed PMID: 32724498. doi:10.1155/2020/9768713

Iadecola, C., and Anrather, J. (2011). The Immunology of Stroke: from Mechanisms to Translation. *Nat. Med.* 17 (7), 796–808. PubMed PMID: 21738161. doi:10.1038/nm.2399

Jin, R., Yang, G., and Li, G. (2010). Inflammatory Mechanisms in Ischemic Stroke: Role of Inflammatory Cells. *J. Leukoc. Biol.* 87 (5), 779–789. PubMed PMID: 20130219. doi:10.1189/jlb.1109766

Kaddour, H., Tranquille, M., and Okeoma, C. M. (2021). The Past, the Present, and the Future of the Size Exclusion Chromatography in Extracellular Vesicles Separation. *Viruses* 13 (11). PubMed PMID: 34835078. doi:10.3390/v13112272

Lachenal, G., Pernet-Gallay, K., Chivet, M., Hemming, F. J., Belly, A., Bodon, G., et al. (2011). Release of Exosomes from Differentiated Neurons and its Regulation by Synaptic Glutamatergic Activity. *Mol. Cel Neurosci* 46 (2), 409–418. PubMed PMID: 21111824. doi:10.1016/j.mcn.2010.11.004

Li, C., Qin, T., Liu, Y., Wen, H., Zhao, J., Luo, Z., et al. (2021). Microglia-Derived Exosomal microRNA-151-3p Enhances Functional Healing after Spinal Cord Injury by Attenuating Neuronal Apoptosis *via* Regulating the p53/p21/CDK1 Signaling Pathway. *Front Cel Dev Biol* 9, 783017. PubMed PMID: 35127706. doi:10.3389/fcell.2021.783017

Li, D., Huang, S., Zhu, J., Hu, T., Han, Z., Zhang, S., et al. (2019). Exosomes from MiR-21-5p-Increased Neurons Play a Role in Neuroprotection by Suppressing Rab11a-Mediated Neuronal Autophagy *In Vitro* after Traumatic Brain Injury. *Med. Sci. Monit.* 25, 1871–1885. PubMed PMID: 30860987. doi:10.12659/msm.915727

Li, Z., Moniruzzaman, M., Dastgheyb, R. M., Yoo, S. W., Wang, M., Hao, H., et al. (2020). Astrocytes Deliver CK1 to Neurons *via* Extracellular Vesicles in Response to Inflammation Promoting the Translation and Amyloidogenic Processing of APP. *J. Extracell Vesicles* 10 (2), e12035. PubMed PMID: 33408815. doi:10.1002/jev2.12035

Li, Z., Song, Y., He, T., Wen, R., Li, Y., Chen, T., et al. (2021). M2 Microglial Small Extracellular Vesicles Reduce Glial Scar Formation *via* the miR-124/STAT3 Pathway after Ischemic Stroke in Mice. *Theranostics* 11 (3), 1232–1248. PubMed PMID: 33391532. doi:10.7150/thno.48761

Liu, J., Guo, Z. N., Yan, X. L., Huang, S., Ren, J. X., Luo, Y., et al. (2020). Crosstalk between Autophagy and Ferroptosis and its Putative Role in Ischemic Stroke. *Front. Cel Neurosci* 14, 577403. PubMed PMID: 33132849. doi:10.3389/fncel.2020.577403

Liu, X., Lv, X., Liu, Z., Zhang, M., and Leng, Y. (2021). MircoRNA-29a in Astrocyte-Derived Extracellular Vesicles Suppresses Brain Ischemia Reperfusion Injury *via* TP53INP1 and the NF-Kb/nlrp3 Axis. *Cell Mol Neurobiol*. PubMed PMID: 33620674. doi:10.1007/s10571-021-01040-3

Liu, Y., Li, Y. P., Xiao, L. M., Chen, L. K., Zheng, S. Y., Zeng, E. M., et al. (2021). Extracellular Vesicles Derived from M2 Microglia Reduce Ischemic Brain Injury through microRNA-135a-5p/TXNIP/NLRP3 axis. *Lab. Invest.* 101 (7), 837–850. PubMed PMID: 33875790. doi:10.1038/s41374-021-00545-1

Long, G., Ma, S., Shi, R., Sun, Y., Hu, Z., and Chen, K. (2022). Circular RNAs and Drug Resistance in Genitourinary Cancers: A Literature Review. *Cancers (Basel)* 14 (4). Epub 2022/02/26PubMed PMID: 35205613; PubMed Central PMCID: PMCPMC8869870. doi:10.3390/cancers14040866

Long, X., Yao, X., Jiang, Q., Yang, Y., He, X., Tian, W., et al. (2020). Astrocyte-derived Exosomes Enriched with miR-873a-5p Inhibit Neuroinflammation *via* Microglia Phenotype Modulation after Traumatic Brain Injury. *J. Neuroinflammation* 17 (1), 89. PubMed PMID: 32192523. doi:10.1186/s12974-020-01761-0

Ma, L., Niu, W., Lv, J., Jia, J., Zhu, M., and Yang, S. (2018). PGC-1α-Mediated Mitochondrial Biogenesis Is Involved in Cannabinoid Receptor 2 Agonist AM1241-Induced Microglial Phenotype Amelioration. *Cel Mol Neurobiol* 38 (8), 1529–1537. PubMed PMID: 30315387. doi:10.1007/s10571-018-0628-z

Ma, Y., Yang, S., He, Q., Zhang, D., and Chang, J. (2021). The Role of Immune Cells in Post-Stroke Angiogenesis and Neuronal Remodeling: The Known and the Unknown. *Front. Immunol.* 12, 784098. PubMed PMID: 34975872. doi:10.3389/fimmu.2021.784098

Marzan, A. L., Nedeva, C., and Mathivanan, S. (2021). Extracellular Vesicles in Metabolism and Metabolic Diseases. *Subcell Biochem.* 97, 393–410. PubMed PMID: 33779925. doi:10.1007/978-3-030-67171-6_15

Marzan, A. L., and Stewart, S. E. (2021). Elucidating the Role of Extracellular Vesicles in Pancreatic Cancer. *Cancers (Basel)* 13 (22). PubMed PMID: 34830825. doi:10.3390/cancers13225669

Mo, Y., Sun, Y. Y., and Liu, K. Y. (2020). Autophagy and Inflammation in Ischemic Stroke. *Neural Regen. Res.* 15 (8), 1388–1396. PubMed PMID: 31997797. doi:10.4103/1673-5374.274331

Möller, A., and Lobb, R. J. (2020). The Evolving Translational Potential of Small Extracellular Vesicles in Cancer. *Nat. Rev. Cancer* 20 (12), 697–709. PubMed PMID: 32958932. doi:10.1038/s41568-020-00299-w

Nagelkerke, A., Ojansivu, M., van der Koog, L., Whittaker, T. E., Cunnane, E. M., Silva, A. M., et al. (2021). Extracellular Vesicles for Tissue Repair and Regeneration: Evidence, Challenges and Opportunities. *Adv. Drug Deliv. Rev.* 175, 113775. PubMed PMID: 33872693. doi:10.1016/j.addr.2021.04.013

Navabi, A., Akbari, B., Abdalsamadi, M., and Naseri, S. (2022). The Role of microRNAs in the Development, Progression and Drug Resistance of Chronic Myeloid Leukemia and Their Potential Clinical Significance. *Life Sci.* 296, 120437. Epub 2022/03/02PubMed PMID: 35231484. doi:10.1016/j.lfs.2022.120437

Nogueras-Ortiz, C. J., Mahairaki, V., Delgado-Peraza, F., Das, D., Avgerinos, K., Eren, E., et al. (2020). Astrocyte- and Neuron-Derived Extracellular Vesicles from Alzheimer's Disease Patients Effect Complement-Mediated Neurotoxicity. *Cells* 9 (7). PubMed PMID: 32635578. doi:10.3390/cells9071618

Norris, G. T., Smirnov, I., Filiano, A. J., Shadowen, H. M., Cody, K. R., Thompson, J. A., et al. (2018). Neuronal Integrity and Complement Control Synaptic Material Clearance by Microglia after CNS Injury. *J. Exp. Med.* 215 (7), 1789–1801. PubMed PMID: 29941548. doi:10.1084/jem.20172244

Palviainen, M., Saari, H., Kärkkäinen, O., Pekkinen, J., Auriola, S., Yliperttula, M., et al. (2019). Metabolic Signature of Extracellular Vesicles Depends on the Cell Culture Conditions. *J. Extracell Vesicles* 8 (1), 1596669. PubMed PMID: 31007875. doi:10.1080/20013078.2019.1596669

Pan, Y., Jiao, Q., Wei, W., Zheng, T., Yang, X., and Xin, W. (2021). Emerging Role of LncRNAs in Ischemic Stroke-Novel Insights into the Regulation of Inflammation. *J. Inflamm. Res.* 14, 4467–4483. PubMed PMID: 34522116. doi:10.2147/jir.S327291

Pei, X., Li, Y., Zhu, L., and Zhou, Z. (2019). Astrocyte-derived Exosomes Suppress Autophagy and Ameliorate Neuronal Damage in Experimental Ischemic Stroke. *Exp. Cel Res* 382 (2), 111474. PubMed PMID: 31229506. doi:10.1016/j.yexcr.2019.06.019

Pei, X., Li, Y., Zhu, L., and Zhou, Z. (2020). Astrocyte-derived Exosomes Transfer miR-190b to Inhibit Oxygen and Glucose Deprivation-Induced Autophagy and Neuronal Apoptosis. *Cell Cycle* 19 (8), 906–917. PubMed PMID: 32150490. doi:10.1080/15384101.2020.1731649

Peker, N., and Gozuacik, D. (2020). Autophagy as a Cellular Stress Response Mechanism in the Nervous System. *J. Mol. Biol.* 432 (8), 2560–2588. PubMed PMID: 31962122. doi:10.1016/j.jmb.2020.01.017

Pluvinage, J. V., Haney, M. S., Smith, B. A. H., Sun, J., Iram, T., Bonanno, L., et al. (2019). CD22 Blockade Restores Homeostatic Microglial Phagocytosis in Ageing Brains. *Nature* 568 (7751), 187–192. PubMed PMID: 30944478. doi:10.1038/s41586-019-1088-4

Potjewyd, G., Moxon, S., Wang, T., Domingos, M., and Hooper, N. M. (2018). Tissue Engineering 3D Neurovascular Units: A Biomaterials and Bioprinting Perspective. *Trends Biotechnol.* 36 (4), 457–472. PubMed PMID: 29422410. doi:10.1016/j.tibtech.2018.01.003

Qi, D., Hou, X., Jin, C., Chen, X., Pan, C., Fu, H., et al. (2021). HNSC Exosome-Derived MIAT Improves Cognitive Disorders in Rats with Vascular Dementia *via* the miR-34b-5p/CALB1 axis. *Am. J. Transl Res.* 13 (9), 10075–10093. PubMed PMID: 34650682.

Radak, D., Katsiki, N., Resanovic, I., Jovanovic, A., Sudar-Milovanovic, E., Zafirovic, S., et al. (2017). Apoptosis and Acute Brain Ischemia in Ischemic Stroke. *Curr. Vasc. Pharmacol.* 15 (2), 115–122. PubMed PMID: 27823556. doi:10.2174/1570161115666161104095522

Raffaele, S., Gelosa, P., Bonfanti, E., Lombardi, M., Castiglioni, L., Cimino, M., et al. (2021). Microglial Vesicles Improve post-stroke Recovery by Preventing Immune Cell Senescence and Favoring Oligodendrogenesis. *Mol. Ther.* 29 (4), 1439–1458. PubMed PMID: 33309882. doi:10.1016/j.ymthe.2020.12.009

Rodríguez, D. A., and Vader, P. (2022). Extracellular Vesicle-Based Hybrid Systems for Advanced Drug Delivery. *Pharmaceutics* 14 (2), 267. PubMed PMID: 35214000. doi:10.3390/pharmaceutics14020267

Roefs, M. T., Sluijter, J. P. G., and Vader, P. (2020). Extracellular Vesicle-Associated Proteins in Tissue Repair. *Trends Cel Biol* 30 (12), 990–1013. PubMed PMID: 33069512. doi:10.1016/j.tcb.2020.09.009

Rojas, C., Barnaeva, E., Thomas, A. G., Hu, X., Southall, N., Marugan, J., et al. (2018). DPTIP, a Newly Identified Potent Brain Penetrant Neutral Sphingomyelinase 2 Inhibitor, Regulates Astrocyte-Peripheral Immune Communication Following Brain Inflammation. *Sci. Rep.* 8 (1), 17715. PubMed PMID: 30531925. doi:10.1038/s41598-018-36144-2

Ruan, L., Wang, B., ZhuGe, Q., and Jin, K. (2015). Coupling of Neurogenesis and Angiogenesis after Ischemic Stroke. *Brain Res.* 1623, 166–173. PubMed PMID: 25736182. doi:10.1016/j.brainres.2015.02.042

Saltarella, I., Lamanuzzi, A., Apollonio, B., Desantis, V., Bartoli, G., Vacca, A., et al. (2021). Role of Extracellular Vesicle-Based Cell-To-Cell Communication in Multiple Myeloma Progression. *Cells* 10 (11). PubMed PMID: 34831408. doi:10.3390/cells10113185

Salucci, S., Bartoletti Stella, A., Battistelli, M., Burattini, S., Bavelloni, A., Cocco, L. I., et al. (2021). How Inflammation Pathways Contribute to Cell Death in Neuro-Muscular Disorders. *Biomolecules* 11 (8). PubMed PMID: 34439778. doi:10.3390/biom11081109

Sierra, A., Abiega, O., Shahraz, A., and Neumann, H. (2013). Janus-faced Microglia: Beneficial and Detrimental Consequences of Microglial Phagocytosis. *Front. Cel Neurosci* 7, 6. PubMed PMID: 23386811. doi:10.3389/fncel.2013.00006

Smith, A. J., Sompel, K. M., Elango, A., and Tennis, M. A. (2021). Non-Coding RNA and Frizzled Receptors in Cancer. *Front. Mol. Biosci.* 8, 712546. Epub 2021/10/22PubMed PMID: 34671643; PubMed Central PMCID: PMCPMC8521042. doi:10.3389/fmolb.2021.712546

Song, H., Zhang, X., Chen, R., Miao, J., Wang, L., Cui, L., et al. (2019). Cortical Neuron-Derived Exosomal MicroRNA-181c-3p Inhibits Neuroinflammation by Downregulating CXCL1 in Astrocytes of a Rat Model with Ischemic Brain Injury. *Neuroimmunomodulation* 26 (5), 217–233. PubMed PMID: 31665717. doi:10.1159/000502694

Song, Y., Li, Z., He, T., Qu, M., Jiang, L., Li, W., et al. (2019). M2 Microglia-Derived Exosomes Protect the Mouse Brain from Ischemia-Reperfusion Injury *via* Exosomal miR-124. *Theranostics* 9 (10), 2910–2923. PubMed PMID: 31244932. doi:10.7150/thno.30879

Sun, Y., Zhu, Y., Zhong, X., Chen, X., Wang, J., and Ying, G. (2018). Crosstalk between Autophagy and Cerebral Ischemia. *Front. Neurosci.* 12, 1022. PubMed PMID: 30692904. doi:10.3389/fnins.2018.01022

Tahir, W., Thapa, S., and Schatzl, H. M. (2022). Astrocyte in Prion Disease: a Double-Edged Sword. *Neural Regen. Res.* 17 (8), 1659–1665. PubMed PMID: 35017412. doi:10.4103/1673-5374.332202

Tallon, C., Picciolini, S., Yoo, S. W., Thomas, A. G., Pal, A., Alt, J., et al. (2021). Inhibition of Neutral Sphingomyelinase 2 Reduces Extracellular Vesicle Release from Neurons, Oligodendrocytes, and Activated Microglial Cells Following Acute Brain Injury. *Biochem. Pharmacol.* 194, 114796. PubMed PMID: 34678224. doi:10.1016/j.bcp.2021.114796

Tang, Y., and Le, W. (2016). Differential Roles of M1 and M2 Microglia in Neurodegenerative Diseases. *Mol. Neurobiol.* 53 (2), 1181–1194. PubMed PMID: 25598354. doi:10.1007/s12035-014-9070-5

Théry, C., Ostrowski, M., and Segura, E. (2009). Membrane Vesicles as Conveyors of Immune Responses. *Nat. Rev. Immunol.* 9 (8), 581–593. PubMed PMID: 19498381. doi:10.1038/nri2567

Thietart, S., and Rautou, P. E. (2020). Extracellular Vesicles as Biomarkers in Liver Diseases: A Clinician's point of View. *J. Hepatol.* 73 (6), 1507–1525. PubMed PMID: 32682050. doi:10.1016/j.jhep.2020.07.014

Tian, Y., Zhu, P., Liu, S., Jin, Z., Li, D., Zhao, H., et al. (2019). IL-4-polarized BV2 Microglia Cells Promote Angiogenesis by Secreting Exosomes. *Adv. Clin. Exp. Med.* 28 (4), 421–430. PubMed PMID: 30684318. doi:10.17219/acem/91826

van Niel, G., D'Angelo, G., and Raposo, G. (2018). Shedding Light on the Cell Biology of Extracellular Vesicles. *Nat. Rev. Mol. Cel Biol* 19 (4), 213–228. PubMed PMID: 29339798. doi:10.1038/nrm.2017.125

Wang, P., Shao, B. Z., Deng, Z., Chen, S., Yue, Z., and Miao, C. Y. (2018). Autophagy in Ischemic Stroke. *Prog. Neurobiol.* 163-164, 98–117. PubMed PMID: 29331396. doi:10.1016/j.pneurobio.2018.01.001

Wu, W., Liu, J., Yang, C., Xu, Z., Huang, J., and Lin, J. (2020). Astrocyte-derived Exosome-Transported microRNA-34c Is Neuroprotective against Cerebral Ischemia/reperfusion Injury *via* TLR7 and the NF-Kb/MAPK Pathways. *Brain Res. Bull.* 163, 84–94. PubMed PMID: 32682816. doi:10.1016/j.brainresbull.2020.07.013

Xie, L., Zhao, H., Wang, Y., and Chen, Z. (2020). Exosomal Shuttled miR-424-5p from Ischemic Preconditioned Microglia Mediates Cerebral Endothelial Cell Injury through Negatively Regulation of FGF2/STAT3 Pathway. *Exp. Neurol.* 333, 113411. PubMed PMID: 32707150. doi:10.1016/j.expneurol.2020.113411

Xin, H., Wang, F., Li, Y., Lu, Q. E., Cheung, W. L., Zhang, Y., et al. (2017). Secondary Release of Exosomes from Astrocytes Contributes to the Increase in Neural Plasticity and Improvement of Functional Recovery after Stroke in Rats Treated with Exosomes Harvested from MicroRNA 133b-Overexpressing Multipotent Mesenchymal Stromal Cells. *Cel Transpl.* 26 (2), 243–257. PubMed PMID: 27677799. doi:10.3727/096368916x693031

Xin, W. Q., Wei, W., Pan, Y. L., Cui, B. L., Yang, X. Y., Bähr, M., et al. (2021). Modulating Poststroke Inflammatory Mechanisms: Novel Aspects of Mesenchymal Stem Cells, Extracellular Vesicles and Microglia. *World J. Stem Cell* 13 (8), 1030–1048. PubMed PMID: 34567423. doi:10.4252/wjsc.v13.i8.1030

Xu, B., Zhang, Y., Du, X. F., Li, J., Zi, H. X., Bu, J. W., et al. (2017). Neurons Secrete miR-132-Containing Exosomes to Regulate Brain Vascular Integrity. *Cell Res* 27 (7), 882–897. PubMed PMID: 28429770. doi:10.1038/cr.2017.62

Xu, J., Camfield, R., and Gorski, S. M. (2018). The Interplay between Exosomes and Autophagy - Partners in Crime. *J. Cel Sci* 131 (15), jcs215210. doi:10.1242/jcs.215210

Xu, L., Cao, H., Xie, Y., Zhang, Y., Du, M., Xu, X., et al. (2019). Exosome-shuttled miR-92b-3p from Ischemic Preconditioned Astrocytes Protects Neurons against Oxygen and Glucose Deprivation. *Brain Res.* 1717, 66–73. PubMed PMID: 30986407. doi:10.1016/j.brainres.2019.04.009

Xu, Q., Zhao, B., Ye, Y., Li, Y., Zhang, Y., Xiong, X., et al. (2021). Relevant Mediators Involved in and Therapies Targeting the Inflammatory Response Induced by Activation of the NLRP3 Inflammasome in Ischemic Stroke. *J. Neuroinflammation* 18 (1), 123. Epub 2021/06/02PubMed PMID: 34059091; PubMed Central PMCID: PMCPMC8166383. doi:10.1186/s12974-021-02137-8

Yang, D., Zhang, W., Zhang, H., Zhang, F., Chen, L., Ma, L., et al. (2020). Progress, Opportunity, and Perspective on Exosome Isolation - Efforts for Efficient Exosome-Based Theranostics. *Theranostics* 10 (8), 3684–3707. PubMed PMID: 32206116. doi:10.7150/thno.41580

Yang, J., Cao, L.-L., Wang, X.-P., Guo, W., Guo, R.-B., Sun, Y.-Q., et al. (2021). Neuronal Extracellular Vesicle Derived miR-98 Prevents Salvageable Neurons from Microglial Phagocytosis in Acute Ischemic Stroke. *Cell Death Dis* 12 (1), 23. PubMed PMID: 33414461. doi:10.1038/s41419-020-03310-2

Yang, M., Weng, T., Zhang, W., Zhang, M., He, X., Han, C., et al. (2021). The Roles of Non-coding RNA in the Development and Regeneration of Hair Follicles: Current Status and Further Perspectives. *Front. Cel Dev Biol* 9, 720879. Epub 2021/10/29PubMed PMID: 34708037; PubMed Central PMCID: PMCPMC8542792. doi:10.3389/fcell.2021.720879

Yang, Y., Boza-Serrano, A., Dunning, C. J. R., Clausen, B. H., Lambertsen, K. L., and Deierborg, T. (2018). Inflammation Leads to Distinct Populations of Extracellular Vesicles from Microglia. *J. Neuroinflammation* 15 (1), 168. PubMed PMID: 29807527. doi:10.1186/s12974-018-1204-7

Zang, J., Wu, Y., Su, X., Zhang, T., Tang, X., Ma, D., et al. (2020). Inhibition of PDE1-B by Vinpocetine Regulates Microglial Exosomes and Polarization through Enhancing Autophagic Flux for Neuroprotection against Ischemic Stroke. *Front. Cel Dev Biol* 8, 616590. PubMed PMID: 33614626. doi:10.3389/fcell.2020.616590

Zhang, D., Cai, G., Liu, K., Zhuang, Z., Jia, K., Pei, S., et al. (2021). Microglia Exosomal miRNA-137 Attenuates Ischemic Brain Injury through Targeting Notch1. *Aging (Albany NY)* 13 (3), 4079–4095. PubMed PMID: 33461167. doi:10.18632/aging.202373

Zhang, L., Zhang, J., and You, Z. (2018). Switching of the Microglial Activation Phenotype Is a Possible Treatment for Depression Disorder. *Front. Cel Neurosci* 12, 306. PubMed PMID: 30459555. doi:10.3389/fncel.2018.00306

Zhang, L., Wei, W., Ai, X., Kilic, E., Hermann, D. M., Venkataramani, V., et al. (2021). Extracellular Vesicles from Hypoxia-Preconditioned Microglia Promote Angiogenesis and Repress Apoptosis in Stroke Mice *via* the TGF-β/Smad2/3 Pathway. *Cel Death Dis* 12 (11), 1068. PubMed PMID: 34753919. doi:10.1038/s41419-021-04363-7

Zhang, Y., Xu, C., Nan, Y., and Nan, S. (2020). Microglia-Derived Extracellular Vesicles Carrying miR-711 Alleviate Neurodegeneration in a Murine Alzheimer's Disease Model by Binding to Itpkb. *Front. Cel Dev Biol* 8, 566530. PubMed PMID: 33240878. doi:10.3389/fcell.2020.566530

Conflict of Interest: The authors declare that the research was conducted in the absence of any commercial or financial relationships that could be construed as a potential conflict of interest.

Publisher's Note: All claims expressed in this article are solely those of the authors and do not necessarily represent those of their affiliated organizations, or those of the publisher, the editors and the reviewers. Any product that may be evaluated in this article, or claim that may be made by its manufacturer, is not guaranteed or endorsed by the publisher.

frontiers | Frontiers in Pharmacology

ORIGINAL RESEARCH
published: 26 April 2022
doi: 10.3389/fphar.2022.851746

Magnetic Resonance Imaging Investigation of Neuroplasticity After Ischemic Stroke in Tetramethylpyrazine-Treated Rats

*Xue-Feng Feng[1,2], Jian-Feng Lei[3], Man-Zhong Li[1,2], Yu Zhan[1,2], Le Yang[1,2], Yun Lu[1,2], Ming-Cong Li[1,2], Yu-Ming Zhuang[1,2], Lei Wang[1,2] and Hui Zhao[1,2]**

[1]School of Traditional Chinese Medicine, Capital Medical University, Beijing, China, [2]Beijing Key Lab of TCM Collateral Disease Theory Research, Beijing, China, [3]Medical Imaging Laboratory of Core Facility Center, Capital Medical University, Beijing, China

OPEN ACCESS

Edited by:
Li-Nan Zhang,
Hebei Medical University, China

Reviewed by:
Yu-Chieh Jill Kao,
National Yang-Ming University, Taiwan
Junxiang Yin,
Barrow Neurological Institute (BNI),
United States

***Correspondence:**
Hui Zhao
zhaohuishouyi@ccmu.edu.cn

Specialty section:
This article was submitted to Neuropharmacology, a section of the journal Frontiers in Pharmacology

Received: 10 January 2022
Accepted: 24 March 2022
Published: 26 April 2022

Citation:
Feng X-F, Lei J-F, Li M-Z, Zhan Y, Yang L, Lu Y, Li M-C, Zhuang Y-M, Wang L and Zhao H (2022) Magnetic Resonance Imaging Investigation of Neuroplasticity After Ischemic Stroke in Tetramethylpyrazine-Treated Rats. Front. Pharmacol. 13:851746. doi: 10.3389/fphar.2022.851746

Ischemic stroke elicits white matter injury typically signed by axonal disintegration and demyelination; thus, the development of white matter reorganization is needed. 2,3,5,6-Tetramethylpyrazine (TMP) is widely used to treat ischemic stroke. This study was aimed to investigate whether TMP could protect the white matter and promote axonal repair after cerebral ischemia. Male Sprague–Dawley rats were subjected to permanent middle cerebral artery occlusion (MCAO) and treated with TMP (10, 20, 40 mg/kg) intraperitoneally for 14 days. The motor function related to gait was evaluated by the gait analysis system. Multiparametric magnetic resonance imaging (MRI) was conducted to noninvasively identify gray-white matter structural integrity, axonal reorganization, and cerebral blood flow (CBF), followed by histological analysis. The expressions of axonal growth-associated protein 43 (GAP-43), synaptophysin (SYN), axonal growth-inhibitory signals, and guidance factors were measured by Western blot. Our results showed TMP reduced infarct volume, relieved gray-white matter damage, promoted axonal remodeling, and restored CBF along the peri-infarct cortex, external capsule, and internal capsule. These MRI findings were confirmed by histopathological data. Moreover, motor function, especially gait impairment, was improved by TMP treatment. Notably, TMP upregulated GAP-43 and SYN and enhanced axonal guidance cues such as Netrin-1/DCC and Slit-2/Robo-1 but downregulated intrinsic growth-inhibitory signals NogoA/NgR/RhoA/ROCK-2. Taken together, our data indicated that TMP facilitated poststroke axonal remodeling and motor functional recovery. Moreover, our findings suggested that TMP restored local CBF, augmented guidance cues, and restrained intrinsic growth-inhibitory signals, all of which might improve the intracerebral microenvironment of ischemic areas and then benefit white matter remodeling.

Keywords: tetramethylpyrazine, ischemic stroke, axonal remodeling, synaptic plasticity, white matter reorganization

INTRODUCTION

Ischemic stroke is a grave cause of long-term neurological deficits globally (Chen et al., 2014). Currently, the tissue plasminogen activator (tPA) is the only FDA-approved therapy for ischemic stroke (Hughes et al., 2021), and mechanical thrombectomy has the superiority in treating acute ischemic stroke (Flottmann et al., 2018). Despite stroke mortality being declined with effective thrombolysis in the acute window (4.5 h) after the onset of ischemic stroke, most patients show significant disabilities. An increasing amount of evidence shows that ischemia results in not only mere neuronal loss but also white matter injury signed with axonal disintegration and demyelination, which is correlated with the severity of neurological deficit (Wang et al., 2016). Therefore, neurorestorative treatments for poststroke white matter reorganization and functional recovery are urgently required.

TMP has been extensively used for cardiovascular and cerebrovascular diseases (Chun-sheng et al., 1978; Guo et al., 1983; Zhao et al., 2016). The pharmacokinetics of TMP revealed that the mean residence time (MRT) of TMP administered intravenously in healthy rat blood and brain tissues are 84.0 and 98.2 min respectively, while the MRT of TMP administered intragastrically are 58.9 and 72.9 min, respectively (Wang et al., 2012). Clinical studies demonstrated TMP treatment strengthened survivability, improved neurological functions, and reduced recurrence in stroke patients (Ni et al., 2013).In addition, TMP could reduce cerebral infarct volume, relieve neuronal injury, and protect the blood–brain barrier in stroke models (Tan et al., 2015; Gong et al., 2019). However, whether TMP could protect the structural integrity of white matter, promote axonal remodeling, and expedite long-term functional recovery related to gait is unknown. In this study, we applied MRI technologies combined with histological analysis to explore the potential effectivity of TMP on white matter remodeling, especially axonal reorganization, and evaluated the effect of TMP on gait function by using DigiGait automated gait analysis in the subacute phase of permanent MCAO rats.

Ample evidence has shown that the intrinsic axonal growth-associated signals play a substantial role in axonal regeneration. GAP-43 participates in regulating axonal elongation, and SYN is beneficial to axonal sprouting and synaptogenesis (Chung et al., 2020; Jing et al., 2020). In particular, the coordinated action of attractive and repulsive extracellular axonal guidance molecules, including Netrins and DCC, Slit-2, and Robo-1, is important for neurite growth and guidance (Chen et al., 2020; Cuesta et al., 2020). In addition to neurite growth and guidance, axonal regeneration could be constrained by neurite growth inhibitors. NogoA binding with NgR by initiating the downstream RhoA/ROCK-2 inhibits axonal regeneration and results in growth cone collapse (Wang et al., 2020). Strategies stimulating axonal growth-promoting factors and suppressing growth-inhibiting signals may greatly improve axonal extension and neurological outcomes (Lu et al., 2021). Therefore, in the present study, we examined the expressions of these intrinsic axonal growth-related proteins to gain an insight into the white matter repair mechanisms underlying TMP treatment.

MATERIALS AND METHODS

Animals and Drugs

A total of 76 adult male Sprague–Dawley rats were purchased from Vital River Laboratory Animal Technology Co., Ltd. (Beijing, China) weighing 300–320 g (aged 8 weeks) and were maintained at a specific pathogen-free (SPF) animal research center in Capital Medical University (SYXK [jing] 2018-0003). Animal care and experimental protocols were performed in accordance with the guidelines set by the National Institute of Health Guide for the Care and Use of Laboratory Animals and approved by the Capital Medical University Animal Ethics Committee (Permit Number: AEEI-2018-052).

TMP hydrochloride injection (HPLC >98%) was purchased from Harbin Medisan Pharmaceutical Co., Ltd., (Lot No. 090923A, Harbin, Heilongjiang, China).

Ischemic Model and Experimental Groups

Focal cerebral ischemia was induced by permanent intraluminal occlusion of the right middle cerebral artery (MCA), according to a previously described method (Laing et al., 1993). The rats were anesthetized with isoflurane (5% for induction and 2% for maintenance) during the surgery. In brief, a right paramidline incision was made to separate the right external carotid artery (ECA) and internal carotid artery (ICA). A small incision was made at the ECA, and a nylon suture (Beijing Sunbio Biotech Co. Ltd., Beijing, China) was inserted into the stump of the ECA. The suture was tightened, and the nylon suture was pushed into the ICA for around 1.8–1.9 cm until a mild sense of resistance was felt to block the origin of the MCA. The rats with successful MCAO showing circling or walking to the contralateral side were included in this experiment (Yu et al., 2013).

Two rats died during MCAO surgery, and four rats that exhibited no obvious neurological symptoms were eliminated from the study. Therefore, 60 MCAO rats were randomly divided into the model group (n = 18), TMP 40 mg/kg group (n = 14), TMP 20 mg/kg (n = 14) group, and TMP 10 mg/kg group (n = 14) by experimenters blinded to the treatment conditions. There were no group differences in neurological deficit scores and body weight before treatment. Another 10 sham-operated rats were grouped into the sham group. TMP dissolved in saline was intraperitoneally injected to rats 4 h after MCAO and once daily for 14 days. The rats in the sham and model groups were injected with the same volume of saline (1 ml/kg/day). The rats from the model group (n = 12), TMP 40 mg/kg group (n = 12), TMP 20 mg/kg group (n = 11), TMP 10 mg/kg group (n = 11), and all the sham-operated rats were able to survive.

Rat Gait Analysis

Gait assessment was carried out on day 14 after MCAO using the DigiGait Imaging and Analysis 15.0 system (Mouse Specifics, Inc., Boston, United States) (Hampton et al., 2004). In brief, rats (n = 10 per group) were trained to walk as the speed was gradually increased to 15 cm/s. A high-speed video camera mounted below captured four paws and their positions relative to the belt, and

qualified videos contained at least three successive footprints (Feng et al., 2019).

Gait parameters were summarized as follows: steps (the number of steps in a stride cycle), cadence (the number of steps taken per second) (Parkkinen et al., 2013), hindlimb shared stance time (the time in contact with the belt with hindlimbs), stride length (the distance between two successive initial postures during the maximal contact), paw area (the maximal paw area in contact with the belt), and ataxia coefficient (Caballero-Garrido et al., 2017). Gait detection and data analysis were conducted by two experimenters blinded to the group assignment.

MRI Acquisition and Analysis

MRI measurements were performed with a 7.0 T MRI scanner (Bruker, PharmaScan, Germany) on the 15th day after TMP intervention (n = 6 per group). The rats were anesthetized (5% isoflurane for induction and 2% isoflurane for maintenance) with an anesthesia system (JD Medical Dist. Co. Inc., United States). MRI images were reconstructed by Paravision version 5.1 software (Bruker, PharmaScan, Germany).

T2-weighted imaging (T2WI) was conducted with a fast spin-echo pulse sequence with the following parameters: repetition time (TR) = 4,400 ms, echo time (TE) = 45 ms, field of view (FOV) = 3 × 3 cm^2 ,and matrix size (MS) = 256 × 256 (Li M Z et al., 2019). Infarct regions were defined by the areas with hyperintensity on T2 images (Chan et al., 2009). The infarct volume was calculated as the summation of infarct areas by the slice thickness (0.7 mm) by ImageJ software (Liu et al., 2011). Similarly, the volumes of bilateral hemispheres and ventricles were calculated. The ipsilateral residual tissue volume was equal to subtracting the infarct and ventricular volumes from the hemisphere volume (Li M et al., 2018).

T2 relaxometry mapping was used to analyze tissue lesions with a multislice multiecho sequence with the following parameters: TR = 2,500 ms, TEs from 11 to 176 ms, FOV = 3.3 × 3.3 cm^2, and MS = 256 × 256 (Zhang et al., 2016). Regions of interest (ROIs) were manually delineated in the bilateral peri-infarct cortex, external capsule, internal capsule, motor cortex, and somatosensory cortex, following a rat atlas (Schober, 1986). T2 values of ROIs were obtained on coronal T2 relaxometry maps by Paravision version 5.1 software. The relative T2 (rT2) was calculated as the ipsilateral T2 value relative to the contralateral T2 value.

Diffusion tensor imaging (DTI) was conducted to detect the microstructural changes with an axial single-shot spin echo-planar imaging sequence with the following parameters: TR/TE = 6,300/25 ms, 30 diffusion encoding directions, and b values = 0, 1,000 s/mm^2 (Zhang et al., 2016). The images of fractional anisotropy (FA), apparent diffusion coefficient (ADC), axial diffusivity (AD), and radial diffusivity (RD) were reconstructed with Paravision version 5.1 software. ROIs were delineated in the bilateral peri-infarct cortex, external capsule, and internal capsule on DTI parametric maps to obtain DTI values (Schober, 1986). Diffusion tensor tractography (DTT) was reconstructed with DSI studio and Diffusion Toolkit software to determine the orientation and integrity of nerve fibers (Liu et al., 2011). The mean fiber length and density of the external capsule and internal capsule were measured (Li M. Z et al., 2018). Data were presented as the ratio of ipsilateral values relative to contralateral values (Guo et al., 2011).

Arterial spin labeling (ASL) was performed to quantify the CBF with an echo-planar imaging fluid-attenuated inversion recovery sequence with the following parameters: TR/TE = 18,000/25 ms, FOV = 3.0 × 3.0 cm^2, matrix size = 128 × 128, and number of excitations = 1. ASL raw data and CBF maps were obtained by Paravision version 5.1 software. The CBF values (mL/100 g/min) of the bilateral peri-infarct cortex, external capsule, and internal capsule were acquired based on our previous method (Zhang et al., 2016; Zhang et al., 2019). The relative CBF (rCBF) was the ratio of the ipsilateral CBF to the contralateral CBF.

Tissue Examination

After MRI scanning, rats were anesthetized for histologic evaluation and ultrastructural detection. The brains of rats were processed as previously described (Zhan et al., 2020). Hematoxylin and eosin (HE) staining was performed to identify the pathological injury of brain tissues (n = 4 per group). The number of nerve cells was measured from three non-overlapping microscopic regions randomly selected in the peri-infarct cortex, according to the previously described method (Li M Z et al., 2019). Data were presented by the average number of cells per mm^2.

Luxol fast blue (LFB) staining was carried out to observe myelinated axon damage (Patro et al., 2019) (n = 4 per group). Three microscopic fields were randomly sampled from the bilateral external capsule and internal capsule. The integrated optical density (IOD) in LFB staining was analyzed with the NIS-Elements Basic Research Image Collection Analysis system (Nikon, Japan). Data were expressed as the ratio of the ipsilateral IOD to the contralateral IOD (Li M Z et al., 2019).

Transmission Electron Microscope Analysis

The ultrastructural changes in axons and synapses in the peri-ischemic cortex were examined with H7700TEM (Hitachi, Tokyo, Japan) (n = 2 per group). In order to evaluate the documentation and arrangement of axonal remyelination, an average of 43 images of axons were captured from each group, and G-ratio (axonal diameter/total fiber diameter) was analyzed (Ramadan et al., 2017). In addition, the synaptic plasticity was analyzed with an average of 20 synapses per group. The number of vesicles in presynaptic membranes was counted, and ultrastructural synaptic junctions including the presynaptic membrane length, synaptic cleft width, postsynaptic density (PSD) thickness, and postsynaptic membrane curvature were analyzed, as described previously (Xu et al., 2009).

Furthermore, the damage degree of mitochondria in axons and synapses was scored, according to the evaluation standard: grade 0, normal structure with intact mitochondrial matrix granules; grade 1, absent mitochondrial matrix granules; grade 2, swollen mitochondria and transparent matrix; grade 3, the disintegrating structure of mitochondrial cristae; and grade 4, destructive bilayer membranes of mitochondria (Hou et al., 2016).

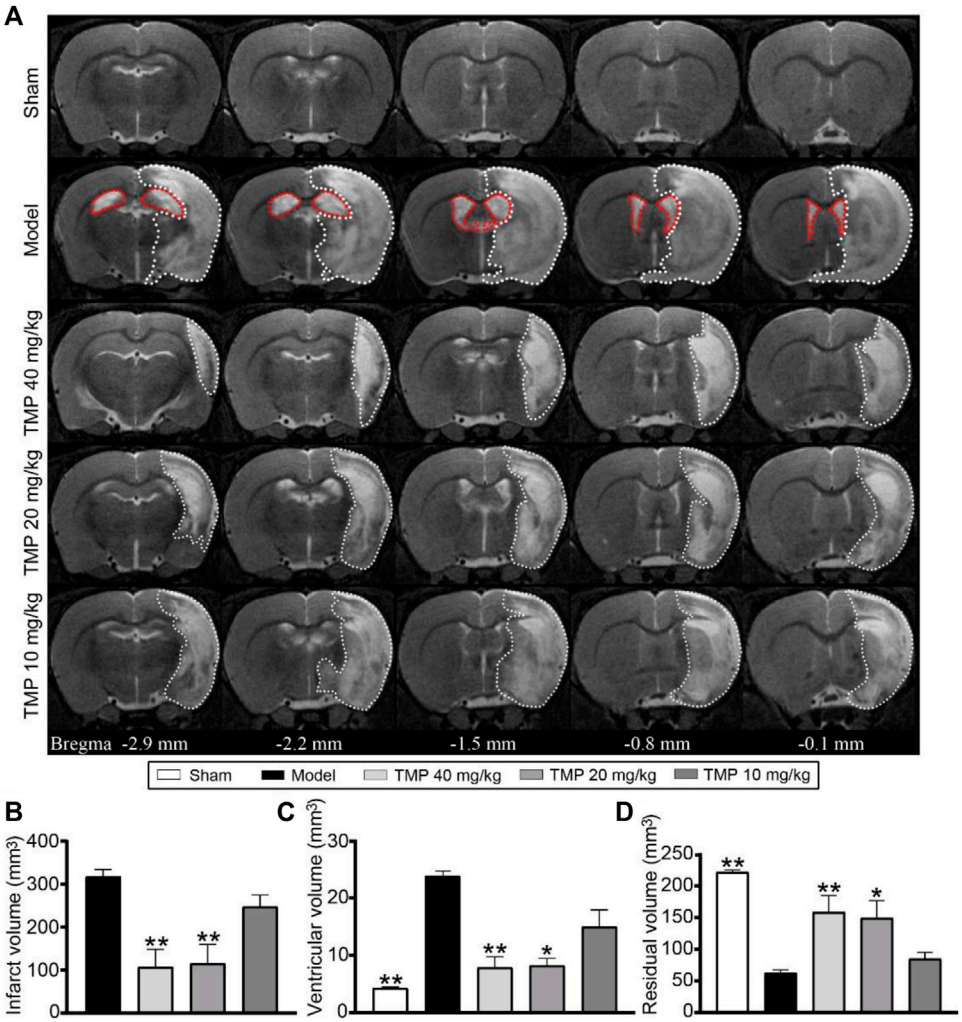

FIGURE 1 | Effect of TMP on cerebral infarction in MCAO rats. **(A)** Typical axial T2 images of each group. The infarct areas are represented with white dotted lines. The ventricles are represented with red dotted lines in the model group (n = 6). Quantitative analysis of the **(B)** infarct volume, **(C)** ventricular volume, and **(D)** residual volume. *p < 0.05 and **p < 0.01 vs. Model group.

Western Blot Analysis

The rats (n = 4 per group) without undergoing MRI experiments were deeply anesthetized. The perilesional cortex was separated, and protein levels were determined by Western blotting, as previously described (Zhan et al., 2020). Proteins were transferred onto polyvinylidene difluoride membranes, followed by blocking them with 5% nonfat milk for 2 h and subsequently incubating membranes at 4°C overnight with primary antibodies: anti-GAP-43 (1:40000; Epitomics, #2259-1), SYN (1:320000; Epitomics, #1870-1), Netrin-1 (1:2,000; Abcam, ab126729), DCC (1:1,000; Abcam, ab125280), Slit-2 (1:10,000; Abcam, ab134166), Robo-1 (1:1,000; Abcam, ab7279), NogoA (1:20,000; Abcam, ab62024), NgR (1:40,000; Abcam, ab62024), RhoA (1:20,000; Cell signaling, 2117s), ROCK-2 (1:50,000; Abcam, ab125025), and GAPDH (1:1,60,000; GeneTex, GTX627408). After washing, membranes were incubated with secondary anti-rabbit (1:20,000; Applygen Technologies Inc., C1309) or anti-mouse (1:20,000; NeoBioscience, cat. ANM 02-1, Lot. 0912) IgG (H + L)-HRP for 1 h at room temperature. Immunoreactive protein bands were detected by using the SuperECL Plus kit (Applygen, China, cat. No. P1050) and chemiluminescent imager (VILBER, United States). The intensities of target proteins were quantified by ImageJ software.

Statistical Analysis

Data were presented as mean ± standard error of the mean (SEM). Statistical analysis was performed using the SPSS 26.0 software (SPSS Inc., United States). Data were analyzed with a one-way analysis of variance (ANOVA), followed by Bonferroni's *post hoc* test. Pearson linear regression was conducted to analyze the correlation between rCBF and DTI metrics. The statistical significance was defined as $p < 0.05$.

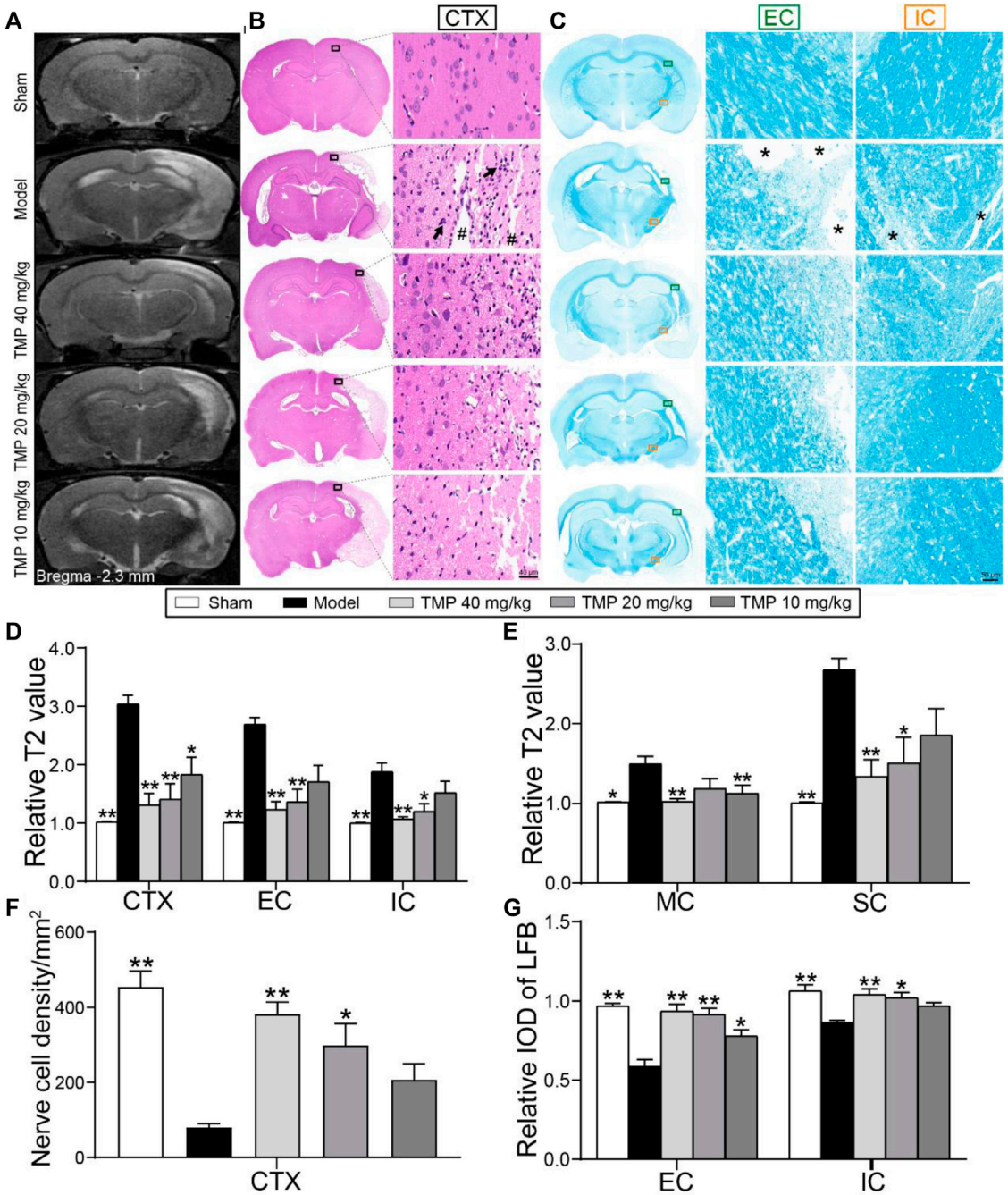

FIGURE 2 | Effect of TMP on cerebral tissue injury in MCAO rats. **(A)** Typical T2 relaxometry mapping of each group (n = 6). **(B)** Typical HE staining photographs showed the degeneration and necrosis of the nerve cells (black arrows) in the peri-infarct cortex (CTX, black boxes) and destructive tissues (#) indicated in the model group (n = 4). **(C)** Typical LFB staining photographs showed myelin sheath of the external capsule (EC, green boxes) and internal capsule (IC, orange boxes). Remarkable cavitation areas with myelin sheath loss (*) in nerve fibers were indicated in the model group (n = 4). Quantitative analysis of relative T2 values of **(D)** CTX, EC, and IC, **(E)** motor cortex (MC), and somatosensory cortex (SC). Quantitative analysis of **(F)** the nerve cell density of CTX and **(G)** relative LFB-IOD of EC and IC. *$p < 0.05$ and **$p <$ 0.01 vs. Model group.

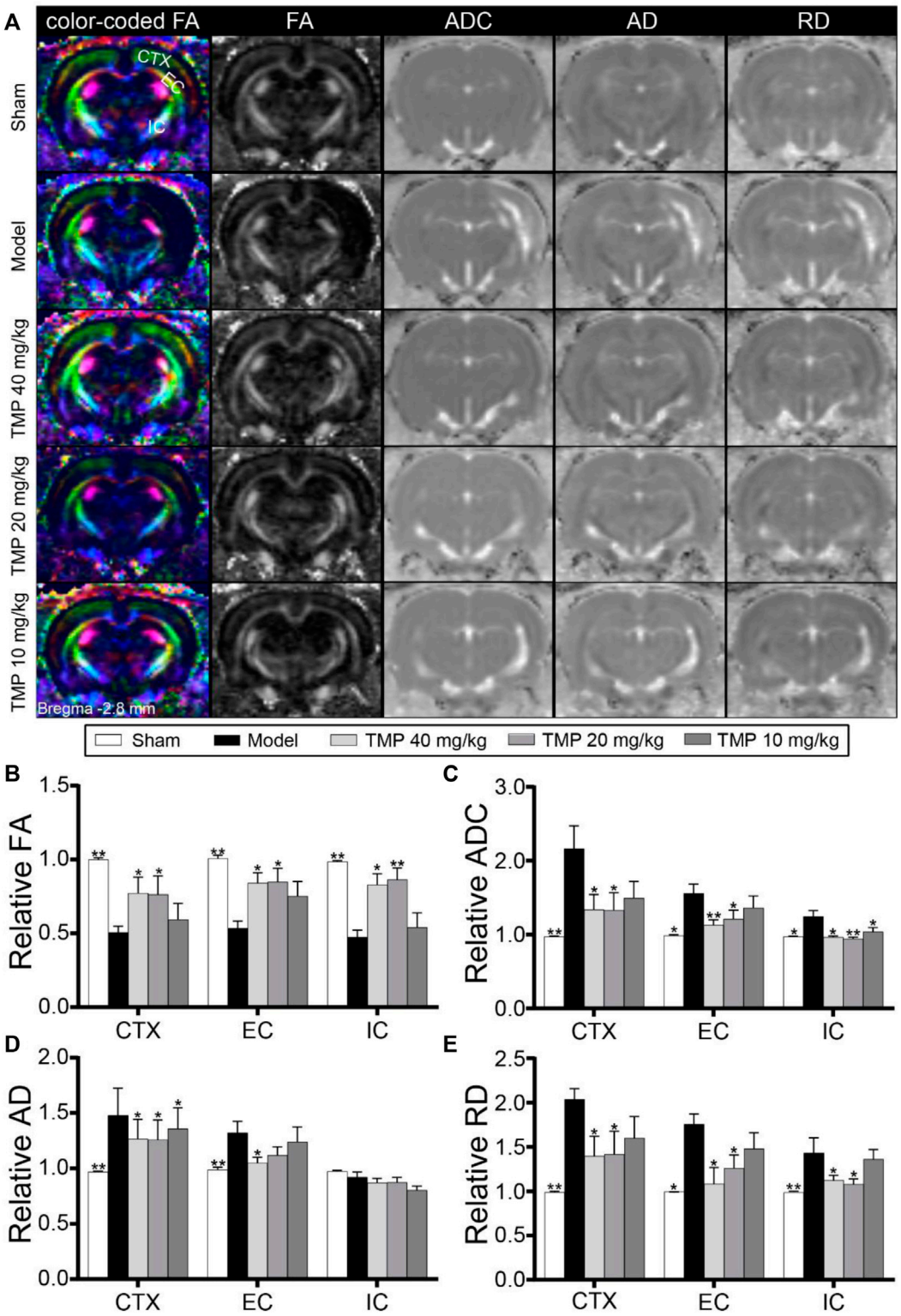

FIGURE 3 | Effect of TMP on the axonal microstructure in MCAO rats. **(A)** Typical axial color-coded FA, FA, ADC, AD, and RD images of each group. ROIs of the peri-infarct cortex (CTX), external capsule (EC), and internal capsule (IC) were identified on the color-coded FA images in the sham group (n = 6). **(B–E)** Quantitative analysis of the relative FA, ADC, AD, and RD of CTX, EC, and IC, respectively. *p < 0.05 and **p < 0.01 vs. Model group.

RESULTS

TMP Alleviated Cerebral Infarction

T2WI revealed a hyperintense signal in the MCA territory, indicating tissue infarction (**Figure 1A**). TMP (20, 40 mg/kg) treatment obviously decreased the infarct volume compared with the model group ($p < 0.01$) (**Figure 1B**). Notably, in comparison with sham rats, the bilateral ventricles were severely enlarged, and the ipsilateral residual volume was decreased after ischemia for 15 days ($p < 0.01$). TMP (20, 40 mg/kg) effectively relieved the ventricular dilatation and preserved the residual tissues in comparison with model rats ($p < 0.05$ or $p < 0.01$) (**Figures 1C,D**).

TMP Relieved Cerebral Tissue Injury and Protected the Myelinated Axons

T2 relaxometry mapping was conducted to determine structural changes in the gray and white matter (**Figure 2A**). Quantitative analysis showed higher rT2 values were detected in the ipsilateral gray matter (the peri-infarct cortex) and white matter (the external capsule and internal capsule) areas of model rats compared with sham rats ($p < 0.01$). In contrast, TMP (20, 40 mg/kg)-treated rats showed lower rT2 in the peri-infarct cortex, somatosensory cortex, external capsule, and internal capsule ($p < 0.05$ or $p < 0.01$), and TMP (10 mg/kg) decreased rT2 of the peri-infarct and motor cortex as compared with model rats ($p < 0.05$ or $p < 0.01$). TMP (40 mg/kg) additionally decreased rT2 of the motor cortex compared to the model group ($p < 0.01$) (**Figures 2D,E**).

Furthermore, HE staining (**Figure 2B**) showed that the nerve cell density of the peri-infarct cortex was sharply decreased when compared with the sham group ($p < 0.01$), whereas a significantly higher number of nerve cells was found in TMP (20, 40 mg/kg) treatment groups than in the model group ($p < 0.05$ or $p < 0.01$) (**Figure 2F**).

LFB staining was performed to examine the alternations of axons and myelin sheath (**Figure 2C**). In comparison with the sham group, the relative LFB-IODs of the external capsule and internal capsule in model rats were sharply decreased ($p < 0.01$). The relative IODs of the external capsule and internal capsule were increased in TMP (20, 40 mg/kg)-treated rats, and TMP (10 mg/kg) also enhanced the relative LFB-IOD of the internal capsule ($p < 0.05$ or $p < 0.01$) (**Figure 2G**). In conclusion, TMP plays a remarkable role in protecting nerve cells in gray matter and myelinated axons in white matter after ischemia.

TMP Ameliorated the Damage of the Axonal Microstructure

DTI was utilized to evaluate the microstructural changes in axons (**Figure 3A**). First, the DTI-derived parameter FA characterizes the alterations of the axonal microstructure. Quantitative data demonstrated that rFA was sharply decreased in the model perilesional cortex, external capsule, and internal capsule compared to the sham group ($p < 0.01$), while it was reversed by TMP (20, 40 mg/kg) ($p < 0.05$ or $p < 0.01$) (**Figure 3B**). In addition, rADC is employed to detect cellular damage. As shown in model rats, the increased rADC was detected in the peri-infarct cortex, external capsule, and internal capsule. In contrast, TMP (20, 40 mg/kg) decreased rADC of the peri-infarct cortex and external capsule compared with the model rats ($p < 0.05$ or $p < 0.01$), and the reduced rADC was also detected in the internal capsule of TMP (10 mg/kg) group rats ($p < 0.05$) (**Figure 3C**).

In particular, rAD and rRD were respectively used to analyze the alterations of axons and myelin sheath. DTI results showed elevated rAD and rRD in the peri-infarct cortex, external capsule, and internal capsule of model rats compared with sham rats ($p < 0.05$ or $p < 0.01$). After the treatment with TMP (10, 20, and 40 mg/kg), the rAD of the peri-infarct cortex was significantly reduced as compared to model rats ($p < 0.05$). Moreover, TMP (40 mg/kg) also decreased rAD of the ipsilateral external capsule (**Figure 3D**). Moreover, TMP (20, 40 mg/kg) remarkably decreased rRD in the peri-infarct cortex, external capsule, and internal capsule in comparison with the model group ($p < 0.05$ or $p < 0.01$). These results suggest that TMP could ameliorate the damage to the axonal microstructure in ischemic rats.

TMP Facilitated Axonal Restoration

DTT was conducted to demonstrate the integrity and connectivity of nerve fibers (**Figure 4A**). The model group rats showed decreased relative fiber length and density in the external capsule and internal capsule compared to sham rats ($p < 0.01$). After treatment with TMP (40 mg/kg), the relative fiber length and density of the external capsule were remarkably increased, and the relative density of internal capsule fibers was also increased in comparison with model rats ($p < 0.05$ or $p < 0.01$). Additionally, TMP (20 mg/kg) elevated the relative density of internal capsule fibers in comparison with model rats ($p < 0.05$ or $p < 0.01$) (**Figures 4B,C**).

TMP Improved the Cerebral Perfusion

Cerebral perfusion was quantitatively evaluated with ASL (**Figure 5A**). *Post hoc* comparisons revealed the rCBF of the peri-infarct cortex, external capsule, and internal capsule in model rats was significantly decreased in comparison to the sham group ($p < 0.01$). TMP treatment (20, 40 mg/kg) significantly increased the rCBF of the peri-infarct cortex, external capsule, and internal capsule ($p < 0.05$ or $p < 0.01$), and TMP (10 mg/kg) also increased the rCBF of the peri-infarct cortex and external capsule compared to model rats ($p < 0.05$ or $p < 0.01$) (**Figure 5B**).

Furthermore, Pearson linear regression analysis showed rFA was significantly in positive correlation with rCBF in the peri-infarct cortex ($R = 0.4938$ and $p < 0.01$), external capsule ($R = 0.6803$ and $p < 0.0001$), and internal capsule ($R = 0.7716$ and $p < 0.0001$). Meanwhile, rADC was strongly in negative correlation with rCBF in the peri-infarct cortex ($R = -0.5093$ and $p < 0.01$), external capsule ($R = -0.7427$ and $p < 0.0001$), and internal capsule ($R = -0.4407$ and $p < 0.05$), suggesting the improvement of the rCBF might contribute to restore the axonal microstructure after ischemia (**Figure 5C**).

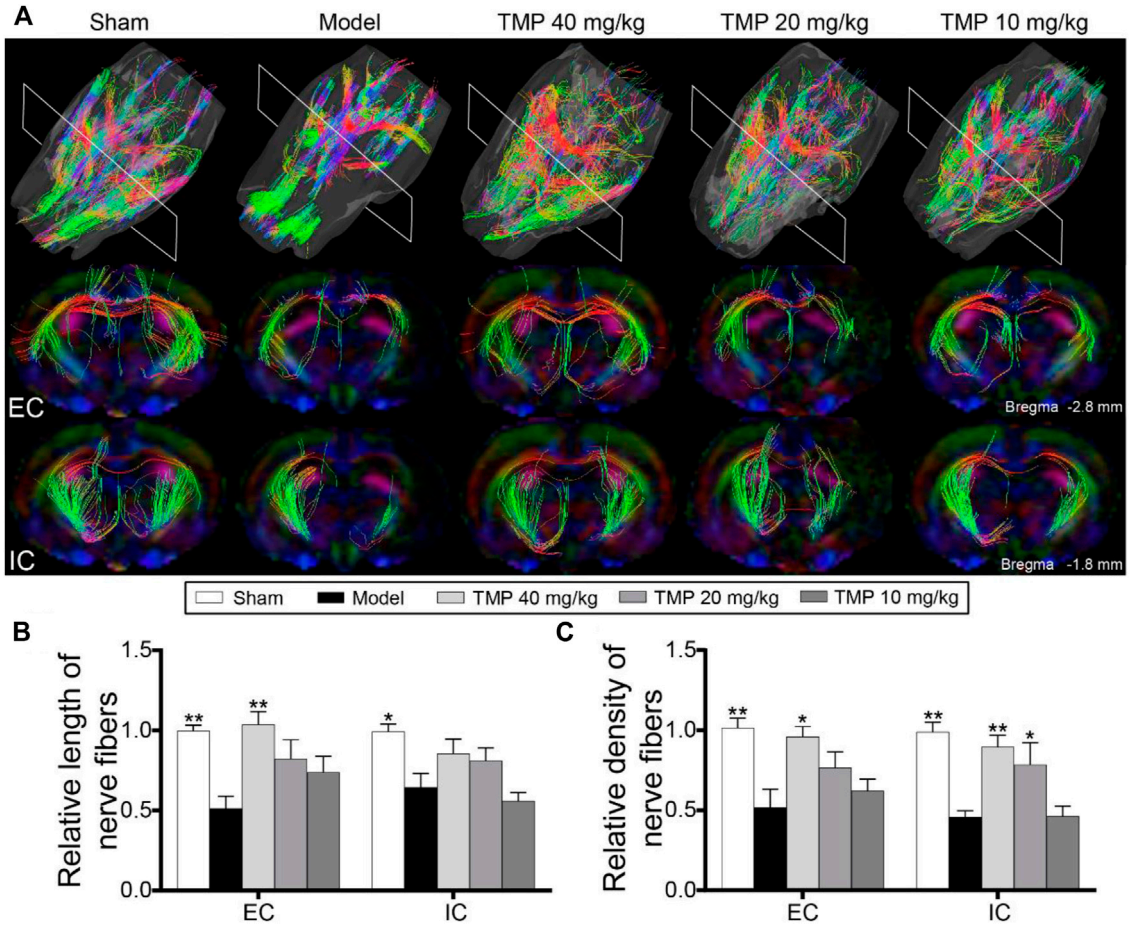

FIGURE 4 | Effect of TMP on axonal restoration in MCAO rats. **(A)** Typical 3D reconstruction DTT images of the whole brain and anatomical pathways of the external capsule (EC) and internal capsule (IC) of each group ($n = 6$). Quantitation of the **(B)** relative length and **(C)** relative density of nerve fibers in EC and IC. $^{*}p < 0.05$ and $^{**}p < 0.01$ vs. Model group.

TMP Elevated GAP-43 and SYN Expressions and Decreased Damage to Axonal and Synaptic Microstructures

To test whether TMP treatment of stroke induces axonal and synaptic plasticity, GAP-43 (a marker for axon growth) and SYN (a marker for synaptogenesis) were examined. Western blot revealed that GAP-43 and SYN in the model perilesional cortex were significantly decreased compared with the sham group ($p < 0.05$ or $p < 0.01$). After TMP (10, 20, and 40 mg/kg) treatment, GAP-43 and SYN were significantly elevated in comparison with the model cortex ($p < 0.05$ or $p < 0.01$) (**Figures 6A,B**).

Notably, electron micrographs showed the ultrastructural alterations of myelinated axons with the swollen myelin lamina after MCAO (**Figure 6C**). Moreover, the measurement of the G-ratio was significantly declined in the model group as compared with the sham group ($p < 0.01$). TMP (10, 20, and 40 mg/kg) dramatically increased the G-ratio in comparison with model rats ($p < 0.01$), suggesting axonal remyelination after TMP intervention (**Figure 6C**).

In addition, the synaptic ultrastructural analysis showed MCAO decreased the number of vesicles in presynaptic membranes, induced structural changes in synaptic junctions including the decreased presynaptic membrane length, PSD thickness, and postsynaptic membrane curvature, and increased the synaptic cleft width. The synaptic parameters were altered after TMP treatment. TMP (10, 20, and 40 mg/kg) increased PSD thickness and postsynaptic membrane curvature and decreased synaptic cleft width in comparison with model rats ($p < 0.01$). In particular, TMP (20, 40 mg/kg) increased the number of presynaptic vesicles ($p < 0.01$), and TMP (40 mg/kg) also extended the presynaptic membrane length ($p < 0.05$) (**Figures 6I–M**-M).

Moreover, quantitation showed that mitochondrial damage scores in axons and synapses were increased in the model group compared to the sham group ($p < 0.01$). TMP (10, 20, and 40 mg/kg) restored the mitochondrial injury in the perilesional cortex ($p < 0.05$ or $p < 0.01$) (**Figures 6F,N**).

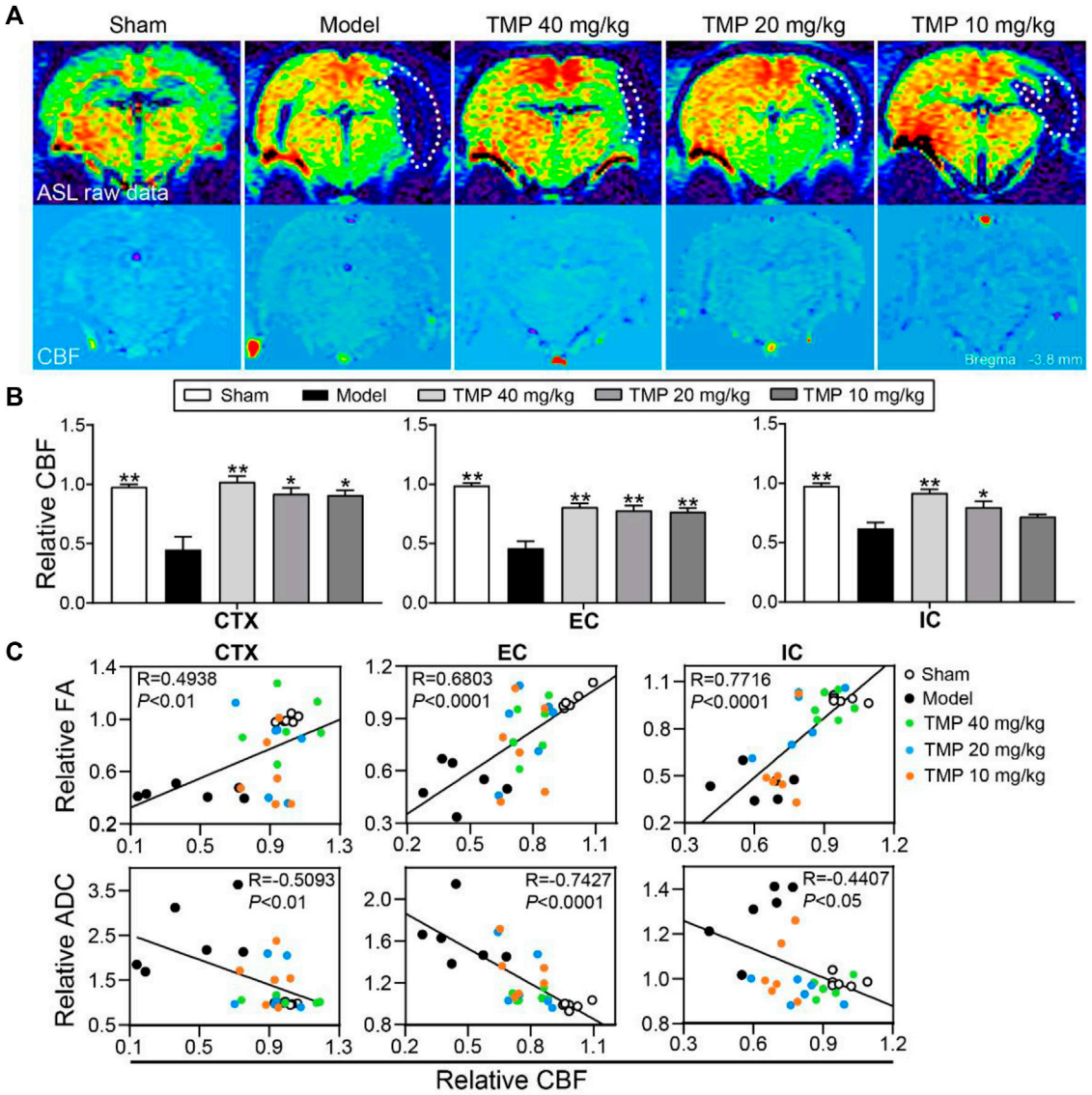

FIGURE 5 | Effect of TMP on cerebral perfusion in MCAO rats. **(A)** Typical ASL raw data and CBF images of each group. The ischemic areas are represented with white dotted lines ($n = 6$). **(B)** Quantitation of relative CBF (rCBF) of the peri-infarct cortex (CTX), external capsule (EC), and internal capsule (IC). **(C)** Correlations between DTI metrics (rFA and rADC) and rCBF of CTX, EC, and IC. *$p < 0.05$ and **$p < 0.01$ vs. Model group.

TMP Regulated Axonal Guidance Signals and Inhibited Axonal Growth-Inhibitory Signals

Western blot results showed that axonal guidance factors DCC, Slit-2, and Robo-1 were notably downregulated in the periischemic cortex of model rats compared to sham rats ($p < 0.05$ or $p < 0.01$), while TMP (10, 20, and 40 mg/kg) significantly upregulated DCC, Slit-2, and Robo-1 expressions compared to the model group ($p < 0.05$ or $p < 0.01$). In addition, TMP (40 mg/kg) also increased the expression of Netrin-1 when compared to model rats ($p < 0.05$) (**Figures 7A,B**).

In particular, the axonal growth inhibitors NogoA/NgR and RhoA/ROCK-2 were distinctly upregulated in model rats compared with the sham group ($p < 0.05$ or $p < 0.01$). In comparison with the model group, TMP (20, 40 mg/kg) treatment downregulated NogoA, NgR, RhoA, and ROCK-2, and TMP (10 mg/kg) also suppressed NgR, RhoA, and ROCK-2 levels in the peri-ischemic cortex (**Figures 7C,D**). To sum up, TMP improves axonal remodeling by regulating axonal guidance and growth-inhibitory signals.

TMP Improved the Gait Function

The gait impairment and functional recovery after TMP treatment were evaluated by the DigiGait-automated gait test (**Figure 8A**). The model rats displayed the significantly increased steps and cadence compared with sham rats ($p < 0.05$ or $p < 0.01$). After TMP (10, 20, and 40 mg/kg) treatment, steps and cadence were decreased in

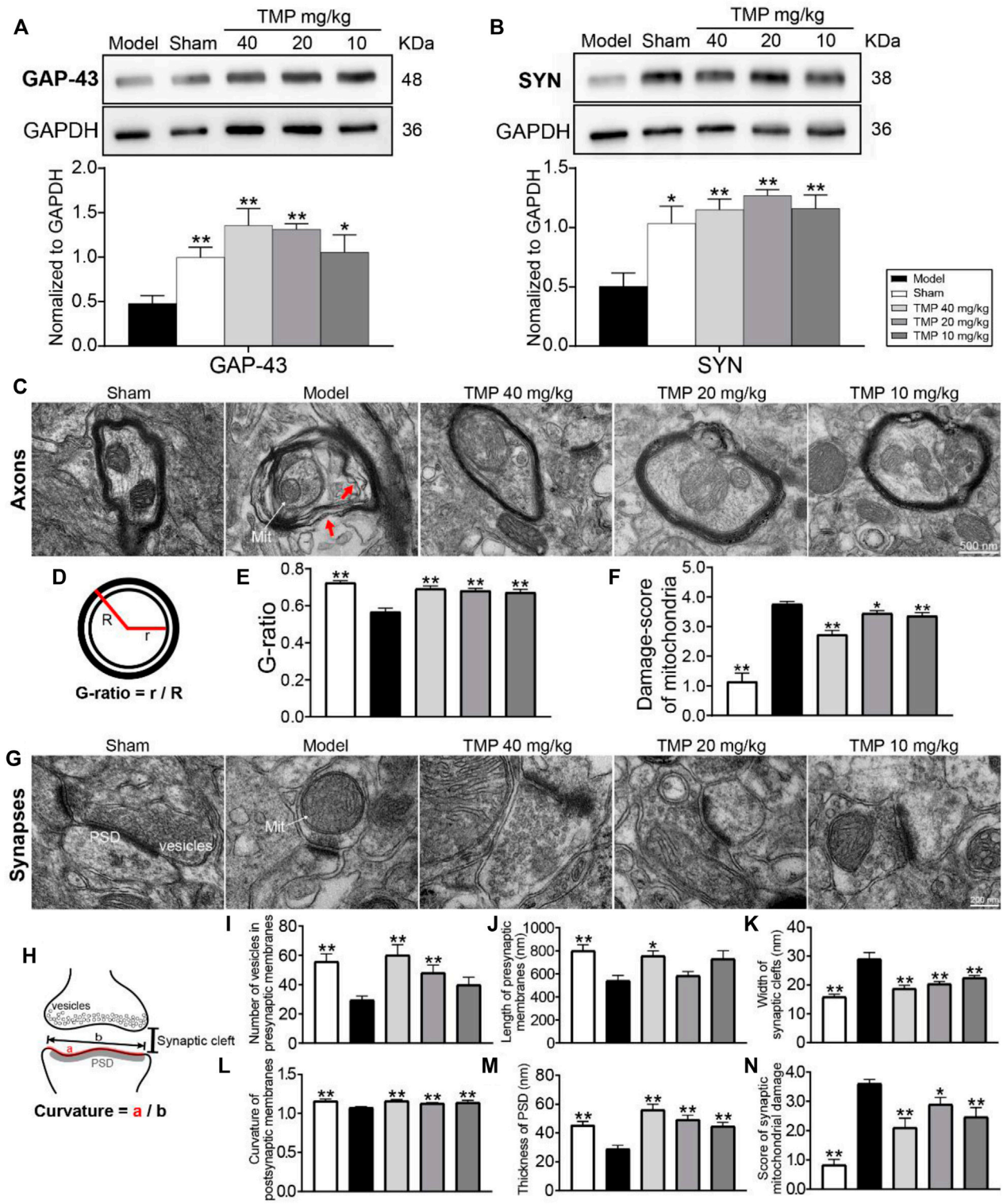

FIGURE 6 | Effects of TMP on GAP-43 and SYN expressions and axonal and synaptic microstructural damage in MCAO rats. Typical Western blot images and analysis for **(A)** GAP-43 and **(B)** SYN ($n = 4$). The protein levels were quantified with GAPDH as the loading control. **(C)** Representative TEM images of myelinated axons in each group, and the axons separating from myelin sheath (red arrows) and abnormal mitochondria (Mit) were indicated in the model group ($n = 2$). **(D)** G-ratio indicated the axonal diameter (r)/total fiber diameter (R). The quantitation of **(E)** G-ratio and **(F)** damage score of mitochondria in axons. **(G)** Representative TEM images of synapses in each group ($n = 2$). **(H)** Vesicles in presynaptic membranes, synaptic cleft, PSD, and postsynaptic membrane curvature are shown on the schematic diagram. The quantitation of **(I)** vesicles in presynaptic membranes, **(J)** presynaptic membrane length, **(K)** synaptic cleft width, **(L)** postsynaptic membrane curvature, **(M)** PSD thickness, and **(N)** damage score of mitochondria in synapses. $^{*}p < 0.05$ and $^{**}p < 0.01$ vs. Model group.

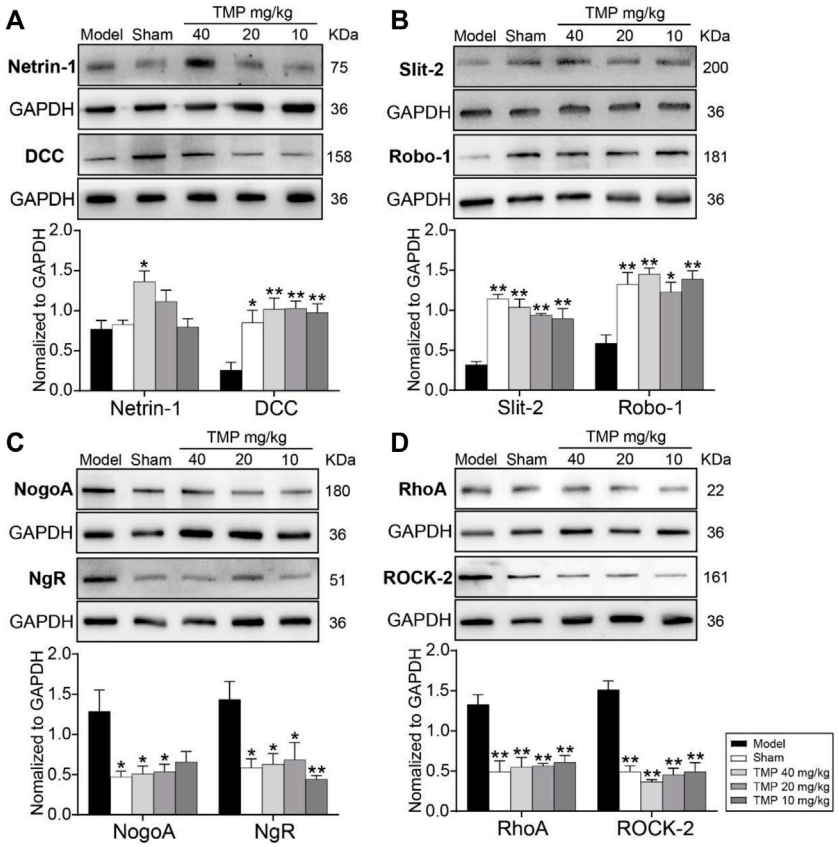

FIGURE 7 | Effects of TMP on the expressions of axonal guidance and growth-inhibitory signals in MCAO rats. Typical Western blot images and analysis for **(A)** Netrin-1/DCC, **(B)** Slit-2/Robo-1, **(C)** NogoA/NgR, and **(D)** RhoA/ROCK-2 ($n = 4$). The protein levels were quantified with GAPDH as the loading control. $^{*}p < 0.05$ and $^{**}p < 0.01$ vs. Model group.

comparison with model rats ($p < 0.05$ or $p < 0.01$) (**Figures 8B,C**). The stride length of the four limbs and hindlimb shared stance time were shortened in model rats compared to sham rats ($p < 0.05$ or $p < 0.01$), which were both reversed by TMP (10, 20, and 40 mg/kg) ($p < 0.05$ or $p < 0.01$) (**Figures 8D,E**).

The paw area of the left hindlimb and right limbs in model rats was smaller than that in sham rats ($p < 0.05$ or $p < 0.01$), which was increased in TMP (10, 20, and 40 mg/kg) groups, and TMP (20, 40 mg/kg) also increased the paw area of the right forelimbs in comparison with the model group ($p < 0.05$) (**Figure 8F**).

Notably, the model rats showed an increased ataxia coefficient of the hindlimbs compared with the sham group, representing the impairment in the interlimb coordination ($p < 0.05$ or $p < 0.01$), whereas it was decreased by TMP (10, 20, and 40 mg/kg) compared with model rats ($p < 0.05$ or $p < 0.01$) (**Figure 8G**). These data elucidate that TMP could alleviate gait impairment and improve the limb locomotor function after ischemic stroke.

DISCUSSION

On the basis of the multiparametric MRI, the present study revealed that TMP had beneficial effects on protecting both gray and white matter, especially promoting axonal remodeling after ischemic stroke, which was coupled with improving cerebral perfusion. With the information obtained from the DigiGait-automated analysis, we demonstrated that TMP facilitated gait function recovery. Meanwhile, intrinsic axonal guidance cues and growth-inhibitory signals would be participated in the process of TMP promoting axonal reorganization. Our research would offer an ideal therapeutic approach to promote post-stroke brain repair.

MRI is an extremely reliable modality to noninvasively reveal tissue damages (Saar and Koretsky, 2019). In the present study, T2WI images exhibited TMP could reduce infarct volumes and protect residual tissues of ischemic brains, and T2 relaxometry mapping displayed decreased T2 values located in the peri-infarct cortex, external capsule, and internal capsule, following TMP treatment. In corresponding areas, histopathological analysis confirmed TMP preserved nerve cells in the peri-infarct cortex and increased LFB positive myelinated nerve fibers in the external capsule and internal capsule which are the integral white matters. Therefore, our data indicated TMP not only relieves gray matter injury but also protects white matter structures.

We noninvasively detected the microstructure and integrity of gray and white matter by DTI (Jung et al., 2017). The decreased rFA but increased rADC, rAD, and rRD predominantly appeared

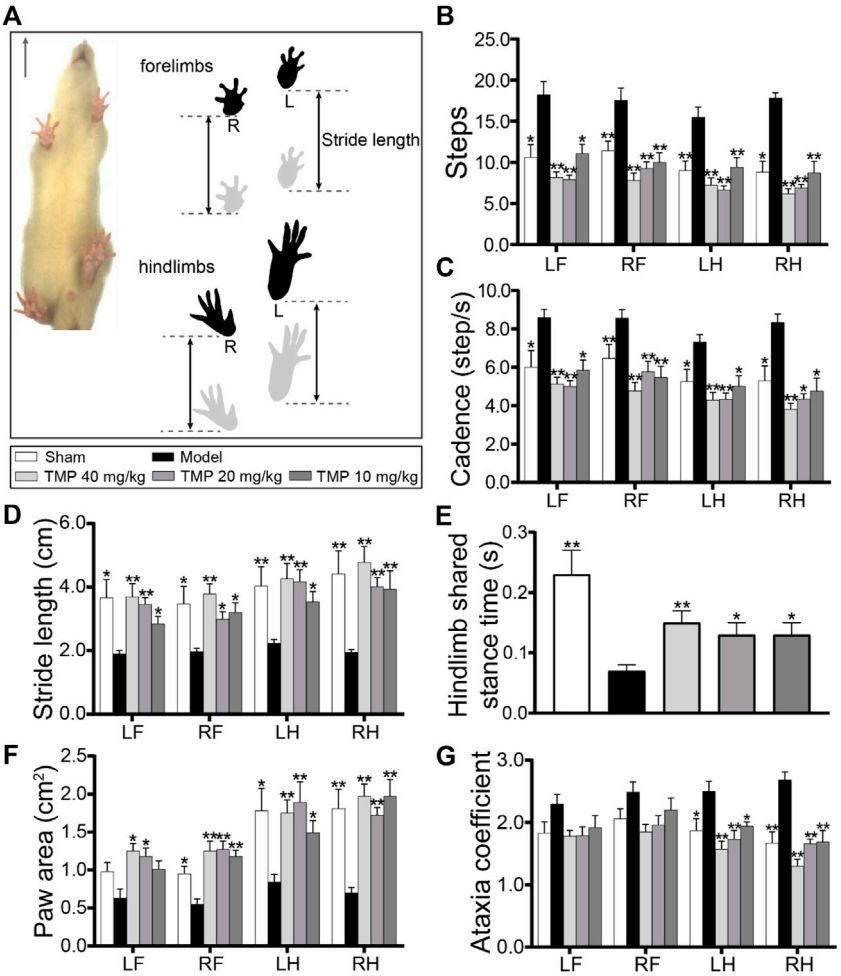

FIGURE 8 | Effects of TMP on gait functions in MCAO rats. **(A)** Schematic diagram exhibited a rat subjected to a gait test (n = 10). The locations of the four paws were painted. Stride length indicated the distance between two successive initial postures during the maximal contact. Quantitative analysis of **(B)** steps, **(C)** cadence, **(D)** stride length, **(E)** hindlimb shared stance time, **(F)** paw area, and **(G)** ataxia coefficient in rats of each group. LF, left forelimb; RF, right forelimb; LH, left hindlimb; RH, right hindlimb. *p < 0.05 and **p < 0.01 vs. Model group.

in the peri-infarct cortex, external capsule, and internal capsule after stroke. FA as a common parameter of DTI reflects the density and integrity of the axonal microstructure, while the reduced FA pixels independently represent demyelination and axonal loss. The increased ADC is a sign of cellular injury, and the elevated AD and RD indicate axonotmesis and myelin degradation, respectively (Mailhard et al., 2013). Notably, a higher rFA but lower rADC, rAD, and rRD were detected in corresponding regions after TMP treatment, suggesting TMP could lessen microstructural injury of axons and myelin sheath and facilitate axonal remodeling after ischemic stroke. In particular, DTT maps revealed that TMP intervention robustly elevated the fiber density and length in the ischemic external capsule and internal capsule, suggesting fiber tract repair. With the information obtained from MRI, this study firmly demonstrated the efficacy of TMP in facilitating white matter reformation involving demyelination and axonal reorganization, following ischemia. However, the intricate mechanism remains unclear and requires further investigation.

Previous studies have revealed that TMP could inhibit platelet aggregation, reduce blood–brain barrier permeability, and promote angiogenesis (Tan et al., 2015; Li L et al., 2019), which were essential for maintaining circulatory homeostasis following ischemia. CBF improvement is favorable for relieving axonal injury and promoting white matter remodeling after ischemia (Hatakeyama et al., 2020). To show the association between CBF and axonal remodeling, we quantitatively investigated the CBF with MRI-ASL images and constructed the correlation between CBF and DTI indices. Our findings demonstrated that MCAO rats treated with TMP showed restoration of the CBF in peri-infarct regions. Interestingly, a strong correlation was observed between rCBF and rFA/rADC, suggesting elevating regional CBF might coordinate axonal remodeling.

On the grounds of the aforementioned results, we further investigated the level of axonal growth protein GAP-43 and synaptogenesis marker SYN. GAP-43 exits in the growth-cone membranes of axons, and SYN lies on the membranes of presynaptic vesicles. The upregulated GAP-43 and SYN are, respectively, related to neurite outgrowth and synaptic plasticity (Chung et al., 2020; Jing et al., 2020). Our results found TMP treatment markedly improved GAP-43 and SYN expressions in the peri-ischemic cortex. Furthermore, TEM images provided direct evidence that TMP could protect the ultrastructure of axons and synapses. The increased G-ratio of axons in MCAO rats treated with TMP reflected that TMP alleviated axonal damage and demyelination (Stikov et al., 2015). In particular, the synaptic ultrastructural analysis revealed that TMP induced structural changes in synaptic junctions. Synapses have dynamic structures, and the ultrastructural alterations are closely related to synaptic plasticity (Li et al., 2016). In addition, TMP could alleviate mitochondrial damage in axons and synapses. Collectively, these data combined with MRI evidence strongly support that improved CBF after TMP treatment is beneficial for axonal outgrowth and synaptic plasticity.

Recently, attractive and repulsive axonal guidance cues such as Netrin-1 and Slit-2 have been recognized to play a major role in guiding axonal growth. In this study, we found TMP could upregulate Netrin-1/DCC and Slit-2/Robo-1 levels after ischemia for 15 days. It was worth noting that TMP (40 mg/kg) significantly increased the Netrin-1 expression compared with the model group. Netrin-1 is initially characterized as a neural guidance factor and has been demonstrated as a potent vascular mitogen that stimulates proliferation, migration, and tube formation (Park et al., 2004). Subsequently, evidence revealed that Netrin-1 could induce angiogenesis and improve the post-stroke neurovascular structure in adult mouse brains (Lu et al., 2012; Ding et al., 2014). These results, along with the information obtained from ASL and DTI, raised the interesting possibility of the beneficial effects of TMP toward CBF augmentation and axonal repair after ischemic stroke.

It is evident that the growth-inhibitory proteins of myelin-associated axons make a critical difference in impeding axonal repair post stroke (Huang et al., 2017). Specifically, NogoA binding to NgR inhibits axonal sprouting by activating the downstream RhoA and its effector ROCK-2, disintegrating axonal growth cones (Zagrebelsky and Korte, 2014). More obviously, TMP-treated rats exhibited significantly reduced growth-inhibitory proteins NogoA/NgR and RhoA/ROCK-2. Our findings were consistent with previous reports showing upregulated NogoA/NgR and RhoA/ROCK-2, following ischemic stroke (Kilic et al., 2010). Overall, our findings proved that axonal guidance and growth-inhibitory signals within the cerebral microenvironment might contribute to TMP promoting brain tissue remodeling post ischemia.

Remodeling of gray and white matter accounts for functional recovery (Rosano et al., 2008; de Laat et al., 2011); thus, we investigated the therapeutic effects of TMP on gait impairment using the DigiGait-assisted automated analysis system. Unilateral ischemia could result in bilateral gait variations (Parkkinen et al., 2013), and clinical studies based on MRI have confirmed that demyelination and axonal degeneration are parallel to the attenuated gait speed, stride length, and double support time [56, 57]. The increase in steps and decline in the stride length are related to the attenuation of gait stability and speed (Krasovsky et al., 2012; van der Holst et al., 2018); in addition , the reduction in paw area is due to the inadequate propulsion and weight-bearing capabilities of the limbs (Zeng et al., 2018). In particular, the shortened hindlimb shared stance time and increased ataxia coefficient suggest that limb coordination is impaired by stroke (Langhorne et al., 2011; Ambrosini et al., 2020). In the present study, gait parameters were effectively improved after TMP treatment for 2 weeks, including steps, cadence, stride length, hindlimb shared stance time, paw area, and ataxia coefficient, demonstrating that TMP has the potential to alleviate the gait deficit of MCAO rats.

In the present research, we proved TMP alleviated gray and white matter injury and enhanced axonal remodeling by improving CBF, inducing endogenous GAP-43 and SYN expressions, augmenting guidance cues Netrin-1/DCC and Slit-2/Robo-1, and interfering with intrinsic growth-inhibitory signals NogoA/NgR and RhoA/ROCK-2. These data provide meaningful evidence that TMP might improve the intracerebral microenvironment of ischemic areas and benefit white matter remodeling, in consequence, contributing to the improvement of functional recovery after stroke.

DATA AVAILABILITY STATEMENT

The original contributions presented in the study are included in the article/**Supplementary Material**; further inquiries can be directed to the corresponding author.

ETHICS STATEMENT

The animal study was reviewed and approved by Capital Medical University Animal Ethics Committee (Permit Number: AEEI-2018-052).

AUTHOR CONTRIBUTIONS

X-FF conducted this study, dealt with data, analyzed results, and finished the manuscript. J-FL and M-ZL performed MRI experiments. YZ collected MRI data. LY prepared samples. YL carried out a gait test. M-CL collected gait data. Y-MZ fed rats. LW supervised the experimental work. HZ programmed the whole work and modified the final manuscript.

FUNDING

This work was supported by the Beijing Municipal Natural Science Foundation (Grant No.7212161).

SUPPLEMENTARY MATERIAL

The Supplementary Material for this article can be found online at: https://www.frontiersin.org/articles/10.3389/fphar.2022.851746/full#supplementary-material

REFERENCES

Ambrosini, E., Parati, M., Peri, E., De Marchis, C., Nava, C., Pedrocchi, A., et al. (2020). Changes in Leg Cycling Muscle Synergies after Training Augmented by Functional Electrical Stimulation in Subacute Stroke Survivors: a Pilot Study. *J. Neuroeng Rehabil.* 17, 35. doi:10.1186/s12984-020-00662-w

Caballero-Garrido, E., Pena-Philippides, J. C., Galochkina, Z., Erhardt, E., and Roitbak, T. (2017). Characterization of Long-Term Gait Deficits in Mouse dMCAO, Using the CatWalk System. *Behav. Brain Res.* 331, 282–296. doi:10.1016/j.bbr.2017.05.042

Chan, K. C., Khong, P. L., Lau, H. F., Cheung, P. T., and Wu, E. X. (2009). Late Measures of Microstructural Alterations in Severe Neonatal Hypoxic-Ischemic Encephalopathy by MR Diffusion Tensor Imaging. *Int. J. Dev. Neurosci.* 27, 607–615. doi:10.1016/j.ijdevneu.2009.05.012

Chen, B., Carr, L., and Dun, X. P. (2020). Dynamic Expression of Slit1-3 and Robo1-2 in the Mouse Peripheral Nervous System after Injury. *Neural Regen. Res.* 15, 948–958. doi:10.4103/1673-5374.268930

Chen, J., Venkat, P., Zacharek, A., and Chopp, M. (2014). Neurorestorative Therapy for Stroke. *Front. Hum. Neurosci.* 8, 382. doi:10.3389/fnhum.2014.00382

Chun-sheng, L., Hsiao-meng, Y., Yun-hsiang, H., Chun, P., and Chi-fen, S. (1978). Radix Salviae Miltiorrhizae and Rhizoma Ligustici Wallichii in Coronary Heart Disease. *Chin. Med. J. (Engl)* 4, 43–46.

Chung, D., Shum, A., and Caraveo, G. (2020). GAP-43 and BASP1 in Axon Regeneration: Implications for the Treatment of Neurodegenerative Diseases. *Front Cel Dev Biol* 8, 567537. doi:10.3389/fcell.2020.567537

Cuesta, S., Nouel, D., Reynolds, L. M., Morgunova, A., Torres-Berrío, A., White, A., et al. (2020). Dopamine Axon Targeting in the Nucleus Accumbens in Adolescence Requires Netrin-1. *Front. Cel Dev Biol* 8, 487. doi:10.3389/fcell.2020.00487

de Laat, K. F., Tuladhar, A. M., van Norden, A. G., Norris, D. G., Zwiers, M. P., and de Leeuw, F. E. (2011). Loss of white Matter Integrity Is Associated with Gait Disorders in Cerebral Small Vessel Disease. *Brain* 134, 73–83. doi:10.1093/brain/awq343

Ding, Q., Liao, S. J., and Yu, J. (2014). Axon Guidance Factor Netrin-1 and its Receptors Regulate Angiogenesis after Cerebral Ischemia. *Neurosci. Bull.* 30, 683–691. doi:10.1007/s12264-013-1441-9

Feng, H., Larrivee, C. L., Demireva, E. Y., Xie, H., Leipprandt, J. R., and Neubig, R. R. (2019). Mouse Models of GNAO1-Associated Movement Disorder: Allele- and Sex-specific Differences in Phenotypes. *Plos One* 14, e0211066. doi:10.1371/journal.pone.0211066

Flottmann, F., Leischner, H., Broocks, G., Nawabi, J., Bernhardt, M., Faizy, T. D., et al. (2018). Recanalization Rate Per Retrieval Attempt in Mechanical Thrombectomy for Acute Ischemic Stroke. *Stroke* 49, 2523–2525. doi:10.1161/STROKEAHA.118.022737

Gong, P., Zhang, Z., Zou, Y., Tian, Q., Han, S., Xu, Z., et al. (2019). Tetramethylpyrazine Attenuates Blood-Brain Barrier Disruption in Ischemia/reperfusion Injury through the JAK/STAT Signaling Pathway. *Eur. J. Pharmacol.* 854, 289–297. doi:10.1016/j.ejphar.2019.04.028

Guo, J., Zheng, H. B., Duan, J. C., He, L., Chen, N., Gong, Q. Y., et al. (2011). Diffusion Tensor MRI for the Assessment of Cerebral Ischemia/reperfusion Injury in the Penumbra of Non-human Primate Stroke Model. *Neurol. Res.* 33, 108–112. doi:10.1179/016164110x12761752770177

Guo, S. K., Chen, K. J., Qian, Z. H., Weng, W. L., and Qian, M. Y. (1983). Tetramethylpyrazine in the Treatment of Cardiovascular and Cerebrovascular Diseases. *Planta Med.* 47, 89.

Hampton, T. G., Stasko, M. R., Kale, A., Amende, I., and Costa, A. C. (2004). Gait Dynamics in Trisomic Mice: Quantitative Neurological Traits of Down Syndrome. *Physiol. Behav.* 82, 381–389. doi:10.1016/j.physbeh.2004.04.006

Hatakeyama, M., Ninomiya, I., and Kanazawa, M. (2020). Angiogenesis and Neuronal Remodeling after Ischemic Stroke. *Neural Regen. Res.* 15, 16–19. doi:10.4103/1673-5374.264442

Hou, S., Shen, P. P., Zhao, M. M., Liu, X. P., Xie, H. Y., Deng, F., et al. (2016). Mechanism of Mitochondrial Connexin43's Protection of the Neurovascular Unit under Acute Cerebral Ischemia-Reperfusion Injury. *Int. J. Mol. Sci.* 17, 679. doi:10.3390/ijms17050679

Huang, S., Huang, D., Zhao, J., and Chen, L. (2017). Electroacupuncture Promotes Axonal Regeneration in Rats with Focal Cerebral Ischemia through the Downregulation of Nogo-A/NgR/RhoA/ROCK Signaling. *Exp. Ther. Med.* 14, 905–912. doi:10.3892/etm.2017.4621

Hughes, R. E., Tadi, P., and Bollu, P. C. (2021). *TPA Therapy*. Eluru, India: StatPearls.

Jing, M., Yi, Y., Jinniu, Z., Xiuli, K., and Jianxian, W. (2020). Rehabilitation Training Improves Nerve Injuries by Affecting Notch1 and SYN. *Open Med. (Wars)* 15, 387–395. doi:10.1515/med-2020-0045

Jung, W. B., Han, Y. H., Chung, J. J., Chae, S. Y., Lee, S. H., Im, G. H., et al. (2017). Spatiotemporal Microstructural white Matter Changes in Diffusion Tensor Imaging after Transient Focal Ischemic Stroke in Rats. *Nmr Biomed.* 30, e3704. doi:10.1002/nbm.3704

Kilic, E., ElAli, A., Kilic, U., Guo, Z., Ugur, M., Uslu, U., et al. (2010). Role of Nogo-A in Neuronal Survival in the Reperfused Ischemic Brain. *J. Cereb. Blood Flow Metab.* 30, 969–984. doi:10.1038/jcbfm.2009.268

Krasovsky, T., Baniña, M. C., Hacmon, R., Feldman, A. G., Lamontagne, A., and Levin, M. F. (2012). Stability of Gait and Interlimb Coordination in Older Adults. *J. Neurophysiol.* 107, 2560. doi:10.1152/jn.00950.2011

Laing, R. J., Jakubowski, J., and Laing, R. W. (1993). Middle Cerebral Artery Occlusion without Craniectomy in Rats. Which Method Works Best? *Stroke* 24, 294–298. doi:10.1161/01.Str.24.2.294

Langhorne, P., Bernhardt, J., and Kwakkel, G. (2011). Stroke Rehabilitation. *Lancet* 377, 1693–1702. doi:10.1016/S0140-6736(11)60325-5

Li, H., Wang, J., Wang, P., Rao, Y., and Chen, L. (2016). Resveratrol Reverses the Synaptic Plasticity Deficits in a Chronic Cerebral Hypoperfusion Rat Model. *J. Stroke Cerebrovasc. Dis.* 25, 122–128. doi:10.1016/j.jstrokecerebrovasdis.2015.09.004

Li, L., Chu, L., Ren, C., Wang, J., Sun, S., Li, T., et al. (2019). Enhanced Migration of Bone Marrow-Derived Mesenchymal Stem Cells with Tetramethylpyrazine and its Synergistic Effect on Angiogenesis and Neurogenesis after Cerebral Ischemia in Rats. *Stem Cell Dev* 28, 871–881. doi:10.1089/scd.2018.0254

Li, M., Ouyang, J., Zhang, Y., Cheng, B. C. Y., Zhan, Y., Yang, L., et al. (2018). Effects of Total Saponins from Trillium Tschonoskii Rhizome on Grey and white Matter Injury Evaluated by Quantitative Multiparametric MRI in a Rat Model of Ischemic Stroke. *J. Ethnopharmacol* 215, 199–209. doi:10.1016/j.jep.2018.01.006

Li, M. Z., Zhang, Y., Zou, H. Y., Ouyang, J. Y., Zhan, Y., Yang, L., et al. (2018). Investigation of Ginkgo Biloba Extract (EGb 761) Promotes Neurovascular Restoration and Axonal Remodeling after Embolic Stroke in Rat Using Magnetic Resonance Imaging and Histopathological Analysis. *Biomed. Pharmacother.* 103, 989–1001. doi:10.1016/j.biopha.2018.04.125

Li, M. Z., Zhan, Y., Yang, L., Feng, X. F., Zou, H. Y., Lei, J. F., et al. (2019). MRI Evaluation of Axonal Remodeling after Combination Treatment with Xiaoshuan Enteric-Coated Capsule and Enriched Environment in Rats after Ischemic Stroke. *Front. Physiol.* 10, 1528. doi:10.3389/fphys.2019.01528

Liu, H. S., Shen, H., Harvey, B. K., Castillo, P., Lu, H., Yang, Y., et al. (2011). Post-treatment with Amphetamine Enhances Reinnervation of the Ipsilateral Side Cortex in Stroke Rats. *Neuroimage* 56, 280–289. doi:10.1016/j.neuroimage.2011.02.049

Lu, H., Wang, Y., He, X., Yuan, F., Lin, X., Xie, B., et al. (2012). Netrin-1 Hyperexpression in Mouse Brain Promotes Angiogenesis and Long-Term Neurological Recovery after Transient Focal Ischemia. *Stroke* 43, 838–843. doi:10.1161/STROKEAHA.111.635235

Lu, W., Chen, Z., and Wen, J. (2021). RhoA/ROCK Signaling Pathway and Astrocytes in Ischemic Stroke. *Metab. Brain Dis.* 36, 1101–1108. doi:10.1007/s11011-021-00709-4

Maillard, P., Carmichael, O., Harvey, D., Fletcher, E., Reed, B., Mungas, D., et al. (2013). FLAIR and Diffusion MRI Signals Are Independent Predictors of White Matter Hyperintensities. *AJNR Am. J. Neuroradiol* 34, 54–61. doi:10.3174/ajnr.A3146

Ni, X., Ni, X., Liu, S., and Guo, X. (2013). Medium- and Long-Term Efficacy of Ligustrazine Plus Conventional Medication on Ischemic Stroke: a Systematic Review and Meta-Analysis. *J. Tradit Chin. Med.* 33, 715–720. doi:10.1016/s0254-6272(14)60002-9

Park, K. W., Crouse, D., Lee, M., Karnik, S. K., Sorensen, L. K., Murphy, K. J., et al. (2004). The Axonal Attractant Netrin-1 Is an Angiogenic Factor. *Proc. Natl. Acad. Sci. U S A.* 101, 16210–16215. doi:10.1073/pnas.0405984101

Parkkinen, S., Ortega, F. J., Kuptsova, K., Huttunen, J., Tarkka, I., and Jolkkonen, J. (2013). Gait Impairment in a Rat Model of Focal Cerebral Ischemia. *Stroke Res. Treat.* 2013, 410972. doi:10.1155/2013/410972

Patro, N., Naik, A. A., and Patro, I. K. (2019). Developmental Changes in Oligodendrocyte Genesis, Myelination, and Associated Behavioral Dysfunction in a Rat Model of Intra-generational Protein Malnutrition. *Mol. Neurobiol.* 56, 595–610. doi:10.1007/s12035-018-1065-1

Ramadan, W. S., Abdel-Hamid, G. A., Al-Karim, S., and Abbas, A. T. (2017). Histological, Immunohistochemical and Ultrastructural Study of Secondary Compressed Spinal Cord Injury in a Rat Model. *Folia Histochem. Cytobiol* 55, 11–20. doi:10.5603/FHC.a2017.0001

Rosano, C., Aizenstein, H., Brach, J., Longenberger, A., Studenski, S., and Newman, A. B. (2008). Special Article: Gait Measures Indicate Underlying Focal gray Matter Atrophy in the Brain of Older Adults. *J. Gerontol. A. Biol. Sci. Med. Sci.* 63, 1380–1388. doi:10.1093/gerona/63.12.1380

Saar, G., and Koretsky, A. P. (2019). Manganese Enhanced MRI for Use in Studying Neurodegenerative Diseases. *Front. Neural Circuit* 12, 114. doi:10.3389/fncir.2018.00114

Schober, W. (1986). The Rat Cortex in Stereotaxic Coordinates. *J. Hirnforsch* 27, 121–143.

Stikov, N., Campbell, J. S., Stroh, T., Lavelée, M., Frey, S., Novek, J., et al. (2015). *In Vivo* histology of the Myelin G-Ratio with Magnetic Resonance Imaging. *Neuroimage* 118, 397–405. doi:10.1016/j.neuroimage.2015.05.023

Tan, F., Fu, W., Cheng, N., Meng, D. I., and Gu, Y. (2015). Ligustrazine Reduces Blood-Brain Barrier Permeability in a Rat Model of Focal Cerebral Ischemia and Reperfusion. *Exp. Ther. Med.* 9, 1757–1762. doi:10.3892/etm.2015.2365

van der Holst, H. M., Tuladhar, A. M., Zerbi, V., van Uden, I. W. M., de Laat, K. F., van Leijsen, E. M. C., et al. (2018). White Matter Changes and Gait Decline in Cerebral Small Vessel Disease. *Neuroimage Clin.* 17, 731–738. doi:10.1016/j.nicl.2017.12.007

Wang, J., Ni, G., Liu, Y., Han, Y., Jia, L., and Wang, Y. (2020). Tanshinone IIA Promotes Axonal Regeneration in Rats with Focal Cerebral Ischemia through the Inhibition of Nogo-A/NgR1/RhoA/ROCKII/MLC Signaling. *Drug Des. Devel Ther.* 14, 2775–2787. doi:10.2147/DDDT.S253280

Wang, L. S., Shi, Z. F., Zhang, Y. F., Guo, Q., Huang, Y. W., and Zhou, L. L. (2012). Effect of Xiongbing Compound on the Pharmacokinetics and Brain Targeting of Tetramethylpyrazine. *J. Pharm. Pharmacol.* 64, 1688–1694. doi:10.1111/j.2042-7158.2012.01546.x

Wang, Y., Liu, G., Hong, D., Chen, F., Ji, X., and Cao, G. (2016). White Matter Injury in Ischemic Stroke. *Prog. Neurobiol.* 141, 45–60. doi:10.1016/j.pneurobio.2016.04.005

Xu, X., Ye, L., and Ruan, Q. (2009). Environmental Enrichment Induces Synaptic Structural Modification after Transient Focal Cerebral Ischemia in Rats. *Exp. Biol. Med. (Maywood)* 234, 296–305. doi:10.3181/0804-Rm-128

Yu, K., Wu, Y., Hu, Y., Zhang, Q., Xie, H., Liu, G., et al. (2013). Prior Exposure to Enriched Environment Reduces Nitric Oxide Synthase after Transient MCAO in Rats. *Neurotoxicology* 39, 146–152. doi:10.1016/j.neuro.2013.09.002

Zagrebelsky, M., and Korte, M. (2014). Maintaining Stable Memory Engrams: New Roles for Nogo-A in the Cns. *Neuroscience* 283, 17–25. doi:10.1016/j.neuroscience.2014.08.030

Zeng, G. R., Zhou, S. D., Shao, Y. J., Zhang, M. H., Dong, L. M., Lv, J. W., et al. (2018). Effect of Ginkgo Biloba Extract-761 on Motor Functions in Permanent Middle Cerebral Artery Occlusion Rats. *Phytomedicine* 48, 94–103. doi:10.1016/j.phymed.2018.05.003

Zhan, Y., Li, M. Z., Yang, L., Feng, X. F., Lei, J. F., Zhang, N., et al. (2020). The Three-phase Enriched Environment Paradigm Promotes Neurovascular Restorative and Prevents Learning Impairment after Ischemic Stroke in Rats. *Neurobiol. Dis.* 146, 105091. doi:10.1016/j.nbd.2020.105091

Zhang, J., Chen, S., Shi, W., Li, M., Zhan, Y., Yang, L., et al. (2019). Effects of Xiaoshuan Enteric-Coated Capsule on White and Gray Matter Injury Evaluated by Diffusion Tensor Imaging in Ischemic Stroke. *Cel Transpl.* 28, 671–683. doi:10.1177/0963689718802755

Zhang, J., Zou, H., Zhang, Q., Wang, L., Lei, J., Wang, Y., et al. (2016). Effects of Xiaoshuan Enteric-Coated Capsule on Neurovascular Functions Assessed by Quantitative Multiparametric MRI in a Rat Model of Permanent Cerebral Ischemia. *BMC Complement. Altern. Med.* 16, 198. doi:10.1186/s12906-016-1184-z

Zhao, Y., Liu, Y., and Chen, K. (2016). Mechanisms and Clinical Application of Tetramethylpyrazine (An Interesting Natural Compound Isolated from Ligusticum Wallichii): Current Status and Perspective. *Oxid Med. Cel Longev* 2016, 2124638. doi:10.1155/2016/2124638

Conflict of Interest: The authors declare that the research was conducted in the absence of any commercial or financial relationships that could be construed as a potential conflict of interest.

Publisher's Note: All claims expressed in this article are solely those of the authors and do not necessarily represent those of their affiliated organizations, or those of the publisher, the editors, and the reviewers. Any product that may be evaluated in this article, or claim that may be made by its manufacturer, is not guaranteed or endorsed by the publisher.

frontiers | Frontiers in Neuroscience

ORIGINAL RESEARCH
published: 09 May 2022
doi: 10.3389/fnins.2022.861059

Diprotin A TFA Exerts Neurovascular Protection in Ischemic Cerebral Stroke

Ming-Yue Zhou[1†], Ya-Jie Zhang[1†], Hong-Mei Ding[1,2†], Wei-Feng Wu[1], Wei-Wei Cai[3], Yan-Qiang Wang[4] and De-Qin Geng[1,2*]*

[1] Department of Neurology, The Affiliated Hospital of Xuzhou Medical University, Xuzhou, China, [2] Department of Neurology, Nanjing Medical University, Nanjing, China, [3] Department of Neurology, The Third Hospital of Huai'an, Huai'an, China, [4] Department of Neurology, The Affiliated Hospital of Weifang Medical University, Weifang, China

Background: It has been established that the dipeptidyl peptidase-4 (DPP-4) inhibitor Diprotin A TFA can reduce vascular endothelial (VE)-cadherin disruption by inhibiting the increase in cleaved β-catenin in response to hypoxia, thereby protecting the vascular barrier of human umbilical vein endothelial cells. In this study, we sought to investigate the possible effect of Diprotin A TFA on the VE barrier after cerebral ischemic stroke in mice.

Methods: C57BL/6J mice were divided into five groups, namely, (1) sham, (2) stroke, (3) stroke + dimethyl sulfoxide (DMSO), (4) stroke + Diprotin A TFA, and (5) stroke + Diprotin A TFA + XAV-939. First, the cerebral ischemia model was established by photothrombotic ischemia, followed by intraperitoneal injection with Diprotin A TFA and XAV-939 at doses of 70 μg/kg and 40 mg/kg 30 min once in the morning and once in the evening for 3 days. Immunofluorescence staining and Western blot methods were used to analyze the expression of vascular and blood-brain barrier (BBB)-associated molecular markers in the peri-infarct area.

Results: Compared with the vehicle control group, we found that mice injected with Diprotin A TFA exhibited reduced cerebral infarction volume, increased vascular area and length around the brain injury, increased pericyte and basement membrane coverage, upregulated expression of BBB tight junction proteins, and improved their BBB permeability, whereas the group injected with both drug and inhibitor exhibited significantly aggravated vascular injury and BBB permeability.

Conclusion: Diprotin A TFA can reduce VE-cadherin disruption by inhibiting ischemia-hypoxia-induced β-catenin cleavage to protect blood vessels.

Keywords: ischemic stroke, blood-brain barrier, VE-cadherin, β-catenin, Diprotin A TFA

OPEN ACCESS

Edited by:
Yongjun Sun,
Hebei University of Science and Technology, China

Reviewed by:
Shinsuke Nakagawa,
Fukuoka University, Japan
Liping Wang,
Shanghai Jiao Tong University, China

***Correspondence:**
Yan-Qiang Wang
wangqiangdoctor@126.com
De-Qin Geng
gengdeqin@hotmail.com

[†]These authors have contributed equally to this work

Specialty section:
This article was submitted to Neuropharmacology, a section of the journal Frontiers in Neuroscience

Received: *24 January 2022*
Accepted: *06 April 2022*
Published: *09 May 2022*

Citation:
Zhou M-Y, Zhang Y-J, Ding H-M, Wu W-F, Cai W-W, Wang Y-Q and Geng D-Q (2022) Diprotin A TFA Exerts Neurovascular Protection in Ischemic Cerebral Stroke. Front. Neurosci. 16:861059. doi: 10.3389/fnins.2022.861059

INTRODUCTION

Stroke is well-established as one of the leading causes of death and long-term disability worldwide. During ischemic stroke, additional injury may occur during arterial reperfusion to the tissue following deficient oxygen supply. Such injuries include oxidative stress and disruption of the blood-brain barrier (BBB), followed by intracerebral hemorrhage. The initial ischemic lesions can

reportedly enlarge within minutes to hours, whereas the process of activating spontaneous repair mechanisms often lasts weeks to months (Lo, 2008).

Recovery after brain injury is often determined by the residual neural tissue's reorganization. These repair mechanisms include the plasticity of vascular structures and the repair of neurovascular units (Freitas-Andrade et al., 2020). An increasing body of evidence suggests that the BBB is a unique barrier composed of endothelial cells, tight junctions, pericytes, astrocytic terminal foot processes, and basement membrane, essential for regulating the microenvironment (Fischer et al., 1999; Sandoval and Witt, 2008). Interestingly, it has been reported that endothelial permeability is regulated to a certain extent by the dynamic opening and closing of intercellular adherens junctions (AJs). Current evidence suggests that the AJ in endothelial cells is mainly composed of vascular endothelial cadherin (VE-cadherin), an endothelial-specific member of the cadherin family that binds to protein partners through its cytoplasmic domain, including p120, β-catenin, and plakoglobin (Dejana et al., 2008). β-catenin is an essential regulatory protein of the Wnt signaling pathway that can partially bind to E-cadherin to stabilize intercellular adhesion. VE-cadherin and β-catenin play a key role in regulating vascular permeability and integrity (Hashimoto et al., 2017).

A study demonstrated that VE-cadherin exhibited a serrated staining pattern under hypoxic conditions and Diprotin A could alleviate VE-cadherin's disruption by inhibiting β-catenin cleavage in human umbilical vein endothelial cells (HUVEC) (Hashimoto et al., 2017). Moreover, the dipeptidyl peptidase-4 (DPP-4) Inhibitor could exacerbate vascular leakage from the retina by increasing phosphorylation of Src and VE-cadherin in a mouse diabetic retinopathy model (Labat-gest and Tomasi, 2013). From the above literature, it can be concluded that Diprotin A attenuates hypoxia-induced disruption of VE-cadherin by inhibiting β-catenin cleavage in HUVEC, whereas it induces vascular leakage by enhancing the SDF-1α/CXCR4/Src/VE-cadherin signaling pathway. Accordingly, we hypothesized that Diprotin A plays a role in maintaining VE structure integrity after ischemic stroke.

MATERIALS AND METHODS

Animal Grouping

Adult male C57BL/6J mice (weighing 22–30 g) were purchased from the Laboratory Animal Center of Xuzhou Medical University. First, the mice were randomly divided into six groups, namely, (1) control group: (sham operation group); (2) experimental group: 6 h, 1 day, 3 days, 5 days, and 7 days after cerebral infarction. Tissue from the ischemic penumbra area of the cortex (i.e., brain tissue at the junction of ischemic necrotic tissue and normal tissue) was extracted for Western blotting to quantify smooth muscle actin (α-SMA), solute carrier family 16 member 1 recombinant protein (SLC16A1), and Zonula Occludens-1 (ZO-1) protein expression levels. Subsequently, the optimal time point to analyze the expression of the above proteins was selected, then the mice were randomly divided into the following five groups, namely, (1) sham, (2) stroke, (3) stroke + dimethyl sulfoxide (DMSO), (4) stroke + Diprotin A TFA (Diprotin A TFA [DA]: chemical structural analog of Diprotin A), and (5) stroke + Diprotin A TFA + XAV-939 (XAV-939: β-catenin inhibitor). The following experiments were performed using methods such as immunofluorescence staining and Western blotting.

Cerebral Focal Ischemia

The cerebral ischemia model was induced by photothrombotic ischemia as previously described (Wester et al., 1995; Labat-gest and Tomasi, 2013). Mice were first anesthetized with 10% chloral hydrate intraperitoneally (i.p.) (300 mg/kg in 0.9% saline) and received i.p. injections of 1% Rose Bengal (100 mg/kg in 0.9% saline; Sigma-Aldrich). The head of the mouse was fixed on an animal brain stereotaxic apparatus to ensure that the bregma and λ were in the same horizontal plane (RWD). The scalp was cut open, the anterior fontanel of the skull was exposed, the forelimb representation area of the sensorimotor cortex was identified, and a diaphragmatic pad was placed. The position of the cold light source probe was adjusted to align it with the diaphragm pad, the mouse was given an i.p. injection of 1% Rose Bengal, and the cold light source switched on for irradiation for 12 min (LEICA). At the end of irradiation, the scalp wound was sutured with sutures and the mice were placed in a cage.

Drug Administration

According to the instructions of the manufacturers, Diprotin A TFA (DA) was diluted in normal saline to a concentration of 20 μg/ml, and the drug was i.p. injected into mice at a dose of 70 μg/kg 30 min before establishing the cerebral ischemia model (Lee et al., 2016). Then, drug injections were given once in the morning and once in the evening 3 days. XAV-939 was diluted to a 3.33 mg/ml concentration in a mixed co-solvent (10% DMSO + 90% corn oil), and XAV-939 was i.p. injected at a dose of 40 mg/kg 30 min before modeling (Wang et al., 2020). The drug was injected once daily for 3 days after the model was established.

Nissl Staining

Mice were perfused transcardially with phosphate-buffered saline (PBS; 0.1 m phosphate buffer) and 4% paraformaldehyde (PFA) sequentially, and brains were removed and fixed in 4% PFA overnight at 4°C. Then, the murine brains were cut into coronal 40-μm-thick sections using an oscillating microtome (LEICA). Brain sections were sequentially attached to hydrophobic adhesion slides (VICMED), and Nissl staining was performed when the brain slices were dried to transparency. The slides were first placed in 100, 95, and 80% ethanol solutions for 30 s each, then treated with FD Cresyl Violet Solution TM (FD NeoroTechnologies, Columbia, MD, USA) for 5 min, and washed three times with deionized water. The brain slices were sequentially dehydrated in 50, 70, 80, 90, 95, and 100% ethanol solutions for 60 s each, then treated with xylene for 10 min, and finally fixed with neutral resin.

Infarct Volume Measurement

The brain infarct volume was quantified as infarct volume percentage as previously described (Renolleau et al., 1998; Rousselet et al., 2012; McBride et al., 2015). Cresyl violet-stained brain sections were scanned and imaged using an Epson scanner. The areas of the contralateral hemisphere (C_i), ipsilateral hemisphere (I_i), and ipsilateral non-ischemic region (N_i) were determined using the ImageJ software (NIH), and the infarct volume (%) was calculated as follows:

$$\text{Infarct volume (\%)} = \left(\frac{\sum_i \left((\frac{I_i - N_i}{I_i}) C_i \right)}{2 \sum_i C_i} \right) x\ 100.$$

Evans Blue

The permeability of the BBB was assessed by Evans blue (EB) exosmosis (Goldim et al., 2019; Ahishali and Kaya, 2021). First, 2% EB (3–4 ml/kg; VICMED) was injected into mice *via* the tail vein, and about 1–2 h later, the brains of the mice were perfused and extracted to observe EB extravasation in the cerebral infarction area and assess BBB permeability. After fixing the mouse brain with 4% PFA, the slices were cut with an oscillating microtome to observe EB extravasation under a laser microscope (Olympus).

Immunofluorescence Staining

Brain sections were blocked with 0.5% TritonX-100 and 10% donkey serum in PBS for 1 h at room temperature, after which the sections were incubated with primary antibodies overnight at 4°C. Primary antibodies included rat anti-CD31 (antiplatelet endothelial cell adhesion molecule-1, labels blood vessels) (Xu et al., 2017) (BD Pharmingen, 553369), rabbit anti-desmin (Cell Signaling, #5332), and rabbit anti-collagen IV (Bio-Rad, 2150-1470). The slides were washed and then incubated with Alexa Fluor 488-conjugated species-appropriate secondary antibody (Vector Labs, DI-1488) and Cy3-conjugated streptavidin (Invitrogen, A10522) for 1 h at room temperature in the dark. Then, the slides were stained with 4′,6-diamidino-2-phenylindole for 5 min in the dark, and the brain slices were washed with PBS, then patched and mounted.

Western Blotting

First, tissue proteins in the cerebral ischemic penumbra (brain tissue at the junction of ischemic necrotic and normal tissue) were placed in a tissue lysis solution. The homogenates were immediately lysed on ice and centrifuged at 4°C to obtain protein from the supernatant. Then, the protein concentration was measured using a BCA protein assay kit (Beyotime). Equal amounts of protein were loaded, separated by sodium dodecyl sulfate-polyacrylamide gel electrophoresis, and transferred to NC membranes. Then, incubation with primary antibodies and β-tubulin (ProteinTech, 10094-1-AP) was performed overnight at 4°C. Primary antibodies included rabbit anti-α-SMA (Cell Signaling, 19245), rabbit anti-SLC16A1 (NovusBio, NBP1-59656), mouse anti-ZO-1 (Invitrogen, 33-9100), rabbit anti-occludin (Invitrogen, 40-4700), and rabbit anti-PDGFR-β (Cell Signaling, 3169). Then, protein samples were incubated with secondary antibodies for 1 h at room temperature. The target proteins were visualized using a ChemiDoc imaging system (Bio-Rad). For quantification, the density of the blots of interest was normalized to that of tubulin, and optical density was assessed using ImageJ analysis software.

Image Analysis

Brain angioarchitecture analyses were performed using the open-source "Angiotool" software (National Cancer Institute, USA) (Zudaire et al., 2011). CD31-stained brain sections were used to analyze blood vessel's area and length. The vascular area was defined as the area of the segmented vessel. The vascular length was defined as the sum of the Euclidean distances between all vessel pixels in the image (Gambardella et al., 2012). Desmin- and CD31-positive fluorescent areas were determined to assess pericyte coverage on vessels using the ImageJ area measurement tool. Pericyte coverage was described as the percentage of desmin-positive fluorescent area covering the CD31-positive capillary area (Bell et al., 2010). The basement membrane coverage was defined as the percentage of collagen IV-positive fluorescent area covering the CD31-positive capillary area (Xu et al., 2017).

Statistical Analysis

All statistical analyses were performed using the GraphPad Prism 8.0 software. For normally distributed measurements, one-way ANOVA followed by Tukey's *post-hoc* test was used for three or more groups. The Kruskal-Wallis test (three or more groups) was used for measurements that were not normally distributed. $p < 0.05$ was considered statistically significant, and data were presented as mean ± SEM from three independent experiments.

RESULTS

Changes in Cerebrovascular Sertoli Cell, Endothelial Cell, and BBB Tight Junction Protein After Photothrombotic Stroke

To understand the expression of pericyte α-SMA (labeled arterioles) (Xu et al., 2017), SLC16A1 (expressed in venous capillary endothelial cells) (Yao et al., 2020), and BBB tight junction protein ZO-1 around ischemic infarcts in the cerebral cortex, Western blot experiments were performed. The mouse brain was intact for 2,3,5-triphenyltetrazolium chloride (TTC) staining after cerebral ischemia (Joshi et al., 2004; Yi et al., 2020), in which the cortex's white area was the cerebral infarction area and the area surrounded by the black line was the ischemic penumbra area; the tissue at this site was harvested for Western blot (**Figure 1A**). First, wildtype mice were subjected to a sham operation and cerebral ischemia and the ischemic penumbra brain tissues were extracted for Western blot (**Figure 1B**). The results revealed that the expression levels of α-SMA, SLC16A1, and ZO-1 were significantly reduced on day 3 (**Figures 1C–E**), indicating that the degree of damage to cerebral vessel structures was the most severe on day 3 after the model was established.

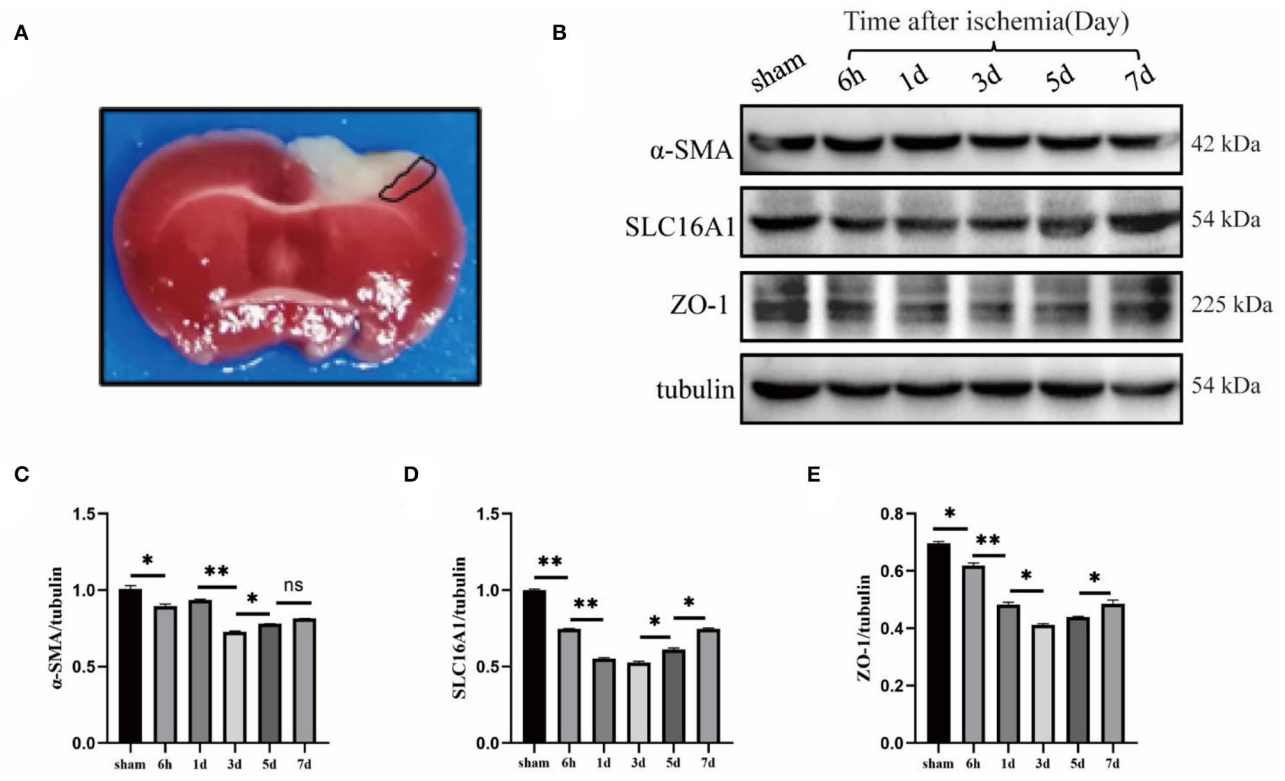

FIGURE 1 | Changes of cerebrovascular Sertoli cell, endothelial cell, and blood-brain barrier tight junction protein after photothrombotic stroke. **(A)** TTC staining image of cerebral ischemia model induced by photothrombosis. The white area of cortex is the cerebral infarction area, and the area surrounded by the black lines is the ischemic penumbra area (i.e., the junction between ischemic necrotic tissue and normal tissue), which is usually used for Western blot (WB) experiment of brain tissue in this area. **(B)** Wildtype mice were used to do sham, 6-h, 1-day, 3-day, 5-day, and 7-day time points of cerebral ischemia model, WB. **(C–E)** The statistical results showed that α-SMA (smooth muscle actin), SLC16A1 (venous-capillary marker) and ZO-1 (Zonula Occludens-1) were all significantly reduced in expression on day 3, which was statistically significant. $n = 3$ in all the experimental groups. Data are represented as mean with SEM. $^{*}p < 0.05$, $^{**}p < 0.01$. α-SMA, smooth muscle actin; SLC16A1, solute carrier family 16 member 1 recombinant protein; ZO-1, Zonula Occludens-1.

The subsequent experiments were performed 3 days after the ischemia model.

DA Reduces Cerebral Ischemic Damage

First, DA was i.p. injected into mice at 60 days, followed by photothrombosis 30 min later to establish a cerebral ischemia model. DA was injected once in the morning and once in the evening for the next 3 days. XAV-939 was injected as described above, and Nissl staining of brain sections was conducted (**Figure 2A**). The area surrounded by a red line in the right upper cortex of the brain slice is the infarct area, which is seen to be lighter in color than the surrounding normal tissue (Joshi et al., 2004; Yi et al., 2020), and the cortical infarct areas are all circled with red circles (**Figure 2B**). The cerebral infarct size was significantly reduced in the DA-treated group and increased in the DA- and XAV-939-treated group (**Figure 2C**). Moreover, the cerebral infarction volume in the DA-treated group was lower than that in the vehicle control group, the degree of brain injury was mild, and the infarct volume in the DA- and XAV-939-treated group was increased, indicating that XAV-939 exerts an inhibitory effect on the efficacy of DA drug (**Figure 2D**).

DA Improves the Permeability of the BBB After Cerebral Ischemic Injury

It is well-recognized that EB is an azo dye preparation for assessing capillary permeability since its molecular weight is similar to plasma albumin and its high affinity for plasma albumin in the blood. As plasma albumin does not normally penetrate the BBB, EB bound to plasma albumin cannot stain the BBB if it is intact. Therefore, the permeability of the BBB can be assessed by the extravasation of EB (Goldim et al., 2019). As shown, EB extravasation in the brain-injured area was significantly reduced in DA-treated mice compared with control mice, indicating that BBB permeability was reduced in DA mice, while EB extravasation in the brain-injured area was increased in mice treated with both DA and XAV-939, indicating that XAV-939 could inhibit the drug efficacy of DA to a certain extent (**Figure 3A**). Statistical analysis of the mean fluorescence intensity of EB extravasation in the cerebral infarction area of the five mice groups showed that EB's mean fluorescence intensity was reduced in the DA-treated group compared with the vehicle control group (**Figure 3B**). Brain sections obtained after EB injection in mice were

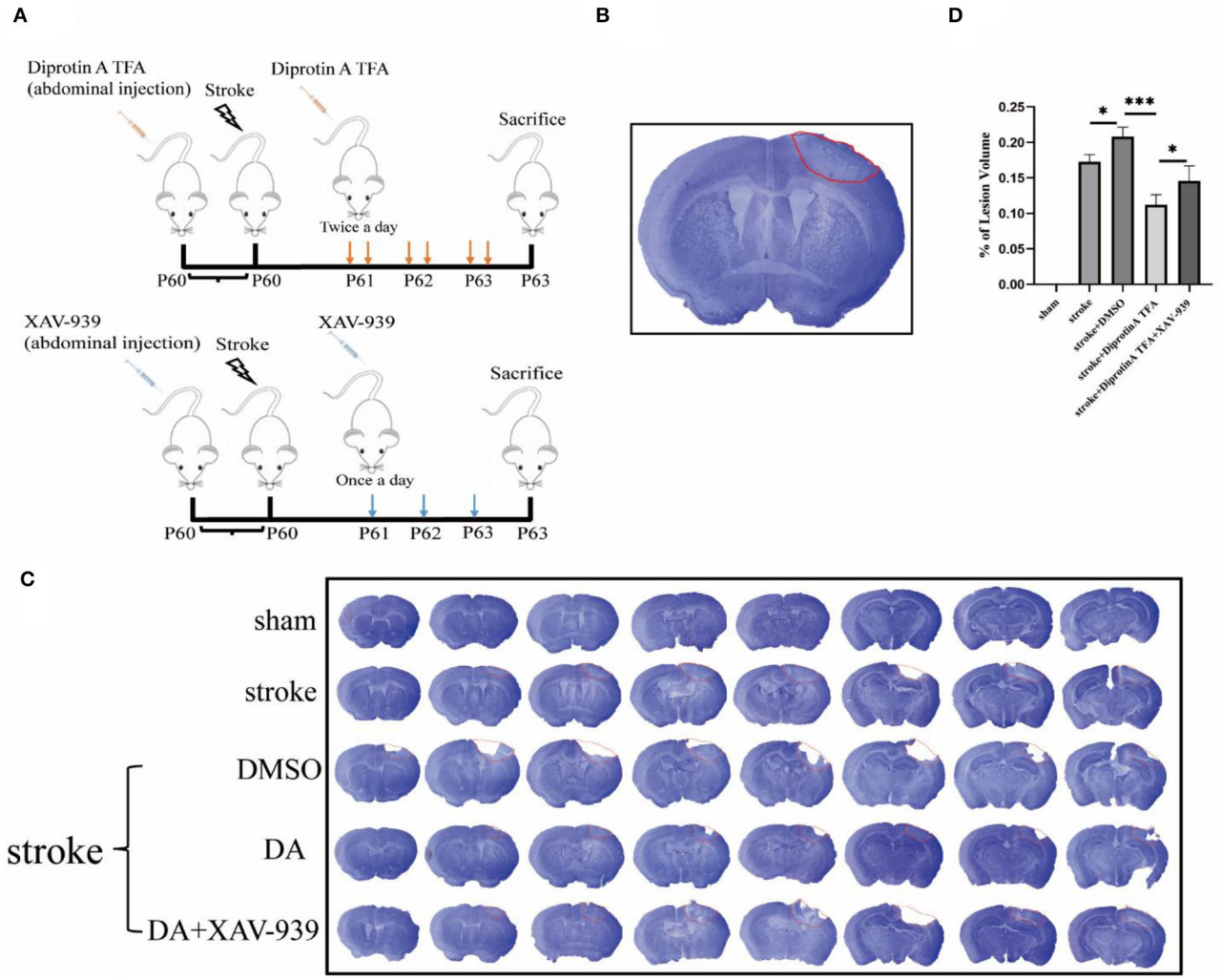

FIGURE 2 | Diprotin A TFA reduces cerebral ischemic damage. **(A)** A simple diagram of the experimental process time of using mice from intraperitoneal injection of drugs to make a model to perfusing the brain or extracting protein. **(B)** A Nissl-stained image of a brain slice, with a section thickness of 40 μm, and the area surrounded by red lines in the upper right part of the brain slice is the infarct area. **(C)** The Nissl staining of five groups of mice after 3 days of photothrombotic cerebral infarction model, The slice thickness is 40 μm. **(D)** Statistical analysis of the cerebral infarction areas of the five groups of mice showed that the cerebral infarction volume of the group injected with DA mice was reduced compared with the vehicle control group. $n = 3$ per group. Data are represented as mean with SEM. $^{*}p < 0.05$, $^{***}p < 0.001$. DA, Diprotin A TFA; XAV-939, β-catenin inhibitor.

observed under a fluorescence microscope, and EB presented red fluorescence only in the cortical infarct area, with red granules as leaky EB (Zhao et al., 2020). Taken together, the above results demonstrated that DA improved BBB permeability (**Figure 3C**).

DA Reduces the Degree of Vascular Injury Around Cerebral Infarction

It is well-established that Diprotin A attenuates hypoxia-induced VE-cadherin destruction by inhibiting β-catenin cleavage in HUVEC (Hashimoto et al., 2017). VE-cadherin is an essential cadherin in VE cells and plays a crucial role in vascular permeability (Dejana et al., 2008). Given that Diprotin A attenuates VE-cadherin destruction after hypoxia, we speculated that DA is essential for the VE structure's integrity. After ischemic brain injury, the vascular density of the surrounding tissue in the cerebral infarction group was reduced compared with the sham group, which was caused by vascular injury after stroke. Accordingly, we explored whether DA induces vascular changes after a cerebral ischemic injury. After conducting immunofluorescence staining for CD31, we found that the vascular density increased in the DA-treated group compared with the vehicle control group (**Figure 4A**). Statistical analysis of staining images in the five groups showed that vascular area and length were increased in the DA-treated group compared with the control group, but decreased in the group that received both DA and XAV-939, indicating that DA did affect the peripheral vessels of the cerebral infarct, thereby reducing the

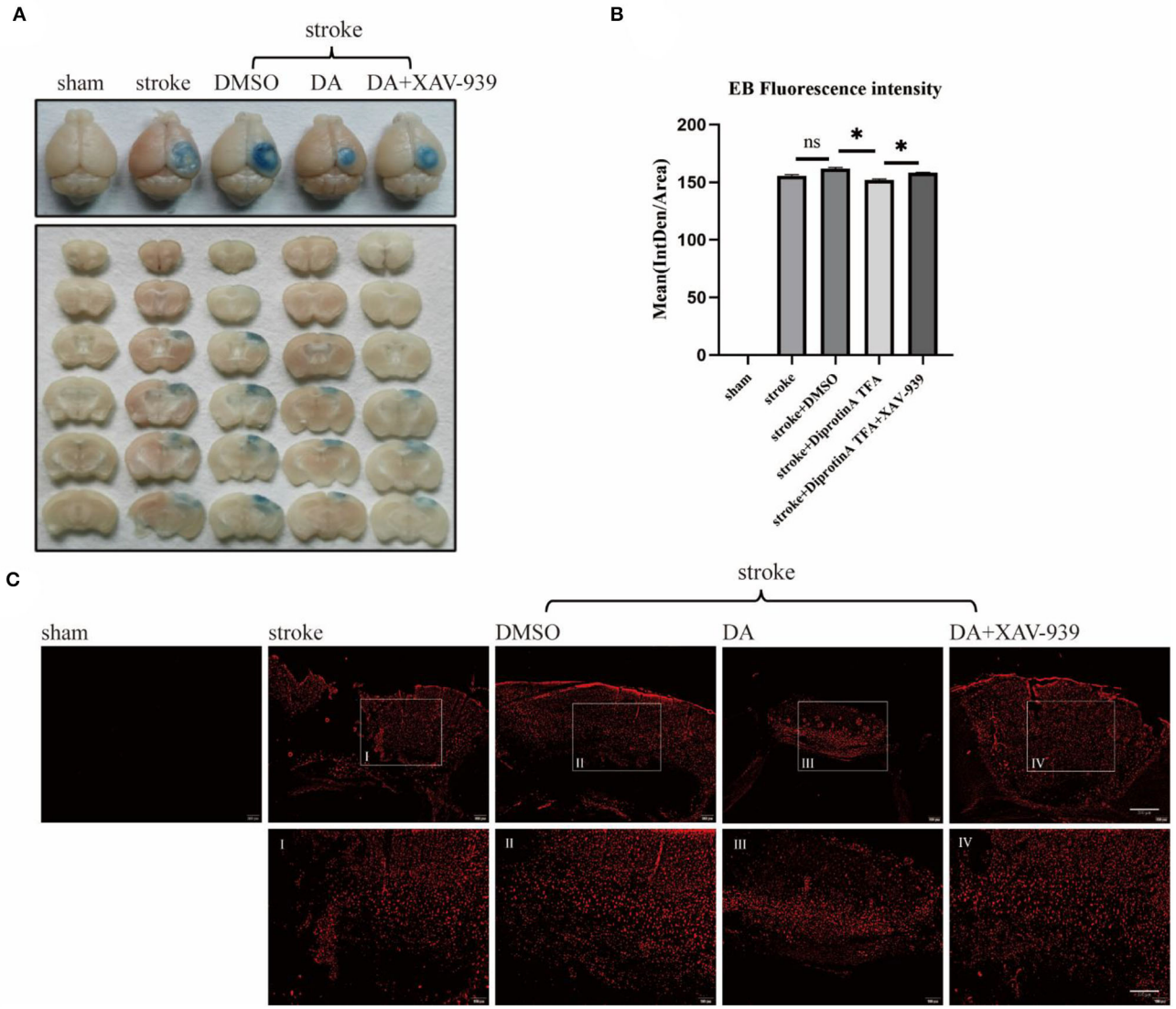

FIGURE 3 | Diprotin A TFA improves the permeability of the BBB after cerebral ischemic injury. **(A)** To inject 2% EB into the tail vein of five groups of mice to observe the extravasation of EB. **(B)** The mean fluorescence intensity of EB extravasation in the cerebral infarction area of the five groups of mice was statistically analyzed. $n = 3$ per group. Data are represented as mean with SEM. $^*p < 0.05$. **(C)** Mice were injected with 2% EB into the tail vein, and the brains were perfused to obtain brain sections for immunofluorescence analysis. The slice thickness is 40 μm. Bar = 200 μm [**(C)**, upper], bar = 100 μ m [**(C)**, bottom]. BBB, blood-brain barrier; EB, Evans blue.

degree of vascular injury and improving vascular remodeling (**Figures 4B,C**).

DA Increases Vascular-Pericyte and Endothelial Basement Membrane Coverage in Peri-Infarct Cortex

Substantial evidence suggests that the structural integrity of the BBB is mainly composed of endothelial cells, tight junctions, pericytes, astrocyte foot processes, and basement membrane (Kadry et al., 2020). Accordingly, we investigated whether DA could affect BBB integrity. Therefore, brain slices from three groups of mice were subjected to immunofluorescence co-staining for CD31, desmin (labeled pericytes) (Xu et al., 2017), and collagen IV (labeled basement membrane) (**Figures 5A,B**) (Yao et al., 2020). The results showed that the pericyte coverage of stained vessels in the peri-infarct cortex increased in the DA-treated group compared with the control group and decreased in the DA- and XAV-939-treated group, indicating that DA improved BBB integrity after ischemic stroke (**Figure 5C**). The statistical analysis results of VE basement membrane coverage were consistent with pericyte coverage, indicating that DA improves BBB integrity after ischemic stroke (**Figure 5D**).

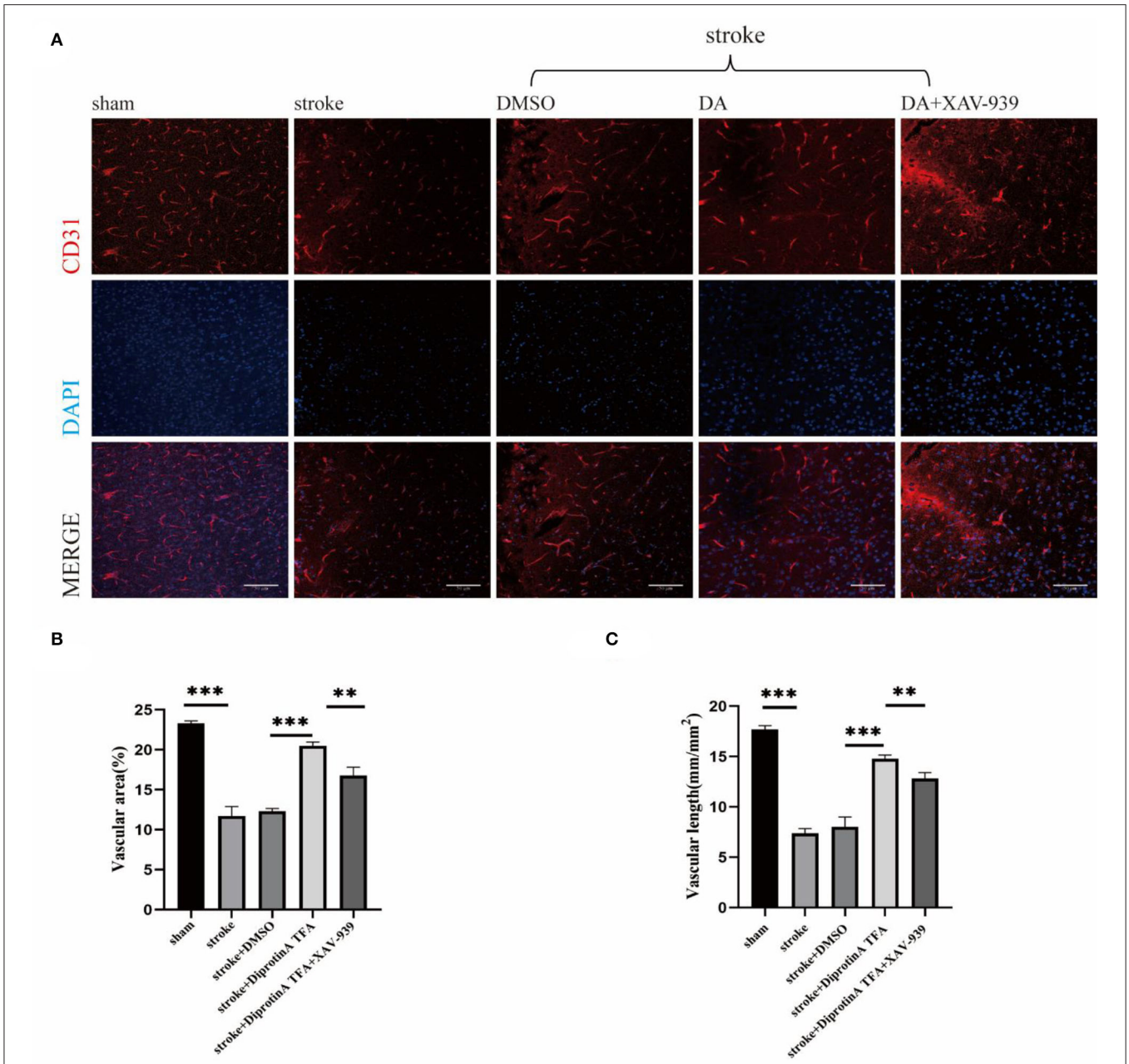

FIGURE 4 | Diprotin A TFA reduces the degree of vascular injury around cerebral infarction. **(A)** There are immunofluorescent staining images of CD31 (red) (antiplatelet endothelial cell adhesion molecule-1), which labels blood vessels. The slice thickness is 40 μm. Bar = 50 μm. **(B)** The statistical plot of vascular area. **(C)** The statistical plot of vascular length. The DA group had a statistically significant increase in the area and length of stained vessels relative to the vehicle control group. $n = 3$ per group. Data are represented as mean with SEM. $^{**}p < 0.01$, $^{***}p < 0.001$.

DA Regulates the Expression of Tight Junction Protein at the BBB and Pericyte

Tight junctions and pericytes are reportedly affected when the BBB is damaged (Castro Dias et al., 2019). We subsequently analyzed the expression levels of the associated proteins. Western blotting analysis of BBB-associated tight junction protein (occludin, ZO-1) and pericyte (PDGFR-β) (Bell et al., 2010) was conducted in penumbra tissues of five groups with cerebral ischemic injury (**Figure 6A**). Statistical analysis showed that occludin and ZO-1 expression levels were increased in the peri-infarct cortex in the DA-treated group compared with the control group, whereas the DA- and XAV-939-treated group exhibited lower levels than in the DA-treated group, and PDGFR-β expression was comparable (**Figures 6B–D**). These results indicate that DA can upregulate BBB tight junction proteins and pericytes, and can maintain BBB integrity after ischemic

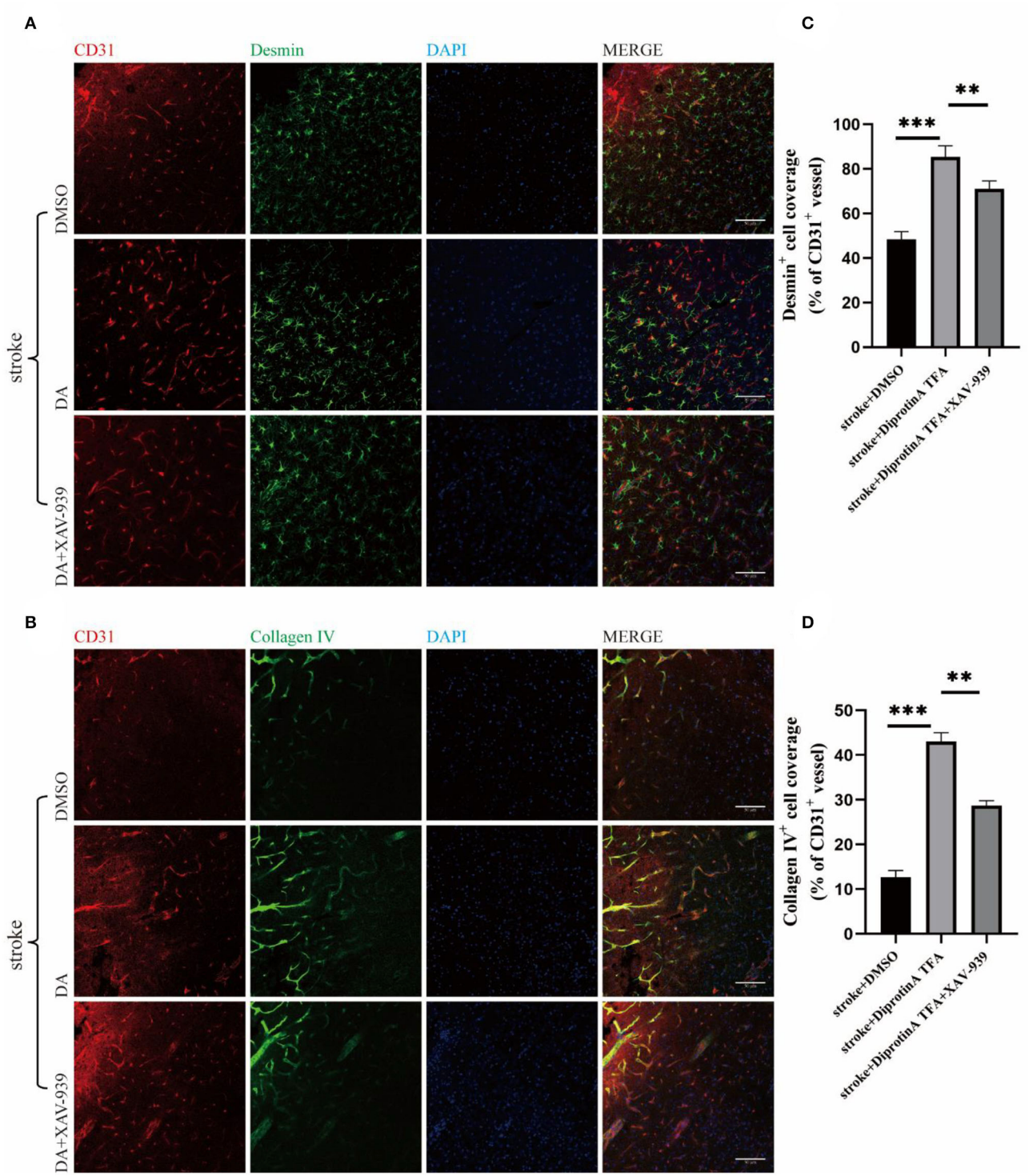

FIGURE 5 | Diprotin A TFA increases vascular-pericyte and endothelial basement membrane coverage in peri-infarct cortex. **(A)** Immunofluorescent staining images of CD31 (red) and desmin (green) (desmin, labeled pericytes) co-staining. The slice thickness is 40 μm. Bar = 50 μm. **(B)** Immunofluorescent staining images of CD31 (red) and collagen IV (green) (type IV collagen, labeled basement membrane) co-staining, with a section thickness of 40 μm. Bar = 50 μm. **(C)** A statistical plot of vascular pericyte coverage. **(D)** A statistical plot of vascular endothelial basement membrane coverage. Compared with the vehicle control group, it can be seen that the coverage rate of stained vascular pericytes in the DA injection group was increased compared with the vehicle control group. Vascular endothelial basement membrane coverage results were the same as above. $n = 3$ per group. Data are represented as mean with SEM. $^{**}p < 0.01$, $^{***}p < 0.001$.

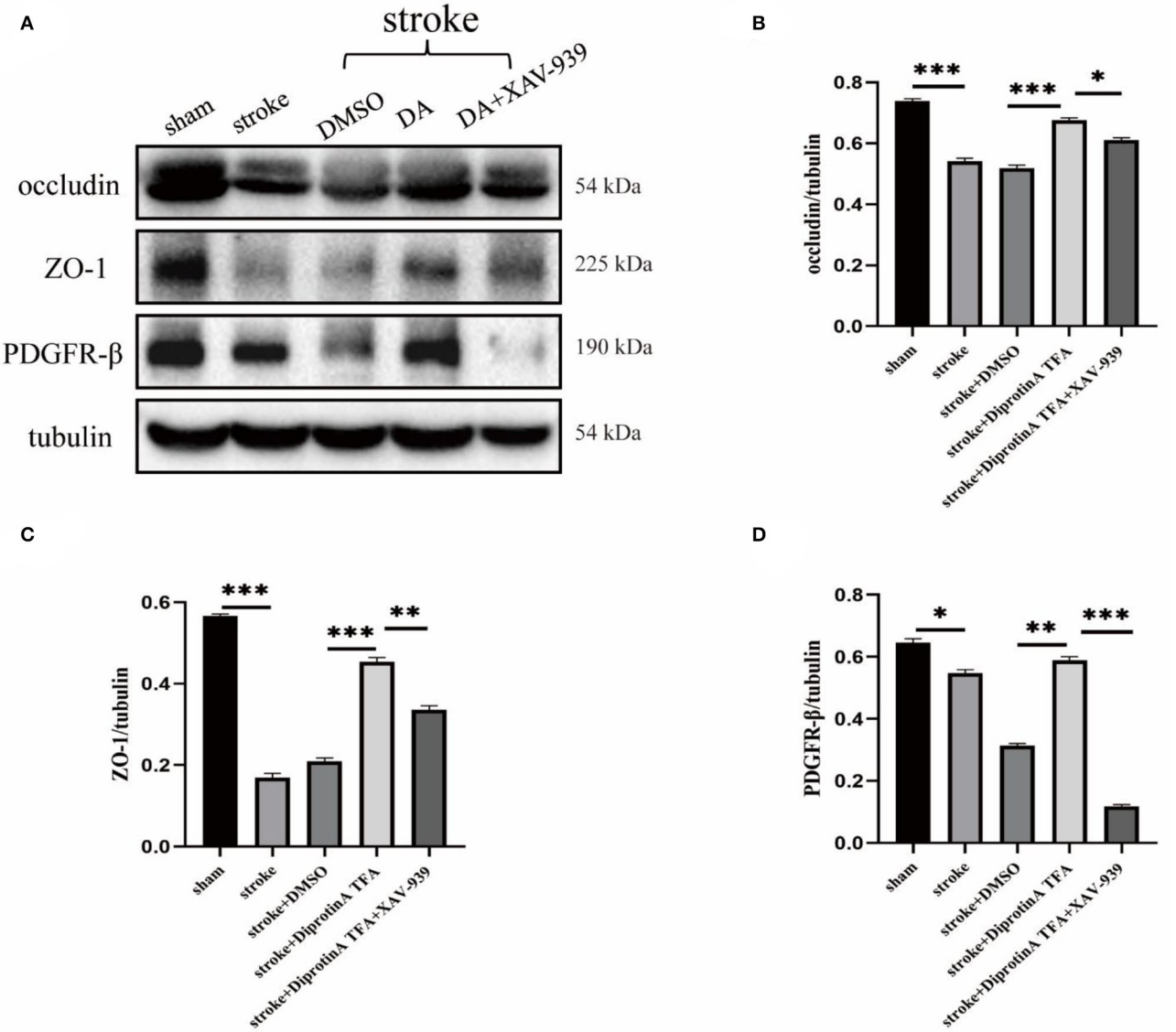

FIGURE 6 | Diprotin A TFA regulates the expression of tight junction protein at the BBB and pericyte. **(A)** Western blot images of BBB-associated tight junction protein (occludin, ZO-1) and pericyte (PDGFR-β) in the penumbra tissue of five groups of mice with cerebral ischemic injury. **(B–D)** The results showed that the expression levels of occludin, ZO-1, and PDGFR-β were upregulated in the group injected with DA compared with the vehicle control group, whereas the expression levels were downregulated in the group injected with DA and β-catenin inhibitor. $n = 3$ per group. Data are represented as mean with SEM. $^{*}p < 0.05$, $^{**}p < 0.01$, $^{***}p < 0.001$.

stroke. Meanwhile, XAV-939 can downregulate DA and inhibit β-catenin cleavage, attenuating the vasoprotective mechanism of VE-cadherin disruption in the DA- and XAV-939-treated group, thereby downregulating BBB tight junction protein levels and increasing BBB permeability.

DISCUSSION

In this study, we aimed to explore the effect of DA on the neurovasculature during cerebral ischemia. Importantly, we found that vascular pericytes and the BBB tight junctions were altered following cerebral ischemia. Then, Nissl staining was used to evaluate the cerebral infarction volume, and EB extravasation to assess the BBB structural integrity, vascular area and length, and the pericyte and basement membrane coverage in blood vessels. Findings of this study indicate that DA reduces vascular injury around cerebral infarction, improves BBB integrity and permeability, contributes to vascular remodeling, and is essential for ischemic brain repair.

In recent years, DPP-4 inhibitors have been widely used to treat diabetes (Sun et al., 2020). Interestingly, DPP-4 inhibition improves cardiac function and reduces myocardial ischemia through SDF-1a/CXCR4-mediated STAT3 signaling (Kubota et al., 2016) and exerts an antiapoptotic effect on HUVEC under

hypoxic conditions (Nagamine et al., 2017). Accordingly, we hypothesized that DPP-4 inhibitors yield a beneficial effect on cardiovascular and cerebrovascular diseases.

AJs in endothelial cells are mainly composed of VE-cadherin, connected to the AJ proteins p120, β-catenin, and plakoglobin through its cytoplasmic tail (Weis and Nelson, 2006). The importance of VE-cadherin has been emphasized in adult mice for maintaining vascular integrity, given that anti-VE-cadherin antibody administration leads to a dramatic increase in permeability, vascular fragility, and hemorrhage (Corada et al., 1999). Another study that assessed the effect of β-catenin on specific gene inactivation in mouse embryonic endothelial cells suggested its role in vascular permeability and integrity (Cattelino et al., 2003). VE-cadherin and β-catenin are known to play key roles in regulating vascular permeability and integrity irrespective of the mechanism of action (Guo et al., 2008; Rho et al., 2017). Intriguingly, it has been documented that Diprotin A can improve the staining pattern of serrated VE-cadherin by attenuating the increase in cleaved β-catenin levels during hypoxia, thus indicating that Diprotin A protects endothelial AJ from hypoxia (Hashimoto et al., 2017). Therefore, we speculate that Diprotin A exerts a protective effect on the VE barrier during ischemia-hypoxia.

Herein, DA (chemical structural similarity of Diprotin A and DPP-4 inhibitor; Lee et al., 2016) was used to establish a mice model of cerebral ischemia to observe the changes in various parameters. Meanwhile, mice were treated with XAV-939 (β-catenin inhibitor, which can stimulate β-catenin degradation; Huang et al., 2009) and DA to assess the effect of XAV-939 on the pharmacological efficacy of DA. Interestingly, we found that the cerebral infarction volume was significantly reduced in the DA injection group and increased in the DA- and XAV-939-treated group, indicating that DA could improve cerebral ischemic injury, and XAV-939 suppressed the efficacy of DA. Next, immunofluorescence staining using CD31 (Lertkiatmongkol et al., 2016) showed that DA-treated mice had increased vascular area and length in the peri-infarct cortex compared with the control group, and DA alleviated the degree of vascular injury around the cerebral infarction. As shown in **Figure 4**, vascular density was increased in the DA-treated group compared with the vehicle control group. This effect was induced by vascular injury after an ischemic stroke. It should be borne in mind that the increase in vascular density may be independent of angiogenesis, given that ample evidence substantiates that microvessels on the infarcted side begin to grow 1–2 days after cerebral infarction and peak on day 7 (Morris et al., 2003). However, the optimal experimental time point selected was day 3 after cerebral infarction. The increased vascular density observed in the DA injection group compared with the DMSO injection group (**Figure 4**) may be attributed to vascular injury. However, the possible role of induction factors of angiogenesis cannot be ruled out. Subsequently, immunofluorescence with CD31 and desmin and collagen IV co-staining were performed. The results showed that the pericyte coverage and endothelial basement membrane coverage of blood vessels in the peri-infarct cortex stained in the DA injection group were increased compared with the control group and decreased in the DA and XAV-939 groups, indicating that DA improved BBB integrity after ischemic stroke. It is widely acknowledged that EB extravasation and tight junction protein expression levels can reflect BBB structure integrity and permeability (Castro Dias et al., 2019; Goldim et al., 2019). Importantly, we demonstrated that DA improves BBB permeability by reducing leakage EB and upregulating tight junction protein content. Our experiments corroborated that DA could alleviate VE-cadherin disruption by inhibiting ischemia-hypoxia-induced β-catenin cleavage, thus exerting a vasoprotective effect. Moreover, the β-catenin inhibitor downregulated this vasoprotective mechanism, which led to the exacerbation of VE-cadherin disruption after hypoxia in the DA and XAV-939 groups, substantiating that DA exerts a protective effect on vascular injury after cerebral ischemia.

DATA AVAILABILITY STATEMENT

The original contributions presented in the study are included in the article/supplementary material, further inquiries can be directed to the corresponding author/s.

ETHICS STATEMENT

The animal study was reviewed and approved by the Committee on the Ethics of Animal Experiments of Xuzhou Medical University (Xuzhou, China).

AUTHOR CONTRIBUTIONS

D-QG and Y-QW formulated the study concept and designed the studies. M-YZ and Y-JZ performed the studies. M-YZ, H-MD, and W-FW executed the experiments and interpreted the results. M-YZ and W-WC assisted in editing the revised manuscript. M-YZ wrote and edited the manuscript. All authors contributed to the article and approved the submitted version.

FUNDING

This work was supported by the National Natural Science Foundation of China (No. 81870943) and the Shandong Provincial Nature Fund Joint Special Fund Project (ZR2018LH006).

REFERENCES

Ahishali, B., and Kaya, M. (2021). Evaluation of blood-brain barrier integrity using vascular permeability markers: evans blue, sodium fluorescein, albumin-alexa fluor conjugates, and horseradish peroxidase. *Methods Mol. Biol.* 2367, 87–103. doi: 10.1007/7651_2020_316

Bell, R. D., Winkler, E. A., Sagare, A. P., Singh, I., LaRue, B., Deane, R., et al. (2010). Pericytes control key neurovascular functions and neuronal

phenotype in the adult brain and during brain aging. *Neuron* 68, 409–427. doi: 10.1016/j.neuron.2010.09.043

Castro Dias, M., Mapunda, J. A., Vladymyrov, M., and Engelhardt, B. (2019). Structure and junctional complexes of endothelial, epithelial and glial brain barriers. *Int. J. Mol. Sci*. 20, 5372. doi: 10.3390/ijms20215372

Cattelino, A., Liebner, S., Gallini, R., Zanetti, A., Balconi, G., Corsi, A., et al. (2003). The conditional inactivation of the beta-catenin gene in endothelial cells causes a defective vascular pattern and increased vascular fragility. *J. Cell Biol*. 162, 1111–1122. doi: 10.1083/jcb.200212157

Corada, M., Mariotti, M., Thurston, G., Smith, K., Kunkel, R., Brockhaus, M., et al. (1999). Vascular endothelial-cadherin is an important determinant of microvascular integrity *in vivo*. *Proc. Natl. Acad. Sci. U.S.A*. 96, 9815–9820. doi: 10.1073/pnas.96.17.9815

Dejana, E., Orsenigo, F., and Lampugnani, M. G. (2008). The role of adherens junctions and VE-cadherin in the control of vascular permeability. *J. Cell Sci*. 121, 2115–2122. doi: 10.1242/jcs.017897

Fischer, S., Clauss, M., Wiesnet, M., Renz, D., Schaper, W., and Karliczek, G. F. (1999). Hypoxia induces permeability in brain microvessel endothelial cells via VEGF and NO. *Am. J. Physiol*. 276, C812–C820. doi: 10.1152/ajpcell.1999.276.4.C812

Freitas-Andrade, M., Raman-Nair, J., and Lacoste, B. (2020). Structural and functional remodeling of the brain vasculature following stroke. *Front. Physiol*. 11, 948. doi: 10.3389/fphys.2020.00948

Gambardella, L., Zudaire, E., and Vermeren, S. (2012). "Quantitative analysis of angiogenesis in the allantois explant model," in *The Textbook of Angiogenesis and Lymphangiogenesis: Methods and Applications* (Dordrecht: Springer), 189–204. doi: 10.1007/978-94-007-4581-0_12

Goldim, M., Della Giustina, A., and Petronilho, F. (2019). Using evans blue dye to determine blood-brain barrier integrity in rodents. *Curr. Protoc. Immunol*. 126, e83. doi: 10.1002/cpim.83

Guo, M., Breslin, J. W., Wu, M. H., Gottardi, C. J., and Yuan, S. Y. (2008). VE-cadherin and beta-catenin binding dynamics during histamine-induced endothelial hyperpermeability. *Am. J. Physiol. Cell Physiol*. 294, C977–C984. doi: 10.1152/ajpcell.90607.2007

Hashimoto, N., Ikuma, K., Konno, Y., Hirose, M., Tadokoro, H., Hasegawa, H., et al. (2017). DPP-4 inhibition protects human umbilical vein endothelial cells from hypoxia-induced vascular barrier impairment. *J. Pharmacol. Sci*.135, 29–36. doi: 10.1016/j.jphs.2017.08.005

Huang, S. M., Mishina, Y. M., Liu, S., Cheung, A., Stegmeier, F., Michaud, G. A., et al. (2009). Tankyrase inhibition stabilizes axin and antagonizes Wnt signalling. *Nature*. 461, 614–620. doi: 10.1038/nature08356

Joshi, C. N., Jain, S. K., and Murthy, P. S. (2004). An optimized triphenyltetrazolium chloride method for identification of cerebral infarcts. *Brain Res. Brain Res. Protoc*. 13, 11–17. doi: 10.1016/j.brainresprot.2003.12.001

Kadry, H., Noorani, B., and Cucullo, L. (2020). A blood-brain barrier overview on structure, function, impairment, and biomarkers of integrity. *Fluids Barriers CNS*. 17, 69. doi: 10.1186/s12987-020-00230-3

Kubota, A., Takano, H., Wang, H., Hasegawa, H., Tadokoro, H., Hirose, M., et al. (2016). DPP-4 inhibition has beneficial effects on the heart after myocardial infarction. *J. Mol. Cell. Cardiol*. 91, 72–80. doi: 10.1016/j.yjmcc.2015.12.026

Labat-gest, V., and Tomasi, S. (2013). Photothrombotic ischemia: a minimally invasive and reproducible photochemical cortical lesion model for mouse stroke studies. *J. Vis. Exp*. 76, 50370. doi: 10.3791/50370

Lee, C. S., Kim, Y. G., Cho, H. J., Park, J., Jeong, H., Lee, S. E., et al. (2016). Dipeptidyl Peptidase-4 inhibitor increases vascular leakage in retina through VE-cadherin Phosphorylation. *Sci. Rep*. 6, 29393. doi: 10.1038/srep 29393

Lertkiatmongkol, P., Liao, D., Mei, H., Hu, Y., and Newman, P. J. (2016). Endothelial functions of platelet/endothelial cell adhesion molecule-1 (CD31). *Curr. Opin. Hematol*. 23, 253–259. doi: 10.1097/MOH.0000000000000239

Lo, E. H. (2008). A new penumbra: transitioning from injury into repair after stroke. *Nat. Med*. 14, 497–500. doi: 10.1038/nm1735

McBride, D. W., Klebe, D., Tang, J., and Zhang, J. H. (2015). Correcting for brain swelling's effects on infarct volume calculation after middle cerebral artery occlusion in rats. *Transl. Stroke Res*. 6, 323–338. doi: 10.1007/s12975-015-0400-3

Morris, D. C., Yeich, T., Khalighi, M. M., Soltanian-Zadeh, H., Zhang, Z. G., and Chopp, M. (2003). Microvascular structure after embolic focal cerebral ischemia in the rat. *Brain Res*. 972, 31–37. doi: 10.1016/S0006-8993(03)02433-8

Nagamine, A., Hasegawa, H., Hashimoto, N., Yamada-Inagawa, T., Hirose, M., Kobara, Y., et al. (2017). The effects of DPP-4 inhibitor on hypoxia-induced apoptosis in human umbilical vein endothelial cells. *J. Pharmacol. Sci*. 133, 42–48. doi: 10.1016/j.jphs.2016.12.003

Renolleau, S., Aggoun-Zouaoui, D., Ben-Ari, Y., and Charriaut-Marlangue, C. (1998). A model of transient unilateral focal ischemia with reperfusion in the P7 neonatal rat: morphological changes indicative of apoptosis. *Stroke*. 29, 1454–1461. doi: 10.1161/01.STR.29.7.1454

Rho, S. S., Ando, K., and Fukuhara, S. (2017). Dynamic regulation of vascular permeability by vascular endothelial cadherin-mediated endothelial cell-cell junctions. *J. Nippon Med. Sch*. 84, 148–159. doi: 10.1272/jnms.84.148

Rousselet, E., Kriz, J., and Seidah, N. G. (2012). Mouse model of intraluminal MCAO: cerebral infarct evaluation by cresyl violet staining. *J. Vis. Exp*. 69, 4038. doi: 10.3791/4038

Sandoval, K. E., and Witt, K. A. (2008). Blood-brain barrier tight junction permeability and ischemic stroke. *Neurobiol. Dis*. 32, 200–219. doi: 10.1016/j.nbd.2008.08.005

Sun, Z. G., Li, Z. N., and Zhu, H. L. (2020). The research progress of DPP-4 inhibitors. *Mini Rev. Med. Chem*. 20, 1709–1718. doi: 10.2174/1389557520666200628032507

Wang, L., Geng, J., Qu, M., Yuan, F., Wang, Y., Pan, J., et al. (2020). Oligodendrocyte precursor cells transplantation protects blood-brain barrier in a mouse model of brain ischemia via Wnt/β-catenin signaling. *Cell Death Dis*. 11, 9. doi: 10.1038/s41419-019-2206-9

Weis, W. I., and Nelson, W. J. (2006). Re-solving the cadherin-catenin-actin conundrum. *J. Biol. Chem*. 281, 35593–35597. doi: 10.1074/jbc.R600027200

Wester, P., Watson, B. D., Prado, R., and Dietrich, W. D. (1995). A photothrombotic 'ring' model of rat stroke-in-evolution displaying putative penumbral inversion. *Stroke* 26, 444–450. doi: 10.1161/01.STR.26.3.444

Xu, H., Cao, Y., Yang, X., Cai, P., Kang, L., Zhu, X., et al. (2017). ADAMTS13 controls vascular remodeling by modifying VWF reactivity during stroke recovery. *Blood*. 130, 11–22. doi: 10.1182/blood-2016-10-747089

Yao, L. L., Hu, J. X., Li, Q., Lee, D., Ren, X., Zhang, J. S., et al. (2020). Astrocytic neogenin/netrin-1 pathway promotes blood vessel homeostasis and function in mouse cortex. *J. Clin. Invest*. 130, 6490–6509. doi: 10.1172/JCI132372

Yi, K. S., Choi, C. H., Jung, C., Lee, Y., Jeon, C. Y., Yeo, H. G., et al. (2020). Which pathologic staining method can visualize the hyperacute infarction lesion identified by diffusion MRI?: a comparative experimental study. *J. Neurosci. Methods*. 344, 108838. doi: 10.1016/j.jneumeth.2020.108838

Zhao, W., Zhao, L., Guo, Z., Hou, Y., Jiang, J., and Song, Y. (2020). Valproate sodium protects blood brain barrier integrity in intracerebral hemorrhage mice. *Oxid. Med. Cell. Longev*. 2020, 8884320. doi: 10.1155/2020/8884320

Zudaire, E., Gambardella, L., Kurcz, C., and Vermeren, S. (2011). A computational tool for quantitative analysis of vascular networks. *PLoS ONE*. 6, e27385. doi: 10.1371/journal.pone.0027385

Conflict of Interest: The authors declare that the research was conducted in the absence of any commercial or financial relationships that could be construed as a potential conflict of interest.

Publisher's Note: All claims expressed in this article are solely those of the authors and do not necessarily represent those of their affiliated organizations, or those of the publisher, the editors and the reviewers. Any product that may be evaluated in this article, or claim that may be made by its manufacturer, is not guaranteed or endorsed by the publisher.

frontiers | Frontiers in Pharmacology

REVIEW
published: 18 May 2022
doi: 10.3389/fphar.2022.854249

Neuroprotective Effects of Quercetin on Ischemic Stroke: A Literature Review

Leilei Zhang[1†], Jingying Ma[2†], Fan Yang[3†], Sishi Li[2], Wangran Ma[2], Xiang Chang[1] and Lin Yang[1*]*

[1]Xi'an Hospital of Traditional Chinese Medicine, Xi'an, China, [2]Shaanxi University of Chinese Medicine, Xianyang, China, [3]Guang'anmen Hospital, Chinese Academy of Chinese Medical Sciences, Beijing, China

Ischemic stroke (IS) is characterized by high recurrence and disability; however, its therapies are very limited. As one of the effective methods of treating acute attacks of IS, intravenous thrombolysis has a clear time window. Quercetin, a flavonoid widely found in vegetables and fruits, inhibits immune cells from secreting inflammatory cytokines, thereby reducing platelet aggregation and limiting inflammatory thrombosis. In pre-clinical studies, it has been shown to exhibit neuroprotective effects in patients with ischemic brain injury. However, its specific mechanism of action remains unknown. Therefore, this review aims to use published data to elucidate the potential value of quercetin in patients with ischemic brain injury. This article also reviews the plant sources, pharmacological effects, and metabolic processes of quercetin *in vivo*, thus focusing on its mechanism in inhibiting immune cell activation and inflammatory thrombosis as well as promoting neuroprotection against ischemic brain injury.

Keywords: quercetin, ischemic stroke, inflammatory thrombus, neuroprotection, immune cell activation, mechanism

OPEN ACCESS

Edited by:
Yongjun Sun,
Hebei University of Science and Technology, China

Reviewed by:
Pallavi Shrivastava,
Louisiana State University, United States
Peng Sun,
Shandong University of Traditional Chinese Medicine, China
Gollapalle L. Viswanatha,
Independent Consultant, Bengaluru, India

***Correspondence:**
Xiang Chang
3590150795@qq.com
Lin Yang
yang_lin2005@126.com

†These authors have contributed equally to this work

Specialty section:
This article was submitted to Neuropharmacology, a section of the journal Frontiers in Pharmacology

Received: *13 January 2022*
Accepted: *28 April 2022*
Published: *18 May 2022*

Citation:
Zhang L, Ma J, Yang F, Li S, Ma W, Chang X and Yang L (2022) Neuroprotective Effects of Quercetin on Ischemic Stroke: A Literature Review. Front. Pharmacol. 13:854249. doi: 10.3389/fphar.2022.854249

1 INTRODUCTION

Quercetin, which is present in many plants, has become a nutraceutical because of its significant antioxidant and anti-inflammatory activities (Shen et al., 2021; Zou et al., 2021), especially with its ability to scavenge free radicals (Anand David et al., 2016). Clinical studies have shown that quercetin has certain therapeutic effects on cardiovascular diseases (Dehghani et al., 2021), metabolic syndrome (Leyva-Soto et al., 2021), COVID-19 (Di Pierro et al., 2021), and central nervous system diseases.

Ischemic stroke (IS) is caused by hypoxic necrosis of brain tissue due to impaired blood supply to the brain, thereby leading to ischemia. It is the third leading cause of death worldwide (GBD, 2021). In 2017, there were 80.5 (UI78.9-82.6) deaths per 100,000 people, of which 45% were related to IS (Avan et al., 2019); IS accounted for 62.4% of stroke events in 2019 (GBD, 2021). Various risk factors, such as hypertension, diabetes, high body mass index, and smoking, determine the prevalence of IS and its complications; the antioxidant and inflammatory balance mechanisms in the body are severely damaged, thus causing an increase in neuronal reactive oxygen species (ROS), dysfunction, calcium excess, and oxidative stress (Lo et al., 2003).

Vitamins, carotenoids, and quercetin, which are natural antioxidants, are effectively used to prevent IS. Their mechanism may be related to the synergistic effects of vitamins and antioxidants (Ratnam et al., 2006). The molecular structure of quercetin is C15H10O7 (Magar and Sohng, 2020), which means that there is one -OH at each of the 3, 3′, 5, 7, and 4′ positions (Rice-Evans et al., 1997),

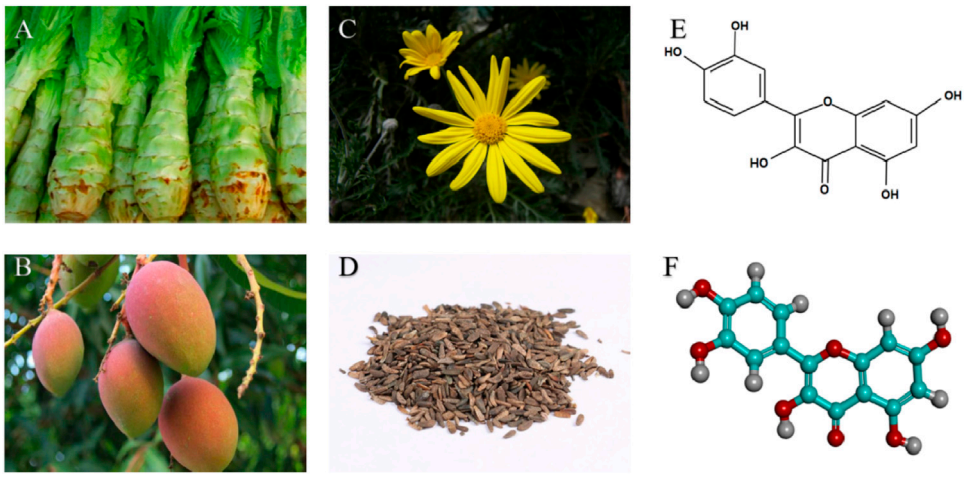

FIGURE 1 | Natural sources and structures of quercetin: **(A)** Lettuce Rootstock; **(B)** Mango fruit; **(C)** Arnica flowering plants; **(D)** Dried ripe fruit of burdock; **(E)** Chemical structure of quercetin; **(F)** 3D structure of quercetin (Visualized by DiscoveryStudio 2016).

and is present in a variety of plants and fruits (**Figure 1**). Quercetin is a polyphenol belonging to the flavonoid family (Brüll et al., 2015). Inflammatory thrombus formation exacerbates nerve damage in IS (De Meyer et al., 2022). Clinical studies have found that oral quercetin can reduce collagen-stimulated platelet tyrosine phosphorylation and thus inhibit platelet aggregation (Hubbard et al., 2004). Quercetin pre-treatment also reduces lipopolysaccharide-induced neutrophil IL-6 secretion (Liu J. et al., 2005). This process slows the formation of inflammatory thrombi, thus reducing the occurrence of IS.

Recent studies have demonstrated the neuroprotective properties of quercetin in *in vivo* and *in vitro* IS models (Yang et al., 2021). Therefore, this article is the first to describe the source and physicochemical properties of quercetin as well as the pathogenesis of ischemic brain injury. The therapeutic potential of quercetin in ischemic brain injury has been highlighted, including its role in limiting the secretion of inflammatory factors by various immune cells, thereby inhibiting inflammatory thrombosis, oxidative stress, apoptosis, autophagy.

2 SOURCE AND PHYSICOCHEMICAL PROPERTIES OF QUERCETIN

The term, "*quercetin*," has been used since the mid-18th century and is derived from the Latin word, "*quercetum*" (Jaimand et al., 2012). Quercetin is highly lipophilic and has poor water solubility, rapid metabolism, short half-life, and low bioavailability (Mukhopadhyay and Prajapati, 2015). Meanwhile, it is a unique polyphenol found in large quantities in various leafy vegetables, fruits, and herbs, such as apples, berries, long-leaf berry cilantro, cumin, lingonberry, lingonberry, wild grapes, and onions (Yang D. et al., 2020; Sharifi-Rad et al., 2021). According to previous research, quercetin has more than seven biological features, including neuroprotection, anti-allergy, anti-oxidation, anti-inflammation, immune regulation, anti-microbial, and anti-tumor properties (Bjeldanes and Chang, 1977; Dajas, 2012; Oboh et al., 2016; Darband et al., 2018; Dhiman et al., 2019; Huang et al., 2020; Shabbir et al., 2021). However, some studies have indicated that quercetin can induce mutations and promote mutagenesis (Bjeldanes and Chang, 1977). Conversely, Sumi et al. (2013) found that quercetin glucoside promoted angiogenesis after ischemia, but did not promote tumor growth.

In addition, the effectiveness of quercetin depends mainly on the plant source, dose, and chemical properties after processing (Najda et al., 2019). It can also be combined with salivary proteins to form soluble protein-quercetin binary aggregates. It is generated in the small intestines and is directly absorbed by the sodium-dependent glucose transporter-1 in the cecum and colon (Manach et al., 2004). Quercetin is also absorbed by intestinal epithelial cells, thus entering the liver through lipophilic dispersion and undergoing metabolism (Shen et al., 2021). In humans, quercetin has very low bioavailability and is highly unstable (0–50%), with a half-life of 1–2 h in the body after ingesting quercetin-rich foods or supplements (Graefe et al., 1999). Furthermore, quercetin poorly crosses the blood-brain barrier (BBB) (Oliveira et al., 2021). After dietary absorption, quercetin is digested and metabolized extremely quickly; therefore, its pharmacological effects are concentrated on *in vitro* studies rather than *in vivo* (Williams et al., 2004; Barnes et al., 2011). Therefore, various approaches have been attempted to improve the bioavailability of quercetin in the brain, such as enzyme modification or nano-encapsulation (Pateiro et al., 2021). Simultaneously, nanotechnology and targeted vectors are solutions to overcome the shortcomings of quercetin, such as low bioavailability and poor BBB passage (Naseri et al., 2015). The bioavailability of quercetin is 50 times higher than that of standard quercetin products after being packaged into nanocapsules (Riva et al., 2019). Alternatively, it changes the basic structure of quercetin to

TABLE 1 | Sources of quercetin.

Scientific Name	Walnut	Active Portions	Family	References
Davidia involucrata Baill	Dove tree	Fruits and seeds	Nyssaceae	Girardelo et al. (2020)
Mangifera indica L.	Mango	Fruits and Kernels	Anacardiaceae	Mwaurah et al. (2020)
Arctium lappa L.	Great Burdock Achene	Fruits and roots	Asteraceae	Moro and T P S Clerici, (2021)
Punica granatum L.	Pomegranate	Leaves and fruits	Lythraceae	Rojas-Garbanzo et al. (2021)
Theobroma speciosum	Theobroma	Shells and beans	Sterculiaceae	Mar et al. (2021)
Allium cepa L.	Onion	Bulbs	Liliaceae	Fredotović et al. (2021)
Capsicum annuum L	Sweet Pepper	fruits	Solanaceae	Guevara et al. (2021)
Syringa vulgaris L.	Lilac	Flowers and leaves	Oleaceae	Hanganu et al. (2021)
Sorbus aucuparia L.	mountain-ash	Fruits	Rosaceae	Rutkowska et al. (2021)
Gracilaria	Seaweed	Fruits	Gracilariaceae	Pourakbar et al. (2021)
Musa nana Lour	Banana	Skins and fruits	Musaceae	Bashmil et al. (2021)
Lactuca sativa L.	Lettuce	Leaves	Asteraceae	Assefa et al. (2021)
Abies alba Mill	Silver fir	Leaves	Pinaceae	Vek et al. (2021)
Juglans regia L.	Walnut	Nuts	Juglandaceae	Kalogiouri and Samanidou, (2021)
Malus pumila Mill	apple	Peels and fruits	Rosaceae	Yousefi-Manesh et al. (2021)
Arnica montana L.	*A. Montana*	Flowers and roots	Asteraceae	Nieto-Trujillo et al. (2021)
Paronychia argentea L	*P. argentea*	Leaves and Herbs	Caryophyllaceae	Abdelkhalek et al. (2021)

improve its pharmacokinetic and neuroprotective abilities (Chen et al., 2005). **Table 1** summarises the sources of quercetin.

3 PATHOGENESIS OF ISCHEMIC STROKE

3.1 Inflammatory Thrombus

In the pathophysiological process of IS, inflammatory thrombi lead to cerebral vascular occlusion, inflammatory response, and severe nerve damage after ischemic events (De Meyer et al., 2022). Early platelet adhesion and activation are key factors for the development of IS inflammatory thrombosis. The main receptors that mediate platelet adhesion are glycoprotein (GP) VI and integrin α2β1, both of which bind to the GPIbα subunit of collagen and the GPIB-IX-V complex, which interact with the von Willebrand factor (vWF) (Poulter et al., 2017; Constantinescu-Bercu et al., 2022; Feitsma et al., 2022). After endothelial injury, vWF interacts with GPIbα, thus causing platelets to decelerate on the fixed vWF (Constantinescu-Bercu et al., 2022; Kanaji et al., 2022) and thereby contributing to platelet aggregation. The use of GPIbα-vWF inhibitors restores vascular patency by specifically breaking down the outer layer of the occlusive thrombus (Le Behot et al., 2014). Subsequently, platelet activation induces a conformational change in the GPIIb/IIIa surface receptor and its affinity to fibrinogen and vWF, thus promoting platelet aggregation (O'Brien and Salmon, 1990).

In addition, vWF was found in different samples of thrombus extracted from IS patients; the thrombus contained 20.3% ± 10.1% vWF on average (Denorme et al., 2016). In a middle cerebral artery occlusion (MCAO) rat model, cerebral infarct size and fibrinogen deposition were significantly increased in platelet-only vWF chimeric rats (Verhenne et al., 2015). Interestingly, vWF can be cleaved by metalloprotease ADAMTS13, a disintegrin and metalloproteinase with a thrombospondin type 1 motif member 13. ADAMTS13 effectively dissolves anti-tissue-plasminogen activator (t-PA) thrombus within 5–60 min of MCAO occlusion (Denorme et al., 2016). Furthermore, caADAMTS13, a ADAMTS13 variant, significantly reduced residual vWF, fibrin, and platelet aggregation as well as neutrophil recruitment in the middle cerebral artery (MCA) (South et al., 2022).

However, thrombosis not only involves simple platelet aggregation, but also includes leukocyte-platelet complexation (Li et al., 2015; Pircher et al., 2019; Schrottmaier et al., 2020). This may be because basic diseases, such as hyperlipidemia and hyperglycemia, stimulate hematopoietic cells in the bone marrow to produce a large number of white blood cells in the circulating blood (Stumvoll et al., 2005; Zhou et al., 2016; Vekic et al., 2019). Neutrophils are closely related to thrombosis in IS patients with COVID-19 (Genchi et al., 2022). Neutrophils account for the majority of leukocytes in IS thrombi, followed by macrophages and T cells (Heo et al., 2020). This difference is partly due to their proportion in the circulating blood under physiological conditions; however, IS is also related to the level of activation of various white blood cells. Thrombus formation is a series of complex events that occur sequentially in the vascular system, including endothelial activation, neutrophil extracellular trap (NET) formation, vWF secretion, blood cell adhesion, aggregation, and activation (Yang J. et al., 2020). Genetic deletion of PKM2 in bone marrow hematopoietic cells reduces NET after cerebral ischemia/reperfusion, which further reduces fibrinogen, platelet deposition, and inflammatory cytokines in the brain (Dhanesha et al., 2022). Similarly, rats lacking CD84 on their platelets or T cells showed reduced cerebral thrombosis and milder nerve damage after MCAO (Schuhmann et al., 2020). In contrast, endothelial CD69 deficiency increases fibrinogen and vWF levels in ischemic tissue and exacerbates nerve injury (Brait et al., 2019). Thus, inhibition of inflammatory thrombi formation is one of the goals of IS prevention.

3.2 Immune Activation

Activation of immune cells, including neutrophils, T cells, and microglia, is involved in brain tissue repair after IS (Ma et al., 2017). Subsequently, neutrophils are attracted along a concentration gradient of chemokines in areas of ischemia to release pro-inflammatory factors, ROS, proteases, and matrix

metalloproteinases (MMPs) (Wang et al., 2007), thus leading to the disruption of the BBB and exacerbation of neurological damage (Rosell et al., 2008). Similarly, in the acute phase of IS, Th1 and Th17 cells degrade tight junction proteins (TJ) by secreting IFN-γ, IL-17, and IL-21, thereby further disrupting the integrity of the BBB (Gelderblom et al., 2012; Clarkson et al., 2014). T cells and their isoforms have also been associated with repair and functional improvement in late brain injury (Liesz et al., 2009). During ongoing inflammation, activated M1 microglia phagocytose astrocyte ends and disrupt the integrity of the BBB by secreting various vascular proteins (Wang et al., 2018; Haruwaka et al., 2019).

3.3 Oxidative Stress

Oxidative stress and mitochondrial dysfunction are important factors for the development of cerebral ischemic injury (Lo et al., 2003). Mitochondria are central to ROS production and cell death (Lo et al., 2003). Cerebral ischemia induces a cascade of excessive ROS production. Excess ROS leads to lipid peroxidation (LPO), exacerbates oxidative damage to proteins and nucleic acids, and contributes to neuronal apoptosis and BBB destruction (Allen and Bayraktutan, 2009; Kleinschnitz et al., 2010; Casas et al., 2017; Sun et al., 2018). Immune activation and oxidative stress also contribute to programmed neuronal death in the ischemic zone.

3.4 Procedural Death

Both hypoxia and ischemia induce autophagy. Shortly thereafter, autophagic vesicles accumulate extensively in the brain tissue (Tuo et al., 2021). Mitochondrial autophagy facilitates the maintenance of cellular homeostasis under mild ischemia or hypoxia. In contrast, sustained ischemia-reperfusion (I/R) results in prolonged autophagy, thus promoting neuronal cell damage or even death (Zhang et al., 2013). Similarly, neuronal apoptosis is the main mechanism through which I/R injury induces cell death. The balance between anti-apoptotic Bcl-2 and pro-apoptotic Bax protein expression is critical for the regulation of apoptosis (Culmsee and Plesnila, 2006). ROS production and mitochondria-dependent apoptosis play an important role in neuronal death following I/R injury (Jordan et al., 2011; Wang et al., 2014). After IS, a series of molecular events induced by oxidative stress overlap with iron sagging/oxidation processes; these have common molecular targets, such as LPO and glutathione (GSH) depletion (Seiler et al., 2008; Choi et al., 2013; Yang et al., 2014). Iron death is dependent on excessive iron accumulation, with the core process being LPO (Cao and Dixon, 2016). In a rat model of MCAO, GSH inhibited iron death by driving glutathione peroxidase 4 (GPx4) expression, thereby protecting neurons and reducing core ischemic areas (Karuppagounder et al., 2016; Alim et al., 2019).

4 PHARMACOLOGICAL EFFECTS OF QUERCETIN ON ISCHEMIC STROKE

4.1 Inhibition of Immune Cell Recruitment

The activation of peripheral immune cells promotes platelet aggregation. Pre-treatment of activated T cells with quercetin blocks IL-12-induced JAK-STAT tyrosine phosphorylation, thereby reducing T cell proliferation and Th1 differentiation (Muthian and Bright, 2004). Quercetin has a similar effect on neutrophils. NETs are closely associated with inflammatory thromboses. Quercetin does not directly affect NET formation, but inhibits it in peripheral blood polykaryotic cells by downregulating TNF-α production in lipopolysaccharide (LPS) peripheral blood monocytes (Yuan et al., 2020; Jo et al., 2021). During inflammation, LPS delays the spontaneous apoptosis of neutrophils, while quercetin accelerates this process (Liu J. J. et al., 2005; Yuan et al., 2020). This is associated with a reduction in the expression of inflammatory cytokines, activation of PKCa, and enhancement of CD95-mediated apoptosis in neutrophils (Russo et al., 2003). Quercetin effectively protects LDL from neutrophil-mediated modification at physiological concentrations (1 μM) and inhibits myeloperoxidase (MPO) oxidative damage (Loke et al., 2008) (**Figure 2**). Subsequently, quercetin downregulates the TLR-NF-κB signaling pathway, reduces the activities of COX, 5-LOx, NOS, MPO, and CRP, inhibits ldL-induced adhesion molecule expression, and ameliorates endothelial dysfunction in atherosclerosis (Bhaskar et al., 2016). Quercetin also reduces the activity of neutrophil MPO and inhibits the production of HOCl, a powerful oxidant, to protect endothelial cells from oxidative damage (Lu et al., 2018). In contrast, Suri et al. (2008) found that quercetin did not exert excessive influence on neutrophils, but only reduced the calcium response induced by N-formyl-methionyl-leucyl-phenylalanine (fMLP).

4.2 Inhibition of Thrombosis

The key factor for the occurrence of IS is the formation of an inflammatory thrombus; thrombolysis significantly alleviates brain injury. Quercetin, a natural flavonol compound, can significantly reduce diabetes-induced platelet aggregation (Mosawy et al., 2014), which may be related to the inhibition of compact platelet granule exocytosis (Mosawy et al., 2013b). Similarly, quercetin inhibits agonists (ADP, collagen, and thrombin) as well as induces platelet aggregation and granule secretion (Liang et al., 2015). Quercetin also binds to the GPIIb/IIIa platelet receptor, thus inhibiting the aggregation-promoting properties of calcium ion carriers and avoiding an increase in platelet-derived particles; these improve hemorheology (Zaragozá et al., 2021) and reduce thrombosis after carotid artery injury induced by FeCl3 in C57BL/6 rats (Mosawy et al., 2013a). Quercetin also effectively blocked *in vivo* FeCl3-induced arterial thrombosis and reduced IS infarct volume by inhibiting glycoprotein VI (GPVI)-mediated platelet signal transduction (Oh et al., 2021).

The binding of collagen to GPVI leads to receptor aggregation, which stimulates tyrosine phosphorylation and thus causes platelet aggregation (Gibbins et al., 1996; Poole et al., 1997). Quercetin inhibits platelet activation by inhibiting various components of the GPVI signaling pathway (e.g., collagenous tyrosine phosphorylation) (Hubbard et al., 2003; Hubbard et al., 2006; Wright et al., 2010), which may be a key factor for improving nerve injury in IS. In clinical trials, platelet aggregation was inhibited 30 and 120 min after oral quercetin administration, with a corresponding reduction in collagen-

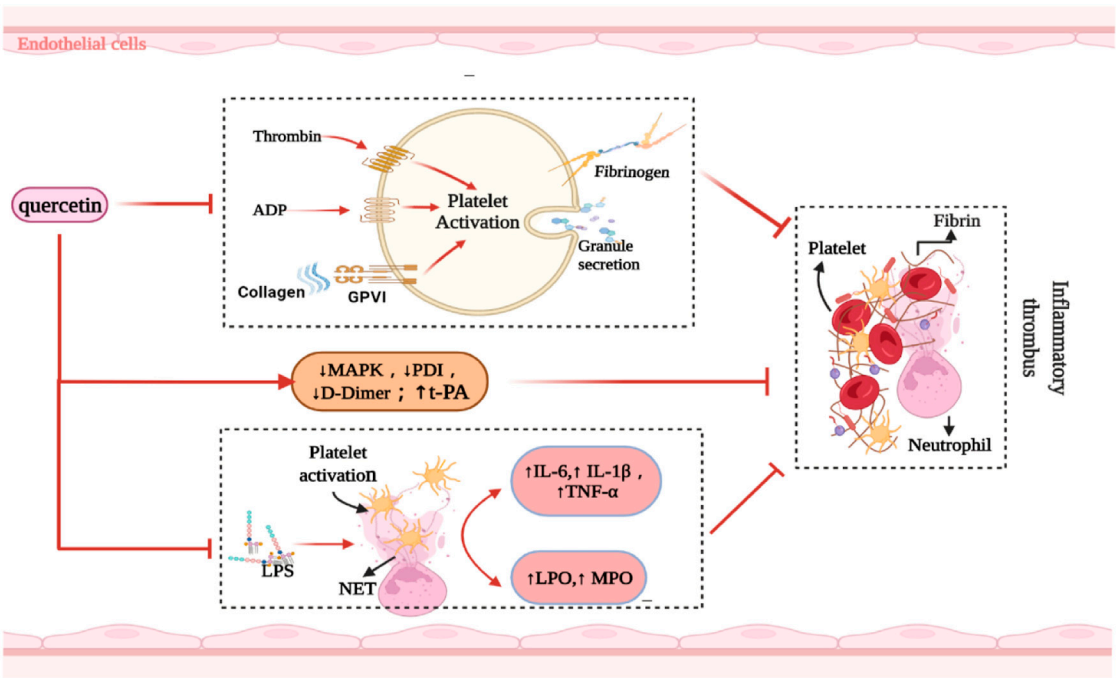

FIGURE 2 | Summarized the mechanism of quercetin inhibiting inflammatory thrombosis. Abbreviations: ↑, increase; ↓, decrease; ADP, Adenosine diphosphate; PDI, Protein disulfide isomerase; NET, neutrophil extracellular trap; LPO, lipid peroxidation; MPO, myeloperoxidase; t-PA, anti-tissue-plasminogen activator; MAPK, mitogen-activated protein kinase; LPS, lipopolysaccharide; GPVI, glycoprotein VI; IL, interleukin; TNF-α, tumor necrosis factor-alfa.

stimulated platelet tyrosine phosphorylation (Hubbard et al., 2004). Quercetin also inhibited platelet aggregation when collagen was stimulated at concentrations between 0.5 and 1.0 μg/ml, with IC50 values below 3 μM (Hubbard et al., 2003). Thus, these results support the clinical transformation of quercetin.

In contrast, Lee et al. (2013) found that quercetin did not reduce PT, aPTT, or platelet aggregation in experimental rats. They revealed that its downregulation of mitogen-activated protein kinase (MAPK) activation restricted tissue factor expression, thereby prolonging the time for atherothrombosis development. In endothelial cells, quercetin transcription induces the human t-PA gene by requiring a specific Sp1 (b) element within the proximal promoter region, which is mediated by the P38 MAPK-dependent signaling pathway (Pan et al., 2008).

Protein disulfide isomerase (PDI), a thiol isomerase secreted by vascular cells, is required for thrombosis. Quercetin-3-rutinoside prevents thrombosis in a PDI-dependent manner in experimental rats (Jasuja et al., 2012). Oral administration of 1,000 mg isoquercetin can reduce the plasma concentration of D-dimer by 21.9% and inhibit the activity of PDI in the plasma, thereby exerting an antithrombotic effect (Zwicker et al., 2019). This was related to the reduction of platelet-dependent thrombin content by blocking the production of platelet factor Va (Stopa et al., 2017). Intravenous administration of quercetin significantly attenuated TNF-α levels and prothrombin activity in a rabbit model of LPS-induced DIC (Yu et al., 2013) (**Figure 2**). Nonetheless, oral quercetin did not prevent thrombo-embolic stroke in an earlier Dutch cohort study (Knekt et al., 2000). This finding may be related to the use of dietary quercetin content as an intervening factor. **Table 2** summarizes the role of quercetin and its derivatives in limiting thrombosis.

4.3 The Role of Histomorphology

In an *in vitro* ischemia model, quercetin-treated cells showed improved tolerance to oxygen-glucose deprivation (OGD) or oxygen glucose recovery (ROG) (Lee et al., 2016). Quercetin administration reduced the corrected total infarct volume and edema percentage by 43.6% and 48.5%, respectively, along with a significant behavioral recovery effect (Lee et al., 2015). Quercetin and Kolaviron pre-treatment significantly improved the I/R-induced changes in brain water content. Significant remission of cerebral infarction was observed in the Kolaviron and quercetin treatment groups (Akinmoladun et al., 2015), which might be linked to the role of quercetin in the Sirt1/nuclear factor-erythroid 2-related factor 2 (Nrf2)/heme oxygenase-1 (HO-1) signaling cascade (Yang et al., 2021). Compared to free quercetin or quercetin-carrying exosome (quercetin-EXO) therapy, treatment with quercetin/mAb gAP43-EXO dramatically reduced infarct size and improved neurological recovery in MCAO reperfusion-induced rats (Guo et al., 2021) (**Figure 3**). Simultaneously, quercetin improved the IS-associated motor and sensory deficits in the dorsal striatum, which may be related to the upregulation of MC4R-mRNA expression (Ulya et al., 2021). More intuitively, quercetin showed 6.79 2 ± 0.41 right turn in rats in the permanent MCAO model and 9.31 ± 0.33 right turn in the control group. Most rats in the treatment group showed mild to moderate

TABLE 2 | Anti-platelet aggregation effect of quercetin.

Ingredient	Dose	Experimental Model	Mechanism	References
quercetin	6 mg/kg	C57BL/6 mice; FeCl3-induced carotid artery injury	↓GPIIb/IIIa activation; ↓platelet granule exocytosis; Inhibits platelet aggregation	Mosawy et al. (2013a)
quercetin-3-rutinoside	0.5 mg/kg	C57BL/6J mice; Laser-induced injury/FeCl3 injury	Inhibit fibrin production; ↓Expression of PDI; Inhibits platelet aggregation and thrombosis	Jasuja et al. (2012)
isoquercetin	500 mg or 1,000 mg	Healthy cohort (a-e) abstaining from quercetin-rich foods 72 h before intervention, excluding those with oral anticoagulants or antiplatelet drugs	↓PDI activity; ↓platelet factor Va; ↓platelet-dependent thrombin	Stopa et al. (2017)
quercetin	2 mg or 10 mg	SD rats, FeCl3-induced carotid artery injury	↓blood triglyceride, ↓glucose levels; ↓tissue factor, ↓MAPK activation	Brüll et al. (2015)
quercetin	–	Healthy non-smokers with normal coagulation function, not using immunologics, antiplatelet, NSAIDsetc.	Blocks GPIIb/IIIa receptors; ↓Platelet activation and aggregation	Zaragozá et al. (2021)
quercetin	0.5 mg/kg, 1 mg/kg, 2 mg/kg	Adult male New Zealand white rabbits, DIC experimental models	↑Protein C and ATIII; ↓APTT, ↓PT, ↓TNF-α; Anti-inflammatory and anticoagulant	Yu et al. (2013)
quercetin	50 mg/kg, 100 mg/kg	Wild-type (WT, C57BL/6 strain, 6–8 weeks old, 18–22 g BW) male mice, FeCl3-induced *in vivo* thrombosis	↓granule secre, ↓ROS; ↓platelet aggregation; tionInhibition of αIIbβ3 integrin and GPVI signaling;	Oh et al. (2021)
quercetin	1 μM	Quercetin pretreated human umbilical vein endothelial cells for 0–24 h	↑ t-PA gene expression; activate p38MAPK	Pan et al. (2008)
quercetin	6 mg/kg	Diabetes C57BL/6 mice; FeCl3-induced carotid artery injury	↓granule exocytosis; Inhibits platelet hyperaggregation and thrombosis	Mosawy et al. (2014)
quercetin	5 mg or 69 mg	A two-treatment, randomized, double-blind, crossover study	↓Syk tyrosine phosphorylation; Inhibits collagen stimulated platelet aggregation	Hubbard et al. (2006)
quercetin-4¢-O-b-D-glucoside	150 mg or 300 mg	Those who did not take aspirin and a low quercetin diet 14 days before the study	↓Syk tyrosine phosphorylation; Inhibition of GPVI signal transduction	Hubbard et al. (2004)
Isoquercetin	500 mg or 1000 mg	Patients with advanced cancer; A multicenter, multidose, open-label phase II clinical trial	↓D-dimer, ↓platelet dependent thrombin; Inhibition of PDI activity	Zwicker et al. (2019)

neuromotor deficits ($p < 0.0001$) (Ahn and Jeon, 2015). In addition, the infarct volume of rats in the control and treatment groups was 26.35 ± 2.25% and 14.87 ± 1.75%, respectively (Park et al., 2020). Quercetin can improve cognitive function in rats with ischemic injury. In the Morris water maze (MWM) test, quercetin therapy restored spatial learning deficits by increasing the time and amount of access to the central region (Le et al., 2020). By boosting the number of new Olig2+ oligodendrocyte progenitors in the subventricular zone, quercetin alleviated hypoxia/ischemia (HI)-induced cognitive impairment (Qu et al., 2014). Compared with the control group, I/R rats pre-treated with quercetin (20 mg/kg) for 7 days showed a significant reduction in cognitive impairment as well as improvement in motor capacity, cerebral edema, and infarct volume ($p < 0.001$) (Viswanatha et al., 2018; Viswanatha et al., 2019). **Table 3** summarizes the neuroprotective effects of quercetin on IS.

4.4 Prevention of Oxidative Stress

4.4.1 Quercetin

The mitochondria are the main source of oxidative stress. Quercetin can activate mitochondrial large-conductance Ca^{2+} to regulate potassium (mitoBKCa) channels, participate in mitochondrial depolarization, and protect brain tissue from HI damage (Kampa et al., 2021). Quercetin synergistically enhances mitochondrial spare respiration, maintains neuronal mitochondrial function, and increases the expression of CREB target genes (PGC-1a), which promote neuronal survival and mitochondrial biogenesis in an OGD model (Nichols et al., 2015). Furthermore, quercetin can control the Sirt1/Nrf2/HO-1 pathway, thus drastically reducing ROS formation following IS (Yang et al., 2021). In several IS models, quercetin revealed a dose-dependent reversal of OGD-induced declines in superoxide dismutase-1 (SOD1), SOD2, glutathione peroxidase-1 (GPX-1), and catalase (CAT) levels (Le et al., 2020), which may be achieved by its LPO-reducing capability (Shalavadi et al., 2020). Another study pointed out that quercetin also regulates the expression of oxidase and other antioxidant enzyme genes, thereby preventing IS-associated oxidative stress (Yamagata, 2019). Further studies showed that quercetin induced the expression of Nrf2 in erythrocytes, thus strongly inhibiting the production of adhesion molecules; this action may be related to the antioxidant effect of HO-1 (Li C. et al., 2016). Lee et al. (2016) discovered that quercetin increased the expression of Nrf2, HO-1, and nitric oxide synthase 1 (NOS1) in SHSY5Y cells, thus indicating its antioxidative stress impact.

4.4.2 Quercetin and Other Herbs

Quercetin and other herbal pre-treatments inhibit I/R-induced decreases in catalase and SOD enzyme activity, prevent LPO production, and increase GSH levels (Viswanatha et al., 2018; Viswanatha et al., 2019). Additionally, reduced NO and hippocampal lactate dehydrogenase (LDH) levels were observed in the cortex, striatum, and hippocampus of I/R rats (Ojo et al., 2019). Furthermore, intragastric injection of quercetin and rutin 10 min before reperfusion significantly reduced malondialdehyde (MDA) and myeloperoxidase (MPO) levels, increased endogenous antioxidant enzyme SOD and CAT levels, and improved I/R-induced inflammatory response (Annapurna et al., 2013).

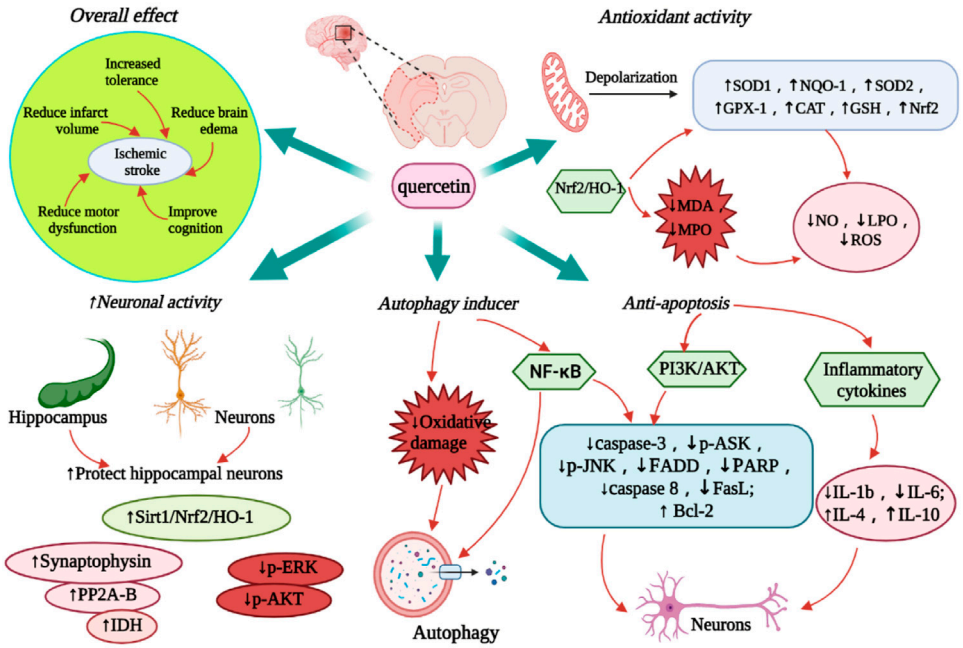

FIGURE 3 | Diagram of the neuroprotective effect of quercetin on IS. The figure highlights the overall therapeutic effect of quercetin, anti-oxidative stress, anti-apoptosis, promoting autophagy and neuroprotective activity. Abbreviations: ↑, increase; ↓, decrease; SOD, Superoxide dismutase; NQO-1, NAD(P)H dehydrogenase quinone-1; GPX-1, glutathione peroxidase-1; CAT, catalase; NOS1, nitric oxide synthase 1; GSH, glutathione; Nrf2, nuclear factor 2-related factor 2; HO-1, Heme oxygenase-1; NO, nitric oxide; LPO, lipid peroxidation; ROS, reactive oxygen species; IL, interleukin; Sirt1, sirtuin 1; NF-kB, nuclear factor kappa B; IDH, isocitrate dehydrogenase; PP2A, Protein phosphatase 2A; FADD, Fas-associated death domain; PARP, poly (ADP-ribose) polymerase; PI3K, phosphoinositide 3-kinase; AKT, protein kinase B; ASK, apoptosis signal-regulating kinase; JNK, c-Jun N-terminal protein kinases; ERK, extracellular-signal-regulated kinase; FasL, factor associated suicide ligand.

4.4.3 Optimization of Quercetin

Optimization of quercetin can significantly improve its efficiency and pharmacological effects across the BBB. Quercetin liposome preparations slow down the decline of GSH levels in the ipsilateral striatum and cortex after ischemia; it also maintains GSH levels in the ischemic areas and increases GSH concentration in neuronal and glial cells (Rivera et al., 2008). During cerebral I/R, intracellular GSH levels significantly increased in young and old rats receiving nano-quercetin (27 mg/kg) (Ghosh et al., 2013). Quercetin/mAb GAP43-Exo targets neurons by mediating mAb GAP43, thus enhancing the accumulation of quercetin in the ischemic areas as well as inhibiting ROS production by activating the Nrf2/HO-1 pathway to increase LDH levels (Guo et al., 2021). Quercetin/mAb GAP43-Exo decreased oxidative stress-induced I/R damage by boosting the nuclear translocation of Nrf2 and upregulating the transcription of NAD(P)H dehydrogenase quinone-1 (NQO-1), HO-1, SOD1 and GPx1 (Guo et al., 2021) (**Figure 3**).

4.5 Protection of Hippocampal Neurons

IS significantly induced endogenous neurogenesis in the dentate gyrus of the hippocampus. However, newborn neurons are difficult to differentiate into mature neurons (Arvidsson et al., 2002; Doeppner et al., 2011). Quercetin maintains isocitrate dehydrogenase levels in MCAO animal models and helps to preserve neuronal cell energy production, thereby reducing IS-induced neuronal cell damage (Shah et al., 2018). Moreover, quercetin attenuates the decrease in PP2A subunit B expression caused by glutamate treatment, thus further reducing neuronal cell death (Park et al., 2019). Through the Sirt1/Nrf2/HO-1 signaling pathway, quercetin restores the normal structure of hippocampal neurons in I/R mice with severe neuronal injury (Yang et al., 2021). Quercetin also reduces the activity and pathophysiology of the following processes: protein tyrosine and serine/threonine phosphatase in rat cortical tissue, oxygen-glucose deprivation/reoxygenation (OGD/R) in hippocampal slices and neuronal/glial cell lines, phosphorylation of ERK and Akt, and I/R-induced hindbrain damage (Wang et al., 2020). Quercetin treatment can also significantly increase the activity of SHSY5Y cells and E18 mouse cortical neurons (Lee et al., 2016), enhance the expression of synaptophysin in PC12 cells in the OGD model, and promote neurite growth in PC12 cells (Orbán-Gyapai et al., 2014). Three days after reperfusion, oral administration of nano-encapsulated quercetin reduced the activity of iNOS and caspase-3, expanded the number of neurons in the hippocampus, and prevented neuronal cell damage (Ghosh et al., 2013) (**Figure 3**).

4.6 Promotion of Autophagy

The mechanism of quercetin-induced autophagy in cell survival is complex because of the large number of biomolecules involved in this process. Based on the scope of the damage caused by HI,

TABLE 3 | Neuroprotective effects of quercetin in different IS models.

Ischemic stroke	*In vitro/In vivo*	Dose	Effective Molecular Mechanism	References
MCAO	*in vitro/in vivo*	10 mg/kg	↓ PP2A subunit B; inhibition of glutamate toxicity	Park et al. (2019)
MCAO/R	*in vitro/in vivo*	3.4 mg/ml	↑NQO-1, ↑HO-1, ↑SOD1, ↑GPx1; ↓ROS activation of Nrf2/HO-1 pathway; reduce I/R damage;	Guo et al. (2021)
OGD	*in vitro*	10 μM	↑synaptophysin; promote the growth of neurites	Orbán-Gyapai et al. (2014)
MCAO/R	*in vivo*	30 mg/kg	↑GPx, ↑SOD, ↑CAT; ↓PARP, ↓caspase-3, ↓p53, ↓LPO; protection of Na_+K_+-ATPase Activity	Ahmad et al. (2011)
MCAO	*in vivo*	30 mg/kg	↓caspase-3, ↓PARP; inhibit the apoptosis pathway; reduce neuronal defects and neuronal degeneration	Park et al. (2018)
Focal cortical ischemia	*in vivo*	25 μmol/kg	↓MMP-9; reduce the damage of BBB	Lee et al. (2011)
pMCAO/Glutamate	*in vitro/in vivo*	10 mg/kg	↑Bcl2; ↓caspase-3, ↓Bax; reduce calcium overload of intracellular and hippocampal neurons	Park et al. (2020)
HIBI/OGD	*in vitro/in vivo*	50 mg/kg	↓IL-1β, ↓IL-6, ↓TNF-α; ↑SOD1,↑ SOD2, ↑GPX-1, ↑CAT; increase cell viability; Inhibit TLR4/NF-κB signaling pathway; improve dyskinesia and cognitive impairment	Le et al. (2020)
pMCAO	*in vivo*	30 mg/kg	↑ GSH; protect neurons and glial cells	Rivera et al. (2008)
MCAO	*in vivo*	10 mg/kg	↑[NAD+], ↑adenosine homocysteinase, ↑pyruvate kinase, ↑carboxy terminal hydrolase L1; ↓HSP60, ↓HSP2	Shah et al. (2018)
MCAO/HUMSCs	*in vivo*	25 mol/kg	↓caspase-3, ↓IL-6, ↓IL-1b; ↑IL-4, ↑IL-10, ↑transforming growth factor-b1; promote nerve function recovery	Zhang et al. (2016)
MCAO	*in vivo*	10 mg/kg	reduce infarct size and edema; antioxidant and neuroprotective activity	Lee et al. (2015)
MCAO/OGDR	*in vitro/in vivo*	25 mg/kg	anti-oxidative, anti-inflammatory, and antiapoptotic effects; reduces changes in ERK/Akt phosphorylation and protein phosphatase activity	Wang et al. (2020)
common carotid artery occlusion and reperfusion	*in vivo*	2.7 mg/kg	↓iNOS,↓ caspase-3, ↓ROS; ↑ HO-1, ↑SOD1, ↑GSH; protect the mitochondrial membrane; protect mitochondrial membranes and neuronal cells	Ghosh et al. (2013)

autophagy is used as a pro-apoptotic signal, wherein quercetin can be used as its inducer (Costa et al., 2016). In models of oxidative damage and ischemia, studies have revealed that the protective impact of quercetin is directly linked to the induction of autophagy (Wu et al., 2017). As a result, autophagy is linked to the pro-survival mechanism of quercetin in IS-induced brain injury and other related events (Wang et al., 2011; Zhi et al., 2016; Granato et al., 2017; Liu et al., 2017) (**Figure 3**). Quercetin has a protective effect against MCAO-induced neuronal cell apoptosis and likewise induces autophagy-mediated neuronal PC12 cell survival (Ahn and Jeon, 2015; Park et al., 2018). In IS, if myeloid cells lack an autophagy response, inflammatory glial cells would thus play a significant role in neuronal cell apoptosis by increasing ischemia; this happens in compensation for the reduced activity of myeloid cells (Kotoda et al., 2018). In this case, autophagy protected the neurons from ischemia-induced cell death. Surprisingly, quercetin, like many other polyphenols, induces autophagy (Pallauf and Rimbach, 2013). Quercetin plays a role in cellular survival by activating autophagy in brain myeloid cells (Chang et al., 2017). Furthermore, in MCAO-induced ischemia, quercetin altered the apoptosis/autophagy interaction and its linkage with the nuclear factor kappa B (NF-κB) signaling pathway by upregulating ubiquitin carboxy-terminal hydrolase L1, which is a related gene enzyme, at almost double the rate (Chirumbolo et al., 2019).

4.7 Inhibition of Apoptosis

Quercetin upregulates the intracellular Ca^{2+} concentration in the cerebral cortical and hippocampal neurons of MCAO rats. It also regulates the gene expression of Bcl-2, Bax, and caspase-3, thereby preventing apoptosis (Park et al., 2020). Another study found that quercetin reduced HI-induced cortical cell death by blocking the neuro-inflammatory response mediated by the toll-like receptor 4 (TLR4)/nuclear factor-kappa B (NF-κB) signaling pathway (Wu et al., 2019). The anti-apoptotic activity of quercetin may be due to its ability to suppress inflammatory genes in BV2 microglia (Mrvová et al., 2015). In addition, quercetin has also been reported to improve I/R-induced cognitive deficits as well as inhibit neuronal apoptosis by increasing p-Akt and decreasing p-ASK1, P-JNK3, cleaved caspase-3, and FADD protein expressions (Pei et al., 2016). Furthermore, quercetin not only inhibits acid toxicity mediated by acid-sensing ion channels, but also improves neuronal apoptosis in focal cerebral ischemia by reducing caspase-3 and PARP expression through the PI3K/Akt pathway (Park et al., 2018). After local cerebral ischemia, human umbilical cord mesenchymal stem cells (HUMSCs) transplanted with quercetin can reduce pro-inflammatory cytokines IL-1B and IL-6, increase anti-inflammatory cytokines IL-4 and IL-10, inhibit the expression of apoptosis factor caspase-3, and promote the recovery of nerve function (Zhang et al., 2016). Furthermore, isorhamnetin (30-methoxy-3,40,5, 7-tetrahydroxy flavanone), a quercetin metabolite, has been demonstrated to lower blood pressure and endothelial dysfunction in spontaneously hypertensive rats (Sánchez et al., 2006; Sanchez et al., 2007). In the methylglyoxal-binding OGD model, isorhamnetin inhibited caspase 8

activation and decreased Fas and FasL expression, thereby lowering the activation and ability of NF-κB to perform an anti-mitochondrial-dependent apoptotic role (Li W. et al., 2016) (**Figure 3**).

5 CONCLUSION AND PERSPECTIVES

Quercetin has a unique chemical structure and is widely found in our daily diet (e.g., vegetables and fruits), thus making it easy to obtain. Quercetin has showed respectable therapeutic effects on IS-induced models. It inhibits inflammatory thrombosis, reduces cerebral edema, infarct size, and oxidative stress, promotes autophagy and anti-apoptosis, and can be used as an adjuvant agent in the treatment of IS. Importantly, quercetin has been found to inhibit platelet activation and limit inflammatory thrombosis in both animal and clinical studies. The anti-inflammatory properties of quercetin are mediated by the regulation of the expression of various inflammatory factors. It also prevents neuronal death by stimulating the NF-κB signaling pathway, which suppresses caspase-3 and Bax, and promotes Bcl-2 expression.

To date, a number of studies have suggested that quercetin can be used as a neuroprotective drug in the treatment of IS. However, owing to its poor bioavailability and ability to cross the BBB, its application in the clinical setting is limited. Therefore, future research should focus on optimizing the conformation of quercetin or developing a quercetin nano-drug delivery system to improve its bioavailability and BBB passing rate. Meanwhile, we should pay attention to the effects of quercetin on neurogenesis and synaptic plasticity after IS. More clinical trials should also be designed to clarify the effective dose of quercetin in the treatment of IS. Quercetin also has a variety of metabolic components in the body; only a few studies have focused on the pharmacological effects of its metabolites, thus warranting further research on its biochemical and metabolic properties.

AUTHOR CONTRIBUTIONS

LZ, LY, JM, and FY were involved in literature search, manuscript writing, draft preparation, graphic production, and content production. XC, WM, and SL were involved in conception, drafting, and editing of the manuscript.

REFERENCES

Abdelkhalek, A., Al-Askar, A. A., Alsubaie, M. M., and Behiry, S. I. (2021). First Report of Protective Activity of Paronychia Argentea Extract against Tobacco Mosaic Virus Infection. *Plants* 10 (11), 2435. doi:10.3390/plants10112435

Ahmad, A., Khan, M. M., Hoda, M. N., Raza, S. S., Khan, M. B., Javed, H., et al. (2011). Quercetin Protects against Oxidative Stress Associated Damages in a Rat Model of Transient Focal Cerebral Ischemia and Reperfusion. *Neurochem. Res.* 36 (8), 1360–1371. doi:10.1007/s11064-011-0458-6

Ahn, T. B., and Jeon, B. S. (2015). The Role of Quercetin on the Survival of Neuron-like PC12 Cells and the Expression of α-synuclein. *Neural Regen. Res.* 10 (7), 1113–1119. doi:10.4103/1673-5374.160106

Akinmoladun, A. C., Akinrinola, B. L., Olaleye, M. T., and Farombi, E. O. (2015). Kolaviron, a Garcinia Kola Biflavonoid Complex, Protects against Ischemia/reperfusion Injury: Pertinent Mechanistic Insights from Biochemical and Physical Evaluations in Rat Brain. *Neurochem. Res.* 40 (4), 777–787. doi:10.1007/s11064-015-1527-z

Alim, I., Caulfield, J. T., Chen, Y., Swarup, V., Geschwind, D. H., Ivanova, E., et al. (2019). Selenium Drives a Transcriptional Adaptive Program to Block Ferroptosis and Treat Stroke. *Cell* 177 (5), 1262–e25. e1225. doi:10.1016/j.cell.2019.03.032

Allen, C. L., and Bayraktutan, U. (2009). Oxidative Stress and its Role in the Pathogenesis of Ischaemic Stroke. *Int. J. Stroke* 4 (6), 461–470. doi:10.1111/j.1747-4949.2009.00387.x

Anand David, A. V., Arulmoli, R., and Parasuraman, S. (2016). Overviews of Biological Importance of Quercetin: A Bioactive Flavonoid. *Pharmacogn. Rev.* 10 (20), 84–89. doi:10.4103/0973-7847.194044

Annapurna, A., Ansari, M. A., and Manjunath, P. M. (2013). Partial Role of Multiple Pathways in Infarct Size Limiting Effect of Quercetin and Rutin against Cerebral Ischemia-Reperfusion Injury in Rats. *Eur. Rev. Med. Pharmacol. Sci.* 17 (4), 491–500.

Arvidsson, A., Collin, T., Kirik, D., Kokaia, Z., and Lindvall, O. (2002). Neuronal Replacement from Endogenous Precursors in the Adult Brain after Stroke. *Nat. Med.* 8 (9), 963–970. doi:10.1038/nm747

Assefa, A. D., Hur, O.-S., Hahn, B.-S., Kim, B., Ro, N.-Y., and Rhee, J.-H. (2021). Nutritional Metabolites of Red Pigmented Lettuce (Lactuca sativa) Germplasm and Correlations with Selected Phenotypic Characters. *Foods* 10 (10), 2504. doi:10.3390/foods10102504

Avan, A., Digaleh, H., Di Napoli, M., Stranges, S., Behrouz, R., and Shojaeianbabaei, G. (2019). Socioeconomic Status and Stroke Incidence, Prevalence, Mortality, and Worldwide Burden: An Ecological Analysis From the Global Burden of Disease Study 2017. *BMC Medicine* 17 (1), 191. doi:10.1186/s12916-019-1397-3

Barnes, S., Prasain, J., D'Alessandro, T., Arabshahi, A., Botting, N., Lila, M. A., et al. (2011). The Metabolism and Analysis of Isoflavones and Other Dietary Polyphenols in Foods and Biological Systems. *Food Funct.* 2 (5), 235–244. doi:10.1039/c1fo10025d

Bashmil, Y. M., Ali, A., Bk, A., Dunshea, F. R., and Suleria, H. A. R. (2021). Screening and Characterization of Phenolic Compounds from Australian Grown Bananas and Their Antioxidant Capacity. *Antioxidants* 10 (10), 1521. doi:10.3390/antiox10101521

Bhaskar, S., Sudhakaran, P. R., and Helen, A. (2016). Quercetin Attenuates Atherosclerotic Inflammation and Adhesion Molecule Expression by Modulating TLR-NF-Kb Signaling Pathway. *Cell Immunol.* 310, 131–140. doi:10.1016/j.cellimm.2016.08.011

Bjeldanes, L. F., and Chang, G. W. (1977). Mutagenic Activity of Quercetin and Related Compounds. *Science* 197 (4303), 577–578. doi:10.1126/science.327550

Brait, V. H., Miró-Mur, F., Pérez-de-Puig, I., Notario, L., Hurtado, B., Pedragosa, J., et al. (2019). CD69 Plays a Beneficial Role in Ischemic Stroke by Dampening Endothelial Activation. *Circ. Res.* 124 (2), 279–291. doi:10.1161/circresaha.118.313818

Brüll, V., Burak, C., Stoffel-Wagner, B., Wolffram, S., Nickenig, G., Müller, C., et al. (2015). Effects of a Quercetin-Rich Onion Skin Extract on 24 H Ambulatory Blood Pressure and Endothelial Function in Overweight-To-Obese Patients with (Pre-)hypertension: a Randomised Double-Blinded Placebo-Controlled Cross-Over Trial. *Br. J. Nutr.* 114 (8), 1263–1277. doi:10.1017/s0007114515002950

Cao, J. Y., and Dixon, S. J. (2016). Mechanisms of Ferroptosis. *Cell Mol. Life Sci.* 73, 2195–2209. doi:10.1007/s00018-016-2194-1

Casas, A. I., Geuss, E., Kleikers, P. W. M., Mencl, S., Herrmann, A. M., Buendia, I., et al. (2017). NOX4-dependent Neuronal Autotoxicity and BBB Breakdown Explain the Superior Sensitivity of the Brain to Ischemic Damage. *Proc. Natl. Acad. Sci. U. S. A.* 114 (46), 12315–12320. doi:10.1073/pnas.1705034114

Chang, J. L., Chow, J. M., Chang, J. H., Wen, Y. C., Lin, Y. W., Yang, S. F., et al. (2017). Quercetin Simultaneously Induces G0/G1 -phase Arrest and Caspase-Mediated Crosstalk between Apoptosis and Autophagy in Human Leukemia HL-60 Cells. *Environ. Toxicol.* 32 (7), 1857–1868. doi:10.1002/tox.22408

Chen, X., Yin, O. Q., Zuo, Z., and Chow, M. S. (2005). Pharmacokinetics and Modeling of Quercetin and Metabolites. *Pharm. Res.* 22 (6), 892–901. doi:10.1007/s11095-005-4584-1

Chirumbolo, S., Vella, A., and Bjørklund, G. (2019). Quercetin Might Promote Autophagy in a Middle Cerebral Artery Occlusion-Mediated Ischemia Model: Comments on Fawad-Ali Shah et al. *Neurochem. Res.* 44 (2), 297–300. doi:10.1007/s11064-018-2692-7

Choi, I. Y., Lim, J. H., Kim, C., Song, H. Y., Ju, C., and Kim, W. K. (2013). 4-hydroxy-2(E)-Nonenal Facilitates NMDA-Induced Neurotoxicity via Triggering Mitochondrial Permeability Transition Pore Opening and Mitochondrial Calcium Overload. *Exp. Neurobiol.* 22 (3), 200–207. doi:10.5607/en.2013.22.3.200

Clarkson, B. D., Ling, C., Shi, Y., Harris, M. G., Rayasam, A., Sun, D., et al. (2014). T Cell-Derived Interleukin (IL)-21 Promotes Brain Injury Following Stroke in Mice. *J. Exp. Med.* 211 (4), 595–604. doi:10.1084/jem.20131377

Constantinescu-Bercu, A., Wang, Y. A., Woollard, K. J., Mangin, P., Vanhoorelbeke, K., Crawley, J. T. B., et al. (2022). The GPIbα Intracellular Tail - Role in Transducing VWF- and collagen/GPVI-Mediated Signaling. *Haematologica* 107 (4), 933–946. doi:10.3324/haematol.2020.278242

Costa, L. G., Garrick, J. M., Roquè, P. J., and Pellacani, C. (2016). Mechanisms of Neuroprotection by Quercetin: Counteracting Oxidative Stress and More. *Oxid. Med. Cell Longev.* 2016, 2986796. doi:10.1155/2016/2986796

Culmsee, C., and Plesnila, N. (2006). Targeting Bid to Prevent Programmed Cell Death in Neurons. *Biochem. Soc. Trans.* 34, 1334–1340. doi:10.1042/bst0341334

Dajas, F. (2012). Life or Death: Neuroprotective and Anticancer Effects of Quercetin. *J. Ethnopharmacol.* 143 (2), 383–396. doi:10.1016/j.jep.2012.07.005

Darband, S. G., Kaviani, M., Yousefi, B., Sadighparvar, S., Pakdel, F. G., Attari, J. A., et al. (2018). Quercetin: A Functional Dietary Flavonoid with Potential Chemo-Preventive Properties in Colorectal Cancer. *J. Cell Physiol.* 233 (9), 6544–6560. doi:10.1002/jcp.26595

De Meyer, S. F., Langhauser, F., Haupeltshofer, S., Kleinschnitz, C., and Casas, A. I. (2022). Thromboinflammation in Brain Ischemia: Recent Updates and Future Perspectives. *Stroke*. 53(5), 101161strokeaha122038733. doi:10.1161/strokeaha.122.038733

Dehghani, F., Sezavar Seyedi Jandaghi, S. H., Janani, L., Sarebanhassanabadi, M., Emamat, H., and Vafa, M. (2021). Effects of Quercetin Supplementation on Inflammatory Factors and Quality of Life in Post-myocardial Infarction Patients: A Double Blind, Placebo-Controlled, Randomized Clinical Trial. *Phytother. Res.* 35 (4), 2085–2098. doi:10.1002/ptr.6955

Denorme, F., Langhauser, F., Desender, L., Vandenbulcke, A., Rottensteiner, H., Plaimauer, B., et al. (2016). ADAMTS13-mediated Thrombolysis of t-PA-resistant Occlusions in Ischemic Stroke in Mice. *Blood* 127 (19), 2337–2345. doi:10.1182/blood-2015-08-662650

Dhanesha, N., Patel, R. B., Doddapattar, P., Ghatge, M., Flora, G. D., Jain, M., et al. (2022). PKM2 Promotes Neutrophil Activation and Cerebral Thromboinflammation: Therapeutic Implications for Ischemic Stroke. *Blood* 139 (8), 1234–1245. doi:10.1182/blood.2021012322

Dhiman, P., Malik, N., Sobarzo-Sánchez, E., Uriarte, E., and Khatkar, A. (2019). Quercetin and Related Chromenone Derivatives as Monoamine Oxidase Inhibitors: Targeting Neurological and Mental Disorders. *Molecules* 24 (3). doi:10.3390/molecules24030418

Di Pierro, F., Iqtadar, S., Khan, A., Ullah Mumtaz, S., Masud Chaudhry, M., Bertuccioli, A., et al. (2021). Potential Clinical Benefits of Quercetin in the Early Stage of COVID-19: Results of a Second, Pilot, Randomized, Controlled and Open-Label Clinical Trial. *Int. J. Gen. Med.* 14, 2807–2816. doi:10.2147/ijgm.S318949

Doeppner, T. R., Kaltwasser, B., ElAli, A., Zechariah, A., Hermann, D. M., and Bähr, M. (2011). Acute Hepatocyte Growth Factor Treatment Induces Long-Term Neuroprotection and Stroke Recovery via Mechanisms Involving Neural Precursor Cell Proliferation and Differentiation. *J. Cereb. Blood Flow. Metab.* 31 (5), 1251–1262. doi:10.1038/jcbfm.2010.211

Feitsma, L. J., Brondijk, H. C., Jarvis, G. E., Hagemans, D., Bihan, D. G., Jerah, N. E., et al. (2022). Structural Insights into Collagen-Binding by Platelet Receptor Glycoprotein VI. *Blood*. doi:10.1182/blood.2021013614

Fredotović, Ž., Puizina, J., Nazlić, M., Maravić, A., Ljubenkov, I., Soldo, B., et al. (2021). Phytochemical Characterization and Screening of Antioxidant, Antimicrobial and Antiproliferative Properties of Allium × Cornutum Clementi and Two Varieties of Allium cepa L. Peel Extracts. *Plants* 10 (5), 832. doi:10.3390/plants10050832

GBD (2021). Global, Regional, and National Burden of Stroke and its Risk Factors, 1990-2019: a Systematic Analysis for the Global Burden of Disease Study 2019. *LancetNeurology*. 20(10). doi:10.1016/s1474-4422(21)00252-0

Gelderblom, M., Weymar, A., Bernreuther, C., Velden, J., Arunachalam, P., Steinbach, K., et al. (2012). Neutralization of the IL-17 axis Diminishes Neutrophil Invasion and Protects from Ischemic Stroke. *Blood* 120 (18), 3793–3802. doi:10.1182/blood-2012-02-412726

Genchi, A., Semerano, A., Schwarz, G., Dell'Acqua, B., Gullotta, G. S., Sampaolo, M., et al. (2022). Neutrophils Predominate the Immune Signature of Cerebral Thrombi in COVID-19 Stroke Patients. *Acta Neuropathol. Commun.* 10 (1), 14. doi:10.1186/s40478-022-01313-y

Ghosh, A., Sarkar, S., Mandal, A. K., and Das, N. (2013). Neuroprotective Role of Nanoencapsulated Quercetin in Combating Ischemia-Reperfusion Induced Neuronal Damage in Young and Aged Rats. *PloS one* 8 (4), e57735. doi:10.1371/journal.pone.0057735

Gibbins, J., Asselin, J., Farndale, R., Barnes, M., Law, C. L., and Watson, S. P. (1996). Tyrosine Phosphorylation of the Fc Receptor Gamma-Chain in Collagen-Stimulated Platelets. *J. Biol. Chem.* 271 (30), 18095–18099. doi:10.1074/jbc.271.30.18095

Girardelo, J. R., Munari, E. L., Dallorsoleta, J. C. S., Cechinel, G., Goetten, A. L. F., Sales, L. R., et al. (202010961). Bioactive Compounds, Antioxidant Capacity and Antitumoral Activity of Ethanolic Extracts from Fruits and Seeds of Eugenia Involucrata DC. *Food Res. Int.* 137, 109615. doi:10.1016/j.foodres.2020.109615

Graefe, E. U., Derendorf, H., and Veit, M. (1999). Pharmacokinetics and Bioavailability of the Flavonol Quercetin in Humans. *Int. J. Clin. Pharmacol. Ther.* 37 (5), 219–233.

Granato, M., Rizzello, C., Gilardini Montani, M. S., Cuomo, L., Vitillo, M., Santarelli, R., et al. (2017). Quercetin Induces Apoptosis and Autophagy in Primary Effusion Lymphoma Cells by Inhibiting PI3K/AKT/mTOR and STAT3 Signaling Pathways. *J. Nutr. Biochem.* 41, 124–136. doi:10.1016/j.jnutbio.2016.12.011

Guevara, L., Domínguez-Anaya, M. Á., Ortigosa, A., González-Gordo, S., Díaz, C., Vicente, F., et al. (2021). Identification of Compounds with Potential Therapeutic Uses from Sweet Pepper (Capsicum Annuum L.) Fruits and Their Modulation by Nitric Oxide (NO). *Int. J. Mol. Sci.* 22 (9). doi:10.3390/ijms22094476

Guo, L., Huang, Z., Huang, L., Liang, J., Wang, P., Zhao, L., et al. (2021). Surface-modified Engineered Exosomes Attenuated Cerebral Ischemia/reperfusion Injury by Targeting the Delivery of Quercetin towards Impaired Neurons. *J. Nanobiotechnol* 19 (1), 141. doi:10.1186/s12951-021-00879-4

Hanganu, D., Niculae, M., Ielciu, I., Olah, N.-K., Muntean, M., Burtescu, R., et al. (2021). Chemical Profile, Cytotoxic Activity and Oxidative Stress Reduction of Different Syringa Vulgaris L. Extracts. *Molecules* 26 (11), 3104. doi:10.3390/molecules26113104

Haruwaka, K., Ikegami, A., Tachibana, Y., Ohno, N., Konishi, H., Hashimoto, A., et al. (2019). Dual Microglia Effects on Blood Brain Barrier Permeability Induced by Systemic Inflammation. *Nat. Commun.* 10 (1), 5816. doi:10.1038/s41467-019-13812-z

Heo, J. H., Nam, H. S., Kim, Y. D., Choi, J. K., Kim, B. M., Kim, D. J., et al. (2020). Pathophysiologic and Therapeutic Perspectives Based on Thrombus Histology in Stroke. *J. Stroke* 22 (1), 64–75. doi:10.5853/jos.2019.03440

Huang, Y. Y., Wang, Z. H., Deng, L. H., Wang, H., and Zheng, Q. (2020). Oral Administration of Quercetin or its Derivatives Inhibit Bone Loss in Animal Model of Osteoporosis. *Oxid. Med. Cell Longev.* 2020, 6080597. doi:10.1155/2020/6080597

Hubbard, G. P., Stevens, J. M., Cicmil, M., Sage, T., Jordan, P. A., Williams, C. M., et al. (2003). Quercetin Inhibits Collagen-Stimulated Platelet Activation through Inhibition of Multiple Components of the Glycoprotein VI Signaling Pathway. *J. Thromb. Haemost.* 1 (5), 1079–1088. doi:10.1046/j.1538-7836.2003.00212.x

Hubbard, G. P., Wolffram, S., de Vos, R., Bovy, A., Gibbins, J. M., and Lovegrove, J. A. (2006). Ingestion of Onion Soup High in Quercetin Inhibits Platelet Aggregation and Essential Components of the Collagen-Stimulated Platelet Activation Pathway in Man: a Pilot Study. *Br. J. Nutr.* 96 (3), 482–488.

Hubbard, G. P., Wolffram, S., Lovegrove, J. A., and Gibbins, J. M. (2004). Ingestion of Quercetin Inhibits Platelet Aggregation and Essential Components of the

Collagen-Stimulated Platelet Activation Pathway in Humans. *J. Thromb. Haemost.* 2 (12), 2138–2145. doi:10.1111/j.1538-7836.2004.01067.x

Jaimand, K., Rezaee, M. B., Behrad, Z., and Najafy-Ashtiany, A. (2012). Comparison of Extraction and Measurement of Quercetin from Stigma, Style, Sepals, Petals and Stamen of Crocus Sativus by HPLC in Combination with Heat and Ultrasonic. *J. Med. Plants Prod.* 2, 167–170.

Jasuja, R., Passam, F. H., Kennedy, D. R., Kim, S. H., van Hessem, L., Lin, L., et al. (2012). Protein Disulfide Isomerase Inhibitors Constitute a New Class of Antithrombotic Agents. *J. Clin. Invest.* 122 (6), 2104–2113. doi:10.1172/jci61228

Jo, H. M., Ahn, C., Kim, H., Kang, B. T., Jeung, E. B., and Yang, M. P. (2021). Effect of Quercetin on Formation of Porcine Neutrophil Extracellular Trap. *Vet. Immunol. Immunopathol.* 241, 110335. doi:10.1016/j.vetimm.2021.110335

Jordan, J., de Groot, P. W., and Galindo, M. F. (2011). Mitochondria: the Headquarters in Ischemia-Induced Neuronal Death. *Cent. Nerv. Syst. Agents Med. Chem.* 11 (2), 98–106. doi:10.2174/187152411796011358

Kalogiouri, N. P., and Samanidou, V. F. (2021). A Validated Ultrasound-Assisted Extraction Coupled with SPE-HPLC-DAD for the Determination of Flavonoids in By-Products of Plant Origin: An Application Study for the Valorization of the Walnut Septum Membrane. *Molecules* 26 (21), 6418. doi:10.3390/molecules26216418

Kampa, R. P., Sęk, A., Szewczyk, A., and Bednarczyk, P. (2021). Cytoprotective Effects of the Flavonoid Quercetin by Activating Mitochondrial BKCa Channels in Endothelial Cells. *Biomed. Pharmacother.* 142, 112039. doi:10.1016/j.biopha.2021.112039

Kanaji, S., Morodomi, Y., Weiler, H., Zarpellon, A., Montgomery, R. R., Ruggeri, Z. M., et al. (2022). The impact of aberrant von Willebrand Factor-GPIbα Interaction on Megakaryopoiesis and Platelets in Humanized Type 2B von Willebrand Disease Model Mouse. *Haematologica*. doi:10.3324/haematol.2021.280561

Karuppagounder, S. S., Alim, I., Khim, S. J., Bourassa, M. W., Sleiman, S. F., John, R., et al. (2016). Therapeutic Targeting of Oxygen-Sensing Prolyl Hydroxylases Abrogates ATF4-dependent Neuronal Death and Improves Outcomes after Brain Hemorrhage in Several Rodent Models. *Sci. Transl. Med.* 8 (328), 328ra29. 328ra329. doi:10.1126/scitranslmed.aac6008

Kleinschnitz, C., Grund, H., Wingler, K., Armitage, M. E., Jones, E., Mittal, M., et al. (2010). Post-stroke Inhibition of Induced NADPH Oxidase Type 4 Prevents Oxidative Stress and Neurodegeneration. *PLoS Biol.* 8 (9). doi:10.1371/journal.pbio.1000479

Knekt, P., Isotupa, S., Rissanen, H., Heliövaara, M., Järvinen, R., Häkkinen, S., et al. (2000). Quercetin Intake and the Incidence of Cerebrovascular Disease. *Eur. J. Clin. Nutr.* 54 (5), 415–417. doi:10.1038/sj.ejcn.1600974

Kotoda, M., Furukawa, H., Miyamoto, T., Korai, M., Shikata, F., Kuwabara, A., et al. (2018). Role of Myeloid Lineage Cell Autophagy in Ischemic Brain Injury. *Stroke* 49 (6), 1488–1495. doi:10.1161/strokeaha.117.018637

Le Behot, A., Gauberti, M., Martinez De Lizarrondo, S., Montagne, A., Lemarchand, E., Repesse, Y., et al. (2014). GpIbα-VWF Blockade Restores Vessel Patency by Dissolving Platelet Aggregates Formed under Very High Shear Rate in Mice. *Blood* 123 (21), 3354–3363. doi:10.1182/blood-2013-12-543074

Le, K., Song, Z., Deng, J., Peng, X., Zhang, J., Wang, L., et al. (2020). Quercetin Alleviates Neonatal Hypoxic-Ischemic Brain Injury by Inhibiting Microglia-Derived Oxidative Stress and TLR4-Mediated Inflammation. *Inflamm. Res.* 69 (12), 1201–1213. doi:10.1007/s00011-020-01402-5

Lee, J. K., Kwak, H. J., Piao, M. S., Jang, J. W., Kim, S. H., and Kim, H. S. (2011). Quercetin Reduces the Elevated Matrix Metalloproteinases-9 Level and Improves Functional Outcome after Cerebral Focal Ischemia in Rats. *Acta Neurochir. (Wien)* 153 (6), 1321–1329. discussion 1329. doi:10.1007/s00701-010-0889-x

Lee, S. M., Moon, J., Chung, J. H., Cha, Y. J., and Shin, M. J. (2013). Effect of Quercetin-Rich Onion Peel Extracts on Arterial Thrombosis in Rats. *Food Chem. Toxicol.* 57, 99–105. doi:10.1016/j.fct.2013.03.008

Lee, Y. H., Kim, H. J., Yoo, H., Jung, S. Y., Kwon, B. J., Kim, N. J., et al. (2015). Synthesis of (2-amino)ethyl Derivatives of Quercetin 3-O-Methyl Ether and Their Antioxidant and Neuroprotective Effects. *Bioorg Med. Chem.* 23 (15), 4970–4979. doi:10.1016/j.bmc.2015.05.023

Lee, Y. J., Bernstock, J. D., Nagaraja, N., Ko, B., and Hallenbeck, J. M. (2016). Global SUMOylation Facilitates the Multimodal Neuroprotection Afforded by Quercetin against the Deleterious Effects of Oxygen/glucose Deprivation and the Restoration of Oxygen/glucose. *J. Neurochem.* 138 (1), 101–116. doi:10.1111/jnc.13643

Leyva-Soto, A., Alejandra Chavez-Santoscoy, R., Porras, O., Hidalgo-Ledesma, M., Serrano-Medina, A., Alejandra Ramírez-Rodríguez, A., et al. (2021). Epicatechin and Quercetin Exhibit *In Vitro* Antioxidant Effect, Improve Biochemical Parameters Related to Metabolic Syndrome, and Decrease Cellular Genotoxicity in Humans. *Food Res. Int.* 142, 110101. doi:10.1016/j.foodres.2020.110101

Li, C., Zhang, W. J., and Frei, B. (2016a). Quercetin Inhibits LPS-Induced Adhesion Molecule Expression and Oxidant Production in Human Aortic Endothelial Cells by P38-Mediated Nrf2 Activation and Antioxidant Enzyme Induction. *Redox Biol.* 9, 104–113. doi:10.1016/j.redox.2016.06.006

Li, J., Kim, K., Barazia, A., Tseng, A., and Cho, J. (2015). Platelet-neutrophil Interactions under Thromboinflammatory Conditions. *Cell Mol. Life Sci.* 72 (14), 2627–2643. doi:10.1007/s00018-015-1845-y

Li, W., Chen, Z., Yan, M., He, P., Chen, Z., and Dai, H. (2016b). The Protective Role of Isorhamnetin on Human Brain Microvascular Endothelial Cells from Cytotoxicity Induced by Methylglyoxal and Oxygen-Glucose Deprivation. *J. Neurochem.* 136 (3), 651–659. doi:10.1111/jnc.13436

Liang, M. L., Da, X. W., He, A. D., Yao, G. Q., Xie, W., Liu, G., et al. (2015). Pentamethylquercetin (PMQ) Reduces Thrombus Formation by Inhibiting Platelet Function. *Sci. Rep.* 5, 11142. doi:10.1038/srep11142

Liesz, A., Suri-Payer, E., Veltkamp, C., Doerr, H., Sommer, C., Rivest, S., et al. (2009). Regulatory T Cells Are Key Cerebroprotective Immunomodulators in Acute Experimental Stroke. *Nat. Med.* 15 (2), 192–199. doi:10.1038/nm.1927

Liu, J. J., Song, C. W., Yue, Y., Duan, C. G., Yang, J., He, T., et al. (2005b). Quercetin Inhibits LPS-Induced Delay in Spontaneous Apoptosis and Activation of Neutrophils. *Inflamm. Res.* 54 (12), 500–507. doi:10.1007/s00011-005-1385-2

Liu, J., Li, X., Yue, Y., Li, J., He, T., and He, Y. (2005a). The Inhibitory Effect of Quercetin on IL-6 Production by LPS-Stimulated Neutrophils. *Cell Mol. Immunol.* 2 (6), 455–460.

Liu, Y., Gong, W., Yang, Z. Y., Zhou, X. S., Gong, C., Zhang, T. R., et al. (2017). Quercetin Induces Protective Autophagy and Apoptosis through ER Stress via the P-STAT3/Bcl-2 axis in Ovarian Cancer. *Apoptosis* 22 (4), 544–557. doi:10.1007/s10495-016-1334-2

Lo, E. H., Dalkara, T., and Moskowitz, M. A. (2003). Mechanisms, Challenges and Opportunities in Stroke. *Nat. Rev. Neurosci.* 4 (5), 399–415. doi:10.1038/nrn1106

Loke, W. M., Proudfoot, J. M., McKinley, A. J., Needs, P. W., Kroon, P. A., Hodgson, J. M., et al. (2008). Quercetin and its *In Vivo* Metabolites Inhibit Neutrophil-Mediated Low-Density Lipoprotein Oxidation. *J. Agric. Food Chem.* 56 (10), 3609–3615. doi:10.1021/jf8003042

Lu, N., Sui, Y., Tian, R., and Peng, Y. Y. (2018). Inhibitive Effects of Quercetin on Myeloperoxidase-dependent Hypochlorous Acid Formation and Vascular Endothelial Injury. *J. Agric. Food Chem.* 66 (19), 4933–4940. doi:10.1021/acs.jafc.8b01537

Ma, Y., Wang, J., Wang, Y., and Yang, G. Y. (2017). The Biphasic Function of Microglia in Ischemic Stroke. *Prog. Neurobiol.* 157, 247–272. doi:10.1016/j.pneurobio.2016.01.005

Magar, R. T., and Sohng, J. K. (2020). A Review on Structure, Modifications and Structure-Activity Relation of Quercetin and its Derivatives. *J. Microbiol. Biotechnol.* 30 (1), 11–20. doi:10.4014/jmb.1907.07003

Manach, C., Scalbert, A., Morand, C., Rémésy, C., and Jiménez, L. (2004). Polyphenols: Food Sources and Bioavailability. *Am. J. Clin. Nutr.* 79 (5), 727–747. doi:10.1093/ajcn/79.5.727

Mar, J. M., da Silva, L. S., Moreira, W. P., Biondo, M. M., Pontes, F. L. D., Campos, F. R., et al. (2021). Edible Flowers from Theobroma Speciosum: Aqueous Extract Rich in Antioxidant Compounds. *Food Chem.* 356, 129723. doi:10.1016/j.foodchem.2021.129723

Moro, T. M. A., and Clerici, M. T. P. S. (2021). Burdock (Arctium Lappa L) Roots as a Source of Inulin-type Fructans and Other Bioactive Compounds: Current Knowledge and Future Perspectives for Food and Non-food Applications. *Food Res. Int.* 141, 109889. doi:10.1016/j.foodres.2020.109889

Mosawy, S., Jackson, D. E., Woodman, O. L., and Linden, M. D. (2013a). Inhibition of Platelet-Mediated Arterial Thrombosis and Platelet Granule Exocytosis by

3',4'-dihydroxyflavonol and Quercetin. *Platelets* 24 (8), 594–604. doi:10.3109/09537104.2012.749396

Mosawy, S., Jackson, D. E., Woodman, O. L., and Linden, M. D. (2014). The Flavonols Quercetin and 3',4'-dihydroxyflavonol Reduce Platelet Function and Delay Thrombus Formation in a Model of Type 1 Diabetes. *Diab Vasc. Dis. Res.* 11 (3), 174–181. doi:10.1177/1479164114524234

Mosawy, S., Jackson, D. E., Woodman, O. L., and Linden, M. D. (2013b). Treatment with Quercetin and 3',4'-dihydroxyflavonol Inhibits Platelet Function and Reduces Thrombus Formation *In Vivo*. *J. Thromb. Thrombolysis* 36 (1), 50–57. doi:10.1007/s11239-012-0827-2

Mrvová, N., Škandík, M., Kuniaková, M., and Račková, L. (2015). Modulation of BV-2 Microglia Functions by Novel Quercetin Pivaloyl Ester. *Neurochem. Int.* 90, 246–254. doi:10.1016/j.neuint.2015.09.005

Mukhopadhyay, P., and Prajapati, A. K. (2015). Quercetin in Anti-diabetic Research and Strategies for Improved Quercetin Bioavailability Using Polymer-Based Carriers - a Review. *RSC Adv.* 5 (118), 97547–97562. doi:10.1039/c5ra18896b

Muthian, G., and Bright, J. J. (2004). Quercetin, a Flavonoid Phytoestrogen, Ameliorates Experimental Allergic Encephalomyelitis by Blocking IL-12 Signaling through JAK-STAT Pathway in T Lymphocyte. *J. Clin. Immunol.* 24 (5), 542–552. doi:10.1023/B:JOCI.0000040925.55682.a5

Mwaurah, P. W., Kumar, S., Kumar, N., Panghal, A., Attkan, A. K., Singh, V. K., et al. (2020). Physicochemical Characteristics, Bioactive Compounds and Industrial Applications of Mango Kernel and its Products: A Review. *Compr. Rev. food Sci. food Saf.* 19 (5), 2421–2446. doi:10.1111/1541-4337.12598

Najda, A., Klimek, K., Balant, S., Wrzesinska-Jedrusiak, E., and Piekarski, W. (2019). Optimization of the Process of Polyphenol Extraction from Mentha Spicata with Various Solvents. *Przemysl Chem.* 98 (8), 1286–1289.

Naseri, N., Valizadeh, H., and Zakeri-Milani, P. (2015). Solid Lipid Nanoparticles and Nanostructured Lipid Carriers: Structure, Preparation and Application. *Adv. Pharm. Bull.* 5 (3), 305–313. doi:10.15171/apb.2015.043

Nichols, M., Zhang, J., Polster, B. M., Elustondo, P. A., Thirumaran, A., Pavlov, E. V., et al. (2015). Synergistic Neuroprotection by Epicatechin and Quercetin: Activation of Convergent Mitochondrial Signaling Pathways. *Neuroscience* 308, 75–94. doi:10.1016/j.neuroscience.2015.09.012

Nieto-Trujillo, A., Cruz-Sosa, F., Luria-Pérez, R., Gutiérrez-Rebolledo, G. A., Román-Guerrero, A., Burrola-Aguilar, C., et al. (2021). Arnica montana Cell Culture Establishment, and Assessment of its Cytotoxic, Antibacterial, α-Amylase Inhibitor, and Antioxidant *In Vitro* Bioactivities. *Plants* 10 (11), 2300. doi:10.3390/plants10112300

O'Brien, J. R., and Salmon, G. P. (1990). An Independent Haemostatic Mechanism: Shear Induced Platelet Aggregation. *Adv. Exp. Med. Biol.* 281, 287–296. doi:10.1007/978-1-4615-3806-6_30

Oboh, G., Ademosun, A. O., and Ogunsuyi, O. B. (2016). Quercetin and its Role in Chronic Diseases. *Adv. Exp. Med. Biol.* 929, 377–387. doi:10.1007/978-3-319-41342-6_17

Oh, T. W., Do, H. J., Jeon, J. H., and Kim, K. (2021). Quercitrin Inhibits Platelet Activation in Arterial Thrombosis. *Phytomedicine* 80, 153363. doi:10.1016/j.phymed.2020.153363

Ojo, O. B., Amoo, Z. A., Saliu, I. O., Olaleye, M. T., Farombi, E. O., and Akinmoladun, A. C. (2019). Neurotherapeutic Potential of Kolaviron on Neurotransmitter Dysregulation, Excitotoxicity, Mitochondrial Electron Transport Chain Dysfunction and Redox Imbalance in 2-VO Brain Ischemia/reperfusion Injury. *Biomed. Pharmacother.* 111, 859–872. doi:10.1016/j.biopha.2018.12.144

Oliveira, A. I., Pinho, C., Sarmento, B., and Dias, A. C. P. (2021). Quercetin-biapigenin Nanoparticles Are Effective to Penetrate the Blood-Brain Barrier. *Drug Deliv. Transl. Res.* 12, 267–281. doi:10.1007/s13346-021-00917-6

Orbán-Gyapai, O., Raghavan, A., Vasas, A., Forgo, P., Hohmann, J., and Shah, Z. A. (2014). Flavonoids Isolated from Rumex Aquaticus Exhibit Neuroprotective and Neurorestorative Properties by Enhancing Neurite Outgrowth and Synaptophysin. *CNS Neurol. Disord. Drug Targets* 13 (8), 1458–1464. doi:10.2174/1871527313666141023154446

Pallauf, K., and Rimbach, G. (2013). Autophagy, Polyphenols and Healthy Ageing. *Ageing Res. Rev.* 12 (1), 237–252. doi:10.1016/j.arr.2012.03.008

Pan, W., Chang, M. J., Booyse, F. M., Grenett, H. E., Bradley, K. M., Wolkowicz, P. E., et al. (2008). Quercetin Induced Tissue-type Plasminogen Activator Expression Is Mediated through Sp1 and P38 Mitogen-Activated Protein Kinase in Human Endothelial Cells. *J. Thromb. Haemost.* 6 (6), 976–985. doi:10.1111/j.1538-7836.2008.02977.x

Park, D. J., Jeon, S. J., Kang, J. B., and Koh, P. O. (2020). Quercetin Reduces Ischemic Brain Injury by Preventing Ischemia-Induced Decreases in the Neuronal Calcium Sensor Protein Hippocalcin. *Neuroscience* 430, 47–62. doi:10.1016/j.neuroscience.2020.01.015

Park, D. J., Kang, J. B., Shah, M. A., and Koh, P. O. (2019). Quercetin Alleviates the Injury-Induced Decrease of Protein Phosphatase 2A Subunit B in Cerebral Ischemic Animal Model and Glutamate-Exposed HT22 Cells. *J. Vet. Med. Sci.* 81 (7), 1047–1054. doi:10.1292/jvms.19-0094

Park, D. J., Shah, F. A., and Koh, P. O. (2018). Quercetin Attenuates Neuronal Cells Damage in a Middle Cerebral Artery Occlusion Animal Model. *J. Vet. Med. Sci.* 80 (4), 676–683. doi:10.1292/jvms.17-0693

Pateiro, M., Gómez, B., Munekata, P. E. S., Barba, F. J., Putnik, P., Kovačević, D. B., et al. (2021). Nanoencapsulation of Promising Bioactive Compounds to Improve Their Absorption, Stability, Functionality and the Appearance of the Final Food Products. *Molecules* 26 (6), 1547. doi:10.3390/molecules26061547

Pei, B., Yang, M., Qi, X., Shen, X., Chen, X., and Zhang, F. (2016). Quercetin Ameliorates Ischemia/reperfusion-Induced Cognitive Deficits by Inhibiting ASK1/JNK3/caspase-3 by Enhancing the Akt Signaling Pathway. *Biochem. Biophys. Res. Commun.* 478 (1), 199–205. doi:10.1016/j.bbrc.2016.07.068

Pircher, J., Engelmann, B., Massberg, S., and Schulz, C. (2019). Platelet-Neutrophil Crosstalk in Atherothrombosis. *Thromb. Haemost.* 119 (8), 1274–1282. doi:10.1055/s-0039-1692983

Poole, A., Gibbins, J. M., Turner, M., van Vugt, M. J., van de Winkel, J. G., Saito, T., et al. (1997). The Fc Receptor Gamma-Chain and the Tyrosine Kinase Syk Are Essential for Activation of Mouse Platelets by Collagen. *Embo J.* 16 (9), 2333–2341. doi:10.1093/emboj/16.9.2333

Poulter, N. S., Pollitt, A. Y., Owen, D. M., Gardiner, E. E., Andrews, R. K., Shimizu, H., et al. (2017). Clustering of Glycoprotein VI (GPVI) Dimers upon Adhesion to Collagen as a Mechanism to Regulate GPVI Signaling in Platelets. *J. Thromb. Haemost.* 15 (3), 549–564. doi:10.1111/jth.13613

Pourakbar, L., Moghaddam, S. S., Enshasy, H. A. E., and Sayyed, R. Z. (2021). Antifungal Activity of the Extract of a Macroalgae, Gracilariopsis Persica, against Four Plant Pathogenic Fungi. *Plants* 10 (9), 1781. doi:10.3390/plants10091781

Qu, X., Qi, D., Dong, F., Wang, B., Guo, R., Luo, M., et al. (2014). Quercetin Improves Hypoxia-Ischemia Induced Cognitive Deficits via Promoting Remyelination in Neonatal Rat. *Brain Res.* 1553, 31–40. doi:10.1016/j.brainres.2014.01.035

Ratnam, D. V., Ankola, D. D., Bhardwaj, V., Sahana, D. K., and Kumar, M. N. (2006). Role of Antioxidants in Prophylaxis and Therapy: A Pharmaceutical Perspective. *J. Control Release* 113 (3), 189–207. doi:10.1016/j.jconrel.2006.04.015

Rice-Evans, C., Miller, N., and Paganga, G. (1997). Antioxidant Properties of Phenolic Compounds. *Trends plant Sci.* 2 (4), 152–159. doi:10.1016/s1360-1385(97)01018-2

Riva, A., Ronchi, M., Petrangolini, G., Bosisio, S., and Allegrini, P. (2019). Improved Oral Absorption of Quercetin from Quercetin Phytosome®, a New Delivery System Based on Food Grade Lecithin. *Eur. J. Drug Metab. Pharmacokinet.* 44 (2), 169–177. doi:10.1007/s13318-018-0517-3

Rivera, F., Costa, G., Abin, A., Urbanavicius, J., Arruti, C., Casanova, G., et al. (2008). Reduction of Ischemic Brain Damage and Increase of Glutathione by a Liposomal Preparation of Quercetin in Permanent Focal Ischemia in Rats. *Neurotox. Res.* 13 (2), 105–114. doi:10.1007/bf03033562

Rojas-Garbanzo, C., Rodríguez, L., Pérez, A. M., Mayorga-Gross, A. L., Vásquez-Chaves, V., Fuentes, E., et al. (2021). Anti-platelet Activity and Chemical Characterization by UPLC-DAD-ESI-QTOF-MS of the Main Polyphenols in Extracts from Psidium Leaves and Fruits. *Food Res. Int.* 141, 110070. doi:10.1016/j.foodres.2020.110070

Rosell, A., Cuadrado, E., Ortega-Aznar, A., Hernández-Guillamon, M., Lo, E. H., and Montaner, J. (2008). MMP-9-positive Neutrophil Infiltration Is Associated to Blood-Brain Barrier Breakdown and Basal Lamina Type IV Collagen Degradation during Hemorrhagic Transformation after Human Ischemic Stroke. *Stroke* 39 (4), 1121–1126. doi:10.1161/strokeaha.107.500868

Russo, M., Palumbo, R., Mupo, A., Tosto, M., Iacomino, G., Scognamiglio, A., et al. (2003). Flavonoid Quercetin Sensitizes a CD95-Resistant Cell Line to Apoptosis

by Activating Protein Kinase Calpha. *Oncogene* 22 (21), 3330–3342. doi:10.1038/sj.onc.1206493

Rutkowska, M., Kolodziejczyk-Czepas, J., Owczarek, A., Zakrzewska, A., Magiera, A., and Olszewska, M. A. (2021). Novel Insight into Biological Activity and Phytochemical Composition of Sorbus Aucuparia L. Fruits: Fractionated Extracts as Inhibitors of Protein Glycation and Oxidative/nitrative Damage of Human Plasma Components. *Food Res. Int.* 147, 110526. doi:10.1016/j.foodres.2021.110526

Sánchez, M., Galisteo, M., Vera, R., Villar, I. C., Zarzuelo, A., Tamargo, J., et al. (2006). Quercetin Downregulates NADPH Oxidase, Increases eNOS Activity and Prevents Endothelial Dysfunction in Spontaneously Hypertensive Rats. *J. Hypertens.* 24 (1), 75–84. doi:10.1097/01.hjh.0000198029.22472.d9

Sanchez, M., Lodi, F., Vera, R., Villar, I. C., Cogolludo, A., Jimenez, R., et al. (2007). Quercetin and Isorhamnetin Prevent Endothelial Dysfunction, Superoxide Production, and Overexpression of P47phox Induced by Angiotensin II in Rat Aorta. *J. Nutr.* 137 (4), 910–915. doi:10.1093/jn/137.4.910

Schrottmaier, W. C., Mussbacher, M., Salzmann, M., and Assinger, A. (2020). Platelet-leukocyte Interplay during Vascular Disease. *Atherosclerosis* 307, 109–120. doi:10.1016/j.atherosclerosis.2020.04.018

Schuhmann, M. K., Stoll, G., Bieber, M., Vögtle, T., Hofmann, S., Klaus, V., et al. (2020). CD84 Links T Cell and Platelet Activity in Cerebral Thrombo-Inflammation in Acute Stroke. *Circ. Res.* 127 (8), 1023–1035. doi:10.1161/circresaha.120.316655

Seiler, A., Schneider, M., Förster, H., Roth, S., Wirth, E. K., Culmsee, C., et al. (2008). Glutathione Peroxidase 4 Senses and Translates Oxidative Stress into 12/15-lipoxygenase Dependent- and AIF-Mediated Cell Death. *Cell Metab.* 8 (3), 237–248. doi:10.1016/j.cmet.2008.07.005

Shabbir, U., Rubab, M., Daliri, E. B.-M., Chelliah, R., Javed, A., and Oh, D.-H. (2021). Curcumin, Quercetin, Catechins and Metabolic Diseases: The Role of Gut Microbiota. *Nutrients* 13 (1), 206. doi:10.3390/nu13010206

Shah, F. A., Park, D. J., and Koh, P. O. (2018). Identification of Proteins Differentially Expressed by Quercetin Treatment in a Middle Cerebral Artery Occlusion Model: A Proteomics Approach. *Neurochem. Res.* 43 (8), 1608–1623. doi:10.1007/s11064-018-2576-x

Shalavadi, M. H., Chandrashekhar, V. M., and Muchchandi, I. S. (2020). Neuroprotective Effect of Convolvulus Pluricaulis Choisy in Oxidative Stress Model of Cerebral Ischemia Reperfusion Injury and Assessment of MAP2 in Rats. *J. Ethnopharmacol.* 249, 112393. doi:10.1016/j.jep.2019.112393

Sharifi-Rad, J., Quispe, C., Shaheen, S., El Haouari, M., Azzini, E., Butnariu, M., et al. (2021). Flavonoids as Potential Anti-Platelet Aggregation Agents: From Biochemistry to Health Promoting Abilities. *Crit. Rev. Food Sci. Nutr.* [Epub ahead of print], 1–14. doi:10.1080/10408398.2021.1924612

Shen, P., Lin, W., Deng, X., Ba, X., Han, L., Chen, Z., et al. (2021). Potential Implications of Quercetin in Autoimmune Diseases. *Front. Immunol.* 12, 689044. doi:10.3389/fimmu.2021.689044

South, K., Saleh, O., Lemarchand, E., Coutts, G., Smith, C. J., Schiessl, I., et al. (2022). Robust Thrombolytic and Anti-inflammatory Action of a Constitutively Active ADAMTS13 Variant in Murine Stroke Models. *Blood* 139 (10), 1575–1587. doi:10.1182/blood.2021012787

Stopa, J. D., Neuberg, D., Puligandla, M., Furie, B., Flaumenhaft, R., and Zwicker, J. I. (2017). Protein Disulfide Isomerase Inhibition Blocks Thrombin Generation in Humans by Interfering with Platelet Factor V Activation. *JCI Insight* 2 (1), e89373. doi:10.1172/jci.insight.89373

Stumvoll, M., Goldstein, B. J., and van Haeften, T. W. (2005). Type 2 Diabetes: Principles of Pathogenesis and Therapy. *Lancet* 365 (9467), 1333–1346. doi:10.1016/s0140-6736(05)61032-x

Sumi, M., Tateishi, N., Shibata, H., Ohki, T., and Sata, M. (2013). Quercetin Glucosides Promote Ischemia-Induced Angiogenesis, but Do Not Promote Tumor Growth. *Life Sci.* 93 (22), 814–819. doi:10.1016/j.lfs.2013.09.005

Sun, M. S., Jin, H., Sun, X., Huang, S., Zhang, F. L., Guo, Z. N., et al. (2018). Free Radical Damage in Ischemia-Reperfusion Injury: An Obstacle in Acute Ischemic Stroke after Revascularization Therapy. *Oxid. Med. Cell Longev.* 2018, 3804979. doi:10.1155/2018/3804979

Suri, S., Taylor, M. A., Verity, A., Tribolo, S., Needs, P. W., Kroon, P. A., et al. (2008). A Comparative Study of the Effects of Quercetin and its Glucuronide and Sulfate Metabolites on Human Neutrophil Function *In Vitro*. *Biochem. Pharmacol.* 76 (5), 645–653. doi:10.1016/j.bcp.2008.06.010

Tuo, Q. z., Zhang, S. t., and Lei, P. (2021). Mechanisms of Neuronal Cell Death in Ischemic Stroke and Their Therapeutic Implications. *Med. Res. Rev.* 42, 259–305. doi:10.1002/med.21817

Ulya, T., Ardianto, C., Anggreini, P., Budiatin, A. S., Setyawan, D., and Khotib, J. (2021). Quercetin Promotes Behavioral Recovery and Biomolecular Changes of Melanocortin-4 Receptor in Mice with Ischemic Stroke. *J. Basic Clin. Physiol. Pharmacol.* 32 (4), 349–355. doi:10.1515/jbcpp-2020-0490

Vek, V., Keržič, E., Poljanšek, I., Eklund, P., Humar, M., and Oven, P. (2021). Wood Extractives of Silver Fir and Their Antioxidant and Antifungal Properties. *Molecules* 26 (21), 6412. doi:10.3390/molecules26216412

Vekic, J., Zeljkovic, A., Stefanovic, A., Jelic-Ivanovic, Z., and Spasojevic-Kalimanovska, V. (2019). Obesity and Dyslipidemia. *Metabolism* 92, 71–81. doi:10.1016/j.metabol.2018.11.005

Verhenne, S., Denorme, F., Libbrecht, S., Vandenbulcke, A., Pareyn, I., Deckmyn, H., et al. (2015). Platelet-derived VWF Is Not Essential for Normal Thrombosis and Hemostasis but Fosters Ischemic Stroke Injury in Mice. *Blood* 126 (14), 1715–1722. doi:10.1182/blood-2015-03-632901

Viswanatha, G. L., Venkataranganna, M. V., Prasad, N. B. L., and Hanumanthappa, S. (2018). Chemical Characterization and Cerebroprotective Effect of Methanolic Root Extract of Colebrookea Oppositifolia in Rats. *J. Ethnopharmacol.* 223, 63–75. doi:10.1016/j.jep.2018.05.009

Viswanatha, G. L., Venkataranganna, M. V., Prasad, N. B. L., and Shylaja, H. (2019). *Achyranthes aspera* Linn. Alleviates Cerebral Ischemia-Reperfusion-Induced Neurocognitive, Biochemical, Morphological and Histological Alterations in Wistar Rats. *J. Ethnopharmacol.* 228, 58–69. doi:10.1016/j.jep.2018.09.018

Wang, J., Wang, P., Li, S., Wang, S., Li, Y., Liang, N., et al. (2014). Mdivi-1 Prevents Apoptosis Induced by Ischemia-Reperfusion Injury in Primary Hippocampal Cells via Inhibition of Reactive Oxygen Species-Activated Mitochondrial Pathway. *J. Stroke Cerebrovasc. Dis.* 23 (6), 1491–1499. doi:10.1016/j.jstrokecerebrovasdis.2013.12.021

Wang, J., Xing, H., Wan, L., Jiang, X., Wang, C., and Wu, Y. (2018). Treatment Targets for M2 Microglia Polarization in Ischemic Stroke. *Biomed. Pharmacother.* 105, 518–525. doi:10.1016/j.biopha.2018.05.143

Wang, K., Liu, R., Li, J., Mao, J., Lei, Y., Wu, J., et al. (2011). Quercetin Induces Protective Autophagy in Gastric Cancer Cells: Involvement of Akt-mTOR- and Hypoxia-Induced Factor 1α-Mediated Signaling. *Autophagy* 7 (9), 966–978. doi:10.4161/auto.7.9.15863

Wang, Q., Tang, X. N., and Yenari, M. A. (2007). The Inflammatory Response in Stroke. *J. Neuroimmunol.* 184, 53–68. doi:10.1016/j.jneuroim.2006.11.014

Wang, Y. Y., Chang, C. Y., Lin, S. Y., Wang, J. D., Wu, C. C., Chen, W. Y., et al. (2020). Quercetin Protects against Cerebral Ischemia/reperfusion and Oxygen Glucose Deprivation/reoxygenation Neurotoxicity. *J. Nutr. Biochem.* 83, 108436. doi:10.1016/j.jnutbio.2020.108436

Williams, R. J., Spencer, J. P., and Rice-Evans, C. (2004). Flavonoids: Antioxidants or Signalling Molecules? *Free Radic. Biol. Med.* 36 (7), 838–849. doi:10.1016/j.freeradbiomed.2004.01.001

Wright, B., Moraes, L. A., Kemp, C. F., Mullen, W., Crozier, A., Lovegrove, J. A., et al. (2010). A Structural Basis for the Inhibition of Collagen-Stimulated Platelet Function by Quercetin and Structurally Related Flavonoids. *Br. J. Pharmacol.* 159 (6), 1312–1325. doi:10.1111/j.1476-5381.2009.00632.x

Wu, L., Zhang, Q., Dai, W., Li, S., Feng, J., Li, J., et al. (20172017). Quercetin Pretreatment Attenuates Hepatic Ischemia Reperfusion-Induced Apoptosis and Autophagy by Inhibiting ERK/NF-κB Pathway. *Gastroenterol. Res. Pract.* 2017, 9724217. doi:10.1155/2017/9724217

Wu, M., Liu, F., and Guo, Q. (2019). Quercetin Attenuates Hypoxia-Ischemia Induced Brain Injury in Neonatal Rats by Inhibiting TLR4/NF-Kb Signaling Pathway. *Int. Immunopharmacol.* 74, 105704. doi:10.1016/j.intimp.2019.105704

Yamagata, K. (2019). Polyphenols Regulate Endothelial Functions and Reduce the Risk of Cardiovascular Disease. *Curr. Pharm. Des.* 25 (22), 2443–2458. doi:10.2174/1381612825666190722100504

Yang, D., Wang, T., Long, M., and Li, P. (2020a). Quercetin: Its Main Pharmacological Activity and Potential Application in Clinical Medicine. *Oxid. Med. Cell Longev.* 2020, 8825387. doi:10.1155/2020/8825387

Yang, J., Wu, Z., Long, Q., Huang, J., Hong, T., Liu, W., et al. (2020b). Insights Into Immunothrombosis: The Interplay Among Neutrophil Extracellular Trap, von

Willebrand Factor, and ADAMTS13. *Front. Immunol.* 11, 610696. doi:10.3389/fimmu.2020.610696

Yang, R., Shen, Y.-J., Chen, M., Zhao, J.-Y., Chen, S.-H., Zhang, W., et al. (2021). Quercetin Attenuates Ischemia Reperfusion Injury by Protecting the Blood-Brain Barrier through Sirt1 in MCAO Rats. *J. Asian Nat. Prod. Res.* 24, 278–289. doi:10.1080/10286020.2021.1949302

Yang, W. S., SriRamaratnam, R., Welsch, M. E., Shimada, K., Skouta, R., Viswanathan, V. S., et al. (2014). Regulation of Ferroptotic Cancer Cell Death by GPX4. *Cell* 156, 317–331. doi:10.1016/j.cell.2013.12.010

Yousefi-Manesh, H., Dehpour, A. R., Nabavi, S. M., Khayatkashani, M., Asgardoon, M. H., Derakhshan, M. H., et al. (2021). Therapeutic Effects of Hydroalcoholic Extracts from the Ancient Apple Mela Rosa dei Monti Sibillini in Transient Global Ischemia in Rats. *Pharmaceuticals* 14 (11), 1106. doi:10.3390/ph14111106

Yu, P. X., Zhou, Q. J., Zhu, W. W., Wu, Y. H., Wu, L. C., Lin, X., et al. (2013). Effects of Quercetin on LPS-Induced Disseminated Intravascular Coagulation (DIC) in Rabbits. *Thromb. Res.* 131 (6), e270–3. doi:10.1016/j.thromres.2013.03.002

Yuan, K., Zhu, Q., Lu, Q., Jiang, H., Zhu, M., Li, X., et al. (2020). Quercetin Alleviates Rheumatoid Arthritis by Inhibiting Neutrophil Inflammatory Activities. *J. Nutr. Biochem.* 84, 108454. doi:10.1016/j.jnutbio.2020.108454

Zaragozá, C., Monserrat, J., Mantecón, C., Villaescusa, L., Álvarez-Mon, M. Á., Zaragozá, F., et al. (2021). Binding and Antiplatelet Activity of Quercetin, Rutin, Diosmetin, and Diosmin Flavonoids. *Biomed. Pharmacother.* 141, 111867. doi:10.1016/j.biopha.2021.111867

Zhang, L. L., Zhang, H. T., Cai, Y. Q., Han, Y. J., Yao, F., Yuan, Z. H., et al. (2016). Anti-inflammatory Effect of Mesenchymal Stromal Cell Transplantation and Quercetin Treatment in a Rat Model of Experimental Cerebral Ischemia. *Cell Mol. Neurobiol.* 36 (7), 1023–1034. doi:10.1007/s10571-015-0291-6

Zhang, X., Yan, H., Yuan, Y., Gao, J., Shen, Z., Cheng, Y., et al. (2013). Cerebral Ischemia-Reperfusion-Induced Autophagy Protects against Neuronal Injury by Mitochondrial Clearance. *Autophagy* 9 (9), 1321–1333. doi:10.4161/auto.25132

Zhi, K., Li, M., Bai, J., Wu, Y., Zhou, S., Zhang, X., et al. (2016). Quercitrin Treatment Protects Endothelial Progenitor Cells from Oxidative Damage via Inducing Autophagy through Extracellular Signal-Regulated Kinase. *Angiogenesis* 19 (3), 311–324. doi:10.1007/s10456-016-9504-y

Zhou, M., Zhu, L., Cui, X., Feng, L., Zhao, X., He, S., et al. (2016). Influence of Diet on Leukocyte Telomere Length, Markers of Inflammation and Oxidative Stress in Individuals with Varied Glucose Tolerance: a Chinese Population Study. *Nutr. J.* 15, 39. doi:10.1186/s12937-016-0157-x

Zou, H., Ye, H., Kamaraj, R., Zhang, T., Zhang, J., and Pavek, P. (2021). A Review on Pharmacological Activities and Synergistic Effect of Quercetin with Small Molecule Agents. *Phytomedicine* 92, 153736. doi:10.1016/j.phymed.2021.153736

Zwicker, J. I., Schlechter, B. L., Stopa, J. D., Liebman, H. A., Aggarwal, A., Puligandla, M., et al. (2019). Targeting Protein Disulfide Isomerase with the Flavonoid Isoquercetin to Improve Hypercoagulability in Advanced Cancer. *JCI Insight* 4 (4). doi:10.1172/jci.insight.125851

Conflict of Interest: The authors declare that the research was conducted in the absence of any commercial or financial relationships that could be construed as a potential conflict of interest.

Publisher's Note: All claims expressed in this article are solely those of the authors and do not necessarily represent those of their affiliated organizations, or those of the publisher, the editors and the reviewers. Any product that may be evaluated in this article, or claim that may be made by its manufacturer, is not guaranteed or endorsed by the publisher.

frontiers | Frontiers in Neuroscience

ORIGINAL RESEARCH
published: 23 May 2022
doi: 10.3389/fnins.2022.889292

Effect of Celastrol on LncRNAs and mRNAs Profiles of Cerebral Ischemia-Reperfusion Injury in Transient Middle Cerebral Artery Occlusion Mice Model

Jiandong Liu[1,2†], Xiangna Guo[1†], Lu Yang[1], Tao Tao[3], Jun Cao[1,4], Zexuan Hong[1], Fanning Zeng[1], Yitian Lu[1], Chunshui Lin[1] and Zaisheng Qin[1*]*

[1] Department of Anesthesiology, Nanfang Hospital, Southern Medical University, Guangzhou, China, [2] Department of Anesthesiology, The Affiliated Dongnan Hospital of Xiamen University, School of Medicine, Xiamen University, Zhangzhou, China, [3] Department of Anesthesiology, The Central People's Hospital of Zhanjiang, Zhanjiang, China, [4] Department of Anesthesiology, Affiliated Shenzhen Maternity and Child Healthcare Hospital, Southern Medical University, Shenzhen, China

Celastrol plays a significant role in cerebral ischemia-reperfusion injury. Although previous studies have confirmed that celastrol post-treatment has a protective effect on ischemic stroke, the therapeutic effect of celastrol on ischemic stroke and the underlying molecular mechanism remain unclear. In the present study, focal transient cerebral ischemia was induced by transient middle cerebral artery occlusion (tMCAO) in mice and celastrol was administered immediately after reperfusion. We performed lncRNA and mRNA analysis in the ischemic hemisphere of adult mice with celastrol post-treatment through RNA-Sequencing (RNA-Seq). A total of 50 differentially expressed lncRNAs (DE lncRNAs) and 696 differentially expressed mRNAs (DE mRNAs) were identified between the sham and tMCAO group, and a total of 544 DE lncRNAs and 324 DE mRNAs were identified between the tMCAO and tMCAO + celastrol group. Bioinformatic analysis was done on the identified deregulated genes through gene ontology (GO) analysis, KEGG pathway analysis and network analysis. Pathway analysis indicated that inflammation-related signaling pathways played vital roles in the treatment of ischemic stroke by celastrol. Four DE lncRNAs and 5 DE mRNAs were selected for further validation by qRT-PCR in brain tissue, primary neurons, primary astrocytes, and BV2 cells. The results of qRT-PCR suggested that most of selected differentially expressed genes showed the same fold change patterns as those in RNA-Seq results. Our study suggests celastrol treatment can effectively reduce cerebral ischemia-reperfusion injury. The bioinformatics analysis of lnRNAs and mRNAs profiles in the ischemic hemisphere of adult mice provides a new perspective in the neuroprotective effects of celastrol, particularly with regards to ischemic stroke.

Keywords: celastrol, ischemic stroke, lncRNA, RNA-sequencing, inflammation

OPEN ACCESS

Edited by:
Yongjun Sun,
Hebei University of Science and Technology, China

Reviewed by:
Lianguo Hou,
Hebei Medical University, China
Fei-Fei Shang,
Chongqing Medical University, China
Hebo Wang,
Hebei General Hospital, China
Jianhua Peng,
The Affiliated Hospital of Southwest Medical University, China

***Correspondence:**
Chunshui Lin
lcsnfyy@126.com
Zaisheng Qin
mzkqzs@smu.edu.cn

† These authors have contributed equally to this work

Specialty section:
This article was submitted to Neuropharmacology, a section of the journal Frontiers in Neuroscience

Received: *04 March 2022*
Accepted: *28 April 2022*
Published: *23 May 2022*

Citation:
Liu J, Guo X, Yang L, Tao T, Cao J, Hong Z, Zeng F, Lu Y, Lin C and Qin Z (2022) Effect of Celastrol on LncRNAs and mRNAs Profiles of Cerebral Ischemia-Reperfusion Injury in Transient Middle Cerebral Artery Occlusion Mice Model. Front. Neurosci. 16:889292. doi: 10.3389/fnins.2022.889292

INTRODUCTION

Ischemic stroke is one of the most common cerebrovascular diseases and is a leading cause of disability and death worldwide (Feigin et al., 2014). In China, the prevalence and incidence of ischemic stroke have been increasing over the past decade (Wu et al., 2019). Traditional treatments for ischemic stroke include endovascular thrombectomy and systemic thrombolysis, but ischemia-reperfusion (I/R) injury is inevitable while restoring blood flow to the brain. Numerous drugs were developed but also failed to show benefit in the therapy of acute ischemic stroke (Chamorro et al., 2016). Hence, there is an urgent need to develop effective neuroprotective drugs for the treatment of cerebral I/R injury. Neuroinflammation and oxidative stress play pivotal roles in the pathophysiological of cerebral I/R injury, which could be an attractive therapy strategy for stroke (Maida et al., 2020).

Celastrol is a pentacyclic triterpene isolated from the traditional Chinese herb "Thunder of God Vine" (Tripterygium wilfordii Hook F.) (Salminen et al., 2010), which exhibits diverse pharmacological activities including anti-inflammatory, anti-oxidative and neuroprotective effects (Chen T. et al., 2017). Many studies have demonstrated that celastrol exerted beneficial effects in the treatment of cancer, inflammatory diseases, neurodegenerative diseases, obesity, and diabetes (Lu et al., 2021; Xu et al., 2021). In recent years, the effect of celastrol on the central nervous system has attracted close attention. Celastrol plays a neuroprotective role in a variety of neurological disorders, including neurodegenerative diseases (Paris et al., 2010; Lin et al., 2019), traumatic brain injury (Eroglu et al., 2014) and ischemic brain injury (Li Y. et al., 2012). Increasing evidence suggests that neuroprotective effect of celastrol in cerebral ischemic injury is associated with antioxidant activity and anti-inflammation property. A previous study illustrated that celastrol dramatically relieved permanent cerebral ischemia injury in rats by downregulating the expression of p-JNK, p-c-Jun and NF-κB (Li Y. et al., 2012). Another study also demonstrated that celastrol ameliorated acute ischemic stroke induced brain injury through promoting IL-33/ST2 axis-mediated microglia/macrophage M2 polarization (Jiang et al., 2018). More recently, celastrol has been reported to exhibit anti-inflammatory and antioxidant actions in rats by targeting HSP70 and NF-κB p65 and directly binding to high mobility group box 1 (HMGB1) in cerebral I/R injury (Zhang et al., 2020; Liu D. D. et al., 2021). These results suggested that celastrol may be a promising therapeutic agent for the treatment of ischemic stroke. However, little is known regarding the neuroprotective effect and the underlying mechanism of celastrol in ischemic stroke.

Long non-coding RNAs (lncRNAs) are the largest class of RNA molecules more than 200 bp in length without protein coding ability (Wang C. et al., 2017). Recently, studies have found that the mechanisms of lncRNA function involve both transcriptional and post-transcriptional regulation (Bao et al., 2018). In the post-transcriptional level, lncRNAs regulate the gene expression either by directly influencing the RNA splicing and RNA degradation, or negatively regulating the functions of miRNA as miRNA sponge (Ebert et al., 2007). Many studies demonstrated that lncRNAs participate in many crucial physiological processes and play significant roles in the occurrence and development of various diseases, including various types of tumors, cardiovascular disorders and cerebrovascular diseases (Chen et al., 2021). Previous research has uncovered that lncRNAs play critical roles in the pathogenesis of ischemic stroke (Bhattarai et al., 2017; Bao et al., 2018). Recent study indicated that lncRNA AK005401 plays an important role in the protective effect of celastrol on ischemia-induced hippocampal damage (Wang et al., 2021). However, the function and mechanism of lncRNAs in ischemic stroke need further research.

In the present study, we established the transient cerebral ischemia model in mice and evaluated the effect of celastrol on infarction volume and neurological function. Then we analyzed the different expression profiles of lncRNAs and mRNAs in the ipsilateral hemisphere after celastrol treatment by RNA-Seq. Through bioinformatics analysis of the different expression genes, we uncover the potential role of celastrol in ischemic stroke and provide a new direction on the functions and mechanisms of lncRNAs in ischemic stroke.

MATERIALS AND METHODS

Experimental Animals

Male C57BL/6 mice (8–10 weeks old, 22–25 g) were purchased from the Experimental Animals Center of Southern Medical University. The mice were kept in a temperature-controlled animal facility under normal light/dark cycle with free access to food and water. All animals adapted to the environment for 7 days before experiments. All animal experiments were approved by the Southern Medical University Administrative Panel on Laboratory Animal Care and conducted in accordance with the guidelines of Animal Use and Care of Southern Medical University.

Transient Middle Cerebral Artery Occlusion Model

To induce cerebral I/R injury, a transient middle cerebral artery occlusion (tMCAO) model was performed on the mice as previously described (Luo et al., 2017).Briefly, mice were anesthetized with sevoflurane (5% for induction and 2–3% for maintenance). Following a midline cervical incision, the right common carotid artery (CCA), external carotid artery (ECA), and internal carotid artery (ICA) were carefully exposed under an operating microscope. Thereafter, a silicone rubber-coated nylon monofilament (Yushun Biological Technology Co. Ltd., Pingdingshan, China) was inserted into the ECA, and advanced to occlude the middle cerebral artery for 90 min. After 90 min occlusion, the monofilament was gently pulled out for reperfusion and the incision was sutured. Mice in sham group adopted a same surgery except the middle cerebral artery occlusion.

Drug Administration

Adult mice were randomized into three groups (sham group, tMCAO group and tMCAO + celastrol group; n = 18 in each

group). Celastrol (Selleckchem, Houston, TX, United States) was dissolved in 1% dimethylsulfoxide (DMSO) (Sigma-Aldrich, St. Louis, MO, United States) at the concentration of 4.5 mg/kg and injected intraperitoneally at the onset of reperfusion. The mice in sham and tMCAO groups without drug treatment were injected with the same volume of DMSO. Mice were re-anesthetized and sacrificed 24 h after tMCAO. The concentration of celastrol used in the experiment was based on the concentration reported in previous study (Chen et al., 2022).

Infarct Size Measurements

The 2,3,5-triphenyltetrazolium chloride (TTC) (Sigma-Aldrich, St. Louis, MO, United States) staining was used to determine cerebral infarction volume. After 90 min of MCAO and 24 h of reperfusion, the mice were anesthetized with 5% sevoflurane, and their brains (n = 5/group) were rapidly removed and coronally cut into six slices at a thickness of 2 mm using a rodent brain matrix. The brain slices were stained with 2% TTC at 37°C for 15 min and subsequently fixed in 4% paraformaldehyde at 4°C overnight. After TTC staining, the red area indicated no infarction while the white area indicated infarction. The brain slices were scanned and the infarct size was analyzed using Image J software (National Institutes of Health, Bethesda, MD, United States) by researchers who were blinded to the study group. In order to exclude the effect of cerebral edema, the following calculation formula was used: (contralateral hemisphere area–ipsilateral non-ischemic hemisphere area)/contralateral hemisphere area × 100% (Liu M. et al., 2021). Five male mice were used in each group.

Neurological Deficit Score

The neurological deficit scores of the mice were evaluated at 24 h after tMCAO by researchers who were blinded to the experimental groups. According to the modified Bederson score, the neurological grading scores range from 0 to 5 (0, no deficit; 1, forelimb flexion; 2, as for 1, plus decreased resistance to lateral push; 3, unidirectional circling; 4, longitudinal spinning or seizure activity; and 5, no movement) (Jin et al., 2015). Seven male mice were used in each group.

Rotarod Test

Motor performance was accessed by accelerating rotarod test after evaluating the neurological deficit scores. The mice were trained to remain on the rotarod at a starting rotation of 5 r/min which was accelerated to 40 r/min over 60 s before the model establishment (Du et al., 2020). The mice were tested under the same accelerated conditions after 24 h of reperfusion. The entire test lasted 300 s and was performed three times for each mouse at 10-min intervals. The latency of falling off of the rod were recorded and averaged.

Primary Cortical Neurons Cultures

Primary cortical neurons were obtained from embryonic day C57BL/6 mice and cultured as previously described (Luo et al., 2017). Briefly, pregnant mice were euthanized and the cerebral cortices of the embryos were dissected and dissociated by mild trypsinization, followed by trituration in DNAase I (Sigma-Aldrich, St. Louis, MO, United States). The cells were suspended in neurobasal medium supplemented with 2% B-27 (Gibco, Grand Island, NY, United States) and 0.5 mM Glutamax (Gibco, Grand Island, NY, United States). The single cell suspension was plated in 6-well plates precoated with poly-L-lysine, and the cell culture was kept in a humidified atmosphere of 5% CO_2 at 37°C. Half of the culture medium was replaced every 3 days and neurons were cultured for 9 days for use in subsequent experiments.

Primary Astrocytes Cultures

Primary cultures of astrocytes were prepared from cortices of C57BL/6 newborn mice (P1–P3). Briefly, the bilateral cortices were dissected in a sterile environment and digested with 0.25% trypsin and DNAase I for 10 min at 37°C. Subsequently, cortical fragments were suspended in Dulbecco's Modified Eagle's medium (DMEM)/F12 (Gibco, Grand Island, NY, United States) with 10% fetal bovine serum (Gibco, Grand Island, NY, United States). Single cell suspensions were made by repeated pipetting and the cells were incubated at 37°C in a humidified 5% CO_2 chamber for 7 days. The culture medium was replaced twice a day.

BV2 Microglial Cell Cultures

BV2 microglial cells, which were bought from Shanghai Gaining Biological Technology Co. Ltd., were cultured in DMEM (Gibco, Grand Island, NY, United States) with 10% fetal bovine serum at 37°C in CO_2/air (5/95%) mixture.

Oxygen-Glucose Deprivation and Drug Treatment

To simulate ischemia-reperfusion injury *in vitro*, primary cortical neurons, primary astrocytes and BV2 microglial cells were subjected to oxygen and glucose deprivation (OGD) followed by reoxygenation. Primary astrocytes and BV2 microglial cells were incubated with glucose-free DMEM and placed within a hypoxic chamber which was continuously maintained with 95% N_2, 5% CO_2, 1% O_2 at 37°C for 5 h, while primary cortical neurons for 4 h. OGD was terminated by replacing the glucose-free DMEM to their normal culture medium in the normoxic incubator with 95% air and 5% CO_2 for 24 h. Cells incubated in normal culture medium under a normoxic incubator were used as the normoxic control. At the same time, celastrol was applied in the culture medium with the final concentration of 0.5 μM for 24 h. In contrast, the same volume of DMSO was applied in the culture medium in the control group cells. All experiments were at least duplicated three times biologically.

RNA Extraction

The total RNA from the ischemic hemisphere or cells was isolated with the TRIzol Reagent (Invitrogen, Carlsbad, CA, United States) according to the manufacturer's instructions. RNA purity and concentration were evaluated by using the Nanodrop ND-2000 spectrophotometer (Thermo Fisher Scientific, Waltham, MA, United States). RNA Integrity Number (RIN) was analyzed

by Bioanalyzer 2100 (Agilent, Palo Alto, CA, United States). If the RIN number is >7, it can be used for high-throughput transcriptome sequencing.

RNA-Sequencing

A total of 5 μg RNA from ischemic hemisphere was utilized for each RNA sample. Firstly, ribosomal RNA (rRNA) was depleted by Ribo-Zero Gold rRNA Removal Kit (Illumina, San Diego, CA, United States). Secondly, the left RNAs were fragmented into short fragments using divalent cations (NEBNext® Magnesium RNA Fragmentation Module, NEB, Ipswich, MA, United States) under high temperature. The complementary DNA (cDNA) was synthesized and purified. Finally, the average insert size for the final cDNA library was 300 ± 50 bp. 2 × 150 bp paired-end sequencing was performed on Illumina Novaseq^{TM}6000 (LC-Bio Technology Co. Ltd., Hangzhou, China) according to the recommended protocol.

Quality Control

Clean reads were obtained by removing reads containing adapter, reads containing ploy-N and low-quality reads from raw data by Cutadapt (Love et al., 2014). Then sequence quality was verified using FastQC (Babraham Bioinformatics, Babraham Institute, Cambridge, United Kingdom), including the Q20, Q30, and GC-content of the clean data. The downstream analysis was done on high-quality clean data.

Differential Expression Analysis

Cuffdiff (v2.1.1) was used to calculate fragments per kilobase million (FPKMs) of both lncRNAs and mRNAs. The differentially expressed lncRNAs and mRNAs were selected with fold change > 2 or fold change < 0.5 and P-value < 0.05 by DESeq2. To outline the characteristics of gene expression profiles, heatmaps and volcano plots were generated by using the R package.

Gene Ontology and Kyoto Encyclopedia of Genes and Genomes Enrichment Analysis

Gene Ontology (GO) and Kyoto Encyclopedia of Genes and Genomes (KEGG) pathway enrichment analysis of differentially expressed genes (DEGs) was implemented with DAVID.[1] GO analysis includes the categories biological processes (BP), cellular components (CC), and molecular functions (MF). GO terms with $P < 0.05$ were defined as significantly enriched GO terms in DEGs. Pathways with $P < 0.05$ were considered as significantly enriched pathways in DEGs.

Soft Cluster Analysis

The soft clustering Mfuzz function is based on the fuzzy c-means algorithm of the e1071 package. The R/Bioconductor package was used for soft clustering of genes, and Mfuzz-specific clusters were selected based on gene expression trends (Yang et al., 2020). The genes were determined by default parameters and the number of clusters were 12.

[1]http://david.ncifcrf.gov/

Construction of ceRNA Network

According to the competitive endogenous RNA (ceRNA) mechanism, miRNA can lead to gene silencing by binding mRNA, while ceRNA can regulate mRNA expression by competitively binding miRNA. In this study, DE lncRNAs and DE mRNAs were constructed for ceRNA network. DE mRNA was put into Starbase database (Starbase V3.0) to predict upstream miRNAs, and DE lncRNA was put into miRcode to determine the targeted miRNAs. Finally, the lncRNA-miRNA-mRNA ceRNA network formed by the intersection of the two groups of predicted miRNAs. The ceRNA network was visualized by Cytoscape (Li et al., 2014).

Quantitative Real-Time PCR

Total RNA (1 μg) was used to synthesize cDNA using a ReverTra Ace qPCR RT Master Mix with gDNA Remover (TOYOBO, Tokyo, Japan). Quantitative real-time PCR was performed on the ABI QuantStudio 6 flex (Applied Biosystems, Carlsbad, CA, United States) using SYBR Green Realtime PCR Master Mix (TOYOBO, Tokyo, Japan). GAPDH was used as a reference gene for quantification. Each experimental group was performed in triplicate to obtain the cycle time (CT) mean and the results of the analyses were calculated using the 2-ΔΔCT equation. The primer sequences were shown in the **Supplementary Table 1**.

Statistical Analysis

Data are expressed as mean ± SEM. Differences were evaluated by one-way analysis of variance (ANOVA; three or more groups). $P < 0.05$ was considered statistical significance. Statistical analyses were performed using SPSS 20.0 Statistics (IBM SPSS Statistics for Version 20.0, IBM Corp, Armonk, NY United States).

RESULTS

Celastrol Reduced Infarction, and Improved Neurological Scores and Motor Function After Transient Middle Cerebral Artery Occlusion

We examined whether celastrol improve infarct volume and neurological behavior after tMCAO. After 90 min occlusion, celastrol was immediately injected at a concentration of 4.5 mg/kg at the beginning of reperfusion. Infarct volume was measured with TTC staining after 24 h of reperfusion. The results show that the infarct volume was apparently larger in the tMCAO group (48.87 ± 2.86%) compared with sham group (0%), whereas celastrol treatment significantly reduced I/R-induced infarct volume to 35.89 ± 2.10% (**Figures 1A,B**). Similarly, the neurological deficit scores of mice in the tMCAO group were significantly increased to 2.85 ± 0.34, but celastrol treatment decreased neurological outcomes to 1.71 ± 0.28 (**Figure 1C**). Subsequently, the mice were subjected to the Rotarod fatigue test. The results showed that the time spent on the rotarod of mice in tMCAO group was 52.21 ± 5.60 s, while celastrol treatment significantly increased the time spent on the rotarod to 113.40 ± 6.40 s (**Figure 1D**).

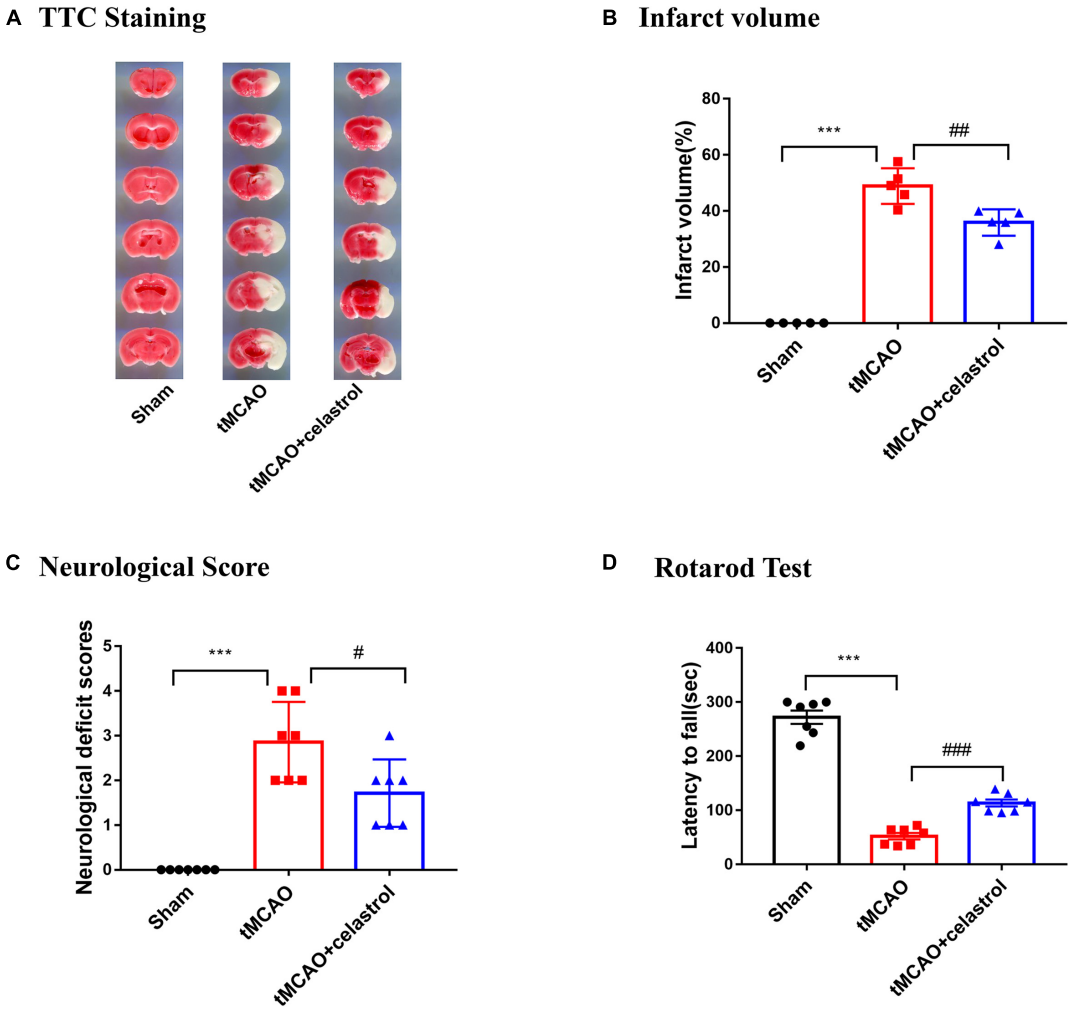

FIGURE 1 | (A,B) Celastrol reduced infarct volume in tMCAO mice. $^{***}P < 0.001$ vs. sham group; $^{\#\#}P < 0.01$ vs. tMCAO group, $n = 5$. **(C,D)** Celastrol improved neurological deficit scores and motor function in tMCAO mice. $^{***}P < 0.001$ vs. sham group; $^{\#}P < 0.05$, $^{\#\#\#}P < 0.001$ vs. tMCAO group, $n = 7$.

RNA-Seq Analysis of Ischemic Hemisphere After Celastrol Post-treatment in Transient Middle Cerebral Artery Occlusion

To explore the mechanism underlying the neuroprotective function of celastrol in tMCAO, RNA-sequencing analysis was performed. Gene expression profiles for sham, tMCAO and tMCAO + celastrol groups were visualized as heatmap (**Figure 2A**). The fold change (FC) > 2 or FC < 0.5 and $P < 0.05$ were used as the threshold to identify the DEGs between each two groups. A total of 50 DE lncRNAs (**Supplementary Table 2**) and 696 DE mRNAs (**Supplementary Table 3**) were identified between the sham and tMCAO group. And a total of 544 DE lncRNAs (**Supplementary Table 4**) and 324 DE mRNAs (**Supplementary Table 5**) were identified between tMCAO and tMCAO + celastrol group. The mRNA profiles were further analyzed, and the distribution of mRNA was displayed by volcano plots. 612 upregulated DE mRNAs and 84 downregulated DE mRNAs were found between the sham and tMCAO group (**Figure 2B**). However, 168 upregulated DE mRNAs and 156 downregulated DE mRNAs were found between the tMCAO and tMCAO + celastrol group (**Figure 2C**). The distribution of mRNA in sham and tMCAO + celastrol group was also shown in **Figure 2D**.

The Gene Ontology and Kyoto Encyclopedia of Genes and Genomes Enrichment Analysis of Differentially Expressed mRNAs

Gene Ontology and KEGG enrichment analysis were performed with DE mRNAs between sham and tMCAO groups. The top 10 results of GO analysis in the biological process on mRNA are shown in **Figure 2E**, including neutrophil migration, granulocyte migration, myeloid leukocyte migration, leukocyte chemotaxis, leukocyte migration, cell chemotaxis, cytokine-mediated signaling pathway, positive regulation of response to

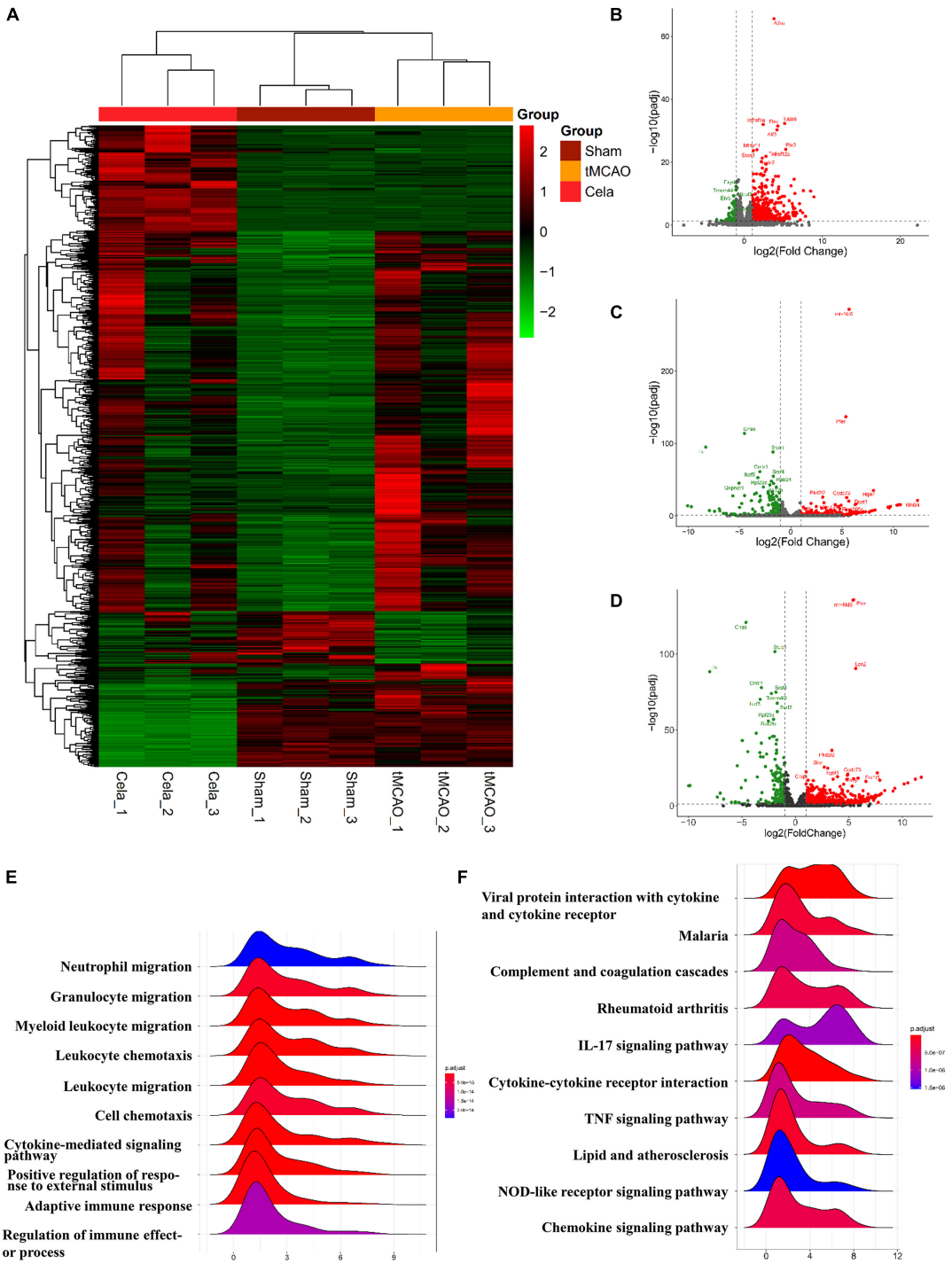

FIGURE 2 | (A) The heatmap of DE lncRNAs and DE mRNAs. **(B–D)** The volcano plot of the mRNAs between sham and tMCAO group, tMCAO and tMCAO + celastrol group, sham and tMCAO + celastrol group. **(E)** Top 10 enrichment biological processes of GO analysis of DE mRNAs between the sham and tMCAO group. **(F)** Top 10 enrichment pathways of KEGG pathway analysis of DE mRNAs between the sham and tMCAO group.

external stimulus, adaptive immune response, and regulation of immune effect or process. The top 10 results of the KEGG analysis of DE mRNAs also appeared in **Figure 2F**, including viral protein interaction with cytokine and cytokine receptor, malaria, complement, and coagulation cascades, rheumatoid arthritis, IL-17 signaling, cytokine-cytokine receptor interaction, TNF signaling pathway, lipid and atherosclerosis, NOD-like receptor signaling and chemokine signaling pathway. The results

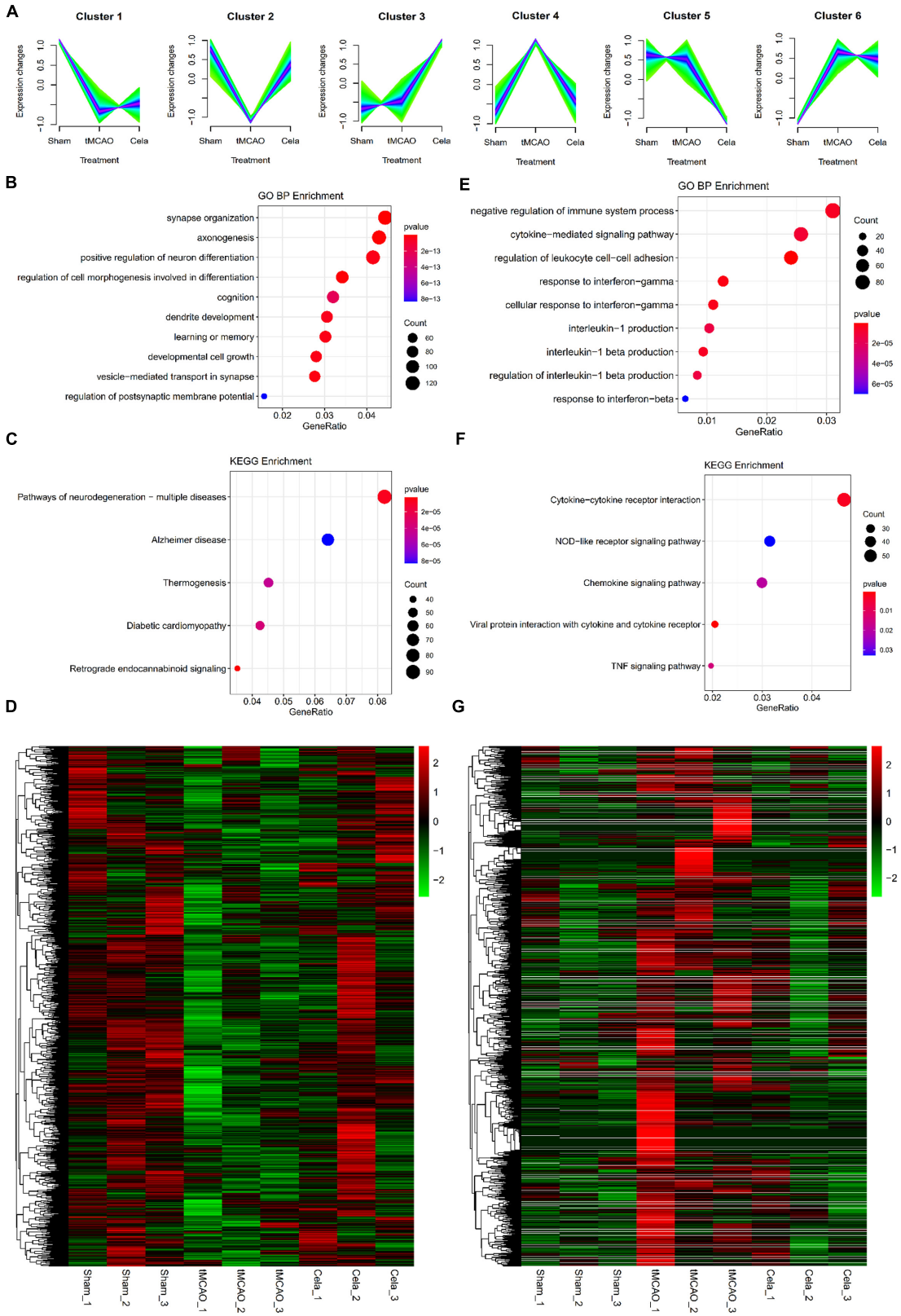

FIGURE 3 | (A) Six clusters of mRNAs among the three groups by Mfuzz analysis. **(B–D)** The enrichment results of GO analysis, KEGG pathway and the heatmap of up-regulated genes in mRNA cluster 2. **(E–G)** The enrichment results of GO analysis, KEGG pathway and the heatmap of down-regulated genes in mRNA cluster 4.

above indicated the potential connection between these pathways and the effects of celastrol. The results above indicated that the neuroprotective effects of celastrol are potentially related to these biological processes and metabolic pathways.

Gene Ontology and Kyoto Encyclopedia of Genes and Genome Pathway Analysis of Two Typical mRNA Clusters

The soft clustering method was used to assign genes to several clusters based on expression patterns. For mRNA, a total of six clusters were obtained by Mfuzz analysis in the three groups (**Figure 3A**). These six clusters could be classified into two large classes. One type of clusters showed upregulation of gene expression between the tMCAO and tMCAO + celastrol group (including cluster 1, 2, and 3), while another showed the downregulation. According to the experimental design, cluster 2 and cluster 4 were selected for further analysis. In order to gain insight into the biological function, GO and KEGG enrichment analysis were performed in these two clusters. The top 10 results of GO analysis in the biological process on cluster 2 and cluster 4 are shown in **Figures 3B,E** respectively. The results showed that genes in these two clusters were associated with different biological processes. Genes in Cluster 2 were mainly associated with neuro-related processes, such as synapse organization, axonogenesis and neuron differentiation. Genes in Cluster 4 were mainly associated with immune and inflammation. The top 5 results of the KEGG analysis also appeared in **Figures 3C,F** respectively. In addition, the expression of mRNA in cluster 2 and cluster 4 were shown in the heatmap respectively (**Figures 3D,G**). The DE mRNAs from mRNA cluster 2 and cluster 4 were respectively listed in **Supplementary Tables 6**, **7**.

Two Typical LncRNA Clusters via Mfuzz Analysis

For lncRNA, a total of six clusters were obtained by Mfuzz analysis in the three groups (**Figure 4A**). These six clusters also could be classified into two large classes. One type of clusters showed downregulation of gene expression between the tMCAO and tMCAO + celastrol group (including cluster 1, 2, and 3), while another showed the upregulation. The expression of lncRNA in cluster 3 and cluster 5&6 were shown in the heatmap respectively (**Figures 4B,C**). The DE lncRNAs from lncRNA cluster 3 and cluster 5&6 were listed in **Supplementary Table 8**.

Construction of LncRNA-MiRNA-mRNA ceRNA Network

Based on differential analyses and interaction prediction, the lncRNA-miRNA-mRNA ceRNA network were established. The ceRNA networks included both positive and negative regulation (**Figure 5**). DE mRNAs in Mfuzz Cluster 2 (up-regulated) and DE lncRNAs in lncRNA Mfuzz Cluster 5&6 (up-regulated) were both used to predict the bound miRNAs, then the intersection of these two groups of miRNAs were formed into ceRNA network. Finally, six up-regulated lncRNAs, nine down-regulated miRNAs, and 16 up-regulated mRNAs were constructed into lncRNA-miRNA-mRNA ceRNA networks (**Figure 5A**). Similarly, DE mRNAs in Mfuzz Cluster 4 (down-regulated) and DE lncRNAs in lncRNA Mfuzz Cluster 3 (down-regulated) were used to predict the bound miRNAs, then the ceRNA network formed by intersection of these two groups of mirnas. Finally, ceRNA

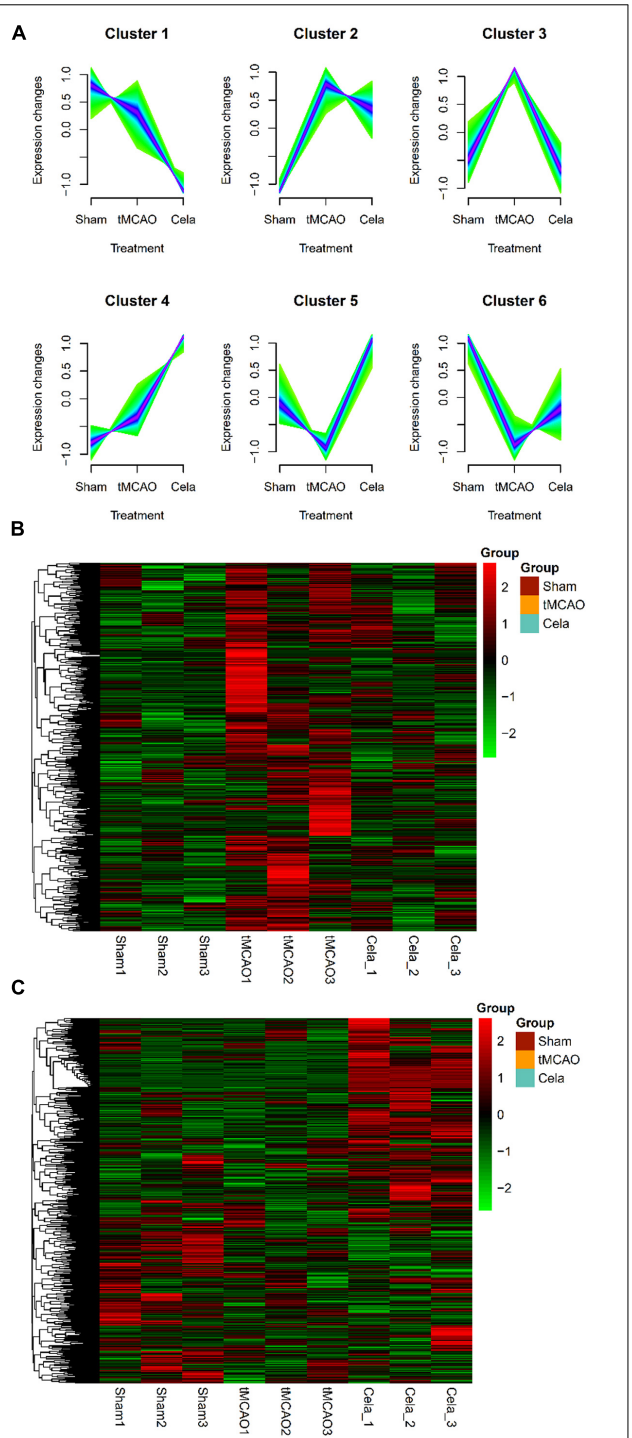

FIGURE 4 | (A) Six clusters of lncRNAs among the three groups by Mfuzz analysis. **(B)** The heatmap of down-regulated genes in lncRNA cluster 3. **(C)** The heatmap of up-regulated genes in lncRNA cluster 5 and 6.

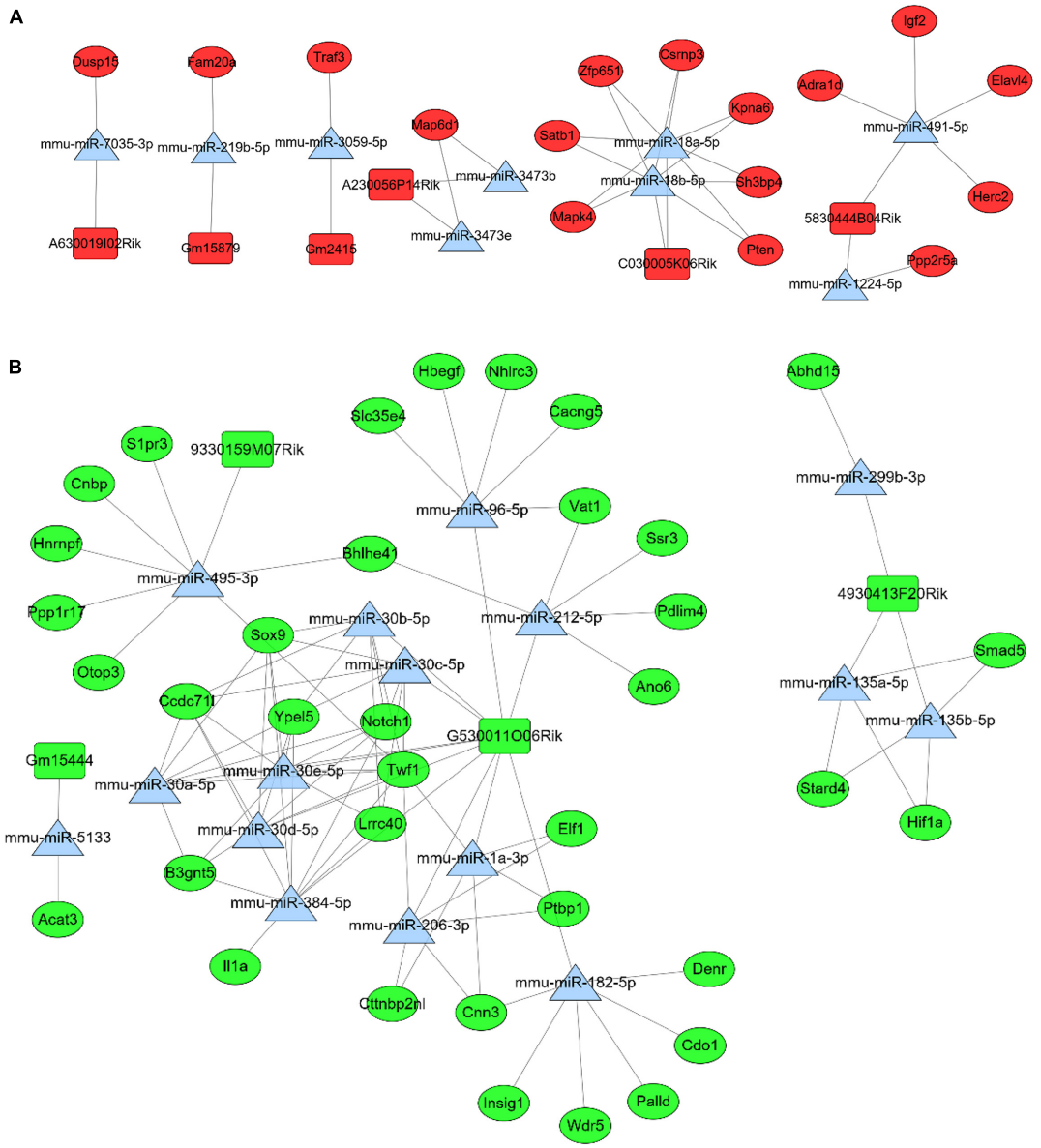

FIGURE 5 | In the ceRNA network, rectangles represent lncRNAs, triangles represent miRNAs, and circles represent mRNAs. And red represents up-regulated genes and green represents down- regulated genes. **(A)** The positive regulation network of lncRNA-miRNA-mRNA ceRNA. **(B)** The negative regulation network of lncRNA-miRNA-mRNA ceRNA.

networks were constructed by 4 up-regulated lncRNAs, 16 down-regulated miRNAs and 36 up-regulated mRNAs (**Figure 5B**). The network consists of lncRNAs (rectangles), miRNAs (triangles), and mRNAs (circles). The red pots represent up-regulated RNAs and the green pots represent down-regulated RNAs. Above of all indicated potential critical RNA interactions involved in celastrol treatment.

LncRNA-mRNA Interaction Network

The relationship between lncRNAs and mRNAs was based on the *Cis* and *Trans* function. **Figure 6A** shows the interaction network of differentially expressed up-regulated lncRNAs with DE mRNAs which is also the target genes of lncRNAs. Similarly, **Figure 6B** shows the interaction network of differentially expressed down-regulated lncRNAs with their differentially expressed target mRNAs. The Triangle node and the round node respectively represent lncRNAs and mRNAs. The red color reveals that the lncRNAs or mRNAs are significantly up-regulated, otherwise indicated with a green color.

Validation of the Selected Differentially Expressed Genes

Based on the above bioinformatic analysis, we selected several DE lncRNAs and DE mRNAs for qRT-PCR validation.

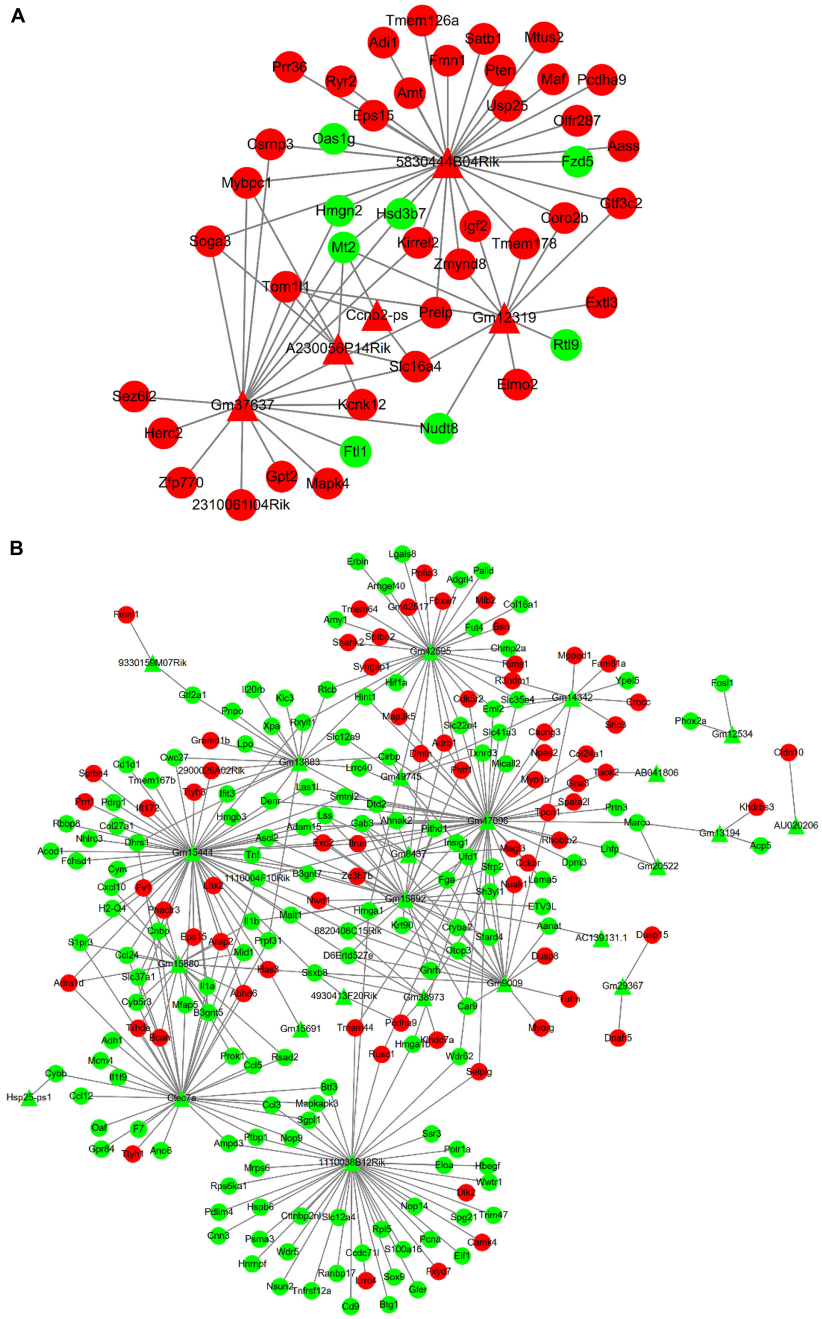

FIGURE 6 | In the interaction network, triangles represent lncRNAs and circles represent mRNAs. And red represents up-regulated genes and green represents down-regulated genes. **(A)** The interaction network between up-regulated DE lncRNAs and DE mRNAs. **(B)** The interaction network between down-regulated DE lncRNAs and DE mRNAs.

5830444B04Rik-Elavl4, C030005K06Rik-Sh3bp4, and 4930413F20Rik- HIF-1α were selected from the ceRNA network, and Gm15444-Ascl2/Acod1 was selected from the DE lncRNA-DE mRNA interaction network. They were selected for further validation in the brain tissue, primary neurons, primary astrocytes, and BV2 cells by qRT-PCR. In the brain tissue, 5830444B04Rik, C030005K06Rik, Elavl4, Sh3bp4, HIF-1α, Ascl2, and Acod1 showed the same fold change patterns as those in the RNA-Seq results (**Figure 7A**). The expression of 4930413F20Rik and Gm15444 were consistent with lncRNA cluster 3, and Ascl2, and Acod1 were also consistent with mRNA cluster 4 in three types of cells. The expression of HIF-1α was consistent with mRNA cluster 4 both in the primary astrocyte and BV2 cells and the expression of Sh3bp4

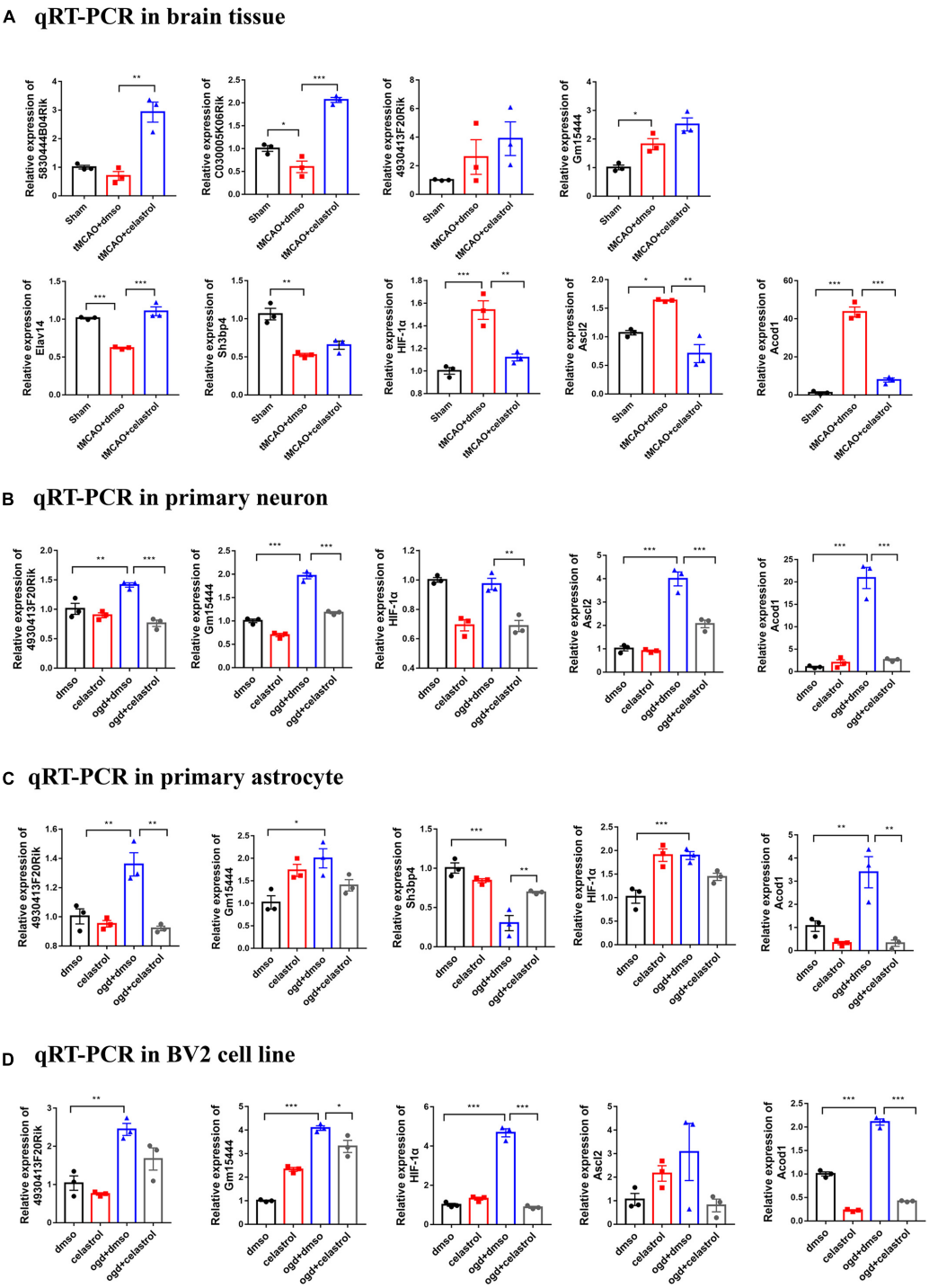

FIGURE 7 | Differentially expressed lncRNAs and mRNAs confirmation by qRT-PCR. **(A)** Validation of DE lncRNAs and DE mRNAs in brain tissue. **(B)** Validation of DE lncRNAs and DE mRNAs in primary neuron. **(C)** Validation of DE lncRNAs and DE mRNAs in primary astrocyte. **(D)** Validation of DE lncRNAs and DE mRNAs in BV2 cells. $^{*}P < 0.05$, $^{**}P < 0.01$, $^{***}P < 0.001$, $n = 3$.

was consistent with mRNA cluster 2 in the primary astrocyte (**Figures 7B–D**). But some of them did not reach statistical significance. The validation of the other DEGs were shown in the **Supplementary Figure 1**.

DISCUSSION

In present study, we found that celastrol reduced the cerebral infarction volume in mice, improved the neurological and motor

function. These results are consistent with the previous studies, which demonstrated that celastrol post-treatment reduces ischemic stroke-induced brain damage in rats (Li Y. et al., 2012; Jiang et al., 2018; Liu D. D. et al., 2021). Biological process of GO and KEGG pathway analysis of DE mRNAs suggested that inflammation and immunity response play important roles in the ischemia stroke. Neuroinflammation is involved in the pathophysiological process of ischemia reperfusion injury and anti-inflammatory is an important target for the development of neuroprotective drugs (Maida et al., 2020). Four lncRNAs and five mRNAs were selected from the lncRNA-miRNA-mRNA ceRNA network and lncRNA-mRNA co-expression network for further validation by qRT-PCR and most of them showed the same fold change patterns in brain tissue as those in the RNA-Seq results. Taken together, these results suggest that DEGs may play a complicated role in the neuroprotective effect of celastrol in ischemic stroke, and the potential function of them required further validation and annotation.

The potential mechanism of celastrol in neuroprotective effect deserves further investigation. Celastrol is the most abundant compound extracted from the root of Tripterygium wilfordii (Salminen et al., 2010), which has exhibited preclinical and clinical efficacy in a broad range of diseases such as cancer, rheumatoid arthritis (Tao et al., 1989), ulcerative colitis (Gao et al., 2020), and central nervous system disease (Schiavone et al., 2021) due to its different pharmacological properties. Celastrol was demonstrated to exert anticancer effects in many types of tumors such as breast cancer (Yang et al., 2011), retinoblastoma (Li Z. et al., 2012), gastric cancer (Sha et al., 2015), and melanoma (Abbas et al., 2007) by suppressing tumor migration, invasion and angiogenesis as well as promoting autophagy and apoptosis. Hsp90, NF-κB, HIF-1α/VEGF, PTEN/PI3K/Akt, Akt/mTOR, and ROS/JNK signaling pathways were identified as relevant anticancer targets and underlying mechanisms of celastrol (Lu et al., 2021). In the past several decades, the anti-inflammatory effects and mechanisms of celastrol also became clearer. Several studies showed that celastrol can alleviate rheumatoid arthritis by inhibiting inflammatory cytokines and oxidative stress as well as regulating the calcium homeostasis (Cascão et al., 2012; Li et al., 2013; Wong et al., 2019). Furthermore, Shaker et al. demonstrated celastrol can ameliorate inflammatory symptoms in mice colitis model, and the relevant mechanism involved the inhibition of the NOD-like receptor protein 3 inflammasome (NLRP3-inflammasome), reduction of the levels of IL- 23 and IL-17A as well as the up-regulated expression of IL-10 and TNF-α (Shaker et al., 2014). As a potent inhibitor of inflammation and oxidative stress, celastrol was confirmed to have a potential neuroprotective effect in central nervous system disease, such as neurodegenerative diseases (Konieczny et al., 2014), neuropsychiatric disorders (Zhu et al., 2021) and ischemic stroke (Li Y. et al., 2012). Inflammatory insult and oxidative stress have been implicated in the pathogenesis of ischemic stroke. Recently, increasing studies demonstrated neuroprotective effects of celastrol in permanent and transient ischemic stroke in rodents (Jiang et al., 2018; Zhang et al., 2020). However, owing to the complexity of the underlying signaling pathways, further effort is needed to further illustrate the neuroprotection mechanism of celastrol in ischemic stroke. In this study, we found "TNF signaling pathway" and "NOD-like receptor signaling pathway," the two signaling pathways are both significantly enriched in the ischemic stroke and celastrol post-treatment process. And the immune response such as "negative regulation of immune system process" and "response to interferon-gamma and interferon beta" also contribute to the transcription profile change of celastrol. These results suggests that anti-inflammatory effect and immune response of celastrol may be the main factor of reducing cerebral ischemia-reperfusion injury, which is consistent with previous studies. What's interesting, the KEGG pathway analysis also suggested that lipid metabolism may play a potential role in neuroprotection of celastrol. More recently, a study found lipid metabolism partially regulated the neuroprotection of celastrol on cerebral I/R injury through the lipidomic analysis (Liu M. et al., 2021), but the underlying mechanism need further investigation.

It is essential to explore the potential targets of celastrol in ischemia stroke. Although previous study has found that the neuroprotective action of celastrol was partly due to its inhibition of neuroinflammation through directly binding with HMGB1 protein (Liu D. D. et al., 2021), it remains essential to explore more direct targets of celastrol. In this study, we selected five DE mRNAs from the ceRNA network or lncRNA-mRNA interaction network for the further validation by qRT-PCR, including Elavl4, Sh3bp4, HIF-1α, Ascl2, and Acod1. In the brain tissue, almost all of them showed the same fold change patterns as those in the RNA-Seq results. Among them, HIF-1α, Acod1, and Elavl4 attracted our great attention. First, hypoxia inducible factor-1 alpha (HIF-1α) is the main subunit of hypoxia-inducible factor, which is an oxygen-dependent transcriptional activator (Lee et al., 2004). Accumulating evidence elucidated that HIF-1α plays an important role in suppressing oxidative stress and inflammation in stroke (Baranova et al., 2007; Amin et al., 2021). In this study, we found that the expression of HIF-1α was consistent with mRNA cluster 4 in mice brain tissue, primary astrocyte and BV2 cells. Combined with previous studies, how celastrol alleviates cerebral ischemia-reperfusion injury via HIF-1α need further study. Secondly, aconitate decarboxylase 1 (ACOD1, also known as immune-responsive gene 1 [IRG1]), has attracted much attention as a multifunctional regulator of immunometabolism in inflammation and infection (Michelucci et al., 2013; Cordes et al., 2016). ACOD1 plays important roles in many diseases by regulating itaconate production, oxidative stress, and inflammation (Wu et al., 2020). ACOD1-mediated itaconate has been demonstrated to play an anti-inflammatory role in macrophages. Recently, ACOD1 has been proved to have an association with neurotoxic microglial activation and chronic neuroinflammation (Lampropoulou et al., 2016). More recently, a study demonstrated that Acod1 KO mice presented significant increase in cerebral lesion volume compared to control mice and illustrated that ACOD1 suppressed cerebral ischemia-reperfusion injury by oxidative stress regulation (Lampropoulou et al., 2016). In present study, we found the expression of ACOD1 presented up-regulation both in the tMCAO mice and three types of cells with OGD/R, which was reversed by celastrol. The role of ACOD1 in cerebral ischemic stroke and how does celastrol

regulate ACOD1 have attracted much attention. Thirdly, ELAVL4 (also known as HuD), an RNA-binding protein, is mainly expressed in neuronal systems and regulates the metabolism of target mRNAs (McKee and Silver, 2007; Singh et al., 2015). ELAVL4 plays important roles in neuronal processes, including neuronal development, differentiation, dendritic maturation, and neural plasticity (Akamatsu et al., 2005; Bronicki and Jasmin, 2013). Several studies have shown that ELAVL4 involved in the pathogenesis of neurodegenerative diseases, such as Alzheimer's disease (Kang et al., 2014), Parkinson's disease (Noureddine et al., 2005), and amyotrophic lateral sclerosis (Dell'Orco et al., 2021). However, whether ELAVL4 is involved in the pathogenesis of ischemic stroke remains unclear. In the brain tissue, ELAVL4 showed the same fold change patterns as those in the RNA-Seq results. These results suggested that celastrol may participate in the regulation of ischemic stroke, but the underling mechanism and whether celastrol can play a neuroprotective role through ELAVL4 need further study.

Further studies on lncRNAs are beneficial to reveal the underlying mechanism of celastrol in cerebral I/R injury. LncRNAs play important roles in brain development, neuron function, neuronal proliferation and apoptosis (Briggs et al., 2015). Numerous studies have demonstrated that lncRNAs are engaged in the occurrence and development of various central nervous system diseases, such as Alzheimer's disease (AD), Parkinson's disease (PD), Huntington's disease (HD), and ischemic stroke (Bao et al., 2018; Vangoor et al., 2021). Increasingly evidence has elucidated that lncRNAs play critical role in the pathogenesis of ischemic stroke. A bulk of aberrantly expressed lncRNAs have been reported in ischemic stroke patients (Dykstra-Aiello et al., 2016), rodent stroke models (Wang J. et al., 2017) or oxygen-glucose deprived (OGD) cells (Zhang et al., 2016) by RNA-seq and microarrays. Notably, Yin at al. confirmed that Malat1 was involved in the protection of cerebral microvasculature and parenchyma after cerebral ischemic insults through inhibiting endothelial cell apoptosis and inflammation. Moreover, Malat1 KO mice appeared larger cerebral infarct size, worsened neurological deficit, and weaken sensorimotor functions (Zhang et al., 2016, 2017). Other lncRNAs, such as ANRIL (Bai et al., 2014), SNHG14 (Qi et al., 2017), TUG1 (Chen S. et al., 2017), and MEG3 (Yan et al., 2016), were also found to affect neuronal apoptosis, inflammation and angiogenesis during ischemic stroke. More recently, Zhang at al. indicated celastrol can reduce I/R-mediated hippocampal injury by downregulating AK005401/MAP3K12 signaling, and its neuroprotection was alleviated by AK005401 overexpression (Wang et al., 2021). However, the above lncRNAs was not found to be the DE lncRNAs in this study, we suggested that the different species and different cerebral ischemic models can explain this problem. In current study, 5830444B04Rik, C030005K06Rik, and 4930413F20Rik from ceRNA network and Gm15444 from lncRNA-mRNA co-expression network were selected for further validation by qRT-PCR in brain tissue and three types of cells. Most of them showed the same fold change patterns as those in the RNA-Seq results, while others showed different fold change patterns probably because of the methodological or statistical differences. In order to elucidate the functions and mechanisms of celastrol on I/R-mediated neuronal injury, further study on these lncRNA is needed.

Undoubtedly, this study has several limitations. First, the RNA-seq tested the expression profile of mRNAs and lncRNAs, but without miRNAs. Second, differences in gene expression detected by RNA-seq and qPCR may be due to methodological or statistical differences. Third, the validated mRNAs and lncRNAs by qRT-PCR and bioinformatic analysis still need deliberately designed experiment to further undermine the regulating mechanism.

In conclusion, the present study demonstrated that celastrol treatment can effectively reduce cerebral ischemia-reperfusion injury. Celastrol can influence the expression of lncRNAs and mRNAs in ischemia stroke, and bioinformatics analysis have identified that inflammation related biological processes and KEGG pathways associated with celastrol treatment. Several lncRNAs or mRNAs of potential therapeutic targets were selected for further validation. Our results provide a framework for further investigation of the role of lncRNAs and their target mRNAs in the neuroprotective effects of celastrol, especially in ischemic stroke.

DATA AVAILABILITY STATEMENT

The data of RNA-sequencing in this study can be obtained from the NCBI GEO database at this link: https://www.ncbi.nlm.nih.gov/geo/query/acc.cgi?acc=GSE202659.

ETHICS STATEMENT

The animal study was reviewed and approved by Southern Medical University Administrative Panel on Laboratory Animal Care.

AUTHOR CONTRIBUTIONS

ZQ, CL, and TT designed the experiments. JL, XG, LY, and JC performed the experiments. XG, ZH, FZ, and YL wrote the manuscript and analyzed the data. All authors contributed to the article and approved the submitted version.

FUNDING

This research was funded by the National Natural Science Foundation of China (Grant Number 81973305) and the Discipline Construction Fund of Central People's Hospital of Zhanjiang (2020A01 and 2020A02).

SUPPLEMENTARY MATERIAL

The Supplementary Material for this article can be found online at: https://www.frontiersin.org/articles/10.3389/fnins.2022.889292/full#supplementary-material

REFERENCES

Abbas, S., Bhoumik, A., Dahl, R., Vasile, S., Krajewski, S., Cosford, N. D., et al. (2007). Preclinical studies of celastrol and acetyl isogambogic acid in melanoma. *Clin. Cancer Res.* 13(22 Pt 1), 6769–6778. doi: 10.1158/1078-0432.Ccr-07-1536

Akamatsu, W., Fujihara, H., Mitsuhashi, T., Yano, M., Shibata, S., Hayakawa, Y., et al. (2005). The RNA-binding protein HuD regulates neuronal cell identity and maturation. *Proc. Natl. Acad. Sci. U.S.A.* 102, 4625–4630. doi: 10.1073/pnas.0407523102

Amin, N., Chen, S., Ren, Q., Tan, X., Botchway, B. O. A., Hu, Z., et al. (2021). Hypoxia Inducible Factor-1α attenuates ischemic brain damage by modulating inflammatory response and glial activity. *Cells* 10:1359. doi: 10.3390/cells10061359

Bai, Y., Nie, S., Jiang, G., Zhou, Y., Zhou, M., Zhao, Y., et al. (2014). Regulation of CARD8 expression by ANRIL and association of CARD8 single nucleotide polymorphism rs2043211 (p.C10X) with ischemic stroke. *Stroke* 45, 383–388. doi: 10.1161/strokeaha.113.003393

Bao, M. H., Szeto, V., Yang, B. B., Zhu, S. Z., Sun, H. S., and Feng, Z. P. (2018). Long non-coding RNAs in ischemic stroke. *Cell Death Dis.* 9:281. doi: 10.1038/s41419-018-0282-x

Baranova, O., Miranda, L. F., Pichiule, P., Dragatsis, I., Johnson, R. S., and Chavez, J. C. (2007). Neuron-specific inactivation of the hypoxia inducible factor 1 alpha increases brain injury in a mouse model of transient focal cerebral ischemia. *J. Neurosci.* 27, 6320–6332. doi: 10.1523/jneurosci.0449-07.2007

Bhattarai, S., Pontarelli, F., Prendergast, E., and Dharap, A. (2017). Discovery of novel stroke-responsive lncRNAs in the mouse cortex using genome-wide RNA-seq. *Neurobiol. Dis.* 108, 204–212. doi: 10.1016/j.nbd.2017.08.016

Briggs, J. A., Wolvetang, E. J., Mattick, J. S., Rinn, J. L., and Barry, G. (2015). Mechanisms of long non-coding RNAs in mammalian nervous system development, plasticity, disease, and evolution. *Neuron* 88, 861–877. doi: 10.1016/j.neuron.2015.09.045

Bronicki, L. M., and Jasmin, B. J. (2013). Emerging complexity of the HuD/ELAVl4 gene; implications for neuronal development, function, and dysfunction. *RNA* 19, 1019–1037. doi: 10.1261/rna.039164.113

Cascão, R., Vidal, B., Raquel, H., Neves-Costa, A., Figueiredo, N., Gupta, V., et al. (2012). Effective treatment of rat adjuvant-induced arthritis by celastrol. *Autoimmun. Rev.* 11, 856–862. doi: 10.1016/j.autrev.2012.02.022

Chamorro, Á, Dirnagl, U., Urra, X., and Planas, A. M. (2016). Neuroprotection in acute stroke: targeting excitotoxicity, oxidative and nitrosative stress, and inflammation. *Lancet Neurol.* 15, 869–881. doi: 10.1016/s1474-4422(16)00114-9

Chen, M., Liu, M., Luo, Y., Cao, J., Zeng, F., Yang, L., et al. (2022). Celastrol protects against cerebral ischemia/reperfusion injury in mice by inhibiting glycolysis through targeting HIF-1α/PDK1 Axis. *Oxid. Med. Cell Longev.* 2022:7420507. doi: 10.1155/2022/7420507

Chen, S., Wang, M., Yang, H., Mao, L., He, Q., Jin, H., et al. (2017). LncRNA TUG1 sponges microRNA-9 to promote neurons apoptosis by up-regulated Bcl2l11 under ischemia. *Biochem. Biophys. Res. Commun.* 485, 167–173. doi: 10.1016/j.bbrc.2017.02.043

Chen, T., Dai, S. H., Jiang, Z. Q., Luo, P., Jiang, X. F., Fei, Z., et al. (2017). The AMPAR antagonist perampanel attenuates traumatic brain injury through anti-oxidative and anti-inflammatory activity. *Cell Mol. Neurobiol.* 37, 43–52. doi: 10.1007/s10571-016-0341-8

Chen, Y., Li, Z., Chen, X., and Zhang, S. (2021). Long non-coding RNAs: from disease code to drug role. *Acta Pharm. Sin. B* 11, 340–354. doi: 10.1016/j.apsb.2020.10.001

Cordes, T., Wallace, M., Michelucci, A., Divakaruni, A. S., Sapcariu, S. C., Sousa, C., et al. (2016). Immunoresponsive Gene 1 and itaconate inhibit succinate dehydrogenase to modulate intracellular succinate levels. *J. Biol. Chem.* 291, 14274–14284. doi: 10.1074/jbc.M115.685792

Dell'Orco, M., Sardone, V., Gardiner, A. S., Pansarasa, O., Bordoni, M., Perrone-Bizzozero, N. I., et al. (2021). HuD regulates SOD1 expression during oxidative stress in differentiated neuroblastoma cells and sporadic ALS motor cortex. *Neurobiol. Dis.* 148:105211. doi: 10.1016/j.nbd.2020.105211

Du, X., Xu, Y., Chen, S., and Fang, M. (2020). Inhibited CSF1R alleviates ischemia injury via inhibition of microglia M1 polarization and NLRP3 pathway. *Neural. Plast.* 2020:8825954. doi: 10.1155/2020/8825954

Dykstra-Aiello, C., Jickling, G. C., Ander, B. P., Shroff, N., Zhan, X., Liu, D., et al. (2016). Altered expression of long noncoding rnas in blood after ischemic stroke and proximity to putative stroke risk Loci. *Stroke* 47, 2896–2903. doi: 10.1161/strokeaha.116.013869

Ebert, M. S., Neilson, J. R., and Sharp, P. A. (2007). MicroRNA sponges: competitive inhibitors of small RNAs in mammalian cells. *Nat. Methods* 4, 721–726. doi: 10.1038/nmeth1079

Eroglu, B., Kimbler, D. E., Pang, J., Choi, J., Moskophidis, D., Yanasak, N., et al. (2014). Therapeutic inducers of the HSP70/HSP110 protect mice against traumatic brain injury. *J. Neurochem.* 130, 626–641. doi: 10.1111/jnc.12781

Feigin, V. L., Forouzanfar, M. H., Krishnamurthi, R., Mensah, G. A., Connor, M., Bennett, D. A., et al. (2014). Global and regional burden of stroke during 1990-2010: findings from the Global Burden of Disease Study 2010. *Lancet* 383, 245–254. doi: 10.1016/s0140-6736(13)61953-4

Gao, Q., Qin, H., Zhu, L., Li, D., and Hao, X. (2020). Celastrol attenuates collagen-induced arthritis via inhibiting oxidative stress in rats. *Int. Immunopharmacol.* 84:106527. doi: 10.1016/j.intimp.2020.106527

Jiang, M., Liu, X., Zhang, D., Wang, Y., Hu, X., Xu, F., et al. (2018). Celastrol treatment protects against acute ischemic stroke-induced brain injury by promoting an IL-33/ST2 axis-mediated microglia/macrophage M2 polarization. *J. Neuroinflammation* 15:78. doi: 10.1186/s12974-018-1124-6

Jin, Z., Liang, J., Wang, J., and Kolattukudy, P. J. (2015). MCP-induced protein 1 mediates the minocycline-induced neuroprotection against cerebral ischemia/reperfusion injury in vitro and in vivo. *J. Neuroinflammation* 12:39. doi: 10.1186/s12974-015-0264-1

Kang, M. J., Abdelmohsen, K., Hutchison, E. R., Mitchell, S. J., Grammatikakis, I., Guo, R., et al. (2014). HuD regulates coding and noncoding RNA to induce APP?Aβ processing. *Cell Rep.* 7, 1401–1409. doi: 10.1016/j.celrep.2014.04.050

Konieczny, J., Jantas, D., Lenda, T., Domin, H., Czarnecka, A., Kuter, K., et al. (2014). Lack of neuroprotective effect of celastrol under conditions of proteasome inhibition by lactacystin in in vitro and in vivo studies: implications for Parkinson's disease. *Neurotox. Res.* 26, 255–273. doi: 10.1007/s12640-014-9477-9

Lampropoulou, V., Sergushichev, A., Bambouskova, M., Nair, S., Vincent, E. E., Loginicheva, E., et al. (2016). Itaconate links inhibition of succinate dehydrogenase with macrophage metabolic remodeling and regulation of inflammation. *Cell Metab.* 24, 158–166. doi: 10.1016/j.cmet.2016.06.004

Lee, J. W., Bae, S. H., Jeong, J. W., Kim, S. H., and Kim, K. W. (2004). Hypoxia-inducible factor (HIF-1)alpha: its protein stability and biological functions. *Exp. Mol. Med.* 36, 1–12. doi: 10.1038/emm.2004.1

Li, G. Q., Liu, D., Zhang, Y., Qian, Y. Y., Zhu, Y. D., Guo, S. Y., et al. (2013). Anti-invasive effects of celastrol in hypoxia-induced fibroblast-like synoviocyte through suppressing of HIF-1α/CXCR4 signaling pathway. *Int. Immunopharmacol.* 17, 1028–1036. doi: 10.1016/j.intimp.2013.10.006

Li, J. H., Liu, S., Zhou, H., Qu, L. H., and Yang, J. H. (2014). StarBase v2.0: decoding miRNA-ceRNA, miRNA-ncRNA and protein-RNA interaction networks from large-scale CLIP-Seq data. *Nucleic Acids Res.* 42, D92–D97. doi: 10.1093/nar/gkt1248

Li, Y., He, D., Zhang, X., Liu, Z., Zhang, X., Dong, L., et al. (2012). Protective effect of celastrol in rat cerebral ischemia model: down-regulating p-JNK, p-c-Jun and NF-κB. *Brain Res.* 1464, 8–13. doi: 10.1016/j.brainres.2012.04.054

Li, Z., Wu, X., Li, J., Yao, L., Sun, L., Shi, Y., et al. (2012). Antitumor activity of celastrol nanoparticles in a xenograft retinoblastoma tumor model. *Int. J. Nanomed.* 7, 2389–2398. doi: 10.2147/ijn.S29945

Lin, M. W., Lin, C. C., Chen, Y. H., Yang, H. B., and Hung, S. Y. (2019). Celastrol inhibits dopaminergic neuronal death of parkinson's disease through activating mitophagy. *Antioxidants* 9:37. doi: 10.3390/antiox9010037

Liu, D. D., Luo, P., Gu, L., Zhang, Q., Gao, P., Zhu, Y., et al. (2021). Celastrol exerts a neuroprotective effect by directly binding to HMGB1 protein in cerebral ischemia-reperfusion. *J. Neuroinflammation* 18:174. doi: 10.1186/s12974-021-02216-w

Liu, M., Chen, M., Luo, Y., Wang, H., Huang, H., Peng, Z., et al. (2021). Lipidomic profiling of ipsilateral brain and plasma after celastrol post-treatment in transient middle cerebral artery occlusion mice model. *Molecules* 26:4124. doi: 10.3390/molecules26144124

Love, M. I., Huber, W., and Anders, S. (2014). Moderated estimation of fold change and dispersion for RNA-seq data with DESeq2. *Genome Biol.* 15:550. doi: 10.1186/s13059-014-0550-8

Lu, Y., Liu, Y., Zhou, J., Li, D., and Gao, W. (2021). Biosynthesis, total synthesis, structural modifications, bioactivity, and mechanism of action of the quinone-methide triterpenoid celastrol. *Med. Res. Rev.* 41, 1022–1060. doi: 10.1002/med.21751

Luo, C., Ouyang, M.-W., Fang, Y.-Y., Li, S.-J., Zhou, Q., Fan, J., et al. (2017). Dexmedetomidine protects mouse brain from ischemia-reperfusion injury via inhibiting neuronal autophagy through up-regulating HIF-1α. *Front. Cell. Neurosci.* 11:197. doi: 10.3389/fncel.2017.00197

Maida, C. D., Norrito, R. L., Daidone, M., Tuttolomondo, A., and Pinto, A. (2020). Neuroinflammatory mechanisms in ischemic stroke: focus on cardioembolic stroke, background, and therapeutic approaches. *Int. J. Mol. Sci.* 21:6454. doi: 10.3390/ijms21186454

McKee, A. E., and Silver, P. A. (2007). Systems perspectives on mRNA processing. *Cell Res.* 17, 581–590. doi: 10.1038/cr.2007.54

Michelucci, A., Cordes, T., Ghelfi, J., Pailot, A., Reiling, N., Goldmann, O., et al. (2013). Immune-responsive gene 1 protein links metabolism to immunity by catalyzing itaconic acid production. *Proc. Natl. Acad. Sci. U.S.A.* 110, 7820–7825. doi: 10.1073/pnas.1218599110

Noureddine, M. A., Qin, X. J., Oliveira, S. A., Skelly, T. J., van der Walt, J., Hauser, M. A., et al. (2005). Association between the neuron-specific RNA-binding protein ELAVL4 and Parkinson disease. *Hum. Genet.* 117, 27–33. doi: 10.1007/s00439-005-1259-2

Paris, D., Ganey, N. J., Laporte, V., Patel, N. S., Beaulieu-Abdelahad, D., Bachmeier, C., et al. (2010). Reduction of beta-amyloid pathology by celastrol in a transgenic mouse model of Alzheimer's disease. *J. Neuroinflammation* 7:17. doi: 10.1186/1742-2094-7-17

Qi, X., Shao, M., Sun, H., Shen, Y., Meng, D., and Huo, W. (2017). Long non-coding RNA SNHG14 promotes microglia activation by regulating miR-145-5p/PLA2G4A in cerebral infarction. *Neuroscience* 348, 98–106. doi: 10.1016/j.neuroscience.2017.02.002

Salminen, A., Lehtonen, M., Paimela, T., and Kaarniranta, K. (2010). Celastrol: molecular targets of thunder god vine. *Biochem. Biophys. Res. Commun.* 394, 439–442. doi: 10.1016/j.bbrc.2010.03.050

Schiavone, S., Morgese, M. G., Tucci, P., and Trabace, L. (2021). The therapeutic potential of celastrol in central nervous system disorders: highlights from in vitro and in vivo approaches. *Molecules* 26:4700. doi: 10.3390/molecules26154700

Sha, M., Ye, J., Luan, Z. Y., Guo, T., Wang, B., and Huang, J. X. (2015). Celastrol induces cell cycle arrest by MicroRNA-21-mTOR-mediated inhibition p27 protein degradation in gastric cancer. *Cancer Cell. Int.* 15:101. doi: 10.1186/s12935-015-0256-3

Shaker, M. E., Ashamallah, S. A., and Houssen, M. E. (2014). Celastrol ameliorates murine colitis via modulating oxidative stress, inflammatory cytokines and intestinal homeostasis. *Chem. Biol. Interact* 210, 26–33. doi: 10.1016/j.cbi.2013.12.007

Singh, G., Pratt, G., Yeo, G. W., and Moore, M. J. (2015). The clothes make the mRNA: past and present trends in mRNP fashion. *Annu. Rev. Biochem.* 84, 325–354. doi: 10.1146/annurev-biochem-080111-092106

Tao, X. L., Sun, Y., Dong, Y., Xiao, Y. L., Hu, D. W., Shi, Y. P., et al. (1989). A prospective, controlled, double-blind, cross-over study of tripterygium wilfodii hook F in treatment of rheumatoid arthritis. *Chin. Med. J.* 102, 327–332.

Vangoor, V. R., Gomes-Duarte, A., and Pasterkamp, R. J. (2021). Long non-coding RNAs in motor neuron development and disease. *J. Neurochem.* 156, 777–801. doi: 10.1111/jnc.15198

Wang, C., Wan, H., Li, M., and Zhang, C. (2021). Celastrol attenuates ischemia/reperfusion-mediated memory dysfunction by downregulating AK005401/MAP3K12. *Phytomedicine* 82:153441. doi: 10.1016/j.phymed.2020.153441

Wang, C., Wang, L., Ding, Y., Lu, X., Zhang, G., Yang, J., et al. (2017). LncRNA structural characteristics in epigenetic regulation. *Int. J. Mol. Sci.* 18:2659. doi: 10.3390/ijms18122659

Wang, J., Zhao, H., Fan, Z., Li, G., Ma, Q., Tao, Z., et al. (2017). Long noncoding RNA H19 promotes neuroinflammation in ischemic stroke by driving histone deacetylase 1-dependent m1 microglial polarization. *Stroke* 48, 2211–2221. doi: 10.1161/strokeaha.117.017387

Wong, V. K. W., Qiu, C., Xu, S. W., Law, B. Y. K., Zeng, W., Wang, H., et al. (2019). Ca(2+) signalling plays a role in celastrol-mediated suppression of synovial fibroblasts of rheumatoid arthritis patients and experimental arthritis in rats. *Br. J. Pharmacol.* 176, 2922–2944. doi: 10.1111/bph.14718

Wu, R., Chen, F., Wang, N., Tang, D., and Kang, R. (2020). ACOD1 in immunometabolism and disease. *Cell Mol. Immunol.* 17, 822–833. doi: 10.1038/s41423-020-0489-5

Wu, S., Wu, B., Liu, M., Chen, Z., Wang, W., Anderson, C. S., et al. (2019). Stroke in China: advances and challenges in epidemiology, prevention, and management. *Lancet Neurol.* 18, 394–405. doi: 10.1016/s1474-4422(18)30500-3

Xu, S., Feng, Y., He, W., Xu, W., Xu, W., Yang, H., et al. (2021). Celastrol in metabolic diseases: progress and application prospects. *Pharmacol. Res.* 167:105572. doi: 10.1016/j.phrs.2021.105572

Yan, H., Yuan, J., Gao, L., Rao, J., and Hu, J. (2016). Long noncoding RNA MEG3 activation of p53 mediates ischemic neuronal death in stroke. *Neuroscience* 337, 191–199. doi: 10.1016/j.neuroscience.2016.09.017

Yang, H. S., Kim, J. Y., Lee, J. H., Lee, B. W., Park, K. H., Shim, K. H., et al. (2011). Celastrol isolated from *Tripterygium regelii* induces apoptosis through both caspase-dependent and -independent pathways in human breast cancer cells. *Food Chem. Toxicol.* 49, 527–532. doi: 10.1016/j.fct.2010.11.044

Yang, Y., Yan, R., Zhang, L., Meng, X., and Sun, W. (2020). Primary glioblastoma transcriptome data analysis for screening survival-related genes. *J. Cell Biochem.* 121, 1901–1910. doi: 10.1002/jcb.29425

Zhang, B., Zhong, Q., Chen, X., Wu, X., Sha, R., Song, G., et al. (2020). Neuroprotective effects of celastrol on transient global cerebral ischemia rats via regulating HMGB1/NF-κB signaling pathway. *Front. Neurosci.* 14:847. doi: 10.3389/fnins.2020.00847

Zhang, J., Yuan, L., Zhang, X., Hamblin, M. H., Zhu, T., Meng, F., et al. (2016). Altered long non-coding RNA transcriptomic profiles in brain microvascular endothelium after cerebral ischemia. *Exp. Neurol.* 277, 162–170. doi: 10.1016/j.expneurol.2015.12.014

Zhang, X., Tang, X., Liu, K., Hamblin, M. H., and Yin, K. J. (2017). Long Noncoding RNA Malat1 regulates cerebrovascular pathologies in ischemic stroke. *J. Neurosci.* 37, 1797–1806. doi: 10.1523/jneurosci.3389-16.2017

Zhu, C., Yang, J., Zhu, Y., Li, J., Chi, H., Tian, C., et al. (2021). Celastrol alleviates comorbid obesity and depression by directly binding amygdala HnRNPA1 in a mouse model. *Clin. Transl. Med.* 11:e394. doi: 10.1002/ctm2.394

Conflict of Interest: The authors declare that the research was conducted in the absence of any commercial or financial relationships that could be construed as a potential conflict of interest.

Publisher's Note: All claims expressed in this article are solely those of the authors and do not necessarily represent those of their affiliated organizations, or those of the publisher, the editors and the reviewers. Any product that may be evaluated in this article, or claim that may be made by its manufacturer, is not guaranteed or endorsed by the publisher.

frontiers | Frontiers in Neuroscience

REVIEW
published: 10 June 2022
doi: 10.3389/fnins.2022.901360

miRNA Involvement in Cerebral Ischemia-Reperfusion Injury

Maria-Adriana Neag[1], Andrei-Otto Mitre[2], Codrin-Constantin Burlacu[2], Andreea-Ioana Inceu[1], Carina Mihu[1], Carmen-Stanca Melincovici[3], Marius Bichescu[2] and Anca-Dana Buzoianu[1]*

[1] Department of Pharmacology, Toxicology and Clinical Pharmacology, Iuliu Haţieganu University of Medicine and Pharmacy, Cluj-Napoca, Romania, [2] Faculty of Medicine, Iuliu Haţieganu University of Medicine and Pharmacy, Cluj-Napoca, Romania, [3] Department of Morphological Sciences, Iuliu Haţieganu University of Medicine and Pharmacy, Cluj-Napoca, Romania

Cerebral ischemia reperfusion injury is a debilitating medical condition, currently with only a limited amount of therapies aimed at protecting the cerebral parenchyma. Micro RNAs (miRNAs) are small, non-coding RNA molecules that *via* the RNA-induced silencing complex either degrade or prevent target messenger RNAs from being translated and thus, can modulate the synthesis of target proteins. In the neurological field, miRNAs have been evaluated as potential regulators in brain development processes and pathological events. Following ischemic hypoxic stress, the cellular and molecular events initiated dysregulate different miRNAs, responsible for long-terming progression and extension of neuronal damage. Because of their ability to regulate the synthesis of target proteins, miRNAs emerge as a possible therapeutic strategy in limiting the neuronal damage following a cerebral ischemic event. This review aims to summarize the recent literature evidence of the miRNAs involved in signaling and modulating cerebral ischemia-reperfusion injuries, thus pointing their potential in limiting neuronal damage and repair mechanisms. An in-depth overview of the molecular pathways involved in ischemia reperfusion injury and the involvement of specific miRNAs, could provide future perspectives in the development of neuroprotective agents targeting these specific miRNAs.

Keywords: miRNAs, ischemia reperfusion, cell death, inflammation, oxidative stress

OPEN ACCESS

Edited by:
Yongjun Sun,
Hebei University of Science and Technology, China

Reviewed by:
Chunhua Chen,
Peking University, China
Slava Rom,
Temple University, United States

****Correspondence:***
Andrei-Otto Mitre
andrei.mitre97@gmail.com

Specialty section:
This article was submitted to Neuropharmacology, a section of the journal Frontiers in Neuroscience

Received: *21 March 2022*
Accepted: *23 May 2022*
Published: *10 June 2022*

Citation:
Neag M-A, Mitre A-O, Burlacu C-C, Inceu A-I, Mihu C, Melincovici C-S, Bichescu M and Buzoianu A-D (2022) miRNA Involvement in Cerebral Ischemia-Reperfusion Injury. Front. Neurosci. 16:901360. doi: 10.3389/fnins.2022.901360

INTRODUCTION

Stroke represents the third leading cause of death and a major debilitating medical condition. It is responsible for permanent disabilities in approximately 80% of post-stroke patients (Moskowitz et al., 2010; Lallukka et al., 2018). Metabolic disruption of neurons activates immune responses, resulting in a complex chain of molecular events, which further promote progressive cellular damage and irretrievable neuronal death (Moskowitz et al., 2010; Khoshnam et al., 2017).

The ischemic/reperfusion (I/R) injury is caused by a sudden restriction of blood supply and oxygen, followed by subsequent restoration of blood flow and reoxygenation, contributing supplementary to the global oxidative stress (Eltzschig and Eckle, 2011). The I/R injury is the main actor in the neuroinflammatory repertoire, triggering different cell death provoking events, which include apoptosis, blood-brain barrier (BBB) disruption and mitochondrial dysfunction (Eltzschig and Eckle, 2011; Khoshnam et al., 2017).

The neuroprotective agents under current research address either the ischemic core, or the viable penumbra region, with the aim of reestablishing the collateral blow flow and ameliorating

the microenvironment damaged tissue (Eltzschig and Eckle, 2011; He et al., 2021). The standard therapeutic strategy for ischemic stroke remains thrombolytic reperfusion therapy provided by intravenous tissue plasminogen activator that is, however, limited by a short therapeutic window of 3-4,5 hours (Del Zoppo et al., 2009; IST-3 collaborative group et al., 2012; Fonarow et al., 2014).

Preclinical translation of neuroprotective drugs into clinical settings is failing. Even with advancing experimental studies on animal models, with excellent human reproducibility provided by thromboembolic stroke models, i.e., reproducible infarct size, and penumbra zone, there are still many promising neuroprotective agents in preclinical studies that fail to show a significant effect on patients (Dirnagl, 2006; Canazza et al., 2014; Luo et al., 2019). Dirnag et al. attributed this limited clinical potential of experimental drugs to statistical errors, lack of blinding and randomization of the animals, and negative publication bias (Dirnagl, 2006). Unexplored impediments steam from the limited ability of drugs to penetrate the BBB and target the ischemic neuronal tissue, resulting in decreased efficient concentration of the neuroprotective agents (Saugstad, 2010; Ponnusamy and Yip, 2019). In this context, selective drug delivery systems such as stroke tissue-related homing peptides and nanoparticles-mediated agents are emerging (Hong et al., 2008; He et al., 2021).

Micro RNAs (miRNAs) are small, non-coding RNA molecules, containing around 18–25 nucleotides, which pose a post-transcriptional regulatory role by down-regulating messenger RNAs (mRNAs) (Jonas and Izaurralde, 2015). Binding to the target mRNAs by base pairing, miRNAs negatively regulate gene expression of mRNAs *via* cleavage of mRNA, translation repression or destabilization of mRNA structure (Bartel, 2009; MacFarlane and Murphy, 2010).

The first pathological condition described, related to miRNAs was chronic lymphocytic leukemia (Calin et al., 2004). Since then, multiple studies outline the potential of miRNAs to mediate several pathological mechanisms of human diseases—i.e., cancer, neurological disorders, immune system disorders, acting as signaling molecules and mediators of cell-cell communication in different cellular processes such as proliferation, differentiation, and apoptosis (Smirnova et al., 2005; Garofalo et al., 2010; Tüfekci et al., 2014). MicroRNAs are key master regulators of gene expression in the brain, in processes related to brain development and its normal functioning, i.e., synaptogenesis, myelination, cerebral vasculogenesis and angiogenesis, but also in different brain disorders: ischemic stroke, neurodegenerative disease, traumatic brain injury, spinal cord injury, hypoxic-ischemic encephalopathy (Saugstad, 2010; Ponnusamy and Yip, 2019).

MicroRNAs also play a pivotal role in I/R injury, the main contributor to reactive oxygen species (ROS) production, cellular metabolic disfunctions associated with/underlying ischemic stroke (Ouyang et al., 2015; Cao et al., 2021). Recent studies have shown that I/R-related miRNAs alter the mitochondrial response and mediate multiple pathways that further promote neuronal survival and apoptosis (Jeyaseelan et al., 2008; Di et al., 2014; Hu et al., 2015; Ouyang et al., 2015). Min et al. highlighted the altered expression profile of miRNAs in brain I/R injury, which consisted of 15 miRNAs upregulated and 44 miRNAs downregulated (Min et al., 2015). MiRNAs modulate critical signaling pathways in I/R injury, associated with fibrosis, neoangiogenesis, necrosis, apoptosis and inflammation (Ghafouri-Fard et al., 2020).

However, miRNAs have also been reported in promoting the pathogenesis of ischemic stroke—i.e., atherosclerosis, hypertension, hyperlipidemia, plaque rupture, bidirectionally influencing the pathological chain of ischemic events, both pathogenesis and pathways (Rink and Khanna, 2011). In this direction, advancing the knowledge in gene functions using agomirs or antagomirs—double stranded miRNA agents, chemically modified at antisense strand that act as miRNA mimickers or inhibitors—could provide potential neuroprotective effects in modulating pathological processes in ischemic injuries (Kadir et al., 2020).

Neuroscience confronts limited therapeutic strategies aimed at protecting ischemic tissue, for which there is a critical and urgent need for advancing our knowledge. A depth overview of the molecular pathways involved in ischemic stroke, which are targeted by specific miRNAs, could provide future perspectives in the development of neuroprotective miRNA agents. This review aims to summarize the recent literature evidence of the miRNAs involved in signaling and modulating cerebral ischemia-reperfusion injuries, thus pointing their potential in limiting neuronal damage and repair mechanisms.

miRNAs IN NEUROLOGICAL DISEASES

Development of the adult brain and its functions are a highly studied subject in today's literature. Normal brain development proceeds *via* complex multistep processes, which involves early embryonic stage- neurogenesis, consisting in proliferation and differentiation of precursor neuronal cells, continuing to myelination and synaptogenesis in the childhood and adulthood period, which contributes to synaptic plasticity and memory (Semple et al., 2013). MiRNAs play essential roles in controlling neurodevelopment processes and normal brain functions, and dysregulation of miRNA expression profiling has been related to perinatal brain injury (Cho et al., 2019). Ponnusamy and Yip (2019) deciphered the role of miRNA involved in normal brain development' processes under normoxic and hypoxic conditions, consisting in myelination, axonal outgrowth, dendric outgrowth, synaptogenesis, neuronal differentiation, neuronal migration, angiogenesis.

Neurodegenerative diseases, which are mainly characterized by intracellular or extracellular protein aggregate formation, resulting to neuron dysfunction in certain brain areas, includes Alzheimer's disease (AD), Parkinson's disease (PD), Huntington's disease and multiple sclerosis (MS) (Quinlan et al., 2017).

Mounting evidence suggested the role of miRNAs-based therapeutics in modulating the prognosis of neurodegenerative diseases, emerging new miRNAs biomarkers for a better disease control (Quinlan et al., 2017). Thus, Juźwik et al. (2019) in a systematic review of 12 neurodegenerative disease identified 10 miRNAs frequently dysregulated, including miR-9-5p,

miR-21-5p, miR-29a-3p, miR-29b-3p, miR-29c-3p, miR-124-3p, miR-132-3p, miR146a-5p, miR-155-5p, and miR-223-3p. Notably, a different expression level of miRNAs, miR-9-5p, miR-21-5p, the miR-29, miR-124-3p, and miR-132-3p have been revealed, suggesting the mixed expression levels of miRNAs.

PD is characterized by dopaminergic neuron loss from the substantia nigra, with dysregulated level of miRNAs expression in the striatal brain areas and dopaminergic neurons (Nies et al., 2021). Prefrontal cortex of post-mortem PD patients exhibited 125 dysregulated miRNAs, of which miR-10b-5p levels being associated with clinical onset in both PD and Huntington's Disease (Hoss et al., 2016). The pathogenesis of PD related to miRNAs have been explained by modulation of PD-associated genes and protein expression related to α-synuclein-induced neuroinflammation, and degeneration of dopaminergic neurons (Nies et al., 2021). Down regulation of miR-425 in MPTP injected mouse PD model contributes to necroptosis and apoptosis activation, disintegration of mitochondrial membrane, ultimately leading to neuron loss and dopamine depletion. Moreover, miR-103a-3p, miR-30b-5p, and miR-29a-3p exhibited high levels of expression after Levodopa treatment, suggesting the role of miRNAs as disease modifier agents in PD (Serafin et al., 2015). Recent studies have shown that suppressing miR-34a can improve neuronal loss related to PD (Chua and Tang, 2019).

Sun et al. (2021) using bioinformatic analysis, reviewed the dysregulated miRNAs expression profiling in tissues of AD patients' brain, blood and CSF, correlated with pathological processes. Therefore, 27 dysregulated miRNAs identified have been related to neuroinflammation, amyloidogenesis, tau phosphorylation, synaptogenesis, apoptosis, and neuron degradation (Sun et al., 2021).

Multiple *in vivo* and *in vitro* animal models revealed the potential of miRNAs to counteracting beta-amyloid or tau reduction, inhibiting of apoptosis, and synaptic protection. In APP/PS1 transgenic mice, miR-137 exhibited reduced levels in the cerebral cortex, hippocampus, and serum, suggesting the neuroprotective potential of miR-137 to suppress p-tau overexpression (Jiang et al., 2018b). Moreover, inhibition of miR-98 in N2a/APP cells suppressed Aβ production by upregulating insulin-like growth factor 1 pathway (Hu et al., 2013, 1).

Neuroinflammation plays critical roles in MS pathogenesis consisting in dysregulation of inflammatory cell events in the brain, resulting in BBB disruption, damage of myelin and oligodendrocytes, neuro-axonal damage and inflammation (Haase and Linker, 2021).

MiR-155 which exhibited upregulated levels in MS, poses important role in BBB disruption under inflammatory conditions, which drives to demyelination processes, i.e., microglial activation, polarization of astrocyte. In 58 MS patients with adult onset, miR-320a, miR-125a-5p, miR-652-3p, miR-185-5p, miR-942-5p, miR-25-3p were significantly upregulated in peripheral blood samples, controlling transcription factors of SP1, NF-κB, TP53, HDAC1, and STAT3 (Nuzziello et al., 2018).

Unbalance of inflammatory reactions including dysfunction of memory T-cells and Treg cells contributed to continuous and progression inflammatory demyelinating of CNS. For instance, in MS patients, miR-19a, miR-19b, miR-25, and miR-106 elicited significantly upregulated levels in Treg cells compared with healthy controls (Gao et al., 2021). Targeting dysregulated miRNAs represents a therapeutic strategy. Thus, inhibiting let-7e decrease the differentiation of Th1 and Th17 cells, reducing the severity of MS in experimental autoimmune encephalomyelitis (Angelou et al., 2019). Increasing evidence ascertained the involvement of miRNAs in the initiation and progression of multifold types of cancer. Petrescu et al. (2019) reviewed the main dysregulated miRNAs related to brain tumors pathogenesis in glioma, meningioma, pituitary adenoma, and astrocytoma.

Multiple pathological processes associated with gliomagenesis were controlled by miRNAs. From disrupting BBB by targeting junctional proteins, zonula occludens-1 (ZO-1), occludin and β-catenin, to angiogenic, infiltration and migration of glioma cells by downregulating MMP2, MMP9, VEGF, all these tumor promoting processes are modulated by several miRNAs (Petrescu et al., 2019).

MiRNAs could be also used as clinical prognosis biomarkers. In 90 serum astrocytoma patients, miR-15b-5p, -16-5p, -19a-3p, -19b-3, 20a-5p, 106a-5p, 130a-3p, 181b-5p and 208a-3p exhibited upregulation levels, with miR-19a-3p, -106a-5p, and -181b-5p being associated with lower survival rate (Zhi et al., 2015).

CEREBRAL ISCHEMIA/REPERFUSION INJURIES

Histopathological Findings in Hypoxic/Ischemic Brain Injury

Hypoxic or ischemic brain injury give rise to a heterogeneity of histological findings, in which the neurons, the glial cells, the neuropile and the brain microvasculature are affected. These alterations in brain histological structures occur in chronological order and depends on the magnitude and duration of ischemia, and the extension of tissue damage. Two areas are examined: the ''ischemic core" or the irreversibly damaged area, and the ''ischemic penumbra," the hypoperfused area, which still contains viable cells.

Neurons and Glial Cells Modifications

The earliest change which occurs in the ischemic core is represented by neuronal swelling, because of the cytotoxic edema caused by ion alteration. The damaged neurons are large, with pale staining cytoplasm and pyknotic nucleus in hematoxylin and eosin (H&E) staining. After hours, in the ischemic core appear the red, eosinophilic, or ischemic neurons, characterized on routine histological sections by cell shrinkage, a pyknotic nucleus without nucleolus, and a highly eosinophilic cytoplasm, devoided of Nissle bodies. These neurons may be found also in the penumbra area for 1 or 2 days. Another aspect of advanced neuronal degeneration is represented by 'ghost neurons', found in the ischemic core and in the ischemic penumbra zone, which exhibits an irregular and very ill-defined cell border, pale staining cytoplasm in H&E staining and pyknotic, dark nucleus. The disintegration of dead neurons leads to parenchymal necrosis and release of cellular debris, which later will be engulfed by

macrophages (Mărgăritescu et al., 2009; Rahaman and Del Bigio, 2018).

Activation and proliferation of microglia, the resident macrophages in the central nervous system, occurs in the ischemic core in the first hours after ischemic injury, being involved in removing the necrotic tissue. During activation, microglia undergo morphological changes, with increase in cell body size and retraction of cytoplasmatic processes, acquiring an amoeboid phenotype in the ischemic core. In the ischemic penumbra and in the marginal zone we can find numerous highly ramified microglia (reactive microglia), which can migrate to the ischemic core, suggesting the fact that microglia may exhibit different morphological patterns, according to degree of ischemia and the time interval after ischemia (Zhang, 2019). After about 3 days, a lot of bone marrow-derived macrophages infiltrated the ischemic core and the ischemic penumbra (mostly), where they phagocytose the cellular and myelin debris, having a foamy appearance on histological sections. Activated microglia express high levels of immunomarker Iba1 +, while bone marrow-derived macrophages are highly positive for CD45 (Mărgăritescu et al., 2009; Li et al., 2014b; Magaki et al., 2018; Washida et al., 2019; Zhang, 2019).

In the ischemic core, swelling or edematous astrocytes may be found in the early phase, with a pale staining cytoplasm and disrupted cytoplasmatic processes; eventually, these cells will die. In the ischemic penumbra, the surviving astrocyte proliferate and undergo hypertrophy (reactive astrogliosis), expressing high amounts of glial fibrillary acidic protein. In routine histological sections, reactive astrocytes are large, star-shaped cells, having a coarse nuclear chromatin, glassy eosinophilic cytoplasm and long, branching cytoplasmatic processes; they are also called gemistocytic astrocytes. Astrogliosis represents a hallmark of nervous tissue injury after ischemia, and always follows the microglial activation and blood-derived macrophages invasion. After several days, the astrocytes and microglial cells from the ischemic penumbra surround the ischemic core and the cells will fill the necrotic areas, forming the glial scar tissue, an eosinophilic zone in H&E staining, with neuron loss and numerous glial cells, mainly reactive astrocytes (Mărgăritescu et al., 2009; Li et al., 2014b; Magaki et al., 2018).

In the first hours after ischemic injury, oligodendrocytes damage may cause axonal degeneration and demyelination, leading to rarefaction of the white matter (Mărgăritescu et al., 2009; Washida et al., 2019).

Microvascular Changes

In the ischemic core, structural changes of the small blood vessels are observed, such as: endothelial cell (ECs) swelling, pericyte and ECs detachment from the basement membrane, narrowing of the lumen, hyalinization and vascular wall thickening and sclerosis, with increase amount of collagen fibers and disintegration of vascular smooth muscle cells. These vascular modifications, in addition to morphological changes of astrocyte foot processes, lead to alteration of the BBB, which cause the vasogenic edema in the neuropil. Disruption of BBB or disintegration of capillaries in the necrotic areas, induce the appearance of microhemorrhages, extravasated and lysed erythrocytes releasing hemosiderin pigment, which is phagocytized by macrophages (siderophages) (Mărgăritescu et al., 2009; Rahaman and Del Bigio, 2018; Liu et al., 2019a).

The ischemic penumbra contains congested blood vessels, surrounded by perivascular edema. After 3 days, neovascularization occurs within the ischemic penumbra, but the newly formed blood vessels are abnormal, thin, highly permeable, thus increasing the pre-existing brain edema (Rahaman and Del Bigio, 2018; Liu et al., 2019a).

Inflammatory Reaction

Polymorphonuclear leukocytes (PMNs) and macrophages play a key role in early inflammatory reaction after brain ischemia, while lymphocytes (mostly T lymphocytes), are involved in the delayed phases of ischemia. An acute inflammatory reaction appears within the first 4-6 hours after ischemic injury, with PMNs infiltration in the necrotic tissue. Within the first 3 days, activated microglia and blood-derived macrophages invade the necrotic area, engulfing the cellular and myelin debris (lipid-laden macrophages) (Kawabori and Yenari, 2015; Anrather and Iadecola, 2016).

General Mechanisms of Cerebral Ischemia/reperfusion Injury

Neuronal damage after recanalization has long been known to occur following ischemic stroke through a unique type of injury that is not expressed during the hypoxic period (S.M. Humphrey et al., 1973; Baird et al., 1994). As ischemic events are responsible for stroke in almost 80% of cases, even with the achievement of reperfusion *via* thrombolysis, stent retrievers or spontaneous reperfusion, I/R injuries have been shown to have deleterious and noteworthy effects of brain function and ischemic area after artery occlusion (Zhang et al., 1994). Animal studies have shown that the area damaged by the initial ischemic event can increase in size after repermeabilization of the affected artery, compared to continuous occlusion (Zhang et al., 1994). As pathophysiological mechanism may be possible targets for therapy and prevention of reperfusion injury, altering the BBB has been thought as the main mechanism involved. New evidence suggests multiple damage mechanism that can alter neuronal function in I/R injury such as the activation of the complement system (inhibition of which may yield less ischemia-reperfusion cardiac injury), the increase in leukocyte taxis to the affected area (the depletion of which can be a target in limiting reperfusion damage), cellular component damage, the stress caused by ROS and the activation of platelets can cause reperfusion damage and cerebral edema (Lin et al., 2016; Wu et al., 2018). Another molecular mechanism for brain damage after I/R concerns matrix metalloproteinases (MMPs) and their ability to interrupt endothelial junctions after restoration of blood flow (Candelario-Jalil et al., 2009). The vasogenic edema is caused by a biphasic "opening" of the BBB, with the early phase occurring several hours after reperfusion and being related to the activation of gelatinase A (MMP-2) and the second, 1 to 2 days after restoration of blood flow, associated with the expression and activation of gelatinase B (MMP-9) and stromelysin-1 (MMP3) (Rosenberg and Yang, 2007).

ROS are responsible for the damage to cellular components, such as mitochondria, nucleic acids and proteins (Brieger et al., 2012). Their role in reperfusion injury has long been presumed and recent data confirm that superoxide molecules can be produced after reperfusion following brain ischemia and molecules such as NADPH oxidase (NOX) can be involved in I/R injury in the brain and altering the BBB through their ability to transfer electrons to molecular oxygen (Kim et al., 2017b; Yang, 2019). The latter can be considered a way through which the mechanisms involved in I/R injury link to each other, especially when referring to the first phase of I/R brain injury related to the BBB in case of ischemic brain injury.

An important pathway that can lead to aggravating I/R injury is related to cellular component damage. ROS are causing damage to nucleic acids and macromolecules, as stated above, but also to mitochondria leading to ATP depletion, anaerobic metabolism and malfunctioning of ion pumps (Sanderson et al., 2013). The ischemia-reperfusion model in mitochondrial injury consists of calcium overload due to the altered function of the endoplasmic reticulum, which can generate ROS that may hyperpolarize the mitochondria membrane and surpass the antioxidants present in the cell (Wu et al., 2018). Excess reactive oxygen may escape from the electron transport chain and activate mechanisms that interfere with apoptosis and necrosis, while mitochondrial disfunction regarding fission and fusion becomes impaired during IR injury (Turrens, 2003; Andreyev et al., 2005). Besides an excess in ROS, reperfusion-induced inflammation also causes the release of cytokines, causing cytokine storm that ultimately injures the surrounding tissue (Eltzschig and Eckle, 2011).

Oxidative stress during I/R injury is thought to be caused by three different systems: xanthine oxidase system, NADPH oxidase (NOX) system and nitric oxide synthase (NOS) system (Cantu-Medellin and Kelley, 2013; Ma et al., 2017b). NOX-derived free oxygen radicals are known to cause the increase in local inflammatory cell presence and may lead to impaired perfusion of multiple organs (Sedeek et al., 2009; Meza et al., 2019). Even though the NOS system has a well-established role in providing nitric oxide as an antioxidant protective agent against I/R injury, it is also known that this type of injury can transform NOS into a superoxide generating system, with a resulting decrease in cellular NO and increase in ROS (Forstermann and Munzel, 2006). The free oxygen radicals can promote inflammation in the affected cells and can lead to cellular death (Lisa and Bernardi, 2006).

Inflammation represents a mechanism that has important implications in determining the amount of damage during reperfusion injury. This mechanism can yield effects through the cytokines, and molecules produced by the endothelium and parenchymal cells during I/R injury, but also by the number of leukocytes attracted to the damaged area. Oxidative stress, as mentioned above, can also be a means of aggravating ROS induced inflammation by increasing the expression of pro-inflammatory factors such as TNF-α and interleukin (IL)-1β (Turovsky et al., 2021). The adhesion of white blood cells to the endothelium, slow-rolling and trans-endothelial migration are augmented by flow restoration after ischemia, together with increased oxygen content. As more free oxygen radicals are produced, and leukocyte activation is ongoing due to danger signals, NADPH oxidase produces more ROS, neutrophils are able to release different cell damaging hydrolytic enzymes and generate hypochlorous acid *via* the activity of myeloperoxidase, pore-forming molecules being produced in the detriment of the vascular and parenchymal cells (Granger et al., 1993; Frangogiannis, 2015). Oxidative stress and NO depletion are also responsible for triggering humoral response to I/R injury as molecules such as TNF-α, IL-1, ANG II, LTB4 and PAF (linking the activation of platelets to neutrophil I/R damage) (García-Culebras et al., 2019). In addition to inflammation, complement system activation (C') has been associated to I/R injury, both by increasing chemotaxis and activation in damage area leukocytes and activating the membrane attack complex to induce cellular damage (Gorsuch et al., 2012). Inhibiting the C5a fragment has also been shown to decrease neutrophile tissue infiltration (Wood et al., 2020). As inflammation is strongly linked to multiple types of cell death, nuclear factors that stimulate the expression of genes related to inflammation have been seen as a mechanism and also as a potential target during I/R injury. Different studies have supported this view, as strategies such as ulinastatin administration to mice undergoing temporary middle cerebral artery occlusion, which downregulates TLR4 and NF-kB expression, sodium butyrate administered during I/R injury of the lung and inhibiting NF-κB and JAK2/STAT3 signaling pathways or combination of octreotide and melatonin to alleviate the inflammasome-induced pyroptosis through the inhibition of TLR4-NF-κB-NLRP3 pathway in liver I/R injury, have clearly showed that NF-kB plays an important role in reperfusion injury (Li et al., 2017b; El-Sisi et al., 2021; Ying et al., 2021).

Neutrophils can adhere to the endothelial wall where necrosis factors expressed by injured cells are exhibited on the luminal surface and contact the leukocytes (such as P-selectin). After flow reestablishment, the cells are able to cytoskeletal shape-shift and adapt to linear flow, moving through an inter-endothelial pattern and eventually localizing points of entry by mechanism of actin polymerization and matrix metalloproteinase activity and gaps between pericytes (Nourshargh and Alon, 2014). Other immune cells such as lymphocytes, thrombocytes, mast cells or macrophages are also believed to play a role in I/R injury by increasing the presence of tissue neutrophils (Rodrigues and Granger, 2010). Platelets are also involved in attracting leukocytes and inducing I/R damage by their activation in the presence of inflammatory cytokines including PAF, due to the damage of endothelial cells, lack of NO, prostacyclin, and abundance of ROS (Esch et al., 2010; Franks et al., 2010).

In response to brain hypoxia/ischemia, miRNAs modulate a complex network of gene expression, for which they were proposed as potential and reproducible biomarkers in ischemic stroke due to a consistent correlation with neuropathological changes and prognosis of stroke (Vijayan and Reddy, 2016; Condrat et al., 2020). Several types of hypoxia/ischemia-sensitive miRNAs, whose blood levels are correlated with their brain circulating levels, were identified as potential clinical biomarkers in stroke: miR-210, miR-125a-5p, miR-125b-5p, and miR-143-3p (Zeng et al., 2011; Tiedt et al., 2017). MiRNAs influence gene expression in response to hypoxic/ischemic injury, and in

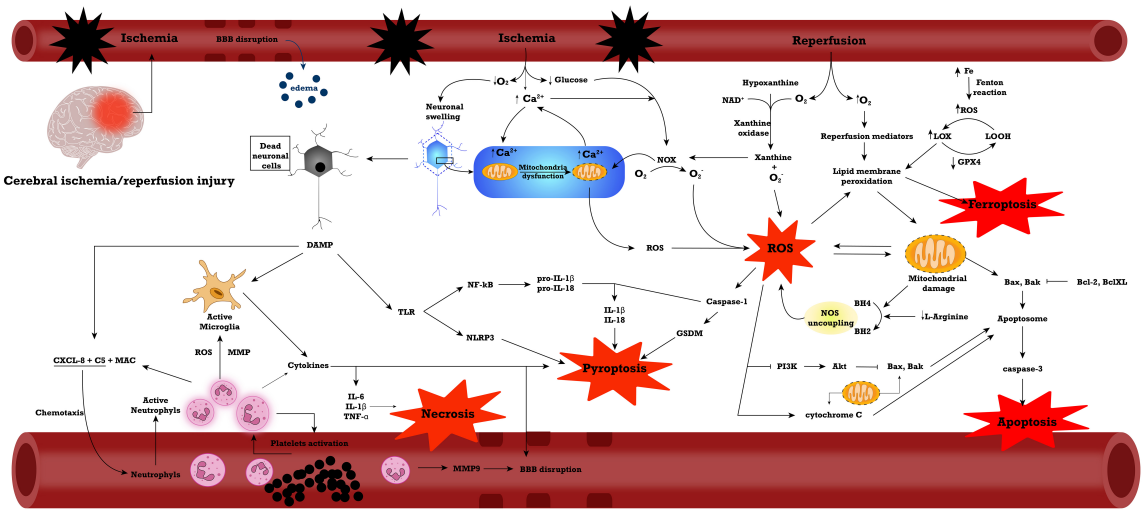

FIGURE 1 | General mechanisms in ischemia/reperfusion injury. Abbreviations: Akt, Protein kinase B; BBB, blood-brain barrier; C5, complement fraction 5; CXCL, C-X-C Motif Chemokine Ligand; DAMP, damage-associated molecular pattern; GPX4, glutathione peroxidase 4; IL, interleukin; LOOH, lipid alcohol; LOX, lipid peroxide; MAC, membrane attack complex; MMP, matrix metalloproteinase; NAD, nicotinamide adenine dinucleotide; NF-kB, nuclear factor kappa-light-chain-enhancer of activated B cells; NOS, nitric oxide synthase; NOX, NADPH oxidase; PI3K, phosphoinositide 3-kinases; ROS, reactive oxygen species; TLR, Toll-like receptor; TNF-α, tumoral necrosis factor α.

turn the inflammatory responses triggered by ischemia-hypoxia dysregulate miRNA expression (Chen et al., 2020b). In the complex array of neuroinflammatory events, microRNAs are at the center of target gene regulation and modulation, microglia activation, cytokine production, cell apoptosis, mitochondrial disfunction and immune cell development, maintaining the vicious processes that lead to the progression and extension of neuronal damage (Chen et al., 2020b).

The most important of these processes are displayed in **Figure 1**.

microRNAs IN ISCHEMIA/REPERFUSION INJURY

Inflammation

The inflammatory response is one of the major consequences of cerebral ischemia and miRNAs play an important role in its regulation. The involvement of several miRNAs in these pathways is presented in **Tables 1**, **2**. Changes in the expression of inflammatory cytokines may occur after cerebral I/R injury (Wu et al., 2020). In lesions caused by I/R, inflammation is initiated by stagnant blood flow (vessel occlusion) and is then maintained by leukocytes activation and release of pro-inflammatory cytokines. Reducing or stopping the blood flow causes changes in the coagulation cascade, activates NF-kB and increases the expression of adhesion molecules on endothelial cells (Jurcau and Simion, 2021). Decreasing the amount of oxygen in the tissue causes varying degrees of damage. The first innate immune mechanism that is involved in this mechanism is the activation of toll-like receptors (TLRs). Activation of these receptors determines the activation of NF-kB, recognized as a pathway with a major role in the inflammatory response and with the ability to modulate several cytokines (TNF-α, IL-1β, and IL-6) and other mediators (iNOS, PGE2) (Shi et al., 2018; Yang et al., 2020). Microglia is the main factor involved in neuroinflammation. Its function and morphology are altered after ischemia. Activation of the microglia leads to its migration in and around the affected area (Hao et al., 2020). Together with the microglia, macrophages accumulate in the lesion (Islam et al., 2018). Following this activation process, the microglia release large amounts of pro-inflammatory cytokines (TNF-α, IL-6, IL-1β) that are considered to be the main factors involved in acute inflammation in ischemic stroke (Hao et al., 2020; Wang et al., 2020c).

I/R damage can be ameliorated by transforming growth factor β1 (TGF-β1), a cytokine with anti-inflammatory effects (Yang et al., 2020). TGF-β1 is a factor produced in large amounts in the lesion, starting on day 5 after reperfusion or later. A source of TGF-β1 may be the microglia and macrophages. The anti-inflammatory effect of TGF-β1 is thought to be a consequence of phosphorylation of the Smad protein by binding of this ligand to TGF-β receptors (Islam et al., 2018). Another member of the TGF family, TGF-β2, has a neuroprotective effect, being considered a neuroprotective factor. The expression of this protein is increased in animals with transient cerebral ischemia. Activation of the TGF-β2/Smad3 signaling pathway is essential for neuroprotection in ischemic brain injury (Peng et al., 2019).

The inflammatory response can be initiated by inflammasomes, complex molecular protein structures that are sensitive to cellular changes when homeostasis is lost (Franke et al., 2021). The main components of an inflammasome are a NLR sensor molecule, a pro-inflammatory caspase, and an adaptor protein (apoptosis-associated speck-like protein (ASC)) with a role in transmitting cellular signals (Hong et al., 2019; Caseley et al., 2020). Currently, the most studied inflammasome

TABLE 1 | Up-regulated miRNAs in cerebral I/R injuries.

miRNA	miRNA or agmonir effect	Study type	References
miR-106b-5p	↑ ROS production, ↓antioxidant ability (SOD) and ↑ apoptosis activation	Experimental (Rat model and PC12 cell line)	Li et al., 2017a
miR-124	Biomarker of AIS	Clinical	Weng et al., 2011; Rainer et al., 2016
miR-124	↓ p-STAT3, ↓ pyroptosis	Experimental (Rat model)	Sun et al., 2020a
miR-125b	↓ CK2α; ↑ NOX2 and NOX4 activation, ↑ ROS	Experimental (Rat model and PC12 cell line)	Liang et al., 2018
miR-125b	↓ Protein kinase CK2	Experimental (PC-12 cell line)	Liang et al., 2018
miR-128	↓ proliferation ability ↓ GFAP and MAP2 ↑ TNF-α, IL-6, and IL-1β ↓ GSH and SOD ↑ MDA ↓ ARPP21 and CREB1 ↓ BDNF	Clinical and Experimental (Mouse model and hippocampal neurons and astrocytes)	Chai et al., 2021
miR-128-3p	↓ Nrf2, ↓ antioxidant ability	Experimental (Rat model and neural stem cells line)	Li et al., 2019a
miR-142-5p	↓ Nrf2/ARE, ↑ ROS	Experimental (Rat model and primary hippocampal neurons)	Wang et al., 2017
miR-143-3p	↓ FSTL1, Bcl-2, ↑ Bax, caspase 3 and cleaved caspase 3, ↑ apoptosis	Experimental (Mice model and human neuroblastoma cell line SH-SY5Y)	Wang and Liu, 2021
miR-145	↑ ERK, p38 and MAPK ↑ Cyclin D1, Nestin, NSE, and GFAP ↓ Cleaved-caspase 3 ↑ NSCs proliferation ↑differentiation of NSCs ↓ apoptosis	Experimental (Rat model and Rat neural stem cells)	Xue et al., 2019
miR-150	↓ BBB permeability ↑ Tie-2 ↓ claudin-5	Experimental (Rat model and BMECs cell line)	Fang et al., 2016, 2
miR-153	↓ Nrf2 and HO-1, ↓ antioxidant levels, ↑ ROS	Experimental (Primary hippocampal neurons)	Ji et al., 2017
miR-16	Biomarker of AIS	Clinical	Rainer et al., 2016
miR-181a	↓ XIAP, Bcl-2, ↑ Bax, cleaved caspase 3, ↑ apoptosis	Experimental (Rat model and primary cortical neurons)	Zhang et al., 2019a
miR-182	↓ mTOR/ ↓ FOXO1 ↓ ZO-1, Occludin, and Claudin-5 ↓ Bcl-2/Bax	Experimental (Mouse model and primary cultures of astrocytes, mouse brain vascular pericytes, N2a mouse neuroblastoma cell line and BV2 microglial cells)	Zhang et al., 2020b
miR-187-3p	↓ Seipin, ↑ apoptosis, ↓ autophagy	Experimental (PC12 cells)	Ren et al., 2020
miR-191-5p	↓ BDNF	Experimental (Mouse model)	Wu et al., 2021
miR-195-5p and miR-451a	↓ BDNF ↓ VEGF-A	Clinical	Giordano et al., 2020
miR-19a-3p	↑ TNF-α, IL-1β, IL-6 ↓ Bcl-2, ↑ Bax ↓ IGFBP3 ↓ cell viability	Experimental (rat model and SH-SY5Y cell line)	Chai et al., 2020
miR-200a	↑ STAT and MAPK, ↑Bax/Bcl-2, p53, cytochrome c, ↑ apoptosis	Experimental (Neural stem cells)	Ma et al., 2017a
miR-200a-3p	↑ neuronal cell death, ↑ ROS levels	Experimental (HT-22 cells)	Wei et al., 2015
miR-200b-3p	↑ neuronal cell death, ↑ ROS levels	Experimental (HT-22 cells)	Wei et al., 2015

(Continued)

TABLE 1 | (Continued)

miRNA	miRNA or agmonir effect	Study type	References
miR-20a	↑ Cadherin 1	Experimental (Rat model)	Yang et al., 2021
miR-210	↑HIF-1α, VEGF, caspase-3, ↑ apoptosis	Experimental (Rat model and rat neuronal cells)	Sun et al., 2019
miR-23a-3p	↓ NO, 3-NT ↑ MnSOD, ↑ antioxidant ability, ↓ caspase 3, ↓ ROS, ↓ apoptosis	*In vivo* and *in vitro* (Mice model and neuro-2a cells)	Zhao et al., 2014
miR-29b	↑ caspase 3, ↓ Bcl-2, MCL-1, ↑ apoptosis	Experimental (neuro-2a cells)	Huang et al., 2018
miR-302b-3p	↓ Nrf2/ARE, FGF15, ↑ caspase 3, ↑ ROS, ↑ apoptosis	Experimental (Murine HT22 cell line)	Zhang et al., 2019b
miR-30a	↑ BBB permeability ↑ zinc accumulation ↓ ZnT4 ↓ occludin and claudin-5	Experimental (Rat model and Brain microvascular EC bEnd3 cell line, pericyte cell line MBVP, astrocytic cell C8-D1A)	Wang et al., 2021c
miR-339	↓ FGF9 and CACNG2 ↓ Cell Proliferation ↑ Induces Apoptosis ↑ p-P38 and p-JNK	Experimental (PC12 cells)	Gao et al., 2020, 2
miR-421	↓ SOD, ↑ ROS, ↑ apoptosis	Experimental (Rat model and PC12 rat pheochromocytoma cell line)	Yue et al., 2020
miR-424	↑ Nrf2, ↑ antioxidant responses, ↓ROS	Experimental (Mouse model)	Liu et al., 2015
miR-429	↑ neuronal cell death, ↑ ROS levels	Experimental (HT-22 cells)	Wei et al., 2015
miR-670	↓ Hippo-Yap, ↑ apoptosis	Experimental (Mouse model and neuro-2a cells)	Yu et al., 2021c
miR-670	↓ phosphorylation of downstream Yap ↓ Yap degradation.	Experimental (Mouse model and neuro-2a cells)	Yu et al., 2020
miR-7-5p	↓ Sirtuin 1, ↑ apoptosis	Experimental (Rat model and SH-SY5Y cells)	Zhao and Wang, 2020
miR-9	Biomarker of AIS	Clinical	Ji et al., 2016
miR-93	↓ Nrf2 and HO-1, ↓ antioxidant levels, ↑ ROS	Experimental (mice model and primary cortical neurons)	Wang et al., 2016

ACSL4, acyl-CoA synthetase long chain family member 4; AIM, absent in melanoma; AIS, acute ischemic stroke; Akt, Protein kinase B; ARE, antioxidant response element; AQP, Aquaporin; BBB, blood-brain barrier; BBC3, Bcl-2-binding component 3; BDNF, Brain-derived neurotrophic factor; CCL, C-C Motif Chemokine Ligand; CXCL, C-X-C motif ligand; CXCR, C-X-C motif chemokine receptor; FIP, FAK family-interacting protein; FOXO1, Forkhead box class O1; FSTL1, follistatin-like protein 1; GPX4, glutathione peroxidase 4; GSK, glycogen synthase kinase; HDAC, histone deacetylase; HIF, hypoxia inducible factor; HO-1, heme oxygenase 1; IGFBP3, Insulin Like Growth Factor Binding Protein 3; IL, interleukin; JAK, Janus kinase; MAPK, mitogen-activated protein kinase; MCL, myeloid leukemia sequence; MDA, malondialdehyde; miR, microRNA; MnSOD, manganese superoxide dismutase; mTOR, mammalian target of rapamycin; NEAT, nuclear paraspeckle assembly transcript; NF-κB, nuclear factor kappa-light-chain-enhancer of activated B cells; NO, nitric oxide; 3-NT, 3-nitrotyrosine; NOX, nicotinamide adenine dinucleotide phosphate (NADPH) oxidase; Nrf2, nuclear factor-erythroid factor 2-related factor 2; PI3K, Phosphoinositide 3-kinase; PUMA, p53-up-regulated modulator of apoptosis; SOD, super oxide dismutase; p-STAT, phosphorylated (activated) signal transducer and activator of transcription; RBFox-1, RNA-binding protein fox-1 homolog 1; SNAI2, Snail Family Transcriptional Repressor 2; SOX7, SRY-Box Transcription Factor 7; TFR1, transferrin receptor 1; TLR4, Toll-like receptor 4; TNF, tumoral necrosis factor; TP53INP1, Tumor Protein P53 Inducible Nuclear Protein 1; VEGF, vascular-epithelial growth factor; XIAP, X chromosome-linked inhibitor of apoptosis protein; ZO, zonula occludens.

is nod-like receptor protein 3 (NLRP3). It plays an important role in various diseases with inflammatory components. Activation of NLRP3 leads to cerebral ischemia by releasing proinflammatory cytokines, such as IL-1β and IL-18. In the first stage after cerebral I/R injury, microglia become the main reservoir for activated NLRP3 inflammasome. In the following stages, NLRP3 are activated in both neurons and endothelial cells (Gao et al., 2017; Gong et al., 2018). The interaction between inflammasomes and TXNIP (thioredoxin interacting protein) leads to the activation of inflammation. In a normal, stress-free state, TXNIP is linked to Trx1 (thioredoxin1). Thus, NLRP3 is in inactive form. In stroke, a state with high oxidative stress, TXNIP and Trx1 dissociate and thus NLRP3 is activated. Nuclear factor erythroid 2-related factor 2 (Nrf2) is involved in the oxidative process and can interfere with processes that are consequences of oxidative stress. Trx1 has a neuroprotective effect against I/R and Nrf2 lesions by regulating the Trx1/TXNIP interaction negatively regulates NLRP3 inflammasome (Hou et al., 2018).

TABLE 2 | Down-regulated miRNAs in cerebral I/R injuries.

miRNA	miRNA or agomiRNA effects	Study type	References
Let-7g* and miR-98	↓ CCL2, CCL5 (both miRNAs) ↓ CCL3, CXCL1 (Let-7g*) ↓ IP-10 (miR-98)	Experimental (Mouse model)	Bernstein and Rom, 2020
miR-124	↑ SOD, ↓ MDA and NOX2, ↓ NF-κB, TNF-α and IL-6, ↓ apoptosis	Experimental (Rat model and PC12 cell line)	Wu et al., 2020c
miR-125b	↓ p53, Bax, cytochrome C and caspase-3, ↓ apoptosis	Experimental (Rat model)	Xie et al., 2018
miR-126a-5p	↓ NOX2	Experimental (Rat model)	Liu et al., 2017
miR-130a	↑ PI3K/AKT	Experimental (Rat model, PC12 cells)	Zheng et al., 2019
miR-132-3p	↓ NOX4	Experimental (Rat model)	Liu et al., 2017
miR-132/212	↓ Claudin-1, TJAP-1, RBFox-1	Experimental (Mouse model and neuronal cultures)	Yan et al., 2021
miR-135b-5p	↓ GSK-3β activation, ↑ Nrf2/ARE, ↓ apoptosis	Experimental (Mouse hippocampal HT22 cell line)	Duan et al., 2018
miR-142-3p	↓ mitochondrial enzymes, ↑ mitochondrial function ↑ NOX2/Rac1, ↑ ROS, ↓ apoptosis	Experimental (Rat cerebrum primary cortical neurons)	Xia et al., 2020
miR-146a	↓ NOX4	Experimental (Rat model and SH-SY5Y cells)	Hong et al., 2018
miR-149-5	↓ S1PR2 ↓ pericyte migration ↑ N-cadherin ↑ BBB integrity	Experimental (Rat model and BMECs cell line and pericytes)	Wan et al., 2018
miR-150	↓ MYB ↓ VEGF	Experimental (BMVECs and 293T cells)	Zhang et al., 2021b
miR-182-5p	↓ TLR4	Experimental (Rat model)	Wang et al., 2018
miR-186	↓ HIF-1α ↓ N2a cell, cleaved caspase-3, Bax, ↑ Bcl-2 ↓ ROS production	Experimental (Rat model and Neuro2a cell line)	Li et al., 2021b
miR-18b	↓ Annexin A3, ↑ PI3K/Akt pathway, ↓TNF-α, IL-1β, ↓apoptosis	Experimental (Mouse model, SH-SY 5Y cells)	Min et al., 2020
miR-18b	↓ ANXA3 ↑ PI3K/Akt ↑ Bcl-2 ↓ Bax ↓ TNF-α, IL-1β ↑ p-PI3K, p-Akt, and p-mTOR	Experimental (Mouse model and SH-SY 5Y cell line)	Min et al., 2020
miR-194	↓ NOX1, ACSL4, Bach1, iron, ↑ GPX4, Nrf2, HO-1, ↓ ferroptosis	Experimental (PC12 cells)	Li et al., 2021d
miR–19a	↓ Syndecan 1, ↑ JAK1/STAT3 signalling pathway	Experimental (Mouse model)	Fang et al., 2021
miR-21	↓ MAPK	Experimental (Rat model)	Yao et al., 2018
miR-211	↓ PUMA, ↓ apoptosis	Experimental (Rat model and PC12 cells)	Liu et al., 2020
miR-214	↓ TFR1 and p53, ↑ GSH/GSSG, GPX4 ↓ ROS ↓ ferroptosis	Clinical and experimental study (Mouse model)	Lu et al., 2020a
miR-216a	↓ JAK2 ↓ p-STAT3 ↓ LDH ↓ cleaved caspase-3 ↓ iNOS, MMP-9, TNF-α, and IL-1b	Experimental (Mouse model and Primary Cortical Neuronal Cells)	Tian et al., 2018, 3
miR-219a-5p	↓ Phosphodiesterase 4D, ↓apoptosis,	Experimental (Mouse neuroblastoma N2a cells)	Lu et al., 2020b
miR-22	↓ NF-kB	Experimental (Rat model)	Yu et al., 2015

(Continued)

TABLE 2 | (Continued)

miRNA	miRNA or agomiRNA effects	Study type	References
miR-22	↓ TNF-α, IL-1β, IL-6, IL-18, MIP-2 and PGE2 ↓ NF-κB ↓ p38 MAPK ↓ p-p38, NF-κB, COX-2 and iNOS	Experimental (Rat model and PC12 cells)	Dong et al., 2019
miR-22	↑ VEGF and Ang-1 ↑ p-PI3K/PI3K and p-Akt/Akt	Experimental (Rat model and	Wang et al., 2020b
miR-22-3p	↓ IL-1β, IL-18, ↓ cleaved caspase 1 ↓ NLRP3, NEAT1, ↓pyroptosis, ↓ apoptosis	Experimental (Rat model and rat primary cortical neurons)	Zhang et al., 2021a
miR-224-3p	↓ FIP200, ↓ cleaved caspase-3, ↓ ROS, ↓ apoptosis	Experimental (Neuro-2a cells)	Deng et al., 2019
miR-25	↓ Fas/FasL, ↓ inhibits apoptosis	Experimental (Human SH-SY5Y and IMR-32 cells)	Zhang et al., 2016
miR-25	↓ NOX4	Experimental (Rat model and SH-SY5Y cells)	Hong et al., 2018
miR-27a-3p	↓ FOXO1, ↓ caspase 3, caspase 9, ↑ Bcl-2, ↑ SOD, GSH, ↓ MDA, ↓ apoptosis, ↓ ROS	Experimental (Rat model and murine HT22 cells)	Li et al., 2021c
miR-27a-3p	↓ BBB permeability ↑ claudin-5 and ↑ occludin, ↓ GSK3ß ↑ Wnt/ß-catenin.	Experimental (hCMEC/D3 cell line)	Harati et al., 2022
miR-29a	↓ BBC3/PUMA, ↓ apoptosis	Experimental (Mouse primary astrocyte cells)	Ouyang et al., 2013
miR-29a-5p	↓ NOX4	Experimental (Rat model)	Liu et al., 2017
miR-29c-3p	↓ NOX4	Experimental (Rat model)	Liu et al., 2017
miR-29b	↓ AQP-4 ↓ Extravasated IgG ↑ CD31/occludin and CD31/ZO-1	Clinical and experimental (Mouse model)	Wang et al., 2015b, 4
miR-320a	↓ AQP-1 and AQP-4	Experimental (Rat model and Human astrocytoma cells)	Sepramaniam et al., 2010
miR-326-5p	↓ STAT3, ↑ Mitofusin 2	Experimental (Rat model)	Huang et al., 2021b
miR-34b	↓ Keap1, ↑Nrf2/ARE, HO-1, ↓ NO, 3-NT, ↑ SOD, MnSOD, ↓ ROS	Experimental (Rat model and cell line)	Huang et al., 2019
miR-34c-5p	↑ Bcl-2, ↓ p65, Bax/β-actin, caspase-3, ↓ IL-6, TNF-α, ↑ IL-10, ↓ apoptosis	Experimental (Rat model and cortical neurons)	Tu and Hu, 2021
miR-34c-5p	↓ p65, NF-kB, ↓ Nuclear Receptor Coactivator 1	Experimental (Rat model)	Tu and Hu, 2021
miR-374	↑ Wnt5a, Bcl-2, Bcl-Xl, ↓ Bax, ↓ apoptosis	Experimental (Rat model)	Xing et al., 2021
miR-374	↓ Wnt5a ↓ BAX ↑ BCL-XL and BCL-2	Experimental (rat model)	Xing et al., 2021
miR-376b-5p	↑ Wnt3a and β-catenin ↓ SOX7 ↓ BBB permeability	Experimental (Mouse model)	Zhao et al., 2021
miR-410	↓ TIMP2 ↓ ERK, ↓ p38 MAPK, ↓ JNK, ↓ p-ERK, and p-JNK ↓ MDA ↑ SOD, GSH-Px	Experimental (Mouse model and culture of hippocampal neurons)	Liu et al., 2018

(Continued)

TABLE 2 | (Continued)

miRNA	miRNA or agomiRNA effects	Study type	References
miR-424	↑ SOD, MnSOD, Nrf2 ↓ MDA, ↓ ROS ↓ apoptosis Increased antioxidant ability (SOD and Nrf2) and decreased ROS and MDA	Experimental (Mice model and primary cortical neurons)	Liu et al., 2015
miR-484	↓ BCL2L13, ↓ apoptosis	Experimental (Mouse model and murine cortical neurons)	Liu et al., 2021
miR-485	↓ AIM2, caspase 1, ↓ IL-1β, IL-18 ↓ apoptosis and pyroptosis	Experimental (Rat model and human neuroblastoma cells)	Liang et al., 2020
miR-489-3p	↓ HDAC2, ↓ apoptosis	Experimental (Rat model and PC12 cells)	Jia et al., 2022
miR-496	↓ BCL-2-like protein 14, ↓ apoptosis	Experimental (Rat model and SH-SY5Y cells)	Yao et al., 2019
miR-532-3p	↓ NOX2, caspase 3 ↓ ROS, ↓ apoptosis	Experimental (Rat model and SH-SY5Y cells)	Mao et al., 2020
miR-532-5p	↓CXCL1/CXCR2/Nf-kB, ↓ apoptosis	Experimental (Rat model and SH-SY5Y cells)	Shi et al., 2021
miR-539	↓ Matrix metallopeptidase 9 ↓ SNAI2	Clinical and Experimental (rat model + RBMVEC cell line)	Li et al., 2021a, 9
miR-652	↓ NOX2, ↓ ROS	Experimental (Rat model and SH-SY5Y cells)	Zuo et al., 2020
miR-7-5p	↓p65, TNF-α, IL-6, IL-1, ↓ROS, ↓ apoptosis	Experimental (Rat model and PC12 cells)	Xu et al., 2019
miR-7a-5p	↓ α-synuclein, ↓ apoptosis	Experimental (Rat model)	Kim et al., 2018
miR-874-3p	↓ Bcl2 Modifying Factor and BCL2 Like 13	Experimental (Rat model, SH-SY5Y cells)	Jiang et al., 2019
miR-92a	↓ NOX4	Experimental (Rat model and SH-SY5Y cells)	Hong et al., 2018
miR-92b	↓ BBB permeability ↑ claudin-5 ↑ occluding, ZO- 1 and VE- cadherin ↑ SOD ↓ ROS ↓ NOX4	Experimental (rat model and BMECs cel line)	Shen et al., 2021, 4
miR-98	↓ leukocyte infiltration and ↓ microglia activation	Experimental (Mouse model and primary BMVEC)	Bernstein et al., 2020
miR-98-5p	↓ Nrf2/ARE, ↑ Bach1, ↓ ROS, ↓ apoptosis	Experimental (murine hippocampal neuronal cells)	Sun et al., 2018b
miR-98-5p	↑ SOD, Bcl-2, HO-1 ↓ Bax2, cleaved caspase 3 ↓ROS, ↓ apoptosis	Experimental (Mouse model)	Yu et al., 2021b
miR-99a	blocks aberrant S phase re-entry, ↓ caspase-3/β-actin ↓apoptosis	Clinical and experimental (Patients, mouse model, neuro-2a cells)	Tao et al., 2015

ACSL4, acyl-CoA synthetase long chain family member 4; AIM, absent in melanoma; AIS, acute ischemic stroke; Akt, Protein kinase B; ARE, antioxidant response element; AQP, Aquaporin; BBB, blood-brain barrier; BBC3, Bcl-2-binding component 3; BDNF, Brain-derived neurotrophic factor; CCL, C-C Motif Chemokine Ligand; CXCL, C-X-C motif ligand; CXCR, C-X-C motif chemokine receptor; FIP, FAK family-interacting protein; FOXO1, Forkhead box class O1; FSTL1, follistatin-like protein 1; GPX4, glutathione peroxidase 4; GSK, glycogen synthase kinase; HDAC, histone deacetylase; HIF, hypoxia inducible factor; HO-1, heme oxygenase 1; IGFBP3, Insulin Like Growth Factor Binding Protein 3; IL, interleukin; JAK, Janus kinase; MAPK, mitogen-activated protein kinase; MCL, myeloid leukemia sequence; MDA, malondialdehyde; miR, microRNA; MnSOD, manganese superoxide dismutase; mTOR, mammalian target of rapamycin; NEAT, nuclear paraspeckle assembly transcript; NF-κB, nuclear factor kappa-light-chain-enhancer of activated B cells; NO, nitric oxide; 3-NT, 3-nitrotyrosine; NOX, nicotinamide adenine dinucleotide phosphate (NADPH) oxidase; Nrf2, nuclear factor-erythroid factor 2-related factor 2; PI3K, Phosphoinositide 3-kinase; PUMA, p53-up-regulated modulator of apoptosis; SOD, super oxide dismutase; p-STAT, phosphorylated (activated) signal transducer and activator of transcription; RBFox-1, RNA-binding protein fox-1 homolog 1; SNAI2, Snail Family Transcriptional Repressor 2; SOX7, SRY-Box Transcription Factor 7; TFR1, transferrin receptor 1; TLR4, Toll-like receptor 4; TNF, tumoral necrosis factor; TP53INP1, Tumor Protein P53 Inducible Nuclear Protein 1; VEGF, vascular-epithelial growth factor; XIAP, X chromosome-linked inhibitor of apoptosis protein; ZO, zonula occludens.

Cell Death

In I/R injuries, the first pathological event is represented by hypoxia due to ischemia. This causes cell death by mitochondrial damage and ROS formation. In the following phases, several inflammatory pathways are activated, besides the initial ROS events, all of which contribute to neuronal damage and loss of function (Jurcau and Simion, 2021).

Necrosis and Necroptosis

Necrosis is the main form of cell death present in the hypoxic regions closest to the ischemic core. It is characterized by plasma membrane permeation and cell and organelle swelling (D'Arcy, 2019). It is caused by the intense stress caused by the lack of oxygen and nutrients in the ischemic areas. Necroptosis shares similar death-pattern characteristics to necrosis, but it is controlled by death signals and therefore, it is considered a form of programmed cell death (Wu et al., 2018). Necroptosis requires the presence of death signals, such as tumoral necrosis factor (TNF) receptor and the activity of receptor-interacting protein 1 (RIP1 or RIPK1) (Festjens et al., 2007; Vandenabeele et al., 2010). In cerebral I/R injuries, inhibiting RIP1 reduces the neuronal damage (Degterev et al., 2008; Kim et al., 2017a). Several other therapeutic approaches have been tested in murine models for reducing necroptosis, however, the data regarding miRNAs is scarce (Liao et al., 2020). Among the studies miRNAs, miR-497 and miR-369 seem to have a role in necroptosis by influencing the cellular response to TNF-α (Hsu et al., 2020; Yin et al., 2022).

Apoptosis

Compared to necrosis, apoptosis is a coordinated formed of programmed cell death. It involves the activation of a complex cascade of processes and the activation of caspases, cysteine proteases with a pivotal role in this process (Elmore, 2007). In I/R injuries, it is present both in the initial hypoxic phase, as well as in the reperfusion state, but activated *via* different pathways (Wu et al., 2018). In the hypoxic phase, the intrinsic pathway plays a more important role, caused by the hypoxia-induces mitochondrial damage, which leads to the formation of apoptosomes and the activation of caspase 9, which leads to the activation of caspase 3 and the execution pathway. In the reperfusion state, the inflammatory mediators present in large amounts are responsible for the activation of the extrinsic pathway, where caspase 8 activation leads to caspase 3 activation and the execution pathway that includes DNA degradation, cytoskeletal reorganization and in the end, the formation of apoptotic bodies and cell death (Radak et al., 2017).

Apoptosis inhibition strategies were found to be effective in cerebral ischemia-reperfusion injury models, by reducing the extent of the infarct volume and improving the neurological score (Gong et al., 2017; Tang et al., 2020; Wang et al., 2021a). Biochanin A, an O-methylated isoflavone, reduced the expression of pro-apoptotic proteins Bax, Bcl-2, caspase-3 and caspase-12 in a model of middle cerebral artery occlusion and reperfusion (MCAO) (Guo et al., 2021b). Also, astragalin, another flavonoid reduced the expression of Bax and caspase-3, while upregulating the expression of Bcl-Xl (Chen et al., 2020a). Among these strategies, miRNA-based therapeutic approaches are presenting promising experimental results (Sun et al., 2018a; Liu et al., 2019b).

One of the most studied miRNAs in I/R pathologies is miR-124 (Liu et al., 2019b). In a rat model of MCAO, miR-124 presented as a promising biomarker for cerebral stroke injuries (Weng et al., 2011). Also, in patients with ischemic stroke, miR-124 as well as miR-9 were significantly elevated, supporting the idea of using miRNAs as biomarkers in I/R injuries (Ji et al., 2016). Another study in stroke patients showed the utility of miR-124-3p and miR-16 as biomarkers (Rainer et al., 2016).

In an experimental study, miR-211 downregulation increased the neurological damage and infarct volume of the mouse brain *via* a loss of Bcl-2-binding component 3 (BBC3) inhibition (Liu et al., 2020). BBC3 is also known as p53-up-regulated modulator of apoptosis and is part of the Bcl-2 protein family. Its main mechanism of action is interacting with other Bcl-2 family members proteins and promoting apoptosis (Nakano and Vousden, 2001). By upregulating miR-211, BBC3 was inhibited and the infarct size, neurological score and apoptosis were decreased. Another miRNA that acts by inhibiting BBC3 is miR-29a. In transient forebrain ischemia, miR-29a levels were decreased in the ischemic areas and its upregulation provided a protective effect in I/R injury (Ouyang et al., 2013). MiR-7-5p was upregulated in I/R injury models, degrading Sirtuin 1, a protein which alleviates I/R injuries, and therefore increasing neuronal apoptosis (Zhao and Wang, 2020; Diwan et al., 2021). In another study, miR-7-5p expression was reduced in MCAO rat models and its increase reduced the formation of ROS and inflammatory molecules and reduced the associated neuronal apoptosis (Xu et al., 2019). Similar results were found by Kim et al. in a rat model of I/R, where miR-7-5p levels were downregulated and pre-ischemic administration of miR-7 reduced I/R associated apoptosis and neuronal injury (Kim et al., 2018). The regulation of several other miRNAs has been studied in correlation with pro-apoptotic proteins or apoptosis, which are presented in **Tables 1**, **2**.

Pyroptosis

Pyroptosis is considered a gasdermin (GSDM)-mediated programmed cell death (Shi et al., 2015). Compared to apoptosis, pyroptosis includes in its characteristics inflammation, as well as pore formation and cell swelling, with loss of cell membrane integrity. It includes the activation of caspases, however, these are different than in apoptosis, pyroptosis being activated by caspases 1, 4, 5, and 11 (Yu et al., 2021a). The canonical pathway in pyroptosis is characterized by cleaved-caspase 1 inflammasome formation, GSDM cleavage and release of IL-1β and IL-18 (Nunes and de Souza, 2013). The process by which pyroptosis is activated has been reviewed in detail by Yu et al. (2021a).

In cerebral I/R injuries, pyroptosis inhibition through the NF-kB pathway reduced the infarct volume and improved the neurological recovery. Also, inhibition of inflammasome formation *via* NLRP3 and NLRP1 regulation proved successful in improving neuronal survival and diminishing the impact of I/R injuries (Chen et al., 2020a; Sun et al., 2020b; Huang et al., 2021a). In this process, several miRNAs have been profiled to be activated and possible therapeutical targets for

pyroptosis inhibition (Wang et al., 2020a). Gastrodin regulated the miR-22/NEAT1 axis and reduced the pro-inflammatory cytokines, reducing pyroptosis and attenuating the I/R injuries both *in vivo* and *in vitro* (Zhang et al., 2021a). MiR-124, which was previously discussed for apoptosis and was described as a marker of I/R injury, inhibits STAT3 expression and thereby reduces pyroptosis and improves the neurological outcome (Sun et al., 2020a). Overall, more studies are needed in order to fully elucidate how miRNAs regulation is related to pyroptosis and how these could potentially be used as therapeutic targets.

Ferroptosis

Ferroptosis is a recently described form of iron dependent cell death (Zhang et al., 2021c). Intracellular iron accumulation leads through the Fenton reaction to the formation of hydroxyl radicals that are ROS. ROS formation leads to lipid peroxidation (mainly phosphatidylethanolamine polyunsaturated fatty acids) that are destroying the lipid membranes, causing cell death. Ferroptosis is involved in several pathologies, including inflammatory pathologies, neurodegenerative diseases, cancers and I/R injuries (Liang et al., 2019; Capelletti et al., 2020; Li et al., 2020; Reichert et al., 2020; Sun et al., 2020c; Mitre et al., 2022). In mice experimental models of I/R injury, ferroptosis inhibition reduces the intestinal ischemic area and also protects the lungs and liver against ischemia-induced remote injuries (Li et al., 2019b, 2020; Qiang et al., 2020; Deng et al., 2021). In acute myocardial infarction, ferroptosis inhibition by liproxstatin-1 presented promising results by reducing the infarct size in experimental studies (Lillo-Moya et al., 2021). More studies are needed to determine the clinical efficiency of ferroptosis-inhibiting strategies in I/R injuries.

In cerebral I/R injury, tau-mediated iron accumulation can trigger ferroptosis (Tuo et al., 2017). Ferroptosis activation increases the neuronal damage and the ischemic area (Zhao et al., 2022). Inhibiting this process by enhancing the expression of GPX4, the main regulatory enzyme of ferroptosis, leads to reduced neuronal deficit after ischemia and reduced neuronal death (Guan et al., 2019, 2021). These results are similar with other experimental studies, where ferroptosis inhibition by inhibiting its various pathways improved the neurological outcome and reduced the affected area in I/R injuries (Chen et al., 2021; Guo et al., 2021a; Wang et al., 2021b; Tuo et al., 2022; Xu et al., 2022).

In patients with acute ischemic stroke, miR-214 levels were downregulated. In mice, upregulating the levels of miR-214 reduced the infarct size and improved the neurological scores (Lu et al., 2020a). In oxygen-glucose deprivation, miR-194 upregulation improved cell survival and viability, as well as reduced the expression of ACSL4, while upregulating GPX4. These results indicate that miR-194 could potentially reduce ferroptosis and thus improve neuronal survival *in vivo* (Li et al., 2021d).

Oxidative Stress Damage

The Role of Oxidative Stress in Cerebral Ischemia-Reperfusion Injury (CIRI)

In I/R injuries, the reperfusion process provides a large amount of oxygen carried by the red blood cells to the ischemic site. At the same time, the rapid alterations in oxygen flow allows the generation of ROS. Ischemia also modifies the concentration of antioxidative agents, which leads to greater damage caused by the generated ROS. In the ischemia stage, ATP production is reduced. Consecutively, the function of ion-exchange channels and enzymes is altered, leading to mitochondrial dysfunction and electrolytes imbalance. In these circumstances, the oxidative stress pathways are further activated: the NADPH oxidase (NOX) complex, the inducible nitric oxide (iNOS) complex and the xanthine oxidase complex (Wu et al., 2018).

Mitochondria is the main source for ROS synthesis due to the electron chains from the mitochondrial inner membrane, NOXs and mitochondrial redox carriers complexes I and III. In physiological states, the generation of ROS, like superoxide anion, hydrogen peroxide and hydroxide radical, is at a low level and antioxidants, like superoxide dismutase (SOD), catalases, glutathione peroxidase (GSHPx) and glutathione, control any excess of ROS (Hu et al., 2015). The excessive production or delayed elimination of ROS is often a starting point for CIRI. An excessive amount of ROS in the brain interacts with structural molecules, such as proteins, lipids, carbohydrates and nucleic acids, affecting the neuronal biochemical processes and promoting neuronal death. The main mechanisms involved in ROS toxicity are: mitochondrial membrane lipid peroxidation, cross-linking of molecules, like nucleic acids, proteins and carbohydrates that alter their function in biochemical processes, endothelial damage of the BBB and consecutively increased permeability, activation of inflammatory key factors, like cytokines and adhesion molecules, and increased synthesis of excitatory amino acids (EAA), involved in delayed neuron death (Wu et al., 2020).

Oxidative Stress

Oxidative stress is involved in DNA damage, local inflammation and endothelial dysfunction. Nuclear factor (erythroid-derived 2) -related factor 2 (Nrf2) is an antioxidant regulator activated in oxidative stress conditions that upregulate the expression of antioxidant genes, like superoxide dismutase (SOD), heme-oxygenase-1 (HO-1), NADPH- quinone oxidoreductase 1 (NQO1) and glutathione S transferase (GST) (Chen et al., 2015).

Li et al. (2019a) showed that theaflavin has an antioxidant and neuroprotective effect in a rat model of I/R injury and in neural stem cells subjected to oxygen-glucose deprivation and reoxygenation (OGD/R), increasing the expression of Nrf2 by downregulating miRNA-128-3p. The study confirmed that the miRNA-128-3p level of expression is increased in CIRI, and it is responsible for ROS generation.

Zhao et al. (2014) demonstrated that miR-23a-3p is increased in a CIRI mice model, a protective trial mechanism activated to increase the antioxidant ability of the neurons and to suppress oxidative stress. MiR-23a-3p agomir decreased the synthesis of nitric oxide (NO), 3-nitrotyrosine and hydrogen peroxide-induced lactate dehydrogenase release and increased the expression of manganese superoxide dismutase, an enzyme that protects the mitochondrial energy network from oxidative stress damage. Another similar study found out that miR-424 levels increased at 1 and 4 h and decreased at 24 h after reperfusion in an I/R mice model. MiR-424 agomir

decreased the level of excessive ROS and lipid peroxidation product malondialdehyde (MDA) generated after reperfusion and increased the expression of SOD and Nrf2. The study concluded that miR-424 activates an antioxidant mechanism in CIRI to limit further damage (Liu et al., 2015).

Huang R and the collaborators suggested that the reduced level of miR-34b expression in focal cerebral I/R is associated with oxidative stress parameters and decreased antioxidant ability. They showed that overexpression of miR-34b ameliorates CIRI through suppression of Keap1 and increase of Nrf2 and heme oxygenase (HO-1). Kelch-like ECH-associated protein 1 (Keap1)/Nrf2/ARE signaling pathway has been proved to be an important antioxidant mechanism and a potential target for miR-34b (Huang et al., 2019). Nrf2/ARE inhibition and excessive ROS production are common mechanisms that involve other miRNAs downregulation, such as miR-98-5p or miR-135b-5p (Duan et al., 2018; Sun et al., 2018b).

Wei et al. (2015) concluded that the miR-200 family increases ROS production, reduces mitochondrial membrane potential and modulates apoptosis network during CIRI, especially miR-200a-3p, miR-200b-3p and miR-429. The imbalance between ROS excessive production (MDA) and reduced antioxidant (SOD) ability causing oxidative stress damage is also determined by miR-106b-5p upregulation. MiR-106b-5p accentuates neurons death by involving the Bcl-2 family proteins, with the pro-apoptotic protein Bax and antiapoptotic protein B cell lymphoma-2 balance dysregulation (Bcl-2). Li et al. (2017a) reported that miR-106b-5p antagomir ameliorates the oxidative stress imbalance and activates antiapoptotic proteins, like Bcl-2 and myeloid cell leukemia-1 (Mcl-1). MiR-421 is also upregulated in CIRI and seems to activate the same pathological mechanisms (Yue et al., 2020). Nrf2/ARE mediated antioxidant pathways inhibition and ROS excessive production were described in a large number of studies referring to miRNAs upregulation: miR-153 (Ji et al., 2017), miR-93 (Wang et al., 2016), miR-142-5p (Wang et al., 2017) and miR-302b-3p that also targets fibroblast growth factor 15 (FGF15) (Zhang et al., 2019b).

Mitochondria Damage

Mitochondrial pathways involved in the survival of the cell are ATP production and synthesis of different molecules used in signaling networks. Mitochondria environment is also a place for miRNAs mediated posttranscriptional regulation, affecting energy metabolism, biochemical homeostasis and the activity of enzymes related to oxidative stress pathways. In CIRI, mitochondrial damage is involved in pathophysiological processes, such as ROS excessive production, reduced antioxidant activity, energy metabolism dysregulation and neuronal apoptosis (Hu et al., 2015).

To establish a possible interaction between miRNAs and mitochondrial damage, Xia et al. (2020) designed a model of OGD/R in primary cortical neuron culture. They proved that the decreased expression of miR-142-3p is involved in mitochondrial dysfunction and suggested that miR-142-3p regulates enzymes involved in mitochondrial biogenesis and function, such as electron transfer chain complexes I-III, peroxisome proliferator-activated receptor- γ coactivator-1α (PGC1α), mitochondrial transcription factor A (TFAM), and nuclear respiratory factor 1 (NRF1). Moreover, miR-142-3p overexpression improves mitochondrial function by decreasing the ROS toxic effects due to inhibition of NOX2/Rac Family Small GTPase 1 (Rac1)/ROS signaling pathway (Xia et al., 2020).

NADPH, iNOS

NADPH oxidase (NOX) is a family of 7 enzymes, NOX1 to NOX5 and dual oxidase (Duox-1 and Duox-2). NOX2 and NOX4 have been described as important enzymes that coordinate neuronal apoptosis and ROS generation in CIRI (Liang et al., 2018; Zuo et al., 2020).

Protein kinase CK2 (casein kinase 2) is a kinase that phosphorylates a large number of different substrates; therefore, it is involved in different cellular processes. It has been outlined that CK2 has a neuroprotective effect in CIRI by downregulating NADPH oxidases NOX2 and NOX4. Both *in vivo* and *in vitro* studies concluded that miR-125b is upregulated in I/R injury, while CK2α is decreased and proved that mi-R-125b binds with 3′UTR of CK2α and directly suppresses CK2 levels, resulting in NOX2 and NOX4 activation and ROS overproduction and neuronal apoptosis (Liang et al., 2018). Zuo et al. (2020) showed that miR-652 is significantly decreased, while the expression of NOX2 is increased in a CIRI rat model and in a cell hypoxia/reoxygenation (H/R) model. Overexpression of miR-652 in H/R cells reduced NOX2 expression and ROS production and ameliorated brain tissue CIRI (Zuo et al., 2020). A similar study that used both *in vitro* and *in vivo* CIRI models found out that miR-532-3p level of expression is reduced and NOX2 level is increased and suggested that miR-532-3p downregulation may be a part of CIRI through the NOX2 pathway (Mao et al., 2020).

The downregulation of several miRNAs in the ischemic brain tissue in hyperglycemic rats has been associated with NOX2 and NOX4 genes: miRNA-29a-5p, miRNA-29c-3p, miRNA-126a-5p, miRNA-132-3p, miRNA-136-3p, miRNA-138-5p, miRNA-139-5p, miRNA-153-5p, miRNA-337-3p, and miRNA-376a-5p. NOX2 was identified as the target gene of miR-126a-5p whereas NOX4 was the target gene of miR-29a-5p, miR-29c-3p and miR-132-3p (Liu et al., 2017). NOX4 was also studied as a target for miR-25, miR-92a and miR-146a. In an experimental study of CIRI, the expression levels of miR-25, miR-92a and miR-146a were decreased, but the NOX4 protein expression was increased in the interventional group. Treatment with isoflavones resulted in decreased ROS generation and neuronal cell death related to the inhibition of NOX4 *via* the induction of NOX4-related miRNAs (Hong et al., 2018).

Other Pathways

Blood Brain Barrier Disruption

Alongside with oxidative stress, apoptosis and inflammation, disruption of BBB and subsequent increased permeability of BBB, results in myelin sheath damage and brain edema, leading to neuronal dysfunction (Haley and Lawrence, 2017; Jiang et al., 2018a; Ma et al., 2020). BBB dysfunction has been ascertained in multiple brain disorders, including stroke, traumatic brain injury (TBI), MS, epilepsy, AD, amyotrophic lateral sclerosis and PD (Daneman, 2012; Kamphuis et al., 2015). The main pathways

activated upon BBB disruption consists of tight junction protein degradation, microvascular endothelial cells (ECs) damage, immune cell infiltration and activation of cytokine expression (Shen and Ma, 2020). MiRNAs have been shown to modulate BBB function under various pathological conditions, from: ischemic brain injury, TBI, spinal cord injury to neurodegenerative diseases (AD, Vascular dementia), brain tumors and cerebral infections (Ma et al., 2020).

In MCAO-induced CRTC1 knockout mice model, reduced levels of miRNA-132/212 have been correlated with aggravated BBB permeability and increased infarct volume. Moreover, miRNA-132 promotes BBB integrity expression, by binding to 3-UTR regions of the target genes of tight junction-associated protein-1 (TJAP-1), claudin-1, thus repressing junction protein's expression (Yan et al., 2021). Peripheral blood samples of 48 cerebrovascular patients revealed decreased levels of miR-539, which was related to impaired BBB. By binding to SNAI2, miR-539 has been shown to restore endothelial cell permeability by repressing MMP9 signaling pathway (Li et al., 2021a).

The expression of intercellular junctions could also be regulated by miR-27a-3p mimics *via* upregulating the protein expression of claudin-5 and occludin, thus impairing BBB permeability in CMEC/D3cells model (Harati et al., 2022). In MCAO-induced miR-182 KD (knockout) mice, the integrity of BBB was restored, with increased expression of tight junction proteins (Zhang et al., 2020b).

The cellular components of BBB have also been regulated by miRNAs upon ischemic insult. In ischemic rat brain and cultured pericytes, miR-149-5 expression was decreased. Downregulation of miR-149-5p expression enhances S1PR2 in pericytes, which was associated with decreased N-cadherin expression and increased pericyte migration, thus aggravating BBB integrity. Intracerebroventricular injection of agomir-149-5p has been shown to increase the level of N-cadherin and decrease pericyte migration, ameliorating BBB dysfunction (Wan et al., 2018).

Vascular endothelium poses important roles in BBB homeostasis and integrity (Hawkins and Davis, 2005). The integrity of BBB depends on the 'injury' status of brain microvascular endothelial cells (BMECs), suggesting that protecting BMECs represents a therapeutic strategy against ischemic stroke. CI/R injury induces autophagy in BMECs, and in turn autophagy further protects BMECs upon CI/R injury, suggesting the protective mechanism of autophagy on BMECs exposed to OGD/R injury (Li et al., 2014a). Ln RNA Malat1 promotes down-regulation of miR-26b to promote neuroprotective effects in CI/R injury by stimulating autophagy of BMECs (Li et al., 2017c).

JAK2, STAT3, MAPK Associated Pathways

Multiple studies evidenced that JAK2/STAT3 signaling pathways have been activated after ischemic stroke, posing neuropathogenic roles in I/R injury (Liang et al., 2016). Interestingly, silencing JAK2/STAT3 pathway has been associated with up-regulation expression levels of miRNAs in various pathological settings, including hepatopulmonary syndrome rat model, pancreatic cancer cells (Wang et al., 2015a; Yin et al., 2022).

In MCAO mice model and OGD-induced neuronal cells dysfunction, miR-216a was down-regulated. Overexpression of miR-216a exhibited neuroprotective effects against I/R injury by negatively regulating JAK2/STAT3 signaling pathway (Tian et al., 2018).

Mitogen-activated protein kinases pathway (MAPKs) participate in signal transduction, exerting regulatory roles on cell death and survival, being involved in different biological processes, including differentiation, cell proliferation and apoptosis (Nozaki et al., 2001; Imajo et al., 2006). Under ischemic conditions, MAPK activated inflammatory processes and promoted neuronal cell death, the expression level of MAPK being highly expressed in the cerebral macrophages from the ischemic core after stroke (Madhyastha et al., 2012; Wang et al., 2019; Xie et al., 2019; Zeng et al., 2019).

MiR-22 ameliorates the neuroinflammatory responses *in vivo* and *in vitro* animal models of I/R injury, by suppressing p38 MAPK/NF-κB pathways (Dong et al., 2019). In ischemic rat model, miR-145 exhibited low expression levels, which was associated with suppressing the MAPK pathways. Interestingly, in rat neuronal stem cells (NSCs), miR-145, p38 and ERK increased in a cultured time-dependent manner, suggesting the neuroprotective mechanisms promoted with growth of the NSCs. miR-145 promoted NSCs proliferation and inhibited apoptosis, whereas MAPK's inhibitor (SB203580) enhanced apoptosis and inhibited NSCs proliferation. After cerebral injection of NSCs in the ischemic rat cortex, the walking ability and neurological impairment of ischemic stroke rats improved over time, miR-145 playing critical roles in NSCs-promoted recovery of ischemic rat cortex, by targeting MAPK pathway (Xue et al., 2019). Moreover, miR-339 accelerated the progression of I/R injury in MCAO-rat model and PC12 cells exposed to OGD/R treatment, by stimulating proliferation and apoptosis of neuronal cells. The deleterious effects of miR-339 on neuronal injury proceed *via* inhibiting FGF9/CACNG2 axis, thus activating MAPK signaling pathway in ischemic stroke (Gao et al., 2020, 2). MiR-410 exhibited low levels in I/R mouse model and miR-410 mimic transfection reversed neuron apoptosis and enhanced hippocampal neuron survival *via* suppressing TIMP2-dependent MAPK pathway (Liu et al., 2018). Moreover, miR-410 overexpression decreased expression levels of TIMP2, p38, JNK and ERK proteins (Liu et al., 2018).

HIF

Hypoxia-inducible factor-1 (HIF-1), transcription factor, activated in response to oxygen levels fluctuations, modulates gene expression aimed at facilitating cell adaptation in hypoxic conditions (Sharp and Bernaudin, 2004; Shi, 2009). Noteworthy, hypoxic/pharmacological induction of HIF-1 *in vivo* and *in vitro* ischemic stroke models elicited neuroprotection against ischemic insult by promoting antiapoptotic mechanisms and contributing to the neuronal cell's survival (Siddiq et al., 2005; Baranova et al., 2007). However, depending on the intensity of the injurious stimulus and duration of ischemia, HIF-1 might promote both cell survival in mild hypoxic conditions or neuron apoptosis in long-term hypoxia (Helton et al., 2005; Baranova et al., 2007). Serum samples of 52 ischemic stroke patients showed a lower

miR-210 expression level, with a variable mean of miR-210 between different time points (time of admission and 3 months after stroke) and a higher HIF-1α levels, which does not change in a time-dependent manner. Increased expression levels of miR-210 and decreased HIF-1α levels exhibited a better survival rate in these patients (Rahmati et al., 2021). In OGD/R induced neuroblastoma cells microRNA-186 elicited antiapoptotic effects, by downregulating HIF-1α (Li et al., 2021b). PC12 cells exposed to OGD/R injury exhibited elevated miR-134 and HIF-1α expression levels. HIF-1α overexpression may alleviate OGD/R-induced injury, by suppressing miR-134 expression (Zhang et al., 2020a). Moreover, by inhibiting miR-134 expression, HIF-1α induces the activation of ERK1/2 and JAK1/STAT3 pathways (Zhang et al., 2020a).

Vascular Endothelial Growth Factor

Vascular endothelial growth factor (VEGF), a pro-angiogenic factor which modulates vasculogenesis and neoangiogenesis, presents essential properties in both physiological and pathological conditions, such as wound healing and repair, pregnancy, diabetic retinopathy, tumor growth and metastasis, and ischemic processes, myocardial infarction, and ischemic stroke (Melincovici et al., 2018; Shim and Madsen, 2018). VEGF regulates cerebral angiogenesis after stroke, promoting either restoration of blood supply after ischemic injury, or promoting BBB disruption by increasing vascular permeability (Zhang et al., 2017; Geiseler and Morland, 2018). The beneficial or deleterious effects promoted by VEGF depends on the level of expression of VEGF. For instance, an elevated VEGF expression leads to neurological deterioration, whereas an appropriate level of VEGF sustains the recovery process of brain in response to hypoxia (Zhang et al., 2021b).

Brain Microvascular Endothelial Cells (BMVEC) exposed to OGD elicited increased level of VEGF and reduced miR-150 expression. In OGD-induced BMVEC cells, downregulation of miR-150 and upregulated its predicted target, MYB induced VEGF expression, thus regulating cerebral angiogenesis after ischemic stroke (Zhang et al., 2021b). Serum samples from 78 diabetic and non-diabetic patients with ischemic stroke (acute ischemic stroke or transient ischemic attack) revealed a high level of miRNA-195-5p and miRNA-451a at 0, 24, and 72 hours after the stroke event, with low levels of BDNF and VEGF-A at the same time-points (Giordano et al., 2020).

Brain Derived Neurotrophic Factor

The brain derived neurotrophic factor (BDNF), crucial neurotrophic factor involved in the regulation process of synaptic transmission and brain plasticity activity, promotes neuroprotective effects in hypoxic and excitotoxic-induced neuron cell death (Degos et al., 2013; Miranda et al., 2019).

Besides transcriptional and translational regulation, BDNF expression might be regulated upon post-transcriptional level, by epigenetic mechanisms, including neuronal activity, hormones environmental factors such as exercise and stress (Metsis et al., 1993; Lubin et al., 2008; Miranda et al., 2019). The expression levels of BDNF have a high reach in hippocampus, being also detected in the cerebellum, cerebral cortex and amygdala (Hofer et al., 1990). In MCAO mice model, upregulated level of miR-191-5p was associated with disturbed angiogenesis, by inhibiting BDNF, suggesting the neuroprotective mechanisms promoted by miR-191-5p inhibition (Wu et al., 2021). In OGD-induced mouse neurons and astrocytes, inhibiting miR-128 by treatment with ARPP21 antagonistic intron exhibited up-regulation of BDNF and CREB1, therefore inhibiting apoptosis and promoting neurological recovery against ischemic stroke (Chai et al., 2021).

PI3K, AKT

Mounting evidence revealed the involvement of PI3K/Akt signaling pathway in cerebral ischemic/hypoxic injury, emerging new promising strategy for ischemic stroke (Zhang et al., 2018). By phosphorylating the inositol group in the plasma membrane phospholipids, PI3K/Akt pathway acts as a critical regulator of multifold cell processes, including cell growth, proliferation, coagulation, inflammation under different physiological and pathological settings (Fruman et al., 1998; Li et al., 2008).

Activation of the PI3K/Akt pathway by increasing miR-18b exhibited decreased apoptosis rate and reduced neuroinflammation in OGDR induced SH-SY 5Y cell dysfunction and MCAO mice model (Min et al., 2020). MiR-22 exhibited low expression level in cerebral I/R injury. Treatment with miR-22 mimic in MCAO rat model revealed increased levels of serum VEGF and Ang-1 and the levels of p-PI3K/PI3K and p-Akt/Akt proteins. Thus, miR-22 promoted angiogenic and neuroprotective effects in ischemia/reperfusion injury by activating PI3K/Akt signaling pathway (Wang et al., 2020b).

Aquaporin

Aquaporin (AQP)-4, the active regulator of water flux, poses critical role in edema formation, emerging new therapeutic targets for counteracting vascular edema in ischemic stroke (Zador et al., 2009). In this context, miR-29b, 130a and -32 were shown to repress AQP-4 (Sepramaniam et al., 2010, 2012; Wang et al., 2015b). MiR-29b overexpression promoted neuroprotection in ischemic stroke, by ameliorating BBB disruption upon ischemic stroke. Moreover, AQP-4 expression significantly decreased after miR-29b overexpression (Wang et al., 2015b, 4). Treatment of OGD-induced human astrocytoma cells injury and MCAO rat model with anti-miR-320a exhibited decreased infarct volume of cerebral ischemia, *via* upregulation of AQP1 and 4 (Sepramaniam et al., 2010).

CONCLUSION

All these mechanisms are simultaneously present during I/R injury and it is hard to separate these events from each other. MiRNAs are interlinked with oxidative stress damage, inflammatory mediators production, inflammation and cell death. As a general rule, "reversing" the expression of the miRNAs involved in cerebral I/R injuries (inhibiting an over-expressed miRNA or mimicking the effect of a down-regulated miRNA) improved the outcome and studied parameters. This holds true for the majority of studies and could mean that a miRNA-centered therapeutic approach could be beneficial.

Although experimental *in vivo* and *in vitro* models showed outcome improvements when analyzing one pathway and miRNA, it is very likely that in a clinical setting these strategies to be insufficient. It could be that by inhibiting one pathway, another one to over-express or that the benefit of such therapies to be clinically insignificant. Further research is needed to determine the exact roles of miRNAs and of miRNAs stimulation or inhibition in I/R injuries and to determine the most favorable candidates as treatment options.

AUTHOR CONTRIBUTIONS

M-AN, A-OM, C-CB, A-II, CM, MB, and C-SM were involved in the literature search and writing of the manuscript. A-OM, C-CB, and MB prepared the figure and tables. M-AN, A-OM, and A-DB performed the critical reading of the manuscript. All authors contributed to manuscript preparation and revision and reviewed the final version making the necessary changes and approved the submitted version.

REFERENCES

Andreyev, A. Y., Kushnareva, Y. E., and Starkov, A. A. (2005). Mitochondrial metabolism of reactive oxygen species. *Biochem. Biokhimiia* 70, 200–214. doi: 10.1007/s10541-005-0102-7

Angelou, C. C., Wells, A. C., Vijayaraghavan, J., Dougan, C. E., Lawlor, R., Iverson, E., et al. (2019). Differentiation of pathogenic Th17 cells is negatively regulated by let-7 micrornas in a mouse model of multiple sclerosis. *Front. Immunol.* 10:3125. doi: 10.3389/fimmu.2019.03125

Anrather, J., and Iadecola, C. (2016). Inflammation and stroke: an overview. neurother. *J. Am. Soc. Exp. Neurother.* 13, 661–670. doi: 10.1007/s13311-016-0483-x

Baird, A. E., Donnan, G. A., Austin, M. C., Fitt, G. J., Davis, S. M., and McKay, W. J. (1994). Reperfusion after thrombolytic therapy in ischemic stroke measured by single-photon emission computed tomography. *Stroke* 25, 79–85. doi: 10.1161/01.STR.25.1.79

Baranova, O., Miranda, L. F., Pichiule, P., Dragatsis, I., Johnson, R. S., and Chavez, J. C. (2007). Neuron-specific inactivation of the hypoxia inducible factor 1 alpha increases brain injury in a mouse model of transient focal cerebral ischemia. *J. Neurosci. Off. J. Soc. Neurosci.* 27, 6320–6332. doi: 10.1523/JNEUROSCI.0449-07.2007

Bartel, D. P. (2009). MicroRNAs: target recognition and regulatory functions. *Cell* 136, 215–233. doi: 10.1016/j.cell.2009.01.002

Bernstein, D. L., and Rom, S. (2020). Let-7g* and miR-98 reduce stroke-induced production of proinflammatory cytokines in mouse brain. *Front. Cell Dev. Biol.* 8:632. doi: 10.3389/fcell.2020.00632

Bernstein, D. L., Zuluaga-Ramirez, V., Gajghate, S., Reichenbach, N. L., Polyak, B., Persidsky, Y., et al. (2020). Mir-98 reduces endothelial dysfunction by protecting blood-brain barrier (BBB) and improves neurological outcomes in mouse ischemia/reperfusion stroke model. *J. Cereb. Blood Flow Metab. Off. J. Int. Soc. Cereb. Blood Flow Metab.* 40, 1953–1965. doi: 10.1177/0271678X19882264

Brieger, K., Schiavone, S., Miller, F. J., and Krause, K.-H. (2012). Reactive oxygen species: from health to disease. *Swiss Med. Wkly.* 142:w13659. doi: 10.4414/smw.2012.13659

Calin, G. A., Liu, C.-G., Sevignani, C., Ferracin, M., Felli, N., Dumitru, C. D., et al. (2004). MicroRNA profiling reveals distinct signatures in B cell chronic lymphocytic leukemias. *Proc. Natl. Acad. Sci. U. S. A.* 101, 11755–11760. doi: 10.1073/pnas.0404432101

Canazza, A., Minati, L., Boffano, C., Parati, E., and Binks, S. (2014). Experimental models of brain ischemia: a review of techniques, magnetic resonance imaging, and investigational cell-based therapies. *Front. Neurol.* 5:19. doi: 10.3389/fneur.2014.00019

Candelario-Jalil, E., Yang, Y., and Rosenberg, G. A. (2009). Diverse roles of matrix metalloproteinases and tissue inhibitors of metalloproteinases in neuroinflammation and cerebral ischemia. *Neuroscience* 158, 983–994. doi: 10.1016/j.neuroscience.2008.06.025

Cantu-Medellin, N., and Kelley, E. E. (2013). Xanthine oxidoreductase-catalyzed reactive species generation: a process in critical need of reevaluation. *Redox. Biol.* 1, 353–358. doi: 10.1016/j.redox.2013.05.002

Cao, M., Song, W., Liang, R., Teng, L., Zhang, M., Zhang, J., et al. (2021). MicroRNA as a potential biomarker and treatment strategy for ischemia-reperfusion injury. *Int. J. Genomics* 2021:e9098145. doi: 10.1155/2021/9098145

Capelletti, M. M., Manceau, H., Puy, H., and Peoc'h, K. (2020). Ferroptosis in liver diseases: an overview. *Int. J. Mol. Sci.* 21:E4908. doi: 10.3390/ijms21144908

Caseley, E. A., Poulter, J. A., Rodrigues, F., and McDermott, M. F. (2020). Inflammasome inhibition under physiological and pharmacological conditions. *Genes Immun.* 21, 211–223. doi: 10.1038/s41435-020-0104-x

Chai, Z., Gong, J., Zheng, P., and Zheng, J. (2020). Inhibition of miR-19a-3p decreases cerebral ischemia/reperfusion injury by targeting IGFBP3 *in vivo* and *in vitro*. *Biol. Res.* 53:17. doi: 10.1186/s40659-020-00280-9

Chai, Z., Zheng, P., and Zheng, J. (2021). Mechanism of ARPP21 antagonistic intron miR-128 on neurological function repair after stroke. *Ann. Clin. Transl. Neurol.* 8, 1408–1421. doi: 10.1002/acn3.51379

Chen, B., Lu, Y., Chen, Y., and Cheng, J. (2015). The role of Nrf2 in oxidative stress-induced endothelial injuries. *J. Endocrinol.* 225, R83–R99. doi: 10.1530/JOE-14-0662

Chen, W., Jiang, L., Hu, Y., Tang, N., Liang, N., Li, X.-F., et al. (2021). Ferritin reduction is essential for cerebral ischemia-induced hippocampal neuronal death through p53/SLC7A11-mediated ferroptosis. *Brain Res.* 1752:147216. doi: 10.1016/j.brainres.2020.147216

Chen, X., Cheng, C., Zuo, X., and Huang, W. (2020a). Astragalin alleviates cerebral ischemia-reperfusion injury by improving anti-oxidant and anti-inflammatory activities and inhibiting apoptosis pathway in rats. *BMC Complement. Med. Ther.* 20:120. doi: 10.1186/s12906-020-02902-x

Chen, Y.-M., He, X.-Z., Wang, S.-M., and Xia, Y. (2020b). δ-opioid receptors, microRNAs, and neuroinflammation in cerebral ischemia/hypoxia. *Front. Immunol.* 11:421. doi: 10.3389/fimmu.2020.00421

Cho, K. H. T., Xu, B., Blenkiron, C., and Fraser, M. (2019). Emerging roles of miRNAs in brain development and perinatal brain injury. *Front. Physiol.* 10:227. doi: 10.3389/fphys.2019.00227

Chua, C. E. L., and Tang, B. L. (2019). miR-34a in neurophysiology and neuropathology. *J. Mol. Neurosci. MN* 67, 235–246. doi: 10.1007/s12031-018-1231-y

Condrat, C. E., Thompson, D. C., Barbu, M. G., Bugnar, O. L., Boboc, A., Cretoiu, D., et al. (2020). miRNAs as biomarkers in disease: latest findings regarding their role in diagnosis and prognosis. *Cells* 9:276. doi: 10.3390/cells9020276

Daneman, R. (2012). The blood-brain barrier in health and disease. *Ann. Neurol.* 72, 648–672. doi: 10.1002/ana.23648

D'Arcy, M. S. (2019). Cell death: a review of the major forms of apoptosis, necrosis and autophagy. *Cell Biol. Int.* 43, 582–592. doi: 10.1002/cbin.11137

Degos, V., charpentier, T. L., Chhor, V., Brissaud, O., Lebon, S., Schwendimann, L., et al. (2013). Neuroprotective effects of dexmedetomidine against glutamate agonist-induced neuronal cell death are related to increased astrocyte brain-derived neurotrophic factor expression. *Anesthesiology* 118, 1123–1132. doi: 10.1097/ALN.0b013e318286cf36

Degterev, A., Hitomi, J., Germscheid, M., Ch'en, I. L., Korkina, O., Teng, X., et al. (2008). Identification of RIP1 kinase as a specific cellular target of necrostatins. *Nat. Chem. Biol.* 4, 313–321. doi: 10.1038/nchembio.83

Del Zoppo, G. J., Saver, J. L., Jauch, E. C., Adams, H. P., and American Heart Association Stroke Council (2009). Expansion of the time window for treatment of acute ischemic stroke with intravenous tissue plasminogen activator: a science advisory from the American Heart Association/American Stroke Association. *Stroke* 40, 2945–2948. doi: 10.1161/STROKEAHA.109.192535

Deng, F., Zhao, B.-C., Yang, X., Lin, Z.-B., Sun, Q.-S., Wang, Y.-F., et al. (2021). The gut microbiota metabolite capsiate promotes Gpx4 expression by activating TRPV1 to inhibit intestinal ischemia reperfusion-induced ferroptosis. *Gut Microbes* 13, 1–21. doi: 10.1080/19490976.2021.1902719

Deng, Y., Ma, G., Dong, Q., Sun, X., Liu, L., Miao, Z., et al. (2019). Overexpression of miR-224-3p alleviates apoptosis from cerebral ischemia reperfusion injury by targeting FIP200. *J. Cell. Biochem.* 120, 17151–17158. doi: 10.1002/jcb.28975

Di, Y., Lei, Y., Yu, F., Changfeng, F., Song, W., and Xuming, M. (2014). MicroRNAs expression and function in cerebral ischemia reperfusion injury. *J. Mol. Neurosci. MN* 53, 242–250. doi: 10.1007/s12031-014-0293-8

Dirnagl, U. (2006). Bench to bedside: the quest for quality in experimental stroke research. *J. Cereb. Blood Flow Metab. Off. J. Int. Soc. Cereb. Blood Flow Metab.* 26, 1465–1478. doi: 10.1038/sj.jcbfm.9600298

Diwan, D., Vellimana, A. K., Aum, D. J., Clarke, J., Nelson, J. W., Lawrence, M., et al. (2021). Sirtuin 1 mediates protection against delayed cerebral ischemia in subarachnoid hemorrhage in response to hypoxic postconditioning. *J. Am. Heart Assoc.* 10:e021113. doi: 10.1161/JAHA.121.021113

Dong, H., Cui, B., and Hao, X. (2019). MicroRNA-22 alleviates inflammation in ischemic stroke *via* p38 MAPK pathways. *Mol. Med. Rep.* 20, 735–744. doi: 10.3892/mmr.2019.10269

Duan, Q., Sun, W., Yuan, H., and Mu, X. (2018). MicroRNA-135b-5p prevents oxygen-glucose deprivation and reoxygenation-induced neuronal injury through regulation of the GSK-3β/Nrf2/ARE signaling pathway. *Arch. Med. Sci.* 14, 735–744. doi: 10.5114/aoms.2017.71076

Elmore, S. (2007). Apoptosis: a review of programmed cell death. *Toxicol. Pathol.* 35:495. doi: 10.1080/01926230701320337

El-Sisi, A. E.-D. E.-S., Sokar, S. S., Shebl, A. M., Mohamed, D. Z., and Abu-Risha, S. E.-S. (2021). Octreotide and melatonin alleviate inflammasome-induced pyroptosis through inhibition of TLR4-NF-κB-NLRP3 pathway in hepatic ischemia/reperfusion injury. *Toxicol. Appl. Pharmacol.* 410:115340. doi: 10.1016/j.taap.2020.115340

Eltzschig, H. K., and Eckle, T. (2011). Ischemia and reperfusion–from mechanism to translation. *Nat. Med.* 17, 1391–1401. doi: 10.1038/nm.2507

Esch, J. S. A., Jurk, K., Knoefel, W. T., Roeder, G., Voss, H., Tustas, R. Y., et al. (2010). Platelet activation and increased tissue factor expression on monocytes in reperfusion injury following orthotopic liver transplantation. *Platelets* 21, 348–359. doi: 10.3109/09537101003739897

Fang, H., Li, H.-F., He, M.-H., Yang, M., and Zhang, J.-P. (2021). HDAC3 Downregulation improves cerebral ischemic injury *via* regulation of the SDC1-Dependent JAK1/STAT3 signaling pathway through miR-19a upregulation. *Mol. Neurobiol.* 58, 3158–3174. doi: 10.1007/s12035-021-02325-w

Fang, Z., He, Q.-W., Li, Q., Chen, X.-L., Baral, S., Jin, H.-J., et al. (2016). MicroRNA-150 regulates blood-brain barrier permeability *via* Tie-2 after permanent middle cerebral artery occlusion in rats. *FASEB J. Off. Publ. Fed. Am. Soc. Exp. Biol.* 30, 2097–2107. doi: 10.1096/fj.201500126

Festjens, N., Vanden Berghe, T., Cornelis, S., and Vandenabeele, P. (2007). RIP1, a kinase on the crossroads of a cell's decision to live or die. *Cell Death Differ.* 14, 400–410. doi: 10.1038/sj.cdd.4402085

Fonarow, G. C., Zhao, X., Smith, E. E., Saver, J. L., Reeves, M. J., Bhatt, D. L., et al. (2014). Door-to-needle times for tissue plasminogen activator administration and clinical outcomes in acute ischemic stroke before and after a quality improvement initiative. *JAMA* 311, 1632–1640. doi: 10.1001/jama.2014.3203

Forstermann, U., and Munzel, T. (2006). Endothelial nitric oxide synthase in vascular disease: from marvel to menace. *Circulation* 113, 1708–1714. doi: 10.1161/CIRCULATIONAHA.105.602532

Frangogiannis, N. G. (2015). Inflammation in cardiac injury, repair and regeneration. *Curr. Opin. Cardiol.* 30, 240–245. doi: 10.1097/HCO.0000000000000158

Franke, M., Bieber, M., Kraft, P., Weber, A. N. R., Stoll, G., and Schuhmann, M. K. (2021). The NLRP3 inflammasome drives inflammation in ischemia/reperfusion injury after transient middle cerebral artery occlusion in mice. *Brain. Behav. Immun.* 92, 221–231. doi: 10.1016/j.bbi.2020.12.009

Franks, Z. G., Campbell, R. A., Weyrich, A. S., and Rondina, M. T. (2010). Platelet-leukocyte interactions link inflammatory and thromboembolic events in ischemic stroke. *Ann. N. Y. Acad. Sci.* 1207, 11–17. doi: 10.1111/j.1749-6632.2010.05733.x

Fruman, D. A., Meyers, R. E., and Cantley, L. C. (1998). Phosphoinositide kinases. *Annu. Rev. Biochem.* 67, 481–507. doi: 10.1146/annurev.biochem.67.1.481

Gao, L., Dong, Q., Song, Z., Shen, F., Shi, J., and Li, Y. (2017). NLRP3 inflammasome: a promising target in ischemic stroke. *Inflamm. Res. Off. J. Eur. Histamine Res. Soc. Al* 66, 17–24. doi: 10.1007/s00011-016-0981-7

Gao, X.-Z., Ma, R.-H., and Zhang, Z.-X. (2020). miR-339 promotes hypoxia-induced neuronal apoptosis and impairs cell viability by targeting FGF9/CACNG2 and mediating MAPK pathway in ischemic stroke. *Front. Neurol.* 11:436. doi: 10.3389/fneur.2020.00436

Gao, Y., Han, D., and Feng, J. (2021). MicroRNA in multiple sclerosis. *Clin. Chim. Acta Int. J. Clin. Chem.* 516, 92–99. doi: 10.1016/j.cca.2021.01.020

García-Culebras, A., Durán-Laforet, V., Peña-Martínez, C., Moraga, A., Ballesteros, I., Cuartero, M. I., et al. (2019). Role of TLR4 (Toll-Like Receptor 4) in N1/N2 neutrophil programming after stroke. *Stroke* 50, 2922–2932. doi: 10.1161/STROKEAHA.119.025085

Garofalo, M., Condorelli, G. L., Croce, C. M., and Condorelli, G. (2010). MicroRNAs as regulators of death receptors signaling. *Cell Death Differ.* 17, 200–208. doi: 10.1038/cdd.2009.105

Geiseler, S. J., and Morland, C. (2018). The janus face of VEGF in stroke. *Int. J. Mol. Sci.* 19:E1362. doi: 10.3390/ijms19051362

Ghafouri-Fard, S., Shoorei, H., and Taheri, M. (2020). Non-coding RNAs participate in the ischemia-reperfusion injury. *Biomed. Pharmacother. Biomedecine Pharmacother.* 129:110419. doi: 10.1016/j.biopha.2020.110419

Giordano, M., Trotta, M. C., Ciarambino, T., D'Amico, M., Galdiero, M., Schettini, F., et al. (2020). Circulating MiRNA-195-5p and -451a in diabetic patients with transient and acute ischemic stroke in the emergency department. *Int. J. Mol. Sci.* 21:E7615. doi: 10.3390/ijms21207615

Gong, L., Tang, Y., An, R., Lin, M., Chen, L., and Du, J. (2017). RTN1-C mediates cerebral ischemia/reperfusion injury *via* ER stress and mitochondria-associated apoptosis pathways. *Cell Death Dis.* 8:e3080. doi: 10.1038/cddis.2017.465

Gong, Z., Pan, J., Shen, Q., Li, M., and Peng, Y. (2018). Mitochondrial dysfunction induces NLRP3 inflammasome activation during cerebral ischemia/reperfusion injury. *J. Neuroinflammation* 15:242. doi: 10.1186/s12974-018-1282-6

Gorsuch, W. B., Chrysanthou, E., Schwaeble, W. J., and Stahl, G. L. (2012). The complement system in ischemia-reperfusion injuries. *Immunobiology* 217, 1026–1033. doi: 10.1016/j.imbio.2012.07.024

Granger, D. N., Kvietys, P. R., and Perry, M. A. (1993). Leukocyte–endothelial cell adhesion induced by ischemia and reperfusion. *Can. J. Physiol. Pharmacol.* 71, 67–75. doi: 10.1139/y93-011

Guan, X., Li, X., Yang, X., Yan, J., Shi, P., Ba, L., et al. (2019). The neuroprotective effects of carvacrol on ischemia/reperfusion-induced hippocampal neuronal impairment by ferroptosis mitigation. *Life Sci.* 235:116795. doi: 10.1016/j.lfs.2019.116795

Guan, X., Li, Z., Zhu, S., Cheng, M., Ju, Y., Ren, L., et al. (2021). Galangin attenuated cerebral ischemia-reperfusion injury by inhibition of ferroptosis through activating the SLC7A11/GPX4 axis in gerbils. *Life Sci.* 264:118660. doi: 10.1016/j.lfs.2020.118660

Guo, H., Zhu, L., Tang, P., Chen, D., Li, Y., Li, J., et al. (2021a). Carthamin yellow improves cerebral ischemia-reperfusion injury by attenuating inflammation and ferroptosis in rats. *Int. J. Mol. Med.* 47:52. doi: 10.3892/ijmm.2021.4885

Guo, M.-M., Qu, S.-B., Lu, H.-L., Wang, W.-B., He, M.-L., Su, J.-L., et al. (2021b). biochanin a alleviates cerebral ischemia/reperfusion injury by suppressing endoplasmic reticulum stress-induced apoptosis and p38MAPK signaling pathway *in vivo* and *in vitro*. *Front. Endocrinol.* 12:646720. doi: 10.3389/fendo.2021.646720

Haase, S., and Linker, R. A. (2021). Inflammation in multiple sclerosis. *Ther. Adv. Neurol. Disord.* 14:17562864211007688. doi: 10.1177/17562864211007687

Haley, M. J., and Lawrence, C. B. (2017). The blood-brain barrier after stroke: structural studies and the role of transcytotic vesicles. *J. Cereb. Blood Flow Metab. Off. J. Int. Soc. Cereb. Blood Flow Metab.* 37, 456–470. doi: 10.1177/0271678X16629976

Hao, T., Yang, Y., Li, N., Mi, Y., Zhang, G., Song, J., et al. (2020). Inflammatory mechanism of cerebral ischemia-reperfusion injury with treatment of stepharine in rats. *Phytomedicine* 79:153353. doi: 10.1016/j.phymed.2020.153353

Harati, R., Hammad, S., Tlili, A., Mahfood, M., Mabondzo, A., and Hamoudi, R. (2022). miR-27a-3p regulates expression of intercellular junctions at the brain endothelium and controls the endothelial barrier permeability. *PLoS ONE* 17:e0262152. doi: 10.1371/journal.pone.0262152

Hawkins, B. T., and Davis, T. P. (2005). The blood-brain barrier/neurovascular unit in health and disease. *Pharmacol. Rev.* 57, 173–185. doi: 10.1124/pr.57.2.4

He, W., Zhang, Z., and Sha, X. (2021). Nanoparticles-mediated emerging approaches for effective treatment of ischemic stroke. *Biomaterials* 277:121111. doi: 10.1016/j.biomaterials.2021.121111

Helton, R., Cui, J., Scheel, J. R., Ellison, J. A., Ames, C., Gibson, C., et al. (2005). Brain-specific knock-out of hypoxia-inducible factor-1alpha reduces rather than increases hypoxic-ischemic damage. *J. Neurosci. Off. J. Soc. Neurosci.* 25, 4099–4107. doi: 10.1523/JNEUROSCI.4555-04.2005

Hong, H.-Y., Choi, J. S., Kim, Y. J., Lee, H. Y., Kwak, W., Yoo, J., et al. (2008). Detection of apoptosis in a rat model of focal cerebral ischemia using a homing peptide selected from *in vivo* phage display. *J. Control. Release Off. J. Control. Release Soc.* 131, 167–172. doi: 10.1016/j.jconrel.2008.07.020

Hong, P., Gu, R.-N., Li, F.-X., Xiong, X.-X., Liang, W.-B., You, Z.-J., et al. (2019). NLRP3 inflammasome as a potential treatment in ischemic stroke concomitant with diabetes. *J. Neuroinflammation* 16:121. doi: 10.1186/s12974-019-1498-0

Hong, S., Kwon, J., Hiep, N. T., Sim, S. J., Kim, N., Kim, K. H., et al. (2018). The isoflavones and extracts from maclura tricuspidata fruit protect against neuronal cell death in ischemic injury *via* induction of Nox4-targeting miRNA-25, miRNA-92a, and miRNA-146a. *J. Funct. Foods* 40, 785–797. doi: 10.1016/j.jff.2017.12.011

Hoss, A. G., Labadorf, A., Beach, T. G., Latourelle, J. C., and Myers, R. H. (2016). microRNA profiles in parkinson's disease prefrontal cortex. *Front. Aging Neurosci.* 8:36. doi: 10.3389/fnagi.2016.00036

Hou, Y., Wang, Y., He, Q., Li, L., Xie, H., Zhao, Y., et al. (2018). Nrf2 inhibits NLRP3 inflammasome activation through regulating Trx1/TXNIP complex in cerebral ischemia reperfusion injury. *Behav. Brain Res.* 336, 32–39. doi: 10.1016/j.bbr.2017.06.027

Hsu, C.-C., Huang, C.-C., Chien, L.-H., Lin, M.-T., Chang, C.-P., Lin, H.-J., et al. (2020). Ischemia/reperfusion injured intestinal epithelial cells cause cortical neuron death by releasing exosomal microRNAs associated with apoptosis, necroptosis, and pyroptosis. *Sci. Rep.* 10:14409. doi: 10.1038/s41598-020-71310-5

Hu, Y., Deng, H., Xu, S., and Zhang, J. (2015). MicroRNAs regulate mitochondrial function in cerebral ischemia-reperfusion injury. *Int. J. Mol. Sci.* 16, 24895–24917. doi: 10.3390/ijms161024895

Hu, Y.-K., Wang, X., Li, L., Du, Y.-H., Ye, H.-T., and Li, C.-Y. (2013). MicroRNA-98 induces an Alzheimer's disease-like disturbance by targeting insulin-like growth factor 1. *Neurosci. Bull.* 29, 745–751. doi: 10.1007/s12264-013-1348-5

Huang, L., Li, X., Liu, Y., Liang, X., Ye, H., Yang, C., et al. (2021a). Curcumin alleviates cerebral ischemia-reperfusion injury by inhibiting NLRP1-dependent neuronal pyroptosis. *Curr. Neurovasc. Res.* 18, 189–196. doi: 10.2174/1567202618666210607150140

Huang, R., Ma, J., Niu, B., Li, J., Chang, J., Zhang, Y., et al. (2019). MiR-34b protects against focal cerebral ischemia-reperfusion (I/R) injury in rat by targeting keap1. *J. Stroke Cerebrovasc. Dis.* 28, 1–9. doi: 10.1016/j.jstrokecerebrovasdis.2018.08.023

Huang, Y., Wang, Y., Duan, Z., Liang, J., Xu, Y., Zhang, S., et al. (2021b). Restored microRNA-326-5p Inhibits neuronal apoptosis and attenuates mitochondrial damage *via* suppressing STAT3 in cerebral ischemia/reperfusion injury. *Nanoscale Res. Lett.* 16:63. doi: 10.1186/s11671-021-03520-3

Huang, Z., Lu, L., Jiang, T., Zhang, S., Shen, Y., Zheng, Z., et al. (2018). miR-29b affects neurocyte apoptosis by targeting MCL-1 during cerebral ischemia/reperfusion injury. *Exp. Ther. Med.* 16, 3399–3404. doi: 10.3892/etm.2018.6622

Imajo, M., Tsuchiya, Y., and Nishida, E. (2006). Regulatory mechanisms and functions of MAP kinase signaling pathways. *IUBMB Life* 58, 312–317. doi: 10.1080/15216540600746393

Islam, A., Choudhury, M. E., Kigami, Y., Utsunomiya, R., Matsumoto, S., Watanabe, H., et al. (2018). Sustained anti-inflammatory effects of TGF-β1 on microglia/macrophages. *Biochim. Biophys. Acta BBA - Mol. Basis Dis.* 1864, 721–734. doi: 10.1016/j.bbadis.2017.12.022

IST-3 collaborative group, Sandercock, P., Wardlaw, J. M., Lindley, R. I, Dennis, M., Cohen, G., et al. (2012). The benefits and harms of intravenous thrombolysis with recombinant tissue plasminogen activator within 6 h of acute ischaemic stroke (the third international stroke trial [IST-3]): a randomised controlled trial. *Lancet Lond. Engl.* 379, 2352–2363. doi: 10.1016/S0140-6736(12)60768-5

Jeyaseelan, K., Lim, K. Y., and Armugam, A. (2008). MicroRNA expression in the blood and brain of rats subjected to transient focal ischemia by middle cerebral artery occlusion. *Stroke* 39, 959–966. doi: 10.1161/STROKEAHA.107.500736

Ji, Q., Gao, J., Zheng, Y., Liu, X., Zhou, Q., Shi, C., et al. (2017). Inhibition of microRNA-153 protects neurons against ischemia/reperfusion injury in an oxygen–glucose deprivation and reoxygenation cellular model by regulating Nrf2/HO-1 signaling. *J. Biochem. Mol. Toxicol.* 31, 1–8. doi: 10.1002/jbt.21905

Ji, Q., Ji, Y., Peng, J., Zhou, X., Chen, X., Zhao, H., et al. (2016). Increased brain-specific MiR-9 and MiR-124 in the serum exosomes of acute ischemic stroke patients. *PLoS ONE* 11:e0163645. doi: 10.1371/journal.pone.0163645

Jia, T., Wang, M., Yan, W., Wu, W., and Shen, R. (2022). Upregulation of miR-489-3p attenuates cerebral ischemia/reperfusion injury by targeting histone deacetylase 2 (HDAC2). *Neuroscience* 484, 16–25. doi: 10.1016/j.neuroscience.2021.12.009

Jiang, D., Sun, X., Wang, S., and Man, H. (2019). Upregulation of miR-874-3p decreases cerebral ischemia/reperfusion injury by directly targeting BMF and BCL2L13. *Biomed. Pharmacother.* 117:108941. doi: 10.1016/j.biopha.2019.108941

Jiang, X., Andjelkovic, A. V., Zhu, L., Yang, T., Bennett, M. V. L., Chen, J., et al. (2018a). Blood-brain barrier dysfunction and recovery after ischemic stroke. *Prog. Neurobiol.* 163–164, 144–171. doi: 10.1016/j.pneurobio.2017.10.001

Jiang, Y., Xu, B., Chen, J., Sui, Y., Ren, L., Li, J., et al. (2018b). Micro-RNA-137 inhibits tau hyperphosphorylation in alzheimer's disease and targets the CACNA1C gene in transgenic mice and human neuroblastoma SH-SY5Y cells. *Med. Sci. Monit. Int. Med. J. Exp. Clin. Res.* 24:5635. doi: 10.12659/MSM.908765

Jonas, S., and Izaurralde, E. (2015). Towards a molecular understanding of microRNA-mediated gene silencing. *Nat. Rev. Genet.* 16, 421–433. doi: 10.1038/nrg3965

Jurcau, A., and Simion, A. (2021). Neuroinflammation in cerebral ischemia and ischemia/reperfusion injuries: from pathophysiology to therapeutic strategies. *Int. J. Mol. Sci.* 23:14. doi: 10.3390/ijms23010014

Juźwik, C. A., Drake, S., Zhang, Y., Paradis-Isler, N., Sylvester, A., Amar-Zifkin, A., et al. (2019). microRNA dysregulation in neurodegenerative diseases: a systematic review. *Prog. Neurobiol.* 182:101664. doi: 10.1016/j.pneurobio.2019.101664

Kadir, R. R. A., Alwjwaj, M., and Bayraktutan, U. (2020). MicroRNA: an emerging predictive, diagnostic, prognostic and therapeutic strategy in ischaemic stroke. *Cell. Mol. Neurobiol.* 42, 1301–1319. doi: 10.1007/s10571-020-01028-5

Kamphuis, W. W., Derada Troletti, C., Reijerkerk, A., Romero, I. A., and de Vries, H. E. (2015). The blood-brain barrier in multiple sclerosis: microRNAs as key regulators. *CNS Neurol. Disord. Drug Targets* 14, 157–167. doi: 10.2174/1871527314666150116125246

Kawabori, M., and Yenari, M. A. (2015). Inflammatory responses in brain ischemia. *Curr. Med. Chem.* 22:1258.

Khoshnam, S. E., Winlow, W., and Farzaneh, M. (2017). The interplay of micrornas in the inflammatory mechanisms following ischemic stroke. *J. Neuropathol. Exp. Neurol.* 76, 548–561. doi: 10.1093/jnen/nlx036

Kim, C. R., Kim, J. H., Park, H.-Y. L., and Park, C. K. (2017a). Ischemia reperfusion injury triggers TNFα induced-necroptosis in rat retina. *Curr. Eye Res.* 42, 771–779. doi: 10.1080/02713683.2016.1227449

Kim, J. Y., Park, J., Lee, J. E., and Yenari, M. A. (2017b). NOX inhibitors - a promising avenue for ischemic stroke. *Exp. Neurobiol.* 26, 195–205. doi: 10.5607/en.2017.26.4.195

Kim, T., Mehta, S. L., Morris-Blanco, K. C., Chokkalla, A. K., Chelluboina, B., Lopez, M., et al. (2018). The microRNA miR-7a-5p ameliorates ischemic brain damage by repressing α-synuclein. *Sci. Signal.* 11:eaat4285. doi: 10.1126/scisignal.aat4285

Lallukka, T., Ervasti, J., Lundström, E., Mittendorfer-Rutz, E., Friberg, E., Virtanen, M., et al. (2018). Trends in diagnosis-specific work disability before and after stroke: a longitudinal population-based study in Sweden. *J. Am. Heart Assoc.* 7:e006991. doi: 10.1161/JAHA.117.006991

Li, H., Gao, A., Feng, D., Wang, Y., Zhang, L., Cui, Y., et al. (2014a). Evaluation of the protective potential of brain microvascular endothelial cell autophagy on blood-brain barrier integrity during experimental cerebral ischemia-reperfusion injury. *Transl. Stroke Res.* 5, 618–626. doi: 10.1007/s12975-014-0354-x

Li, H., Han, G., He, D., Wang, Y., Lin, Y., Zhang, T., et al. (2021a). miR-539 targeting SNAI2 regulates MMP9 signaling pathway and affects blood-brain barrier permeability in cerebrovascular occlusive diseases: a study based on head and neck ultrasound and CTA. *J. Healthc. Eng.* 2021:5699025. doi: 10.1155/2021/5699025

Li, H., Zhang, N., Lin, H.-Y., Yu, Y., Cai, Q.-Y., Ma, L., et al. (2014b). Histological, cellular and behavioral assessments of stroke outcomes after photothrombosis-induced ischemia in adult mice. *BMC Neurosci.* 15:58. doi: 10.1186/1471-2202-15-58

Li, L., Qu, Y., Mao, M., Xiong, Y., and Mu, D. (2008). The involvement of phosphoinositid 3-kinase/Akt pathway in the activation of hypoxia-inducible factor-1alpha in the developing rat brain after hypoxia-ischemia. *Brain Res.* 1197, 152–158. doi: 10.1016/j.brainres.2007.12.059

Li, P., Shen, M., Gao, F., Wu, J., Zhang, J., Teng, F., et al. (2017a). An antagomir to MicroRNA-106b-5p ameliorates cerebral ischemia and reperfusion injury in rats *via* inhibiting apoptosis and oxidative stress. *Mol. Neurobiol.* 54, 2901–2921. doi: 10.1007/s12035-016-9842-1

Li, R., Li, X., Wu, H., Yang, Z., Li, F. E. I., and Jianhong, Z. H. U. (2019a). Theaflavin attenuates cerebral ischemia/reperfusion injury by abolishing miRNA-128-3p-mediated Nrf2 inhibition and reducing oxidative stress. *Mol. Med. Rep.* 20, 4893–9404. doi: 10.3892/mmr.2019.10755

Li, S., Wang, Y., Wang, M., Chen, L., Chen, S., Deng, F., et al. (2021b). microRNA-186 alleviates oxygen-glucose deprivation/reoxygenation-induced injury by directly targeting hypoxia-inducible factor-1α. *J. Biochem. Mol. Toxicol.* 35, 1–11. doi: 10.1002/jbt.22752

Li, W., Zhu, Q., Xu, X., and Hu, X. (2021c). MiR-27a-3p suppresses cerebral ischemia-reperfusion injury by targeting FOXO1. *Aging* 13, 11727–11737. doi: 10.18632/aging.202866

Li, X., Su, L., Zhang, X., Zhang, C., Wang, L., Li, Y., et al. (2017b). Ulinastatin downregulates TLR4 and NF-kB expression and protects mouse brains against ischemia/reperfusion injury. *Neurol. Res.* 39, 367–373. doi: 10.1080/01616412.2017.1286541

Li, X., Zhang, X., Liu, Y., Pan, R., Liang, X., Huang, L., et al. (2021d). Exosomes derived from mesenchyml stem cells ameliorate oxygen-glucose deprivation/reoxygenation-induced neuronal injury *via* transferring MicroRNA-194 and targeting Bach1. *Tissue Cell* 73:101651. doi: 10.1016/j.tice.2021.101651

Li, Y., Cao, Y., Xiao, J., Shang, J., Tan, Q., Ping, F., et al. (2020). Inhibitor of apoptosis-stimulating protein of p53 inhibits ferroptosis and alleviates intestinal ischemia/reperfusion-induced acute lung injury. *Cell Death Differ.* 27, 2635–2650. doi: 10.1038/s41418-020-0528-x

Li, Y., Feng, D., Wang, Z., Zhao, Y., Sun, R., Tian, D., et al. (2019b). Ischemia-induced ACSL4 activation contributes to ferroptosis-mediated tissue injury in intestinal ischemia/reperfusion. *Cell Death Differ.* 26, 2284–2299. doi: 10.1038/s41418-019-0299-4

Li, Z., Li, J., and Tang, N. (2017c). Long noncoding RNA Malat1 is a potent autophagy inducer protecting brain microvascular endothelial cells against oxygen-glucose deprivation/reoxygenation-induced injury by sponging miR-26b and upregulating ULK2 expression. *Neuroscience* 354, 1–10. doi: 10.1016/j.neuroscience.2017.04.017

Liang, C., Zhang, X., Yang, M., and Dong, X. (2019). Recent progress in ferroptosis inducers for cancer therapy. *Adv. Mater. Deerfield Beach Fla* 31:e1904197. doi: 10.1002/adma.201904197

Liang, J., Wang, Q., Li, J.-Q., Guo, T., and Yu, D. (2020). Long non-coding RNA MEG3 promotes cerebral ischemia-reperfusion injury through increasing pyroptosis by targeting miR-485/AIM2 axis. *Exp. Neurol.* 325:113139. doi: 10.1016/j.expneurol.2019.113139

Liang, Y., Xu, J., Wang, Y., Tang, J. Y., Yang, S. L., Xiang, H. G., et al. (2018). Inhibition of MiRNA-125b decreases cerebral ischemia/reperfusion injury by targeting CK2α/NADPH oxidase signaling. *Cell. Physiol. Biochem.* 45, 1818–1826. doi: 10.1159/000487873

Liao, S., Apaijai, N., Chattipakorn, N., and Chattipakorn, S. C. (2020). The possible roles of necroptosis during cerebral ischemia and ischemia / reperfusion injury. *Arch. Biochem. Biophys.* 695:108629. doi: 10.1016/j.abb.2020.108629

Lillo-Moya, J., Rojas-Solé, C., Muñoz-Salamanca, D., Panieri, E., Saso, L., and Rodrigo, R. (2021). Targeting ferroptosis against ischemia/reperfusion cardiac injury. *Antioxidants* 10:667. doi: 10.3390/antiox10050667

Lin, L., Wang, X., and Yu, Z. (2016). Ischemia-reperfusion injury in the brain: mechanisms and potential therapeutic strategies. *Biochem. Pharmacol. Open Access* 5:213. doi: 10.4172/2167-0501.1000213

Lisa, F. D., and Bernardi, P. (2006). Mitochondria and ischemia-reperfusion injury of the heart: fixing a hole. *Cardiovasc. Res.* 70, 191–199. doi: 10.1016/j.cardiores.2006.01.016

Liu, N.-N., Dong, Z.-L., and Han, L.-L. (2018). MicroRNA-410 inhibition of the TIMP2-dependent MAPK pathway confers neuroprotection against oxidative stress-induced apoptosis after ischemic stroke in mice. *Brain Res. Bull.* 143, 45–57. doi: 10.1016/j.brainresbull.2018.09.009

Liu, P., Zhao, H., Wang, R., Wang, P., Tao, Z., Gao, L., et al. (2015). MicroRNA-424 protects against focal cerebral ischemia and reperfusion injury in mice by suppressing oxidative stress. *Stroke* 46, 513–519. doi: 10.1161/STROKEAHA.114.007482

Liu, Q., Radwanski, R., Babadjouni, R., Patel, A., Hodis, D. M., Baumbacher, P., et al. (2019a). Experimental chronic cerebral hypoperfusion results in decreased pericyte coverage and increased blood-brain barrier permeability in the corpus callosum. *J. Cereb. Blood Flow Metab. Off. J. Int. Soc. Cereb. Blood Flow Metab.* 39, 240–250. doi: 10.1177/0271678X17743670

Liu, W., Miao, Y., Zhang, L., Xu, X., and Luan, Q. (2020). MiR-211 protects cerebral ischemia/reperfusion injury by inhibiting cell apoptosis. *Bioengineered* 11:189. doi: 10.1080/21655979.2020.1729322

Liu, X., Feng, Z., Du, L., Huang, Y., Ge, J., Deng, Y., et al. (2019b). The potential role of MicroRNA-124 in cerebral ischemia injury. *Int. J. Mol. Sci.* 21:E120. doi: 10.3390/ijms21010120

Liu, X., Wang, X., Zhang, L., Zhou, Y., Yang, L., and Yang, M. (2021). By targeting apoptosis facilitator BCL2L13, microRNA miR-484 alleviates cerebral ischemia/reperfusion injury-induced neuronal apoptosis in mice. *Bioengineered* 12, 948–959. doi: 10.1080/21655979.2021.1898134

Liu, Z., Tuo, Y. H., Chen, J. W., Wang, Q. Y., Li, S., Li, M. C., et al. (2017). NADPH oxidase inhibitor regulates microRNAs with improved outcome after mechanical reperfusion. *J. NeuroInterventional Surg.* 9, 702–706. doi: 10.1136/neurintsurg-2016-012463

Lu, J., Xu, F., and Lu, H. (2020a). LncRNA PVT1 regulates ferroptosis through miR-214-mediated TFR1 and p53. *Life Sci.* 260:118305. doi: 10.1016/j.lfs.2020.118305

Lu, M.-Y., Wu, J.-R., Liang, R.-B., Wang, Y.-P., Zhu, Y.-C., Ma, Z.-T., et al. (2020b). Upregulation of miR-219a-5p decreases cerebral ischemia/reperfusion injury *in vitro* by targeting Pde4d. *J. Stroke Cerebrovasc. Dis.* 29:104801. doi: 10.1016/j.jstrokecerebrovasdis.2020.104801

Lubin, F. D., Roth, T. L., and Sweatt, J. D. (2008). Epigenetic regulation of bdnf gene transcription in the consolidation of fear memory. *J. Neurosci.* 28, 10576–10586. doi: 10.1523/JNEUROSCI.1786-08.2008

Luo, Y., Tang, H., Li, H., Zhao, R., Huang, Q., and Liu, J. (2019). Recent advances in the development of neuroprotective agents and therapeutic targets in the treatment of cerebral ischemia. *Eur. J. Med. Chem.* 162, 132–146. doi: 10.1016/j.ejmech.2018.11.014

Ma, F., Zhang, X., and Yin, K.-J. (2020). MicroRNAs in central nervous system diseases: a prospective role in regulating blood-brain barrier integrity. *Exp. Neurol.* 323:113094. doi: 10.1016/j.expneurol.2019.113094

Ma, J., Shui, S., Han, X., Guo, D., Li, T., and Yan, L. (2017a). microRNA-200a silencing protects neural stem cells against cerebral ischemia/reperfusion injury. *PLoS One* 12:e0172178. doi: 10.1371/journal.pone.0172178

Ma, M. W., Wang, J., Zhang, Q., Wang, R., Dhandapani, K. M., Vadlamudi, R. K., et al. (2017b). NADPH oxidase in brain injury and neurodegenerative disorders. *Mol. Neurodegener.* 12:7. doi: 10.1186/s13024-017-0150-7

MacFarlane, L.-A., and Murphy, P. R. (2010). MicroRNA: biogenesis. *Funct. Role Cancer. Curr. Genomics* 11, 537–561. doi: 10.2174/138920210793175895

Madhyastha, R., Madhyastha, H., Nakajima, Y., Omura, S., and Maruyama, M. (2012). MicroRNA signature in diabetic wound healing: promotive role of miR-21 in fibroblast migration. *Int. Wound J.* 9, 355–361. doi: 10.1111/j.1742-481X.2011.00890.x

Magaki, S. D., Williams, C. K., and Vinters, H. V. (2018). Glial function (and dysfunction) in the normal & ischemic brain. *Neuropharmacology* 134, 218–225. doi: 10.1016/j.neuropharm.2017.11.009

Mao, L., Zuo, M. L., Wang, A. P., Tian, Y., Dong, L. C., Li, T. M., et al. (2020). Low expression of miR-532-3p contributes to cerebral ischemia/reperfusion oxidative stress injury by directly targeting NOX2. *Mol. Med. Rep.* 22, 2415–2423. doi: 10.3892/mmr.2020.11325

Mărgăritescu, O., Mogoantă, L., Pirici, I., Pirici, D., Cernea, D., and Mărgăritescu, C. (2009). Histopathological changes in acute ischemic stroke. *Romanian J. Morphol. Embryol. Rev. Roum. Morphol. Embryol.* 50, 327–339.

Melincovici, C. S., Boşca, A. B., Şuşman, S., Mărginean, M., Mihu, C., Istrate, M., et al. (2018). Vascular endothelial growth factor (VEGF) - key factor in

normal and pathological angiogenesis. *Romanian J. Morphol. Embryol. Rev. Roum. Morphol. Embryol.* 59, 455–467.

Metsis, M., Timmusk, T., Arenas, E., and Persson, H. (1993). Differential usage of multiple brain-derived neurotrophic factor promoters in the rat brain following neuronal activation. *Proc. Natl. Acad. Sci. U.S.A* 90, 8802–8806. doi: 10.1073/pnas.90.19.8802

Meza, C. A., La Favor, J. D., Kim, D.-H., and Hickner, R. C. (2019). Endothelial dysfunction: is there a hyperglycemia-induced imbalance of NOX and NOS? *Int. J. Mol. Sci.* 20:E3775. doi: 10.3390/ijms20153775

Min, X., Wang, T., Cao, Y., Liu, J., Li, J., and Wang, T. (2015). MicroRNAs: a novel promising therapeutic target for cerebral ischemia/reperfusion injury? *Neural Regen. Res.* 10, 1799–1808. doi: 10.4103/1673-5374.170302

Min, X.-L., He, M., Shi, Y., Xie, L., Ma, X.-J., and Cao, Y. (2020). miR-18b attenuates cerebral ischemia/reperfusion injury through regulation of ANXA3 and PI3K/Akt signaling pathway. *Brain Res. Bull.* 161, 55–64. doi: 10.1016/j.brainresbull.2020.04.021

Yin, K. J., Deng, Z., Huang, H., Hamblin, M., Xie, C., Zhang, J., et al. (2022). miR-497 regulates neuronal death in mouse brain after transient focal cerebral ischemia. *Neurobiol. Dis.* 38, 17–26. doi: 10.1016/j.nbd.2009.12.021

Miranda, M., Morici, J. F., Zanoni, M. B., and Bekinschtein, P. (2019). Brain-derived neurotrophic factor: a key molecule for memory in the healthy and the pathological brain. *Front. Cell. Neurosci.* 13:363. doi: 10.3389/fncel.2019.00363

Mitre, A.-O., Florian, A. I., Buruiana, A., Boer, A., Moldovan, I., Soritau, O., et al. (2022). Ferroptosis involvement in glioblastoma treatment. *Medicina* 58:319. doi: 10.3390/medicina58020319

Moskowitz, M. A., Lo, E. H., and Iadecola, C. (2010). The science of stroke: mechanisms in search of treatments. *Neuron* 67, 181–198. doi: 10.1016/j.neuron.2010.07.002

Nakano, K., and Vousden, K. H. (2001). PUMA, a novel proapoptotic gene, is induced by p53. *Mol. Cell* 7, 683–694. doi: 10.1016/S1097-2765(01)00214-3

Nies, Y. H., Mohamad Najib, N. H., Lim, W. L., Kamaruzzaman, M. A., Yahaya, M. F., and Teoh, S. L. (2021). MicroRNA dysregulation in parkinson's disease: a narrative review. *Front. Neurosci.* 15:660379. doi: 10.3389/fnins.2021.660379

Nourshargh, S., and Alon, R. (2014). Leukocyte migration into inflamed tissues. *Immunity* 41, 694–707. doi: 10.1016/j.immuni.2014.10.008

Nozaki, K., Nishimura, M., and Hashimoto, N. (2001). Mitogen-activated protein kinases and cerebral ischemia. *Mol. Neurobiol* 23, 1–19. doi: 10.1385/MN:23:1:01

Nunes, T., and de Souza, H. S. (2013). Inflammasome in intestinal inflammation and cancer. *Mediators Inflamm.* 2013:654963. doi: 10.1155/2013/654963

Nuzziello, N., Vilardo, L., Pelucchi, P., Consiglio, A., Liuni, S., Trojano, M., et al. (2018). Investigating the role of MicroRNA and transcription factor co-regulatory networks in multiple sclerosis pathogenesis. *Int. J. Mol. Sci.* 19:3652. doi: 10.3390/ijms19113652

Ouyang, Y.-B., Stary, C. M., White, R. E., and Giffard, R. G. (2015). The use of microRNAs to modulate redox and immune response to stroke. *Antioxid. Redox Signal.* 22, 187–202. doi: 10.1089/ars.2013.5757

Ouyang, Y.-B., Xu, L., Lu, Y., Sun, X., Yue, S., Xiong, X.-X., et al. (2013). Astrocyte-enriched miR-29a targets PUMA and reduces neuronal vulnerability to forebrain ischemia. *Glia* 61, 1784–1794. doi: 10.1002/glia.22556

Peng, L., Yin, J., Wang, S., Ge, M., Han, Z., Wang, Y., et al. (2019). TGF-β2/Smad3 signaling pathway activation through enhancing VEGF and CD34 Ameliorates cerebral ischemia/reperfusion injury after isoflurane post-conditioning in rats. *Neurochem. Res.* 44, 2606–2618. doi: 10.1007/s11064-019-02880-8

Petrescu, G. E. D., Sabo, A. A., Torsin, L. I., Calin, G. A., and Dragomir, M. P. (2019). MicroRNA based theranostics for brain cancer: basic principles. *J. Exp. Clin. Cancer Res. CR* 38:231. doi: 10.1186/s13046-019-1180-5

Ponnusamy, V., and Yip, P. K. (2019). The role of microRNAs in newborn brain development and hypoxic ischaemic encephalopathy. *Neuropharmacology* 149, 55–65. doi: 10.1016/j.neuropharm.2018.11.041

Qiang, Z., Dong, H., Xia, Y., Chai, D., Hu, R., and Jiang, H. (2020). Nrf2 and STAT3 alleviates ferroptosis-mediated IIR-ALI by regulating SLC7A11. *Oxid. Med. Cell. Longev.* 2020:5146982. doi: 10.1155/2020/5146982

Quinlan, S., Kenny, A., Medina, M., Engel, T., and Jimenez-Mateos, E. M. (2017). MicroRNAs in neurodegenerative diseases. *Int. Rev. Cell Mol. Biol.* 334, 309–343. doi: 10.1016/bs.ircmb.2017.04.002

Radak, D., Katsiki, N., Resanovic, I., Jovanovic, A., Sudar-Milovanovic, E., Zafirovic, S., et al. (2017). Apoptosis and acute brain ischemia in ischemic stroke. *Curr. Vasc. Pharmacol.* 15, 115–122. doi: 10.2174/1570161115666161104095522

Rahaman, P., and Del Bigio, M. R. (2018). Histology of brain trauma and hypoxia-ischemia. *Acad. Forensic Pathol.* 8, 539–554. doi: 10.1177/1925362118797728

Rahmati, M., Ferns, G. A., and Mobarra, N. (2021). The lower expression of circulating miR-210 and elevated serum levels of HIF-1α in ischemic stroke; possible markers for diagnosis and disease prediction. *J. Clin. Lab. Anal.* 35:e24073. doi: 10.1002/jcla.24073

Rainer, T. H., Leung, L. Y., Chan, C. P. Y., Leung, Y. K., Abrigo, J. M., Wang, D., et al. (2016). Plasma miR-124-3p and miR-16 concentrations as prognostic markers in acute stroke. *Clin. Biochem.* 49, 663–668. doi: 10.1016/j.clinbiochem.2016.02.016

Hofer, M., Pagliusi, S. R., Hohn, A., Leibrock, J., and Barde, Y. A. (1990). Regional distribution of brain-derived neurotrophic factor mRNA in the adult mouse brain. *EMBO J.* 9, 2459–2464. doi: 10.1002/j.1460-2075.1990.tb07423.x

Reichert, C. O., de Freitas, F. A., Sampaio-Silva, J., Rokita-Rosa, L., Barros, P., de, L., et al. (2020). Ferroptosis mechanisms involved in neurodegenerative diseases. *Int. J. Mol. Sci.* 21:E8765. doi: 10.3390/ijms21228765

Ren, Z., Xie, P., Lv, J., Hu, Y., Guan, Z., Chen, L., et al. (2020). miR-187-3p inhibitor attenuates cerebral ischemia/reperfusion injury by regulating Seipin-mediated autophagic flux. *Int. J. Mol. Med.* 46, 1051–1062. doi: 10.3892/ijmm.2020.4642

Rink, C., and Khanna, S. (2011). MicroRNA in ischemic stroke etiology and pathology. *Physiol. Genomics* 43, 521–528. doi: 10.1152/physiolgenomics.00158.2010

Rodrigues, S. F., and Granger, D. N. (2010). Role of blood cells in ischaemia-reperfusion induced endothelial barrier failure. *Cardiovasc. Res.* 87, 291–299. doi: 10.1093/cvr/cvq090

Rosenberg, G. A., and Yang, Y. (2007). Vasogenic edema due to tight junction disruption by matrix metalloproteinases in cerebral ischemia. *Neurosurg. Focus 22* 5, 1–9. doi: 10.3171/foc.2007.22.5.5

Sanderson, T. H., Reynolds, C. A., Kumar, R., Przyklenk, K., and Hüttemann, M. (2013). Molecular mechanisms of ischemia–reperfusion injury in brain: pivotal role of the mitochondrial membrane potential in reactive oxygen species generation. *Mol. Neurobiol.* 47, 9–23. doi: 10.1007/s12035-012-8344-z

Saugstad, J. A. (2010). MicroRNAs as effectors of brain function with roles in ischemia and injury, neuroprotection, and neurodegeneration. *J. Cereb. Blood Flow Metab. Off. J. Int. Soc. Cereb. Blood Flow Metab.* 30, 1564–1576. doi: 10.1038/jcbfm.2010.101

Sedeek, M., Hébert, R. L., Kennedy, C. R., Burns, K. D., and Touyz, R. M. (2009). Molecular mechanisms of hypertension: role of nox family NADPH oxidases. *Curr. Opin. Nephrol. Hypertens.* 18, 122–127. doi: 10.1097/MNH.0b013e32832923c3

Semple, B. D., Blomgren, K., Gimlin, K., Ferriero, D. M., and Noble-Haeusslein, L. J. (2013). Brain development in rodents and humans: identifying benchmarks of maturation and vulnerability to injury across species. *Prog. Neurobiol.* 106–107, 1–16. doi: 10.1016/j.pneurobio.2013.04.001

Sepramaniam, S., Armugam, A., Lim, K. Y., Karolina, D. S., Swaminathan, P., Tan, J. R., et al. (2010). MicroRNA 320a functions as a novel endogenous modulator of aquaporins 1 and 4 as well as a potential therapeutic target in cerebral ischemia. *J. Biol. Chem.* 285, 29223–29230. doi: 10.1074/jbc.M110.144576

Sepramaniam, S., Ying, L. K., Armugam, A., Wintour, E. M., and Jeyaseelan, K. (2012). MicroRNA-130a represses transcriptional activity of aquaporin 4 M1 promoter. *J. Biol. Chem.* 287, 12006–12015. doi: 10.1074/jbc.M111.280701

Serafin, A., Foco, L., Zanigni, S., Blankenburg, H., Picard, A., Zanon, A., et al. (2015). Overexpression of blood microRNAs 103a, 30b, and 29a in L-dopa-treated patients with PD. *Neurology* 84, 645–653. doi: 10.1212/WNL.0000000000001258

Sharp, F. R., and Bernaudin, M. (2004). HIF1 and oxygen sensing in the brain. *Nat. Rev. Neurosci.* 5, 437–448. doi: 10.1038/nrn1408

Shen, G., and Ma, Q. (2020). MicroRNAs in the blood-brain barrier in hypoxic-ischemic brain injury. *Curr. Neuropharmacol.* 18, 1180–1186. doi: 10.2174/1570159X18666200429004242

Shen, J., Li, G., Zhu, Y., Xu, Q., Zhou, H., Xu, K., et al. (2021). Foxo1-induced miR-92b down-regulation promotes blood-brain barrier damage after ischaemic stroke by targeting NOX4. *J. Cell. Mol. Med.* 25, 5269–5282. doi: 10.1111/jcmm.16537

Shi, C.-X., Ding, Y.-B., Jin, F. Y. J., Li, T., Ma, J.-H., Qiao, L.-Y., et al. (2018). Effects of sevoflurane post-conditioning in cerebral ischemia-reperfusion injury *via*

TLR4/NF-κB pathway in rats. *Eur. Rev. Med. Pharmacol. Sci.* 22, 1770–1775. doi: 10.26355/eurrev_201803_14595

Shi, H. (2009). Hypoxia inducible Factor 1 as a therapeutic target in ischemic stroke. *Curr. Med. Chem.* 16:4593. doi: 10.2174/092986709789760779

Shi, J., Zhao, Y., Wang, K., Shi, X., Wang, Y., Huang, H., et al. (2015). Cleavage of GSDMD by inflammatory caspases determines pyroptotic cell death. *Nature* 526, 660–665. doi: 10.1038/nature15514

Shi, Y., Yi, Z., Zhao, P., Xu, Y., and Pan, P. (2021). MicroRNA-532-5p protects against cerebral ischemia-reperfusion injury by directly targeting CXCL1. *Aging* 13, 11528–11541. doi: 10.18632/aging.202846

Shim, J. W., and Madsen, J. R. (2018). VEGF signaling in neurological disorders. *Int. J. Mol. Sci.* 19:E275. doi: 10.3390/ijms19010275

Siddiq, A., Ayoub, I. A., Chavez, J. C., Aminova, L., Shah, S., LaManna, J. C., et al. (2005). Hypoxia-inducible factor prolyl 4-hydroxylase inhibition. a target for neuroprotection in the central nervous system. *J. Biol. Chem.* 280, 41732–41743. doi: 10.1074/jbc.M504963200

Humphrey, S. M., Hearse, D. J., and Chain, E. B. (1973). Abrupt reoxygenation of the anoxic potassium-arrested perfused rat heart: a study of myocardial enzyme release. *J Mol Cell Cardiol* 5, 395–407. doi: 10.1016/0022-2828(73)90030-8

Smirnova, L., Gräfe, A., Seiler, A., Schumacher, S., Nitsch, R., and Wulczyn, F. G. (2005). Regulation of miRNA expression during neural cell specification. *Eur. J. Neurosci.* 21, 1469–1477. doi: 10.1111/j.1460-9568.2005.03978.x

Sun, C., Liu, J., Duan, F., Cong, L., and Qi, X. (2021). The role of the microRNA regulatory network in Alzheimer's disease: a bioinformatics analysis. *Arch. Med. Sci.* 18, 206–222. doi: 10.5114/aoms/80619

Sun, H., Li, J.-J., Feng, Z.-R., Liu, H.-Y., and Meng, A.-G. (2020a). MicroRNA-124 regulates cell pyroptosis during cerebral ischemia-reperfusion injury by regulating STAT3. *Exp. Ther. Med.* 20:227. doi: 10.3892/etm.2020.9357

Sun, J.-J., Zhang, X.-Y., Qin, X.-D., Zhang, J., Wang, M.-X., and Yang, J.-B. (2019). MiRNA-210 induces the apoptosis of neuronal cells of rats with cerebral ischemia through activating HIF-1α-VEGF pathway. *Eur. Rev. Med. Pharmacol. Sci.* 23, 2548–2554. doi: 10.26355/eurrev_201903_17403

Sun, P., Liu, D. Z., Jickling, G. C., Sharp, F. R., and Yin, K.-J. (2018a). MicroRNA-based therapeutics in central nervous system injuries. *J. Cereb. Blood Flow Metab. Off. J. Int. Soc. Cereb. Blood Flow Metab.* 38, 1125–1148. doi: 10.1177/0271678X18773871

Sun, R., Peng, M., Xu, P., Huang, F., Xie, Y., Li, J., et al. (2020b). Low-density lipoprotein receptor (LDLR) regulates NLRP3-mediated neuronal pyroptosis following cerebral ischemia/reperfusion injury. *J. Neuroinflammation* 17:330. doi: 10.1186/s12974-020-01988-x

Sun, X., Li, X., Ma, S., Guo, Y., and Li, Y. (2018b). MicroRNA-98-5p ameliorates oxygen-glucose deprivation/reoxygenation (OGD/R)-induced neuronal injury by inhibiting Bach1 and promoting Nrf2/ARE signaling. *Biochem. Biophys. Res. Commun.* 507, 114–121. doi: 10.1016/j.bbrc.2018.10.182

Sun, Y., Chen, P., Zhai, B., Zhang, M., Xiang, Y., Fang, J., et al. (2020c). The emerging role of ferroptosis in inflammation. *Biomed. Pharmacother. Biomedecine Pharmacother.* 127:110108. doi: 10.1016/j.biopha.2020.110108

Tang, H., Gamdzyk, M., Huang, L., Gao, L., Lenahan, C., Kang, R., et al. (2020). Delayed recanalization after MCAO ameliorates ischemic stroke by inhibiting apoptosis *via* HGF/c-Met/STAT3/Bcl-2 pathway in rats. *Exp. Neurol.* 330:113359. doi: 10.1016/j.expneurol.2020.113359

Tao, Z., Zhao, H., Wang, R., Liu, P., Yan, F., Zhang, C., et al. (2015). Neuroprotective effect of microRNA-99a against focal cerebral ischemia–reperfusion injury in mice. *J. Neurol. Sci.* 355, 113–119. doi: 10.1016/j.jns.2015.05.036

Liang, Z., Wu, G., Fan, C., Xu, J., Jiang, S., Yan, X., et al. (2016). The emerging role of signal transducer and activator of transcription 3 in cerebral ischemic and hemorrhagic stroke. *Prog. Neurobiol.* 137, 1–16. doi: 10.1016/j.pneurobio.2015.11.001

Tian, Y. S., Zhong, D., Liu, Q. Q., Zhao, X. L., Sun, H. X., Jin, J., et al. (2018). Upregulation of miR-216a exerts neuroprotective effects against ischemic injury through negatively regulating JAK2/STAT3-involved apoptosis and inflammatory pathways. *J. Neurosurg.* 130, 977–988. doi: 10.3171/2017.5.JNS163165

Tiedt, S., Prestel, M., Malik, R., Schieferdecker, N., Duering, M., Kautzky, V., et al. (2017). RNA-seq identifies circulating miR-125a-5p, miR-125b-5p, and miR-143-3p as potential biomarkers for acute ischemic stroke. *Circ. Res.* 121, 970–980. doi: 10.1161/CIRCRESAHA.117.311572

Tu, Y., and Hu, Y. (2021). MiRNA-34c-5p protects against cerebral ischemia/reperfusion injury: involvement of anti-apoptotic and anti-inflammatory activities. *Metab. Brain Dis.* 36, 1341–1351. doi: 10.1007/s11011-021-00724-5

Tüfekci, K. U., Oner, M. G., Meuwissen, R. L. J., and Genç, S. (2014). The role of microRNAs in human diseases. *Methods Mol. Biol. Clifton NJ* 1107, 33–50. doi: 10.1007/978-1-62703-748-8_3

Tuo, Q.-Z., Lei, P., Jackman, K. A., Li, X.-L., Xiong, H., Li, X.-L., et al. (2017). Tau-mediated iron export prevents ferroptotic damage after ischemic stroke. *Mol. Psychiatry* 22, 1520–1530. doi: 10.1038/mp.2017.171

Tuo, Q.-Z., Liu, Y., Xiang, Z., Yan, H.-F., Zou, T., Shu, Y., et al. (2022). Thrombin induces ACSL4-dependent ferroptosis during cerebral ischemia/reperfusion. *Signal Transduct. Target. Ther.* 7:59. doi: 10.1038/s41392-022-00917-z

Turovsky, E. A., Varlamova, E. G., and Plotnikov, E. Y. (2021). Mechanisms underlying the protective effect of the peroxiredoxin-6 are mediated *via* the protection of astrocytes during ischemia/reoxygenation. *Int J Mol Sci* 22:8805. doi: 10.3390/ijms22168805

Turrens, J. F. (2003). Mitochondrial formation of reactive oxygen species. *J. Physiol.* 552, 335–344. doi: 10.1113/jphysiol.2003.049478

Vandenabeele, P., Galluzzi, L., Vanden Berghe, T., and Kroemer, G. (2010). Molecular mechanisms of necroptosis: an ordered cellular explosion. *Nat. Rev. Mol. Cell Biol.* 11, 700–714. doi: 10.1038/nrm2970

Vijayan, M., and Reddy, P. H. (2016). Peripheral biomarkers of stroke: focus on circulatory microRNAs. *Biochim. Biophys. Acta* 1862, 1984–1993. doi: 10.1016/j.bbadis.2016.08.003

Wan, Y., Jin, H.-J., Zhu, Y.-Y., Fang, Z., Mao, L., He, Q., et al. (2018). MicroRNA-149-5p regulates blood-brain barrier permeability after transient middle cerebral artery occlusion in rats by targeting S1PR2 of pericytes. *FASEB J. Off. Publ. Fed. Am. Soc. Exp. Biol.* 32, 3133–3148. doi: 10.1096/fj.201701121R

Wang, J., Xu, Z., Chen, X., Li, Y., Chen, C., Wang, C., et al. (2018). MicroRNA-182-5p attenuates cerebral ischemia-reperfusion injury by targeting toll-like receptor 4. *Biochem. Biophys. Res. Commun.* 505, 677–684. doi: 10.1016/j.bbrc.2018.09.165

Wang, K., Ru, J., Zhang, H., Chen, J., Lin, X., Lin, Z., et al. (2020a). Melatonin enhances the therapeutic effect of plasma exosomes against cerebral ischemia-induced pyroptosis through the TLR4/NF-κB pathway. *Front. Neurosci.* 14:848. doi: 10.3389/fnins.2020.00848

Wang, L., Zhuang, L., Rong, H., Guo, Y., Ling, X., Wang, R., et al. (2015a). MicroRNA-101 inhibits proliferation of pulmonary microvascular endothelial cells in a rat model of hepatopulmonary syndrome by targeting the JAK2/STAT3 signaling pathway. *Mol. Med. Rep.* 12, 8261–8267. doi: 10.3892/mmr.2015.4471

Wang, M., Chen, Z., Yang, L., and Ding, L. (2021a). Sappanone a protects against inflammation, oxidative stress and apoptosis in cerebral ischemia-reperfusion injury by alleviating endoplasmic reticulum stress. *Inflammation* 44, 934–945. doi: 10.1007/s10753-020-01388-6

Wang, N., Zhang, L., Lu, Y., Zhang, M., Zhang, Z., Wang, K., et al. (2017). Down-regulation of microRNA-142-5p attenuates oxygen-glucose deprivation and reoxygenation-induced neuron injury through up-regulating Nrf2/ARE signaling pathway. *Biomed. Pharmacother.* 89, 1187–1195. doi: 10.1016/j.biopha.2017.03.011

Wang, P., Cui, Y., Ren, Q., Yan, B., Zhao, Y., Yu, P., et al. (2021b). Mitochondrial ferritin attenuates cerebral ischaemia/reperfusion injury by inhibiting ferroptosis. *Cell Death Dis.* 12:447. doi: 10.1038/s41419-021-03725-5

Wang, P., Liang, X., Lu, Y., Zhao, X., and Liang, J. (2016). MicroRNA-93 downregulation ameliorates cerebral ischemic injury through the Nrf2/HO-1 defense pathway. *Neurochem. Res.* 41, 2627–2635. doi: 10.1007/s11064-016-1975-0

Wang, P., Pan, R., Weaver, J., Jia, M., Yang, X., Yang, T., et al. (2021c). MicroRNA-30a regulates acute cerebral ischemia-induced blood–brain barrier damage through ZnT4/zinc pathway. *J. Cereb. Blood Flow Metab.* 41, 641–655. doi: 10.1177/0271678X20926787

Wang, Q.-C., Lu, L., and Zhou, H.-J. (2019). Relationship between the MAPK/ERK pathway and neurocyte apoptosis after cerebral infarction in rats. *Eur. Rev. Med. Pharmacol. Sci.* 23, 5374–5381. doi: 10.26355/eurrev_201906_18206

Wang, S., and Liu, Z. (2021). Inhibition of microRNA-143-3p Attenuates cerebral ischemia/reperfusion injury by targeting FSTL1. *Neuromolecular Med.* 23, 500–510. doi: 10.1007/s12017-021-08650-6

Wang, X., Shi, C., Pan, H., Meng, X., and Ji, F. (2020b). MicroRNA-22 exerts its neuroprotective and angiogenic functions *via* regulating PI3K/Akt signaling pathway in cerebral ischemia-reperfusion rats. *J. Neural Transm. Vienna Austria* 1996, 35–44. doi: 10.1007/s00702-019-02124-7

Wang, Y., Huang, J., Ma, Y., Tang, G., Liu, Y., Chen, X., et al. (2015b). MicroRNA-29b is a therapeutic target in cerebral ischemia associated with aquaporin 4. *J. Cereb. Blood Flow Metab. Off. J. Int. Soc. Cereb. Blood Flow Metab.* 35, 1977–1984. doi: 10.1038/jcbfm.2015.156

Wang, Y., Xiao, G., He, S., Liu, X., Zhu, L., Yang, X., et al. (2020c). Protection against acute cerebral ischemia/reperfusion injury by QiShenYiQi *via* neuroinflammatory network mobilization. *Biomed. Pharmacother.* 125:109945. doi: 10.1016/j.biopha.2020.109945

Washida, K., Hattori, Y., and Ihara, M. (2019). Animal models of chronic cerebral hypoperfusion: from mouse to primate. *Int. J. Mol. Sci.* 20:E6176. doi: 10.3390/ijms20246176

Wei, R., Zhang, R., Xie, Y., Shen, L., and Chen, F. (2015). Hydrogen suppresses hypoxia/reoxygenation-induced cell death in hippocampal neurons through reducing oxidative stress. *Cell. Physiol. Biochem.* 36, 585–598. doi: 10.1159/000430122

Weng, H., Shen, C., Hirokawa, G., Ji, X., Takahashi, R., Shimada, K., et al. (2011). Plasma miR-124 as a biomarker for cerebral infarction. *Biomed. Res. Tokyo Jpn.* 32, 135–141. doi: 10.2220/biomedres.32.135

Wood, A. J., Vassallo, A. M., Ruchaud-Sparagano, M.-H., Scott, J., Zinnato, C., Gonzalez-Tejedo, C., et al. (2020). C5a impairs phagosomal maturation in the neutrophil through phosphoproteomic remodeling. *JCI Insight* 5:137029. doi: 10.1172/jci.insight.137029

Wu, L., Xiong, X., Wu, X., Ye, Y., Jian, Z., Zhi, Z., et al. (2020). Targeting oxidative stress and inflammation to prevent ischemia-reperfusion injury. *Front. Mol. Neurosci.* 13:28. doi: 10.3389/fnmol.2020.00028

Wu, M. Y., Yiang, G. T., Liao, W. T., Tsai, A. P. Y., Cheng, Y. L., Cheng, P. W., et al. (2018). Current mechanistic concepts in ischemia and reperfusion injury. *Cell. Physiol. Biochem.* 46, 1650–1667. doi: 10.1159/000489241

Wu, Y., Yang, S., Zheng, Z., Pan, H., Jiang, Y., Bai, X., et al. (2021). MiR-191-5p disturbed the angiogenesis in a mice model of cerebral infarction by targeting inhibition of bdnF. *Neurol. India* 69, 1601–1607. doi: 10.4103/0028-3886.333459

Wu, Y., Yao, J., and Feng, K. (2020c). miR-124-5p/NOX2 axis modulates the ROS production and the inflammatory microenvironment to protect against the cerebral I/R injury. *Neurochem. Res.* 45, 404–417. doi: 10.1007/s11064-019-02931-0

Xia, P. P., Zhang, F., Chen, C., Wang, Z. H., Wang, N., Li, L. Y., et al. (2020). Rac1 relieves neuronal injury induced by oxygenglucose deprivation and re-oxygenation *via* regulation of mitochondrial biogenesis and function. *Neural Regen. Res.* 15, 1937–1946. doi: 10.4103/1673-5374.280325

Xie, W., Zhu, T., Dong, X., Nan, F., Meng, X., Zhou, P., et al. (2019). HMGB1-triggered inflammation inhibition of notoginseng leaf triterpenes against cerebral ischemia and reperfusion injury *via* MAPK and NF-κB signaling pathways. *Biomolecules* 9:512. doi: 10.3390/biom9100512

Xie, Y.-L., Zhang, B., and Jing, L. (2018). MiR-125b blocks Bax/Cytochrome C/Caspase-3 apoptotic signaling pathway in rat models of cerebral ischemia-reperfusion injury by targeting p53. *Neurol. Res.* 40, 828–837. doi: 10.1080/01616412.2018.1488654

Xing, F., Liu, Y., Dong, R., and Cheng, Y. (2021). miR-374 improves cerebral ischemia reperfusion injury by targeting Wnt5a. *Exp. Anim.* 70, 126–136. doi: 10.1538/expanim.20-0034

Xu, H., Nie, B., Liu, L., Zhang, C., Zhang, Z., Xu, M., et al. (2019). Curcumin prevents brain damage and cognitive dysfunction during ischemic-reperfusion through the regulation of miR-7-5p. *Curr. Neurovasc. Res.* 16, 441–454. doi: 10.2174/1567202616666191029113633

Xu, Y., Liu, Y., Li, K., Yuan, D., Yang, S., Zhou, L., et al. (2022). COX-2/PGE2 pathway inhibits the ferroptosis induced by cerebral ischemia reperfusion. *Mol. Neurobiol.* 59, 1619–1631. doi: 10.1007/s12035-021-02706-1

Xue, W.-S., Wang, N., Wang, N.-Y., Ying, Y.-F., and Xu, G.-H. (2019). miR-145 protects the function of neuronal stem cells through targeting MAPK pathway in the treatment of cerebral ischemic stroke rat. *Brain Res. Bull.* 144, 28–38. doi: 10.1016/j.brainresbull.2018.08.023

Yan, H., Kanki, H., Matsumura, S., Kawano, T., Nishiyama, K., Sugiyama, S., et al. (2021). MiRNA-132/212 regulates tight junction stabilization in blood-brain barrier after stroke. *Cell Death Discov.* 7:380. doi: 10.1038/s41420-021-00773-w

Yang, C., Wei, X., Fu, X., Qian, L., Xie, L., Liu, H., et al. (2021). Down-regulating microRNA-20a regulates CDH1 to protect against cerebral ischemia/reperfusion injury in rats. *Cell Cycle* 20, 54–64. doi: 10.1080/15384101.2020.1856498

Yang, J. (2019). The role of reactive oxygen species in angiogenesis and preventing tissue injury after brain ischemia. *Microvasc. Res.* 123, 62–67. doi: 10.1016/j.mvr.2018.12.005

Yang, T., Feng, C., Wang, D., Qu, Y., Yang, Y., Wang, Y., et al. (2020). Neuroprotective and anti-inflammatory effect of tangeretin against cerebral ischemia-reperfusion injury in rats. *Inflammation* 43, 2332–2343. doi: 10.1007/s10753-020-01303-z

Yao, X., Wang, Y., and Zhang, D. (2018). microRNA-21 Confers neuroprotection against cerebral ischemia-reperfusion injury and alleviates blood-brain barrier disruption in rats *via* the MAPK signaling pathway. *J. Mol. Neurosci.* 65, 43–53. doi: 10.1007/s12031-018-1067-5

Yao, X., Yao, R., Yi, J., and Huang, F. (2019). Upregulation of miR-496 decreases cerebral ischemia/reperfusion injury by negatively regulating BCL2L14. *Neurosci. Lett.* 696, 197–205. doi: 10.1016/j.neulet.2018.12.039

Ying, X.-D., Wei, G., and An, H. (2021). Sodium butyrate relieves lung ischemia-reperfusion injury by inhibiting NF-κB and JAK2/STAT3 signaling pathways. *Eur. Rev. Med. Pharmacol. Sci.* 25, 413–422. doi: 10.26355/eurrev_202101_24409

Yu, H., Wu, M., Zhao, P., Huang, Y., Wang, W., and Yin, W. (2015). Neuroprotective effects of viral overexpression of microRNA-22 in rat and cell models of cerebral ischemia-reperfusion injury. *J. Cell. Biochem.* 116, 233–241. doi: 10.1002/jcb.24960

Yu, P., Zhang, X., Liu, N., Tang, L., Peng, C., and Chen, X. (2021a). Pyroptosis: mechanisms and diseases. *Signal Transduct. Target. Ther.* 6, 1–21. doi: 10.1038/s41392-021-00507-5

Yu, S., Zhai, J., Yu, J., Yang, Q., and Yang, J. (2021b). miR-98-5p protects against cerebral ischemia/reperfusion injury through anti-apoptosis and anti-oxidative stress in mice. *J. Biochem.* 169, 195–206. doi: 10.1093/jb/mvaa099

Yu, S.-J., Yu, M.-J., Bu, Z.-Q., He, P.-P., and Feng, J. (2020). MicroRNA-670 aggravates cerebral ischemia/reperfusion injury *via* the Yap pathway. *Neural Regen. Res.* 16, 1024–1030. doi: 10.4103/1673-5374.300455

Yu, S.-J., Yu, M.-J., Bu, Z.-Q., He, P.-P., and Feng, J. (2021c). MicroRNA-670 aggravates cerebral ischemia/reperfusion injury *via* the yap pathway. *Neural Regen. Res.* 16, 1024–1030. doi: 10.4103/1673-5374.300455

Yue, Y., Zhao, H., Yue, Y., Zhang, Y., and Wei, W. (2020). Downregulation of microrna-421 relieves cerebral ischemia/reperfusion injuries: involvement of anti-apoptotic and antioxidant activities. *NeuroMolecular Med.* 22, 411–419. doi: 10.1007/s12017-020-08600-8

Zador, Z., Stiver, S., Wang, V., and Manley, G. T. (2009). Role of aquaporin-4 in cerebral edema and stroke. *Handb. Exp. Pharmacol.* 190, 159–170. doi: 10.1007/978-3-540-79885-9_7

Zeng, L., Liu, J., Wang, Y., Wang, L., Weng, S., Tang, Y., et al. (2011). MicroRNA-210 as a novel blood biomarker in acute cerebral ischemia. *Front. Biosci. Elite Ed.* 3:1265–1272. doi: 10.2741/e330

Zeng, Z., Zhang, Y., Liang, X., Wang, F., Zhao, J., Xu, Z., et al. (2019). Qingnao dripping pills mediate immune-inflammatory response and MAPK signaling pathway after acute ischemic stroke in rats. *J. Pharmacol. Sci.* 139, 143–150. doi: 10.1016/j.jphs.2018.12.009

Zhang, H., Liu, X., Yang, F., Cheng, D., and Liu, W. (2020a). Overexpression of HIF-1α protects PC12 cells against OGD/R-evoked injury by reducing miR-134 expression. *Cell Cycle Georget. Tex* 19, 990–999. doi: 10.1080/15384101.2020.1743903

Zhang, H.-S., Ouyang, B., Ji, X.-Y., and Liu, M.-F. (2021a). Gastrodin alleviates cerebral ischaemia/reperfusion injury by inhibiting pyroptosis by regulating the lncRNA NEAT1/miR-22-3p axis. *Neurochem. Res.* 46, 1747–1758. doi: 10.1007/s11064-021-03285-2

Zhang, H.-T., Zhang, P., Gao, Y., Li, C.-L., Wang, H.-J., Chen, L.-C., et al. (2017). Early VEGF inhibition attenuates blood-brain barrier disruption in ischemic rat brains by regulating the expression of MMPs. *Mol. Med. Rep.* 15, 57–64. doi: 10.3892/mmr.2016.5974

Zhang, J., Shi, L., Zhang, L., Zhao, Z., Liang, F., Xu, X., et al. (2016). MicroRNA-25 negatively regulates cerebral ischemia/reperfusion injury-induced cell apoptosis through Fas/FasL pathway. *J. Mol. Neurosci.* 58, 507–516. doi: 10.1007/s12031-016-0712-0

Zhang, R. L., Chopp, M., Chen, H., and Garcia, J. H. (1994). Temporal profile of ischemic tissue damage, neutrophil response, and vascular plugging following permanent and transient (2H) middle cerebral artery occlusion in the rat. *J. Neurol. Sci.* 125, 3–10. doi: 10.1016/0022-510x(94)90234-8

Zhang, S. (2019). Microglial activation after ischaemic stroke. *Stroke Vasc. Neurol.* 4, 71–74. doi: 10.1136/svn-2018-000196

Zhang, S., Chen, A., and Chen, X. (2021b). A feedback loop involving MicroRNA-150 and MYB regulates VEGF expression in brain microvascular endothelial cells after oxygen glucose deprivation. *Front. Physiol.* 12:619904. doi: 10.3389/fphys.2021.619904

Zhang, T., Tian, C., Wu, J., Zhang, Y., Wang, J., Kong, Q., et al. (2020b). MicroRNA-182 exacerbates blood-brain barrier (BBB) disruption by downregulating the mTOR/FOXO1 pathway in cerebral ischemia. *FASEB J. Off. Publ. Fed. Am. Soc. Exp. Biol.* 34, 13762–13775. doi: 10.1096/fj.201903092R

Zhang, Y., Lu, X., Tai, B., Li, W., and Li, T. (2021c). Ferroptosis and Its multifaceted roles in cerebral stroke. *Front. Cell. Neurosci.* 15:615372. doi: 10.3389/fncel.2021.615372

Zhang, Y., Shan, Z., Zhao, Y., and Ai, Y. (2019a). Sevoflurane prevents miR-181a-induced cerebral ischemia/reperfusion injury. *Chem. Biol. Interact.* 308, 332–338. doi: 10.1016/j.cbi.2019.06.008

Zhang, Z., Wang, N., Zhang, Y., Zhao, J., and Lv, J. (2019b). Downregulation of microRNA-302b-3p relieves oxygen-glucose deprivation/re-oxygenation induced injury in murine hippocampal neurons through up-regulating Nrf2 signaling by targeting fibroblast growth factor 15/19. *Chem. Biol. Interact.* 309:108705. doi: 10.1016/j.cbi.2019.06.018

Zhang, Z., Yao, L., Yang, J., Wang, Z., and Du, G. (2018). PI3K/Akt and HIF-1 signaling pathway in hypoxia-ischemia (Review). *Mol. Med. Rep.* 18, 3547–3554. doi: 10.3892/mmr.2018.9375

Zhao, B., Wang, P., Yu, J., and Zhang, Y. (2021). MicroRNA-376b-5p targets SOX7 to alleviate ischemic brain injury in a mouse model through activating Wnt/β-catenin signaling pathway. *Life Sci.* 270:119072. doi: 10.1016/j.lfs.2021.119072

Zhao, H., Tao, Z., Wang, R., Liu, P., Yan, F., Li, J., et al. (2014). MicroRNA-23a-3p attenuates oxidative stress injury in a mouse model of focal cerebral ischemia-reperfusion. *Brain Res.* 1592, 65–72. doi: 10.1016/j.brainres.2014.09.055

Zhao, J., and Wang, B. (2020). MiR-7-5p Enhances cerebral ischemia-reperfusion injury by degrading sirt1 mRNA. *J. Cardiovasc. Pharmacol.* 76, 227–236. doi: 10.1097/FJC.0000000000000852

Zhao, J., Wu, Y., Liang, S., and Piao, X. (2022). Activation of SSAT1/ALOX15 axis aggravates cerebral ischemia/reperfusion injury *via* triggering neuronal ferroptosis. *Neuroscience* 485, 78–90. doi: 10.1016/j.neuroscience.2022.01.017

Zheng, T., Shi, Y., Zhang, J., Peng, J., Zhang, X., Chen, K., et al. (2019). MiR-130a exerts neuroprotective effects against ischemic stroke through PTEN/PI3K/AKT pathway. *Biomed. Pharmacother.* 117:109117. doi: 10.1016/j.biopha.2019.109117

Zhi, F., Shao, N., Wang, R., Deng, D., Xue, L., Wang, Q., et al. (2015). Identification of 9 serum microRNAs as potential noninvasive biomarkers of human astrocytoma. *Neuro-Oncol.* 17, 383–391. doi: 10.1093/neuonc/nou169

Zuo, M. L., Wang, A. P., Song, G. L., and Yang, Z. B. (2020). miR-652 protects rats from cerebral ischemia/reperfusion oxidative stress injury by directly targeting NOX2. *Biomed. Pharmacother.* 124:109860. doi: 10.1016/j.biopha.2020.109860

Conflict of Interest: The authors declare that the research was conducted in the absence of any commercial or financial relationships that could be construed as a potential conflict of interest.

Publisher's Note: All claims expressed in this article are solely those of the authors and do not necessarily represent those of their affiliated organizations, or those of the publisher, the editors and the reviewers. Any product that may be evaluated in this article, or claim that may be made by its manufacturer, is not guaranteed or endorsed by the publisher.

frontiers | Frontiers in Pharmacology

ORIGINAL RESEARCH
published: 13 June 2022
doi: 10.3389/fphar.2022.889404

Panax notoginseng Saponins Stimulates Neurogenesis and Neurological Restoration After Microsphere-Induced Cerebral Embolism in Rats Partially *Via* mTOR Signaling

Jiale Gao[1], *Jianxun Liu*[1]*, *Mingjiang Yao*[1], *Wei Zhang*[2], *Bin Yang*[2] *and Guangrui Wang*[1]

[1]Beijing Key Laboratory of Pharmacology of Chinese Materia Medica, Institute of Basic Medical Sciences of Xiyuan Hospital, China Academy of Chinese Medical Sciences, Beijing, China, [2]Department of Pathology, Xiyuan Hospital, China Academy of Chinese Medical Sciences, Beijing, China

P. Notoginseng Saponins (PNS), the main active component of herbal medicine Panax notoginseng, has been widely used to treat cerebrovascular diseases. It has been acknowledged that PNS exerted protection on nerve injuries induced by ischemic stroke, however, the long-term impacts of PNS on the restoration of neurological defects and neuroregeneration after stroke have not been thoroughly studied and the underlying molecular mechanism of stimulating neurogenesis is difficult to precisely clarify, much more in-depth researches are badly needed. In the present study, cerebral ischemia injury was induced by microsphere embolism (ME) in rats. After 14 days, PNS administration relieved cerebral ischemia injury as evidenced by alleviating neurological deficits and reducing hippocampal pathological damage. What's more, PNS stimulated hippocampal neurogenesis by promoting cell proliferation, migration and differentiation activity and modulated synaptic plasticity. Increased number of BrdU/Nestin, BrdU/DCX and NeuroD1-positive cells and upregulated synapse-related GAP43, SYP, and PSD95 expression were observed in the hippocampus. We hypothesized that upregulation of brain-derived neurotrophic factor (BDNF) expression and activation of Akt/mTOR/p70S6K signaling after ME could partially underlie the neuroprotective effects of PNS against cerebral ischemia injury. Our findings offer some new viewpoints into the beneficial roles of PNS against ischemic stroke.

Keywords: ***Panax notoginseng*** **saponins, cerebral ischemia, neurogenesis, synaptic plasticity, Akt/mTOR/p70S6K pathway**

OPEN ACCESS

Edited by:
Li-Nan Zhang,
Hebei Medical University, China

Reviewed by:
Yi Wang,
Zhejiang University, China
Norio Takagi,
Tokyo University of Pharmacy and Life Sciences, Japan

***Correspondence:**
Jianxun Liu
liujx0324@sina.com

Specialty section:
This article was submitted to Neuropharmacology, a section of the journal Frontiers in Pharmacology

Received: *04 March 2022*
Accepted: *23 May 2022*
Published: *13 June 2022*

Citation:
Gao J, Liu J, Yao M, Zhang W, Yang B and Wang G (2022) Panax notoginseng Saponins Stimulates Neurogenesis and Neurological Restoration After Microsphere-Induced Cerebral Embolism in Rats Partially Via mTOR Signaling. Front. Pharmacol. 13:889404. doi: 10.3389/fphar.2022.889404

1 INTRODUCTION

Ischemic stroke is one of the leading causes of long-term lethality and disability in the world (Zhu et al., 2018), and the incidence and prevalence are on the rise with an aging population globally (Koh and Park, 2017), which seriously threatens human health and brings heavy mental and economic burden to families and society (Liu et al., 2012). Stroke patients often suffer from sensory-motor and

cognitive dysfunction, such as dementia, aphasia, paralysis, etc. However, ischemia stroke is involved in complex pathological mechanism and there is currently no effective preparation especially for neural restoration after stroke, so it is of great significance to develop drugs or preparations with neuroprotective and restorative effects in order to promote the recovery of neurological functions for stoke patients those who are out of 4.5-hour time window of thrombolysis.

In the past decade, much interest has been focused on neurogenesis, which provides fundamental support for remodeling and restoration of brain architecture and function (Yamaguchi et al., 2016) and may open up a novel therapeutic method to restore impaired neurological function after ischemic stroke. Nevertheless, neurogenesis from the embryonic brain throughout adulthood requires a well-controlled external and internal signal that guides the neural stem cells (NSCs) to transition into a properly functioning neuron, which involves the complex process of cell proliferation, division, differentiation, migration, and functional integration into neuronal circuits. In the adult brain, neurogenesis mainly happens in two canonical neurogenic areas: subgranular zone (SGZ) of dentate gyrus (DG) in the hippocampus and the subventricular zone (SVZ) of the lateral ventricle (Fh, 2000; Kempermann et al., 2015; Dillen et al., 2020), where endogenous NSCs proliferate, migrate and differentiate to replace dead neurons following cerebral ischemia (Kong et al., 2016; Piermartiri et al., 2020). However, due to limited repair capacity, ischemia-induced neurogenesis alone is not enough to restore neurological deficits, thus enhancing endogenous neurogenesis through drug stimulation might be an attractive strategy.

The main active ingredients of herbal medicine *P. notoginseng* are *P. notoginseng* saponins (PNS) whose major constituents are saponins, including Ginsenoside Rb1 (32.7 %), Ginsenoside Rg1 (32.1%), Notoginsenoside R1 (5.9%), Ginsenoside Rd (6.3%), and Ginsenoside Re (4.1%). It's reported that PNS could modulate the inflammatory response and promote proliferation and differentiation of hippocampal NSCs *in vitro* (Si et al., 2011; Luo et al., 2021), indicating its potential benefits on neurogenesis after ischemic brain injury. Although the protection of PNS on neural damage induced by ischemic stroke is well characterized, the mechanism behind its actions concerning cerebral ischemia is not fully known. Further, the long-term effects of PNS on the recovery of neurological defects and neuroregeneration after stroke have not been thoroughly studied and the underlying molecular mechanism of stimulating neurogenesis is difficult to precisely clarify, much more in-depth researches are badly needed.

The mammalian target of rapamycin (mTOR), a large serine/threonine protein kinase, plays a vital role in cell growth, proliferation, survival, nutrient metabolism, autophagy, and protein translation, at present, great endeavor has been made to transfer targeting mTOR for cancer to CNS diseases and the extensive role of mTOR has attracted much interest in this field (Park et al., 2008; Guo and Yu, 2019). Multiple proteins combined with mTOR constitute two divergent complexes, designed as mTORC1 and mTORC2, in which mTORC1 is essential to maintain endogenous neural progenitor pool and for NSC differentiation into daughter cells (Licausi and Hartman, 2018). Studies have shown that AKT/mTOR signaling pathway could mediate the development of NSC, including NSC proliferation, differentiation, neural progenitor migration, dendrite development, synapse formation, and neuron maturation, playing a critical role in enhancing neurogenesis following ischemic stroke (Corsini et al., 2009; Liang et al., 2016; Zhang et al., 2016).

Regulation of cell signaling towards mTOR may exert profound effects on neurogenesis and initiate neuroprotection during cerebral ischemia, however, involvement of mTOR in cerebral ischemia-induced endogenous neurogenesis is not yet fully known, much more related researches are still needed to demonstrate this viewpoint. Here, we firstly demonstrated that PNS stimulated hippocampal neurogenesis by promoting NSC/NPC proliferation, migration, and differentiation activity and modulated synaptic plasticity by increasing synaptic formation-related proteins synthesis. Meanwhile, upregulation of brain-derived neurotrophic factor (BDNF) expression and activation of Akt/mTOR/p70S6K signaling after ME could partially underlie the neuroprotective effects of PNS against cerebral ischemia injury.

2 MATERIALS AND METHODS

2.1 Main Chemicals and Reagents

PNS was offered by Chengdu Ruifen Si Biotechnology Co., Ltd. (Batch No. RFS-DFZY-SQZZG201225, Chengdu, China). CMC-Na was purchased from Dalian Meilun Biotechnology Co., Ltd. (Batch No. J1204A, Dalian, China). Sucrose was provided by Beijing Beihua Fine Chemicals Co., Ltd. (Batch No. 20051012, Beijing, China). Goat serum was purchased from Proteintech Group, Inc. (B900780, Wuhan, China). DAPI solution (C00650), 5′-Bromo-2′-deoxyuridine (BrdU, No. 2011031) and TritonX-100 (No. 1109F0524) were purchased from Solarbio Life Sciences & Technology Co., Ltd. (Beijing, China). GAP43 (ab75810), BDNF (ab108319), β-actin (ab8226-100), SYP (ab32127), PSD95 (ab238135), Anti-BrdU Rat mAb (ab6326), Anti-DCX Rabbit mAb (ab207175), Anti-NeuroD1 Rabbit mAb (ab213725), Anti-Nestin Rabbit mAb (ab221260) and Anti-Fade Fluorescence-aqueous, Fluoroshield (ab104135) were purchased from abcam (Cambridge, United Kingdom). Fluorescence microspheres (106–125 μm and 180–212 μm in diameter, UVPMS-BY2) were purchased from Cospheric (US). Cy3-labeled Goat Anti-Rat IgG (H&L) (CSA1041) and DyLight 488-labeled Goat Anti-Rabbit IgG (H&L) (CSA1029) were purchased from Cohesion (Cambridge, United Kingdom). Akt (4685s), Phospho-Akt (Ser473) (D9E) XP Rabbit mAb (p-Akt, 4060s), mTOR (2983), Phospho-mTOR (Ser2448) (D9C2) XP® Rabbit mAb (p-mTOR, 5536), p70S6K (2708s), and Phospho-p70 S6 Kinase (Thr389) (D5U1O) Rabbit mAb (p-p70S6K, 97596s) were purchased from Cell Signaling Technology, Inc. (CST) (Boston, United States).

2.2 Experimental Animals

Male 8-week-old Sprague-Dawley (SD) rats (weighing 210 ± 10 g) were purchased from Beijing Sibafu Biotechnology Co., Ltd.

[Beijing, China; laboratory animal certificate number: SYXK (jing), 2019-0010]. Animals were kept three to six per cage on a 12 h light/dark cycle with free access to water and food in a temperature (22°C ± 2°C) and humidity (55% ± 5%)-controlled Xiyuan hospital Animal Center. The experimental protocols were approved by Experimental Ethics Committee at Xiyuan hospital.

2.3 Animal Model and Drug Administration

2.3.1 Experiment I

To evaluate the effect of PNS on the neurological protection of microsphere-induced cerebral embolism (ME) rats and screen out the effective doses of PNS, the rats were randomly divided into seven groups: sham, ME, ME + PNS 15 mg/kg, ME + PNS 30 mg/kg, ME + PNS 60 mg/kg, ME + PNS 120 mg/kg and ME + PNS 240 mg/kg groups (n = 9 per group). Microsphere-induced cerebral embolism (ME) was conducted to induce sustained cerebral ischemia according to Takeo et al., 1989 with slight modifications based on previous research in our laboratory.

In short, the rats were fastened in the supine position after their anesthesia by intraperitoneal injection of 80 mg/kg pentobarbital sodium. The right common carotid artery (CCA), internal carotid artery (ICA) and external carotid artery (ECA) were isolated and exposed, then the right pterygopalatine arteries were twisted off by electric coagulation pen and the right ECA were ligated with strings. Next, the right CCA for the rats were temporarily occluded with vascular clamp. Fluorescence microspheres, suspended in 200 ul of 5% dextran solution, were injected into the right ICA through a syringe inserted into the ECA, then the vascular clamp occluding CCA was simultaneously removed, allowing 273 microspheres to move to the various arteries of the brain and lead to embolisms, and the wound was closed by sutures. The sham rats received equal volume of vehicle without microspheres.

PNS was prepared fresh daily in 0.5% CMC-Na. The rats in PNS groups were administrated with 15, 30, 60, 120, or 240 mg/kg PNS accordingly once a day for 14 days *via* gavage after surgery. The rats in Sham and ME groups were given equal volume of vehicle *via* gavage. The fresh sterile solution of BrdU was made daily in 0.9% saline at a dilution of 10 mg/ml. For tracking the neurogenesis, all the rats were injected intraperitoneally with BrdU (50 mg/kg) once daily for 14 days in order to identify the proliferative cells. Fourteen days after ME, animals were killed by decapitation under anesthesia after the last BrdU injection.

In this part, we set five doses of PNS and explored the pharmacological protection effects of PNS on ME rats through animal behaviors, ELISA as well as HE staining experiments.

2.3.2 Experiment II

Based on the results of Experiment I, we have selected three appropriately effective doses of PNS 30, 60, and 120 mg/kg to further investigate the effect of PNS on neurogenesis and synaptic plasticity, and finally identified the probable underlying mechanism through immunofluorescence and Western Blot experiments.

The experimental protocols are presented in **Figure 1**.

2.4 Behavioral Test

The modified neuro-functional assessment, forepaw outreaching test and rope-climbing test were performed by a person blinded to group designation as previously described (Garcia et al., 1995; Ohlsson and Johansson, 1995; Wu et al., 2019b). Neuro-functional assessment and forepaw outreaching test were conducted at day 1, 3, 7, and 14 after operation, rope-climbing test were conducted at day 14 after operation.

2.4.1 Weight Percentage

The body weight was measured every day until the end of experiment and the data were collected at day 1, 3, 7 and 14 after surgery for statistical analysis. Weight percentage = post-surgery body weight/pre-surgery body weight.

2.4.2 Neuro-Functional Assessment

The neurological functional score was rated from 0 to 4 (0, no neurological deficit symptoms; 1, unable to completely stretch left forepaw; 2, circling to the left; 3, falling to the left or rolling on the ground; 4, no spontaneous activity with consciousness disorder). Rats with the score between one and three were included in the following experiments.

2.4.3 Forepaw Outreaching Test

The rats were made to walk on forelimbs while being held by the tail. Symmetry in the outreaching of both forelimbs was observed with the hindlimbs of rats kept in the air, and the scores are as follows. 0, both forelimbs were outstretched symmetrically, and the rats walked in a straight line; 1, left forelimb outstretched less than right forelimb, and the rats leaned slightly to the left when walking; 2, left forelimb outstretched minimally, and the rats circled to the left when walking; 3, left forelimb did not move.

2.4.4 Rope-Climbing Test

The rats were allowed to seize the steel rope (2 mm in diameter) 80 cm above the ground with their forelimbs while the hindlimbs were kept in the air and the time hanging on the steel rope was evaluated, the scores are the following: 0, seize the steel rope for more than 5 s with their hindlimbs tight to the rope; 1, seize the steel rope for 5 s without their hindlimbs tight to the rope; 2, seize the steel rope for 3~4 s; 3, seize the steel rope for 0~2 s.

2.5 Enzyme-Linked Immunosorbent Assay

The BDNF (brain derived neurotrophic factor) concentrations in the serum of rats after centrifugation (3000 rpm/min, 15 min) were measured using commercial ELISA kits (Human/Mouse/Rat Brain Derived Neurotrophic Factor Enzyme-Linked ImmunoSorbent Assay Kit, Beyotime Biotechnology) based on the manufacturer's instructions.

2.6 Hematoxylin-Eosin Staining

Brains of rats in each group were separated and fixed using 10% formalin overnight, and were then dehydrated through graded alcohol and embedded in paraffin wax. Then paraffin-embedded tissue sections (5 μm thick) were stained routinely for HE staining

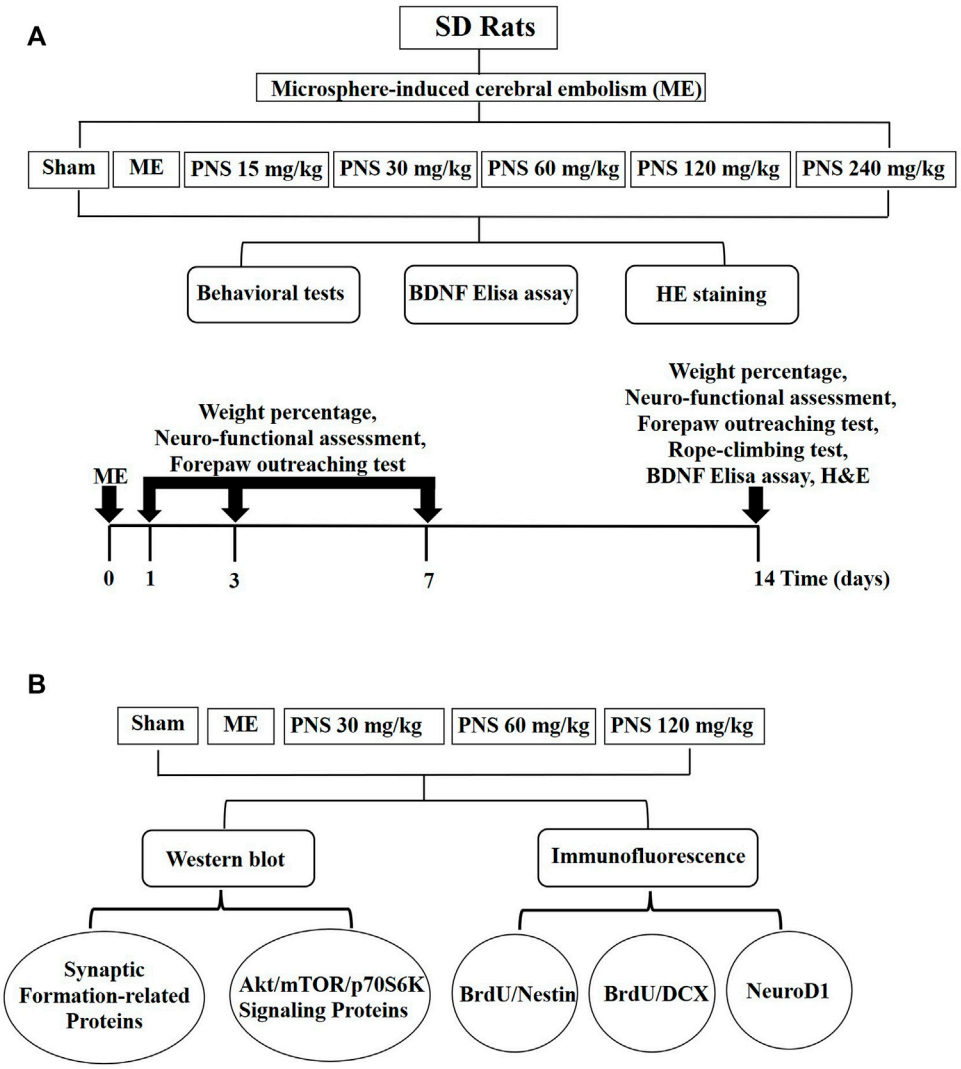

FIGURE 1 | Diagram of experimental protocols. **(A)** Screening scheme of the appropriately effective PNS does **(B)** Mechanism of PNS promoting neural repair after cerebral ischemia.

in order to observe the neuronal pathological changes in the hippocampus.

2.7 Immunofluorescence

To explore the function of PNS on proliferation and migration of newly neural progenitor cells (NPC), expressions of BrdU/Nestin and BrdU/DCX in brain hippocampus were detected by double immunofluorescence staining. To study the impact of PNS on differentiation of neural progenitor cells, expressions of neurogenic differentiation1 (NeuroD1) in brain hippocampus were examined by immunofluorescence staining. Brains of rats were separated and fixed in 4% paraformaldehyde overnight at 4°C and then transferred into 25% sucrose in 0.1 M PB until sinking to the bottom. After that, the brains were embedded and frozen in optimal cutting temperature compound (OCT compound) and a series of brain coronal sections (40 μm) were cut at −20°C by a freezing microtome (Leica, CM1950, German). The frozen sections were then immediately processed for free-floating immunohistochemistry.

For BrdU/Nestin and BrdU/DCX double immunofluorescence staining, brain sections were washed in 0.1 M PB for 5 mins, then sections were incubated in 1 M HCl for 46 mins at 37°C to denature DNA, followed by 0.1 M sodium borate buffer (pH 8.5) for 10 mins at room temperature and rinsed three times for 5 mins each with 0.1 M PB. After that, brain sections were incubated in a blocking solution containing 3% normal goat serum and 1.5% TritonX-100 in 0.1 M PB for 30 min at room temperature prior to incubating at 4°C overnight in a solution containing 1% normal goat serum, 1.5% Triton X-100, with the primary antibodies [Rabbit anti-Nestin monoclonal antibody (1:100) or Rabbit anti-DCX monoclonal antibody (1: 100)]. After rinsing three times for 5 mins each with 0.1 M PB, the

sections were incubated 1.5 h at room temperature in the dark with corresponding secondary antibody [DyLight 488-labeled Goat Anti-Rabbit IgG (H&L) (1:400)]. Followed by rinsing in 0.1 M PB, brain sections were incubated in a blocking solution containing 3% normal goat serum and 1.5% TritonX-100 in 0.1 M PB prior to incubating in a solution containing 1% normal goat serum, 1.5% Triton X-100, with another primary antibody [Rat anti-BrdU monoclonal antibody (1:500)] at 37°C 1.5 h, and after rinsing three times for 5 mins each with 0.1 M PB, the sections were incubated 1.5 h at room temperature in the dark with corresponding secondary antibody [Cy3-labeled Goat Anti-Rat IgG (H&L) (1:500)]. DAPI solution was added for nuclear counterstaining.

For NeuroD1 immunofluorescence staining, brain sections were washed in 0.1 M PB for 5 mins, then sections were incubated in a blocking solution containing 3% normal goat serum and 1.5% TritonX-100 in 0.1 M PB for 30 min at room temperature prior to incubating at 4°C overnight in a solution containing 1% normal goat serum, 1.5% Triton X-100, with the primary antibody [Rabbit anti-NeuroD1 monoclonal antibody (1:200)]. After rinsing three times for 5 mins each with 0.1 M PB, the sections were incubated 1.5 h at room temperature in the dark with corresponding secondary antibody [DyLight 488-labeled Goat Anti-Rabbit IgG (H&L) (1:400)].

The images of immunofluorescence staining including NeuroD1 and double immunofluorescence staining including BrdU+/Nestin+ and BrdU+/DCX+ positive cells in ipsilateral subgranular zone (SGZ) and granule cell layer (GCL) of the hippocampal dentate gyrus were observed under the fluorescence microscope (Olympus, Olympus BX53, Japan) at a magnification of ×200. And the number of positive cells (Nestin/BrdU, DCX/BrdU and NeuroD1) was counted using ImageJ based on single-positive or double-positive cells and their nucleus in three coronal sections per animal (three animals in each group and three coronal sections per animal were used to separately determine the number of Nestin/BrdU, DCX/BrdU and NeuroD1-positive cells), which areas corresponded to coronal coordinates of −2.8 mm to −4.52 mm from bregma.

2.8 Western Blot

Fifteen rats were killed by decapitation ($n = 3$ per group) and their brains were rapidly taken and then frozen by liquid nitrogen. The ipsilateral hippocampus was isolated and homogenized in RIPA lysis solution containing phosphatase inhibitors, protein phosphatase inhibitors and PMSF on ice for thorough lysis of proteins, then the supernatant was gathered by centrifugation. Bradford method was adopted to detect the protein contents and then protein concentration was adjusted to the same level after quantification. Then it was mixed with 5× loading buffer to prepare sample solutions of a certain concentration and samples were separated by SDS-PAGE, and then transferred to PVDF membranes (Millipore, United States). Membranes were blocked with 5% non-fatty milk or 5% BSA for 2 h, followed by incubation overnight at 4°C with the primary antibodies [Akt (1:1000), p-Akt (1:1000), mTOR (1:1000), p-mTOR (1:1000), p70S6K (1:1000), p-p70S6K (1:500), GAP43 (1:1000), SYP(1:1000), PSD95 (1:1000), BDNF (1:1000) and β-actin (1:1000)]. Then, the membranes were washed with TBST for 5 min three times, and were incubated for another 1 h at room temperature with corresponding secondary antibodies. Immunoreactive bands were detected using BeyoECL Moon reagent (beyotime, China) and the average gray value of each band was calculated using the software ImageJ, β-actin was used as an internal control.

2.9 Statistical Analysis

All data were presented as mean ± standard deviation and were analyzed using appropriate statistical methods with SPSS 25.0 software (IBM, Chicago, United States). Differences between two groups were evaluated by a non-parametric *U*-test when data were out of normal distribution. Statistical comparison among multiple groups was determined through a one-way analysis of variance or two-way repeated-measures analysis of variance followed by the LSD test, and $p < 0.05$ indicates a significant difference.

3 RESULTS

3.1 *P. notoginseng* Saponins Treatment Improved the Recovery of Neurological Functions in Microsphere Embolism Rats

As shown in **Figures 2A–C**, the effect of PNS on ME-induced neurological defects was evaluated by neurological score, forepaw outreaching and rope-climbing test score. The higher the scores were, the severer the damage was. The neurological score, forepaw outreaching test score as well as rope-climbing test score were all strikingly increased in ME group compared with sham group at different time nodes, indicating a severe neurological impairment. However, both the neurological score and forepaw outreaching score of ME rats obviously decreased over time after surgery, which means mild recovery after ME, and PNS administration effectively attenuated the neurological deficits in ME rats at different time nodes. Compared with ME group, on day 1 after surgery, PNS 120 mg/kg significantly reduced the neurological score and forepaw outreaching score, on day 3 after surgery, PNS 120 mg/kg significantly reduced the forepaw outreaching score and PNS 60 mg/kg significantly reduced neurological score, on day 7 after surgery, PNS 30, 60, 120, and 240 mg/kg significantly reduced the neurological score and forepaw outreaching score, on day 14 after surgery, PNS 30, 60, 120, and 240 mg/kg significantly reduced the neurological score and forepaw outreaching score, PNS 15 mg/kg significantly reduced the forepaw outreaching score, and PNS 120 and 240 mg/kg significantly reduced the rope-climbing test score. Overall, PNS 30, 60, and 120 mg/kg group appeared to function relatively well. As shown in **Figure 2D**, remarkedly time-dependent increase in weight percentage of Sham, ME and PNS treatment rats were all observed, and the weight percentage was obviously decreased in ME group compared with sham group at different time nodes, however, treatment with PNS treatment exhibited an increase in ME rats on day 3, 7, and 14 after surgery. Compared with ME group, on day 3 after surgery, PNS 15 and 30 mg/kg significantly increased the weight percentage, on day 7

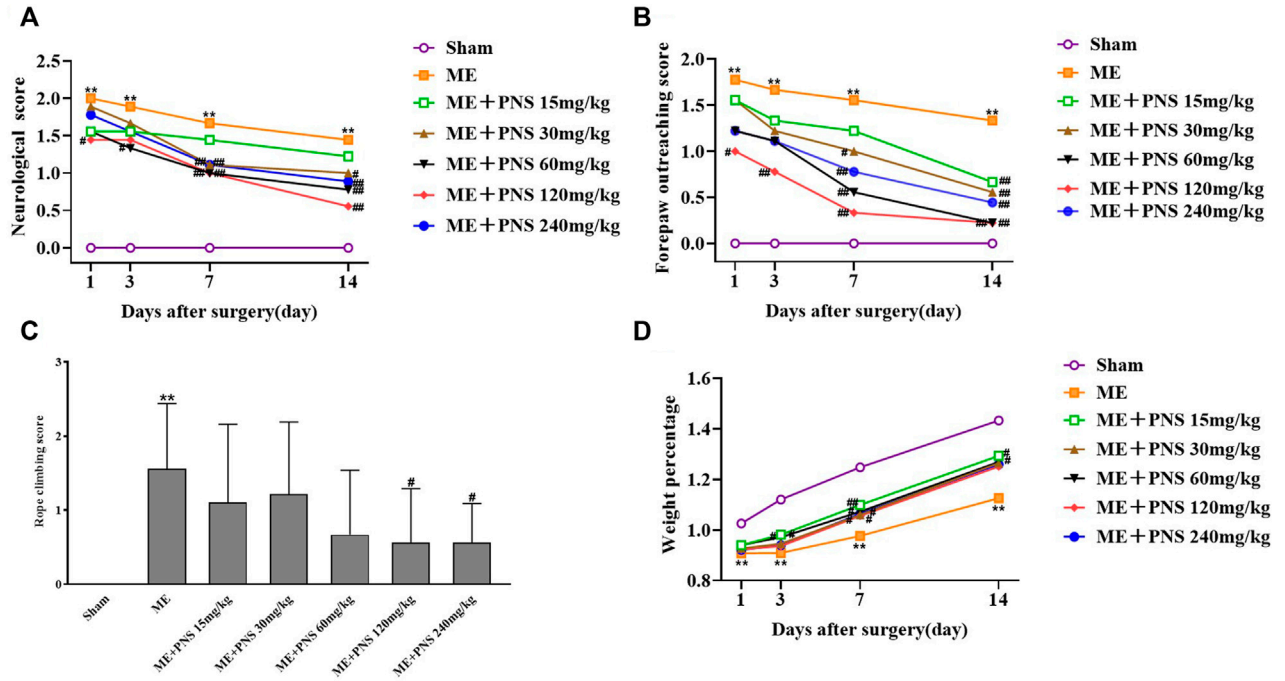

FIGURE 2 | PNS treatment improved the recovery of neurological functions in ME rats. Comparison of neurological score, forepaw outreaching score and weight percentage were measured at day 1, 3, 7, and 14 after ME surgery at different time nodes. Rope climbing test score were detected at day 14 after ME surgery. **(A)** Neurological score **(B)** Forepaw outreaching test score **(C)** Rope climbing test score **(D)** Weight percentage. The data in experiment **(A,B,D)** were shown as means and the data in experiment **(C)** were presented as means ± standard deviation (n = 9 animals per group). $^{*}p < 0.05$, $^{**}p < 0.01$ versus Sham group; $^{\#}p < 0.05$, $^{\#\#}p < 0.01$ versus ME group.

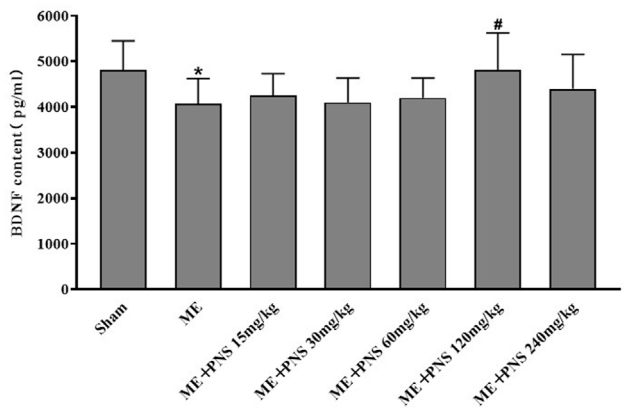

FIGURE 3 | PNS administration promoted BDNF protein levels in the serum of ME rats. Expression level of BDNF was measured by ELISA and data were presented as means ± standard deviation, n = 8 in sham and ME, n = 7 in other groups. $^{*}p < 0.05$, $^{**}p < 0.01$ versus Sham group; $^{\#}p < 0.05$, $^{\#\#}p < 0.01$ versus ME group.

after surgery, PNS 15, 30, 60, 120, and 240 mg/kg significantly increased the weight percentage, and on day 14 after surgery, PNS 15 and 60 mg/kg significantly increased the weight percentage. Taken together, these results indicated that PNS treatment ameliorated neurological function deficits induced by ME in rats.

3.2 *P. notoginseng* Saponins Administration Attenuated Microsphere Embolism-Induced Decrease of Brain-Derived Neurotrophic Factor Content in the Serum

As shown in **Figure 3**, ME-induced cerebral ischemia led to an obvious downregulation of BDNF protein level in the serum compared with sham group, whereas administration with 15, 30, 60, 120, and 240 mg/kg PNS for 14 days all attenuated ME-induced decrease of BDNF content. Among which, ME + PNS 120 mg/kg group significantly increased the BDNF concentration after ME.

3.3 *P. notoginseng* Saponins Administration Increased the Number of Viable Neurons and Alleviated Pathological Damage in Hippocampus of Microsphere Embolism Rats

HE staining was carried out to investigate the morphological changes of brain tissue. As shown in **Figure 4**, neuronal cells in the CA1, CA3, and DG regions of hippocampus were intact without vacuoles and necrosis, the cytoplasm was rich and uniform, cells were arranged neatly and connected tightly in sham group. But in ME group, obvious neuronal injuries were observed, including infarctions and a large area of vacuoles,

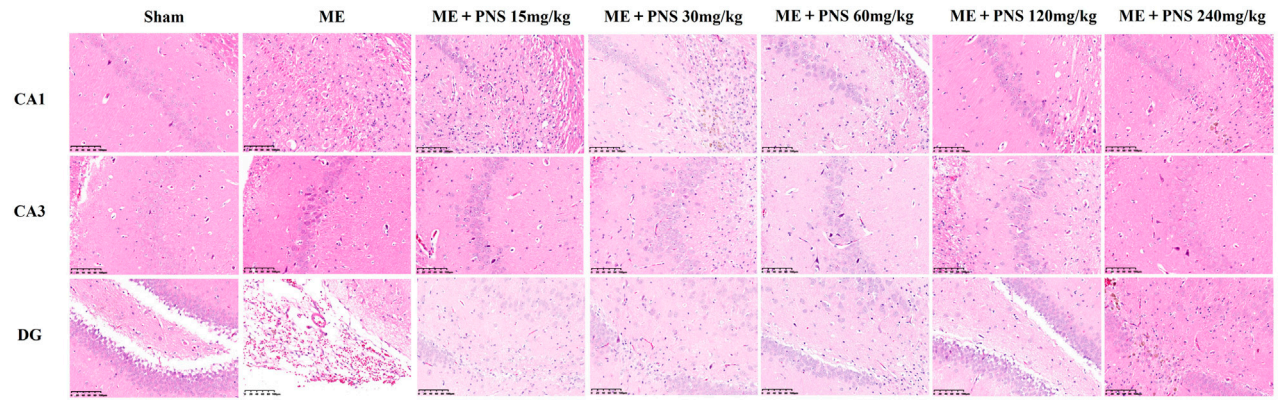

FIGURE 4 | Effect of PNS on histopathological changes of hippocampal CA1, CA3, and DG in ME rats under a ×200 light microscope (scale bar = 100 μm).

accompanied by inflammatory cell infiltration. The neuronal cells were loosed and disordered, the widened intercellular space and decreased intact neurons could be clearly seen. However, these histopathological injuries were attenuated after PNS treatment and smaller infarctions, reduced inflammatory cell infiltration and more intact neurons were found in PNS-treated groups, among which ME + PNS 30, 60, or 120 mg/kg group seemed to play a relatively good effect.

These above experimental results showed that PNS 30, 60, or 120 mg/kg presented the optimal effect, may be the appropriate doses and were then enrolled in the following experiments to further explore the effect of PNS on neurogenesis, synaptic plasticity and underlying mechanism through immunofluorescence and Western Blot.

3.4 *P. notoginseng* Saponins Administration Stimulated Post-ischemic Hippocampal Neurogenesis in Microsphere Embolism Rats

To determine whether the long-term effect of PNS on ischemic stroke benefits from the proliferation, migration and differentiation of newborn neuronal cells, we detected the BrdU/Nestin, BrdU/DCX double labelled and NeuroD1 single labelled, presumably NSC/NPCs, migrating neuroblasts and differentiated immature neurons respectively.

As illustrated in **Figures 5A,B,D**, in sham group, almost few BrdU/Nestin and BrdU/DCX were found in DG, however, both the numbers of BrdU/Nestin and BrdU/DCX were remarkably increased in damaged DG zone of ME rats, demonstrating that the proliferation and migration of NSC/NPC were triggered in response to cerebral ischemia. Besides, both the double-positive cells of BrdU/Nestin and BrdU/DCX in PNS 120 mg/kg group were significantly upregulated compared with ME rats, showing that PNS owned the ability to promote NSC/NPC proliferation and migration after cerebral ischemia.

Similarly, as we can see from **Figures 5C,D**, in the impaired DG of ME rats, NeuroD1 obviously expanded as compared with sham group. Besides, the number of NeuroD1-positive cell of PNS 60 and 120 mg/kg group was obviously higher than that of ME group, showing that PNS could further promote the neuronal differentiation.

These findings suggested that PNS could enhance the proliferation, migration and differentiation of NSC/NPC in the DG after ME.

3.5 *P. notoginseng* Saponins Administration Modulated Synaptic Plasticity by Increasing the Expressions of Brain-Derived Neurotrophic Factor and Synaptic Formation-Related Proteins GAP43, SYP, and PSD95 in the Hippocampus of Microsphere Embolism Rats

BDNF, a key neurotrophic factor produced in the brain, has been proved to protect neurons and promote neurogenesis and synaptic plasticity during ischemic stroke. To evaluate the effects of PNS on synaptic connectivity after cerebral ischemia, BDNF, GAP43 (the crucial component of axonal outgrowth), SYP (presynaptic marker), PSD95 (postsynaptic marker) were examined. As presented in **Figures 6A–D**, the expression levels of BDNF, GAP43, SYP, and PSD95 were all significantly downregulated in response to ME, which was reversely promoted by PNS administration in a dose-dependent manner, indicating that PNS was possibly involved in the beneficial effect of synaptic plasticity in ME rats.

3.6 *P. notoginseng* Saponins Administration Activated Akt/mTOR/p70S6K Pathway in Microsphere Embolism Rats

AKT/mTOR signaling plays a crucial role in stimulating neurogenesis and synaptic plasticity. To further explore the potential molecular mechanisms of PNS in promoting neurogenesis and expression of synaptic formation-related proteins induced by ME, we investigated whether PNS results in some changes in the AKT-mTOR-p70S6K pathway. The protein levels of p-Akt, Akt, p-mTOR, mTOR, p-p70S6K, and p70S6K were

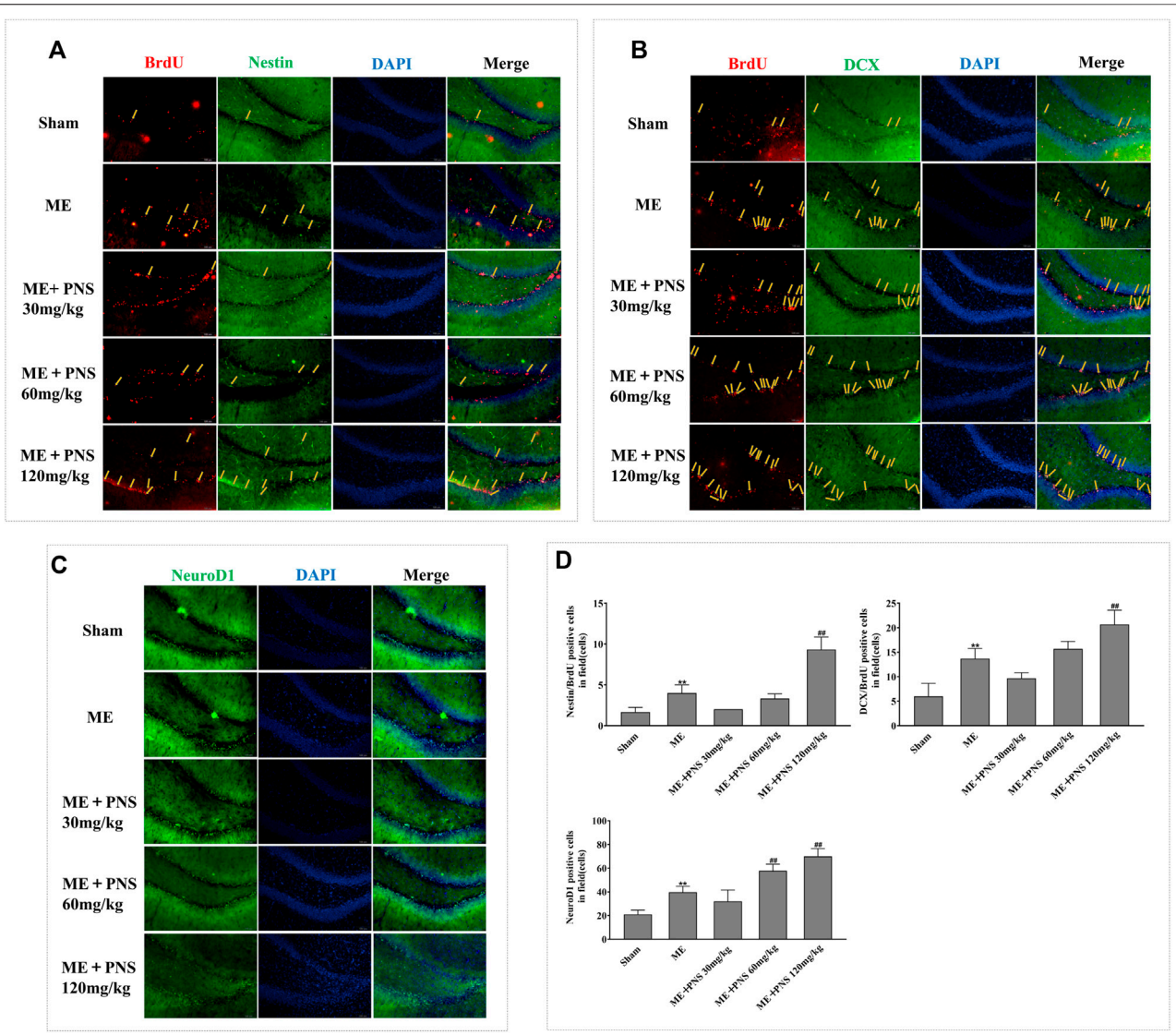

FIGURE 5 | PNS administration stimulated post-ischemic hippocampal neurogenesis in ME rats. Representative images of ipsilateral hemisphere sctions under a fluorescence microscope at a magnification of ×200 (scale bar =100 μm) were shown as **(A)** BrdU (red, a marker of proliferating cells) and Nestin (green, a marker of NSC/NPC); **(B)** BrdU (red) and DCX (green, a marker of migrating neuroblasts); **(C)** NeuroD1 (green, a marker of differentiation factor). **(D)** The numbers of double-positive of BrdU/Nestin, BrdU/DCX, and single-positive NeuroD1 were analyzed and data were presented as means ± standard deviation (n = 3 animals per group). $^{*}p < 0.05$, $^{**}p < 0.01$ versus Sham group; $^{\#}p < 0.05$, $^{\#\#}p < 0.01$ versus ME group.

measured by Western blot. As depicted in **Figures 7A–C**, the ratios of p-Akt/Akt, p-mTOR/mTOR, and p-p70S6K/p70S6K remarkably descended after ME. However, PNS administration dramatically raised the p-Akt/Akt, p-mTOR/mTOR, and p-p70S6K/p70S6K ratios in a dose-dependent manner, suggesting that Akt/mTOR/p70S6K pathway might participate in the protective mechanisms of PNS against cerebral ischemia injury.

4 DISCUSSION

Stroke is a leading cause of physical disability and death worldwide, characterized by high rates of morbidity, mortality, disability and recurrence, including hemorrhagic and ischemic stroke, and the latter accounts for a large proportion (Liu et al., 2019; Sun et al., 2020b). Although there are many drugs developed to cure stroke symptoms, the effective treatment for management in patients is limited and sequelae of severe neurological damage remain irreversible. Ischemia-induced spontaneous neurogenesis is beneficial but not sufficient, therefore in the present study, we explored the effect of PNS on endogenous NSCs/NPCs in a rat of ME model.

Oral clinical preparations with PNS as the main component, such as Xueshuantong soft capsule, Xuesaitong tablet or granule, were often used to treat cerebrovascular sequelae, and the clinical PNS dosage was 2.5–10 mg/kg individually per day, which could be transformed into 15.75–63 mg/kg daily for rats (obversion

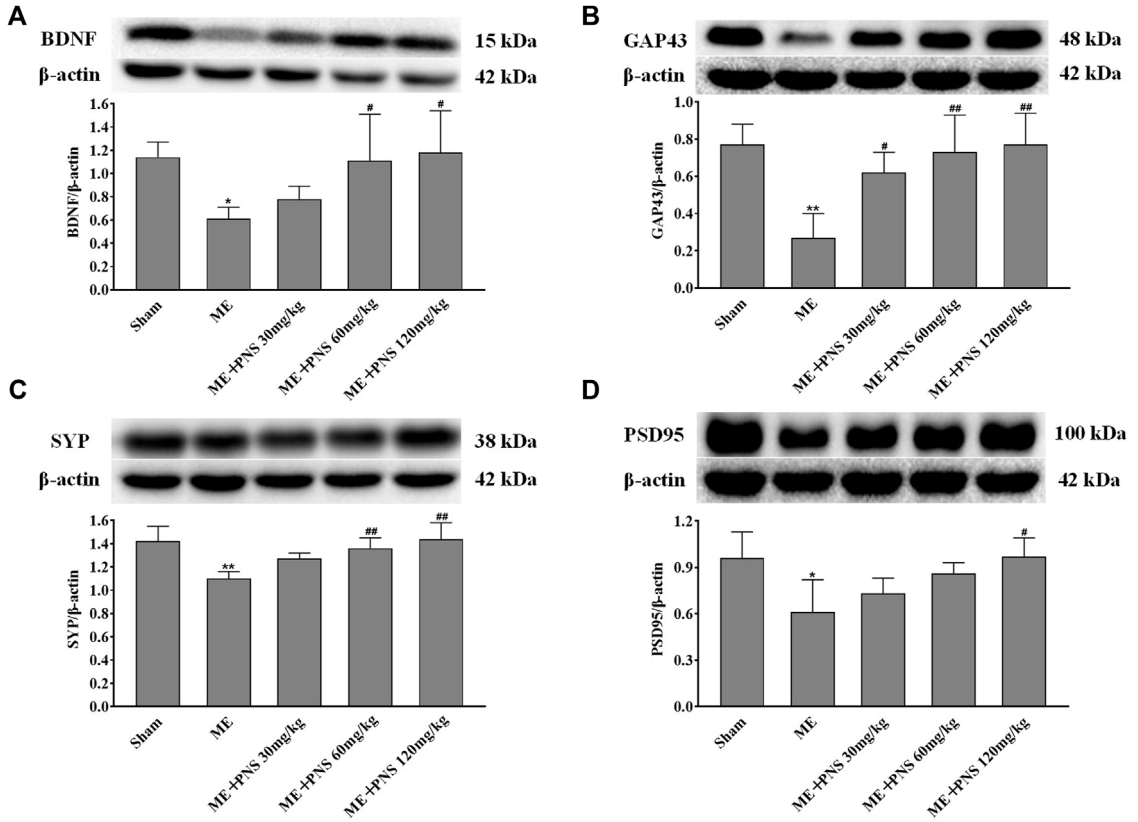

FIGURE 6 | PNS administration enhanced synaptic plasticity by increasing the expressions of BDNF and synaptic formation-related proteins GAP43, SYP, and PSD95 in hippocampus of ME Rats. The expressions of BDNF **(A)**, GAP43 **(B)**, SYP **(C)**, and PSD95 **(D)** in hippocampus tissues were assessed by Western blot. Data were presented as means ± standard deviation (n = 3 animals per group). $^{*}p < 0.05$, $^{**}p < 0.01$ versus Sham group; $^{\#}p < 0.05$, $^{\#\#}p < 0.01$ versus ME group.

coefficient = 6.3). What's more, plenty of previous studies have shown that 30–120 mg/kg PNS is optimal for protection against cerebral ischemia injuries in animal models (Wu et al., 2016), and lower or higher dose, such as 10 or 300 mg/kg, has also been orally given to the rats in some studies (Fan et al., 2015; Zhou et al., 2018). Therefore, in this study, PNS dosage was selected as 15, 30, 60, 120, and 240 mg/kg, which is 1.5, 3, 6, 12, and 24 times the maximum clinical dose (10 mg/kg) respectively. Our results showed that PNS treatment ameliorated neurological function deficits induced by ME in rats, and PNS 30, 60 and 120 mg/kg seemed to play a relatively good effect.

Our findings revealed that PNS relieved neurological deficits and hippocampal pathological damage caused by cerebral ischemia. Moreover, PNS increased hippocampal neurogenesis by reinforcing the proliferation, migration and differentiation activity of NSC/NPCs in the post-ischemic DG and modulated synaptic plasticity by strengthening the expression of synaptic formation-related proteins GAP43, SYP, and PSD95 in the hippocampus. Meanwhile, BDNF upregulation and activation of Akt/mTOR/p70S6K pathway could partially underlie the neuroprotective effects of PNS against cerebral ischemia injury.

Cerebral ischemia could stimulate neurogenesis in the DG and enhanced hippocampal neurogenesis may be a compensatory adaptive response to ischemia-induced injuries, which contributes to improvement of neurological function and remodeling of brain structures after stroke (Liu et al., 1998; Sun et al., 2020a). Enhancing endogenous neurogenesis is important for recovery of neurological function after stroke, and some studies have shown that neurological deficits were improved in ischemic stroke rat *via* increasing neurogenesis (Li et al., 2018; Cheng et al., 2020). Our results showed that PNS alleviated neurological deficits and hippocampal pathological damage after ischemic stroke, then to determine whether improved neurological function benefited from enhanced neurogenesis in hippocampal dentate gyrus, we detected major indicators of neurogenesis by immunofluorescence. In the DG, newly born neurons are locally generated at the border between the hilus and the granule cell layer and then migrate into the granule cell layer, where they gradually matured both morphologically and functionally and finally integrated into neural circuits (Stanfield and Trice, 1988). Here, we used BrdU (5-Bromo-2-deoxyUridine) as a principal proliferative marker of only dividing cells during neurogenesis, which is an analogue for an endogenous DNA base thymidine, could track the fate of divided cells and their progeny *via* the substitution of thymidine during the S phase of mitosis and participate in the process of newly synthesized DNA (Moon et al., 2016). As an initial response to neurogenesis, it is necessary to enhance endogenous NSC proliferation, which helps to promote the migration, differentiation and survival of newborn neurons. Nestin

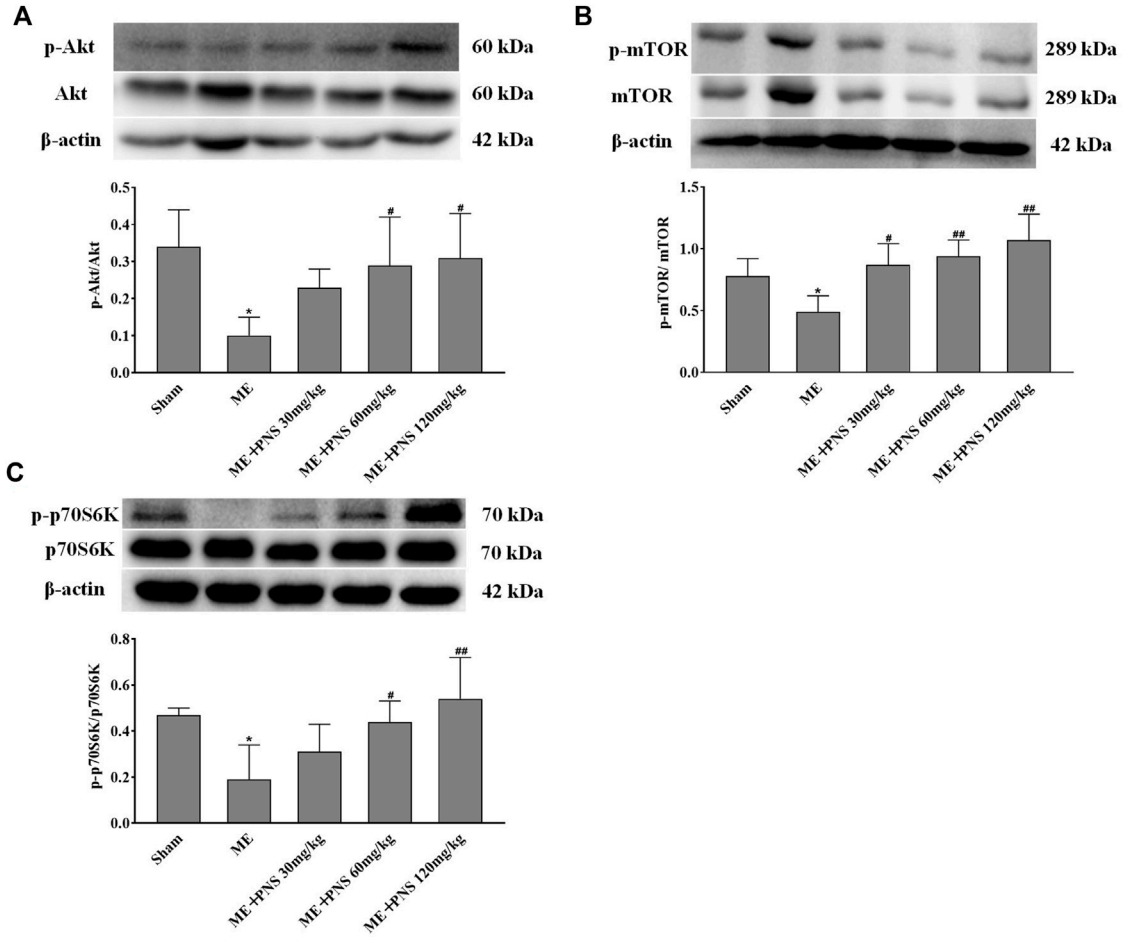

FIGURE 7 | PNS administration activated Akt/mTOR/p70S6K pathway in ME rats. (**A–C**) The protein levels of p-Akt, Akt, p-mTOR, mTOR, p-p70S6K, and p70S6K in hippocampus tissues were detected by Western blot. Data were shown as means ± standard deviation (n = 3 animals per group). $^{*}p < 0.05$, $^{**}p < 0.01$ verssus Sham group; $^{\#}p < 0.05$, $^{\#\#}p < 0.01$ versus ME group.

has been widely recognized as a marker of NSC/NPCs and double-labelled BrdU/Nestin was used for the identification of newly generated NSCs in the DG (von Bohlen und Halbach, 2011; Zhang et al., 2020). Therefore, we used BrdU/Nestin to evaluate DG cellular proliferative ability at day 14 post-ME, and the immunofluorescence staining results presented that BrdU/Nestin expression in the DG began to increase after ME, which denoted an activated proliferative characteristic of NSC as a response to cerebral ischemia, and PNS 120 mg/kg administration remarkedly advanced BrdU/Nestin expression, suggesting that PNS could augment the number of NSC populations in the hippocampus. Doublecortin (DCX) is a microtubule-associated protein, to better specify whether PNS have potential benefits on immature neuroblasts, we detected BrdU/DCX double-labelled cell, which is usually accepted as a marker of newborn migrating neuroblasts (Gleeson et al., 1999). Researchers reported that PNS treatment enhanced DCX^{+} expressions in the olfactory bulb at day 14 after global brain ischemia/reperfusion (He et al., 2015). Similar to these results, our findings revealed that expressions of BrdU/DCX in the DG of PNS 60 and 120 mg/kg groups were higher than ME groups, showing that PNS boosted NSCs to differentiate into immature neuroblasts. NeuroD1, a bHLH transcription factor indispensable for granule neuron differentiation, could foster the precursor cell lineage into immature neuron through differentiation (Hodge and Hevner, 2011; Brulet et al., 2017). In accordance with previous studies (Kisoh et al., 2017), our results also exhibited significantly upregulated expression of NeuroD1-positive cells in the DG after ME, which was further strengthened by PNS 60 and 120 mg/kg administration. All these results demonstrated that PNS advanced neurogenesis by reinforcing the proliferation, migration and differentiation ability of newborn cells after ME. And we speculated that enhancing the proliferation, migration, and differentiation of NSC/NPC after ME by PNS administration might be involved in the recovery of neurological function.

BDNF is regarded as an instructive intermedia of functional and structural plasticity in the brain, playing a critical role in enhancing adult hippocampal neurogenesis (Liu et al., 2018; Colucci-D'Amato et al., 2020). And low BDNF concentration has been associated with the rising risk of stroke. Researchers found that patients with acute stroke had significantly lower

BDNF levels in the serum compared to healthy controls and decreased concentration of BDNF in the serum was also found in cerebral ischemic rat model (Chen et al., 2012; Karantali et al., 2021). Moreover, previous studies have shown that levels of BDNF in the hippocampus were found to be obviously lower in ischemic rats than sham rats (Moriyama et al., 2011; Sheikholeslami et al., 2021). Therefore, in this study, we detected the levels of BDNF both in the serum and hippocampus tissue, consistent with these observations, our studies showed that BDNF levels in the serum and hippocampus of ME rats were both obviously decreased compared with sham rats, however, administration with 15, 30, 60, 120, and 240 mg/kg PNS for 14 days all attenuated ME-induced decrease of BDNF content in the serum. Among which, PNS 120 mg/kg group remarkedly increased the BDNF concentration in the serum after ME surgery. And BDNF expression in the hippocampus of PNS 30, 60, and 120 mg/kg groups was higher than ME group. We speculated that BDNF induction may be related to the protective mechanisms of PNS against cerebral ischemia injury.

Activating the mTOR signaling pathway revitalizes the NSCs, restores their proliferation and enhances hippocampal neurogenesis (Romine et al., 2015). The activity of mTOR is regulated through phosphorylation on its specific residue serine 2448, which is the target of upstream Akt and downstream p70 ribosomal S6 kinase (p70S6K), and phosphorylation of threonine 389 residue by mTOR is critical for p70S6K activation and serves as a marker for mTOR activity (Chong et al., 2010; Chong et al., 2013). When AKT/mTOR pathway is activated, the phosphorylation level of downstream substrate p70S6K is remarkably upregulated, thus the development, differentiation, survival and regeneration of neurons as well as protein translation can be promoted (Li et al., 2020).To further explore potential mechanisms of enhanced neurogenesis in the hippocampal DG after PNS treatment, we next chose hippocampus tissue to examine the expression of Akt-mTOR-p70S6K signaling. Our western blot results have shown that the ratio of p-Akt/Akt, p-mTOR/mTOR, and p-p70S6K/p70S6K was obviously reduced after ME compared with sham group, however, PNS administration enhanced phosphorylation of Akt, mTOR, and p70S6K dose-dependently after ME. We supposed that these quantitative changes of Akt, mTOR and p70S6K were caused by NSC in the hippocampal DG, and induction of neurogenesis was possibly associated with activation of Akt/mTOR/p70S6K signaling pathway.

After cerebral ischemia, axon remodeling and synaptic connectivity are critical for neurorehabilitation. Differentiated mature neurons are highly polarized cells that own two units, namely axons and dendrites, and transmission information between axons and dendrites in neurons mainly depends on synaptic function and plasticity. As a principal modulator of translation, activation of mTOR has also been linked with synapse-related protein synthesis and synaptic plasticity (Li et al., 2010; Xie et al., 2018; Xiong et al., 2018). Not only does BDNF have the ability to promote neurogenesis, but also appears to be vital to synaptic function and plasticity in the adult hippocampus (Rauti et al., 2020). Having proved that PNS increased BDNF expression and activated the Akt/mTOR/p70S6K pathway after ME in this study, we then focused on the expression of synapse-related proteins in the hippocampus to further identify whether PNS could also restore the disrupted synaptic function after cerebral ischemia. GAP43 (growth associated protein 43), a crucial component of axonal outgrowth, is involved in neurite outgrowth and axon regeneration during neuronal development (Abe et al., 2010; Yang et al., 2020). Previous studies found that GAP43 expression was obviously decreased after cerebral ischemia/reperfusion insults (Zhang et al., 2019; Chen et al., 2020) and similar to these results, GAP43 level was also dramatically declined after ME in our study, whereas PNS administration enhanced axonal growth capacity by upregulating GAP43 expression with a dose-dependent trend. The presynaptic marker SYP (synaptophysin) and postsynaptic marker PSD95 (post-synaptic density protein 95) are two major synaptic proteins, which were associated closely with synaptic formation and neurotransmission (Wu et al., 2019a). The nerve terminal of neurons is filled with some small synaptic vesicles, specialized secretory organelles participated in the storage and release of neurotransmitters, and SYP (presynaptic marker) is the major integral membrane protein of synaptic vesicles, indicates connections between neurons (Thiel, 1993; Cousin, 2021). PSD95 (postsynaptic scaffold protein) has been proved to be required for the final stages of morphological maturation and formation of dendritic spines, which are vital for the integration of hippocampal granule neurons (Mardones et al., 2019). Our results found that the expression of SYP and PSD95 proteins profoundly decreased after ME, which was in agreement with previous study showing downregulation of synaptic proteins after ischemia in adult animals (Zhang et al., 2018), indicating a failure in synaptic functioning. However, rats treated with PNS showed a higher expression of SYP and PSD95 than ME rats. We speculated the upregulation of GAP43, SYP, and PSD95 in the hippocampus by PNS administration were originated from nerve cells, mainly from neurons, implying that PNS probably induced production of synaptic connectivity between neurons. Overall, the above results revealed that PNS may contribute to mediating hippocampal synaptic plasticity through invoking the synapse-related proteins expression of GAP43, SYP, and PSD95.

Enhancing endogenous neurogenesis through drug stimulation might be an attractive strategy to recover the damaged neurons after stroke, and the ability of PNS to synchronously offer neuroprotection, promote neurogenesis and modulate synaptic plasticity perhaps make it a promising candidate for developing strategies to stimulate NSC/NPCs for neural repair after cerebral ischemia. In spite of these encouraging findings, whether these newborn NSC/NPC could gradually develop into mature neurons both structurally and functionally, forming appropriate synapse between newly NPC-derived neurons and host neurons and finally integrating into existing neural circuits needs to be explored in-depth in the future.

5 CONCLUSION

Taken together, our study demonstrated that PNS administration enhanced the recovery of neurological deficits and improved hippocampal pathological damage caused by cerebral ischemia. What's more, PNS stimulated hippocampal neurogenesis by promoting NSC/NPC proliferation, migration and differentiation activity and modulated synaptic plasticity. Meanwhile, upregulation of BDNF expression and activation of Akt/mTOR/p70S6K signaling

after ME could partially underlie the neuroprotective effects of PNS against cerebral ischemia injury. Our findings offer some new standpoints into the beneficial roles of PNS against ischemic stroke.

DATA AVAILABILITY STATEMENT

The original contributions presented in the study are included in the article/Supplementary Materials, further inquiries can be directed to the corresponding author.

ETHICS STATEMENT

The animal study was reviewed and approved by the Experimental Ethics Committee at Xiyuan hospital, China Academy of Chinese Medical Sciences. (No. 2019XLC016-2).

AUTHOR CONTRIBUTIONS

Study concepts and design: JL, JG, and MY; Experimental studies: MY and GW participated in partial preparation of ME rats, WZ helped cut the frozen brain sections, BY heartedly provided important guidance on HE staining and double immunofluorescence staining, and the preparation of other ME rats and following experiments were finished by JG; Reagents, materials, and analysis tools: JG; Writing manuscript: JG; Review and editing manuscript: JL; Funding acquisition: JL. All authors approved the final manuscript after reading.

FUNDING

This study was supported by grants from the National Nature Science Foundation of China (Grant No. 82030124) and Innovation Team and Talents Cultivation Program of National Administration of Traditional Chinese Medicine (No. ZYYCXTD-C-202007).

ACKNOWLEDGMENTS

We sincerely thank the Department of Pathology of Xiyuan Hospital for their support.

REFERENCES

Abe, N., Borson, S. H., Gambello, M. J., Wang, F., and Cavalli, V. (2010). Mammalian Target of Rapamycin (mTOR) Activation Increases Axonal Growth Capacity of Injured Peripheral Nerves. *J. Biol. Chem.* 285, 28034–28043. doi:10.1074/jbc.M110.125336

Brulet, R., Zhu, J., Aktar, M., Hsieh, J., and Cho, K. O. (2017). Mice with Conditional NeuroD1 Knockout Display Reduced Aberrant Hippocampal Neurogenesis but No Change in Epileptic Seizures. *Exp. Neurol.* 293, 190–198. doi:10.1016/j.expneurol.2017.04.005

Chen, A., Lin, Z., Lan, L., Xie, G., Huang, J., Lin, J., et al. (2012). Electroacupuncture at the Quchi and Zusanli Acupoints Exerts Neuroprotective Role in Cerebral Ischemia-Reperfusion Injured Rats via Activation of the PI3K/Akt Pathway. *Int. J. Mol. Med.* 30, 791–796. doi:10.3892/ijmm.2012.1074

Chen, S., Wang, H., Xu, H., Zhang, Y., and Sun, H. (2020). Electroacupuncture Promotes Axonal Regrowth by Attenuating the Myelin-Associated Inhibitors-Induced RhoA/ROCK Pathway in Cerebral Ischemia/reperfusion Rats. *Brain Res.* 1748, 147075. doi:10.1016/j.brainres.2020.147075

Cheng, J., Shen, W., Jin, L., Pan, J., Zhou, Y., Pan, G., et al. (2020). Treadmill Exercise Promotes Neurogenesis and Myelin Repair via Upregulating Wnt/β-catenin S-ignaling P-athways in the J-uvenile B-rain F-ollowing F-ocal C-erebral I-schemia/reperfusion. *Int. J. Mol. Med.* 45, 1447–1463. doi:10.3892/ijmm.2020.4515

Chong, Z. Z., Shang, Y. C., Zhang, L., Wang, S., and Maiese, K. (2010). Mammalian Target of Rapamycin: Hitting the Bull's-Eye for Neurological Disorders. *Oxid. Med. Cell Longev.* 3, 374–391. doi:10.4161/oxim.3.6.14787

Chong, Z. Z., Yao, Q., and Li, H. H. (2013). The Rationale of Targeting Mammalian Target of Rapamycin for Ischemic Stroke. *Cell Signal* 25, 1598–1607. doi:10.1016/j.cellsig.2013.03.017

Colucci-D'amato, L., Speranza, L., and Volpicelli, F. (2020). Neurotrophic Factor BDNF, Physiological Functions and Therapeutic Potential in Depression, Neurodegeneration and Brain Cancer. *Int. J. Mol. Sci.* 21. doi:10.3390/ijms21207777

Corsini, N. S., Sancho-Martinez, I., Laudenklos, S., Glagow, D., Kumar, S., Letellier, E., et al. (2009). The Death Receptor CD95 Activates Adult Neural Stem Cells for Working Memory Formation and Brain Repair. *Cell Stem Cell* 5, 178–190. doi:10.1016/j.stem.2009.05.004

Cousin, M. A. (2021). Synaptophysin-dependent Synaptobrevin-2 Trafficking at the Presynapse-Mechanism and Function. *J. Neurochem.* 159, 78–89. doi:10.1111/jnc.15499

Dillen, Y., Kemps, H., Gervois, P., Wolfs, E., and Bronckaers, A. (2020). Adult Neurogenesis in the Subventricular Zone and its Regulation after Ischemic Stroke: Implications for Therapeutic Approaches. *Transl. Stroke Res.* 11, 60–79. doi:10.1007/s12975-019-00717-8

Fan, J. Z., Wang, Y., Meng, Y., Li, G. W., Chang, S. X., Nian, H., et al. (2015). Panax Notoginseng Saponins Mitigate Ovariectomy-Induced Bone Loss and Inhibit Marrow Adiposity in Rats. *Menopause* 22, 1343–1350. doi:10.1097/GME.0000000000000471

Fh, G. (2000). Mammalian Neural Stem Cells. *Science* 287, 1433–1438.doi:10.1126/science.287.5457.1433

Garcia, J. H., Wagner, S., Liu, K. F., and Hu, X. J. (1995). Neurological Deficit and Extent of Neuronal Necrosis Attributable to Middle Cerebral Artery Occlusion in Rats. Statistical Validation. *Stat. validationStroke* 26, 627–635. doi:10.1161/01.str.26.4.627

Gleeson, J. G., Lin, P. T., Flanagan, L. A., and Walsh, C. A. (1999). Doublecortin Is a Microtubule-Associated Protein and Is Expressed Widely by Migrating Neurons. *Neuron* 23, 257–271. doi:10.1016/s0896-6273(00)80778-3

Guo, Z., and Yu, Q. (2019). Role of mTOR Signaling in Female Reproduction. *Front. Endocrinol. (Lausanne)* 10, 692. doi:10.3389/fendo.2019.00692

He, X., Deng, F. J., Ge, J. W., Yan, X. X., Pan, A. H., and Li, Z. Y. (2015). Effects of Total Saponins of Panax Notoginseng on Immature Neuroblasts in the Adult Olfactory Bulb Following Global Cerebral Ischemia/reperfusion. *Neural Regen. Res.* 10, 1450–1456. doi:10.4103/1673-5374.165514

Hodge, R. D., and Hevner, R. F. (2011). Expression and Actions of Transcription Factors in Adult Hippocampal Neurogenesis. *Dev. Neurobiol.* 71, 680–689. doi:10.1002/dneu.20882

Karantali, E., Kazis, D., Papavasileiou, V., Prevezianou, A., Chatzikonstantinou, S., Petridis, F., et al. (2021). Serum BDNF Levels in Acute Stroke: A Systematic Review and Meta-Analysis. *Med. Kaunas.* 57. doi:10.3390/medicina57030297

Kempermann, G., Song, H., and Gage, F. H. (2015). Neurogenesis in the Adult Hippocampus. *Cold Spring Harb. Perspect. Biol.* 7, a018812. doi:10.1101/cshperspect.a018812

Kisoh, K., Hayashi, H., Itoh, T., Asada, M., Arai, M., Yuan, B., et al. (2017). Involvement of GSK-3β Phosphorylation through PI3-K/Akt in Cerebral

Ischemia-Induced Neurogenesis in Rats. *Mol. Neurobiol.* 54, 7917–7927. doi:10.1007/s12035-016-0290-8

Koh, S. H., and Park, H. H. (2017). Neurogenesis in Stroke Recovery. *Transl. Stroke Res.* 8, 3–13. doi:10.1007/s12975-016-0460-z

Kong, X., Zhong, M., Su, X., Qin, Q., Su, H., Wan, H., et al. (2016). Tetramethylpyrazine Promotes Migration of Neural Precursor Cells via Activating the Phosphatidylinositol 3-Kinase Pathway. *Mol. Neurobiol.* 53, 6526–6539. doi:10.1007/s12035-015-9551-1

Li, N., Lee, B., Liu, R. J., Banasr, M., Dwyer, J. M., Iwata, M., et al. (2010). mTOR-Dependent Synapse Formation Underlies the Rapid Antidepressant Effects of NMDA Antagonists. *Science* 329, 959–964. doi:10.1126/science.1190287

Li, N., Song, X., Wu, L., Zhang, T., Zhao, C., Yang, X., et al. (2018). Miconazole Stimulates Post-ischemic Neurogenesis and Promotes Functional Restoration in Rats. *Neurosci. Lett.* 687, 94–98. doi:10.1016/j.neulet.2018.09.035

Li, W., Ye, A., Ao, L., Zhou, L., Yan, Y., Hu, Y., et al. (2020). Protective Mechanism and Treatment of Neurogenesis in Cerebral Ischemia. *Neurochem. Res.* 45, 2258–2277. doi:10.1007/s11064-020-03092-1

Liang, Q., Luo, Z., Zeng, J., Chen, W., Foo, S. S., Lee, S. A., et al. (2016). Zika Virus NS4A and NS4B Proteins Deregulate Akt-mTOR Signaling in Human Fetal Neural Stem Cells to Inhibit Neurogenesis and Induce Autophagy. *Cell Stem Cell* 19, 663–671. doi:10.1016/j.stem.2016.07.019

Licausi, F., and Hartman, N. W. (2018). Role of mTOR Complexes in Neurogenesis. *Int. J. Mol. Sci.* 19. doi:10.3390/ijms19051544

Liu, B., Zhang, Q., Ke, C., Xia, Z., Luo, C., Li, Y., et al. (2019). Ginseng-Angelica-Sansheng-Pulvis Boosts Neurogenesis against Focal Cerebral Ischemia-Induced Neurological Deficiency. *Front. Neurosci.* 13, 515. doi:10.3389/fnins.2019.00515

Liu, D., Ye, Y., Xu, L., Yuan, W., and Zhang, Q. (2018). Icariin and Mesenchymal Stem Cells Synergistically Promote Angiogenesis and Neurogenesis after Cerebral Ischemia via PI3K and ERK1/2 Pathways. *Biomed. Pharmacother.* 108, 663–669. doi:10.1016/j.biopha.2018.09.071

Liu, J., Solway, K., Messing, R. O., and Sharp, F. R. (1998). Increased Neurogenesis in the Dentate Gyrus after Transient Global Ischemia in Gerbils. *J. Neurosci.* 18, 7768–7778. doi:10.1523/jneurosci.18-19-07768.1998

Liu, J., Wang, L. N., Tan, J. P., Ji, P., Gauthier, S., Zhang, Y. L., et al. (2012). Burden, Anxiety and Depression in Caregivers of Veterans with Dementia in Beijing. *Arch. Gerontol. Geriatr.* 55, 560–563. doi:10.1016/j.archger.2012.05.014

Luo, H., Vong, C. T., Tan, D., Zhang, J., Yu, H., Yang, L., et al. (2021). Panax Notoginseng Saponins Modulate the Inflammatory Response and Improve IBD-like Symptoms via TLR/NF-[Formula: See Text]B and MAPK Signaling Pathways. *Am. J. Chin. Med.* 49, 925–939. doi:10.1142/S0192415X21500440

Mardones, M. D., Jorquera, P. V., Herrera-Soto, A., Ampuero, E., Bustos, F. J., Van Zundert, B., et al. (2019). PSD95 Regulates Morphological Development of Adult-Born Granule Neurons in the Mouse hippocampus. *J. Chem. Neuroanat.* 98, 117–123. doi:10.1016/j.jchemneu.2019.04.009

Moon, M., Jeong, H. U., Choi, J. G., Jeon, S. G., Song, E. J., Hong, S. P., et al. (2016). Memory-enhancing Effects of Cuscuta Japonica Choisy via Enhancement of Adult Hippocampal Neurogenesis in Mice. *Behav. Brain Res.* 311, 173–182. doi:10.1016/j.bbr.2016.05.031

Moriyama, Y., Takagi, N., and Tanonaka, K. (2011). Intravenous Injection of Neural Progenitor Cells Improved Depression-like Behavior after Cerebral Ischemia. *Transl. Psychiatry* 1, e29. doi:10.1038/tp.2011.32

Ohlsson, A. L., and Johansson, B. B. (1995). Environment Influences Functional Outcome of Cerebral Infarction in Rats. *Stroke* 26, 644–649. doi:10.1161/01.str.26.4.644

Park, Kk., Liu, K., Hu, Y., Smith, P. D., Wang, C., Cai, B., et al. (2008). Promoting Axon Regeneration in the Adult CNS by Modulation of the PTEN/mTOR Pathway. *Science* 322, 963–966. doi:10.1126/science.1161566

Piermartiri, T. C. B., Dos Santos, B., Barros-Aragão, F. G. Q., Prediger, R. D., and Tasca, C. I. (2020). Guanosine Promotes Proliferation in Neural Stem Cells from Hippocampus and Neurogenesis in Adult Mice. *Mol. Neurobiol.* 57, 3814–3826. doi:10.1007/s12035-020-01977-4

Rauti, R., Cellot, G., D'andrea, P., Colliva, A., Scaini, D., Tongiorgi, E., et al. (2020). BDNF Impact on Synaptic Dynamics: Extra or Intracellular Long-Term Release Differently Regulates Cultured Hippocampal Synapses. *Mol. Brain* 13, 43. doi:10.1186/s13041-020-00582-9

Romine, J., Gao, X., Xu, X. M., So, K. F., and Chen, J. (2015). The Proliferation of Amplifying Neural Progenitor Cells Is Impaired in the Aging Brain and Restored by the mTOR Pathway Activation. *Neurobiol. Aging* 36, 1716–1726. doi:10.1016/j.neurobiolaging.2015.01.003

Sheikholeslami, M. A., Ghafghazi, S., Pouriran, R., Mortazavi, S. E., and Parvardeh, S. (2021). Attenuating Effect of Paroxetine on Memory Impairment Following Cerebral Ischemia-Reperfusion Injury in Rat: The Involvement of BDNF and Antioxidant Capacity. *Eur. J. Pharmacol.* 893, 173821. doi:10.1016/j.ejphar.2020.173821

Si, Y. C., Zhang, J. P., Xie, C. E., Zhang, L. J., and Jiang, X. N. (2011). Effects of Panax Notoginseng Saponins on Proliferation and Differentiation of Rat Hippocampal Neural Stem Cells. *Am. J. Chin. Med.* 39, 999–1013. doi:10.1142/S0192415X11009366

Stanfield, B. B., and Trice, J. E. (1988). Evidence that Granule Cells Generated in the Dentate Gyrus of Adult Rats Extend Axonal Projections. *Exp. Brain Res.* 72, 399–406. doi:10.1007/BF00250261

Sun, L., Zhang, H., Wang, W., Chen, Z., Wang, S., Li, J., et al. (2020a). Astragaloside IV Exerts Cognitive Benefits and Promotes Hippocampal Neurogenesis in Stroke Mice by Downregulating Interleukin-17 Expression via Wnt Pathway. *Front. Pharmacol.* 11, 421. doi:10.3389/fphar.2020.00421

Sun, X., Wang, D., Zhang, T., Lu, X., Duan, F., Ju, L., et al. (2020b). Eugenol Attenuates Cerebral Ischemia-Reperfusion Injury by Enhancing Autophagy via AMPK-mTOR-P70s6k Pathway. *Front. Pharmacol.* 11, 84. doi:10.3389/fphar.2020.00084

Takeo, S., Miyake, K., Minematsu, R., Tanonaka, K., and Konishi, M. (1989). *In Vitro* effect of Naftidrofuryl Oxalate on Cerebral Mitochondria Impaired by Microsphere-Induced Embolism in Rats. *J. Pharmacol. Exp. Ther.* 248, 1207–1214.

Thiel, G. (1993). Synapsin I, Synapsin II, and Synaptophysin: Marker Proteins of Synaptic Vesicles. *Brain Pathol.* 3, 87–95. doi:10.1111/j.1750-3639.1993.tb00729.x

Von Bohlen Und Halbach, O. (2011). Immunohistological Markers for Proliferative Events, Gliogenesis, and Neurogenesis within the Adult hippocampus. *Cell Tissue Res.* 345, 1–19. doi:10.1007/s00441-011-1196-4

Wu, L., Cao, J., Li, N., Chen, H., Liu, W., Zhang, G., et al. (2019a). Novel Neuroprotective Tetramethylpyrazine Analog T-006 Promotes Neurogenesis and Neurological Restoration in a Rat Model of Stroke. *Neuroreport* 30, 658–663. doi:10.1097/WNR.0000000000001256

Wu, T., Jia, Z., Dong, S., Han, B., Zhang, R., Liang, Y., et al. (2019b). Panax Notoginseng Saponins Ameliorate Leukocyte Adherence and Cerebrovascular Endothelial Barrier Breakdown upon Ischemia-Reperfusion in Mice. *J. Vasc. Res.* 56, 1–10. doi:10.1159/000494935

Wu, T., Sun, J., Kagota, S., Maruyama, K., Wakuda, H., and Shinozuka, K. (2016). Panax Notoginseng Saponins Ameliorate Impaired Arterial Vasodilation in SHRSP.Z-Lepr(fa) /lzmDmcr Rats with Metabolic Syndrome. *Clin. Exp. Pharmacol. Physiol.* 43, 459–467. doi:10.1111/1440-1681.12547

Xie, Y. C., Yao, Z. H., Yao, X. L., Pan, J. Z., Zhang, S. F., Zhang, Y., et al. (2018). Glucagon-Like Peptide-2 Receptor Is Involved in Spatial Cognitive Dysfunction in Rats after Chronic Cerebral Hypoperfusion. *J. Alzheimers Dis.* 66, 1559–1576. doi:10.3233/JAD-180782

Xiong, T., Qu, Y., Wang, H., Chen, H., Zhu, J., Zhao, F., et al. (2018). GSK-3beta/mTORC1 Couples Synaptogenesis and Axonal Repair to Reduce Hypoxia Ischemia-Mediated Brain Injury in Neonatal Rats. *J. Neuropathol. Exp. Neurol.* 77, 383–394. doi:10.1093/jnen/nly015

Yamaguchi, M., Seki, T., Imayoshi, I., Tamamaki, N., Hayashi, Y., Tatebayashi, Y., et al. (2016). Neural Stem Cells and Neuro/gliogenesis in the Central Nervous System: Understanding the Structural and Functional Plasticity of the Developing, Mature, and Diseased Brain. *J. Physiol. Sci.* 66, 197–206. doi:10.1007/s12576-015-0421-4

Yang, K., Zhou, Y., Zhou, L., Yan, F., Guan, L., Liu, H., et al. (2020). Synaptic Plasticity after Focal Cerebral Ischemia Was Attenuated by Gap26 but Enhanced by GAP-134. *Front. Neurol.* 11, 888. doi:10.3389/fneur.2020.00888

Zhang, B., Chen, X., Lv, Y., Wu, X., Gui, L., Zhang, Y., et al. (2019). Cdh1 Overexpression Improves Emotion and Cognitive-Related Behaviors via Regulating Hippocampal Neuroplasticity in Global Cerebral Ischemia Rats. *Neurochem. Int.* 124, 225–237. doi:10.1016/j.neuint.2019.01.015

Zhang, G., Zhang, T., Li, N., Wu, L., Gu, J., Li, C., et al. (2018). Tetramethylpyrazine Nitrone Activates the BDNF/Akt/CREB Pathway to Promote Post-ischaemic Neuroregeneration and Recovery of Neurological Functions in Rats. *Br. J. Pharmacol.* 175, 517–531. doi:10.1111/bph.14102

Zhang, Q., Zhao, Y., Xu, Y., Chen, Z., Liu, N., Ke, C., et al. (2016). Sodium Ferulate and N-Butylidenephthalate Combined with Bone Marrow Stromal Cells (BMSCs) Improve the Therapeutic Effects of Angiogenesis and Neurogenesis after Rat Focal Cerebral Ischemia. *J. Transl. Med.* 14, 223. doi:10.1186/s12967-016-0979-5

Zhang, X., Hei, Y., Bai, W., Huang, T., Kang, E., Chen, H., et al. (2020). Toll-Like Receptor 2 Attenuates Traumatic Brain Injury-Induced Neural Stem Cell Proliferation in Dentate Gyrus of Rats. *Neural Plast.* 2020, 9814978. doi:10.1155/2020/9814978

Zhou, Z., Wang, J., Song, Y., He, Y., Zhang, C., Liu, C., et al. (2018). Panax Notoginseng Saponins Attenuate Cardiomyocyte Apoptosis through Mitochondrial Pathway in Natural Aging Rats. *Phytother. Res.* 32, 243–250. doi:10.1002/ptr.5961

Zhu, S. Z., Szeto, V., Bao, M. H., Sun, H. S., and Feng, Z. P. (2018). Pharmacological Approaches Promoting Stem Cell-Based Therapy Following Ischemic Stroke Insults. *Acta Pharmacol. Sin.* 39, 695–712. doi:10.1038/aps.2018.23

Conflict of Interest: The authors declare that the research was conducted in the absence of any commercial or financial relationships that could be construed as a potential conflict of interest.

Publisher's Note: All claims expressed in this article are solely those of the authors and do not necessarily represent those of their affiliated organizations, or those of the publisher, the editors and the reviewers. Any product that may be evaluated in this article, or claim that may be made by its manufacturer, is not guaranteed or endorsed by the publisher.

frontiers | Frontiers in Pharmacology

TYPE Original Research
PUBLISHED 15 July 2022
DOI 10.3389/fphar.2022.949290

OPEN ACCESS

EDITED BY
Yongjun Sun,
Hebei University of Science and Technology, China

REVIEWED BY
Yuhua Chen,
Central South University, China
Jae Sang Oh,
Soon Chun Hyang University Cheonan Hospital, South Korea

*CORRESPONDENCE
Yangmin Zheng,
zhengyangmin@xwhosp.org
Yumin Luo,
yumin111@ccmu.edu.cn

SPECIALTY SECTION
This article was submitted to Neuropharmacology, a section of the journal Frontiers in Pharmacology

RECEIVED 20 May 2022
ACCEPTED 28 June 2022
PUBLISHED 15 July 2022

CITATION
Zhao F, Wang R, Huang Y, Li L, Zhong L, Hu Y, Han Z, Fan J, Liu P, Zheng Y and Luo Y (2022), Elevated plasma syndecan-1 as glycocalyx injury marker predicts unfavorable outcomes after rt-PA intravenous thrombolysis in acute ischemic stroke.
Front. Pharmacol. 13:949290.
doi: 10.3389/fphar.2022.949290

Elevated plasma syndecan-1 as glycocalyx injury marker predicts unfavorable outcomes after rt-PA intravenous thrombolysis in acute ischemic stroke

Fangfang Zhao[1], Rongliang Wang[1,2], Yuyou Huang[1,2], Lingzhi Li[1,2], Liyuan Zhong[1,2], Yue Hu[1,2], Ziping Han[1,2], Junfen Fan[1,2], Ping Liu[1], Yangmin Zheng[1,2]* and Yumin Luo[1,2,3]*

[1]Institute of Cerebrovascular Disease Research and Department of Neurology, Xuanwu Hospital of Capital Medical University, Beijing, China, [2]Beijing Geriatric Medical Research Center and Beijing Key Laboratory of Translational Medicine for Cerebrovascular Diseases, Beijing, China, [3]Beijing Institute for Brain Disorders, Capital Medical University, Beijing, China

Purpose: We aimed to examine the prognostic value of syndecan-1 as a marker of glycocalyx injury in patients with acute ischemic stroke (AIS) receiving rt-PA intravenous thrombolysis.

Methods: The study included 108 patients with AIS treated with rt-PA intravenous thrombolysis and 47 healthy controls. Patients were divided into unfavorable and favorable prognosis groups based on modified Rankin Scale scores. Univariate and multivariate logistic regression analyses were used to determine risk factors affecting prognosis. Risk prediction models presented as nomograms. The predictive accuracy and clinical value of the new model were also evaluated.

Results: Plasma levels of syndecan-1 were significantly higher in patients with AIS than in controls ($p < 0.05$). Univariate analysis indicated that higher levels of syndecan-1 were more frequent in patients with poor prognosis than in those with good prognosis ($t = -4.273$, $p < 0.001$). Syndecan-1 alone and in combination with other factors predicted patient outcomes. After adjusting for confounding factors, syndecan-1 levels remained associated with poor prognosis [odds ratio, 1.024; 95% confidence interval (CI), 1.010–1.038]. The risk model exhibited a good fit, with an area under the receiver operating characteristic curve of 0.935 (95% CI, 0.888–0.981). The categorical net reclassification index (NRI) and continuous NRI values were >0. The integrated discrimination improvement value was 0.111 (95% CI, 0.049–0.174, $p < 0.001$). Decision curve analysis indicated that the model incorporating syndecan-1 levels was more clinically valuable than the conventional model.

Conclusion: Plasma syndecan-1 levels represent a potential marker of prognosis of AIS following intravenous thrombolysis. Adding syndecan-1 to the conventional model may improve risk stratification.

KEYWORDS
syndecan-1, acute ischemic stroke, rt-PA, prognosis, glycocalyx

Introduction

Ischemic stroke is the leading cause of disability and the third leading cause of death worldwide, following heart disease and cancer, accounting for approximately 5.5 million deaths globally, two-thirds of which occur in developing countries. In addition, many survivors with ischemic stroke live with disabilities. Treatment for acute ischemic stroke (AIS) involves restoring perfusion to the affected cerebral area (i.e., reperfusion therapy) as soon as possible. Recombinant tissue plasminogen activator (rt-PA), an ischemic stroke treatment approved by the Food and Drug Administration, has been shown to increase the number of patients with good prognosis by 11%–13% when administered within 3 h of AIS onset. The same study conducted by the National Institute of Neurological Disorders and Stroke reported that tPA treatment reduced the frequency of disability and death at 3 months post-AIS (National Institute of Neurological Disorders and Stroke rt-PA Stroke Study Group, 1995). Subsequently, the time window for administering intravenous thrombolytic therapy with rt-PA was extended to 4.5 h, which remained associated with significant improvements in clinical outcomes.

Despite its demonstrated efficacy, rt-PA has adverse effects, including brain edema and intracranial hemorrhage (Tsuji et al., 2005). A growing body of evidence suggests that tPA mediates increases in blood–brain barrier permeability induced by cerebral ischemia (Yepes et al., 2003; Zhu et al., 2019). Animal experiments have also demonstrated that tPA treatment can induce Evans dye extravasation, increasing the expression and activity of matrix metallopeptidase 9 (MMP-9) (Zhu et al., 2019), which has been associated with late neurotoxicity (Yepes et al., 2003).

Recent studies have identified endothelial glycocalyx as an integral part of the expanded neurovascular unit given its important role in maintaining neuronal homeostasis (Stanimirovic and Friedman, 2012). Endothelial glycocalyx is composed of proteoglycan and GAG chains (van Vliet et al., 2014), forming a barrier between the blood and vessels. Notably, injury to endothelial glycocalyx appears to be the first step in blood–brain barrier dysfunction (Wang et al., 2016). Syndecans are members of the transmembrane heparan sulfate glycoprotein family that are mainly expressed on the surface of cells, including vascular endothelial cells (Chronopoulos et al., 2020). In addition, their complete extracellular domains can be shed into the extracellular environment (Faria-Ramos et al., 2021). Changes in the expression or distribution of syndecan-1 may affect the integrity of the endothelial glycocalyx and endothelial barrier function (Kim et al., 2020). Increased levels of syndecan-1 in the blood may also represent a marker of glycocalyx degradation (Yao et al., 2019), and decreased thickness of the endothelial glycocalyx has been reported in syndecan-1$^{-/-}$ mice (Lu et al., 2020). In this study, we aimed to examine the prognostic value of syndecan-1 levels as a marker of glycocalyx injury after thrombolysis in patients with AIS.

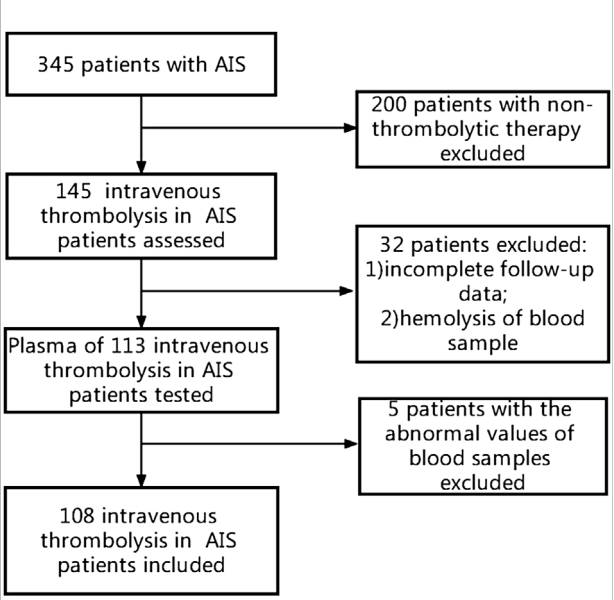

FIGURE 1
Study flow chart.

Methods

This cohort study included 345 patients with acute cerebral infarction who had presented to Xuanwu Hospital of Capital Medical University within 24 h of onset between September 2018 and May 2019. A total of 145 patients received intravenous thrombolysis with rt-PA. Thirty-two patients were excluded due to incomplete medical records, incomplete follow-up data, or blood sample hemolysis. Data were analyzed for 113 patients who had received thrombolytic therapy; five patients were excluded due to abnormal plasma test results. Thus, the final analysis included 108 patients (Figure 1). A total of 47 age- and sex-matched healthy participants were included in the control group. This study was approved by the Ethics Committee of the Xuanwu Hospital of Capital Medical University.

Patients were eligible for this study if they met the following criteria: diagnosis of AIS, as defined by the relevant Chinese guidelines (Zhong et al., 2019); absence of low-density changes on brain computed tomography scans; willingness to participate and provide informed consent; clear neurological deficits; onset time <4.5 h; no previous cerebral infarction; and complete case and follow-up data. Exclusion criteria were as follows: history of

cerebral infarction; diagnosis of hemorrhagic disease; diagnosis of malignant tumors, blood disease, or severe infection; pregnancy; diagnosis of epilepsy, mental illness, coagulation disorders, or liver/kidney dysfunction.

Collection of clinical data and blood samples

Patients with AIS were treated with rt-PA at a dose of 0.9 mg/kg. An intravenous injection containing 10% of the total amount of the drug was administered within 1 min, while a micropump was used to infuse the remaining 90% of the prescribed dose within 1 h, up to a maximum dose of <90 mg. In addition to rt-PA intravenous thrombolysis, other treatments include routine treatment of acute cerebral infarction and corresponding treatment of associated diseases (such as antihypertensive drugs for hypertension and hypoglycemic drugs for diabetes). Demographic and clinical characteristics of interest included age, sex, body mass index, medical history, smoking history, blood pressure, blood glucose levels, blood C-reactive protein (CRP) levels, blood homocysteine levels, and routine blood and biochemical indices at admission. In this study, AIS was divided into large-artery atherosclerosis (LAA), small-artery occlusion (SAO), and others (cardioembolism, unknown causes, and other causes) in accordance with the TOAST classification. In the AIS group, the degree of neurological deficits was evaluated by experienced neurologists immediately after admission using the National Institutes of Health Stroke Scale (NIHSS). The modified Rankin Scale (mRS) was used to predict patient outcomes at 3 months, with mRS scores of 0–2 and 3–6 points representing good and poor prognosis, respectively. An mRS score of 6 was defined as death. An EDTA tube was used to collect blood samples from each patient within 15 min after admission, following which rt-PA was administered for those meeting the criteria for intravenous thrombolysis. The separated plasma was stored at −80°C after centrifugation.

Plasma levels of syndecan-1

Plasma levels of syndecan-1 were detected using a Human Syndecan-1 ELISA kit (cargo number: ab46506; batch number: GR3368280-5), in accordance with the manufacturer's instructions, using a Bio-Tek Elx800 instrument. If a sample concentration exceeded the upper limit of the detection range, the sample was diluted and re-examined.

Statistical analyses

SPSS (version 22.0; IBM Corp., Armonk, NY, United States) and R software (version 4.1.1) were used for statistical analyses. Continuous variables conforming to a normal distribution are reported as the mean ± SD and were compared using t-tests or analyses of variance. Variables not conforming to a normal distribution assumption are represented as the median (interquartile range) and were compared using Mann–Whitney U-tests. Correlations were analyzed using Spearman correlation coefficients. Categorical variables are reported as frequencies (%) and were compared using chi-square tests. Multivariate prognostic analysis was performed using a binary logistic regression model.

Least absolute shrinkage and selection operator (LASSO) regression was performed to screen variables relevant to the risk assessment model, including lambda.min and lambda.1se. Variables with non-zero regression coefficients were included in the final model. The LASSO logistic regression model was built using the glmpath package in R software. The risk prediction model was constructed by integrating the candidate independent risk factors. A nomogram was created based on the results of the logistic regression analysis. The consistency index (C-index), area under (AUC) the receiver operating characteristic curve (ROC), and smooth-fitting curve values were used to evaluate the discriminative ability of the nomogram. A calibration diagram was used to evaluate its consistency. The net reclassification improvement (NRI) and integrated discrimination improvement (IDI) values were used to examine the accuracy of the risk model and provide a baseline reference for model improvements. Decision curve analysis (DCA) was used to evaluate the clinical value of the line chart. *P*-values < 0.05 were considered statistically significant.

Results

Patient characteristics

The distributions of age and sex were similar in the AIS (n = 108) and control groups (n = 47). Plasma levels of syndecan-1 were significantly higher in patients with AIS who had received intravenous thrombolysis than in healthy controls (t = 3.066, p = 0.0026, Figure 2A).

Baseline factors influencing prognosis in patients with AIS treated with rt-PA

Based on the mRS score at 3 months, 39 (36.11%) patients had an unfavorable prognosis; among them, 29 (74.36%) were male. Older age, history of atrial fibrillation, high CRP, treatment with mechanical thrombectomy, high blood glucose, high neutrophil count, high neutrophil/lymphocyte ratio, high NIHSS score, and high blood syndecan-1 levels were more common in patients with unfavorable prognosis than in those with favorable prognosis. Patients with LAA also tended to have

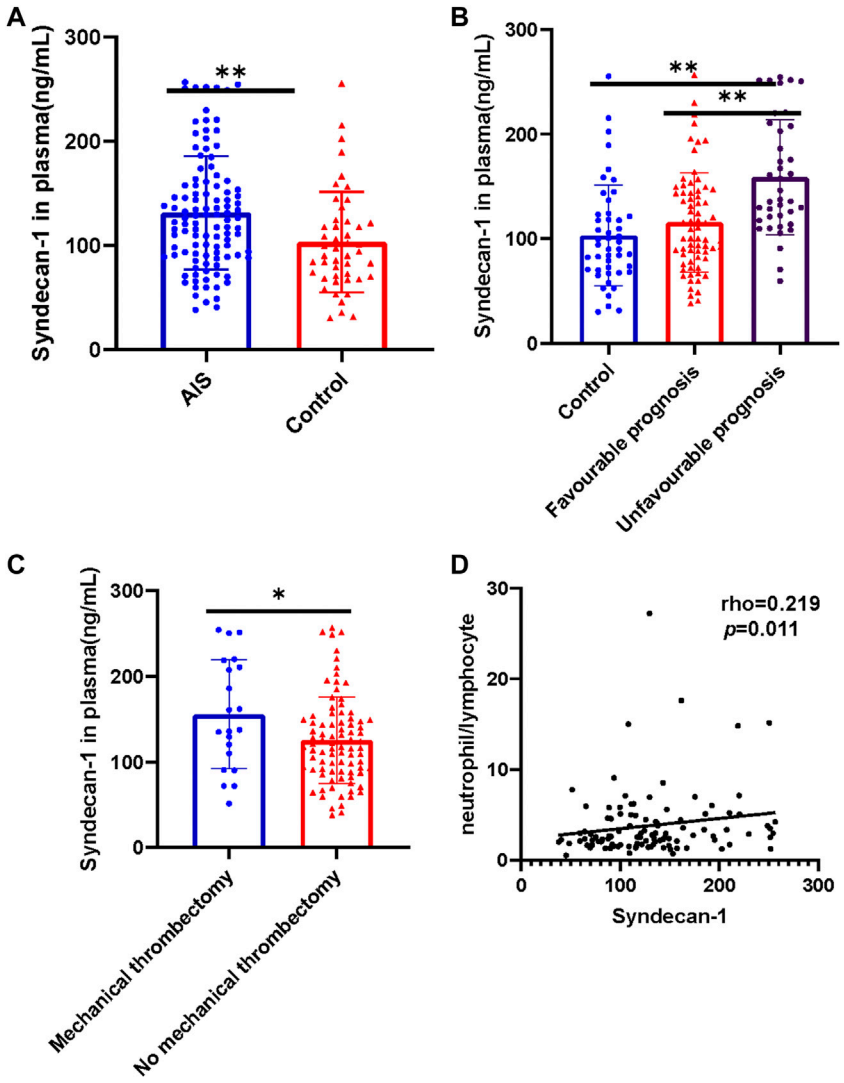

FIGURE 2
Plasma levels of syndecan-1 protein and their relationship with the neutrophil/lymphocyte ratio in different subgroups. **(A)** Comparison of plasma syndecan-1 levels between patients with AIS treated using intravenous thrombolysis and controls; **(B)** among the control group (n = 47), favorable prognosis group (n = 69), and unfavorable prognosis group (n = 39); **(C)** between patients treated with and without mechanical thrombectomy. **(D)** Correlation between syndecan-1 levels and neutrophil/lymphocyte ratio. The control group included healthy participants, while the AIS group included patients treated with intravenous thrombolysis (n = 108). *p < 0.05, **p < 0.01. AIS, acute ischemic stroke.

poor prognosis; in contrast, patients with SAO had relatively good prognosis (p < 0.05, Table 1).

Syndecan-1 levels and prognosis

Plasma levels of syndecan-1 were significantly higher in the unfavorable prognosis group than in the favorable prognosis group (p < 0.001, Figure 2B and Table 1). In addition, plasma syndecan-1 levels were significantly lower in the control group than in the unfavorable prognosis group (p < 0.001, Figure 2B) and significantly higher in the mechanical embolectomy group than in the non-mechanical embolectomy group (t = 2.335, p = 0.0214, Figure 2C). Syndecan-1 levels were also positively correlated with the neutrophil-to-lymphocyte ratio (p = 0.011, Figure 2D).

Variable selection

Thirty variables were screened as candidate predictors. The LASSO regression analysis yielded seven variables that most strongly correlated with adverse prognosis after thrombolysis

TABLE 1 Baseline characteristics of AIS patients with mRS of ≤2 and that of >2 at 3 months.

	All (108)	Favourable prognosis (n = 69)	Unfavourable prognosis (n = 39)	p value
Demographic characteristics[n(%) OR median (IQR) OR $\bar{x}$ ± s]				
Male, n (%)	85 (78.70)	56 (81.16)	29 (74.36)	0.466
Age, y, (x ± s)	64.30 ± 12.61	61.23 ± 10.92	69.72 ± 13.68	0.001
Body mass index, kg/m2	24.84 (23.85, 26.74)	25 (23.75, 26.73)	24.59 (23.85, 26.80)	0.595
Medical history [n (%)]				
Hypertension	78 (72.22)	50 (72.46)	28 (71.79)	0.556
Diabetes mellitus	37 (34.26)	23 (33.33)	14 (35.90)	0.835
Hypercholesterolemia	50 (46.30)	34 (49.28)	16 (41.03)	0.266
Coronary artery disease	21 (19.44)	13 (18.84)	8 (20.51)	0.511
Atrial fibrillation	9 (8.33)	3 (4.35)	6 (15.38)	0.046
Smoking habit	46 (42.59)	33 (47.83)	13 (33.33)	0.103
Stroke characteristics and treatment [n(%) OR median (IQR)]				
Onset-to-treatment time, h	2.20 (1.20, 3.38)	2.5 (1.20, 3.40)	2 (1.20, 3.30)	0.699
Mechanical thrombectomy	21 (19.44)	6 (8.70)	15 (38.46)	<0.001
Stroke classification[n (%)]				
LAA	65 (60.19)	36 (52.17)	29 (74.36)	0.024
SAO	36 (33.33)	28 (40.58)	8 (20.51)	0.034
Others	7 (6.48)	5 (7.25)	2 (5.13)	0.668
Complication				
sICH	2 (1.9)	1 (1.4)	2 (5.1)	0.295
General evaluation of admission[n(%) OR median (IQR) OR $\bar{x}$ ± s]				
Systolic blood pressure, mm Hg	150 (140, 168)	150 (139.50, 168.00)	150 (140.00, 168.00)	0.734
Diastolic blood pressure, mm Hg	82.50 (74.25, 92.75)	82 (73.50, 93.00)	86 (75.00, 92.00)	0.885
Blood glucose concentration, g/L	7.90 (6.52, 10.30)	7.40 (6.20, 9.70)	8.90 (7.60, 11.10)	0.026
Glycated hemoglobin	6.15 (5.60, 7.30)	6 (5.60, 7.20)	6.20 (5.70, 7.30)	0.512
CRP, mg/L	2.13 (1.12, 5.89)	1.89(0.80, 4.17)	5.89 (1.75, 12.31)	<0.001
Homocysteine, μmol/L	14.80 (11.60, 17.40)	14.5 (11.40, 18.35)	14.9 (12.20, 16.10)	0.883
TC, mmol/L	1.71 (1.03, 2.70)	1.76 (1.10, 2.74)	1.7 (0.99, 2.63)	0.468
Cholesterol, mmol/L	4.62 ± 1.06	4.62 ± 1.11	4.6 ± 1.0	0.922
HDL, mmol/L	1.12 (0.94, 1.30)	1.12 (0.96, 1.36)	1.06 (0.89, 1.27)	0.359
LDL, mmol/L	2.65 ± 0.92	2.64 ± 0.97	2.7 ± 0.82	0.786
NIHSS score	5 (3, 12)	5 (3, 6.50)	12.00 (6, 18)	<0.001
WBC, ×109/L	7.38 (6.14, 9.14)	7.20 (576, 8.79)	7.87 (6.52, 10.61)	0.120
Neutrophils, ×109/L	4.71 (3.71, 6.54)	4.47 (3.53, 5.67)	5.37 (4.06, 7.95)	0.025
Lymphocytes, ×109/L	1.83 (1.32, 2.26)	1.90 (1.52, 2.33)	1.48 (1.16, 2.19)	0.053
Neutrophil-to-lymphocyte ratio	2.61 (1.84, 4.47)	2.35 (1.66, 3.46)	3.35 (2.42, 5.55)	0.010
Platelet count, ×1,000/mm3	208.5 (175, 242)	220 (177.50, 245)	201 (167, 232)	0.065
Syndecan-1,ng/mL	131.19 ± 54.35	115.60 ± 47.71	158.77 ± 54.97	<0.001

NIHSS, NIH stroke scale; IQR, interquartile range; CRP, C-reactive protein; HDL, high-density lipoprotein; LDL, low-density lipoprotein; TC, triglyceride; sICH, symptomatic intracranial hemorrhage.

in AIS, including age, NIHSS score, history of atrial fibrillation, mechanical thrombectomy, blood CRP level, stroke classification, and syndecan-1 level. Models with different variable configurations were tested and fitted using 10-fold cross validation. The log value of λ and AUC values were used for plotting. The model with the best performance and fewest independent variables corresponded to the λ of 0.04902451 (Figures 3A,B).

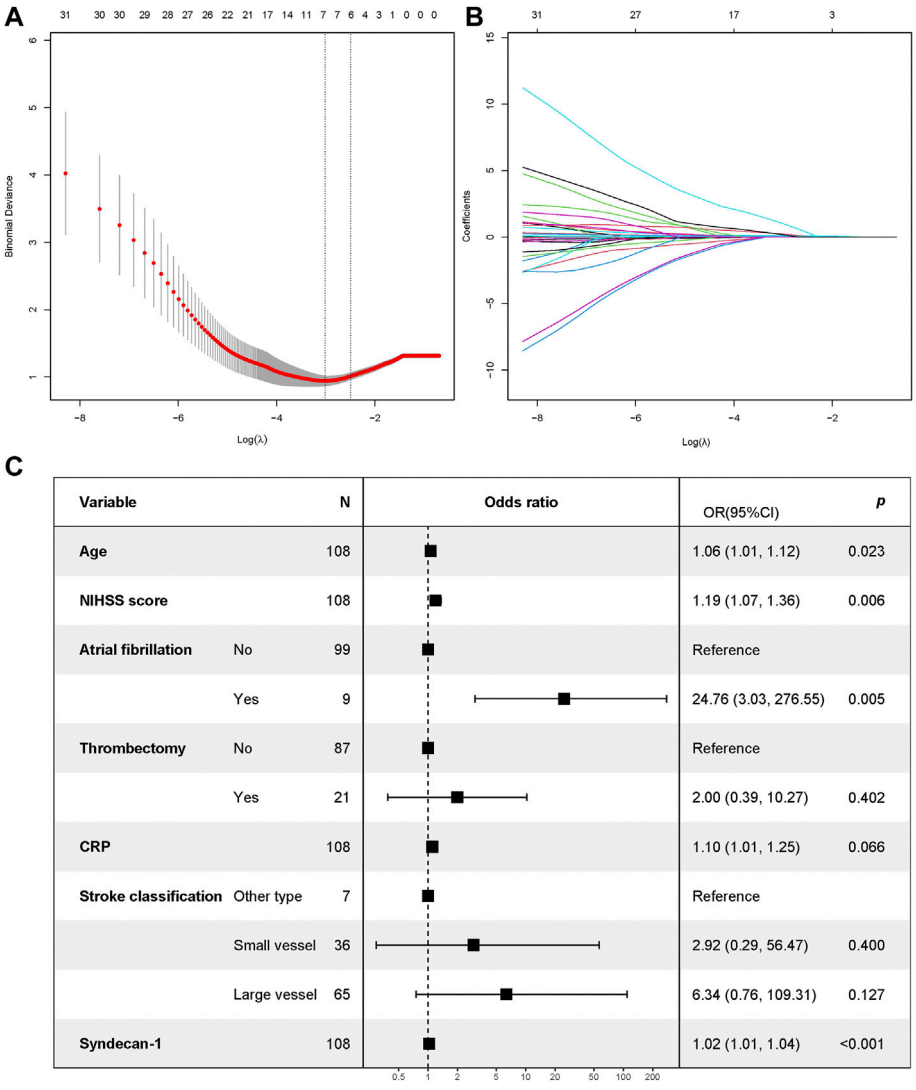

FIGURE 3
Screening of characteristic variables based on LASSO regression and forest map of factors influencing prognosis as determined using logistic regression. **(A)** The process of selecting the most suitable value for λ in the LASSO model via cross-validation method. When λ = 0.04902451 and seven parameters are selected, the LASSO regression model is most suitable; **(B)** The figure shows the characteristics of the variable coefficients. LASSO, least absolute shrinkage and selection operator; **(C)** Forest map. Note: An mRS of >2 points at 3 months was used as the dependent variable. The independent variables included age, NIHSS score, atrial fibrillation, mechanical thrombectomy, CRP, stroke classification, and syndecan-1 levels (screened out via LASSO regression). mRS, modified Rankin scale; NIHSS, National Institutes of Health Stroke Scale; CRP, C-reactive protein; LASSO, least absolute shrinkage and selection operator.

Plasma syndecan-1 levels can better predict poor prognosis

After adjusting for age, NIHSS score, history of atrial fibrillation, mechanical thrombectomy status, blood CRP levels, stroke classification, and syndecan-1 levels, logistic regression analysis (Model 2) revealed that syndecan-1 levels remained significantly associated with unfavorable prognosis in patients with AIS treated with intravenous thrombolysis ($p < 0.001$, Table 2). After multivariate correction, the odds ratio (OR) (95% confidence interval, 95% CI) for syndecan-1 levels was 1.024 (1.010–1.038). The optimal cutoff value of plasma syndecan-1 for determining unfavorable prognosis was 102.82 ng/ml. Subsequently, syndecan-1 levels were dichotomized into ≥102.82 and <102.82 ng/ml. Syndecan-1 levels were associated with poor prognosis as a continuous variable (OR, 1.024; 95% CI, 1.010–1.038); moreover, values of ≥102.82 ng/ml were associated with poor prognosis (OR, 34.551; 95% CI, 5.408–220.732) at 3 months in patients with AIS treated with intravenous thrombolysis (Table 2).

TABLE 2 Syndecan-1 alone and in combination predicted the prognosis of AIS patients treated with intravenous thrombolysis.

	Model1		Model2	
	OR (95%CI)	*p* value	OR (95%CI)	*p* value
Biomarkers (as continuous variables)				
Syndecan-1[a]	1.016 (1.008, 1.025)	<0.001	1.024 (1.010, 1.038)	<0.001
Biomarkers (as categorical variables)				
Syndecan-1, ≥102.82 ng/ml[b]	11.657 (3.278, 41.461)	<0.001	34.551 (5.408, 220.732)	<0.001

MODEL 2: mRS of >2 points at 3 months was the dependent variable; covariates included age, NIHSS score, history of atrial fibrillation, mechanical thrombectomy, blood CRP, stroke classification, blood syndecan-1(screened out by the LASSO regression).

[a]Continuous variable.

[b]Categorical variable.

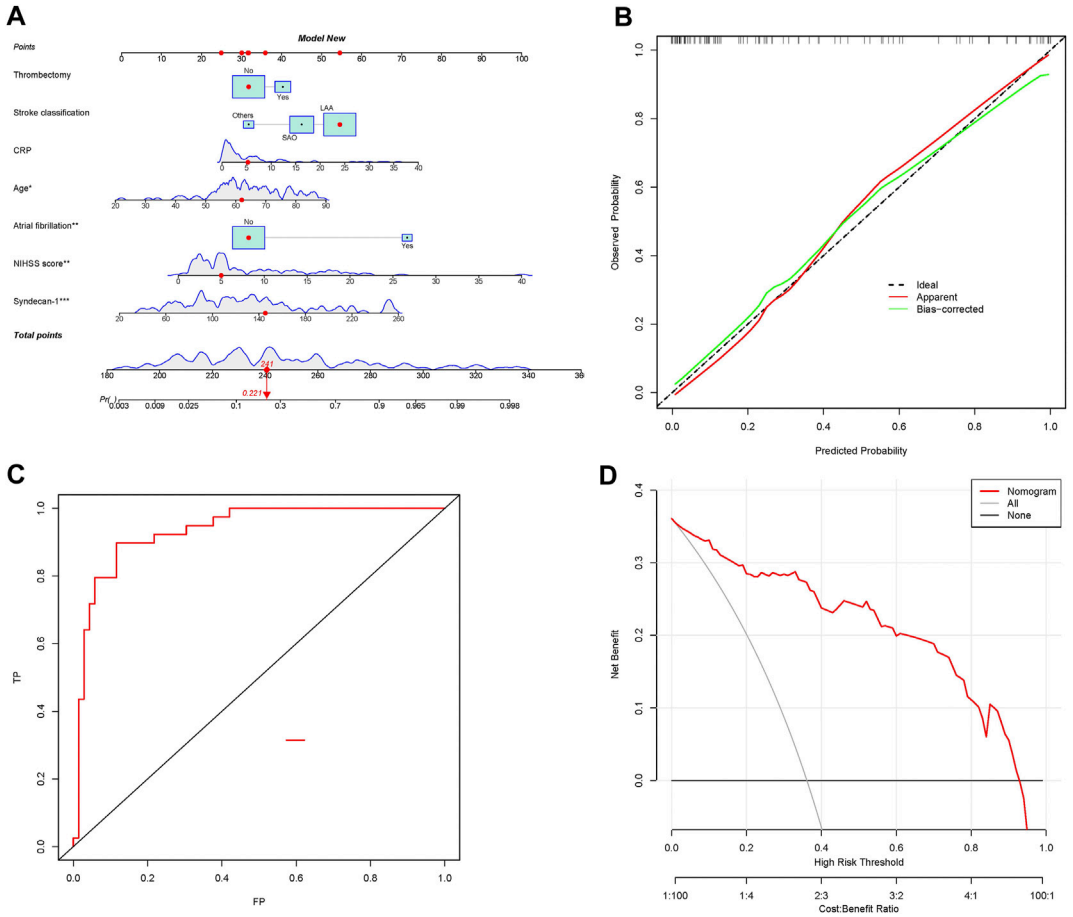

FIGURE 4
Nomograms for predicting prognosis using the risk model and evaluation of the prediction model. **(A)** Nomograms for predicting prognosis based on the risk model; **(B)** plots depicting the calibration of the risk model; **(C)** ROC plot based on nomograms for prognosis; **(D)** decision curve analysis of the model for predicting AIS prognosis following thrombolytic treatment. ROC, receiver operating characteristic.

Based on the seven variables selected by LASSO regression, an additional binary logistic regression analysis was performed. This analysis indicated that age, NIHSS score, history of atrial fibrillation, and high plasma syndecan-1 levels were associated with poor prognosis ($p < 0.05$, Figure 3C).

TABLE 3 NRI and IDI differences between the old and new models.

		Estimate	Lower	Upper	*p*
NRI (Categorical)	NRI	0.069	-0.027	0.403	0.541
	NRI+	0.026	-0.051	0.203	0.684
	NRI-	0.043	-0.028	0.252	0.554
NRI (Continuous)	NRI	0.776	0.169	1.596	0.046
	NRI+	0.385	-0.042	0.825	0.090
	NRI-	0.391	0.079	0.833	0.050
IDI		0.111	0.049	0.174	<0.001

TABLE 4 Accuracy of the Prediction Score of the Nomogram for Estimating the Risk of prognosis of AIS patients treated with intravenous thrombolysis.

Variable	Risk model (OR,95% CI)
Area of ROC curve	0.93 (0.89–0.98)
Threshold	133.92
Sensitivity, %	0.90 (0.75, 0.97)
Specificity, %	0.88 (0.78, 0.95)
Accuracy	0.89 (0.81, 0.94)
PPV, %	0.81 (0.66, 0.91)
NPV, %	0.94 (0.84, 0.98)

Prognostic nomogram

The risk assessment models were converted into nomograms (Figure 4A). The crude and bootstrap-corrected C-index values for the nomogram were 0.935 (95% CI, 0.888–0.981) and 0.898, respectively. The predictive probability of the nomogram was in good agreement with the actual probability observed. The risk model exhibited a better fit (Figure 4B), with an AUC of 0.935 (95% CI, 0.888–0.981) (Figure 4C), as well as good discriminative ability and accuracy. The classification and continuous NRI values for the unfavorable and favorable prognosis groups were greater than 0, indicating that the predictive accuracy of the risk model was better. The IDI was 0.111 (95% CI, 0.049–0.174, $p < 0.001$), also highlighting the better predictive ability of the risk model (Table 3).

Risk following rt-PA treatment for AIS patients based on nomogram scores

The optimal threshold for the nomogram based on the risk model was a score of 133.92. The sensitivity, specificity, accuracy, positive predictive value (PPV), and negative predictive value (NPV) of the risk model for differentiating prognosis were 90%, 88%, 89%, 81%, and 94%, respectively (Table 4).

Clinical application

DCA quantifies the net benefit of different threshold probabilities in a dataset to determine the clinical value of a nomogram. The DCA results suggested that the risk model, which included syndecan-1 levels, exhibited a better ability to predict AIS prognosis following rt-PA treatment than the conventional model (Figure 4D). These findings suggest that the nomogram has some clinical value.

Discussion

Ischemic stroke is the leading cause of death and disability worldwide, and its incidence is expected to increase given aging of the global population (Paul and Candelario-Jalil, 2021). Diagnostic biomarkers have been used in the context of stroke diagnosis for decades (Bsat et al., 2021), although rapid assessment and management are essential for improving patient prognosis. Syndecan-1 is a major marker of glycocalyx degradation, levels of which are elevated in the peripheral plasma of affected patients. In this study, we examined the prognostic value of syndecan-1 levels as a marker of post-thrombolysis glycocalyx injury in patients with AIS.

Previous studies have reported that ischemia/reperfusion injury can promote glycocalyx degradation (Rehm et al., 2007). However, DellaValle et al. observed no changes in syndecan-1 levels following onset in 10 patients with AIS (DellaValle et al., 2019). An animal study by Zhu et al. demonstrated that, after acute middle cerebral artery occlusion, plasma syndecan-1 levels began to rise at 1 h, peaking at 6 h, gradually decreasing thereafter, and increasing again on days 5 and 7 (Zhu et al., 2021). However, to our knowledge, no previous studies have examined the correlation between syndecan-1 levels and poor prognosis in patients with acute cerebral infarction undergoing thrombolysis. The present study is first to show that elevated plasma syndecan-1 levels may be associated with poor prognosis in patients with AIS treated with intravenous thrombolysis. Moreover, adding syndecan-1 levels to the conventional risk assessment model increased model discrimination and accuracy. These findings indicate that syndecan-1 levels may play an important role in the pathophysiology of AIS, highlighting their potential as a target in the diagnosis and treatment of patients with AIS following intravenous thrombolysis.

Previous studies have demonstrated that inflammation plays a role in the development of AIS (Gasbarrino et al., 2019; Rivera-Caravaca et al., 2019) and may affect patient prognosis. High levels of circulating syndecan-1 may contribute to such inflammation (Johansson et al., 2011). Stroke severity is typically evaluated using the NIHSS, with higher scores generally indicating a worse prognosis following AIS. In addition, age has been identified as a risk factor for poor AIS

prognosis following treatment with intravenous thrombolysis. Age also increases the risk of ischemic stroke and reduces the likelihood of recovery following damage to the neurovascular unit (Soriano-Tárraga et al., 2017). In the present study, patients with AIS that underwent concurrent mechanical thrombectomy exhibited poorer prognosis than their counterparts, which may have been related to the severity of cerebrovascular disease and the extent of the infarction. Atrial fibrillation has also been associated with poor prognosis and may be a marker of poor cardiac function. Patients with macrovascular disease may present with cerebral infarction of a larger extent, resulting in more severe neurological deficits and poor prognosis.

In the univariate analysis, plasma syndecan-1 levels were higher among patients with poor prognosis after intravenous thrombolysis than among those with good prognosis. Multivariate logistic regression analysis verified that syndecan-1 levels were associated with poor prognosis. Furthermore, addition of syndecan-1 levels to the conventional risk prediction model significantly improved its prognostic efficiency. In this study, a nomogram was used to visualize the prediction model; the AUC and fitting curve were used to determine the discrimination and consistency of the prediction model. The NRI and IDI values were used to evaluate model accuracy. Overall, the new risk model incorporating syndecan-1 exhibited better discriminative ability, consistency, and accuracy than the conventional model. DCA revealed that the new model had greater clinical value than the conventional model. This study is first to report that syndecan-1 levels in patients with AIS undergoing intravenous thrombolysis may predict prognosis, highlighting its potential value as a biomarker for risk stratification. Improved stratification may aid in identifying patients at the greatest risk for poor prognosis, which may in turn facilitate early diagnosis and treatment, thereby improving outcomes.

Presently, rt-PA thrombolysis is the only AIS treatment approved by the Food and Drug Administration. However, the clinical use of rt-PA is limited to less than 5% of patients because of the narrow treatment window (Kleindorfer et al., 2008). Delayed rt-PA treatment increases the risk of cerebral edema and hemorrhage, increasing the risk of mortality in this patient group (Mohr, 2000). In general, rt-PA may trigger bleeding by weakening the blood–brain barrier. Upon entering the brain, rt-PA induces cytokine production and activates MMP-9 (Tsuji et al., 2005). Research has indicated that use of hyperbaric oxygen with rt-PA can reduce the extent of rt-PA-related bleeding, likely by strengthening the blood–brain barrier (Kim et al., 2005). Preventing damage to the blood–brain barrier can help protect the brain and reduce the risk of tPA-related adverse events, thereby extending the treatment window. In rodent experiments, rt-PA has been shown to aggravate ischemia-induced damage to the blood–brain barrier by enhancing the proteolytic activity of MMP-9 (Pfefferkorn and Rosenberg, 2003; Wang et al., 2003). Studies involving human patients with stroke have demonstrated that high plasma MMP-9 levels before treatment are more likely to result in cerebral hemorrhage complications after rt-PA therapy (Zhong et al., 2019). MMP inhibitors may prevent the premature opening of the blood–brain barrier and reduce the risk of bleeding and death when rt-PA is administered during stroke (Lapchak et al., 2000). Since glycocalyx is an important component of the blood–brain barrier, inhibiting glycocalyx degradation may protect the blood–brain barrier and reduce rates of bleeding, especially in patients with nerve damage caused by rt-PA. This may help to reduce mortality following rt-PA thrombolysis and safely extend the treatment window. Glycocalyx degradation inhibitors combined with rt-PA thrombolytic therapy may therefore help to improve the treatment of acute cerebral infarction.

Conclusion

The current findings demonstrate that incorporating plasma syndecan-1 levels may help to improve the risk stratification of patients with acute cerebral infarction undergoing intravenous thrombolysis. Plasma syndecan-1 levels combined with clinical and imaging test results may therefore aid in identifying patients at the greatest risk for poor outcomes. However, large-scale, multi-center studies are required to validate the present findings.

Data availability statement

The raw data supporting the conclusion of this article will be made available by the authors, without undue reservation.

Ethics statement

The studies involving human participants were reviewed and approved by This study was approved by the Ethics Committee of the Xuanwu Hospital of Capital Medical University. The patients/participants provided their written informed consent to participate in this study.

Author contributions

FZ wrote the manuscript. YZ performed experiments and modified the procedures. RW, YH, LL, ZH, JF, LZ, YH, and PL also performed experiments and modified the relevant procedures. YL designed the study and critically revised the manuscript.

Funding

This work was supported by grants from Capital Funds for Health Improvement and Research (2020-2-1032), the National

Natural Science Foundation of China (NSFC, Grant/Award Number: 82171301, 82001390, 81971222).

Conflict of interest

The authors declare that the research was conducted in the absence of any commercial or financial relationships that could be construed as a potential conflict of interest.

Publisher's note

All claims expressed in this article are solely those of the authors and do not necessarily represent those of their affiliated organizations, or those of the publisher, the editors and the reviewers. Any product that may be evaluated in this article, or claim that may be made by its manufacturer, is not guaranteed or endorsed by the publisher.

References

Bsat, S., Halaoui, A., Kobeissy, F., Moussalem, C., El Houshiemy, M. N., Kawtharani, S., et al. (2021). Acute ischemic stroke biomarkers: a new era with diagnostic promise. *Acute Med. Surg.* 8 (1), e696. doi:10.1002/ams2.696

Chronopoulos, A., Thorpe, S. D., Cortes, E., Lachowski, D., Rice, A. J., Mykuliak, V. V., et al. (2020). Syndecan-4 tunes cell mechanics by activating the kindlin-integrin-RhoA pathway. *Nat. Mat.* 19 (6), 669–678. doi:10.1038/s41563-019-0567-1

DellaValle, B., Hasseldam, H., Johansen, F. F., Iversen, H. K., Rungby, J., Hempel, C., et al. (2019). Multiple soluble components of the glycocalyx are increased in patient plasma after ischemic stroke. *Stroke* 50 (10), 2948–2951. doi:10.1161/STROKEAHA.119.025953

Faria-Ramos, I., Poças, J., Marques, C., Santos-Antunes, J., Macedo, G., Reis, C. A., et al. (2021). Heparan sulfate glycosaminoglycans: (Un)Expected allies in cancer clinical management. *Biomolecules* 11 (2), 136. doi:10.3390/biom11020136

Gasbarrino, K., Hafiane, A., Zheng, H., and Daskalopoulou, S. S. (2019). Intensive statin therapy compromises the adiponectin-AdipoR pathway in the human monocyte-macrophage lineage. *Stroke* 50 (12), 3609–3617. doi:10.1161/STROKEAHA.119.026280

Johansson, P. I., Stensballe, J., Rasmussen, L. S., and Ostrowski, S. R. (2011). A high admission syndecan-1 level, a marker of endothelial glycocalyx degradation, is associated with inflammation, protein C depletion, fibrinolysis, and increased mortality in trauma patients. *Ann. Surg.* 254 (2), 194–200. doi:10.1097/SLA.0b013e318226113d

Kim, H. B., Soh, S., Kwak, Y. L., Bae, J. C., Kang, S. H., Song, J. W., et al. (2020). High preoperative serum syndecan-1, a marker of endothelial glycocalyx degradation, and severe acute kidney injury after valvular heart surgery. *J. Clin. Med.* 9 (6), E1803. doi:10.3390/jcm9061803

Kim, H. Y., Singhal, A. B., and Lo, E. H. (2005). Normobaric hyperoxia extends the reperfusion window in focal cerebral ischemia. *Ann. Neurol.* 57 (4), 571–575. doi:10.1002/ana.20430

Kleindorfer, D., Lindsell, C. J., Brass, L., Koroshetz, W., and Broderick, J. P. (2008). National US estimates of recombinant tissue plasminogen activator use: ICD-9 codes substantially underestimate. *Stroke* 39 (3), 924–928. doi:10.1161/STROKEAHA.107.490375

Lapchak, P. A., Chapman, D. F., and Zivin, J. A. (2000). Metalloproteinase inhibition reduces thrombolytic (tissue plasminogen activator)-induced hemorrhage after thromboembolic stroke. *Stroke* 31 (12), 3034–3040. doi:10.1161/01.str.31.12.3034

Lu, R., Sui, J., and Zheng, X. L. (2020). Elevated plasma levels of syndecan-1 and soluble thrombomodulin predict adverse outcomes in thrombotic thrombocytopenic purpura. *Blood Adv.* 4 (21), 5378–5388. doi:10.1182/bloodadvances.2020003065

Mohr, J. P. (2000). Thrombolytic therapy for ischemic stroke: from clinical trials to clinical practice. *JAMA* 283 (9), 1189–1191. doi:10.1001/jama.283.9.1189

National Institute of Neurological Disorders and Stroke rt-PA Stroke Study Group (1995). Tissue plasminogen activator for acute ischemic stroke. *N. Engl. J. Med.* 333 (24), 1581–1587. doi:10.1056/NEJM199512143332401

Paul, S., and Candelario-Jalil, E. (2021). Emerging neuroprotective strategies for the treatment of ischemic stroke: an overview of clinical and preclinical studies. *Exp. Neurol.* 335, 113518. doi:10.1016/j.expneurol.2020.113518

Pfefferkorn, T., and Rosenberg, G. A. (2003). Closure of the blood-brain barrier by matrix metalloproteinase inhibition reduces rtPA-mediated mortality in cerebral ischemia with delayed reperfusion. *Stroke* 34 (8), 2025–2030. doi:10.1161/01.STR.0000083051.93319.28

Rehm, M., Bruegger, D., Christ, F., Conzen, P., Thiel, M., Jacob, M., et al. (2007). Shedding of the endothelial glycocalyx in patients undergoing major vascular surgery with global and regional ischemia. *Circulation* 116 (17), 1896–1906. doi:10.1161/CIRCULATIONAHA.106.684852

Rivera-Caravaca, J. M., Marín, F., Vilchez, J. A., Galvez, J., Esteve-Pastor, M. A., Vicente, V., et al. (2019). Refining stroke and bleeding prediction in atrial fibrillation by adding consecutive biomarkers to clinical risk scores. *Stroke* 50 (6), 1372–1379. doi:10.1161/STROKEAHA.118.024305

Soriano-Tárraga, C., Mola-Caminal, M., Giralt-Steinhauer, E., Ois, A., Rodriguez-Campello, A., Cuadrado-Godia, E., et al. (2017). Biological age is better than chronological as predictor of 3-month outcome in ischemic stroke. *Neurology* 89 (8), 830–836. doi:10.1212/WNL.0000000000004261

Stanimirovic, D. B., and Friedman, A. (2012). Pathophysiology of the neurovascular unit: disease cause or consequence. *J. Cereb. Blood Flow. Metab.* 32 (7), 1207–1221. doi:10.1038/jcbfm.2012.25

Tsuji, K., Aoki, T., Tejima, E., Arai, K., Lee, S. R., Atochin, D. N., et al. (2005). Tissue plasminogen activator promotes matrix metalloproteinase-9 upregulation after focal cerebral ischemia. *Stroke* 36 (9), 1954–1959. doi:10.1161/01.STR.0000177517.01203.eb

van Vliet, E. A., Aronica, E., and Gorter, J. A. (2014). Role of blood-brain barrier in temporal lobe epilepsy and pharmacoresistance. *Neuroscience* 277, 455–473. doi:10.1016/j.neuroscience.2014.07.030

Wang, L., Huang, X., Kong, G., Xu, H., Li, J., Hao, D., et al. (2016). Ulinastatin attenuates pulmonary endothelial glycocalyx damage and inhibits endothelial heparanase activity in LPS-induced ARDS. *Biochem. Biophys. Res. Commun.* 478 (2), 669–675. doi:10.1016/j.bbrc.2016.08.005

Wang, X., Lee, S. R., Arai, K., Lee, S. R., Tsuji, K., Rebeck, G. W., et al. (2003). Lipoprotein receptor-mediated induction of matrix metalloproteinase by tissue plasminogen activator. *Nat. Med.* 9 (10), 1313–1317. doi:10.1038/nm926

Yao, W., Rose, J. L., Wang, W., Seth, S., Jiang, H., Taguchi, A., et al. (2019). Syndecan 1 is a critical mediator of macropinocytosis in pancreatic cancer. *Nature* 568 (7752), 410–414. doi:10.1038/s41586-019-1062-1

Yepes, M., Sandkvist, M., Moore, E. G., Bugge, T. H., Strickland, D. K., Lawrence, D. A., et al. (2003). Tissue-type plasminogen activator induces opening of the blood-brain barrier via the LDL receptor-related protein. *J. Clin. Invest.* 112 (10), 1533–1540. doi:10.1172/JCI19212

Zhong, Di, Zhang, Shuting, and Wu, Bo (2019). Interpretation of ' guidelines for the diagnosis and treatment of acute ischemic stroke in china 2018. *Chin. J. Mod. Neurology* 19 (11), 897–901.

Zhu, J., Li, Z., Ji, Z., Wu, Y., He, Y., Liu, K., et al. (2021). Glycocalyx is critical for blood-brain barrier integrity by suppressing caveolin1-dependent endothelial transcytosis following ischemic stroke. *Brain Pathol.* 32, e13006. doi:10.1111/bpa.13006

Zhu, J., Wan, Y., Xu, H., Wu, Y., Hu, B., Jin, H., et al. (2019). The role of endogenous tissue-type plasminogen activator in neuronal survival after ischemic stroke: friend or foe. *Cell. Mol. Life Sci.* 76 (8), 1489–1506. doi:10.1007/s00018-019-03005-8

frontiers | Frontiers in Pharmacology

TYPE Original Research
PUBLISHED 15 August 2022
DOI 10.3389/fphar.2022.950376

OPEN ACCESS

EDITED BY
Yongjun Sun,
Hebei University of Science and Technology, China

REVIEWED BY
Liqun Yang,
Shanghai Jiao Tong University, China
Sumio Ohtsuki,
Kumamoto University, Japan

*CORRESPONDENCE
Qi Wan,
qiwan1@hotmail.com
Fengyuan Che,
che1971@126.com

†These authors have contributed equally to this work

SPECIALTY SECTION
This article was submitted to Neuropharmacology, a section of the journal Frontiers in Pharmacology

RECEIVED 22 May 2022
ACCEPTED 29 June 2022
PUBLISHED 15 August 2022

CITATION
Chen J, Zhuang Y, Zhang Y, Liao H, Liu R, Cheng J, Zhang Z, Sun J, Gao J, Wang X, Chen S, Zhang L, Che F and Wan Q (2022), A synthetic BBB-permeable tripeptide GCF confers neuroprotection by increasing glycine in the ischemic brain.
Front. Pharmacol. 13:950376.
doi: 10.3389/fphar.2022.950376

A synthetic BBB-permeable tripeptide GCF confers neuroprotection by increasing glycine in the ischemic brain

Juan Chen[1,2†], Yang Zhuang[2†], Ya Zhang[2], Huabao Liao[2], Rui Liu[2], Jing Cheng[2], Zhifeng Zhang[2], Jiangdong Sun[3], Jingchen Gao[3], Xiyuran Wang[3], Shujun Chen[3], Liang Zhang[4], Fengyuan Che[5*] and Qi Wan[3,6*]

[1]Department of Neurology, The Central Hospital of Wuhan, Tongji Medical College, Huazhong University of Science and Technology, Wuhan, China, [2]Department of Physiology, School of Medicine, Wuhan University, Wuhan, China, [3]Department of Pathophysiology, School of Basic Medicine, Institute of Neuroregeneration and Neurorehabilitation, Qingdao University, Qingdao, China, [4]Krembil Research Institute, University Health Network, University of Toronto, Toronto, ON, Canada, [5]Central Laboratory, Department of Neurology, Linyi People's Hospital, Qingdao University, Linyi, China, [6]Qingdao Gui-Hong Intelligent Medical Technology Co., Ltd., Qingdao, China

Background: We and others have previously demonstrated that glycine is neuroprotective in cerebral ischemia-reperfusion injury. But glycine has low permeability to the blood–brain barrier (BBB). To deliver glycine into the ischemic brain to confer neuroprotection, we designed a novel glycine-containing and BBB-permeable tripeptide, the H-glycine-cysteine-phenylalanine-OH (GCF).

Methods: For the synthesis of GCF, phenylalanine was included to increase the BBB permeability of the tripeptide. Cysteine was conjugated with glycine to enable the release of glycine from GCF. With the use of immunofluorescence labeling and HPLC assays, we measured the distribution and level of GCF. We used TTC labeling, LDH release, and MTT assays to evaluate the neuroprotective effect of GCF.

Results: Following intravenous injection in a rat model of cerebral ischemia-reperfusion injury, GCF was intensively distributed in the ischemic neurons. Intravenous injection of GCF, but not the non-cleavable acetyl-GCF, resulted in the elevation of glycine in the ischemic brain. GCF but not acetyl-GC conferred neuroprotection in ischemic stroke animals.

Conclusion: GCF protects against cerebral ischemia-reperfusion injury in the rat. In contrast to peptide drugs that exert therapeutic effect by interfering with signaling interaction, GCF acts as a BBB shuttle and prodrug to deliver glycine to confer neuroprotection, representing a novel therapeutic strategy for acute ischemic stroke.

KEYWORDS

ischemic stroke, glycine, BBB, tripeptide, neuroprotection

Introduction

Glycine is the simplest non-essential amino acid that plays a fundamental role in cell metabolism (Perez-Torres et al., 2017; Razak et al., 2017). Glycine provides essential precursors for the synthesis of proteins, nucleic acids, and lipids that are crucial to cell growth and survival (Locasale, 2013). Glycine is an integral component of glutathione that is the main antioxidant molecule of the cell (Amelio et al., 2014). Glycine is also required to maintain the cellular redox balance (Petrat et al., 2012). In mitochondria, glycine fuels heme biosynthesis and sustains oxidative phosphorylation (Petrat et al., 2012).

In the central nervous system, glycine functions as an agonist of inhibitory glycine receptors and a co-agonist of excitatory NMDA receptors (Paul and de Belleroch e, 2014; Lynch et al., 2017), We and others have demonstrated that glycine exerted a neuroprotective effect *in vitro* and in cerebral ischemia injury *in vivo* (Yang et al., 2000; Zhao et al., 2005; Liu et al., 2007; Tanabe et al., 2010; Chen et al., 2016; Hu et al., 2016).

As the blood–brain barrier (BBB) prevents most drugs from reaching their targets in the brain, delivery of drugs into the brain is a major challenge in the drug development of neurological disorders. Peptides, acting as BBB shuttles, have recently received growing attention because of their lower cost, reduced immunogenicity, and higher chemical versatility, providing feasibility for the development of BBB-permeable CNS drugs (Oller-Salvia et al., 2016).

In this study, we showed that glycine had low BBB permeability in ischemic conditions. We, therefore, designed a glycine-containing and BBB-permeable tripeptide GCF. Intravenous injection of GCF led to the elevation of glycine in

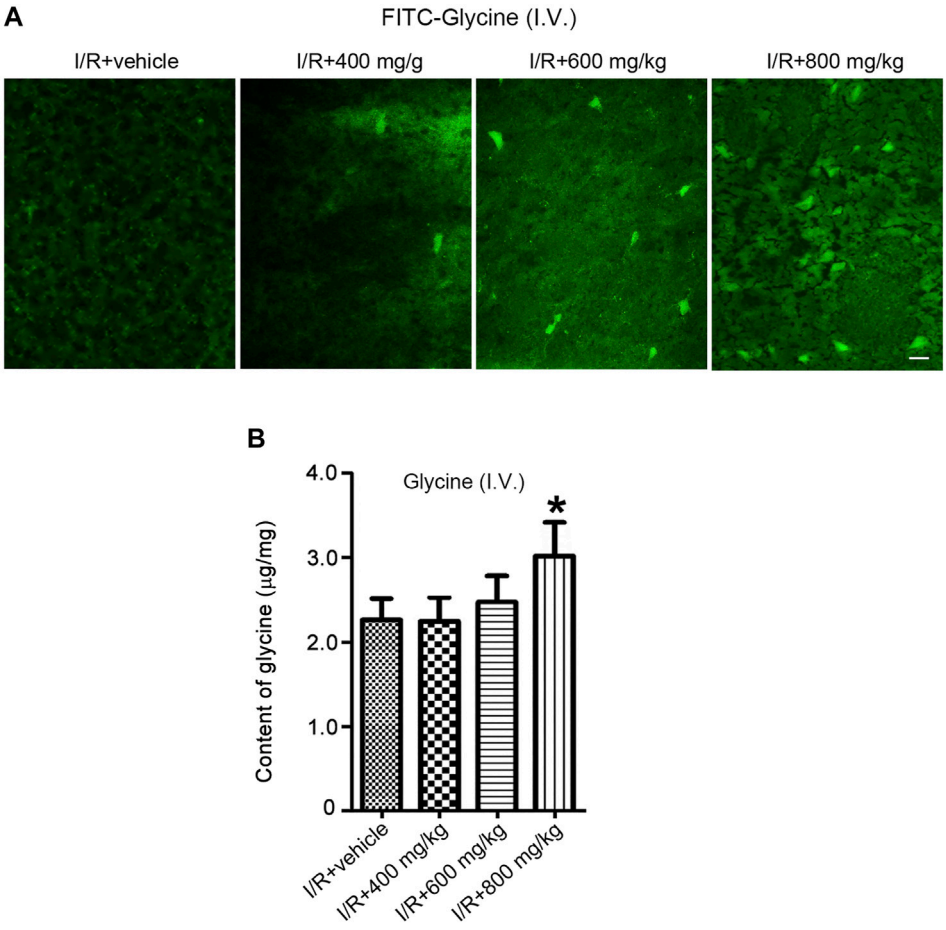

FIGURE 1
A high dose is required for glycine to pass through BBB after rat cerebral ischemia-reperfusion injury. **(A)** FITC-Glycine at different concentrations is intravenously injected at 1.0 h after rat cerebral I/R injury. Fluorescent images show the labeling of FITC-Glycine in the ischemia brain at 1.0 h after intravenous injection of FITC-Glycine. I/R: ischemia-reperfusion. Scale bar = 20 μm. **(B)** Glycine at different concentrations is intravenously injected at 1.0 h after rat cerebral I/R injury. The levels of glycine are measured by HPLC in the ischemic brain at 1.0 h after the intravenous injection of various concentrations of glycine (n = 8, *p < 0.05 vs. I/R + vehicle; ANOVA test). I/R: ischemia-reperfusion.

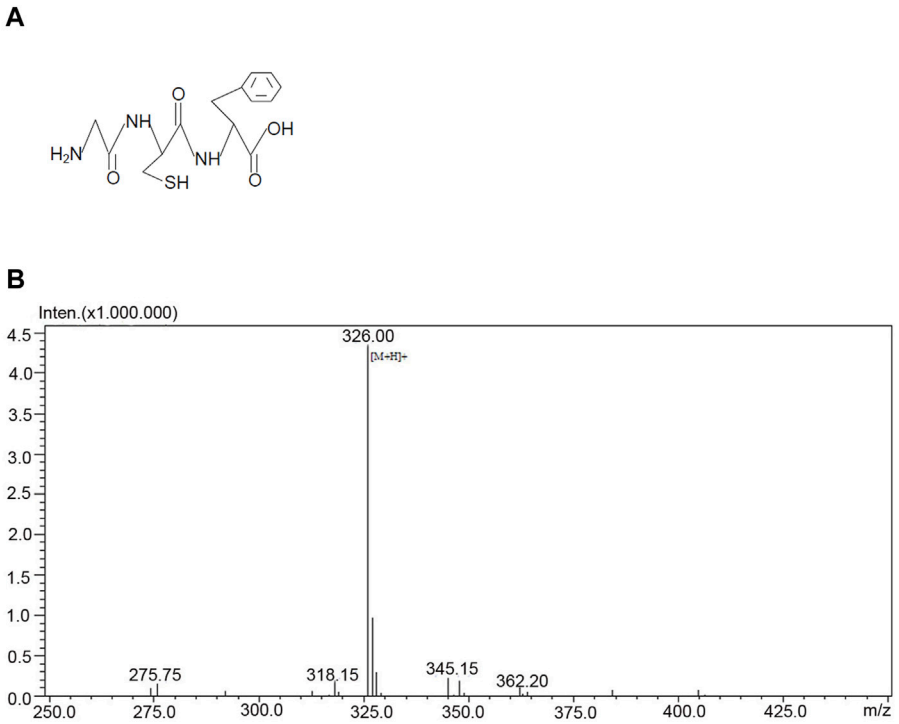

FIGURE 2
Structure and the mass spectrometry analysis of GCF. **(A)** The structure of GCF. **(B)** Mass spectrometry analysis of GCF.

the ischemic neurons and protected against ischemic neuronal death in stroke animals.

Results

Glycine has low BBB permeability in cerebral ischemia conditions

Glycine is known to protect against cerebral ischemia injury. However, the permeability of glycine to BBB is not clear. We set up to test whether glycine is permeable to BBB in rats subjected to middle cerebral artery occlusion (MCAO, an experimental model of cerebral ischemia injury). To enable the visualization of glycine in the brain, we conjugated fluorescein isothiocyanate (FITC) with glycine. FITC-Glycine was injected intravenously 1 h after cerebral ischemia-reperfusion injury in the MCAO rats. We found that only an extra high dose of FITC-Glycine (800 mg/kg) led to the significant detection of FITC-Glycine in the ipsilateral ischemic brain at 1.0 h after intravenous injection of FITC-Glycine (Figure 1A). To further confirm the low BBB permeability of glycine in the ischemic brain, we injected glycine intravenously 1 h after ischemia-reperfusion injury in the MCAO rats. HPLC assay showed that the levels of glycine were elevated in the ischemic brain at the concentration of 800 mg/kg after intravenous injection (Figure 1B). Thus, these results indicate that glycine has low BBB permeability in the ischemic brain and is unlikely to be directly used as a practical neuroprotectant for the treatment of stroke patients.

Design a glycine-containing tripeptide that is BBB-permeable

To develop a practical approach that allowed glycine to pass through BBB and entered the injured brain to confer neuroprotection, we designed a glycine-containing tripeptide, the H-glycine-cysteine-phenylalanine-OH (GCF) (Figures 2A,B). As the aromatic amino acid phenylalanine has a high permeability to BBB (Rautio et al., 2013; Oller-Salvia et al., 2016), we included phenylalanine in the GCF to increase the permeability of GCF through BBB. We conjugated cysteine with glycine in the GCF as we reasoned that the bond between glycine and cysteine was cleavable.

We first tested whether GCF was able to cross BBB and entered the ischemic brain in the rat MCAO model. To trace the location of GCF in the brain, we conjugated FITC with the amino terminal of GCF. FITC-GCF (150 mg/kg) was intravenously injected at 1.0 h after rat cerebral ischemia-reperfusion. At

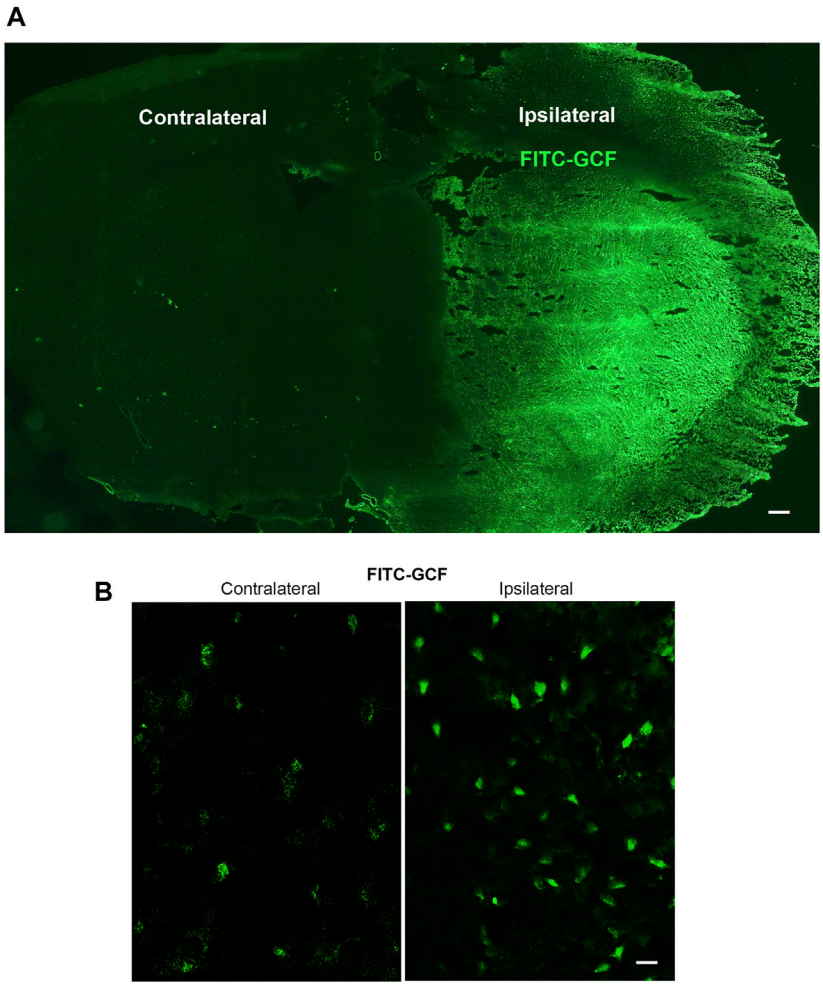

FIGURE 3
Intravenous injection of GCF leads to the distribution of GCF in the ischemic brain. **(A,B)** FITC-GCF (150 mg/kg) is intravenously injected at 1.0 h after rat cerebral ischemia-reperfusion injury. Brain sections are examined 1.0 h after intravenous FITC-GCF injection. **(A)** The low power sample image shows that FITC-GCF is distributed in the ipsilateral ischemic brain and the contralateral brain. Scale bar = 100 μm. **(B)** High-power images show the cell labeling by intravenous FITC-GCF injection in the ipsilateral and contralateral brain regions. Scale bar = 30 μm.

1.0 h after intravenous injection, FITC-GCF was found to distribute both in the ipsilateral ischemic brain and the contralateral brain, but with high intensities in the ipsilateral brain (Figures 3A,B). These data suggest that GCF is permeable to rat BBB.

We further showed that few FITC-labeled cells were localized in the ipsilateral ischemia brain but not in the ipsilateral sham brain (Figure 4A). However, FITC-GCF-labelled cells were localized in both ipsilateral ischemic and the sham brain with more FITC-GCF-labelled cells in the ischemic brain (Figure 4A). We then examined the colocalization of FITC or FITC-GCF with NeuN (a mature neuronal marker) in Sham and I/R animals. Immunocytochemical staining showed that the number of NeuN-positive neurons labeled with FITC-GCF was higher than that labeled with FITC in the ischemic brain (Figure 4B). The number of NeuN-positive neurons labeled with FITC-GCF was higher than that of the Sham brain (Figure 4B). These results together indicate that GCF, but not FITC, efficiently passes through BBB and enters the damaged neurons after ischemia-reperfusion injury.

PhT1 is an oligopeptide transporter that is known to regulate the cellular uptake of di/tripeptides (Wang et al., 2010; Smith et al., 2013). It has been reported that PhT1 is abundantly expressed in the rodent brain (Yamashita et al., 1997; Shen et al., 2004; Smith et al., 2004). However, the function of PhT1 in the brain is largely unknown. To test whether PhT1 mediates GCF transport through BBB, brain uptakes of FITC-GCF were determined in the absence and presence of L-histidine, a specific inhibitor of PhT1. As shown in Figure 4C, in the presence of 10 mmol L-histidine, the uptake

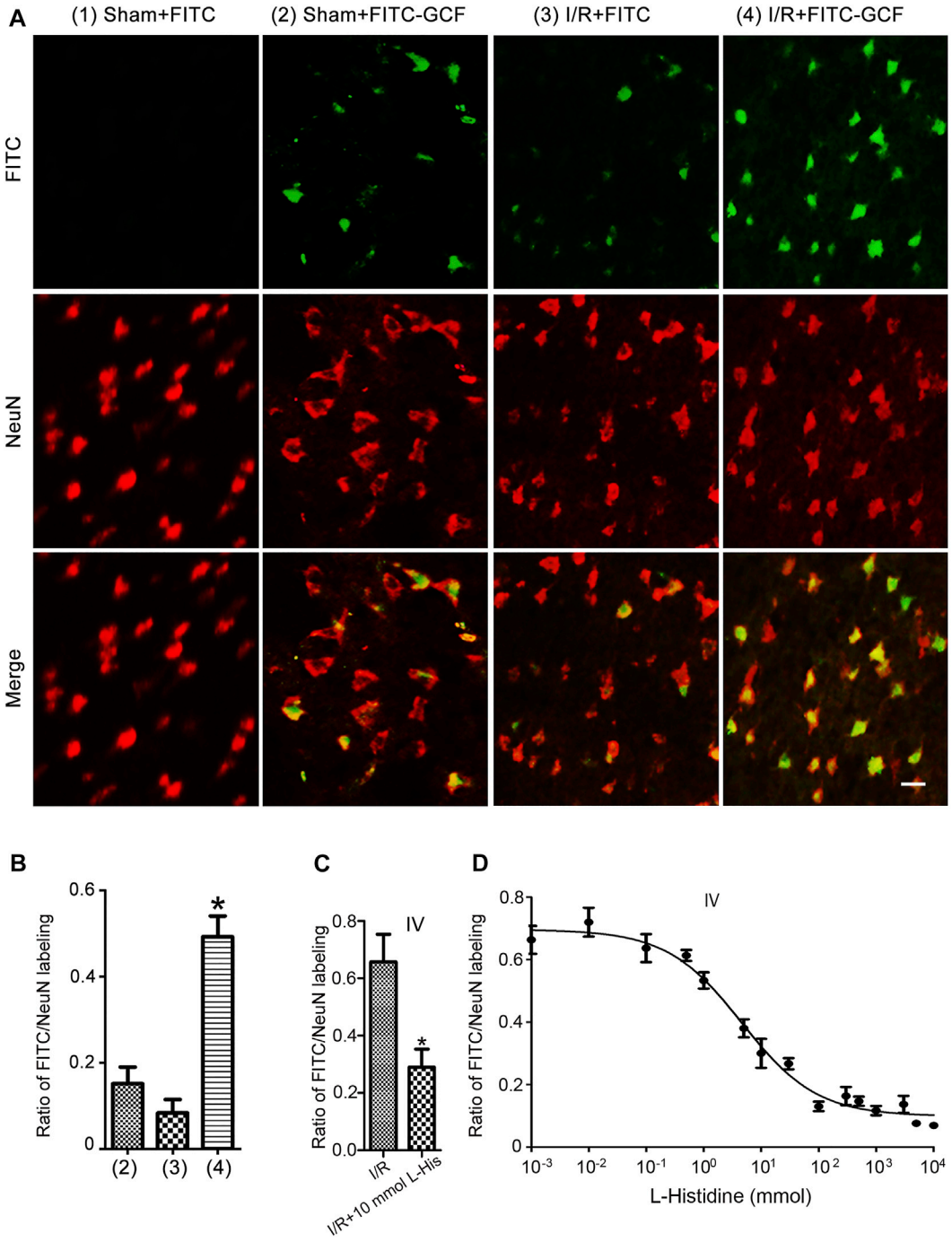

FIGURE 4
Intravenous injection of GCF leads to the distribution of GCF in the ischemic neurons. **(A)** Intravenous injection of FITC or FITC-GCF (150 mg/kg) is performed in rats at 1.0 h following I/R. The brain sections are collected to detect FITC or FITC-GCF at 1.0 h after injection. Sample fluorescent images show that FITC-GCF but not FITC are detected in the neurons of the ipsilateral brain in Sham animals. Both FITC and FITC-GCF are detected in the neurons of the ipsilateral brain in ischemic animals. FITC-GCF is colocalized with NeuN-positive neurons. Scale bar = 50 μm. **(B)** Summarized data indicate that the number of NeuN-positive neurons labeled with FITC-GCF is remarkably higher than that labeled with FITC in the ischemic brain. The number of NeuN-positive neurons labeled with FITC-GCF is remarkably higher in the ischemic brain than in the Sham brain. ($n = 7$, $^*p < 0.05$ vs. I/R + FITC or Sham + FITC-GCF; ANOVA test). I/R: ischemia-reperfusion. **(C)** L-histidine (10 mmol) and FITC-GCF (150 mg/kg) are intravenously injected in rats at 3.0 h following ischemia-reperfusion. The brain sections are collected to detect FITC-GCF at 1.0 h after intravenous injection. The summarized data indicate that the uptake of FITC-GCF is inhibited by L-Histidine ($n = 6$, $^*p < 0.05$ vs. I/R; Student t-test). **(D)** Dose-response inhibition of FITC-GCF (150 mg/kg) uptake by L-Histidine in the ischemic brain. IV: intravenous injection; I/R: ischemia-reperfusion; L-histidine: L-His.

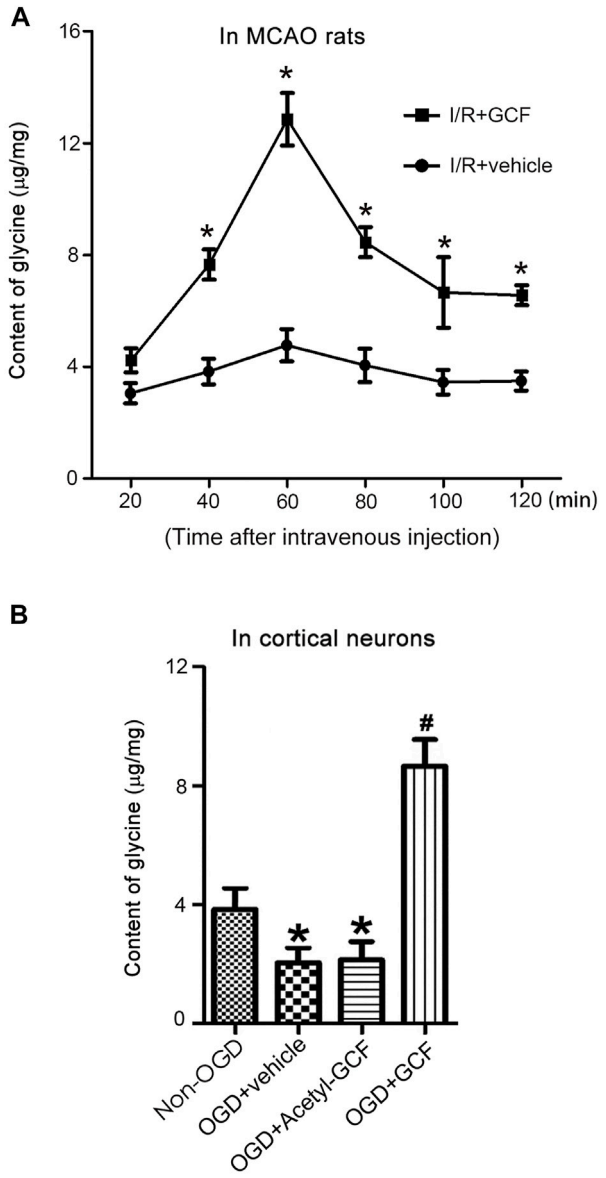

FIGURE 5
GCF injection results in increased level of glycine in the ischemic brain. **(A)** Intravenous injection of GCF (150 mg/kg) at 1.0 h after rat I/R increases the levels of glycine in the ischemic brain tissue at 40, 60, 80, 100 and 120 min following GCF injection (n = 6, $^{*}p < 0.05$ vs. I/R + vehicle; ANOVA test). I/R: ischemia reperfusion; Vehicle: 0.9% NaCl. **(B)** HPLC measurement in the neuronal cultures show that GCF (15 μM) but not acetyl-GCF at 1.0 h after reoxygenation increases the level of intraneuronal glycine at 60 min following GCF treatment (n = 6, $^{*}p < 0.05$ vs. Non-OGD, $^{\#}p < 0.05$ vs. OGD + vehicle; ANOVA test). Vehicle: 0.9% NaCl.

of FITC-GCF was reduced by 57%. Dose-response inhibitory analysis indicated that the uptake of FITC-GCF (150 mg/kg) was inhibited by L-histidine in the ischemic brain region with IC50 of 4.61 mmol (Figure 4D). These data suggest that the transport of GCF through BBB requires oligopeptide transporter PhT1.

Interestingly, we revealed that the intranasal administration of FITC-GCF led to the distribution of FITC-GCF in the damaged rat brain region after ischemia-reperfusion injury (Supplementary Figure S1). This result further confirmed the permeability of GCF to BBB and also provides a possibility for the future development of GCF as a pre-hospital oneself therapy immediately following stroke onset.

Intravenous GCF injection leads to an increased level of glycine in the ischemic brain

To determine whether the tripeptide GCF released glycine in the ischemic brain region, we performed HPLC to measure the levels of glycine in the ipsilateral ischemic brain tissues after intravenous GCF injection. Our results showed that the treatment of GCF (150 mg/kg) increased the level of glycine in the ischemic brain tissue at 40, 60 80, 100, and 120 min after GCF injection while compared with the vehicle group (Figure 5A). We also treated the neuronal cultures, subjected to oxygen-glucose deprivation (OGD, an *in vitro* model of cerebral ischemia injury), with GCF or acetyl-GCF [a stabilized form of GCF that was difficult to be cleaved (Xiong et al., 2009)] at 1.0 h after reoxygenation. HPLC was used to measure the level of intraneuronal glycine. We found that the level of glycine was increased at 60 min after the treatment of GCF but not acetyl-GCF (Figure 5B). These data support the possibility that GCF may release glycine in the ischemic brain.

Intravenous GCF injection protects against cerebral ischemia-reperfusion injury

We then set up to determine whether the intravenous injection of GCF was neuroprotective after ischemia-reperfusion injury. GCF was intravenously injected at 1.0 h after ischemia-reperfusion in rats subjected to 2 h MCAO. Animals were sacrificed to measure the infarct volume at 24 h after ischemia onset. The cerebral infarction was measured in the brain sections stained with TTC (2,3,5-triphenyltetrazolium chloride). Our data showed that intravenous injection of GCF (10, 50, and 150 mg/kg) reduced the infarct volume of MCAO rats (Figure 6A). Glycine (800 mg/kg) was also intravenously injected in the same experimental conditions. We found that an extra high concentration of glycine exerted a neuroprotective effect (Figure 6A).

We further verified the neuroprotective effect of GCF in the OGD-insulted cultured neurons. Double labeling of propidium iodide (PI) and fluorescein diacetate (FDA) was performed to

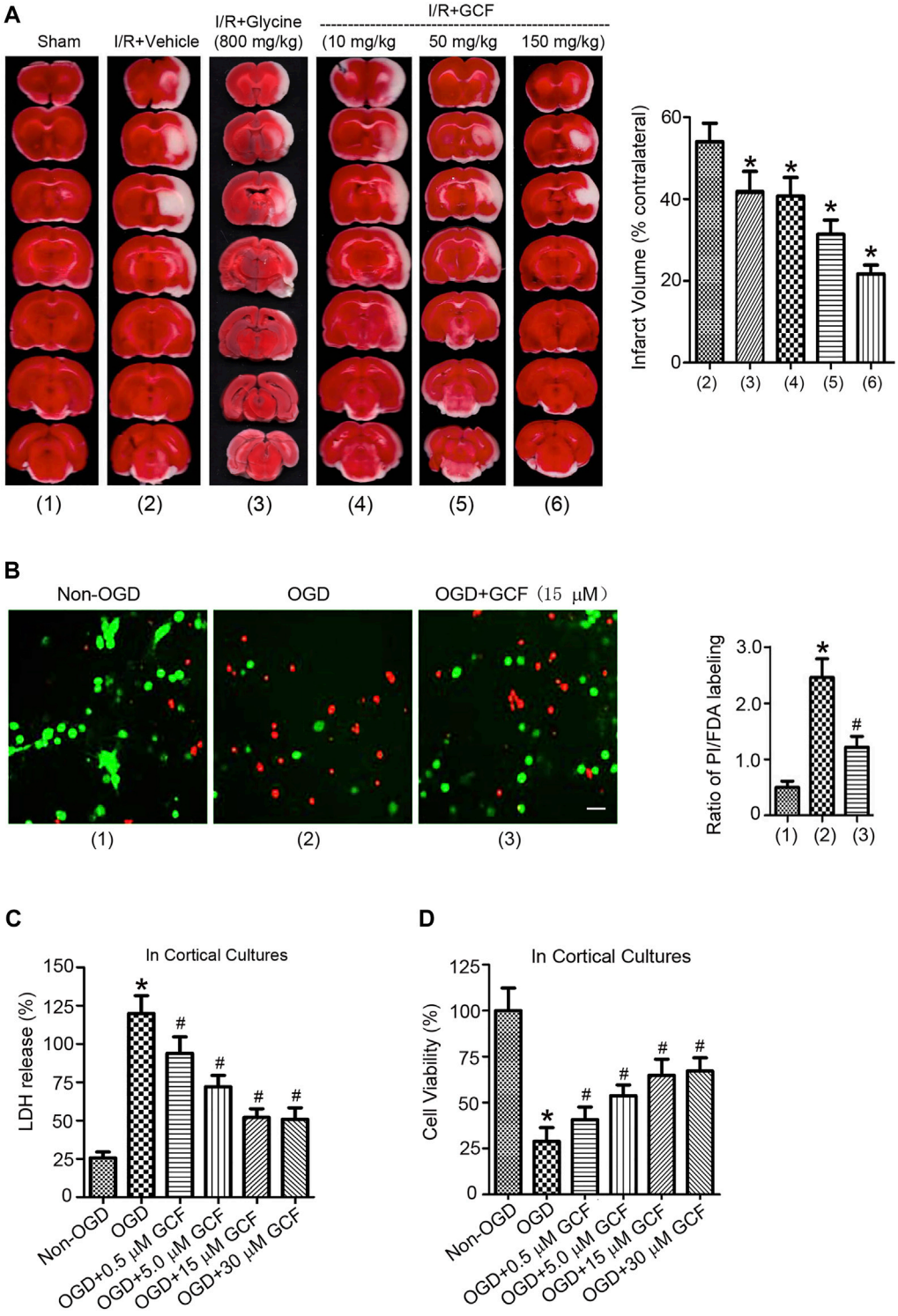

FIGURE 6
The neuroprotective effect of GCF. **(A)** Left: sample images of TTC staining show that intravenous injection of glycine (800 mg/kg) and GCF (10, 50 and 150 mg/kg) at 1.0 h following I/R reduces the infarct volume of ischemic brain at 24 h following ischemia onset. Right: the summarized data indicate that GCF is neuroprotective (n = 8, *p < 0.05 vs. I/R + Vehicle; ANOVA test). IV: intravenous injection. I/R: ischemia-reperfusion. Vehicle: 0.9% NaCl. **(B)** GCF (15 μM) reduces OGD-induced cortical neuronal death (n = 6, *p < 0.05 vs. Non-OGD; $^{\#}p$ < 0.05 vs. OGD; ANOVA test). Green: FDA; Red: PI. **(C,D)** LDH and MTT assays show that GCF is neuroprotective in OGD-insulted neurons (n = 7 for each group, *p < 0.05 vs. Non-OGD; $^{\#}p$ < 0.05 vs. OGD; ANOVA test).

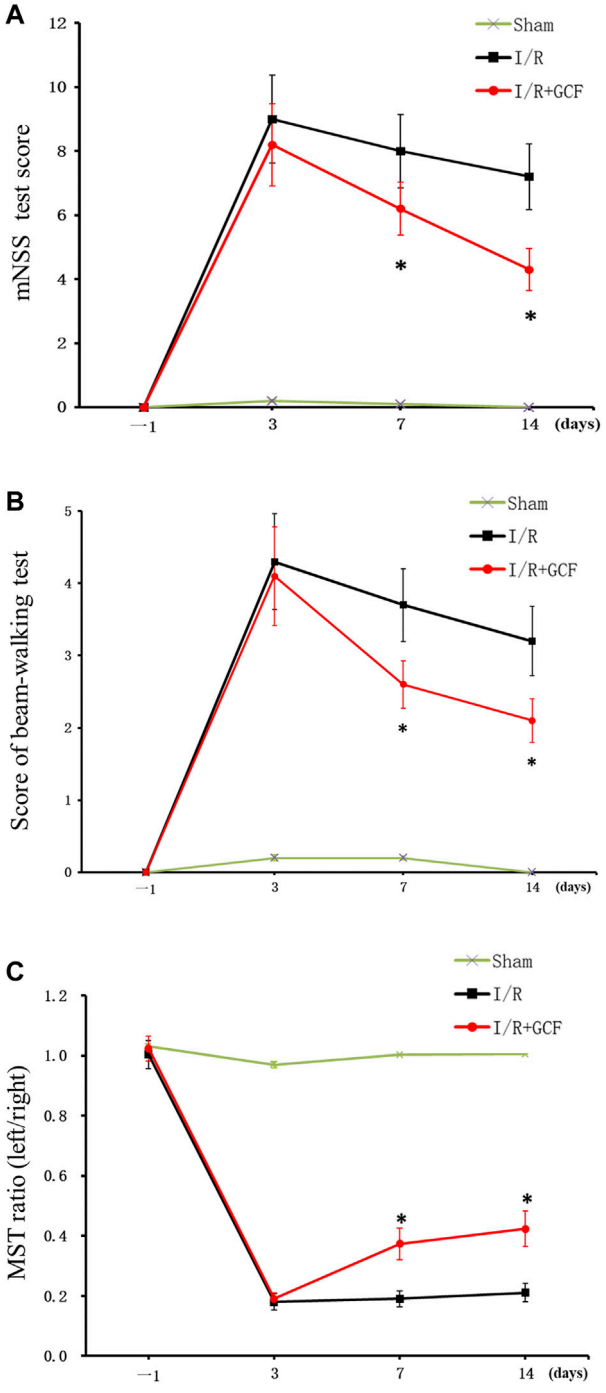

FIGURE 7
GCF Improves the neurobehavioral function of stroke animals. (A) Summarized data show that rats treated with GCF have significantly lower scores on mNSS tests on days 7 and 14 after MCAO (n = 8 rats for each group, *p < 0.05 vs. I/R, ANOVA test). (B) Summarized data show that rats treated with GCF have significantly lower scores on the beam-walking test on days 7 and 14 after MCAO (n = 9 rats for each group, *p < 0.05 vs. I/R, ANOVA test) (C) Summarized data show that rats treated with GCF have a
(*Continued*)

FIGURE 7
significantly higher ratio of a modified sticky-tape test at day 7 and 14 after MCAO (n = 8 rats for each group, *p < 0.05 vs. I/R, ANOVA test).

determine the ratio of neuronal death/viability. We found that treatment of GCF (15 μM) at 1.0 h after reoxygenation increased the ratio of cortical neuronal viability at 24 h after OGD onset (Figure 6B). In a dose-dependent manner, GCF reduced the level of lactate dehydrogenase (LDH) released from the injured neurons and increased the rate of neuronal survival determined by 3-(4,5-dimethylthiazol-2-yl)-2,5-diphenyltetrazolium bromide (MTT) assay (Figures 6C,D).

GCF promotes functional recovery of stroke animals

To determine the functional consequence of GCF in stroke animals, we performed a battery of neurobehavioral tests including modified neurological severity scores (mNSS) test, beam-walking test, and modified sticky-tape (MST) test 1 day before MCAO, and at 3, 7, and 14 days after MCAO. Our data showed that rats treated with GCF had significantly lower scores on the mNSS test on day 7 and 14 after MCAO (Figure 7A), and lower scores on a beam-walking test on day 7 and 14 after MCAO (Figure 7B), and a higher ratio of modified sticky-tape (MST) test at days 7 and 14 after MCAO (Figure 7C). Together, these results provide functional evidence for the neuroprotective role of GCF in stroke animals.

The neuroprotection of GCF depends on GCF-induced increase of glycine in the ischemic brain

The preceding HPLC data suggest that intravenous GCF injection led to an increase of glycine in the ischemic brain (Figure 5). To further verify whether the increased level of glycine contributed to GCF-induced neuroprotection, we synthesized a stabilized form of GCF, the Acetyl-GCF, which was difficult to cleave (Xiong et al., 2009). FITC-Acetyl-GCF (150 mg/kg) was intravenously injected at 1.0 h following ischemia-reperfusion. At 1.0 h after injection, FITC-Acetyl-GCF was found to localize in the ischemic neurons (Figure 8A). However, the level of glycine was not increased at 1.0 h after injection of Acetyl-GCF (Figure 8B). We also found that intravenous injection of Acetyl-GCF (150 mg/kg) 1.0 h after ischemia-reperfusion had no effect on the infarct volume at 24 h after ischemia onset (Figure 8C). In addition, Acetyl-GCF (15 μM) did not reduce

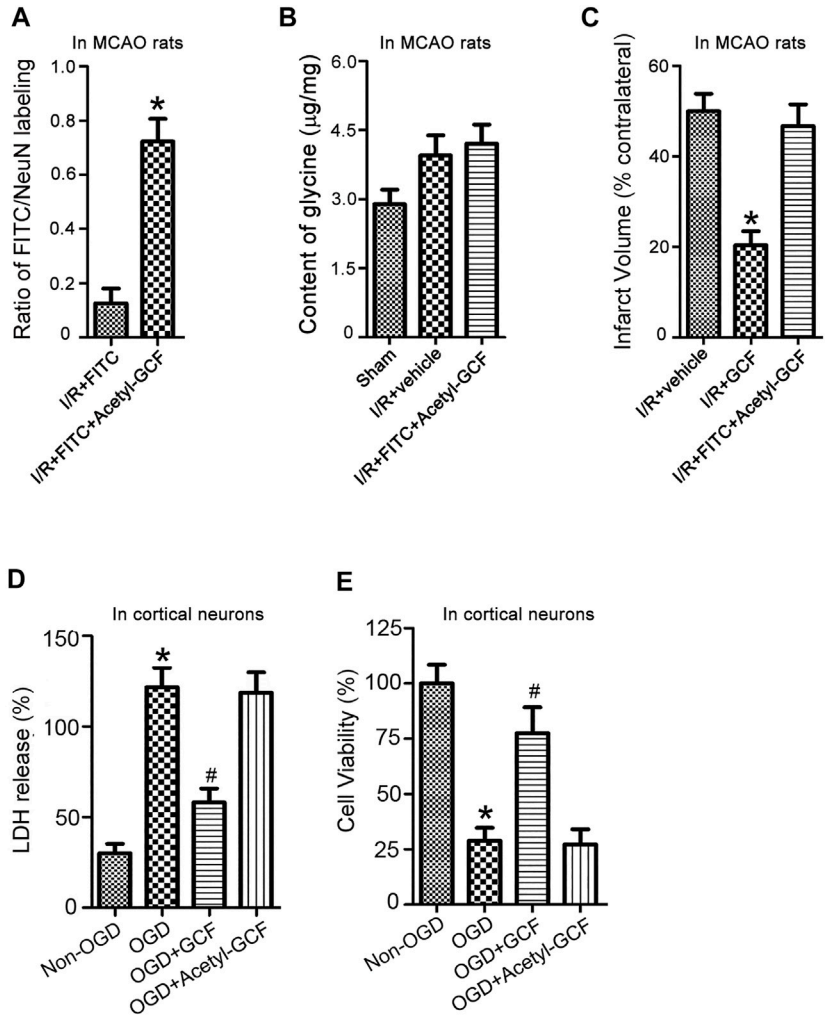

FIGURE 8
GCF-mediated increase of glycine in the ischemic brain is required for GCF-induced neuroprotection. **(A)** FITC-Acetyl-GCF (150 mg/kg) is intravenously injected in rats at 1.0 h following I/R. At 1.0 h after injection, FITC-Acetyl-GCF is localized in NeuN-labeled neurons ($n = 7$, $^{*}p < 0.05$ vs. I/R + FITC; Student's *t*-test). I/R: ischemia-reperfusion. **(B)** Compared with the group of I/R + Vehicle, the level of glycine is not increased in the ischemic brain at 1.0 h after the intravenous injection of Acetyl-GCF (150 mg/kg; n = 7). I/R: ischemia-reperfusion. **(C)** TTC staining data show that intravenous injection of Acetyl-GCF (150 mg/kg) at 1.0 h after I/R does not reduce the infarct volume at 24 h after ischemia onset (n = 7, $^{*}p < 0.05$ vs. I/R + Vehicle; ANOVA test). I/R: ischemia-reperfusion. Vehicle: 0.9% NaCl. **(D,E)** LDH and MTT assays show that Acetyl-GCF (15 μM) does not reduce OGD-induced cortical neuronal death at 24 h after injury ($n = 6$ for each group, $^{*}p < 0.05$ vs. Non-OGD; $^{\#}p < 0.05$ vs. OGD; ANOVA test).

OGD-induced cortical neuronal death (Figures 8D,E). Thus, these results suggest that intravenous injection of GCF confers neuroprotection by increasing the level of glycine in the ischemic brain region.

Discussion

We and the others have previously shown that glycine exerts a neuroprotective effect *in vitro* and in cerebral ischemia injury *in vivo* (Yang et al., 2000; Zhao et al., 2005; Liu et al., 2007; Tanabe et al., 2010; Chen et al., 2016; Hu et al., 2016). However, whether these amino acids can efficiently cross the BBB to confer neuroprotection remains largely unknown. In this study we showed that a high dose of glycine was required for intravenous injection-induced neuroprotection in ischemic stroke rats, indicating a low BBB permeability of glycine in cerebral ischemia conditions. In order to deliver glycine through the BBB into the ischemic brain, we designed a novel glycine-containing and BBB-permeable tripeptide GCF. To ensure the tripeptide crosses the BBB, we included the aromatic amino acid phenylalanine in the tripeptide GCF. Indeed, our results showed that GCF was distributed in both Sham and ischemic brains but with a larger amount of GCF

localized in the ischemic neurons following intravenous injection of GCF. These data support the notion that GCF can pass BBB efficiently. Since the GCF distribution is high in the ipsilateral brain compared with the contralateral side, it is expected that enhanced distribution of GCF is possibly due to BBB breakdown by ischemic damage or the induction of LAT1 expression at the BBB in the ischemic brain region.

Another key design for the GCF is the inclusion of cysteine with glycine to enable the release of glycine from GCF. It is possible that the specific peptidase expressed in neurons cleaves glycine in GCF. We showed that intravenous GCF injection led to an increased level of glycine in the ischemic brain and conferred neuroprotection. But the intravenous injection of acetyl-GCF, a non-cleaved form of GCF, resulted in no change in the level of glycine and exerted no neuroprotective effect on ischemic neuronal death. These data suggest that intravenous GCF injection-induced neuroprotection may be mediated by the released glycine from GCF in the ischemic brain.

Interestingly, intranasal administration of GCF also leads to the distribution of GCF in the ischemic brain region. This finding not only further supports the permeability of GCF to BBB but also provides an attractive possibility for the development of GCF as a pre-hospital neuroprotection therapy immediately after stroke onset.

Recent studies indicate that developing peptide-based neuroprotectants is a promising strategy in stroke therapy (Aarts et al., 2002; Cui et al., 2007; Hill et al., 2012; Hill et al., 2020). The peptide Tat-NR2B9c (also termed NA-1) is developed from the discovery that postsynaptic density protein-95, the NMDA receptor-interacting protein, is a hub for excitotoxic signaling and a stroke therapeutic target (Aarts et al., 2002; Cui et al., 2007). The Phase 3 clinical trial of NA1 has provided encouraging human efficacy data (Hill et al., 2020). In contrast to NA-1 and other existing peptides that use peptides themselves to interfere in signaling interaction or degrade target proteins (Aarts et al., 2002; Hill et al., 2012; Schaible et al., 2013; Fan et al., 2014), GCF acts as a BBB shuttle and prodrug to deliver its own amino acid to confer therapeutic effect, representing a new design of peptide drug and a novel therapeutic mechanism.

As a small peptide, GCF has a simple structure, low immunogenicity, and higher chemical versatility than traditional peptide approaches (Oller-Salvia et al., 2016). Tripeptide is easier to be characterized, synthesized, and purified and has a lower cost. Thus, the design of the BBB-permeable small peptide offers a safe, simple and efficient approach for the development of ischemic stroke therapeutics.

Substantial evidence indicates that amino acids, including glycine, have cytoprotective property (King et al., 2010; Petrat et al., 2012). Because of the low permeability of these amino acids to the BBB, amino acid supplement therapy for CNS diseases is lacking. The GCF design provides a novel therapeutic strategy by which low BBB-permeable amino acids are delivered into the brain of CNS diseases. In addition, the efficient membrane permeability of GCF also offers the possibility to develop GCF in treating a variety of periphery organ diseases including injuries to the liver, small intestine, lung, skeletal muscle, and heart following ischemia–reperfusion, hemorrhagic shock, or resuscitation (Petrat et al., 2012).

Methods and materials

Animals

All animal experiments were approved and carried out in compliance with the IACUC guidelines of the Wuhan University School of Medicine and Qingdao University School of Medicine. All animal use and experimental protocols were approved and carried out in compliance with the IACUC guidelines and the Animal Care and Ethics Committee of Wuhan University School of Medicine and Qingdao University School of Medicine. Randomization was used to assign samples to the experimental groups, and to collect and process data. The experiments were performed by investigators blinded to the groups for which each animal was assigned. All studies involving animals are reported in accordance with the ARRIVE guidelines for reporting experiments involving animals (Curtis et al., 2015; McGrath and Lilley, 2015).

Reagents

GCF, Acetyl-GCF, FITC, FITC-GCF, FITC-Acetyl-GCF, and FITC-Glycine were obtained from Top-peptide Co., Ltd. (Shanghai, China). Glycine was purchased from Sigma-Aldrich (St. Louis, MO, United States). DNFB was purchased from Xiya Reagent (Chengdu, China). HPLC-grade acetonitrile and methanol were purchased from Sinopharm Chemical Reagent (Shanghai, China). All other chemicals of analytical reagent grade were purchased from Sinopharm Chemical Reagent (Shanghai, China).

Middle cerebral artery occlusion in rats and infarct measurement

Adult male Sprague–Dawley (SD) rats, weighing 250–270 g, were group-housed with two to three rats per cage on a 12 h light/dark cycle in a temperature-controlled room (23–25°C) with free access to food and water. Animals were allowed at least 3 days to acclimatize before experimentation. Transient focal cerebral ischemia was induced using the suture occlusion technique (Wexler et al., 2002; Chen et al., 2017; Zhang et al., 2017). Male Sprague–Dawley rats weighing 250–270 g were anesthetized with 4% isoflurane in 70% N_2O and 30% O_2 using a mask. A midline incision was made in the neck, the right external carotid artery (ECA) was carefully exposed and dissected, and a 3–0 monofilament nylon suture was inserted from the ECA into the right internal carotid artery to occlude the

origin of the right middle cerebral artery (MCA) (approximately 22 mm). After 1.5 h of occlusion, the suture was removed to allow reperfusion, the ECA was ligated, and the wound was closed. Non-OGD-operated rats underwent identical surgery except that the suture was inserted and withdrawn immediately. Rectal temperature was maintained at 37.0 ± 0.5°C using a heating pad and heating lamp.

Rats were sacrificed at various times following reperfusion after being anesthetized, and the brains were removed for TTC (2,3,5-triphenyltetrazolium chloride) staining. The brain was placed in a cooled matrix and 2.0 mm coronal sections were cut. Individual sections were placed in 10 cm Petri dishes and incubated for 30 min in a solution of 2% TTC in phosphate buffered saline at 37°C. The slices were fixed in 4% paraformaldehyde at 4°C. All image collection, processing, and analysis were performed in a blind manner. The scanned images were analyzed using image analysis software (Image-Pro Plus Version 6.0, United States). The infarct volume was calculated to correct for edema. The normal volume of the contralateral hemisphere and the normal volume of the ipsilateral hemisphere were measured, and the infarct percentage was calculated as % contralateral structure to avoid mismeasurement secondary to edema.

Intravenous injection

Male Sprague-Dawley rats weighing 250–270 g were anesthetized with 4% isoflurane in 70% N_2O and 30% O_2 using a mask. FITC, FITC-GCF, GCF, and Acetyl-GCF at the designed concentration were dissolved in 0.5 ml saline and then injected into the right femoral vein per animal.

Immunohistochemistry

The method has been described previously (Ning et al., 2004). Rats were sacrificed after being anesthetized, and the brains were removed. The tissue was then frozen in Tissue-Tek OCT mounting medium and 15 μm coronal sections were cut. Sections were subsequently spread on microscope slides and allowed to air dry. Air dried sections were fixed in 4% paraformaldehyde in PBS for 30 min then washed 3 times in PBS for 5 min each. After post-fixation, the sections were blocked and permeabilized in 0.1 M PBS with 0.3% TX-100 (sigma) and 5% bovine serum albumin (BSA) for 1 h. Following permeabilization, a primary anti-NeuN or anti-glycine antibody (Millipore, United States) was applied overnight at 4°C. Primary antibody was removed with three washes in PBS and secondary antibody (Alexa 594 conjugated to goat anti-mouse) was applied for 1 h at room temperature. Secondary antibody was removed with three washes in PBS and the sections were observed under an Olympus BX51 microscope or a Zeiss LSM 510 META confocal microscope.

Neuronal culture and OGD insult

The cortical neuronal cultures were prepared from Sprague–Dawley rats at gestation day 17 as described (Brewer et al., 1993; Liu et al., 2006). Briefly, dissociated neurons were suspended in a plating medium (Neurobasal medium, 2% B-27 supplement, 0.5% FBS, 0.5 μM L-glutamine, and 25 μM glutamic acid) and plated on poly-D-lysine coated Petri dishes. After 1.0 days in culture, half of the plating medium was removed and replaced with a maintenance medium (Neurobasal medium, 2% B-27 supplement, and 0.5 mM L-glutamine). Thereafter, the maintenance medium was changed in the same manner every 3.0 days. To suppress glial cell growth, the cultures were exposed to 10 μM cytosine arabinoside (Ara C) for 48 h between days 3 and 5 after plating. The cultured neurons were used for experiments 12 days after plating.

The method of OGD insult was described in our previous study (Liu et al., 2006). To initiate the OGD challenge, cells were transferred to a deoxygenated glucose-free extracellular solution (ECS) (in mM: 116 NaCl, 5.4 KCl, 0.8 $MgSO_4$, 1.0 NaH_2PO_4, 1.8 $CaCl_2$, and 26 $NaHCO_3$), introduced into a specialized chamber, and maintained at 37°C in 85% N_2/10% H_2/5% CO_2 for 2 h. Neurons were removed from the chamber, transferred to the maintenance medium, and returned to the incubator. For non-OGD group treatment, cultures were transferred to the standard ECS (in mM: 116 NaCl, 5.4 KCl, 0.8 $MgSO_4$, 1.0 $NaH2PO_4$, 1.8 $CaCl_2$, 26 $NaHCO_3$, and 33 glucose), introduced into the chamber maintained at 37°C in 95% air/5% CO_2. After 2 h incubation, the neurons were transferred to the maintenance medium and returned to the original incubator.

High-performance liquid chromatography

The neuronal cultures were first washed with ECS three times before sample collection. Brain samples were collected after the animals were sacrificed and transcardially perfused with PBS. The samples were then homogenized in 200 μL of chilled saline solution (0.9%). The homogenate was centrifuged at 14,000 rpm for 20 min at 4°C. The supernatant was used to measure the level of proteins. The remaining samples were mixed with two x volume of methanol and centrifuged to remove protein. The supernatant was transferred for derivatization (Mao et al., 2012). An aliquot of mixed amino acids solution (40 μL) or sample supernatant (40 μL) was mixed with 0.5 M sodium bicarbonate solution (40 μL) and 0.5% of DNFB (20 μL) in a 500 μL centrifuge tube. The well-mixed solution was incubated at 60°C in the water bath for 1 h. DNFB was reacted with an amino group and enabled amino acids to be detected with UV detection. After cooling to room temperature, the solution (30 μL) was injected into the equilibrated HPLC system. Analysis was carried out on a Waters HPLC system

(United States) equipped with a UV detector (360 nm). The analyte was separated on a Hypersil BDS C_{18} (200 mm length × 4.6 mm, 5.0 μm particle diameter) manufactured by Elite Analytical Instrument (Dalian, China). The mobile phase was composed of 0.05 M (PH = 6.5) sodium acetate buffer (A), a mixture of acetonitrile and water (1:1, v:v, B) was carried out in a gradient elution mode with a flow rate of 1.0 ml/min (Supplementary Table S1). The column temperature was maintained at 30°C (Zhang et al., 2012).

PI and FDA labeling

Double staining of propidium iodide (PI) and fluorescein diacetate (FDA) was performed to detect neuronal death/viability (Jones and Senft, 1985; Zheng et al., 2012). Briefly, cultures were rinsed with an extracellular solution and incubated with FDA (5.0 μM) and PI (2.0 μM) for 30 min. The cultures were washed with ECS and then viewed on an Olympus fluorescent microscope (IX51, Olympus). Neuronal death/viability was determined by calculating the number of PI-labeled cells over FDA-labeled cells. The investigator for the cell count was blinded to the experimental treatment.

LDH assay

The lactate dehydrogenase (LDH) is a cytoplasmic enzyme retained by viable cells with intact plasma membranes and released from cells with damaged membranes. The LDH release was measured using CytoTox 96 cytotoxicity kit based on the manufacturer's instructions (Promega, United States) (Zheng et al., 2012). The levels of maximal LDH release were measured by treating the cultures with a 10× lysis solution (provided by the manufacturer) to yield complete lysis of the cells. Absorbance data were obtained using a 96-well plate reader (Molecular Devices, United States) at 490 nm. According to the manufacturer's instructions, the LDH release (%) was calculated by calculating the ratio of experimental LDH release to maximal LDH release.

MTT assay

The viability of the cells in the neuronal cultures was assessed by their ability to uptake thiazolyl blue tetrazolium bromide (MTT) (Chang et al., 2010; Chien et al., 2015; Chen et al., 2016). The cells were incubated with MTT for 1.0 h, then lysed with dimethyl sulfoxide (DMSO) and left at room temperature in the dark overnight. The lysates were then read on a plate reader (PowerWave X, Bio-Tek) at the absorbance wavelength of 540 nm.

Neurobehavioral tests

The modified neurological severity score (mNSS) test for evaluating neurological function (Panahpour et al., 2019), the Beam walk test for measuring animals' complex neuromotor function (Petullo et al., 1999; Chen et al., 2001), and the Adhesive-removal test, a modified sticky-tape (MST) test, for evaluating forelimb function (Aronowski et al., 1996) were described in detail in our previous study (Chen et al., 2017; Zhang et al., 2017).

Statistical analysis

The data and statistical analysis in this study comply with the recommendations on experimental design and analysis (Curtis et al., 2015). The group sizes per experiment were based on a power analysis (Charan and Kantharia, 2013). The criterion for significance (alpha) was set at 0.05. The power of 80% was considered to yield a statistically significant result. Student's *t*-test or ANOVA test was used where appropriate to examine the statistical significance of the differences between groups of data. Bonferroni tests were used for *post hoc* comparisons when appropriate. All results are presented as mean ± SEM. Significance was placed at $p < 0.05$.

Data availability statement

The raw data supporting the conclusion of this article will be made available by the authors, without undue reservation.

Ethics statement

The animal study was reviewed and approved by Animal Care and Ethics Committee of Wuhan University School of Medicine and Qingdao University School of Medicine.

Author contributions

JuC and YZ performed the experiment, analyzed data, and wrote the manuscript. YZ, HL, RL, JiC, XW, and SC performed the *in vivo* experiments and analyzed the data. ZZ, JS, and JG performed the *in vitro* experiments and analyzed the data. LZ, FC, and QW conceived the project and wrote the manuscript.

Funding

This work was supported by the National Key R&D Program of China (2019YFC0120000; 2018YFC1312300), National

Natural Science Foundation of China (NSFC: 82071385), Key Research and Development Project of Shandong (2019JZZY021010), and TaiShan Industrial Experts Programme (No. tscy20200412) to QW. This work was also supported by NSFC (81701291) to JC.

Conflict of interest

QW is employed as a part-time scientist by the company Qingdao Gui-Hong Intelligent Medical Technology Co, Ltd.

The remaining authors declare that the research was conducted in the absence of any commercial or financial relationships that could be construed as a potential conflict of interest.

Publisher's note

Supplementary material

The Supplementary Material for this article can be found online at: https://www.frontiersin.org/articles/10.3389/fphar.2022.950376/full#supplementary-material

References

Aarts, M., Liu, Y., Liu, L., Besshoh, S., Arundine, M., Gurd, J. W., et al. (2002). Treatment of ischemic brain damage by perturbing NMDA receptor- PSD-95 protein interactions. *Science* 298, 846–850. doi:10.1126/science.1072873

Amelio, I., Cutruzzola, F., Antonov, A., Agostini, M., and Melino, G. (2014). Serine and glycine metabolism in cancer. *Trends biochem. Sci.* 39, 191–198. doi:10.1016/j.tibs.2014.02.004

Aronowski, J., Samways, E., Strong, R., Rhoades, H. M., and Grotta, J. C. (1996). An alternative method for the quantitation of neuronal damage after experimental middle cerebral artery occlusion in rats: Analysis of behavioral deficit. *J. Cereb. Blood Flow. Metab.* 16, 705–713. doi:10.1097/00004647-199607000-00022

Brewer, G. J., Torricelli, J. R., Evege, E. K., and Price, P. J. (1993). Optimized survival of hippocampal neurons in B27-supplemented Neurobasal, a new serum-free medium combination. *J. Neurosci. Res.* 35, 567–576. doi:10.1002/jnr.490350513

Chang, N., Li, L., Hu, R., Shan, Y., Liu, B., Li, L., et al. (2010). Differential regulation of NMDA receptor function by DJ-1 and PINK1. *Aging Cell* 9, 837–850. doi:10.1111/j.1474-9726.2010.00615.x

Charan, J., and Kantharia, N. D. (2013). How to calculate sample size in animal studies? *J. Pharmacol. Pharmacother.* 4, 303–306. doi:10.4103/0976-500X.119726

Chen, J., Hu, R., Liao, H., Zhang, Y., Lei, R., Zhang, Z., et al. (2017). A non-ionotropic activity of NMDA receptors contributes to glycine-induced neuroprotection in cerebral ischemia-reperfusion injury. *Sci. Rep.* 7, 3575. doi:10.1038/s41598-017-03909-0

Chen, J., Li, Y., Wang, L., Zhang, Z., Lu, D., LuM., et al. (2001). Therapeutic benefit of intravenous administration of bone marrow stromal cells after cerebral ischemia in rats. *Stroke* 32, 1005–1011. doi:10.1161/01.str.32.4.1005

Chen, J., Zhuang, Y., Zhang, Z. F., Wang, S., Jin, P., He, C., et al. (2016). Glycine confers neuroprotection through microRNA-301a/PTEN signaling. *Mol. Brain* 9, 59. doi:10.1186/s13041-016-0241-3

Chien, L., Chen, W. K., Liu, S. T., Chang, C. R., Kao, M. C., Chen, K. W., et al. (2015). Low-dose ionizing radiation induces mitochondrial fusion and increases expression of mitochondrial complexes I and III in hippocampal neurons. *Oncotarget* 6, 30628–30639. doi:10.18632/oncotarget.5790

Cui, H., Hayashi, A., Sun, H. S., Belmares, M. P., Cobey, C., Phan, T., et al. (2007). PDZ protein interactions underlying NMDA receptor-mediated excitotoxicity and neuroprotection by PSD-95 inhibitors. *J. Neurosci.* 27, 9901–9915. doi:10.1523/JNEUROSCI.1464-07.2007

Curtis, M. J., Bond, R. A., Spina, D., Ahluwalia, A., Alexander, S. P. A., Giembycz, M. A., et al. (2015). Experimental design and analysis and their reporting: New guidance for publication in BJP. *Br. J. Pharmacol.* 172, 3461–3471. doi:10.1111/bph.12856

Fan, X., Jin, W. Y., Lu, J., Wang, J., and Wang, Y. T. (2014). Rapid and reversible knockdown of endogenous proteins by peptide-directed lysosomal degradation. *Nat. Neurosci.* 17, 471–480. doi:10.1038/nn.3637

Hill, M. D., Goyal, M., Menon, B. K., Nogueira, R. G., McTaggart, R. A., Demchuk, A. M., et al. (2020). Efficacy and safety of nerinetide for the treatment of acute ischaemic stroke (ESCAPE-NA1): A multicentre, double-blind, randomised controlled trial. *Lancet* 395, 878–887. doi:10.1016/S0140-6736(20)30258-0

Hill, M. D., Martin, R. H., Mikulis, D., Wong, J. H., Silver, F. L., Terbrugge, K. G., et al. (2012). Safety and efficacy of NA-1 in patients with iatrogenic stroke after endovascular aneurysm repair (ENACT): A phase 2, randomised, double-blind, placebo-controlled trial. *Lancet. Neurol.* 11, 942–950. doi:10.1016/S1474-4422(12)70225-9

Hu, R., Chen, J., Lujan, B., Lei, R., Zhang, M., Wang, Z., et al. (2016). Glycine triggers a non-ionotropic activity of GluN2A-containing NMDA receptors to confer neuroprotection. *Sci. Rep.* 6, 34459. doi:10.1038/srep34459

Jones, K. H., and Senft, J. A. (1985). An improved method to determine cell viability by simultaneous staining with fluorescein diacetate-propidium iodide. *J. Histochem. Cytochem.* 33, 77–79. doi:10.1177/33.1.2578146

King, N., Lin, H., and Suleiman, M. S. (2010). Cysteine protects freshly isolated cardiomyocytes against oxidative stress by stimulating glutathione peroxidase. *Mol. Cell. Biochem.* 343, 125–132. doi:10.1007/s11010-010-0506-6

Liu, B., Liao, M., Mielke, J. G., Ning, K., Chen, Y., Li, L., et al. (2006). Ischemic insults direct glutamate receptor subunit 2-lacking AMPA receptors to synaptic sites. *J. Neurosci.* 26, 5309–5319. doi:10.1523/JNEUROSCI.0567-06.2006

Liu, Y., Wong, T. P., Aarts, M., Rooyakkers, A., Liu, L., Lai, T. W., et al. (2007). NMDA receptor subunits have differential roles in mediating excitotoxic neuronal death both *in vitro* and *in vivo*. *J. Neurosci.* 27, 2846–2857. doi:10.1523/JNEUROSCI.0116-07.2007

Locasale, J. W. (2013). Serine, glycine and one-carbon units: Cancer metabolism in full circle. *Nat. Rev. Cancer* 13, 572–583. doi:10.1038/nrc3557

Lynch, J. W., Zhang, Y., Talwar, S., and Estrada-Mondragon, A. (2017). Glycine receptor drug discovery. *Adv. Pharmacol.* 79, 225–253. doi:10.1016/bs.apha.2017.01.003

Mao, K. B., Ma, Y., Shen, X. Y., Li, B. P., Li, C. Y., and Li, Z. L. (2012). Estimation of broadband emissivity (8-12 um) from ASTER data by using RM-NN. *Opt. Express* 20, 20096–20101. doi:10.1364/OE.20.020096

McGrath, J. C., and Lilley, E. (2015). Implementing guidelines on reporting research using animals (ARRIVE etc.): New requirements for publication in BJP. *Br. J. Pharmacol.* 172, 3189–3193. doi:10.1111/bph.12955

Ning, K., Li, L., Liao, M., Liu, B., Mielke, J. G., Chen, Y., et al. (2004). Circadian regulation of GABAA receptor function by CKI epsilon-CKI delta in the rat suprachiasmatic nuclei. *Nat. Neurosci.* 7, 489–490. doi:10.1038/nn1236

Oller-Salvia, B., Sanchez-Navarro, M., Giralt, E., and Teixido, M. (2016). Blood-brain barrier shuttle peptides: An emerging paradigm for brain delivery. *Chem. Soc. Rev.* 45, 4690–4707. doi:10.1039/c6cs00076b

Panahpour, H., Terpolilli, N. A., Schaffert, D., Culmsee, C., and Plesnila, N. (2019). Central application of aliskiren, a renin inhibitor, Improves outcome after experimental stroke independent of its blood pressure lowering effect. *Front. Neurol.* 10, 942. doi:10.3389/fneur.2019.00942

Paul, P., and de Belleroche, J. (2014). The role of D-serine and glycine as co-agonists of NMDA receptors in motor neuron degeneration and amyotrophic

lateral sclerosis (ALS). *Front. Synaptic Neurosci.* 6, 10. doi:10.3389/fnsyn.2014.00010

Perez-Torres, I., Zuniga-Munoz, A. M., and Guarner-Lans, V. (2017). Beneficial effects of the amino acid Glycine. *Mini Rev. Med. Chem.* 17, 15–32. doi:10.2174/1389557516666160609081602

Petrat, F., Boengler, K., Schulz, R., and de Groot, H. (2012). Glycine, a simple physiological compound protecting by yet puzzling mechanism(s) against ischaemia-reperfusion injury: Current knowledge. *Br. J. Pharmacol.* 165, 2059–2072. doi:10.1111/j.1476-5381.2011.01711.x

Petullo, D., Masonic, K., LinColn, C., WibberLey, L., TeliskaM., and Yao, D. L. (1999). Model development and behavioral assessment of focal cerebral ischemia in rats. *Life Sci.* 64, 1099–1108. doi:10.1016/s0024-3205(99)00038-7

Rautio, J., Gynther, M., and Laine, K. (2013). LAT1-mediated prodrug uptake: A way to breach the blood-brain barrier? *Ther. Deliv.* 4, 281–284. doi:10.4155/tde.12.165

Razak, M. A., Begum, P. S., Viswanath, B., and Rajagopal, S. (2017). Multifarious beneficial effect of nonessential amino acid, Glycine: A review. *Oxidative Med. Cell. Longev.* 2017, 1716701. doi:10.1155/2017/1716701

Schaible, E. V., SteinstraBer, A., Jahn-Eimermacher, A., Luh, C., Sebastiani, A., Kornes, F., et al. (2013). Single administration of tripeptide alpha-MSH(11-13) attenuates brain damage by reduced inflammation and apoptosis after experimental traumatic brain injury in mice. *PloS one* 8, e71056. doi:10.1371/journal.pone.0071056

Shen, H., Smith, D. E., Keep, R. F., and Brosius, F. C., 3rd. (2004). Immunolocalization of the proton-coupled oligopeptide transporter PEPT2 in developing rat brain. *Mol. Pharm.* 1, 248–256. doi:10.1021/mp049944b

Smith, D. E., Clemencon, B., and Hediger, M. A. (2013). Proton-coupled oligopeptide transporter family SLC15: Physiological, pharmacological and pathological implications. *Mol. Asp. Med.* 34, 323–336. doi:10.1016/j.mam.2012.11.003

Smith, D. E., Johanson, C. E., and Keep, R. F. (2004). Peptide and peptide analog transport systems at the blood-CSF barrier. *Adv. Drug Deliv. Rev.* 56, 1765–1791. doi:10.1016/j.addr.2004.07.008

Tanabe, M., Nitta, A., and Ono, H. (2010). Neuroprotection via strychnine-sensitive glycine receptors during post-ischemic recovery of excitatory synaptic transmission in the hippocampus. *J. Pharmacol. Sci.* 113, 378–386. doi:10.1254/jphs.10150fp

Wang, M., Zhang, X., Zhao, H., Wang, Q., and Pan, Y. (2010). Comparative analysis of vertebrate PEPT1 and PEPT2 genes. *Genetica* 138, 587–599. doi:10.1007/s10709-009-9431-6

Wexler, E. J., Peters, E. E., Gonzales, A., Gonzales, M. L., Slee, A. M., and Kerr, J. S. (2002). An objective procedure for ischemic area evaluation of the stroke intraluminal thread model in the mouse and rat. *J. Neurosci. Methods* 113, 51–58. doi:10.1016/s0165-0270(01)00476-9

Xiong, Z. M., Kitagawa, K., Nishiuchi, Y., Kimura, T., Nakamura, T., and Inagaki, C. (2009). Acetyl-Ile-Gly-Leu protects neurons from Abeta(1-42) induced toxicity *in vitro* and in V337M human tau-expressing mice. *Life Sci.* 84, 132–138. doi:10.1016/j.lfs.2008.11.011

Yamashita, T., Shimada, S., Guo, W., Sato, K., Kohmura, E., Hayakawa, T., et al. (1997). Cloning and functional expression of a brain peptide/histidine transporter. *J. Biol. Chem.* 272, 10205–10211. doi:10.1074/jbc.272.15.10205

Yang, L., Zhang, B., ToKu, K., MaedaN., SakanakaM., and Tanaka, J. (2000). Improvement of the viability of cultured rat neurons by the non-essential amino acids L-serine and glycine that upregulates expression of the anti-apoptotic gene product Bcl-w. *Neurosci. Lett.* 295, 97–100. doi:10.1016/s0304-3940(00)01597-4

Zhang, X., Zhao, T., Cheng, T., Liu, X., and Zhang, H. (2012). Rapid resolution liquid chromatography (RRLC) analysis of amino acids using pre-column derivatization. *J. Chromatogr. B Anal. Technol. Biomed. Life Sci.* 906, 91–95. doi:10.1016/j.jchromb.2012.08.030

Zhang, Z. F., Chen, J., Han, X., Zhang, Y., Liao, H. B., Lei, R. X., et al. (2017). Bisperoxovandium (pyridin-2-squaramide) targets both PTEN and ERK1/2 to confer neuroprotection. *Br. J. Pharmacol.* 174, 641–656. doi:10.1111/bph.13727

Zhao, P., Qian, H., and Xia, Y. (2005). GABA and glycine are protective to mature but toxic to immature rat cortical neurons under hypoxia. *Eur. J. Neurosci.* 22, 289–300. doi:10.1111/j.1460-9568.2005.04222.x

Zheng, M., Liao, M., Cui, T., Tian, H., Fan, D. S., and Wan, Q. (2012). Regulation of nuclear TDP-43 by NR2A-containing NMDA receptors and PTEN. *J. Cell Sci.* 125, 1556–1567. doi:10.1242/jcs.095729

frontiers | Frontiers in Pharmacology

TYPE Review
PUBLISHED 05 September 2022
DOI 10.3389/fphar.2022.948889

OPEN ACCESS

EDITED BY
Li-Nan Zhang,
Hebei Medical University, China

REVIEWED BY
Tom L Broderick,
Midwestern University, United States
Letizia Giampietro,
University G.d'Annunzio, Italy
Félix Javier Jiménez-Jiménez,
Hospital Universitario del Sureste, Spain
Wladyslaw - Lason,
Maj Institute of Pharmacology, Poland

*CORRESPONDENCE
Min Wu,
Wumin175@126.com

†These authors have contributed equally to this work

SPECIALTY SECTION
This article was submitted to Neuropharmacology, a section of the journal Frontiers in Pharmacology

RECEIVED 20 May 2022
ACCEPTED 01 August 2022
PUBLISHED 05 September 2022

CITATION
Wang Q, Yu Q and Wu M (2022), Antioxidant and neuroprotective actions of resveratrol in cerebrovascular diseases. *Front. Pharmacol.* 13:948889. doi: 10.3389/fphar.2022.948889

Antioxidant and neuroprotective actions of resveratrol in cerebrovascular diseases

Qing Wang[1,2†], Qi Yu[2,3,4†] and Min Wu[1*]

[1]Shaanxi Prov Peoples Hospital, Shaanxi Prov Key Lab Infect and Immune Dis, Xian, China, [2]Shaanxi Key Laboratory of Ischemic Cardiovascular Diseases and Institute of Basic and Translational Medicine, Xi'an Medical University, Xi'an, China, [3]Department of Histology and Embryology, Xi'an Medical University, Xi'an, China, [4]Department of Pharmacology, College of Pharmacy, Shaanxi University of Chinese Medicine, Xianyang, China

Cerebralvascular diseases are the most common high-mortality diseases worldwide. Despite its global prevalence, effective treatments and therapies need to be explored. Given that oxidative stress is an important risk factor involved with cerebral vascular diseases, natural antioxidants and its derivatives can be served as a promising therapeutic strategy. Resveratrol (3, 5, 4′-trihydroxystilbene) is a natural polyphenolic antioxidant found in grape skins, red wine, and berries. As a phytoalexin to protect against oxidative stress, resveratrol has therapeutic value in cerebrovascular diseases mainly by inhibiting excessive reactive oxygen species production, elevating antioxidant enzyme activity, and other antioxidant molecular mechanisms. This review aims to collect novel kinds of literature regarding the protective activities of resveratrol on cerebrovascular diseases, addressing the potential mechanisms underlying the antioxidative activities and mitochondrial protection of resveratrol. We also provide new insights into the chemistry, sources, and bioavailability of resveratrol.

KEYWORDS

resveratrol, anti-oxidant, neuroprotection, stroke, vascular dementia

Introduction

Cerebrovascular disease (CVD) has become one of the most life-threatening diseases and represents the second leading cause of death and the main cause of serious disability, which predominantly clinically presents as acute neurological deficits (Ledbetter et al., 2021). CVD mainly includes fatal or non-fatal ischemic stroke, hemorrhagic stroke, transient ischemic attack, and vascular dementia (VaD). Due to vessel narrowing, thrombosis and emboli, these disorders may lead to reduced cerebral blood flow and even cerebrovascular rupture (Chowdhury et al., 2012). As the most common type of CVD, stroke is defined as an acute focal or global neurologic injury caused by the blockage of cerebral blood flow (ischemic stroke) and the sudden rupture of cerebral blood vessels (hemorrhage). Ischemic stroke accounts for approximately 80% of all strokes, and hemorrhagic stroke accounts for 20% (Strong, Mathers, and Bonita 2007). VaD is a cognitive disorder caused by impaired blood flow and vascular injury (Braun et al., 2019),

which is the second most common type of dementia, being ranked behind Alzheimer's disease. VaD accounts for 10–20% of all dementia, and the incidence of VaD among 65-year-old population has risen steadily over the years (Østergaard et al., 2016; Wolters and MA, 2019). Following changes in lifestyle and people getting older, the morbidity, mortality and disability rates of CVD have therefore risen sharply (Fu et al., 2021). However, there is still a lack of efficient therapy, particularly in medicine, protecting against oxidative stress.

Recently, plant-derived natural antioxidants such as resveratrol (RES), quercetin, curcumin, and naringin are extensively used to treat and prevent various types of brain damage. It has been shown that RES has better antioxidant activity than other phyto-antioxidants (Khanduja and Bhardwaj 2003; Salehi et al., 2018). RES (3,5,40- trihydroxystilbene) is a natural polyphenolic compound, which is mainly extracted from grape skin/seed, vegetables, cereals, peanut skins, red wine, and tea (Yu, Fu, and Wang 2012) (Figure 1). Both *in vitro* and *in vivo* studies have shown that RES possesses diverse biological and pharmacological properties, which may be applied through antioxidant, anti-inflammatory, anti-apoptosis, anti-cancer, cardio-cerebrovascular protection (Shankar, Singh, and Srivastava 2007; Lopez, Dempsey, and Vemuganti 2015; Yang et al., 2015; Elshaer et al., 2018). It has been suggested that RES had cerebral-protective effects whereby it reduced radicals and upregulated the expression of antioxidant-related genes, including the endothelial nitric oxide synthase (eNOS) (Wang et al., 2011), superoxide dismutase (SOD) (Kovacic and Somanathan 2010), heme oxygenase-1 (HO-1) (Ren et al., 2011) and catalase (CAT) (Khan et al., 2013). Moreover, Sirtuin1 (SIRT1) is a nicotinamide adenine dinucleotide (NAD)-dependent deacetylase involved in both cellular stress and longevity (Horio et al., 2011). RES, as a chemical SIRT1 activator, can target the SIRT1 to maintain the homeostasis between prooxidants and antioxidants in mitochondria and exerts anti-inflammatory effects (Li et al., 2013). More evidence implicates that RES can attenuate various kinds of acute CVD, suggesting that the underlying mechanism is involved with its antioxidative effects (Ma et al., 2013; Hou et al., 2018). Here, we have summarized these novel works of literature to present the pharmacological role of RES in CVD, further assessing the anti-oxidative effect of RES and its potential mechanism.

Structure and metabolism of RES

RES ($C_{14}H_{12}O_3$; MW: 228.25 Da) is a natural antibacterial compound that binds to Flavin mononucleotide riboswitches and

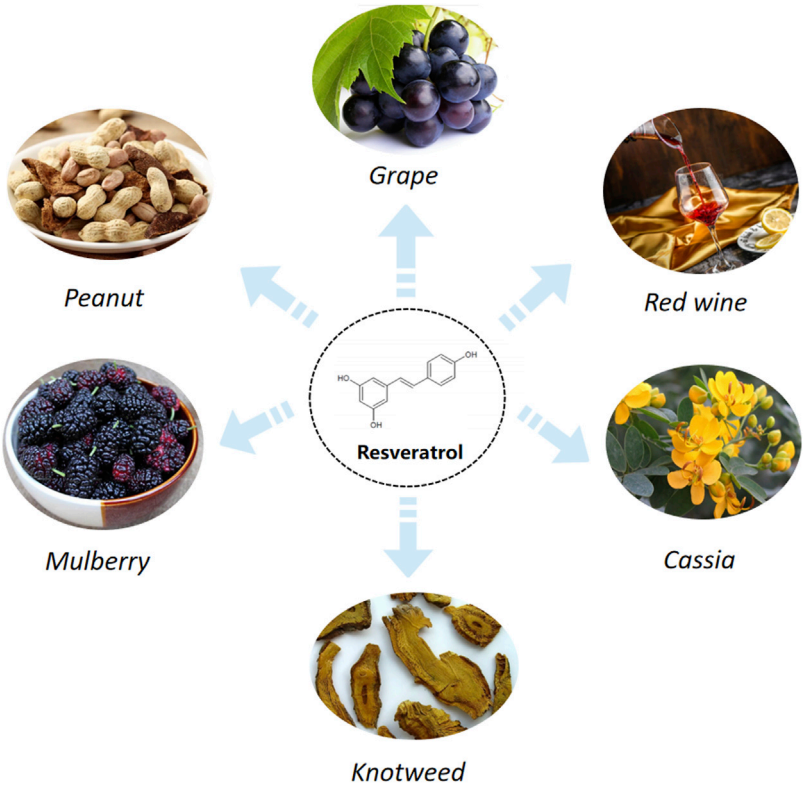

FIGURE 1
Resveratrol sources.

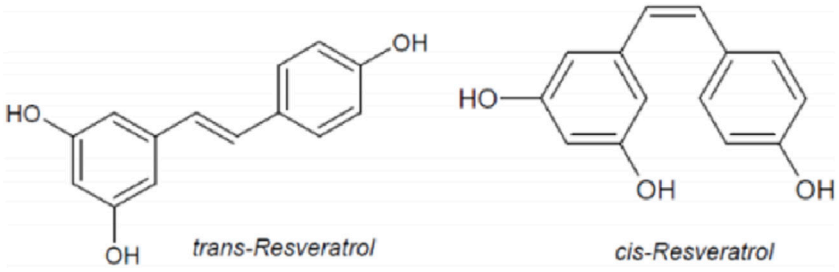

FIGURE 2
Chemical structures of trans-resveratrol and cis-resveratrol.

regulates gene expression (Sung and Dyck 2015). RES is a class of stilbene polyphenol molecules with dual structural isomeric forms: cis and trans (Figure 2). They possess comparable lipophilicity, but trans-resveratrol has a wider range of applications due to higher stability (Wallerath et al., 2002; Orallo 2006). Trans-resveratrol can be synthesized by pcoumaroyl coenzymes A (CoA) and malonyl CoA, whereas trans-resveratrol can also be converted into other cis-isomers after exposure to heat and ultraviolet irradiations (Shankar, Singh, and Srivastava 2007). RES is mainly transported through passive diffusion due to its small molecular weight and non-polar properties, but the oral bioavailability of RES is only 20% because of extensive metabolism in the gastrointestinal tract and poor intestinal absorption (Walle et al., 2004; Chen F et al., 2013). RES is quickly metabolized in the liver and binds to plasma albumin to promote drug uptake (Kuhnle et al., 2000). After oral and intravenous administration of RES, it has been shown that the main metabolites include sulfatesulfonylurea, 2-monosulfates, monofluorourea, 2-resveratrol monoglucuronides and dihydro resveratrol glucuronide (Calamini et al., 2010). In human urine, these metabolites were found in high concentrations (Boocock et al., 2007; Rotches-Ribalta et al., 2012). It is also reported that there was a ten folds increase in the half-life and plasma concentration of RES metabolites compared to native RES compounds in the human blood (Baur and Sinclair 2006). It suggested that even though its bioavailability was low and its metabolism and elimination were relatively rapid, RES had a relevant biological efficacy, which possibly was due to its conversion or interconversion into sulfonate and glucuronide metabolites (Vitaglione et al., 2005; Delmas et al., 2011). Besides, in animal studies, blood and serum levels of RES peaked 15 min after administration and then rapidly declined. Conversely, RES's metabolites decreased rather slowly (Soleas et al., 2001). Above these results indicated that the bioavailability of RES metabolites was greater than that of RES (Goldberg, Yan, and Soleas 2003). It is reported that RES readily crossed the blood-brain barrier (BBB) and penetrated into brain tissue (Wang et al., 2002; Wang et al., 2004). They also demonstrated the levels of RES in the brain 4 h after intraperitoneal injection. A multicentric placebo-controlled phase II trial found that RES and its metabolites could penetrate the BBB based on the analysis of cerebrospinal fluid biomarkers (Turner et al., 2015). Besides, RES preserves BBB integrity. The study found that RES attenuated the BBB dysfunction by regulating the matrix metalloproteinase-9 (MMP-9) to limit the infiltration of leukocytes and other inflammatory mediators into the brain (Moussa et al., 2017). Nevertheless, there was no significant difference in the half-life times between the oral and intravenous administration. The half-life was 9.2 h after oral administration and 11.4 h after intravenous injection, and plasma concentrations of RES declined exponentially in a parallel of 72 h (Wang and Sang 2018).

On lipid peroxidation injury of brain synaptosomes, RES exerts the antioxidative potency. In this study, RES significantly scavenged the superoxide anion generated from rat forebrain mitochondria and inhibited ATPase activity with two EC50 values, 0.39 ± 0.15 nano-moles (nM) and 23.1 ± 6.4 micro-moles (μM) (Zini et al., 1999). Another study confirmed that the oxygen consumption of mitochondria was significantly inhibited by RES with a low EC50 of 18.34 picomole (pM) (Zini et al., 2002). Above these results showed that the RES had neuroprotection in CVDs via valuable anti-oxidant activities.

Protective effects of RES on CVD

RES and ischemic stroke

Ischemic stroke is caused by a reduction in cerebral blood flow, leading to energy dysmetabolism, neurological disorders, and cell death. Currently, the principal therapeutic treatment is to restore the cerebral blood flow whereby treatment with recombinant tissue plasminogen activator (rt-PA) destroys thrombi (clots), while rt-PA is also limited by the narrow therapeutic window (Warner et al., 2019). The main reason is that cerebral ischemia is a series of complicated pathological processes involving oxidative stress, inflammation, autophagy,

TABLE 1 Summary of the most relevant preclinical studies *in vivo* evaluating the effects of resveratrol administration on animals subjected to cerebrovascular diseases, including ischemic stroke, hemorrhage stroke, and vascular dementia.

Disease	Experimental model	Animal Sex/Age	Dose and duration of study	Outcome of study	References
Ischemic stroke	Occlusion of the middle cerebral artery 2 h by insertion of a silicone-coated 8-0 and the suture was removed to restore the blood flow	Male SD rats/ age 8–12 weeks	RES30 mg/kg, intraperitoneally, for 7 days	RES reduced neurological deficit scores, promoted proliferation of neural stem cells, inhibited astrocyte and microglia activation by the Shh signaling pathway	Yu et al. (2021)
Ischemic stroke	Occlusion of the right common carotid artery (RCCA) and right middle cerebral artery for 60 min	Male SD rats/ not mentioned	RES 20 mg/kg, intraperitoneally, for 10days	RES reduced levels of MDA, Ferrum (Fe), Copper (Cu), and Aluminum (Al) and increased the anti-oxidants enzyme SOD and CAT activity	Lin et al. (2021)
Ischemic stroke	Ligation of the right middle cerebral Artery (RMCA) and RCCA for 1 h	Male SD rats/ not mentioned	RES20 mg/kg, intraperitoneally, for 10 days	RES increased trace element concentrations of Magnesium (Mg), Zinc (Zn), Selenium (Se), SOD and CAT antioxidant activity	Ro, Liu, and Lin (2021)
Ischemic stroke	Occlusion of the middle cerebral artery 2 h by insertion of a silicone-coated 8-0 and the suture was removed to restore the blood flow	Male Wistar rats/not mentioned	RES1.9 mg/kg, tail vein injection, at the onset of reperfusion	RES reduced the cerebral region damage and diminishes glucose transporter 3 (GLUT3) expression at the mRNA and protein level in astrocytes which might depend on adenosine 5′-monophosphate (AMP)-activated protein kinase (AMPK) activation	Aguilar et al. (2020)
Ischemic stroke	Occlusion of middle cerebral artery 24 h	Male SD rats/ Adult	RES 30 mg/kg, intraperitoneally	RES improved the neurological behavior, brain edema and brain infarction by upregulating the p-Akt and p-glycogensynthasekinase-3β (p-GSK-3β) expression levels	Park et al. (2019)
Ischemic stroke	Occlusion of the middle cerebral artery 2 h and the suture was removed to restore the blood flow for 24 h	Male Wistar rats/not mentioned	RES1.8 mg/kg, tail vein injection	RES decreased the infarct area,the production of superoxide anion, the overload of intracellular Ca^{2+} and increased the levels of phosphorylated AMPK.	Pineda-Ramírez et al. (2020)
Ischemic stroke	Right middle cerebral artery occlusion for 90 min and reperfusion immediately for 20days	Male SD rats/ 8 weeks	RES (10,100 mg/kg),intraperitoneally at 2 h on the onset of ischemia	RES significantly reduced the neurological deficit, cerebral infarct sizes, neuronal injury, decreased inflammation, and BBB disruption by downregulation of the toll-like receptor 4 (TLR4) pathway	Lei et al. (2019)
Ischemic stroke	Occlusion of the middle cerebral artery for 60 min, followed by reperfusion	Male C57BL/ 6 mice/ 8–10 weeks	RES 200 mg/kg, intraperitoneally for 3 days	RES attenuated systemic inflammation and neuroinflammation by modulating intestinal fora-mediated Th17/Tregs and Th1/Th2 polarity shift in SI-LP.	Dou et al. (2019)
Ischemic stroke	Occlusion of the middle cerebral artery 2 h and reperfusion immediately for 24 h	Male SD rats/ Adult	RES 30 mg/kg, intraperitoneally, for 7 days	RES significantly decreased neuronal damage, and attenuated neuronal apoptosis via upregulating the PI3K/AKT/mTOR pathway by activating Janus kinase 2 (JAK2)/signal transducer and activator of transcription3(STAT3)	Hou et al. (2018)
Ischemic stroke	Occlusion of middle cerebral artery 24 h	Male SD rats/ not mentioned	RES 100 mg/kg, intraperitoneally at 2 and 12 h after the onset of ischemia	RES significantly reduced the enzymatic activity of myeloperoxidase (MPO),suppressed the inflammatory factors, and upregulated the expression of cyclo-oxygen-ase 2(COX2) by activating PI3K/Akt pathway	Lei et al. (2019)
Ischemic stroke	Occlusion of the middle cerebral artery 2 h and reperfusion immediately	SD rats/not mentioned	RES 20 mg/kg, intraperitoneally for 7 days	RES alleviated cognitive impairment, downregulated inflammatory cytokines via modulating JAK/ERK/STAT pathway	Chang et al. (2018)
Ischemic stroke	Occlusion of the middle cerebral artery 60min and reperfusion immediately	Male SD rats/ not mentioned	RES 100 mg/kg, intraperitoneally at the onset of reperfusion	RES attenuated inflammation, and upregulated autophagy by inhibiting NOD-like receptor protein 3 inflammasome (NLRP3) inflammasome activation through Sirt1-dependent autophagy activity	He et al. (2017)

(Continued on following page)

TABLE 1 (*Continued*) Summary of the most relevant preclinical studies *in vivo* evaluating the effects of resveratrol administration on animals subjected to cerebrovascular diseases, including ischemic stroke, hemorrhage stroke, and vascular dementia.

Disease	Experimental model	Animal Sex/Age	Dose and duration of study	Outcome of study	References
Ischemic stroke	Occlusion of both carotid arteries for 30min	Male Wistar rats/Adult	RES 20 mg/kg, intraperitoneally, for30 days	RES exerted cerebral protection and inhibited inflammation by reducing interleukin-1β (IL-1β) and upregulating osteopontin	Al Dera (2017)
Ischemic stroke	Occlusion of the middle cerebral artery 90 min and reperfusion immediately for 24 h	Male Wistar rats/Adult	RES 20 mg/kg, orally, for 30 days	RES pre-administration reduced oxidative stress, inflammation, apoptosis, enhanced the levels of oxidized forms of DJ-1, and increased the Nrf2 expression via PI3K/Akt pathway activation	Abdel-Aleem et al. (2016)
Ischemic stroke	Occlusion of the middle cerebral artery 90 min and reperfusion immediately for 24 h	Male SD rats/ not mentioned	RES 50 mg/kg, intraperitoneally, for 7 days	RES increased levels of IL-10, decreased tumor necrosis factor-α (TNF-α) and IL-6, increased frequencies of Tregs in the spleens and ischemic hemisphere, and improved the frequency and suppressive function of Tregs in the spleens	Yang et al. (2016)
Ischemic stroke	Occlusion of the middle cerebral artery 90 min and reperfusion immediately for 24 h	Male adult SD rats/2 months of age	RES 30 mg/kg, intraperitoneally at 1, 4, 6, 12, or 24 h before ischemia	RES before ischemia exerts a potent neuroprotective effect with an efficacious time window of at least 4 h via the national marine distributors association (NMDA) receptor-mediated ERK1/2-cAMP-response element binding protein (CREB) pathway	Li H et al. (2016)
Ischemic stroke	Occlusion of the middle cerebral artery 2 h and reperfusion immediately for 24 h	Male SD rats/ 7–8 weeks of age	RES 20 mg/kg, intraperitoneally, for 5 days	RES significantly reduced adenosine triphosphate (ATP) energy consumption and exerted neuroprotection by inhibiting PDEs and regulating the cyclic adenosine monophosphate (cAMP)/AMPK/ SIRT1 pathway	Wan et al. (2016)
Ischemic stroke	Occlusion of the middle cerebral artery 90min and reperfusion immediately for 24 h	Male SD rats/ Adult	RES 20 mg/kg, intraperitoneally at 0 and 20 h following reperfusion	RES prevented brain injury through ameliorating oxidative stress and reducing AQP4 expression	Li et al. (2015)
Ischemic stroke	Occlusion of the 4-vessel	Male Wistar rats/not mentioned	RES (1.10 mg/kg), intraperitoneally, for 21 day	RES attenuated doublecortin (DCX)/ polysialylated-neural cell adhesion molecule (PSA-NCAM) expression, increased angiogenesis, improved spatial memory rete1ntion, and regulated corticosterone secretion	Girbovan et al. (2016)
Ischemic stroke	Occlusion of the 4-vessel	Male Wistar rats/not mentioned	RES (1.10 mg/kg), intraperitoneally, for 21day	RES exerted brain protection by increasing GLT-1 expression and inhibiting CD11b/c and glial fibrillary acidic protein (GFAP) expression	Girbovan and Plamondon (2015)
Ischemic stroke	Middle cerebral artery occlusion and reperfusion immediately for 24 h	Male SD rats/ not mentioned	RES 50 mg/kg, intraperitoneally	RES attenuated the cerebral ischemia by maintaining the integrity of BBB via regulation of MMP-9 and tissue inhibitor of matrix metalloproteinases-1 (TIMP-1)	Wei et al. (2015)
Ischemic stroke	Middle cerebral artery Occlusion 30min and reperfusion immediately for 5.5 h	Male SD rats/ not mentioned	RES (0.1 and 1 μM), Intracortical injection	RES exerted neuroprotection by activating either estrogen receptor subtype within the ischemic cortex of rats	Saleh, Connell, and Saleh. (2013)
Ischemic stroke	Middle cerebral artery occlusion 2 h and reperfusion immediately for 24 h	Male SD rats/ not mentioned	RES 200 mg/kg, intraperitoneally, for 6 days	RES protected the brain through the Transient receptor potential channel 6/ methyl ethyl ketone (TRPC6-MEK)-CREB and TRPC6-CaMKIV-CREB pathways	Lin et al. (2013)

(Continued on following page)

TABLE 1 (*Continued*) Summary of the most relevant preclinical studies *in vivo* evaluating the effects of resveratrol administration on animals subjected to cerebrovascular diseases, including ischemic stroke, hemorrhage stroke, and vascular dementia.

Disease	Experimental model	Animal Sex/Age	Dose and duration of study	Outcome of study	References
Ischemic stroke	Middle cerebral artery occlusion for 90 min and reperfusion immediately	Male SD rats/ 8 weeks of age	RES 10 mg/kg, intravenously, for 20 days	RES ameliorated brain injury and attenuated neuronal apoptosis by downregulating the TGF-β-ERK pathway	Zhao et al. (2019)
Cerebral hemorrhage	Over-insertion of the intracranial internal carotid artery	Male SD rats/ not mentioned	RES 100 mg/kg, intraperitoneally, 48 h prior to SAH	RES exerted neuroprotective effects, and prevented BBB disruption through the SIRT1/p53 signal pathway	Qian et al. (2017)
Cerebral hemorrhage	Fresh autologous arterial blood was slowly injected into the suprachiasmatic cistern for the 20s	Male SD rats/ Adult	RES 60 mg/kg,intraperitoneally, 2 and 12 h post-SAH	RES provided neuroprotection, inhibited mitochondrial-dependent apoptosis, and improved mitochondrial biogenesis and antioxidative ability by activating the PGC-1α signaling pathway	Zhou et al. (2021)
Cerebral hemorrhage	Fresh autologous arterial blood was slowly injected into the suprachiasmatic cistern for the 20s	Male SD rats/ not mentioned	RES (20,60) mg/kg, intraperitoneally, at 2 and 24 h after initial bleeding	RES attenuated neuronal apoptosis by the PI3K/Akt signaling	Zhou et al. (2014)
Cerebral hemorrhage	Over-insertion of the internal carotid artery	SD rats/not mentioned	RES 30 ml/kg, intraperitoneally, at 6 h after SAH	RES promoted functional brain recovery, prevented BBB disruption, and inhibited the activation of nuclear factor kappa-B(NF-κB) and downregulation of MMP-9 expression	Shao et al. (2014)
Vascular dementia	Induction of chronic cerebral hypoperfusion (CCH) induced by bilateral common carotid artery occlusion	Male Wistar/ not mentioned rats/not mentioned	RES 40 mg/kg, intraperitoneally, for 4 weeks	RES effectively restored the synaptic plasticity and improved spatial memory via PKA-CREB activation	Li Z et al. (2016)
Vascular dementia	Occlusion of the 2-vessel	Male Wistar rats/3 months of age	RES 20 mg/kg,intraperitoneally, for 7 days	RES attenuated pyramidal cell death in the CA1 hippocampal subfield, prevented both spatial working and References memory impairments, and increased the nerve growth factor (NGF) levels	Anastácio et al. (2014)
Vascular dementia	Bilateral common carotid artery occlusion (BCCAO)	Male SD rats/ 2 months of age	RES 20 ml/kg, intraperitoneally, for 4 weeks	RES exhibited neuroprotective effects, and inhibited apoptosis and oxidative stress injury	Zhang et al. (2019)
Vascular dementia	BCCAO	Male SD rats/ not mentioned	RES 50 mg/kg, intragastrically, for 9 weeks	RES improved cognitive function and reduced neuronal damage and neuronal apoptosis by activating autophagy and regulating the Akt/ mTOR signaling pathway	Wang et al. (2019)

mitochondrial dysfunction, and various signaling pathways (Tao et al., 2020). Chen et al. have revealed that RES extended the clinical therapeutic window of the rt-PA, suggesting that such an effect may be applied by reducing the MMP expression (Chen et al., 2016). Meanwhile, a study has demonstrated that RES preconditioning (RPC) provides a novel long-term window of cerebral ischemic tolerance for 2 weeks in mice (Khoury et al., 2019). These results provide evidence that RPC promotes a beneficial effect on cellular metabolisms such as glycolysis, mitochondrial respiration efficiency, elevated energy production (increased tricarboxylic acid cycle) as well as regulated oxidative phosphorylation and pyruvate uptake (Khoury et al., 2019). Numerous studies have shown that RES exerts neuroprotection in ischemic stroke by increasing antioxidant capacity as well as attenuating oxidative stress and inflammation (Al Dera 2017; Lei and Chen 2018). In such a process, SIRT1 is deemed as the primary molecular target of RES pharmacological actions (Borra, Smith, and Denu 2005; Della-Morte et al., 2009). In the cerebral ischemia-reperfusion-induced brain injury mice model, the mice were administered intraperitoneally with 30 mg/kg of RES and SIRT1/2 selective inhibitor before ischemia (Grewal, Singh, and Singh 2019). The results have shown that RES activates SIRT1, further promoting the improvement in neurobehavioral functions, the reduction in cerebral infarct volume, oxidative stress level, and acetylcholinestrase activity (Grewal, Singh, and Singh 2019).

TABLE 2 Summary of the most relevant preclinical studies *in vitro* evaluating the effects of RES administration on animals subjected to CVD, including ischemic stroke, hemorrhage stroke and vascular dementia.

Disease	Experimental model	Dose and duration of study	Outcome of study	Reference
Ischemic stroke	Primary cortical neurons were subjected to oxygen-glucose deprivation/reperfusion *in vitro*	RES 5 μM	RES reduced neurological deficit scores, promoted proliferation of neural stem cells, inhibited astrocyte and microglia activation by the Shh signaling pathway	Yu et al. (2021)
Ischemic stroke	Primary cortical neurons were subjected to oxygen-glucose deprivation/reperfusion *in vitro*	RES 10 μM	RES improved cell viability and suppressed oxidative stress by stimulating the PTEN-PINK1/Parkin-mediated pathway	Ye, Wu, and Li (2021)
Ischemic stroke	SH-SY5Y cells were subjected to oxygen-glucose deprivation	RES 10 μM	RES rescued mitochondrial deficiency, increased the Bcl-2 and CREB expression, and inhibited caspase 3 and 9 activity via increasing expression of AMPK and p-AMPK	Lin et al. (2020)
Ischemic stroke	Primary rat cortical neurons were subjected to oxygen-glucose deprivation/reperfusion *in vitro*	RES 40 mM	RES treatment at different times increased neuronal viability, decreased the LDH and SOD activity, and inhibited neuronal apoptosis via enhancing the activation of the Nrf2 pathway	Yang et al. (2018)
Ischemic stroke	HT22 cells were subjected to oxygen-glucose deprivation/reperfusion *in vitro*	RES 10 μM	RES attenuated cytotoxicity, and oxidative stress and repaired DNA damage by upregulating APE1 activity and level	Jia et al. (2017)
Ischemic stroke	PC12 cells were subjected to oxygen-glucose for 6 h deprivation/reperfusion 24 h*in vitro*	RES 25 μM	RES significantly increased the cell viability and decreases ROS generation, intracellular Ca^{2+} levels, and hypoxia associated transcription factors	Yu, Fu, and Wang. (2012)
Cerebral hemorrhage	Primary cultured cortical neurons were stimulated with oxyhemoglobin (oxyHb) to induce SAH.	RES 20 μM	RES protected primary cortical neurons against oxyHb insults, including reducing the proportion of neuronal apoptosis, alleviating neuronal degeneration, and improved cell viabilities	Zhang X et al. (2017)

Other studies have also found that RES inhibited sulfonylurea receptor1 (SUR1) and aquaporin 4 (AQP4) expression by targeting specificity proteins transcription factors, thereby improving BBB damage, infarct area, cerebral edema and neurological deficit (Alquisiras-Burgos et al., 2020). In addition, Ma et al. have indicated that RES activated microglia and alleviated neuroinflammation via down-regulating the miR-155 expression (Ma et al., 2020). Even in the experimental stroke of aged female mice, the study shows that RES mitigates ischemic brain injury and inflammation (Jeong et al., 2016). The neuroprotective effects of RES on various ischemic brain injury models are shown in Tables 1, 2.

RES and hemorrhage stroke

Cerebral hemorrhage is a cause of cerebral brain vasospasm (Souissi et al., 2010). More importantly, subarachnoid hemorrhage (SAH) results in long-term cognitive and neurological outcomes (Bederson et al., 2009; Suzuki 2015). Studies have revealed that oxidative damage and endoplasmic reticulum (ER) stress lead to the early stage of brain injury (Ayer and Zhang 2008; Nakka, Prakash-Babu, and Vemuganti 2016). In recent years, there has been a functional link between oxidative stress and ER stress (Ilieva et al., 2007; Zhang 2010). He et al. showed that oxidative stress increased the accumulation of reactive oxygen species (ROS) in the ER stress, and upregulated the expression of Glucose-regulated protein 78 (GRP78) (He et al., 2008). Zhang et al. also proposed that ROS can target ER-based calcium channels, leading to the release of calcium from the ER to the cytosol (Zhang 2010). Increased cytosolic calcium can form a positive feedback loop to produce more ROS. GRP78 is a molecular chaperone with important functions at the cellular level, including the regulation of intracellular calcium, protein folding, and ER stress (Chiang et al., 2011). As a monitor of ER stress, GRP78 is associated with oxidative stress and stabilization of calcium homeostasis (Kudo et al., 2008). It is reported that reduction of GRP78 expression inhibited the ER stress induced by oxidative stress (Pan et al., 2010). Xie et al. have revealed that RES ameliorated SAH-induced brain injury by attenuating oxidative damage, ER stress, and neuroinflammation (Xie et al., 2019). Regarded rats were treated with 60 mg/kg RES after SAH-induced brain injury. And they showed that it alleviated neurological deficits and brain edema, and reduced ROS and malondialdehyde (MDA) levels, indicating that the NF-E2-related factor 2 (Nrf2)/HO-1 pathway and suppressed GRP78 may involve with these effects (Xie et al., 2019). Another study demonstrated that RES significantly prevented the brain injury in hypertension-induced cerebral microhemorrhages, diminished hypertension-induced oxidative stress, and inhibited vascular MMP activation

(Toth et al., 2015). Moreover, Post-SAH administration of RES attenuated neurological deficits, cerebral vasospasm, and microvessel thrombi through SIRT1-dependent activation (Diwan et al., 2021). A number of studies suggested that RES prevented BBB disruption, inhibited mitochondrial-dependent apoptosis, and was correlated with transforming growth factor-β-extracellular-signal regulated kinases (TGF-β-ERK), peroxisome proliferator-activated receptor-gamma coactivator (PGC)-1α, phosphatidylinositol three kinase/protein kinase B (PI3K/Akt) and et al. (Tables 1, 2).

RES and vascular dementia

VaD is the second largest cause of dementia in the elderly and is mainly associated with cerebrovascular lesions as well as cognitive decline (Kovacic and Somanathan 2010). The primary pathological cause of VaD is the reduction of blood flow in cerebrovascular (Enciu et al., 2011). Chronic cerebral hypoperfusion is one of the most significant risk factors, which can lead to cerebrovascular degeneration, energy loss, oxidative stress, and inflammation (Jellinger 2007). Ma et al. showed that RES improved learning and memory ability in VaD rats. Specifically, RES exerted an anti-oxidative role via diminishing the MDA but increasing the SOD and glutathione (GSH) levels (Ma et al., 2013). Gocmez et al. established a streptozotocin-induced diabetic VaD rat model, and RES (20 mg/kg) was administrated intraperitoneally for 4 weeks, showing that RES prevented endothelial dysfunction, inflammation, and impairment of neurotrophin expression (Gocmez et al., 2019). Studies showed that a significant reduction of estrogens and progesterone was related to the onset of Alzheimer's disease (Resnick and Henderson 2002; Jankowska 2017). Note, in the chronic cerebral hypoperfused and ovariectomized-female rats model, RES significantly alleviated brain injury by reducing astrocyte activation and its antioxidant and antiapoptotic effects. Above these findings may provide new insight into the potential clinical application in postmenopausal elderly women who suffer from VaD (Ozacmak, Sayan-Ozacmak, and Barut 2016). In addition, as shown in Table 1, RES regulates various proteins and signal pathways involved in the pathogenesis of VaD.

Molecular mechanisms of RES on CVD

Antioxidant actions of RES on CVD

A major mechanism of CVD may be ascribed to oxidative stress, which is mainly caused by the excessive accumulation of ROS and depleted activities of antioxidant enzymes (Orellana-Urzúa et al., 2020). Excess ROS includes superoxide anion, hydrogen peroxide (H_2O_2), and nitric oxide (NO), resulting in severe damage to cellular DNA, proteins, and lipids. It has been reported that the MDA and 4-hydroxynonenal were products of lipid peroxidation (Adibhatla, Hatcher, and Dempsey 2006). On the another hand, a variety of antioxidants such as SOD, CAT, GSH, and glutathione peroxidase (GSH-Pxs) protect from brain injury by eliminating ROS. Of note, the levels and activities of these antioxidants were markedly reduced in the animal model of CVD (Bharti and Garg 2019). Therefore, an increase in antioxidant defenses is an important strategy for blunting oxidative damage. Studies have shown that RES directly attenuates oxidative stress by inhibiting lipid peroxidation and upregulating the SOD and GSH activity in brain injury (Ma et al., 2013; Toth et al., 2015; Ozacmak, Sayan-Ozacmak, and Barut 2016; Zhao et al., 2019). Given that extensive ROS inhibits the generation of endothelial NOS (eNOS) and causes vascular endothelial damage, RES can prevent endothelial dysfunction by reducing oxidative stress and inflammation (Gocmez et al., 2019).

In addition, RES regulates trace elements to avoid ROS-induced oxidative damage. A variety of trace elements are important for maintaining normal brain functions. It is reported that Mg depressed oxidative stress and stabilizes the cell membrane (de Baaij, Hoenderop, and Bindels 2012). Zn is a part of the SOD structure and involves antioxidant production (Fang et al., 2013). Se has various beneficial effects, including protecting neurons, increasing antioxidant enzyme activity, and repairing DNA damage (Van Eersel et al., 2010; Song et al., 2014). Besides, increased Fe and Cu levels produce toxic hydroxyl radicals, leading to deleterious lipid peroxidation and oxidative injury (Allen et al., 2008; Murphy and Oudit 2010). Al and As are also considered to induce oxidative stress (Good et al., 1992; Miller et al., 2002; Cohen et al., 2006; Jomova and Valko 2011; Jaishankar et al., 2014). In a recent report, researchers have discovered that RES diminished the overload of Fe, Cu, As and Al, but increased Mg, Zn and Se levels to exert antioxidant effects in cerebral ischemic injury (Lin et al., 2021; Ro, Liu, and Lin 2021).

Nrf2 is a molecular target of oxidative stress through regulating abundant antioxidant enzymes and defense proteins (Vomund et al., 2017). Under normal physiological conditions, Nrf2 forms a Kelch-like ECH-associated protein 1 (Keap1)-Nrf2 complex in the cytoplasm. After stressful or inflammatory responses, Nrf2 is released from the Keap1/Nrf2 complex and translocates into the nucleus to combine with the antioxidant response element (ARE), initiating the transcription of downstream target genes (Kobayashi et al., 2004; Hayes et al., 2010). Many target genes are involved in the regulation of cellular redox homeostasis, such as NAD(P)H quinone oxidoreductase 1 (NQO1), HO-1, glutathione-s-transferase (GST) (Kumar and Mittal 2017). A recent study suggested that RES inhibited oxidative stress by upregulating the Nrf2 and HO-1 mRNA, thus protecting brain function (Yang et al., 2018).

Noteworthy, DJ-1 is activated during oxidative stress, which is therefore deemed as a crucial antioxidant regulator in brain science (Taira et al., 2004). Indeed, DJ-1 is an important modulator of Nrf2 and negatively regulates PI3K/Akt signal pathway (McNally et al., 2011). A number of studies have revealed that PI3K/Akt activation is apparently associated with antioxidative stress and anti-apoptosis (Liu et al., 2017; Yang et al., 2020). In contrast, PI3K activity is negatively regulated by phosphatase and tensin homolog deleted on chromosome ten (PTEN) (Almazari et al., 2012). In the central nervous system, PTEN has been considered a mediator of ROS production and cell apoptosis (Shang et al., 2022). At present, some studies have reported that DJ-1 activates the PI3K/Akt signal pathway by inhibiting PTEN to avert damage due to oxidative stress (Kim et al., 2005; Kim et al., 2009). In another study, RES reduced ROS generation and enhanced antioxidant enzyme activity. This effect is clearly linked to the reduction in oxidized levels of DJ-1, inhibiting PTEN activity and PI3K/Akt survival pathway activation (Abdel-Aleem et al., 2016).

PGC-1α is a transcription co-activator involved in mitochondrial biogenesis and function (Wareski et al., 2009). In addition, increasing evidence suggests that PGC-1α upregulates a serious of oxidative stress protective genes such as manganese SOD (Mn-SOD) to remove the ROS production (Valle et al., 2005; Orallo 2006). This remarkable antioxidant mechanism was also observed in the protective role of RES in the SAH model. In this study, RES increased PGC-1α expression and promoted PGC-1α nuclear translocation. Moreover, RES can apply to scavenge excess ROS, increasing the activity of SOD and improving the mitochondrial function and ATP levels to prevent neurological impairment after SAH. These results indicate that RES promotes mitochondrial biogenesis and decreases oxidative stress by activation of the PGC-1α signaling pathway in SAH (Zhou et al., 2021).

Oxidative stress commonly causes DNA peroxidation, which gives rise to DNA damage (Chen et al., 1997; Lan et al., 2003; Chen et al., 2011). APE1 is a ubiquitous and multifunctional DNA repair enzyme and participates in protein redox regulation (Dyrkheeva, Lebedeva, and Lavrik 2016; Laev, Salakhutdinov, and Lavrik 2017). Moreover, regulation of APE1 in neurons protects against ischemia-induced neuronal death (Ludwig et al., 1998; Vasko, Guo, and Kelley 2005). It has been reported that endogenous upregulation of APE1 reduced white matter infarct, promoting neurologic functional recovery after stroke (Stetler et al., 2016). Leak et al. have also revealed that the upregulation of APE1, either endogenously or through transgene overexpression, reduces oxidative DNA damage and protects neurons against acute ischemic damage (Leak et al., 2015). Consistent with prior studies, Jia et al. have found that RES obviously elevated the activity and level of APE1 (Jia et al., 2017). On the other hand, previous research has shown that strand breaks of apurinic/apyrimidinic sites are considered a marker of oxidative DNA damage, and 8-OHdG is also the specific product of DNA oxidative damage (Chen et al., 1997; Lan et al., 2003). Notedly, this study also demonstrated that RES reduced the level of 8-OHdG and AP sites in OGD/R-induced cell damage. In addition, the knockdown of APE1 blocked the neuroprotective and antioxidant effects of RES. The above results further showed that RES exerted a neuroprotective role in ischemic stroke, which was related to the APE1-induced oxidative DNA damage reduction and antioxidant defense system enhancement (Jia et al., 2017) (Figure 3).

Mitochondrial protective effects of RES on CVD

Mitochondria are the major organelles involved in the synthesis of ATP in mammalian cells, which are essential for maintaining cellular homeostasis and function (Papa et al., 2012; Chaban, Boekema, and Dudkina 2014). Mitochondrial dysfunction plays an important role in the pathogenesis of CVD (Correia et al., 2010; Li et al., 2012; Chen et al., 2020; Han et al., 2020). Mitochondrial biogenesis is the process responsible for the synthesis of new mitochondria, which is the main component of the mitochondrial mass control system. Mammalian mitochondrial biogenesis and function require the coordinated action of both nuclear and mitochondrial genomes (Scarpulla 2008; Jornayvaz and Shulman 2010; Ungvari et al., 2011). PGC-1α regulates mitochondrial biogenesis by activating the nuclear respiratory factors 1 and 2 (NRF-1 and NRF-2) and increases the expression of mitochondrial proteins encoded by nuclear DNA (Virbasius, Virbasius, and Scarpulla 1993; Schreiber et al., 2004; Anderson and Prolla 2009; Scarpulla 2011). Among these proteins, Transcription factor A mitochondrial (TFAM) is an essential mitochondria transcriptor playing both a transcription and replication role in mitochondrial DNA (mtDNA) (Canugovi et al., 2010). Additionally, TFAM has been viewed as an important modulator of mtDNA homeostasis and repair (Picca and Lezza 2015; Filograna et al., 2021). The D-loop (mitochondrial displacement loop) was an mtDNA noncoding region, and it was the major control region for the regulation of mitochondrial genome replication and expression. The expression of the D-loop was used in evaluating mtDNA copy number and mitochondrial biogenesis (Shuwen, Xi, and Yuefen 2017). Recent evidence implicates the increasing mitochondrial biogenesis is thought to prevent mitochondrial dysfunction as well as attenuate CVD progression (Yin et al., 2008; Chen et al., 2010). Lin et al. have evidenced that RES rescued SH-SY5Y cells from OGD-mediated mitochondrial lower D-loop level and mitochondrial mass dimension. RES also rescued the transcript expression levels of PGC1-α, and mitochondrial genes (NRF-1 and TFAM) in OGD-treated SH-SY5Y cells (Lin et al., 2020). Besides, AMPK activity is important for maintaining mitochondrial biogenesis homeostasis (Zhang J

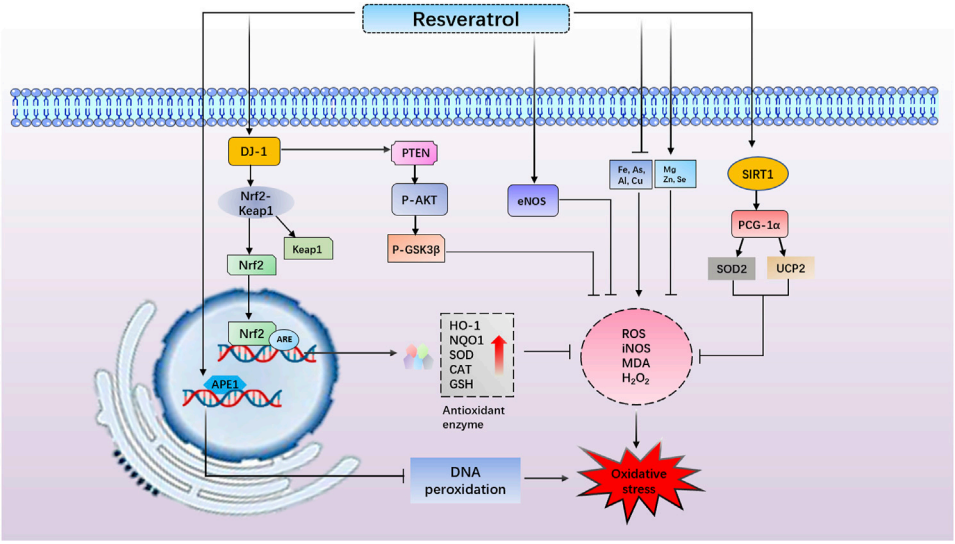

FIGURE 3
Resveratrol (RES) reduces apurinic/apyrimidinic endonuclease 1–induced oxidative DNA damage. RES increases DJ-1 protein expression, promotes NF-E2-related factor 2 (Nrf2) dissociating from Kelch-like ECH- associated protein l and induces Nrf2/antioxidant response element–dependent antioxidant enzyme (heme oxygenase-1 and NAD(P)H quinone oxidoreductase 1) transcriptions, thus exerting antioxidant effects. RES reduces reactive oxygen species generation and enhances antioxidant enzyme activity through reduction in oxidized levels of DJ-1, inhibiting phosphatase and tensin homolog deleted on chromosome ten activity and phosphatidylinositol 3 kinase/protein kinase B survival pathway activation. RES increases the generation of endothelial nitric oxide synthase to prevent oxidative stress. RES diminishes the overload of Fe, Cu, As, and Al but increases Mg, Zn, and Se levels to exert an antioxidant role. RES activates peroxisome proliferator–activated receptor–gamma coactivator–1alpha and increases superoxide dismutase 2 and UCP2 levels to promote mitochondrial biogenesis and thus decreases oxidative stress.

et al., 2017). These studies have shown that activation of AMPK protected neurons against mitochondrial dysfunction, and oxidative stress, further suggesting that AMPK may be critically important in preventing neuronal cell damage (Zhang J et al., 2017; Nanjaiah and Vallikannan 2019). Lin et al. also have found that RES improved the expression of AMPK and p-AMPK in OGD-exposed SH-SY5Y cells. It implies that RES reverses OGD-induced SH-SY5Y cell damage caused by mitochondrial dysfunction in an AMPK-dependant manner (Lin et al., 2020).

Mitochondria also have crucial functions in a number of essential cellular processes, such as the regulation of ROS production, tricarboxylic acid cycle (TAC) and respiratory chain regulation (Madamanchi and Runge 2007; Peng et al., 2019). In the brain, oxidative damage decreases enzyme activity of the respiratory chain, resulting in mitochondrial dysfunction (Szeto 2008; Huang et al., 2013; Han et al., 2020). The respiratory chain dysfunction promotes electrons leakage and excess ROS production (Murphy 2009). ROS forms a positive feedback loop, which can cause damage to the inner membrane integrity of the mitochondrial, mitochondrial depolarization, and the opening of mitochondrial permeability transition pore (MPTP) (Szeto 2008). ROS mainly consists of H_2O_2 and superoxide anion radical. H_2O_2 and superoxide anion radical lead to alterations in the function of the respiratory chain (Turrens 2003). There are several antioxidant defense mechanisms in mitochondria, including enzyme and non-enzymatic defenses. Among the enzymatic antioxidant defenses, Mn-SOD takes a crucial role in the converting superoxide anion radical into H_2O_2 through reacting with glutathione peroxidase (GPx) or CAT, generating water (Flynn and Melov 2013; Lu 2013; Morris et al., 2014; Barrera et al., 2016). Reduced GSH is the main nonenzymatic antioxidant defense (Lu 2013). GSH is produced in the cytosol and is necessary to attenuate redox impairment through the reactions of Mn-SOD (Flynn and Melov 2013) and from mitochondrial complexes (Zorov, Juhaszova, and Sollott 2014). Therefore, protective intervention in the mitochondrial function might contribute to the amelioration of ischemia-related brain damage. Studies have shown that RES and mitochondrial function have also been linked to ischemia-reperfusion injury (Zini et al., 1999; Kipp and Ramirez 2001; Zini et al., 2002). The RES can preserve the function of brain mitochondria by reducing the generation of ROS in the mitochondria after hypoxia-reoxygenation (Morin et al., 2003). The mitochondrial respiratory enzyme COX was also examined to evaluate the mitochondrial function (Ortiz-Ruiz et al., 2021). In the present study, it is very likely that RES significantly rescues SH-SY5Y cells from OGD-mediated mitochondrial deficiency (maximal respiratory function, ATP content, COX activity, and mitochondrial membrane potential) (Yousuf et al., 2009; Lin

et al., 2020). Remarkably, Khoury et al. reported that RPC promoted an increase in glycolysis and mitochondrial respiration efficiency. Additionally, genes involved in pyruvate uptake, TAC cycle, and oxidative phosphorylation were more highly expressed, indicating protection on mitochondrial energy-producing pathways during cerebral ischemia (Khoury et al., 2019). For the treatment of SAH, RES resulted in the activation of Sirt5. The activation restored mitochondrial metabolism dysfunction and alleviated early brain injury as well as desuccinylation of citrate synthase and ATP synthase (Xiao et al., 2021). There is also evidence that in the VaD model, RES significantly reduces mitochondrial ROS generation, lipid peroxidation, and protein carbonyls. Beyond this, significant improvements in redox ratio and Mn-SOD activity were observed with RES (Yadav et al., 2018).

The adverse reactions and clinical efficacy of RES

Although RES intake has potent pleiotropic effects in humans and is well tolerated (Ramírez-Garza et al., 2018), others have reported toxic effects of RES *in vitro* and *in vivo* (Calabrese, Mattson, and Calabrese 2010; Cottart et al., 2010; Salehi et al., 2018). It is known that RES has beneficial antioxidant activity, but it appears that RES intake has negative effects on metabolic function, endothelial health, inflammation, and cardiovascular markers in human patients (Ramírez-Garza et al., 2018). In one study, healthy volunteers were given RES doses of 25 mg, 50 mg, 100 mg, and 150 mg at intervals of 4 hours for 48 h. Finally, in some participants, mild adverse effects were reported, such as headaches, dizziness, and epididymitis (Almeida et al., 2009). In obese postmenopausal women, administration of 1 g RES for 12 weeks resulted in negative effects. The liver enzyme levels of one of the 34 subjects were elevated. In addition, 30% of the subjects experienced diarrhea, and 27% had increased total cholesterol (Chow et al., 2014). It is reported that a 450 mg/day dose of RES was a safe dose for a 60 kg person (Moon et al., 2004). RES (1,000 mg/day) was found to inhibit cytochrome P450 isoenzymes such as CYP1A2 and CYP2C9, resulting in interactions with many other drugs (Detampel et al., 2012). In most cases, these interactions could diminish the activity of these drugs. It indicates that RES administration (over 1000 mg/day) causes differences in the pharmacokinetics of drugs administered concurrently (Detampel et al., 2012). Moreover, intracellular redox imbalance in endothelial cells can lead to endothelial dysfunction, which is an important step in the progression of CVD (Cai and Harrison 2000). Numerous studies have demonstrated RES provided protection via its antioxidant impact on the endothelium (Cao and Li 2004; Chen M et al., 2013). However, RES has been shown to increase intracellular oxidative state at tissue-achievable doses, according to Posadino et al. It leads to mitochondrial damage and endothelial cell death (Posadino et al., 2015). Finally, the researchers concluded RES affected endothelial cells biphasically depending on the concentration. *In vitro*, RES at low concentrations reduced the oxidative state of endothelial cells. RES (≥10 μM) increased the status of oxidative stress at higher concentrations *in vitro* (Posadino et al., 2015). Overall, the adverse effects associated with RES use correlate with drug dose. Compared with the overwhelming benefits of RES, its side effects appear mild and sporadic.

Currently, there are many clinical cases that support the use of RES in the prevention and treatment of nervous system disorders. In patients with acute ischemic stroke, rt-PA is one of the most successful treatment options. However, their narrow therapeutic window limits their therapeutic benefits (Lansberg et al., 2012). As is reported, co-administration of RES and rt-PA could extend the time-bound therapeutic window in cerebral stroke patients (Chen et al., 2016). Additionally, they also suggest a potential role for the combination of RES and rt-PA treatment to improve BBB integrity. There has also been researching on the effects of RES on neurological and cognitive disorders in overweight but otherwise healthy individuals as well. Memory performance was improved by RES by increasing hippocampal functional connectivity and improving glucose metabolism (Witte et al., 2014). Interestingly, it was found that RES altered cerebral blood flow in healthy adults. During this study, a dose-dependent increase in cerebral blood flow was observed following two doses of trans-resveratrol (250 and 500 mg) (Kennedy et al., 2010). While RES has been reported to be beneficial for a number of human diseases, it is currently not prescribed for them. Many clinical trials still ongoing. As knowledge of the health benefits of RES increases, the clinical utility is likely to become more apparent and widely accepted.

Conclusion and future direction

CVD severely impacts the patient's quality of life. Treatments of cerebrovascular disorders have developed significantly, such as intravenous (IV) tissue plasminogen activator (IV-tPA), intra-arterial therapy (IAT) for ischemic stroke, and endovascular embolization of vascular malformations. However, thrombolysis has a relatively narrow therapeutic time window (4.5 h) and the risk of severe adverse effects such as hemorrhagic transformation. These treatments are effective, but it is limited to use in a small proportion of patients. Therefore, developing new therapeutic agents are necessary for the treatment of CVD.

Natural products and their derivatives are widely used as treatments for many diseases. RES has various properties like low cytotoxicity, low cost, and extensive sources. More

importantly, oxidative stress also becomes a prominent target of RES. Taken together, RES has therapeutic value in CVD mainly by inhibiting excessive ROS production and elevating antioxidant enzyme activity. Despite that, RES is limitedly used because of its low aqueous solubility and bioavailability. To overcome these defects, cyclodextrins and nanoparticles are developed as drug carriers, which can be applied for enhancement of the solubility, stability, and absorption rate. In addition, an effective sustained-release drug delivery system may decrease the early degradation in the intestine and liver. These innovative approaches have significantly improved the pharmacokinetics of RES, providing a promising treatment for CVD.

Author contributions

QW and QY contributed to the design of the review. MW revised the manuscript. All the authors read and approved the final version of the manuscript.

Funding

The present work was supported by the National Natural Science of China (81400328 and 81773795), Innovation Support Plan and Key Research and Development Program of Shaanxi Province of China (2020PT-003) and Research Found of Xi'an Medical University (2018XNRC02 and 2018PT23).

Conflict of interest

The authors declare that the research was conducted in the absence of any commercial or financial relationships that could be construed as a potential conflict of interest.

Publisher's note

All claims expressed in this article are solely those of the authors and do not necessarily represent those of their affiliated organizations, or those of the publisher, the editors and the reviewers. Any product that may be evaluated in this article, or claim that may be made by its manufacturer, is not guaranteed or endorsed by the publisher.

Supplementary material

The Supplementary Material for this article can be found online at: https://www.frontiersin.org/articles/10.3389/fphar.2022.948889/full#supplementary-material

References

Abdel-Aleem, G. A., Khaleel, E. F., Mostafa, D. G., and Elberier, L. K. (2016). Neuroprotective effect of resveratrol against brain ischemia reperfusion injury in rats entails reduction of DJ-1 protein expression and activation of PI3K/Akt/GSK3b survival pathway. *Arch. Physiol. Biochem.* 122, 200–213. doi:10.1080/13813455.2016.1182190

Adibhatla, R. M., Hatcher, J. F., and Dempsey, R. J. (2006). Lipids and lipidomics in brain injury and diseases. *Aaps J.* 8, E314–E321. doi:10.1007/BF02854902

Aguilar, G. F., Alquisiras-Burgos, I., Franco-Pérez, J., Pineda-Ramírez, N., Ortiz-Plata, A., Torres, I., et al. (2020). Resveratrol prevents GLUT3 up-regulation induced by middle cerebral artery occlusion. *Brain Sci.* 10, E651. doi:10.3390/brainsci10090651

Al Dera, H. (2017). Neuroprotective effect of resveratrol against late cerebral ischemia reperfusion induced oxidative stress damage involves upregulation of osteopontin and inhibition of interleukin-1beta. *J. Physiol. Pharmacol.* 68, 47–56.

Allen, K. J., Gurrin, L. C., Constantine, C. C., Osborne, N. J., Delatycki, M. B., Nicoll, A. J., et al. (2008). Iron-overload-related disease in HFE hereditary hemochromatosis. *N. Engl. J. Med.* 358, 221–230. doi:10.1056/NEJMoa073286

Almazari, I., Park, J. M., Park, S. A., Suh, J. Y., Na, H. K., Cha, Y. N., et al. (2012). Guggulsterone induces heme oxygenase-1 expression through activation of Nrf2 in human mammary epithelial cells: PTEN as a putative target. *Carcinogenesis* 33, 368–376. doi:10.1093/carcin/bgr259

Almeida, L., Vaz-da-Silva, M., Falcão, A., Soares, E., Costa, R., Loureiro, A. I., et al. (2009). Pharmacokinetic and safety profile of trans-resveratrol in a rising multiple-dose study in healthy volunteers. *Mol. Nutr. Food Res.* 53 (1), S7–S15. doi:10.1002/mnfr.200800177

Alquisiras-Burgos, I., Ortiz-Plata, A., Franco-Pérez, J., Millán, A., and Aguilera, P. (2020). Resveratrol reduces cerebral edema through inhibition of de novo SUR1 expression induced after focal ischemia. *Exp. Neurol.* 330, 113353. doi:10.1016/j.expneurol.2020.113353

Anastácio, J. R., Netto, C. A., Castro, C. C., Sanches, E. F., Ferreira, D. C., Noschang, C., et al. (2014). Resveratrol treatment has neuroprotective effects and prevents cognitive impairment after chronic cerebral hypoperfusion. *Neurol. Res.* 36, 627–633. doi:10.1179/1743132813Y.0000000293

Anderson, R., and Prolla, T. (2009). PGC-1alpha in aging and anti-aging interventions. *Biochim. Biophys. Acta* 1790, 1059–1066. doi:10.1016/j.bbagen.2009.04.005

Ayer, R. E., and Zhang, J. H. (2008). Oxidative stress in subarachnoid haemorrhage: Significance in acute brain injury and vasospasm. *Acta Neurochir. Suppl.* 104, 33–41. doi:10.1007/978-3-211-75718-5_7

Barrera, G., Gentile, F., Pizzimenti, S., Canuto, R. A., Daga, M., Arcaro, A., et al. (2016). Mitochondrial dysfunction in cancer and neurodegenerative diseases: Spotlight on fatty acid oxidation and lipoperoxidation products. *Antioxidants (Basel)* 5, 7. doi:10.3390/antiox5010007

Baur, J. A., and Sinclair, D. A. (2006). Therapeutic potential of resveratrol: The *in vivo* evidence. *Nat. Rev. Drug Discov.* 5, 493–506. doi:10.1038/nrd2060

Bederson, J. B., Connolly, E. S., Jr., Batjer, H. H., Dacey, R. G., Dion, J. E., Diringer, M. N., et al. (2009). Guidelines for the management of aneurysmal subarachnoid hemorrhage: A statement for healthcare professionals from a special writing group of the stroke council. *Am. Heart Assoc.* 40, 994–1025. doi:10.1161/STROKEAHA.108.191395

Bharti, A., and Garg, N. (2019). SA and AM symbiosis modulate antioxidant defense mechanisms and asada pathway in chickpea genotypes under salt stress. *Ecotoxicol. Environ. Saf.* 178, 66–78. doi:10.1016/j.ecoenv.2019.04.025

Boocock, D. J., Patel, K. R., Faust, G. E., Normolle, D. P., Marczylo, T. H., Crowell, J. A., et al. (2007). Quantitation of trans-resveratrol and detection of its metabolites in human plasma and urine by high performance liquid chromatography. *J. Chromatogr. B Anal. Technol. Biomed. Life Sci.* 848, 182–187. doi:10.1016/j.jchromb.2006.10.017

Borra, M. T., Smith, B. C., and Denu, J. M. (2005). Mechanism of human SIRT1 activation by resveratrol. *J. Biol. Chem.* 280, 17187–17195. doi:10.1074/jbc.M501250200

Cai, H., and Harrison, D. G. (2000). Endothelial dysfunction in cardiovascular diseases: The role of oxidant stress. *Circ. Res.* 87, 840–844. doi:10.1161/01.res.87.10.840

Calabrese, E. J., Mattson, M. P., and Calabrese, V. (2010). Resveratrol commonly displays hormesis: Occurrence and biomedical significance. *Hum. Exp. Toxicol.* 29, 980–1015. doi:10.1177/0960327110383625

Calamini, B., Ratia, K., Malkowski, M. G., Cuendet, M., Pezzuto, J. M., Santarsiero, B. D., et al. (2010). Pleiotropic mechanisms facilitated by resveratrol and its metabolites. *Biochem. J.* 429, 273–282. doi:10.1042/BJ20091857

Canugovi, C., Maynard, S., Bayne, A. C., Sykora, P., Tian, J., de Souza-Pinto, N. C., et al. (2010). The mitochondrial transcription factor A functions in mitochondrial base excision repair. *DNA Repair (Amst)* 9, 1080–1089. doi:10.1016/j.dnarep.2010.07.009

Cao, Z., and Li, Y. (2004). Potent induction of cellular antioxidants and phase 2 enzymes by resveratrol in cardiomyocytes: Protection against oxidative and electrophilic injury. *Eur. J. Pharmacol.* 489, 39–48. doi:10.1016/j.ejphar.2004.02.031

Chaban, Y., Boekema, E. J., and Dudkina, N. V. (2014). Structures of mitochondrial oxidative phosphorylation supercomplexes and mechanisms for their stabilisation. *Biochim. Biophys. Acta* 1837, 418–426. doi:10.1016/j.bbabio.2013.10.004

Chang, C., Zhao, Y., Song, G., and She, K. (2018). Resveratrol protects hippocampal neurons against cerebral ischemia-reperfusion injury via modulating JAK/ERK/STAT signaling pathway in rats. *J. Neuroimmunol.* 315, 9–14. doi:10.1016/j.jneuroim.2017.11.015

Chen, F., Qian, L. H., Deng, B., Liu, Z. M., Zhao, Y., and Le, Y. Y. (2013). Resveratrol protects vascular endothelial cells from high glucose-induced apoptosis through inhibition of NADPH oxidase activation-driven oxidative stress. *CNS Neurosci. Ther.* 19, 675–681. doi:10.1111/cns.12131

Chen, H., Yoshioka, H., Kim, G. S., Jung, J. E., Okami, N., Sakata, H., et al. (2011). Oxidative stress in ischemic brain damage: Mechanisms of cell death and potential molecular targets for neuroprotection. *Antioxid. Redox Signal.* 14, 1505–1517. doi:10.1089/ars.2010.3576

Chen, J., Bai, Q., Zhao, Z., Sui, H., and Xie, X. (2016). Resveratrol improves delayed r-tPA treatment outcome by reducing MMPs. *Acta Neurol. Scand.* 134, 54–60. doi:10.1111/ane.12511

Chen, J., Jin, K., Chen, M., Pei, W., Kawaguchi, K., Greenberg, D. A., et al. (1997). Early detection of DNA strand breaks in the brain after transient focal ischemia: Implications for the role of DNA damage in apoptosis and neuronal cell death. *J. Neurochem.* 69, 232–245. doi:10.1046/j.1471-4159.1997.69010232.x

Chen, M. L., Yi, L., Jin, X., Xie, Q., Zhang, T., Zhou, X., et al. (2013). Absorption of resveratrol by vascular endothelial cells through passive diffusion and an SGLT1-mediated pathway. *J. Nutr. Biochem.* 24, 1823–1829. doi:10.1016/j.jnutbio.2013.04.003

Chen, S. D., Lin, T. K., Lin, J. W., Yang, D. I., Lee, S. Y., Shaw, F. Z., et al. (2010). Activation of calcium/calmodulin-dependent protein kinase IV and peroxisome proliferator-activated receptor γ coactivator-1α signaling pathway protects against neuronal injury and promotes mitochondrial biogenesis in the hippocampal CA1 subfield after transient global ischemia. *J. Neurosci. Res.* 88, 3144–3154. doi:10.1002/jnr.22469

Chen, W., Guo, C., Jia, Z., Wang, J., Xia, M., Li, C., et al. (2020). Inhibition of mitochondrial ROS by MitoQ alleviates white matter injury and improves outcomes after intracerebral haemorrhage in mice. *Oxid. Med. Cell. Longev.* 2020, 8285065. doi:10.1155/2020/8285065

Chiang, C. K., Hsu, S. P., Wu, C. T., Huang, J. W., Cheng, H. T., Chang, Y. W., et al. (2011). Endoplasmic reticulum stress implicated in the development of renal fibrosis. *Mol. Med.* 17, 1295–1305. doi:10.2119/molmed.2011.00131

Chow, H. H., Garland, L. L., Heckman-Stoddard, B. M., Hsu, C. H., Butler, V. D., Cordova, C. A., et al. (2014). A pilot clinical study of resveratrol in postmenopausal women with high body mass index: Effects on systemic sex steroid hormones. *J. Transl. Med.* 12, 223. doi:10.1186/s12967-014-0223-0

Chowdhury, R., Stevens, S., Gorman, D., Pan, A., Warnakula, S., Chowdhury, S., et al. (2012). Association between fish consumption, long chain omega 3 fatty acids, and risk of cerebrovascular disease: Systematic review and meta-analysis. *Bmj* 345, e6698. doi:10.1136/bmj.e6698

Cohen, S. M., Arnold, L. L., Eldan, M., Lewis, A. S., and Beck, B. D. (2006). Methylated arsenicals: The implications of metabolism and carcinogenicity studies in rodents to human risk assessment. *Crit. Rev. Toxicol.* 36, 99–133. doi:10.1080/10408440500534230

Correia, S. C., Carvalho, C., Cardoso, S., Santos, R. X., Santos, M. S., Oliveira, C. R., et al. (2010). Mitochondrial preconditioning: A potential neuroprotective strategy. *Front. Aging Neurosci.* 2, 138. doi:10.3389/fnagi.2010.00138

Cottart, C. H., Nivet-Antoine, V., Laguillier-Morizot, C., and Beaudeux, J. L. (2010). Resveratrol bioavailability and toxicity in humans. *Mol. Nutr. Food Res.* 54, 7–16. doi:10.1002/mnfr.200900437

de Baaij, J. H., Hoenderop, J. G., and Bindels, R. J. (2012). Regulation of magnesium balance: Lessons learned from human genetic disease. *Clin. Kidney J.* 5, i15–i24. doi:10.1093/ndtplus/sfr164

Della-Morte, D., Dave, K. R., DeFazio, R. A., Bao, Y. C., Raval, A. P., and Perez-Pinzon, M. A. (2009). Resveratrol pretreatment protects rat brain from cerebral ischemic damage via a sirtuin 1-uncoupling protein 2 pathway. *Neuroscience* 159, 993–1002. doi:10.1016/j.neuroscience.2009.01.017

Delmas, D., Aires, V., Limagne, E., Dutartre, P., Mazué, F., Ghiringhelli, F., et al. (2011). Transport, stability, and biological activity of resveratrol. *Ann. N. Y. Acad. Sci.* 1215, 48–59. doi:10.1111/j.1749-6632.2010.05871.x

Detampel, P., Beck, M., Krähenbühl, S., and Huwyler, J. (2012). Drug interaction potential of resveratrol. *Drug Metab. Rev.* 44, 253–265. doi:10.3109/03602532.2012.700715

Diwan, D., Vellimana, A. K., Aum, D. J., Clarke, J., Nelson, J. W., Lawrence, M., et al. (2021). Sirtuin 1 mediates protection against delayed cerebral ischemia in subarachnoid hemorrhage in response to hypoxic postconditioning. *J. Am. Heart Assoc.* 10, e021113. doi:10.1161/JAHA.121.021113

Dou, Z., Rong, X., Zhao, E., Zhang, L., and Lv, Y. (2019). Neuroprotection of resveratrol against focal cerebral ischemia/reperfusion injury in mice through a mechanism targeting gut-brain Axis. *Cell. Mol. Neurobiol.* 39, 883–898. doi:10.1007/s10571-019-00687-3

Dyrkheeva, N. S., Lebedeva, N. A., and Lavrik, O. I. (2016). AP endonuclease 1 as a Key enzyme in repair of apurinic/apyrimidinic sites. *Biochemistry.* 81, 951–967. doi:10.1134/S0006297916090042

Elshaer, M., Chen, Y., Wang, X. J., and Tang, X. (2018). Resveratrol: An overview of its anti-cancer mechanisms. *Life Sci.* 207, 340–349. doi:10.1016/j.lfs.2018.06.028

Enciu, A. M., Constantinescu, S. N., Popescu, L. M., Mureşanu, D. F., and Popescu, B. O. (2011). Neurobiology of vascular dementia. *J. Aging Res.* 2011, 401604. doi:10.4061/2011/401604

Fang, K. M., Cheng, F. C., Huang, Y. L., Chung, S. Y., Jian, Z. Y., and Lin, M. C. (2013). Trace element, antioxidant activity, and lipid peroxidation levels in brain cortex of gerbils after cerebral ischemic injury. *Biol. Trace Elem. Res.* 152, 66–74. doi:10.1007/s12011-012-9596-1

Filograna, R., Mennuni, M., Alsina, D., and Larsson, N. G. (2021). Mitochondrial DNA copy number in human disease: The more the better? *FEBS Lett.* 595, 976–1002. doi:10.1002/1873-3468.14021

Flynn, J. M., and Melov, S. (2013). SOD2 in mitochondrial dysfunction and neurodegeneration. *Free Radic. Biol. Med.* 62, 4–12. doi:10.1016/j.freeradbiomed.2013.05.027

Fu, M., Guo, J., Zhao, Y., Zhang, Y., Zhang, Y., Wang, Z., et al. (2021). Characteristics of fall-related fractures in older adults with cerebrovascular disease: A cross-sectional study. *Clin. Interv. Aging* 16, 1337–1346. doi:10.2147/CIA.S316739

Girbovan, C., Kent, P., Merali, Z., and Plamondon, H. (2016). Dose-related effects of chronic resveratrol administration on neurogenesis, angiogenesis, and corticosterone secretion are associated with improved spatial memory retention following global cerebral ischemia. *Nutr. Neurosci.* 19, 352–368. doi:10.1179/1476830515Y.0000000020

Girbovan, C., and Plamondon, H. (2015). Resveratrol downregulates type-1 glutamate transporter expression and microglia activation in the hippocampus following cerebral ischemia reperfusion in rats. *Brain Res.* 1608, 203–214. doi:10.1016/j.brainres.2015.02.038

Gocmez, S. S., Şahin, T. D., Yazir, Y., Duruksu, G., Eraldemir, F. C., Polat, S., et al. (2019). Resveratrol prevents cognitive deficits by attenuating oxidative damage and inflammation in rat model of streptozotocin diabetes induced vascular dementia. *Physiol. Behav.* 201, 198–207. doi:10.1016/j.physbeh.2018.12.012

Goldberg, D. M., Yan, J., and Soleas, G. J. (2003). Absorption of three wine-related polyphenols in three different matrices by healthy subjects. *Clin. Biochem.* 36, 79–87. doi:10.1016/s0009-9120(02)00397-1

Good, P. F., Perl, D. P., Bierer, L. M., and Schmeidler, J. (1992). Selective accumulation of aluminum and iron in the neurofibrillary tangles of alzheimer's disease: A laser microprobe (LAMMA) study. *Ann. Neurol.* 31, 286–292. doi:10.1002/ana.410310310

Grewal, A. K., Singh, N., and Singh, T. G. (2019). Effects of resveratrol postconditioning on cerebral ischemia in mice: Role of the sirtuin-1 pathway. *Can. J. Physiol. Pharmacol.* 97, 1094–1101. doi:10.1139/cjpp-2019-0188

Han, B., Jiang, W., Liu, H., Wang, J., Zheng, K., Cui, P., et al. (2020). Upregulation of neuronal PGC-1α ameliorates cognitive impairment induced by chronic cerebral hypoperfusion. *Theranostics* 10, 2832–2848. doi:10.7150/thno.37119

Hayes, J. D., McMahon, M., Chowdhry, S., and Dinkova-Kostova, A. T. (2010). Cancer chemoprevention mechanisms mediated through the Keap1-Nrf2 pathway. *Antioxid. Redox Signal.* 13, 1713–1748. doi:10.1089/ars.2010.3221

He, Q., Li, Z., Wang, Y., Hou, Y., Li, L., and Zhao, J. (2017). Resveratrol alleviates cerebral ischemia/reperfusion injury in rats by inhibiting NLRP3 inflammasome activation through Sirt1-dependent autophagy induction. *Int. Immunopharmacol.* 50, 208–215. doi:10.1016/j.intimp.2017.06.029

He, S., Yaung, J., Kim, Y. H., Barron, E., Ryan, S. J., and Hinton, D. R. (2008). Endoplasmic reticulum stress induced by oxidative stress in retinal pigment epithelial cells. *Graefes Arch. Clin. Exp. Ophthalmol.* 246, 677–683. doi:10.1007/s00417-008-0770-2

Horio, Y., Hayashi, T., Kuno, A., and Kunimoto, R. (2011). Cellular and molecular effects of sirtuins in health and disease. *Clin. Sci.* 121, 191–203. doi:10.1042/CS20100587

Hou, Y., Wang, K., Wan, W., Cheng, Y., Pu, X., and Ye, X. (2018). Resveratrol provides neuroprotection by regulating the JAK2/STAT3/PI3K/AKT/mTOR pathway after stroke in rats. *Genes Dis.* 5, 245–255. doi:10.1016/j.gendis.2018.06.001

Huang, L., Wan, J., Chen, Y., Wang, Z., Hui, L., Li, Y., et al. (2013). Inhibitory effects of p38 inhibitor against mitochondrial dysfunction in the early brain injury after subarachnoid hemorrhage in mice. *Brain Res.* 1517, 133–140. doi:10.1016/j.brainres.2013.04.010

Ilieva, E. V., Ayala, V., Jové, M., Dalfó, E., Cacabelos, D., Povedano, M., et al. (2007). Oxidative and endoplasmic reticulum stress interplay in sporadic amyotrophic lateral sclerosis. *Brain* 130, 3111–3123. doi:10.1093/brain/awm190

Jaishankar, M., Tseten, T., Anbalagan, N., Mathew, B. B., and Beeregowda, K. N. (2014). Toxicity, mechanism and health effects of some heavy metals. *Interdiscip. Toxicol.* 7, 60–72. doi:10.2478/intox-2014-0009

Jankowska, K. (2017). Premature ovarian failure. *Przeglad menopauzalny = Menopause Rev.* 16, 51–56. doi:10.5114/pm.2017.68592

Jellinger, K. A. (2007). The enigma of vascular cognitive disorder and vascular dementia. *Acta Neuropathol.* 113, 349–388. doi:10.1007/s00401-006-0185-2

Jeong, S. I., Shin, J. A., Cho, S., Kim, H. W., Lee, J. Y., Kang, J. L., et al. (2016). Resveratrol attenuates peripheral and brain inflammation and reduces ischemic brain injury in aged female mice. *Neurobiol. Aging* 44, 74–84. doi:10.1016/j.neurobiolaging.2016.04.007

Jia, J. Y., Tan, Z. G., Liu, M., and Jiang, Y. G. (2017). Apurinic/apyrimidinic endonuclease 1 (APE1) contributes to resveratrol-induced neuroprotection against oxygen-glucose deprivation and re-oxygenation injury in HT22 cells: Involvement in reducing oxidative DNA damage. *Mol. Med. Rep.* 16, 9786–9794. doi:10.3892/mmr.2017.7799

Jomova, K., and Valko, M. (2011). Advances in metal-induced oxidative stress and human disease. *Toxicology* 283, 65–87. doi:10.1016/j.tox.2011.03.001

Jornayvaz, F. R., and Shulman, G. I. (2010). Regulation of mitochondrial biogenesis. *Essays Biochem.* 47, 69–84. doi:10.1042/bse0470069

Kennedy, D. O., Wightman, E. L., Reay, J. L., Lietz, G., Okello, E. J., Wilde, A., et al. (2010). Effects of resveratrol on cerebral blood flow variables and cognitive performance in humans: A double-blind, placebo-controlled, crossover investigation. *Am. J. Clin. Nutr.* 91, 1590–1597. doi:10.3945/ajcn.2009.28641

Khan, M. A., Chen, H. C., Wan, X. X., Tania, M., Xu, A. H., Chen, F. Z., et al. (2013). Regulatory effects of resveratrol on antioxidant enzymes: A mechanism of growth inhibition and apoptosis induction in cancer cells. *Mol. Cells* 35, 219–225. doi:10.1007/s10059-013-2259-z

Khanduja, K. L., and Bhardwaj, A. (2003). Stable free radical scavenging and antiperoxidative properties of resveratrol compared *in vitro* with some other bioflavonoids. *Indian J. biochem. Biophys.* 40, 416–422.

Khoury, N., Xu, J., Stegelmann, S. D., Jackson, C. W., Koronowski, K. B., Dave, K. R., et al. (2019). Resveratrol preconditioning induces genomic and metabolic adaptations within the long-term window of cerebral ischemic tolerance leading to bioenergetic efficiency. *Mol. Neurobiol.* 56, 4549–4565. doi:10.1007/s12035-018-1380-6

Kim, R. H., Peters, M., Jang, Y., Shi, W., Pintilie, M., Fletcher, G. C., et al. (2005). DJ-1, a novel regulator of the tumor suppressor PTEN. *Cancer Cell* 7, 263–273. doi:10.1016/j.ccr.2005.02.010

Kim, Y. C., Kitaura, H., Taira, T., Iguchi-Ariga, S. M., and Ariga, H. (2009). Oxidation of DJ-1-dependent cell transformation through direct binding of DJ-1 to PTEN. *Int. J. Oncol.* 35, 1331–1341. doi:10.3892/ijo_00000451

Kipp, J. L., and Ramirez, V. D. (2001). Effect of estradiol, diethylstilbestrol, and resveratrol on F0F1-ATPase activity from mitochondrial preparations of rat heart, liver, and brain. *Endocrine* 15, 165–175. doi:10.1385/ENDO:15:2:165

Kobayashi, A., Kang, M. I., Okawa, H., Ohtsuji, M., Zenke, Y., Chiba, T., et al. (2004). Oxidative stress sensor Keap1 functions as an adaptor for Cul3-based E3 ligase to regulate proteasomal degradation of Nrf2. *Mol. Cell. Biol.* 24, 7130–7139. doi:10.1128/MCB.24.16.7130-7139.2004

Kovacic, P., and Somanathan, R. (2010). Multifaceted approach to resveratrol bioactivity: Focus on antioxidant action, cell signaling and safety. *Oxid. Med. Cell. Longev.* 3, 86–100. doi:10.4161/oxim.3.2.11147

Kudo, T., Kanemoto, S., Hara, H., Morimoto, N., Morihara, T., Kimura, R., et al. (2008). A molecular chaperone inducer protects neurons from ER stress. *Cell Death Differ.* 15, 364–375. doi:10.1038/sj.cdd.4402276

Kuhnle, G., Spencer, J. P., Chowrimootoo, G., Schroeter, H., Debnam, E. S., Srai, S. K., et al. (2000). Resveratrol is absorbed in the small intestine as resveratrol glucuronide. *Biochem. Biophys. Res. Commun.* 272, 212–217. doi:10.1006/bbrc.2000.2750

Kumar, A., and Mittal, R. (2017). Nrf2: A potential therapeutic target for diabetic neuropathy. *Inflammopharmacology* 25, 393–402. doi:10.1007/s10787-017-0339-y

Laev, S. S., Salakhutdinov, N. F., and Lavrik, O. I. (2017). Inhibitors of nuclease and redox activity of apurinic/apyrimidinic endonuclease 1/redox effector factor 1 (APE1/Ref-1). *Bioorg. Med. Chem.* 25, 2531–2544. doi:10.1016/j.bmc.2017.01.028

Lan, J., Li, W., Zhang, F., Sun, F. Y., Nagayama, T., O'Horo, C., et al. (2003). Inducible repair of oxidative DNA lesions in the rat brain after transient focal ischemia and reperfusion. *J. Cereb. Blood Flow. Metab.* 23, 1324–1339. doi:10.1097/01.WCB.0000091540.60196.F2

Lansberg, M. G., O'Donnell, M. J., Khatri, P., Lang, E. S., Nguyen-Huynh, M. N., Schwartz, N. E., et al. (2012). Antithrombotic and thrombolytic therapy for ischemic stroke: Antithrombotic therapy and prevention of thrombosis, 9th ed: American college of chest physicians evidence-based clinical practice guidelines. *Chest* 141, e601S–e636S. doi:10.1378/chest.11-2302

Leak, R. K., Li, P., Zhang, F., Sulaiman, H. H., Weng, Z., Wang, G., et al. (2015). Apurinic/apyrimidinic endonuclease 1 upregulation reduces oxidative DNA damage and protects hippocampal neurons from ischemic injury. *Antioxid. Redox Signal.* 22, 135–148. doi:10.1089/ars.2013.5511

Ledbetter, L. N., Burns, J., Shih, R. Y., Ajam, A. A., Brown, M. D., Chakraborty, S., et al. (2021). ACR appropriateness Criteria® cerebrovascular diseases-aneurysm, vascular malformation, and subarachnoid hemorrhage. *J. Am. Coll. Radiol.* 18, S283–S304. doi:10.1016/j.jacr.2021.08.012

Lei, J., and Chen, Q. (2018). Resveratrol attenuates brain damage in permanent focal cerebral ischemia via activation of PI3K/Akt signaling pathway in rats. *Neurol. Res.* 40, 1014–1020. doi:10.1080/01616412.2018.1509826

Lei, J. R., Tu, X. K., Wang, Y., Tu, D. W., and Shi, S. S. (2019). Resveratrol downregulates the TLR4 signaling pathway to reduce brain damage in a rat model of focal cerebral ischemia. *Exp. Ther. Med.* 17, 3215–3221. doi:10.3892/etm.2019.7324

Li, H., Wang, J., Wang, P., Rao, Y., and Chen, L. (2016). Resveratrol reverses the synaptic plasticity deficits in a chronic cerebral hypoperfusion rat model. *J. Stroke Cerebrovasc. Dis.* 25, 122–128. doi:10.1016/j.jstrokecerebrovasdis.2015.09.004

Li, J., Ma, X., Yu, W., Lou, Z., Mu, D., Wang, Y., et al. (2012). Reperfusion promotes mitochondrial dysfunction following focal cerebral ischemia in rats. *PLoS One* 7, e46498. doi:10.1371/journal.pone.0046498

Li, W., Tan, C., Liu, Y., Liu, X., Wang, X., Gui, Y., et al. (2015). Resveratrol ameliorates oxidative stress and inhibits aquaporin 4 expression following rat cerebral ischemia-reperfusion injury. *Mol. Med. Rep.* 12, 7756–7762. doi:10.3892/mmr.2015.4366

Li, Y. G., Zhu, W., Tao, J. P., Xin, P., Liu, M. Y., Li, J. B., et al. (2013). Resveratrol protects cardiomyocytes from oxidative stress through SIRT1 and mitochondrial biogenesis signaling pathways. *Biochem. Biophys. Res. Commun.* 438, 270–276. doi:10.1016/j.bbrc.2013.07.042

Li, Z., Fang, F., Wang, Y., and Wang, L. (2016). Resveratrol protects CA1 neurons against focal cerebral ischemic reperfusion-induced damage via the ERK-CREB signaling pathway in rats. *Pharmacol. Biochem. Behav.* 146-147, 21–27. doi:10.1016/j.pbb.2016.04.007

Lin, C. H., Nicol, C. J. B., Cheng, Y. C., Yen, C., Wang, Y. S., and Chiang, M. C. (2020). Neuroprotective effects of resveratrol against oxygen glucose deprivation induced mitochondrial dysfunction by activation of AMPK in SH-SY5Y cells with 3D gelatin scaffold. *Brain Res.* 1726, 146492. doi:10.1016/j.brainres.2019.146492

Lin, M. C., Liu, C. C., Lin, Y. C., and Liao, C. S. (2021). Resveratrol protects against cerebral ischemic injury via restraining lipid peroxidation, transition elements, and toxic metal levels, but enhancing anti-oxidant activity. *Antioxidants (Basel)* 10, 1515. doi:10.3390/antiox10101515

Lin, Y., Chen, F., Zhang, J., Wang, T., Wei, X., Wu, J., et al. (2013). Neuroprotective effect of resveratrol on ischemia/reperfusion injury in rats through TRPC6/CREB pathways. *J. Mol. Neurosci.* 50, 504–513. doi:10.1007/s12031-013-9977-8

Liu, L., Huang, W., Wang, J., Song, H., Cen, J., and Ji, B. (2017). Anthraquinone derivative exerted hormetic effect on the apoptosis in oxygen-glucose deprivation-induced PC12 cells via ERK and Akt activated Nrf2/HO-1 signaling pathway. *Chem. Biol. Interact.* 262, 1–11. doi:10.1016/j.cbi.2016.12.001

Lopez, M. S., Dempsey, R. J., and Vemuganti, R. (2015). Resveratrol neuroprotection in stroke and traumatic CNS injury. *Neurochem. Int.* 89, 75–82. doi:10.1016/j.neuint.2015.08.009

Lu, S. C. (2013). Glutathione synthesis. *Biochim. Biophys. Acta* 1830, 3143–3153. doi:10.1016/j.bbagen.2012.09.008

Ludwig, D. L., MacInnes, M. A., Takiguchi, Y., Purtymun, P. E., Henrie, M., Flannery, M., et al. (1998). A murine AP-endonuclease gene-targeted deficiency with post-implantation embryonic progression and ionizing radiation sensitivity. *Mutat. Res.* 409, 17–29. doi:10.1016/s0921-8777(98)00039-1

Ma, S., Fan, L., Li, J., Zhang, B., and Yan, Z. (2020). Resveratrol promoted the M2 polarization of microglia and reduced neuroinflammation after cerebral ischemia by inhibiting miR-155. *Int. J. Neurosci.* 130, 817–825. doi:10.1080/00207454.2019.1707817

Ma, X., Sun, Z., Liu, Y., Jia, Y., Zhang, B., and Zhang, J. (2013). Resveratrol improves cognition and reduces oxidative stress in rats with vascular dementia. *Neural Regen. Res.* 8, 2050–2059. doi:10.3969/j.issn.1673-5374.2013.22.004

Madamanchi, N. R., and Runge, M. S. (2007). Mitochondrial dysfunction in atherosclerosis. *Circ. Res.* 100, 460–473. doi:10.1161/01.RES.0000258450.44413.96

McNally, R. S., Davis, B. K., Clements, C. M., Accavitti-Loper, M. A., Mak, T. W., and Ting, J. P. (2011). DJ-1 enhances cell survival through the binding of Cezanne, a negative regulator of NF-kappaB. *J. Biol. Chem.* 286, 4098–4106. doi:10.1074/jbc.M110.147371

Miller, W. H., Jr., Schipper, H. M., Lee, J. S., Singer, J., and Waxman, S. (2002). Mechanisms of action of arsenic trioxide. *Cancer Res.* 62, 3893–3903.

Moon, R. T., Kohn, A. D., De Ferrari, G. V., and Kaykas, A. (2004). WNT and beta-catenin signalling: Diseases and therapies. *Nat. Rev. Genet.* 5, 691–701. doi:10.1038/nrg1427

Morin, C., Zini, R., Albengres, E., Bertelli, A. A., Bertelli, A., and Tillement, J. P. (2003). Evidence for resveratrol-induced preservation of brain mitochondria functions after hypoxia-reoxygenation. *Drugs Exp. Clin. Res.* 29, 227–233.

Morris, G., Anderson, G., Dean, O., Berk, M., Galecki, P., Martin-Subero, M., et al. (2014). The glutathione system: A new drug target in neuroimmune disorders. *Mol. Neurobiol.* 50, 1059–1084. doi:10.1007/s12035-014-8705-x

Moussa, C., Hebron, M., Huang, X., Ahn, J., Rissman, R. A., Aisen, P. S., et al. (2017). Resveratrol regulates neuro-inflammation and induces adaptive immunity in Alzheimer's disease. *J. Neuroinflammation* 14, 1. doi:10.1186/s12974-016-0779-0

Murphy, C. J., and Oudit, G. Y. (2010). Iron-overload cardiomyopathy: Pathophysiology, diagnosis, and treatment. *J. Card. Fail.* 16, 888–900. doi:10.1016/j.cardfail.2010.05.009

Murphy, M. P. (2009). How mitochondria produce reactive oxygen species. *Biochem. J.* 417, 1–13. doi:10.1042/BJ20081386

Nakka, V. P., Prakash-Babu, P., and Vemuganti, R. (2016). Crosstalk between endoplasmic reticulum stress, oxidative stress, and autophagy: Potential therapeutic targets for acute CNS injuries. *Mol. Neurobiol.* 53, 532–544. doi:10.1007/s12035-014-9029-6

Nanjaiah, H., and Vallikannan, B. (2019). Enhanced phosphorylation of AMPK by lutein and oxidised lutein that lead to mitochondrial biogenesis in hyperglycemic HepG2 cells. *J. Cell. Biochem.* 120, 15255–15267. doi:10.1002/jcb.28793

Orallo, F. (2006). Comparative studies of the antioxidant effects of cis- and trans-resveratrol. *Curr. Med. Chem.* 13, 87–98. doi:10.2174/092986706775197962

Orellana-Urzúa, S., Rojas, I., Líbano, L., and Rodrigo, R. (2020). Pathophysiology of ischemic stroke: Role of oxidative stress. *Curr. Pharm. Des.* 26, 4246–4260. doi:10.2174/1381612826666200708133912

Ortiz-Ruiz, A., Ruiz-Heredia, Y., Morales, M. L., Aguilar-Garrido, P., García-Ortiz, A., Valeri, A., et al. (2021). Myc-related mitochondrial activity as a novel target for multiple myeloma. *Cancers (Basel)* 13, 1662. doi:10.3390/cancers13071662

Østergaard, L., Engedal, T. S., Moreton, F., Hansen, M. B., Wardlaw, J. M., Dalkara, T., et al. (2016). Cerebral small vessel disease: Capillary pathways to stroke and cognitive decline. *J. Cereb. Blood Flow. Metab.* 36, 302–325. doi:10.1177/0271678X15606723

Ozacmak, V. H., Sayan-Ozacmak, H., and Barut, F. (2016). Chronic treatment with resveratrol, a natural polyphenol found in grapes, alleviates oxidative stress and apoptotic cell death in ovariectomized female rats subjected to chronic cerebral hypoperfusion. *Nutr. Neurosci.* 19, 176–186. doi:10.1179/1476830515Y.0000000027

Pan, C., Giraldo, G. S., Prentice, H., and Wu, J. Y. (2010). Taurine protection of PC12 cells against endoplasmic reticulum stress induced by oxidative stress. *J. Biomed. Sci.* 17 (1), S17. doi:10.1186/1423-0127-17-S1-S17

Papa, S., Martino, P. L., Capitanio, G., Gaballo, A., De Rasmo, D., Signorile, A., et al. (2012). The oxidative phosphorylation system in mammalian mitochondria. *Adv. Exp. Med. Biol.* 942, 3–37. doi:10.1007/978-94-007-2869-1_1

Park, D. J., Kang, J. B., Shah, F. A., and Koh, P. O. (2019). Resveratrol modulates the Akt/GSK-3β signaling pathway in a middle cerebral artery occlusion animal model. *Lab. Anim. Res.* 35, 18. doi:10.1186/s42826-019-0019-8

Peng, W., Cai, G., Xia, Y., Chen, J., Wu, P., Wang, Z., et al. (2019). Mitochondrial dysfunction in atherosclerosis. *DNA Cell Biol.* 38, 597–606. doi:10.1089/dna.2018.4552

Picca, A., and Lezza, A. M. (2015). Regulation of mitochondrial biogenesis through TFAM-mitochondrial DNA interactions: Useful insights from aging and calorie restriction studies. *Mitochondrion* 25, 67–75. doi:10.1016/j.mito.2015.10.001

Pineda-Ramírez, N., Alquisiras-Burgos, I., Ortiz-Plata, A., Ruiz-Tachiquín, M. E., Espinoza-Rojo, M., and Aguilera, P. (2020). Resveratrol activates neuronal autophagy through AMPK in the ischemic brain. *Mol. Neurobiol.* 57, 1055–1069. doi:10.1007/s12035-019-01803-6

Posadino, A. M., Cossu, A., Giordo, R., Zinellu, A., Sotgia, S., Vardeu, A., et al. (2015). Resveratrol alters human endothelial cells redox state and causes mitochondrial-dependent cell death. *Food Chem. Toxicol.* 78, 10–16. doi:10.1016/j.fct.2015.01.017

Qian, C., Jin, J., Chen, J., Li, J., Yu, X., Mo, H., et al. (2017). SIRT1 activation by resveratrol reduces brain edema and neuronal apoptosis in an experimental rat subarachnoid hemorrhage model. *Mol. Med. Rep.* 16, 9627–9635. doi:10.3892/mmr.2017.7773

Ramírez-Garza, S. L., Laveriano-Santos, E. P., Marhuenda-Muñoz, M., Storniolo, C. E., Tresserra-Rimbau, A., Vallverdú-Queralt, A., et al. (2018). Health effects of resveratrol: Results from human intervention trials. *Nutrients* 10, E1892. doi:10.3390/nu10121892

Ren, J., Fan, C., Chen, N., Huang, J., and Yang, Q. (2011). Resveratrol pretreatment attenuates cerebral ischemic injury by upregulating expression of transcription factor Nrf2 and HO-1 in rats. *Neurochem. Res.* 36, 2352–2362. doi:10.1007/s11064-011-0561-8

Resnick, S. M., and Henderson, V. W. (2002). Hormone therapy and risk of alzheimer disease: A critical time. *Jama* 288, 2170–2172. doi:10.1001/jama.288.17.2170

Ro, J. H., Liu, C. C., and Lin, M. C. (2021). Resveratrol mitigates cerebral ischemic injury by altering levels of trace elements, toxic metal, lipid peroxidation, and antioxidant activity. *Biol. Trace Elem. Res.* 199, 3718–3727. doi:10.1007/s12011-020-02497-x

Rotches-Ribalta, M., Andres-Lacueva, C., Estruch, R., Escribano, E., and Urpi-Sarda, M. (2012). Pharmacokinetics of resveratrol metabolic profile in healthy humans after moderate consumption of red wine and grape extract tablets. *Pharmacol. Res.* 66, 375–382. doi:10.1016/j.phrs.2012.08.001

Saleh, M. C., Connell, B. J., and Saleh, T. M. (2013). Resveratrol induced neuroprotection is mediated via both estrogen receptor subtypes, ER(α) and ER(β). *Neurosci. Lett.* 548, 217–221. doi:10.1016/j.neulet.2013.05.057

Salehi, B., Mishra, A. P., Nigam, M., Sener, B., Kilic, M., Sharifi-Rad, M., et al. (2018). Resveratrol: A double-edged sword in health benefits. *Biomedicines* 6, E91. doi:10.3390/biomedicines6030091

Scarpulla, R. C. (2011). Metabolic control of mitochondrial biogenesis through the PGC-1 family regulatory network. *Biochim. Biophys. Acta* 1813, 1269–1278. doi:10.1016/j.bbamcr.2010.09.019

Scarpulla, R. C. (2008). Transcriptional paradigms in mammalian mitochondrial biogenesis and function. *Physiol. Rev.* 88, 611–638. doi:10.1152/physrev.00025.2007

Schreiber, S. N., Emter, R., Hock, M. B., Knutti, D., Cardenas, J., Podvinec, M., et al. (2004). The estrogen-related receptor alpha (ERRalpha) functions in PPARgamma coactivator 1alpha (PGC-1alpha)-induced mitochondrial biogenesis. *Proc. Natl. Acad. Sci. U. S. A.* 101, 6472–6477. doi:10.1073/pnas.0308686101

Shang, Y., Xue, W., Kong, J., Chen, Y., Qiu, X., An, X., et al. (2022). Ultrafine black carbon caused mitochondrial oxidative stress, mitochondrial dysfunction and mitophagy in SH-SY5Y cells. *Sci. Total Environ.* 813, 151899. doi:10.1016/j.scitotenv.2021.151899

Shankar, S., Singh, G., and Srivastava, R. K. (2007). Chemoprevention by resveratrol: Molecular mechanisms and therapeutic potential. *Front. Biosci.* 12, 4839–4854. doi:10.2741/2432

Shao, A. W., Wu, H. J., Chen, S., Ammar, A. B., Zhang, J. M., and Hong, Y. (2014). Resveratrol attenuates early brain injury after subarachnoid hemorrhage through

inhibition of NF-κB-dependent inflammatory/MMP-9 pathway. *CNS Neurosci. Ther.* 20, 182–185. doi:10.1111/cns.12194

Shuwen, H., Xi, Y., and Yuefen, P. (2017). Can mitochondria DNA provide a novel biomarker for evaluating the risk and prognosis of colorectal cancer? *Dis. Markers* 2017, 5189803. doi:10.1155/2017/5189803

Soleas, G. J., Angelini, M., Grass, L., Diamandis, E. P., and Goldberg, D. M. (2001). Absorption of trans-resveratrol in rats. *Methods Enzymol.* 335, 145–154. doi:10.1016/s0076-6879(01)35239-4

Song, E., Su, C., Fu, J., Xia, X., Yang, S., Xiao, C., et al. (2014). Selenium supplementation shows protective effects against patulin-induced brain damage in mice via increases in GSH-related enzyme activity and expression. *Life Sci.* 109, 37–43. doi:10.1016/j.lfs.2014.05.022

Souissi, R., Boubakker, A., Souissi, H., Abdelrazek, A., Badri, M., Bziouech, S., et al. (2010). Prediction of cerebral vasospasm in patients with aneurysmal subarachnoid hemorrhage using jugular bulb oximetry monitoring: Preliminary results. *Crit. Care (Houten).* 14, 343. doi:10.1186/cc8575

Stetler, R. A., Gao, Y., Leak, R. K., Weng, Z., Shi, Y., Zhang, L., et al. (2016). APE1/Ref-1 facilitates recovery of gray and white matter and neurological function after mild stroke injury. *Proc. Natl. Acad. Sci. U. S. A.* 113, E3558–E3567. doi:10.1073/pnas.1606226113

Strong, K., Mathers, C., and Bonita, R. (2007). Preventing stroke: Saving lives around the world. *Lancet. Neurol.* 6, 182–187. doi:10.1016/S1474-4422(07)70031-5

Sung, M. M., and Dyck, J. R. (2015). Therapeutic potential of resveratrol in heart failure. *Ann. N. Y. Acad. Sci.* 1348, 32–45. doi:10.1111/nyas.12839

Suzuki, H. (2015). What is early brain injury? *Transl. Stroke Res.* 6, 1–3. doi:10.1007/s12975-014-0380-8

Szeto, H. H. (2008). Mitochondria-targeted cytoprotective peptides for ischemia-reperfusion injury. *Antioxid. Redox Signal.* 10, 601–619. doi:10.1089/ars.2007.1892

Taira, T., Saito, Y., Niki, T., Iguchi-Ariga, S. M., Takahashi, K., and Ariga, H. (2004). DJ-1 has a role in antioxidative stress to prevent cell death. *EMBO Rep.* 5, 213–218. doi:10.1038/sj.embor.7400074

Tao, T., Liu, M., Chen, M., Luo, Y., Wang, C., Xu, T., et al. (2020). Natural medicine in neuroprotection for ischemic stroke: Challenges and prospective. *Pharmacol. Ther.* 216, 107695. doi:10.1016/j.pharmthera.2020.107695

Toth, P., Tarantini, S., Springo, Z., Tucsek, Z., Gautam, T., Giles, C. B., et al. (2015). Aging exacerbates hypertension-induced cerebral microhemorrhages in mice: Role of resveratrol treatment in vasoprotection. *Aging Cell* 14, 400–408. doi:10.1111/acel.12315

Turner, R. S., Thomas, R. G., Craft, S., van Dyck, C. H., Mintzer, J., Reynolds, B. A., et al. (2015). A randomized, double-blind, placebo-controlled trial of resveratrol for Alzheimer disease. *Neurology* 85, 1383–1391. doi:10.1212/WNL.0000000000002035

Turrens, J. F. (2003). Mitochondrial formation of reactive oxygen species. *J. Physiol.* 552, 335–344. doi:10.1113/jphysiol.2003.049478

Ungvari, Z., Sonntag, W. E., de Cabo, R., Baur, J. A., and Csiszar, A. (2011). Mitochondrial protection by resveratrol. *Exerc. Sport Sci. Rev.* 39, 128–132. doi:10.1097/JES.0b013e3182141f80

Valle, I., Alvarez-Barrientos, A., Arza, E., Lamas, S., and Monsalve, M. (2005). PGC-1alpha regulates the mitochondrial antioxidant defense system in vascular endothelial cells. *Cardiovasc. Res.* 66, 562–573. doi:10.1016/j.cardiores.2005.01.026

Van Eersel, J., Ke, Y. D., Liu, X., Delerue, F., Kril, J. J., Götz, J., et al. (2010). Sodium selenate mitigates tau pathology, neurodegeneration, and functional deficits in Alzheimer's disease models. *Proc. Natl. Acad. Sci. U. S. A.* 107, 13888–13893. doi:10.1073/pnas.1009038107

Vasko, M. R., Guo, C., and Kelley, M. R. (2005). The multifunctional DNA repair/redox enzyme Ape1/Ref-1 promotes survival of neurons after oxidative stress. *DNA Repair (Amst)* 4, 367–379. doi:10.1016/j.dnarep.2004.11.006

Virbasius, C. A., Virbasius, J. V., and Scarpulla, R. C. (1993). NRF-1, an activator involved in nuclear-mitochondrial interactions, utilizes a new DNA-binding domain conserved in a family of developmental regulators. *Genes Dev.* 7, 2431–2445. doi:10.1101/gad.7.12a.2431

Vitaglione, P., Sforza, S., Galaverna, G., Ghidini, C., Caporaso, N., Vescovi, P. P., et al. (2005). Bioavailability of trans-resveratrol from red wine in humans. *Mol. Nutr. Food Res.* 49, 495–504. doi:10.1002/mnfr.200500002

Vomund, S., Schäfer, A., Parnham, M. J., Brüne, B., and von Knethen, A. (2017). Nrf2, the master regulator of anti-oxidative responses. *Int. J. Mol. Sci.* 18, E2772. doi:10.3390/ijms18122772

Walle, T., Hsieh, F., DeLegge, M. H., Oatis, J. E., Jr., and Walle, U. K. (2004). High absorption but very low bioavailability of oral resveratrol in humans. *Drug Metab. Dispos.* 32, 1377–1382. doi:10.1124/dmd.104.000885

Wallerath, T., Deckert, G., Ternes, T., Anderson, H., Li, H., Witte, K., et al. (2002). Resveratrol, a polyphenolic phytoalexin present in red wine, enhances expression and activity of endothelial nitric oxide synthase. *Circulation* 106, 1652–1658. doi:10.1161/01.cir.0000029925.18593.5c

Wan, D., Zhou, Y., Wang, K., Hou, Y., Hou, R., and Ye, X. (2016). Resveratrol provides neuroprotection by inhibiting phosphodiesterases and regulating the cAMP/AMPK/SIRT1 pathway after stroke in rats. *Brain Res. Bull.* 121, 255–262. doi:10.1016/j.brainresbull.2016.02.011

Wang, N., He, J., Pan, C., Wang, J., Ma, M., Shi, X., et al. (2019). Resveratrol activates autophagy via the AKT/mTOR signaling pathway to improve cognitive dysfunction in rats with chronic cerebral hypoperfusion. *Front. Neurosci.* 13, 859. doi:10.3389/fnins.2019.00859

Wang, P., and Sang, S. (2018). Metabolism and pharmacokinetics of resveratrol and pterostilbene. *Biofactors* 44, 16–25. doi:10.1002/biof.1410

Wang, Q., Xu, J., Rottinghaus, G. E., Simonyi, A., Lubahn, D., Sun, G. Y., et al. (2002). Resveratrol protects against global cerebral ischemic injury in gerbils. *Brain Res.* 958, 439–447. doi:10.1016/s0006-8993(02)03543-6

Wang, Q., Yu, S., Simonyi, A., Rottinghaus, G., Sun, G. Y., and Sun, A. Y. (2004). Resveratrol protects against neurotoxicity induced by kainic acid. *Neurochem. Res.* 29, 2105–2112. doi:10.1007/s11064-004-6883-z

Wang, S., Qian, Y., Gong, D., Zhang, Y., and Fan, Y. (2011). Resveratrol attenuates acute hypoxic injury in cardiomyocytes: Correlation with inhibition of iNOS-NO signaling pathway. *Eur. J. Pharm. Sci.* 44, 416–421. doi:10.1016/j.ejps.2011.08.029

Wareski, P., Vaarmann, A., Choubey, V., Safiulina, D., Liiv, J., Kuum, M., et al. (2009). PGC-1{alpha} and PGC-1{beta} regulate mitochondrial density in neurons. *J. Biol. Chem.* 284, 21379–21385. doi:10.1074/jbc.M109.018911

Warner, J. J., Harrington, R. A., Sacco, R. L., and Elkind, M. S. V. (2019). Guidelines for the early management of patients with acute ischemic stroke: 2019 update to the 2018 guidelines for the early management of acute ischemic stroke. *Stroke* 50, 3331–3332. doi:10.1161/STROKEAHA.119.027708

Wei, H., Wang, S., Zhen, L., Yang, Q., Wu, Z., Lei, X., et al. (2015). Resveratrol attenuates the blood-brain barrier dysfunction by regulation of the MMP-9/TIMP-1 balance after cerebral ischemia reperfusion in rats. *J. Mol. Neurosci.* 55, 872–879. doi:10.1007/s12031-014-0441-1

Witte, A. V., Kerti, L., Margulies, D. S., and Flöel, A. (2014). Effects of resveratrol on memory performance, hippocampal functional connectivity, and glucose metabolism in healthy older adults. *J. Neurosci.* 34, 7862–7870. doi:10.1523/JNEUROSCI.0385-14.2014

Wolters, F. J., and Ma, I. (2019). Epidemiology of vascular dementia. *Arterioscler. Thromb. Vasc. Biol.* 39, 1542–1549. doi:10.1161/ATVBAHA.119.311908

Xiao, Z. P., Lv, T., Hou, P. P., Manaenko, A., Liu, Y., Jin, Y., et al. (2021). Sirtuin 5-mediated lysine desuccinylation protects mitochondrial metabolism following subarachnoid hemorrhage in mice. *Stroke* 52, 4043–4053. doi:10.1161/STROKEAHA.121.034850

Xie, Y. K., Zhou, X., Yuan, H. T., Qiu, J., Xin, D. Q., Chu, X. L., et al. (2019). Resveratrol reduces brain injury after subarachnoid hemorrhage by inhibiting oxidative stress and endoplasmic reticulum stress. *Neural Regen. Res.* 14, 1734–1742. doi:10.4103/1673-5374.257529

Yadav, A., Sunkaria, A., Singhal, N., and Sandhir, R. (2018). Resveratrol loaded solid lipid nanoparticles attenuate mitochondrial oxidative stress in vascular dementia by activating Nrf2/HO-1 pathway. *Neurochem. Int.* 112, 239–254. doi:10.1016/j.neuint.2017.08.001

Yang, H., Zhang, A., Zhang, Y., Ma, S., and Wang, C. (2016). Resveratrol pretreatment protected against cerebral ischemia/reperfusion injury in rats via expansion of T regulatory cells. *J. Stroke Cerebrovasc. Dis.* 25, 1914–1921. doi:10.1016/j.jstrokecerebrovasdis.2016.04.014

Yang, J., Huang, J., Shen, C., Cheng, W., Yu, P., Wang, L., et al. (2018). Resveratrol treatment in different time-attenuated neuronal apoptosis after oxygen and glucose deprivation/reoxygenation via enhancing the activation of nrf-2 signaling pathway *in vitro*. *Cell Transpl.* 27, 1789–1797. doi:10.1177/0963689718780930

Yang, T., Wang, L., Zhu, M., Zhang, L., and Yan, L. (2015). Properties and molecular mechanisms of resveratrol: A review. *Trans. Tianjin Univ.* 70, 501–506. doi:10.1007/s12209-015-2629-z

Yang, Y., Ding, Z., Zhong, R., Xia, T., Wang, W., Zhao, H., et al. (2020). Cardioprotective effects of a Fructus Aurantii polysaccharide in isoproterenol-induced myocardial ischemic rats. *Int. J. Biol. Macromol.* 155, 995–1002. doi:10.1016/j.ijbiomac.2019.11.063

Ye, M., Wu, H., and Li, S. (2021). Resveratrol alleviates oxygen/glucose deprivation/reoxygenation-induced neuronal damage through induction of mitophagy. *Mol. Med. Rep.* 23, 73. doi:10.3892/mmr.2020.11711

Yin, W., Signore, A. P., Iwai, M., Cao, G., Gao, Y., and Chen, J. (2008). Rapidly increased neuronal mitochondrial biogenesis after hypoxic-ischemic brain injury. *Stroke* 39, 3057–3063. doi:10.1161/STROKEAHA.108.520114

Yousuf, S., Atif, F., Ahmad, M., Hoda, N., Ishrat, T., Khan, B., et al. (2009). Resveratrol exerts its neuroprotective effect by modulating mitochondrial dysfunctions and associated cell death during cerebral ischemia. *Brain Res.* 1250, 242–253. doi:10.1016/j.brainres.2008.10.068

Yu, P., Wang, L., Tang, F., Guo, S., Liao, H., Fan, C., et al. (2021). Resveratrol-mediated neurorestoration after cerebral ischemic injury - sonic Hedgehog signaling pathway. *Life Sci.* 280, 119715. doi:10.1016/j.lfs.2021.119715

Yu, W., Fu, Y. C., and Wang, W. (2012). Cellular and molecular effects of resveratrol in health and disease. *J. Cell. Biochem.* 113, 752–759. doi:10.1002/jcb.23431

Zhang, J., Wang, Y., Liu, X., Dagda, R. K., and Zhang, Y. (2017). How AMPK and PKA interplay to regulate mitochondrial function and survival in models of ischemia and diabetes. *Oxid. Med. Cell Longev.* 2017, 4353510. doi:10.1155/2017/4353510

Zhang, K. (2010). Integration of ER stress, oxidative stress and the inflammatory response in health and disease. *Int. J. Clin. Exp. Med.* 3, 33–40.

Zhang, X., Wu, Q., Zhang, Q., Lu, Y., Liu, J., Li, W., et al. (2017). Resveratrol attenuates early brain injury after experimental subarachnoid hemorrhage via inhibition of NLRP3 inflammasome activation. *Front. Neurosci.* 11, 611. doi:10.3389/fnins.2017.00611

Zhang, Y., Li, Y., Wang, Y., Wang, G., Mao, L., Zhang, D., et al. (2019). Effects of resveratrol on learning and memory in rats with vascular dementia. *Mol. Med. Rep.* 20, 4587–4593. doi:10.3892/mmr.2019.10723

Zhao, R., Zhao, K., Su, H., Zhang, P., and Zhao, N. (2019). Resveratrol ameliorates brain injury via the TGF-β-mediated ERK signaling pathway in a rat model of cerebral hemorrhage. *Exp. Ther. Med.* 18, 3397–3404. doi:10.3892/etm.2019.7939

Zhou, J., Yang, Z., Shen, R., Zhong, W., Zheng, H., Chen, Z., et al. (2021). Resveratrol improves mitochondrial biogenesis function and activates PGC-1α pathway in a preclinical model of early brain injury following subarachnoid hemorrhage. *Front. Mol. Biosci.* 8, 620683. doi:10.3389/fmolb.2021.620683

Zhou, X. M., Zhou, M. L., Zhang, X. S., Zhuang, Z., Li, T., Shi, J. X., et al. (2014). Resveratrol prevents neuronal apoptosis in an early brain injury model. *J. Surg. Res.* 189, 159–165. doi:10.1016/j.jss.2014.01.062

Zini, R., C Morin, A. B., Bertelli, A. A., and Tillement, J. P. (1999). Effects of resveratrol on the rat brain respiratory chain. *Drugs Exp. Clin. Res.* 25, 87–97.

Zini, R., Morin, C., Bertelli, A., Bertelli, A. A., and Tillement, J. P. (2002). Resveratrol-induced limitation of dysfunction of mitochondria isolated from rat brain in an anoxia-reoxygenation model. *Life Sci.* 71, 3091–3108. doi:10.1016/s0024-3205(02)02161-6

Zorov, D. B., Juhaszova, M., and Sollott, S. J. (2014). Mitochondrial reactive oxygen species (ROS) and ROS-induced ROS release. *Physiol. Rev.* 94, 909–950. doi:10.1152/physrev.00026.2013

Glossary

Al: Aluminum
AMPK: Adenosine 5′-monophosphate (AMP)-activated protein kinase
APE1: Apurinic/apyrimidinic endonuclease one
AQP4: Aquaporin four
ARE: Antioxidant response element
ATP: Adenosine triphosphate
BBB: Blood-brain barrier disruption
BCCAO: Bilateral common carotid artery occlusion
CaMKIV: Calmodulin kinase IV
cAMP: Cyclic adenosine monophosphate
CAT: Catalase
CCH: Chronic cerebral hypoperfusion
CoA: CoenzymeA
COX2: Cyclo-oxygenase two
CREB: cAMP-response element binding protein
Cu: Copper
CVD: Cerebrovascular diseases
DCX: Doublecortin
DNA: Deoxyribonucleic acid
eNOS: Endothelial nitric oxide synthase
ER: Endoplasmic reticulum
Fe: Ferrum
GPx: Glutathione peroxidase
GFAP: Glial fibrillary acidic protein
GLUT3: Glucose transporter3
GRP78: Glucose-regulated protein 78
GSH: Glutathione
GSH-Pxs: Glutathione peroxidase
GST: Glutathione-s-transferase
H_2O_2: Hydrogen peroxide
HO-1: Heme oxygenase-1
I/R: Ischemic reperfusion
IL-1β: Interleukin-1β
JAK: Janus kinase
Keap1: Kelch-like ECH- associated protein l
LDH: Lactate dehydrogenase
MCAO/R: Middle cerebral artery occlusion/reperfusion
MDA: Malondialdehyde
Mg: Magnesium
MMP: Matrix metalloproteinase
MnSOD: Manganese superoxide dismutase
MPO: Myeloperoxidase
MPTP: Mitochondrial permeability transition pore
mTOR: Mechanistic target of rapamycin
mtDNA: Mitochondrial DNA
NF-κB: Nuclear factor kappa-B
NGF: Nerve growth factor
NLRP3: NOD-like receptor protein three inflammasome
NMDA: National Marine Distributors Association
NO: Nitric oxide
NQO1: NAD(P)H qui-none oxidoreductase one
NRF-1: Respiratory factors 1
Nrf2: NF-E2-related factor 2
OGD/R: Oxygen-glucose deprivation/reperfusion
PGC-1α: Peroxisome proliferator-activated receptor-gamma coactivator (PGC)-1alpha
PI3K/Akt: Phosphatidylinositol three kinase/Protein Kinase B
PINK1: PTEN-induced putative kinase protein one
PKA: Protein kinase A
PSA-NCAM: Polysialylated-neural cell adhesion molecule
PTEN: Phosphatase and tensin homolog deleted on chromosome ten
RCCA: Right common carotid artery
RES: Resveratrol
RMCA: Right Middle Cerebral Artery
ROS: Reactive oxygen species
RPC: RES preconditioning
rt-PA: Recombinant tissue plasminogen activator
SAH: Subarachnoid hemorrhage
Se: Selenium
SIRT1: Sirtuin1
SOD: Superoxide dismutase
STAT3: Signal transducer and activator of transcription3
SUR1: Sulfonylurea Receptor1
TAC: tricarboxylic acid cycle
TFAM: Transcription factor A mitochondrial
TGF-β-ERK: Transforming growth factor-β-Extracellular-signal-regulated kinases
TIMP-1: Tissue inhibitor of matrix metalloproteinases
TLR4: Toll-like receptor four
TNF-α: Tumor necrosis factor-α
TRPC6-MEK: Transient receptor potential channel 6/methyl ethyl ketone
VaD: Vascular dementia
VO: Vessel occlusion
Zn: Zinc

frontiers | Frontiers in Pharmacology

TYPE Original Research
PUBLISHED 11 January 2023
DOI 10.3389/fphar.2022.987293

OPEN ACCESS

EDITED BY
Yongjun Sun,
Hebei University of Science and Technology, China

REVIEWED BY
Vinod Tiwari,
Indian Institute of Technology (BHU), India
Xiaoping Liang,
Johns Hopkins Medicine, United States

*CORRESPONDENCE
Wenhu Zhou,
zhouwenhuyaoji@163.com
Yanhui Cui,
cuiyanhui0110@163.com

†These authors have contributed equally to this work and share first authorship

SPECIALTY SECTION
This article was submitted to Neuropharmacology, a section of the journal Frontiers in Pharmacology

RECEIVED 06 July 2022
ACCEPTED 30 December 2022
PUBLISHED 11 January 2023

CITATION
Zhang H, Wang L, Yang Y, Cai C, Wang X, Deng L, He B, Zhou W and Cui Y (2023), DL-3-n-butylphthalide (NBP) alleviates poststroke cognitive impairment (PSCI) by suppressing neuroinflammation and oxidative stress.
Front. Pharmacol. 13:987293.
doi: 10.3389/fphar.2022.987293

DL-3-n-butylphthalide (NBP) alleviates poststroke cognitive impairment (PSCI) by suppressing neuroinflammation and oxidative stress

Hui Zhang[1†], Laifa Wang[1†], Yongping Yang[1], Chuanhai Cai[1], Xueqin Wang[1], Ling Deng[1], Binsheng He[1,2], Wenhu Zhou[1,2,3*] and Yanhui Cui[1*]

[1]Neuroscience and Behavioral Research Center, Academician Workstation, Changsha Medical University, Changsha, China, [2]Hunan Key Laboratory of the Research and Development of Novel Pharmaceutical Preparations, Changsha Medical University, Changsha, China, [3]Xiangya School of Pharmaceutical Sciences, Central South University, Changsha, Hunan, China

Currently, the recovery of cognitive function has become an essential part of stroke rehabilitation. DL-3-n-butylphthalide (NBP) is a neuroprotective reagent and has been used in stroke treatment. Clinical studies have confirmed that NBP can achieve better cognitive outcomes in ischemic stroke patients than in healthy controls. In this study, we aimed to investigate the influences of NBP on cognitive function in an ischemic reperfusion (I/R) rat model. Our results showed that NBP profoundly decreased neurological scores, reduced cerebral infarct areas and enhanced cerebral blood flow (CBF). NBP potently alleviated poststroke cognitive impairment (PSCI) including depression-like behavior and learning, memory and social cognition impairments, in I/R rats. NBP distinctly suppressed the activation of microglia and astrocytes and improved neuron viability in the ischemic brain. NBP inhibited the expression of inflammatory cytokines, including interleukin-6 (IL-6), interleukin-1β (IL-1β) and tumor necrosis factor-α (TNF-α), by targeting the nuclear factor kappa B/inducible nitric oxide synthase (NF-κB/iNOS) pathway and decreased cerebral oxidative stress factors, including reactive oxygen species (ROS) and malondialdehyde (MDA), by targeting the kelch like ECH associated protein 1/nuclear factor-erythroid 2 p45-related factor 2 (Keap1/Nrf2) pathway in the ischemic brain. The current study revealed that NBP treatment improved neurological function and ameliorated cognitive impairment in I/R rats, possibly by synergistically suppressing inflammation and oxidative stress.

KEYWORDS

Dl-3-n-butylphthalide, neuroprotectants, acute ischemic stroke, inflammation, stress oxidation

Introduction

Currently, stroke is still the leading cause of disability and the second most common of mortality worldwide (Mendelson and Prabhakaran, 2021). Stroke is generally classified into hemorrhagic stroke and ischemic stroke and the latter accounts for 71% of all stroke cases (Sacks et al., 2018). Functional outcomes of stroke involve not only physical disability, but also cognitive impairment in approximately 1/3 of patients, severely affecting their capability to live independently (Kalaria et al., 2016). Poststroke cognitive impairment (PSCI) is a type of

vascular cognitive impairment and likely develops into dementia (Teng et al., 2017). PSCI is quite common in acute ischemic stroke patients, with an incidence ranging from 7.4% to 41.3% (Huang et al., 2022). PSCI, including memory and learning disorders, emotional disorders, attention disorders, sensory and perceptual disorders, executive dysfunction, personality changes and behavioral abnormalities, has become one of the primary challenges faced in stroke rehabilitation (Liu et al., 2020). Lesions in cerebral areas, such as the hippocampus, white matter, and cortex, induced by ischemic reperfusion (I/R) might contribute to the pathogenesis of PSCI (Sun et al., 2014). Currently, drugs available for PSCI treatment mainly include calcium antagonists, excitatory amino acid receptor antagonists and cholinesterase inhibitors (Grupke et al., 2015). However, the effects of these reagents are still far from satisfactory, necessitating the development of novel preventive approaches to improve the cognitive function of AIS patients.

DL-3-n-butylphthalide (NBP) is a chiral compound synthesized from L-3-n-butylphthalide, which was originally extracted from the seeds of *Apium graveolens* Linn (Fan et al., 2022). NBP was licensed by the State Food and Drug Administration of China (SFDA) in 2002 for ischemic stroke treatment (Peng et al., 2013). Fundamental or clinical studies have demonstrated that NBP could alleviate PSCI (Sun et al., 2017; Yan et al., 2017). Multiple mechanisms are involved in the neuroprotective function of NBP, such as inhibiting neuroinflammation (Wang et al., 2019), resisting oxidative stress (Wang et al., 2021), promoting cerebral blood flow (CBF) (Li et al., 2019), and reducing neuronal damage (Li H Q et al., 2021). Oxidative stress and inflammation play essential roles in the pathogenesis of cognitive deficits induced by various risk factors (Tiwari et al., 2009; Tiwari and Chopra, 2012). Increasing evidence has suggested that neuroinflammation is an important factor contributing to PSCI, and the relevant mechanisms include neuronal cell injury, brain function impairment and inflammasome activation (Gold et al., 2011; Swardfager et al., 2013; Kim et al., 2020). Oxidative stress is another major mechanism participating in the pathogenesis of PSCI. Augmenting of oxidative stress levels damages neurons and contributes to aggravated PSCI (Bahader et al., 2021). Both neuroinflammation and oxidative stress provide targets for PSCI treatment (Zhang and Bi, 2020). In the present study, we hypothesized that NBP protects neurological function and alleviates PSCI, possibly by synergistically suppressing inflammation and oxidative stress. Therefore, the influences of NBP on neurological function and PSCI were investigated, and the underlying mechanisms were further probed.

Materials and methods

Ischemic reperfusion (I/R) model

Animal experiments were licensed by the Institutional Animal Care and Use Committee of Changsha Medical University. Animal suffering was minimized according to the guidelines. Sprague-Dawley (SD) rats with body weights ranging from 250 g to 280 g were purchased from Hunan SJA Laboratory (Changsha, China). The rats were housed in a room with a temperature of 20°C–24°C, humidity of 45%–65% and 12-h light/dark cycle.

I/R models were established by middle cerebral artery occlusion (MCAO) according to Longa's method (Longa et al., 1989) with minor modifications. The rats were anesthetized by pentobarbital sodium (30 mg/kg i.p.,). The right common carotid artery, external carotid artery (ECA) and internal carotid artery (ICA) were carefully separated and exposed. The common carotid artery was first ligated. A small incision was made at the ECA, and a Nylon suture with a .36-mm diameter (Cinontech, Beijing, China) was inserted and guided through the ICA to the middle cerebral artery (MCA). After 1 h of occlusion, the suture was withdrawn from the ICA for reperfusion. The sham group was subjected to a surgical procedure similar to that of the I/R group except for MCA occlusion. The rats in the vehicle + I/R group (I/R group) were administered saline (450 μL, i. p.), and the rats in the NBP + I/R group were administered NBP (9 mg/kg, i. p.) (CSPC Pharmaceutical Group Co., Ltd., Shijiazhuang, China). The flowchart of the animal experiment is generalized in Figure 1.

Neurological deficit scoring

The neurological deficit score was evaluated on the 7th day after surgery by researchers blinded to the animal grouping. No deficit was scored 0; forelimb weakness was scored 1; circling to one side was scored 2; inability to bear weight on the affected side was scored 3; and no spontaneous motor activity was scored 4 (Shah et al., 2006). Rats scored 0 after I/R surgery were deemed failed models and were excluded from subsequent experiments.

Laser speckle imaging

Laser speckle imaging (RWD Life Technologies, Shenzhen, China) was utilized to monitor CBF before MCAO, after MCAO, after reperfusion and on the 7th day after I/R surgery. Briefly, a scalp incision was made in the middle of the head. Bilateral skulls were ground and polished by a cranial perforator until the scull was sufficiently thin for CBF detection. The detector was positioned above the skull. Videos were obtained, and CBF in the region of interest (ROI) was recorded. Relative CBF for each rat was expressed as the ratio of CBF in the right hemisphere to the left hemisphere.

Infarct area analysis

The cerebral infarct area was evaluated by 2,3,5-triphenyltetrazolium chloride (TTC) staining (Solarbio, Beijing, China). Briefly, the rats were anesthetized and sacrificed by cervical dislocation. Brains were rapidly removed and cut into slices of approximately 2-mm thickness on ice. The slices were immersed in TTC solution for 30 min at 37°C and fixed in 4% paraformaldehyde for 2 h. Photos of the slices were obtained. The infarct area was measured by ImageJ software (Media Cybernetics, Bethesda, MD, United States). The infarct volume was calculated through multiplying the area by the thickness of the slices. The percentage of the infarct volume was calculated.

Sucrose preference test (SPT)

The SPT was performed to evaluate depression-like behavior (Lu et al., 2017). During the SPT procedure, the rats were kept separately. In the adaptation phase, each rat was supplied with two bottles of 1% (w/v) sucrose. After 24 h, one bottle of sucrose was replaced with water for another 24 h. Subsequently, the rat was deprived of water for 24 h. In the test phase, the rat was simultaneously supplied with one bottle

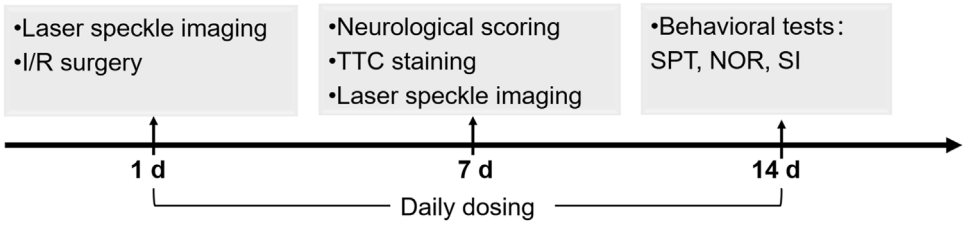

FIGURE 1
Schedule of the animal experiments including I/R model establishment, NBP dosing, cerebral infarction analysis, CBF analysis, neurological scoring and behavioral tests.

of water and one bottle of 1% sucrose for 2 h. Sucrose preference (SP) was calculated according to the following formula: SP = sucrose intake/(sucrose intake + water intake) × 100%.

Novel object recognition (NOR) test

The NOR test was performed to evaluate animal learning and memory capability (Lueptow, 2017). In the adaptive phase, two identical objects were placed in a square opaque box (20 cm × 20 cm). The rat was allowed to acclimate to the box for 5 min and then removed from the box to its home cage. In the test phase, one of the objects was replaced with a novel object with different materials, shapes and colors. The rat was returned to the box and allowed to freely explore for 5 min. The time spent sniffing or climbing each object by the rat was analyzed by Smart software, version 3.0 (Panlab, Spain). The Discrimination ratio was calculated according to the following formula ($Time_{Novel}$—$Time_{Familiar}$)/($Time_{Novel}$ + $Time_{Familiar}$).

Social interaction (SI) test

The SI test was performed to evaluate animal social cognitive capability (Liu et al., 2019). The device consisted three opaque square boxes (40 × 40 × 40 cm), with a passage connecting the boxes. One clear cage of the same size, sufficiently large to hold a rat, was positioned in the left box and the right box. In the first phase, the three boxes were separated with clear Plexiglas, and the subject rat was placed in the middle box to acclimate for 5 min. In the second phase, a stimulus rat (familiar rat) was placed to the left cage. The Plexiglas was removed to allow the subject rat to explore freely in the three boxes for 10 min. In the third phase, a second rat (unfamiliar rat) was placed in the right cage. The subject rat was allowed to freely explore for another 10 min. The time spent communicating with the familiar rat and the unfamiliar rat by the subject rat was analyzed by Smart software, version 3.0. The Discrimination ratio was calculated according to the following formula ($Time_{Unfamiliar}$—$Time_{Familiar}$)/($Time_{Unfamiliar}$ + $Time_{Familiar}$) × 100%.

Enzyme-linked immunosorbent assay (ELISA)

Inflammatory cytokines, including interleukin-6 (IL-6), interleukin-1β (IL-1β) and tumor necrosis factor-α (TNF-α), in the ischemic cerebral hemisphere were analyzed by ELISA kits according to the manufacturer's instructions (Meiman, Jiangsu, China). A dose of 10 μL of supernatants of ischemic brain homogenate or standard sample was mixed with 40 μL of sample diluent and added to the wells. A dose of 100 μL of HRP-conjugated reagent was added to each well except for the blank wells. The plate was incubated at 37°C for 1 h. Chromogen Solution A (50 μL) and Chromogen Solution B (50 μL) were added to each well. The plate was incubated at 37°C for 15 min in the dark. The absorbance was measured at 450 nm.

Reactive oxygen species (ROS) and malondialdehyde (MDA) analysis

The ischemic hemisphere of the brain was collected and homogenized. The homogenate was centrifuged at 4000 × g at 4°C for 20 min. The supernatant was collected. The protein concentration was determined by a BCA Protein Assay Kit (Kangwei Century Biotechnology, Jiangsu, China).

ROS were measured by an ROS assay kit (Jiancheng Bioengineering Institute, Nanjing, China) according to the manufacturer's instructions. Briefly, 1 μL of sample, 5 μL of DCFH probe (5 μM) and PBS were mixed into a 96-well plate and incubated at 37°C for 40 min. The fluorescent value was measured under an excitation wavelength of 500 nm and an emission wavelength of 525 nm. The ROS level was expressed as a fold change in the fluorescent value compared with the sham group.

The MDA level was measured by an MDA assay kit (Jiancheng Bioengineering Institute, Nanjing, China) according to the manufacturer's instructions. The test mixture contained 20 μL of sample, 20 μL of solution I, 1 mL of solution II and 330 μL of solution III. The blank mixture contained 20 μL of ethanol instead of sample and the standard mixture contained 20 μL standard substance (10 nM) instead of sample, with the other components the same. All of the mixtures were incubated in 95°C water bath for 40 min and centrifuged at 1000 × g for 10 min. The absorbance value at 532 nm was recorded. The MDA level was expressed as: OD_{Sample} × 10 nM/($OD_{Standard}$—OD_{Blank})/protein concentration (nM/mgprot).

Western blot

The proteins extracted from the ischemic brain (10 μg per lane) were separated by 10% SDS–PAGE gel and transferred to a .45 μm nitrocellulose membrane (Boster Biological Technology, CA, United States). The membranes were blocked with 5% nonfat milk at room temperature for 1 h and incubated with primary

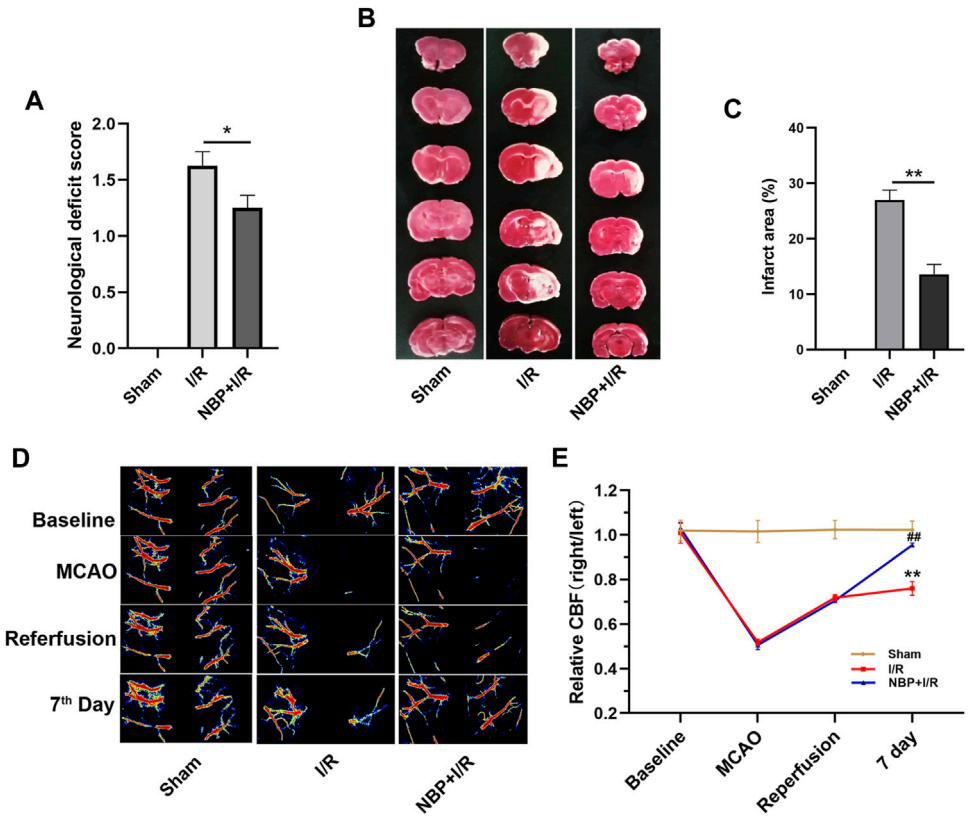

FIGURE 2
Effects of NBP on neurological scores, cerebral infarction and CBF in I/R rats. **(A)** Effects of NBP on neurological scores (n = 16). Rats showed obvious neurological deficits after I/R surgery, while NBP treatment significantly improved neurological function. **(B and C)** Effects of NBP on the infarct area in the right hemisphere of the brains in I/R rats (n = 3). I/R surgery resulted in obvious infarction in the right hemisphere of the brain, while NBP significantly reduced the infarct area in I/R rats. **(D and E)** Effects of NBP on CBF and the ratio of CBF in the right hemisphere to the left hemisphere (n = 3). Data are expressed as the mean ± SEM and were analyzed by one-way ANOVA (*post hoc* analysis: Tukey's *post hoc* analysis test). * ($p < .05$) and ** ($p < .01$) represent significance compared to the I/R group. ## ($p < .01$) represents significance compared to the sham group. NBP dose: NBP + I/R, 9 mg/kg.

antibodies at 4°C overnight. After washing with TBST buffer 3 times, the membrane was incubated with HRP-conjugated secondary antibody at room temperature for 70 min. The bands were detected by an Odyssey Clx system (Li-COR Biosciences, United States). The protein expression level was quantified by ImageJ software and normalized to GAPDH. The primary antibodies included anti-Keap1 antibody (1:1000, ab119403, Abcam, United States), anti-Nrf2 antibody (1:500, ab92946, Abcam, United States), anti-NF-κB P65 antibody (1:500, ab194726, Abcam, United States), anti-iNOS antibody (1:500, ab283655, Abcam, United States), and anti-GAPDH antibody (1: 2000, 10494-1-AP, ProteinTech, United States).

Immunohistochemistry

The rats were anesthetized and perfused with saline solution and 4% paraformaldehyde. The brain was removed and sequentially immersed in 4% paraformaldehyde, 15% sucrose, 30% sucrose and 35% sucrose, each step for 12 h and imbedded into Tissue-Tek® O.C.T (Sakura Finetek, United States). The brains were cut into slices with a thickness of 15 μm. The slices were incubated with primary antibodies at 4°C overnight. After washing with PBS, the slices were incubated with donkey anti-rabbit and donkey anti-mouse secondary antibodies at room temperature for 2 h. Subsequently, the slices were stained with 3,3′-diaminobenzidine (DAB) (ZSGB-BIO, Beijing, China) and washed with PBS. The primary antibodies included anti-NeuN antibody (1:200, ab177487, Abcam, United States), anti- GFAP polyclonal antibody (1:200, ab7260, Abcam, United States), and anti-Iba-1 antibody (1:200, 019-19741, Wako, Japan). The slides were dehydrated by ethanol, cleared by xylene and sealed. The same zone of brain sections was scanned using a Panoramic 250 FLASH II digital slide scanner (3DHISTECH, Budapest, Hungary). The numbers of positive cells per field were counted (×40 magnification). At least three sections for each rat were analyzed.

Statistical analysis

The data are presented as the mean ± SEM and were analyzed by Graphpad Prism software, version 8 (San Diego, CA, United States). Group comparisons were performed by one-way ANOVA followed by Tukey's *post hoc* test. $p < .05$ was considered significantly different.

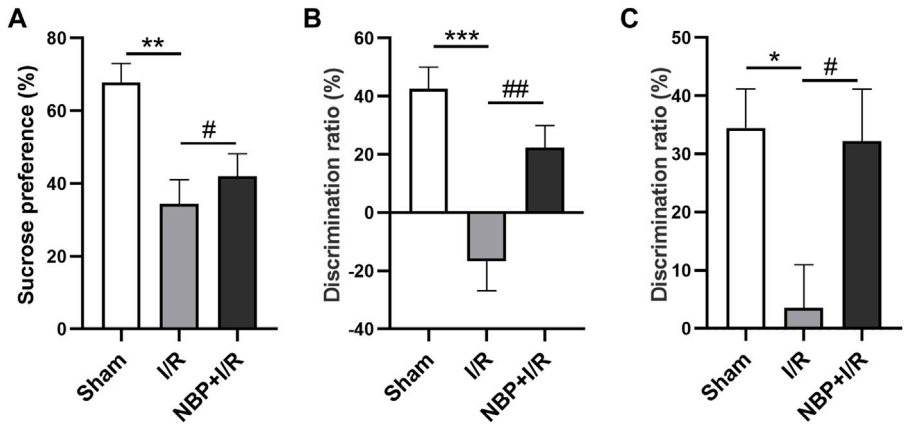

FIGURE 3
Effects of NBP on the cognitive behavior of I/R rats. **(A)** Effects of NBP on depression-like behavior in I/R rats as assessed by the SPT. Sucrose consumption was significantly decreased in I/R rats, while NBP significantly enhanced sucrose preference. **(B)** Effects of NBP on social cognition in I/R rats by SI testing. The discrimination ratio was significantly decreased in the I/R group and significantly increased after NBP treatment on the SI test. **(C)** Effects of NBP on study and memory in I/R rats by the NOR test. The discrimination ratio was significantly decreased in the I/R group and significantly increased after NBP treatment on the NOR test. Data are expressed as the mean ± SEM (n = 10) and were analyzed by one-way ANOVA (*post hoc* analysis: Tukey's *post hoc* analysis test). * ($p < .05$), ** ($p < .01$) and *** ($p < .001$) represent significance compared to the sham group. # ($p < .05$) and ## ($p < .01$) represent significance compared to the I/R group ($p < .01$). NBP dose: NBP + I/R, 9 mg/kg.

Results

Effects of NBP on neurological scores, cerebral infarction and CBF in I/R rats

Neurological function was evaluated on the 7th day after I/R surgery. As shown in Figure 2A, the rats in the I/R group showed obvious neurological deficits compared with the sham group. NBP significantly improved neurological function ($p < .05$). TTC staining results showed that an obvious infarct area was observed in the I/R group, while NBP significantly reduced the infarct area in I/R rats ($p < .01$) (Figures 2B, C). CBF was monitored during I/R surgery and, on the 7th day after I/R surgery, by laser speckle imaging. CBF in the ischemic hemisphere of I/R rats was obviously reduced after MCAO and partially recovered after reperfusion, indicative of successful cerebral blood occlusion and reperfusion. On the 7th day, NBP significantly enhanced the CBF in the ischemic hemispheres of I/R rats ($p < .01$) (Figures 2D, E).

Effects of NBP on cognitive behavior in I/R rats

The sucrose consumption by I/R rats was significantly decreased ($p < .01$). NBP significantly enhanced sucrose preference in I/R rats ($p < .05$) (Figure 3A), indicating that NBP could alleviate depression-like behavior in I/R rats. The SI test was performed to evaluate animal social cognition. Compared with the sham group, the discrimination ratio in the I/R group was significantly decreased ($p < .001$). NBP treatment significantly increased the discrimination ratio ($p < .05$), indicating that NBP could improve the social cognitive ability of I/R rats (Figure 3B). The NOR test was performed to investigate animal learning and memory capability. Compared with the sham group, the I/R group exhibited a significantly decreased discrimination ratio ($p < .001$). NBP treatment significantly increased the discrimination ratio compared with the I/R group ($p < .05$), suggesting that NBP could effectively improve the learning and memory abilities of I/R rats (Figure 3C).

Effects of NBP on oxidative stress in I/R rats

To evaluate the effects of NBP on oxidative stress, the levels of ROS and MDA in the right hemispheres of the rats were measured. The results suggested that transient ischemia significantly elevated ROS levels ($p < .05$) and MDA levels ($p < .05$). ROS ($p < .01$) and MDA ($p < .01$) were significantly decreased in the NBP + I/R group compared with the I/R group, indicating that NBP could suppress oxidative stress in I/R rats (Figures 4A, B). The oxidative stress-associated kelch like ECH associated protein 1/nuclear factor-erythroid 2 p45-related factor 2 (Keap1/Nrf2) pathway was further analyzed. The expression of both Keap1 and Nrf2 was low in the sham group. Keap1 protein expression was significantly elevated in the I/R group ($p < .01$). NBP significantly downregulated Keap1 levels ($p < .05$) and upregulated Nrf2 levels ($p < .05$), suggesting that NBP alleviated oxidative stress by targeting the Keap1/Nrf2 pathway (Figures 4C, D).

Effects of NBP on neuroinflammation in I/R rats

Cytokines including IL-6, IL-1β and TNF-α, in the ischemic brain were assayed to investigate the effects of NBP on inflammatory levels in I/R rats. The concentrations of cerebral cytokines (IL-6, $p < .01$; IL-1β, $p < .01$; TNF-α, $p < .01$) were significantly increased after transient ischemia. NBP significantly decreased IL-6 ($p < .01$), IL-1β ($p < .001$) and TNF-α ($p < .01$) levels in the ischemic brains of the I/R rats (Figures 5A–C). The nuclear factor kappa B/inducible nitric oxide synthase (NF-κB/iNOS) was further analyzed. The expression of both NF-κB P65 ($p < .05$) and iNOS ($p < .05$) was significantly increased in the I/R group. NBP significantly

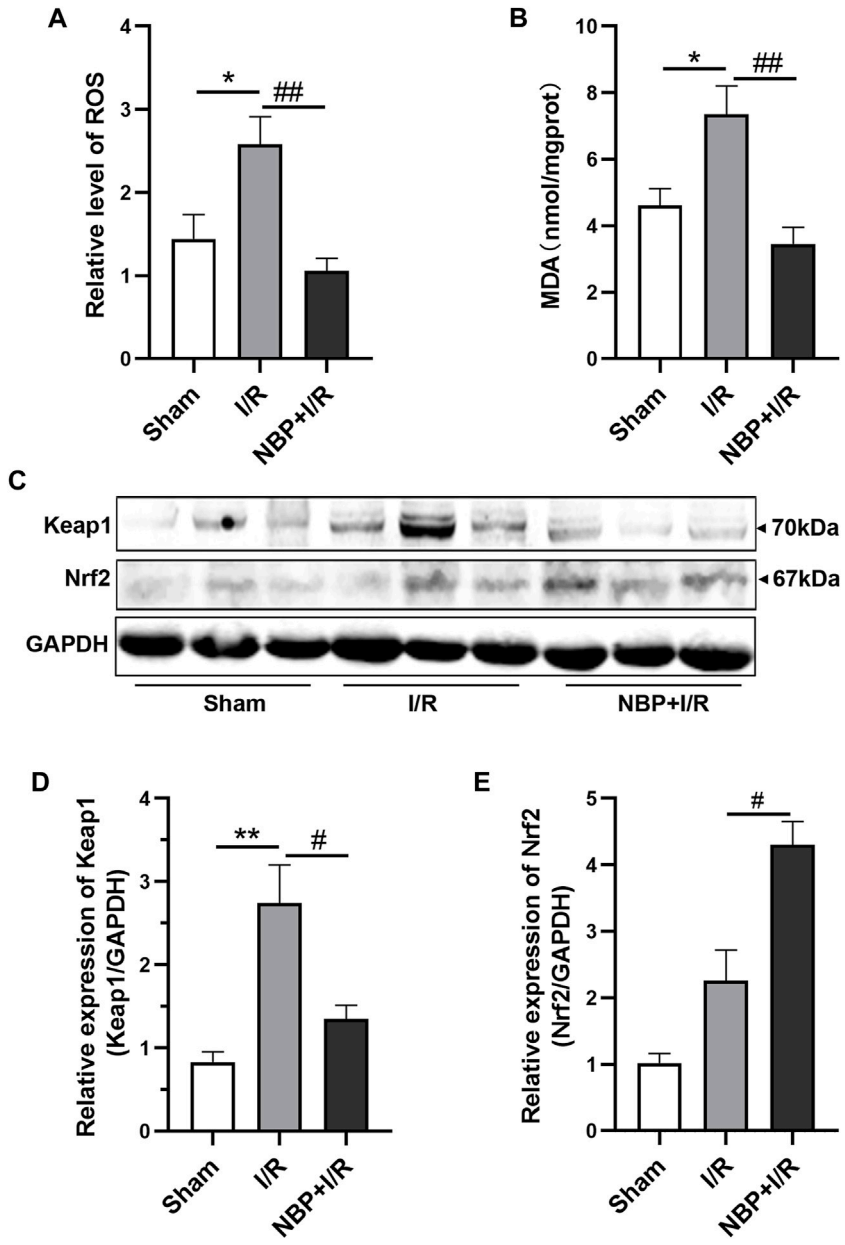

FIGURE 4
Effects of NBP on oxidative stress in the infarcted cerebral hemisphere in I/R rats. **(A and B)** Effects of NBP on ROS levels and MDA leves (n = 6). I/R surgery significantly elevated ROS levels and MDA levels, while NBP significantly decreased ROS levels and MDA levels in I/R rats. **(C–E)** Effects of NBP on Keap1/Nrf2 pathway (n = 3). NBP significantly downregulated Keap1 expression and upregulated Nrf2 expression in I/R rats. Data are expressed as the mean ± SEM and were analyzed by one-way ANOVA (*post hoc* analysis: Tukey's *post hoc* analysis test). * ($p < .05$) and ** ($p < .01$) represent significance compared to the sham group. # ($p < .05$) and ## ($p < .01$) represent significance compared to the I/R group ($p < .01$). NBP dose: NBP + I/R, 9 mg/kg.

downregulated NF-κB P65 ($p < .05$) and iNOS expression ($p < .05$). The above data suggested that NBP attenuated neuroinflammation by targeting the NF-κB/iNOS pathway (Figures 5D–F).

Effects of NBP on neurons, microglia and astrocytes in I/R rats

According to the immunohistochemistry results, neuron-specific nuclear protein (NeuN)-positive cells were significantly decreased in the I/R group compared with the sham group ($p < .01$). NBP significantly increased the number of NeuN-positive cells in the ischemic penumbra zone ($p < .05$) (Figures 6A, B), suggesting that NBP could preserve the viability of neurons in I/R rats. Glial fibrillary acidic protein (GFAP) and ionized calcium binding adaptor molecule 1 (Iba1) were analyzed to verify the activation of microglia and astrocytes in the ischemic penumbra, respectively. Compared with the sham group, GFAP-positive cells and Iba1-positive cells were significantly increased in the I/R group ($p < .01$). NBP significantly decreased GFAP-positive cells and Iba1-positive cells ($p < .05$), indicating that NBP could effectively protect microglia and astrocytes against overactivation (Figures 6A, C, D).

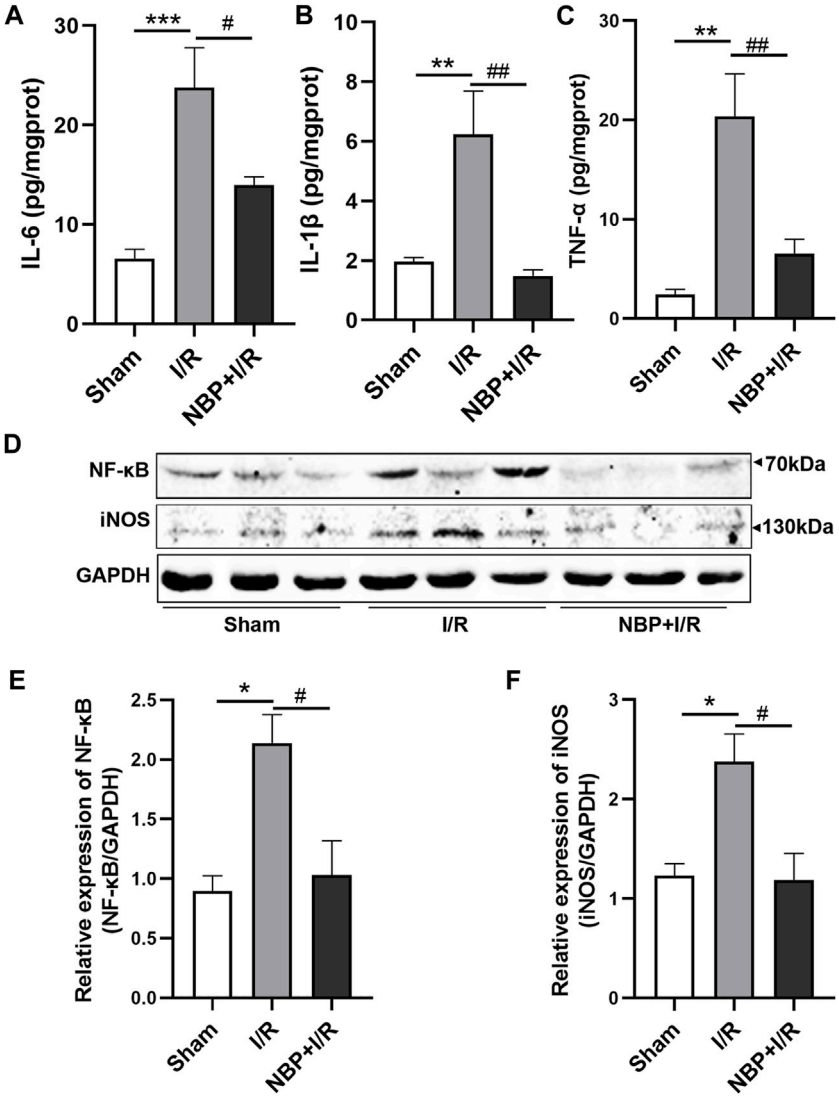

FIGURE 5
Effects of NBP on inflammation on the infarcted cerebral hemisphere in I/R rats. **(A–C)** Effects of NBP on inflammatory cytokines including IL-6, IL-1β and TNF-α. The concentrations of the three cytokines were significantly increased after I/R surgery and significantly decreased after NBP treatment. **(D–F)** Effects of NBP on the NF-κB/iNOS pathway. Data are expressed as the mean ± SEM and were analyzed by one-way ANOVA (*post hoc* analysis: Tukey's *post hoc* analysis test). * ($p < .05$), ** ($p < .01$) and *** ($p < .001$) represent significance compared to the sham group. # ($p < .05$) and ## ($p < .01$) represent significance compared to the I/R group ($p < .01$). NBP dose: NBP + I/R, 9 mg/kg.

Discussion

At the beginning of ischemic stroke, an irreversible necrotic zone in the brain is first formed, followed by second-phase damage in the peri-infarct area surrounding the core (Darwish et al., 2020). The peri-infarct area, which is called the ischemic penumbra, plays an important role in the clinical deficits of ischemic stroke and can be recovered by rapid reperfusion or neuroprotective treatment (Belayev et al., 2018). PSCI developing after stroke usually leads to worse clinical outcomes (Douven et al., 2018). Compared with healthy controls, ischemic stroke patients with even mild neurological impairment exhibit PSCI, including depressive symptoms, fading memory and decreased social cognitive performance (Pedroso et al., 2018). The pathogenesis of ischemic stroke is quite complex. It has been suggested that the injured brain following ischemic stroke is a functional unit to be protected, and neuroprotective reagents with multiple targets might be a promising option for PSCI treatment (Terasaki et al., 2014).

Our study showed that NBP profoundly ameliorated depression-like disorder, enhanced study and memory competence and promotes social cognition as judged by the SPT, NOR test and SI test, respectively. The protective effect of NBP on neurological function was evaluated in our study. According to neurological scoring and TTC staining results, NBP potently attenuated neurological deficits and reduced infarct volume, consistent with previously reported studies (Zhang et al., 2012; Li et al., 2019). In addition, by laser speckle imaging, we confirmed that NBP was able to enhance CBF in the ischemic cerebral hemisphere in I/R rats, which has been reported to be responsible for neurological deficits (El Amki and Wegener,

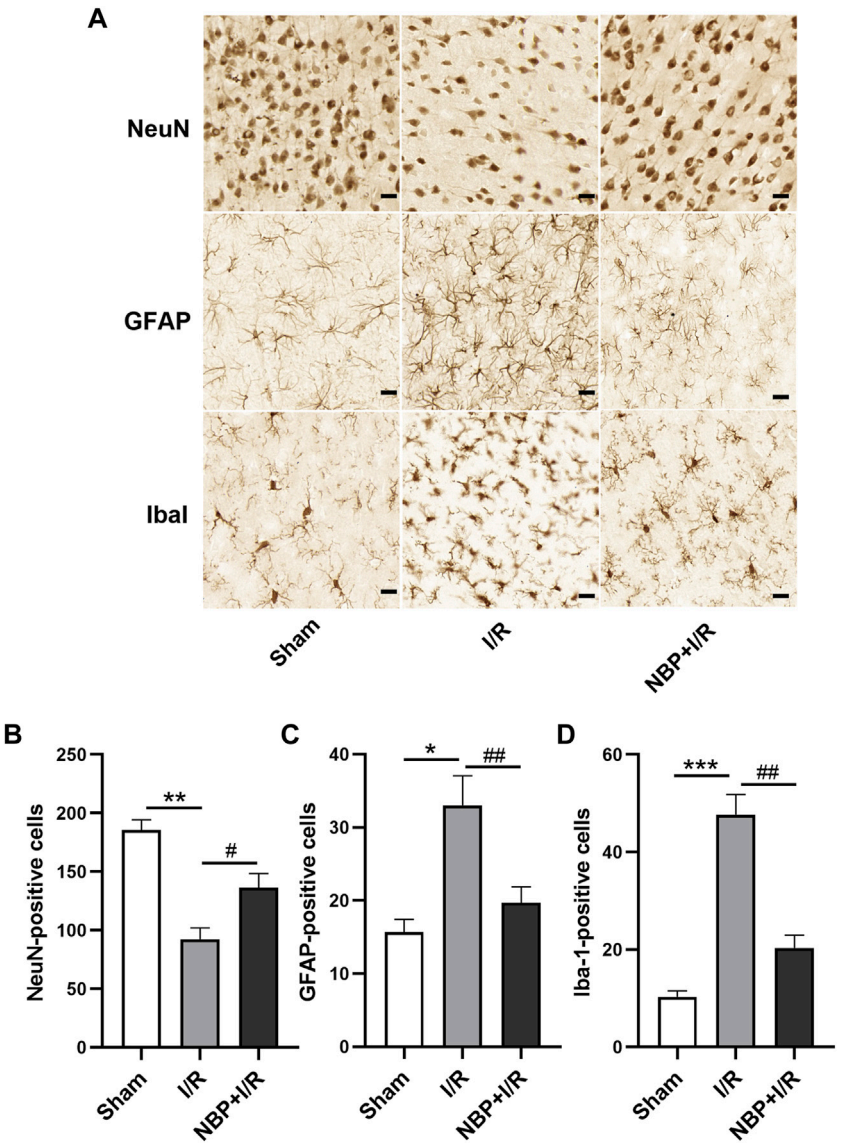

FIGURE 6
Effects of NBP on nerve cells in the ischemic penumbra in I/R rats. **(A)** NeuN, GFAP and Iba1 staining by immunochemistry (scale bar = 20 μm). NBP significantly increased NeuN-positive cells **(B)** and decreased GFAP-positive cells **(C)** and Iba1-positive cells **(D)**, suggesting that NBP could preserve the viability of neurons and protect microglia and astrocytes against overactivation in I/R rats. Data are expressed as the mean ± SEM (n = 3) and were analyzed by one-way ANOVA (*post hoc* analysis: Tukey's *post hoc* analysis test). ** ($p < .01$) represents significance compared to the sham group. # ($p < .05$) represents significance compared to the I/R group ($p < .01$). NBP dose: NBP + I/R, 9 mg/kg.

2017). Loss of neurons, and excessive activation of microglia and astrocytes play vital roles in cerebral injury and cognitive dysfunction after ischemic stroke (Chamorro et al., 2016; Xu et al., 2017). Suppression of microglia and astrocyte activation and protection of neuronal viability contribute to functional recovery in brain (Wang et al., 2022). In our study, we showed that NBP significantly suppressed the activation of microglia and astrocytes and protected neurons in the ischemic penumbra in I/R rats, indicating that NBP is an effective neuroprotective reagent.

It has been demonstrated that NBP is a multitarget neuroprotectant that suppresses neuroinflammation, reduces oxidative stress, improves mitochondrial function and inhibits neuronal apoptosis (Yang et al., 2015). It is proposed in our study that NBP alleviates PSCI by targeting multiple signaling pathways. Oxidative stress plays a pivotal role in the progression of ischemic stroke by initiating a series of biochemical cascades. ROS are essential signaling molecules that are overexpressed during cerebral ischemia and reperfusion and cause cellular damage and death (Li W et al., 2021). MDA, a kind of lipid peroxide, is another major oxidative stress indicator reflecting the degree of lipid peroxidation and cell damage in the injured brain (Hua et al., 2015). In our study, we show that NBP significantly inhibits ROS and MDA production, indicating that NBP is a potent antioxidant. Nrf2 is a key regulator in antioxidative response. Nrf2 initiates the transcription of a number of antioxidative genes by binding nucleus antioxidant response elements (AREs) after redox stimulation (Hassanein et al., 2020). The cytoplasmic protein Keap1 is a negative regulator of Nrf2. Overexpression of Keap1 inhibits Nrf2 levels and aggravates

oxidative stress induced brain injury. In contrast, inhibition of Keap1 releases Nrf2 to the nucleus, thus activating the antioxidant defense system (Byun and Lee, 2015). Recently, a clinical study showed that NBP exerts a neuroprotective effect on ischemic stroke patients by regulating the Keap1/Nrf2 pathway (Zhang et al., 2022). In addition, activation of the Nrf2 pathway suppresses oxidative stress and further attenuates brain injury and improves PSCI in I/R rats (Zhang et al., 2021). Combined with the above research and our results, it is concluded that the Keap1/Nrf2 pathway is also associated with PSCI alleviation by NBP.

Conversely, increasing evidences has shown that inflammation after ischemic stroke poses a second wave of damage to the brain (Veltkamp and Gill, 2016). Neuroinflammation provides potential targets for the treatment of neurological diseases (Chopra et al., 2010; Sharma et al., 2019). It has been proved in both clinical studies and animal experiments that the NF-κB signaling pathway plays an important role in inflammation-induced injury in ischemic stroke (Ran et al., 2021). The involvement of the NF-κB pathway in ischemic stroke makes it an attractive target for the development of anti-inflammatory drugs to treat ischemia-reperfusion injury (Howell and Bidwell, 2020). Our data showed that the levels of inflammatory cytokines, including IL-6, IL-1β and TNF-α, were significantly increased and that NF-κB and iNOS were significantly overexpressed in I/R rats. NBP significantly downregulated the cytokine, NF-κB protein and iNOS protein expression levels, indicating that the NF-κB/iNOS pathway is another important target for NBP.

Conclusion

In summary, our data suggest that NBP effectively protects neurological function and alleviates PSCI in I/R rats by synergistically suppressing inflammation and oxidative stress by targeting the Keap1/Nrf2 pathway and NF-κB/iNOS pathway, respectively. Therefore, NBP is a promising neuroprotective agent for PSCI treatment.

Data availability statement

The original contributions presented in the study are included in the article/supplementary material, further inquiries can be directed to the corresponding authors.

Ethics statement

The animal study was reviewed and approved by the Institutional Animal Care and Use Committee of Changsha Medical University. Written informed consent was obtained from the owners for the participation of their animals in this study.

Author contributions

Conceived and designed the experiments: HZ, WZ, BH, and YC. Performed the experiments: HZ, LW, YY, CC, XW, and LD. Analyzed the data: HZ, LW, WZ, and YC. Wrote the paper: HZ, WZ, and YC. All of the authors reviewed the manuscript and approved it for publication.

Funding

This work was supported by the Research Foundation of Education Bureau of Hunan Province (Program No. 22C0673, 19B069, 19C0197, 19C0220), the Natural Science Foundation of Hunan Province (Program No. 2021JJ40644), the Basic Ability Enhancement Program for Young and Middle-aged Teachers of Guangxi Wuzhou Medical College (Program No. 2021KY 1943, 2021KY 1947, 2021KY 1945), and the Hunan College Students Innovation and Entrepreneurship Training Program "The role of voltioxetine in posttraumatic stress disorder" to YY. The Natural Science Foundation of Changsha, China (kq2014117).

Conflict of interest

The authors declare that the research was conducted in the absence of any commercial or financial relationships that could be construed as a potential conflict of interest.

Publisher's note

All claims expressed in this article are solely those of the authors and do not necessarily represent those of their affiliated organizations, or those of the publisher, the editors and the reviewers. Any product that may be evaluated in this article, or claim that may be made by its manufacturer, is not guaranteed or endorsed by the publisher.

References

Bahader, G. A., Nash, K. M., Almarghalani, D. A., Alhadidi, Q., McInerney, M. F., and Shah, Z. A. (2021). Type-I diabetes aggravates post-hemorrhagic stroke cognitive impairment by augmenting oxidative stress and neuroinflammation in mice. *Neurochem. Int.* 149, 105151. doi:10.1016/j.neuint.2021.105151

Belayev, L., Hong, S. H., Menghani, H., Marcell, S. J., Obenaus, A., Freitas, R. S., et al. (2018). Docosanoids promote neurogenesis and angiogenesis, blood-brain barrier integrity, penumbra protection, and neurobehavioral recovery after experimental ischemic stroke. *Mol. Neurobiol.* 55 (8), 7090–7106. doi:10.1007/s12035-018-1136-3

Byun, H. G., and Lee, J. K. (2015). Chlorella ethanol extract induced phase II enzyme through NFE2L2 (nuclear factor [Erythroid-Derived] 2-like 2, NRF2) activation and protected ethanol-induced hepatoxicity. *J. Med. Food.* 18 (2), 182–189. doi:10.1089/jmf.2014.3159

Chamorro, Á., Dirnagl, U., Urra, X., and Planas, A. M. (2016). Neuroprotection in acute stroke: Targeting excitotoxicity, oxidative and nitrosative stress, and inflammation. *Lancet. Neurol.* 15 (8), 869–881. doi:10.1016/S1474-4422(16)00114-9

Chopra, K., Tiwari, V., Arora, V., and Kuhad, A. (2010). Sesamol suppresses neuro-inflammatory cascade in experimental model of diabetic neuropathy. *J. Pain.* 11 (10), 950–957. doi:10.1016/j.jpain.2010.01.006

Darwish, E. A. F., Abdelhameed-El-Nouby, M., and Geneidy, E. (2020). Mapping the ischemic penumbra and predicting stroke progression in acute ischemic stroke: The overlooked role of susceptibility weighted imaging. *Insights Imaging* 11 (1), 6. doi:10.1186/s13244-019-0810-y

Douven, E., Aalten, P., Staals, J., Schievink, S. H. J., van Oostenbrugge, R. J., Verhey, F. R. J., et al. (2018). Co-Occurrence of depressive symptoms and executive dysfunction after

stroke: Associations with brain pathology and prognosis. *J. Neurol. Neurosurg. Psychiatry.* 89 (8), 859–865. doi:10.1136/jnnp-2017-317548

El Amki, M., and Wegener, S. (2017). Improving cerebral blood flow after arterial recanalization: A novel therapeutic strategy in stroke. *Int. J. Mol. Sci.* 18 (12), 2669. doi:10.3390/ijms18122669

Fan, X., Shen, W., Wang, L., and Zhang, Y. (2022). Efficacy and safety of DL-3-n-butylphthalide in the treatment of poststroke cognitive impairment: A systematic review and meta-analysis. *Front. Pharmacol.* 12, 810297. doi:10.3389/fphar.2021.810297

Gold, A. B., Herrmann, N., Swardfager, W., Black, S. E., Aviv, R. I., Tennen, G., et al. (2011). The relationship between indoleamine 2, 3-dioxygenase activity and post-stroke cognitive impairment. *J. Neuroinflammation.* 8, 17. doi:10.1186/1742-2094-8-17

Grupke, S., Hall, J., Dobbs, M., Bix, G. J., and Fraser, J. F. (2015). Understanding history, and not repeating it. Neuroprotection for acute ischemic stroke: From review to preview. *Clin. Neurol. Neurosurg.* 129, 1–9. doi:10.1016/j.clineuro.2014.11.013

Hassanein, E. H. M., Sayed, A. M., Hussein, O. E., and Mahmoud, A. M. (2020). Coumarins as modulators of the keap1/nrf2/ARE signaling pathway. *Med. Cell. Longev.* 2020, 1675957. doi:10.1155/2020/1675957

Howell, J. A., and Bidwell, G. L., 3rd. (2020). Targeting the NF-κB pathway for therapy of ischemic stroke. *Ther. Deliv.* 11 (2), 113–123. doi:10.4155/tde-2019-0075

Hua, K., Sheng, X., Li, T. T., Wang, L. N., Zhang, Y. H., Huang, Z. J., et al. (2015). The edaravone and 3-n-butylphthalide ring-opening derivative 10b effectively attenuates cerebral ischemia injury in rats. *Acta. Pharmacol. Sin.* 36 (8), 917–927. doi:10.1038/aps.2015.31

Huang, Y. Y., Chen, S. D., Leng, X. Y., Kuo, K., Wang, Z. T., Cui, M., et al. (2022). Post-stroke cognitive impairment: Epidemiology, risk factors, and management. *J. Alzheimers. Dis.* 86 (3), 983–999. doi:10.3233/JAD-215644

Kalaria, R. N., Akinyemi, R., and Ihara, M. (2016). Stroke injury, cognitive impairment and vascular dementia. *Biochim. Biophys. Acta.* 1862 (5), 915–925. doi:10.1016/j.bbadis.2016.01.015

Kim, H., Seo, J. S., Lee, S. Y., Ha, K. T., Choi, B. T., Shin, Y. I., et al. (2020). AIM2 inflammasome contributes to brain injury and chronic post-stroke cognitive impairment in mice. *Brain Behav. Immun.* 87, 765–776. doi:10.1016/j.bbi.2020.03.011

Li, H. Q., Xia, S. N., Xu, S. Y., Liu, P. Y., Gu, Y., Bao, X. Y., et al. (2021). γ-Glutamylcysteine alleviates ischemic stroke-induced neuronal apoptosis by inhibiting ros-mediated endoplasmic reticulum stress. *Oxid. Med. Cell. Longev.* 2021, 2961079. doi:10.1155/2021/2961079

Li, J., Liu, Y., Zhang, X., Chen, R., Zhang, L., Xue, J., et al. (2019). Dl-3-N-butylphthalide alleviates the blood-brain barrier permeability of focal cerebral ischemia reperfusion in mice. *Neuroscience* 413, 99–107. doi:10.1016/j.neuroscience.2019.06.020

Li, W., Wei, D., Zhu, Z., Xie, X., Zhan, S., Zhang, R., et al. (2021). Dl-3-n-Butylphthalide alleviates hippocampal neuron damage in chronic cerebral hypoperfusion *via* regulation of the CNTF/CNTFRα/JAK2/STAT3 signaling pathways. *Front. Aging. Neurosci.* 12, 587403. doi:10.3389/fnagi.2020.587403

Liu, Y., Kong, C., Gong, L., Zhang, X., Zhu, Y., Wang, H., et al. (2020). The association of post-stroke cognitive impairment and gut microbiota and its corresponding metabolites. *J. Alzheimers Dis.* 73 (4), 1455–1466. doi:10.3233/JAD-191066

Liu, Z. W., Yu, Y., Lu, C., Jiang, N., Wang, X. P., Xiao, S. Y., et al. (2019). Postweaning isolation rearing alters the adult social, sexual preference and mating behaviors of male Cd-1 mice. *Front. Behav. Neurosci.* 13, 21. doi:10.3389/fnbeh.2019.00021

Longa, E. Z., Weinstein, P. R., Carlson, S., and Cummins, R. (1989). Reversible middle cerebral artery occlusion without craniectomy in rats. *Stroke* 20 (1), 84–91. doi:10.1161/01.str.20.1.84

Lu, Y., Ho, C. S., Liu, X., Chua, A. N., Wang, W., McIntyre, R. S., et al. (2017). Chronic administration of fluoxetine and pro-inflammatory cytokine change in a rat model of depression. *PLoS One* 12 (10), e0186700. doi:10.1371/journal.pone.0186700

Lueptow, L. M. (2017). Novel object recognition test for the investigation of learning and memory in mice. *J. Vis. Exp.* 126, 55718. doi:10.3791/55718

Mendelson, S. J., and Prabhakaran, S. (2021). Diagnosis and management of transient ischemic attack and acute ischemic stroke: A review. *JAMA* 325 (11), 1088–1098. doi:10.1001/jama.2020.26867

Pedroso, V. S. P., Brunoni, A. R., Vieira, É. L. M., Jorge, R. E., Lauterbach, E. C., and Teixeira, A. L. (2018). Early psychiatric morbidity in a Brazilian sample of acute ischemic stroke patients. *Clin. (Sao Paulo.* 73, e55. doi:10.6061/clinics/2018/e055

Ran, Y., Su, W., Gao, F., Ding, Z., Yang, S., Ye, L., et al. (2021). Curcumin ameliorates white matter injury after ischemic stroke by inhibiting microglia/macrophage pyroptosis through NF-κB suppression and NLRP3 inflammasome inhibition. *Oxid. Med. Cell. Longev.* 2021, 1552127. doi:10.1155/2021/1552127

Sacks, D., Baxter, B., Campbell, B. C. V., Carpenter, J. S., Cognard, C., Dippel, D., et al. (2018). Multisociety consensus quality improvement revised consensus statement for endovascular therapy of acute ischemic stroke. *Int. J. Stroke.* 13 (6), 612–632. doi:10.1177/1747493018778713

Shah, Z. A., Namiranian, K., Klaus, J., Kibler, K., and Doré, S. (2006). Use of an optimized transient occlusion of the middle cerebral artery protocol for the mouse stroke model. *J. Stroke Cerebrovasc. Dis.* 15 (4), 133–138. doi:10.1016/j.jstrokecerebrovasdis.2006.04.002

Sharma, D., Gondaliya, P., Tiwari, V., and Kalia, K. (2019). Kaempferol attenuates diabetic nephropathy by inhibiting rhoa/rho-kinase mediated inflammatory signalling. *Biomed. Pharmacother.* 109, 1610–1619. doi:10.1016/j.biopha.2018.10.195

Sun, J. H., Tan, L., and Yu, J. T. (2014). Post-stroke cognitive impairment: Epidemiology, mechanisms and management. *Ann. Transl. Med.* 2 (8), 80. doi:10.3978/j.issn.2305-5839.2014.08.05

Sun, Y., Cheng, X., Wang, H., Mu, X., Liang, Y., Luo, Y., et al. (2017). Dl-3-n-butylphthalide promotes neuroplasticity and motor recovery in stroke rats. *Behav. Brain. Res.* 329, 67–74. doi:10.1016/j.bbr.2017.04.039

Swardfager, W., Winer, D. A., Herrmann, N., Winer, S., and Lanctôt, K. L. (2013). Interleukin-17 in post-stroke neurodegeneration. *Neurosci. Biobehav. Rev.* 37 (3), 436–447. doi:10.1016/j.neubiorev.2013.01.021

Teng, Z., Dong, Y., Zhang, D., An, J., and Lv, P. (2017). Cerebral small vessel disease and post-stroke cognitive impairment. *Int. J. Neurosci.* 127 (9), 824–830. doi:10.1080/00207454.2016.1261291

Terasaki, Y., Liu, Y., Hayakawa, K., Pham, L. D., Lo, E. H., Ji, X., et al. (2014). Mechanisms of neurovascular dysfunction in acute ischemic brain. *Curr. Med. Chem.* 21 (18), 2035–2042. doi:10.2174/09298673216613122822340O

Tiwari, V., and Chopra, K. (2012). Attenuation of oxidative stress, neuroinflammation, and apoptosis by curcumin prevents cognitive deficits in rats postnatally exposed to ethanol. *Psychopharmacol. Berl.* 224 (4), 519–535. doi:10.1007/s00213-012-2779-9

Tiwari, V., Kuhad, A., and Chopra, K. (2009). Suppression of neuro-inflammatory signaling cascade by tocotrienol can prevent chronic alcohol-induced cognitive dysfunction in rats. *Behav. Brain. Res.* 203 (2), 296–303. doi:10.1016/j.bbr.2009.05.016

Veltkamp, R., and Gill, D. (2016). Clinical trials of immunomodulation in ischemic stroke. *Neurotherapeutics* 13 (4), 791–800. doi:10.1007/s13311-016-0458-y

Wang, B. N., Wu, C. B., Chen, Z. M., Zheng, P. P., Liu, Y. Q., Xiong, J., et al. (2021). DL-3-n-butylphthalide ameliorates diabetes-associated cognitive decline by enhancing PI3K/akt signaling and suppressing oxidative stress. *Acta. Pharmacol. Sin.* 42 (3), 347–360. doi:10.1038/s41401-020-00583-3

Wang, C. Y., Xu, Y., Wang, X., Guo, C., Wang, T., and Wang, Z. Y. (2019). Dl-3-n-Butylphthalide inhibits NLRP3 inflammasome and mitigates alzheimer's-like pathology via nrf2-TXNIP-TrX Axis. *Antioxid. Redox Signal.* 30 (11), 1411–1431. doi:10.1089/ars.2017.7440

Wang, L., Wang, X., Deng, L., Zhang, H., He, B., Cao, W., et al. (2022). Pexidartinib (PLX3397) through restoring hippocampal synaptic plasticity ameliorates social isolation-induced mood disorders. *Int. Immunopharmacol.* 113, 109436. doi:10.1016/j.intimp.2022.109436

Xu, J., Dong, H., Qian, Q., Zhang, X., Wang, Y., Jin, W., et al. (2017). Astrocyte-derived CCL2 participates in surgery-induced cognitive dysfunction and neuroinflammation via evoking microglia activation. *Behav. Brain. Res.* 332, 145–153. doi:10.1016/j.bbr.2017.05.066

Yan, H., Yan, Z., Niu, X., Wang, J., Gui, Y., and Zhang, P. (2017). Dl-3-n-butylphthalide can improve the cognitive function of patients with acute ischemic stroke: A prospective intervention study. *Neurol. Res.* 39 (4), 337–343. doi:10.1080/01616412.2016.1268775

Yang, L. C., Li, J., Xu, S. F., Cai, J., Lei, H., Liu, D. M., et al. (2015). L-3-n-Butylphthalide promotes neurogenesis and neuroplasticity in cerebral ischemic rats. *CNS. Neurosci. Ther.* 21 (9), 733–741. doi:10.1111/cns.12438

Zhang, L., Yu, W. H., Wang, Y. X., Wang, C., Zhao, F., Qi, W., et al. (2012). DL-3-n-Butylphthalide, an anti-oxidant agent, prevents neurological deficits and cerebral injury following stroke per functional analysis, magnetic resonance imaging and histological assessment. *Curr. Neurovasc. Res.* 9 (3), 167–175. doi:10.2174/156720212801618956

Zhang, X., and Bi, X. (2020). Post-stroke cognitive impairment: A review focusing on molecular biomarkers. *J. Mol. Neurosci.* 70 (8), 1244–1254. doi:10.1007/s12031-020-01533-8

Zhang, X., Wu, Q., Wang, Z., Li, H., and Dai, J. (2022). Keap1-Nrf2/ARE signal pathway activated by butylphthalide in the treatment of ischemic stroke. *Am. J. Transl. Res.* 14 (4), 2637–2646. PMID: 35559381.

Zhang, X., Yuan, M., Yang, S., Chen, X., Wu, J., Wen, M., et al. (2021). Enriched environment improves post-stroke cognitive impairment and inhibits neuroinflammation and oxidative stress by activating nrf2-ARE pathway. *Int. J. Neurosci.* 131 (7), 641–649. doi:10.1080/00207454.2020.1797722

Frontiers in Pharmacology

Explores the interactions between chemicals and living beings

The most cited journal in its field, which advances access to pharmacological discoveries to prevent and treat human disease.

Discover the latest Research Topics

See more →

Frontiers

Avenue du Tribunal-Fédéral 34
1005 Lausanne, Switzerland
frontiersin.org

Contact us

+41 (0)21 510 17 00
frontiersin.org/about/contact